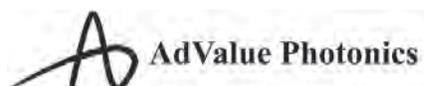


Table of Contents

Schedule-at-a-Glance	2
General Chairs' Welcome Letter	3
Conference Services	5
Sponsoring Societies' Booths	7
Conference Materials	8
Plenary Sessions and Awards Ceremony	9
Special Symposia	13
Applications & Technology Topical Reviews	16
Short Courses	19
Special Events	29
CLEO:EXPO	
Exhibitors	32
CLEO: Industry Focus	34
CLEO Committees	36
Explanation of Session/Presentation Codes	41
Agenda of Sessions	41
Technical Program	
Abstracts	52
Key to Authors	250

CLEO Management thanks the following corporate sponsors for their generous support:



Conference on Lasers and Electro-Optics®

Schedule-at-a-Glance

	Sunday 13 May	Monday 14 May	Tuesday 15 May	Wednesday 16 May	Thursday 17 May	Friday 18 May
GENERAL						
Registration	07:00–17:00	07:00–18:00	07:00–18:30	07:30–18:30	07:30–18:00	07:30–15:30
Speaker Ready Room	13:00–17:00	07:00–18:00	07:00–18:00	07:00–17:30	07:00–18:00	07:30–15:30
Coffee Breaks *on show floor		10:00–10:30 15:30–16:00	10:00–11:30 * 15:00–17:00*	10:00–11:30* 15:00–17:00*	10:00–11:30* 16:00–16:30	10:00–10:30
CLEO TECHNICAL PROGRAMMING						
Short Courses	08:30–17:30	12:30–16:30	12:00–16:00			
Technical Sessions		08:00–18:00	13:00–19:00	13:00–19:00	08:00–18:30	08:00–16:00
Special Symposium and A&T Topical Reviews		08:00–12:30	13:00–19:00	13:00–19:00	08:00–18:30	08:00–16:00
Plenary Sessions			08:00–10:00	08:00–10:00		
 Dynamic e-Posters			11:30–13:00	11:30–13:00	11:30–13:00	
Postdeadline Paper Sessions					20:00–22:00	
CLEO:EXPO AND SHOW FLOOR ACTIVITIES						
CLEO:EXPO			10:00–17:00	10:00–17:00	10:00–15:00	
Poster Sessions and Free Lunches in Exhibit Hall			11:30–13:00 Free Lunch	11:30–13:00 Free Lunch	11:30–13:00 12:30–14:00 Free Lunch	
OIDA VIP Industry Leaders Speed Meetings Lunch			12:00–13:30			
CLEO Theaters I & II			10:00–17:00	10:00–17:00	10:00–14:00	
Meet the OSA Editors’ Reception			15:30–17:00			
KMLabs Lunch and Learn Event				12:00–13:30		
Technology Transfer Program					10:15–13:00	
SPECIAL EVENTS						
OSAF Data Science & Career Opportunities	08:30–17:00					
OSAF Cheeky Scientist Workshop	13:00–14:00 16:00–17:00					
OIDA Executive Forum on the Exploding Role of Optics in Sensing		08:30–18:00				
OSA Technical Group Events		12:00–13:00 19:00–20:30	19:00–20:30	12:00–13:00	18:30–20:00	
Social Media 102		13:00–14:00				
Workshop: Understanding Unconscious Bias		14:00–15:30 16:00–17:30				
Diversity & Inclusion in Optics and Photonics Reception		17:30–18:30				
Conference Reception				19:30–20:30		

Welcome to CLEO!

It is our pleasure to welcome you to CLEO 2018 in San Jose, CA. CLEO continues to be the world's premier international forum for scientific and technical optics, uniting the fields of lasers and optoelectronics by bringing together all aspects of laser technology, from basic research to industry applications. Within the scope of a single conference, CLEO provides a forum where attendees can explore new scientific ideas, engineering concepts, and emerging applications in fields such as biophotonics, optical communications, and novel light sources. While the quality of work presented remains assured by CLEO's world-renowned technical program, the conference continues to evolve with new features to enhance your experience.

CLEO offers high quality content in five core event elements:

Fundamental Science: The premier venue for discussion of basic research in optical and laser physics and related fields. Topics include modern spectroscopy, ultrafast and nonlinear light-matter interactions, quantum optics, low-dimensional optical materials, quantum information science, nanophotonics, plasmonics, and metamaterials.

Science & Innovations: World-leading scientific research and innovation in lasers, optical materials, and photonic devices. Topics include laser processing of materials, terahertz science and technologies, ultrafast optics, biophotonics, nanophotonics, fiber photonics, nonlinear optical and laser technologies, metrology, sensing, and energy-efficient "green" photonics.

Applications & Technology: Exploration of the transition of fundamental research into emerging applications and products. The scope spans innovative laser and EO components and systems and applications. This topic includes biomedical devices for diagnostics and therapeutics, high power laser systems for industry and defense, photonics instrumentation and technologies for metrology, industrial processes, environmental sensing, and energy conservation.

CLEO:EXPO: The exhibition will showcase more than 200 participating companies featuring a wide range of photonics innovations, products and services. It is expected to attract more than 4,000 attendees including researchers, engineers, and leaders from top research institutions and major businesses who represent the fastest growing markets in optics and photonics.

CLEO Theaters: This program focuses on the latest trends in the photonics marketplace and provides a forum to discuss new products and emerging technologies. All presentations and discussions are focused on the latest in photonics products and services that have been playing an important role in the industry and those that potentially hold a future business opportunity.

This year's CLEO features 5 extraordinary plenary speakers. On Tuesday morning, Nader Engheta and Vasilis Ntziachristos are our featured speakers. Engheta will describe exciting features and novel opportunities arising from light-matter interaction in metastructures, while Ntziachristos will discuss exciting recent progress in optoacoustic microscopy and its potential clinical impact. On Wednesday morning, featured speakers are Jian-Wei Pan and Sara Seager. Pan will highlight new developments that could lead to a satellite-based global quantum communication network, and Seager will discuss the dramatic advances in the discovery and characterization of exoplanets.

The International Day of Light is celebrated across the world on 16 May as the anniversary of the first successful operation of the laser in 1960 by physicist and engineer Theodore Maiman. CLEO is the perfect home to recognize this day. This conference epitomizes "how a scientific discovery can yield revolutionary benefits to society in communications, healthcare and many other fields," as quoted on the IDL site. In recognition of the International Day of Light, CLEO is excited have a third Wednesday plenary speaker, John C. Mather, Nobel Laureate, who will talk about our exploration of the universe through light waves.

The CLEO Technical Program committee maintains a rigorous peer review system that emphasizes and maintains high technical quality in all presentations. This rigorous process is made possible by the combined efforts of over 300 volunteers in 25 technical committees. In 2018, the conference features an outstanding collection of contributed paper presentations, invited speakers and tutorials. We are excited to offer more than 1300 oral presentations, 230 invited talks by some of the most respected researchers in our international community, and 23 tutorials. This year's poster sessions include an outstanding list of more than 500 posters, including a specially selected subset of posters that are dynamic E-posters. Furthermore, selected topics are highlighted in special symposia and topical reviews comprising tutorials and invited talks. Participation from industry is particularly encouraged through these topical reviews. Finally, we are pleased to offer a comprehensive short course program featuring 17 courses.

We extend our sincere thanks to the Technical Program Co-Chairs; Michael M. Mielke and Jin Ung Kang in Applications & Technology; and Stewart Aitchison and Todd Pittman in Fundamental Science, Amr S. Helmy and Shinji Yamashita in Science & Innovations for coordinating the work of our subcommittees to compile this outstanding CLEO program. We also thank Robert Fisher and Ben Eggleton, Short Course Co-Chairs, and all of the program committee members whose leadership, dedication, and hard work has been critical to maintaining the high quality of the meeting. Additionally, we would like to thank the APS Division of Laser Science, the IEEE Photonics Society, The Optical Society (OSA), and the exhibitors for their support and contributions to the meeting. Finally, we thank the OSA staff for their professional assistance and dedication in organizing this event.

We welcome you to the conference and thank you for your participation.



Peter Andersen
*Technical University of
Denmark, Denmark*
General Chair



Zhigang Chen
*San Francisco State
University, USA*
General Chair



Nicusor Iftimia
*Physical Sciences, Inc.,
Germany*
General Chair



Nathan Newbury
*National Institute of Standards
& Technology, USA*
General Chair



Jessie Rosenberg
*International Business Machines
Corp., USA*
General Chair



Jeff Shapiro
*Massachusetts Institute of
Technology, USA*
General Chair

Conference Services

Registration

Concourse Level

Sunday, 13 May	07:00–17:00
Monday, 14 May	07:00–18:00
Tuesday, 15 May	07:00–18:30
Wednesday, 16 May	07:30–18:30
Thursday, 17 May	07:30–18:00
Friday, 18 May	07:30–15:30

CLEO:EXPO

Exhibit Hall

The CLEO:EXPO is open to all registered attendees. Visit a diverse group of companies representing every facet of the lasers and electro-optics industries. Exhibition information can be found on page 32.

Tuesday, 15 May	10:00–17:00
Wednesday, 16 May	10:00–17:00
Thursday, 17 May	10:00–15:00

Speaker and Presider Ready Room

Room 211A

All technical presentation speakers and session presidors are required to check in to the Speaker Ready Room located on the Concourse Level in Room 211A. Speakers are required to check in 24 hours before their session begins.

Session presidors should check in one to two hours prior to their session for instructions on how to use in-room equipment and check for speaker cancellations and changes. Computers will be available to review uploaded slides.

Sunday, 13 May	13:00–17:00
Monday, 14 May	07:00–18:00
Tuesday, 15 May	07:00–18:00
Wednesday, 16 May	07:00–17:30
Thursday, 17 May	07:00–18:00
Friday, 18 May	07:30–15:30

Coat and Baggage Check

Lower Lobby, Street Level

Coat and baggage check is available to conference attendees for a nominal fee.

Thursday, 17 May	07:30–22:00
Friday, 18 May	07:30–16:30

Customer Service & Information Center

Concourse Level

For questions about the program, locating sessions or general conference information, visit the Conference Information Center. Lost and Found items will be left at the Conference Information Center for 24 hours. Please put your name on all conference materials (Program Book and Short Course Notes).

There is a replacement fee for Program Books and badges.

Sunday, 13 May	13:30–17:30
Monday, 14 May	07:00–17:00
Tuesday, 15 May	08:00–17:00
Wednesday, 16 May	08:00–17:00
Thursday, 17 May	08:00–16:00

E-Center Kiosks

Concourse Level

The E-Center provides multiple viewing stations allowing attendees to check email. The E-Center Kiosks will be open during registration hours. Please limit your time on a station between 10 to 15 minutes so others may have time to check their emails. Kiosk hours will mirror Registration hours.

First Aid and Emergency Information

The First Aid room, staffed with emergency medical personnel, is located on the Exhibit Level. This room will be open during all conference hours. In the event of an emergency, please contact a security guard or a CLEO staff member. All accidents, injuries or illnesses in the San Jose Convention Center should be reported to the Public Safety Office immediately; call the office at extension 3500 from any white courtesy phone.

Wireless Access

San Jose Convention Center offers free Wi-Fi experience. To access the network just connect to the SSID, **“Wickedlyfastwifi”**, a return, SSID is easily readable.

No personal information or password needed with unlimited Wi-Fi access provided in the Convention Center.

All conference locations are in the San Jose Convention Center unless otherwise noted.

CLEO Announces CLEO KIDS - Child Care Options

This will be the first time CLEO has offered subsidized on-site childcare to attendees who want to bring their kids. We have contracted with KiddieCorp, an established childcare provider service that other conferences have used for childcare with great success.

Childcare reservations must be made 24 hours prior to date of service. Childcare services is based on space availability. Please contact Debbie Leffall at +1 916-595-7033 for reservation options.

Monday, 14 May	08:00–18:30
Tuesday, 15 May	08:00–19:30
Wednesday, 16 May	08:00–19:30
Thursday, 17 May	08:00–19:00
Friday, 18 May	08:00–16:30

All conference locations are in the San Jose Convention Center unless otherwise noted.

Sponsoring Societies' Booths

APS Booth

Concourse Level

Email: meetings@aps.org

Website: www.aps.org

The American Physical Society (APS) is a non-profit membership organization working to advance and diffuse the knowledge of physics through its outstanding research journals, scientific meetings, education and diversity programs, outreach, advocacy, and international activities. APS represents over 54,000 members, including physicists in academia, national laboratories, and industry in the United States and throughout the world. Throughout 2018, APS is celebrating the 125th anniversary of the Physical Review journals. Please stop by our booth near registration to learn more about APS programs, services, and world-class journals.

IEEE Photonics Society Booth & Membership Lounge

Concourse Level

Email: photonicsociety@ieee.org

Website: www.PhotonicsSociety.org

The IEEE Photonics Society is the professional home for a global network of scientists and engineers who represent the laser, optoelectronics and photonics community. The Society provides its members with professional growth opportunities, publishes journals, sponsors conferences and supports local chapter and student activities around the world. Visit the IEEE Photonics Society booth on the Concourse Level, near registration, for more information.

When you join or renew an IEEE Membership at the booth, eligible members will receive 50% off membership dues and all benefits through 31 December 2018. An IEEE Photonics Society Membership is as low as \$17 USD and only \$8.50 USD for students.

IEEE members are also welcome to visit the IEEE Member Lounge, sponsored by the IEEE Photonics Society. Come to the IEEE members-only lounge to relax, grab a snack and connect to the internet.

IEEE Lounge Schedule:

Monday, 14 May	10:00–16:00
Tuesday, 15 May	10:00–16:00
Wednesday, 16 May	10:00–16:00
Thursday, 17 May	10:00–14:00

IEEE Photonics Fund

The IEEE Photonics Society, in partnership with the IEEE Foundation, is proud to announce the establishment of the IEEE Photonics Fund. This fund will be used to enhance the humanitarian and educational initiatives of the Society by providing members and the photonics community with the ability to contribute directly to mission-driven imperatives, such as Humanitarian Projects, Student Resources, STEM Outreach and Diversity Initiatives.

All conference locations are in the San Jose Convention Center unless otherwise noted.

The IEEE Photonics Society has contributed USD \$100K to The IEEE Photonics Fund. Will you match us with your donation? With the establishment of this fund, you too can play a direct role in this vital work. Visit the IEEE Photonics Society booth or www.PhotonicsSociety.org for more information.

The Optical Society Booth

Exhibit Hall, #1927

Email: info@osa.org

Website: www.osa.org

Founded in 1916, The Optical Society (OSA) is the leading professional association in optics and photonics, home to accomplished science, engineering, and business leaders from all over the world.

Through world-renowned publications, meetings, and membership programs, OSA provides quality information and inspiring interactions that power achievements in the science of light. More than 21,000 OSA members, residing in over 100 countries and spanning academia, government and industry, call OSA their professional home.

Stop by to meet OSA staff, and learn more about our publications, conferences and meetings, and membership for individuals and companies.

The Optical Society Member Lounge

Concourse Level

OSA members are invited to take a brief respite from the conference at the Member Lounge. Whether it's to plan your schedule, meet up with other members or print your boarding pass, the lounge offers comfortable seating, light refreshments, coffee service and a computer/printer. In addition, take advantage of renewing your membership at 50% discount for one-year! You can renew at the OSA Member Lounge or the OSA Booth on the Exhibit Floor. This special rate is available whether you're rejoining for the first time or renewing for another year.

OSA Member Lounge Schedule:

Monday, 14 May	10:00–17:00
Tuesday, 15 May	10:00–17:00
Wednesday, 16 May	10:00–17:00
Thursday, 17 May	10:00–16:00

OSA CAM Lounge

Room 213

The Celebrating All Members (CAM) videos are an opportunity for OSA members to share their stories in 3 minutes or less about what/who inspired them to get into their field, what excites them about their current work and what OSA means to them. These short vignettes are shown on our website (osa.org/100), on social media and at some of our conferences. Stop by on Monday or Tuesday between 09:00–16:00 for a quick interview.

Conference Materials

Access to Technical Digest and Postdeadline Papers

Technical attendees have *early* and *continuous* access to the CLEO:2018 Technical Digest, including the Postdeadline Papers. The Technical Digest is comprised of the two-page summaries of tutorial, invited and accepted contributed/post-deadline papers. They can be downloaded individually or by downloading daily .zip files. (.zip files are available for 60 days after the conference).

1. Visit the conference website, www.cleoconference.org.
2. Select the Access Digest Papers link on the right side of the web page.
3. Log in using the same email address and password you used to register for the meeting. You will be directed to the conference page where you will see the .zip file links at the top of the page. Please note: if you are logged in successfully, you will see your name in the upper right-hand corner.

Access is limited to Full Conference attendees only, not Exhibits Pass Plus or One-Day attendees. If you need assistance with your login information, please use the "forgot password" utility or "Contact Help" link.

The available paper summaries will be submitted to the IEEE Xplore Digital Library (www.ieeeexplore.ieee.org), provided that the paper is presented by a co-author during CLEO 2018.

Poster PDFs

Authors presenting posters have the option to submit the PDF of their poster, which will be attached to their papers in OSA Publishing's Digital Library. If submitted, poster PDFs will be available three weeks after the conference. Submit your poster PDF no later than 31 May to cstech@osa.org. Your PDF should be named using your presentation number with "-1" added at the end (JTh2A.24-1.pdf.)

Short Course Notes

Notes typically include a copy of the presentation and any additional materials provided by the instructor. Each course has a unique set of notes, which are distributed on-site to registered course attendees only. Notes are not available for purchase separately from the course.

CLEO App

Manage your conference experience by downloading the CLEO App to your Smartphone or tablet.

Download the app one of three ways

1. Search for 'CLEO Conference' in the app store.
2. Go to cleoconference.org/app
3. Scan the QR code

Schedule

Search for conference presentations by day, topic, speaker or program type. Plan your schedule by setting bookmarks on programs of interest. Technical attendees can access technical papers within session descriptions.

Exhibit Hall

Search for exhibitors in alphabetical order and set a bookmark reminder to stop by their booth. Tap on the map icon within a description, and you'll find their location on the EXPO floor map. View a daily schedule of all activities occurring on the show floor.

Access Technical Digest Papers

Full technical registrants can navigate directly to the technical papers right from the CLEO mobile app. Locate the session or talk in "Event Schedule" and click on the "Download PDF" link that appears in the description .

IMPORTANT: You will need to log in with your registration email and password to access the technical papers. Access is limited to Full Conference attendees only.



Need assistance?

Contact our support team, available 24 hours a day Monday through Friday, and from 09:00 to 21:00 EDT on weekends, at +1.888.889.3069 option 1.

Android users who downloaded the app for CLEO 2017 or earlier years may need to download a new version of the app. Scan the QR code or search for 'CLEO Conference' in the Google Play Store.

All conference locations are in the San Jose Convention Center unless otherwise noted.

Plenary Sessions and Awards Ceremony

Plenary Session I

Tuesday, 15 May, 08:00–10:00
Grand Ballroom



Metaphotonics

Nader Engheta, *University of Pennsylvania, USA*

Materials are often used to control and manipulate photons. Metamaterials and metasurfaces are two representative classes of judiciously designed structures that provide unprecedented platforms for sculpting waves and fields. Their extreme properties lead to novel opportunities in photonics. Light-matter interaction in metastructures exhibits unusual functionalities with numerous exciting features and potential applications.

Nader Engheta is the H. Nedwill Ramsey Professor at the University of Pennsylvania. He received his PhD from Caltech. His current research activities span various areas of nanophotonics, metamaterials, nano-optics, electrodynamics, graphene optics, optical circuits, imaging and sensing inspired by eyes of animal species, and physics and engineering of light-matter interaction. His most recent awards include William Streifer Scientific Achievement Award, SPIE Gold Medal, Fellow of US National Academy of Inventors, Vannevar Bush Faculty Fellow Award, IEEE Electromagnetics Award, and URSI Balthasar van der Pol Gold Medal. He is a Fellow of OSA, APS, MRS, SPIE, IEEE, URSI, and AAAS.



Listening to Light: Advances in Opto-acoustic Imaging

Vasilis Ntziachristos, *Technical University of Munich, Germany*

Optical imaging is unequivocally the most versatile and widely used visualization modality in the life sciences. Yet it has been significantly limited by photon scattering, which complicates imaging beyond a few hundred microns. Progress with fast tunable lasers, spectral techniques and advanced instrumentation have allowed the development of multi-spectral opto-acoustic tomography (MSOT) for clinical use, offering unprecedented optical imaging performance and assessment of disease pathophysiology. The talk illuminates progress with opto-acoustic macroscopy and mesoscopy and its implication toward clinical impact.

Vasilis Ntziachristos is Professor of Medicine, Professor of Electrical Engineering and Director of the Chair for Biological Imaging (CBI) at the Technical University of Munich, Director of the Institute for Biological and Medical Imaging (IBMI) at the Helmholtz Zentrum Munchen and Director of Bioengineering at the Helmholtz Pioneering Campus. He has received the Diploma in Electrical Engineering and Computer Science from the Aristotle University of Thessaloniki, Greece and the MSc and PhD degrees in Bioengineering from the University of Pennsylvania in Philadelphia. Prior to his current appointment he served as faculty at Harvard University and the Massachusetts General Hospital.

Plenary Session II & International Day of Light

Wednesday, 16 May, 08:00–10:00
Grand Ballroom



Quantum Communication Network and Future Aspects

Jian-Wei Pan, *University of Science and Technology of China, China*

Based on state of the art fiber technologies, the prevailing quantum communication technology allows practical communication in the metropolitan area. However, the distance of fiber-based quantum communications is limited due to intrinsic fiber loss. To overcome these problems, we are taking two paths in parallel: quantum repeaters and through satellite, to establish a global quantum communication network.

Jian-Wei Pan obtained his PhD degree of Experimental Physics from the University of Vienna in 1999. In 2001, he was appointed as full professor of physics by the University of Science and Technology of China (USTC). In 2011, he was elected as the academician of Chinese Academy of Sciences (CAS). In 2012, he was elected as the World Academy of Science (TWAS) Fellow. His research focuses on quantum optics, quantum information and quantum foundations. He has accomplished a series of profound achievements in experimental quantum information science. Due to his numerous progresses on quantum communication and multi-photon entanglement manipulation, quantum information science has become one of the most rapidly developing fields of physical science in China in recent years.



Mapping the Nearest Stars for Habitable Worlds

Sara Seager, *Massachusetts Institute of Technology, USA*

For thousands of years people have wondered, "Are there planets like Earth?"; "Are such planets common?"; and "Do any have signs of life?" Today, astronomers are poised to answer these ancient questions, having recently found thousands of planets that orbit nearby Sun-like stars, called "exoplanets." The presentation will share the latest advances in this revolutionary field and work to answer the question, "Are we alone?" Or put another way, where are the neighbors, and how far away are they? In a few decades of research in opto-electronics and spectroscopy, we could know an answer.

Sara Seager is a planetary scientist and astrophysicist at the Massachusetts Institute of Technology. She has pioneered many research areas in the characterization of exoplanets. Her present research focus is on the search for life by way of exoplanet atmospheric "biosignature" gases. She works on space missions for exoplanets including as: the PI of the CubeSat ASTERIA; the Deputy Science Director of the MIT-led NASA Explorer-class mission TESS; and as a lead of the Starshade Rendezvous Mission (a space-based direct imaging exoplanet discovery concept under technology development)

All conference locations are in the San Jose Convention Center unless otherwise noted.

to find a true Earth analog orbiting a Sun-like star. Among other accolades, she was elected to the US National Academy of Sciences in 2015 and is a 2013 MacArthur Fellow.



**International
Day of Light**

16 May

Exploring the Universe at the Speed of Light

John C. Mather, *NASA's Goddard Space Flight Center, USA*

Astronomers travel the universe with imagination and observation, and most of the information arrives as light waves, showing the distant universe as it was when the light was sent out. We can now see at wavelengths ranging from over 10 meters to less than a picometer, limited only by our ingenuity and the opacity of our environment. We are beginning to learn the story of our own origins, from the expanding early universe, to the formation of galaxies, stars, and black holes, to the stellar nuclear processes producing the heavy elements of life, to the formation of planets. That history is full of catastrophic events, apparently necessary for our own existence. I will show some of the future discoveries we hope to see through NASA's James Webb Space Telescope (JWST), discuss the expanding views of the universe, and outline the technology that will lead us to deeper understanding.

John C. Mather is a Senior Astrophysicist in the Observational Cosmology Laboratory at NASA's Goddard Space Flight Center (GSFC). His research centers on infrared astronomy and cosmology. As an NRC postdoctoral fellow at the Goddard Institute for Space Studies, he led the proposal efforts for the Cosmic Background Explorer (74-76), and came to GSFC to be the Study Scientist (76-88), Project Scientist (88-98) and also the Principal Investigator for the Far IR Absolute Spectrophotometer (FIRAS) on COBE. He showed that the cosmic microwave background radiation has a blackbody spectrum within 50 ppm. As Senior Project Scientist (95-present) for the James Webb Space Telescope, he leads the science team, and represents scientific interests within the project management. He has received many awards including the Nobel Prize in Physics, 2006, for his precise measurements of the cosmic microwave background radiation using the COBE satellite. He was elected as an OSA Honorary Member in 2016.

Awards Ceremony

Tuesday, 15 May
Grand Ballroom

OSA Charles Hard Townes Medal



The Optical Society (OSA) established this medal in 1980 to honor Charles Hard Townes, whose pioneering contributions to masers and lasers led to the development of the field of quantum electronics. It is given to an individual or a group for outstanding experimental or theoretical work, discovery or invention in the field of quantum electronics.

The 2018 recipient is Peter Fritschel, Kavli Institute for Astrophysics and Space Research, Massachusetts Institute of Technology, USA, recognized for advances in quantum-limited precision measurement in the Advanced LIGO detectors, leading to the first direct detection of gravitational waves.

The Optical Society 2018 Fellows

These Fellows are being recognized at CLEO. Visit osa.org/fellows for a complete list of 2018 Fellows.

Andrea Armani, *University of Southern California, USA*
For contributions to integrated photonics with applications in telecommunication and chemical and biological detection

Hou-Tong Chen, *Los Alamos National Laboratory, USA*
For seminal contributions to the field of metamaterials, including active metamaterials and the realization of novel electromagnetic structures at terahertz frequencies

Yu-Ao Chen, *University of Science and Technology of China, China*
For outstanding contributions on photonic quantum information and quantum simulation

Stavros Demos, *Laboratory for Laser Energetics, University of Rochester, USA*
For pioneering and sustained contributions to understanding dynamic behaviors and improved performance in optical materials for high power lasers and developing multimodal imaging and characterization methods for medical and other applications

Heike Ebendorff-Heidpriem, *University of Adelaide, Australia*
For ground breaking science contributions to the field of optical glasses and fibers

Sasan Fathpour, *CREOL, The College of Optics and Photonics, University of Central Florida, USA*
For pioneering contributions to the field of integrated photonics, particularly heterogeneous integration in silicon photonics for second- and third-order nonlinear optics and mid-infrared wavelengths applications

Almantas Galvanauskas, *Center for Ultrafast Optical Science (CUOS), EECS Department, University of Michigan, USA*
For pioneering contributions to the science and technology of ultrashort pulse and high power fiber lasers, novel fiber structures, nonlinear interactions in fibers and fiber lasers, and fiber laser beam and pulse combining

All conference locations are in the San Jose Convention Center unless otherwise noted.

Goëry Genty, *Tampere University of Technology, Finland*
For pioneering research in the study of supercontinuum generation and nonlinear instabilities in optical fibers

Dr. Constantin Haefner, *Lawrence Livermore National Laboratory, USA*

For pioneering next generation, high average power Petawatt laser systems enabling a new arena of applications and sustained advancement of state-of-the art technologies in large-scale, high intensity, peak-power laser systems

Sivanandan S. Harilal, *Pacific Northwest National Laboratory, USA*

For pioneering contributions to the fundamentals of laser ablation, optical spectroscopy of laser ablation plumes and laser-plasma light sources

John E. Heebner, *Lawrence Livermore National Laboratory, USA*

For numerous innovations, achievements, and technical leadership in high energy laser systems and integrated optics including nonlinear optical microresonators and ultrafast light deflectors

Nicusor Iftimia, *Physical Sciences Inc., USA*

For original contributions in biomedical optics, especially pioneering the use of optical coherence tomography for interstitial tissue imaging and biopsy guidance, as well as for outstanding service to the biomedical optics community

Mona Jarrahi, *University of California, Los Angeles, USA*

For pioneering contributions to terahertz optoelectronics and microwave photonics through development of novel engineered materials, plasmonic nanostructures, and quantum well devices

Jungsang Kim, *Duke University, USA*

For research on scalable modular quantum computers and networks using trapped ions, large-scale optical switches, quantum optics with single-photon sources and detectors, and gigapixel-scale cameras

Tobias Kippenberg, *Ecole Polytechnique Federale de Lausanne, Switzerland*

For pioneering fundamental and applied research on microresonator frequency combs and cavity optomechanics

Tien-Chang Lu, *National Chiao Tung University, Taiwan*

For pioneering and outstanding contributions to wide band-gap semiconductor vertical-cavity surface-emitting lasers, light-emitting diodes, microcavity polariton lasers and surface plasmon polariton lasers

Zhenqiang Ma, *University of Wisconsin-Madison, USA*

For pioneering contributions to flexible optoelectronics and semiconductor nanomembrane based photonics

Arash Mafi, *University of New Mexico, USA*

For pioneering contributions to fundamental understanding of quantum and nonlinear behavior of optical waveguides, light propagation in disordered media, and development of Anderson localizing optical fibers

Mo Mojahedi, *Department of Electrical and Computer Engineering, University of Toronto, Canada*

For seminal contributions to the field of plasmonics and hybrid plasmonics with important applications to nanophotonics and sensing

John Nees, *University of Michigan, USA*

For contributions to the development of short pulse high rep rate laser technology as well as to the science of high intensity short pulse laser interactions with matter

Valdas Pasiskevicius, *Royal Institute of Technology (KTH), Sweden*

For substantial contributions to the development of novel applications of structured nonlinear optical materials and service to the optics community, particularly OSA

Alan B. Petersen, *Spectra-Physics, MKS Instruments, Inc., USA*

For significant and innovative contributions to the design of commercial scientific and industrial UV laser systems and for long term service to the optics community

Pepijn Pinkse, *Universiteit Twente, Netherlands*

For original and pioneering contributions in the fields of nanophotonics, quantum optics, and quantum secure authentication

Innocenzo Pinto, *University of Sannio, INFN, LVC, and KAGRA, Italy*

For fundamental contributions to thermal noise reduction in the mirror coatings of the LIGO interferometric gravitational wave detectors, and for original contributions to the science of Electromagnetics

Derryck T. Reid, *Heriot-Watt University, United Kingdom*

For the invention of two-photon autocorrelation using photodiodes and the development of frequency combs based on ultrafast optical parametric oscillators

Pascale Senellart, *Center for Nanoscience and Nanotechnology, France*

For inventing in-situ optical lithography that couples quantum dots and optical cavities with nanometric precision, realising solid-state single and entangled photon sources of unsurpassed performance that are moving quantum optics towards a scalable future

Glenn Solomon, *Joint Quantum Institute, USA*

For pioneering the development of semiconductor quantum dot optical materials and device structures for solid-state quantum optics

Kartik Srinivasan, *National Institute of Standards & Technology, USA*

For outstanding contributions to nanophotonics and quantum optics, including cavity-QED, frequency conversion, and integrated optics such as photonic crystals

Thomas Sudmeyer, *Universite de Neuchatel, Switzerland*

For seminal contributions to ultrafast photonics, in particular in the area of ultrafast thin disk lasers, nonlinear frequency conversion, and optical frequency combs

Hong-Bo Sun, *Tsinghua University, China*

For pioneering contributions to the field of laser nanofabrication in both fundamental research and industrial applications, as well as ultrafast spectroscopy and their applications on deep insight into nanophotonic materials and devices

Sergei Tochitsky, *University of California, Los Angeles, USA*

For outstanding contributions to the development of high-power picosecond CO₂ lasers and their applications in nonlinear optics and laser-driven particle acceleration

All conference locations are in the San Jose Convention Center unless otherwise noted.

M. Selim Ünlü, *Boston University, USA*

For pioneering contributions in utilization of optical interference in enhanced photodetectors and biological sensing and imaging

Mu Wang, *Nanjing University and American Physical Society, China*

For original contributions in designing of metallic subwavelength microstructures to control the polarization, propagation and intensity of light, optimizing physical properties and striving for their applications in optics and opto-electric exchange

IEEE Photonics Society 2018 Fellows**Michael Krames**, *Pacific Bell, USA*

For leadership in GaN-based light-emitting device physics and its commercialization

Hong-Bo Sun, *Tsinghua University, China*

For contributions to laser nanofabrication and ultrafast spectroscopy

James P. Gordon Memorial Speakership

Established in 2014 with the support of the Gordon family, The James P. Gordon Memorial Endowment funds a speakership on Quantum Information and Quantum Optics to a CLEO invited speaker. This speakership pays tribute to Dr. Gordon for his numerous high-impact contributions to quantum electronics and photonics, including the demonstration of the maser.

The recipient receives a \$1,500 honorarium and their presentation will be recorded and archived in OSA's media library. The contents will serve as an educational resource for the next generation of optics and photonics leaders.

Congratulations to

Mikhail Lukin, *Harvard University, USA***Tingye Li Innovation Prize**

The Tingye Li Innovation Prize, established in 2013, honors the global impact Dr. Li made to the field of Optics and Photonics. This prize is presented to a young professional with an accepted paper that has demonstrated innovative and significant ideas and/or contributions to the field of optics. The recipient of this prize receives a \$3,000 stipend, an invitation to the Chairs' Reception, and special recognition at the conference.

Congratulations to

Logan G. Wright, *Cornell University, USA***Maiman Student Paper Competition**

The Maiman Student Paper Competition honors American physicist Theodore Maiman for his demonstration of the first working laser and his other outstanding contributions to optics and photonics. It recognizes student innovation and research excellence in the areas of laser technology and electro-optics. The competition results will be announced during the meeting. The prize is endowed by a grant from HRL Laboratories LLC, the IEEE Photonics Society and the APS Division of Laser Science and is administered by the OSA Foundation.

Congratulations to our finalists:

Sheldon Kwok, *Massachusetts Institute of Technology, USA***Nils Otterstrom**, *Yale University, USA***Dominik Peller**, *University of Regensburg, Germany***Brian Stern**, *Cornell University, USA***Incubic/Milton Chang Travel Grant**

The OSA Foundation is pleased to award 10 recipients this year's Incubic/Milton Chang Student Travel Grant, endowed by Milton and Rosalind Chang. The list of recipients can be viewed at www.osa.org/foundation.

Plenary Speaker Meet-n-Greet

Tuesday, 15 May, 10:15–10:45

Theater I, Exhibit Hall, #2433

Meet Nader Engheta, Vasilis Ntziachristos and Jian-Wei Pan, ask questions and network with your colleagues.

Plenary Speaker Meet-n-Greet

Wednesday, 16 May, 10:15–10:45

Theater I, Exhibit Hall, #2433

Meet John Mather and Sara Seager, ask questions and network with your colleagues.

All conference locations are in the San Jose Convention Center unless otherwise noted.

Special Symposia

Future Directions in Terahertz Nanoscopy

Monday, 14 May, Session I: 08:00–10:00,
Session II: 10:30–12:30
Executive Ballroom 210A

Organizers

Tyler Cocker, *Universität Regensburg, Germany*
Daniel Mittleman, *Brown University, USA*

Terahertz and multi-terahertz microscopy with subwavelength spatial resolution has recently progressed from proof-of-principle demonstrations to scientific studies capable of revealing unique information. For example, the ability of terahertz nanoscopy to combine spatial resolution on the nanometer (or even sub-nanometer) scale with ultrafast temporal resolution may ultimately make it a 'killer application' for terahertz technology—one that can address scientific questions that are inaccessible via any other experimental approach. It may even be possible to obtain a comprehensive picture of nanoscale dynamics by combining cutting-edge terahertz-based techniques like near-field scanning optical microscopy and lightwave-driven scanning tunneling microscopy. Still, technical challenges remain that must be solved before the full potential of these techniques can be realized, either individually or together. In this symposium, we will discuss the latest results and future prospects of terahertz nanoscopy, as well as scientific goals for the field.

Invited Speakers

Joanna Atkin, *Univ. of North Carolina at Chapel Hill, USA*,
Towards Quantitative Conductivity Measurements with Infrared Near-Field Optical Microscopy

Dmitri Basov, *Columbia University, USA*, **Nano-THz Imaging of Quantum Materials**

Frank Hegmann, *University of Alberta, Canada*, **Future Directions in Terahertz Scanning Tunneling Microscopy**

Pernille Klarskov Pedersen, *Brown University, USA*, **Pushing Terahertz Emission Microscopy to the Nanoscale**

Jun Takeda, *Yokohama National University, Japan*, **Nanoscale Electron Manipulation Using Phase-controlled THz Near-fields**

Multimodal and Molecular Contrast Optical Imaging

Tuesday, 15 May, Session I: 13:00–15:00,
Session II: 17:00–19:00
Salon I & II, San Jose Marriott

Organizer

Wolfgang Drexler, *Medizinische Universität Wien, Austria*

Momentary clinical medical imaging technologies are expensive and complex with limited sensitivity and specificity. Multimodal and molecular contrast optical imaging offers low-cost, non-invasive, accurate, rapid alternatives and the potential to address global medical needs. This symposium focuses on the combination of state-of-the-art optical imaging modalities to enable enhanced clinical diagnosis in a variety of medical fields. A special emphasis will be on approaches enabling molecular contrast as well as endoscopic imaging.

Tutorial Speaker

Irene Georgakoudi, *Tufts University, USA*, **Bringing Functional High Resolution Diagnostics to the Bedside Using Multimodal, Label-free, Two-photon Imaging**

Invited Speakers

Thomas Bocklitz, *IPHT Jena, Germany*, **Nonlinear Optical Endoscopy**

Audrey Bowden, *Stanford University, USA*, **Multimodal Endoscopic Bladder Imaging**

Zhongping Chen, *University of California Irvine, USA*, **Intravascular Multimodal Imaging**

Johannes de Boer, *Vrije Univ Amsterdam, Netherlands*, **Combined Optical Coherence Tomography and Near Infrared Fluorescence of Cancer-specific Antibodies**

Adam de la Zerda, *Stanford University, USA*, **Molecular Imaging with Optical Coherence Tomography**

Kristen Maitland, *Texas A&M University, USA*, **Reflectance Confocal Microscopy and Fluorescence Lifetime Imaging in the Oral Cavity**

New Advances in Adaptive Optics Retinal Imaging

Wednesday, 16 May, Session I: 13:00–15:00,
Session II: 17:00–19:00
Salon VI, San Jose Marriott

Organizer

Mircea Mujat, *Physical Sciences Inc., USA*

Adaptive optics (AO) has recently achieved success in a range of high resolution retinal imaging applications in ophthalmology using instruments from flood illumination full-field retinal cameras and confocal scanning laser ophthalmoscopes (SLO) to optical coherence tomography (OCT). AO is being used as a tool to understand structural and functional aspects of vision, the elegant but complex retinal circuitry, and the dissolution of that structure, wiring and processes during the progression of disease. It has been used in direct measurements of the foveal avascular zone, retinal capillary erythrocyte and leukocyte velocity, pulsatility, and other functional dynamics. The RPE cell mosaic is being mapped in monkeys and humans and correlated to the cone mosaic. Diseases such as rod-cone dystrophy and genetic defects are confirmed and explored directly in the live eye. High-resolution retinal imaging is being applied to advanced molecular and gene therapies, both in their development and as the primary method to determine treatment efficacy at the cellular level. Systems are slowly migrating from the research lab into the clinic for use on patients with a variety of diseases and conditions. New developments such as dark-field imaging methods and OCT Angiography are clearly making their mark on ophthalmology research and practice.

Invited Speakers

Jacque Duncan, *University of California San Francisco, USA*, **Adaptive Optics Scanning Laser Ophthalmoscopy in Retinal Degenerations: New Insights in Structure and Function**

All conference locations are in the San Jose Convention Center unless otherwise noted.

Alfredo Dubra, *Stanford University, USA*, **Adaptive Optics Scanning Light Ophthalmoscopy: Beyond Structural Imaging**

Ethan Rossi, *University of Pittsburgh, USA*, **Imaging Single Cells in the Living Eye from the Retinal Pigment Epithelium to the Ganglion Cell Layer**

Robert Zawadzki, *University of California Davis, USA*, **Progress on Functional Retinal Imaging with OCT: Recent Advancements in Measurements and Modeling of Photoreceptor Optophysiology**

Advances in Integrated Microwave Photonics

Thursday, 17 May, Session I: 14:00–16:00,
Session II: 16:30–18:30
Executive Ballroom 210D

Organizers

David Marpaung, *University of Twente, Netherlands*
Maurizio Burla, *ETH Zurich, Switzerland*
Jose Capmany, *Universidad Politecnica de Valencia, Spain*

The field of integrated microwave photonics explores the incorporation of photonic integration technology for the generation, processing and measurement of radio-frequency and microwave signals and is one of the fastest growing fields in signal processing. At present, the field of integrated microwave photonics has adopted significantly distinct approaches, technological tools, and focused applications compared to the recent past. A new research paradigm is to explore general purpose and programmable signal processor capable of synthesizing a multitude of on-demand signal processing tasks. On the other hand, incorporation of new technological tools such as on-chip frequency combs, opto-acoustic interactions, and plasmonics open new ways of manipulating RF signals. From the applications side, emerging concepts such as 5G communications and the Internet of Things (IoT) are expected to shape development of new systems focusing on high operating frequencies in the millimeter-waves, low power consumption, and high level of integration with electronics. This symposium emphasizes on these recent advances in integrated microwave photonics and their application to emerging massive takeover applications. It seeks for transformative ideas about the future developments field and, at the same time, attempts to bridge dialogues between device-focused and application-driven approaches.

Invited Speakers

Richard DeSalvo, *Harris Corporation, USA*, **Advanced Microwave Photonics Applications and Routes to Hybrid Integration**

Jonathan Klamkin, *Univ. of California Santa Barbara, USA*, **Integrated Microwave Photonic Component Technologies**

Juerg Leuthold, *ETH Zurich, Switzerland*, **Plasmonics for RF Photonics**

Chris Roeloffzen, *LioniX International, Netherlands*, **Integrated Microwave Photonics for 5G**

Xiaoxiao Xue, *Tsinghua University, China*, **Microcomb Engine for Microwave Photonics**

Jianping Yao, *University of Ottawa, Canada*, **Photonic Integrated Circuits for Microwave Signal Generation and Processing**

Integrated Sources of Non-Classical Light: Perspectives and Challenges

Thursday, 17 May, Session I: 14:00–16:00,
Session II: 16:30–18:30
Executive Ballroom 210C

Organizers

Marco Liscidini, *Universita degli Studi di Pavia, Italy*
Alireza Marandi, *Stanford University, USA*
John Sipe, *University of Toronto, Canada*

Parametric fluorescence in bulk crystals for generating non-classical light, such as a single photon, photon pairs, and squeezed states, has been an essential part of quantum optics for more than three decades. Recently, the use of integrated photonic structures has attracted attention as a promising strategy for generation and manipulation of non-classical states of light. This is particularly interesting because light confinement at the micro- and nano-scale can enhance the nonlinear light-matter interaction by several orders of magnitude, and the optical properties of these structures can be engineered beyond what can be achieved in bulk materials, for instance in terms of dispersion. Moreover, using integrated structures offers the promise of better stability, scalability, and lower cost, which are typical of integrated devices. Hence, "Great Expectations" have been raised for using integrated photonics toward development of scalable quantum technologies as well as extending the frontiers of light-matter interactions. Despite recent advances, the generation and control of non-classical light on a chip for the realization of practical and scalable quantum devices is still a major challenge. The goal of this symposium is to provide a forum for discussing the state-of-the-art developments in integrated photonics for generation and manipulation of non-classical light as well as major challenges and potential directions in using them toward practical quantum technologies.

Invited Speakers

Andrea Fiore, *Technische Universiteit Eindhoven, Netherlands*, **Tailoring Radiative Emission in Integrated Quantum Light Sources**

Matteo Galli, *Universita degli Studi di Pavia, Italy*, **Nonclassical Light Sources for Silicon Photonics**

Roberto Morandotti, *INRS-Energie Mat & Tele Site Varennes, Canada*, **Scalable On-chip Generation and Coherent Control of Complex Optical Quantum States**

Sven Ramelow, *Humboldt Universität zu Berlin, Germany*, **Nonlinear Quantum Optics in Si₃N₄ micro-ring Resonators**

Andrey Sukhorukov, *The Australian National Univ., Australia*, **Photon-pair Generation and Quantum-classical Correspondence in Nonlinear Nanostructures**

All conference locations are in the San Jose Convention Center unless otherwise noted.

Emerging Quantum Sensing Techniques and Applications

Friday, 18 May, Session I: 10:30–12:30,
Session II: 14:00–16:00
Executive Ballroom 210B

Organizers

Peter Humphreys, *Delft University of Technology, Netherlands*
Marina Radulaski, *Stanford University, USA*

There has been substantial recent progress in developing novel quantum sensing techniques by building on the latest developments in a diverse range of quantum optics platforms. These new sensors will enable unprecedented scientific inquiries through a combination of enhancing temporal and spatial resolutions, enabling robust and compact sensing devices and through extending the range of conditions over which signals can be detected. For instance, NV-center magnetometers can provide sub-nanometer and sub-millihertz precision, enabling sensing of individual electron spins, and have even been embedded in nanodiamonds for in-situ detection of temperatures at the sub-cellular level. Drawing on research on atomic vapors, entangled atom metrology can reduce noise 100 times below the standard quantum limit. New optomechanical devices will enable compact sensors able to detect minute variations in the gravitational field. The challenges facing this nascent field are: harnessing quantum phenomena to move sensing beyond classical boundaries, and refining these techniques to move beyond laboratory. This symposium will focus on emerging quantum sensing concepts and experiments, aiming to bring together researchers from across this new field along with potential future beneficiaries of these techniques.

Invited Speakers

Ania Bleszynski Jayich, *UCSB, USA*, **Quantum Sensing and Imaging with Diamond Spins**

Alexey Gorshkov, *Univ. of Maryland, USA*, **Optimal and Secure Measurement Protocols for Quantum Sensor Networks**

Sebastien Gleyzes, *College de France – CNRS, France*, **Quantum Metrology with Rydberg Atoms**

Lee McCuller, *MIT Kavli Institute for Astrophysics and Space Research, USA*, **The LIGO Squeezed Light Upgrade**

Morgan Mitchell, *ICFO -The Institute of Photonic Sciences, Spain*, **Quantum Sensing with Extreme-coherence Spin Ensembles**

Lasers in Accelerator Science and Technology

Friday, 18 May, Session I: 08:00–10:00,
Session II: 10:30–12:30
Executive Ballroom 210C

Organizer

Sergio Carbajo, *Stanford University and SLAC National Accelerator Laboratory, USA*

Unifying laser and accelerator physics is essential for the development of future accelerators, light sources, and other scientific instruments due to increasingly synergistic advances at the cross-section between these two fields. Laser fields are ideal agents to tailor the 6-D phase-space distribution of charged particle beams because they can imprint correlations with extremely high spatio-temporal precision. In addition to long-standing uses in photo-injectors and compact acceleration, recent laser applications to free electron laser seeding, accelerators on a chip, hybrid x-ray light sources, and more have highlighted the need for further research into laser-particle interactions. The goal of this symposium is to fill this breach and to bring experts in various aspects of this interdisciplinary field to expose present and future opportunities in laser research and development to serve accelerator technology and applications, from instrumentation requirements to science cases.

Invited Speakers

Félicie Albert, *Lawrence Livermore National Laboratory, USA*, **Light Sources from Laser Wakefield Acceleration: Development and Applications**

Jerome Faure, *LOA-ENSTA, France*, **Recent Progress on High-Repetition Rate Laser-Plasma Acceleration**

William Graves, *Arizona State University, USA*, **X-ray Laser Based on Inverse Compton Scattering**

Peter Hommelhoff, *Friedrich-Alexander-Universität Erlangen, Germany*, **Hotonics-based Laser-driven Particle Acceleration: from Proof-of-concept Structures to the Accelerator on a Chip**

Agostino Marinelli, *SLAC National Accelerator Laboratory, USA*, **Laser-shaping of Electron Beams for X-ray Free-electron Laser Applications**

Liang Jie Wong, *SIMTech, Singapore*, **Linear-Field Particle Acceleration in Free Space by Spatiotemporally Structured Laser Pulses**

CALL FOR 2019 CLEO SYMPOSIUM PROPOSALS

The 2019 CLEO Program Committee is seeking special symposium proposals for consideration from members of the optics and photonics community. Submissions should consist of timely, cutting-edge topics and/or new material in rapidly advancing areas.

Submissions need to address the following questions:

1. Why is this symposium topic important now and needed in contrast to other years?
2. Which existing topic subcommittees if any, would this topic be most aligned with?
3. Proposed invited speaker list and talk titles.

Submission Deadline: 9 July 2018

cleoconference.org/symposia

All conference locations are in the San Jose Convention Center unless otherwise noted.

Applications & Technology Topical Reviews

Photonics-enabled Quantum Technologies in Transition

Monday, 14 May, Session I: 08:00–10:00,
Session II: 10:30–12:30
Salon VI, San Jose Marriott

Organizers

Dana Anderson, *University of Colorado at Boulder, USA*
Wilhelm Kaenders, *Toptica Photonics AG & Inc., Germany*

With applications ranging from computing to navigation, quantum technology starts to make its way into the mainstream economy through both startups and well-established corporations. The evolution reflects a maturation of science and technology from novel laboratory demonstrations and prototypes to sophisticated and highly-engineered instruments. The challenges facing deployment of quantum-enabled systems are often more of a classical rather than quantum nature: Questions regarding how best to imbed quantum performance in classical systems such as for navigation and communication define a new regime for systems engineering while questions addressing size, weight, power and cost present new challenges for systems integration and manufacturing. In so many cases quantum and photonics technologies are intimately intertwined. Advances in optics and photonics technology will thus go hand-in-hand with the evolution and deployment of quantum technology. This symposium will focus on maturing quantum-enabled instruments and systems and their application in quantum information, metrology, and sensing domains. We aim to bring together researchers in both quantum-enabled classical applications such as navigation and timekeeping, and quantum applications such as quantum computing and secure communications.

Invited Speakers

David Andersen, *Rydberg Technologies, USA*, **Quantum RF electric-field Sensing with Rydberg-atom Vapors**

John Burke, *DARPA, USA*, **The Challenge of Complexity, Control, and Low Reliability in Quantum Sensors**

Tatjana Curcic, *Quantum Valley Innovations, Canada*, **From Basic Research to Quantum Technologies: Challenges and Opportunities**

Bruno Desruelle, *MUQUANS, France*, **Innovative Laser Solutions for Operational Quantum sensors**

Karl Nelson, *Honeywell, USA*, **Photonics-enabled Quantum Timing and Navigation at Honeywell**

Max Perez, *ColdQuanta, USA*, **Engineering Challenges in Commercial Photonics-enabled Quantum Technologies**

Rik van Gorsel, *id Quantique, USA*, **10 Years of Commercial Quantum Key Distribution: Engineering Achievements and Market Challenges**

Brent Young, *AOsense, USA*, **Photonics for Quantum Sensing**

Advanced Applications of Laser Radar and Remote Sensing

Tuesday, 15 May, Session I: 13:00–15:00
Wednesday, 16 May, Session II: 13:00–15:00
Theater I

Organizer

Fabio Di Teodoro, *The Aerospace Corporation, USA*

This topical review will address cutting-edge research and development of laser-based standoff sensors from a system standpoint to include new laser transmitters, detectors, and advanced sensing concepts. Examples include sensors deployed in ground, airborne and space-based platforms for reconnaissance and imaging, environmental/meteorological studies, chemical/biological detection as well as autonomous navigation. Such systems must address many technological challenges including the design, performance improvement, maturation, and qualification of suitable laser transmitters and detectors; minimization of size, weight, power consumption, and cost; increase in ruggedness and support for operation in thermo-mechanically harsh environments; and improvement of long-term reliability.

Invited Speakers

Gerald Buller, *Heriot-Watt University, UK*, **Three-Dimensional Imaging Under Extreme Conditions Using Single-Photon Counting**

Lute Maleki, *OEwaves Inc, USA*, **LiDAR for Autonomous Vehicles: Challenges and Opportunities for Photonics**

Paul McManamon, *Exciting Technology LLC, USA*

Marcos Sirota, *Sigma Space Corp, USA*, **Recent Advances in Single Photon Sensitive Mapping Lidars**

Mariano Troccoli, *Evolution Photonics Inc, USA*, **High Performance Mid-IR Devices and Applications to Gas Sensing**

Advances in Supercontinuum Technologies

Tuesday, 15 May, Session I: 13:00–15:00
Wednesday, 16 May, Session II: 13:00–15:00
Theater II

Organizer

Adam Devine, *Fianium Ltd., UK*

Advances in Supercontinuum Technologies I: Supercontinuum Generation

Almost two decades after the pivotal experiments of supercontinuum generation in photonic crystal fibers, significant advances continue to be made in the area of broadband light generation within waveguides. This topical review session will focus on recent advances and cutting edge research in supercontinuum generation technology.

All conference locations are in the San Jose Convention Center unless otherwise noted.

Advances in Supercontinuum Technologies II: New Application Areas for Supercontinuum Light Sources

Supercontinuum broadband light sources represent a disruptive technology for traditional light sources such as xenon lamps, laser diodes and plasma driven light sources. From telecommunication to medical imaging and metrology, these light sources are enabling advances in exciting new application areas. This session will focus on new and emerging fields exploiting these broadband light sources.

Invited Speakers

David Castaneda-Castellanos, *Leica Microsystems, Germany*, **Biological Applications of Supercontinuum Lasers in Optical Light Microscopy**

Frans J.M. Harren, *Radboud Univ., Netherlands*, **Mid-infrared Supercontinuum-based Trace Gas Sensing**

Michal Lipson, *Columbia Univ., USA*, **Ultra Low Loss Waveguides for Extreme Nonlinear Optics**

Peter Moselund, *NKT Photonics Inc, Denmark*, **Supercontinuum from Labs to Factories**

Adrian Podoleanu, *Univ. of Kent, UK*, **Supercontinuum Applications in High Resolution Non Invasive Optical Imaging**

Jonathan Price, *Univ. of Southampton, UK*, **The Development of Tailored Supercontinuum Sources in Silica and Non-silica Fibers**

Peter John Rodrigo, *Technical Univ. of Denmark, Denmark*, **Mid-IR Hyperspectral Imaging of Gases Using a Supercontinuum Source and Frequency Upconversion**

John Travers, *Heriot-Watt Univ., UK*, **Ultraviolet Supercontinuum Generation in Optical Fibers**

Topical Review on Neurophotonic

Thursday, 17 May, Session I: 08:00–10:00,
Session II: 14:00–16:00
Willow Glen, San Jose Marriott

Organizers

Kishan Dholakia, *Univ. of St Andrews, UK*
Chris Xu, *Cornell Univ., USA*

Advanced neurophotonic enable recording and stimulation of a population of neurons at high spatial and temporal resolution, deep within a living, intact animal brain. Research in neurophotonic is a major part of the multibillion-dollar BRAIN Initiative, and will likely play an essential role in understanding how the brain works at the level of neural circuits, which will provide a bridge between microscopic interactions at the neuronal level and the complex computations performed at larger scales. This topical review session will focus on the development of optical tools for neuroscience and brain research.

Tutorial Speaker

Jerome Mertz, *Boston Univ., USA*, **The Challenge of Large-scale Neuronal Imaging**

Scientific and Commercial Progress in Semiconductor Laser Technology

Thursday, 17 May, Session I: 16:30–18:30
Friday, 18 May, Session II: 08:00–10:00
Willow Glen, San Jose Marriott

Organizer

Bojan Resan, *Univ. of Applied Sciences Northwestern Switzerland, Switzerland*

Semiconductor lasers continue to pave the way towards practical use in numerous applications. Many scientific ideas are on the horizon, but many challenges remain to be solved. Semiconductor lasers are a large and fruitful field and capture the largest share of the commercial laser market. We will review the recent developments in optically pumped VECSELs (semiconductor disc lasers), edge emitters, and their applications. Particular focus will be devoted to devices operating in challenging wavelength regions, efficient wavelength conversion architectures, boundaries for power scaling and ultrashort pulse generation.

Invited Speakers

Mircea Guina, *Optoelectronics Research Centre, Finland*, **Progress in VECSELs: from Gain Mirror Technology to New Applications**

Nils Hempler, *M Squared Lasers, UK*, **Commercial Semiconductor Disk Lasers**

Peter Skovgaard, *Norlase ApS, Denmark*, **New Platform for High Power IR and Visible Diode Laser Modules: Towards Yellow Wavelengths**

Time-Stretch Technology: Principles and Applications

Friday, 18 May, Session I: 10:30–12:30, Session II: 14:00–16:00
Willow Glen, San Jose Marriott

Organizers

Hongwei Chen, *Tsinghua Univ., China*
Keisuke Goda, *Univ. of Tokyo, Japan*

Optical time stretch is a method based on the exploitation of temporal dispersion for temporally stretching information-encoded ultrashort optical pulses such that the information is detected and digitized by a slow photodetector and a slow digitizer, respectively. With pulse repetition, such a measurement can be performed at a rate of MHz to GHz, allowing for fast, continuous, real-time measurements. Since it was conceived, optical time stretch has been mainly used in data acquisition for femtosecond digitization, data compression, and spectroscopy. In recent years, the method has been further studied and advanced, enabling the observation of non-repetitive and statistically rare events on ultrashort time scales such as soliton explosions, soliton molecules, optical rogue waves, and the birth of mode-locking. Furthermore, it has led to the development of ultrafast imaging, high-throughput imaging flow cytometry, ultrafast optical coherence tomography, and ultrafast surface vibrometry. This special symposium provides a forum for introducing the fundamental principles, emerging applications, and recent advances of optical time stretch as well as for discussing its technical challenges and future perspectives.

All conference locations are in the San Jose Convention Center unless otherwise noted.

Invited Speakers

Dale Capewell, *Roguescope Technologies, USA*, **Coherent RogueScope**

Goëry Genty, *Tampere Univ. of Technology, Finland*, **Real-time Measurements of Nonlinear Instabilities in Optical Fibers**

Cheng Lei, *Univ. of Tokyo, Japan*, **Optofluidic Time-stretch Microscopy for Precision Medicine**

Ray Man, *Amonics Limited, Hong Kong*, **Studying Nonlinear Pulse Interactions using Time Stretch**

Adam C. Scofield, *Aerospace Corporation, USA*, **Demonstration of GHz-band RF Receiver and Spectrometer Using Random Speckle Patterns**

Kevin Tsia, *Univ. of Hong Kong, Hong Kong*, **Large-scale, Deep Single-cell Analysis by All-optical Laser-scanning Imaging Cytometry**

Short Courses

Short Course Chairs

Robert Fisher, *R. A. Fisher Associates, USA*
Ben Eggleton, *Univ. of Sydney, Australia*

The CLEO Short Course Program includes a range of topics at a variety of educational levels. Widely recognized experts in industry and academia lead attendees in building skills and/or achieving new insight, and the small-classroom setting provides a tremendous, interactive learning opportunity. Short Courses are an excellent opportunity to learn about new products, cutting edge technology and vital information at the forefront of the laser science and electro-optics fields.

Certificates of Attendance are available for those who register and attend a course. You may request a certificate upon completion of the online course evaluation. If you have any questions about receiving a Certificate of Attendance or completing the course evaluation, please email shortcourses@cleoconference.org with your name and course name(s).

Sunday, 13 May 2018

08:30–12:30

SC361: Coherent MidInfrared Sources and Applications

Instructor: Konstantin Vodopyanov; CREOL, The College of Optics & Photonics, Univ. Central Florida, USA

SC149: Foundations of Nonlinear Optics

Instructor: Robert Fisher, R. A. Fisher Associates, USA

SC466: Silicon Integrated Nanophotonics NEW

Instructor: Yurii A. Vlasov, Univ. of Illinois at Urbana-Champaign, USA

08:30–15:00

SC456: How to Start A Company

Instructor: Jes Broeng, DTU, Denmark, and Milton Chang, Incubic, USA

13:30–16:30

SC439: Attosecond Optics

Instructor: Zenghu Chang, Univ. of Central Florida, USA

SC403: NanoCavity Quantum Electrodynamics and Applications

Instructor: Jelena Vuckovic, Stanford Univ., USA

13:30–17:30

SC396: Frontiers of Guided Wave Nonlinear Optics

Instructor: Ben Eggleton, Univ. of Sydney, Australia

SC157: Laser Beam Analysis, Propagation, and Shaping Techniques

Instructor: James Leger, Univ. of Minnesota, USA

SC301: Quantum Cascade Lasers: Science, Technology, Applications and Markets

Instructor: Federico Capasso, Harvard Univ., USA

Monday, 14 May 2018

12:30–15:30

SC362: Cavity Optomechanics: Fundamentals and Applications of Controlling and Measuring Nano- and Micro-mechanical Oscillators with Laser Light

Instructor: Tobias Kippenberg, Ecole Polytechnique Federale de Lausanne, Switzerland

12:30–16:30

SC455: Integrated Photonics for Quantum Information Science and Technology

Instructor: Dirk Englund; MIT, USA

SC378: Introduction to Ultrafast Optics

Instructor: Rick Trebino, Georgia Institute of Technology, USA

Tuesday, 15 May 2018

12:00–15:00

SC410: Finite Element Modeling Methods for Photonics and Optics

Instructor: Arti Agrawal, City Univ., UK

SC352: Introduction to Ultrafast Pulse Shaping--Principles and Applications

Instructor: Marcos Dantus, Michigan State Univ., USA

SC376: Plasmonics

Instructor: Mark Brongersma, Stanford Univ., USA

12:00–16:00

SC270: High Power Fiber Lasers and Amplifiers

Instructor: W. Andrew Clarkson, Optoelectronics Res. Ctr., Univ. of Southampton, UK

SC438: Photonic Metamaterials

Instructor: Nader Engheta, Univ. of Pennsylvania, USA

All conference locations are in the San Jose Convention Center unless otherwise noted.

Short Course Descriptions

Courses are listed by date and time. Complete course descriptions are available at: www.cleoconference.org/shortcourses.

SC361 - Coherent Midinfrared Sources and Applications

Konstantin Vodopyanov, *CREOL, The College of Optics & Photonics, Univ. Central Florida, USA*
Sunday, 13 May, 08:30–12:30

This course will make a comprehensive review of different techniques for producing coherent light in this important yet challenging spectral region. It will examine different state-of-the-art approaches from diverse areas of photonics that include: solid-state lasers based on rare-earth and transition metals, fiber lasers, semiconductor lasers (including intra- and intersubband cascade lasers), laser sources based on nonlinear optical frequency downconversion (including difference frequency generators, optical parametric oscillators, generators and amplifiers), Raman sources and others. Since the course is focused mostly on modern-day techniques, such traditional areas as carbon dioxide lasers and free electron lasers will not be covered. Explaining fundamental principles behind a given technique will precede discussions on each topic. The course will review several emerging technologies such as supercontinuum generation in fibers and waveguides, as well as frequency combs generation. Several important mid-IR applications will be also reviewed and include molecular sensing, spectroscopy with frequency combs, and medical and military applications.

Short Course Benefits:

This course will enable you to:

- Get a clear idea of existing laser sources in the mid-IR spectral region (2-20 μm) and understand their operational principles, as well as advantages and disadvantages
- Distinguish between different operational regimes, from continuous-wave to few optical cycle pulsed operation
- Distinguish between broadband and narrow-band sources, as well as between the supercontinuum and the frequency comb regimes
- Learn about new applications of mid-IR coherent sources, from trace molecular detection and remote sensing to ultrafast spectroscopy and attosecond physics
- Identify what kind of laser source you need for your particular application

Short Course Level: Intermediate

Short Course Audience: Students, academics, researchers and engineers in various disciplines who require a broad introduction to the subject and would like to learn more about the state-of-the-art and upcoming trends in mid-infrared coherent source development and applications. Undergraduate training in either engineering or science is assumed.

SC149 - Foundations of Nonlinear Optics

Robert Fisher, *R. A. Fisher Associates, USA*
Sunday, 13 May, 08:30–12:30

This introductory and intermediate level course provides the basic concepts of nonlinear optics. Although some mathematical formulas are provided, the emphasis is on simple explanations. It is recognized that the beginning practitioner in nonlinear optics is overwhelmed by a constellation of complicated nonlinear optical effects, including second-harmonic generation, optical Kerr effect, self-focusing, self-phase modulation, self-steepening, fiberoptic solitons, chirping, stimulated Raman and Brillouin scattering, and photorefractive phenomena. It is our job in this course to demystify this daunting collection of seemingly unrelated effects by developing simple and clear explanations for how each works, and learning how each effect can be used for the modification, manipulation or conversion of light pulses. Examples will address the nonlinear optical effects that occur inside optical fibers and those that occur in liquids, bulk solids, and gases. This course will incorporate the creation of cartoons to lock in the basic concepts.

Short Course Benefits:

This course will enable you to:

- Explain and manipulate the Slowly-Varying Envelope Approximation (SVEA)
- Recognize what nonlinear events come into play in different effects
- Appreciate the intimate relationship between nonlinear events which at first appear quite different
- Discuss how a variety of different nonlinear events arise, and how they affect the propagation of light
- Describe how wavematching, phase-matching, and index matching are related
- Summarize how self-phase modulation impresses “chirping” on pulses
- Explain basic two-beam interactions in photorefractive materials
- Develop an appreciation for the extremely broad variety of ways in which materials exhibit nonlinear behavior”

Short Course Level: Beginner and Intermediate

Short Course Audience: Although we start at the very beginning of each topic, we move quite rapidly in order to grasp a deep understanding of each topic. Therefore, both beginners and intermediates will benefit greatly from this course. The material will be of interest to graduate students, to researchers, to members of the legal profession, to experts who are just transferring to this field, to managers, and to anyone else who just wants to learn how nonlinear optics works. This course, offered on Sunday Morning, will also give an excellent nonlinear optics foundation for those feeling the need so they can also take any of the following more specialized nonlinear optics courses at this CLEO conference: SC396: Frontiers of Guided Wave Nonlinear Optics; SC378: Introduction to Ultrafast Optics; SC270: High Power Fiber Lasers and Amplifiers; SC410: Finite Element Modeling Methods for Photonics and Optics; and SC352: Introduction to ultrafast pulse shaping—principles and applications.

All conference locations are in the San Jose Convention Center unless otherwise noted.

SC466 - Silicon Integrated Nanophotonics **NEW**

Yurii A. Vlasov, *Univ. of Illinois at Urbana-Champaign, USA*
Sunday, 13 May, 08:30–12:30

Silicon photonics is a rapidly growing industry as well as an active area of advanced research. This course will focus on practical applications of advanced EM concepts to silicon photonics integrated circuits. It combines the rigorous derivation of major physical concepts like matrix optics, waveguiding, coupled mode theory, pin junctions, etc. with the applications of these knowledge towards the design of practical silicon photonic devices like passive wavelength filters, active switches and modulators for optical communications, as well as germanium photodetectors. The emphasis will be given to interaction of guided EM waves with electrical charges in pin junction that would allow participants to understand the operation and design principles of a new class of photonic devices (modulators, switches, photodetectors, etc.) based on carrier-injection/depletion in silicon/germanium integrated optics. Fabrication approaches and CMOS integration challenges will be reviewed. System-level analysis of short-reach and long-haul optical links will be analyzed that will drive the design considerations for optical transmitter and receiver subsystems and individual devices.

Short Course Benefits:

This course will enable you to:

- Get a clear idea of basic principles of integrated silicon optical devices and circuits including wavelength filters, modulators, switches, and photodetectors
- Learn about approaches to fabrication and challenges with CMOS integration of silicon integrated photonics that define the current landscape
- Understand how system-level requirements for optical communications as channel bandwidth, optical link error penalties, and power constraints, define the design considerations for subsystems and silicon photonic devices
- Understand the figures of merit for silicon photonic devices and compare various technical concepts for applications in short-reach and long-haul optical communications

Short Course Level: Beginner

Short Course Audience: Students, scientists, and engineers who are interested in learning about the rapidly developing field of silicon photonics and its impact on optical communications. Broad introduction to the subject and comprehensive review of basic concepts and the state-of-the-art trends allow beginners to take full advantage of this course with assumed undergraduate training in optical engineering or science.

SC456 - How to Start A Company

Jes Broeng¹ and Milton Chang², ¹DTU, Denmark, ²Incubic, USA
Sunday, 13 May, 08:30–15:00

Starting a new business is one of the most rewarding experiences one can imagine. The journey from an idea to a successful company is, however, paved with challenges and puts high demands on technology, business and social skills. The upside, though, is tremendous in personal learning and potentially also in an economic sense.

This short course is aimed to help people thinking about starting their own company and provide practice-oriented tools to help aspiring entrepreneurs who have a scientific or engineering background.

To commercialize a new technology, the short course will help answer the following questions:

- How do I know I have a viable business idea?
- What to look for in co-founders?
- What financing strategy is appropriate for my kind of business?
- How to pitch and work with investors?
- How to bootstrap if all fails?

The course will include a mix of business theory and start-up experience based on a number of successful high-tech companies familiar to the scientists and engineers at CLEO. The short course will also include a workshop session, where start-up ideas from the attendees may be introduced and strengthened under the instructor's guidance. The course includes an informal networking lunch.

Short Course Benefits:

This course will enable you to:

- Recognize a potential high-tech business opportunity
- Have an understanding of different business models and to identify the right one for your start-up
- Knowledge of how investors think and how you may attract funding for a new venture
- Understand the principles to set up an effective organization
- Establish an eco-system to support your business, including lead customers and R&D partners.

Short Course Audience: This course is intended for scientists & engineers with interest in starting up their own high-tech business. This short course limited to an enrollment of 25.

SC439 - Attosecond Optics

Zenghu Chang, *Univ. of Central Florida, USA*
Sunday, 13 May, 13:30–16:30

Since the invention of lasers in 1960, various techniques such as mode-locking have been developed to push the pulse duration down first to picoseconds and then to femtoseconds, which is the oscillation period of infrared and visible light. The generation of attosecond pulses requires new methods to produce broadband coherent electromagnetic waves in the UV to X-ray range because of the lack of proper gain media. The discovery of high-order harmonic generation in high intensity laser-atom interaction at the end of 1980s paved the way. In 2001, attosecond light pulses, a train of attosecond bursts or single isolated attosecond pulses, were measured for the first time. It was accomplished by first converting the attosecond photons to photoelectrons in a combination of weak extreme ultraviolet and strong infrared fields, and then retrieve the spectral phase of the attosecond pulse by reconstructing the photoelectron spectrum. Since then, various sub-optical-cycle gating schemes such as polarization gating and Double Optical Gating have been demonstrated

All conference locations are in the San Jose Convention Center unless otherwise noted.

to generation isolated attosecond pulses. By properly compensating the intrinsic chirp, 53 as pulses were characterized in 2017, which is so far the shortest light pulses. The new frontier in attosecond optics research is to significantly increase the photon flux and to extend the spectrum to the "water window." This course covers: (1) High harmonic generation. (2) Carrier-envelope phase of femtosecond driving lasers. (3) Semi-classical model and Strong Field Approximation. (4) Phase-matching in partially ionized media. (5) Sub-cycle gating and attosecond pulse characterization. (6) Attosecond streaking and transient absorption spectroscopy.

Short Course Benefits:

This course will enable you to:

- Specify parameters of femtosecond driving lasers that are critical to the generation of attosecond pulse trains and single isolated attosecond pulses
- Compare pros and cons of driving lasers based on Ti:Sapphire Chirped Pulse Amplification and Optical Parametric Amplifiers
- Explain the principle and techniques of locking the carrier-envelope offset frequency of femtosecond oscillators and carrier-envelope phase of amplified pulses
- Define short and long trajectories in the attosecond generation process using the Strong Field Approximation in the Lewenstein model
- Estimate the cutoff photon energy and attosecond chirp using the semi-classical model
- Calculate ionization probability of atoms in an intense laser field with the Ammosov-Delone-Krainov (ADK) tunneling rate
- Describe the principle of attosecond streak camera for characterizing attosecond pulses, as well as identify the major factors that affects the phase matching of high harmonic generation in partially ionized media

Short Course Level: Beginner (No background or minimal training is necessary to understand course material)

Short Course Audience: This short course targets senior undergraduate students, graduate students, postdoc fellows, scientists and engineers seeking to enter attosecond optics. The audience should have studied electromagnetism, optics, lasers, quantum mechanics and atomic physics at undergraduate or graduate levels. Prior knowledge of femtosecond lasers is required. Although basic theory is covered, it emphasizes on experimental aspects of attosecond optics, such as locking the carrier-envelope phase of the driving lasers and designing time-of-flight spectrometers for attosecond streak cameras.

SC403 - NanoCavity Quantum Electrodynamics and Applications

Jelena Vuckovic, *Stanford Univ., USA*
Sunday, 13 May, 13:30–16:30

Strong localization of light in nanophotonic structures leads to enhanced light-matter interaction, which can be employed in a variety of applications, ranging from improved (higher speed, lower threshold) optoelectronic devices, to biophotonics, quantum information and low threshold nonlinear optics. In particular, quantum dots in optical nanocavities are interesting as a test-bed for fundamental studies of such light-

matter interaction (cavity quantum electrodynamics - QED), as well as an integrated platform for information processing. As a result of the strong field localization inside of sub-cubic wavelength volumes, they enable very large emitter-field interaction strengths (vacuum Rabi frequencies in the range of 10's of GHz – a few orders of magnitude larger than in atomic cavity QED). In addition to the study of new regimes of cavity QED, this can also be employed to build devices for quantum information processing, such as ultrafast quantum gates, nonclassical light sources, and spin-photon interfaces. Beside quantum information systems, many classical information processing devices greatly benefit from the enhanced light matter interaction in such structures; examples include all-optical switches operating at the single photon level, electro-optic modulators controlled with sub-fJ energy and operating at GHz speed, and lasers with threshold currents of 100nA.

This course will introduce cavity QED (e.g., strong and weak coupling regimes, Purcell effect, etc.), with particular emphasis on semiconductor nanocavities. We will also describe state of the art in solid state cavity QED experiments and applications.

Short Course Benefits:

This course will enable you to:

- Explain light matter interaction in optical nanostructures
- Discuss state of the art in solid state cavity QED
- Identify benefits of employing nano-cavity QED for certain applications

Short Course Level: Beginner

Short Course Audience: Scientists and engineers interested in cavity QED and nanophotonic devices in general. Some background in electromagnetics, quantum mechanics, and optoelectronics is helpful, but not required

SC396 - Frontiers of Guided Wave Nonlinear Optics

Ben Eggleton, *Univ. of Sydney, Australia*
Sunday, 13 May, 13:30–17:30

This course will review recent research and applications in the field of nonlinear guided wave optics with emphasis on both fundamentals and emerging applications. Starting from a strong foundation in the principles of nonlinear optics, we will review recent progress in emerging nonlinear optical platforms with an emphasis on the different materials, including silicon, chalcogenide, III-V semiconductors, lithium niobate, photonic crystal fibres, nanophotonic circuits and others. We will establish key figures of merit for these different material systems and a general framework for nonlinear guided wave optics with emphasis on the applications in emerging areas of science and technology. We will then review recent progress and breakthroughs in the following areas: All-optical processing, Ultra-fast optical communications, Slow light, highly nonlinear and emerging waveguides, Ultrafast measurement and pulse characterization, Frequency combs and optical clock, Optical parametric amplifiers and oscillators, Generation and applications of optical super-continuum, Nonlinear localization effects and solitons, Nonlinear optics for quantum information.

All conference locations are in the San Jose Convention Center unless otherwise noted.

Short Course Benefits:

This course should enable the participants to:

- Get state of the art knowledge of nonlinear optics in emerging waveguides and materials
- Understand the applications of nonlinear optics in key applications
- Have a foundation of nonlinear waveguide physics for emerging applications and science

Short Course Level: Advanced Beginner

Short Course Audience: This course assumes some basic knowledge/familiarity of nonlinear optics. Individuals lacking such knowledge should consider taking SC149: Foundations of Nonlinear Optics first.

SC157 - Laser Beam Analysis, Propagation, and Shaping Techniques

James Leger; *Univ. of Minnesota, USA*
Sunday, 13 May, 13:30–17:30

The propagation and focusing properties of real laser beams are greatly influenced by beam shape, phase distortions, degree of coherence, polarization, and aperture truncation effects. The ability to understand, predict, and correct these real-world effects is essential to modern optical engineering. Attendees of this course will learn a variety of techniques for measuring and quantifying the important characteristics of real laser beams, be able to calculate the effects of these characteristics on optical system performance, and explore a variety of beam shaping techniques to optimize specific optical systems.

The course starts with a basic and intuitive description of Gaussian beam characteristics from an ideal laser. These concepts are extended to non-Gaussian beams (e.g. high-order Hermite Gaussian beams, top-hat shapes, laser arrays, and non-diffracting beams) and the relative merits of various beam shapes are discussed. The properties of optical vortex beams, cylindrical vector beams, and orbital angular momentum are then explored. Beam characterization methods such as M^2 , Strehl ratio, and TDL are reviewed. Simple expressions for estimating the effects of laser aberrations and coherence on beam focusing and propagation are developed. Coupling of light into single and multi-mode fibers, as well as far-field light concentration limits are explored as real-world examples. The constant radiance theorem and étendue are employed as engineering tools to optimize optical design, and simple analytical tools are presented to estimate the effects of spatial beam shape, phase aberrations, and coherence on beam concentration. The course ends with a description of internal and external cavity beam shaping techniques using phase and polarization modulation.

Short Course Benefits:

This course will enable you to:

- Measure the quality of a laser beam using several methods
- Interpret the meaning of various laser specifications
- understand Gaussian laser beam properties from an intuitive standpoint

- Predict the propagation and focusing properties of non-ideal and aberrated laser beams
- Determine the concentration limits of a light field
- Design optimal beam concentration optics
- Compare different beam profiles for specific applications and calculate ideal performance
- Design beam shaping optics using polarization and phase manipulation

Short Course Level: Advanced Beginner

Short Course Audience: This course is designed to provide laser engineers, optical system designers, and technical management professionals with a working knowledge of laser beam characterization, analysis, and modification. Physical and intuitive explanations of most topics are designed to make the concepts accessible to a wide range of participants.

SC301 - Quantum Cascade Lasers: Science, Technology, Applications and Markets

Federico Capasso; *Harvard Univ., USA*
Sunday, 13 May, 13:30–17:30

Quantum Cascade Lasers (QCLs) are fundamentally different from diode lasers due to their physical operating principle, which makes it possible to design and tune their wavelength over a wide range by simple tailoring of active region layer thicknesses, and due to their unipolar nature. Yet they use the same technology platform as conventional semiconductor lasers. These features have revolutionized applications (spectroscopy, sensing, etc.) in the mid-infrared region of the spectrum, where molecules have their absorption fingerprints, and in the far-infrared or so called Terahertz spectrum. In these regions until the advent of QCLs there were no semiconductor lasers capable of room temperature operation in pulsed or cw, as well high output power and stable/wide single mode tunability. The unipolar nature of QCL, combined with the capabilities of quantum engineering, leads to unprecedented design flexibility and functionality compared to other lasers. The physics of QCLs, design principles, supported by modeling, will be discussed along with the electronic, optical and thermal properties. State-of-the-art performance in the mid-ir and Terahertz will be reviewed. In particular high power CW room temperature QCLs, broadly tunable QCL, short wavelength MWIR QCLs and recent breakthroughs in THz room temperature operation will be presented. A broad range of applications (IR countermeasures, stand-off detection, chem-bio sensing, trace gas analysis, industrial process control, medical and combustion diagnostics, imaging, etc.) and their ongoing commercial development will be discussed.

Short Course Benefits:

This course will enable you to:

- Describe underlying QC Laser physics, operating principles and fundamental differences between standard semiconductor lasers and QC lasers
- Explain quantum design of the key types of QC lasers, which have entered real world applications, and how their electrical and optical properties can be tailored to optimize performance in the mid-infrared and THz regions.

All conference locations are in the San Jose Convention Center unless otherwise noted.

- Discuss experimental device performance, including physical limits, design constraints and comparison with theory and determine device characteristics (current-voltage and light-current curves; differential and power efficiency, threshold, gain and losses; spectral behavior, single mode operation; high speed operation)
- Explain the basics of QC laser device technology: fabrication process, materials growth options
- Illustrate the basics of a chemical sensing system; discuss applications of state-of-the-art mid-infrared QC lasers to sensing and present several examples of QC laser commercialization
- Discuss current and future markets of QC lasers

Short Course Level: Beginner

Short Course Audience: Graduate students; qualified undergraduates (mostly senior level) majoring in EE or physics/applied physics; researchers in industry, academia and government labs; engineers, sales reps and technical managers.

Education: Undergraduate degree or a Ph.D or pursuing a Ph.D in EE, Physics or Applied Physics, with knowledge of introductory level semiconductor devices.

SC362 - Cavity Optomechanics: Fundamentals and Applications of Controlling and Measuring Nano- and Micro-mechanical Oscillators with Laser Light

Tobias Kippenberg, *Ecole Polytechnique Federale de Lausanne, Switzerland*

Monday, 14 May, 12:30–15:30

Radiation pressure denotes the force that optical fields exert and which have wide ranging applications in both fundamental science and applications such as Laser cooling or optical tweezers. Radiation pressure can, however, also have a profound influence on micro- and nanophotonic devices, due to the fact that radiation pressure can couple optical and mechanical modes. This optomechanical coupling gives rise to a host of new phenomena and applications in force, displacement and mass sensing. This course is intended to give an introduction of the Physics and Applications of cavity optomechanics and highlight the rapid developments in this emerging field. Optomechanical coupling can be used to both cool and amplify mechanical motion and thereby allow new light driven photon clocks. Optomechanical refrigeration of mechanical modes gives insights into the quantum limits of mechanical motion. In addition, radiation pressure coupling enables new way of processing light all optically enabling optical mixers, delay lines or storage elements. Moreover, the basic limitations of optomechanical displacement measurements, due to quantum noise and practical laser phase noise limitations, will be reviewed, relevant across a wide range of sensing experiments.

The course will make contact to practical applications of optomechanics in Metrology (force sensors, mass sensors and light driven optical clocks) and review fundamental design principles of optomechanical coupling and the design of high Q mechanical oscillators. The use of finite element simulations will be covered.

Short Course Benefits:

This course will enable you to:

- Explain gradient and scattering light forces in microcavities and micromechanical systems
- Design high $-Q$ nano- and micro- mechanical oscillators (finite element modeling, FEM)
- Discuss the fundamental limits of mechanical Q in NEMS/MEMS
- Describe of the fundamental and practical limits of displacement sensors
- Summarize Applications of optomechanics in mass and force sensing
- Explain the basic optomechanical phenomena (amplification, cooling)
- Discuss the standard quantum limit (SQL)
- Characterize radiation pressure driven oscillations in terms of fundamental oscillator metrics
- Define Phase and frequency noise of oscillators
- Know the influence of phase and amplitude noise of a wide variety of laser systems (fiber lasers, TiSa, diode lasers) in optomechanical systems

Short Course Level: Advanced Beginner

Short Course Audience: This course is intended for physicists and optical and electrical engineers desiring both focused fundamental knowledge of cavity optomechanical coupling (i.e., radiation pressure coupling of light and NEMS/MEMS) but also a view of emerging applications of this new technology. The instruction will be at a level appropriate for graduate students and will assume some basic knowledge of laser.

SC455 - Integrated Photonics for Quantum Information Science and Technology

Dirk Englund, *MIT, USA*

Monday, 14 May, 12:30–16:30

The rules of quantum mechanics enable applications that are inherently more powerful than their classical counterparts. Quantum key distribution now makes it possible to transmit information with unconditional security; quantum simulation is beginning to address problems that are intractable on classical computers; and quantum metrology techniques push the boundaries of precision measurements.

Many of these quantum technologies rely fundamentally on advanced photonics that place extremely demanding requirements on precision, efficiency, and mode complexity. Over the past decade, new generations of photonic integrated circuits have been developed to begin to address these requirements.

This course will cover basic concepts and recent progress in photonic integrated circuits technology for quantum information processing, with a focus on two primary application areas: quantum communications -- from quantum cryptography to entanglement distribution over quantum networks -- and quantum computing, including analog and digital approaches. Motivated by these applications, the course will discuss nonclassical light sources, photonic interfaces with atomic memories, high-fidelity mode transformation circuits,

All conference locations are in the San Jose Convention Center unless otherwise noted.

nonlinear photonic quantum gates, and waveguide-integrated single photon resolving detectors.

Short Course Benefits:

This course will enable you to:

- Describe a practical quantum key distribution system, estimate performance, and identify central limitations
- Propose methods to extend the reach of quantum secure communications
- Describe the main classes of quantum communications
- Categorize the major areas of quantum computing
- Diagram quantum networks
- Design photonic integrated circuits for quantum key distribution and quantum repeaters

Short Course Level: Advanced Beginner

Short Course Audience: The course is designed for an audience interested in the key ideas and technology of photonic quantum communication and computation. It will probably be most valuable to participants who have some background in quantum information science or integrated optics and who want to better understand where the intersections of these fields and where the challenges and opportunities lie. The course should be useful for graduate students and industrial and academic researchers with an interest in applied photonic quantum technologies.

SC378 - Introduction to Ultrafast Optics

Rick Trebino, *Georgia Institute of Technology, USA*
Monday, 14 May, 12:30–16:30

Ultrafast Optics—the science and technology of ultrashort laser pulses—is one of the most exciting and dynamic fields of science. While ultrashort laser pulses seem quite exotic (they're the shortest events ever created!), their applications are many, ranging from the study of ultrafast fundamental events to telecommunications to micro-machining to biomedical imaging - to name a few. Interestingly, these lasers are readily available, and they are easy to understand. But their use requires some sophistication. This course is a basic introduction to the nature of these lasers and the pulses they generate. It will discuss the principles of their generation and amplification and describe their most common distortions in space and time and how to avoid them—or take advantage of them. In addition, it will cover the nonlinear optics of ultrashort pulses for converting pulses to almost any color, as well as the additional interesting and potentially deleterious effects nonlinear optical processes can cause. Finally, it will cover techniques for ultrashort-pulse measurement.

Short Course Benefits:

This course will enable you to:

- Explain how ultrashort-pulse lasers and amplifiers work
- Describe ultrashort pulses and their many distortions
- Use nonlinear optics to convert ultrashort laser pulse to virtually any wavelength
- Take advantage of—or avoid—nonlinear-optical high-intensity effects
- Meaningfully measure ultrashort pulses

Short Course Level: Beginner

Short Course Audience: Any scientist or engineer interested in the science and technology of the shortest events ever created, especially those new to it.

SC410 - Finite Element Modeling Methods for Photonics and Optics

Arti Agrawal, *City Univ., UK*
Tuesday, 15 May, 12:00–15:00

Numerical modelling and simulation of optical devices and components is a key tool in improving performance by reducing time and monetary costs, design optimization and characterization as well as innovating new ideas. Both passive and active devices are modelled and optimized numerically. In some cases simulation is the only way to explore phenomena where technology is not advanced enough for fabrication. The interaction of the optical beam with physical effects such as non-linearity, stress, strain, change in refractive index due to temperature, application of electric fields etc. are now extremely important. Modelling complements experimental work perfectly and almost no research is conducted without it.

The Finite Element (FE) method is one of the most popular and powerful methods for modelling in Photonics. This short course starts with Maxwell's equations and explains the basic principles of numerical modelling and the key assumptions involved. This foundation is used to develop the FE method, including a brief tour of the mathematics. How the method can be applied to various optical devices is discussed in detail. How can physical effects be included with the FE method for modelling is considered. The course ends with an explanation of FE based beam propagation methods and how these can be used to find the evolution of the optical fields.

Some salient features of the short course include:

- Emphasis on practical application of FEM for modelling of devices
- Discussion on developing code
- Perfectly Matched Layer and Periodic boundary condition
- Generating mesh for structures, post-processing of results
- Discussion on popular commercial software such as COMSOL and how to best utilize them

Methods covered include:

- Full vector Finite Element method for modal solution
- Introduction to inclusion of physical effects with the optical model

Practical illustrations include:

- Optical fibers including photonic crystal fibers
- Si slot waveguides, nanowires and high index contrast structures
- Bent waveguides and loss
- Plasmonic waveguides

All conference locations are in the San Jose Convention Center unless otherwise noted.

Short Course Benefits:

This course will enable you to:

- Identify and explain basic principles of numerical modelling in Photonics
- Discuss and explain Full vector Finite Element Method (FEM) for modal solutions
- Introduction to FEM with physical effects (non-linearity, stress/strain, acousto-optic, electro-optic effect etc.)
- Discuss and explain how to incorporate Perfectly Matched Layer and Periodic boundary condition
- Summarize how to generate mesh for structures and post-processing of results
- Tips on how to best utilise commercial software
- Discuss the application of the method to practical devices: nano wires, optical fibers, sensors etc.
- Identify the appropriate modeling method for their problem
- How to incorporate PML boundary conditions and write your own code

Short Course Audience: This course is intended for researchers, engineers and students who use simulation in their work in both fundamental and applied aspects of Optics and Photonics, especially for components and devices. The course is useful for members of both academic and industrial institutions. Basic background and familiarity in Optics will be sufficient.

SC352 - Introduction to Ultrafast Pulse Shaping-- Principles and Applications

Marcos Dantus, *Michigan State Univ., USA*
Tuesday, 15 May, 12:00–15:00

Pulse shaping is an integral part of every femtosecond laser, and learning about pulse shaping can help us better understand dispersion, pulse characterization and pulse compression. This course begins by describing how the spectral phase affects the temporal characteristics of a femtosecond pulse with a hands-on computer simulation. The essential physics and a brief background of the development of shapers are provided. The course goes over the experimental implementation requirements and then covers some of the most salient applications of pulse shapers, among them: (a) pulse compression, (b) pulse characterization, (c) creation of two or more pulse replicas, and (d) control of nonlinear optical processes such as selective two-photon excitation and selective vibrational mode excitation (e) material processing, (f) microscopy and others. The course provides a good foundation for those wanting to explore the more fundamental aspects of light-matter interactions, and it also provides multiple examples of practical applications that are made possible by pulse shaping.

Short Course Benefits:

This course will enable you to:

- Gain a better understanding of femtosecond laser pulses and their applications
- Learn pulse shaper design principles
- Compare among different pulse shaper designs and

to determine which one is best suited for a particular application

- Simulate the output pulse from a pulse shaper given a particular phase and amplitude modulation
- Predict the effect caused by introducing a simple phase such as a linear, quadratic or cubic function on a transform-limited pulse
- Learn two different approaches to creating pulse replica that can be independently controlled with attosecond precision in the time domain using the pulse shaper
- Measure the spectral phase of laser pulses using the pulse shaper itself as the measurement tool, and eliminating phase distortions to compress the output pulses
- Summarize the advantages of having an adaptive pulse shaper for controlling the output of ultrafast lasers

Short Course Level: Advanced Beginner (basic understanding of topic is necessary to follow course material)

Short Course Audience:

This course, updated yearly, is intended for everyone that uses or intends to use femtosecond laser pulses in academic research or industry. Attendees will learn how pulse shaping can greatly enhance femtosecond laser applications. No prior knowledge about pulse shaping is required.

SC376 - Plasmonics

Mark Brongersma, *Stanford Univ., USA*
Tuesday, 15 May, 12:00–15:00

Plasmonics is an exciting new field of science and technology that aims to exploit the unique optical properties of metallic nanostructures to enable routing and active manipulation of light at the nanoscale. Nanometallic objects derive these properties from their ability to support collective electron excitations, known as surface plasmons (SPs). Presently we are witnessing an explosive growth in both the number and range of plasmonics applications; it is becoming eminently clear that both new fundamental science and device technologies are being enabled by the current plasmonics revolution. The intention of this tutorial is to give the participants a fundamental background and working knowledge of the main physical ideas used in plasmonics, as well as an overview of modern trends in research and applications.

The Short Course will begin with a general overview of the field of plasmonics. This will be followed by an introduction to the basic concepts that enable one to understand and design a range of plasmonic functionalities. This part will be followed by an in-depth discussion of a range of active and passive plasmonic devices that have recently emerged. Particular attention will be given to nanometallic structures in which surface plasmons can be generated, routed, switched, amplified, and detected. It will be shown that the intrinsically small size of plasmonic devices directly results in higher operating speeds and facilitates an improved synergy between optical and electronic components. The field of plasmonics is rapidly growing and has started to provide a whole range of exciting new research and development opportunities that go well beyond chip-scale components. A number of such developments will be investigated, including new types of optical sensors, solar cells, quantum plasmonic components, non-linear, and ultrafast devices. At the end of the tutorial, a critical assessment of the entire field is given and some of the

All conference locations are in the San Jose Convention Center unless otherwise noted.

truly exciting new opportunities for plasmonics are identified. A comparison of metallic and high-index semiconductor antennas and metamaterials will be made as well.

Short Course Benefits:

This course will enable you to:

- Obtain a working knowledge of the key physical concepts used in Plasmonics that enable light manipulation at ultra small length- and time-scales
- Understand choices of different metal types, shapes, and sizes to accomplish different plasmonic functionalities
- Find out about common electromagnetic computational tools to design plasmonic structures and devices
- Get a feel for the current state of the field in terms of fundamental understanding as well as device applications
- Learn about the most recent trends and developments in research and applications

Short Course Level: Beginner

Short Course Audience: Optical engineers and scientists who are interested in learning about the rapidly emerging field of plasmonics and its potential impact.

SC270 - High Power Fiber Lasers and Amplifiers

W. Andrew Clarkson, *Optoelectronics Res. Ctr., Univ. of Southampton, UK*

Tuesday, 15 May, 12:00–16:00

Short Course Description:

Recent advances in cladding-pumped fiber lasers and amplifiers have been dramatic, leading to unprecedented levels of performance in terms of output power, efficiency, beam quality and wavelength coverage. These achievements have attracted growing interest within the community and have fueled thoughts that fiber-based sources may one day replace conventional “bulk” solid-state lasers in many application areas. The main attractions of cladding-pumped fiber sources are derived directly from their geometry, which simultaneously allows very efficient generation of coherent light and almost complete immunity from the effects of heat generation, which are so detrimental to the performance of other types of lasers.

This course aims to provide an introduction to high power fiber lasers and amplifiers, starting from the basic principles of operation and ending with examples of current state-of-the-art devices and some thoughts on future prospects. The course will cover a range of topics, including basic fiber laser and amplifier theory, spectroscopy of the relevant rare earth ions for high power devices, a discussion of the factors influencing laser and amplifier performance, fiber design and fabrication, pump sources and pump launching schemes, fiber resonator design, master-oscillator and power-amplifier configurations, linewidth control and wavelength selection, transverse mode selection, nonlinear loss processes (SBS and SRS) and their impact on performance, and heat generation and its impact on power scalability. The course will also give an overview of techniques (e.g. coherent and spectral beam combining) for further scaling of output power and provide an introduction to hybrid fiber-bulk laser schemes for scaling pulse energy.

Short Course Benefits:

This course will enable you to:

- Calculate threshold pump power and slope efficiency, and estimate the maximum output power that can be obtained from a given fiber laser oscillator or amplifier configuration
- Select the optimum pump source for a given rare earth ion transition and fiber design
- Design the pump light collection and coupling scheme and estimate the pump launch efficiency
- Specify the fiber parameters (e.g. cladding design, core size, rare earth ion concentration) required for a particular laser or amplifier configuration
- Design the fiber laser resonator and amplifier and select the operating wavelength
- Estimate thermally induced damage limit
- Estimate the power scaling limit
- Measure fiber laser performance characteristics and relate these to fiber design and resonator parameters

Short Course Level: Advanced Beginner

Short Course Audience: This course is intended for individuals with a basic knowledge of lasers and optics who wish to learn about the basic principles and capabilities of fiber lasers and amplifiers when operating at high power levels. The course will also cover some of the practical issues of operating these devices and provide an update for those wishing to learn about some of the latest developments in this rapidly advancing field.

SC438 - Photonic Metamaterials

Nader Engheta, *Univ. of Pennsylvania, USA*

Tuesday, 15 May, 12:00–16:00

Controlling electromagnetic and optical fields and waves can be achieved via materials. The wave-matter interaction can be engineered using structures made of materials with required parameters and structures with selected shapes, dimensions and sizes. Recent advances in materials science and engineering, condensed matter physics, optical materials, nanoscience and nanotechnology have made it possible to tailor materials with unusual parameters and characteristics. The field of metamaterials, along with its two-dimensional version known as metasurfaces, has seen growing interest and extensive development in recent years. Metamaterials are engineered composite structures made of subwavelength inclusions with suitable materials and proper arrangements. The compositions, arrangements, alignments, densities and distributions of these building blocks in host media provide a variety of degrees of freedom in the design of light-matter interaction with such structures. Manipulation of light at the nano-, micro-, meso- and macroscales using metamaterials and metasurfaces provides rich platforms for tailoring electromagnetic waves with desired functionalities.

In this tutorial, we will begin with the basics of electromagnetic wave interaction with material media and structures. Then the course will get into some of the specifics of the characteristics of metamaterials and metasurfaces including the dispersion properties, scattering mechanisms, effective-medium phenomena, and unconventional features of waves in

All conference locations are in the San Jose Convention Center unless otherwise noted.

such environments. We will then discuss some of the specific topics in photonic metamaterials such as extreme-parameter metamaterials (i.e., epsilon-near-zero (ENZ), mu-near-zero (MNZ), and epsilon-and-mu-near-zero (EMNZ) structures) and their specialized wave-matter interactions, graphene metamaterials as a platform for ideas for one-atom-thick optical device concepts, optical metatronics (“lumped” nanocircuitry) and informatic metastuctures for photonic information processing and computing at the nanoscale, scattering engineering using metamaterials (such as cloaking), guided waves in metamaterials, and nonreciprocal metastructures. Various features and potential applications of these topics will also be presented and discussed. During the course, we will have interactive discussions and question-answer sessions.

Short Course Benefits:

This course will enable you to:

- Describe the basics of electromagnetic field and wave interaction with metamaterials and metasurfaces
- Explain some of the important properties of photonic metamaterials
- Discuss some of the scenarios in light-matter interaction with “extreme-parameter” metamaterials
- Describe the fundamentals of optical nanocircuits (“optical metatronics”), with potentials for information processing in nanophotonics
- Explain some of the salient features of scattering and guidance of lights in metamaterials and metasurfaces

Short Course Level: Beginner

Short Course Audience: Graduate students and senior undergraduates with EE, Physics, and Applied Physics interests; Engineers, researchers and technical managers from industry, government labs, and universities; Introductory knowledge of electromagnetics and optics is required.

Special Events

OSAF Data Science Career Opportunities

Sunday, 13 May, 08:30–17:00

Market 1, Hilton San Jose

Instructor: Roberto Reif, *Metis, USA*

Sponsored by the OSA Foundation and Milton and Rosalind Chang, this course provides an introduction to careers in data science. It incorporates interactive lectures and group exercises. By attending this course, attendees will learn how their technical skills can transition into the data science field and what a career in data science is like, understand what the field of data science is and the roles, necessary skills, and types of problems data scientists work on, and gain insight into the data science project lifecycle and outputs.

Roberto Reif is a senior data scientist at Metis. Prior to Metis, he led the signal processing team at Sensoria Inc. and was a program manager at Microsoft. He has worked on applications in the healthcare, internet of things, biomedical optics, and business intelligence. He has a PhD in Biomedical Engineering from Boston University's Biomedical Optics Laboratory and completed a senior postdoctoral research fellowship at the University of Washington's Biophotonics and Imaging Laboratory. He has co-authored several scientific publications, book chapters, and patents.

Attendance is limited to 50 people. The required registration fee of \$25 includes lunch.

Hosted by: 

OSAF Cheeky Scientist Career Development Workshops

Sunday, 13 May, Session I: 13:00–14:00,

Session II: 16:00–17:00

Winchester 1&2, Hilton San Jose

Instructor: Isaiah Hankel, *Cheeky Scientist, USA*

Isaiah Hankel works with hundreds of graduate students and postdocs daily assisting them to transition to industry by first showing them how to present themselves as business professionals. These programs will provide you with a strong understanding of what it takes to have a tailored industry resume and how to showcase your transferrable skills.

Session Schedule

Session I: The Modern Job Search:

Using online profiles to maximize the effectiveness of the job seeking/transition process. Hiring managers use LinkedIn to determine whether they will bring in a candidate for an interview, this topic will cover all the key elements of the LinkedIn profile and how each section should be used to strategically maximize its impact. In addition, we will show candidates how to use LinkedIn algorithms to support their job search, and sell themselves to perspective employers.

Session II: Networking: An Art & Science:

This section is created based on the networking strategies of some of the most strategic networkers in the world and also goes into the science of building rapport and why this is important for the job seeking professional. While this topic tends to be popular, it seems people are still not using it effectively and thus we have detailed specific action steps job seekers can take, and specific scripts to use while networking.

Workshops are complimentary for OSA Members. There is limited space at each. RSVP online through CLEO Special Events site.

Hosted by: 

OIDA Executive Forum on the Exploding Role of Optics in Sensing

Monday, 14 May, 08:30–18:00

Almaden Ballroom, Hilton San Jose

This event aims to match applications leaders needing new solutions with early-stage technologies in a range of sectors, spanning consumer to industrial markets. While the ultimate activity is "matchmaking" the emphasis will be on the end-product vendors' needs and investor perspectives. The workshop will focus on segments within the field that have particular promise today, such as mobility and automation, Big Data and AI, and manufacturing issues related to these products. Some key questions for discussion will be:

- What is needed from the photonics industry? Which are the problems that optics and photonics can have the greatest impact on?
- What are the enabling technologies that have the most promise?
- What are the bottlenecks or "showstoppers" among photonics technologies today, and potential solutions?

OSA Optical Material Studies Technical Group Special Talk

Monday, 14 May, 12:00–13:00

Room 230A

Students and recent graduates are invited to join the OSA Optical Material Studies Technical Group for a special talk on potential career paths during lunch on Monday. Attendees will have the opportunity to hear from two recent graduates, one who has pursued a career in industry and one who has pursued a career in academia, who will provide insight into their current research and their career paths. An RSVP is required for this technical group event; please contact TGactivities@osa.org to register, pending availability.

Hosted by: 

All conference locations are in the San Jose Convention Center unless otherwise noted.

Workshop: Understanding Unconscious Bias

Monday, 14 May, 14:00–15:30, 16:00–17:30

Winchester 1&2, Hilton San Jose

Speaker: Sara Bendoraitis, *American Univ., USA*

Research demonstrates that we all have unconscious biases. These biases can result in best and brightest talent made to feel unwelcome, invisible, and not important to the success of the organization. This training will explore concepts and engage participants to better understand implicit bias, increase awareness and understanding the impact on organizational culture and identify ways to promote greater engagement with diversity and inclusion.

Programs are open to OSA Members. There is limited space. RSVP required through CLEO Special Events Page.

Hosted by:



Diversity & Inclusion in Optics and Photonics Reception

Monday, 14 May, 17:30–18:30

Market 1&2, Hilton San Jose

Join us for a reception to connect with the optics and photonics community to discuss diversity in the field. Come to learn, share and engage with colleagues around this important topic. Please RSVP by going to CLEO Special Events site to let us know you are attending.

Hosted by: This inclusive event has been organized by OSA, IEEE and APS

OSA Nanophotonics Technical Group 20x20 Talks

Monday, 14 May, 19:00–20:30

Room 230A

This special session hosted by OSA Nanophotonics Technical Group offers a unique platform for individuals to present their research in a creative and concise fashion that differs from the usual oral or poster session. Selected participants will showcase their research in a presentation of 20 images, in which each image is displayed for 20 seconds. Presenters will talk along to the images as the slides advance automatically. Immediately following presentations, attendees are invited to join the technical group for small reception where they can telework with colleagues over refreshments.

Hosted by: 

OSA Technical Group Poster Session

Tuesday, 15 May, 19:00 – 20:30

Room 230A/B

Join the OSA Technical Groups for a series of focused poster sessions, bringing together students and colleagues for an opportunity to share their latest research findings and exchange ideas. After listening to the poster presentations and connecting with fellow attendees over refreshments, you'll have a chance to cast your vote for the best poster from each of the four participating technical groups. Among the technical groups participating this year will be the Optical Material Studies Technical Group, the Ultrafast Optical Phenomena Technical Group, the Systems and Instrumentation Technical Group and the Environmental Sensing Technical Group.

Hosted by: 

Meet OSA Publishing Journal Editors Reception

Tuesday, 15 May, 15:30–17:00

Exhibit Hall #2425

Join OSA Publishing's Journal Editors for conversation and ice cream. The Editors welcome your questions, concerns, and ideas for any of OSA's Journals. Topics for discussion can include best practices when submitting a manuscript; elements of a useful manuscript review; criteria editors look for in submitted manuscripts; or the process to propose a Feature Issue topic for publication in an OSA Journal. All are welcome.

OSA Photonic Metamaterials Technical Group Tutorial on Metasurface Design and Simulation

Wednesday, 16 May, 12:00–13:00

Room 230A

Join the OSA Photonic Metamaterials Technical Group for a tutorial on metasurface design and simulation during lunch on Wednesday. This tutorial, aimed at students and new researchers, will focus on hands-on skills. Dr. Wei Ting Chen from Harvard University, with assistance from Alexander Zhu and Yao-Wei Huang, will provide an overview of metasurfaces followed by a tutorial on how to perform the simulation. An RSVP is required for this technical group event; please contact TGactivities@osa.org to register, pending availability.

Hosted by: 

Conference Reception

Wednesday, 15 May, 19:30–20:30
Grand Ballroom

Enjoy a festive evening with your colleagues, while intermingling with the exhibitors and viewing the first poster session. The reception is open to all attendees and badges must be worn to enter the reception.

Sponsored by: 

Lunch at the CLEO:EXPO

Tuesday and Wednesday, 16 & 17 May, 11:30–13:00
Thursday, 18 May, 12:30–14:00
Exhibit Hall

Grab some lunch and network with exhibitors to check out their innovative products and services that can help your organization.

Emerging Trends in Nonlinear Optics – A Review of CLEO: 2018

Thursday, 17 May, 18:30 – 20:00
Room 230A

OSA Members are invited to join the OSA Nonlinear Optics Technical Group for a special panel discussion presenting the exciting and hot topics in nonlinear optics that were presented during CLEO: 2018. Short presentations from our panelists highlighting important themes from the conference will be followed by moderated question and answer sessions. Following the conclusion of the panel discussion, members are invited to join the technical group for a small reception where they can network with colleagues over refreshments. This technical group event is open to OSA Members; please contact TGactivities@osa.org to register, pending availability.

Hosted by: 

Postdeadline Paper Sessions

Thursday, 17 May, 20:00–22:00
Locations announced on the Conference Update Sheet

The Technical Program Committee has accepted a limited number of postdeadline papers for oral presentation. The purpose of postdeadline papers is to give participants the opportunity to hear new and significant materials in rapidly advancing areas.

All conference locations are in the San Jose Convention Center unless otherwise noted.

CLEO:EXPO

Exhibit Hall

Make sure to visit the show floor which features a diverse group of companies, representing every facet of the lasers and electro-optics industries. Learn about new products, find technical and business solutions, and gain the most up-to-date perspective of the laser-related business environment. Review the list of exhibitors on the following pages to see the companies you'll meet at CLEO.

CLEO:EXPO is free of charge for all conference registrants.

Tuesday, 15 May exhibit-only time	10:00–17:00 10:00–13:00; 15:00–17:00
Wednesday, 16 May exhibit-only time	10:00–17:00 10:00–13:00; 15:00–17:00
Thursday, 17 May Exhibit-only time	10:00–15:00 10:00–14:00

Exhibit Hall Rules

Children 12 and under must be accompanied by an adult at all times. Strollers are not allowed on the show floor at any time.

Neither photography nor videotaping is permitted in the Exhibit Hall. Exhibitors need to get permission from Show Management to photograph their own booths. Non-compliance may result in the surrendering of film and removal from the hall.

For further questions, visit Registration on the Concourse Level.

Exhibitors (as of 9 April 2018)

3DOptix
 AdValue Photonics, Inc.
 Advanced Research Systems
 AdvR
 AIP Publishing
 Allied Laser Solutions
 ALPAO
 Alpes Lasers SA
 Alpine Research Optics
 Altos Photonics, Inc.
 American Elements
 American Institute of Physics
 American Physical Society (APS)
 AMPHOS, Inc.
 Amplitude Laser Group
 APE - Applied Physics & Electronics, Inc.
 Aspen Systems - Laser Cooling
 Attocube Systems, Inc.
 AUREA Technology
 Azur Light Systems
 Boston Electronics Corporation
 Bristol Instruments, Inc.
 Calmar Laser, Inc.
 CASTECH, Inc.
 Changchun New Industries Optoelectronics Tech. Co.
 Chinese Laser Press
 Chromacity
 Class 5 Photonics GmbH
 Cobolt AB
 Coherent Solutions
 Coherent, Inc.
 Cornell NanoScale Facility
 CREOL, University of Central Florida
 Crestec Corporation
 Cristal Laser SA
 Crystalline Mirror Solutions, GmbH
 CST of America, Inc.
 Cybel, LLC
 Cycle GmbH
 DataRay, Inc.
 Daylight Solutions, Inc.
 DCM Tech
 Double Helix LLC
 Edmund Optics, Inc.
 EEOptics Corp.
 EKSMA Optics
 EKSPLA
 Elas
 Electro-Optics Technology, Inc.
 Energetiq Technology, Inc.
 EOSPACE, Inc.
 EXFO
 FASTLITE
 Femtochrome Research, Inc.
 few-cycle Inc.

All conference locations are in the San Jose Convention Center unless otherwise noted.

Gentec Electro-Optics, Inc.
 GTAT Corp.
 Hagitec Ltd
 Hamamatsu Corporation
 HC Photonics Corp.
 Hindsight Imaging
 Hiwin Corporation
 HJ Optronics, Inc.
 HOLOEYE Photonics AG
 HTA Photomask
 Ibsen Photonics A/S
 IEEE Photonics Society
 IMRA America, Inc.
 Industrial Technology Research Institute
 INNOLAS
 InPhenix
 Inrad Optics
 Integrated Fiber Optics
 IPG Photonics Corp.
 IRflex Corporation
 Keopsys US
 KMLabs, Inc.
 LaCroix Precision Optics
 Laser and Engineering Technologies Cluster
 Laser Focus World
 Laser Quantum, Inc.
 Lattice Electro Optics, Inc.
 Light Conversion, Ltd.
 Lighthouse Photonics
 Liquid Instruments
 Lumentron
 Luvantix ADM Co., Ltd.
 M Squared Lasers Ltd.
 McPherson Inc.
 Menlo Systems
 Mesa Photonics, LLC
 Micro Photon Devices
 Mindrum Precision, Inc.
 MIRTHE + Photonics Sensing Center
 MKS Instruments
 MPS Micro Precision Systems AG
 Nanjing Ninke Photoelectric Tech., Co., Ltd.
 NANOGRASS
 National Energetics
 National Reconnaissance Office
 Newport Corporation
 Nikon Corporation
 NKT Photonics
 Northrop Grumman Cutting Edge Optronics, Inc.
 NPI Lasers
 NTT Electronics Corporation
 NuCrypt LLC
 Nuphoton Technologies Inc.
 OEwaves, Inc.
 Ophir
 Optiforms
 OptiGrate
 Optimax Systems, Inc.
 OptoSigma Corporation
 Optronics Co., Ltd., The
 OSA - The Optical Society
 Osela, Inc.
 Oxford University Press
 Oxide Corporation
 OZ Optics
 PHASICS Corp.
 Photodigm, Inc.
 Photon Design
 Photonics Media/Laurin Publishing
 Photonix Edge, LLC
 Photop Technologies, Inc
 Physics Today
 PI (Physik Instrumente) LP
 PicoQuant
 Princeton Scientific Corporation
 PriTel, Inc.
 Pure Photonics
 Quantel
 Quantum Design, Inc.
 Quantum Opus
 Raicol Crystals Ltd.
 Resolved Instruments
 Sacher Lasertechnik GmbH
 Sandia National Laboratories
 Santec USA Corporation
 Seiwa Optical America, Inc.
 Shasta Crystals
 SHI Cryogenics Group
 SILIOS Technologies S.A.
 Siskiyou Corporation
 SmarAct, Inc.
 Solid Sealing Technology
 Specialised Imaging
 Spectra Quest Lab
 Spectral Energies, LLC
 Spectra-Physics
 SPIE: The Intl Society for Optics and Photonics
 Springer
 Srico, Inc.
 Stable Laser Systems
 STANDA
 Stanford Research Systems
 StellarNet, Inc.
 Swabian Instruments GmbH
 Swamp Optics, LLC
 Synopsys, Inc.
 ThermoTek, Inc.
 Thorlabs
 Timbercon, Inc.
 Toptica Photonics, Inc.
 TRUMPF Inc.
 University of Arizona, College of Optical Sciences
 University of Campinas (UNICAMP)
 Vescent Photonics, Inc.
 Vigo Systems SA
 Wasatch Photonics
 YSL Photonics Co., Ltd.
 Zaber Technologies
 Zurich Instruments

All conference locations are in the San Jose Convention Center unless otherwise noted.

CLEO:EXPO Technology Playground

Using the game card placed in your attendee bag (obtained at Registration), stop by participating exhibitor booths to hear about their products and services. They'll stamp your card; and when you've met with all of them, you'll be entered into a daily drawing to win a \$100 gift card.

Exhibitors Participating:

Calmar Laser
Edmund Optics
Gentec-EO USA, Inc.
KMLabs
MKS Newport Corporation
Optimax
Optosigma
OZ Optics
Sacher Lasertechnik GmbH
Thorlabs

Exhibit Hall Coffee Breaks

The exhibit floor is the perfect place to build and maintain professional contacts, and these breaks provide ideal networking opportunities. Complimentary coffee will be served at these times:

Tuesday, 15 May	10:00–11:30 and 15:00–17:00
Wednesday, 16 May	10:00–11:30 and 15:00–17:00
Thursday, 17 May	10:00–11:30

Sponsored by **THORLABS**

MKS Student Lounge

#1340

All student attendees are invited to the MKS Student Lounge, co-sponsored by OSA. The lounge provides an opportunity to relax and spend time networking with other students, while enjoying complimentary, wireless internet and refreshments.

Sponsored by **mks**

Co-sponsored by **OSA** | **100**
The Optical Society | Since 1916

OIDA VIP Industry Leaders Speed Meetings Lunch

Tuesday, 15 May, 12:00–13:30
#2605

This session brings together Industry Executives to share their business experience with Young Professionals, Recent Graduates and Students – how they started their careers, lessons learned and using their degree in an executive position. Informal networking during lunch is followed by a transition to “speed meetings” – brief, small-group visits with each executive to discuss industry trends or career topics.

If you have any questions about this event or are a Student or Recent Graduate and interested in attending, please email vipevents@osa.org

Sponsored by 

Plenary Speaker Meet-n-Greets

Theater I, #2433

Meet CLEO Plenary speakers, ask questions and network with your colleagues.

Tuesday, 15 May 10:15–10:45
Nader Engheta and Vasilis Ntziachristos

Wednesday, 16 May 10:15–10:45
John Mather, Jian-Wei Pan and Sara Seager

Free Lunch at the CLEO:EXPO

Tuesday and Wednesday, 16 & 17 May, 11:30–13:00
Thursday, 18 May, 12:30–14:00
Exhibit Hall

Grab some lunch and network with exhibitors to check out their innovative products and services that can help your organization.

Poster Sessions

Exhibit Hall

Poster Sessions are an integral part of the Technical program. Each author is provided with a board with eight-foot-high by four-foot-wide (243cm x121cm) of usable space on which to display the summary and results of his or her paper. Authors should remain in the vicinity of their presentation board for the duration of the sessions to answer questions from attendees. Authors may set up one hour prior to their assigned session must remove their poster one hour following the session. Authors may submit their poster PDF to cstech@osa.org for publication. New this year are the Dynamic e-Posters. This new presentation method combines the richness of multimedia content of oral presentations with the personalized one-on-one interaction of posters.

Tuesday, 15 May	11:30–13:00
Wednesday, 16 May	11:30–13:00
Thursday, 17 May	11:30–13:00

All conference locations are in the San Jose Convention Center unless otherwise noted.

KMLabs Lunch & Learn Event

Wednesday, 15 May, 12:00–13:30
VIP Industry Networking, #2605

Tabletop Laser Sources at Short Wavelengths Beyond the Ultraviolet—Implementation and Application

Speaker: Henry C. Kapteyn, *Kapteyn-Murnane Laboratories Inc. and Department of Physics, Univ. of Colorado Boulder*

The recent availability of commercial tabletop-scale lasers at wavelengths in the vacuum-UV to EUV to soft x-ray spectral regions (i.e. $h\nu \sim 5\text{-}500$ eV) presents new opportunities for next-generation optical nanometrology as well as studies of fundamental processes in materials science, chemistry, and biology. In this talk, we will discuss the enabling high-harmonic generation technology, the characteristics of the light, its applications, and what it takes to put these sources to use in your lab.

Sponsored by



Technology Transfer Program

Thursday, 17 May
Theater I, #2433

The Technology Transfer Program includes a Keynote presentation, a Technology Transfer Tutorial and a Pitch Panel. The Technology Transfer Tutorial provides attendees an opportunity to learn more about the licensing process: funding, entrepreneurship, technology transfer, and intellectual property. The Pitch Panel provides entrepreneurs an opportunity to showcase their technology, explain why it's valuable and discuss the next steps to commercialization.

- 10:15 – 10:45 Keynote Speaker:
Ruth Houbertz, *Multiphoton Optics GmbH, Germany*
- 10:45 – 11:30 Tech Transfer Tutorial
Presenters:
Hossin Abdeldayem, *NASA-Goddard Space Flight Center, USA*
Newton Frateschi, *INOVA - UNICAMP, Brazil*
Yuzuru Takashima, *Univ. of Arizona, USA*
- 11:30 – 13:00 Pitch Panel w/ Feedback from Panelists
Pitch Panelist:
Leslie Kimerling, *Double Helix, USA*
Presenters:
Kristan Corwin, *Kansas State Univ., Department of Physics, College of Arts and Sciences, USA*
Aykutlu Dana, *Nanoeye, Inc., USA*
Pouya Dianat, *Drexel University and Nanograss Solar LLC, USA*
Lu Lan, *Boston Univ., USA*

Visit www.cleoconference.org/techtransfer for complete information.

All conference locations are in the San Jose Convention Center unless otherwise noted.

CLEO Committees

Applications & Technology

Peter Andersen, *Technical Univ. of Denmark, Denmark*,
General Chair
Nicusor Iftimia, *Physical Sciences, Inc., Germany*, General
Chair
Michael M. Mielke, *Iradion Laser, USA*, Program Chair
Jin Ung Kang, *Johns Hopkins Univ., USA*, Program Chair

CLEO A&T 1: Biomedical Applications

Ilko Ilev, *U.S. Food and Drug Administration, USA*,
Subcommittee Chair
Benjamin Vakoc, *Harvard Medical School, USA*,
Subcommittee Chair
Andrea Armani, *Univ. of Southern California, USA*
Brian Cullum, *Univ. of Maryland, USA*
Qiyin Fang, *McMaster Univ., Canada*
Irene Georgakoudi, *Tufts Univ., USA*
Thomas Huser, *Univ. of Bielefeld, Germany*
Beop-Min Kim, *Korea Univ., South Korea*
Xingde Li, *Johns Hopkins Univ., USA*
Laura Marcu, *University of California Davis, USA*
Brian Pryor, *Lite Cure, LLC, USA*
Sean Wang, *B&W Tek, Inc, USA*
Yicong Wu, *National Institutes of Health, USA*

CLEO A&T 2: Industrial Applications

Andrius Marcinkevicius, *TRUMPF Inc., USA*, Subcommittee
Chair
Nicolas Falletto, *ESI, USA*
Peter Morten Moselund, *NKT Photonics, Denmark*
Michael Krainak, *NASA Goddard Space Flight Center, USA*
Oleg Khodykin, *KLA-Tencor, USA*
Manyalibo Matthews, *LLNL, USA*
Dirk Mueller, *Coherent, USA*
Jie Qiao, *RIT, USA*

CLEO A&T 3: Laser-Based Instrumentation for Measurements and Monitoring

Paul Williams, *National Institute of Standards & Technology, USA*, Subcommittee Chair
Giorgio Brida, *INRIM, Italy*
Peter Fendel, *Thorlabs, USA*
Kara Peters, *North Carolina State Univ., USA*
Greg Rieker, *Univ. of Colorado, USA*
Brian Simonds, *NIST, USA*
Mike Thorpe, *Bridger Photonics Inc., USA*

CLEO A&T 4: Applications in Energy & Environment

Stephanie Tomasulo, *Naval Research Laboratory, USA*,
Subcommittee Chair
Mark Zondlo, *Princeton Univ., USA*, Subcommittee Chair
David Bomse, *Mesa Photonics, Inc. USA*
Bernhard Buccholz, *PTB, Germany*
David Canteli, *Universidad Politecnica de Madrid, Spain*
Amir Khan, *Delaware State Univ., USA*
Jan Nekarda, *Fraunhofer ISE, Germany*
Joel Silver, *Southwest Sciences, Inc., USA*

Fundamental Science

Zhigang Chen, *San Francisco State Univ., USA*, General Chair
Jeff Shapiro, *Massachusetts Institute of Technology, USA*,
General Chair
Stewart Aitchison, *Univ. of Toronto, Canada*, Program Chair
Todd Pittman, *Univ. of Maryland Baltimore County, USA*,
Program Chair

FS 1: Quantum Optics of Atoms, Molecules and Solids

Tracy Northup, *Universität Innsbruck, Austria*, Subcommittee
Chair
Takao Aoki, *Waseda Univ., Japan*
Daniel Felinto Pires Barbosa, *Universidade Federal de
Pernambuco, Brazil*
Adam Black, *US Naval Research Laboratory, USA*
Nathalie de Leon, *Princeton Univ., USA*
Hugues de Riedmatten, *ICFO -The Institute of Photonic
Sciences, Spain*
Edward Flagg, *West Virginia Univ., USA*
Elizabeth Goldschmidt, *US Army Research Laboratory, USA*
Peter Humphreys, *Technische Universiteit Delft, Netherlands*
Virginia Lorenz, *Univ. of Illinois at Chicago, USA*
Andreas Muller, *Univ. of South Florida, USA*
Marina Radulaski, *Stanford Univ., USA*

FS 2: Quantum Science, Engineering and Technology

Joshua Bienfang, *National Institute of Standards and
Technology, USA*, Subcommittee Chair
Konrad Banaszek, *Uniwersytet Warszawski, Poland*
Michael Brodsky, *U.S. Army Research Laboratory, USA*
Maria Chekhova, *Max-Planck-Institut für die Physik des Lichts,
Germany*
John Howell, *Univ. of Rochester, USA*
Yoon-Ho Kim, *Pohang Univ. of Science & Technology, South
Korea*
Olivier Pfister, *Univ. of Virginia, USA*
Raphael Pooser, *Oak Ridge National Laboratory, USA*
Kevin Resch, *Univ. of Waterloo, Canada*
John Sipe, *Univ. of Toronto, Canada*
Martin Stevens, *National Institute of Standards & Technology,
USA*
Shigeki Takeuchi, *Kyoto Univ., Japan*
Philip Walther, *Universität Wien, Austria*

All conference locations are in the San Jose Convention Center unless otherwise noted.

FS 3: Metamaterials and Complex Media

Alexey Yamilov, *Missouri Univ. of Science and Technology, USA*, Subcommittee Chair
 Viktoriia Babicheva, *Georgia State Univ., USA*
 Igal Brener, *Sandia National Labs, USA*
 Yaron Bromberg, *The Hebrew Univ., Israel*
 Yidong Chong, *Nanyang Technological Univ., Singapore*
 Xu Fang, *Univ. of Southampton, UK*
 Liang Feng, *Univ. of Pennsylvania, USA*
 Sylvain Gigan, *Laboratoire Kastler Brossel, France*
 Zubin Jacob, *Purdue Univ., USA*
 Boubacar Kante, *Univ. of California San Diego, USA*
 Andrei Lavrinenko, *Danmarks Tekniske Universitet, Denmark*
 Junsuk Rho, *POSTECH, South Korea*
 Ekatarina Shamonina, *Univ. of Oxford, UK*

FS 4: Optical Excitations and Ultrafast Phenomena in Condensed Matter

Keshav Dani, *Okinawa Institute of Science and Technology, Japan*, Subcommittee Chair
 Elbert Chia, *Nanyang Technological Univ., Singapore*
 Hui Deng, *Univ. of Michigan, USA*
 Mackillo Kira, *Univ. of Michigan, USA*
 Chih-Wei Lai, *US Army Research Laboratory, USA*
 Xiaoqin Li, *Univ. of Texas at Austin, USA*
 Kaihui Liu, *Peking Univ., China*
 Noa Marom, *Carnegie Mellon Univ., USA*
 Ilias Perakis, *Univ. of Alabama at Birmingham, USA*
 Denis Seletskiy, *Univ. of Konstanz, Germany*
 Mark Sherwin, *Univ. of California Santa Barbara, USA*
 Diyar Talbayev, *Tulane Univ., USA*
 Jerome Tignon, *CNRS - Laboratoire Pierre Aigrain, France*
 Lyubov Titova, *Univ. of Alberta, USA*
 Ulrike Woggon, *Technische Universität Berlin, Germany*

FS 5: Nonlinear Optics and Novel Phenomena

Mercedeh Khajavikhan, *CREOL, Univ. of Central Florida, USA*, Subcommittee Chair
 Tal Carmon, *Technion Israel Institute of Technology, Israel*
 Demetrios Christodoulides, *Univ. of Central Florida, USA*
 Scott Diddams, *National Institute of Standards & Technology, USA*
 Sara Ducci, *Université Paris Diderot, France*
 Arash Mafi, *Univ. of New Mexico, USA*
 Konstantinos Makris, *Univ. of Crete, Greece*
 David Moss, *Swinburne Univ. of Technology, Australia*
 Peter Rakich, *Yale Univ., USA*
 Mikael Rechtsman, *Pennsylvania State Univ., USA*

FS 6: Nano-Optics and Plasmonics

Amit Agrawal, *National Institute of Standards and Technology, USA*, Subcommittee Chair
 Andrea Baldi, *Dutch Institute for Fundamental Energy Research, Netherlands*
 Palash Bharadwaj, *Rice Univ., USA*
 Peter Catrysse, *Stanford Univ., USA*
 Andrea Di Falco, *SUPA, Univ. of St Andrews, UK*
 Monika Fleischer, *Universität Tübingen, Germany*
 Hayk Harutyunyan, *Emory Univ., USA*
 Ido Kaminer, *Technion Israel Institute of Technology, Israel*
 Mo Mojahedi, *Univ. of Toronto, Canada*
 Esther Wertz, *Rensselaer Polytechnic Institute, USA*
 Wei Zhou, *Virginia Tech, USA*
 Rashid Zia, *Brown Univ., USA*

FS 7: High-Field Physics and Attoscience

Michael Chini, *Univ. of Central Florida, USA*, Subcommittee Chair
 Luca Argenti, *Univ. of Central Florida, USA*
 Jens Biegert, *ICFO - The Institute of Photonic Sciences, Spain*
 Francesca Calegari, *DESY, Hamburg, Italy*
 Oren Cohen, *Technion Israel Institute of Technology, Israel*
 Matthias Fuchs, *Univ. of Nebraska Lincoln, USA*
 Shambhu Ghimire, *SLAC/Stanford Univ., USA*
 Nobuhisa Ishii, *Institute for Solid State Physics, Japan*
 Julia Mikhailova, *Princeton Univ., USA*
 Arvinder Sandhu, *The Univ. of Arizona, USA*
 Olga Smirnova, *Max Born Institute, Germany*
 Xiaoming Wang, *Washington State Univ., USA*
 Amelle Zair, *Kings College London, UK*

Science & Innovations

Nathan Newbury, *National Institute of Standards & Technology, USA*, General Chair
 Jessie Rosenberg, *International Business Machines Corp., USA*, General Chair
 Amr S. Helmy, *Univ. of Toronto, Canada*, Program Chair
 Shinji Yamashita, *Univ. of Tokyo, Japan*, Program Chair

CLEO S&I 1: Light-Matter Interactions and Materials Processing

Tsing-Hua Her, *Univ. of North Carolina at Charlotte, USA*, Subcommittee Chair
 Feng Chen, *Shandong Univ., China*
 Ya Cheng, *Shanghai Institute of Optics and Fine Mechanics, China*
 James Fitz-Gerald, *Univ. of Virginia, USA*
 Carl Liebig, *Air Force Research Laboratory, USA*
 Chih Wei Luo, *National Chiao Tung Univ., Taiwan*
 Renee Sher, *Wesleyan Univ., USA*
 Javier Solis, *Instituto de Óptica "Daza de Valdés," Spain*
 Zijie Yan, *Clarkson Univ., USA*

CLEO S&I 2: Advanced Science and Technology for Laser Systems and Facilities

Jake Bromage, *Univ. of Rochester, USA*, Subcommittee Chair
 M J Daniel Esser, *Heriot-Watt Univ., UK*
 Erhard Gaul, *Univ. of Texas at Austin, USA*
 Max Lederer, *European XFEL, Germany*
 Seong Ku Lee, *CoREeLS IBS-GIST, South Korea*
 Xiaoyan Liang, *Shanghai Institute of Optics & Fine Mechanics, China*
 Thomas Metzger, *TRUMPF Scientific Lasers GmbH + Co. KG, Germany*
 Dimitrios Papadopoulos, *LULI, France*
 Brendan Reagan, *Colorado State Univ., USA*
 Clara Saraceno, *Ruhr Universität Bochum, Germany*
 David Spence, *Macquarie Univ., Australia*
 Thomas Spinka, *Lawrence Livermore National Laboratory, USA*

All conference locations are in the San Jose Convention Center unless otherwise noted.

CLEO S&I 3: Semiconductor Lasers

Mikhail Belkin, *Univ. of Texas at Austin, USA*, Subcommittee Chair

Chadwick Canedy, *NRL, USA*

Connie Chang, *UC Berkeley, USA*

Lan Fu, *Australian National Univ., Australia*

Nicolas Grandjean, *EPFL, Switzerland*

Qing Gu, *UT Dallas USA*

Peter Heim, *Thorlabs Quantum Electronics, USA*

Ted Masselink, *Humboldt Univ. of Berlin, Germany*

Nobuhiko Nishiyama, *Tokyo Institute of Technology, Japan*

Boon Siew Ooi, *KAUST, Saudi Arabia*

Leon Shterengas, *SUNY - Stony Brook, USA*

Gottfried Strasser, *TU Vienna, Austria*

Qijie Wang, *Nanyang Technological Univ., Singapore*

Hongping Zhao, *Case Western Reserve Univ., USA*

CLEO S&I 4: Nonlinear Optical Technologies

Michelle Y. Sander, *Boston Univeristy, USA*, Subcommittee Chair

Amol Choudhary, *Univ. of Sydney, Australia*

Katia Gallo, *KTH Royal Institute of Technology, Sweden*

Shu-Wei Huang, *UCLA Engineering IV, USA*

Yoshitomo Okawachi, *Columbia Univ., USA*

Kartik Srinivasan, *National Inst of Standards & Technology, USA*

Markku Vainio, *Univ. of Helsinki, Finland*

Sergey Vasilyev, *IPG Photonics Corp., Mid-IR Lasers, USA*

CLEO S&I 5: Terahertz Science and Technologies

Matthias Hoffmann, *SLAC National Accelerator Laboratory, USA*, Subcommittee Chair

Tyler Cocker, *Universität Regensburg, Germany*

Martin Koch, *Philipps-Universität Marburg, Germany*

Juliette Mangeney, *École normale supérieure, France*

Daniel Mittleman, *Brown Univ., USA*

Tadao Nagatsuma, *Osaka Univ., Japan*

Rohit Prasankumar, *Los Alamos National Laboratory, USA*

Masayoshi Tonouchi, *Osaka Univ., Japan*

Miriam Vitiello, *Scuola Normale Superiore di Pisa, Italy*

Stephan Winnerl, *Forschungszentrum Dresden-Rossendorf, Germany*

CLEO S&I 6: Optical Materials, Fabrication and Characterization

Thomas Murphy, *Univ. of Maryland at College Park, USA*, Subcommittee Chair

Guang-Hua Duan, *Alcatel-Thales III-V Laboratory, France*

Matthew Escarra, *Tulane Univ., USA*

Frederic Gardes, *Univ. of Southampton, UK*

Juejun Hu, *Massachusetts Institute of Technology, USA*

Eiichi Kuramochi, *NTT Corporation, Japan*

Robert Norwood, *The Univ. of Arizona, USA*

Roberto Paiella, *Boston Univ., USA*

Zhipei Sun, *Aalto Yliopisto, Finland*

Frank (Fengqiu) Wang, *Nanjing Univ., China*

CLEO S&I 7: Micro- and Nano-Photonic Devices

Takasumi Tanabe, *Keio Univ., Japan*, Subcommittee Chair

Ali Adibi, *Georgia Institute of Technology, USA*

Vladimir Aksyuk, *National Institute of Standards & Technology, USA*

Paul Barclay, *Univ. of Calgary, Canada*

Daryl Beggs, *Cardiff Univ., UK*

Alfredo De Rossi, *Thales Research & Technology, France*

Dirk Englund, *Massachusetts Institute of Technology, USA*

Karen Grutter, *Univ. Technical Services, Inc., USA*

Zhihong Huang, *Hewlett Packard Laboratories, USA*

Wei Jiang, *Rutgers Univ., USA*

Jin Liu, *Sun Yat-Sen Univ., China*

Nobuyuki Matsuda, *NTT Basic Research Laboratories, Japan*

Jeremy Munday, *Univ. of Maryland at College Park, USA*

Sharon Weiss, *Vanderbilt Univ., USA*

Lan Yang, *Washington Univ. in St Louis, USA*

CLEO S&I 8: Ultrafast Optics, Optoelectronics & Applications

Christophe Dorrer, *Univ. of Rochester, USA*, Subcommittee Chair

Jose Azana, *INRS-Énergie, Matériaux et Télécommunications, Canada*

Alan Fry, *SLAC National Accelerator Laboratory, USA*

Igor Jovanovic, *Univ. of Michigan, USA*

Fumihiko Kannari, *Keio Univ., Japan*

Thomas Planchon, *Delaware State Univ., USA*

Liejia Qian, *Shanghai Jiao Tong Univ., China*

Bojan Resan, *Univ. of Applied Sciences, Switzerland*

Lawrence Shah, *Luminar Technologies, USA*

Catherine Teisset, *TRUMPF Scientific Lasers, Germany*

Andreas Vaupel, *IPG Photonics Corp, USA*

Laszlo Veisz, *Umea Univ., Sweden*

Tobias Witting, *Max-Born-Institut, Germany*

CLEO S&I 9: Components, Integration, Interconnects and Signal Processing

Weidong Zhou, *Univ. of Texas at Arlington, USA*, Subcommittee Chair

Sasan Fathpour, *CREOL, Univ. of Central Florida, USA*

Qiaoqiang Gan, *State Univ. of New York at Buffalo, USA*

Zetian Mi, *Univ. of Michigan, Ann Arbor, USA*

Richard Pentyl, *Univ. of Cambridge, UK*

Haisheng Rong, *Intel Corporation, USA*

Jian Wang, *Huazhong Univ. of Science and Technology, China*

Winnie Ye, *Carleton Univ., Canada*

All conference locations are in the San Jose Convention Center unless otherwise noted.

CLEO S&I 10: Biophotonics and Optofluidics

Andreu Llobera, *Carl Zeiss Vision GmbH, Germany*,
Subcommittee Chair
Haticce Altug, *Ecole Polytechnique Federale de Lausanne, Switzerland*
Michelle Digman, *Univ. of California, Irvine, USA*
Emily Gibson, *Univ. of Colorado Boulder, USA*
Ewa Goldys, *Macquarie Univ., Australia*
Aaron Hawkins, *Brigham Young Univ., USA*
Jessica Houston, *New Mexico State Univ., USA*
Rainer Andreas Leitgeb, *Medical Univ. Vienna, Austria*
Ute Neugebauer, *Center for Sepsis Control and Care Jena, Germany*
Maria Moya-Payan, *Instituto de Microelectronica de Barcelo, Spain*
Katarina Svanberg, *Lund Laser Centre, Sweden*

CLEO S&I 11: Fiber Photonics

Sze Yun Set, *Univ. of Tokyo, Japan*, Subcommittee Chair
Kazi Abedin, *OFS Laboratories, USA*
Shaif-Ul Alam, *Univ. of Southampton, UK*
Camille-Sophie Bres, *École polytechnique fédérale de Lausanne, Switzerland*
Neil Broderick, *Univ. of Auckland, New Zealand*
Gregory Cowle, *Lumentum, USA*
Liang Dong, *Clemson Univ., USA*
Julien Fatome, *Université de Bourgogne, France*
Stuart Jackson, *Macquarie Univ., Australia*
Khanh Kieu, *The Univ. of Arizona, USA*
William Renninger, *Yale Univ., USA*
Masaki Tokurakawa, *Univ. of Electro-communications, ILS, Japan*
Kenneth Kin-Yip Wong, *Univ. of Hong Kong, Hong Kong*
Meng Zhang, *Beihang Univ., China*

CLEO S&I 12: Lightwave Communications and Optical Networks

David Geisler, *Massachusetts Institute of Technology Lincoln Lab, USA*, Subcommittee Chair
Anjali Agarwal, *Vencore Labs, USA*
Xi Chen, *Nokia Bell Labs, USA*
Francesco Da Ros, *Technical Univ. Of Denmark, Denmark*
Marija Furdek, *KTH Royal Institute of Technology, Sweden*
Vladimir Grigoryan, *Ciena Corporation, USA*
Yue-Kai Huang, *NEC Laboratories America Inc, USA*
Masayuki Matsumoto, *Wakayama Univ., Japan*
Ryan Scott, *Keysight Technologies, Inc, USA*
Yikai Su, *Shanghai Jiao Tong Univ., China*
Stylianios Sygletos, *Aston Univ., UK*

CLEO S&I 13: Active Optical Sensing

Todd Stievater, *US Naval Research Laboratory, USA*, Subcommittee Chair
Brian Brumfield, *Pacific Northwest National Laboratory, USA*
Adam Fleisher, *National Institute of Standards & Technology, USA*
Jason Guicheteau, *USA RDECOM ECBC, USA*
R. Jason Jones, *The Univ. of Arizona, USA*
Gamani Karunasiri, *Naval Postgraduate School, USA*
Waruna Kulatilaka, *Texas A&M Univ., USA*
Bernhard Lendl, *Technische Universität Wien, Austria*
Michal Nikodem, *Wroclaw Research Centre EIT+, Poland*
Ian White, *Univ. of Maryland at College Park, USA*
Michael Wojcik, *Space Dynamics Laboratory, USA*

CLEO S&I 14: Optical Metrology

Ian Coddington, *National Institute of Standards & Technology, USA*, Subcommittee Chair
E. Anne Curtis, *National Physical Laboratory, UK*
Tara Fortier, *National Institute of Standards & Technology, USA*
Jungwon Kim, *Korea Advanced Institute of Science & Technology, South Korea*
Nathan Lemke, *Air Force Research Laboratory, USA*
Marco Marangoni, *Politecnico di Milano, Italy*
Mark Notcutt, *Stable Laser Systems, USA*
Laura Sinclair, *National Institute of Standards & Technology, USA*
Guanhao Wu, *Tsinghua Univ., China*

CLEO Steering Committee**IEEE/Photonics Society**

Ann Catrina Coleman, *Univ. of Texas at Dallas, USA*, Chair
Seth Bank, *Univ. of Texas at Austin, USA*
Kent Choquette, *Univ. of Illinois at Urbana-Champaign, USA*
Peter Smowton, *Cardiff Univ., UK*
Weidong Zhou, *Univ. of Texas at Arlington, USA*

The Optical Society

Craig Arnold, *Princeton Univ., USA*
Ingmar Hartl, *DESY, Germany*
Jessie Rosenberg, *IBM TJ Watson Research Center, USA*
Yurii Vlasov, *Univ. of Illinois at Urbana-Champaign, USA*
Jonathan Zuegel, *Laboratory for Laser Energetics, Univ. of Rochester, USA*

APS/Division of Laser Science

Nicholas Bigelow, *Univ. of Rochester, USA*
Rohit Prasankumar, *Los Alamos National Laboratory, USA*

Exhibitor Representative

Anjul Loiacono, *Thorlabs Inc, USA*

Ex-Officio

Peter Andersen, *Danmarks Tekniske Universitet, Denmark*
Stewart Aichison, *Univ. of Toronto, Canada*
Sterling J. Backus, *Kapteyn-Murnane Labs., USA*
Zhigang Chen, *San Francisco State Univ., USA*
Christophe Dorrer, *Univ. of Rochester, USA*
Ben Eggleton, *Univ. of Sydney, Australia*
Robert A. Fisher, *RA Fisher Associates, LLC, USA*
Amr Helmy, *Univ. of Toronto, Canada*
Nicusor Iftimia, *Physical Sciences Inc., USA*
Jin Kang, *Johns Hopkins Univ., USA*
Michal Lipson, *Columbia Univ., USA*
Natalia M Litchinitser, *State Univ. of New York at Buffalo, USA*
Michael M. Mielke, *Iradion Laser Inc., USA*
Eric Mottay, *Amplitude Systemes, France*, Chair
Nathan Newbury, *National Institute of Standards & Technology, USA*
Irina Novikova, *College of William & Mary, USA*
Todd Pittman, *Univ. of Maryland Baltimore County, USA*
Sergey V. Polyakov, *NIST, USA*
Jeff Shapiro, *MIT, USA*
Christine Silberhorn, *Universität Paderborn, Germany*
Stephanie Tomasulo, *Naval Research Laboratory, USA*
Shinji Yamashita, *Univ. of Tokyo, Japan*

All conference locations are in the San Jose Convention Center unless otherwise noted.

CLEO Budget Committee

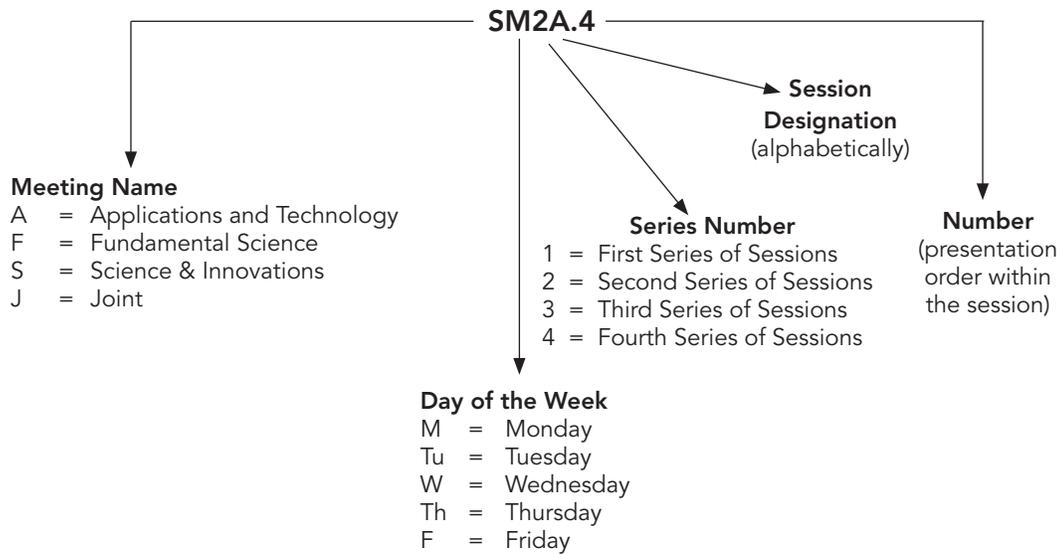
Craig Arnold, *Princeton Univ., USA*
Joe Haus, *Univ. of Dayton, USA*
Kent Choquette, *Univ. of Illinois at Urbana-Champaign, USA*
Chris Jannuzzi, *IEEE Photonics Society, USA*
Anne Kelley, *Univ. of California Merced, USA*
Kate Kirby, *American Physical Society, USA*
Elizabeth A. Rogan, *The Optical Society, USA*

Joint Council on Applications

Eric Mottay, *Amplitude Systemes, France, Chair*
Wilhelm G. Kaenders, *Toptica Photonics Inc, Germany*
Amy Eskilson, *Inrad Optics, USA*
Peter Fendel, *Thorlabs Inc., USA*
Klause Klein, *Coherent, Inc., US*
Tyler Morgus, *Thorlabs Inc., USA*
Rick Plympton, *Optimax Systems, USA*
Carsten Thomsen, *NKT Photonics, Denmark*
Mark Tolbert, *Toptica Photonics, USA*
Chris Wood, *Insight Photonic Solutions, USA*

All conference locations are in the San Jose Convention Center unless otherwise noted.

Explanation of Session/Presentation Codes



The first letter of the code designates the meeting (For instance, A=Applications & Technology, F=Fundamental Science, S=Science and Innovations, J=Joint). The second element denotes the day of the week (Monday=M, Tuesday=Tu, Wednesday=W, Thursday=Th, Friday=F). The third element indicates the session series in that day (for instance, 2 would denote the second parallel sessions in that day). Each series of sessions begins with the letter A in the fourth element and continues alphabetically through a series of parallel sessions. The number on the end of the code (separated from the session code with a period) signals the position of the talk within the session (first, second, third, etc.). For example, a presentation coded SM2A.4 indicates that this paper is part of Science and Innovations (S) and is being presented on Monday (M) in the second series of sessions (2), and is the first parallel session (A) in that series and the fourth paper (4) presented in that session.

Agenda of Sessions — Sunday, 13 May

07:00–17:00	Registration, Concourse Level
08:30–17:00	OSAF Data Science Career Opportunities Course, Market 1, Hilton San Jose
08:30–12:30	SC149: Foundations of Nonlinear Optics SC361: Coherent MidInfrared Sources and Applications SC466: Silicon Integrated Nanophotonics
08:30–15:00	SC456: How to Start A Company
13:00–14:00	OSAF Cheeky Scientist Career Development Workshop (Session I), Winchester 1&2, Hilton San Jose
13:30–16:30	SC439: Attosecond Optics SC403: NanoCavity Quantum Electrodynamics and Applications
13:30–17:30	SC157: Laser Beam Analysis, Propagation, and Shaping Techniques SC301: Quantum Cascade Lasers: Science, Technology, Applications and Markets SC396: Frontiers of Guided Wave Nonlinear Optics
16:00–17:00	OSAF Cheeky Scientist Workshop (Session II), Winchester 1&2, Hilton San Jose

Agenda of Sessions — Monday, 14 May

	Executive Ballroom 210A	Executive Ballroom 210B	Executive Ballroom 210C	Executive Ballroom 210D	Executive Ballroom 210E	Executive Ballroom 210F	Executive Ballroom 210G	Executive Ballroom 210H	Meeting Room 211 B/D
07:00–18:00	Registration, Concourse Level								
08:00–10:00	JM1A • Symposium on Future Directions in Terahertz Nanoscopy I	SM1B • Nonlinear and Microwave Integrated Photonics	SM1C • RF Photonic & Radio-over-fiber	SM1D • Nonlinear Resonators	FM1E • Topological Optics	FM1F • Highly Correlated and Topological States of Matter	FM1G • Quantum Photonic Devices	FM1H • Solid State Spin-Photon Interfaces	SM1I • Modulator on Integrated Platform
08:30–18:00	OIDA Executive Forum on the Exploding Role of Optics in Sensing, Almaden Ballroom, Hilton San Jose								
10:00–10:30	Coffee Break, Concourse Level								
10:30–12:30	JM2A • Symposium on Future Directions in Terahertz Nanoscopy II	SM2B • Novel Nanophotonic Structures and Devices	SM2C • Short Reach Communication	SM2D • Nonlinear Optical Phenomena	FM2E • Topological Photonics and Lasers	FM2F • Exciton-polaritons and Other Excitation in Semiconductors	FM2G • Novel Nonphotonic Light Sources	FM2H • Quantum Optics with Single Atoms	SM2I • Integrated Detectors
12:00–13:00	OSA Optical Material Studies Technical Group Special Talk, Room 230A								
12:30–13:30	Lunch Break (on your own)								
12:30–15:30	SC362: Cavity Optomechanics: Fundamentals and Applications of Controlling and Measuring Nano- and Micro-mechanical Oscillators with Laser Light								
12:30–16:30	SC455: Integrated Photonics for Quantum Information Science and Technology SC378: Introduction to Ultrafast Optics								
13:00–14:00	Social Media 102, Market Room 1, Hilton San Jose								
13:30–15:30	SM3A • Terahertz Nonlinear Spectroscopy	SM3B • Optical Modulators	SM3C • SDM Communications I	SM3D • Nonlinear Optics in Fibers and Waveguides	FM3E • Symmetries in Optics	FM3F • High Harmonic Generation in Solids	FM3G • Quantum Sources I	FM3H • Chiral and Topological Quantum Optics	SM3I • Optical Phase Arrays
14:00–15:30	Workshop: Understanding Unconscious Bias, Winchester 1&2, Hilton San Jose								
15:30–16:00	Coffee Break, Concourse Level								
16:00–18:00	SM4A • THz High-field Generation and Detection	SM4B • Microrings and Novel Modulation Schemes	SM4C • SDM Communication II	SM4D • Optical Meteorology Nonlinear Optical Technologies	FM4E • PT-Symmetry and Non-Hermitian Photonics	FM4F • Probing Materials with Ultrafast Electricity and Extreme Light	FM4G • Quantum Sources II	FM4H • Quantum Optics with Atomic and Molecular Ensembles	SM4I • Novel Emitters
16:00–17:30	Workshop: Understanding Unconscious Bias, Winchester 1&2, Hilton San Jose								
17:30–18:30	Diversity & Inclusion in Optics and Photonics Reception, Market 1&2, Hilton San Jose								
19:00–20:30	OSA Nonphotonic Technical Group 20x20 Talks, Room 230A								

Meeting Room 212 A/C	Meeting Room 212 B/D	Marriott, Salon I & II	Marriott, Salon III	Marriott, Salon IV	Marriott, Salon V	Marriott, Salon VI	Marriott, Willow Glen
Registration, <i>Concourse Level</i>							
AM1J • Advanced Microscopy and Imaging Techniques	SM1K • Raman Scattering and Applications	SM1L • Precision Clocks and Time Transfer	AM1M • Laser-based Advanced Manufacturing & Materials Processing	SM1N • Advanced Laser Technologies	SM1O • Fundamentals of Light-matter Interaction	AM1P • A&T Topical Review on Photonics-enabled Quantum Technologies in Transition I	FM1Q • Optical Filamentation and X-rays
OIDA Executive Forum on the Exploding Role of Optics in Sensing, <i>Almaden Ballroom, Hilton San Jose</i>							
Coffee Break, <i>Concourse Level</i>							
AM2J • Biomedical Imaging	SM2K • Fiber Sensing and Measurement	SM2L • Optical Microwave Generation	AM2M • Material Processing Lasers and Sensing Technologies	SM2N • Fiber and Wave Guide Lasers	SM2O • Light Matter Interaction in Plasmonic & Metamaterials	AM2P • A&T Topical Review on Photonics-enabled Quantum Technologies in Transition II	FM2Q • Non-Hermitian and PT Photonics
OSA Optical Material Studies Technical Group Special Talk, <i>Room 230A</i>							
Lunch Break (<i>on your own</i>)							
SC362: Cavity Optomechanics: Fundamentals and Applications of Controlling and Measuring Nano- and Micro-mechanical Oscillators with Laser Light							
SC455: Integrated Photonics for Quantum Information Science and Technology SC378: Introduction to Ultrafast Optics							
Social Media 102, <i>Market Room 1, Hilton San Jose</i>							
FM3J • Imaging and Cloaking in Metamaterials	SM3K • Billouim Scattering and Applications	SM3L • Photonic Frequency References and Sources	FM3M • Sources and Technology for Attosecond and High-field Physics	SM3N • High Power Lasers	SM3O • Fundamentals of Laser Material Processing	AM3P • Photobiomodulation Therapeutics	FM3Q • Topological Photonic Structure
Workshop: Understanding Unconscious Bias, <i>Winchester 1&2, Hilton San Jose</i>							
Coffee Break, <i>Concourse Level</i>							
FM4J • Fundamentals of Metamaterials	SM4K • Nonlinear Fiber Optics	SM4L • Frequency Comb Development & Technology	SM4M • Power Scaling of Ultrafast Sources	SM4N • Laser Materials	SM4O • Structured Light for Material Processing	AM4P • Biosensing Technologies	FM4Q • Valley-Hall and Active Topological Photonics
Workshop: Understanding Unconscious Bias, <i>Winchester 1&2, Hilton San Jose</i>							
Diversity & Inclusion in Optics and Photonics Reception, <i>Market 1&2, Hilton San Jose</i>							
OSA Nonophotonics Technical Group 20x20 Talks, <i>Room 230A</i>							

Agenda of Sessions — Tuesday, 15 May

	Executive Ballroom 210A	Executive Ballroom 210B	Executive Ballroom 210C	Executive Ballroom 210D	Executive Ballroom 210E	Executive Ballroom 210F	Executive Ballroom 210G	Executive Ballroom 210H	Meeting Room 211 B/D
07:00–18:30	Registration, <i>Concourse Level</i>								
08:00–10:00	JTU1A • Plenary Session I & Awards Ceremony, <i>Grand Ballroom</i>								
10:00–17:00	Exhibition Open, <i>Exhibit Hall</i>								
10:00–11:30	Coffee Break & Exhibit Only Time, <i>Exhibit Hall</i>								
11:30–13:00	JTU2A • Poster Session I, <i>Exhibit Hall</i> Exhibit Hall Free Lunch								
12:00–13:30	OIDA VIP Industry Leaders Speed Meetings Lunch, <i>Exhibit Hall, #2605</i>								
12:00–15:00	SC352: Introduction to Ultrafast Pulse Shaping--Principles and Applications SC376: Plasmonics SC410: Finite Element Modeling Methods for Photonics and Optics								
12:00–16:00	SC270: High Power Fiber Lasers and Amplifiers SC438: Photonic Metamaterials								
13:00–15:00	STu3A • Quantum Photonic Technology	STu3B • OAM and Photodetective	STu3C • Advanced Short Reach and Free Space Communications	STu3D • Terahertz Communications	FTu3E • Thermal and Quantum Applications of Metasurfaces	STu3F • Nonlinear Integrated Photonic Platforms	FTu3G • Quantum Key Distribution	FTu3H • Quantum Optics with Solid-state Single Emitters	ATu3I • OCT and LIDAR
15:00–17:00	Coffee Break & Exhibit Only Time, <i>Exhibit Hall</i>								
15:30–17:00	Meet the OSA Editors Reception, <i>Exhibit Hall, #2425</i>								
17:00–19:00	FTu4A • Quantum Information Processing	STu4B • Wavelength and Phase-sensitive Integrated Devices	STu4C • Nonlinearity Compensation	STu4D • Terahertz QCLs	FTu4E • Quantum and Non-local Plasmonics	STu4F • Nonlinear Optical Phononics & Optomechanics	FTu4G • Continuous Variable Quantum Computing	FTu4H • Novel Solid State Systems for Quantum Optics	ATu4I • Combustion and Hypersonic Flow Diagnostics
19:00–20:30	OSA Technical Group Poster Session, <i>230A/B</i>								

Meeting Room 212 A/C	Meeting Room 212 B/D	Marriott, Salon I & II	Marriott, Salon III	Marriott, Salon IV	Marriott, Salon V	Marriott, Salon VI	Marriott, Willow Glen	Theatre I	Theatre II
Registration, Concourse Level									
JTU1A • Plenary Session I & Awards Ceremony, Grand Ballroom									
Exhibition Open, Exhibit Hall									
Coffee Break & Exhibit Only Time, Exhibit Hall									
JTU2A • Poster Session I, Exhibit Hall Exhibit Hall Free Lunch									
OIDA VIP Industry Leaders Speed Meetings Lunch, Exhibit Hall, #2605									
SC352: Introduction to Ultrafast Pulse Shaping--Principles and Applications SC376: Plasmonics SC410: Finite Element Modeling Methods for Photonics and Optics									
SC270: High Power Fiber Lasers and Amplifiers SC438: Photonic Metamaterials									
ATu3J • Nanobiophotonics	STu3K • Novel Fibers	JTu3L • Symposium on Multimodal and Molecular Contrast Optical Imaging I	STu3M • High Peak Power Lasers & Technologies	STu3N • Chemical Sensing	JTu3O • Laser Modification of Materials	STu3P • Precision Spectroscopy	STu3Q • Advances in VCSELS	ATu3R • A&T Topical Review on Advanced Applications of Laser Radar and Remote Sensing I	ATu3S • A&T Topical Review on Advances in Supercontinuum Technologies I
Coffee Break & Exhibit Only Time, Exhibit Hall									
Meet the OSA Editors Reception, Exhibit Hall, #2425									
ATu4J • Medical Devices & Systems	STu4K • Fiber Frequency Combs	JTu4L • Symposium on Multimodal and Molecular Contrast Optical Imaging II	ATu4M • Thin Film & Metrology for Laser Processing	STu4N • 2D Materials in Photonic Structures	STu4O • Laser Facilities	STu4P • Advanced Sensing Concepts	STu4Q • UV-visible Semiconductor Lasers		
OSA Technical Group Poster Session, 230A/B									

Agenda of Sessions — Wednesday, 16 May

	Executive Ballroom 210A	Executive Ballroom 210B	Executive Ballroom 210C	Executive Ballroom 210D	Executive Ballroom 210E	Executive Ballroom 210F	Executive Ballroom 210G	Executive Ballroom 210H	Meeting Room 211 B/D
07:30–18:30	Registration, <i>Concourse Level</i>								
08:00–10:00	JW1A • Plenary Session II & International Day of Light, <i>Grand Ballroom</i>								
10:00–17:00	Exhibition Open, <i>Exhibit Hall</i>								
10:00–11:30	Coffee Break & Exhibit Only Time, <i>Exhibit Hall</i>								
11:30–13:00	JW2A • Poster Session II, <i>Exhibit Hall</i> Exhibit Hall Free Lunch								
12:00–13:00	OSA Photonic Metamaterials Technical Group Tutorial on Metasurface Design and Simulation, <i>Room 230A</i>								
13:00–15:00	SW3A • Microresonator Combs	SW3B • Hybrid Lasers on Silicon	SW3C • High Capacity Transmission	SW3D • Terahertz Nano-imaging and Spectroscopy	FW3E • Frequency Combs & Precision Metrology	FW3F • Single-Photon Detectors	FW3G • Nonlinear Nano-optics	FW3H • Active and Tunable Metasurfaces	SW3I • Low-dimensional and Phase-change Materials
15:00–17:00	Coffee Break & Exhibit Only Time, <i>Exhibit Hall</i>								
17:00–19:00	SW4A • High-Q Microcavities	SW4B • Nitride-based Integrated Photonics	SW4C • Optical Switching	SW4D • Novel THz Techniques	FW4E • Quantum and Nonlinear Phenomena	FW4F • Beyond Qubits	FW4G • Plasmon-mediated Control of Light Emission	FW4H • Shaping Emission Using Metasurfaces	SW4I • Silicon Hybrid Integration
19:30–20:30	Conference Reception, <i>Grand Ballroom</i>								

Meeting Room 212 A/C	Meeting Room 212 B/D	Marriott, Salon I & II	Marriott, Salon III	Marriott, Salon IV	Marriott, Salon V	Marriott, Salon VI	Marriott, Willow Glen	Theatre I	Theatre II
Registration, Concourse Level									
JW1A • Plenary Session II & International Day of Light, Grand Ballroom									
Exhibition Open, Exhibit Hall									
Coffee Break & Exhibit Only Time, Exhibit Hall									
JW2A • Poster Session II, Exhibit Hall Exhibit Hall Free Lunch									
OSA Photonic Metamaterials Technical Group Tutorial on Metasurface Design and Simulation, Room 230A									
SW3J • Biosensors & Photonic Devices	SW3K • Few Mode Fibers and OAM	SW3L • Fiber and Waveguide Sensing	SW3M • Beam Control & Measurement	SW3N • Few-cycle Sources	AW3O • Optical Enhancement of Photovoltaics	JW3P • Symposium on New Advances in Adaptive Optics Retinal Imaging I	SW3Q • Semiconductor Lasers for Integration	AW3R • A&T Topical Review on Advanced Applications of Laser Radar and Remote Sensing II	AW3S • A&T Topical Review on Advances in Supercontinuum Technologies II
Coffee Break & Exhibit Only Time, Exhibit Hall									
SW4J • Advanced Microscopy Methods	SW4K • Fiber Lasers and Amplifiers	SW4L • NIR Dual Combs	SW4M • Application of Microresonator Frequency Combs	SW4N • Ultrafast Phenomena	AW4O • Novel Laser Characterization	JW4P • Symposium on New Advances in Adaptive Optics Retinal Imaging II	SW4Q • Novel Semiconductor Emitters		
Conference Reception, Grand Ballroom									

Agenda of Sessions — Thursday, 17 May

	Executive Ballroom 210A	Executive Ballroom 210B	Executive Ballroom 210C	Executive Ballroom 210D	Executive Ballroom 210E	Executive Ballroom 210F	Executive Ballroom 210G	Executive Ballroom 210H
07:30–18:00	Registration, <i>Concourse Level</i>							
08:00–10:00	STh1A • Novel Structures and Devices	STh1B • Integrated Photonic Sensors	STh1C • Machine Learning for Communication	FTh1D • Nonlinear Metamaterials and Metasurfaces	FTh1E • Nonlinear Optics in Microresonator Systems	FTh1F • Novel Phenomena in van der Waals Heterostructure	FTh1G • Integrated Quantum Sources	FTh1H • Quantum Interference, Imaging and Spectroscopy
10:00–15:00	Exhibition Open, <i>Exhibit Hall</i>							
10:15–13:00	Technology Transfer Program, <i>Exhibit Hall Theater</i>							
10:00–11:30	Coffee Break & Exhibit Only Time, <i>Exhibit Hall</i>							
11:30–13:00	JTh2A • Poster Session III, <i>Exhibit Hall</i>							
12:30–14:00	Exhibit Hall Free Lunch							
14:00–16:00	STh3A • Photonic Crystals	STh3B • Networks on a Chip	JTh3C • Symposium on Integrated Sources of Non-Classical Light: Perspectives and Challenges I	JTh3D • Symposium on Advances in Integrated Microwave Photonics I	FTh3E • Non-diffracting and Vortex Beams	STh3F • Mid-IR Nonlinear Devices	STh3G • Quantum Information Processing on Photonic Nanostructures	ATH3H • Control of Quantum Optical and Opto-mechanical Systems
16:00–16:30	Coffee Break, <i>Concourse Lobby</i>							
16:30–18:30	STh4A • Waveguide Structures	STh4B • On-chip and Offchip Coupling Schemes	JTh4C • Symposium on Integrated Sources of Non-Classical Light: Perspectives and Challenges II	JTh4D • Symposium on Advances in Integrated Microwave Photonics II	FTh4E • Multimode Nonlinear Fiber Optics	STh4F • Optical Parametric Oscillators	FTh4G • Cats and Kets	FTh4H • Nanophotonic Emitters, Detectors and Modulators
18:30–20:00	Dinner Break (<i>on your own</i>)							
18:30–20:00	Emerging Trends in Nonlinear Optics – A Review of CLEO: 2018							
20:00–22:00	Postdeadline Paper Sessions, <i>Location TBD</i>							

Meeting Room 211 B/D	Meeting Room 212 A/C	Meeting Room 212 B/D	Marriott, Salon I & II	Marriott, Salon III	Marriott, Salon IV	Marriott, Salon V	Marriott, Salon VI	Marriott, Willow Glen
Registration, <i>Concourse Level</i>								
STh1I • Novel Fabrication Methods	STh1J • OCT & Biomedical Imaging	FTh1K • Optical Near-field and Thermal Imaging	STh1L • MIR to the THz Dual Combs	FTh1M • Nonlinear Dynamics in Resonators and Fibers	STh1N • Ultrafast Applications	ATH1O • Trace Gas Detection	FTh1P • Engineering and Metrology of Thermal Radiation	ATH1Q • A&T Topical Review on Neurophotonics I
Exhibition Open, <i>Exhibit Hall</i>								
Technology Transfer Program, <i>Exhibit Hall Theater</i>								
Coffee Break & Exhibit Only Time, <i>Exhibit Hall</i>								
JTh2A • Poster Session III, <i>Exhibit Hall</i>								
Exhibit Hall Free Lunch								
STh3I • Integrated Photonic Platforms	STh3J • Optofluidics & High Throughput Florescence	STh3K • Multimode Fiber Optics	STh3L • Imaging and Ranging	FTh3M • Chirality Vortices and Topological Effects	STh3N • Ultrafast Metrology I	ATH3O • Novel Spectroscopic Approaches I	ATH3P • Sensing in Extreme Environments & Organic Optical Materials	ATH3Q • A&T Topical Review on Neurophotonics II
Coffee Break, <i>Concourse Lobby</i>								
STh4I • Mid-IR Optoelectronics	FTh4J • Random and Alternative Materials Metasurfaces	STh4K • Long Wavelength Fiber Sources	STh4L • Optical Sensing in Combustion	FTh4M • Functional Nanophotonics Using Metasurfaces	STh4N • Ultrafast Metrology II	ATH4O • Novel Spectroscopic Approaches II	ATH4P • Environmental Greenhouse Gas Sensing	ATH4Q • A&T Topical Review on Scientific and Commercial Progress in Semiconductor Laser Technology I
Dinner Break (<i>on your own</i>)								
Emerging Trends in Nonlinear Optics – A Review of CLEO: 2018								
Postdeadline Paper Sessions, <i>Location TBD</i>								

Agenda of Sessions — Friday, 18 May

	Executive Ballroom 210A	Executive Ballroom 210B	Executive Ballroom 210C	Executive Ballroom 210D	Executive Ballroom 210E	Executive Ballroom 210F	Executive Ballroom 210G	Executive Ballroom 210H
07:30–15:30	Registration, <i>Concourse Level</i>							
08:00–10:00	SF1A • Si Photonics	FF1B • Quantum Enhanced Measurements	JF1C • Symposium on Lasers in Accelerator Science and Technology I	FF1D • Ultrafast Spectroscopy of 2D Materials	FF1E • THz Generation and Novel Phenomena	FF1F • Spatial and Temporal Control of Light Using Metasurfaces	SF1G • Surface Emitting Lasers	FF1H • Nanophotonic Strategies for Controlling Light-Matter Interaction
10:00–10:30	Coffee Break, <i>Concourse Level</i>							
10:30–12:30	SF2A • Nonlinear Photonics in Integrated Structures	JF2B • Symposium on Emerging Quantum Sensing Techniques and Applications I	JF2C • Symposium on Lasers in Accelerator Science and Technology II	FF2D • THz Electrodynamics and control of Electronic Degrees of Freedom	FF2E • Novel Nonlinear Optical Materials	FF2F • Fundamental Nanophotonics: Sensing and Infrared Applications	SF2G • Mid-infrared Semiconductor Lasers	FF2H • Interference and Localization Phenomena in Complex Media
12:30–14:00	Lunch Break (<i>on your own</i>)							
14:00–16:00	SF3A • Integrated Photonics (III-V Heterogeneous)	JF3B • Symposium on Emerging Quantum Sensing Techniques and Applications II	FF3C • Optimization and Design of Metasurfaces	FF3D • Spectroscopy of Low Dimensional Systems	FF3E • Photon-Phonon Interactions and Cooling	FF3F • Optomechanical Interactions and Single Particle Tracking	SF3G • Quantum Cascade Lasers	FF3H • Wavefront Shaping in Complex Media

Meeting Room 211 B/D	Meeting Room 212 A/C	Meeting Room 212 B/D	Marriott, Salon I & II	Marriott, Salon III	Marriott, Salon IV	Marriott, Salon V	Marriott, Salon VI	Marriott, Willow Glen
<i>Registration, Concourse Level</i>								
SF1I • Perovskites and Organics	SF1J • Metasurfaces	SF1K • Hollow Core Fibers		AF1M • Fiber-Optic Based Sensing	SF1N • Ultrafast Mid-IR Sources		FF1P • Attosecond and X-Ray Spectroscopy	AF1Q • A&T Topical Review on Scientific and Commercial Progress in Semiconductor Laser Technology II
<i>Coffee Break, Concourse Level</i>								
SF2I • Electrooptic and Nanophotonic Materials	SF2J • Cavity Optomechanics	SF2K • Novel Fiber Technology	FF2L • Polaritons in 2D Materials	AF2M • Imaging & Microscopy	SF2N • Ultrafast Oscillators		FF2P • High-order Harmonic Generation in Solids	AF2Q • A&T Topical Review on Time-Stretch Technology: Principles and Applications I
<i>Lunch Break (on your own)</i>								
SF3I • Materials for Fiber and Solid State Lasers	SF3J • Mid IR Sensing and Optical Forces	SF3K • Mode-Locked Fiber Lasers		AF3M • Instruments and Components for Spectroscopy	SF3N • Ultrafast Pulse Manipulation		FF3P • Strong-field Physics in Solids	AF3Q • A&T Topical Review on Time-Stretch Technology: Principles and Applications II

Executive Ballroom
210A

Joint

08:00–10:00

JM1A • Symposium on Future Directions in Terahertz Nanoscopy I

Presider: Tyler Cocker; *Universität Regensburg, Germany*

JM1A.1 • 08:00 **Invited**

Pushing Terahertz Emission Microscopy to the Nanoscale, Pernille Klarskov Pedersen^{1,2}, Angela C. Pizzuto¹, Hyewon Kim¹, Vicki Colvin¹, Daniel M. Mittleman¹; ¹*Brown Univ., USA*; ²*DTU Fotonik, Technical Univ. of Denmark, Denmark*. Using a scattering-type optical nearfield microscope the spatial resolution of Laser Terahertz Emission Microscopy (LTEM) can be improved dramatically. With this material properties can be studied optically with a resolution of only 20 nm.

JM1A.2 • 08:30 **Invited**

Towards Quantitative Conductivity Measurements with Infrared Near-Field Optical Microscopy, Joanna M. Atkin¹; ¹*Chemistry, Univ of North Carolina at Chapel Hill, USA*. Mid-infrared scattering-type scanning near-field optical microscopy (s-SNOM) is a non-destructive optical method to extract nanoscale conductivity maps in semiconductors. Combined with spectroscopic analysis, we can extract quantitative local dielectric properties.

Executive Ballroom
210B

CLEO: Science & Innovations

08:00–10:00

SM1B • Nonlinear and Microwave Integrated Photonics

Presider: Richard Penty; *Univ. of Cambridge, UK*

SM1B.1 • 08:00

Heterogeneously Integrated InP Widely Tunable Laser and SiN Microring Resonator for Integrated Comb Generation, Keith A. McKinzie¹, Cong Wang¹, Abdullah Al Noman¹, David Mathine², Kyunghun Han¹, Daniel E. Leaird¹, Maria Anagnost², Vikrant Lal², Gloria Hoefler², Fred Kish², Minghao Qi¹, Andrew M. Weiner¹; ¹*Purdue Univ., USA*; ²*Infinera Corporation, USA*. Optical microresonator frequency combs are inherently compact but require an external pump laser. We demonstrate heterogeneous assembly of an InP high power tunable laser and SiN microring resonator with an eye towards integrated comb generation.

SM1B.2 • 08:15

Random Quasi-Phase-Matching on a Nanophotonic Heterogeneous Silicon Chip, Ashutosh Rao¹, Tracy Sjaardema¹, Guillermo Camacho-Gonzalez¹, Amirmahdi Honardoost¹, Marcin Malinowski¹, Kenneth Schepler¹, Sasan Fathpour¹; ¹*CREOL, Univ Central Florida, USA*. We demonstrate grating-assisted random quasi-phase-matching in unpoled thin-film lithium niobate waveguides on a silicon substrate via second-harmonic generation from near-infrared to visible wavelengths.

SM1B.3 • 08:30

Demonstration of Stimulated Raman Scattering on a Silicon Nitride Photonic Integrated Waveguide, Haolan Zhao^{1,2}, Stephane Clemmen^{1,2}, Ali Raza^{1,2}, Roel Baets^{1,2}; ¹*Photonics Research Group, INTEC, Ghent Univ., Belgium*; ²*Center for Nano- and Biophotonics, Ghent Univ., Belgium*. We report the first demonstration of stimulated Raman scattering (SRS) enabled by an integrated nanophotonic waveguide with CW excitations. It constitutes an important step towards all-on-chip Raman sensor suitable for both gas and liquid detection.

SM1B.4 • 08:45

High-Order Microwave Photonic Intensity Differentiator Based on CMOS-Compatible Micro-Combs, Xingyuan Xu¹, Jiayang Wu¹, Thach Nguyen², Sai T. Chu³, Brent Little⁴, Roberto Morandotti⁵, Arnan Mitchell², David J. Moss¹; ¹*Swinburne Univ. of Technology, Australia*; ²*RMIT Univ., Australia*; ³*City Univ. of Hong Kong, Hong Kong*; ⁴*Chinese Academy of Science, China*; ⁵*INRS-Energie, Matériaux et Télécommunications, Canada*. We demonstrate a third-order microwave photonic intensity differentiator based on micro-combs generated by a CMOS-compatible integrated micro-ring resonator (MRR). The micro-combs serve as a multi-wavelength source, which reduced the cost, and complexity of the differentiator.

Executive Ballroom
210C

08:00–10:00

SM1C • RF Photonic & Radio-over-fiber

Presider: Masayuki Matsumoto; *Wakayama Univ., Japan*

SM1C.1 • 08:00

Reconfigurable Filter-free Sinc-shaped RF Photonic Filters Based on Rectangular Optical Frequency Comb, Jianqi Hu¹, Simon J. Fabbri¹, Camille-Sophie Bres¹; ¹*École polytechnique fédérale de Lausanne, Switzerland*. We demonstrate reconfigurable sinc-shaped RF photonic filters based on rectangular optical frequency comb synthesized from cascaded modulators. Simplicity of the approach and flexibility in bandwidth for fixed free-spectral-range is shown. Phase response is also investigated.

SM1C.2 • 08:15

Noise-resistant all-optical sampling based on a temporal integrator, Zihan Geng^{1,2}, Deming Kong^{1,2}, Bill Corcoran^{1,2}, Arthur Lowery^{1,2}; ¹*Monash Univ., Australia*; ²*CUDOS, Australia*. We propose a novel noise-resistant all-optical sampling with temporal integration. A proof-of-concept experiment shows a receiver sensitivity improvement up to 8-dB for a 1.25 Gbaud PAM 4 signal.

SM1C.3 • 08:30 **Invited**

Optically Powered Radio-Over-Fiber Systems, Motoharu Matsuura¹; ¹*Univ. of Electro-Communications, Japan*. This paper introduces recent works on optically powered radio-over-fiber systems, which drive remote antenna units by power-over-fiber without any other external power supplies. This paper also discusses the perspective on future mobile communications.

Executive Ballroom
210D

CLEO: Science & Innovations

08:00–10:00

SM1D • Nonlinear Resonators

President: Yoshitomo Okawachi; Columbia Univ., USA

SM1D.1 • 08:00

Searching for New Regimes in Microresonator Frequency Combs Using a Pulsed Pump Laser, Jordan Stone¹, Daniel C. Cole¹, Scott Papp¹; ¹NIST, USA. We show how microresonators driven by optical pulses enable the efficient, low-power generation of Kerr solitons and potentially open the door to new nonlinear regimes. We observe two new kinds of low-noise Kerr frequency combs.

SM1D.2 • 08:15

Tunable Insertion of Uniform-Amplitude Multiple Coherent Lines into a Kerr Frequency Comb Using Nyquist Pulse Generation, Fatemeh Alishahi¹, Peicheng Liao¹, Amirhossein Mohajerin Ariaei¹, Ahmad Fallahpour¹, Ahmed Almaiman¹, Yinwen Cao¹, Arne Kordts², Maxim Karpov², Martin Pfeiffer², Tobias J. Kippenberg², Alan E. Willner¹; ¹Univ. of Southern California, USA; ²EPFL, Switzerland. We experimentally achieve tunable insertion of uniform-amplitude multiple coherent lines into a Kerr frequency comb. Coherent, flat lines with spacings of 7GHz and 6GHz are inserted into the Kerr combs with FSRs of 71.7GHz and 192GHz respectively. The Nyquist pulses are compared to the theory.

SM1D.3 • 08:30

Spatial-mode-coupling-based dispersion engineering for integrated optical waveguide, Yu Li¹, Jiachen Li¹, Yuandong Huo¹, Minghua Chen¹, Sigang Yang¹, Hongwei Chen¹; ¹Tsinghua Univ., China. The proposed spatial-mode-coupling-based dispersion engineering method achieves anomalous dispersion on a micro-ring resonator over a range of 25 nm with high Q of 0.8 million on the double-strip TriPleX™ waveguide platform for the first time.

SM1D.4 • 08:45

Switching Dynamics of Counter-propagating Light States in Microresonators, Leonardo Del Bino^{1,2}, Michael T. Woodley^{1,2}, Jonathan M. Silver¹, Shuangyou Zhang¹, Pascal Del'Haye¹; ¹National Physical Lab (NPL), UK; ²CDT Applied Photonics, Heriot-Watt Univ., UK. We present a dynamical analysis of the transition between counter-propagating light states in a nonlinear microresonator. Our results provide important information for the use of these states in optical memories and for dynamical routing in photonic circuits.

Executive Ballroom
210E

CLEO: QELS-Fundamental Science

08:00–10:00

FM1E • Topological Optics

President: Mikael Rechtsman; Pennsylvania State Univ., USA

FM1E.1 • 08:00

Experimental Observation of the Coupling of a Nonlinear Wave to a Topological Edge State, Arstan Bisianov¹, Mark Kremer², Martin Wimmer¹, Alexander Szameit², Ulf Peschel¹; ¹Inst. of Condensed Matter Theory and Optics, Friedrich Schiller Univ. Jena, Germany; ²Inst. for Physics, Univ. of Rostock, Germany. We experimentally investigate a topologically non-trivial edge state of the SSH model. In the presence of nonlinearity topological protection breaks down resulting in efficient energy transfer from a nonlinear wave to the edge state.

FM1E.2 • 08:15

Observation of Aharonov-Bohm Suppression of Optical Tunneling in Twisted Multicore Fibers, Midya Parto¹, Helena Lopez¹, Jose Enrique Antonio-Lopez¹, Juan Carlos Alvarado Zacarias¹, Mercedesh Khajavikhan¹, Rodrigo Amezcua Correa¹, Demetrios N. Christodoulides¹; ¹CREOL, USA. We report the first observation of Aharonov-Bohm-like topological suppression of optical tunneling in twisted multicore fibers. Experimental results show that this effect is insensitive to imperfections, nonlinearities and mode-mixing processes, in agreement with theoretical predictions.

FM1E.3 • 08:30

Topological Lossless Optical Digitizer, Yonatan Sharabi¹, Yonatan Plotnik¹, Yonatan Nemirovski¹, Mordechai Segev¹; ¹Technion, Israel. We present an optical digitizer, based on Bragg reflections and nonlinear index change that restricts the output intensity to two pre-designed values. This device is a manifestation of an intensity-dependent topological phase transition.

FM1E.4 • 08:45

Localization, Time-reversal, and Unidirectional Guiding of Light Pulses Using Dynamic Modulation, Momchil Minkov¹, Shanhui Fan¹; ¹Stanford Univ., USA. We study a coupled-cavity waveguide in which the resonance frequency of each cavity is sinusoidally modulated in time, and demonstrate a range of interesting dynamics that can be achieved in various regimes defined by the underlying parameters.

Executive Ballroom
210F

08:00–10:00

FM1F • Highly Correlated and Topological States of Matter

President: Robert Kaindl; Lawrence Berkeley National Lab, USA

FM1F.1 • 08:00

Controlling electron-phonon interaction in the Bi₂Se₃ topological insulator by Dirac-plasmon engineering, Chihun In¹, Sangwan Sim¹, Beom Kim¹, Hyemin Bae¹, Hyunseung Jung², Woosun Jang¹, Myungwoo Son³, Jisoo Moon⁴, Maryam Salehi⁴, Seung Young Seo⁵, Aloysius Soon¹, Moon-Ho Ham³, Hojin Lee², Seongshik Oh⁴, Dohun Kim⁶, Moon-Ho Jo⁵, Hyunyong Choi¹; ¹Yonsei Univ., South Korea; ²Soongsil Univ., South Korea; ³Gwangju Inst. of Science and Technology, South Korea; ⁴Rutgers Univ., USA; ⁵Pohang Univ. of Science and Technology, South Korea; ⁶Seoul National Univ., South Korea. We performed the time-domain and time-resolved ultrafast THz spectroscopy on the topological insulator (TI) Bi₂Se₃ Dirac plasmons. The distinct dynamics of phonon broadening and phonon stiffening were observed when Dirac plasmon moves across the TI phonon.

FM1F.2 • 08:15

Ultrafast Photocurrent Measurements of Bulk-Conduction Induced Spin Hall Effect in the Topological Insulator Bi₂Se₃, Jekwan Lee², Sangwan Sim², Sungjun Park², Soohyun Park², Seungwan Cho², Sooun Lee¹, Hoil Kim³, Jehyun Kim⁴, Wooyoung Shim¹, Junsung Kim³, Dohun Kim⁴, Hyunyong Choi²; ¹Materials Science & Engineering, Yonsei Univ., South Korea; ²Electrical & Electronic Engineering, Yonsei Univ., South Korea; ³Physics, Pohang Univ. of Science and Technology, South Korea; ⁴Physics & Astronomy, Seoul National Univ., South Korea. We have measured the temporally-resolved helicity-dependent photocurrent at the Bi₂Se₃ topological insulator and identified that the skew scattering induces spin Hall effect while the spin suffers Elliott-Yafet relaxation at the bulk state of the Bi₂Se₃.

FM1F.3 • 08:30 **Invited**

Title To Be Determined, Alessandra Lanzara¹; ¹Univ. of California Berkeley, USA. TBD

**Executive Ballroom
210G**
CLEO: QELS-Fundamental Science
08:00–10:00
FM1G • Quantum Photonic Devices
Presider: Joshua Bienfang; NIST, USA
FM1G.1 • 08:00

A Universal Two-Qubit Photonic Quantum Processor, Xiaogang Qiang^{1,2}, Xiaoqi Zhou^{3,1}, Jianwei Wang¹, Callum Wilkes¹, Thomas Loke⁴, Sean O'Gara¹, Laurent Kling¹, Graham Marshall¹, Raffaele Santagati¹, Jingbo Wang⁴, Jeremy L. O'Brien¹, Mark G. Thompson¹, Jonathan Matthews⁵; ¹Quantum Engineering Technology Labs, Univ. of Bristol, UK; ²State Key Lab of High Performance Computing, NUDT, China; ³State Key Lab of Optoelectronic Materials and Technologies and School of Physics, Sun Yat-sen Univ., China; ⁴School of Physics, The Univ. of Western Australia, Australia. We report a universal two-qubit silicon photonic quantum processor, able to initialise, operate and analyze arbitrary two-qubit states and processes applications in quantum information processing.

FM1G.2 • 08:15

A Large-Number and Multilayer Quantum Walk using Silicon Nano-photonic Chip, Lingxiao Wan¹, Libin Yan¹, Gong Zhang¹, Jianguo Huang¹, Leong Chuan Kwok², Joseph F. Fitzsimons³, Yidong Chong¹, Jiangbin Gong², Alexander Szameit⁴, Xiaoqi Zhou⁵, Man-Hong Yung⁶, Xianmin Jin⁷, Xiaolong Su⁸, Wee Ser¹, Weibo Gao¹, Aiqun Liu¹; ¹Nanyang Technological Univ., Singapore; ²National Univ. of Singapore, Singapore; ³Singapore Univ. of Technology and Design, Singapore; ⁴Univ. of Rostock, Germany; ⁵Sun Yat-sen Univ., China; ⁶Southern Univ. of Science and Technology, China; ⁷Shanghai Jiaotong Univ., China; ⁸Shanxi Univ., China. We experimentally demonstrated 2D quantum walks in a Si₃N₄ chip and study how different parameters affect light distribution. Such scalable quantum device will have a promising application in the field of quantum communication and simulation.

FM1G.3 • 08:30

Monolithically Integrated Hong-Ou-Mandel Experiment in LiNbO₃, Kai-Hong Luo¹, Sebastian Brauner¹, Christof Eigner¹, Raimund Ricken¹, Polina Sharapova¹, Torsten Meier¹, Harald Herrmann¹, Christine Silberhorn¹; ¹Dept. of Physics, Univ. of Paderborn, Germany. We implemented a fully integrated Hong-Ou-Mandel (HOM) interference circuit which comprises a qubit generation, passive routing, fast active polarization manipulation, electro-optic balanced switching, and a variable time delay based on Ti:LiNbO₃ waveguides.

FM1G.4 • 08:45

Investigation of Deep Learning Attacks on Nonlinear Silicon Photonic PUFs, Iskandar Atakhodjaev¹, Bryan Bosworth¹, Brian Grubel¹, Michael Kossey¹, Jesus Villalba¹, A. B. Cooper¹, Najim Dehak¹, Amy Foster¹, Mark A. Foster¹; ¹Johns Hopkins Univ., USA. We demonstrate that nonlinear silicon photonic Physical Unclonable Functions (PUFs) are resistant to adversarial deep learning attacks. We find that this resistance is rooted in the optical nonlinearity of the silicon photonic PUF token.

**Executive Ballroom
210H**
08:00–10:00
FM1H • Solid State Spin-Photon Interfaces
Presider: Elizabeth Goldschmidt; US Army Research Lab, USA
FM1H.1 • 08:00

Spin-photon Quantum Interfaces in Solids, Mete Atature¹; ¹Cambridge Univ., UK. TBD

FM1H.2 • 08:30

Frequency Control of Single Quantum Emitters in Integrated Photonic Circuits, Emma Schmidgall¹, Srivatsa Chakravarthi¹, Michael Gould¹, Ian Christen¹, Karine Hestoffer², Fariba Hatami², Kai-Mei Fu¹; ¹Univ. of Washington, USA; ²Physics, Humboldt-Universität zu Berlin, Germany. We demonstrate a potential integrated-circuit architecture for quantum computation with nitrogen vacancy centers in diamond. The combination of photonic device integration and electrodes enables both high emission rates and tuning of the emission frequency.

FM1H.3 • 08:45

Nanocavity Design for Reduced Spectral Diffusion of Solid-State Defects, Sara L. Mouradian¹, Noel Wan¹, Michael Walsh¹, Eric A. Bersin¹, Matthew Trusheim¹, Tim Schröder², Dirk . Englund¹; ¹MIT, USA; ²Niels Bohr Inst., Denmark. We report on the reduced spectral diffusion of nitrogen vacancy (NV) centers in waveguides and cavities. We also design a novel cavity that provides both high quality factor and isolation from diamond surfaces.

**Meeting Room
211 B/D**
CLEO: Science & Innovations
08:00–10:00
SM11 • Modulator on Integrated Platform
Presider: Judson Ryckman; Clemson Univ., USA
SM11.1 • 08:00

Enhanced Polling and Infiltration of Highly-Linear Mach-Zehnder Modulators on Si/SiN-Organic Hybrid Platform, Iman Taghavi¹, Razi Dehghannasiri¹, Tianren Fan¹, Hesam Moradinejad¹, Hossein Taghinejad¹, Amir H. Hosseini¹, Ali Asghar Eftekhari¹, Ali . Adibi¹; ¹Georgia Inst. of Technology, USA. Effective infiltration and polling of electro-optic polymer (EOP) inside world-record vertical slot of 40 nm is demonstrated for a Mach-Zehnder modulator on a hybrid Si/SiN/EOP platform with highly-linear and high-power handling performance capabilities.

SM11.2 • 08:15

High-speed silicon-organic hybrid modulator enabled by sub-wavelength grating waveguide ring resonator, Zeyu Pan¹, Xiaochuan Xu², Chi-Jui Chung¹, Hamed Dalir², Hai Yan¹, Ke Chen¹, Yaguo Wang¹, Baohua Jia³, Ray Chen¹; ¹Univ. of Texas at Austin, USA; ²Omega Optics, Inc., USA; ³Swinburne Univ. of Technology, Australia. We present a high-speed modulator based on electro-optic polymer infiltrated sub-wavelength grating waveguide ring resonator. A 3-dB small signal modulation bandwidth of 41.36 GHz has been demonstrated.

SM11.3 • 08:30

Silicon-conductive oxide nano-cavity modulator with extremely small active volume, Erwen Li¹, Qian Gao¹, Ray Chen², Alan X. Wang¹; ¹Oregon State Univ., USA; ²Univ. of Texas at Austin, USA. We design and experimentally demonstrated an ultra-compact modulator using transparent conductive oxide as the gate on 1-D silicon photonic crystal cavity. The device offers an ultra-small active volume (<0.06 μm³) and 46 fJ/bit energy efficiency.

SM11.4 • 08:45

100 GBd Plasmonic IQ Modulator, Wolfgang Heni¹, Benedikt Baeuerle¹, Yuriy Fedoryshyn¹, Arne Josten¹, Christian Haffner¹, Tatsuhiko Watanabe¹, David Hillerkuss^{1,2}, Delwin Elder³, Larry R. Dalton³, Juerg Leuthold¹; ¹ETH Zurich, Switzerland; ²Huawei Technologies, Germany; ³Univ. of Washington, USA. Demonstration of a plasmonic IQ modulator operating at 100 GBd QPSK and at 32 GBd 16QAM. The device is orders of magnitude smaller than any photonic counterpart.

Meeting Room
212 A/CCLEO: Applications
& Technology

08:00–10:00

AM1J • Advanced Microscopy and Imaging
Techniques

President: Ilko Ilev; U.S. Food and Drug
Administration, USA

AM1J.1 • 08:00 **Invited**

Brillouin Microscopy for cell and tissue biomechanics,
Giuliano Scarcelli¹; ¹Univ. of Maryland at College Park, USA.
We will describe recent progress of Brillouin microscopy, an
all-optical imaging modality to map mechanical properties
of material based on Brillouin scattering. In ophthalmology,
Brillouin microscopy is in clinical trials; at cell level, Brillouin
microscopy enables characterization of intracellular elasticity.

AM1J.2 • 08:30

**Excitation wavelength optimization of harmonic gen-
eration microscopy in human skin enabled by fiber-based
femtosecond source tunable in 1.15-1.35 μm** , Hsiang-Yu
Chung^{1,2}, Wei Liu^{1,2}, Qian Cao^{1,2}, Rüdiger Greinert³, Franz
X. Kaertner^{1,2}, Guoqing Chang^{1,4}; ¹Center for Free-Electron
Laser Science, DESY, Germany; ²Physics, Universität Hamburg,
Germany; ³Skin Cancer Center Buxtehude, Germany; ⁴The
Hamburg Centre for Ultrafast Imaging, Universität Hamburg,
Germany. We demonstrate a fiber-based tunable femto-
second source covering 1.15-1.35 μm based on self-phase
modulation enabled spectral selection, which allows us to
optimize the excitation wavelength for harmonic generation
imaging in ex vivo human skin.

AM1J.3 • 08:45

**Study of Bacterial Inner Structures with 4π Raman Micros-
copy**, Alejandro Diaz Tormo¹, Dmitry Khalenkov², Andre G.
Skirtach², Nicolas Le Thomas¹; ¹Photonics Research Group,
Belgium; ²Dept. of Molecular Biotechnology, Ghent Univ.,
Belgium. 4π Raman microscopy provides better resolution and
Raman signal than standard Raman microscopy. We determine
the improvement using a silicon layer and show its applicability
to biological specimen for the first time.

Meeting Room
212 B/D

CLEO: Science & Innovations

08:00–10:00

SM1K • Raman Scattering and Applications

President: Kenneth Kin-Yip Wong; Univ. of
Hong Kong, Hong Kong

SM1K.1 • 08:00

**Ultrafast, High Energy, Wideband Wavelength Conversion
Via Continuous Intra-pulse and Discrete Intermodal Raman
Scattering**, Boyin Tai¹, Lars Rishøj¹, Siddharth Ramachandran¹;
¹Boston Univ., USA. We demonstrate energetic (~30nJ) ul-
trashort pulse wavelength conversion from ~1045-1600nm
with ~38% overall efficiency, achieved by a combination of
intra-pulse Raman soliton shifting and discrete, cascaded
intermodal Raman scattering in a step-index multimode fiber.

SM1K.2 • 08:15

**All-fiber dissipative soliton Raman laser for deep tissue
multiphoton imaging**, Khanh Q. Kieu¹, Orkhongua Batjargal¹,
Jennifer Barton¹; ¹Univ. of Arizona, USA. We propose and
demonstrate an all-fiber Raman laser based on phosphosili-
cate fiber. It produces ~5 ps chirped dissipative soliton pulses
with energy up to 8 nJ, average power of 0.3 W at 1230 nm
center wavelength.

SM1K.3 • 08:30

**Demonstration of a Frequency Quadrupled Tunable Soliton
Self-Frequency Shifted Ultra-Short Pulse Fiber Laser with
High Energy Output**, Armin Zach¹, Martin Enderlein¹, Frank
Lison¹, Jeffrey Nicholson², Man Yan², Patrick Wisk², Anthony
DeSantolo²; ¹TOPTICA Projects GmbH, Germany; ²OFS Labs,
USA. We demonstrate a frequency quadrupled soliton self-
frequency shifted femtosecond fiber laser with multiple
tunable outputs in the near infrared and blue spectral range
providing up to 120fs and 6nJ pulse energy.

SM1K.4 • 08:45

**High Power, Ultra-Widely Tunable Wavelength, Cascaded
Raman Fiber Laser**, V Balaswamy¹, Santosh Aparanji¹, S Arun¹,
Siddharth Ramachandran², V R Supradeepa¹; ¹Indian Inst. of
Science, India; ²Boston Univ., USA. We demonstrate a high
power, continuously tunable cascaded Raman fiber laser,
based on filtered distributed feedback. Output powers of
up to 33W is achieved with >450nm tuning from 1118nm-
1575nm, bridging the Ytterbium, Erbium emission bands.

Marriott
Salon I & II

08:00–10:00

SM1L • Precision Clocks and Time Transfer

President: Mark Notcutt; Stable Laser Systems,
USA

SM1L.1 • 08:00

**Real signal generation of a time scale based on an opti-
cal clock**, Hidekazu Hachisu¹, Fumimaru Nakagawa¹, Yuko
Hanado¹, Tetsuya Ido¹; ¹NICT, Japan. Over five months, we
continuously generated real signal of a time scale steered by
an optical clock, showing a long-term instability of low 10^{-16}
level. We also demonstrated the capability to calibrate TAL.

SM1L.2 • 08:30

**Sub-picosecond resolution time-offset measurement over
fiber link with asynchronous optical sampling**, Abulikemu
Abuduweili¹, Xing Chen¹, Jianmin Shang³, Wanpeng Zhang²,
Cheng Ci², Song Yu³, Yingxin Zhao², Bo Liu², Zhigang Zhang¹;
¹Peking Univ., China; ²Nankai Univ., China; ³Beijing Univ. of
Posts and Telecommunications, China. We demonstrate a
sub-picosecond resolution time-offset measurement over
100 km long fiber using asynchronized dual-comb linear
optical sampling.

SM1L.3 • 08:45

**Femtosecond Synchronization through Turbulent Air Off
a Quadcopter**, Laura C. Sinclair¹, Hugo Bergeron², William
C. Swann¹, Isaac Khader¹, Michael Cermak¹, Jean-Daniel
Deschênes², Nathan R. Newbury¹; ¹National Inst. of Stan-
dards and Technology, USA; ²Universite Laval, Canada. We
demonstrate femtosecond-level synchronization of optical
oscillators connected via a moving quadcopter. Synchroniza-
tion is achieved despite 20 m/s motion and 500 m pathlength
changes.

Marriott
Salon IIICLEO: Applications
& Technology

08:00–10:00

AM1M • Laser-based Advanced Manufacturing & Materials Processing
President: TBD**AM1M.1 • 08:00** **Invited****Ultrafast Laser Microwelding of Optical Materials**, Duncan P. Hand¹, Richard Carter¹, Robert R. Thomson¹, M J Daniel Esser¹, Michael Troughton², Ian Elder², Robert Lamb²; ¹Heriot-Watt Univ., UK; ²Leonardo Airborne and Space Systems, UK. Construction of precision optical systems (e.g. lasers) involves bonding optical materials (glasses and crystals - mirrors, beamsplitters, laser crystals) to structural materials (typically metals). I will describe an ultrafast laser welding process for such applications.**AM1M.2 • 08:30****Controlling Femtosecond Laser Ablation of Germanium for Laser Polishing Applications**, Lauren L. Taylor¹, Jing Xu², Thomas Smith², Michael Pomerantz², John Lambropoulos², Jie Qiao¹; ¹Rochester Inst. of Technology, USA; ²Univ. of Rochester, USA. Sensitivity of femtosecond laser ablation to laser parameters was investigated to evaluate controllability of germanium material removal. A processing metric was determined, enabling a method to control laser polishing with flexible combinations of laser parameters**AM1M.3 • 08:45****Process Optimization by Bursts of Ultrafast Laser Pulses and Considerations of Absorbance and Residual Heat**, Beat Neuenschwander¹, Daniel J. Foerster², Beat Jaeggi^{3,1}; ¹Bern Univ. of Applied Sciences, Switzerland; ²Institut für Strahlwerkzeuge ifsw, University of Stuttgart, Germany; ³LASEA AG, Switzerland. It will be shown that an increased absorbance of a copper surface machined with an ultrafast 3 pulse burst may be responsible for the detected increase of the specific removal rate in this case.Marriott
Salon IV

CLEO: Science & Innovations

08:00–10:00

SM1N • Advanced Laser Technologies
President: Erhard Gaul; Univ. of Texas at Austin, USA**SM1N.1 • 08:00****Ultrashort Pulse Laser Irradiation Tests on Silica Glass with Random Antireflective Surface Structures**, Lynda E. Busse¹, Steven R. Flom¹, Jesse Frantz¹, Brandon Shaw¹, Christopher Wilson², Ishwar D. Aggarwal³, Jas Sanghera¹; ¹US Naval Research Lab, USA; ²Univ. of North Carolina at Charlotte, USA; ³Sotera Defense Solutions, USA. We show similar laser induced damage results for silica glass with and without random antireflective surface structures under high intensity fs-laser irradiation.**SM1N.2 • 08:15****High Stability Time-Lens-Based Picosecond Seed Source**, Christophe Dorrer¹, Richard Brown¹; ¹Univ. of Rochester, USA. The design of an optical source based on an electro-optic time lens is described. Excellent pulse-duration stability, short-term jitter, and long-term drift performance are demonstrated, making it suitable as a seed for high-energy laser systems.**SM1N.3 • 08:30****Large-Mode Optical Cavity for UV Laser Power Recycling**, Yun. Liu¹, Abdurahim Rakhman¹; ¹Oak Ridge National Lab, USA. A large-mode Fabry-Perot cavity has been developed for power enhancement of UV laser. Megawatt peak power has been realized inside the cavity through power recycling of 50ps/402.5MHz UV pulses operating in a 10ms/10Hz burst mode.**SM1N.4 • 08:45****Passive compensation of beam misalignment caused by air convection in thin-disk lasers**, Tom Dietrich¹, Stefan Piehler¹, Christoph Röcker¹, Martin Rumpel², Marwan Abdou Ahmed¹, Thomas Graf¹; ¹Universität Stuttgart, Germany; ²MarTec Photonics, Germany. We present a new approach to passively compensate for the misalignment instabilities caused by convection of heated ambient air in front of a thin-disk laser crystal by means of exploiting the spectral dispersion of a diffractive grating-waveguide mirror.Marriott
Salon V

08:00–10:00

SM1O • Fundamentals of Light-matter Interaction
President: Chih Wei Luo; National Chiao Tung Univ., Taiwan**SM1O.1 • 08:00****How Conducting 2D Materials Overlay Modify the Brewster Angle of a Substrate?**, Bruno Majerus¹, Mirko Cormann¹, Nicolas Reckinger¹, Matthieu Paillet³, Luc Henrard¹, Philippe Lambin¹, Michaël Lobet^{2,1}; ¹Univ. of Namur, Belgium; ²John A. Paulson School of Engineering and Applied Sciences, Harvard Univ., USA; ³Laboratoire Charles Coulomb, Univ. of Montpellier, France. Inserting 2D conducting material between dielectrics modifies the Brewster angle. We theoretically and experimentally demonstrate this influence using mono-, bi- and trilayer graphene samples. It provides an original optical measurement of 2D materials' conductivity.**SM1O.2 • 08:15****Optomechanical coupling to ultra-high Q-factor phononic resonators on-chip at cryogenic temperatures**, Prashanta Kharel¹, Yiwen Chu¹, Michael Power¹, Robert J. Schoelkopf¹, Peter T. Rakich¹; ¹Yale Univ., USA. Through engineerable optomechanical coupling to bulk acoustic modes of plano-convex resonators fabricated on-chip, we demonstrate ultra-high acoustic Q-factors of 28 million (6.6 million) for phonons at high frequencies of 12.7 GHz (37.8 GHz) in quartz (silicon) at cryogenic temperatures.**SM1O.3 • 08:30** **Invited****Laser Ablation by Femtosecond Synthesized Waveforms**, Ci-Ling . Pan¹, Chih-Hsuan Lin¹, Chan-Shan Yang¹, Alexey Zaytsev¹; ¹National Tsing Hua Univ., Taiwan. Laser ablation of polymethylmethacrylate by two-color synthesized waveforms show a dependence on the relative phase between the ω and 2ω beams, a manifestation of photoionization in the intermediate regime (Keldysh parameter $g \approx 1.5$).

Marriott
Salon VICLEO: Applications
& Technology

08:00–10:00

AM1P • A&T Topical Review on Photonics-enabled Quantum Technologies in Transition I

Presider: Wilhelm Kaenders; Toptica Photonics AG & Inc., Germany

AM1P.1 • 08:00 **Invited**

From Basic Research to Quantum Technologies: Challenges and Opportunities, Tatjana Curcic¹; ¹US Air Force Office of Scientific Res, USA. Quantum Science research has laid foundations for many new technologies, with applications ranging from brain imaging to information security. In this talk, I will discuss challenges and opportunities accompanying the development of quantum technologies.

AM1P.2 • 08:30 **Invited**

Innovative Laser Solutions for Operational Quantum Sensors, Bruno Desruelle; MUQUANS, France. We present the innovative laser technologies developed for our Absolute Quantum Gravimeter. We describe the work we have done to develop a solution capable of meeting the demanding requirements associated to quantum manipulation of laser cooled atoms, in a compact fibered architecture.

Marriott
Willow GlenCLEO: QELS-Fundamental
Science

08:00–10:00

FM1Q • Optical Filamentation and X-rays

Presider: Alexander Gaeta; Columbia University, USA

FM1Q.1 • 08:00

Precise Holographic Measurements Reveal High Electron Densities in Mid-Infrared Laser Filaments in Air, Dimitris Papazoglou^{2,3}, Valentina Shumakova¹, Skirmantas Ališauskas¹, Vladimir Fedorov^{5,3}, Andrius Pugzlys^{1,4}, Andrius Baltuska^{1,4}, Stylianos Tzortzakis^{5,2}; ¹Vienna Univ. of Technology, Austria; ²Foundation for Research and Technology-Hellas, Greece; ³Univ. of Crete, Greece; ⁴Center for Physical Sciences & Technology, Lithuania; ⁵Texas A&M Univ. at Qatar, Qatar. We report on precise experimental measurements of the electron plasma density in plasma strings generated in air by 3.9 μ m laser filaments using holography. We discuss the origin and impact of the high electron densities observed.

FM1Q.2 • 08:15

Impact of Polarization on Mid-IR Air Filaments, Valentina Shumakova¹, Claudia Gollner¹, Andrius Baltuska^{1,2}, Vladimir Fedorov^{3,4}, Stylianos Tzortzakis^{3,5}, Alexander Voronin^{6,7}, Alexander Mitrofanov^{6,7}, Aleksei Zheltikov^{6,8}, Daniil Kartashov⁹, Andrius Pugzlys^{1,2}; ¹Vienna Univ. of Technology, Austria; ²Center for Physical Sciences & Technology, Lithuania; ³Texas A&M Univ. at Qatar, Qatar; ⁴Lebedev Physical Inst. of the Russian Academy of Sciences, Russia; ⁵Foundation for Research and Technology-Hellas, Greece; ⁶Lomonosov Moscow State Univ., Russia; ⁷Russian Quantum Center, Russia; ⁸Texas A&M Univ., USA; ⁹Friedrich-Schiller Univ. Jena, Germany. We report results of experimental investigation on polarization evolution and losses in linearly and circularly polarized mid-IR filaments in air under different focusing conditions.

FM1Q.3 • 08:30

Shaping Long-lived Electron Wavepackets to Create Customizable Optical Spectra, Rumen R. Dangovski¹, Nicholas Rivera¹, Marin Soljacic¹, Ido Kaminer²; ¹MIT, USA; ²Electrical Engineering, Technion Israel Inst. of Technology, Israel. We introduce new shape-invariant electron wavepackets constructed via superpositions of states in the ionization continuum, enabling customizable optical emission spectra in the eV-keV range. Their shape-invariance is prolonged indefinitely in exchange for larger spatial spreads.

FM1Q.4 • 08:45

Near-infrared Filament Conductivity in Multi-Filament Regime, Milos Burger¹, Patrick J. Skrodzki¹, Igor Jovanovic¹; ¹Univ. of Michigan, USA. Scaling of the electrical conductive properties of femtosecond laser filaments with energy is of significant interest. We observe that the formation of multiple filaments does not impede the increase of air conductivity with laser power.

Executive Ballroom
210A

Joint

JM1A • Symposium on Future Directions in Terahertz Nanoscopy I—Continued

JM1A.3 • 09:00

Bias Dependence of Laser Terahertz Emission Nanoscopy, Angela C. Pizzuto¹, Pernille Klarskov Pedersen^{1,2}, Daniel M. Mittleman¹; ¹*Brown Univ., USA*; ²*Photonics Engineering, Technical Univ. of Denmark, Denmark*. We demonstrate depletion of terahertz emission from semiconductors by applying a DC bias between a substrate and an AFM probe operating in tapping mode. The depletion is strongly dependent on the probe tapping amplitude.

JM1A.4 • 09:15

All-electronic THz Nanoscopy, Clemens Liewald^{1,2}, Fritz Keilmann¹; ¹*Faculty of Physics and Center for NanoScience (CeNS), LMU Munich, Germany*; ²*Nanosystems Initiative Munich, Germany*. We demonstrate 50-nm resolved near-field imaging at $\lambda=500\ \mu\text{m}$ for the first time, using a high-harmonic microwave circuit for emitting/detecting via free space to a standard s-SNOM, and map conductivity contrasts at near single-charge sensitivity.

JM1A.5 • 09:30 **Invited**

Nano-THz Imaging of Quantum Materials, Dimitri Basov¹; ¹*Columbia Univ., USA*. We developed THz nano-spectroscopy and nano-imaging operational at liquid helium temperatures. I will discuss first low-temperature nano-imaging data for ballistic plasmonic transport in graphene, correlated oxides and cuprate high temperature superconductors.

Executive Ballroom
210B

CLEO: Science & Innovations

SM1B • Nonlinear and Microwave Integrated Photonics—Continued

SM1B.5 • 09:00

A highly versatile microwave photonic filter based on an integrated optical frequency comb source, Jiayang Wu¹, Xingyuan Xu¹, Thach Nguyen², Sai T. Chu³, Brent Little⁴, Roberto Morandotti⁵, Arnan Mitchell⁶, David J. Moss⁷; ¹*Swinburne Univ. of Technology, Australia*; ²*RMIT Univ., Australia*; ³*City Univ. of Hong Kong, China*; ⁴*Chinese Academy of Science, China*; ⁵*INRS-Énergie, Matériaux et Télécommunications, Canada*. We experimentally demonstrate a highly versatile microwave photonic filter (MPF) based on Kerr optical comb generated by an integrated microring resonator (MRR). The MPF features improved Q factors, wideband tunability, and highly reconfigurable filtering shapes.

SM1B.6 • 09:15

Chaos synchronization over 50 kilometers using monolithic silicon optomechanical cavities, Jia-Gui Wu^{1,2}, Jaime G. Flor Flores¹, Mingbin Yu³, Guoqiang Lo³, Dim-Lim Kwong³, Shukai Duan², Chee-Wei Wong¹; ¹*Univ. of California, Los Angeles, Fang Lu Mesoscopic Optics and Quantum Electronics Lab, USA*; ²*Southwest Univ., College of Electronic and Information Engineering, China*; ³*Inst. of Microelectronics, Singapore*. High quality chaos synchronization has been experimentally achieved between micro-cavities over 50 kilometers distance. The silicon micro-cavities have been fabricated using fully CMOS-compatible processes, which makes low-cost, scalable solution for secure-communications and networks feasible

SM1B.7 • 09:30

Optical spectral shaping with MHz resolution for arbitrary RF waveform generation, Come Schnebelin¹, Hugues Guillet de Chatellus¹; ¹*LIPhy, France*. We demonstrate a new technique of arbitrary optical spectral shaping with a MHz resolution. The system, based on a single CW laser, enables the generation of radio-frequency arbitrary waveforms with bandwidth exceeding 25 GHz.

Executive Ballroom
210C

SM1C • RF Photonic & Radio-over-fiber—Continued

SM1C.4 • 09:00

Coherently Driven Ultrafast Complex-Valued Photonic Reservoir Computing, Mitsumasa Nakajima¹, Masanobu Inubushi², Takashi Goh¹, Toshikazu Hashimoto¹; ¹*NTT Device Technology Labs., Japan*; ²*NTT Communication Science Labs., Japan*. We propose a complex-valued photonic reservoir computing system implemented using coherent detection and an all-photon wave-forming technique, which achieves gigahertz-order processing with complex-valued inputs and outputs.

SM1C.5 • 09:15

Multi-band carrierless amplitude and phase modulation in RoF system for enhanced reliable mobile fronthaul, Li Di¹, lei deng¹, mengfan cheng¹, Songnian Fu¹, Ming Tang¹, Deming Liu¹; ¹*Huazhong Univ. of Sci. & Tech., China*. We firstly propose to apply multi-band CAP technique in RoF system below 6GHz, and demonstrate a bidirectional 2Gbps CAP signal transmission over 25km-SSMF and 40cm-air, resulting in improved robustness to interference from existing wireless services and asynchronization among different users.

SM1C.6 • 09:30 **Invited**

Microwave Photonics at DARPA: Past, Present and Future, Vincent J. Urick¹; ¹*DARPA, USA*. Microwave photonics research at DARPA is briefly reviewed. The need to focus on multi-use applications of the technology is stressed. Photonics for radio-frequency interference mitigation is identified as such an opportunity.

08:30–18:00 OIDA Executive Forum on the Exploding Role of Optics in Sensing, Almaden Ballroom, Hilton San Jose

10:00–10:30 Coffee Break, Concourse Level

CLEO: Science & Innovations

SM1D • Nonlinear Resonators—Continued

SM1D.5 • 09:00 **Invited**

Widely Tunable Sidebands and Optical Frequency Combs in Passive Nonlinear Resonators, Miro J. Erkintalo¹; ¹Univ. of Auckland, New Zealand. We review recent results on nonlinear frequency conversion in passive resonators, focussing in particular on the generation of widely tunable parametric sidebands in Kerr microresonators and optical frequency combs in quadratically nonlinear cavities.

SM1D.6 • 09:30

Fully Integrated Chip Platform for Electrically Pumped Frequency Comb Generation, Brian Stern^{1,2}, Xingchen Ji^{1,2}, Yoshitomo Okawachi², Alexander L. Gaeta², Michal Lipson²; ¹Cornell Univ., USA; ²Columbia Univ., USA. We demonstrate the first chip-based microresonator comb source consisting of a semiconductor laser integrated with a silicon nitride microresonator. For electrical powers as low as 130 mW, we generate a single-soliton comb spanning 90 nm.

SM1D.7 • 09:45

Ultra-low Power Wavelength Conversion in a Hydrogenated Amorphous Silicon Microring Resonator, Kangmei Li¹, Michael Kossey¹, Amy Foster¹; ¹Johns Hopkins Univ., USA. We demonstrate ultra-low power wavelength conversion via four-wave mixing in a hydrogenated amorphous silicon microring resonator with 10- μ m radius. The results show 22.8-dB conversion efficiency enhancement in the ring compared to a 3.8-mm long waveguide.

CLEO: QELS-Fundamental Science

FM1E • Topological Optics—Continued

FM1E.5 • 09:00

Topological Knotted and Tangled Solitons in Laser Media, Nikolay A. Veretenov^{1,2}, Sergei V. Fedorov^{2,1}, Nikolay N. Rosanov^{1,2}; ¹S.I. Vavilov State Optical Inst., Russia; ²ITMO Univ., Russia. Three-dimensional solitons with the topology of knots and tangles are predicted in laser media with saturable amplification and absorption. Their skeletons consist of unclosed vortex lines forming some axis, and closed ones encircling the axis.

FM1E.6 • 09:15

Classifying Photonic Topological Phases Using Manifold Learning, Or Yair¹, Eran Lustig¹, Ronen Talmon¹, Mordechai Seggev¹; ¹Technion Israel Inst. of Technology, Israel. We use Manifold Learning to classify topological phases of photonic systems, from an arbitrary set of measurements without any prior knowledge or assumptions.

FM1E.7 • 09:30

Observation of Unconventionally Extended Flat-band States in Photonic Lieb Lattices, Shiqi Xia¹, Ajith Ramachandran², Shiqiang Xia¹, Denghui Li¹, Xiuying Liu¹, Liqin Tang¹, Daohong Song^{1,4}, Sergej Flach², Zhigang Chen^{1,3}; ¹The MOE Key Lab of Weak-Light Nonlinear Photonics, TEDA Applied Physics Inst. and School of Physics, Nankai Univ., China; ²Center for Theoretical Physics of Complex Systems, Inst. for Basic Science (IBS), South Korea; ³Dept. of Physics and Astronomy, San Francisco State Univ., USA; ⁴Collaborative Innovation Center of Extreme Optics, Shanxi Univ., China. We propose and demonstrate unconventional flat-band states (compact localized lines) in photonic Lieb lattices. A simple yet effective writing technique leads to desired lattice boundaries that support linear localized modes (lines and necklaces) unrealized before.

FM1E.8 • 09:45

Experimental Realization of Photonic Topological Insulators in Synthetic Dimensions, Eran Lustig¹, Steffen Weimann², Yonatan Plotnik¹, Miguel Bandres¹, Alexander Szameit², Mordechai Seggev¹; ¹Technion Israel Inst. of Technology, Israel; ²Institut für Physik, Universität Rostock, Germany. We report the first experimental realization of photonic topological insulators in synthetic dimensions.

FM1F • Highly Correlated and Topological States of Matter—Continued

FM1F.4 • 09:00

Light-induced Transient State in the Weyl Semimetal TaAs Revealed by Time-resolved Second Harmonic Generation, Nicholas Sirica¹, Yaomin Dai¹, Lingxiao Zhao², Genfu Chen², Run Yang², Bing Xu², Bing Shen², Ni Ni³, Dmitry Yarotski¹, Stuart Trugman¹, Jianxiu Zhu¹, Xianggang Qiu², Toni Taylor¹, Rohit P. Prasankumar¹; ¹Los Alamos National Lab, USA; ²Inst. of Physics Chinese Academy of Sciences, China; ³Dept. of Physics and Astronomy, Univ. of California, Los Angeles, USA. We performed time-resolved second harmonic generation (SHG) spectroscopy on the Weyl semimetal TaAs. These measurements reveal a potential transient photoinduced state as well as an ultrafast dependence of the SHG signal on pump polarization.

FM1F.5 • 09:15

Superconductor sandwiches: cuprate-manganite multilayers with a remarkable new ground state., Benjamin Mallett¹, Premysl Marsik², Jarji Khmaladze², Matteo Minola³, M.C. Simpson^{1,4}, Christian Bernhard²; ¹Univ. of Auckland, New Zealand; ²Physics, Fribourg Univ., Switzerland; ³Festkörperforschung, Max Planck Inst., Germany; ⁴Dodd Walls Centre, New Zealand. In thin-film sandwiches of a cuprate superconductor and specific manganite, the superconductor adopts a startling new ground state. THz ellipsometry and resistivity show it's granular-like, but becomes a 'normal' superconducting state in strong magnetic fields.

FM1F.6 • 09:30

Optically Induced Correlated Phase in CaKFe₂As₄ Superconductor, Richard H. Kim¹, William R. Meier¹, Chirag Vaswani¹, Xin Zhao¹, Xu Yang¹, Martin Mootz², Yongxin Yao¹, Mingyu Xu¹, Ilias E. Perakis², Cai-Zhuang Wang¹, Kai-Ming Ho¹, Serguei Budko¹, Paul Canfield¹, Jigang Wang¹; ¹Iowa State Univ., USA; ²Univ. of Alabama at Birmingham, USA. Ultrafast correlation phenomena is studied on a newly discovered, 1144-type superconductor CaKFe₂As₄ for the first time. Broadband spectral-temporal visualization follows distinct pair-breaking processes and reveal the build-up of a hidden quasiparticle phase with an estimated gap of ~10 meV.

FM1F.7 • 09:45

Probing Charge Density Wave Dynamics in Superconducting YBCO via Ultrafast X-Ray Scattering, Scott Wandel¹, F. Boschini^{2,3}, E.H. da Silva Neto^{2,3}, G. Welch¹, M.H. Seaberg¹, J.D. Koralek¹, G.L. Dakovski¹, W. Hettel¹, M.-F. Lin¹, S.P. Moeller¹, R. Coffee¹, Robert Kaindl⁴, R. Liang^{2,3}, D. Bonn^{2,3}, W. Hardy^{2,3}, M.P. Minitti¹, D.G. Hawthorn⁵, A. Damascelli^{2,3}, C. Giannetti⁶, J.J. Turner¹, G. Coslovich¹; ¹Linac Coherent Light Source, SLAC National Accelerator Lab, USA; ²Dept. of Physics and Astronomy, Univ. of British Columbia, Canada; ³Quantum Matter Inst., Univ. of British Columbia, Canada; ⁴Materials Sciences Division, Lawrence Berkeley National Lab, USA; ⁵Dept. of Physics and Astronomy, Univ. of Waterloo, Canada; ⁶Dept. of Mathematics and Physics, Università Cattolica del Sacro Cuore, Italy. We report optical pump-soft X-ray scattering probe studies of YBCO single crystals. The experiments reveal a picosecond relaxation dynamics of charge density waves, which is in turn strongly modified by the onset of superconductivity.

08:30–18:00 OIDA Executive Forum on the Exploding Role of Optics in Sensing, Almaden Ballroom, Hilton San Jose

10:00–10:30 Coffee Break, Concourse Level

CLEO: QELS-Fundamental Science

FM1G • Quantum Photonic Devices—
ContinuedFM1G.5 • 09:00 **Invited**

Stopped and stationary light with cold atomic ensembles and machine learning., Ben C. Buchler¹; ¹Research School of Physics and Engineering, The Australian National Univ., Australia. Using a cold atomic ensemble, we show the creation of bright stationary light and 87% efficient optical quantum memory. We also demonstrate the use of machine learning to maximise the optical depth of the atoms.

FM1G.6 • 09:30

Plasmon-Mediated Entanglement Dynamics, Benjamin Lawrie¹, Matthew A. Feldman^{1,2}, Ali Passian¹, Phil Evans¹, Matthew Chisholm¹, Jordan Hachtel¹, Richard Haglund², Eugene Dumitrescu¹; ¹Oak Ridge National Lab, USA; ²Vanderbilt Univ., USA. We explore the steady state entanglement of quantum emitters coupled to a lossy plasmonic reservoir and driven by laser or electron-beam pump fields with picosecond antibunching dynamics.

FM1G.7 • 09:45

Ultra Broadband Squeezing and Pairwise Mode-Locking of Coupled Parametric Oscillators, Leon Bello¹, Yaakov Shaked¹, Avi Pe'er¹; ¹Bar-Ilan Univ., Israel. We present a source of bright and broadband, squeezed-light, using active coupling of two parametric oscillators. We demonstrate this design in a radio-frequency experiment, achieving pairwise mode-locking across the entire bandwidth between DC and the pump.

FM1H • Solid State Spin-Photon
Interfaces—Continued

FM1H.4 • 09:00

Quantum dot single photon sources with ultra-low multi-photon error rate, Lukas Hanschke¹, Kevin Fischer², Stefan Appel¹, Daniil Lukin², Jonathan Finley¹, Jelena Vuckovic², Kai Müller¹; ¹Walter Schottky Institut, TU Munich, Germany; ²E.L. Ginzton Lab, Stanford Univ., USA. We demonstrate single-photon generation from self-assembled quantum dots with ultra-low multi-photon probability. While resonant excitation of a two-level system suffers from re-excitation, two-photon excitation of the biexciton state improves multi-photon errors by orders of magnitude.

FM1H.5 • 09:15

Quantum dot single photon sources transfer-printed on wire waveguides, Ryota Katsumi¹, Yasutomo Ota², Masahiro Kakuda², Satoshi Iwamoto^{1,2}, Yasuhiko Arakawa^{1,2}; ¹Inst. of Industrial Science, Japan; ²Inst. for Nano Quantum Information Electronics, Japan. We report quantum dot single photon sources coupled to glass-clad wire waveguides by transfer printing, which enables the heterogeneous source integration in a simple pick-and-place manner. A high waveguide coupling efficiency >60% is experimentally demonstrated.

FM1H.6 • 09:30

Highly Indistinguishable Room Temperature Single Photon Sources with Quantum Emitters in Bad Cavity Regime, Hyeonrak Choi¹, Di Zhu¹, Dirk Englund¹; ¹MIT, USA. We propose room temperature indistinguishable single photon sources based on quantum emitters in solid and nanophotonic cavities. Our approach does not require ultrafast pumping as plasmonic approaches and ultra-high quality factor cavity as funneling regime.

FM1H.7 • 09:45

Near Lifetime-Limited Emitter in a Nanophotonic Waveguide, Henri T. Nielsen¹, Gabija Kirsanskė¹, Hanna Le Jeannic¹, Tommaso Pregnolato¹, Liang Zhai¹, Leonardo Midolo¹, Nir Rotenberg¹, Alisa Javadi¹, Rüdiger Schott², Andreas Wieck², Arne Ludwig², Matthias Löbl³, Immo Söllner³, Richard Warburton³, Peter Lodahl¹; ¹Niels Bohr Inst., Univ. of Copenhagen, Denmark; ²Lehrstuhl für Angewandte Festkörperphysik, Ruhr-Universität Bochum, Germany; ³Dept. of Physics, Univ. of Basel, Switzerland. Coherent light-matter interactions are key to a range of quantum optical technologies and experiments. We present measurements showing near-life-time limited transitions, for quantum dots embedded in nanoguides, demonstrating the robust suppression of environmental decoherence processes.

CLEO: Science & Innovations

SM1I • Modulator on Integrated Platform—
Continued

SM11.5 • 09:00

110 Attojoule-per-bit Efficient Graphene-based Plasmon Modulator on Silicon, Rubab Amin¹, Sikandar Khan¹, Cheol J. Lee², Hamed Dalir³, Volker J. Sorger¹; ¹George Washington Univ., USA; ²Korea Univ., South Korea; ³Omega Optics Inc., USA. We demonstrate a plasmonic Graphene-based electro-absorption modulator heterogeneously integrated in Silicon photonics consuming 110 aJ/bit and being 15 μm compact. We show how the plasmonic metal enables steep switching via improved contact resistance.

SM11.6 • 09:15

Ultra-Fast Compact Plasmonic Modulator based on Adiabatic Coupled Waveguides, Rui Wang¹, Hamed Dalir³, Farzad Koushyari¹, Xiaochuan Xu³, Zeyu Pan¹, Shuai Sun², Volker J. Sorger², Ray Chen¹; ¹ECE, Univ. of Texas, Austin, USA; ²ECE, The George Washington Univ., USA; ³Omega Optics, USA. Compact plasmonic modulator based on adiabatic coupled waveguides obtains insertion loss as low as <0.1 dB with the extinction ratio exceeding 40 dB. In addition the speed of 400 GHz with footprint of 2.7 μm^2 is expected

SM11.7 • 09:30

Microwave-to-Optical Converter based on Integrated Lithium Niobite Coupled-Resonators, Mian Zhang¹, Cheng Wang¹, Yaowen Hu^{1,2}, Amirhassan Shams-Ansari^{1,3}, Guilhem Ribeill⁴, Mohammad Soltani⁴, Marko Loncar¹; ¹John A. Paulson School of Applied and Engineering Sciences, Harvard Univ., USA; ²Dept. of Physics, Tsinghua Univ., China; ³Dept. of Electrical Engineering and Computer Science, Howard Univ., USA; ⁴BBN, Raytheon, USA. We experimentally demonstrate an efficient classical microwave-to-optical converter using coupled optical microresonators on lithium niobite with $Q = 2.7 \times 10^6$. We measure full-depth optical modulation with a 7 GHz microwave driving voltage $V_{\text{rms}} = 70$ mV.

SM11.8 • 09:45

Nonreciprocal Modulation via Intermodal Brillouin Scattering in a Silicon Waveguide, Eric Kittlaus¹, Nils T. Otterstrom¹, Prashanta Kharel¹, Shai Gertler¹, Peter T. Rakich¹; ¹Yale Univ., USA. We report non-reciprocal optical modulation and mode conversion mediated by an optically-driven acoustic wave. Through this process, we experimentally demonstrate >20 dB of nonreciprocity over a >1 nm optical bandwidth in an integrated silicon waveguide.

08:30–18:00 OIDA Executive Forum on the Exploding Role of Optics in Sensing, Almaden Ballroom, Hilton San Jose

10:00–10:30 Coffee Break, Concourse Level

CLEO: Applications
& TechnologyAM1J • Advanced Microscopy and Imaging
Techniques—Continued

AM1J.4 • 09:00

Plasmonics Improves the Sensitivity of Smartphone Fluorescence Microscopy, Qingshan Wei¹, Guillermo Acuna², Seungkyeum Kim³, Carolin Vietz², Derek Tseng³, Jongjae Chae³, Daniel Shir³, Wei Luo³, Philip Tinnfeld², Aydogan Ozcan³; ¹North Carolina State Univ., USA; ²Braunschweig Univ. of Technology, Germany; ³Univ. of California, Los Angeles, USA. We developed a handheld and cost-effective surface-enhanced smartphone fluorescence microscope that showed ~10-fold improvement in signal by using a thin silver film as a plasmonic substrate, enabling the detection of ~80 fluorophores per diffraction-limited spot.

AM1J.5 • 09:15

Deep Learning Microscopy: Enhancing Resolution, Field-of-View and Depth-of-Field of Optical Microscopy Images Using Neural Networks, Yair Rivenson¹, Zoltán Göröcs¹, Harun Günaydin¹, Yibo Zhang¹, Hongda Wang¹, Aydogan . Ozcan¹; ¹Univ. of California Los Angeles, USA. We demonstrate the ability of deep convolutional neural networks to significantly enhance the spatial resolution, field-of-view and depth-of-field of optical microscopy images, without any hardware modification to the imaging system.

AM1J.6 • 09:30

High-resolution optical coherence tomography *in vivo* using a nano-optic endoscope, Hamid Pahlevaninezhad^{1,2}, Mohammadreza Khorasaninejad², Yao-Wei Huang^{2,3}, Zhujun Shi⁴, Lida Hariri¹, David Adams¹, Alexander Zhu², Cheng-Wei Qiu³, Federico Capasso², Melissa Suter¹; ¹Harvard Medical School, USA; ²School of Engineering and Applied Science, Harvard Univ., USA; ³Electrical and Computer Engineering, National Univ. of Singapore, Singapore; ⁴Physics, Harvard Univ., USA. This work establishes a new class of endoscopic optical imaging catheters, termed nano-optic endoscopes, that uses metalenses with the ability to modify the phase of incident light at sub-wavelength level.

AM1J.7 • 09:45

Robust Holographic Autofocusing Based on Edge Sparsity, Yibo Zhang¹, Hongda Wang¹, Yichen Wu¹, Miu Tamamitsu¹, Aydogan . Ozcan¹; ¹Univ. of California Los Angeles, USA. A robust holographic autofocusing criterion based on the edge sparsity of refocused images is presented. Its performance is experimentally validated by imaging various samples with different complex-valued optical transmission functions.

CLEO: Science & Innovations

SM1K • Raman Scattering and
Applications—Continued

SM1K.5 • 09:00

Power Combined, Octave-spanning, CW Supercontinuum using Standard Telecom Fiber with Output Power of 70W, Arun S¹, Vishal Choudhury¹, V Balaswamy¹, V R Supradeepa¹; ¹Centre for Nano Science and Engineering, Indian Inst. of Science (IISc), India. We demonstrate a high power 70W continuous-wave supercontinuum laser using standard telecom fiber, spanning over an octave (850-1900nm). A novel, nonlinear, Raman based power-combining scheme of two independent fiber lasers is used to pump the supercontinuum.

SM1K.6 • 09:15

Multi-Wavelength Diode-Pumping of Fiber Raman Laser, Soonki Hong¹, Yutong Feng¹, Johan Nilsson¹; ¹Optoelectronic research centre, UK. A fiber Raman laser pumped by two wavelength-combined multimode diode lasers at 950 nm and 976 nm generates up to 23 W of output power at a single wavelength (1020 nm) with 51% slope efficiency.

SM1K.7 • 09:30

Enhancing the Detection Sensitivity of Temporal Imaging by Distributed Raman Amplification, Lingxiao Yang¹, Sheng Wang^{1,2}, Chi Zhang², Bowen Li¹, Kenneth Kin-Yip Wong¹; ¹the Univ. of Hong Kong, China; ²Wuhan National Lab for Optoelectronics, Huazhong Univ. of Science and Technology, China. Distributed Raman amplification is integrated into the temporal imaging system for the first time to enhance the detection sensitivity. 6.7-dB sensitivity improvement has been experimentally demonstrated for a 20-nm-bandwidth signal by a 170-mW Raman pump.

SM1L • Precision Clocks and Time
Transfer—Continued

SM1L.4 • 09:00

Absolute Frequency Comb Comparisons and the Measurement of Optical Atomic Clock Transitions, Holly F. Leopardi^{1,2}, Josue Davila-Rodriguez², Jeff Sherman², Franklyn Quinlan², Scott Diddams^{2,1}, Tara M. Fortier²; ¹Univ. of Colorado Boulder, USA; ²NIST, USA. We present agreement in the measurement of optical clock transition frequencies using two independent optical frequency combs to sub-millihertz levels and discuss experiments to improve the measurement instability via coherent atomic clock spectroscopy.

SM1L.5 • 09:15

Sub-mHz Spectral Purity Transfer for Next Generation Strontium Optical Atomic Clocks, Michele Giunta^{1,2}, Wolfgang Hänsel¹, Matthias Lezius¹, Marc Fischer¹, Ronald Holzwarth^{1,2}; ¹Menlo Systems GmbH, Germany; ²Max Planck Inst. of Quantum Optics, Germany. We report on a Er: fiber-based optical frequency comb transferring the stability of ultra-stable lasers from 194THz to 429THz. Sub-mHz level transfer to a fiber-delivered 698.44nm output port for future Strontium QPN-limited lattice clocks is demonstrated.

SM1L.6 • 09:30 **Invited**

Portable Optical Lattice Clocks, Christian Lisdat¹, Jacopo Grotti¹, Silvio Koller¹, Sofia Herbers¹, Stefan Vogt¹, Sebastian Häfner¹, Uwe Sterr¹, Stefano Origlia², Mysore Pramod², Stephan Schiller²; ¹Physikalisch-Technische Bundesanstalt, Germany; ²Heinrich-Heine-Universität Düsseldorf, Germany. I will report on two transportable lattice clocks with strontium. The first was built by PTB and is installed in a car trailer. It was used to demonstrate 'chronometric levelling', i.e. height measurements with clocks by frequency comparisons against a reference clock via optical fibre links. The second apparatus originates from the Space Optical Clock consortium, which has the goal to prepare a space mission with an optical lattice clock. The work is supported by CRC 1128 geo-Q and iSOC.

08:30–18:00 OIDA Executive Forum on the Exploding Role of Optics in Sensing, Almaden Ballroom, Hilton San Jose

10:00–10:30 Coffee Break, Concourse Level

Marriott
Salon IIICLEO: Applications
& TechnologyAM1M • Laser-based Advanced
Manufacturing & Materials Processing—
Continued

AM1M.4 • 09:00

Study for Black Marking of Steel with Short Pulsed and Ultrashort Pulsed Lasers, Daniel Albrecht¹, Tobias Schneider², Claudia Unger¹, Jürgen Koch¹, Oliver Suttman¹, Ludger Overmeyer^{1,2}; ¹Laser Zentrum Hannover e.V., Germany; ²Institut für integrierte Produktion Hannover gGmbH, Germany. Black marking as micrometer scaled binary coding applied on shafts by ultrashort pulsed lasers with high contrast and without ablation as a non-contact sensor system for combined measurement of angular position and torque.

AM1M.5 • 09:15

Laser-based Fabrication of Microfluidic Devices for Porous Media Applications, Krystian L. Włodarczyk¹, Amir Jahanbakhsh¹, Richard Carter¹, Robert R. Maier¹, Duncan P. Hand¹, Mercedes Maroto-Valer¹; ¹Heriot-Watt Univ., UK. A picosecond laser is used for rapid prototyping of enclosed microfluidic devices from borosilicate glass substrates. The fabrication method and applications of these devices for the investigation of subsurface flow processes in porous media are presented.

AM1M.6 • 09:30

Ultrafast Laser Texturing on Si with Burst-mode Picosecond Laser Pulses, Iaroslav Gnilytskyi^{3,1}, Leonardo Orazi¹, Tommi White², Vitaly Gruzdev²; ¹UNIMORE, Italy; ²Dept. of Mechanical & Aerospace Engineering, Univ. of Missouri, USA; ³NoviNano Inc., Ukraine. Picosecond laser-induced periodic surface structures (PLIPSS) have been fabricated on surface of Si in uniform and burst-mode regimes at a high speed. The effects of burst-mode respect to uniform one are examined in term of chemical, mechanical and morphological properties.

AM1M.7 • 09:45

Influence of Laser Power and Scanning Velocity in One- and Two-Step Laser Cladding on Ultra-Thin Substrates, Tobias Gabriel¹, Florian Scherm¹, Marek Gorywoda², Uwe Glatzel¹; ¹Metals and Alloys, Univ. Bayreuth, Germany; ²Materials Engineering, Univ. of Applied Sciences Hof, Germany. Laser cladding on 200 μm thin substrates is a challenge due to poor heat dissipation. Successful coatings were produced using Yb fiber laser with closed-loop controlled laser power. Samples were investigated by SEM and EDS.

Marriott
Salon IV

CLEO: Science & Innovations

SM1N • Advanced Laser Technologies—
Continued

SM1N.5 • 09:00

In situ 3-D temperature mapping of high average power cryogenic laser amplifiers, Han Chi¹, Kristian Dehne², Cory Baumgarten³, Hanchen Wang³, Liang Yin¹, Brendan Reagan^{1,2}, Jorge Rocca^{1,2}; ¹Dept. of Electrical and Computer Engineering, Colorado State Univ., USA; ²XUV Lasers, Inc, PO Box 273251, USA; ³Dept. of Physics, Colorado State Univ., USA. We demonstrate an accurate, in situ, noninvasive optical technique to generate 2-D and 3-D maps of the temperature profile within cryogenic amplifiers operating at high average power.

SM1N.6 • 09:15

Transition-metal-doped solid-state saturable absorbers for passively Q-switched visible Pr:YLF lasers, Hiroki Tanaka^{1,2}, Elena Castellano-Hernández², Christian Kränkel^{2,3}, Fumihiko Kannari¹; ¹Keio Univ., Japan; ²Center for Laser Materials, Leibniz Inst. for Crystal Growth, Germany; ³Inst. of Laser-Physics, Universität Hamburg, Germany. We report the first visibly emitting Q-switched laser based on $\text{Co}^{2+}:\text{Gd}_2\text{Ga}_2\text{O}_{12}$ as the saturable absorber material and present a detailed characterization of the visible saturable absorption properties of various Co^{2+} -doped materials.

SM1N.7 • 09:30

Spectrally tunable, temporally shaped parametric front end to seed high-energy laser systems, Christophe Dorner¹, Albert Consentino¹, Robert Cuffney¹, Ildar Begishev¹, Elizabeth Hill¹, Jake Bromage¹; ¹Univ. of Rochester, USA. We demonstrate the generation of temporally shaped pulses at the 200-mJ level with a tuning range greater than 15 nm via parametric amplification as a high-performance alternative to Nd-doped laser systems.

SM1N.8 • 09:45

Generation of high-fidelity few-cycle pulses via nonlinear ellipse rotation in a stretched hollow-fiber compressor, Nikita Khodakovskiy^{1,2}, Mikhail Kalashnikov², Andreas Blumenstein^{3,4}, Peter Simon⁴, Tamas Nagy², Melek Merve Toktamis⁵, Magali Lozano⁵, Brigitte Mercier⁵, Rodrigo Lopez-Martens⁵; ¹ELI-ALPS Research Inst., Hungary; ²Max-Born-Inst., Germany; ³Univ. of Kassel, Germany; ⁴Laser-Laboratorium Göttingen e.V., Germany; ⁵Laboratoire d'Optique Appliquée, France. We report the generation of high-fidelity few-cycle pulses by nonlinear ellipse rotation in a hollow-fiber compressor. The use of flexible hollow-fiber technology and a pressure gradient enables simultaneous temporal filtering and spectral broadening with record-high efficiency.

Marriott
Salon VSM1O • Fundamentals of Light-matter
Interaction—Continued

SM1O.4 • 09:00

Variable Pattern Projection via a Spatial Light Modulator for Laser Machining on Curved Surfaces, Benjamin Mills¹, Daniel Heath¹, James Grant-Jacob¹, Richard Oreffo¹, Robert Eason¹; ¹Univ. of Southampton, UK. A spatial light modulator can enable precise laser machining on highly curved surfaces without the need for sample rotation, via a beam intensity profile transformation that takes into account the local gradient on the sample.

SM1O.5 • 09:15

Cavity Coupled Hexagonal Boron Nitride Emitters, Sejeong Kim¹, Minh Nguyen¹, Johannes E. Frösch¹, Milos Toth¹, Igor Aharonovich¹; ¹Univ. of Technology Sydney, Australia. We present methods to integrate quantum emitters embedded in hBN to plasmonic and dielectric cavities. Precisely positioned gold nanoparticles in the vicinity of hBN flakes led to emission enhancement. Furthermore, we propose photonic crystal cavities for diverse photonic and quantum applications.

SM1O.6 • 09:30

Waveguide-coupling of pillar microcavities for efficient single quantum dot emission., Tobias Huber¹, Olivier Gazzano¹, Yichen Shuai¹, Glenn S. Solomon¹; ¹JQI (NIST/UMD), USA. We demonstrate a series of pillar microcavities integrated in an optical waveguide. The structure can be used for resonant excitation and single photon emission with spatially orthogonal pump-probe geometry, or for on-chip/off-chip optical coupling.

SM1O.7 • 09:45

Utilization of self-absorption for high resolution laser induced breakdown spectroscopy, Ali Rastegari¹, Matthias Lenzner², Ladan Arissian¹, Jean-Claude M. Diels¹, Kristen Peterson³; ¹UNM, USA; ²Lenzner Research LLC, USA; ³Southwest Sciences, USA. The shock wave created by a high energy UV filament is sufficient to create a low density region in the ablation plume enabling higher resolution in laser induced breakdown spectroscopy. Isotopic selectivity is demonstrated.

08:30–18:00 OIDA Executive Forum on the Exploding Role of Optics in Sensing, Almaden Ballroom, Hilton San Jose

10:00–10:30 Coffee Break, Concourse Level

**CLEO: Applications
& Technology**

AM1P • A&T Topical Review on Photonics-enabled Quantum Technologies in Transition I—Continued

AM1P.3 • 09:00 **Invited**
Engineering Challenges in Commercial Photonics-enabled Quantum Technologies, Max Perez¹; ¹*ColdQuanta, Inc., USA*. As quantum technologies mature, their physical potential clarify but the practical engineering challenges remain. We describe the challenges and trade-offs made when transitioning quantum devices from the Lab to the commercial domain.

AM1P.4 • 09:30
10 years of commercial quantum key distribution: engineering achievements and market challenges, Rik van Gorsel, *id Quantique, USA*. Quantum communication needs good and reliable instrumentation. ID Quantique (IDQ) started in 2002. In order to launch our QKD system in 2007 for elections in the Swiss canton of Genève, we needed to develop the necessary instrumentation as very little existed. For example, a good NIR-SPAD (near infrared single photon avalanche photodiode detector). We have continuously been improving the detectors, so that now we have a NIR-SPAD with single digit dark count rates per second. With such a low dark count rate instrument, we have been able to show quantum key distribution through more than 300 km of high quality optical communication fiber. Our developments in electronics have paralleled the developments in single photon instrumentation. Good hardware is not enough for good technology. Quantum physics-based hardware, firmware, and QKD software needs to be integrated. It also requires the ability and flexibility to integrate new technological developments in any area of quantum communication. For example, originally systems were all-fiber. Current developments in free space communication are rapid and it is not unlikely that a reliable, robust infrastructure will mean a distributed hybrid system with a combination of free space (large distances) and wired communication (in hubs, and free space complement). Good technology is not enough for a good quantum communication network. Trust probably is the most precious element. Trust takes years to build and is very valuable to us. Trust cannot be abstract, but has to be practical and verifiable. For example, our quantum random number generator (QRNG) has been time-proven, and certified by independent organizations in different countries. Current progress in quantum communication is rapid and accelerating and makes the development of solutions to technology and implementation bottlenecks more urgent. I look forward to detail both the technological achievements and discuss the constraints, including limitations by the current infrastructure, solutions to national security concerns of global quantum communication network(s), and the feasibility of cross-border partnerships, e.g. IDQ and US partners.

**CLEO: QELS-Fundamental
Science**

FM1Q • Optical Filamentation and X-rays—Continued

FM1Q.5 • 09:00
Picosecond backward-propagating lasing of atomic hydrogen via femtosecond 2-photon-excitation in a flame, PengJi Ding¹, Maria Ruchkina¹, Yi Liu², Andreas Ehn¹, Marcus Aldén¹, Joakim Bood¹; ¹*Division of Combustion Physics, Dept. of Physics, Lund Univ., Sweden*; ²*Univ. of Shanghai for Science and Technology, China*. We report on the observation of backward-propagating 656-nm lasing of atomic hydrogen in flame using 205-nm femtosecond laser pulses. It shows a donut-shaped spatial mode and smooth temporal profile, suggesting spatially-resolved measurements in few-millimeters resolution.

FM1Q.6 • 09:15
Few-Cycle-Culose-Driven Metasurface-Based Multi-Color X-ray Source, Gilles D. Rosolen¹, Liang Jie Wong², Nicholas Rivera³, Bjorn Maes¹, Marin Soljagic³, Ido Kaminer^{4,3}; ¹*Univ. of Mons, Belgium*; ²*Singapore Inst. of Manufacturing Technology, Singapore*; ³*MIT, USA*; ⁴*Technion - Israel Inst. of Technology, Israel*. We present a multi-harmonic metasurface-based hard X-ray source in which velocity-matched few-cycle laser pulses lead to output brightness enhancements of over 1000 times compared with the non-optimized case.

FM1Q.7 • 09:30
Parametric-Down Conversion of X-rays into the Optical Regime, Aviad Schori¹, Christina Bömer², Denis Borodin¹, Steve Collins³, Blanka Detlefs⁴, Marco Moretti Sala⁴, Shimon Yudovich¹, Sharon Shwartz¹; ¹*Bar-Ilan Univ., Israel*; ²*European XFEL, Germany*; ³*Diamond Light Source, UK*; ⁴*European Synchrotron Radiation Facility, France*. We observe parametrically down converted x-ray signal photons that correspond to idler photons at optical wavelengths. The results represent a new method for probing valence-electron charges and microscopic optical responses of crystals with atomic-scale resolution.

FM1Q.8 • 09:45
Resonance-Enhanced Harmonics From Air Plasma In The Perturbative Regime, Rostyslav Danylo^{1,2}, Yi Liu^{1,2}, Mingwei Lei⁴, An Zhang⁴, Qingqing Liang¹, Zhengquan Fan¹, Xiang Zhang¹, Hongbing Jiang⁴, Chengyin Wu⁴, Aurélien Houard², Vladimir Tikhonchuk³, Qihuang Gong⁴, André Mysyrowicz²; ¹*Shanghai Key Lab of Modern Optical System, Univ. of Shanghai for Science and Technology, China*; ²*Laboratoire d'Optique Appliquée, ENSTA ParisTech, CNRS, Ecole Polytechnique, Université Paris-Saclay, France*; ³*Centre Lasers Intenses et Applications, Université de Bordeaux, CEA, CNRS UMR, France*; ⁴*State Key Lab for Mesoscopic Physics, Inst. of Modern Optics, Dept. of Physics, Peking Univ., China*. Air pumped by mid-infrared femtosecond pulses gives rise to coherent emission at 391 nm. Based on ellipticity dependence measurement and time-resolved characterization, we attribute this emission to resonance-enhanced harmonics in perturbative regime.

08:30–18:00 OIDA Executive Forum on the Exploding Role of Optics in Sensing, Almaden Ballroom, Hilton San Jose

10:00–10:30 Coffee Break, Concourse Level

Executive Ballroom
210A

Joint

10:30–12:30

JM2A • Symposium on Future Directions in Terahertz Nanoscopy II

Presider: Daniel Mittleman; Brown Univ., USA

JM2A.1 • 10:30 **Invited**

Nanoscale Electron Manipulation Using Phase-controlled THz Near-fields, Jun Takeda¹, Katsumasa Yoshioka¹, Yusuke Arashida¹, Ikufumi Katayama¹; ¹Yokohama National Univ., Japan. By utilizing terahertz scanning tunneling microscopy (THz-STM) with phase-controlled THz near-fields, we could successfully implement the phase-resolved sub-cycle electron dynamics in a tunnel junction.

JM2A.2 • 11:00

Sampling the Terahertz Near-Field in Ultrafast Terahertz Scanning Tunneling Microscopy, Vedran Jelic¹, Peter H. Nguyen¹, Yang Luo¹, Daniel Mildenberger¹, Jesus A. Calzada¹, Tianwu Wang¹, Frank A. Hegmann¹; ¹Univ. of Alberta, Canada. We demonstrate that 800 nm femtosecond pulses focused onto the tip of an ultrafast terahertz scanning tunneling microscope (THz-STM) can be used to sample the terahertz electric near-field at the tip apex.

JM2A.3 • 11:15

Nonlinear Plasmonic Response of Doped GaAs Nanowires Observed in s-SNIM, Denny Lang¹, Leila Balaghi^{1,2}, Emmanouil Dimakis¹, René Hübner¹, Susanne Kehr³, Lukas Eng^{3,2}, Oleksiy Pashkin¹, Stephan Winnerl¹, Harald Schneider¹, Manfred Helm^{1,3}; ¹Helmholtz-Zentrum Dresden-Rossendorf, Germany; ²cfaed - Center for Advancing Electronics Dresden, Germany; ³Inst. of Applied Physics, Technische Universität Dresden, Germany. We present nanoscopic infrared-optical investigations on highly n-type doped GaAs-based nanowires, revealing interesting nonlinear phenomena such as a pronounced redshift of the plasma resonance by the strong THz fields of a free-electron laser.

JM2A.4 • 11:30

Watching a Single Molecular Orbital Move, Dominik Peller¹, Tyler Cocker¹, Ping Yu¹, Jascha Repp¹, Rupert Huber¹; ¹Univ. of Regensburg, Germany. We explore a new arena of ultrafast microscopy capturing the femtosecond motion of an individual molecule. Entering a novel, single-electron tunneling regime with lightwave-driven scanning tunneling microscopy, we resolve femtosecond vibrations of a single molecule with sub-angstrom precision.

Executive Ballroom
210B

CLEO: Science & Innovations

10:30–12:30

SM2B • Novel Nanophotonic Structures and Devices

Presider: Weidong Zhou; Univ. of Texas at Arlington, USA

SM2B.1 • 10:30 **Invited**

Subwavelength Engineered Metamaterial Devices for Integrated Photonics, Pavel Cheben¹; ¹National Research Council Canada, Canada. Subwavelength grating (metamaterial) waveguide devices are becoming established as key building blocks for advanced integrated photonic circuits. In this talk we will present an overview and recent advances of this surging field.

SM2B.2 • 11:00

Separating Valley Excitons in a MoS₂ Monolayer at Room Temperature with a Metasurface, Liuyang Sun¹, Chun-Yuan Wang^{1,2}, Alexandr Krasnok³, Junho Choi¹, Jinwei Shi⁴, Andre' Zepeda¹, Shangji Gwo², Chih-Kang Shih¹, Xiaoqin Li¹; ¹Dept. of Physics, The Univ. of Texas at Austin, USA; ²Dept. of Physics, National Tsing-Hua Univ., Taiwan; ³Dept. of Electrical and Computer Engineering, The Univ. of Texas at Austin, USA; ⁴Dept. of Physics and Applied Optics Beijing Area Major Lab, Beijing Normal Univ., China. We demonstrate that by placing a MoS₂ monolayer onto a metasurface consisting of asymmetric grooves, valley polarized excitons can be spatially separated even at room temperature.

SM2B.3 • 11:15

Broadband Waveguide Integrated Black Phosphorus Modulator for Mid Infrared Application, Ruoming Peng¹, che chen¹, mo li¹; ¹Univ. of Minnesota Twin Cities, USA. The optical absorption in black phosphorus could be modulated by electric field due to the QCfK effect. We extracted the extinction coefficient from free space BP device and showed 5dB modulation would be promising for integrated device.

SM2B.4 • 11:30

Small-signal model for heterogeneous integrated graphene-silicon photonics, Dun Mao¹, Thomas M. Kananen¹, Po Dong², Tingyi Gu¹; ¹Univ. of Delaware, USA; ²Nokia Bell Labs, USA. We demonstrate directly contacted graphene-silicon p-i-n junction for ultrafast response. The two-dimensional junction is parameterized by fitting a small-signal model to RF response. The model extrapolates a maximum bandwidth up to 70 GHz.

Executive Ballroom
210C

10:30–12:30

SM2C • Short Reach Communication

Presider: Xi Chen; Nokia Bell Labs, USA

SM2C.1 • 10:30

2.6-km All-Fiber Orbital Angular Momentum (OAM) Multiplexing Link for Data Center Networks (DCNs) using Mode Select Coupler and Commercial SFP+ Transceivers, Yize Liang¹, Xinzhou Su¹, Yifan Zhao¹, Jie Hu¹, Wei Zhou¹, Yan Luo¹, Zongyuan Huang¹, Shuhui Li¹, Jian Wang¹; ¹Wuhan National-Lab for Optoelectron, China. We report an all-fiber orbital angular momentum (OAM) multiplexing transmission link over 2.6-km conventional OM-3 fiber for data center networks. OAM modes are excited, multiplexed and demultiplexed by commercial SFP+ transceivers and mode selective couplers.

SM2C.2 • 10:45

Intensity-Modulation Direct-Detection OCDM System Based on Digital Up-Conversion, Xing Ouyang¹, Cleitus Antony¹, Jian Zhao¹, Giuseppe Talli¹, Paul Townsend¹; ¹Tyndall National Inst., Ireland. We propose for the first time an OCDM for IM/DD system based on digital up-conversion for access network applications. It exhibits better resilience to impairments to chromatic-dispersion-induced fading and noise than OFDM, with ~5 dB improved receiver sensitivity at 37.5 Gbit/s line rate at 80 km.

SM2C.3 • 11:00

128 x 2 Gb/s WDM PON System with a Single TDM Time Lens Source using an AlGaAs-On-Insulator Waveguide, Pengyu Guan¹, Francesco Da Ros¹, Minhao Pu¹, Mads Lilieholm¹, Yi Zheng¹, Elizaveta Semenova¹, Pierre-Yves Bony¹, Michael Galili¹, Toshio Morioka¹, Kresten Yvind¹, Leif K. Oxenlowe¹; ¹DTU Fotonik, Denmark. We demonstrate a WDM-PON transmitter based on optical Fourier transformation of a single-source TDM-PON. Using a single AlGaAs-on-insulator waveguide, 128 WDM-PON signals at 2 Gb/s are generated and transmitted over a 100-km unamplified link.

SM2C.4 • 11:30

First Demonstration of Sensitivity Improvement using APD Receiver for a 100 G Single Channel PAM4 Link, Hao Huang¹, Enis Akbaba¹, Kejia Li¹, Hatem Akell¹, Tedros Tsegaye¹, Sunil Khatana¹; ¹Lumentum Operations LLC, USA. We demonstrate sensitivity improvement for 100 G single wavelength PAM4 link using an APD receiver. 2.7 dB OMA sensitivity advantage is observed as compared to a PIN receiver using the same TIA

CLEO: Science & Innovations

10:30–12:30

SM2D • Nonlinear Optical Phenomena

President: Amol Choudhary; Univ. of Sydney, Australia

SM2D.1 • 10:30

Power and Bandwidth Scaling of Electro-Optic Frequency Comb using Cascaded Four-Wave Mixing in a loop augmented by Tailored Optical Feedback, Roopa Prakash¹, B S Vikram¹, Nagarjun KP¹, Shankar Kumar Selvaraja¹, V R Sureshpradeepa¹; ¹Centre for Nano Science and Engineering, Indian Inst. of Science, Bangalore, India. We demonstrate power and bandwidth scaling of electro-optic frequency combs using cascaded four-wave mixing in a loop augmented by tailored optical feedback. We achieve ~98 lines in a 25GHz C-band frequency comb spanning 20nm.

SM2D.2 • 10:45

Widely-Tunable Optical Parametric Oscillation in MgF₂ Microresonators, Noel Lito B. Sayson¹, Hoan Pham¹, Karen E. Webb¹, Luke S. Trainor², Harald G. Schwefel², Stephane Coen¹, Miro J. Erkintalo¹, Stuart G. Murdoch¹; ¹The Univ. of Auckland, New Zealand, New Zealand; ²The Univ. of Otago, New Zealand. We present a widely-tunable microresonator optical parametric oscillator based on a high-finesse MgF₂ microdisk. The oscillator operates at low-power with output parametric sidebands discretely tunable from 1166 nm to 2226 nm.

SM2D.3 • 11:00 **Invited**

Generation of Quantum States in Nonlinear Whispering Gallery Resonators, Christoph Marquardt^{1,2}; ¹Max-Planck-Inst Physik des Lichts, Germany; ²Univ. of Erlangen-Nuremberg, Germany. We will review a compact and highly tunable source of photon-pairs and squeezed light based on efficient parametric down conversion in a triply resonant whispering-gallery resonator (WGR) made out of lithium niobate.

SM2D.4 • 11:30

Two-Beam Coupling in Dual-Seeded Four-Wave Mixing, Nicholas Brewer¹, Meng-Chang Wu¹, Bonnie L. Schmittberger¹, Paul D. Lett^{1,2}; ¹Univ. of Maryland, USA; ²National Inst. of Standards and Technology, USA. We observe the two-beam coupling effect in dual-seeded four-wave mixing. The effect adds excess noise to the probe seeds at frequencies below 5 MHz when both probe seed powers are over 10 μW.

CLEO: QELS-Fundamental Science

10:30–12:30

FM2E • Topological Photonics and Lasers

President: Mikael Rechtsman; Pennsylvania State Univ., USA

FM2E.1 • 10:30 **Tutorial**

Topological Photonics, Mordechai Segev¹; ¹Technion, Israel. The fundamentals of the new field of Topological Photonics will be described, along with recent discoveries such as photonic topological insulators in synthetic dimensions, topological protection of quantum states, and topological insulator lasers.



Moti Segev is the Robert J. Shillman Distinguished Professor of Physics, at the Technion, Israel. He received his BSc and PhD from the Technion in 1985 and 1990. After postdoc at Caltech, he joined Princeton as Assistant Professor (1994), becoming Associate Professor in 1997, and Professor in 1999. Subsequently, Moti went back to Israel, and in 2009 was appointed as Distinguished Professor. Moti's interests are mainly in nonlinear optics, photonics, solitons, sub-wavelength imaging, lasers, quantum simulators and quantum electronics, although he finds entertainment in more demanding fields such as basketball and hiking. He has won numerous international and national awards, among them the 2007 Quantum Electronics Prize of the EPS, the 2008 Landau Prize (Israel), the 2009 Max Born Award of the OSA, and the 2014 Arthur Schawlow Prize of the APS. In 2011, he was elected to the Israel Academy of Sciences and Humanities, and in 2015 he was elected to the National Academy of Science of the USA. In 2014 Moti Segev won the Israel Prize in Physics (highest honor in Israel). However, above all his personal achievements, he takes pride in the success of his graduate students and postdocs, among them are currently 19 professors in the USA, Germany, Taiwan, Croatia, Italy, India and Israel, and many holding senior R&D positions in the industry.

FM2E.2 • 11:30

Nonlinear nanophotonics and bound states in the continuum, Luca Carletti², Kirill Koshelev^{1,3}, Costantino De Angelis², Yuri S. Kivshar¹; ¹Nonlinear Physics Centre, Australian National Univ., Australia; ²Dept. of Information Engineering, Univ. of Brescia, Italy; ³ITMO Univ., Russia. We reveal that nonlinear effects at the nanoscale can be enhanced by bound states in the continuum. We demonstrate SHG from subwavelength AlGaAs nanoantennas with record-high conversion efficiency when resonator parameters match the proper conditions.

10:30–12:30

FM2F • Exciton-polaritons and Other Excitation in Semiconductors

President: Vinod Menon; City University of New York, USA

FM2F.1 • 10:30

Giant AC Stark Effect in a Strongly-Coupled Light-Matter System, Dimitry Panna¹, Nadav Landau¹, Shlomi Bouscher¹, Leonid Rybak¹, Shai Tsesses¹, Sebastian Brodbeck², Christian Schneider², Sven Höfling², Alex Hayat¹; ¹Technion-Israeli Inst. of technology, Israel; ²Universität Würzburg, Germany. We present the first experimental observation of a giant non-resonant dynamic Stark effect in strongly coupled microcavity exciton-polaritons – stronger than the Rabi splitting and over an order of magnitude stronger than previous observations.

FM2F.2 • 10:45

Long-Range Transport of Organic Exciton-Polaritons Revealed by Ultrafast Microscopy, Georgi Rozenman^{1,2}, Katherine Akulov^{1,2}, Adina Golombek^{1,2}, Tal Schwartz^{1,2}; ¹School of Chemistry, Tel-Aviv Univ., Israel; ²Center for light-matter interaction, Tel Aviv Univ., Israel. We directly measure micron-scale transport in organic materials, induced by strong coupling and formation of cavity polaritons. Using ultrafast microscopy we follow the motion of polaritons in real-time, finding that their propagation is surprisingly slow.

FM2F.3 • 11:00

Microcavity Exciton Polaritons with Exceptional Points Induced by Polarization-Controllable Ultrastrong Coupling, Weilu Gao¹, Xinwei Li¹, Motoaki Bamba^{2,3}, Junichiro Kono^{1,4}; ¹Dept. of Electrical and Computer Engineering, Rice Univ., USA; ²Dept. of Materials Engineering Science, Osaka Univ., Japan; ³PRESTO, Japan Science and Technology Agency, Japan; ⁴Dept. of Physics and Astronomy, Rice Univ., USA. We demonstrate the existence of exceptional points in the dispersion of microcavity exciton polaritons, originating from the polarization-controlled ultrastrong coupling of 1D excitons in aligned single-chirality single-wall carbon nanotubes with microcavity photons.

FM2F.4 • 11:15

Control of coherently coupled exciton-polaritons in atomic crystals, Xiaoze Liu¹, Wei Bao¹, Quanwei Li¹, Chad Ropp¹, Yuan Wang^{1,2}, Xiang Zhang^{1,2}; ¹Univ. of California Berkeley, USA; ²Materials Sciences Division, Lawrence Berkeley National Lab, USA. We demonstrate, for the first time, controlled polariton emission with hybrid composition in monolayer tungsten disulfide due to robust coherent exciton-photon coupling over a broad temperature range of 110–230 K in a single cavity.

FM2F.5 • 11:30

Ultrafast Near-Field Dynamics of Polariton-Exciton in WSe₂ Slab Waveguides at Room Temperature, Michael Mrejen¹, Lena Yadgarov¹, Assaf Levanon¹, Haim Suchowski¹; ¹Tel Aviv Univ., Israel. We observe the propagation of an exciton-polariton wave in a WSe₂ nanometric slab. We directly visualize with unprecedented spatio-temporal resolution (50 nm, <70 fs) a strikingly slow polaritonic wave with a velocity of ~0.017c.

CLEO: QELS-Fundamental Science

CLEO: Science & Innovations

10:30–12:30

FM2G • Novel Nonphotonic Light Sources

Presider: Mo Mojahedi; Univ. of Toronto, Canada

FM2G.1 • 10:30

Reconstructing the Scattering Matrix of Photonic Systems from Their Quasinormal Modes, Filippo Alpegiani^{1,2}, Nikhil Parappurath², Ewold Verhagen², Laurens K. Kuipers^{1,2}; ¹Dept. of Quantum Nanoscience, TU Delft, Netherlands; ²Center for Nanophotonics, AMOLF, Netherlands. We demonstrate that the scattering matrix of nanophotonic systems is completely determined by their quasinormal modes and present a first-principle expansion technique which is directly applicable to an arbitrary number of modes and input-output channels.

FM2G.2 • 10:45

High harmonic plasmon generation by dressed electrons, Nicholas Rivera¹, Liang Jie Wong², Marin Soljagic¹, Ido Kaminer³; ¹MIT, USA; ²SimTECH, Singapore; ³Technion Israel Inst. of Technology, Israel. We show that high harmonics of highly spatially confined plasmons can be generated via free electrons using light intensities 10^4 – 10^6 times smaller than is required for an equivalent multiphoton effect in free space.

FM2G.3 • 11:00 **Invited**

A New Class of Light Sources Based on Electrically-Driven Optical Antennas, Claire Deeb¹; ¹C2N - CNRS, France. A new class of nanoscopic light sources that are not limited by quantum states, but rather depend on the antenna architecture and the applied bias is proposed. These compact light sources, based on electrically-driven optical nanogap antennas, feature a tunable emission wavelength, a high quantum efficiency, and operate at room temperature.

FM2G.4 • 11:30

Generation of Vortex Beams using a Plasmonic Quadramer Nanocluster, Apurv Chaitanya Nellikka¹, Pawel Wozniak^{2,4}, Peter Banzer^{2,3}, Israel De Leon^{1,4}; ¹School of Engineering and Sciences, Tecnológico de Monterrey, Mexico; ²Max Planck Inst. for the Science of Light, Germany; ³Inst. of Optics, Information and Photonics, Germany; ⁴Max Planck - Univ. of Ottawa Centre for Extreme and Quantum Photonics, Canada. We show that the interaction of tightly-focused circularly-polarized Gaussian beams with a nanoplasmonic quadramer can generate orbital angular momentum beams in the farfield. These quadramer can act like a nano-plate, generating desired vortex order.

10:30–12:30

FM2H • Quantum Optics with Single Atoms

Presider: Virginia Lorenz; U. Illinois at Urbana-Champaign, USA

FM2H.1 • 10:30

Atom-mediated Spontaneous Parametric Down-conversion Using Evanescent Modes in Nonlinear Periodic Waveguides, Sina Saravi^{1,4}, Alexander N. Poddubny^{2,3}, Thomas Pertsch¹, Frank Setzpfandt¹, Andrey A. Sukhorukov²; ¹Abbe Center of Photonics, Friedrich Schiller Univ. Jena, Germany; ²ITMO Univ., Russia; ³Ioffe Inst., Russia; ⁴Nonlinear Physics Centre, Australian National Univ., Australia. Relying on the bandgap modes of a nonlinear periodic waveguide, we propose the concept of atom-mediated spontaneous parametric down-conversion, where photon-pairs are only generated with a single 2-level emitter present, creating a heralded excitation mechanism.

FM2H.2 • 10:45

Towards Quantum-Enabled Flow Cytometry, Ivan A. Burenkov¹, Yu-Hsiang Cheng¹, Sergey Polyakov²; ¹Joint Quantum Inst., NIST and UMD, USA; ²PML, National Inst. of Standards and Technology, USA. We enhance an optical flow cytometer with a photon-number statistics measurement. Our technique allows for an absolute measurement of biomarker concentration and proves sensitivity to a single biomarker (a colloidal quantum dot).

FM2H.3 • 11:00

Purcell-enhanced single-photon emission from an atom in a fiber-based cavity, Deepak Pandey¹, Jose Gallego¹, Tobias Macha¹, Miguel Martinez-Dorantes¹, Wolfgang Alt¹, Dieter Meschede¹; ¹Inst. for Applied Physics, Univ. of Bonn, Germany. We report a sixfold Purcell broadening of a resonance line of a ^{87}Rb atom, by strongly coupling it to a single-sided fiber-based Fabry-Perot cavity which collects 90% of the enhanced single photon emission.

FM2H.4 • 11:15

A Hybrid Nanophotonic-Magnetic Chip-Based Atom Trap, Adam T. Black¹, Marcel W. Pruessner¹, Doewon Park¹, Charles T. Fancher¹, Dmitry Kozak¹, Rita Mahon¹, Mark Bashkansky¹, Fredrik K. Fatemi², Todd Stievater¹; ¹US Naval Research Lab, USA; ²U.S. Army Research Lab, USA. We report progress toward the development of a chip-based cold atom trap based on nanoscale waveguides, which incorporates a fabricated two-wire magnetic trap to assist in transferring laser-cooled atoms to the waveguides.

FM2H.5 • 11:30

Coherent Superradiance by Single Atoms, Kyungwon An¹, Junki Kim¹, Daeho Yang¹, Seunghoon Oh¹; ¹Seoul National Univ., South Korea. We report cavity-mediated coherent single-atom superradiance, where single atoms with predefined correlation traverse a cavity one by one, emitting photons cooperatively with the atoms already gone through the cavity during the cavity field decay time.

10:30–12:30

SM2I • Integrated Detectors

Presider: Zhihong Huang; Hewlett Packard Labs, USA

SM2I.1 • 10:30

High-performance InGaAs/InP photodiodes on silicon using low-temperature wafer-bonding, Qianhuan Yu¹, Ye Wang¹, Linli Xie¹, Souheil Nadri¹, Keye Sun¹, jizhao zang¹, Qinglong Li¹, Robert M. Weikle¹, Andreas Beling¹; ¹Univ. of Virginia, USA. We demonstrate back-illuminated III-V modified uni-traveling carrier photodiodes on silicon using SU-8 as the bonding layer. Responsivity at 1620nm, bandwidth, output RF power and OIP3 are 0.8A/W, 18GHz, 4dBm and 22.5dBm at 9GHz, respectively.

SM2I.2 • 10:45

Germanium Photodetector with Carrier Acceleration, De Zhou¹, Yu Yu¹, Yan Zuo¹, Xinliang Zhang¹; ¹Wuhan National Lab for Optoelectronics, China. We propose and demonstrate a carrier acceleration technique, which alleviates the transit-time delay by introducing a pair of on-chip accelerative electrodes. Equivalent circuit simulation and experimental results validate the improved performance.

SM2I.3 • 11:00

100 GHz Photoconductive Plasmonic Germanium Detector, Ping Ma¹, Yannick Salamin¹, Benedikt Bäuerle¹, Alexandros Emboras¹, Yuriy Fedoryshyn¹, Wolfgang Heni¹, Bojun Cheng¹, Arne Josten¹, Juerg Leuthold¹; ¹Eidgenössische Tech Hochschule Zurich, Switzerland. A compact and high-speed integrated photoconductive plasmonic photodetector is demonstrated. The proposed photodetector features a bandwidth beyond 100 GHz with an internal quantum efficiency of 36 % around 1310 nm.

SM2I.4 • 11:15

Nanostructured Fishnet Silicon Photodetector Pixels as a Fully-Contained Microspectrometer Chip, Jasper Cadusch¹, Jiajun Meng¹, Kenneth B. Crozier^{1,2}; ¹Dept. of Electrical and Electronic Engineering, Univ. of Melbourne, Australia; ²School of Physics, Univ. of Melbourne, Australia. We experimentally demonstrate a microspectrometer comprising twenty silicon photodetector pixels, whose responsivities are engineered via nanostructured fishnet patterns. We computationally reconstruct the spectrum of light that illuminates the chip from the measured pixel photocurrents.

SM2I.5 • 11:30

High-speed Si plasmonic photodetector based on internal photoemission and two-photon absorption, Hidetaka Nishi¹, Tai Tsuchizawa¹, Masaaki Ono¹, Masaya Notomi¹, Hiroshi Fukuda¹, Shinji Matsuo¹; ¹NTT, Japan. A Si-Al plasmonic waveguide enables detection of 1550-nm light by internal photoemission and two-photon absorption. We achieve a differential responsivity of 25 mA/W including 6-dB photonic-plasmonic coupling loss and eye openings with over 40-Gbit/s signals.

CLEO: Applications
& Technology

10:30–12:30

AM2J • Biomedical Imaging

President: Irene Georgakoudi; Tufts Univ., USA

AM2J.1 • 10:30 **Invited**

Interrogating Biological Dynamics in Five Dimensions with Multispectral Optoacoustic Tomography, Daniel Razansky^{2,1}; ¹Inst. for Biological and Medical Imaging, Helmholtz Center Munich, Germany; ²Faculty of Medicine, Technical Univ. of Munich, Germany. The talk focuses on the recent advances in multi-spectral optoacoustic tomography and microscopy, an emerging new technology that attains versatile endogenous and exogenous optical absorption contrast from deep tissues with excellent spatial and temporal resolution not achievable with other bio-imaging modalities.

AM2J.2 • 11:00 **Invited**

Optical Coherence Polarimetry, Martin Villiger¹; ¹Wellman Center for Photomedicine, USA. Tissue polarimetry offers valuable insight into the microstructure and composition of biological samples. Recent developments enable accurate reconstruction of depth-resolved polarization properties, including vectorial birefringence, with fiber and catheter-based polarization sensitive optical coherence tomography.

AM2J.3 • 11:30

Speckle-Free Non-Invasive Imaging with Speckle-Modulating Optical Coherence Tomography, Orly Liba¹, Matthew D. Lew¹, Elliott SoReille¹, Rebecca Dutta¹, Debasish Sen¹, Darius Moshfeghi¹, Steven Chu¹, Adam de la Zerda¹; ¹Stanford Univ., USA. Speckle-Modulating Optical Coherence Tomography (SM-OCT) is a method based on light manipulation for removing speckle noise without significant loss of resolution. By removing speckle noise, SM-OCT reveals small structures in the tissues of living animals.

CLEO: Science & Innovations

10:30–12:30

SM2K • Fiber Sensing and Measurement

President: Stuart Jackson; Macquarie Univ., Australia

SM2K.1 • 10:30

Self-triggered Asynchronous Optical Sampling THz Spectroscopy With a Single Bidirectional Fiber Oscillator, Robert D. Baker², Nezih T. Yardimci¹, Khanh Q. Kieu², Mona Jarrahi¹; ¹Dept. of Electrical & Computer Engineering, Univ. of California Los Angeles, USA; ²College of Optical Sciences, Univ. of Arizona, USA. We report a self-triggered single-laser THz spectroscopy system with no moving parts or locking electronics. The simplicity of this architecture demonstrates the possibility of portable THz spectrometers with smaller size, weight and power requirements.

SM2K.2 • 10:45

Helical Long-period Fiber Grating Written in Polarization-maintaining Fiber by CO₂-laser, Chen Jiang¹, Yunqi Liu¹, Yunhe Zhao¹, Liang Zhang¹, Chengbo Mou¹, Tingyun Wang¹; ¹Shanghai Univ., China. We propose the fabrication of helical long-period fiber grating in polarization-maintaining fiber using CO₂-laser. The polarization and sensing characteristics of the gratings were investigated experimentally.

SM2K.3 • 11:00

Frequency-Shifted Interferometry with Bidirectional Electro-Optic Modulation, Huiyong Guo^{1,2}, Zhou Zheng², Yi Liu^{1,2}, Zeng Xiong², Yiwen Ou², Ciming Zhou², Li Qian^{1,2}; ¹Univ. of Toronto, Canada; ²Wuhan Univ. of Technology, China. Efficient bi-directional electro-optic modulation over 2-8 GHz enables location-resolved and spectral-resolved fiber grating sensor multiplexing, achieving ~3 cm spatial resolution over 1 km sensing range using low-power incoherent broadband source without optical amplification.

SM2K.4 • 11:15

Fiber Fault Detection Using Brillouin Amplification and Two-Photon Absorption Process in Si-APD, Yosuke Tanaka¹, Masaya Nemoto¹; ¹Tokyo Univ of Agriculture and Technology, Japan. We experimentally demonstrate a novel method for detecting weak reflection point in an optical fiber using Brillouin amplification and two-photon absorption process in a Si-avalanche photodiode. Weak reflection after a 20-dB attenuator is successfully observed.

SM2K.5 • 11:30

Broadband Multi-Species CARS in Gas-Filled Hollow-Core Photonic Crystal Fiber, Rinat Tyumeneyev¹, Barbara M. Trabold¹, Luisa Späth¹, Michael H. Frosz¹, Philip S. Russell¹; ¹Max Planck Inst. for Light, Germany. We report CARS in hollow-core gas-filled PCF. The results pave the way to single-shot broadband (>4000 cm⁻¹) CARS under ambient conditions. A detection limit of 300 ppm was reached with 200 mW overall laser power.

10:30–12:30

SM2L • Optical Microwave Generation

President: Tara Fortier; NIST, USA

SM2L.1 • 10:30 **Tutorial**

Synthesizing Ultrastable Radio Waves from Light, William Loh¹; ¹Massachusetts Inst of Tech Lincoln Lab, USA. The continual development of advanced laser sources with ever-increasing spectral purity gives rise to the possibility of using light as the underlying means for the generation of ultrastable radio waves. In this tutorial, we review the techniques by which laser light can be used to synthesize some of the purest forms of RF oscillation known today.



William Loh is technical staff of the Quantum Information and Integrated Nanosystems group at MIT Lincoln Laboratory. He was previously at NIST Boulder and obtained his Ph.D. from MIT. His research focuses on the interplay between photonics and electronics for the generation of precision oscillators in both the optical and RF domains.

SM2L.2 • 11:30

Reduction of Amplitude-to-Phase Conversion in Charge-Compensated Modified Uni-traveling Carrier Photodiodes, Jizhao Zang¹, Xiaojun Xie¹, Qianhuan Yu¹, Keye Sun¹, Andreas Beling¹, Joe C. Campbell¹; ¹Univ. of Virginia, USA. We report optimization of charge-compensated modified untravelling carrier photodiodes to reduce amplitude-to-phase conversion. Phase variation with photocurrent is decreased by up to 5 times.

CLEO: Applications
& Technology

10:30–12:30

AM2M • Material Processing Lasers and
Sensing Technologies

Presider: TBD

AM2M.1 • 10:30 **Invited**

Industrial Applications Enabled by Energetic Next-generation High Average Power Diode-pumped Solid-state Lasers, Craig W. Siders¹; ¹Lawrence Livermore National Lab, USA. We will review the needs for next-generation applications of high-power lasers, compare with state-of-the-art technical performances, and discuss DPSSL architectures, evolved from Inertial Confinement Fusion and Inertial Fusion Energy lasers, to deliver multi-100-kW, PW-class performances.

AM2M.2 • 11:00

Normal dispersion thulium fiber for ultrafast near-2 μm fiber laser, Yuhao Chen¹, Raghuraman Sidharthan¹, Daryl Ho¹, Dingyuan Tang¹, Seongwoo Yoo¹; ¹Nanyang Technological Univ., Singapore. We report fabrication of a normal dispersion thulium-doped fiber with a W-type index profile. The fiber is employed in a ring cavity to demonstrate mode-locked laser near 2 μm with a saturable absorber.

AM2M.3 • 11:15

Single-frequency Mod-hop Free Tunable 3 μm Laser Pumped by a 2W Diode for Isotopic Gas Sensing, Jui-Yu Lai^{2,1}, Hsuan-Tse Guo², Yu-Chen Chen², Cheng-Wei Hsu^{2,1}, Dong-Yi Wu², Ming-Hsien Chou², Shang-Da Yang¹; ¹Inst. of Photonics Technologies, National Tsing Hua Univ., Taiwan; ²HC Photonics Corp., Taiwan. A diode-pumped intracavity optical parametric oscillator is built to demonstrate single-frequency and mod-hop free tuning operation over 20 GHz range around 3 μm . Performance is verified by measuring absorption spectrum of isotopic methane.

AM2M.4 • 11:30

Industrial GHz femtosecond amplified laser source for high efficiency laser ablation, Guillaume Bonamis¹, Konstantin Mishchik¹, Inka Manek-Hoenninger², Clemens Hoenninger¹, Eric Mottay¹; ¹Amplitude Systemes, France; ²Université Bordeaux, France. We present a new high power industrial GHz femtosecond laser. The laser source provides GHz-bursts with up to 100W average power. First ablation tests show a three times increase in ablation efficiency.

CLEO: Science & Innovations

10:30–12:30

SM2N • Fiber and Wave Guide Lasers

Presider: Thomas Spinka; Lawrence Livermore
National Lab, USA

SM2N.1 • 10:30

Self-seeded high-power Mamyshev oscillator, Pavel Sidorenko¹, Walter P. Fu¹, Logan Wright¹, Frank W. Wise¹; ¹School of Applied and Engineering Physics, Cornell, USA. We demonstrate an environmentally stable, self-seeded fiber oscillator based on spectral reshaping and reamplification. The oscillator delivers 140 nJ, linearly chirped pulses with 110 nm spectral bandwidth that can be compressed externally to 65 fs.

SM2N.2 • 10:45

Tunable Deep UV to UV radiation source in plasma-core fiber, Frédéric Delahaye¹, Foued Amrani¹, Benoit Debord^{1,2}, Luis Lemos Alves³, Frédéric Gérôme^{1,2}, Fetah Benabid^{1,2}; ¹GPPMM, XLIM, UMR 7252 Univ. de Limoges, France; ²Glo-Photonics, France; ³Instituto de Plasmas e Fusão Nuclear, Portugal. We report on the first tunable plasma-core fiber based DUV-UV radiation source. The emission spans over 236-450 nm range. The source is a made with microwave-driven plasma-core photonic-crystal-fiber and with a fixed beam output-coupling configuration.

SM2N.3 • 11:00

Mechanically exfoliated Rhenium disulfide onto D-shaped optical fiber for sub-300 fs EDFL mode-locking, David Steinberg¹, Juan Zapata¹, Eunézio Thoroh de Souza¹, Lúcia Saito¹; ¹Universidade Presbiteriana Mackenzie, Brazil. For the first time, we present the ultrashort pulse generation of sub 300-fs mode-locked Erbium doped fiber laser using mechanically exfoliated ReS₂ deposited onto the polished surface of a D-shaped optical fiber.

SM2N.4 • 11:15

All Fiber Laser with the Gain Medium of Tm³⁺ Doped ZBLAN Fiber at 785 nm, Masoud Mollaei^{1,2}, Xiushan Zhu¹, kort Wiersma², Jie zong², arturo Chavez-Pirson², Nasser Peyghambarian¹; ¹Univ. of Arizona, USA; ²NP Photonics, USA. All fiber laser with about 0.5 W continuous-wave single transverse mode obtained with 0.1 %mol 3-m thulium doped fluoride fiber. Ytterbium doped fiber laser at 1125 nm was used as the pump source.

SM2N.5 • 11:30

Hybrid mode-locked 2 μm fiber laser with sub-megahertz repetition rate, Sun Do Lim^{3,1}, Jinhwa Gene³, Seung Kwan Kim^{3,1}, Dong-il Yeom²; ¹Measurement Science, Korea Univ. of Science and Technology, South Korea; ²Physics, Ajou Univ., South Korea; ³Physical Metrology, Korea Research Inst. of Standards and Science, South Korea. We demonstrated a high pulse energy, hybrid mode-locked thulium-doped fiber laser with a repetition rate of 427 kHz, the lowest repetition rate at 2 μm to the best of our knowledge.

10:30–12:30

SM2O • Light Matter Interaction in
Plasmonic & Metamaterials

Presider: Zijie Yan; , USA

SM2O.1 • 10:30

Welding Dynamics of Plasmonic Gold Nanorods Under Femtosecond Laser Excitation, Ryan J. Suess¹, Paul Johns², Jawad Naciri¹, Nicholas Charipar¹, Jacob Fontana¹; ¹U.S. Naval Research Lab, USA; ²American Society for Engineering Education Postdoctoral Fellow, U.S. Naval Research Lab, USA. Suspensions of isolated and molecularly linked gold nanorods are investigated using time-domain spectroscopy. Unique dynamics are observed for each configuration, and indicate laser-induced concatenation of the linked nanorods occurs on picosecond timescales.

SM2O.2 • 10:45

Tuning Optical Matter Chains by Polarization Modulation, Fan Nan¹, Zijie Yan¹; ¹Clarkson Univ., USA. We show that the optical binding interactions among metal nanoparticles can be tuned by modulating the polarization states of light, and the spatio-temporal stability of optical matter can be explored by introducing polarization perturbation.

SM2O.3 • 11:00 **Invited**

Light-Matter Interactions in Hybrid Plasmonic Systems, Stephen K. Gray¹; ¹Argonne National Lab, USA. Models of quantum dots interacting with plasmonic systems show lead to optical transparencies and more general Fano resonances. The approach to the strong coupling is also discussed and, with two or more quantum dots, the possibility of quantum entanglement mediated through the plasmon arises.

SM2O.4 • 11:30

Using Planar Hyperbolic Metamaterials to Enhance Spontaneous Emission in Two-dimensional Transition Metal Dichalcogenides, Chen-An Lin¹, Cheng-Li Yu¹, Hsiang-Ting Lin², Chiao-Yun Chang², Hao-Chung Kuo¹, Min-Hsiung Shih^{1,2}; ¹Dept. of Photonics & Inst. of Electro-Optical Engineering, National Chiao Tung Univ., Taiwan; ²Research Center for Applied Sciences (RCAS), Academia Sinica, Taiwan. We designed one-dimensional planar hyperbolic metamaterials (P-HMMs) which supported high k modes and had better coupling compared to multilayers HMMs. Therefore, spontaneous emission enhancement and the strong coupling between P-HMMs and 2D materials were achieved.

**CLEO: Applications
& Technology**

10:30–12:30
AM2P • A&T Topical Review on Photonics-enabled Quantum Technologies in Transition II
Presider: TBD

AM2P.1 • 10:30 **Invited**
The Challenge of Complexity, Control, and Low Reliability in Quantum Sensors, John H. Burke¹; ¹*US Air Force Research Lab, USA, TBD*

AM2P.2 • 11:00 **Invited**
Photonics for Quantum Sensing, Brenton C. Young¹; ¹*AOSense, Inc., USA. Critical defense and civilian assets currently rely on the exquisite accuracy of atomic clocks. The rapidly expanding capabilities of quantum sensors will soon revolutionize high-accuracy navigation. AOSense is developing robust quantum technology components and systems.*

AM2P.3 • 11:30 **Invited**
Quantum RF Electric-field Sensing with Rydberg-atom Vapors, David Andersen; *Rydberg Technologies LLC, USA.* The emergence of quantum sensor technologies is driving a paradigm shift in modern sensing and measurement instrumentation by enabling fundamentally new detection capabilities and performance metrics that are unmatched by those of traditional sensor technology. Quantum sensing of radio-frequency (RF) electric fields using Rydberg electromagnetically-induced transparency (EIT) in atomic vapors has recently been established as a viable new quantum technology, and rapid progress is being made towards practical measurement devices. In this talk I will provide an overview of the technology, from the underlying measurement method to notable recent advances, including the realization of compact sensing elements capable of broadband RF measurement for MHz to >100 GHz electric fields, and measurement ranges spanning sub-10 mV/m to >10 kV/m (120 dB dynamic range in intensity). Existing challenges in extending RF field sensitivity limits, as well as new measurement capabilities and future directions will be discussed.

**CLEO: QELS-Fundamental
Science**

10:30–12:30
FM2Q • Non-Hermitian and PT Photonics
Presider: Yuan Wang; Univ. of Berkeley, USA

FM2Q.1 • 10:30
Non-Hermiticity-induced flat bands, Hamidreza Ramezani¹; ¹*Univ. of Texas, Rio Grande Valley, USA.* We show increasing the non-Hermiticity in PT-symmetric Lieb lattices results in generating a robust entire flat band at the exceptional point. The obtained flat band is embedded in between dispersive bands and can be considered as BIC [1].

FM2Q.2 • 10:45
Photonic Parity-Time Symmetric Topological Edge States in a Two-Dimensional Lattice, Jiho Noh¹, Wladimir A. Benalcazar², Taylor L. Hughes², Mikael C. Rechtsman¹; ¹*Dept. of Physics, Pennsylvania State Univ., USA;* ²*Dept. of Physics, Univ. of Illinois at Urbana-Champaign, USA.* We propose the realization of topological edge states in two-dimensional non-Hermitian parity-time symmetric structure with C_4 symmetry. Also, we study the bulk topological invariants that explain the topological phase of the non-Hermitian Hamiltonian.

FM2Q.3 • 11:00
Non-Hermitian Topological Photonics, Bo Zhen¹, Hengyun Zhou², Chao Peng², Yoseob Yoon², Chia Wei Hsu³, Keith Nelson², Huitao Shen², Liang Fu², John Joannopoulos², Marin Soljacic²; ¹*Univ. of Pennsylvania, USA;* ²*MIT, USA;* ³*Yale Univ., USA.* We present recent results in developing topological band theory for non-Hermitian systems as well our experimental discovery of two phenomena: bulk Fermi arcs and fractional topological charges in polarization, both arising from paired exceptional points.

FM2Q.4 • 11:30
Effects of non-Hermitian perturbations on Weyl Hamiltonians with arbitrary topological charges, Alexander Cerjan¹, Meng Xiao¹, Luqi Yuan¹, Shanhui Fan¹; ¹*Stanford Univ., USA.* We provide a systematic study of non-Hermitian topologically charged systems, demonstrating that adding an arbitrary non-Hermitian perturbation transforms the Weyl points to one-dimensional exceptional contours, and can yield a topological phase transition.

Joint

CLEO: Science & Innovations

JM2A • Symposium on Future Directions in Terahertz Nanoscopy II—Continued

SM2B • Novel Nanophotonic Structures and Devices—Continued

SM2C • Short Reach Communication—Continued

JM2A.5 • 12:00 **Invited**

Future Directions in Terahertz Scanning Tunneling Microscopy, Frank A. Hegmann¹; ¹Physics, Univ. of Alberta, Canada. Terahertz scanning tunneling microscopy (THz-STM) has recently enabled new approaches for exploring ultrafast dynamics in materials with sub-nanometer spatial resolution. The basic physics of THz-STM, recent developments and future directions will be discussed.

SM2B.5 • 11:45

WDM Si Photonic crystal beam scanner for high-throughput parallel 3D sensing, Hiroyuki Ito¹, Tomoki Tatebe¹, Hiroshi Abe¹, Toshihiko Baba¹; ¹Yokohama National Univ., Japan. We fabricated a WDM optical beam scanner consisting of thermally-controlled Si photonic crystal beam steering devices. We demonstrate the parallel scanning of light beams for the different angular ranges using four multiplexed wavelengths.

SM2C.5 • 11:45

Impact of Phase-Filtering on Optical Spectral Reshaping with Microring Resonators for Directly-Modulated 4-PAM Signals, Oskars Ozolins¹, Francesco Da Ros², Valentina Cristofori², Xiaodan Pang^{3,1}, Aleksejs Udalcovs¹, Richard Schatz², Leif K. Oxenlowe², Sergei Popov³, Gunnar Jacobsen¹, Christophe Peucheret⁴; ¹RISE Acreo AB, Sweden; ²DTU Fotonik, Technical Univ. of Denmark, Denmark; ³KTH Royal Inst. of Technology, Sweden; ⁴Univ Rennes, CNRS, FOTON – UMR 6082, France. We investigate microring resonator (MRRs)-based optical spectral reshaping for directly-modulated 4-PAM signals. The phase-filtering of MRR, and consequent dispersion added to the signal, yields 120% reach increase compared to the 95% of amplitude-only filtering.

SM2C.6 • 12:00

224Gb/s Single Carrier Doubly Differential 2ASK-8PSK System without Carrier Recovery, Tingting Zhang¹, Christian Sánchez Costa¹, Mohammad A. Al-Khateeb¹, Ian Phillips¹, Andrew Ellis¹; ¹Aston Univ., UK. A carrier-recovery-free 224Gb/s dual-polarization doubly differential 16-point constellation (2ASK-8PSK) is experimentally demonstrated for the first time. Utilizing 10-symbol decision feedback in the 2nd differential stage, the penalty with respect to conventional 16QAM is only 4.8dB.

SM2B.6 • 12:15

Transfer printing of photonic nanostructures to silicon integrated circuits, Charalambos Klitis¹, Benoit Guilhabert², John McPhillimy², Stuart May¹, Ning Zhang¹, Michael J. Strain², Marc Sorel¹; ¹Univ. of Glasgow, UK; ²Univ. of Strathclyde, UK. Optical systems require the integration of technologies fabricated on different materials. We use a transfer printing technique to integrate pre-processed III-V, polymer and silicon membrane devices onto passive optical circuits with nano-metric positional accuracy.

12:00–13:00 OSA Optical Material Studies Technical Group Special Talk, Room 230A

12:30–13:30 Lunch Break (on your own)

12:30–15:30 SC362: Cavity Optomechanics: Fundamentals and Applications of Controlling and Measuring Nano- and Micro-mechanical Oscillators with Laser Light

12:30–16:30 SC455: Integrated Photonics for Quantum Information Science and Technology
SC378: Introduction to Ultrafast Optics

13:00–14:00 Social Media 102, Market 1, Hilton San Jose

CLEO: Science & Innovations

SM2D • Nonlinear Optical Phenomena—
Continued

SM2D.5 • 11:45

Using Temperature to Reduce Noise in Quantum Frequency Conversion, Paulina S. Kuo¹, Jason Pelc², Carsten Langrock², M. M. Fejer²; ¹NIST, USA; ²Stanford Univ., USA. A main source of noise in quantum frequency conversion is spontaneous Raman scattering, which can be reduced by lowering the operating temperature. We show reduction in dark count rates that agrees well with theory.

FM2E • Topological Photonics and Lasers—
Continued

FM2E.3 • 11:45

Experimental Realization of Magnetic-free Topological Insulator Laser, Miguel A. Bandres¹, Steffen Wittek², Gal Harari¹, Midya Parto², Jinhan Ren², Mordechai Segev¹, Demetrios N. Christodoulides², Mercedeh Khajavikhan²; ¹Technion, Israel; ²CREOL, USA. We demonstrate a nonmagnetic topological insulator laser exhibiting topologically-protected transport. The topological properties of the system give rise to single mode lasing, robustness against fabrication defects, and higher slope efficiencies compared to its trivial counterpart.

FM2E.4 • 12:00

Nonlinear Unidirectional Topological States in Zigzag Arrays of Bianisotropic Dielectric Nanoparticles, Sergey S. Kruk¹, Alexey Slobozhanyuk¹, Alexander Shorokhov², Daria Smirnova³, Ivan Kravchenko⁴, Alexander N. Poddubny¹, Yuri S. Kivshar¹; ¹Australian National Univ., Australia; ²Moscow State Univ., Russia; ³Russian Academy of Science, Russia; ⁴Oak Ridge National Lab, USA. We generate a third-harmonic field from topological photonic edge states in zigzag arrays of silicon nanoparticles. The effect is unidirectional due to the interplay of nonlinearity and bianisotropic coupling between electric and magnetic Mie resonances.

FM2E.5 • 12:15

Complex Edge-State Phase Transitions in 1D Topological Laser Arrays, Midya Parto¹, Steffen Wittek¹, Hossein Hodaei¹, Gal Harari², Miguel Bandres², Jinhan Ren¹, Mikael Rechtsman³, Mordechai Segev², Demetrios N. Christodoulides¹, Mercedeh Khajavikhan¹; ¹CREOL, USA; ²Technion, Israel; ³Pennsylvania State Univ., USA. We report the first observation of complex lasing transitions in a topological 1D Su-Schrieffer-Heeger active array. The effect of gain saturation nonlinearities and carrier dynamics on the edge-state is investigated both theoretically and experimentally.

CLEO: QELS-Fundamental Science

FM2F • Exciton-polaritons and Other
Excitation in Semiconductions—Continued

FM2F.6 • 11:45

Observation of Rydberg exciton-polaritons in 2D transition metal dichalcogenides, Jie Gu^{1,2}, Alexandra Boehmke¹, Rian Koots¹, Vinod M. Menon^{1,2}; ¹Dept. of Physics, City College of New York, USA; ²Dept. of Physics, The Graduate Center of City Univ. of New York, USA. We report the strong coupling between Rydberg excitons (2S state) and cavity photons in monolayer WSe₂ with the Rabi splitting of ~ 20meV at 77K. Rydberg exciton-polaritons are crucial for solid state quantum non-linear optics.

FM2F.7 • 12:00

Dressed Excitons in Carbon Nanotubes, Kankan Cong¹, G. Timothy Noe II¹, Huaping Liu², Hiromichi Kataura³, Junichiro Kono¹; ¹Electrical and Computer Engineering, Rice Univ., USA; ²Inst. of Physics, Chinese Academy of Sciences, China; ³Nanomaterials Research Inst., National Inst. of Advanced Industrial Science and Technology, Japan. Ultrafast spectroscopy of semiconducting carbon nanotubes reveals transient modifications in the lowest exciton absorption peak. Below-gap excitation induces a blue-shift due to the optical Stark effect, while a Rabi doublet appears under resonant excitation.

FM2F.8 • 12:15

Microscopic Theory for Spatially Local Excitations in Semiconductor Nanostructures, Markus Borsch¹, Eric Martin², Steven T. Cundiff^{2,1}, Mackillo Kira^{1,2}; ¹Dept. of Electrical Engineering and Computer Science, Univ. of Michigan, USA; ²Physics Dept., Univ. of Michigan, USA. We develop a cluster-expansion approach further to include spatially local excitations up to two-particle correlations. Our results show that this level is needed to explain the decreasing excitation-spot size measured in resonantly excited quantum wells.

12:00–13:00 OSA Optical Material Studies Technical Group Special Talk, Room 230A

12:30–13:30 Lunch Break (on your own)

12:30–15:30 SC362: Cavity Optomechanics: Fundamentals and Applications of Controlling and Measuring Nano- and Micro-mechanical Oscillators with Laser Light

12:30–16:30 SC455: Integrated Photonics for Quantum Information Science and Technology
SC378: Introduction to Ultrafast Optics

13:00–14:00 Social Media 102, Market 1, Hilton San Jose

CLEO: QELS-Fundamental Science

CLEO: Science & Innovations

FM2G • Novel Nonphotonic Light Sources—Continued

FM2G.5 • 11:45

Direct Generation of Structured Light in Metallic Nanolaser Arrays, William Hayenga¹, Midya Parto¹, Enrique Sanchez Cristobal¹, Demetrios N. Christodoulides¹, Mercedeh Khajavikhan¹; ¹Univ. of Central Florida, CREOL, USA. The interplay between array geometry and the whispering gallery-like modes of individual nanolasers can lead to the direct generation of structured light in nanoscale. Such nanolaser lattices emitting OAM beams are experimentally demonstrated.

FM2G.6 • 12:00

Plasmonic-assisted perovskite submicron lasers, Sangyeon Cho^{2,1}, Andreas C. Liapis², Seok-Hyun Yun^{2,1}; ¹Harvard-MIT Health Sciences and Technology, MIT, USA; ²Wellman Center for Photomedicine, Massachusetts General Hospital and Harvard Medical School, USA. We synthesized micro- and submicron particles containing CsPbBr₃ nanocrystals and silver nanoparticles. Optically-pumped metal-perovskite particles showed lasing, owing to high gain from perovskite and light confinement by plasmonic scattering.

FM2G.7 • 12:15

MXenes for Plasmonic and Metamaterial Devices, Zhuoxian Wang¹, Krishnakali Chaudhuri¹, Mohamed Alhabeb², Xiangeng Meng¹, Shaimaa Azzam¹, Alexander Kildishev¹, Young L. Kim¹, Vladimir M. Shalaev¹, Yury Gogotsi², Alexandra Boltas-seva¹; ¹Purdue Univ., USA; ²Drexel Univ., USA. We explore the applications of MXenes, a new material class of growing interest, in the area of nanophotonics and plasmonics. A broadband plasmonic metamaterial absorber and a random laser device have thus been demonstrated.

FM2H • Quantum Optics with Single Atoms—Continued

FM2H.6 • 12:00

Quantum State Teleportation from a Single Ion to a Single Photon by Heralded Absorption, Jan Arenskötter¹, Stephan Kucera¹, Matthias Kreis¹, Pascal Eich¹, Philipp Müller¹, Jürgen Eschner¹; ¹Universität des Saarlandes, Germany. Using a high-brightness narrowband source of ⁴⁰Ca⁺-ion-resonant entangled photon pairs at 854 nm, we teleport a qubit from the D_{5/2} Zeeman sub-levels of the ion onto the polarization qubit of a single photon by heralded absorption.

FM2H.7 • 12:15

Ultrafast Rabi and Ramsey measurements with reconfigurable single-atom tweezer traps, Yunheung Song¹, Hanlae Jo¹, Han-gyeol Lee¹, Geol Moon¹, Jaewook Ahn¹; ¹Korean Adv Inst of Science and Tech, South Korea. We simultaneously measured fine-structure state Rabi oscillations of rubidium atoms in reconfigurable single-atom tweezer traps driven by shaped ultrafast laser pulses, which are in a good agreement with the characterized laser beam profiles.

SM2I • Integrated Detectors—Continued

SM2I.6 • 11:45

Quantum dot micro-lasers integrated with photodetectors and optical amplifiers on (001) Si via waveguide coupling, Chen Shang¹, Yating Wan¹, Daehwan Jung¹, Justin Norman¹, MJ Kennedy¹, Di Liang², Chong Zhang², Arthur Gossard¹, John E. Bowers¹; ¹UCSB, USA; ²HPE, USA. We demonstrate the first integrated electrically pumped quantum dot micro-ring lasers epitaxially grown on (001) silicon. On-chip photodetection under continuous-wave excitation was achieved with a low threshold current of 3 mA.

SM2I.7 • 12:00

30-GHz graphene-on-silicon nitride waveguide photodetector, Yun Gao¹, Hon Ki Tsang¹, Chester Shu¹; ¹Chinese Univ. of Hong Kong, Hong Kong. We observed 30 GHz dynamic response and 12 mA/W photoresponsivity in a graphene-on-Si₃N₄ photodetector. Our chemical vapor deposited graphene based photodetector is found to have an operating bandwidth comparable to the best pristine graphene photodetector.

SM2I.8 • 12:15

Mid-infrared waveguide integrated chalcogenide glass on black phosphorus photodetectors, Hongtao Lin¹, Skylar Deckoff-Jones¹, Derek Kita¹, Hanyu Zheng¹, Duanhui Li¹, Wei Zhang², Juejun Hu¹; ¹Dept. of Materials Science & Engineering, MIT, USA; ²Key Lab of Photoelectric Materials and Devices of Zhejiang Province, Ningbo Univ., China. The first mid-infrared waveguide integrated black phosphorus photodetector was fabricated and characterized with a responsivity of 40 mA/W at 2185 nm wavelength.

12:00–13:00 OSA Optical Material Studies Technical Group Special Talk, Room 230A

12:30–13:30 Lunch Break (on your own)

12:30–15:30 SC362: Cavity Optomechanics: Fundamentals and Applications of Controlling and Measuring Nano- and Micro-mechanical Oscillators with Laser Light

12:30–16:30 SC455: Integrated Photonics for Quantum Information Science and Technology
SC378: Introduction to Ultrafast Optics

13:00–14:00 Social Media 102, Market 1, Hilton San Jose

**CLEO: Applications
& Technology**

AM2J • Biomedical Imaging—Continued

AM2J.4 • 11:45

In vivo Images of Rat Peripheral Cornea and Limbus With Full-Field Optical Coherence Tomography, Yu Tung Chen¹, Ting Way Hsu¹, Wei Li Chen², Sheng Lung Huang¹; ¹National Taiwan Univ., Taiwan; ²National Taiwan Univ. Hospital, Taiwan. The anatomical structure of rat's peripheral cornea and limbus were delineated *in vivo* with cellular resolution. The loop-like limbal palisades of Vogt, the blood vessel, and peripheral nerve bundles in the peripheral cornea were identified.

AM2J.5 • 12:00

First Demonstration of *in vivo* Mueller Polarimetric Imaging on Human Uterine Cervix, Jérémy Vizet¹, Jean Rehbindler¹, Stanislas Deby¹, Stéphane Roussel¹, André Nazac², Ranya Soufan³, Catherine Genestie³, Christine Haie-Meder⁴, Hervé Fernandez⁵, François Moreau¹, Angelo Pierangelo¹; ¹LPICM, CNRS, Ecole Polytechnique, France; ²Dept. of Obstetrics and Gynecology, Univ. Hospital Brugmann, Université Libre de Bruxelles, Belgium; ³Service d'anatomie pathologique gynécologique, Institut Gustave Roussy, France; ⁴Service de Curiothérapie, Institut Gustave Roussy, France; ⁵Service de Gynécologie Obstétrique, CHU de Bicêtre AP-HP, France. A very first prototype of a Mueller polarimetric colposcope was used for *in vivo* analysis of the human uterine cervix. We believe this device of great interest to improve early detection of cervical cancer.

AM2J.6 • 12:15

Mirau Based Ti³⁺:Al₂O₃ Spectroscopic Full-Field Optical Coherence Tomographic *in vivo* Skin Imaging, Rajendran Soundararajan¹, Ting-Wei Hsu¹, Manuel C. Delgado¹, Yanding Qin², Sheng Lung Huang¹; ¹National Taiwan Univ., Taiwan; ²Inst. of Robotics and Automatic Information System, Nankai Univ., China. Hysteresis compensated piezoelectric transducer enables precise depth-dependent spectral information extracted from the optical coherence tomography raw interferometric data. Preliminary spectral analysis shows melanin absorptions at ~285.5 THz and ~325 THz.

CLEO: Science & Innovations

SM2K • Fiber Sensing and Measurement—Continued

SM2K.6 • 11:45

Packaged Multi-core Fiber Interferometric Vibration Sensor, Joel Villatoro^{1,2}, J. A. Flores-Bravo³, E. Arrospe¹, O. Arrizabalaga¹, Jose Enrique Antonio-Lopez⁴, J. Zubia¹, A. Schülzgen⁴, Rodrigo Amezcua Correa⁴; ¹Univ. of the Basque Country, Spain; ²IKERBASQUE, Spain; ³Centro de Investigación e Innovación Tecnológica, IPN, Mexico; ⁴CREOL, The College of Optics & Photonics, Univ. of Central Florida, USA. We report on a packaged interferometer built with strongly-coupled multi-core optical fiber (MCF) for vibration sensing. An ultra-miniature test mass induces cyclic bending to the MCF which results in periodic shifts of the interference pattern.

SM2K.7 • 12:00

Single-shot phase measurement and fluctuation analysis of Yb-doped fiber amplifier for nanosecond pulses, Yujun Feng¹, Huaqin Lin¹, Johan Nilsson¹; ¹Univ. of Southampton, UK. We demonstrate temporal-based single-shot ns pulse characterization on a nanosecond 1064-nm Yb-doped fiber amplifier system. Both the amplitude and phase stability of bursts containing 35 1-ns pulses are measured and analyzed.

SM2L • Optical Microwave Generation—Continued

SM2L.3 • 11:45

Controllable Amplitude-to-Phase Distortion in High-Speed Photodiodes under Pulsed Illumination, Josue Davila-Rodriguez¹, Xiaojun Xie², Holly F. Leopardi¹, Tara M. Fortier¹, Scott Diddams¹, Joe Campbell², Franklyn Quinlan¹; ¹NIST, Time and Frequency Division, USA; ²Dept. of Electrical and Computer Engineering, Univ. of Virginia, USA. We show <-50 dB AM-to-PM conversion over a wide photocurrent range in MUTC photodiodes. By controlling the AM-to-PM coefficient minimum, we generate 15 dBm microwave power with 60 dB AM rejection onto the microwave phase.

SM2L.4 • 12:00

High-Dynamic Range Optical to Microwave Comparison with Dual-Output Mach-Zehnder Modulators, Mamoru Endo¹, Tyko D. Shoji¹, Thomas R. Schibli^{1,2}; ¹Dept. of Physics, Univ. of Colorado, USA; ²JILA, NIST, and Univ. of Colorado, USA. A high-dynamic range microwave phase noise measurement has been demonstrated with two dual-output Mach-Zehnder modulators and a cross-spectrum analyzer. The noise floor reaches the thermal limit (-186 dBc/Hz above 10-kHz offset from the carrier).

SM2L.5 • 12:15

Transportable Ultra-low Noise Photonic Microwave Synthesizer, Michele Giunta^{1,2}, Wolfgang Hänsel¹, Maurice Lessing¹, Matthias Lezius¹, Marc Fischer¹, Xiaopeng Xie³, Romain Bouchand², Daniele Nicolodi², Pierre-Alain Tremblin⁴, Giorgio Santarelli⁴, Abhai Joshi⁵, Shubhashish Datta⁵, Yann Le Coq³, Ronald Holzwarth^{1,2}; ¹Menlo Systems GmbH, Germany; ²Max-Planck-Institut für Quantenoptik, Germany; ³LNE-SYRTE, Observatoire de Paris, France; ⁴LP2N, Université de Bordeaux, France; ⁵Discovery Semiconductors Inc., USA. We report on a transportable photonic microwave synthesizer comprising an ultra-stable laser and a ultra-low noise frequency comb. The last acts as a frequency divider, transferring the spectral purity from the optical to microwave domain.

12:00–13:00 OSA Optical Material Studies Technical Group Special Talk, Room 230A

12:30–13:30 Lunch Break (on your own)

12:30–15:30 SC362: Cavity Optomechanics: Fundamentals and Applications of Controlling and Measuring Nano- and Micro-mechanical Oscillators with Laser Light

12:30–16:30 SC455: Integrated Photonics for Quantum Information Science and Technology
SC378: Introduction to Ultrafast Optics

13:00–14:00 Social Media 102, Market 1, Hilton San Jose

Monday, 10:30–12:30

CLEO: Applications
& TechnologyAM2M • Material Processing Lasers and
Sensing Technologies—Continued

AM2M.5 • 11:45

The 5.4 kW output power of the ytterbium-doped tandem-pumping fiber amplifier, Xuejiao Wang¹, Ping Yan¹, Zehui Wang¹, Yusheng Huang¹, Jiading Tian¹, Dan Li¹, Qirong Xiao¹, Mali Gong¹; ¹Tsinghua Univ., China. We present our results of a high-power tandem pumping fiber laser amplifier via optimizing the parameters. A 75 W 1080 nm seed was amplified to 5448 W successfully, along with the efficiency of 91.3%.

AM2M.6 • 12:00

Ultrafast Experimental Analysis and Comparative Performance of a Graphene Saturable Mirror at 2 μ m Wavelength, Gaozhong Wang¹, Werner Blau¹, Kangpeng Wang¹; ¹Trinity College Dublin, Ireland. We conducted systematic comparisons on nonlinear optical properties of graphene and that of commercial semiconductor saturable absorber mirror (SESAM) at 2 μ m. Graphene shows significant advantages over the SESAM, exhibiting 50 times faster relaxation time.

AM2M.7 • 12:15

A triple quantum cascade laser based sulfur species sensor for H₂S, CH₃SH and COS in petrochemical process streams, Harald Moser¹, Johannes P. Waclawek¹, Andreas Genner¹, Christoph Gasser¹, Bernhard Lendl¹; ¹Vienna Univ. of Technology, Austria. Hydrogen sulfide (H₂S), methyl mercaptan (CH₃SH) and carbonyl sulfide (COS) gas detection based on second harmonic wavelength modulation spectroscopy (2F-WMS) using three modulation frequency multiplexed continuous wave quantum cascade lasers (cw QCLs) tunable is presented.

CLEO: Science & Innovations

SM2N • Fiber and Wave Guide Lasers—
Continued

SM2N.6 • 11:45

Highly-Efficient Femtosecond-Laser-Written Waveguide Lasers at ~2 μ m in Monoclinic Tm:MgWO₄, Esrom Kifle³, Pavel Loiko², Javier Vázquez de Aldana⁴, Airán Ródenas^{3,5}, Lizhen Zhang¹, Zhoubin Lin¹, Haifeng Lin¹, Ge Zhang¹, Valentin Petrov⁶, Uwe Griebner⁶, Magdalena Aguiló³, Francesc Diaz³, Xavier Mateos³, Weidong Chen¹; ¹Fujian Inst of Res Structure of Matter, China; ²ITMO Univ., Russia; ³Universitat Rovira i Virgili (URV), Spain; ⁴Univ. of Salamanca, Spain; ⁵Istituto di Fotonica e Nanotecnologie, Italy; ⁶Max Born Inst. for Nonlinear Optics and Short Pulse Spectroscopy, Germany. A channel waveguide (propagation loss: ~0.1 dB/cm) laser femtosecond-laser-written in monoclinic Tm:MgWO₄ generated up to 320 mW slightly above 2 μ m (slope efficiency up to 71%) and vibronic laser emission extending up to ~2.08 μ m.

SM2N.7 • 12:00

Compact bi-direction pumped hybrid double-cladding EYDF amplifier, Xiaolei Bai^{1,2}, Quan Sheng^{1,2}, Shijie Fu^{1,2}, Zhaoxin Xie^{1,2}, Shi Wei^{1,2}, Jianquan Yao^{1,2}; ¹Inst. of Laser and Optoelectronics, School of Precision Instrument and Optoelectronic Engineering, Tianjin Univ., China; ²Key Lab of Optoelectronic Information Science and Technology (Ministry of Education), Tianjin Univ., China. The double-cladding EYDF with different core diameter is connected by an asymmetric cladding light stripper (CLS) to realize bi-direction pumping and increase the loss of counter-propagating light. The experimental results shows that this amplifier has benefit to enhance the SBS threshold.

SM2N.8 • 12:15

Coherent Beam Combining of Seven Femtosecond Chirped-Pulse Fiber Amplifiers Using an Interferometric Phase Measurement Technique, Anke Heilmann¹, Jérémy Le Dortz², Séverine Bellanger¹, Louis Danialt¹, Ihsan Fsaïfes¹, Marie Antier³, Jérôme Bourderionnet², Christian Larat², Eric Lallier², Arnaud Brignon², Eric Durand³, Christophe Simon-Boisson³, Jean-Christophe Chanteloup¹; ¹Ecole Polytechnique, France; ²Thales Research & Technology, France; ³Thales Optronique SAS, France. We report on the coherent combination of seven fiber amplifiers in the femtosecond regime using an interferometric phase measurement technique. A combination efficiency of 54 % and a compressed pulse length of 225 fs were achieved.

SM2O • Light Matter Interaction in
Plasmonic & Metamaterials—Continued

SM2O.5 • 11:45

All-optically reconfigurable chiral metamolecules, Linhan Lin¹, Xiaolei Peng¹, Yuebing Zheng¹; ¹Univ. of Texas at Austin, USA. We experimentally demonstrate the optothermal assembly of various metal and dielectric colloidal nanoparticles into chiral metamolecules with reconfigurability.

SM2O.6 • 12:00

Surface Magnon Polaritons for Strong Magnetic Interactions with Light, Jamison M. Sloan¹, Nicholas Rivera¹, John Joannopoulos¹, Marin Soljacic¹, Ido Kaminer^{2,1}; ¹MIT, USA; ²Electrical Engineering and Solid State Inst., Technion, Israel. We propose using surface magnon polaritons, an electromagnetically dual concept to surface plasmon polaritons, to access normally very inefficient spin-flip and other magnetic spontaneous emission processes.

SM2O.7 • 12:15

Strong coupling of 2D excitons to surface lattice modes of plasmonic crystals, Sriram Guddala¹, Robert Collison^{2,4}, Mandeep Khatoniar^{1,3}, Hussai Bhokari¹, Jacob Trevino^{3,4}, Vinod M. Menon^{1,3}; ¹Dept. of Physics, City College, City Univ. of New York (CUNY), USA; ²Dept. of Chemistry, City College, City Univ. of New York (CUNY), USA; ³PhD program in Physics, Graduate Center, City Univ. of New York (CUNY), USA; ⁴PhD program in Chemistry, Graduate Center, City Univ. of New York (CUNY), USA. We demonstrate strong coupling of 2D excitons in monolayer WSe₂ to surface lattice modes of a plasmonic crystal resulting in large Rabi splitting of 95 meV at room temperature.

12:00–13:00 OSA Optical Material Studies Technical Group Special Talk, Room 230A

12:30–13:30 Lunch Break (on your own)

12:30–15:30 SC362: Cavity Optomechanics: Fundamentals and Applications of Controlling and Measuring Nano- and Micro-mechanical Oscillators with Laser Light

12:30–16:30 SC455: Integrated Photonics for Quantum Information Science and Technology
SC378: Introduction to Ultrafast Optics

13:00–14:00 Social Media 102, Market 1, Hilton San Jose

Marriott
Salon VI

**CLEO: Applications
& Technology**

AM2P • A&T Topical Review on Photonics-enabled Quantum Technologies in Transition II—Continued

AM2P.4 • 12:00 **Invited**
Photonics-enabled Quantum Timing and Navigation at Honeywell, Karl D. Nelson¹; ¹Honeywell Aerospace, USA. Quantum technologies such as atom interferometry and atomic clocks are a promising pathway to more precise navigation. We show several ways in which Honeywell uses photonics as enabling technology for quantum control as we work toward putting devices in the field.

Marriott
Willow Glen

**CLEO: QELS-Fundamental
Science**

FM2Q • Non-Hermitian and PT Photonics—Continued

FM2Q.5 • 11:45
Evanescence fields at the gain/loss interface, Radoslaw Kolkowski¹, Hanan Herzig Sheinfux¹, Shai Tsesses², Anna Kodanev², Meir Orenstein², Guy Bartal², Mordechai Segev¹; ¹Physics Dept., Technion - Israel Inst. of Technology, Israel; ²Electrical Engineering Dept., Technion - Israel Inst. of Technology, Israel. We experimentally investigate the branch-cut transition at Total Internal Reflection from a gain medium, and explore the ability to control the branch-cut selection by evanescent coupling of *PT*-symmetric gain/loss plasmon waves.

FM2Q.6 • 12:00
Exceptional Point Engineered Glass Slide for Microscopic Thermography, Han Zhao¹, Zhaowei Chen², Ruogang Zhao², Liang Feng³; ¹Dept. of Electrical and Systems Engineering, Univ. of Pennsylvania, USA; ²Dept. of Biomedical Engineering, The State Univ. of New York at Buffalo, USA; ³Dept. of Materials Science and Engineering, Univ. of Pennsylvania, USA. We demonstrate a thermosensitive glass slide with enhanced sensitivity by exploiting an optical exceptional point. The non-Hermitian exceptional point of the glass slide creates novel functionality for highly-sensitive thermal mapping compatible with conventional microscope systems.

FM2Q.7 • 12:15
Controllable Photonic Topological Insulating Chain Based on Non-Hermiticity, Kenta Takata^{1,2}, Masaya Notomi^{1,3}; ¹NTT Nanophotonics Center, Japan; ²NTT Basic Research Labs, Japan; ³Tokyo Inst. of Technology, Japan. We determine theoretically a one-dimensional photonic insulating lattice whose bulk topology is controllable simply by tuning gain and loss. The system with four-cavity periods realizes a non-Hermiticity-induced topological transition and reconfigurable midgap topological interface states.

12:00–13:00 OSA Optical Material Studies Technical Group Special Talk, Room 230A

12:30–13:30 Lunch Break (on your own)

12:30–15:30 SC362: Cavity Optomechanics: Fundamentals and Applications of Controlling and Measuring Nano- and Micro-mechanical Oscillators with Laser Light

12:30–16:30 SC455: Integrated Photonics for Quantum Information Science and Technology
SC378: Introduction to Ultrafast Optics

13:00–14:00 Social Media 102, Market 1, Hilton San Jose

Monday, 10:30–12:30

CLEO: Science & Innovations

13:30–15:30

SM3A • Terahertz Nonlinear Spectroscopy*Presider: Andrea Markelz; Univ. at Buffalo, SUNY, USA***SM3A.1 • 13:30**

Development of a THz Pump MeV Ultrafast Electron Diffraction Probe Apparatus, Ben Ofori-Okai¹, Matthias C. Hoffmann¹, Alexander H. Reid¹, Renkai Li¹, Xiaozhe Shen¹, Jie Yang¹, Su Ji Park¹, Ehren Mannenbach¹, R. Keith Jobe¹, Stephen Weathersby¹, Steve Edstrom¹, Wayne Polzin¹, Aaron Lindenberg¹, Siegfried Glenzer¹, Xijie Wang¹; ¹SLAC National Accelerator Lab, USA. We demonstrate a terahertz pump-ultrafast electron diffraction probe apparatus. Using the instrument, we show that intense focused THz pulses can characterize ultrashort electron bunches.

SM3A.2 • 13:45

Scalable setup for efficient terahertz generation using a segmented tilted-pulse-front excitation, László Pálfalvi¹, György Tóth², Levente Tokodi¹, Zsuzsanna Mátrón¹, József A. Fülöp^{2,3}, Gábor Almási^{1,3}, János Hebling^{1,2}; ¹Pecsi Tudományegyetem, Hungary; ²MTA-PTE High-Field Terahertz Research Group, Hungary; ³Szentágotthai Research Centre, Hungary. A nonlinear echelon slab structure is proposed for high-energy THz pulse generation. The most important advantage of the setup is the possibility of using plane parallel nonlinear optical crystal for producing good-quality, symmetric THz beam.

SM3A.3 • 14:00 **Invited**

Terahertz Strong-Field Physics without a Strong Field, Junichiro Kono¹; ¹Rice Univ., USA. We discuss cooperative ultrastrong coupling of two-level systems with THz bosonic fields in two situations: a quantum Hall system interacting with high-Q cavity photons, and Er spins interacting with Fe magnons in ErFeO₃.

SM3A.4 • 14:30

Ultrafast Photocarrier Dynamics in Single-Layer Graphene Driven by Strong Terahertz Pulses, Ali Mousavian¹, Byoungwak Lee^{1,2}, Andrew D. Stickle¹, Yun-Shik Lee¹; ¹Physics, Oregon State Univ., USA; ²Physics & Chemistry, Korea Military Academy, South Korea. Strong THz field enhances the THz transmission of photoexcited graphene, increasing carrier scattering rates. High-field also reduces the relaxation time of the photocarriers by opening up the unoccupied states, while photoexcitation retards the relaxation process.

13:30–15:30

SM3B • Optical Modulators*Presider: Jian Wang; Huazhong Univ of Science and Technology, China***SM3B.1 • 13:30**

Electrically Packaged Silicon-Organic Hybrid Modulator for Communication and Microwave Photonic Applications, Heiner Zwickel¹, Juned N. Kemal¹, Clemens Kieninger¹, Yasar Kutuvantavida¹, Matthias Lauermann^{1,2}, Jonas Rittershofer¹, Rastko Pajković¹, Daniel Lindt¹, Sebastian Randel¹, Wolfgang Freude¹, Christian Koos¹; ¹Karlsruher Institut für Technologie, Germany; ²Vanguard Photonics GmbH, Germany. We demonstrate electrical packaging of a silicon-organic hybrid (SOH) modulator. Gold traces on an Al₂O₃ substrate define the electrical connections to an IQ-modulator having a Pi-voltage of 1.5V. Signal generation up to 128Gbit/s is demonstrated.

SM3B.2 • 14:00

96 Gbit/s PAM-4 Generation using an Electro-Optic Polymer Modulator with High Thermal Stability, Shiyoshi Yokoyama¹, Guo-Wei Lu², Hiroki Miura¹, Feng Qiu¹, Andrew Spring¹; ¹Kyushu Univ., Japan; ²Tokai Univ., Japan. The thermal stability of electro-optic polymer modulators is improved using a common ridge and hybrid silicon-to-polymer waveguide-structure. It reveals excellent thermal resistance at 105°C for ~2,000 hours and generates 56Gbit/s OOK and 96Gbit/s PAM-4 successfully.

SM3B.3 • 14:15

Demonstration of Long-Term Thermal Stability of a Silicon-Organic Hybrid (SOH) Modulator at 85°C, Clemens Kieninger^{1,2}, Yasar Kutuvantavida^{1,2}, Juned N. Kemal¹, Heiner Zwickel¹, Hiroki Miura¹, Sebastian Randel¹, Wolfgang Freude¹, Shiyoshi Yokoyama^{3,4}, Christian Koos^{1,2}; ¹Inst. of Photonics and Quantum Electronics, Karlsruhe Inst. of Technology, Germany; ²Inst. of Microstructure Technology, Karlsruhe Inst. of Technology, Germany; ³Inst. for Materials Chemistry and Engineering, Kyushu Univ., Japan; ⁴Dept. of Molecular and Material Sciences, Kyushu Univ., Japan. We demonstrate highly stable silicon-organic hybrid (SOH) modulators fulfilling Telcordia standards for high-temperature storage. We show error-free 40 Gbit/s signaling with drive voltages of 1.65 V_{pp} using a device stored at 85°C for 2700 hours.

SM3B.4 • 14:30

100-GHz Low Voltage Integrated Lithium Niobate Modulators, Cheng Wang¹, Mian Zhang¹, Xi Chen², Maxime Bertrand^{1,3}, Amirhassan Shams-Ansari^{1,4}, Sethumadhavan Chandrasekhar², Peter Winzer², Marko Loncar¹; ¹Harvard Univ., USA; ²Nokia Bell Labs, USA; ³Univ. of Bordeaux, France; ⁴Dept. of Electrical Engineering and Computer Science, Howard Univ., USA. We demonstrate monolithically integrated lithium niobate modulators consisting of sub-wavelength waveguides and velocity-matched RF transmission lines. We measure an RF V_π as low as 2.3V and an electro-optic bandwidth up to 100 GHz.

13:30–15:30

SM3C • SDM Communications I*Presider: Yikai Su; Shanghai Jiao Tong Univ., China***SM3C.1 • 13:30** **Invited**

Multimode and multicore fiber amplifiers for space-division multiplexed communication systems, Nicolas K. Fontaine¹, Haoshuo Chen¹, Roland Ryf¹, Juan Carlos Alvarado Zacarias², Zeinab Sanjabi Eznaveh², Jose Enrique Antonio-Lopez², Rodrigo Amezcua Correa²; ¹Nokia Bell Labs, USA; ²CREOL, Univ. of Central Florida, USA. Multimode and multi-core fiber amplifiers must amplify all modes with uniform gain in each mode while simultaneously producing large output powers per mode (20-dBm) with low noise figures. Leveraging the dense packing of modes, they can be built with less components than an array of single-mode fiber amplifiers. We will discuss several amplifier designs to improve these metrics.

SM3C.2 • 14:00

System Benefits of Coupled-Core Multicore Fibers with Different Coupling Lengths, Rene-Jean Essiambre¹, Roland Ryf¹, Georg F. Rademacher²; ¹Nokia Corporation, USA; ²Photonic Network System Lab, National Inst. of Information and Communications Technology, Japan. We study the impact of the linear coupling length and the number of cores on the nonlinear benefit of the coupled-core multicore fiber having up to 19 cores. Coupling lengths as short as a few meters improves transmission.

SM3C.3 • 14:15

Accurate modal dispersion measurements using maximally-orthogonal Stokes vectors, Ioannis G. Roudas¹, Jaroslav Kwapisz¹; ¹Montana State Univ.-Bozeman, USA. We propose optimal launch modes minimizing the noise error in the estimation of the fiber modal dispersion vector. For a 20-mode fiber, the SNR is improved by 4 dB compared to conventional mode combinations.

SM3C.4 • 14:30

Experimental Demonstration of 400-Gbit/s Free-Space Mode-Division-Multiplexing by Varying Both Indices when using Four Laguerre-Gaussian Modes or Four Hermite-Gaussian Modes, Kai Pang¹, Haoqian Song¹, Zhe Zhao¹, Runzhou Zhang¹, Hao Song¹, Guodong Xie¹, Long Li¹, Cong Liu¹, Jing Du¹, Andreas F. Molisch¹, Moshe Tur¹, Alan E. Willner¹; ¹University of Southern California, USA. We experimentally demonstrate a 400-Gbit/s mode-division-multiplexed free-space-optical communication link using four Laguerre-Gaussian modes or four Hermite-Gaussian modes, achieving a power penalty < 4 dB. The influence of displacement and rotation on system performance is investigated.

CLEO: Science & Innovations

13:30–15:30

SM3D • Nonlinear Optics in Fibers and Waveguides

President: Michelle Sander; Boston Univ., USA

SM3D.1 • 13:30

Coherent Directional Supercontinuum Generation, Yoshitomo Okawachi¹, Mengjie Yu^{1,2}, Jaime Cardenas³, Xingchen Ji^{3,2}, Michal Lipson³, Alexander L. Gaeta¹; ¹Dept. of Applied Physics and Applied Mathematics, Columbia Univ., USA; ²School of Electrical and Computer Engineering, Cornell Univ., USA; ³Dept. of Electrical Engineering, Columbia Univ., USA. We present a novel approach for coherent, directional supercontinuum and cascaded dispersive waves in dispersion-engineered waveguides. Operating in the normal group-velocity-dispersion regime, we demonstrate octave-spanning spectra generated primarily to one side of the pump.

SM3D.2 • 13:45

Mid-IR Supercontinuum Generation in Ultrafast Laser Inscribed Waveguides, James Morris^{2,1}, Mark Mackenzie¹, Christian R. Petersen³, Ajoy K. Kar¹, Ole . Bang³, Henry T. Bookey²; ¹Inst. of Photonics and Quantum Sciences, Heriot-Watt Univ., UK; ²Fraunhofer Centre for Applied Photonics, UK; ³Dept. of Photonics Engineering, DTU Fotonik, Denmark. Supercontinuum from 2.5 to 6.5 μm has been generated in ULL waveguides pumped with femtosecond pulses centered at 4.6 μm . Dispersion measurements show the zero dispersion wavelength for the waveguides to be around 5.3 μm .

SM3D.3 • 14:00 **Invited**

Nonlinear Multimode Fiber Optics, Stefan Wabnitz^{1,2}, Katarzyna Krupa¹, Daniele Modotto¹, Alessandro Tonello³, Alain Barthelemy³, Vincent Couderc³, Guy Millot⁴; ¹Univ. of Brescia, Italy; ²Istituto Nazionale di Ottica del Consiglio Nazionale delle Ricerche (INO-CNR), Italy; ³XLIM, Universite de Limoges, France; ⁴ICB, Universite de Bourgogne, France. We overview recent advances in the nonlinear optics of multimode optical fibers, including ultrabroadband sideband and supercontinuum generation, Kerr and Raman beam cleanup, modal modulation instabilities, four wave mixing, and second harmonic beam cleaning.

SM3D.4 • 14:30

Adiabatic Broadband Four-Wave Mixing Frequency Conversion in Optical Fibers, Xiaoyue Ding¹, Kerriane Harrington², Logan Wright¹, Wei-Zung Chang¹, Frank W. Wise¹, Tim Birks², Haim Suchowski³, Jeffrey Moses¹; ¹School of Applied and Engineering Physics, Cornell Univ., USA; ²Dept. of Physics, Univ. of Bath, UK; ³Raymond and Beverly Sackler School of Physics and Astronomy, Tel Aviv Univ., Israel. We find adiabatic four-wave mixing in optical fibers allows efficient, near-octave-spanning near-infrared to mid-infrared conversion. Simulations indicate several possible fiber platforms, extending one-to-one broadband frequency conversion both to high-repetition-rate and high-energy applications

CLEO: QELS-Fundamental Science

13:30–15:30

FM3E • Symmetries in Optics

President: Konstantinos Makris; Univ. of Crete, Greece

FM3E.1 • 13:30 **Invited**

Chirality and Nonreciprocity in Optomechanical Resonator Systems, Gaurav Bahl¹; ¹Univ of Illinois at Urbana-Champaign, USA. TBD

FM3E.2 • 14:00

Spin-Glass Behavior in Nonlinear Optical Waves, Davide Pierangeli^{1,2}, Mariano Flammini¹, Andrea Tavani¹, Fabrizio Di Mei¹, Aharon Agranat³, Lifu Zhang², Claudio Conti^{1,4}, Eugenio DelRe^{1,4}; ¹Università di Roma La Sapienza, Italy; ²College of Optoelectronic Engineering, Shenzhen Univ., China; ³Dept. of Applied Physics, Hebrew Univ. of Jerusalem, Israel; ⁴Inst. for Complex Systems, ISC-CNR, Italy. We report the observation of replica symmetry breaking in optical wave propagation, a phenomenon that emerges from the interplay of disorder and nonlinearity and demonstrates a spin-glass phase for light.

FM3E.3 • 14:15

Interaction of Counter-Propagating Light in Microresonators: Theoretical Model and Oscillatory Regimes, Michael T. Woodley^{1,2}, Leonardo Del Bino¹, Jonathan M. Silver¹, Shuangyou Zhang¹, Pascal Del'Haye¹; ¹National Physical Lab, UK; ²Heriot-Watt Univ., UK. An analytical model is presented for the recently observed spontaneous symmetry breaking in nonlinear microresonators. Conditions for the symmetry breaking are obtained, and further models for sensing applications are produced, together with a stability analysis.

FM3E.4 • 14:30 **Invited**

Spatial coherence engineering of lasers for imaging applications, Hui Cao¹; ¹Applied Physics, Yale Univ., USA. We design and build the lasers with low spatial coherence to achieve speckle-free full-field imaging. We further proposed and demonstrated a simple method to switch the spatial coherence of a laser for multimodality biomedical imaging.

13:30–15:30

FM3F • High Harmonic Generation in Solids

President: Mark Sherwin; Univ. of California Santa Barbara, USA

FM3F.1 • 13:30 **Tutorial**

Controlling Electronic Quantum Motion on Subcycle and Atomic Scales, Fabian Langer¹, Stefan Schlauderer¹, Christoph P. Schmid¹, Christoph Lange¹, Dominik Peller¹, Tyler Cocker¹, Jascha Repp¹, Johannes T. Steiner², Ulrich Huttner², Peter G. Hawkins², Stephan W. Koch², Mackillo Kira³, Rupert Huber¹; ¹Univ. of Regensburg, Germany; ²Univ. of Marburg, Germany; ³Univ. of Michigan, USA. Atomically strong multi-terahertz waves drive novel subcycle quantum motions of electrons, generating high-harmonics, dynamical Bloch oscillations, quasiparticle collisions etc. Lightwave-driven scanning tunneling microscopy allows us to take the first femtosecond movie of a single-molecule orbital.



Rupert Huber received his PhD from Technical University Munich in 2004. Following his postdoctoral stay as a Humboldt Fellow at Lawrence Berkeley Laboratory he led an Emmy Noether Junior Group at the University of Konstanz. He has been a full professor of physics at the University of Regensburg since 2010.

FM3F.2 • 14:30

Wannier-Bloch approach to localization in high-order harmonic generation in solids, Alexis A. Chacon^{1,2}; ¹Los Alamos National Lab, USA; ²Quantum Optics Group, Inst. of Photonic Sciences, Spain. High harmonic generation, HHG, in solids is a delocalized process, which is still intensely debated. Here, we develop a model what connects the well-understood HHG in atoms to the delocalization problem of HHG in solids.

CLEO: QELS-Fundamental Science

CLEO: Science & Innovations

13:30–15:30

FM3G • Quantum Sources I

President: Joshua Bienfang; NIST, USA

FM3G.1 • 13:30 **Invited**

Single photons in and out of single molecules, Vahid . Sandoghdar¹; ¹Max-Planck-Inst Physik des Lichts, Germany. I shall present high-fidelity single-photon guns based on single molecules in a planar antenna. In addition, we shall discuss the use of single or handful of photons for efficient linear and nonlinear coupling to molecules.

FM3G.2 • 14:00

All-Optical Frequency Multiplexed Single-Photon Source, Chaitali Joshi^{1,2}, Alessandro Farsi², Stephane Clemmen³, Sven Ramelow⁴, Alexander L. Gaeta²; ¹Cornell Univ., USA; ²Applied Physics and Applied Mathematics, Columbia Univ., USA; ³Universite Libre de Bruxelles, Belgium; ⁴Humboldt-Universitat zu Berlin, Germany. We demonstrate a scalable, low-loss fiber-based frequency multiplexed single-photon source based on efficient parametric frequency conversion. We achieve a record count rate of 4.6×10^4 multiplexed photons with a low $g^{(2)}(0)$ of 0.07.

FM3G.3 • 14:15

Heralded Single-photon Source Based on Intermodal Four-wave Mixing in a Few-mode Fiber, Erik N. Christensen¹, Jesper B. Christensen¹, Søren M. Friis¹, Jacob G. Koefoed¹, Mario A. Castaneda¹, Karsten Rottwitz¹; ¹DTU Fotonik, Denmark. We experimentally demonstrate a heralded single-photon source based on intermodal four-wave mixing in a step-index few-mode fiber, and measure a maximum coincidence-to-accidental ratio of 39, and a $g_s^{(2)}(0)$ of 0.13.

FM3G.4 • 14:30

High-visibility interference between two heralded pure-state photons without spectral filtering, Changchen Chen¹, Jeffrey H. Shapiro¹, Franco N. Wong¹; ¹Electrical Engineering and Computer Science, MIT, USA. We measure 90% visibility in Hong-Ou-Mandel interference between two independent heralded single photons from pulsed spontaneous parametric downconversion with a Gaussian spectral phase-matching profile, and study its dependence on the pump spectral properties

13:30–15:30

FM3H • Chiral and Topological Quantum Optics

President: Tracy Northup; Univ. of Innsbruck, Austria

FM3H.1 • 13:30 **Tutorial**

Chiral Quantum Optics, Peter Lodahl¹; ¹Niels Bohr Inst., Univ. of Copenhagen, Denmark. Nanophotonic waveguides may be engineered to constitute a one-dimensional directional photonic reservoir enabling new ways to control light-matter interaction. We review the underlying physics and potential applications of such chiral quantum interaction.



Peter Lodahl is professor at the Niels Bohr Institute, University of Copenhagen. His research focus on solid-state quantum-information processing with quantum dots. He is the recipient of an ERC consolidator/advanced grant (2010/2015), and serves as Director of the Danish National Research Foundation Center of Excellence for Hybrid Quantum Networks (Hy-Q).

FM3H.2 • 14:30

Unbiased photo-carrier transport in the quantum Hall regime, Olivier Gazzano¹, Bin Cao^{1,2}, Jiuning Hu¹, Tobias Grass¹, Tobias Huber¹, Dave Newell³, Mohammad Hafezi^{1,2}, Glenn S. Solomon³; ¹Joint Quantum Inst., USA; ²Dept. of Physics, Univ. of Maryland, USA; ³National Inst. of Standards and Technology, USA. Photocurrent oscillating with respect to backgate voltage is observed in graphene in the quantum Hall regime. The relationship between edge states chirality and carrier type is explored and interplay among various processes is investigated.

13:30–15:30

SM3I • Optical Phase Arrays

President: Wei Jiang; Rutgers Univ., USA

SM3I.1 • 13:30

Planar-lens Enabled Beam Steering for Chip-scale LIDAR, Josue Lopez¹, Scott Skirlo¹, Dave Kharas², Jamison Sloan¹, Jeffrey Herd², Paul W. Juodawlkis², Marin Soljagic¹, Cheryl Sorace-Agaskar²; ¹MIT, USA; ²MIT Lincoln Lab, USA. A lens-enabled chip-scale beam steering device for LIDAR is theoretically analyzed and experimentally demonstrated with azimuthal, $\Phi_{\text{range}} = 38.8^\circ$, and polar, $\theta_{\text{range}} = 12.0^\circ$, beam-steering. The device allows for beam-steering at low power and low cost.

SM3I.2 • 14:00

Silicon Optical Phased Array with Grating Lobe-Free Beam Formation Over 180 Degree Field of View, Christopher T. Phare^{1,2}, Min Chul Shin¹, Jahnvi Sharma¹, Sohail Ahasan¹, Harish Krishnaswamy¹, Michal Lipson¹; ¹Electrical Engineering, Columbia Univ., USA; ²Electrical and Computer Engineering, Cornell Univ., USA. Using index-mismatched waveguides, we demonstrate the first optical phased array with half-wavelength emitter pitch. We show operation without grating lobes over an entire 180° field of view and beam formation up to 60° off-axis.

SM3I.3 • 14:15

160x160 MEMS Based 2-D Optical Phased Array, Youmin Wang¹, Guangya Zhou², Xiaosheng Zhang¹, Kyoungsik Yu³, Ming C. Wu¹; ¹UC Berkeley, USA; ²National Univ. of Singapore, Singapore; ³Korea Advanced Inst. of Science & Technology, South Korea. We present a two-dimensional ultra large aperture optical phase array (OPA) with 160×160 elements enabled with optical microelectromechanical system (MEMS). The random access beamsteering up to $4.4^\circ \times 4.6^\circ$ scanning range at 1550nm is demonstrated.

SM3I.4 • 14:30

Two-Dimensional Beam Steering Using Slow-Light Waveguide Deflector Array with Optical Gain, Keisuke Kondo¹, Xiaodong Gu¹, Zeuku Ho¹, Akihiro Matsutani², Fumio Koyama¹; ¹Photonics Integration System Research Center, Tokyo Inst. of Technology, Japan; ²Semiconductor and MEMS Processing Center, Tokyo Inst. of Technology, Japan. We demonstrated two-dimensional beam steering by using slow-light deflector array with large angular dispersion of $1.3^\circ/\text{nm}$ and chip gain of 2 dB. We show the steering range of $38^\circ \times 10^\circ$, supporting resolvable point of over 270×7 .

CLEO: QELS-Fundamental
Science

13:30–15:30

FM3J • Imaging and Cloaking in
Metamaterials

Presider: Alexandra Boltasseva; Purdue University, USA

FM3J.1 • 13:30

Dispersion engineering of metasurfaces and its applications in the visible, Wei-Ting Chen¹, Alexander Zhu¹, Jared Sisler^{1,2}, Vyshakh Sanjeev^{1,2}, Eric Lee^{1,2}, Federico Capasso¹; ¹Harvard University, USA; ²Univ. of Waterloo, Canada. We show how to finely tune metasurface dispersion up to 2nd order terms in the visible, using coupled TiO₂ dielectric nano-pillars. We demonstrate white-light imaging and aberration-correction in lenses using these dispersion-engineered metasurfaces.

FM3J.2 • 13:45

Far-field Metamaterial Superlens, Guanghui Yuan¹, Katrine S. Rogers², Edward T. Rogers^{3,4}, Nikolay I. Zheludev^{1,3}; ¹Nanyang Technological Univ., Singapore; ²School of Mathematics and Statistics, The Open Univ., UK; ³Optoelectronics Research Centre and Centre for Photonic Metamaterials, Univ. of Southampton, UK; ⁴Inst. for Life Sciences, Univ. of Southampton, UK. We demonstrate a radically new type of metamaterial 'super-lens' that exploits the phenomenon of super-oscillations, giving a smallest hotspot size of 0.33λ and effective numerical aperture as high as 1.52 in air.

FM3J.3 • 14:00

High NA Silicon Metalens at Visible Wavelengths, Haowen Liang¹, Qiaoling Lin¹, Yin Wang¹, Qian Sun¹, Juntao Li¹; ¹Sun Yat-sen Univ., China. We present a crystalline silicon based metalens with effectively low loss and high-NA in air. This metalens can be further front-immersed in high index liquids, presenting much higher NA and diffraction-limited focusing.

FM3J.4 • 14:15

High De-Magnification Hyperlens, Jingbo Sun¹, Natalia Litchinitser¹; ¹State Univ. of New York at Buffalo, USA. We design and fabricate a hyperlens with a large demagnification of 3.75. We experimentally demonstrate such hyperlens' capability to compress the original patterns with feature size of 300nm down to 80nm using 405nm light.

FM3J.5 • 14:30

Subwavelength imaging of collective modes in silicon nanopillar honeycomb lattices, Siying Peng¹, Nick Schilder², Sophie Meuret², Femius Koenderink², Albert Polman², Harry Atwater¹; ¹Applied physics, California Inst. of Technology, USA; ²Center for Nanophotonics, AMOLF, Netherlands. We report fabrication and direct imaging of silicon Mie resonators with molecular-orbital-like bonding and anti-bonding local photonic density of states, as well as selective excitation of collective Bloch modes at specific frequencies and lattice sites.

CLEO: Science & Innovations

13:30–15:30

SM3K • Billouim Scattering and
Applications

Presider: Siddharth Ramachandran; Boston Univ., USA

SM3K.1 • 13:30

Sensing Outside Polyimide-Coated Fibers Using Guided Acoustic Waves Brillouin Scattering, Hilel Hagai Diamandi¹, Yosef London¹, Gil Bashan¹, Avi Zadok¹; ¹Bar-Ilan Univ., Israel. The spectra of guided acoustic waves Brillouin scattering in polyimide-coated single-mode fibers are characterized analytically and experimentally. The measurements distinguish between water and air outside coated fibers

SM3K.2 • 13:45

Fiber-optic cascaded forward Brillouin scattering seeded by backward SBS, Neisei Hayashi¹, Yosuke Mizuno², Nakamura Kentaro², Sze Y. Set¹, Shinji Yamashita¹; ¹The Univ. of Tokyo, Japan; ²Inst. of Innovative Research, Tokyo Inst. of Technology, Japan. We propose a novel principle for generating the cascaded forward Brillouin scattering (CFBS) using a counter-propagating pump-probe technique. The basic concept of this principle is the use of backward SBS as the seed of CFBS.

SM3K.3 • 14:00

Averaging-free Vector BOTDA assisted by a Reference Probe Lightwave, Nan Guo¹, Tao Gui¹, Chao Jin¹, Liang Wang², Hwa-Yaw Tam¹, Chao Lu¹; ¹The Hong Kong Polytechnic Univ., Hong Kong; ²The Chinese Univ. of Hong Kong, Hong Kong. We propose and experimentally demonstrate an averaging-free vector BOTDA system, which enables both distributed Brillouin gain and Brillouin phase shift detection without trace averaging. A 4m spatial resolution over 18.3 km is realized.

SM3K.4 • 14:15

Performance Enhancement for BOFDA Based on Convexity Extraction Algorithm, Bin Wang¹, Xinyu Fan¹, Zuyuan He¹; ¹Shanghai Jiao Tong Univ., China. We propose an approach to enhance the performance of BOFDA by exploiting the ignored information contained on the measured data. A potentially unlimited dynamic range, as well as a fivefold-enhanced spatial resolution, has been achieved.

SM3K.5 • 14:30

Invited

Brillouin-based Optomechanics, Peter T. Rakich¹, Eric Kittlaus¹, Nils T. Otterstrom¹, Ryan O. Behunin², Zheng Wang³; ¹Yale Univ., USA; ²Physics, Northern Arizona Univ., USA; ³Electrical Engineering, Univ. of Texas at Austin, USA. We use a new class of optomechanical waveguides to we create strong stimulated Brillouin scattering in silicon. Harnessing these interactions, we create Brillouin-based RF-photonic filters, optical amplifiers, and lasers in silicon photonics, and explore new optomechanical phenomena.

13:30–15:30

SM3L • Photonic Frequency References and
Sources

Presider: Laura Sinclair; NIST, USA

SM3L.1 • 13:30

Silicon-photonics-based optical frequency synthesizer, Neetesh Singh¹, Ming Xin¹, Nanxi Li¹, Diedrik Vermeulen¹, Alfonso Ruocco¹, Emir Magden¹, Katia Shtyrkova¹, Patrick Callahan¹, Christopher Baiocco², Erich Ippen¹, Franz X. Kaertner¹, Michael Watts¹; ¹MIT, USA; ²SUNY polytechnic, USA. We demonstrate silicon-photonics-based octave spanning optical frequency combs phase coherently locked to a microwave oscillator for optical frequency synthesis. This system offers capability for precision optical synthesis of CW laser over the entire C-band

SM3L.2 • 13:45

Integrated Pound-Drever-Hall Laser Stabilization System in a Standard CMOS SOI Process, Mohamad Hossein Idjadi¹, Firooz Aflatouni¹; ¹Univ. of Pennsylvania, USA. The first integrated Pound-Drever-Hall stabilization system with an on-chip MZI as the frequency reference is demonstrated which suppresses the frequency noise of semiconductor lasers by more than 25 dB while occupying a 2.38 mm² area.

SM3L.3 • 14:00

Narrow electromagnetically induced transparencies in Rb confined large-core core inner-wall coated Kagome HC-PCFs, Ximeng Zheng¹, Maxime Delgrange¹, Jenny Jouin², Philippe Thomas², Benoit Debord¹, Frédéric Gérôme¹, Fetah Benabid¹; ¹GPPMM group, Xlim Research Inst., France; ²SPCTS UMR CNRS 7315, Centre Européen de la Céramique, France. We compare electromagnetically induced transparencies in large-core anti-relaxation materials inner-wall coatings Kagome HC-PCF with thermal Rb confinement in situ. A minimum transparency linewidth of ~150 KHz in OTS coated fiber was observed.

SM3L.4 • 14:15

In-situ dwell-time measurement of Rb at the inner-wall coated-surface of HC-PCF, Ximeng Zheng¹, Jenny Jouin², Maxime Delgrange¹, Christine Restouin¹, Benoit Debord¹, Philippe Thomas², Frédéric Gérôme¹, Fetah Benabid¹; ¹GPPMM group, Xlim Research Inst., France; ²SPCTS UMR CNRS 7315, Centre Européen de la Céramique, France. We report on a new in-situ technique to measure dwell-time of Rb at coated surfaces of the inner-wall core of Kagome HC-PCFs. Surfaces made with silica, Alumino-silicate, PDMS and OTS were measured using this technique.

SM3L.5 • 14:30

Integration of Acetylene into chip scale photonic circuits for telecom frequency referencing, Roy T. Zektzer¹, Matthew Hummon², Liron Stern², Yefim Barash¹, Noa Mazurski¹, John Kitching², Uriel Levy¹; ¹The Hebrew Univ. of Jerusalem, Israel; ²Time and Frequency Division, National Inst. of Standards and Technology, USA. We experimentally demonstrate a chip-scale integration of photonic waveguides and Acetylene for optical telecom frequency reference. The functionality of the hybrid molecular-photonic chip was demonstrated by locking a telecom laser to a molecular line.

CLEO: QELS-Fundamental
Science

13:30–15:30

FM3M • Sources and Technology for
Attosecond and High-field Physics

President: Kyung-Han Hong; MIT, USA

FM3M.1 • 13:30 **Invited**

Approaching the Attosecond keV X-ray Frontier, Zenghu Chang¹; ¹Univ. of Central Florida, CREOL, USA. We demonstrate the generation of isolated 53-as soft X-ray pulses reaching the water window. Mid-infrared lasers centered at 2.5 to 8 μm are being developed to extend the attosecond X-rays to the keV range.

FM3M.2 • 14:00

High-flux Soft X-ray Source for Time-resolved Probing of Magnetization Dynamics in Rare-earth Ferromagnets, Guangyu Fan¹, Vincent Cardin², Katherine Légaré², Edgar Kaksis¹, Giedrius Andriukaitis¹, Bruno E. Schmidt⁴, Jean-Pierre Wolf⁵, François Légaré², Jan Luning³, Andrius Baltuska¹, Tadas Balciunas^{1,3}; ¹Inst. of Photonics, TU Wien, Austria; ²Institut national de la recherche scientifique, Canada; ³Laboratoire de Chimie Physique Matière et Rayonnement, France; ⁴few-cycle, Inc, Canada; ⁵GAP-Biophotonics, Université de Genève, Switzerland. We present high flux table-top 220eV HHG source driven directly by a <20fs, 10mJ, kHz Yb laser amplifier system. For the first time for a table-top system, measurement of magnetization dynamics at the N-edge at 155 eV with fs temporal resolution was demonstrated.

FM3M.3 • 14:15

Relativistic, Ultra-short Mid-infrared Pulse Generation Through Photon Frequency Downconversion in Plasmas, Zan Nie¹, Chih-Hao Pai¹, Jie Zhang¹, Xiaonan Ning¹, Jianfei Hua¹, Chaojie Zhang², Yipeng Wu¹, Yang Wan¹, Fei Li^{1,2}, Qianqian Su¹, Shuang Liu¹, Yue Ma¹, Yunxiao He¹, Zhi Cheng¹, Wei Lu¹, Hsu-Hsin Chu³, Jyhpyng Wang^{3,4}, Warren B. Mori², Chan Joshi²; ¹Tsinghua Univ., China; ²Univ. of California Los Angeles, USA; ³National Central Univ., Taiwan; ⁴National Taiwan Univ., Taiwan. Generation of relativistically intense mid-infrared pulses in the spectral range of 2–6 μm with 15.5mJ pulse energy by frequency downconversion from a 800nm Ti:sapphire laser is demonstrated. The conversion efficiency is as high as 5.2%.

FM3M.4 • 14:30

Self-channeling of Terawatt-power CO₂ laser Pulses in Air, Sergei . Tochitsky¹, Eric Welch¹, Misha Polyanskiy², Igor Pogorelsky², Paris Panagiotopoulos³, Jerome Moloney³, Chan Joshi¹; ¹Univ. of California Los Angeles, USA; ²Accelerator Test Facility, Brookhaven National Lab, USA; ³College of Optical Sciences, Univ. of Arizona, USA. We report the first observation of Kerr self-focusing of 3 ps TW CO₂ laser pulse in atmosphere. A centimeter diameter, 30m long, 10- μm light channel containing a few Joules of energy is generated and characterized.

CLEO: Science & Innovations

13:30–15:30

SM3N • High Power Lasers

President: Jake Bromage; Univ. of Rochester, USA

SM3N.1 • 13:30

Power scaling end-pumped slab lasers: comparison of Tm:YLF and Tm:LuLF, Antoine Berrou¹, Daniel Morris¹, Oliver J. Collett¹, M J Daniel Esser¹; ¹EPS/IPAQS, Heriot-Watt Univ., UK. High brightness diode stack end-pumped Tm:YLF and Tm:LLF slab lasers are compared under identical pump conditions in continuous-wave regime. A maximum output power of 160 W was obtained for 428 W of pump power.

SM3N.2 • 13:45

Highly stable, 54mJ Yb-InnoSlab laser platform at 0.5kW average power, Bruno E. Schmidt¹, arvid hage², Torsten Mans², François Légaré³, Hans Jakob Wörner⁴; ¹few-cycle Inc, Canada; ²AMPHOS GmbH, Germany; ³INRS-EMT, Canada; ⁴ETH Zürich, Switzerland. We present a compact 1.5ps, 10kHz, 54mJ Yb InnoSlab pump laser with sub-% level power stability and different output ports. 10fs seed pulses are derived via white light generation in bulk followed by subsequent compression.

SM3N.3 • 14:00 **Tutorial**

Current State-of-the-art in High-power Ultrafast Lasers, Peter F. Moulton¹; ¹Massachusetts Inst of Tech Lincoln Lab, USA. We review the technologies, both past, present, and future that are behind operation of PW (10¹⁵ W)-class laser systems, survey the installations worldwide and explain their scientific and practical applications.



Peter F. Moulton is presently a Senior Staff member in the Laser Applications and Applications Group at MIT Lincoln Laboratory. He has worked in the fields of solid state lasers, nonlinear optics, and laser applications since the 1970s in industry and in Government-funded facilities, and recently served on a National Academies study on intense, ultrafast lasers.

13:30–15:30

SM3O • Fundamentals of Laser Material
Processing

President: Carl Liebig; Air Force Research Lab, USA

SM3O.1 • 13:30

Visible Waveguide Lasers Based on Femtosecond Laser Inscribed Cladding Waveguides in Pr:YLF Crystal, Hongliang Liu¹, Minghui Hong², Pengfei Wu¹, Feng Chen³; ¹Nankai Univ., China; ²Dept. of Electrical and Computer Engineering, National Univ. of Singapore, Singapore; ³Dept. of Physics, Shandong Univ., China. Channel waveguide in Pr:YLF has been fabricated by femtosecond laser micromachining. π -polarized waveguide lasers at wavelengths of 605 nm and 720 nm were achieved with a pumping laser at a wavelength of 444.5 nm with a maximum output power of 66 mW with slope efficiencies of 9.5%.

SM3O.2 • 13:45

Femtosecond Laser Writing of Lithium Tantalate Crystals for Waveguide Fabrication, Hongshen Song¹, Chen Cheng¹, Ziqi Li¹, Carolina Romero², Javier Vázquez de Aldana², Feng Chen¹; ¹Shandong Univ., China; ²Universidad de Salamanca, Spain. We report on the direct fabrication of type I and type II waveguides in z-cut lithium tantalate crystal by varying the parameters of femtosecond laser. The waveguiding properties and reflectance spectrum of the fabricated waveguides were also characterized in this work.

SM3O.3 • 14:00 **Invited**

Impacts of Spatio-Temporal Coupling in Ultrashort Laser Pulses on Laser Energy Absorption by Transparent Dielectrics in Bulk Modification Regimes, Nadezhda M. Bulgakova¹, Vladimir P. Zhukov^{1,2}, Selçuk Aktürk³; ¹HiLASE Centre, Inst. of Physics CAS, Czechia; ²Inst. of Computational Technologies SB RAS, Russia; ³Eğercili Mah., Turkey. Sophisticated modeling of propagation of ultrashort laser pulses with spatio-temporal coupling through transparent medium has enabled reproducing the effect of directional asymmetry in direct laser writing and gaining a deep insight into the underlying physics.

SM3O.4 • 14:30

Influence of crystal structure on the ultrafast ionization of cubic wide-band-gap crystals by ultrashort laser pulses, Vitaly Gruzdev¹, Olga Sergaeva¹; ¹Univ. of Missouri-Columbia, USA. The Keldysh photoionization-rate formula is used for arbitrary solids by neglecting their specific structure. By deriving analogs of the Keldysh formula for cubic crystals, we show that the ultrafast ionization and absorption are crystal-specific effects.

CLEO: Applications
& Technology

13:30–15:30

AM3P • Photobiomodulation Therapeutics

Presider: Brian Pryor; LiteCure, USA

AM3P.1 • 13:30 **Invited**

Transcranial Photobiomodulation for Psychiatric Disorders: Past and Future Directions, Paolo Cassano^{1,2}, ¹Massachusetts General Hospital, USA; ²Harvard Medical School, USA. Transcranial photobiomodulation with near-infrared and red radiation for the treatment of psychiatric conditions is reviewed. While still experimental, preliminary data on the use of both laser and LED devices for brain disorders are promising.

AM3P.2 • 14:00

Optimization of Irradiation Conditions for Upconversion Nanoparticle Assisted Photobiomodulation of Neuronal Cells, Sumeyra Tek¹, Brandy A. Vincent¹, Christopher A. Baker¹, Kelly L. Nash¹; ¹Univ. of Texas at San Antonio, USA. Photoluminescence from upconversion nanoparticles provides a nanoplatfrom for desired photochemical effects on neuron cells resulting proliferation and outgrowth with NIR light irradiation, when overcoming the unwanted heating issues by optimizing irradiation conditions.

AM3P.3 • 14:15

Optical Scattering of Structured Light, Romanus Hutchins¹, John Rogers¹, Jonathan Williams¹, Ping Yu¹; ¹Univ. of Missouri, USA. Optical scattering of diffraction-free structured light beams was studied using a diffuser at the far field in a forward direction. Generated Speckle is determined by the phase difference in the structured light beams.

AM3P.4 • 14:30 **Invited**

Annihilation of Methicillin-Resistant *Staphylococcus Aureus* (MRSA) via Photobleaching of Staphyloxanthin, Ji-Xin Cheng¹; ¹Boston Univ., USA. We report a drug-free approach to eliminate MRSA through photobleaching of staphyloxanthin, an indispensable membrane-bound antioxidant. Staphyloxanthin bleaching by low-level blue light eradicates MRSA synergistically with external or internal reactive oxygen species.

CLEO: QELS-Fundamental
Science

13:30–15:30

FM3Q • Topological Photonic Structure

Presider: Liang Feng; Univ. of Pennsylvania, USA

FM3Q.1 • 13:30

Edge-State Dynamics in a One-Dimensional Topological Photonic Lattice of Multiple Quantum Numbers, Zhifeng Zhang¹, Mohammad Teimourpour², Jake Arkinstall¹, Mingsen Pan^{4,5}, Pei Miao^{4,5}, Henning Schomerus³, Ramy El-Ganainy², Liang Feng⁵; ¹Electrical and Systems Engineering, Univ. of Pennsylvania, USA; ²Dept. of Physics and Henes Center for Quantum Phenomena, Michigan Technological Univ., USA; ³Dept. of Physics, Lancaster Univ., UK; ⁴Electrical Engineering, SUNY at Buffalo, USA; ⁵Materials Science and Engineering, Univ. of Pennsylvania, USA. By manipulating the couplings in a flexible topological waveguide lattice with multiple nontrivial dispersion bands, we demonstrate the independent control of edge states associated with different quantum numbers through ultrafast heterodyne measurements.

FM3Q.2 • 13:45

Weyl exceptional ring in a helical waveguide array, Alexander Cerjan¹, Sheng Huang², Kevin P. Chen², Yidong Chong³, Mikael Rechtsman¹; ¹Physics, Pennsylvania State Univ., USA; ²Engineering, Univ. of Pittsburgh, USA; ³Physics, Nanyang Technological Univ., Singapore. We demonstrate the existence of a topologically charged contour consisting entirely of exceptional points in a non-Hermitian helical waveguide array. We observe both protected chiral edge states and the lack of conical diffraction.

FM3Q.3 • 14:00

Topology of Photonic Time-Crystals, Eran Lustig¹, Yonatan Sharabi¹, Mordechai Segev¹; ¹Technion Israel Inst. of Technology, Israel. We introduce topological phases in Photonic Time-Crystals. We show that dispersion bands, which are gapped in momentum, can have non-trivial topology, that affect the propagation of light in the temporal crystal.

FM3Q.4 • 14:15

Creation of Semi-Dirac Photons Through Topological Phase Transitions in Photonic Honeycomb Lattices, Marijana Milicevic¹, Gilles Montambaux², Tomoki Ozawa³, Aristide Lemaître¹, Luc Le Gratiet¹, Isabelle Sagnes¹, Jacqueline Bloch¹, Alberto Amo^{1,4}; ¹Centre de Nanosciences et de Nanotechnologies, CNRS, France; ²Laboratoire de Physique de Solids, Université Paris-Sud, France; ³INO-CNR BEC Center and Dipartimento di Fisica, Università di Trento, Italy; ⁴Université Lille, CNRS, UMR 8523, Physique des Lasers Atomes et Molécules (PhLAM), France. Tuning the band structure of photonic Dirac materials allows engineering novel optical properties. We use photonic honeycomb lattices to tailor semi-Dirac photons that combine zero, finite and infinite effective masses.

FM3Q.5 • 14:30

Exceptional Points of Degeneracy in lossless Periodic Coupled Waveguides, Mohamed Y. Nada¹, Mohamed A. Othman¹, Filippo Capolino¹; ¹UCI, USA. We present general aspects of exceptional points of degeneracy (EPD) of order 2, 3, and 4, that appear also in lossless periodic waveguides. We report unconventional scaling of the quality factor in coupled resonators optical waveguides.

CLEO: Science & Innovations

SM3A • Terahertz Nonlinear Spectroscopy—Continued

SM3A.5 • 14:45

Carrier Multiplication in Bismuth Investigated with Intense THz pump-THz Probe Spectroscopy, Yasuo Minami^{1,2}, Thang Dao^{3,4}, Tadaaki Nagao^{3,4}, Masahiro Kitajima⁵, Jun Takeda², Iku-fumi Katayama²; ¹Tokushima Univ., Japan; ²Yokohama National Univ., Japan; ³International Center for Materials Nanoarchitectonics (WPI-MANA), National Inst. for Materials Science, Japan; ⁴CREST, Japan Science and Technology Agency, Japan; ⁵LxRay Co. Ltd., Japan. By utilizing intense terahertz (THz) pump and THz probe spectroscopy, we revealed the carrier dynamics of a semi-metallic bismuth ultrathin film, originating from the THz-induced electron acceleration and a subsequent carrier multiplication process.

SM3A.6 • 15:00

Hot-Carrier Induced Photoluminescence Enhancement and Quenching in GaAs and InP Driven by Intense THz Pulses, David Purschke¹, Frank A. Hegmann¹; ¹Univ. of Alberta, Canada. We show how intense terahertz pulses can modulate photoluminescence lineshape and efficiency in direct gap semiconductors through hot carrier-enhancement of high energy PL and diffusion induced quenching of low energy photoluminescence. We compare these effects in the GaAs and InP.

SM3A.7 • 15:15

High-field Terahertz Switching of Plasmonic Resonance in Photoexcited Nano Antennas on GaAs, Ali Mousavian¹, Andrew D. Stickel¹, Byoungwhak Lee^{1,2}, Yun-Shik Lee¹; ¹Physics, Oregon State Univ., USA; ²Physics & Chemistry, Korea Military Academy, South Korea. Strong terahertz pulses transiently revive the plasmonic resonance of a nano-antenna-array-patterned GaAs film, which was initially turned off by photoexcitation. The high-field THz effect has potential to ultrafast optical/THz switching in plasmonic devices.

SM3B • Optical Modulators—Continued

SM3B.5 • 14:45

20Gbps silicon lateral MOS-Capacitor electro-optic modulator, Weiwei Zhang¹, Kapil Debnath¹, Graham T. Reed¹, David J. Thomson¹, Ali Z. Khokhar¹, Callum Littlejohns¹, James Byers¹, Lorenzo Mastronardi¹, Muhammad K. Husain¹, Frederic Gardes¹, Shinichi Saito¹; ¹Univ. of Southampton, UK. This work presents an experimental demonstration of a 500 μ m long lateral MOS-capacitor silicon modulator. A modulation efficiency ($V_{\pi/2}$) of 1.53V-cm, moderate modulation speed of 20Gbit-s⁻¹ and extinction ratio of 3.65dB have been obtained.

SM3B.6 • 15:00

Compact, High Extinction Ratio Silicon Mach-Zehnder Modulator with Corrugated Waveguides, Seyedreza Hosseini¹, Aroutin Khachaturian², Mircea Cătuneanu¹, Parham Porsandeh Khial², Reza Fatemi², Ali Hajimiri², Kambiz Jamshidi¹; ¹Technische Universität of Dresden, Germany; ²California Inst. of Technology, USA. An integrated silicon photonic MZM modulator with a slow-wave architecture to reduce V π *L is presented. This structure achieves an 80% enhancement in extinction ratio and has a 14GHz bandwidth with 1mm long modulator arms.

SM3B.7 • 15:15

Silicon Photonic Modulators with Coupled Electrodes, David Patel¹, Mahdi Parvizi², Naim Ben-Hamida², Michel Poulin², Claude Rolland², David V. Plant¹; ¹McGill Univ., Canada; ²Ciena Corporation, Canada. We show that differential signaling with coupled electrodes for silicon photonic modulators increases the electro-optic bandwidth in low-resistive substrates. We also show that high DC resistance of transmission lines negates the benefit of longer modulators.

SM3C • SDM Communications I—Continued

14:00–15:30 **Workshop: Understanding Unconscious Bias, Winchester 1&2, Hilton San Jose**

15:30–16:00 **Coffee Break, Concourse Level**

16:00–17:30 **Workshop: Understanding Unconscious Bias Workshop, Winchester 1&2, Hilton San Jose**

CLEO: Science & Innovations

SM3D • Nonlinear Optics in Fibers and Waveguides—Continued

SM3D.5 • 14:45

Octave-Spanning Supercontinuum Generation in a Dispersion Managed Tapered Crystalline Silicon Core Fiber, Haonan Ren¹, Li Shen², Joseph Campling¹, Antoine Runge¹, Ozan Aktas¹, Thomas Hawkins², Peter Horak¹, John Ballato³, Ursula J. Gibson⁴, Anna C. Peacock¹; ¹Univ. of Southampton, UK; ²Wuhan National Lab for Optoelectronics, Huazhong Univ. of Science and Technology, China; ³School of Materials Science and Engineering, Clemson Univ., USA; ⁴Dept. of Physics, Norwegian Univ. of Science and Technology, Norway. We demonstrate octave spanning supercontinuum from 1.35 μm to 3 μm generated in a tapered crystalline silicon core fiber pumped at 2.4 mm using a femtosecond OPO.

SM3D.6 • 15:00

Kerr and Raman beam cleanup with supercontinuum generation in multimode microstructure fiber, Richard Dupiol¹, Katarzyna Krupa², Alessandro Tonello¹, Marc Fabert¹, Daniele Modotto², Stefan Wabnitz^{2,3}, Guy Millot³, Vincent Couderc¹; ¹Université de Limoges, France; ²Università degli Studi di Brescia, Italy; ³Université Bourgogne Franche-Comté, France. We experimentally study the interplay of Kerr and Raman beam cleanup in multimode air-silica microstructure optical fiber. The interplay of modal four-wave mixing and Raman scattering leads to high-brightness multimode supercontinuum.

SM3D.7 • 15:15

Light Sources based on Multiple Solitons in Segmented Fiber Amplifiers, Francisco R. Arteaga-Sierra¹, Aku J. Antikainen¹, Govind P. Agrawal¹; ¹Univ. of Rochester, USA. We propose a novel technique to design light sources producing multiple frequency channels potentially applicable in wavelength-division multiplexing networks. The sources are based on spectral interference of solitons generated in non-uniform fiber amplifiers.

CLEO: QELS-Fundamental Science

FM3E • Symmetries in Optics—Continued

FM3E.5 • 15:00

Optical time reversal from time-dependent Epsilon-Near-Zero media, Vincenzo Bruno¹, Stefano Vezzoli¹, Daniele Faccio^{1,2}, Marcello Ferrara¹, Vladimir M. Shalaev³, Clayton DeVault⁴, Matteo Clerici⁵, Alexandra Boltasseva³, Thomas Roger¹, Audrius Dubietis⁶; ¹Inst. of Photonics and Quantum Sciences, Heriot Watt Univ., UK; ²School of Physics and Astronomy, Univ. of Glasgow, UK; ³School of Electrical and Computer Engineering and Birk Nanotechnology Center, Purdue Univ., USA; ⁴Dept. of Physics and Astronomy and Birk Nanotechnology Center, Purdue Univ., USA; ⁵School of Engineering, Univ. of Glasgow, UK; ⁶Dept. of Quantum Electronics, Vilnius Univ., Lithuania. We provide an efficient surface time-reversal of the incident electric field in an ENZ material producing both phase-conjugated and negative refracted beams. The results obtained exploiting degenerate four-wave mixing show an efficiency conversion over 200%.

FM3E.6 • 15:15

Suppressing laser instabilities with microcavities exhibiting chaotic ray dynamics, Stefan Bittner¹, Hasan Yilmaz¹, Kyungduk Kim¹, Xiaonan Hu², Yongquan Zeng², Qijie Wang², Stefano Guazzotti³, Sang Soon Oh³, Ortwin Hess³, Hui Cao¹; ¹Dept. of Applied Physics, Yale Univ., USA; ²School of Electrical and Electronic Engineering, Nanyang Technological Univ., Singapore; ³Dept. of Physics, Imperial College, UK. We demonstrate experimentally that spatio-temporal instabilities of broad-area semiconductor lasers are strongly suppressed in microcavities with chaotic ray-dynamics. This stabilization of lasing dynamics is attributed to the modifications of the nonlinear interaction of the lasing modes.

FM3F • High Harmonic Generation in Solids—Continued

FM3F.3 • 14:45

High-Order Harmonic Generation from Solids Dressed by an Intense Terahertz Field, Haoyu Huang^{1,2}, Liwei Song^{1,3}, Nicolas Tancogne-Dejean^{4,5}, Nicolai Klemke^{1,2}, Angel Rubio^{4,5}, Franz X. Kaertner^{1,2}, Oliver Muecke^{1,6}; ¹Center for Free-Electron Laser Science CFEL, Deutsches Elektronen Synchrotron, Germany; ²Dept. of Physics, Univ. of Hamburg, Germany; ³State Key Lab of High Field Laser Physics, Shanghai Inst. of Optics and Fine Mechanics, Chinese Academy of Sciences, China; ⁴Max Planck Inst. for the Structure and Dynamics of Matter, Germany; ⁵European Theoretical Spectroscopy Facility (ETSF), Germany; ⁶The Hamburg Centre for Ultrafast Imaging CUI, Univ. of Hamburg, Germany. Using an intense transient terahertz electric field, we observe the appearance of even-order harmonics in silicon, normally forbidden in centrosymmetric crystals. Reducing the symmetry via transient dressing might lead to ultrafast symmetry control in crystals.

FM3F.4 • 15:00

Polarimetry of THz High-Order Sideband Generation: Towards a Measurement of Berry Curvature, Darren C. Valovcin^{1,2}, Qile Wu³, Shawn Mack¹, Arthur Gossard⁵, Ren-Bao Liu³, Mark S. Sherwin^{1,2}; ¹Physics, Univ. of California, Santa Barbara, USA; ²Inst. for Terahertz Science and Technology, Univ. of California, Santa Barbara, USA; ³Physics, The Chinese Univ. of Hong Kong, China; ⁴U.S. Naval Research Lab, USA; ⁵Materials, Univ. of California, Santa Barbara, USA. Dynamical birefringence associated with high-order sideband generation is a consequence of Berry curvature of the driven material. Careful polarimetry opens the way to measuring Berry curvature in solids.

FM3F.5 • 15:15

Emission Phase of Extreme Ultraviolet High Harmonics from Bulk Crystals, Jian Lu¹, Yongsing You¹, David Reis^{1,2}, Shambhu Ghimire¹; ¹SLAC National Accelerator Lab, USA; ²Dept. of Applied Physics, Stanford Univ., USA. We measure the chirp in extreme ultraviolet high-harmonics from bulk MgO crystals pumped by strong near-infrared pulses using the two-color approach. By performing measurements in both reflection and transmission we separate propagation effects.

14:00–15:30 Workshop: Understanding Unconscious Bias, Winchester 1&2, Hilton San Jose

15:30–16:00 Coffee Break, Concourse Level

16:00–17:30 Workshop: Understanding Unconscious Bias Workshop, Winchester 1&2, Hilton San Jose

CLEO: QELS-Fundamental Science

CLEO: Science & Innovations

FM3G • Quantum Sources I—Continued

FM3G.5 • 14:45

Effective $\chi^{(2)}$ in a Rb-Filled Hollow-Core Photonic Bandgap Fiber for Coherent Photon Conversion, Yun Zhao², Prathamesh Donvalkar¹, Chaitali Joshi¹, Bok Young Kim², Alexander L. Gaeta²; ¹*School of Applied and Engineering Physics, Cornell Univ., USA*; ²*Dept. of Applied Physics and Applied Mathematics, Columbia Univ., USA*. We demonstrate a large effective $\chi^{(2)}$ in a rubidium-filled photonic bandgap fiber by an spontaneous parametric down conversion process. This system can be used for the coherent photon conversion scheme in quantum information processing.

FM3G.6 • 15:00

Adiabatic Fock State Generation Scheme Using Kerr Nonlinearity, Ryotatsu Yanagimoto¹, Tatsuhiro Onodera¹, Edwin Ng¹, Hideo Mabuchi¹; ¹*Stanford Univ., USA*. We introduce a theoretical scheme for generating Fock states using a Kerr cavity by adiabatic variation of the detuning and driving field amplitude. We perform numerical calculations to determine requirements for experimental feasibility.

FM3G.7 • 15:15

Energy-entangled W-state in optical fiber, Bin Fang¹, Matteo Menotti², Marco Liscidini², John E. Sipe³, Virginia O. Lorenz¹; ¹*Physics, Univ. of Illinois at Urbana-Champaign, USA*; ²*Physics, Univ. of Pavia, Italy*; ³*Physics, Univ. of Toronto, Canada*. We demonstrate progress towards the generation of an energy-entangled three-photon W-state via spontaneous four-wave mixing in a polarization-maintaining fiber and characterize it by reduced density matrix tomography, without involving frequency conversion.

FM3H • Chiral and Topological Quantum Optics—Continued

FM3H.3 • 14:45

Pancharatnam-Berry Phase in a Condensate of Indirect Excitons, Jason R. Leonard¹, Alexander High¹, Aaron Hammack¹, Michael Fogler¹, Leonid Butov¹, Kenneth Campman², Arthur Gossard²; ¹*Dept. of Physics, Univ. of California at San Diego, USA*; ²*Materials Dept., Univ. of California at Santa Barbara, USA*. We report on the observation of the Pancharatnam-Berry phase in a condensate of indirect excitons realized in a GaAs coupled quantum well structure. Our measurements indicate long range coherent spin transport.

FM3H.4 • 15:00

Scattering of Coherent Pulses from Quantum-Optical Systems, Kevin Fischer¹, Rahul Trivedi¹, Vinay Ramasesh², Irfan Siddiqi², Jelena Vuckovic¹; ¹*Ginzton Lab, Stanford Univ., USA*; ²*Dept. of Physics, Univ. of California, USA*. We develop a new computational tool and framework for characterizing the scattering of photons by energy-nonconserving Hamiltonians into unidirectional (chiral) waveguides, e.g., with coherent pulsed excitation. We demonstrate this approach for two prototypical quantum systems.

FM3H.5 • 15:15

Quantum Čerenkov radiation in weakly and strongly-coupled regimes, Charles Roques-Carnes¹, Nicholas Rivera², John Joannopoulos², Marin Soljacic^{1,2}, Ido Kaminer^{1,3}; ¹*Research Lab of Electronics, MIT, USA*; ²*Dept. of Physics, MIT, USA*; ³*Technion – Israel Inst. of Technology, Dept. of Electrical Engineering, Israel*. We present the time-dependent quantum electrodynamic theory of Čerenkov radiation, which reveals orders of magnitude corrections to the decay rate from the conventional theory, as well as significant modifications to the well-established Čerenkov dispersion relation.

SM3I • Optical Phase Arrays—Continued

SM3I.5 • 14:45

Bessel-Beam-Generating Integrated Optical Phased Arrays, Jelena Notaros¹, Christopher V. Poulton¹, Matthew Byrd¹, Manan Raval¹, Michael Watts¹; ¹*MIT, USA*. Generation of Bessel beams using integrated optical phased arrays is proposed and experimentally demonstrated for the first time. A quasi-Bessel beam with a ~14mm Bessel length and ~30 μ m FWHM is generated using a splitter-tree-based architecture.

SM3I.6 • 15:00

3D integrated silicon photonic unit cell with vertical U-turn for scalable optical phase array, Yu Zhang¹, Kuanping Shang¹, Yi-Chun Ling¹, S. J. Ben Yoo¹; ¹*Univ. of California, Davis, USA*. We demonstrate a 3D integrated silicon photonic unit cell with ultra-compact vertical U-turn interlayer coupling structures. A 120-channel folded single tile optical phase array with 2mm pitch is fabricated as a proof-of-concept.

SM3I.7 • 15:15

Broadband Imaging and Wireless Communication with an Optical Phased Array, Steven Spector¹, Benjamin F. Lane¹, Michael Watts², Lucas Benney¹, Justin Delva¹, Alva Hare¹, Adam Kelsey¹, Jacqueline Mlynarczyk^{1,3}, Ehsan Hosseini², Christopher Poulton², J. P. Laine¹; ¹*Charles Stark Draper Lab, USA*; ²*Analog Photonics, USA*; ³*Carderock Division, Naval Surface War Center, USA*. An optical phased array designed for broadband applications has been demonstrated. Using this architecture, imaging under natural light conditions and free space optical communications at a data rate of 10 Gbps have been achieved.

14:00–15:30 **Workshop: Understanding Unconscious Bias, Winchester 1&2, Hilton San Jose**

15:30–16:00 **Coffee Break, Concourse Level**

16:00–17:30 **Workshop: Understanding Unconscious Bias Workshop, Winchester 1&2, Hilton San Jose**

**CLEO: QELS-Fundamental
Science**

CLEO: Science & Innovations

**FM3J • Imaging and Cloaking in
Metamaterials—Continued**

FM3J.6 • 14:45

"Invisible" Nanotextured Substrates for Quantum Optics and Microscopy, Andreas C. Liapis¹, Charles T. Black², Seok-Hyun Yun¹; ¹Wellman Center for Photomedicine, Massachusetts General Hospital, USA; ²Center for Functional Nanomaterials, Brookhaven National Lab, USA. We show that nanotextured antireflective metasurfaces, fabricated by block copolymer self-assembly, can be used to suppress the influence of the substrate in quantum optical experiments and microscopy.

FM3J.7 • 15:00

Infrared Invisibility Cloak Using Rolled Metamaterial Film, Tomo Amemiya¹, Satoshi Yamasaki¹, Toru Kanazawa¹, Zhichen Gu¹, Daisuke Inoue¹, Atsushi Ishikawa², Nobu Nishiyama¹, takuo tanaka³, Tatsuhiro Urakami⁴, Shigehisa Arai¹; ¹Tokyo Inst. of Technology, Japan; ²Okayama Univ., Japan; ³RIKEN, Japan; ⁴Mitsui Chemicals, Inc., Japan. We propose and demonstrate a method of making an infrared (~60 THz) invisibility cloaking device by simply rolling a metamaterial film around an object that we want to hide.

FM3J.8 • 15:15

Electrically Controllable Reconfiguration of Terahertz Meta-Atoms into Meta-Molecules, Hyunseung Jung¹, Jaemok Koo², Wonwoo Lee³, Moon Sung Kang², Hojin Lee^{1,3}; ¹School of Electronic Engineering, Soongsil Univ., South Korea; ²Dept. of Chemical Engineering, Soongsil Univ., South Korea; ³Dept. of Information Communication, Materials, and Chemistry Convergence Technology, Soongsil Univ., South Korea. We report structural methodology for electrically switchable terahertz metamaterials between atom- and molecule-states by using limited conductance variation of graphene bridges. Based on experimental verification, we confirmed 39% of wide resonance tuning of terahertz metamaterials.

**SM3K • Brillouin Scattering and
Applications—Continued**

SM3K.6 • 15:00

Suppression of Stimulated Brillouin Scattering using Off-Axis Twisted Core Fiber, Kazi S. Abedin¹, Raja Ahmad¹, Kenneth Feder¹, David DiGiovanni¹; ¹OFS Labs, USA. We propose a method of suppression of Brillouin scattering by using offset-core twisted fiber. A 5.2dB increase in SBS-threshold is observed by offsetting the fiber-core from center by 35µm and winding in a 45mm spool.

SM3K.7 • 15:15

Opto-Mechanical Time-Domain Reflectometry: Distributed Sensing Outside the Cladding of Standard Fiber, Gil Bashan¹, Hilel Hagai Diamandi¹, Yosef London¹, Eyal Preter¹, Avi Zadok¹; ¹Bar-Ilan Univ., Israel. Distributed sensing of liquids outside the cladding of standard, unmodified fiber is demonstrated, with 3 km range and 100 m resolution. Guided light remains confined to the core. Measurements rely on fiber opto-mechanics.

**SM3L • Photonic Frequency References and
Sources—Continued**

SM3L.6 • 14:45

Characterization of Large-Area Crystalline Coatings for Next-Generation Gravitational Wave Detectors, Garrett Cole^{1,2}, Christoph Deustch², David Follman¹, Paula Heu¹, Tobias Zederbauer², Ashish Rai², Dominic Bachmann², Alexander von Finck³, Sven Schröder³, Philip Koch⁴, Harald Lück⁴; ¹Crystalline Mirror Solutions LLC, USA; ²Crystalline Mirror Solutions GmbH, Austria; ³Fraunhofer Inst. for Applied Optics and Precision Engineering (IOF), Germany; ⁴Albert Einstein Inst. (AEI) Hannover, Max Planck Inst. for Gravitational Physics, Germany. Through in-depth optical characterization including thickness uniformity and optical scatter measurements, we demonstrate that large-area crystalline coatings are a promising alternative to ion-beam sputtered multilayers for low-noise mirrors employed in next-generation gravitational wave detectors.

SM3L.7 • 15:00

All-Fiber Delay Line-Based Repetition-Rate Stabilization, Dohyeon Kwon¹, Jungwon Kim¹; ¹Korea Advanced Inst of Science & Tech, South Korea. We demonstrate all-fiber repetition-rate stabilization method with 10⁻¹⁴-level frequency instability and 1-fs-level integrated timing jitter over 1-s using all-fiber Michelson interferometer with compactly packaged 10-km-long fiber delay.

14:00–15:30 Workshop: Understanding Unconscious Bias, Winchester 1&2, Hilton San Jose

15:30–16:00 Coffee Break, Concourse Level

16:00–17:30 Workshop: Understanding Unconscious Bias Workshop, Winchester 1&2, Hilton San Jose

CLEO: QELS-Fundamental
Science

CLEO: Science & Innovations

FM3M • Sources and Technology for
Attosecond and High-field Physics—
Continued

FM3M.5 • 14:45

Efficient laser wakefield acceleration by using mid-infrared pulses, Eiji J. Takahashi¹, Shin-ichi Masuda², Eisuke Miura², ¹RIKEN, Japan; ²National Inst. of Advanced Industrial Science and Technology, Japan; ³Photon Pioneers Center, Osaka Univ., Japan. We discuss the feasibility of an efficient laser wakefield acceleration driven by an intense mid-infrared pulse. TW-scale 1.5 μm laser pulse can improve the number of accelerated electrons as an order of magnitude, compared with that driven by a Ti:sapphire laser (0.8 μm).

FM3M.6 • 15:00

Ultrafast electron emission assisted by grating-coupled propagating surface plasmons in the mid-IR range, Kengo Takeuchi¹, Tomoya Mizuno¹, Keisuke Kaneshima¹, Nobuhisa Ishii¹, Teruto Kanai¹, Jiro Itatani¹; ¹The Univ. of Tokyo, Japan. We observed propagating-surface plasmon-assisted photoemission from a grating irradiated by mid-IR laser pulses by measuring the incidence-angle dependence of photoelectron spectra. The results reveal that emitted electrons are further accelerated by locally enhanced electric fields.

FM3M.7 • 15:15

Phase-Dependent Dielectric Laser Acceleration of 99keV Electrons with Symmetrically Driven Silicon Dual Pillar Gratings, Kenneth Leedle¹, Dylan S. Black¹, Yu Miao¹, Karel Urbanek¹, Andrew Ceballos¹, Huiyang Deng¹, James S. Harris¹, Olav Solgaard¹, Robert L. Byer¹; ¹Stanford Univ., USA. We present phase-dependent laser acceleration and deflection of electrons using a symmetrically driven silicon dual pillar grating. We demonstrate cosh accelerator modes and sinh deflecting modes at gradients of 200 MeV/m over 15 μm distance.

SM3N • High Power Lasers—Continued

SM3N.4 • 15:00

High Average Power Type II Frequency Doubling with a Predelay for Pulse Compression and Peak Intensity Enhancement, Sabrina Beyer^{1,2}, Christian Grebing¹, Marcel Schultze¹, Knut Michel¹, Georg Korn³, Thomas Metzger¹; ¹TRUMPF Scientific Lasers GmbH + Co. KG, Germany; ²Fakultät für angewandte Naturwissenschaften und Mechatronik, Munich Univ. of Applied Sciences, Germany; ³Extreme Light Infrastructure - Beamlines, Czechia. Fourfold pulse compression from 840 fs to 192 fs was obtained by inserting a time delay between the ordinary- and extraordinary fundamental pulses prior to type II frequency doubling in a BBO crystal. Despite a conversion efficiency of 26 %, an increase of peak power of nearly 20 % was achieved.

SM3N.5 • 15:15

Gas Lens in kW-Class Thin-Disk Lasers, Francesco Saltarelli¹, Andreas Diebold¹, Ivan J. Graumann¹, Clara J. Saraceno^{1,2}, Christopher R. Phillips¹, Ursula Keller¹; ¹ETH Zurich, Switzerland; ²Ruhr Universität Bochum, Germany. We measured, for the first time, a gas-lens effect accounting for 33% of the total disk thermal lensing. By helium flooding the laser, we obtain optimal beam quality ($M^2 < 1.10$) over a 70% broader power range.

SM3O • Fundamentals of Laser Material
Processing—Continued

SM3O.5 • 14:45

Femtosecond laser writing of 3-D NLO structures in glass, Carl M. Liebig¹, Jonathan Goldstein¹, Sean McDanniel^{1,2}, Douglas Krein^{1,3}, Gary Cook¹; ¹Air Force Research Lab, USA; ²Leidos, USA; ³General Dynamics Information Technology, USA. Femtosecond laser pulses have been used to precipitate 3-dimensional LiNbO₃ structures in supersaturated glass for second harmonic generation (SHG). Measurements for successive layers with parallel and antiparallel optical axes compare nicely with calculations.

SM3O.6 • 15:00

Wavelength-Dependent Coupling of Ultrafast Filaments to Solid Surfaces, Milos Burger¹, Patrick J. Skrodzki¹, John Nees¹, Igor Jovanovic¹; ¹Univ. of Michigan, USA. Plasma luminosity is essential to remote sensing based on filament-induced breakdown spectroscopy. We present the measurements of dynamics and luminosity of plasmas produced by 0.4, 0.8, and 2.0 μm filaments on a copper surface.

SM3O.7 • 15:15

Time-Resolved Surface Microscopy of Single Shot Few-Cycle Pulse Laser Ablation of Single Layer TiO₂ Thin Films, Noah Talisa¹, Kevin Werner¹, Enam Chowdhury¹; ¹Dept. of Physics, The Ohio State Univ., USA. The dynamics of the few-cycle pulse laser ablation process of a single layer TiO₂ thin film from 6 ps to 1.1 ns after a single pulse hits the surface are studied using time-resolved microscopy.

14:00–15:30 Workshop: Understanding Unconscious Bias, Winchester 1&2, Hilton San Jose

15:30–16:00 Coffee Break, Concourse Level

16:00–17:30 Workshop: Understanding Unconscious Bias Workshop, Winchester 1&2, Hilton San Jose

**CLEO: Applications
& Technology**

**AM3P • Photobiomodulation
Therapeutics—Continued**

AM3P.5 • 15:00

Controlled laser biochemistry in room-temperature polar liquids by ultrashort laser pulses, Vitaly Gruzdev¹, Dmitry Korkin², Brian P. Mooney^{3,4}, Jesper F. Havelund^{5,6}, Ian M. Møller⁶, Jay J. Thelen³; ¹Univ. of Missouri-Columbia, USA; ²Dept. of Computer Science, Bioinformatics and Computational Biology Program, Worcester Polytechnic Inst., USA; ³Dept. of Biochemistry, Bond Life Sciences Center, Univ. of Missouri, USA; ⁴Charles W Gehrke Proteomics Center, Univ. of Missouri, USA; ⁵Dept. of Biochemistry and Molecular Biology, Univ. of Southern Denmark, Denmark; ⁶Dept. of Molecular Biology and Genetics, Aarhus Univ., Denmark. Traditional laser methods to control chemical modifications of biomolecules are not applicable under biologically relevant conditions. We report controlled modifications of peptides and insulin by femtosecond laser in water, methanol, and acetonitrile at room temperature.

AM3P.6 • 15:15

Parylene Photonic Waveguide Arrays: A Platform for Implantable Optical Neural Implants, Jay W. Reddy¹; ¹Carnegie Mellon Univ., USA. We demonstrate compact, low-loss (<10dB/cm) Parylene-C waveguide arrays in a flexible, biocompatible, polymer platform suitable for implantable neural probes. Mechanisms of optical loss are investigated and fabrication techniques to reduce propagation loss in the optical waveguides are presented.

**CLEO: QELS-Fundamental
Science**

**FM3Q • Topological Photonic Structure—
Continued**

FM3Q.6 • 14:45

All-dielectric topological meta-optics, Alexey Slobozhanyuk^{2,4}, Alena Shchelokova^{3,4}, Xiang Ni^{1,2}, Hossein Mousavi^{5,1}, Daria Smirnova¹, Pavel Belov³, Andrea Alù⁵, Yuri S. Kivshar⁴, Alexander B. Khanikaev^{1,2}; ¹City College of New York, USA; ²Physics, Graduate Center of CUNY, USA; ³ITMO Univ., Russia; ⁴Australian National Univ., Australia; ⁵Univ. of Texas at Austin, USA. We present all-dielectric resonant structured surfaces for the realization of lossless compact photonic topological metadevices. We demonstrate spin-Hall effect of light for spin-polarized topological edge states through proof-of-concept near-field spectroscopy measurements.

FM3Q.7 • 15:00

Photonic Chern insulator through homogenization of an array of particles, Meng Xiao¹, Shanhui Fan¹; ¹Stanford University, USA. We propose a route towards creating a photonic Chern insulator through homogenization with an array of gyromagnetic cylinders. The non-trivial band topology of such a system is independent of the lattice structure.

FM3Q.8 • 15:15

Experiments on topological nodal chains, Qinghui Yan^{1,2}, Rongjuan Liu¹, Zhongbo Yan³, Boyuan Liu¹, Hongsheng Chen², Zhong Wang³, Ling Lu¹; ¹Inst. of Physics, Chinese Academy of Sciences, China; ²College of Information Science and Electronic Engineering, Zhejiang Univ., China; ³Inst. for Advanced Study, Tsinghua Univ., China. We theoretically predicted and experimentally verified mirror-protected nodal chains in a metallic-mesh photonic crystal at microwave frequencies. The bulk states were detected through angle-resolved transmission and drumhead surface states were mapped out by field scans.

14:00–15:30 Workshop: Understanding Unconscious Bias, Winchester 1&2, Hilton San Jose

15:30–16:00 Coffee Break, Concourse Level

16:00–17:30 Workshop: Understanding Unconscious Bias Workshop, Winchester 1&2, Hilton San Jose

CLEO: Science & Innovations

16:00–18:00

SM4A • THz High-field Generation and Detection*Presider: Masayoshi Tonouchi; Osaka Univ., Japan***SM4A.1 • 16:00****Terahertz Wave Generation from Water**, Yiwen E¹, Qi Jin¹, Kaia Williams¹, Jianming Dai², Xicheng Zhang^{1,3}; ¹Univ. of Rochester, USA; ²Tianjin Univ. of China, China; ³Capital Normal Univ., China. Terahertz wave generation from liquid water has been experimentally demonstrated by focusing femtosecond laser pulses in a water film, which shows that the signal of water is 1.8 times stronger than that of ambient air.**SM4A.2 • 16:15****Simultaneous generation and compression of broadband terahertz pulses in aperiodically poled crystals**, Koustuban Ravi^{1,2}, Franz X. Kaertner^{1,2}; ¹MIT, USA; ²Ultrafast optics and X-rays, Center for free electron lasers, Germany. A non-uniform sequence of pump pulses in aperiodically poled crystals is shown to generate transform-limited terahertz pulses. Tunable, compressed terahertz output with single-stage conversion efficiencies > 2% and pulse energies ~ 10 mJ are predicted.**SM4A.3 • 16:30****Scaling of THz Generation in DSTMS to High Repetition Rates**, Matthew Windeler^{1,2}, Katalin Mecsek¹, Franz Tavella¹, Matthias C. Hoffmann¹; ¹SLAC National Accelerator Lab, USA; ²Queen's Univ., Canada. We explore the scaling behavior of THz generation through optical rectification in DSTMS as function of repetition rate from 100 Hz to 200 kHz. We observe a strong drop-off in conversion efficiency above 10 kHz.**SM4A.4 • 16:45****Segmented Terahertz driven device for ultrashort electron acceleration, compression, focusing and streaking**, Dongfang Zhang¹, Arya Fallahi¹, Michael Hemmer¹, Xiaojun Wu¹, Moein Fakhari¹, Yi Hua¹, Huseyin Cankaya¹, Anne-Laure Calendron¹, Luis Zapata¹, Nicholas H. Matlis¹, Franz X. Kaertner¹; ¹DESY, Germany. We present a novel THz based device (STEAM) capable of performing multiple high-field operations of electron acceleration, compression, focusing and streaking.**SM4A.5 • 17:00** **Invited****Developments and Applications of Echelon-Based Single-shot Terahertz Spectroscopy**, Ben Ofori-Okai¹, Stephanie Teo², Christopher Werley³, Zhijiang Chen¹, Samuel Teitelbaum¹, Brandon Russell⁴, Matthias C. Hoffmann¹, Keith Nelson⁵, Siegfried Glenzer¹; ¹SLAC National Accelerator Lab, USA; ²Samsung Research America, USA; ³Q-State Biosciences, USA; ⁴Univ. of Michigan, USA; ⁵MIT, USA. We present recent advancements in echelon-based single-shot terahertz spectroscopy for broadband spectroscopic applications. We also apply an echelon-based scheme to study photo-induced changes in correlated electron materials and warm dense matter.

16:00–18:00

SM4B • Microrings and Novel Modulation Schemes*Presider: Jian Wang; Huazhong Univ of Science and Technology, China***SM4B.1 • 16:00****Plasmonic-Organic Hybrid Modulators for Optical Interconnects beyond 100G/A**, Benedikt Baeuerle¹, Wolfgang Heni¹, Yuriy Fedoryshyn¹, Arne Josten¹, Christian Haffner¹, Tatsuhiko Watanabe¹, Delwin Elder², Larry R. Dalton², Juerg Leuthold¹; ¹ETH Zurich, Switzerland; ²Dept. of Chemistry, Univ. of Washington, USA. We demonstrate a short-reach optical interconnect with a plasmonic intensity modulator. Data rates of 56 GbD PAM-4 and 100 GbD PAM-2 are demonstrated over 2 km and 1 km SSMF with direct detection at 1544nm.**SM4B.2 • 16:15****Electrically-Induced Absorption Silicon-Plasmonic Modulator with 70nm Bandwidth**, Qian Gao¹, Erwen Li¹, Alan X. Wang¹; ¹Oregon State Univ., USA. We present an electrically-induced absorption plasmonic modulator on silicon platform with 3 μm length using transparent conductive oxide filled in Au slot waveguide. We experimentally demonstrated 1.5dB/μm extinction ratio over 70 nm optical bandwidth**SM4B.3 • 16:30** **Invited****Commercializing Silicon Microring Resonators: Technical Challenges and Potential Solutions**, Po Dong¹, Argishti Melikyan¹, Kwangwoong Kim¹; ¹Nokia Bell Labs, USA. Silicon microrings can find a wide range of applications in optical interconnects and communications. However, their resonant wavelengths are extremely sensitive to fabrication and temperature variations. Here we review possible solutions to address this challenge.**SM4B.4 • 17:00****112-Gb/s PAM-4 using Integrated Germanium on Silicon Franz Keldysh Modulator**, Yeyu Tong¹, Zhouyi Hu², Xinru Wu¹, Jie Liu¹, Chun-Kit Chan², Chester Shu¹, Hon Ki Tsang¹; ¹Electronic Engineering, Chinese Univ. of Hong Kong, Hong Kong; ²Information Engineering, The Chinese Univ. of Hong Kong, Hong Kong. We evaluate the performance of 112-Gb/s PAM-4 modulation using integrated Ge electro-absorption modulator operating at 1622 nm. Using pre-equalization with 25-GHz bandwidth limited arbitrary waveform generator we demonstrated 1-km fiber transmission at 112 Gb/s.

16:00–18:00

SM4C • SDM Communication II*Presider: Ryan Scott; Keysight Technologies Inc., USA***SM4C.1 • 16:00****Crosstalk Impact on a 535 Tb/s 172 km Transmission Using a Homogeneous 19-Core Multicore Fiber**, Ruben S. Luis¹, Benjamin Puttnam¹, Georg F. Rademacher¹, Yoshinari Awaji¹, Naoya Wada¹; ¹National Inst Information & Comm Tech, Japan. We show the feasibility of a 535 Tb/s link with 172.8 km reach using a 19-core homogeneous multicore fiber. We demonstrate an average crosstalk penalty below 0.25 dB, enabling the transmission of 115x24.5 Gbaud PDM-64QAM signals in the C-band.**SM4C.2 • 16:15****Modal Crosstalk Mitigated IM/DD Mode-Multiplexed Transmission Based on Pilot Assisted Least Square Algorithm**, Qianwu Zhang¹, Fang Wang¹, Qingqing Huang¹, Haoshuo Chen², Nicolas K. Fontaine², Roland Ryff², Minwen Liu¹, Jian Chen¹; ¹Shanghai Univ., China; ²Nokia Bell Labs, USA. We experimentally demonstrate mode group crosstalk mitigation in IM/DD mode-multiplexed OFDM transmission using pilot assisted least square algorithm. Transmission performance is improved through mitigating the crosstalk between the LP01 and LP11 mode groups.**SM4C.3 • 16:30** **Invited****Modulation and Detection for Multicore Superchannels with Correlated Phase Noise**, Erik Agrell¹, Arni Alfredsson¹, Benjamin Puttnam², Ruben S. Luis², Georg Rademacher², Magnus Karlsson³; ¹Dept. of Electrical Engineering, Chalmers Univ. of Technology, Sweden; ²Photonic Network System Lab, NICT, Japan; ³Dept. of Microtechnology and Nanoscience, Chalmers Univ. of Technology, Sweden. SDM fibers offer new opportunities and challenges for joint transmitter and receiver processing. We review multidimensional modulation and detection theory, describe algorithms for phase tracking and detection over spatial superchannels, and present some experimental results.**SM4C.4 • 17:00****7x149 Gbit/s PAM4 Transmission over 1 km Multicore Fiber for Short-Reach Optical Interconnects**, Oskars Ozolins¹, Xiaodan Pang^{2,1}, Aleksajs Udalcovs¹, Rui Lin^{2,3}, Joris Van Kerrebrouck⁴, Lin Gan³, Lu Zhang², Ming Tang³, Songnian Fu³, Richard Schatz², Urban Westergren², Gunnar Jacobsen¹, Deming Liu³, Weijun Tong⁵, Guy Torfs⁴, Johan Bauwelinck⁴, Jiajia Chen², Sergei Popov², Xin Yin⁴; ¹RISE Acreo AB, Sweden; ²KTH Royal Inst. of Technology, Sweden; ³Huazhong Univ. of Science and Technology, China; ⁴INTEC, Ghent Univ. – imec, Belgium; ⁵Yangtze Optical fiber and Cable Joint Stock Limited Company, China. We transmit 80 Gbaud/1-core PAM4 signal enabled by 1.55 μm EML over 1 km 7-core fiber. The solution achieves single-wavelength and single-fiber 1.04 Tbit/s post-FEC transmission enhancing bandwidth-density for short-reach optical interconnects.

CLEO: Science & Innovations

16:00–18:00

SM4D • Optical Metrology Nonlinear Optical Technologies

Presider: Michelle Sander; Boston Univ., USA

SM4D.1 • 16:00

High rep-rate, high peak power 1450 nm laser source based on optical parametric chirped pulse amplification, Pengfei Wang¹, Yanyan Li¹, Wenkai Li¹, Hongpeng Su¹, Yujie Peng¹, Yuxin Leng¹; ¹Shanghai Inst of Optics & Fine Mechanics, China. A high peak power 1450 nm laser running at 100 Hz repetition rate is demonstrated, which can generate 20 mJ energy and 60 fs pulse width, corresponding the peak power of more than 0.3 terawatt.

SM4D.2 • 16:15

Near-infrared to visible upconversion detection for active imaging using a broadband pump laser, Romain Demur^{1,2}, Arnaud Grisard¹, Eric Lallier¹, Loic Morvan¹, Luc Leviandier¹, Nicolas Treps², Claude Fabre²; ¹Thales Research & Technology, France; ²Laboratoire Kastler Brossel, UPMC-Sorbonne universités, CNRS, ENS-PSL Research Univ., France. Upconversion is a promising technique to increase sensitivity in active imaging. Using a pump laser with a wide spectrum, the field of view of our system is increased with image characteristics compatible with practical applications.

SM4D.3 • 16:30

Intra-cavity Self-illuminated Image Up-conversion System based on SHG in a Compact Laser, Adrian J. Torregrosa¹, Haroldo Maestre¹, María Luisa Rico², Juan Capmany¹; ¹Universidad Miguel Hernandez, Spain; ²Universidad de Alicante, Spain. We present a compact laser for image up-conversion from infrared to visible based on intra-cavity SHG by type-II phase matching. Reflected images by Nd³⁺:YVO₄ laser illumination at 1342 are intra-cavity frequency-doubled into a KTP crystal.

SM4D.4 • 16:45

Mid-Infrared (6 - 10 μm) upconversion in LiInS₂ using 1064 nm CW pump, Ajanta Barh¹, Lasse Høgstedt², Peter Tidemand-Lichtenberg¹, Christian Pedersen¹; ¹Technical Univ. of Denmark (DTU), Denmark; ²NLIR Aps, Denmark. For the first time wide-band mid-infrared (6-10 μm) frequency upconversion in a LiInS₂ crystal is obtained using a 1064 nm pump. The absorption spectrum of polystyrene is characterized using a near-infrared grating and a Si-CCD.

SM4D.5 • 17:00

Optical Comanding, Yunshan Jiang¹, Bahram Jalali¹; ¹Univ. of California Los Angeles, China. We introduce a new nonlinear analog optical computing concept that compresses the signal's dynamic range and realizes non-uniform quantization that reshapes and improve the signal-to-noise ratio in the digital domain.

CLEO: QELS-Fundamental Science

16:00–18:00

FM4E • PT-Symmetry and Non-Hermitian Photonics

Presider: Stefan Rotter; Technische Universität Wien, Austria

FM4E.1 • 16:00

Manipulation and detection of optical coherence in non-conservative PT photonic structures, Kai Wang^{1,2}, Sergey V. Suchkov¹, James Titchener¹, Steffen Weimann², Demetrios N. Christodoulides³, Alexander Szameit², Andrey A. Sukhorukov¹; ¹Nonlinear Physics Centre, RSPE, Australian National Univ., Australia; ²Inst. for Physics, Rostock Universität, Germany; ³CREOL, The College of Optics and Photonics, Univ. of Central Florida, USA. We predict a periodic variation of the coherence between optical modes in parity-time symmetric photonic structures, and demonstrate experimentally reversible purification of fully spatially incoherent input light state propagating along coupled conservative and lossy waveguides.

FM4E.2 • 16:15

Extreme dynamics near exceptional points, QI ZHONG^{1,2}, Konstantinos Makris³, Ramy El-Ganainy^{1,2}; ¹Dept. of Physics, Michigan Technological Univ., USA; ²Henes Center for Quantum Phenomena, Michigan Technological Univ., USA; ³Dept. of Physics, Univ. of Crete, Greece. We investigate the extreme dynamics of non-Hermitian photonic systems near higher order exceptional points (EP) and we show that the maximum possible power amplification follows a power-law dependence on the order of the EP.

FM4E.3 • 16:30

Unidirectional Light Generation in PT-symmetric Microring Lasers, Jinhan Ren¹, Midya Parto¹, Steffen Wittek¹, Mohammad Parvinnezhad Hokmabadi¹, Demetrios N. Christodoulides¹, Mercedeh Khajavikhan¹; ¹CREOL UCF, USA. At resonance, microring resonators tend to support two counter-propagating degenerate modes. By incorporating S-bend chiral elements in each resonator, unidirectional single mode lasing below and above PT-symmetry breaking point is experimentally demonstrated.

FM4E.4 • 17:00

Saturation-Induced Perfect Absorbers, Ali Kazemi Jahromi¹, Ayman Abouraddy¹; ¹Univ. of Central Florida, CREOL, USA. We introduce a new regime of optical absorption where increasing the incoming intensity – equivalently inducing optical saturation – leads to the enhancement of total absorption in the device, and always reaches 100% at a critical value.

16:00–18:00

FM4F • Probing Materials with Ultrafast Electricity and Extreme Light

Presider: Rupert Huber; Universität Regensburg, Germany

FM4F.1 • 16:00

Quantum Coherent Transverse and Longitudinal Control for Attosecond Shaping of Free Electron Beams, Armin Feist¹, Katharina E. Priebe¹, Christopher Rathje^{1,2}, Thomas Rittmann¹, Sergey V. Yalunin¹, Thorsten Hohage², Sascha Schäfer^{1,3}, Claus Ropers¹; ¹4th Physical Inst., Univ. of Göttingen, Germany; ²Inst. for Numerical and Applied Mathematics, Univ. of Göttingen, Germany; ³Inst. of Physics, Univ. of Oldenburg, Germany. We demonstrate coherent control of free-electron momentum states in the longitudinal and transverse dimensions, including a temporal shaping of electron densities. A novel quantum state reconstruction scheme is employed to measure attosecond electron pulse trains.

FM4F.2 • 16:30

Investigation of Trap States and Their Dynamics in Hybrid Organic-inorganic Mixed Cation Perovskite Films Using Time Resolved Photoemission Electron Microscopy, Andrew Winchester¹, Christopher Petoukhoff¹, Mojtaba Abdi-Jalebi², Zahra Andaji-Garmaroudi², Vivek Pareek¹, E Laine Wong¹, Julien Madeo¹, Michael Man¹, Samuel D. Stranks², Keshav M. Dani¹; ¹Femtosecond Spectroscopy Unit, Okinawa Inst. of Science and Technology, Japan; ²Cavendish Lab, Univ. of Cambridge, UK. We use time-resolved photoemission electron microscopy to investigate hybrid organic perovskite thin films. We observe heterogeneous trap state densities varying on the nanometer scale. Further, we study the photo-excited carrier dynamics within these nanoscale regions.

FM4F.3 • 16:45

Nanoscale Magnetic Imaging using High-Harmonic Radiation, Sergey Zayko¹, Ofer Kfir^{1,2}, Michael Heigl³, Murat Sivis¹, Manfred Albrecht³, Claus Ropers^{1,4}; ¹IV. Physical Inst. – Solids and Nanostructures, Univ. of Göttingen, Germany; ²Solid State Inst. and Physics Dept., Technion – Israel Inst. of Technology, Israel; ³Inst. of Physics, Univ. of Augsburg, Germany; ⁴International Center for Advanced Studies of Energy Conversion (ICASEC), Univ. of Göttingen, Germany. We demonstrate high-resolution magneto-optical imaging using circularly-polarized high-harmonic radiation. We quantitatively map amplitude and phase of the x-ray magnetic circular dichroism at the Co M-edge using coherent diffractive imaging.

FM4F.4 • 17:00

Ultrafast X-ray Diffraction Reveals a Soft-Mode Driven Reversal of Polarity in Ferroelectrics, Christoph Hauf¹, Antonio-Andres Hernandez Salvador¹, Marcel Holtz¹, Michael Woerner¹, Thomas Elsaesser¹; ¹Max-Born-Inst., Germany. Transient charge density maps of photoexcited ferroelectric ammonium sulfate are determined by femtosecond x-ray diffraction. We observe a previously unknown soft-mode that induces a transient reversal of the full macroscopic electric polarization.

CLEO: QELS-Fundamental Science

CLEO: Science & Innovations

16:00–18:00

FM4G • Quantum Sources II

President: Joshua Bienfang; NIST, USA

FM4G.1 • 16:00

Frequency entanglement swapping, Sofiane Merkouche¹, Valerian Thiel², Alex O. Davis², Brian J. Smith^{1,2}; ¹Univ. of Oregon, USA; ²Univ. of Oxford, UK. Entanglement swapping of spectrally-entangled photons is experimentally demonstrated. Idler photons from independent entangled pairs are jointly detected after a beamsplitter and frequency filters, projecting the signal photons onto a frequency-bin singlet state.

FM4G.2 • 16:15

Hong-Ou-Mandel interference in the frequency domain using linear optical components, Poolad Imany¹, Ogaga D. Odele¹, Mohammed S. Al Alshaykh¹, Hsuan-Hao Lu¹, Daniel E. Leaird¹, Andrew M. Weiner¹; ¹Purdue Univ., USA. We demonstrate a Hong-Ou-Mandel interference pattern in the frequency domain with an electro-optic phase modulator and programmable pulse shapers, using energy-time entangled photons.

FM4G.3 • 16:30

Parallel Characterization of Two-Qubit Frequency-Bin Entanglement, Ogaga D. Odele¹, Poolad Imany¹, Daniel E. Leaird¹, Andrew M. Weiner¹; ¹Purdue Univ., USA. We examine multiple sets of frequency bins exhibiting two-dimensional entanglement in parallel using pulse shapers and electro-optic phase modulation. With this technique, we also demonstrate the retrieval of the dispersion constant of a single-mode fiber.

FM4G.4 • 16:45

Shaping photon-pairs time-frequency correlations in inhibited-coupling hollow-core fibers, Martin Cordier¹, Adeline Orieux², Benoit Debord³, Frédéric Gérôme³, Alexandre Gorse⁴, Matthieu Chafer³, Eleni Diamanti², Philippe Delaye⁵, Fetah Benabid³, Isabelle Zaquine¹; ¹Telecom ParisTech, France; ²LIP6, France; ³XLIM, France; ⁴GloPhotonics, France; ⁵Laboratoire Charles Fabry, France. We experimentally show how multiband dispersion properties of inhibited-coupling hollow-core fibers allow to control the spectral correlations of photon pairs generated through four-wave-mixing in a fiber filled with non-linear gas.

FM4G.5 • 17:00

Generation of NIR correlated photon pairs in optical nano-fibers, Jin-Hun Kim¹, Yong Sup Ihn¹, Heedeuk Shin¹, Yoon-Ho Kim¹; ¹Pohang Univ of Science & Technology, South Korea. We report the generation of near-IR (NIR) nondegenerate correlated photon pairs in an 13-cm-long optical nano-fiber (ONF). The coincidence-to-accidental ratio (CAR), 400 has been achieved at a very low average pump power of 70 μ W

16:00–18:00

FM4H • Quantum Optics with Atomic and Molecular Ensembles

President: Adam Black; US Naval Research Lab, USA

FM4H.1 • 16:00

Synthetic Two-dimensional Spin-orbit Coupling in Ultracold Fermi Gases, Jing Zhang¹; ¹Shanxi Univ., China. We report the experimental realization of 2D spin-orbit coupling in ultracold 40K Fermi gases using three lasers, each of which dresses one atomic hyperfine spin state.

FM4H.2 • 16:15

Strong Low-Frequency Squeezed Light from Dual-Seeded Four-Wave Mixing, Meng-Chang Wu¹, Nicholas Brewer¹, Bonnie L. Schmittberger¹, Paul D. Lett^{1,2}; ¹Univ. of Maryland, College Park, USA; ²National Inst. of Standards and Technology, USA. We have obtained -7 dB of intensity-difference squeezing below 15 Hz via four-wave mixing in a rubidium vapor. This was accomplished by locking the laser and using two seed beams to balance the power.

FM4H.3 • 16:30

Sub-Shot Noise Stimulated Raman Spectroscopy with Parametric Homodyne Detection, Yoad H. Michael¹, Michael Rosenbluh¹, Avi Pe'er¹; ¹Bar-Ilan Univ., Israel. We present a method for Raman spectroscopy based on nonlinear phase detection in SU(1,1) interferometer. This method utilizes squeezed light to eliminate the noise associated with the stimulated Raman interactions and enhance the Raman gain.

FM4H.4 • 16:45

Experimental demonstration of Rabi Oscillations produced by adiabatic pulse due to initial atomic coherence, Zhenhuan Yi¹, Xingchen Zhao¹, Zhiguo Wang^{1,2}, Tao Peng¹, Anatoly A. Svidzinsky¹, Hichem Eleuch¹, Marlan Scully^{1,3}; ¹Texas A&M Univ., USA; ²Xi'an Jiaotong Univ., China; ³Baylor Univ., USA. We experimentally demonstrate that initial atomic coherence yields Rabi oscillations in a two-level system driven by an adiabatic pulse. This method can be used to achieve Quantum Amplification by Superradiant Emission of Radiation (QASER) in atomic vapors.

FM4H.5 • 17:00

Spatial Multiplexing of Atom-Photon Entanglement Sources, Zhongxiao Xu¹, Long Tian¹, Shujing Li¹, Hai Wang¹; ¹Shanxi Univ., China. We build a multiplexed light-matter interface and then demonstrate a \sim sixfold (\sim fourfold) probability increase in generating entangled atom-photon (photon-photon) pairs. The measured compositive Bell parameter for the multiplexed interface is 2.49 ± 0.03 and a memory lifetime of up to $\sim 51 \mu$ s.

16:00–18:00

SM4I • Novel Emitters

President: Yasutomo Ota; Univ. of Tokyo, Japan

SM4I.1 • 16:00

Accelerating Emission dynamics in Perovskites Plasmonic Nanolasers, Sui Yang¹, Wei Bao¹, Xiaozhe Liu¹, Jeongmin Kim¹, Rongkuo Zhao¹, Yuan Wang¹, Xiang Zhang¹; ¹Univ. of California Berkeley, USA. Slow exciton recombination in recent emerging perovskite semiconductors brings a fundamental limitation for nanophotonic devices. Here we demonstrate a perovskite nanolaser under hybrid plasmonic confinement with dramatically accelerated emission dynamics via a scalable solution process.

SM4I.2 • 16:15

Electron beam-induced tunable radiation from silicon-only structures in the near-infrared, Charles Roques-Carmes¹, Steven E. Kooi², Aviram Massuda¹, Aun Zaidi¹, Yi Yang¹, Yujia Yang¹, Karl K. Berggren¹, Ido Kaminer^{1,3}, Marin Soljacic^{1,4}; ¹Research Lab of Electronics, MIT, USA; ²Inst. for Soldier Nanotechnologies, USA; ³Dept. of Electrical Engineering, Technion - Israel Inst. of Technology, Israel; ⁴Dept. of Physics, MIT, USA. We experimentally demonstrate the generation of tunable radiation from silicon-only periodic structures in the near-infrared. Spontaneous emission from low-energy electrons is recorded in a modified scanning electron microscope, matching our theoretical predictions.

SM4I.3 • 16:30

Inverse Design for Single-Mode Waveguide Coupling of Electrically Injected Optical Antenna Based NanoLED, Nicolas M. Andrade¹, Sean M. Hooten¹, Seth Fortuna¹, Kevin Han¹, Eli Yablonovitch¹, Ming C. Wu¹; ¹EECS, Univ. of California, Berkeley, USA. We propose a broadband and efficient structure for single-mode spontaneous emission coupling of an electrically-injected slot antenna based nanoLED. Using FDTD simulations and inverse design, we achieved 93% waveguide coupling and 50.77% spontaneous emission coupling.

SM4I.4 • 16:45

Deep Ultraviolet Smith-Purcell Radiation, Yu Ye¹, Fang Liu¹, Mengxuan Wang¹, Yidong Huang¹; ¹Tsinghua Univ., China. We demonstrated high order Smith-Purcell radiation in deep ultraviolet wavelength region. Having free electrons passing through a slot in a 2 μ m-long two-dimensional Aluminum grating, the radiation with wavelength as short as 237nm has been derived.

SM4I.5 • 17:00

Hybrid Metallo-Dielectric Structure for Spontaneous Emission Enhancement, Sean M. Hooten¹, Nicolas Andrade¹, Seth Fortuna¹, Kevin Han¹, Ming C. Wu¹, Eli Yablonovitch¹; ¹UC Berkeley, USA. The rate of spontaneous emission can be enhanced using either a metallic antenna or a dielectric cavity. Here we adapt elements of both types for a novel metallo-dielectric structure that exhibits ultra-low mode volume, $V_{eff} = 4.53e-6 (\lambda/bda)^3$.

CLEO: QELS-Fundamental
Science

16:00–18:00

FM4J • Fundamentals of Metamaterials

President: Mikhail Noginov; Norfolk State Univ., USA

FM4J.1 • 16:00

Epsilon-Near-Zero Systems for Quantum Optics Applications, Larissa Vertchenko¹, Nika Akopian¹, Andrei V. Lavrinenko¹; ¹Technical Univ. of Denmark, Denmark. We propose Epsilon-Near-Zero materials to facilitate the interaction between distant quantum emitters by employing the supercoupling effect and form what we call an ENZ network for quantum applications. We show that such systems present very low losses and are able to coherently transmit radiation.

FM4J.2 • 16:15

Broadband Epsilon Near Zero Conducting Oxide Absorbers Fabricated by Atomic Layer Deposition, Long Tao¹, Aleksei Anopchenko¹, Sudip Gurung¹, Catherine Arndt¹, Jason Myers², Ho Wai H. Lee^{1,3}; ¹Baylor Univ, USA; ²Optical Sciences Division, U.S. Naval Research Lab, USA; ³The Inst. for Quantum Science and Engineering, Texas A&M Univ., College Station, USA. We demonstrate an excitation of broadband epsilon-near-zero resonance in multi-layer conducting oxides grown by atomic layer deposition. Absorption bandwidth (>90%) of 214 nm for Berreman-mode and 294 nm for ENZ-mode in NIR region is realized.

FM4J.3 • 16:30

Hyperbolic modes of a metal-dielectric interface., Evgenii E. Narimanov¹; ¹Purdue Univ., USA. The inherent mobility of free electrons leads to the formation of hyperbolic layers at any high-quality metal-dielectric interface, which support new surface waves with longer propagation distance and stronger field confinement, at the same time.

FM4J.4 • 16:45

Variable Environmental Index Spectroscopy in Metamaterials, Wei-Yi Tsai^{1,2}, Vassili Savinov¹, Jun-Yu Ou¹, Din Ping Tsai^{3,2}, Nikolay I. Zheludev^{1,4}; ¹Univ. of Southampton, UK; ²Dept. of Physics, National Taiwan Univ., Taiwan; ³Research Center for Applied Sciences, Academia Sinica, Taiwan; ⁴Centre for Disruptive Photonic Technologies, Nanyang Technological Univ., Singapore. By immersing metamaterial nanostructures into liquids with different refractive indices, we obtain valuable information on role of different multipoles in their electromagnetic response. Applications to detection of anapole modes are discussed.

FM4J.5 • 17:00

Optoelectronic Plasmonic Metamaterials with a Quantum Cascade Structure, Yezhezi M. Zhang¹, Wentao Fan¹, Alex Y. Song^{1,2}, Deborah Sivco^{1,3}, Claire F. Gmachl¹; ¹Princeton Univ., USA; ²Stanford Univ., USA; ³Trumpf Photonics Inc., USA. Through transmission and reflection measurements, we show that optical properties are preserved when a quantum cascade structure is incorporated into a plasmonic semiconductor metamaterial with negative refraction.

CLEO: Science & Innovations

16:00–18:00

SM4K • Nonlinear Fiber Optics

President: Anna Peacock; Univ. of Southampton, UK

SM4K.1 • 16:00 **Invited**

Mid-IR Supercontinuum Sources using Double Cascading, Ole . Bang^{1,2}, Christian R. Petersen¹, Peter Moselund², Laurent Brilland³; ¹DTU Fotonik, Technical Univ. of Denmark, Denmark; ²NKT Photonics A/S, Denmark; ³SelenOptics, France. Supercontinuum generation in softglass fibers can offer a spatially coherent source covering the spectral region 1-12 μm . However, it requires to control double supercontinuum cascading in a setup with 3 or more vastly different fibers.

SM4K.2 • 16:30

A Watt-level Supercontinuum Source from a Fiber-laser pumped Fluorindate Fiber Spanning 750 nm to 5 μm , Sijing Liang¹, Lin Xu¹, Qiang Fu¹, David Shepherd¹, David Richardson¹, Shaif-UI Alam¹; ¹Optoelectronics Research Centre, Univ. of Southampton, UK. Supercontinuum generation from 750 nm to 5 μm , with an output power of 1.76 W and a 3-dB spectral-bandwidth of 1870 nm, was achieved by pumping a 10-m-long fluorindate-fiber with a 2- μm picosecond fiber MOPA.

SM4K.3 • 16:45

Normal-Dispersion Fiber Optical Parametric Chirped-Pulse Amplification, Walter P. Fu¹, Frank W. Wise¹; ¹Cornell Univ., USA. We demonstrate normal-dispersion fiber optical parametric chirped-pulse amplification pumped with high-power, chirped pulses and seeded with continuous-wave light. We generate 47 nJ, 1310 nm idlers compressible to 210 fs, and anticipate further energy scaling.

SM4K.4 • 17:00

Megawatt peak power femtosecond source at 1.3 μm based on self-phase modulation enabled spectral selection, Hsiang-Yu Chung^{1,2}, Liwei Song^{1,3}, Wei Liu^{1,2}, Qian Cao^{1,2}, Franz X. Kaertner^{1,2}, Guoqing Chang^{1,4}; ¹Center for Free-Electron Laser Science, DESY, Germany; ²Physics, Universität Hamburg, Germany; ³State Key Lab of High Field Laser Physics, Shanghai Inst. of Optics and Fine Mechanics, Chinese Academy of Sciences, China; ⁴The Hamburg Centre for Ultrafast Imaging, Germany. We demonstrate a megawatt peak power femtosecond source at 1.3 μm based on self-phase modulation enabled spectral selection by pumping optical fibers with negative group-velocity dispersion.

16:00–18:00

SM4L • Frequency Comb Development & Technology

President: Jungwon Kim; Korea Advanced Inst of Science & Tech, South Korea

SM4L.1 • 16:00

Operating an Optical Frequency Comb Using a 5-W Handheld USB Charger, Paritosh Manurkar¹, Edgar Perez¹, Daniel Hickstein¹, David R. Carlson¹, Jeff Chiles¹, Daron Westly², Esther Baumann¹, Scott Diddams¹, Nathan R. Newbury¹, Kartik Srinivasan², Scott Papp¹, Ian R. Coddington¹; ¹NIST Boulder, USA; ²NIST Gaithersburg, USA. We present a 100-MHz frequency comb that can be fully stabilized using less than 5 W of electrical power. We demonstrate full repetition-rate and offset-frequency stabilization while powering the comb with a handheld USB charger.

SM4L.2 • 16:15

CEO Stabilization of a Fiber Laser by Cross Gain Modulation, Kutan Gurel¹, Stephane Schilt¹, Thomas Südmeyer¹; ¹Universite de Neuchatel, Switzerland. We present the first CEO stabilization of a fiber laser by cross gain modulation. A low-power CW-laser modulates the fiber gain, achieving 40-times larger modulation bandwidth than standard pump-current control. A tight CEO lock is demonstrated.

SM4L.3 • 16:30

All-fiber-based mode-filtering technique with high side-mode suppression ratio and high multiplication factor, Yoshiaki Nakajima^{1,2}, Akiko Nishiyama^{1,2}, Takuya Hariki^{1,2}, Kaoru Minoshima^{1,2}; ¹Univ. of Electro-Communications, Japan; ²ERATO MINOSHIMA IOS Project, Japan. All-fiber-based mode filtering technique is developed for repetition rate multiplication of fiber-based frequency comb with multiplication factor of 11. Record high side-mode suppression ratio of approximately 40 dB is achieved with 536.0-MHz repetition-rate fiber-based mode-filtered-comb.

SM4L.4 • 16:45

Injection-Locking-Based Tunable Repetition-Rate Multiplication of Mode-Locked Lasers, Chan-Gi Jeon¹, Jungwon Kim¹; ¹Korea Advanced Inst of Science & Tech, South Korea. We demonstrate all-fiber repetition-rate multiplication of mode-locked laser based on injection-locked slave laser. The fundamental repetition-rate of 78.4 MHz can be multiplied by a factor of 13 to 102 (1-GHz to 8-GHz).

SM4L.5 • 17:00

Carrier-envelope-offset locking of 25-GHz EOM comb based on a free-running CW Laser Diode, Atsushi Ishizawa¹, Tadashi Nishikawa², Kazutaka Hara^{1,2}, Kenichi Hitachi¹, Tetsuomi Sogawa¹, Hideki Gotoh¹; ¹NTT Basic Research Labs, Japan; ²Tokyo Denki Univ., Japan. We demonstrate a carrier-envelope-offset (CEO)-locked electro-optics-modulation (EOM) comb with 25-GHz mode spacing at telecommunications wavelengths. The mode spacing of the CEO-locked EOM comb—the widest ever reported—is achieved with a free-running CW laser diode.

CLEO: Science & Innovations

16:00–18:00

SM4M • Power Scaling of Ultrafast Sources*Presider: Tobias Witting; Max-Born-Inst., Germany*SM4M.1 • 16:00 **Invited**

Isolated Pulse Parametric Frequency Conversion under Burst-Mode Pumping, Andrius Baltuska¹, Edgar Kaksis¹, Ignas Astrauskas¹, Tobias Flöry¹, Giedrius Andriukaitis¹, Pavel Malevich¹, Tadas Balciunas¹, Audrius Pugzlys¹; ¹Photonics Inst., TU Wien, Austria. Burst-mode regenerative amplifiers permit substantial energy and average-power scaling of pump lasers. We demonstrate advantages of parametric burst-to-single-pulse up- and down-conversion in the generation of optical harmonics and in multicolor pumping of long-wave parametric amplifiers.

SM4M.2 • 16:30

High-Energy Soliton Dynamics in Gas-Filled Hollow Capillary Fibers, John C. Travers¹, Teodora Grigorova¹, Federico Belli¹; ¹Heriot-Watt Univ., UK. We show that soliton dynamics scale to millijoule energies and terrawatt peak powers in simple hollow capillary fibers. We numerically model sub-femtosecond pulse self-compression, and experimentally demonstrate high-brightness μ J-scale ultraviolet (125–330 nm) pulse generation.

SM4M.3 • 16:45

High power hollow-core fiber compression of Yb lasers as ideal drivers for HHG, Vincent Cardin^{2,1}, Young-Gyun Jeong², Guangyu Fan³, Tadas Balciunas³, Riccardo Piccoli², Denis Ferachou^{2,1}, Jens Limpert⁴, Steffen Hädrich⁶, Roberto Morandotti², Hans Jakob Wörner⁵, Luca Razzari², François Légaré², Andrius Baltuska³, Bruno E. Schmidt¹; ¹few-cycle Inc, Canada; ²INRS-EMT, Canada; ³TU Wien, Austria; ⁴Inst. of Applied Physics, Abbe Center of Photonics, Friedrich-Schiller-Univ. Jena, Germany; ⁵ETH Zürich, Switzerland; ⁶Active Fiber Systems GmbH, Germany. We present recent achievements of single stage hollow-core fiber compression as HHG driving sources enabling: large compression factors (x24), highest output energies of 10mJ and operation at >100W of average power with generally >70% efficiency.

SM4M.4 • 17:00 **Invited**

High Power Ultrashort Amplifiers Based on Yb Doped Single Crystal Fibers, Patrick Georges^{1,2}, Fabien Lesparre^{1,2}, Jean-Thomas Gomes¹, Xavier Delen¹, Igor Martial², Julien Didierjean², Frédéric Druon¹, François Balembois¹; ¹Laboratoire Charles Fabry, Institut d'Optique Graduate School - CNRS, France; ²FiberCryst, France. We will present the advantages of the single-crystal-fiber (SCF) concept and review the main results obtained in ultrashort multi-stages Yb:YAG SCF amplifiers for high average power (100W) and high energy (mJ) regimes using Divided-Pulse-Amplification technic.

16:00–18:00

SM4N • Laser Materials*Presider: Clara Saraceno; Ruhr Universität Bochum, Germany*SM4N.1 • 16:00 **Invited**

Novel Solid-state Laser Materials, Christian Kraenkel^{2,1}; ¹Institut für Laser-Physik, Universität Hamburg, Germany; ²Center for Laser Materials, Leibniz Inst. for Crystal Growth, Germany. Novel materials enable unprecedented laser performance in the visible and near-infrared spectral range. Tb³⁺:LiLuF₄ delivers watt-level output in the green and yellow and the first cw Er:Sc₂O₃ laser emits 0.28 W at 2856 nm.

SM4N.2 • 16:30

Efficient and Broadly Tunable Eye-Safe Laser Operation in a Single Crystal of Tm-Doped Strontium Fluoride (Tm:SrF₂), Alberto Sottile^{1,2}, Eugenio Damiano^{2,3}, Martina Rabe⁴, Rainer Bertram⁴, Detlef Klimm⁴, Mauro Tonelli^{1,2}; ¹NEST, Istituto Nanoscienze - CNR, Italy; ²Dipartimento di Fisica, Università di Pisa, Italy; ³Dipartimento di Scienze Fisiche, della Terra e dell'Ambiente - Sez. di Fisica, Università di Siena, Italy; ⁴IKZ - Leibniz-Institut für Kristallzüchtung, Germany. We report on the growth, spectroscopic characterization, and first laser operation in this material, with a slope efficiency of 50% at 2015 nm. The laser was also continuously tunable between 1840 and 2020 nm.

SM4N.3 • 16:45

Q-switched Cryogenic Ho:YAG Laser, Miftar Ganija¹, Alexander Hemming², Nikita Simakov², Neil Carmody², Peter Veitch¹, John Haub², Jesper Munch¹; ¹Univ. of Adelaide, Australia; ²Cyber and Electronic Warfare Division, Defence Science & Technology Group, Australia. We describe the first power scalable Q-switched, cryogenically cooled, resonantly-pumped, Ho:YAG laser. The output energy was extracted from a confocal resonator with a single-pass pump geometry. Pulsed operation at higher average powers will be reported.

SM4N.4 • 17:00

Electrooptic Active Q switching at the 2 μ m Wavelength Range using KLTN:Cu Crystals, Salman Noach¹, Rotem Naheer^{2,1}, Yehuda Vidal², Aharon J. Agranat²; ¹Jerusalem College of Technology, Israel; ²The Hebrew Univ. of Jerusalem, Israel. An actively Q switched Tm:YLF laser operating at 1880 nm, generating 5 mJ, 34 nsec pulse duration is presented. Q switching was done by an electrooptic 2 mm long KLTN crystal driven at 3.6 kV/cm.

16:00–18:00

SM4O • Structured Light for Material Processing*Presider: Tsing-Hua Her; Univ of North Carolina at Charlotte, USA*SM4O.1 • 16:00 **Tutorial**

Creation of Structured Materials with Optical Vortices, Takashige Omatsu^{1,2}; ¹Chiba Univ., Japan; ²Molecular Chirality Research Center, Chiba Univ., Japan. We review optical vortex materials processing, in which the orbital angular momentum twists materials irradiated by optical vortices to establish chiral structured materials on the nano-/micro-scale. Also, we address recent progress concerning the optical vortex sources for materials processing.



Prof. Omatsu has been pioneering structured materials fabrication by optical vortex illumination. He published over 150 journal papers. He is serving as a deputy editor of Optics Express, and a director of photonics division, Japan Society of Applied Physics (JSAP). He was elected a OSA fellow and a JSAP fellow.

SM4O.2 • 17:00

Acceleration of Micro-Hole Drilling by an Azimuthally Polarized Laser Beam under Tight Focusing Condition, Shugo Matsusaka¹, Yuichi Kozawa¹, Shunichi Sato¹; ¹Inst. of Multidisciplinary Research for Advanced Materials, Tohoku Univ., Japan. We examined the laser micro-hole drilling using radially and azimuthally polarized beams for various types of metallic thin plates. We observed remarkable reduction of drilling time for the tight focusing of an azimuthally polarized beam.

CLEO: Applications
& Technology

16:00–18:00

AM4P • Biosensing Technologies

President: Ilko Ilev; U.S. Food and Drug Administration, USA

AM4P.1 • 16:00 **Invited**

Miniature Biomedical Optical Sensors and Imaging Systems, Ofer Levi¹; ¹Univ. of Toronto, Canada. Miniature integrated optical systems for sensing and imaging can be portable, enabling long-term studies in living tissues. We present our miniature sensitive optical sensors and imaging systems for Lab-on-a-chip and in vivo imaging applications.

AM4P.2 • 16:30

Electric Field Sensing with Graphene Optoelectronics for Action Potential Detection, Jason Horng^{1,2}, Halleh B. Balch¹, Allister McGuire³, Feng Wang¹, Bianxiao Cui³; ¹Univ. of California Berkeley, USA; ²Physics, Univ. of Michigan, Ann Arbor, USA; ³Chemistry, Stanford Univ., USA. Graphene, exhibiting field-dependent optical absorption, offers great opportunities for action potential sensing for bioelectric researches. We demonstrate two novel schemes of graphene opto-electronic realizing high voltage sensitivity and large bandwidth electric field imaging techniques.

AM4P.3 • 16:45

Remote Photonic Sensing of Vocal Cords Vibrations, Nisan Ozana¹, Adi Primov-Fever², Michael Wolf², Zeev Zalevsky¹; ¹Faculty of Engineering and the Nano Technology Center, Bar Ilan Univ., Israel; ²ENT Dept., Sheba Medical Center, Tel-Hashomer, Israel, and Sackler School of Medicine, Tel-Aviv Univ., Israel. The ability to remotely extract vibrations from specific locations on the vocal cords using time varied speckle patterns is innovative. The first step towards characterization of spatial and temporal vocal cords vibrations remotely is presented.

AM4P.4 • 17:00

Self-powered Ultrasensitive Glucose Detection Based on Graphene Multi-Heterojunctions, Cheng Han Chang¹, Wei-Ju Lin¹, Yu-Ming Liao¹, Han-Yi Chou¹, Yang-Fang Chen¹; ¹National Taiwan Univ., Taiwan. A highly sensitive glucose biosensor based graphene/ZnO/p-Si heterojunctions is demonstrated. Its sensing mechanism makes use of the large variation in the Fermi energy of graphene at the presence of glucose molecules, resulting in a superb detection sensitivity.

CLEO: QELS-Fundamental
Science

16:00–18:00

FM4Q • Valley-Hall and Active Topological Photonics

President: Xiaobo Yin; Univ. of Colorado at Boulder, USA

FM4Q.1 • 16:00

Chirality-locked valley polarization in photonic graphene, Yuan Li¹, Yong Sun^{1,2}, Yunhui Li¹, Haitao Jiang¹, Zhigang Chen^{2,3}, Hong Chen¹; ¹MOE Key Lab of Advanced Micro-Structured Materials, School of Physics Science and Engineering, Tongji Univ., China; ²Dept. of Physics and Astronomy, San Francisco State Univ., USA; ³MOE Key Lab of Weak-Light Nonlinear Photonics, TEDA Applied Physics Inst. and School of Physics, Nankai Univ., China. We demonstrate experimentally chirality-locked valley polarization in photonic graphene. A point source without chirality excites two inequivalent (K, K') valleys equally, whereas a chiral source selectively excites only one preferred valley depending on its chirality.

FM4Q.2 • 16:15

Observation of Valley-based Transport for Valley-pseudospin Polarized Photonic Edge State, Yuhao Kang^{1,2}, Xiaojun Cheng^{1,2}, Xiang Ni^{3,2}, Alexander B. Khanikaev^{3,2}, Azriel Z. Genack^{1,2}; ¹Queens College, CUNY, USA; ²Physics, The Graduate Center of the City Univ. of New York, USA; ³The City College of the City Univ. of New York, USA. We demonstrate the photonic valley-pseudospin polarized edge state experimentally. The contrast between transmission spectra demonstrates the conservation of valley degree of freedom at the Y-junction between domains emulating quantum valley-Hall and spin-Hall effects.

FM4Q.3 • 16:30

Experimental demonstration of valley-Hall topological photonic crystal at telecommunication wavelengths, Mikhail I. Shalaev¹, Wiktor Walasik¹, Natalia Litchinitser¹; ¹Buffalo State SUNY, USA. We experimentally demonstrate silicon-based topological valley-Hall photonic crystals operating at near-infrared frequencies. Robust and reflection-less light propagation around sharp turns is demonstrated. This work is an important step towards integrated topological photonics.

FM4Q.4 • 16:45

Valley Waves Sorting and Routing Based on Photonic Topological Insulators, Kueifu Lai^{2,1}, Yang Yu¹, Yuchen Han¹, Fei Gao³, Baile Zhang³, Gennady Shvets¹; ¹Cornell Univ., USA; ²Dept. of Physics, Univ. of Texas at Austin, Austin, USA; ³Nanyang Technological Univ., Singapore. We experimentally demonstrate a platform based on valley-spin locked propagation at heterogeneous photonic topological insulator interfaces. This platform is capable of sorting valley waves and routing it to desired destinations by topology switching.

FM4Q.5 • 17:00

Electrically Reconfigurable Topological Bound-state Laser Array, Ruizhe Yao¹, Hang Li¹, Jun Ding², Chi-sen Lee¹, Hualiang Zhang¹, Wei Guo¹; ¹Univ. of Massachusetts Lowell, USA; ²East China Normal Univ., China. We demonstrate a topological bound-state laser array in a Su-Schrieffer-Heeger array with topological defect. It is shown experimentally that the phase transition exists between the topological bound and bulk state lasing by adjusting the gain.

CLEO: Science & Innovations

SM4A • THz High-field Generation and Detection—Continued**SM4A.6 • 17:30**

Single-Shot Electro-Optic Measurement of Mid-Infrared Pulses, Michael Kozina¹, Matthias C. Hoffmann¹; ¹Linac Coherent Light Source, SLAC National Accelerator Lab, USA. We generate temporally chirped white light through self-phase-modulation in glass. By mixing the white light with ultrafast mid-infrared pulses in GaSe via the electro-optic effect, we observe the phase of the mid-infrared light via spectrally resolving the electro-optic signal.

SM4A.7 • 17:45

Single-shot spectral measurement of THz radiation from elliptically focused two-color laser filamentation in air, Yung Jun Yoo^{1,2}, Zheqiang Zhong¹, Ki-Yong Kim¹; ¹Univ. of Maryland, USA; ²Thorlabs Imaging Systems, USA. We report a single-shot method to measure the spectrum of THz radiation emitted from two-color laser filamentation in air. This method does not require multi-shot pump-probe scanning, and it is invulnerable to shot-to-shot laser fluctuation.

SM4B • Microrings and Novel Modulation Schemes—Continued**SM4B.5 • 17:15**

Fast and Ultra-compact Multi-channel All-optical Switches Based on Silicon Photonic Crystal Nanobeam Cavities, Dong Gaoneng¹, Wentao Deng¹, Xinliang Zhang¹; ¹Wuhan National Lab of Optoelectronic & School of Optical and Electronic Information, Huazhong Univ. of Science and Technology, China. By performing blue-detuned filtering on the output signal light, we achieve multi-channel all-optical switches with a processing density of 320 Tb/s/mm², which is the highest processing density shown in silicon based multi-channel switches.

SM4B.6 • 17:30

Monolithically Integrated Stokes Vector Modulator Based on Quantum-Confined Stark Effect, Mohiyuddin Kazi¹, Samir Ghosh¹, Masakazu Sugiyama¹, Takuo Tanemura¹, Yoshiaki Nakano¹; ¹Univ. of Tokyo, Japan. We demonstrate a monolithically integrated Stokes vector modulator using quantum-confined Stark effect in a simple straight-line configuration. Efficient polarization modulation over Poincaré sphere is observed by applying reverse-bias voltages to MQW-based polarization-dependent phase modulators.

SM4B.7 • 17:45

InP Based Mach Zehnder Modulators With Ultra-low V_π, Ye Liu¹, Quanan Chen¹, Xiang Ma¹, Wei Sun¹, Gongyuan Zhao¹, Gonghai Liu¹, Qiaoyin Lu¹, Weihua Guo¹; ¹Wuhan National Lab. For Optoelectronics, China. We designed and fabricated Mach-Zehnder Modulators (MZMs) with 0.65V V_π based on InP substrate. And the expected bandwidth is >60GHz with a coplanar waveguide electrode (CPW) structure.

SM4C • SDM Communication II—Continued**SM4C.5 • 17:15**

MCF-Enabled Self-Homodyne 16/64QAM Transmission for SDM Optical Access Networks, Aleksejs Udalcovs¹, Xiaodan Pang^{2,1}, Oskars Ozolins¹, Rui Lin², Lin Gan³, Richard Schatz², Anders Djupsjöbacka¹, Jonas Mårtensson¹, Ming Tang³, Songnian Fu³, Deming Liu³, Weijun Tong⁴, Jiajia Chen², Sergej Popov², Gunnar Jacobsen¹; ¹RISE Acreo AB, Sweden; ²KTH Royal Inst. of Technology, Sweden; ³Huazhong Univ. of Science and Technology, China; ⁴Yangtze Optical Fiber and Cable Joint Stock Limited Company, China. We experimentally demonstrate a 28-Gbaud circular and square 16/64QAM transmission over a 33.6-km long seven-core fiber with the LO passed through one of the cores for self-homodyne coherent detection employing a low-complexity digital signal processing.

17:30–18:30 Diversity & Inclusion in Optics and Photonics Reception, Market 1&2, Hilton San Jose

19:00–20:30 OSA Nonophotonics Technical Group 20x20 Talks, Room 230A

CLEO: Science & Innovations

SM4D • Optical Metrology Nonlinear Optical Technologies—Continued

SM4D.6 • 17:15

Nonlinear Dielectric Metasurfaces for Wavefront Control, Lei Wang¹, Sergey S. Kruk¹, Kirill Koshelev¹, Ivan Kravchenko², Barry Luther-Davies¹, Yuri S. Kivshar¹; ¹*Australian National Univ., Australia*; ²*Oak Ridge National Lab, USA*. We demonstrate Si-based metasurfaces for third-harmonic generation of an arbitrary wavefront. The nonlinear metasurfaces produce phase gradients within a full 0–2 π phase range. We achieve 92% diffraction efficiency of the nonlinear wavefront control.

SM4D.7 • 17:30

Giant nonlinear frequency shift in epsilon-near-zero aluminum zinc oxide thin films, Enrico Giuseppe Carnemolla¹, Vincenzo Bruno¹, Lucia Caspani², Matteo Clerici³, Stefano Vezzoli¹, Thomas Roger¹, Clayton DeVault⁴, Jongbum Kim^{5,4}, Amr Shaltout^{4,6}, Vladimir M. Shalaev⁴, Alexandra Boltasseva⁴, Daniele Faccio^{1,3}, Marcello Ferrara¹; ¹*Heriot Watt Univ., IPAQS, UK*; ²*Strathclyde Univ., UK*; ³*Univ. of Glasgow, UK*; ⁴*Purdue Univ., USA*; ⁵*Univ. of Maryland, USA*; ⁶*Stanford Univ., USA*. Degenerate pump/probe experiments have been performed on aluminum zinc oxide thin films at their epsilon-near-zero wavelength. A remarkable spectral shift of the reflected beam is reported to be approximately twice the pulse bandwidth.

CLEO: QELS-Fundamental Science

FM4E • PT-Symmetry and Non-Hermitian Photonics—Continued

FM4E.5 • 17:15

PT-Symmetric Microring Laser Gyroscopes, Jinhan Ren¹, Gal Harari², Absar U. Hassan¹, Weng Chow³, Mohammad Soltani⁴, Mohammad Parvinnezhad Hokmabadi¹, Demetrios N. Christodoulides¹, Mercedeh Khajavikhan¹; ¹*CREOL UCF, USA*; ²*Physics Dept. and Solid State Inst., Technion, Israel*; ³*Sandia National Labs, USA*; ⁴*Raytheon BBN Technologies, USA*. A new scheme for ultrasensitive micro-ring laser gyroscopes based on the physics of exceptional points is proposed. In such systems, the sensitivity to low rotation rates can be enhanced by several orders of magnitude.

FM4E.6 • 17:30

Multi-dimensional synthetic space and state measurement with spectral photonic lattices, Kai Wang¹, James Titchener¹, Bryn Bell², Alexander S. Solntsev^{3,1}, Dragomir N. Neshev¹, Benjamin J. Eggleton², Andrey A. Sukhorukov¹; ¹*Nonlinear Physics Centre, Research School of Physics and Engineering, The Australian National Univ., Australia*; ²*Centre for Ultrafast Bandwidth Devices for Optical Systems (CUDOS), Inst. of Photonics and Optical Science (IPOS), School of Physics, Univ. of Sydney, Australia*; ³*School of Mathematical and Physical Sciences, Univ. of Technology Sydney, Australia*. We propose and experimentally realize spectral photonic lattices with pump-induced frequency couplings, which can emulate multi-dimensional dynamics with synthetic gauge fields and enable single-shot measurement of the signal phase and coherence.

FM4E.7 • 17:45

Single Mode Supersymmetric Laser Array, Mohammad Parvinnezhad Hokmabadi¹, Sanaz Faryadras¹, Ramy El-Ganainy², Demetrios N. Christodoulides¹, Mercedeh Khajavikhan¹; ¹*Univ. of Central Florida, USA*; ²*Michigan Technological Univ., USA*. Multimode emission adversely affects phased-locked laser arrays resulting in chaotic behaviors. Utilizing optical supersymmetry, we experimentally demonstrate a single mode laser array where a superpartner array eliminates undesired higher order transverse modes.

FM4F • Probing Materials with Ultrafast Electricity and Extreme Light—Continued

FM4F.5 • 17:15

Fourier-transform inelastic x-ray scattering: A new kind of gas-phase vibrational spectroscopy, Matthew Ware^{1,2}, James Glowonia³, Adi Natan^{2,3}, James Cryan^{2,3}, Phillip Bucksbaum^{1,2}; ¹*Stanford Univ., USA*; ²*PULSE, USA*; ³*SLAC, USA*. We use the temporal Fourier transform of time-resolved x-ray scattering, known as Fourier-transform inelastic x-ray scattering (FT-IXS), to examine the harmonic, anharmonic, and dissociative dynamics of molecular iodine. This method can directly extract dissociation velocities.

FM4F.6 • 17:30

Ultrafast Separation of Photoexcited Electron Cloud, E Laine Wong¹, Andrew Winchester¹, Michael Man¹, Vivek Pareek¹, Julien Madeo¹, Keshav M. Dani¹; ¹*OIST, Japan*. Separation of photoexcited electron cloud is induced on a homogeneous GaAs surface via the exploitation of intensity variation within the photoexcitation beam. We show that the rate of separation can be controlled by tuning the photoexcitation intensity.

FM4F.7 • 17:45

Ultrafast quantum interference control of photocurrents beyond the perturbative regime, Rodrigo A. Muniz², Kai Wang², Steven T. Cundiff², John E. Sipe¹, Mackillo Kira²; ¹*Univ. of Toronto, Canada*; ²*Univ. of Michigan, USA*. We explore the use of high-intensity ultrashort lightwave waveforms for quantum interference control of photocurrents in semiconductor quantum wells. We analyze the quantum interference between nonlinear optical absorption processes in real time.

17:30–18:30 Diversity & Inclusion in Optics and Photonics Reception, Market 1&2, Hilton San Jose

19:00–20:30 OSA Nonophotonics Technical Group 20x20 Talks, Room 230A

CLEO: QELS-Fundamental Science

CLEO: Science & Innovations

FM4G • Quantum Sources II—Continued

FM4G.6 • 17:15

Real-time spectral characterization of a photon pair source using a chirped supercontinuum seed, Jennifer Erskine^{1,2}, Duncan England², Connor Kupchak^{1,2}, Ben Sussman^{2,1}; ¹Univ. of Ottawa, Canada; ²National Research Council, Canada. We perform joint spectral intensity measurements by studying stimulated four wave mixing in a birefringent fiber photon pair source. Seeding the process with a chirped supercontinuum beam, measurements are acquired in as little as 5 s.

FM4G.7 • 17:30

Quantum interferometry through cascading broadband entanglement sources, Arash Riazi¹, Chang j. Chen¹, Eric Y. Zhu¹, Alexey Gladyshev³, Peter Kazansky², John E. Sipe¹, Li Qian¹; ¹Univ. of Toronto, Canada; ²Univ. of Southampton, UK; ³Russian Academy of Sciences, Russia. We demonstrate broadband (~100nm) quantum interference in telecom frequencies in an all-fiber system with cascaded SPDC sources. Its applications in dispersion metrology and quantum state engineering are also demonstrated.

FM4G.8 • 17:45

A Compact All-fiber Polarization-Entangled Photon Source Pumped by a Laser Diode, Chang j. Chen¹, Arash Riazi¹, Eric Y. Zhu¹, Alexey Gladyshev², Mili Ng³, Peter Kazansky⁴, Li Qian¹; ¹Univ. of Toronto, Canada; ²Russian Academy of Sciences, Russia; ³Oz Optics, Canada; ⁴Univ. of Southampton, UK. We demonstrate a compact, all-fiber broadband polarization-entangled photon source pumped by a cw Fabry-Perot laser diode. Robust and stable operation yields a concurrence of 0.966 ± 0.015 and a fidelity to $|\Psi^+\rangle$ of $98.1 \pm 0.8\%$

FM4H • Quantum Optics with Atomic and Molecular Ensembles—Continued

FM4H.6 • 17:15

Wavevector-multiplexed and memory-enabled source of multimode nonclassical light, Michal Parniak¹, Michal Dabrowski¹, Mateusz Mazelanik¹, Adam Leszczynski¹, Michal Lipka¹, Wojciech Wasilewski¹; ¹Univ. of Warsaw, Poland. We demonstrate a quantum memory based on cold atomic ensemble generating and storing nonclassical light in 665 modes. With novel spin-wave manipulation techniques our system surfaces as a universal platform for quantum state preparation.

FM4H.7 • 17:30

Establishing and storing of quantum entanglement among three Rubidium atomic ensembles, Xiaojun Jia¹; ¹Shanxi Univ., China. Tripartite entanglement of optical modes is mapped into three distant atomic ensembles to establish entanglement of atomic spin waves via electromagnetically-induced-transparency light-matter interaction. Then the stored atomic entanglement is transferred into a tripartite entangled state.

FM4H.8 • 17:45

Entanglement Generation in Green Fluorescent Proteins, Siyuan Shi¹, Kim F. Lee¹, Prem Kumar¹; ¹Northwestern Univ., USA. We demonstrate generating polarization-entangled state through spontaneous four-wave mixing in enhanced green fluorescent proteins. We report coincident-to-accidental ratio of ~145 and entangled state fidelity of ~94% for the generated photon pairs.

SM4I • Novel Emitters—Continued

SM4I.6 • 17:15

Lasing in Si₃N₄-Organic Hybrid (SiNOH) Spiral Resonators, Daria Kohler^{2,1}, Sentayehu Fetene Wondimu^{2,1}, Lothar Hahn², Isabel Allegro², Matthias Blaicher^{2,1}, Wolfgang Freude¹, Christian Koos^{2,1}; ¹Inst. of Photonics and Quantum Electronics, Karlsruhe Inst. of Technology, Germany; ²Inst. of Microstructure Technology, Karlsruhe Inst. of Technology, Germany. We demonstrate lasing in optically pumped hybrid devices that combine passive Si₃N₄ waveguides with active organic cladding materials. Si₃N₄-organic hybrid (SiNOH) lasers lend themselves to low-cost integration and parallel read-out of large-scale sensor arrays.

SM4I.7 • 17:30 **Invited**

Physics and Applications of Active High-Q Microcavities, Jean-Baptiste Ceppe^{1,2}, Vincent Huet¹, Michel Mortier², Philippe Rochard¹, Ariel Levenson⁴, Kamel Bencheikh⁴, Alejandro Yacomotti⁴, Patrice Féron¹, Yannick Dumeige¹; ¹Université de Rennes, CNRS, Institut FOTON, France; ²IR-CICA (CNRS USR 3380) - PhLAM (CNRS UMR 8523), France; ³IRCP, Chimie ParisTech, France; ⁴C2N, France. High-quality factor whispering gallery mode microcavities doped with rare earth materials are used i) to study the dynamical and noise properties of micro-lasers and ii) to demonstrate slow-light effects in miniaturized devices.

17:30–18:30 Diversity & Inclusion in Optics and Photonics Reception, Market 1&2, Hilton San Jose

19:00–20:30 OSA Nonphotonics Technical Group 20x20 Talks, Room 230A

CLEO: QELS-Fundamental
Science

CLEO: Science & Innovations

FM4J • Fundamentals of Metamaterials—
Continued

FM4J.6 • 17:15

Controlling Cherenkov Angles with Resonance Transition Radiation, Xiao Lin¹, Sajan Easo², Yichen Shen³, Hongsheng Chen⁴, Baile Zhang¹, John Joannopoulos³, Marin Soljagic³, Ido Kaminer²; ¹Physics and Applied Physics, Nanyang Technological Univ., Singapore; ²Particle Physics Dept., Rutherford-Appleton Lab (STFC), UK; ³Physics, MIT, USA; ⁴Zhejiang Univ., China. We propose a new mechanism using the constructive interference of resonance transition radiation from photonic crystals to generate Cherenkov radiation into controllable Cherenkov angles with high sensitivity to any desired range of velocities.

FM4J.7 • 17:30

Time Domain Modeling of Bi-Anisotropic Homogenized Media with Analytical Dispersion, Ludmila J. Prokopeva¹, Zhaxylyk A. Kudyshev¹, Alexander Kildishev¹; ¹Purdue Univ., USA. We present a bi-anisotropic (BA) homogenization technique combined with derivation of the analytical dispersion of BA parameters. This formulation enables time domain modeling of the BA homogenized media and allows characterizing the geometry of the nanostructure with the dispersion parameters.

FM4J.8 • 17:45

The Superlight Inverse Doppler Effect, Xihang Shi¹, Xiao Lin¹, Ido Kaminer², Fei Gao¹, Zhaoju Yang¹, John Joannopoulos³, Marin Soljagic³, Baile Zhang¹; ¹Nanyang Technological Univ., Singapore; ²Physics, MIT, USA. An inverse Doppler frequency shift of light, i.e., superlight inverse Doppler effect, is shown possible even in homogeneous media with positive-refractive index, contrary to the status quo ante. We show an example with graphene plasmons.

SM4K • Nonlinear Fiber Optics—Continued

SM4K.5 • 17:15

High-peak-power, high-efficiency, frequency doubled and quadrupled Thulium fiber laser, Lin Xu¹, Sijing Liang¹, Qiang Fu¹, David Shepherd¹, David Richardson¹, Shaif-Ul Alam¹; ¹Univ. of Southampton, UK. We report frequency doubling and quadrupling of a short-pulsed (~80 ps) thulium-doped fiber laser, generating 976-nm and 488-nm wavelengths with peak powers of 34 kW and 10 kW, at conversion efficiencies of 75% and 22%, respectively.

SM4K.6 • 17:30

Phase-preserving Multilevel Amplitude Regeneration in Conjugate Nonlinear-Optical Loop Mirror Pair, Feng Wen^{1,2}, Mariia Sorokina¹, Christos P. Tsekrekos¹, Yong Geng², Xingyu Zhou², Baojian Wu², Kun Qiu², Sergei K. Turitsyn¹, Stylianos Sygletos¹; ¹Aston Inst. of Photonic Technologies, UK; ²Univ. of Electronic Science and Technology of China, China. We propose a conjugate nonlinear-optical loop mirror pair scheme (Conj-NOLM) for phase-preserving multilevel amplitude regeneration, by cascading two identical NOLMs with an intermediate phase conjugation stage. Q²-factor improvements of 2.42dB are achieved for 16-QAM signals.

SM4K.7 • 17:45

Fundamental Limits to Duration and Bandwidth of Temporal Cavity Solitons due to Raman Scattering, Yadong Wang¹, Miles Anderson¹, Stephane Coen¹, Stuart Murdoch¹, Miro J. Erkintalo¹; ¹Univ. of Auckland, New Zealand. We theoretically and experimentally show that stimulated Raman scattering destabilizes temporal cavity solitons at large pump-cavity detunings. Significantly, the identified instability imposes fundamental limits on the duration and bandwidth of temporal CSs.

SM4L • Frequency Comb Development &
Technology—Continued

SM4L.6 • 17:15

Frequency Comb Stabilization of a 50-fs Thin-Disk Laser Oscillator Operating in a Strongly SPM-broadened Regime, Norbert Modsching¹, Clément Paradis¹, Pierre Brochard¹, Nayara Jornod¹, Kutan Gurel¹, Christian Kränke^{2,3}, Stephane Schilt¹, Valentin J. Wittwer¹, Thomas Südmeyer¹; ¹Laboratoire Temps-Fréquence, Institut de Physique, Université de Neuchâtel, Switzerland; ²Center for Laser Materials, Leibniz Inst. for Crystal Growth, Germany; ³Inst. of Laser-Physics, Univ. of Hamburg, Germany. An Yb:LuO thin-disk laser generating 50-fs pulses at 4-W average output power and 50-MW intracavity peak power is CEO stabilized with 200-mrad integrated phase noise. Effects of repetition-rate stabilization onto the CEO noise are discussed.

SM4L.7 • 17:30

Fully Stabilized Optical Frequency Comb from a Semiconductor Disk Laser, Dominik Waldburger¹, Aline S. Mayer¹, Cesare Alfieri¹, Jacob Nürnberg¹, Adrea R. Johnson^{2,3}, Xingchen Ji^{4,5}, Alexander Klenner², Yoshitomo Okawachi², Michal Lipson⁴, Alexander L. Gaeta², Ursula Keller¹; ¹Inst. for Quantum Electronics, ETH Zürich, Switzerland; ²Dept. of Applied Physics and Applied Mathematics, Columbia Univ., USA; ³School of Applied and Engineering Physics, Cornell Univ., USA; ⁴Dept. of Electrical Engineering, Columbia Univ., USA; ⁵School of Electrical and Computer Engineering, Cornell Univ., USA. We demonstrate pulse repetition rate and carrier-envelope offset (CEO) frequency stabilization of a gigahertz SESAM-modelocked VECSEL. The CEO-detection is enabled by lowpower supercontinuum generation in a silicon-nitride waveguide without external pulse amplification.

17:30–18:30 Diversity & Inclusion in Optics and Photonics Reception, Market 1&2, Hilton San Jose

19:00–20:30 OSA Nonphotonics Technical Group 20x20 Talks, Room 230A

CLEO: Science & Innovations

SM4M • Power Scaling of Ultrafast Sources—Continued

SM4M.5 • 17:30

Two-dimensional, Eight-beam Combination of Ultrashort Pulses Using Two Diffractive Optics, Tong Zhou¹, Qiang Du¹, Tyler Sano¹, Russell Wilcox¹, Wim Leemans¹; ¹Lawrence Berkeley National Lab, USA. We demonstrate beam combination of eight 120fs pulses, using a diffractive optic pair. This highly scalable technique preserves input pulse width, and achieves 89.5% combining efficiency, limited by the diffractive optic.

SM4M.6 • 17:45

Cavity Phase Measurement via Modulated Impulse Response for Coherent Temporal Pulse Stacking, Yawei Yang¹, Jay Dawson², Lawrence Doolittle¹, Qiang Du¹, Almantas Galvanauskas³, Gang Huang¹, Tong Zhou¹, Russell Wilcox¹, Wim Leemans¹; ¹Lawrence Berkeley National Lab, USA; ²Lawrence Livermore National Lab, USA; ³Univ. of Michigan, USA. We have temporally combined 25 equal-amplitude pulses using four cavities, stabilizing cavity round-trip phase by measuring the response to a probe pulse train. Energy enhancement of 18.4 is maintained within 1% RMS.

SM4N • Laser Materials—Continued

SM4N.5 • 17:15

Radiation Balanced Thin Disk Lasers, Zhou Yang¹, Alexander Albrecht¹, Junwei Meng¹, Mansoor . Sheik-Bahae¹; ¹Univ. of New Mexico, USA. We demonstrate the first radiation balanced thin disk lasers. Ytterbium-doped YLF and YAG thin disks are pumped by a fiber laser in multipass geometry and an InGaAs/GaAs VECSEL in intracavity geometry.

SM4N.6 • 17:30

Q-switched Laser Oscillation in Micro-Domain Controlled Yb:FAP Anisotropic Laser Ceramics, Yoichi Sato¹, Jun Akiyama¹, Takunori Taira¹; ¹Inst. for Molecular Science, Japan. Using polycrystalline Yb³⁺-doped fluoroapatite (Yb:FAP), we investigated quantum mechanics for orientation-control of microdomains in anisotropic laser ceramics with 4f-electrons of RE³⁺-ion. Kilowatt-level sub-ns laser pulses were generated with the extraction density of 0.34 J/cm².

SM4N.7 • 17:45

Inversion caused spectral phase shift in a broadband Ti:Sapphire amplifier at room and cryogenic temperatures, Roland Nagymihály¹, Huabao Cao¹, Peter Jójart¹, Viktor Zuba², Mikhail Kalashnikov^{1,3}, Adam Borzsonyi^{1,2}, Vladimir V. Chvykov¹, Karoly Osvay¹; ¹ELI-HU Non-Profit Ltd., Hungary; ²Dept. of Optics and Quantum Electronics, Univ. of Szeged, Hungary; ³Max Born Inst. for Nonlinear Optics and Short Pulse Spectroscopy, Germany. Spectral phase shift of ultra-broadband pulses due to inversion was measured along the two axes of Ti:Sapphire at room and cryogenic temperatures. Results are crucial for CEP stabilization and compression of high energy few-cycle pulses.

SM4O • Structured Light for Material Processing—Continued

SM4O.3 • 17:15

Surface Relief Structuring via Multiple Pulse Femtosecond Ablation using an Intensity Spatial Light Modulator, Benjamin Mills¹, Daniel Heath¹, Rupert Bapty¹, Taimoor Rana¹, Behrad Gholipour¹, James Grant-Jacob¹, Robert Eason¹; ¹Univ. of Southampton, UK. Subtractive femtosecond laser machining using multiple pulses with different spatial intensity profiles on the same position on a sample enables surface relief structuring with up to 60 layers, 330nm spatial resolution, 3µm maximum depth.

SM4O.4 • 17:30

Two-photon induced 'super-resolution' single-armed relief in azo-polymer film, Keigo Masuda¹, Shogo Nakano¹, Yoshinori Kinezuka¹, Mitsuki Ichijo¹, Ryo Shinozaki¹, Katsuhiko Miyamoto^{1,2}, Takashige Omatsu^{1,2}; ¹Chiba Univ., Japan; ²Molecular chirality research center, Chiba Univ., Japan. We present the formation of a 'super-resolution' single-armed chiral relief in an azo-polymer film through a two-photon absorption process by the illumination of circularly polarized picosecond optical vortex pulses.

SM4O.5 • 17:45

STED-inspired Laser Lithography Based on Spirothiopyran Chromophores, Patrick Mueller^{1,2}, Larissa Hammer³, Rouven Mueller³, Eva Blasco³, Christopher Barner-Kowollik^{3,4}, Martin Wegener^{1,2}; ¹Inst. of Nanotechnology, Karlsruhe Inst. of Technology, Germany; ²Inst. of Applied Physics, Karlsruhe Inst. of Technology, Germany; ³Macromolecular Architectures, Inst. of Technical Chemistry and Polymer Chemistry, Karlsruhe Inst. of Technology, Germany; ⁴School of Chemistry, Physics, and Mechanical Engineering, Queensland Univ. of Technology, Australia. We present a photoresist based on the photochromic spirothiopyran moiety capable of creating free-standing 3D structures and offering an inhibition channel, which potentially allows for STED-inspired sub-diffraction laser lithography. Reversible inhibition and linewidth narrowing are demonstrated.

17:30–18:30 Diversity & Inclusion in Optics and Photonics Reception, Market 1&2, Hilton San Jose

19:00–20:30 OSA Nonophotonics Technical Group 20x20 Talks, Room 230A

**CLEO: Applications
& Technology**

**AM4P • Biosensing Technologies—
Continued**

AM4P.5 • 17:15

Multifunctional Optophoresis for Biomolecular Detection by Using Integrated Silicon Photonic Waveguide Arrays, Zhenyu Li^{1,2}, Haitao Zhao², Gong Zhang², Yanyu Chen², Jianguo Huang², qihua xiong², Aiqun Liu²; ¹Peking Univ., China; ²Nanyang Technological Univ., Singapore. A multifunctional optophoresis for biomolecular detection in integrated silicon photonic chip is demonstrated. Sample fractionation part is to avoid contamination and reduce interference. Signal is enhanced 5 more times after integrating sensors with waveguide arrays.

AM4P.6 • 17:30

Trapping and Optical Identification of Microparticles in a Liquid with a Functional Optical Fiber Probe, Fredrik Laurell¹, Sebastian Etcheverry¹, Walter Margulis¹; ¹Kungliga Tekniska Hogskolan, Sweden. A fiber probe traps single micrometer-particles by fluid suction into a hollow microstructure and enables optical identification by the fluorescence light collected in a fiber core. The probe finds applications in life-science and environmental monitoring.

AM4P.7 • 17:45

All-fiber, Portable, Online Raman Biosensor with Enhancement of Signal Excitation and Collection Efficiency, Qian Chu¹, Guanghui Wang¹, Zhiqiang Jin¹, Jie Tan¹, Hao Cai¹, Bo Lin², Xuping Zhang¹; ¹Nanjing Univ., China; ²China Academy of Electronics and Information Technology, China. We demonstrate an all-fiber online Raman biosensor with enhancement of signal excitation and collection efficiency by inserting a gold-coated-fiber-tip reflector into the metal-lined capillary for transmission mode collection, which provides nearly 2 times of enhancement.

**CLEO: QELS-Fundamental
Science**

**FM4Q • Valley-Hall and Active Topological
Photonics—Continued**

FM4Q.6 • 17:15

Topological Hybrid Silicon Microlasers, Han Zhao¹, Pei Miao^{2,3}, Mohammad H. Teimourpour⁴, Simon Malzard⁵, Ramy El-Ganainy⁴, Henning Schomerus⁵, Liang Feng²; ¹Dept. of Electrical and Systems Engineering, Univ. of Pennsylvania, USA; ²Dept. of Materials Science and Engineering, Univ. of Pennsylvania, USA; ³Dept. of Electrical Engineering, The State Univ. of New York at Buffalo, USA; ⁴Dept. of Physics and Henes Center for Quantum Phenomena, Michigan Technological Univ., USA; ⁵Dept. of Physics, Lancaster Univ., UK. We present an active topological hybrid silicon microlaser array respecting the charge-conjugation symmetry. The created symmetry favors the lasing of a protected zero-mode, where robust single-mode laser action prevails even with intentionally introduced perturbations.

FM4Q.7 • 17:30

Robust Radiation from Photonic Topological Insulators, Yaakov Lumer¹, Nader Engheta¹; ¹Electrical and Systems Engineering, Univ. of Pennsylvania, USA. We numerically demonstrate how a photonic topological insulator can be exploited to feed an antenna array, resulting in robust radiation performance free from unwanted interferences, mutual coupling and matching challenges among feed points.

FM4Q.8 • 17:45

Robust non-reciprocal lasing in topological cavities of arbitrary geometries, Babak Bahari¹, Abdoulaye Ndao¹, Felipe Vallini¹, Abdelkrim El Amili¹, Yeshaiahu Fainman¹, Boubacar Kante¹; ¹Univ. of California San Diego, USA. We present non-reciprocal topological cavities operating at telecommunication wavelengths. The unidirectional stimulated emission has an isolation ratio of about 10 dB between the output ports.

17:30–18:30 Diversity & Inclusion in Optics and Photonics Reception, Market 1&2,
Hilton San Jose

19:00–20:30 OSA Nonophotonics Technical Group 20x20 Talks, Room 230A

07:00–18:30 Registration, Concourse Level

08:00–10:00 JTu1A • Plenary Session I & Awards Ceremony, Grand Ballroom

10:00–17:00 Exhibition Open, Exhibit Hall

10:00–11:30 Coffee Break & Exhibit Only Time, Exhibit Hall

Exhibit Hall

11:30–13:00 JTu2A • Poster Session I

JTu2A.1

Cladding Waveguides in Aminoacid Crystal: Fabrication and Second Harmonic Generation, Gustavo Almeida¹, Renato Martins¹, Jonathas Siqueira¹, Juliana Almeida¹, Jose J. Rodrigues Jr.², Cleber R. Mendonca¹; ¹USP - Instituto de Fisica de Sao Carlos, Brazil; ²Physics Dept., Federal Univ. of Sergipe, Brazil. Cladding waveguides were inscribed in L-threonine aminoacid crystals by fs-laser pulses. Guided second harmonic generation was observed at 390 nm, with an efficiency of $1.3\%(\text{MW cm}^2)^{-1}$. Such results open new opportunities in organic nonlinear photonics.

JTu2A.2

Optothermal Nanoscissors for Versatile Low-Power Patterning of Atomic-Thin Two-Dimensional Materials, Jingang Li¹, Linhan Lin^{1,2}, Xiaolei Peng¹, Yuebing Zheng^{1,2}; ¹Materials Science & Engineering Program, The Univ. of Texas at Austin, USA; ²Dept. of Mechanical Engineering, The Univ. of Texas at Austin, USA. We report a new technique - optothermal nanoscissors - to achieve fast, on-demand and arbitrary patterning of different atomic-thin two-dimensional materials using the highly localized plasmonic heating effect.

JTu2A.3

Laser Direct Writing of Waveguides in Flexible Glass and Ultrafast Visualization of Its Dynamics via Time-Resolved Interferometry, Garima C. Nagar¹, Dennis Dempsey¹, James Sutherland², Rostislav Grynkó¹, Bonggu Shim¹; ¹BINGHAMTON UNIV., USA; ²Corning Incorporated, USA. Waveguides are inscribed onto flexible Corning Willow™ glass using femtosecond laser pulses. Interferometric phase imaging is used to elucidate the fabrication process by measuring dynamically-evolving plasma densities on ultrashort time scales.

JTu2A.4

Femtosecond-Laser Ablation of Monolayer Tungsten Diselenide (WSe₂) on Sapphire, Yu-Ling Chen¹, Ya-Hsin Tseng¹, Yen-Chun Chen¹, Wen-Hao Chang¹, Tsing-Hua Her², Chih Wei Luo¹; ¹National Chiao Tung Univ., Taiwan; ²Dept. of Physics and Optical Science, The Univ. of North Carolina at Charlotte, USA. Near-IR femtosecond laser ablation of monolayer tungsten diselenide WSe₂ on sapphire is demonstrated. The ablation threshold is found low (below 10 mJ/cm²), due to its low dimensionality and weak coupling to substrates. Substrate-dependent ablation threshold is predicted and will be discussed.

JTu2A.5

Femtosecond Laser- Colored ITO Films for Blue Light Attenuation and Image Screening, Ya-Hsin Tseng¹, Hung Yang¹, Chih Wei Luo¹; ¹National Chiao Tung Univ., Taiwan. Laser-colored ITO films are fabricated using femtosecond laser annealing. The fluence-dependent nanostructures on ITO significantly attenuate blue light, which are suited to eye protection and the screening of images behind ITO for information security.

JTu2A.6

Free-Space Optical Switching of GST Phase-Change Thin Films via 1550 nm Light, Gary A. Sevison^{1,4}, Joshua Burrow¹, Andrea Aboujaoude², Matthew Mircovich³, Andrew Sarangan¹, Josh Hendrickson⁴, Imad Agha^{1,3}; ¹Electro-Optics, Univ. of Dayton, USA; ²Electrical and Computer Engineering, Univ. of Dayton, USA; ³Physics, Univ. of Dayton, USA; ⁴Sensors Directorate, Air Force Research Lab, Wright-Patterson AFB, USA. We experimentally demonstrate free-space phase change of Germanium Antimony Telluride (GST), switching between the amorphous and hexagonal crystalline states utilizing telecom-band laser pulses.

JTu2A.7

Graphene/III-V Hybrid Diode Optical Modulator, Ruizhe Yao¹, Bowen Zheng¹, Hyun Kum², Yunjo Kim², Sanghoon Bae², Jeehwan Kim², Hualiang Zhang¹, Wei Guo¹; ¹Univ. of Massachusetts Lowell, USA; ²MIT, USA. We demonstrate a graphene/III-V hybrid diode optical modulator working over a large frequency range from NIR to THz. The hybrid diode is achieved by heterogeneous integration of graphene and III-V heterostructures by remote epitaxy growth.

JTu2A.8

Long-lived Quantum Emitters in hBN-WSe₂ Van-Der-Waals Heterostructures, Jakob Wierzbowski¹, Malte Kremser¹, Christian Straubinger¹, Florian Sigger¹, Julian Klein¹, Michael Kaniber¹, Kai Müller¹, Jonathan Finley¹; ¹Walter Schottky Institut - TU München, Germany. We present a significant linewidth narrowing (12.5%) of free excitons in hBN encapsulated TMDs and localized (< 350 nm) single-photon emitters with long lifetimes of ~18 ns in hBN/WSe₂ heterostructures.

JTu2A.9

Mode-switching phenomena in periodic InGaN-based hexagon microcavity array, Chia-Yen Huang¹, Tsu-Ying Tai¹, Jing-Jie Lin¹, Tsu-Chi Chang¹, Che-Yu Liu¹, Kuo-Bin Hong¹, Tien-Chang Lu¹, Hao-Chung Kuo¹; ¹Dept. of Photonics, NCTU, Taiwan. The lasing behavior of InGaN-based microcavity array was strongly relevant to the excitation area. The stronger rod-to-rod optical interaction between the fundamental axial mode resulted its dominance in the collective lasing behavior.

JTu2A.10

Frequency-Doubled Wafer-Fused 638 nm VCSEL with an Output Power of 5.6 W, Emmi L. Kantola¹, Tomi Leinonen¹, Antti Rantamäki¹, Mircea D. Guina¹, Vladimir Iakovlev², Alexei Sirbu²; ¹ORC, Tampere Univ. of Technology, Finland; ²RTI-Research SA, Switzerland. We report on a frequency doubled vertical-external-cavity surface-emitting laser emitting 5.6 W at 635 nm. The cavity employed a wafer-fused AlInGaAs/InP-AlAs/GaAs gain mirror in a V-shaped configuration. The heatsink temperature was 20 °C.

JTu2A.11

VCSEL Amplifier with High Power and Narrow Divergence Applying a Folded Waveguide Layout, Mizuki Morinaga¹, Xiaodong Gu¹, Keisuke Shimura¹, Masanori Nakahama¹, Fumio Koyama¹; ¹Tokyo Inst. of Technology, Japan. We demonstrated a compact VCSEL amplifier with a folded waveguide layout. Light propagation and amplification are realized in all 8 arms of the waveguide. Output power of 330mW and narrow divergence of 0.1° were obtained.

JTu2A.12

1.5 μm GaInAsP Stripe Laser Comparison Between InP Substrate and Directly Bonded InP/Si Substrate, Gandhi Kallarasani Periyanyagam¹, Naoki Kamada¹, Yuya Onuki¹, Kazuki Uchida¹, Hirokazu Sugiyama¹, Xu Han¹, Natsuki Hayasaka¹, Masaki Aikawa¹, Kazuhiko Shimomura¹; ¹Sophia Univ., Japan. Crystal growth on the Si substrate for 1.5 μm GaInAsP stripe laser diode has been demonstrated via MOVPE and successfully achieved the lasing operation in the pulse regime. We have compared the lasing characteristics between directly bonded InP/Si substrate and InP substrate as a reference.

JTu2A.13

A Large Area Monolayer WS₂ Laser Based on Surface-Emitting Heterostructure Photonic Crystal Cavities, Xiaochen Ge¹, Momchil Minkov², Xiuling Li³, Shanhui Fan², Weidong Zhou¹; ¹Univ. of Texas at Arlington, USA; ²Electrical Engineering, Stanford Univ., USA; ³Electrical and Computer Engineering, Univ. of Illinois Urbana-Champaign, USA. An optically pumped continuous wave room temperature operation monolayer WS₂ laser is presented. The cavity is formed around Γ point above lightline in a large area heterostructure photonic crystal slab for energy efficient surface emission.

JTu2A.14

High-Power DBR-Free Membrane Semiconductor Disk Lasers, Zhou Yang¹, David Follman², Alexander Albrecht¹, Paula Heu², Garrett Cole², Mansoor. Sheik-Bahae¹; ¹Univ. of New Mexico, USA; ²Crystalline Mirror Solutions LLC, USA. We compare the performance of DBR-free membrane semiconductor disk lasers (SDLs) with single and dual SiC intracavity heatspreaders. A record output power of 16.1 W is achieved and a fluorescence-based temperature characterization technique is demonstrated.

JTu2A.15

Demonstration of 1-um-band Si-Photonics-Based Quantum Dot Heterogeneous Tunable Laser, Atsushi Matsumoto¹, Kouichi Akahane¹, Toshimasa Umezawa¹, Naokatsu Yamamoto¹, Hirohito Yamada², Tomohiro Kita²; ¹NICT, Japan; ²Tohoku Univ., Japan. We present a Si-photonics-based quantum dot heterogeneous tunable lasers in the 1-mm band. Optical devices using Si-photonics-based PIC in the 1-mm band probably have not been reported yet.

JTu2A.16

Generation of Cylindrical Vector Beams from Vertical-Cavity Surface-Emitting Laser with Optical Feedback, Yuki Nara¹, Yuichi Kozawa¹, Shunichi Sato¹; ¹*Inst. of Multidisciplinary Research for Advanced Materials, Tohoku Univ., Japan*. We demonstrated the direct and selective generation of radially and azimuthally polarized beams from a VCSEL which was optically feedbacked from an external cavity including a birefringent lens to select polarization.

JTu2A.17

Frequency-Doubled VECSEL Employing a Volume Bragg Grating for Linewidth Narrowing, Emmi L. Kantola¹, Jussi-Pekka Penttinen¹, Tomi Leinonen¹, Sanna Ranta¹, Mircea D. Guina¹; ¹*ORC, Tampere Univ. of Technology, Finland*. We report on a frequency-doubled VECSEL emitting at 512.6 nm. The laser spectrum was narrowed with a Volume Bragg Grating and the intracavity frequency-doubling was achieved with a periodically poled MgO-doped lithium niobate.

JTu2A.18

Tunable External Cavity Quantum Cascade Laser using Intra-cavity Out-coupling, Yohei Matsuoka¹, Sven Peters², Mykhaylo P. Semtsiv¹, W. T. Masselink¹; ¹*Humboldt Univ. of Berlin, Germany*; ²*Sentech Instruments GmbH, Germany*. We describe an external-cavity quantum cascade laser with an intra-cavity out-coupling optical configuration. We achieved more than twice the output power compared to the Littrow design, while keeping the tunability.

JTu2A.19

Suppressing High Order Transverse Modes in Broad-Area Quantum Cascade Lasers, Ron Kaspi¹, Chi Yang¹, Sanh Luong¹, Timothy Bate¹, Chunte Lu¹, Timothy C. Newell¹, Don Gianardi¹; ¹*Directed Energy Directorate, Air Force Research Lab, USA*. Intracavity lateral constrictions and distributed loss through metallic sidewalls are two distinct methods that provide preferential losses to the high order transverse modes in broad-ridge quantum cascade lasers and increase brightness.

JTu2A.20

Simultaneous Oscillation of Two-Color Laser Lights from a GaAs/AlGaAs Coupled Multilayer Cavity, Yasuo Minami¹, Xiangmeng Lu¹, Naoto Kumagai², Ken Morita³, Takahiro Kitada¹; ¹*Tokushima Univ., Japan*; ²*National Inst. of Advanced Industrial Science and Technology, Japan*; ³*Chiba Univ., Japan*. We succeeded in simultaneous two-color laser oscillation from a GaAs/AlGaAs coupled multilayer cavity by current injection at room temperature. The simultaneous lasing was confirmed by detecting SFG generated by the two color laser lights.

JTu2A.21

Optical gain characterization of nano-ridge amplifiers epitaxially grown on a standard Si wafer, Yuting Shi¹, Bernardette Kunert², Marina Baryshnikova², Marianna Pantouvakis², Joris Van Campenhout², Dries VanThourhout^{1,2}; ¹*INTEC, UGent, Belgium*; ²*Ivec, Belgium*. With this paper, the authors report optical gain characterization of InGaAs/GaAs nano-ridge amplifiers epitaxially grown on a standard 300-mm Si wafer, by varying strip length (VSL) method. The measured material gain is ~ 4000 cm⁻¹, which is comparable with conventional GaAs material.

JTu2A.22

Demonstration of A Novel Two-Section DFB Laser, Gonghai Liu¹, Gongyuan Zhao¹, Weihua Guo¹, Qiaoyin Lu¹; ¹*Huazhong Univ. of Science & Technol, China*. TS-DFB laser containing an unbiased reflection section that has the same MQWs and grating pitch as the gain section, has 0.38 mW/mA slope efficiency, outstanding single mode yield and wavelength controlling reliability.

JTu2A.23

Free-standing III-V Semiconductor Microdisk Laser Particles, Andreas C. Liapis¹, Nicola Martino¹, Sheldon Kwok¹, Paul Dannenberg¹, Dong-Hoon Jang², Yong-Hee Lee², Seok-Hyun Yun¹; ¹*Wellman Center for Photomedicine, Massachusetts General Hospital, USA*; ²*Dept. of Physics, Korea Advanced Inst. of Science and Technology (KAIST), South Korea*. Semiconductor microdisks can be detached from their substrate and used as free-standing laser "particles" exhibiting room-temperature single-mode lasing. Silica-coated laser particles embedded in hydrogels display sub-nm linewidths and sub-20-pJ thresholds.

JTu2A.24

The Effect of Temperature on the Dynamical States of a Time Delayed Mid-infrared Quantum Cascade Oscillator, Olivier Spitz^{1,2}, Jiagui Wu^{3,4}, Sudeep Khanal⁵, Mathieu Carras², Benjamin Williams⁵, Chee Wei Wong³, Frédéric Grillot^{1,6}; ¹*Télécom ParisTech, France*; ²*mirSense, France*; ³*Fang Lu Mesoscopic Optics and Quantum Electronics Lab, Univ. of California Los Angeles, USA*; ⁴*College of Electronics and Information Engineering, Southwest Univ., China*; ⁵*Electrical and Computer Engineering, Univ. of California Los Angeles, USA*; ⁶*Center for High Technology Materials, Univ. of New-Mexico, USA*. Carrier-to-photon lifetime ratio is a key parameter in the non-linear dynamics study of quantum cascade lasers under external optical feedback. We experimentally investigate the influence of temperature on this parameter and hence on chaotic behaviors.

JTu2A.25

Temperature Dependence of Electrically Injected Quantum-Dot Photonic-Crystal Surface-Emitting Lasers, Ming-Yang Hsu¹, Gray Lin¹, Yu-Chen Chen¹, Chien-Hung Pan²; ¹*National Chiao Tung Univ., Taiwan*; ²*Truelight Corporation, Taiwan*. We have simplified fabrication of electrically injected quantum-dot photonic-crystal surface-emitting lasers and demonstrated lasing emissions at 1313 nm. Excellent threshold temperature characteristics was exhibited in range of 20–45 °C with characteristics temperature of almost infinity.

JTu2A.26

Design Optimization for Semiconductor Lasers with High-Order Surface Gratings having Multiple Periods, Gaurav Jain¹, Michael J. Wallace¹, Qiaoyin Lu², Wei-Hua Guo², John F. Donegan¹; ¹*School of Physics and CRANN, Trinity College Dublin, Ireland*; ²*Wuhan National Lab for Optoelectronics, Huazhong Univ. of Science and Technology, China*. A ridge waveguide multi period structure within 37th order surface grating semiconductor laser is presented. These gratings allow wide tuning over the C-band while allowing for low threshold and high SMSR.

JTu2A.27

GaSb-based 2.7µm laser diode with GaAs top cladding, Timothy Bate¹, Chunte Lu¹, Robert Palomino¹, Chi Yang¹, Timothy C. Newell¹, Sanh Luong¹, Ron Kaspi¹; ¹*Directed Energy Directorate, Air Force Research Lab, USA*. GaSb-based ~2.7µm diode lasers were grown with highly mismatched GaAs top clad using MBE. Only ~27% reduction in slope efficiency was observed, with peak power >300mW at room temperature, despite fully relaxed clad.

JTu2A.28

High performance GaSb superluminescent diodes for tunable light source at 2 µm and 2.55 µm, Nouman Zia¹, Jukka Viheriälä¹, Eero Koivusalo¹, Antti Aho¹, Soile Suomalainen¹, Mircea D. Guina¹; ¹*Optoelectronics research centre Tampere, Finland*. We report on GaSb-based superluminescent diodes emitting an output power of 70 mW at 2 µm and the first demonstration of 2.55µm SLD with mW-level output power at room temperature for compact gas sensors.

JTu2A.29

Enhanced Performance of 450 nm GaN Laser Diodes with an Optical Feedback for High bit-rate Visible Light Communication, Md. Hosne Mobarok Shamim¹, Mohamed Shemis¹, Chao Shen², Hassan Oubei², Tien Khee Ng², Boon S. Ooi², Mohammed Khan¹; ¹*King Fahd Univ. of Petroleum & Mine, Saudi Arabia*; ²*King Abdullah Univ. of Science and Technology, Saudi Arabia*. First report on significant performance improvement of 450 nm blue edge-emitting laser in terms of optical linewidth (~6.5 times), modulation bandwidth (~16%) and SMSR (~7.4 times) by employing self-injection locking scheme.

JTu2A.30

Coupling in Densely Integrated Metallo-dielectric Nanolasers, Suruj Deka¹, Si Hui Pan¹, Qing Gu², Yeshiahu Fainman¹, Abdelkrim El Amili¹; ¹*Electrical and Computer Engineering, Univ. of California, San Diego, USA*; ²*Electrical Engineering, Univ. of Texas, USA*. We demonstrated coupling between two metallo-dielectric nanolasers using three-dimensional finite-element method simulations. Splits in resonant wavelength and quality factor were observed due to bonding and anti-bonding states. To prevent coupling, cavity resonances were slightly detuned.

JTu2A.31

Stabilization and jitter reduction in mode-locked quantum dash lasers by asymmetric dual-loop optical feedback, Haroon Asghar^{1,2}, Ehsan Sooudi^{1,2}, John McInerney^{1,2}; ¹*Univ. College Cork, Ireland*; ²*Tyndall National Inst., Ireland*. A novel asymmetric dual-loop configuration suppresses parasitic noise-resonances when single- and dual-loop optical feedback is used to stabilize mode-locked quantum-dash lasers at 1550 nm. Conditions for optimum suppression are determined and compared with published theory.

JTu2A.32

QoT estimation for Unestablished Lightpaths Using Artificial Neural Networks, Min Zhang¹, Dong Fu¹, Bo Xu¹, Baojian Wu¹, Kun Qiu¹; ¹*Univ of Electronic Science & Tech China, China*. Estimating the quality of transmission (QoT) for lightpaths is crucial for reducing provisioned margins. We investigate an artificial neural network framework to estimate the QoT of unestablished lightpaths considering interference effects and optical monitoring uncertainties.

JTu2A.34

Coherent Free-space/Fiber L-band Optical Communication using Self-Injection Locked InAs/InP Quantum-dash Laser, Mohamed Shemis¹, Emad Alkhazraji^{1,2}, Muhammed Talal Khan¹, Amr Ragheb³, Maged Esmail³, Habib Fathallah^{4,5}, Saleh Alshebeili^{3,4}, Mohammed Zayed Khan¹; ¹*Optoelectronics Research Lab, Electrical Engineering Dept., Saudi Arabia*; ²*Dept. of Electrical and Electronics Engineering Technology, Jubail Industrial College, Saudi Arabia*; ³*KACST-TIC in Radio Frequency and Photonics for the e-Society, Saudi Arabia*; ⁴*Electrical Engineering Dept., King Saud Univ., Saudi Arabia*; ⁵*Computer Dept. of the College of Science of Bizerte, Univ. of Carthage, Tunisia*. Demonstration of mid-L-band (~1602–1613nm) broadly tunable self-injection locked quantum-dash laser diode is reported with ~11nm tunability and ~30dB SMSR. Record 168(176) Gb/s DP-QPSK transmission over 10km SMF (16m FSO) link is achieved at ~1610nm.

JTu2A.35

Phase Noise of Diode Laser Frequency Comb and its Impact in Coherent Communication Systems, Mustafa A. Al-Qadi¹, Govind Vedala¹, Rongqing Hui¹; ¹*Univ. of Kansas, USA*. Phase noise performance of QD-based diode laser comb sources in coherent communication systems is reported. The performance results show that much higher linewidths can be tolerated compared to single frequency lasers, like DFB, due to unique phase noise characteristics.

JTu2A.36

Single-stage Phase-sensitive Amplifier Based Quadrature De-multiplexer for De-aggregating QAM Signals into In-phase and Quadrature Components, Jiabin Cui¹, Guo-Wei Lu^{2,3}, Hongxiang Wang¹, Lin Bai¹, Yuefeng Ji¹; ¹State Key Lab of Information Photonics and Optical Communications, School of Information and Communication Engineering, Beijing Univ. of Posts and Telecom., China; ²Inst. of Innovative Science and Technology, Tokai Univ., Japan; ³National Inst. of Information and Communications Technology (NICT), Japan. A single-stage phase-sensitive amplifier based quadrature de-multiplexer is proposed and validated for de-aggregating QAM signals into in-phase and quadrature components with wavelength and polarization preserved. A 10Gbaud 16QAM/64QAM is successfully de-aggregated into two PAM4s/PAM8s.

JTu2A.37

Few-Mode EDFA Based All-Optical Relaying System for Atmospheric Channels, Shanyong Cai¹, Zhiguo Zhang¹, Xue Chen¹; ¹Beijing Univ of Posts & Telecom, China. We present a scheme of all-optical relaying system based on few-mode erbium-doped fiber amplifier (EDFA) to resist turbulence for atmospheric channels with improved bit error rate.

JTu2A.38

Dual-phase-conjugation Coded Digital Multicarrier Transmission for Long-haul Coherent Optical Systems, Takahiro Kodama¹, Masanori Hanawa¹, Yamanashi Univ., Japan. A dual phase-conjugated multicarrier DP-QPSK system for chromatic dispersion and nonlinear tolerant transmission has been demonstrated. We show Q-factor improvement by balancing a nonlinear distortion over 10000 km SMF transmission with 6-dB worst case PDL.

JTu2A.39

512-Gbit/s PAM-4 Signals Direct-Detection using Silicon Photonics Receiver with Volterra Equalization, Yung Hsu¹, Chun-Yen Chuang¹, Liang-Yu Wei¹, Chi-Wai Chow¹, Xinru Wu², Hon Ki Tsang², Jyehong Chen¹, Chien-Hung Yeh³; ¹National Chiao Tung Univ., Taiwan; ²Dept. of Electronic Engineering, The Chinese Univ. of Hong Kong, Hong Kong; ³Dept. of Photonics, Feng Chia Univ., Taiwan. A 400-Gbit/s Ethernet (GbE) pulse-amplitude-modulation-4 (PAM-4) over 10-km single-mode-fiber (SMF) transmission direct-detected by an integrated silicon-photonics-receiver satisfying the IEEE P802.3bs requirement; and its feasibility to support 512-Gbit/s were illustrated.

JTu2A.40

2-Gbit/s Visible Light Modulation Using GaN-Based Photonic Crystal Light-Emitting Diodes without Pre- and Post-Emphasis, Zi-Xuan You¹, Tung-Ching Lin¹, Yu-Feng Yin¹, Yung-Tsan Chen¹, Hsuan-Yun Kao¹, Cheng-Yi Huang¹, Yu-Hong Lin¹, Jian-Jang Huang¹; ¹National Taiwan Univ., Taiwan. Recently, GaN based light-emitting diodes (LEDs) have become a promising candidate for visible light communication (VLC). In this work, we demonstrated 2-Gbit/s data rate transmission using GaN-based LEDs with photonic crystal (PhC) structure.

JTu2A.41

Set-Partitioned QAM Fast-OFDM with Real-Valued Orthogonal Circulant Matrix Transform Pre-Coding, Zhouyi Hu¹, Jian Zhao², Yang Hong¹, Shuang Gao¹, Chun-Kit Chan¹, Lian-Kuan Chen¹; ¹The Chinese Univ. of Hong Kong, Hong Kong; ²Tyndall National Inst. and Univ. College Cork, Ireland. We propose SP-QAM based Fast-OFDM with a novel real-valued OCT pre-coding scheme for IM/DD systems. For 19.76-Gbit/s 20-km transmission, the proposed scheme achieves 3.5-dB sensitivity improvement and higher filtering tolerance over conventional PAM Fast-OFDM.

JTu2A.42

Multi-Format and Low-Complexity Carrier Phase Estimation Scheme Based on Linear Approximation for Elastic Optical Networks, Yang Tao¹, Chen Shi², Xue Chen¹, Lijian Wang¹, Huan Chen¹; ¹Beijing Univ of Posts & Telecom, China; ²Iowa State Univ., USA. We propose an innovative multi-format CPE scheme outperforming existing CPEs in both performance and complexity for m-QAM formats in elastic optical networks. Simulation and experimental results demonstrate its effectiveness, flexibility and excellent linewidth tolerance.

JTu2A.43

Towards 400Gb/s Data Center Interconnect Using Coherent Detection with Higher-Order QAM Formats, Xuan He¹, Yang Yue¹, Qiang Wang¹, Andre Vovan¹, Jon Anderson¹; ¹Juniper Networks, USA. We experimentally studied the capacity-reach matrix for single-carrier high baud rate x-QAM signals in unamplified link. We show that 400Gbit/s (64GBd 16-QAM) can be achieved over 80 km link, potentially for data center interconnect application.

JTu2A.44

Machine Learning Enabling Traffic-Aware Dynamic Slicing for 5G Optical Transport Networks, Chuang Song¹, Min Zhang¹, Xuetian Huang², Yueying Zhan³, Danshi Wang¹, Min Liu¹, Yanhong Rong¹; ¹State Key Lab of Information Photonics and Optical Communications, Beijing Univ. of Posts and Telecom., China; ²China Telecom Corporation, China; ³Technology and Engineering Center for Space Utilization, Chinese Academy of Science (CAS), China. We demonstrate a machine-learning-based traffic-aware approach for dynamic network slicing in optical networks. Experimental results indicate that the proposed framework achieves 96% traffic prediction accuracy, 49% blocking reduction and 29% delay reduction compared with conventional solutions.

JTu2A.45

Silicon Photonic Deserialization for Energy Efficient Links, Nathan Abrams¹, Robert Polster¹, Michail Oikonomou¹, Liang Yuan Dai¹, Keren Bergman¹; ¹Columbia Univ., USA. We develop a novel optical deserialization system in silicon photonics to reduce electrical deserialization power consumption and improve receiver sensitivity. Results demonstrate a path to increasing receiver sensitivity by 2.5 dB with improved modulators.

JTu2A.46

Reduced Complexity Interleaved Multi-Carrier CDMA for Passive Optical Networks, Abdallah M. Abdelaziz¹, Mostafa Khalil¹, mohamed El-Shimy¹, Masoud Alghoniemy¹, Hossam M. Shalaby^{1,2}; ¹Electrical Engineering, Alexandria Univ., Egypt; ²Egypt-Japan Univ. of Science and Technology (E-JUST), Egypt. A reduced complexity interleaved multi-carrier CDMA technique is proposed for passive optical networks (PONs). The proposed technique provides performance improvement compared to traditional O-OFDMA with less complexity than MC-CDMA.

JTu2A.47

RSOP Equalization through an Extend Kalman Filter Scheme in Stokes Vector Direct Detection System, Qisong Shang¹, Zibo Zheng¹, Nan Cui¹, Nannan Zhang¹, Wenbo Zhang¹, Hengying Xu^{1,2}, Xianfeng Tang¹, Lixia Xi¹, Xiaoguang Zhang¹; ¹Beijing Univ of Posts & Telecom, China; ²Liaocheng Univ., China. A new scheme for RSOP equalization in Stokes Vector Direct Detection (SV-DD) is proposed. The scheme is using Extended Kalman Filter (EKF) to tracking and compensation, which has a good performance in fast dynamic RSOP.

JTu2A.48

Cost-effective Demultiplexing Scheme for Two PDM-PAM4 Joint IM/DD Links Utilizing Stokes Receiver, Yan Pan¹, Lianshan Yan¹, Anlin Yi¹, Lin Jiang¹, Wei Pan¹, Bin Luo¹; ¹Southwest Jiaotong Univ., China. We propose a cost-effective demultiplexing scheme for two PDM-PAM4 signals in IM/DD system based on a single Stokes receiver. About 1-dB power penalty is observed after 25-km NZDSF transmission at 160-Gbit/s data rate.

JTu2A.49

Fine and Coarse Tunability over a Continuous 8.1-ns Delay Range with Access to Multiple Possible Delays using a Frequency Comb, Ahmed Almainan¹, Yinwen Cao¹, Amirhossein Mohajerin Ariaei¹, Fatemeh Alishahi¹, Ahmad Fallahpour¹, Dmitry Starodubov¹, Kaiheng Zou¹, Peicheng Liao¹, Changjing Bao¹, Shlomo Zach², Nadav Cohen², Moshe Tur², Alan E. Willner¹; ¹Univ. of Southern California, USA; ²School of Electrical Engineering, Tel Aviv Univ., Israel. A continuous delay range of 8.1 ns is achieved with simultaneous access to four different delays. Our system's penalty is ~2 dB for a 10 Gbaud QPSK signal. We also add a HNLF to convert one of the delays to the original wavelength, adding ~0.3 dB penalty.

JTu2A.50

A Cost-Effective demodulator for the Next Generation of Optical Access Networks Receivers, Ana R. Bastos¹, Ali Shahpari¹, Luis D. Carlos², Mário Lima¹, Paulo S. Andre¹, Maria R. Ferreira²; ¹Instituto de Telecomunicacoes, Portugal; ²CICECO, Portugal. We introduce a cost-effective organic-inorganic hybrid photonic integrated circuit suitable for coherent access networks and demonstrate a 3.5±0.3 dB power penalty, relatively to back-to-back, for 20 Gb/s QPSK transmission over 40 km of G.652 fiber.

JTu2A.51

Programmable sub-harmonic optical clock recovery based on dispersion-induced inverse temporal self-imaging, Jinwoo Jeon¹, Reza M. Qartavol¹, James van Howe², Jose Azana¹; ¹INRS-Energie Materiaux et Telecom, Canada; ²Dept. of Physics and Astronomy, Augustana College, USA. We propose and experimentally demonstrate the first design of a fiber-optics programmable base/sub-harmonic optical clock recovery circuit, involving a phase modulator and linear dispersion, in which the rate division factor can be electrically reconfigurable.

JTu2A.52

Impact of differential group-velocity dispersion on intermodal four-wave mixing in few-mode fibers, Georg Rademacher¹, Ruben S. Luis¹, Benjamin Puttnam¹, Hideaki Furukawa¹, Yoshinari Awaji¹, Naoya Wada¹, Ryo Maruyama², Kazuhiko Aikawa²; ¹National Inst of Information & Comm Tech, Japan; ²Fujikura Ltd, Japan. We investigate the impact of differential group-velocity dispersion between modes of a few-mode fiber on intermodal four-wave mixing. We find that differences of the chromatic dispersion lead to a reduced bandwidth with full phase-matching.

JTu2A.53

Enhancing the Performance of an Optical High-Order QAM Communication Channel by Adding Correlated Data to Robust Neighboring Channels in a Heterogeneous Network, Yinwen Cao¹, Kaiheng Zou¹, Ahmed Almainan¹, Amirhossein Mohajerin Ariaei¹, Changjing Bao¹, Peicheng Liao¹, Fatemeh Alishahi¹, Ahmad Fallahpour¹, Alan E. Willner¹; ¹Univ. of Southern California, USA. An enhanced high-order QAM communication using data correlation with neighboring channels is demonstrated. The effectiveness of this approach is verified by using 10-Gbaud 4/16/64/256-QAM channels in simulation and 5/10-Gbaud 16-QAM channels in experiment.

JTu2A.54

Single-Source Duplex High-Speed FSO Communications Using Electro-Optic Modulator-Based MRR, Xianglian Feng¹, Hexin Jiang¹, Zhihang Wu¹, Tianshu Wang², Hongwei He¹, Shiming Gao¹; ¹Zhejiang Univ., China; ²Changchun Univ. of Science and Technology, China. A single-source 10 Gb/s duplex free-space optical communication is demonstrated using electro-optic modulator-based modulating retro-reflector. The power penalty is <2.3 (8.0) dB for downlink DPSS (uplink OOK) signal at 1×10⁻³ BER in an atmospheric cell.

JTu2A.55

Nyquist-WDM Super-Channel Using an On-Chip Frequency Comb enabled by a Silicon Dual-drive MZM, Jiachuan Lin¹, Yelong Xu¹, Hassan Sepehrian¹, Leslie A. Rusch¹, Wei Shi¹; ¹Université Laval, Canada. We experimentally generate a 20 GHz spaced 5-line comb using a silicon modulator, with good performance to support 16Gbaud 32QAM and 20Gbaud 16QAM, aggregating net rates of 667 Gb/s and 747 Gb/s.

JTu2A.56

Terabit optical OFDM data transmission carried by coherent Kerr soliton frequency comb lines, Xiaotao Huang¹, Yong Geng¹, Wenwen Cui¹, Yun Ling¹, Xingwen Yi¹, Baojian Wu¹, Kun Qiu¹, Shu-Wei Huang³, Chee Wei Wong², Heng Zhou¹; ¹Univ of Electronic Science & Tech China, China; ²Univ. of California, Los Angeles, USA; ³Dept. of Electrical, Computer, and Energy Engineering, Univ. of Colorado, Boulder, USA. We demonstrate seamless multiplexing of 180-channel optical-orthogonal-frequency-division-multiplexing utilizing dissipative Kerr soliton microcomb aided by sinc-pulse modulation. Mutual coherence among Kerr comb lines is exploited for the first time to achieve 6.885 Tb/s data transmission.

JTu2A.57

2¹⁴ (=16,384) Level Intensity Modulation at 10 Gbaud for Y-00 Quantum Stream Cipher, Ken Tanizawa¹, Fumio Futami¹; ¹Tamagawa Univ., Japan. Coarse-to-fine driving of an MZI is proposed for multilevel intensity modulation beyond a resolution limit of a D/A converter. We demonstrate noise masking with record-high 2¹⁴ (=16,384) intensity levels in 10-Gbaud Y-00 quantum stream cipher.

JTu2A.58

192-Gbit/s PAM-4 Optical Interconnect using Mode-Division Multiplexing, Yung Hsu¹, Xinru Wu², Chun-Yen Chuang¹, Chi-Wai Chow¹, Hon Ki Tsang², Jyehong Chen¹, Chien-Hung Yeh²; ¹National Chiao Tung Univ., Taiwan; ²Dept. of Electronic Engineering, The Chinese Univ. of Hong Kong, Hong Kong; ³Dept. of Photonics, Feng Chia Univ., Taiwan. 192-Gbit/s pulse-amplitude-modulation-4 (PAM-4) signal transmission for on-chip optical interconnects using mode-division-multiplexing (MDM) is experimentally investigated. 3 channels are successfully mode multiplexed and de-multiplexed satisfying the forward-error correction (FEC) requirement.

JTu2A.59

Third-Order Nonlinear Optical Coefficients of Si and GaAs in the Near-Infrared Spectral Region, Joel M. Hales^{2,3}, San-Hui Chi¹, Taylor Allen¹, Sepehr Benis⁴, Natalia Munera⁴, Joseph W. Perry¹, Dale McMorrow², David J. Hagan⁴, Eric W. Van Stryland²; ¹Georgia Inst. of Technology, USA; ²Naval Research Lab, USA; ³Sotera Defense Solutions, USA; ⁴Univ. of Central Florida, USA. The third-order optical nonlinearities of Si and GaAs have been characterized throughout the near-infrared spectral region (1.1–2 μm) using multiple ultrafast spectroscopic techniques. These results have been independently confirmed at two different Labs.

JTu2A.60

Stable, high-average-power, narrow-linewidth source at 2.1 μm pumped at 1.064 μm, Biplob K. Nandy², Hanyu Ye², Chaitanya Kumar Suddapalli^{1,2}, Majid Ebrahim-Zadeh^{2,3}; ¹Radiantis, Spain; ²ICFO-The Inst. of Photonic Sciences, Spain; ³Instituto Catalana de Recerca i Estudis Avancats (ICREA), Passeig Lluís Companys 23, Spain. We report stable, narrow-bandwidth operation of nanosecond degenerate OPO at 2.1 μm, for the first time, generating >2 W of average power in good beam-quality (M²<3.7) and passive power-stability of 0.6% rms over 1 hour.

JTu2A.61

Compact Femtosecond Optical Parametric Oscillator Based on an Integrated Fibre Retroreflector, Callum F. O'Donnell^{1,2}, Chaitanya Kumar Suddapalli¹, Therese Paoletta², M. Ebrahim-Zadeh²; ¹Radiantis, Spain; ²ICFO - Institut de Ciències Fotòniques, Spain. We report a compact femtosecond optical parametric oscillator based on MgO:PPLN, incorporating an integrated-mirror, single-mode fibre-feedback loop, generating up to 50 mW across 1128–1243 nm and 1358–1600 nm, and exhibiting interesting spectral features.

JTu2A.62

Broadband Comb Upconversion in an Apodized Step-Chirped PPLN Waveguide for the Quantum Memories, Susu He¹, Yoo Seung Lee¹, Hao Liu¹, Jinghui Yang¹, Chee Wei Wong¹; ¹UCLA, USA. We present theoretical modeling and characteristics of an apodized step-chirped PPLN waveguide for efficient and uniform broadband upconversion from 1580-nm comb to ~984-nm comb with a 3dB bandwidth of 48.6-nm to interface with rare-earth solid-state quantum memories.

JTu2A.63

Four-Wave Mixing in Highly Nonlinear Chalcogenide Glass-in-Silica Waveguides, Moshe Katzman¹, Dvir Munk¹, Mirit Hen¹, Arik Bergman¹, Mark Oksman¹, Yuri Kaganovskii¹, Michael Rosenbluh¹, Avi Zadok¹; ¹Bar-Ilan Univ., Israel. Highly nonlinear waveguides are fabricated through deposition of chalcogenide glass into pre-patterned trenches in a silica cladding. No processing of the chalcogenide glass is required. Four-wave mixing is demonstrated with nonlinear coefficient of 6.5±1 [W*²m]⁻¹.

JTu2A.64

All-optical Wavelength Conversion of Phase-encoded Signals in Silicon-rich Silicon Nitride Waveguides, Cosimo Lacava¹, Stuart May², David Richardson¹, Graham T. Reed¹, Marc Sorel², Periklis Petropoulos¹; ¹Univ. of Southampton, UK; ²Univ. of Glasgow, UK. We show the design and characterization of a silicon-rich silicon nitride-based all-optical wavelength converter, for phase-encoded signals. We demonstrate successful conversion of a 40 Gb/s 16-QAM signal with negligible penalty and no-signs of TPA.

JTu2A.65

Millijoule single-cycle angularly dispersed optical parametric amplifier, Xiao Zou^{2,1}, Houkun Liang², Shizhen Qu^{2,1}, Kun Liu^{2,1}, Cheng Liu^{2,1}, Qijie Wang¹, Ying Zhang²; ¹Nanyang Technological Univ., Singapore; ²Singapore Inst. of Manufacturing Technology, Singapore. We propose an angularly dispersed optical parametric amplifier to compensate the phase mismatch over 1.3–4.1 μm, and generate carrier-envelope phase stable, millijoule, ~1.1 cycle pulses centered at 2 μm wavelength.

JTu2A.66

Controlling Brillouin-Induced Optical Delay via Four-Wave-Mixing Bragg Scattering, Ning Zhang¹, Xuelei Fu², Jie Liu¹, Chester Shu¹; ¹The Chinese Univ. of Hong Kong, Hong Kong; ²School of Information Engineering, Wuhan Univ. of Technology, China. To rapidly tune the Brillouin-induced optical delay, we perform vector sum of Brillouin-delayed pulse with non-delayed pulse through four-wave-mixing (FWM) Bragg scattering. Output pulse delay is effectively amplified and tuned by controlling FWM pump power.

JTu2A.67

Tunable, Multi-Milliwatt, Continuous-Wave Difference-Frequency-Generation Across 4.6–4.7 μm Based on Orientation-Patterned GaP, Kavita Devi¹, Anuja Padhye¹, Peter G. Schunemann², M. Ebrahim-Zadeh^{1,3}; ¹ICFO - The Inst. of Photonic Sciences, Spain; ²BAE Systems, Inc., USA; ³Instituto Catalana de Recerca i Estudis Avancats (ICREA), Spain. We report the first realization of tunable continuous-wave difference-frequency generation across 4608–4694 nm in OP-GaP, with maximum power of 43 mW at 4608 nm and passive power stability of 2.5% rms (1.5 mins), in good beam quality.

JTu2A.68

Characterization of the Impact of β₂ and β₃ in Four-Wave Mixing Optical Time Lenses using Input-Output Cross-Correlations, Frederik Klejs¹, Mads Lilliehölm¹, Michael Galili¹, Leif K. Oxenlowe¹; ¹DTU, Denmark. We propose the use of input-output cross correlations to quantify the performance of four-wave mixing time lenses with dispersion-induced degradation. The impact of dispersion variations is investigated.

JTu2A.69

Stable UV-extended Supercontinuum Generation in Bulk Material by Picosecond Pulses, Veselin Aleksandrov^{1,2}, Anton Trifonov^{1,2}, Velizar Stoyanov¹, Kaloyan Georgiev¹, Ivan C. Buchvarov¹; ¹Physics Dept., Sofia Univ. "St. Kliment Ohridski", Bulgaria; ²IBPhotonics Ltd., Bulgaria. Stable UV-extended supercontinuum generation by self-action of picosecond pulses in bulk materials is demonstrated. The stability and spectral properties of the continuum show a strong dependence on the focusing parameters in 120-mm long CaF₂ rod.

JTu2A.70

Harmonic Generation in Cascaded Raman Fiber Lasers, Santosh Aparanji¹, V Balaswamy¹, S Arun¹, V R Supradeepa¹; ¹Indian Inst. of Science, India. We report the surprising observation of visible harmonics in an infrared cascaded Raman fiber laser. A transition from 2nd to 3rd harmonic is seen with increasing locally propagating wavelengths, which we attribute to Cherenkov-type phase-matching.

JTu2A.71

Characterization of linear and nonlinear carrier generation in silicon nano-waveguides at 1550 nm, Andres Gil-Molina^{1,2}, Ivan A. Aldaya^{1,3}, Julian L. Pita², Lucas Gabrielli², Hugo Fragrino^{1,4}, Paulo C. Dainese¹; ¹Inst. of Physics, Univ. of Campinas, Brazil; ²School of Electrical Engineering, Univ. of Campinas, Brazil; ³State Univ. of Sao Paulo, Brazil; ⁴Mackgrahpe, Mackenzie Presbyterian Univ., Brazil. We characterize the generation of free-carriers in a silicon strip nano-waveguide at 1550nm performing pump-and-probe measurements. Compared with bulk silicon, we identified a higher effective two-photon absorption coefficient and a significant carrier-generation via single-photon absorption.

JTu2A.72

Characterization of Ultra-High-Q Si₃N₄ Micro-Ring Resonators with High-Precision Temperature Control, Paul Kaufmann¹, Xingchen Ji², Kevin Luke², Alexander L. Gaeta³, Michal Lipson², Sven Ramelow¹; ¹Institut für Physik, Humboldt Universität zu Berlin, Germany; ²Dept. of Applied and Engineering Physics, Columbia Univ., USA; ³Dept. of Applied Physics and Applied Mathematics, Columbia Univ., USA. We observe ultra-high Q-factors in Si₃N₄ micro-ring resonators exceeding 2×10⁸ at 850 nm. We characterize them with a novel method harnessing high-precision temperature scanning and determine their thermal tuning coefficient with an uncertainty of only 4 MHz/K.

JTu2A.73

PbO-based ultrafast fiber lasers, Yufeng Song¹, Chenyang Xing¹, Yunxiang Chen¹, Han Zhang¹; ¹Shenzhen Univ., China. A novel 2D material PbO was used as saturable absorber in a fiber laser. Passive mode locking pulse was as short as 850 fs. Passive Q-switching pulse is repetition tunable from 20kHz–50kHz. This finding suggests that PbO could be developed as a device in the applications of optical communication.

JTu2A.74

Measurement of Constant Power Contours for Dissipative Kerr Solitons, Xinbai Li^{2,1}, Boqiang Shen², Heming Wang², Ki Youl Yang², Xu Yi², Qifan Yang², Zhiping Zhou¹, Kerry Vahala²; ¹Peking Univ., China; ²Applied physics and materials science, California Inst. of Technology, USA. Dissipative Kerr solitons are generated within an existence region of pumping power versus cavity-pump detuning frequency. By comparing modeling with measurement in microcavities, the contours of constant soliton power are studied within this existence region.

JTu2A.75

Adaptive Wavefront Control for Optimized Coherent Raman Multi-sideband Generation, Mariia Shutova¹, Anton Shutov¹, Jonathan Thompson¹, Alexandra A. Zhdanova¹, Alexei V. Sokolov¹; ¹*Inst. for Quantum Science and Engineering, Dept. of Physics and Astronomy, Texas A&M Univ., USA*. We demonstrate that the wavefront optimization algorithm with feedback loop allows the extension of the total bandwidth of coherent Raman sidebands towards UV wavelengths, which will provide broader bandwidths for subcycle UV-VIS-NIR pulse synthesis.

JTu2A.76

Breather solitons dynamics and period-doubling transitions in 19 GHz microresonator frequency combs, Wenting Wang¹, Abhinav K. Vinod¹, Jinghui Yang¹, Mingbin Yu², Dim-Lim Kwong², Chee Wei Wong¹; ¹*Univ. of California, Los Angeles, USA*; ²*Inst. of Microelectronics, Singapore*. We observed breather soliton dynamics and period-doubling transitions in 19 GHz dispersion-engineered dissipative microresonator frequency combs. The low-noise comb breather frequency is deterministically controlled via effective pump detuning with 18 kHz/MHz slope efficiencies.

JTu2A.77

Hybrid Silicon-Nitride / Polymer Waveguide for Nonlinear-Optics Applications, Subrata Das¹, Brett R. Wenner², Jeffery W. Allen³, Monica S. Allen³, Michael Vasilyev¹; ¹*Univ. of Texas at Arlington, USA*; ²*Air Force Research Lab Sensors Directorate, USA*; ³*Air Force Research Lab Munitions Directorate, USA*. We describe a hybrid silicon-nitride / polymer slot waveguide for generation of second harmonic of a 1550 nm beam. Modal phase-matching and optimized geometry yield order-of-magnitude improvement over a channel waveguide.

JTu2A.78

Efficient tuning of second-harmonic generation in a lithium niobate nanophotonic waveguide, Rui Luo¹, Yang He¹, Hanxiao Liang¹, Mingxiao Li¹, Qiang Lin¹; ¹*Univ. of Rochester, USA*. We report flexible spectral tuning of second-harmonic generation in a lithium niobate nanophotonic waveguide, with a thermal tuning slope of 0.84 nm/K for a telecom pump, by utilizing the significant thermo-optic birefringence of lithium niobate.

JTu2A.80

Distributed Monitoring of Cascaded Four-Wave Mixing due to Kerr and Opto-Mechanical Nonlinearities, Hilel Hagai Diamandi¹, Yosef London¹, Gil Bashan¹, Avi Zadok¹; ¹*Bar-Ilan Univ., Israel*. Distributed monitoring of cascaded four-wave processes along an optical fiber is performed using a multi-tone optical time-domain reflectometry setup. The interplay between Kerr nonlinearity and guided acoustic waves Brillouin scattering is observed.

JTu2A.81

Continuous-Time Electro-Optic PLL with Decimated Optical Delay/Loss and Spur Cancellation for LIDAR, Jahnvi Sharma¹, Sohail Ahasan¹, Christopher T. Phare¹, Michal Lipson¹, Harish Krishnaswamy¹; ¹*Electrical Engineering, Columbia Univ., USA*. Current EO-PLLs for laser chirp modulation require large, lossy delay waveguides in an MZI to detect chirp slope. EO-PLLs, and electronic control loops generally, are dominantly digital. A new analog EO-PLL breaks the trade-off between chirp bandwidth and MZI delay, reducing area and loss by 10x.

JTu2A.82

Absorption-enhanced Imaging through Scattering Medium, Mehbuba Tanzid¹, Ashok Veeraraghavan¹, Naomi Halas¹; ¹*Rice Univ., USA*. Using carbon-black absorbers, we show 80% image resolution-enhancement in isotropic polystyrene medium, compared to only 8% in a forward-scattering-medium. Subsequently, by increasing imaging wavelength from visible to NIR, resolution-enhancement for the forward-scattering-medium is increased (4x).

JTu2A.83

A Compact and Portable Laser Radioactive Decontamination System Using a Fiber Laser and a Polygon Scanner, Yu-Chieh Lin¹, Yen-Yin Lin¹, An-Chung Chiang¹; ¹*National Tsing Hua Univ., Taiwan*. We designed a compact and portable laser radioactive decontamination system using a fiber laser and a polygon scanner. By varying the spinning speed of the polygon mirror, we achieved a processing speed exceeding 88500 mm/s.

JTu2A.84

Level-set Fabrication Constraints for Gradient-based Optimization of Optical Devices, Dries Verduyck^{1,2}, Logan Su¹, Rahul Trivedi¹, Neil V. Saprà¹, Alexander Y. Piggott¹, Jelena Vuckovic¹; ¹*Stanford Univ., USA*; ²*KU Leuven, Belgium*. When designing integrated optical devices, fabrication constraints need to be satisfied. We present an analytical constraint for level-set parameterizations that limits the gap/feature size and can be combined with higher order gradient-based optimization algorithms.

JTu2A.85

Kerr-comb generation in a dispersion engineered coupled thin silicon nitride microresonators, Ali Eshaghian Dorche¹, Ali Asghar Eftekhari¹, Ali. Adibi¹; ¹*Georgia Inst. of Technology, USA*. We numerically demonstrate the first wideband Kerr-comb generation at telecommunication wavelength (1550 nm) using thin silicon nitride platform based on coupled-resonator for dispersion engineering.

JTu2A.86

Silicon Nitride Grating Couplers with High Efficiency and Wide Bandwidth, Chi Xu¹, Mercedesh Khajavikhan¹, Patrick LiKamWa¹; ¹*Creol, Univ. of Central Florida, USA*. A grating coupler for coupling vertically emitted laser light into planar silicon nitride waveguides is presented. The waveguide coupling efficiency was measured at 30% with a 3-dB bandwidth of 100 nm using an optical fiber.

JTu2A.87

Long-Term Stable Operation of Coherent Ising Machine for Cloud Service, Toshimori Honjo¹, Takahiro Inagaki¹, Kensuke Inaba¹, Takuya Ikuta¹, Hiroki Takesue¹; ¹*NTT Basic Research Labs, Japan*. A 24-hour stable operation of a coherent Ising machine, an Ising model solver based on a network of degenerate optical parametric oscillators, was successfully demonstrated. The average success probability of computation exceeds 94%.

JTu2A.88

Sub-500 fs pulses from a hybrid architecture for high energy lasers, Damien Sangla¹, Pierre Sevilano¹, Jean-Gabriel Brisset¹, Magali Durand¹, Olivier Alexaline¹, Antoine Courjaud¹; ¹*Amplitude Systemes, France*. An hybrid architecture for high energy laser is presented, based on Yb:CaF₂ regenerative amplifier and Yb:YAG thin-disk multipass amplifier at room temperature delivering pulses 74 mJ with a 450 fs duration at 100 Hz.

JTu2A.89

Multiplexed static FBG strain sensors by dual-comb spectroscopy with a free running fiber laser, Jingjing Guo¹, Yihang Ding¹, Xiaosheng Xiao¹, Lingjie Kong¹, Changxi Yang¹; ¹*Tsinghua Univ., China*. We demonstrate a novel FBG sensor system by dual-comb spectroscopy with a single fiber laser cavity, which enables interrogation of multiplexed FBG strain sensors with 0.5 μe resolution in a large dynamic range of 520 μe .

JTu2A.90

Laser induced thermomechanical cracking for fatigue life determination of coated steel, Jeffrey Warrender¹, Gregory Vigilante¹; ¹*US Army, ARDEC RDECOM, USA*. A pulsed Yb fiber laser was used to irradiate steel coated with chromium to induce thermomechanical cracks; the resultant part showed a reduced fatigue life. This provides a path to accelerated fatigue tests.

JTu2A.91

Ti/TaN Bilayer for Efficient Injection and Reliable AlGaIn Nanowires LEDs, Davide Priante¹, Bilal Janjua², Aditya Prabaswara¹, Ram Chandra Subedi¹, Rami Elafandy¹, Sergei Lopatin¹, Dalaver Anjum¹, Chao Zhao¹, Tien Khee Ng¹, Boon S. Ooi¹; ¹*KAUST, Saudi Arabia*; ²*Univ. of Toronto, Canada*. Reliable operation of UV AlGaIn-based nanowires-LED at high injection current was realized by incorporating a Ti-pre-orienting/TaN-diffusion-barrier bilayer, thus enhancing external quantum efficiency, and resolving the existing device degradation issue in group-III-nanowires-on-silicon devices.

JTu2A.92

High efficiency continuous-wave Ti:sapphire laser, Tomoki Kanetake¹, Kesuke Hayashi¹, Motoki Morioka¹, Shunji Kataoka¹, Hiroki Kadoya¹, Toru Sato¹, Naoya Nakajima¹, Fumihiko Sugiki¹, Ryo Kobayashi¹, Sakae Kawato¹; ¹*Univ. of Fukui, Japan*. Highest efficiencies of CW-Ti:sapphire laser were obtained by using the high gain architecture. The maximum optical-to-optical conversion efficiency and slope efficiency are 31.7% and 41.9% for the incident pump power, respectively.

JTu2A.93

Hotspot Detection in Integrated Circuits by Two-photon fluorescence-based Thermal Microscope, Ming-Che Chan¹, Guan-Yu Zhuo², ZuPo Yang¹; ¹*Inst. of Photonic System, Taiwan*; ²*Inst. of Medical Science and Technology, National Sun Yat-sen Univ., No. 70, Lienhai Rd, Taiwan*. For thermal images and related hotspot diagnosis on integrated circuits (ICs) during operation, we present a high temporal, spatial, and temperature resolution thermal microscope based on the thermal-optical properties of R6G thin film.

JTu2A.94

Full ocular biometry through dual-depth whole-eye optical coherence tomography, Hyung-Jin Kim¹, Minji Kim¹, Min Gyu Hyeon¹, Youngwoon Choi¹, Beop-Min Kim¹; ¹*Korea Univ., South Korea*. There are important geometric parameters in a human eye including three major axes and two angles between them. It is known that identification of those parameters may be helpful when performing some ophthalmic surgeries. We propose a new method to measure them using dual-depth whole-eye OCT.

JTu2A.95

Diffraction-free, Self-reconstructing Bessel beam generation using thermal nonlinear optical effect, qian Zhang¹, xue m. cheng¹, zhaoyu ren¹, hao w. chen¹, bo he¹, ying Zhang², jintao bai¹; ¹*Northwest Univ., China*; ²*School of Science, Engineering Univ. of PAP, China*. We propose a method to generate Bessel beam based on thermal nonlinear optical effect without the restriction to the laser wavelength. And the beam generated demonstrates superior non-diffraction and self-reconstruction properties.

JTu2A.96

Optical System for Multi-Channel Real-Time PCR, Sangheon Kim^{1,2}, Sunjak Choi^{1,3}, Yeji Lee^{1,3}, Sangyoon Jung³, Minhyoung Jung³, Jieun Baek³, Hyeonuk Sim³, Donghyun Kang³, Junho Lee¹; ¹*Korea Electronics Technology Inst., South Korea*; ²*Korea Univ., South Korea*; ³*Gachon Univ., South Korea*. Optical module for multi-channel real-time PCR detection system is designed and implemented. By using hyperspectral band-pass filter integrated on CMOS photo sensor, Multi-channel optical fluorescence excitation and detection system are realized in experiments.

JTu2A.97

Optical fluorescence to assess abnormal tryptophan metabolic activity in brain samples from Alzheimer's patients, Laura Sordillo^{1,2}, Lin Zhang¹, Lingyan Shi^{1,3}, Vidyasagar Sriramamoji¹, Peter Sordillo¹, Robert Alfano^{1,2}; ¹physics and electrical engineering, CCONY, USA; ²electrical engineering, grove school of engineering, USA; ³chemistry, columbia Univ., USA. Brain samples from Alzheimer's patients and aged-matched controls were studied using label-free fluorescence. Increased tryptophan metabolite to tryptophan ratios were seen in the hippocampus and Brodmann's area 9 in Alzheimer's patients as compared to normal.

JTu2A.98

Dermis-simulating phantom for noninvasive blood glucose sensing with OCT, Guoqing Yang¹, Xiaotian S. Yao^{1,2}, Ya Su¹, Suling Liu¹, Ting Feng¹, Lei Chen¹, Hongjie Wang¹, Wenping Li¹; ¹Hebei Univ., China; ²General Photonics Corporation, USA. We developed a tissue phantom to mimic the optical properties of dermis layer and expect that it may serve as a useful tool to evaluate and standardize the theoretical model of noninvasive blood glucose sensing.

JTu2A.99

SVM Based Automatic Classification of Human Stomach Cancer with Optical Coherence Tomography Images, Site Luo¹, Yingwei fan¹, Hao Liu², Huikai Xie³, Peng Li⁴, Hongen Liao¹, Li Huo¹, Xin An⁵; ¹Tsinghua Univ., China; ²South China Medical Univ., China; ³Dept. of Electrical and Computer Engine, Univ. of Florida, USA; ⁴Shenzhen Moptim Imaging Technique, China; ⁵Foshan Optomedic Technologies, China. Classification is carried out by SVM and human with 1539 normal and 1567 cancerous OCT images. Accuracy, sensitivity and specificity of human are 82.8%, 73.9%, 93.5%, and that of SVM are 91.3%, 95.3%, 87.2%.

JTu2A.100

Quantitative Analysis of Keratinocytes in Human Skin Using Full-Field Optical Coherence Tomography, Chia-Kai Chang¹, Sheng Lung Huang¹; ¹National Taiwan Univ., Taiwan. The three-dimensional spatial distribution and morphometry of the keratinocytes of *in vivo* human skin are analyzed quantitatively using the full-field optical coherence tomography. The depth dependent volume and ellipticity of the keratinocyte nuclei are extracted.

JTu2A.101

In Depth Flow Inspection based on Spatial Analysis of Dynamic Laser Speckle, Mark Golberg², Ran Califa², Sagi Polani², Javier G. Monreal², Zeev Zalevsky²; ²ContinUse Biometrics Ltd., Israel. A novel optical approach based on statistical analysis of spatial laser speckle pattern for tissue in-depth flow characteristics is presented. Properties such as flow orientation and speed can be estimated. In-vitro experimental results are demonstrated

JTu2A.102

Laser Speckle Contrast Imaging under the breaking ergodicity conditions for intravital visualization of brain vasculature, Anton U. Sdobnov¹, Alexander Bykov¹, Vyacheslav Kalchenko², Guillaume Molodij², Alexey Popov¹, Igor Meglinski¹; ¹Univ. of Oulu, Finland; ²Weizmann Inst. of Science, Israel. In current study, the laser speckle contrast imaging has been considered at different ergodicity conditions with a final aim of accurate and valid quantitative assessment and intravital visualization of brain vasculature and blood flow.

JTu2A.103

Endoscopic optical coherence tomography probe with large scan range, Site Luo¹, Donglin Wang², Hao Liu³, Hui Zhao⁴, Huikai Xie⁵, Li Huo¹; ¹Tsinghua Univ., China; ²School of Physics and Electronic Engineering, Zhengzhou Univ. of Light Industry, China; ³South China Medical Univ., China; ⁴Foshan Optomedic Technologies, China; ⁵Dept. of Electrical and Computer Engine, Univ. of Florida, USA. A novel miniature endoscopic OCT probe with a diameter of 2.5 mm, scan a large range of 6 mm based on electric-thermal microelectro-mechanical system (MEMS) and C-lens.

JTu2A.104

Label Free Imaging of Endogenous Chromophore in Biological Tissues with High Speed Photothermal Microscopy, Jun Miyazaki¹, Yuya Ishikawa¹, Takayoshi Kobayashi²; ¹Wakayama Univ., Japan; ²Advanced Ultrafast Laser Research Center, The Univ. of Electro-Communications, Japan. A high-sensitivity and high-speed photothermal microscope was developed with a new detection scheme. The system demonstrates label free imaging of endogenous chromophores in brain and skeletal muscle with the image acquisition time of 0.76 s.

JTu2A.105

Seed-Based Hemodynamic Connectivity Mapping to Analyze the Effect of Hemi-Parkinson's Disease using NIR Imaging, Seung-ho Paik¹, Sedef Erdogan¹, Zeph Phillips¹, Young-Kyu Kim¹, Kang-Il Song², Sunghee Park², Youngwoon Choi¹, Inchan Youn², Beop-Min Kim¹; ¹Bio-convergence Engineering, Korea Univ., South Korea; ²Korea Inst. of Science and Technology, Biomedical Research Inst., South Korea. A single camera near infrared hemodynamic imaging system was developed to analyze the effects hemi-Parkinson's disease on the functional organization of the brain using seed-based connectivity mapping during resting state.

JTu2A.106

Suture Maps Based on Structural Enhanced Imaging Endoscope for Laparoscopic Robotic Surgery, Hanh N. Le¹, Shuwen Wei¹, Simon Leonard¹, Justin Opfermann², Axel Krieger³, Jin U. Kang¹; ¹Johns Hopkins Univ., USA; ²Children's National Health System, USA; ³Univ. of Maryland, USA. A detection method for cutting scheme in 3D is proposed to assist robotic surgical manipulation, leading to an automatic suturing suggestion mapping.

JTu2A.107

Lens-less Micro-endoscopy through highly scattering media, Omer Wagner¹, Aditya Pandya², Yoav Chemla³, Hadar Pinhas¹, Irina Schelkanova², Asaf Shamoon¹, Yossi Mandel³, Alexandre Douplik², Zeev Zalevsky¹; ¹engineering, Bar-Ilan Univ., Israel; ²Physics, Ryerson Univ., Canada; ³Faculty of Life Sciences, School of Optometry and Visual Science, Bar Ilan Univ., Israel. We demonstrate a setup based on lensless, minimally invasive micro-endoscope to image biological samples through scattering medium. We present in-vitro results of Polydimethylsiloxane micro-channels filled with Hemoglobin covered by intralipid mimicking epidermis of human skin.

JTu2A.108

Compressive OCT based on spectral domain random encoding, Xuan Liu¹, Yahui Wang¹; ¹New Jersey Inst. of Technology, USA. We developed and validated a compressive OCT system based on spectral domain random encoding that achieves random modulation of OCT signal for hardware compressive sampling and allows information beyond Nyquist limit to be extracted.

JTu2A.109

High Pulse Energy Supercontinuum Laser for Photoacoustic Detection and Identification of Lipids in the 1650-1850 nm Wavelength Region, Manoj Kumar Dasa¹, Christos Markos¹, Michael Maria^{2,1}, Ivan Bravo Gonzalo¹, Christian R. Petersen¹, Deepak Jain¹, Peter Moselund², Ole. Bang^{1,2}; ¹Technical Univ. of Denmark, Denmark; ²NKT Photonics, Denmark. Lipids are highly coveted for the interrogation of fatal chronic diseases. We propose cost-efficient high pulse energy supercontinuum source, using telecom range diode laser and standard optical fiber for photoacoustic detection and identification of lipids.

JTu2A.110

Longitudinal Control of Topological Charge and Polarization of Attenuation-Resistant OAM Modes, Ahmed Dorrah¹, Mateus Corato-Zanarella^{2,3}, Michel Zamboni-Rached², Mo Mojahedi¹; ¹Dept. of Electrical and Computer Engineering, Univ. of Toronto, Canada; ²School of Electrical Engineering, Univ. of Campinas, Brazil; ³Dept. of Electrical Engineering, Columbia Univ., USA. We experimentally demonstrate non-diffracting and attenuation-resistant beams with orbital angular momentum (OAM) and whose topological charge and polarization can be controlled independently along the beam's axis. This can address many challenges in micromanipulation and optical communications.

JTu2A.111

Dispersion Control in Silicon Oxide Wedge Microdisks, Laís Fujii dos Santos¹, Marvyn Inga¹, Jorge H. Soares¹, Thiago P. Alegre¹, Gustavo S. Wiederhecker¹; ¹Unicamp, Brazil. We demonstrate the generation of optical frequency combs by engineering the dispersion of a small radius (100 microns) thin wedge microcavity. The phase-matching of the excitation taper is also employed to inhibit avoided-crossings.

JTu2A.112

Investigation of the Effect of Stimulated Raman Scattering on Parametric Pumping of Microring Resonators, Mohammed S. Al Alshaykh¹, Daniel E. Leaird¹, Andrew M. Weiner¹; ¹Purdue Univ., USA. We numerically investigate the effect of stimulated Raman scattering on parametric pumping of microring resonators. Furthermore, we re-derive the LLE for a generalized pump including a FSR mismatch term to determine the locking range.

JTu2A.113

Extremely Bright THz Radiation from Two-color Filamentation of Mid-infrared Laser Pulses, Vladimir Fedorov^{1,2}, Stylianos Tzortzakis^{1,3}; ¹Texas A & M Univ. at Qatar, Qatar; ²P.N. Lebedev Physical Inst. of the Russian Academy of Sciences, Russia; ³Inst. of Electronic Structure and Laser (IESL), Foundation for Research and Technology - Hellas (FORTH), Greece. We show numerically that two-color filamentation of mid-infrared 3.9 μ m laser pulses allows one to generate THz pulses of multi-millijoule energies and extreme conversion efficiencies, with electric and magnetic fields of GV/cm and kT level, exceeding by far any available quasi-DC field source today.

JTu2A.114

Size Dependent Ultra-low Upconverted Lasing Threshold in CsPbBr₃ Perovskites Quantum Dots, Gabriel Nagamine¹, Jaqueline O. Rocha¹, Luiz G. Bonato¹, Ana Flávia Nogueira¹, Carlos Henrique B. Cruz¹, Lazaro Padilha¹; ¹Universidade Estadual de Campinas, Brazil. We report on the size dependent of up-converted lasing threshold for CsPbBr₃ perovskite quantum dots, excited via two-photon absorption, showing threshold as low as 1.6 mJ/cm² under femtosecond excitation.

JTu2A.115

Negative Irradiance-Dependent Nonlinear Refraction in Single-Layer Graphene, Giorgos Demetriou¹, Ajoy K. Kar², Fabio Biancalana², Eitan Abraham³, Wei Ji⁴, Yu Wang⁵; ¹Inst. of Photonics, Strathclyde Univ., UK; ²Inst. of Photonics and Quantum Sciences, School of Engineering and Physical Sciences, Heriot-Watt Univ., UK; ³Inst. of Biological Chemistry, Biophysics and Bioengineering, School of Engineering and Physical Sciences, Heriot-Watt Univ., UK; ⁴Dept. of Physics, National Univ. of Singapore, Singapore; ⁵State Key Lab of Multiphase Complex Systems, Inst. of Process Engineering, Chinese Academy of Sciences, China. We show that single-layer graphene presents negative irradiance-dependent nonlinear refraction. We discriminate between a low-irradiance regime, where the conventional Kerr effect applies and a high-irradiance regime where the nonlinear refraction becomes irradiance-dependent.

JTu2A.116

THz Pulse Generation from CSP and ZGP by Tilted Pulse Front Scheme, Wenchao Qiao¹, Huseyin Cankaya¹, Anthony Hartin¹, Peter G. Schunemann², Kevin Zawilski², Nicholas H. Matlis¹, Franz X. Kaertner¹, ¹DESY, Germany; ²BAE System, USA. We report single-cycle THz-pulse generation with a 2 μm laser in CdSiP₂ and ZnGeP₂ using the tilted-pulse-front scheme and compare with LiNbO₃. Initial conversion efficiencies for both crystals are promising relative to LiNbO₃.

JTu2A.117

Experimental Investigation of All-optical Dynamic Photonic Bandgap Control in an All-solid Tellurite Photonic Bandgap Fiber, Tonglei Cheng¹, Shunta Tanaka¹, Takenobu Suzuki¹, Yasutake Ohishi¹; ¹ofmlab, Japan. All-optical dynamic photonic bandgap control by optical Kerr effect is investigated in an all-solid double-clad tellurite photonic bandgap fiber. This is the first demonstration of all-optical dynamic PBG control in optical fibers.

JTu2A.118

Tunable Backward THz-Wave Parametric Oscillation Using a Periodically Poled Lithium Niobate, Kouji Nawata¹, Yu Tokizane¹, Yuma Takida¹, Hiroaki Minamide¹; ¹RIKEN, Japan. We demonstrated tunable backward terahertz-wave parametric oscillation using a slant-stripe-type periodically poled lithium niobate with a poling period of 53 μm . A novel noncollinear phase-matching scheme, quasi-collinear phase-matching condition, produces the wide tunability.

JTu2A.119

Buffering optical topological data using passive Kerr resonators, Bruno Garbin¹, Julien Fatome², Yadong Wang¹, François Léo³, Gian-Luca Oppo⁴, Stuart G. Murdoch¹, Mirosław J. Erkartalo¹, Stéphane Coen¹; ¹The Dodd-Walls Centre for Photonic and Quantum Technologies, Dept. of Physics, The Univ. of Auckland, New Zealand; ²Laboratoire Interdisciplinaire Carnot de Bourgogne (ICB), UMR 6303 CNRS, Université de Bourgogne Franche-Comté, France; ³OPERA-photonique, Université Libre de Bruxelles, Belgium; ⁴SUPA and Dept. of Physics, Univ. of Strathclyde, UK. We experimentally demonstrate the existence of dissipative polarization domain walls, in a normally dispersive Kerr resonator. Through deterministic manipulation of the laser driving the resonator, we achieve systematic excitation and locking of the domain walls.

JTu2A.120

Frequency Comb Generation in Crack-free CMOS Si-photonics Compatible Si₃N₄ Microresonator Chip, Ayman N. Kamel¹, Houssein El Dirani², Marco Casale², Sébastien Kerdiles², Carole Socquet-Clerc², Minhao Pu¹, Leif K. Oxenlowe¹, Kresten Yvind¹, Corrado SCIANCALEPORE²; ¹Danmarks Tekniske Universitet, Denmark; ²Univ. Grenoble Alpes, CEA-LETI Minatoc, France. We present frequency comb generation in crack- and annealing-free Si₃N₄ microresonator chips fabricated using novel CMOS Si-photonics compatible processing.

JTu2A.121

THz Emissions from Air-Plasmas Created by Mid- and Far-Infrared Two-Color Femtosecond Pulses, Alisee Nguyen¹, Luc Bergé¹, Pedro González de Alaiza Martínez², Illia Thiele², Stefan Skupin³; ¹CEA, DAM, DIF, France; ²Univ. Bordeaux - CNRS - CEA, Centre Lasers Intenses et Applications, UMR 5107, France; ³Institut Lumière Matière, UMR 5306 Université Lyon 1 - CNRS, Université de Lyon, France. We study THz emission by two-color femtosecond filaments in air using mid-to far-infrared pump wavelengths. 3D numerical simulations show that 10.6- μm laser pulses can produce THz fields with unequaled mJ energies and GV/m amplitudes.

JTu2A.122

Deterministic Single Soliton Formation and Manipulation in Anomalous Dispersion Microresonators via Parametric, Jinghao Wong¹, Minming Zhang², Deming Liu¹; ¹Huazhong Univ. of Science and Technology, China; ²Huazhong Univ. of Science and Technology, China. We propose a novel method for the deterministic transition from multiple solitons to a single soliton in anomalous dispersion microresonators via parametric seeding. Then the temporal position of the single soliton are flexibly manipulated.

JTu2A.123

Ten-Fold Enhancement in the Small Signal Modulation of Differentially Pumped Coupled Quantum Well Lasers, Yan-nis Kominis¹, Vassilios I. Kovanis², Tassos Bountis³; ¹National Technical Univ. of Athens, Greece; ²Physics, Nazarbayev Univ., Kazakhstan; ³Mathematics, Nazarbayev Univ., Kazakhstan. We unexpectedly found theoretically a 10-fold enhancement in the small signal modulation response of differentially pumped coupled quantum well lasers due to the existence of novel stable asymmetric phase-locked states under differential pumping.

JTu2A.124

Optical Meta-Molecules for Non-Hermitian Photonics, Yan-nis Kominis¹, Vassilios I. Kovanis², Tassos Bountis³; ¹National Technical Univ. of Athens, Greece; ²Physics, Nazarbayev Univ., Kazakhstan; ³Mathematics, Nazarbayev Univ., Kazakhstan. A photonic dimer consisting of two optically coupled lasers is dissected as an optical meta-molecule for non-Hermitian photonic applications. Spectral signatures of exceptional points and Hopf bifurcations are shown for generic asymmetric configurations.

JTu2A.125

Ultrafast Mid-infrared Non-Perturbative Nonlinear Optics in Polycrystalline Zinc Selenide, Kevin Werner¹, Noah Talisa¹, Brian Wilmer², Laura Vanderhoeft³, Aaron Schweinsberg⁴, Christopher Wolfe³, Anthony Valenzuela³, Enam Chowdhury¹; ¹Dept. of Physics, The Ohio State Univ., USA; ²SURVICE Engineering, USA; ³Weapons and Materials Research Directorate, U.S. Army Research Lab, USA; ⁴Oak Ridge Inst. For Science and Education, USA. Strong-field MIR laser-solid interactions have recently generated great interest. Harmonic continuum was generated in ZnSe with MIR pulses. Power scaling of the harmonics was non-perturbative with conversion efficiency as high as 26%.

JTu2A.126

Near-infrared to Mid-infrared wavelength conversion by chalcogenide suspended-core fiber, Kenshiro Nagasaka¹, Tong Hoang Tuan¹, Nguyen Phuoc Trung Hoa¹, Morio Matsumoto², Shigeki Cho², Takenobu Suzuki¹, Yasutake Ohishi¹; ¹Research Center for Advanced Photon Technology, Toyota Technological Inst., Japan; ²Furukawa Denshi Co., Ltd., Japan. We experimentally demonstrated mid-infrared wavelength conversion using a chalcogenide suspended-core fiber pumped with a pico-second pulse.

JTu2A.127

Highly Coherent Mid-Infrared Supercontinuum Spanning From 1.8-10 μm Pumped By A 2- μm Laser, Hoa P. Nguyen¹, Kenshiro Nagasaka¹, Hoang Tuan Tong¹, Takenobu Suzuki¹, Yasutake Ohishi¹; ¹Toyota Technological Inst., Japan. We simulated a 2-step supercontinuum generation with tellurite and chalcogenide fibers pumped by a 2 μm femto second laser. The output SC expands from 1.8 to 10 μm with coherence of unity all over the spectrum.

JTu2A.128

Four-Wave Mixing in a Silicon Self-Pumped Ring Resonator, Micol Previde Massara¹, Federico Sabatoli¹, Matteo Galli¹, Daniele Bajoni²; ¹Dept. of Physics, Univ. of Pavia, Italy; ²Dipartimento di Ingegneria Industriale e dell'Informazione, Univ. of Pavia, Italy. We report on four-wave mixing in a silicon micro-ring resonator using a self-pumping scheme instead of an external laser. We study the correlation of the emitted photons.

JTu2A.129

Consideration on a mechanism of pure circular polarization electroluminescence in a lateral spin-LED, Hiro Muneoka¹, Nozomi Nishizawa¹; ¹Tokyo Inst. of Technology, Japan. A mechanism that the spin axis of minority-spin electrons is converted into majority spin axis with a relatively strong CP light field in the event of radiative recombination in an active layer is addressed.

JTu2A.130

Epsilon Near-Zero Nonlinear Optical Measurements of Titanium Nitride Thin Films, Manuel R. Ferdinandus^{1,2}, Jamie Gengler², Nathaniel Kinsey³, Augustine Urbas³; ¹Air Force Inst. of Technology, USA; ²Air Force Research Lab, USA; ³Virginia Commonwealth Univ., USA. Using the optical beam deflection method we measure the transient optical nonlinearity of titanium nitride thin films deposited at 350° and 800° C around their respective epsilon near-zero wavelengths.

JTu2A.131

Engineered quasi-phase matching for conversion efficiency optimization of coupled X⁽²⁾ processes, Cheng-Wei Hsu¹, Jui-Yu Lai¹, Shang-Da Yang¹; ¹National Tsing Hua Univ., Taiwan. We propose an algorithm to optimize the efficiency of coupled X⁽²⁾ processes in an aperiodic optical superlattice, achieving record high efficiency of frequency tripling. Feasibility is confirmed by controlled experiment with three different design methods.

JTu2A.132

Sub-Cycle Light Bullets in the Long-Wavelength Infrared, Rostislav Grynko¹, Garima Nagar¹, Bonggu Shim¹; ¹Binghamton Univ., USA. Carrier-resolved unidirectional pulse propagation equations are used to model mid- and long-wavelength infrared laser filamentation in ZnSe, revealing a novel propagation regime where sub-cycle light bullets propagate stably with a critical dependence on plasma.

JTu2A.133

Second Harmonic Generation from UV to Visible in KDP Single-crystalline Fibers, Kam Sing . Wong¹; ¹Hong Kong Univ. of Science & Technology, Hong Kong. Second harmonic generation (SHG) from UV to visible in KDP single-crystal fiber without the need of angle or temperature tuning is demonstrated. This wide SHG tunability is attributed to the unique automatic 'quasi-random' phase matching.

JTu2A.134

Non-Resonant Enhancement of Second-harmonic Generation from Metal Nanoislands Coated with Dielectric Layers, Kalle O. Koskinen¹, Sergey Scherbak^{2,3}, Semyon Chervinskii^{2,4}, Andrey Lipovskii^{2,3}, Martti Kauranen¹; ¹Lab of Photonics, Tampere Univ. of Technology, Finland; ²Inst. of Physics, Nanotechnology and Telecommunication, Peter the Great St. Petersburg Polytechnic Univ., Russia; ³Dept. of Physics and Technology of Nanostructures, St. Petersburg Academic Univ., Russia; ⁴Inst. of Photonics, Univ. of Eastern Finland, Finland. Second-harmonic generation from gold nanoisland films increases with the dielectric TiO₂ coating thickness. This occurs although the plasmon resonance shifts away from the second-harmonic wavelength, due to enhanced non-resonant local fields at the fundamental wavelength.

JTU2A.135

Detection of Orbital Angular Momentum Superposition States in Optical Vortices, Mariia Shutova¹, Alexandra A. Zhdanova¹, Alexei V. Sokolov¹; ¹*Inst. for Quantum Science and Engineering, Dept. of Physics and Astronomy, Texas A&M Univ., USA*. Orbital angular momentum (OAM) transfer through nonlinear processes such as coherent Raman generation often distorts the original spatial mode of light, resulting in OAM superposition states. We characterize such modes and quantify their distortion by astigmatic focusing of the laser beam.

JTU2A.136

Second Harmonic Radiation from Rectangular Gold Antenna: Far-field Contributions of Different Nonlinear Polarizations, Kyungwan Yoo¹, Simon F. Becker², Martin Sillies², Sunkyu Yu¹, Christoph Lienau², Namkyoo Park¹; ¹*Seoul National Univ., South Korea*; ²*Carl von Ossietzky Universität, Germany*. We investigate the second harmonic generation from rectangular gold antenna. By comparing measurement and hydrodynamic model based calculation, we show different contributions of each nonlinear polarization to second harmonic radiation.

JTU2A.137

Anomalous Trapping of Temporal Cavity Solitons by Amplitude Modulated Driving Fields, Ian Hendry¹, Wei Chen^{1,2}, Yadong Wang¹, Julien Javaloyes³, Gian-Luca Oppo⁴, Stephane Coen¹, Stuart Murdoch¹, Miro J. Erkintalo¹; ¹*Univ. of Auckland, New Zealand*; ²*National Univ. of Defense Technology, China*; ³*Univ. of the Balearic Islands, Spain*; ⁴*Univ. of Strathclyde, UK*. We report a systematic study of cavity soliton motion in the presence of amplitude modulated driving fields. We show that, contrary to conventional wisdom, cavity solitons are trapped to particular values of the driving field.

JTU2A.138

Design of a GaInP/AlGaInP electrically-driven photon-pair source near 1.3-micrometer wavelengths, Xiaoya Xie¹, Xiaoming Chi¹, Kaiyu Cui², Xiaolong Hu¹; ¹*Tianjin Univ., China*; ²*Electronic Engineering, Tsinghua Univ., China*. We present our design of an electrically-driven device based on a GaInP/AlGaInP quantum well and a Bragg-reflection waveguide to generate photon pairs near 1.3-micrometer wavelengths through internal spontaneous parametric down-conversion.

JTU2A.139

Enhanced Free-space Coupling to Whispering-gallery-mode Resonators by Accelerating Beams, Xu Liu¹, Yi Hu¹, Fang Bo¹, Zhenzhong Hao¹, Zhigang Chen¹, Jingjun Xu¹; ¹*The MOE Key Lab of Weak-Light Nonlinear Photonics, TEDA Applied Physics Inst. and School of Physics, Nankai Univ., China*. We propose free-space coupling to whispering-gallery-mode resonators via accelerating beams propagating along a semi-circle, and demonstrate nearly three-fold enhancement in coupling efficiency as compared with conventional Gaussian beams.

JTU2A.140

Towards the Manipulation of Relativistic Laguerre-Gaussian Laser Pulse, Cheonha Jeon¹, Seong Geun Lee^{1,2}, Hwang Woon Lee¹, Jae Hee Sung^{1,3}, Seong Ku Lee^{1,3}, Il Woo Choi^{1,3}, Chang Hee Nam^{1,2}; ¹*Center for Relativistic Laser Science, Inst. for Basic Science, South Korea*; ²*Dept. of Physics and Photon Science, Gwangju Inst. of Science and Technology, South Korea*; ³*Advanced Photonics Research Inst., Gwangju Inst. of Science and Technology, South Korea*. The effect of Laguerre-Gaussian beam compare to Gaussian beam on the characteristics of laser driven proton beams is presented using 150 TW beam. The LG beam experiment with the 4 PW laser is being conducted.

JTU2A.141

Collapsing dynamics of elliptic-symmetry vector optical fields with hybrid states of polarization, Dan Wang¹, Yue Pan¹, Jiaqi Lyu¹, PingPing Li¹, GuiGeng Liu¹, MengQiang Cai¹, YongNan Li¹, ChengHou Tu¹, HuiTian Wang^{1,2}; ¹*Nankai Univ., China*; ²*Nanjing Univ., China*. The eccentricity of the spatial polarization distribution provides a new degree of freedom to achieve the controllable collapse. The coupling between the intensity and polarization affects the nonlinear dynamic properties of the structured optical fields.

JTU2A.142

Simultaneous generation of 1D and 2D Airy beams and their frequency doubling characteristics, Raghwinder S. Grewal¹, Anirban Ghosh¹, Goutam K. Samanta¹; ¹*Physical Research Lab, India*. We report on simultaneous generation of high power, 1D and 2D Airy beam using a pair of concave and convex cylindrical lenses in a novel experimental scheme and studied their frequency doubling characteristics.

JTU2A.143

Coherent Mid-infrared Supercontinuum Generation using Rib Waveguide Pumped with Femtosecond Laser, Than Singh Saini¹, Nguyen Phuoc Trung Hoa¹, Kenshiro Nagasaka¹, Xing Luo¹, Tong Hoang Tuan¹, Takenobu Suzuki¹, Yasutake Ohishi¹; ¹*Research Center for Advanced Photon Technology, Toyota Technological Inst., Japan*. Coherent mid-infrared supercontinuum spectrum spanning 1.2 to 7.2 μm has been reported using an As₂Se₃-chalcogenide rib waveguide pumped with 200 fs laser pulses of a moderately low peak power of 2.5 kW at 2.8 μm .

JTU2A.144

Electromagnetic Ghost Waves., Evgenii E. Narimanov¹; ¹*Purdue Univ., USA*. Anisotropic dielectrics support ghost waves that combine properties of propagating and evanescent fields. Similarly to negative index media, these modes can grow exponentially through the transparent anisotropic material, leading to dramatic enhancement of local intensity.

JTU2A.145

Light-Actuated Electrohydrodynamics in Plasmonic Nanofluids, Luat Vuong^{1,2}, James McQuade¹, Vera Zarubin¹, Heriberto Vasquez¹; ¹*Queens College of CUNY, USA*; ²*Graduate Center, CUNY, USA*. The light-actuated electrohydrodynamics in plasmonic nanofluids represent harvestable energy in an open system. Here we demonstrate thermoelectric responses and analyze the energy conversion. Future efforts will require scrutiny of the negative-Soret-coefficient thermophoretic dynamics.

JTU2A.146

Quantum Spectroscopy with Extreme Nonlinear Effects, Benjamin J. Girodias¹, Mackillo Kira¹; ¹*Univ. of Michigan, USA*. We present a new method to study extreme nonlinearities with quantum spectroscopy. Our spectroscopy approach increases the sensitivity to detect nonlinearities by an order of magnitude while remaining robust against experimental noise.

JTU2A.147

Ultra-efficient and stable EO dendrimers containing supramolecular homodimers of dipolar semifluorinated aromatics, JieYun Wu¹, Bo Wu¹, Wen Wang¹, Kin S. Chiang^{1,2}, Alex K. Jen³, Jingdong Luo³; ¹*Univ. of Science and Tech of China, China*; ²*Electronic Engineering, City Univ. of Hong Kong, Hong Kong*; ³*Chemistry, City Univ. of Hong Kong, Hong Kong*. We demonstrated the supramolecular homodimerization of semifluorinated dipolar aromatics to self-assemble electro-optic dendrimers. The self-assembled dendritic films showed large electro-optic coefficients (248 pm/V) and excellent temporal stability (>95%) after 1000 h.

JTU2A.148

Precision generation and control of dissipative Kerr solitons with suppressed cavity thermal disturbance, Yong Geng¹, Wenwen Cui¹, Yun Ling¹, Baojian Wu¹, Kun Qiu¹, Chee-Wei Wong², Heng Zhou¹; ¹*Univ. of Electronic Science and Technology of China, China*; ²*Univ. of California, Los Angeles, USA*. Dissipative Kerr soliton formation with unprecedented detuning control precision is demonstrated using an auxiliary-laser-heating method to suppress cavity thermal disturbance. New existence region of dissipative Kerr soliton in low pump power regime is originally discovered.

JTU2A.149

Resonance-enhanced nonlinear optical effects in strong-field ionized nitrogen molecules, Jinping Yao¹, Wei Chu¹, Zhaoxiang Liu¹, Bo Xu¹, Jinming Chen¹, Ya Cheng^{1,2}; ¹*State Key Lab of High Field Laser Physics, Shanghai Inst. of Optics and Fine Mechanics, Chinese Academy of Sciences, China*; ²*State Key Lab of Precision Spectroscopy, East China Normal Univ., China*. We report on lasing actions and extraordinary supercontinuum generation in strong-field ionized nitrogen molecules. It was revealed that these unexpected emissions result from a series resonant nonlinear optical processes in molecular ions.

JTU2A.150

Spatio-Spectral Structures in High Harmonic Generation Driven by a High Repetition Rate OPCPA at 1.55 μm , Gaëtan Jargot^{1,6}, Aura Gonzalez², Philippe Rigaud¹, Antoine Comby³, Olivier Sublemontier⁴, Michel Bougeard⁵, Thierry Ruchon⁵, Marc Hanna¹, Patrick Georges¹; ¹*Institut d'Optique, Laboratoire Charles Fabry, France*; ²*Amplitude Laser Group, France*; ³*CELI, France*; ⁴*NIMBE, CEA, France*; ⁵*CEA, LIDyL, France*; ⁶*Fastlite, France*. We investigate the spatio-spectral properties of high-harmonic generation driven by an optical parametric chirped pulse amplifier at 1.55 μm wavelength operating at 125 kHz. Ring-like structures are observed and explained by the transverse atomic-induced phase.

JTU2A.151

Progress towards a high acquisition rate attosecond pump-probe beamline, Federico J. Furch¹, Tobias Witting¹, Felix Schell¹, Dominik Hoff¹, Chih-Hsuan Lu^{3,4}, Peter Šušnjar¹, Fabio Cavalcante⁵, Carmen Menoni⁵, Claus P. Schulz², Gerhard G. Paulus², A. H. Kung^{3,4}, Marc J. Vrakking¹; ¹*Max Born Inst., Germany*; ²*Helmholtz-Institut Jena Institut für Optik und Quantenelektronik, Friedrich-Schiller-Universität, Germany*; ³*National Tsing Hua Univ., Taiwan*; ⁴*Inst. of Atomic and Molecular Sciences, Academia Sinica, Taiwan*; ⁵*Dept. of Electrical and Computer Engineering, Colorado State Univ., USA*. The development of an attosecond pump-probe beamline based on a 100 kHz laser system is presented. Results on high harmonic generation, pulse shortening towards the single-cycle limit and single-shot carrier-envelope phase characterization are discussed.

JTU2A.152

Circularly Polarized High Harmonic Generation from Chiral Molecules, Yoichi Harada¹, Eisuke Haraguchi¹, Keisuke Kaneshima¹, Tarō Sekikawa¹; ¹*Hokkaido Univ., Japan*. Circularly polarized high harmonic generation from a chiral molecule was found to depend both on the chirality and on the rotating direction of the circularly polarized counter-rotating two-color driving laser fields.

JTU2A.153

Time-resolved ARPES Based on 8-fs High-harmonic Source in the Extreme Ultraviolet Region, Kento Toume^{1,2}, Katsuya Oguri¹, Hiroki Mashiko¹, Keiko Kato¹, Yoshiaki Sekine¹, Hiroki Hibino³, Akira Suda², hideki gotoh¹; ¹*NTT Basic Research Labs, NTT Corporation, Japan*; ²*Faculty of Science and Technology, Tokyo Univ. of Science, Japan*; ³*School of Science and Technology, Kwansei Gakuin Univ., Japan*. We demonstrate time-resolved ARPES based on the 27th harmonic pulse with sub-10-fs duration. The measurement for the initial stage of carrier photoexcitation near the Dirac point of graphite confirms duration of 8 fs.

JTu2A.154

Reconstructing band structure of a crystalline solid from drive-laser-intensity dependence of a single harmonic produced by intraband current, Peiyu Xia¹, Faming Lu¹, Teruto Kanai¹, Nobuhisa Ishii¹, Jiro Itatani¹; ¹*Inst. for Solid State Physics, The Univ. of Tokyo, Japan*. We propose and numerically simulate all-optical reconstruction of band structure from drive-laser-intensity dependence of a single harmonic produced from crystalline solids. This method assumes that a low-order harmonic is mainly produced by intraband current.

JTu2A.155

Energy scaling of soft-x-ray high harmonics driven by a loosely-focused TW-scale mid-infrared pulse, Kataro Nishimura^{1,2}, Yuxi Fu², Akira Suda¹, Katsumi Midorikawa², Eiji J. Takahashi¹; ¹*Tokyo Univ. of Science, Japan*; ²*RIKEN Center for Advanced Photonics, Japan*. We establish an energy-scaling strategy of high-order harmonic driven by a loosely focused mid-infrared pulse. Using a 4-cm Ne gas cell with a 3.5-m laser focusing length, soft x-ray harmonics beyond 200 eV are clearly enhanced by phase-matching effect.

JTu2A.156

High-order Harmonic Generation in Femtosecond laser-Micromachined Devices, Anna Gabriella Ciriolo¹, Rebeca Martinez Vazquez¹, Gabriele Crippa¹, Davide Faccialà¹, Matteo Negro¹, Michele Devetta¹, Diogo Pereira Lopes¹, Aditya Pusala¹, Caterina Vozzi¹, Roberto Osellame¹, Salvatore Stagira¹; ¹*Dipartimento di Fisica, Politecnico di Milano, IFN-CNR, Italy*. We demonstrate the generation of high-order harmonics in a fused-silica chip produced by femtosecond laser micromachining. This achievement paves the way for the miniaturization of HHG applications from large-scale Labs to microstructures.

JTu2A.157

A Time-preserving Ultra-narrow-bandwidth Multilayer-mirror Monochromator for Extreme Ultraviolet Pulses, Yudong Yang^{1,2}, Julia Hengster^{3,4}, Tanja Neumann^{3,4}, Roland E. Mainz^{1,3}, Oliver Muecke^{1,2}, Franz X. Kaertner^{1,3}, Thorsten Uphues^{3,4}; ¹*Center for Free-Electron Laser Science CFEL, Deutsches Elektronen-Synchrotron DESY, Germany*; ²*The Hamburg Centre for Ultrafast Imaging CUI, Univ. of Hamburg, Germany*; ³*Dept. of Physics, Univ. of Hamburg, Germany*; ⁴*Center for Free-Electron Laser Science CFEL, Universität Hamburg, Germany*. We present a multilayer-mirror-based monochromator providing ultra-narrow bandwidth and compact footprint for easy integration into HHG-based or FEL sources. The bandwidth ($\Delta E < 0.5\text{eV}$, $E_e \sim 91\text{eV}$) of the monochromator is characterized experimentally in a HHG-based source.

JTu2A.158

Generation of Few-Cycle UV pulses Synchronized with Attosecond XUV Pulses, Vincent Wanie^{2,1}, Mara Galli^{3,1}, Erik Månsson^{4,1}, Mattea C. Castrovillani^{5,1}, François Légaré², Fabio Frassetto⁶, Luca Poletto⁶, Mauro Nisoli^{3,1}, Francesca Calegari^{4,1}; ¹*Inst. for Photonics and Nanotechnologies CNR-IFN, Italy*; ²*Institut National de la Recherche Scientifique, Canada*; ³*Dept. of Physics, Politecnico di Milano, Italy*; ⁴*Center for Free-Electron Laser Science, DESY, Germany*; ⁵*Inst. for the Structure of Matter CNR-ISM, Italy*; ⁶*Inst. for Photonics and Nanotechnologies CNR-IFN, Italy*. Few-femtosecond UV and isolated attosecond pulses were implemented into a Mach-Zehnder like interferometer. The ultraviolet light is obtained via frequency up-conversion of few-optical-cycle NIR pulses in a gas medium to achieve an optimal temporal resolution.

JTu2A.159

Scaling and Spectral Structure of Relativistic High-Order-Harmonic Generation, Matthew Edwards¹, Julia Mikhailova¹; ¹*Princeton Univ., USA*. We develop scaling models for the behavior of relativistic high-order-harmonic generation, showing how the spectrum, attosecond pulse intensity, and the formation of secondary pulses depend on a simplified set of parameters.

JTu2A.160

THz Emission by Underdense Relativistic Plasma, Jeremy Dechard¹, Arnaud Debayle¹, Xavier Davoine¹, Laurent Gremillet¹, Luc Bergé¹; ¹*CEA-DAM, DIF, France*. Terahertz emissions by gas-based relativistic plasmas created by two-color laser pulses are investigated. PIC simulations reveal that coherent transition radiation driven by wakefield-accelerated electrons is the dominant process, compared to photocurrents, and they yield unprecedented THz energies.

JTu2A.161

Investigation of the waveguide generated by UV filamentation, Ali Rastegari¹, Chengyong Feng^{1,2}, Jean-Claude M. Diels¹; ¹*UNM, USA*; ²*Lab for Laser Energetics, Univ. of Rochester, USA*. The waveguides generated by UV filaments in different focusing schemes have been investigated using the shadowgraphy technique. It was observed that these waveguides have a transverse width of the order of 400µm.

JTu2A.162

MEMS-Based Fast Tunable Laser, Alvaro Jimenez Galindo^{2,1}, Sebastian Schmidtman¹, Herve Tatenguem Fankem¹, Tobias Milde¹, Christian Abmann¹, Guillermo Carpintero del Barrio², Joachim Sacher¹; ¹*Sacher Lasertechnik GmbH, Germany*; ²*Electronic Technology, Universidad Carlos III de Madrid, Spain*. MEMS-based tunable diode lasers inherit the benefits of conventional ECDLs while improving the tuning speed. These lasers are here presented with an example and measurements are shown of the spectral characterization of these devices together with switching speed and stability experimental results.

JTu2A.163

A high energy sapphire-cooled multi-slab Nd:glass amplifier, Wenfa Huang¹, Tingrui Huang¹, Jiangfeng Wang¹, Xinghua Lu¹, Dajie Huang¹, Wei Fan¹, Xuechun Li¹; ¹*SJOM, China*. We present amplification results for a sapphire-cooled multi-slab Nd:glass amplifier, an output energy of 562 mJ at 1 Hz with energy stability of 0.39% RMS was achieved.

JTu2A.164

210 W kHz-linewidth linearly-polarized all-fiber single-frequency MOPA laser, Changsheng Yang¹, Xianchao Guan¹, Shanhui Xu¹, Zhongmin Yang¹; ¹*South China Univ. of Technology, China*. An all-fiber high-power kHz-linewidth linearly-polarized Yb³⁺-doped single-frequency MOPA laser is experimentally demonstrated with a stable CW output power of >210 W and a laser linewidth of <9 kHz.

JTu2A.165

Dual-Pulse Passively Q-switched Microchip Laser for Two-Color Tandem THz-Wave Pulse Generation, Toshiyuki Ikeo¹, Yuma Takida², Kouji Nawata², Yasuhiro Higashi¹, Hiroaki Minamide²; ¹*Ricoh Company, LTD, Japan*; ²*RIKEN, Japan*. Two-color, tandem THz-wave pulses are generated from an injection-seeded THz-wave parametric generator driven by a dual-pulse passively Q-switched microchip laser whose center frequency difference is 11 GHz within a single excitation cycle.

JTu2A.166

High Energy Pulse Compression by a Solid Medium, Seong Ku Lee^{1,2}, Je Yoon Yoo¹, Ji In Kim^{1,3}, Yeong Gyu kim^{1,3}, Jin Woo Yoon^{1,2}, Hwang Woon Lee¹, Jae Hee Sung^{1,2}, Chang Hee Nam^{1,3}; ¹*CoREeLS IBS-GIST, South Korea*; ²*APRI, GIST, South Korea*; ³*Dept. of Physics and Photon Science, GIST, South Korea*. A high energy pulse with the energy of 3.5 J was spectrally broadened by a supercontinuum generation and it was recompressed from 31 fs to 14.5 fs by the dispersion compensation.

JTu2A.167

Bound States of Solitons in a Spatiotemporal Mode-locked Multimode Fiber Laser, Huaqiang Qin¹, Xiaosheng Xiao¹, Pan Wang¹; ¹*Tsinghua Univ., China*. We report on experimental observation of bound states of solitons in a spatiotemporal mode-locked multimode fiber laser.

JTu2A.168

Multi-mJ, high efficiency, picosecond deep ultraviolet source, Pierre Sevillano¹, Jean-Gabriel Brisset¹, Magali Durand¹, Benoit Tropheime¹, Antoine Courjaud¹; ¹*Amplitude systemes, France*. We report a 4.1 mJ, 100 Hz, ~1.7 ps DUV laser at 257.5 nm from a frequency-quadrupled Yb:YAG chirped-pulse amplifier. An infrared-to-DUV conversion efficiency of ~20% is achieved with a good beam quality.

JTu2A.169

Laser performance of RE³⁺:YAG Double-Clad Crystalline Fiber Waveguides, Da Li¹, Huai-chuan Lee¹, Stephanie K. Meissner¹, Helmut E. Meissner¹; ¹*Onyx Optics, Inc, USA*. We report on laser performance and modeling of Yb:YAG and Tm:YAG double-clad crystalline fiber waveguide for high power applications, with 53.6% slope efficiency and 27.5-W output for Yb:YAG, and 31.6% and 46.7-W for Tm:YAG.

JTu2A.170

Development of an Auxiliary OPCPA Beamline for the Vulcan PW Laser Facility., Ian O. Musgrave¹, Alexis Boyle¹, Robert Clarke¹, John Collier¹, Marco Galimberti¹, Cristina Hernandez-Gomez², Pedro Oliviera¹, Waseem Shaikh¹, Adam Wyatt¹; ¹*Science & Technology Facilities Council, UK*. In this paper we present our plans for an auxiliary OPCPA beamline for the Vulcan PW laser facility. It will be capable of delivering 30J <30fs in combination with the existing beams.

JTu2A.171

Wavefront Degradation of a 200 TW Laser from Heat-Induced Deformation of In-Vacuum Compressor Gratings, Vincent Leroux^{1,2}, Spencer Jolly^{1,2}, Matthias Schnepp¹, Timo Eichner¹, Sören Jalas¹, Manuel Kirchen¹, Philipp Messner¹, Christian Werle¹, Paul Winkler¹, Andreas R. Maier¹; ¹*Center for Free-Electron Laser Science, Germany*; ²*Institute of Physics of the ASCR, ELI-Beamlines project, Czechia*. We report laser wavefront degradation of a 200 TW laser from heat absorbed by the in-vacuum compressor gratings, while scanning laser energy and rep-rate. Laser induced damages are investigated.

JTu2A.172

Q-switched optical vortex pulses generated by the coherent superposition of off-axis modes in an azimuthal symmetry breaking laser resonator, YuanYao Lin¹; ¹*National Sun Yat-Sen Univ., Taiwan*. Optical vortex pulse trains are generated by the superposition of coherently phase-locked off-axis laser beamlets resonating independently in an unconventional azimuthal symmetry breaking optical resonator bumped by conventional diode laser without critical beam shaping.

JTu2A.173

Radially polarized and wavelength switchable mode locking Yb-doped fiber laser, Fan Shi¹, Yiping Huang¹, Teng Wang¹, Fufei Pang¹, Tingyun Wang¹, Xianglong Zeng¹; ¹*Shanghai Univ., China*. We experimentally demonstrated the generation of radially polarized and wavelength switchable mode locking pulse at a 1 mm spectral region by using a broadband few mode coupler in a Nonlinear Polarization Rotation fiber ring cavity.

11:30–13:00 JTu2A • Poster Session I

JTu2A.174

Carbon Nanoparticles as an Optical Modulator for Passively Q-switched Fiber Laser, Huiyi Li¹, Jie Ma¹, Mengying Zhang¹, Jun Wang¹, Dingyuan Tang¹, Seongwoo Yoo¹; ¹Nanyang Technological Univ., Singapore. We present the first demonstration of carbon nanoparticles (CNP) as an optical modulator to generate short laser pulses. An ytterbium-doped fiber ring cavity is successfully Q-switched with CNPs prepared in-house via a simple flame synthesis.

JTu2A.175

10 kHz, 10 ns, 13.4 mJ Burst-mode MOPA Nd:YAG Based Frequency-tripled Source at 355 nm, Wentao Wu¹, XuDong Li¹, Renpeng Yan¹, Deying Chen¹; ¹Harbin Inst. of Technology, China. We demonstrated a Nd:YAG based Q-switched burst-mode MOPA laser with ultraviolet output by nonlinear harmonic generation. Single-pulse energy of 13.4 mJ at 355 nm, 10 kHz was obtained. The pulse width reached 10 ns.

JTu2A.176

Gaussian-shaped pulses oscillation of gain-switched Cr:ZnSe laser pumped with nanosecond pulses, Masaki Yumoto¹, Norihito Saito¹, Satoshi Wada¹; ¹RIKEN, Japan. We demonstrated Gaussian-shaped pulses oscillation of gain-switched nanosecond Cr:ZnSe laser based on numerical and experimental research. The Gaussian-shaped pulses with pulse width of 56 ns were obtained without any Q-switch devices inside the laser cavity.

JTu2A.177

Extra-cavity amplification of the digital laser modes using Nd: YAG amplifier, Teboho Bell¹; ¹CSIR National Laser Centre, South Africa. In this paper, we demonstrate experimentally how the laser output power of higher-order LG_p_q modes generated from the digital laser is amplified by using an extra-cavity Nd: YAG amplifier. Amplification of 42% was realized.

JTu2A.178

Transverse Stimulated Raman Scattering Induced Large Aperture KDP Coating Damages of SG-II Facility, Shunxing Tang¹, Yajing Guo¹, Qing Jiang¹, Lin Yang¹, Baoqiang Zhu¹; ¹SIOM, China. Coating damage of large aperture KDP crystal on SG-II laser facility is observed. A simulation model is setup, and it indicates that TSRS can induce energy lose and coating damage in large aperture KDP crystals.

11:30–13:30 Exhibit Hall Free Lunch

12:00–13:30 OIDA VIP Industry Leaders Speed Meetings Lunch, Exhibit Hall, #2605

12:00–15:00 SC352: Introduction to Ultrafast Pulse Shaping--Principles and Applications
SC376: Plasmonics
SC410: Finite Element Modeling Methods for Photonics and Optics

12:00–16:00 SC270: High Power Fiber Lasers and Amplifiers
SC438: Photonic Metamaterials

CLEO: Science & Innovations

13:00–15:00

STu3A • Quantum Photonic Technology*President: Jonathan Matthews; University of Bristol UK*STu3A.1 • 13:00 **Invited**

Scaling Quantum Photonic Technologies, Mark G. Thompson¹; ¹Quantum Engineering Technology Labs, H. H. Wills Physics Lab & Dept. of Electrical and Electronic Engineering, Univ. of Bristol, UK. Silicon Quantum Photonics has emerged as a promising approach to realizing complex large-scale quantum photonic circuits. Here we overview recent developments presenting circuits comprising hundreds of photonic components integrated into single coherent quantum systems.

STu3A.2 • 13:30 **Invited**

Multi-photon Quantum Boson-sampling Machines, Chaoyang Lu¹; ¹Univ of Science and Technology of China, China. We develop single-photon sources that simultaneously combines high purity, efficiency, and indistinguishability. We demonstrate entanglement among ten single photons. We construct high-performance multi-photon boson sampling machines to race against classical computers to reach the goal of quantum computational supremacy.

13:00–15:00

STu3B • OAM and Photodetective*President: Richard Penty; Univ. of Cambridge, UK*STu3B.1 • 13:00 **Tutorial**

Advances in Components and Integrated Devices for OAM-Based Systems, Alan E. Willner¹; ¹Univ. of Southern California, USA. This tutorial will highlight various types of compact components that might be important for future deployment of optical systems based on beams carrying orbital-angular-momentum. Such elements may include: generators, (de) multiplexers, detectors, filters, and fibers.



Alan Willner is the Sample Chair at USC. He received: Member US National Academy of Eng., Int'l Fellow UK Royal Academy of Eng., IEEE Eric Sumner Award, NSF Presidential Faculty Fellows Award from White House, IET JJ Thomson Medal, Packard Foundation Fellowship, OSA Forman Eng. Excellence Award, and SPIE President's Award. He was co-chair National Academies' Committee on Optics and Photonics; president OSA; president IEEE Photonics Society; and CLEO general co-chair.

13:00–15:00

STu3C • Advanced Short Reach and Free Space Communications*President: David Geisler; Massachusetts Inst of Tech Lincoln Lab, USA*

STu3C.1 • 13:00

50 Gb/s Transmission over Uncompensated Link up to 20 km Exploiting DSP-Free Direct-Detection, Francesco Fresi^{1,2}, Mohamed Morsy-Osman³, Enrico Forestieri^{1,2}, Marco Secondini^{1,2}, Fabio Cavaliere⁴, David V. Plant³, Stephane Lessard⁵, Luca Poti²; ¹TeCIP Inst., Scuola Sant'Anna, Italy; ²PNTLab, CNIT, Italy; ³Photonics System Group, Electrical and Computer Engineering Dept., McGill Univ., Canada; ⁴Ericsson, Italy; ⁵Ericsson Canada, Canada. We experimentally transmit 50Gb/s over 20km uncompensated SMF with a conventional DSP-free OOK direct detection receiver, exploiting combined amplitude phase shift codes. A simplified implementation based on analog electronics is also validated at 50Gb/s.

STu3C.2 • 13:15

Carrier Regeneration Assisted Kramers-Kronig Detection of an Independent Sideband Signal, Qiulin Zhang¹, Chester Shu¹; ¹Chinese Univ. of Hong Kong, Hong Kong. We experimentally demonstrate Kramers-Kronig detection of an independent sideband (ISB) signal by Brillouin amplifying a weak pilot tone at the receiver side. A 30Gbit/s ISB signal with mixed modulation formats is successfully transmitted over 80 km.

STu3C.3 • 13:30 **Invited**

The Kramers-Kronig Receiver: a Coherent Receiver Based on Intensity Detection and Phase Recovery, Antonio Mecozzi¹, Cristian Antonelli¹, Mark Shtaiif²; ¹Univ. of L'Aquila, Italy; ²School of Electrical Engineering, Tel Aviv Univ., Israel. We review the operation principles and the various implementations of the Kramers-Kronig receiver. We will show that this receiver permits to extract the full complex envelope of the optical field by simple intensity detection.

Executive Ballroom
210D

CLEO: Science & Innovations

13:00–15:00

STu3D • Terahertz Communications

President: Tyler Cocker; Universität Regensburg, Germany

STu3D.1 • 13:00 **Tutorial**

100s Gigabit/s THz Communication, Leif K. Oxenlowe¹, Michael Galili¹, Darko Zibar¹, Toshio Morioka¹, Hao Hu¹, Francesco Da Ros¹, Pengyu Guan¹, Shi Jia¹, Xiaodan Pang², Oskars Ozolins², Xianbin Yu³, Gunnar Jacobsen², Sergei Popov⁴; ¹DTU Fotonik, Denmark; ²ACREO RISE, Sweden; ³College of Information Science and EE, Zhejiang Univ., China; ⁴KTH, Sweden. This paper gives an overview of recent progress on the topic of using around 0.4 THz carriers for communications. Experimental demonstrations will be described, and concepts and pros&cons of various system-platforms discussed.



Leif Katsuo Oxenlowe, Ph.D. 2002 from DTU, is Professor of Photonic Communication Technologies, group leader of the High-Speed Optical Communications group at DTU Fotonik, and Centre Leader of the DNRF Centre of Excellence SPOC. He has authored or co-authored more than 350 peer reviewed publications.

Executive Ballroom
210E

CLEO: QELS-Fundamental
Science

13:00–15:00

FTu3E • Thermal and Quantum Applications
of Metasurfaces

President: Zubin Jacob; Purdue Univ., USA

FTu3E.1 • 13:00 **Invited**

Metafilms for Large Scale Thermal Management, Xiaobo Yin¹; ¹Univ. of Colorado Boulder, USA. Scalably procured optical metamaterial thin films could enable advance applications including passive radiative cooling. We will discuss the advancement in radiative cooling metafilms and other applications of metafilms in food-energy-water system (FEWS).

FTu3E.2 • 13:30

Near-field Thermo-photovoltaic Platform, Gaurang Bhatt¹, Samantha Roberts¹, Raphael St-Gelais³, Tong Lin¹, Aseema Mohanty¹, Bo Zhao², Jean-Michel Hartmann⁴, Shanhui Fan², Michal Lipson¹; ¹Columbia Univ., New York, USA, USA; ²Electrical Engineering, Stanford Univ., USA; ³Mechanical Engineering, Univ. of Ottawa, Canada; ⁴CEA - Laboratoire d'Électronique des Technologies de l'Information (LETI), France. We demonstrate a platform for heat-to-electricity conversion based on near-field radiative heat transfer. The platform is based on tens-of- μm long suspended micro-heaters at $>400\text{deg.C}$, placed $<100\text{nm}$ away from a room temperature photodetector.

FTu3E.3 • 13:45

Aligned and Packed Single-Wall Carbon Nanotubes as Hyperbolic Thermal Emitters, Weilu Gao¹, Chloe Doiron¹, Xinwei Li¹, Junichiro Kono^{1,2}, Gururaj Naik¹; ¹Dept. of Electrical and Computer Engineering, Rice Univ., USA; ²Dept. of Physics and Astronomy, Rice Univ., USA. We demonstrate a broadly tunable, polarized and selective thermal emitter from highly aligned and densely packed single-wall carbon nanotubes (SWCNTs) operating at $700\text{ }^\circ\text{C}$, originating from their optical topological transition.

Executive Ballroom
210F

CLEO: Science & Innovations

13:00–15:00

STu3F • Nonlinear Integrated Photonic
Platforms

President: Kartik Srinivasan; NIST, USA

STu3F.1 • 13:00

Low Loss Silicon-Rich Silicon Nitride for Nonlinear Optics, Zhichao Ye¹, Attila Fulop¹, Oskar B. Helgason¹, Peter A. Andrekson¹, Victor Torres-Company¹; ¹Microtechnology and Nanoscience, Chalmers Univ. of Technology, Sweden. We demonstrate low loss ($\sim 0.4\text{ dB/cm}$) silicon-rich silicon nitride waveguides and high Q microresonators ($Q_i \sim 10^6$) featuring broadband anomalous dispersion. Microresonator combs are generated for the first time in this emerging material platform.

STu3F.2 • 13:15

Harmonic Generation in Silicon Rich Nitride Photonic Crystal Cavities, Marco Clementi¹, Kapil Debnath^{2,3}, Moise Sotto², Thalia Domínguez Bucio³, Marco Liscidini¹, Daniele Bajoni¹, Frederic Gardes³, Matteo Galli¹; ¹Dipartimento di Fisica, Università di Pavia, Italy; ²Faculty of Physical Sciences and Engineering, Univ. of Southampton, UK; ³Optoelectronics Research Centre, Univ. of Southampton, UK. We demonstrate the cavity-enhanced second and third harmonic generation in silicon rich nitride 2D photonic crystal resonators under low-power continuous-wave excitation. Results show high generation efficiencies and suggest the absence of two-photon absorption.

STu3F.3 • 13:30

On-chip second order nonlinear generation in lithium niobate photonic crystal nanocavity, Haowei Jiang^{1,2}, Hanxiao Liang³, Rui Luo², Xianfeng Chen¹, Yuping Chen¹, Qiang Lin^{3,2}; ¹School of Physics and Astronomy, Shanghai Jiao Tong Univ., China; ²Inst. of Optics, Univ. of Rochester, USA; ³Dept. of Electrical and Computer Engineering, Univ. of Rochester, USA. We report the first observation of the second harmonic generation and the sum frequency generation in the one-dimensional lithium niobate photonic crystal nanocavity.

STu3F.4 • 13:45

Integrated Thin-film Lithium-Niobate Waveguides on Silicon for Second-Harmonic Generation Pumped at 1875 nm, Saeed Khan¹, Marcin Malinowski¹, Jean-Etienne Tremblay², Ashutosh Rao¹, Guillermo Camacho-Gonzalez¹, Ricardo Bustos Ramirez¹, Michael E. Plascak¹, Kathleen Richardson¹, Peter Delfyett^{1,3}, Ming C. Wu², Sasan Fathpour^{1,3}; ¹CREOL, The College of Optics and Photonics, Univ. of Central Florida, USA; ²Dept. of Electrical Engineering and Computer Sciences, Univ. of California, USA; ³Dept. of Electrical and Computer Engineering, Univ. of Central Florida, USA. A thin-film periodically-poled lithium niobate (PPLN) on silicon wavelength converter is demonstrated for application in carrier-envelope offset stabilization. Supercontinuum generation, amplified at about 1900 nm wavelength, is used to generate second harmonic generation.

CLEO: QELS-Fundamental Science

CLEO: Applications
& Technology

13:00–15:00

FTu3G • Quantum Key Distribution

President: Michael Brodsky; U.S. Army Research Lab, USA

FTu3G.1 • 13:00 **Invited**

Handheld Quantum Key Distribution, Gwenaëlle Melen^{1,2}, Peter Freiwang¹, Jannik Luhn¹, Tobias Vogl³, Markus Rau⁴, Wenjamin Rosenfeld¹, Harald Weinfurter^{1,5}; ¹Faculty of Physics, Univ. of Munich, Germany; ²Walter Schottky Inst., Technical Univ. Munich, Germany; ³Centre for Quantum Comp. and Comm. Technology, Australian National Univ., Australia; ⁴Qtools GmbH, Germany; ⁵Max-Planck Inst. for Quantum Optics, Germany. Using integrated optics enabled us to miniaturize QKD optics and to demonstrate handheld QKD. The robust device could be integrated with classical free space communication systems for links in metropolitan areas and to flying platforms.

FTu3G.2 • 13:30

Integrated Chip for Continuous-variable Quantum Key Distribution using Silicon Photonic Fabrication, Gong Zhang¹, Lin Cao², Jing Yan Haw³, Xiaojun Jia⁴, Xiaolong Su¹, Leong Chuan Kwek⁵, Joseph F. Fitzsimons^{5,6}, Ping Koy Lam³, Xiaoqi Zhou⁷, Weibo Gao⁸, Jiangbin Gong⁹, Yidong Chong⁹, Alexander Szameit¹⁰, Wee Ser¹, Ai-Qun Liu¹; ¹School of Electrical and Electronic Engineering, Nanyang Technological Univ., Singapore; ²School of Electronics Engineering and Computer Science, Peking Univ., China; ³Research School of Physics and Engineering, The Australian National Univ., Australia; ⁴Inst. of Opto-Electronics, Shanxi Univ., China; ⁵Centre for Quantum Technologies, National Univ. of Singapore, Singapore; ⁶Singapore Univ. of Technology and Design, Singapore; ⁷State Key Lab of Optoelectronic Materials and Technologies and School of Physics, Sun Yat-Sen Univ., China; ⁸School of Physical & Mathematical Sciences, Nanyang Technological Univ., Singapore; ⁹Dept. of Physics and Centre for Computational Science and Engineering, National Univ. of Singapore, Singapore; ¹⁰Inst. for Physics, Univ. of Rostock, Germany. A continuous-variable quantum key distribution system based on silicon photonic chip is designed and tested. A proof-of-principle test shows the secure key-rate can reach 1.92 Mbit/s at 0 km and 37 kbit/s at 45 km distance.

FTu3G.3 • 13:45

High-rate Time-bin Quantum Key Distribution Using Quantum-controlled Measurement, Nurul T. Islam¹, Charles Lim³, Clinton Cahall¹, Bing Qi², Jungsang Kim¹, Daniel J. Gauthier¹; ¹Duke Univ., USA; ²Oak Ridge National Lab, USA; ³National Univ. of Singapore, Singapore; ⁴The Ohio State Univ., USA. We realize a time-bin qudit-based quantum key distribution system that uses two-photon interference for measuring the phase-basis states, allowing us to generate a secret key at a megabits-per-second rate.

13:00–15:00

FTu3H • Quantum Optics with Solid-state Single Emitters

President: Peter Lodahl; Univ. of Copenhagen, Denmark

FTu3H.1 • 13:00

Two-photon Bundles from a Single Two-level System, Lukas Hanschke¹, Kevin Fischer², Jakob Wierzbowski¹, Tobias Simmet¹, Constantin Dory², Jonathan Finley³, Jelena Vuckovic², Kai Müller¹; ¹Walter Schottky Institut, TU München, Germany; ²E. L. Ginzton Lab, Stanford Univ., USA. Resonantly excited two-level systems are well-known as single-photon emitters. Here, we demonstrate the generation of two-photon bundles from a single quantum two-level transition in a self-assembled InAs quantum dot.

FTu3H.2 • 13:15

A Solid State Source of Photon Triplets based on Quantum Dot Molecules, Milad Khoshnevar^{3,4}, Tobias Huber^{1,2}, Ana Predojević², Dan Dalacu⁵, Maximilian Prilmüller², Jean Lapointe⁵, Xiaohua Wu⁵, Philippe Tamarat⁶, Brahim Lounis⁶, Philip Poole⁵, Gregor Weihs^{4,2}, Hamed Majedi^{3,7}; ¹Joint Quantum Inst., Univ. of Maryland & NIST, USA; ²Institut für Experimentalphysik, Universität Innsbruck, Austria; ³Dept. of Electrical and Computer Engineering, Univ. of Waterloo, Canada; ⁴Inst. for Quantum Computing, Univ. of Waterloo, Canada; ⁵National Research Council of Canada, Canada; ⁶LP2N Institut d'Optique and CNRS, Université Bordeaux, France; ⁷Waterloo Inst. for Nanotechnology, Univ. of Waterloo, Canada. We present a triple cascade recombination and sequential emission of three photons with strong correlations from a quantum dot molecule. We record 65.62 photon triplets per minute under continuous-wave pumping, surpassing rates of earlier reported sources.

FTu3H.3 • 13:30 **Invited**

A quantum knitting machine generating on demand cluster states of entangled photons, David . Gershoni¹; ¹Technion Israel Inst. of Technology, Israel. Repeated timed excitations of a quantum dot confined electronic spin is used to entangle the polarization of the emitted photons with that of the precessing spin and thereby also with the polarizations of the previously emitted photons

13:00–15:00

ATu3I • OCT and LIDAR

President: Peter Fendel; Thorlabs Inc, USA

ATu3I.1 • 13:00 **Invited**

High-Speed Coherent and Incoherent Monitoring of Laser Processing: from Closed-Loop Keyhole Welding to Additive Manufacturing, James M. Fraser¹; ¹Queen's Univ. at Kingston, Canada. In-process monitoring capable of fully resolving high-power laser processing has long been the goal of advanced manufacturing. We have achieved kHz-rate micron-resolution morphology and temperature monitoring and applied it to welding and selective laser melting.

ATu3I.2 • 13:30

Signal Reconstruction in SS-OCT using Compressed Sensing, Takuma Shirahata¹, Shinji Yamashita¹; ¹Univ. of Tokyo, Japan. We applied compressed sensing to SS-OCT for the first time. We use dispersion-tuned fiber laser for non-uniform k-space sampling. We achieved the same resolution and less noise of PSF with less sampling.

ATu3I.3 • 13:45

Spatially-offset optical coherence tomography, Mingzhou Chen¹, Josep Mas¹, Kishan Dholakia¹; ¹School of Physics and Astronomy, Univ. of St. Andrews, UK. We introduce a new geometry of spatially-offset optical coherence tomography (SO-OCT) to improve signal detection and reveal structural information from depth in the presence of strongly scattering layers.

Meeting Room
212 A/C

**CLEO: Applications
& Technology**

13:00–15:00

ATu3J • Nanobiophotonics

Presider: Andrea Armani; Univ. of Southern California, USA

ATu3J.1 • 13:00 **Invited**

Interferometric Microscopy for Detection and Visualization of Biological Nanoparticles, M. Selim Ünlü¹; ¹*Boston Univ., USA*. The sensitive detection and quantitative measurement of biological nanoparticles, such as viruses and exosomes, is of growing importance. We present a label-free optical biosensing method based on interferometric reflectance imaging to detect and characterize individual biological nanoparticles.

ATu3J.2 • 13:30

Broadband Fluorescence Enhancement and Ultrasensitive DNA Detection Using Plasmonic Open-Ring Nanoarrays, Akash Kannegulla¹, Ye Liu¹, Bo Wu¹, Li-Jing Cheng¹; ¹*Oregon State Univ., USA*. Silver open-ring nanostructures were designed for broadband fluorescence enhancement of quantum dots (QDs) and molecular beacons. The plasmon-enhanced fluorescence permits high signal-to-noise ratio yielding a ~300fM detection limit, superior to those on plane silver surfaces.

ATu3J.3 • 13:45

Spatial frequency projection super resolution imaging, Randy A. Bartels¹, Keith Wernsing¹, Patrick Stockton¹, Jeff Field¹, Jeff Squier²; ¹*Colorado State Univ., USA*; ²*Physics, Colorado School of Mines, USA*. Spatial Frequency Modulated Imaging (SPIFI) with nonlinear excitation is shown to enable super-resolved imaging of specimens via real or virtual state contrast. Extension of 1D enhancement to 2D through inverse domain tomography is discussed.

Meeting Room
212 B/D

CLEO: Science & Innovations

13:00–15:00

STu3K • Novel Fibers

Presider: Misha Sumetsky; Aston Univ., UK

STu3K.1 • 13:00 **Invited**

Towards in-fiber Silicon Photonics, Anna C. Peacock¹; ¹*Univ. of Southampton, UK*. This paper reviews recent advances in the fabrication and application of silicon optical fibers. Particular focus is placed on novel materials and device designs that facilitate integration with standard fiber systems.

STu3K.2 • 13:30

Nearly diffraction limited beam qualities in an Anderson localizing optical fiber, Behnam Abaie¹, Mostafa Peysokhan¹, Jian Zhao², Jose Antonio-Lopez², Rodrigo Amezcua Correa², A. Schülzgen², Arash Mafi¹; ¹*Univ. of New Mexico, USA*; ²*Univ. of Central Florida, CREOL, USA*. Nearly diffraction limited beams are demonstrated in a disordered optical fiber. High quality beams with M²~1 are obtained at various transverse positions across the output facet of the fiber.

STu3K.3 • 13:45

Deep-Learning-Based Imaging through Glass-Air Disordered Fiber with Transverse Anderson Localization, JIAN ZHAO¹, Yangyang Sun¹, Zheyuan Zhu¹, Donghui Zheng², Jose Enrique Antonio-Lopez¹, Rodrigo Amezcua Correa¹, Shuo Pang¹, A. Schülzgen¹; ¹*CREOL, College of Optics and Photonics, Univ. of Central Florida, USA*; ²*School of Electronic and Optical Engineering, Nanjing Univ. of Science and Technology, China*. We demonstrate for the first time that deep neural networks (DNNs) can be trained to recover images transported through a 90 cm-long silica-air disordered optical fiber at variable working distances without any distal optics.

Marriott
Salon I & II

Joint

13:00–15:00

JTu3L • Symposium on Multimodal and Molecular Contrast Optical Imaging I

Presider: Wolfgang Drexler, Medizinische Universität Wien, Austria

JTu3L.1 • 13:00 **Invited**

Molecular Imaging with Optical Coherence Tomography, Adam de la Zorda¹; ¹*Stanford Univ., USA*. We developed nanoparticles that produce strong spectral OCT signal, which we use to visualize molecular information in live animals, including key lymphatic markers and tumor-associated macrophages moving about a brain tumor of a live mouse.

JTu3L.2 • 13:30 **Invited**

Reflectance Confocal Microscopy and Fluorescence Lifetime Imaging in the Oral Cavity, Kristen C. Maitland¹, Taylor Hinsdale¹, Rodrigo Cuenca¹, Bilal H. Malik¹, Yi-Shing L. Cheng², John Wright², Javier A. Jo¹; ¹*Biomedical Engineering, Texas A&M Univ., USA*; ²*College of Dentistry, Texas A&M Univ. Health Science Center, USA*. Confocal microscopy provides high resolution optical sectioning of epithelial tissue, but with limited field of view. Fluorescence lifetime imaging is employed for macroscopic guidance with biochemical contrast to complement the microscopic morphologic imaging of reflectance confocal microscopy.

Tuesday, 13:00–15:00

CLEO: Science & Innovations

Joint

13:00–15:00

STu3M • High Peak Power Lasers & Technologies

President: Thomas Spinka; Lawrence Livermore National Lab, USA

STu3M.1 • 13:00

PW-class Laser Operation at 3.3 Hz and High Contrast Ultra-intense $\lambda=400$ nm Beamline, Shoujun Wang¹, Yong Wang¹, Alex Rockwood², Bradley Luther³, Reed Hollinge¹, Alden Curtis¹, Chase Calvi², Carmen Menoni^{1,3}, Jorge Rocca^{1,2}; ¹Electrical and Computer Engineering Dept., Colorado State Univ., USA; ²Physics Dept., Colorado State Univ., USA; ³Chemistry Dept., Colorado State Univ., USA. We demonstrated 0.85PW, 30fs pulses at a repetition rate of 3.3Hz from a Ti:Sapphire laser. Ultra-high contrast $\lambda=400$ nm fs pulses were generated with > 40% efficiency and focused to an intensity of 6.5×10^{21} W/cm².

STu3M.2 • 13:30

Hybrid OPCPA/Glass 10 PW Laser at 1 Shot a Minute, Erhard W. Gaul¹, Gilles Cheriaux¹, roman antipenkov², Frantisek Batysta², Ted borger¹, Gavin Friedman¹, Jonathan T. greene², axel jochmann¹, daniel kramer², bedrich rus², pavel trojek², stepan vyhlidka², todd ditmire¹; ¹National Energetics, USA; ²Extreme Light Infrastructure-Beamlines, Czechia. The 10PW OPCPA/glass laser under construction for ELI-Beamlines will exhibit output pulses delivered every minute with an energy of 1.5kJ within 150fs duration. We will show results of the sub-sections as well as output performances.

STu3M.3 • 13:45

First Intense, phase controlled, few cycle laser sources in the ELI Attosecond Facility, Karoly Osvay¹, Adam Borzsonyi¹, Dimitris Charalambidis¹, Eric Cormier¹, Lajos Fulop¹, Mikhail Kalashnikov¹, Christos Kamperidis¹, Balint Kiss¹, Rodrigo Lopez-Martens¹, Giuseppe Sansone¹, Zoltan Varallyay¹, Katalin Varju¹; ¹ELI-ALPS, Hungary. Laser systems operating in the 100W average power regime provide ELI-ALPS with TW-to-PW peak power pulses for generation of single and few cycle light sources from THz to XUV for basic and applied researches.

13:00–15:00

STu3N • Chemical Sensing

President: Erik Emmons; ECBC, USA

STu3N.1 • 13:00

Gas Sensing Using Heterogeneously Integrated Quantum Cascade Lasers on Silicon, Christopher C. Evans¹, Alexander Spott², Charles D. Merritt³, William W. Bewley³, Igor Vurgaftman³, Chul Soo Kim³, Jerry R. Meyer³, Joel M. Hensley¹, John E. Bowers², Michael B. Frish¹; ¹Physical Sciences Inc., USA; ²Univ. of California, Santa Barbara, USA; ³Naval Research Lab, USA. We demonstrate tunable diode-laser absorption spectroscopy (TDLAS) gas sensing near 4.8 μ m using a distributed-feedback quantum cascade laser heterogeneously integrated on a silicon-on-nitride-on-insulator platform. This platform enables sensors operating at wavelengths up to 6.7 μ m.

STu3N.2 • 13:15

Line-locked Cavity Ring-Down Faraday Rotation Spectroscopy with High Repetition Rate, Jakob Hayden², Jonas Westberg¹, Charles L. Patrick¹, Bernhard Lendl², Gerard Wysocki¹; ¹Dept. of Electrical Engineering, Princeton Univ., USA; ²Inst. of Chemical Technologies and Analytics, Technische Universitaet Wien, Austria. We present a line-locked cavity ring-down Faraday rotation spectrometer for trace gas detection of oxygen. The system reaches a ring-down rate of 8-10 kHz and a noise-equivalent angle of $\sim 9 \times 10^{-10}$ rad/ $\sqrt{\text{Hz}}$.

STu3N.3 • 13:30

Ultrashort-Pulse LIBS for Detecting Airborne Metal Particles from Energetic Material Reactions, Morgan O'Neil¹, Nicholas Niemiec¹, Andrew Demko¹, Eric Petersen¹, Waruna Kulatilaka¹; ¹Texas A&M Univ., USA. Ultrashort-pulse, femtosecond-duration laser-induced breakdown spectroscopy (fs-LIBS), has been demonstrated for enhanced detection of metal particles such as Al, Pb, Cu, and Hg, released to the gas phase during energetic material reactions.

STu3N.4 • 13:45

Standoff detection of bulk and trace elements using laser-induced fluorescence of laser ablation plumes, Sivanandan S. Harilal¹, Brian Brumfield¹, Mark Phillips¹; ¹Pacific Northwest National Lab, USA. We demonstrate 10 m standoff analysis of bulk and trace elements in laser-produced plasmas using tunable laser-induced fluorescence (LIF). LIF of laser-ablation plumes provides emission enhancement, higher spectral resolution in comparison with thermally-excited emission.

13:00–15:00

JTu3O • Laser Modification of Materials

President: Renee Sher; Wesleyan Univeristy, USA

JTu3O.1 • 13:00

Mechanism of Single-pulse Ablative Generation of Laser-induced Periodic Surface Structures, Iaroslav Gnilytskyi^{2,1}, Maxim Shugaev³, Tommi White⁴, Leonid Zhigilei³; ¹UNIMORE, Italy; ²NoviNano Inc., Ukraine; ³Univ. of Virginia, USA; ⁴Univ. of Missouri, USA. Experimental and computational analysis of the mechanisms of ablative LIPSS formation is reported. The results of large-scale molecular dynamics simulation performed for Cr target reveal a complex interplay of material removal and redistribution in the course of spatially modulated ablation.

JTu3O.2 • 13:15

Self-organized nanogratings induced by femtosecond laser pulse direct writing in optical fibers, Jiafeng Lu¹, Qin Li³, Ye Dai³, Yali Zhang¹, Chunhua Wang¹, Fufei Pang¹, Tingyun Wang¹, Xianglong Zeng^{1,2}; ¹Key Lab of Specialty Fiber Optics and Optical Access Networks, Joint International Research Lab of Specialty, Fiber Optics and Advanced Communication, Shanghai Univ., China; ²Shanghai Inst. for Advanced Communication and Data Science, Shanghai Univ., China; ³Dept. of Physics, Shanghai Univ., China. Self-organized nanogratings induced by femtosecond laser pulse direct writing are demonstrated in optical fibers. The results reveal strong anisotropic birefringence of nanogratings. Depolarization and retardation of nanograting are investigated through analyzing Mueller matrices method.

JTu3O.3 • 13:30

Spectrally tunable Airy beam generation using cholesteric liquid crystals, Matthew S. Mills¹, Ben Kowalski^{1,2}, Vincent Tondiglia^{1,2}, Kyungmin Lee^{1,2}, Aubrey Steele^{1,2}, Timothy White¹, Dean Evans¹; ¹RXA, AFRL, USA; ²Azimuth Corporation, USA. We demonstrate spectrally tunable Airy beams via a chiral Bragg reflector. Specifically, we photo-align a cholesteric liquid crystal such that it conditionally imparts a cubic phase dependent on voltage applied across the sample.

JTu3O.4 • 13:45

Photopolymerization differences by using nanosecond and picosecond laser pulses, Evaldas Stankevicius¹; ¹FTMC, Lithuania. Formation of polymeric pillars by using laser interference lithography will be compared for nanosecond and picosecond laser pulses. The experimental results will be explained by dynamics of laser-excited radicals.

CLEO: Science & Innovations

13:00–15:00

STu3P • Precision Spectroscopy

President: Marco Marangoni;
Politecnico di Milano, Italy

STu3P.1 • 13:00

Erbium-Fiber-Based Visible Astro-Comb with 42-GHz Mode Spacing, Sho Okubo¹, Keisuke Nakamura¹, Malte Schramm¹, Hiroki Yamamoto², Jun Ishikawa¹, Feng-Lei Hong², Ken Kashiwagi¹, Kaoru Minoshima³, Hironori Tsutsui⁴, Eiji Kambe⁴, Hideyuki Izumiura⁴, Hajime Inaba¹; ¹National Metrology Inst. of Japan, Japan; ²Yokohama National Univ., Japan; ³Univ. of Electro-Communications, Japan; ⁴Okayama Astrophysical Observatory, NAOJ, Japan. We developed an erbium-fiber-based astro-comb with 42-GHz spacing and wavelength coverage from 500 to 520 nm to calibrate a high dispersion spectrograph for radial velocity measurements and observed the comb spectrum at Okayama astrophysical observatory.

STu3P.2 • 13:15

Ultra-Broadband, Infrared Astro-Comb Generation, Tilo Steinmetz², Yuanjie Wu², Rafael Probst², Heinar Hoogland^{2,3}, Mathäus Halder², Peter Adel², Olaf Mandel², Sascha Donath², Johanna Adelung², Ronald Holzwarth^{2,1}; ¹Max-Planck-Institut für Quantenoptik, Germany; ²Menlo Systems GmbH, Germany; ³Lehrstuhl für Laserphysik, Friedrich-Alexander-Universität, Germany. We present a concept for spectral broadening of an Er: fiber based astronomical frequency comb to cover more than two octaves ranging from 0.45 μm to at least 2.4 μm .

STu3P.3 • 13:30 **Invited**

Measuring Temperature with Atoms and Molecules, Gar-Wing Truong¹, Sarah Scholten¹, Faisal Karim¹, James Anstie¹, Chris Perrella¹, Philip Light¹, Dong Wei², Eric May³, Tom Stace⁴, Andre N. Luiten¹; ¹Univ. of Adelaide, Australia; ²Xi'an Univ., China; ³Univ. of Western Australia, Australia; ⁴Univ. of Queensland, Australia. We have developed atomic and molecular spectrometers that deliver quantum-limited measurements of the absorption lineshape. We use this to deduce the temperature of the gas and thereby measure Boltzmann's constant with high precision and uncertainty.

13:00–15:00

STu3Q • Advances in VCSELS

President: Connie Chang-Hasnain;
Univ. of California Berkeley, USA

STu3Q.1 • 13:00 **Invited**

Recent Progress in GaSb-based VCSELS with Emission Wavelengths up to 4 μm , Ralf Meyer¹, G.K. Veerabathran¹, A. Andrejew¹, S. Sprengel¹, M.-C. Amann¹; ¹TU Munich, Germany. The wavelength of commercially InP-based VCSELS is limited to 2.3 μm . Applying type-II active regions allowed the fabrication of devices emitting at 2.5 μm . Adapting this concept to GaSb, even wavelengths of up to 4 μm were achieved.

STu3Q.2 • 13:30

High-Speed Modulation of 1.55- μm VCSELS with Spin Polarization Modulation, Nobuhide Yokota¹, Kunpei Nisaka¹, Hiroshi Yasaka¹, Kazuhiro Ikeda²; ¹Tohoku Univ., Japan; ²National Inst. of Advanced Industrial Science and Technology, Japan. We investigate a novel high-speed direct modulation scheme of InAlGaAs VCSELS using optical spin injection and modulation. A wide 3-dB bandwidth drastically enhanced by the birefringence of VCSEL is demonstrated in both calculations and experiments.

STu3Q.3 • 13:45

Precise Two-step Growth of 940-nm VCSEL on a GaAsP-capped DBR Wafer, Jiaying Wang¹, Jonas Kapraun¹, Emil Kolev¹, Jipeng Qi¹, Kevin Cook¹, Connie J. Chang-Hasnain¹; ¹Univ. of California Berkeley, USA. We report a 2-step growth for 940-nm VCSELS on DBRs capped by a novel protective GaAsP layer, desorbed during the secondary growth including laser region to yield precise high quality VCSELS with sub-mA threshold.

CLEO: Applications
& Technology

13:00–15:00

ATu3R • A&T Topical Review on Advanced Applications of Laser Radar and Remote Sensing I

President: TBD

ATu3R.1 • 13:00 **Invited**

TBD, McManamon Paul¹; ¹Exciting Technology LLC, USA. TBD

ATu3R.2 • 13:30

High-Performance Integrated Optical Phased Arrays for Chip-Scale Beam Steering and LiDAR, Christopher V. Poulton¹, Peter Russo¹, Erman Timurdogan¹, Michael Whitson¹, Matthew Byrd¹, Ehsan Hosseini¹, Benjamin Moss¹, Zhan Su¹, Diedrik Vermeulen¹, Michael Watts¹; ¹Analog Photonics, USA. We present high-performance integrated optical phased arrays and LiDAR on diffusive targets for the first time at 25m with velocity extraction. This work shows the promise for optical phased arrays in solid-state LiDARs.

ATu3R.3 • 13:45

Vernier Transceiver Architecture for Side-Lobe-Free and High-Entendue LiDAR, Sergio Pinna¹, Bowen Song¹, Larry A. Coldren¹, Jonathan Klamkin¹; ¹Electrical and Computer Engineering, Univ. of California Santa Barbara, USA. Vernier-based LiDAR transceiver for high side-modesuppression optical phased arrays is proposed and investigated. This architecture enables side-lobe-free 180° viewing angle with multiple-wavelength waveguide spacing thereby easing fabrication requirements.

13:00–15:00

ATu3S • A&T Topical Review on Advances in Supercontinuum Technologies I: Supercontinuum Generation

President: Adam Devine; Fianium Ltd., UK

ATu3S.1 • 13:00 **Invited**

Ultra Low Loss Waveguides for Extreme Nonlinear Optics, Michal Lipson¹; ¹Columbia Univ., USA. TBD

ATu3S.2 • 13:30 **Invited**

Ultraviolet Supercontinuum Generation in Optical Fibers, John C. Travers¹, Teodora Grigoro¹, Federico Belli¹; ¹Heriot-Watt Univ., UK. We review the physics and techniques for the extension of multi-octave near-infrared pumped supercontinuum generation to the deep ultraviolet in solid-core photonic-crystal fibers (200 nm) and the vacuum-ultraviolet in gas-filled hollow-core fibers (113 nm).

CLEO: Science & Innovations

STu3A • Quantum Photonic Technology—
Continued

STu3A.3 • 14:00

Enhanced Silicon Single-photon Avalanche Diode Based on Light Trapping, Kai Zang¹, Xiao Jiang^{2,3}, Yijie Huo¹, Tianzhe Zheng^{2,3}, Yueyang Fei^{2,3}, Xun Ding^{2,3}, Matthew Morea¹, Muyu Xue⁴, Ching-Ying Lu¹, Theodore I. Kamins¹, Qiang Zhang^{2,3}, Jian-Wei Pan^{2,3}, James S. Harris^{1,4}; ¹Electrical Engineering, Stanford Univ., USA; ²Hefei National Lab for Physical Sciences at Microscale and Dept. of Modern Physics, Univ. of Science and Technology of China, China; ³CAS center for Excellence and Synergetic Innovation Center in Quantum Information and Quantum Physics, Univ. of Science and Technology of China, China; ⁴Materials Science and Engineering, Stanford, USA. We present a nano-structured light-trapping Si SPAD with improved detection efficiency, without sacrificing jitter distribution or dark count rate. The design can be adopted for CMOS-compatible SPAD image sensors and silicon photomultipliers.

STu3A.4 • 14:15

Metallic Nano-Rings for Efficient, Broadband Light Extraction from Solid-State Single-Photon Sources, Oliver J. Trojak¹, Christopher Woodhead², Jin Dong Song³, Robert Young², Luca Sapienza¹; ¹Dept. of Physics and Astronomy, Univ. of Southampton, UK; ²Physics Dept., Lancaster Univ., UK; ³Center for Opto-Electronic Materials and Devices Research, Korea Inst. of Science and Technology, South Korea. Metallic nano-rings deposited on the sample surface, centered around single InAs/GaAs quantum dots, enhance the brightness of the emission up to $\times 20$, further enhanced by $\times 10$ by epoxy solid-immersion lenses, in a scalable broadband device.

STu3A.5 • 14:30 **Invited**

CMOS Photonic Circuits for Trapped Ion Quantum Computing and Molecular Sensing, Rajeev Jagga Ram¹; ¹MIT, USA. Photonic integrated circuits for UV and visible light offer a scalable approach to the classical optics and electronics required for large-scale trapped-ion quantum information processing as well as for self-contained lab-on-a-chip systems for molecular diagnostics.

STu3B • OAM and Photodetective—
Continued

STu3B.2 • 14:00

Demonstration of Chip-to-Chip Communication Based on Ultra-Compact Orbital Angular Momentum (de)Multiplexers, Shimao Li¹, Zhichao Nong¹, Xiong Wu¹, Wen Yu¹, Mingbo He¹, Yuntao Zhu¹, Shengqian Gao¹, Jie Liu¹, Zhaohui Li¹, Liu Liu², Si-Yuan Yu¹, Xinlun Cai¹; ¹Sun Yat-sen Univ., China; ²South China Normal Univ., China. In this work we demonstrate chip-to-chip orbital angular momentum (OAM) multiplexing transmission using a pair of ultra-compact silicon integrated (de)multiplexer. Four OAM beams were multiplexed and then were demultiplexed by the devices.

STu3B.3 • 14:15

Multi-octave image-reject mixer with large suppression of mixing spurs based on balanced photodetectors, Wenjuan Chen¹, Dan Zhu¹, Shilong Pan¹; ¹Nanjing Univ Aeronautics & Astronautics, China. A multi-octave photonic image-reject mixer is proposed based on two balanced photodetectors and an optical hybrid. More than 60-dB image rejection and mixing spurs suppression are realized simultaneously over a wide frequency range.

STu3B.4 • 14:30

100GHz Balanced Photodetector Module, Patrick Runge¹, Gan Zhou¹, Tobias Beckerwerth¹, Shahram Keyvaninia¹, Sven Mutschall¹, Angela Seeger¹, Robert Klötzer¹, Sebastian Wünsch¹, Greta Ropers¹; ¹Fraunhofer Institut, Germany. We demonstrate a 100GHz balanced photodetector module. Regarding the bandwidth the module exceeds all other state of the art balanced modules. The module focuses on next generation optical networks with 112GBaud and operates in C-band and L-band.

STu3B.5 • 14:45

Zero-bias Photovaractor with 60 GHz Resonant Network for Optically Modulated Scatterer (OMS) Application, Jesse S. Morgan¹, Jizhao Zang¹, Keye Sun¹, Bassem Tossoun¹, Joe C. Campbell¹, Andreas Beling¹; ¹Univ. of Virginia, USA. We report a zero-bias photovaractor flip-chip bonded to a coplanar-waveguide resonant network for use as a probe designed to measure near-field characteristics of antennas operating at 60 GHz.

STu3C • Advanced Short Reach and Free
Space Communications—Continued

STu3C.4 • 14:00

Large Scale Optical Interconnection Using Kerr Frequency Comb and Direct-Detection Kramers-Kronig Receiver, Mingyue Zhu¹, Yong Geng¹, Xingwen Yi^{2,1}, Jing Zhang¹, Heng Zhou¹; ¹Univ. of Electronic Science and Technology of China, China; ²School of Electronics and Information Technology, Sun Yat-Sen Univ., China. We demonstrate large scale optical interconnection using Kerr frequency comb within 1540-1560 nm wavelength. An optical SSB-PAM-4 signal with total bitrate of 325-Gb/s (13 \times 25 Gb/s) are successfully transmitted over 80-km SSMF by a Kramers-Kronig receiver.

STu3C.5 • 14:15

A Phase Retrieval Method Using Dispersion for Direct Detection of Biased QAM Signals, Masayuki Matsumoto¹; ¹Wakayama Univ., Japan. Phase retrieval using dispersion in direct-detection receiver for biased Nyquist 16QAM signals is numerically examined. Processing error can be small at high bias power ratio. The continuous wave acting as a bias can be located within the signal spectrum.

STu3C.6 • 14:30

112 Gb/s PAM-4 Signal Transmission Over 80 km SSMF with Digital CD Pre-compensation Enabled SPM Mitigation, Xiang Li¹, Fan Gao², Ming Luo¹, Jianqiang Li³, Songnian Fu²; ¹WRI, China; ²HUST, China; ³BUPT, China. We demonstrate single-lane 112 Gb/s PAM-4 signal over 80 km SSMF by digital CD pre-compensation. Thanks for the residual positive CD enabled SPM mitigation, simplified Volterra filter equalizer secures BER below the 7% HD-FEC threshold.

STu3C.7 • 14:45

Directly Modulated Laser Transmitters for Scalable Multi-rate DPSK Communications, David O. Caplan¹, P. S. Bedrosian¹, Jade P. Wang¹, Barry R. Romkey¹, Mark L. Stevens¹, Clement Burton¹, Andrew Horvath¹, Scott A. Hamilton¹; ¹MIT Lincoln Lab, USA. We present a new approach for generating multi-rate burst-mode DPSK waveforms using time and frequency-windowed directly modulated laser transmitters. Near-theoretical performance is demonstrated over a wide range of data rates using a WDM-scalable implementation.

15:00–17:00 Coffee Break & Exhibit Only Time, Exhibit Hall

15:30–17:00 Meet the OSA Editors Reception, Exhibit Hall, #2425

CLEO: Science & Innovations

STu3D • Terahertz Communications—
Continued

STu3D.2 • 14:00

Channel Characteristics for Terahertz Wireless Communications, Jianjun Ma¹, Rabi Shrestha¹, Lothar Moeller², Daniel M. Mittleman¹; ¹*School of Engineering, Brown Univ., USA*; ²*New Jersey Inst. of technology, USA*. We investigate channel performances for indoor terahertz (THz) wireless links with carrier frequencies at 100, 200, 300 and 400 GHz. We demonstrate error-free data links using both line-of-sight and non-line-of-sight configurations.

STu3D.3 • 14:15

Seamless connection between high-speed THz-wave and optical signals with high spectral efficiency, Koichi Takiguchi¹; ¹*Dept. of Electrical and Electronic Engineering, Ritsumeikan Univ., Japan*. I report seamless connection between THz-wave and optical signals. A 40 Gbit/s THz-wave signal, which was generated from an optical signal shaped with a Nyquist-filter, was flexibly converted into an optical signal through an optical-modulator.

STu3D.4 • 14:30

Terahertz-to-Optical Conversion Using a Plasmonic Modulator, Sandeep Ummethala^{1,2}, Tobias Harter^{1,2}, Kira Köhnle^{1,2}, Sascha Muehlbrandt^{1,2}, Yasar Kutuvantavida^{1,2}, Juned N. Kemal², Jochen Schaefer³, Hermann Massler⁴, Axel Tessmann⁴, Suresh Kumar Garlapati⁵, Andreas Bacher¹, Lothar Hahn¹, Martin Walther⁴, Thomas Zwick³, Sebastian Randel², Wolfgang Freude², Christian Koos^{1,2}; ¹*Inst. of Microstructure Technology, Karlsruhe Inst. of Technology, Germany*; ²*Inst. of Photonics and Quantum Electronics, Karlsruhe Inst. of Technology, Germany*; ³*Inst. of Radio Frequency Engineering and Electronics, Karlsruhe Inst. of Technology, Germany*; ⁴*Fraunhofer Inst. for Applied Solid State Physics, Germany*; ⁵*Inst. of Nanotechnology, Karlsruhe Inst. of Technology, Germany*. We show a THz plasmonic modulator with flat frequency response from 40 MHz to 0.325 THz and employ it to demonstrate THz-to-optical conversion of a 30 Gbit/s signal on a 0.294 THz carrier.

STu3D.5 • 14:45

Monolithically Integrated THz Transceiver for 1550 nm Excitation, Robert Kohlhaas¹, Simon Nellen¹, Lars Liebermeister¹, Steffen Breuer¹, Bjoern Globisch¹; ¹*Fraunhofer Heinrich Hertz Inst., Germany*. We present a monolithically integrated transceiver based on InGaAs:Fe for THz TDS in reflection geometry. With 70 dB signal-to-noise ratio and 5 THz bandwidth, the transceiver is a competitive alternative to individual THz modules.

CLEO: QELS-Fundamental
ScienceFTu3E • Thermal and Quantum Applications
of Metasurfaces—Continued

FTu3E.4 • 14:00

Dirac-Maxwell correspondence: Spin-1 bosonic topological insulator, Todd F. Van Mechelen¹, Zubin Jacob¹; ¹*Purdue Univ., USA*. We introduce photonic Dirac monopoles and strings, proving the existence of a spin-1 bosonic topological phase for light. Fundamentally different from pseudo-spin-1/2 based photonic crystals, we discover quantized spin in symmetry protected helical edge states of continuous media.

FTu3E.5 • 14:15

Generating Entanglement of Spin and Orbital Angular Momentum by Metasurfaces, Tomer Stav¹, Arkady Faerman², Elhanan Maguid², Dikla Oren¹, Vladimir Kleiner², Erez Hasman², Mordechai Segev¹; ¹*Physics, Technion, Israel*; ²*Mechanical Engineering, Technion, Israel*. We design an experiment that uses a highly efficient dielectric metasurface to create entanglement on a single photon. The spin-orbit interaction mediated by the metasurface entangles the polarization and orbital angular momentum degrees of freedom.

FTu3E.6 • 14:30

Angular Momentum Contribution of Topologically Structured Darkness, Samuel N. Alperin¹, Mark E. Siemens¹; ¹*Univ. of Denver, USA*. We explain the discrepancy between the fractional winding number of a generating spiral phase optic with the OAM of the resulting beam, and demonstrate the first direct measurement of intrinsic OAM of fractional vortex beams.

FTu3E.7 • 14:45

Broadband Control of Topological Nodes in Electromagnetic Fields, Alex Y. Song¹, Peter B. Catrysse¹, Shanhui Fan¹; ¹*Stanford Univ., USA*. The topological nodes in electromagnetic waves are shown to bound to a symmetry plane in a dielectric structure over a broad wavelength range. As an implication, broadband hiding of objects can be realized.

CLEO: Science & Innovations

STu3F • Nonlinear Integrated Photonic
Platforms—Continued

STu3F.5 • 14:00

A gallium arsenide nonlinear platform on silicon, Lin Chang¹, Xiaowen Guo¹, Daryl Spencer², Jeff Chiles², Abijith Kowligy², Nima Nader², Daniel Hickstein², MJ Kennedy¹, Andreas Boes¹, Nicolas Volet¹, Scott Diddams², Scott Papp², John E. Bowers¹; ¹*Univ. of California Santa Barbara, USA*; ²*National Inst. of Standards and Technology, USA*. A nonlinear platform using gallium arsenide (GaAs) waveguides cladded with SiO₂ has been demonstrated on silicon substrates. It is suitable for efficient nonlinear applications. Second harmonic generation (SHG) with record-high efficiency of 38,000% W⁻¹cm⁻² has been achieved.

STu3F.6 • 14:30

Supercontinuum generation in angle-etched diamond waveguides, Pawel Latawiec¹, Amirhassan Shams-Ansari^{1,4}, Yoshitomo Okawachi², Vivek Venkataraman^{1,3}, Mengjie Yu², Haig Atikian¹, Gary Harris⁴, Nathalie Picque⁵, Alexander L. Gaeta², Marko Loncar¹; ¹*Harvard Univ., USA*; ²*Columbia Univ., USA*; ³*Indian Inst. of Technology, India*; ⁴*Howard Univ., USA*; ⁵*Max Plank Inst. for Quantum Optics, Germany*. On-chip supercontinuum generation in visible is demonstrated experimentally in angle-etched diamond waveguides. The output spectrum spans from 670-920 nm in response to a 100 femtosecond pulse input at 15 mW average power and 80 MHz repetition rate.

STu3F.7 • 14:45

Enhanced four-wave mixing in graphene oxide coated waveguides, Yunyi Yang¹, Jiayang Wu¹, Xingyuan Xu¹, Sai T. Chu², Brent Little³, Roberto Morandotti⁴, Baohua Jia¹, David J. Moss¹; ¹*Swinburne Univ. of Technology, Australia*; ²*City Univ. of Hong Kong, China*; ³*Chinese Academy of Science, China*; ⁴*INRS-Energie, Matériaux et Télécommunications, Canada*. We experimentally demonstrate enhanced four-wave mixing (FWM) in an integrated waveguide coated with graphene oxide (GO). Owing to the high Kerr nonlinearity of GO and strong mode overlap, we achieve ~9.5-dB enhancement in FWM conversion efficiency.

15:00–17:00 Coffee Break & Exhibit Only Time, Exhibit Hall

15:30–17:00 Meet the OSA Editors Reception, Exhibit Hall, #2425

CLEO: QELS-Fundamental Science

CLEO: Applications
& TechnologyFTu3G • Quantum Key Distribution—
Continued

FTu3G.4 • 14:00

Experimental Demonstration of a 10-Mbit/s Quantum Link using Data Encoding on Orthogonal Laguerre-Gaussian Modes, Kai Pang¹, Cong Liu¹, Guodong Xie¹, Yongxiang Ren¹, Zhe Zhao¹, Runzhou Zhang¹, Yinwen Cao¹, Jiapeng Zhao¹, Long Li¹, Haoqian Song¹, Hao Song¹, Moshe Tur², Robert Boyd³, Alan E. Willner¹; ¹University of Southern California, USA; ²Tel Aviv Univ., Israel; ³Univ. of Rochester, USA. We experimentally investigate the performance of a quantum communication link using Laguerre-Gaussian (LG) modes with different radial indices. Quantum symbol error rate (QSER) <5% is achieved at an encoding rate of 10 Mbits/s.

FTu3G.5 • 14:15

Experimental Quantum Key Distribution at 1.3 Gbit/s Secret-Key Rate over a 10-dB-Loss Channel, Zheshen Zhang^{2,1}, Changchen Chen², Quntao Zhuang², Jane E. Heyses², Franco N. Wong², Jeffrey H. Shapiro²; ¹The Univ. of Arizona, USA; ²Research Lab of Electronics, Massachusetts Inst. of Technology, USA. We demonstrate quantum key distribution at 1.3-Gbit/s secret-key rates over a 10-dB-loss channel. By transmitting many photons per bit with multi-mode encoding our protocol overcomes channel loss to achieve gigabit-per-second rates without compromising security.

FTu3G.6 • 14:30

Birefringent Interferometry for Quantum Key Distribution, Amos Martinez¹, Bernd Fröhlich¹, James F. Dynes¹, Andrew W. Sharpe¹, Winci Tam¹, Alan Plevins¹, Marco Lucamarini¹, Zhiliang Yuan¹, Andrew Shields¹; ¹Toshiba UK, UK. We report quantum key distribution using an all-fiber, highly birefringent interferometer to implement the BB84 protocol. With this approach, we demonstrate point-to-point operation over 15.5 km drop fiber and an 8-port passive optical network splitter.

FTu3G.7 • 14:45

Entanglement loss and recovery due to arbitrarily oriented polarization dependent loss for telecom band photon pairs., Daniel E. Jones¹, Brian T. Kirby¹, Michael Brodsky¹; ¹US Army Research Lab, USA. Interplay of residual fiber birefringence and modal loss impairs propagation of polarization entangled photons in fibers. We introduce an illustrative Stokes space model of the effect, verify it experimentally, and demonstrate a simple compensating scheme.

FTu3H • Quantum Optics with Solid-state
Single Emitters—Continued

FTu3H.4 • 14:00

Colossal Photon Bunching Driven by Phonon Recombination Dynamics, Matthew A. Feldman^{1,2}, Eugene Dumitrescu², Denzel Bridges³, Matthew Chisholm⁴, Roderick Davidson^{1,2}, Phil Evans⁵, Jordan Hachtel⁵, Anming Hu³, Raphael C. Pooser², Richard Haglund¹, Benjamin Lawrie²; ¹Dept. of Physics and Astronomy, Vanderbilt Univ., USA; ²Quantum Information Science Group, Oak Ridge National Lab, USA; ³Mechanical Engineering, Univ. of Tennessee, USA; ⁴Material Science and Technology Division, Oak Ridge National Lab, USA; ⁵Center for Nanophase Materials Science, Oak Ridge National Lab, USA. We report photon bunching $g^{(2)}(0) \approx 49$ due to phonon sidebands in spectrally filtered cathodoluminescence from NV centers in diamond. The result is consistent with fast, phonon-mediated recombination dynamics, and supported by a stochastic model.

FTu3H.5 • 14:15

Strong Cavity Enhancement of Spontaneous Emission from Silicon-Vacancy Centers in Diamond, Jingyuan Linda Zhang¹, Shuo Sun¹, Michael J. Burek², Constantin Dory¹, Yan-Kai Tzeng³, Kevin Fischer¹, Yousif Kelaita¹, Konstantinos Lagoudakis¹, Marina Radulaski¹, Zhu-Xun Shen^{3,5}, Nicholas Melosh^{4,5}, Steven Chu^{3,6}, Marko Loncar², Jelena Vuckovic¹; ¹E. L. Ginzton Lab, Stanford Univ., USA; ²School of Engineering and Applied Sciences, Harvard Univ., USA; ³Dept. of Physics, Stanford Univ., USA; ⁴Geballe Lab for Advanced Materials, Stanford Univ., USA; ⁵Stanford Inst. for Materials and Energy Sciences, SLAC National Accelerator Lab, USA; ⁶Dept. of Molecular and Cellular Physiology, Stanford Univ., USA. We demonstrate strong enhancement of spontaneous emission of a single silicon-vacancy (SiV) center in diamond embedded in a monolithic optical cavity, with 10-fold lifetime reduction and 42-fold enhancement in emission intensity under resonant condition.

FTu3H.6 • 14:30

Reducing phonon-induced decoherence of solid-state artificial atoms with cavity quantum electrodynamics, Pascale Senellart¹, Alexia Auffeves², Thomas Grange², Carlos Anton¹, Niccolo Somaschi¹, Lorenzo De Santis¹, Aristide Lemaître¹, Guillaume Coppola¹, Valerian Giesz¹; ¹CNRS-Center for Nanoscience and Nanotechnology, France; ²CNRS, Institut Néel, France. We show how cavity quantum electrodynamics can be used to strongly suppress phonon-assisted emission from solid-state artificial atoms such as semiconductor quantum dots. This results in substantially enhanced performances in single-photon sources

FTu3H.7 • 14:45

A solid-state single photon filter, Pascale Senellart¹, Lorenzo De Santis¹, Carlos Anton¹, Alexia Auffeves², Bogdan Reznichenkov², Niccolo Somaschi¹, Guillaume Coppola¹, Aristide Lemaître¹, Andrew White³, Loic Lanco¹; ¹CNRS-Center for Nanoscience and Nanotechnology, France; ²CNRS-Institut Néel, France; ³Univ. of Queensland, Australia. A single semiconductor quantum dot in a microcavity is shown to filter single photon Fock states. The device presents a non-linearity threshold of 0.3 photons and strongly suppresses the multi-photon components of an incident coherent beam.

ATu3I • OCT and LIDAR—Continued

ATu3I.4 • 14:00

Synthetic-Wavelength-Based Dual-Comb Interferometry for High-Speed and High-Precision Distance Measurement, Zebin Zhu¹, Kai Ni², Qian Zhou², Guanhao Wu^{1,2}; ¹Dept. of Precision Instrument, Tsinghua Univ., China; ²Division of Advanced Manufacturing, Graduate School at Shenzhen, Tsinghua Univ., China. We propose a dual-comb ranging system based on synthetic-wavelength interferometry. It can realize absolute distance measurement with ~2.7m ambiguity range, ~3nm precision within ~10ms averaging time.

ATu3I.5 • 14:15

Speckle mitigation in laser Doppler vibrometry based on a compact silicon photonics chip, Yanlu Li^{1,2}, Jinghao Zhu^{1,2}, Matthieu Duperron³, Peter O'Brien³, Ralf Schüler³, Soren Aasmul⁴, Mirko de Melis⁴, Roel Baets^{1,2}; ¹Photonics Research Group, Ghent Univ.-imec, Belgium; ²Center for Nano- and Biophotonics, Ghent Univ., Belgium; ³Tyndall National Inst., Ireland; ⁴Medtronic Bakken Research Center, Netherlands; ⁵SIOS Messtechnik GmbH, Germany. A compact six-beam homodyne laser Doppler vibrometry (LDV) system is realized based on a silicon-on-insulator (SOI) photonic integrated circuit. We demonstrate a speckle mitigation method by averaging signals from the six channels.

ATu3I.6 • 14:30

High spatial resolution LIDAR for detection of cracks on tunnel surfaces, Takeharu Murakami¹, Norihito Saito¹, Yuichi Komachi¹, Takashi Michikawa¹, Michio Sakashita¹, Shigeru Kogure¹, Kiwamu Kase¹, Satoshi Wada¹, Katsumi Midorikawa¹; ¹RIKEN, Japan. We developed a high resolution LIDAR to detect cracks on a concrete placed 5 m away. The LIDAR can detect cracks with 200 μ m width which is difficult to detect by existing remote inspections.

15:00–17:00 Coffee Break & Exhibit Only Time, Exhibit Hall

15:30–17:00 Meet the OSA Editors Reception, Exhibit Hall, #2425

Meeting Room
212 A/C

CLEO: Applications
& Technology

ATu3J • Nanobiophotonics—Continued

ATu3J.4 • 14:00

A Nanoplasmonic Sensor Fabricated by Laser Interference Lithography (LIL) for Immunoglobulin Detection, Chi-Chen Lin¹, Jian-Fu Luo¹, Lon A. Wang¹, Nien-Tsu Huang¹; ¹National Taiwan Univ., Taiwan. We fabricated a nanoplasmonic sensor using laser interference lithography (LIL) for label-free biomolecule sensing. This sensor is able to achieve 236 nm/RIU sensitivity and has high uniformity over a large area (~ 1 cm²).

ATu3J.5 • 14:15

High-throughput holographic monitoring of nanoparticle degradation for drug delivery applications, Aniruddha Ray¹, Shuoran Li¹, Tatiana Segura¹, Aydogan . Ozcan¹; ¹Univ. of California, Los Angeles, USA. We present computational holographic imaging methods for high-throughput quantification of nanoparticle degradation for drug delivery applications. These techniques enable accurate monitoring of the dynamics of nanocarrier degradation over a large field-of-view.

ATu3J.6 • 14:30

Semiconductor Laser Particles in Biological Cells, Sheldon J. Kwok^{2,1}, Nicola Martino², Andreas C. Liapis², Sarah Wu¹, Sarah Forward², Seok-Hyun Yun^{2,1}; ¹MIT, USA; ²Wellman Center for Photomedicine, Massachusetts General Hospital, USA. We develop a method for fabricating biocompatible, semiconductor laser particles for integration into biological systems. Micron-sized laser particles coated with a passivating silica shell are readily and safely uptaken by several cell lines *in vitro*.

ATu3J.7 • 14:45

Sub-nano-Tesla, Shield-less, Field Compensation-Free Inelastic Wave Mixing Magnetometry for Bio-magnetism, Lu Deng¹, Yvonne Y. Li², Feng Zhou¹, Eric Y. Zhu³, Edward W. Hagley¹; ¹NIIST, USA; ²Dana-Farber Cancer Inst., Harvard Medical School, USA; ³Univ. of Toronto, Canada. We report an inelastic-wave-mixing-enhanced Zeeman-coherence atomic magnetometry scheme that results in sub-nT magnetic field detection at human-body temperatures without employing magnetic field shielding, field compensation, and RF-modulation spectroscopy.

Meeting Room
212 B/D

CLEO: Science & Innovations

STu3K • Novel Fibers—Continued

STu3K.4 • 14:00

Demonstration the single mode performance of all-solid large mode area center-sunken cladding-trench fiber, Liu YeHui¹, Fangfang Zhang¹, Nan Zhao¹, Haiqing Li¹, Luyun Yang¹, Nengli Dai¹, Jinyan Li¹, Wang Yibo¹; ¹Huazhong Univ of Science and Technology, China. We report a novel center-sunken and cladding-trenched Yb-doped fiber. A 456 W laser output was observed in a MOPA structure. The laser slope efficiency was measured to be 79% and the M² was 1.17.

STu3K.5 • 14:15

115 W Large-mode-area Multi-core Fiber Laser with All Solid Structure, Junhua Ji¹, Raghuraman Sidharthan¹, Xiaosheng Huang¹, Jichao Zang¹, Daryl Ho¹, Yehuda Benudiz², Udi Ben Ami², Amiel Ishaaya², Seongwoo Yoo¹; ¹The Photonics Inst., Nanyang Technological Univ., Singapore; ²Dept. of Electrical and Computer Engineering, Ben-Gurion Univ. of the Negev, Israel. We demonstrate a multicore Yb-doped fiber laser with an all-solid large-core fiber fabricated in-house and an external Talbot resonator for mode selection. 115W output power with an overall 61% slope efficiency was achieved.

STu3K.6 • 14:30

Low Quantum Defect Fiber Lasers via Yb-Doped Multicomponent Fluorosilicate Optical Fiber, Nanjie Yu¹, Maxime Cavillon², Courtney Kucera², Thomas Hawkins², John Ballato², Peter Dragic¹; ¹Univ. of Illinois Urbana Champaign, USA; ²Center for Optical Materials Science and Engineering Technologies, Clemson Univ., USA. A low quantum defect (QD <1.5%) fiber laser based on an Yb-doped multicomponent fluorosilicate optical fiber is presented. Modeling results indicate that the fiber laser is scalable and that QD values below 1% are feasible.

Marriott
Salon I & II

Joint

JTu3L • Symposium on Multimodal and Molecular Contrast Optical Imaging I—Continued

JTu3L.3 • 14:00 **Invited**

Multimodal Endoscopic Bladder Imaging, Audrey Bowden¹; ¹Stanford Univ., USA. TBD

JTu3L.4 • 14:30 **Invited**

TBD, Zhongping Chen¹; ¹Univ. of California Irvine, USA. TBD

15:00–17:00 Coffee Break & Exhibit Only Time, Exhibit Hall

15:30–17:00 Meet the OSA Editors Reception, Exhibit Hall, #2425

CLEO: Science & Innovations

Joint

STu3M • High Peak Power Lasers & Technologies—Continued

STu3M.4 • 14:00 **Invited**

High-resolution Hyperspectral Imaging based on Liquid-crystal Cells, Aurelie Jullien¹, Remy Pascal¹, Umberto Bor-tolozzo², Nicolas Forget², Stefania Residori¹; ¹INPHYNI - CNRS - UNS, France; ²FASTLITE, France. A compact, integrable and low-cost hyperspectral imaging device is proposed. It relies on cascaded liquid-crystal cells dynamically driven, calibrated through broadband spectral interferometry. 6 nm spectral resolution is demonstrated over 400–1000 nm.

STu3M.5 • 14:30

Pulse-Compressor Grating-Alignment Tolerances for Varied Geometries and Bandwidths, Benjamin Webb¹, Mark J. Guardalben¹, Christophe Dorner¹, Sara Bucht¹, Jake Brom-age¹; ¹Lab for Laser Energetics, Univ. of Rochester, USA. The effects of pulse compressor grating misalignment on pulse duration and focusability are simulated in FRED and MATLAB to specify tolerances over a broad range of design parameters.

STu3M.6 • 14:45

Variable Astigmatism Corrector for High-Power Lasers, Seung-Whan Bahk¹, Brian Kruschwitz¹, Amy Rigatti¹, Jim Oliver¹, Jake Bromage¹; ¹Univ. of Rochester, USA. We present a variable astigmatism corrector whose magnitude and sign in the astigmatism can be deterministically adjusted without separate wavefront measurement. The experimental results agree well with the calculation.

STu3N • Chemical Sensing—Continued

STu3N.5 • 14:00

Rapid Scanning Cavity Ring-down Spectrometer for the Precision Measurement of ¹³C/¹²C for CO₂ in Air, Adam J. Fleisher¹, Hongming Yi¹, Abneesh Srivastava¹, Hodges Joseph¹; ¹NIST, USA. We report a dual-wavelength rapid scanning spectrometer with < 0.1 % measurement reproducibility for ¹³C/¹²C isotope ratios in air. Initial evaluations of accuracy were performed using gas samples with known $\delta^{13}\text{C}$.

STu3N.6 • 14:15

High-Speed Line-Locked Heterodyne Phase Sensitive Dispersion Spectroscopy, Pedro Martín-Mateos¹, Jakob Hayden¹, Bernhard Lendl¹, Pablo Acedo¹; ¹Universidad Carlos III de Madrid, Spain. We present a method for high-speed optical gas analysis based on an line-locked HPSDS system that enables data output rates that are unmatched by any directly comparable optical gas detection and analysis technique.

STu3N.7 • 14:30

Backscatter Absorption Gas Imaging with a Narrow-Line-width Picosecond Optical Parametric Oscillator, Guillaume Walter¹, Jean-Baptiste Dherbecourt¹, Jean-Michel Melkonian¹, Myriam Raybaut¹, Didier Henry¹, Cyril Drag², Antoine Godard¹; ¹ONERA - The French Aerospace Lab, France; ²Laboratoire de Physique des Plasmas, France. Backscatter absorption gas imaging of nitrous oxide at atmospheric pressure is carried out with a narrow-linewidth OPO tunable over 215 nm around 3.82 μm in 130 ms. This setup is promising for multi-species gas-leak detection.

STu3N.8 • 14:45

Optical Cavity Mode Measurements at Hz-Level Precision With a Comb-Based VIPA Spectrometer, Grzegorz A. Kowzan¹, Dominik Charczun¹, Agata Cygan¹, Ryszard S. Trawinski¹, Daniel Lisak¹, Piotr Maslowski¹; ¹Nicolaus Copernicus Univ., Poland. We present cavity mode width and frequency measurements over 60-cm⁻¹ range at Hz-level precision. We utilize a near-infrared frequency comb and a VIPA spectrometer to retrieve absorption and dispersion of a CO-N₂ sample in a high-finesse cavity.

JTu3O • Laser Modification of Materials—Continued

JTu3O.5 • 14:00 **Invited**

Laser Hyperdoping Silicon for Infrared Optoelectronics, Jeffrey Warrender¹; ¹US Army, ARDEC RDECOM, USA. Silicon may be laser hyperdoped with transition metals above the equilibrium solubility. I will describe this process and the optical and optoelectronic properties of layers fabricated with it, emphasizing the most promising hyperdopant, gold.

JTu3O.6 • 14:30

Evaluating carrier lifetimes in laser hyperdoped silicon using terahertz spectroscopy, Senali Dissanayake¹, Philippe Chow², Shao Qi Lim³, Matthew Wilkins⁴, Eduard Dumitrescu⁴, Wenjie Yang³, Quentin Hudspeth², Jacob Krich⁴, Jim Williams³, Jeffrey Warrender², Renee Sher¹; ¹Dept. of Physics, Wesleyan University, USA; ²U.S. Army ARDEC - Benet Labs, USA; ³Research School of Physics and Engineering, The Australian National Univ., Australia; ⁴Dept. of Physics, Univ. of Ottawa, Canada. Silicon doped with gold at supersaturated concentrations is promising for infrared photodetectors and photovoltaic applications. Ion implantation followed by pulsed laser processing creates high quality hyperdoped material, and we investigate material properties using terahertz spectroscopy.

JTu3O.7 • 14:45

Silicon nanofibers formed at room temperature following laser irradiation of silicon in SF₆, Jeffrey Warrender¹, Quentin Hudspeth¹, Philippe Chow¹, Stephen Bartolucci¹, Joshua Maurer¹; ¹US Army, ARDEC RDECOM, USA. Silicon nanofibers were observed to form after several months at room temperature following laser irradiation of silicon in SF₆ in an aluminum chamber.

15:00–17:00 Coffee Break & Exhibit Only Time, Exhibit Hall

15:30–17:00 Meet the OSA Editors Reception, Exhibit Hall, #2425

CLEO: Science & Innovations

STu3P • Precision
Spectroscopy—Continued

STu3P.4 • 14:00

Broadband Complex Refractive Index Spectroscopy via Measurement of Cavity Modes, Alexandra C. Johansson¹, Lucile Rutkowski¹, Anna Filipsson¹, Thomas Hausmaninger¹, Gang Zhao^{1,2}, Ove Axner¹, Aleksandra Foltynowicz¹; ¹Umeå Univ., Sweden; ²Shanxi Univ., China. We retrieve high precision absorption and dispersion spectra of the $3\nu_1 + \nu_3$ band of CO₂ from direct measurement of cavity transmission modes using an optical frequency comb and a mechanical Fourier transform spectrometer with sub-nominal resolution.

STu3P.5 • 14:15

Application of Cavity-Enhanced Comb-Based Fourier-Transform Spectroscopy to Line Shape Study of Carbon Monoxide in Argon, Akiko Nishiyama^{2,1}, Grzegorz Kowzan², Dominik Charczun², Vinicius S. Oliveira³, Axel Ruehl^{3,4}, Ingmar Hartl³, Kaoru Minoshima¹, Ryszard S. Trawinski², Piotr Maslowski²; ¹Univ. of Electro-Communications, Japan; ²Inst. of Physics, Faculty of Physics, Astronomy and Informatics, Nicolaus Copernicus Univ. in Torun, Poland; ³Deutsches Elektronen-Synchrotron (DESY), Germany; ⁴Leibniz Univ. Hannover, QUEST-Leibniz-Research School, Inst. for Quantum Optics, Germany. We performed measurements of overtone band of CO using cavity-enhanced Fourier-transform spectrometer with sub-nominal resolution. The system's performance allows to study collisional effects not described by the Voigt profile and precise determination of line parameters.

STu3P.6 • 14:30

CO₂ Line Parameter Retrieval Beyond the Voigt Profile Using Comb-Based Fourier Transform Spectroscopy, Alexandra C. Johansson¹, Anna Filipsson¹, Lucile Rutkowski¹, Piotr Maslowski², Aleksandra Foltynowicz¹; ¹Umeå Univ., Sweden; ²Nicolaus Copernicus Univ., Poland. We measure absorption spectra of the CO₂ $3\nu_1 + \nu_3$ band at 1.57 μm using optical frequency comb Fourier transform spectroscopy with sub-nominal resolution and retrieve line shape parameters using multiline fitting with the speed-dependent Voigt profile.

STu3Q • Advances in VCSELS—
Continued

STu3Q.4 • 14:00

36 Gb/s Error Free Modulation of 850nm Monolithic Injection Locked VCSEL Arrays, Harshil Dave¹, Peicheng Liao², Stewart Fryslie³, Zihe Gao¹, Bradley J. Thompson¹, Alan E. Willner², Kent D. Choquette¹; ¹Univ. of Illinois, USA; ²Electrical Engineering, Univ. of Southern California, USA; ³Freedom Photonics, USA. We report direct modulation of 2x1 proton-implanted index-confined photonic crystal coherently-coupled VCSEL array operating error free at 36 Gb/s. The high-speed modulation is attributed to modulation-bandwidth enhancement.

STu3Q.5 • 14:15

Air-Cavity Dominated HCG-VCSEL with a Wide Continuous Tuning, Jonas Kapraun¹, Jipeng Yi¹, Jiaying Wang¹, Philippe Tingzon², Kevin Cook¹, Emil Kolev¹, Larry Coldren³, Connie J. Chang-Hasnain¹; ¹Dept. of Electrical Engineering and Computer Sciences and Tsinghua-Berkeley Shenzhen Inst., UC Berkeley, USA; ²Univ. of the Philippines – Diliman, Philippines; ³Electrical and Computer Engineering, UC Santa Barbara, USA. We present continuously tuned emission of 940-1000 nm wavelength from an electrically-pumped VCSEL without top DBR layers via an electrostatically controlled HCG mirror. Large tuning range results from a high optical intensity in the air cavity.

STu3Q.6 • 14:30

Novel Oxide Spacer High-Contrast Grating VCSELS, Kevin T. Cook¹, Jipeng Qi¹, Jiaying Wang¹, Neil Cabello^{2,1}, Connie J. Chang-Hasnain^{1,3}; ¹Univ. of California, Berkeley, USA; ²Univ. of the Philippines Diliman, Philippines; ³Tsinghua-Berkeley Shenzhen Inst., China. VCSELS using high-contrast grating mirrors defined by wet oxidation of an AlGaAs spacer layer are demonstrated. The devices, operating near 960nm, have threshold current as low as 0.6mA and peak power as high as 1mW.

STu3Q.7 • 14:45

Control and Simulation of Coherent Array Modes in Vertical Cavity Laser Arrays, Bradley J. Thompson¹, Zihe Gao¹, Harshil Dave¹, Stewart Fryslie², Katherine Lakomy¹, Kent D. Choquette¹; ¹Univ. of Illinois, USA; ²Freedom Photonics, USA. A 3x1 vertical-cavity surface-emitting laser array is resonantly tuned to multiple coherent modes. Experimental near-field and far-field coherent modes profiles are characterized and simulated. The center element bias demonstrates control of the coherent mode.

CLEO: Applications
& TechnologyATu3R • A&T Topical Review on
Advanced Applications of Laser
Radar and Remote Sensing I—
ContinuedATu3R.4 • 14:00 **Invited**

Recent Advances in Single Photon Sensitive Mapping Lidars, Jacobo Marcos Sirota¹, John Degnan¹, Joshua Gluckman¹, Ed Leventhal¹, Spencer Disque¹; *Sigma Space Corp, USA*. Latest developments in single-photon-sensitive based mapping systems are presented, including detection, timing, intensity measurement, multi-photon bias correction, and near real time processing techniques. Performance is evaluated from data collected in a variety of urban and natural landscapes.

ATu3S • A&T Topical Review on
Advances in Supercontinuum
Technologies I: Supercontinuum
Generation—ContinuedATu3S.3 • 14:00 **Invited**

The Development of Tailored Supercontinuum Sources in Silica and Non-silica Fibers, Jonathan H. Price¹, Sijing Liang¹, Lin Xu¹, Qiang Fu¹, Yongmin Jung¹, Krzysztof P. Herdzik^{1,2}, Sumeet Mahajan², David Shepherd¹, David Richardson¹, Shaif-UI Alam¹; ¹Optoelectronics Research Centre, Univ. of Southampton, UK; ²Inst. for Life Sciences, Univ. of Southampton, UK. Applications such as bio-imaging and mid-IR sensing demand tailored sources often using different fibers as their basis. A review of source development work using silica and non-silica fibers will be presented with relevant underpinning concepts.

ATu3S.4 • 14:30 **Invited**

Supercontinuum from Labs to Factories, Peter Moselund¹, Patrick Bowen¹, Magalie Bondu¹, Lucy Hooper², Adam Devine²; ¹NKT Photonics Inc, Denmark; ²NKT Photonics UK, UK. We review recent trends in supercontinuum research and the challenges involved in maturing supercontinuum from being a cutting edge lab instrument replacing exotic lasers to an industrially mature light source in its own right.

15:00–17:00 Coffee Break & Exhibit Only Time, Exhibit Hall

15:30–17:00 Meet the OSA Editors Reception, Exhibit Hall, #2425

CLEO: QELS-Fundamental
Science

17:00–19:00

FTu4A • Quantum Information Processing

President: Michael Brodsky; U.S. Army
Research Lab, USA

FTu4A.1 • 17:00 Tutorial

Large Scale Quantum Simulations Using Ultracold Atomic Gases in Optical Lattices, Immanuel Bloch^{1,2}; ¹Quantum Many-Body Systems Division, Max-Planck-Institut für Quantenoptik, Germany; ²Physics, Ludwig Maximilians Univ., Germany. Large scale quantum simulations in computationally intractable regimes offer the opportunity to address fundamental problems across different fields of science. I will introduce the field of atomic quantum simulations with ultracold atoms.



Immanuel Bloch is scientific director at the Max Planck Institute of Quantum Optics (Garching) and professor at the Ludwig-Maximilians-University (Munich). His scientific work is among the most highly cited in the field of quantum physics and has helped to open the new interdisciplinary research field of quantum simulations.

FTu4A.2 • 18:00

Quantum vs. Optical Annealing: Benchmarking the OPO Ising Machine and D-Wave, Ryan Hamerly^{2,1}, Takahiro Inagaki³, Peter L. McMahon^{4,1}, Davide Venturelli⁵, Alireza Marandi⁴, Tatsuhiro Onodera⁴, Edwin Ng⁴, Eleanor Rieffel⁵, M. M. Fejer⁴, Shoko Utsunomiya¹, Hiroki Takesue³, Yoshihisa Yamamoto⁶; ¹National Inst. for Informatics, USA; ²Research Lab of Electronics, MIT, USA; ³NTT Basic Research Labs, Japan; ⁴Applied Physics, Stanford Univ., USA; ⁵NASA Ames Research Center, USA; ⁶Japan Science and Technology Agency, Japan. We benchmark the OPO-based Coherent Ising Machine (CIM) against the D-Wave quantum annealer for Ising problems up to size N=200. The CIM exhibits exponential speedup relative to D-Wave for Ising problems with dense connectivity.

CLEO: Science & Innovations

17:00–19:00

STu4B • Wavelength and Phase-sensitive
Integrated Devices

President: Haisheng Rong; Intel, USA

STu4B.1 • 17:00

MEMS-Actuated 8x8 Silicon Photonic Wavelength-Selective Switches with 8 Wavelength Channels, Tae Joon Seok^{1,2}, Jianheng Luo², Zhilei Huang², Kyungmok Kwon², Johannes Henriksson², John Jacobs³, Lane Ochikubo³, Richard Muller², Ming C. Wu²; ¹Gwangju Inst. of Science and Technol., South Korea; ²EECS, Univ. of California, Berkeley, USA; ³TSI Semiconductors, USA. We report on a fully integrated 8x8 silicon photonic MEMS wavelength-selective switch with 8 wavelength channels on a 9.7mm x 6.7mm chip. Total on-chip loss including switches and echelle grating mux/demux is 13.3 dB.

STu4B.2 • 17:30

CMOS-Compatible Optical Phased Arrays with Monolithically-Integrated Erbium Lasers, Jelena Notaros¹, Nanxi Li^{1,2}, Christopher V. Poulton¹, Zhan Su¹, Matthew Byrd¹, Emir Magden¹, Michael Watts¹; ¹MIT, USA; ²Harvard Univ., USA. An electronically-steerable integrated optical phased array powered by an on-chip erbium-doped laser is experimentally demonstrated. This system represents the first demonstration of a rare-earth-doped laser monolithically integrated with an active CMOS-compatible silicon photonics system.

STu4B.3 • 17:45

Silicon Photonic 50GHz Wavelength (De)Multiplexer with Low Crosstalk and Flat Passband, Liangshun Han¹, Bill P. Kuo¹, Motohiko Eto¹, Ana Pejic¹, Jin Zhang¹, Nikola Alic¹, Stojan Radic¹; ¹Dept. of Electrical and Computer Engineering, Univ. of California, San Diego, USA. We demonstrated an eight-channel flat-topped wavelength (de)multiplexer with 50GHz channel spacing on a SOI chip. The measured crosstalk is < -26.0 dB at central wavelengths of the channels and 1-dB bandwidth is 33.0 GHz.

STu4B.4 • 18:00

Reconfigurable Mode (De)multiplexer with Integrated Thermo-Optic Long-Period Grating and Y-junction, Wei ke Zhao¹, Jing Feng¹, Kaixin Chen¹, Kin S. Chiang²; ¹Univ of Electronic Science & Tech China, China; ²City Univ. of Hong Kong, China. We demonstrate reconfigurable mode (de)multiplexing with an integrated thermo-optic long-period grating and an asymmetric Y-junction. Our fabricated device achieves a mode selectivity >12 dB over the C+L band with a switching power of 198 mW.

17:00–19:00

STu4C • Nonlinearity Compensation

President: Vladimir Grigoryan; Ciena
Corporation, USA

STu4C.1 • 17:00

Nonlinearity Compensation for Dual-Polarization Signals using Optical Phase Conjugation in a Silicon Waveguide, Francesco Da Ros¹, Edson P. da Silva¹, Andrzej Gajda², Pawel M. Kaminski¹, Valentina Cristofori¹, Anna Peczek³, Andreas Mai², Klaus Petermann⁴, Lars Zimmermann², Leif K. Oxenlowe¹, Michael Galili¹; ¹DTU Fotonik, Denmark; ²IHP, Germany; ³IHP Solutions, Germany; ⁴TU Berlin, Germany. Improvements in signal-to-noise ratio (1.2 dB) and transmission reach (16 %) are demonstrated for dual-polarization WDM 16-QAM signals through nonlinearity compensation by optical phase conjugation in a silicon waveguide with a lateral p-i-n diode.

STu4C.2 • 17:15

Experimental Comparison of Probabilistic Shaping with on-line PMF Optimization and Mid-link OPC, Metodi Yankov^{1,2}, Francesco Da Ros¹, Edson P. da Silva¹, Michael Galili¹, Leif K. Oxenlowe¹; ¹DTU Fotonik, Denmark; ²Fingerprint Cards ApS, Denmark. Gains offered by mid-link OPC and probabilistic shaping are compared in a dispersion-managed link with 64QAM input. Probabilistic shaping is optimized online and tailored to the specific channel and transceiver conditions, including the OPC stage.

STu4C.3 • 17:30

Polarization-Division-Multiplexed Nonlinear Frequency Division Multiplexing, Tao Gui^{1,2}, Wasyhun A. Gemechu^{1,3}, Jan-Willem Goossens^{1,4}, Mengdi Song¹, Stefan Wabnitz², Mansoor I. Yousefi¹, Hartmut Hafermann², Alan Pak Tao Lau², Yves Jaouen¹; ¹LTCL, Telecom ParisTech, Université Paris-Saclay, France; ²Photonics Research Centre, Dept. of Electrical Engineering, The Hong Kong Polytechnic Univ., China; ³Dipartimento di Ingegneria dell'Informazione, Università di Brescia, Italy; ⁴Mathematical and Algorithmic Sciences Lab, Paris Research Center, Huawei Technologies France SASU, France. We experimentally demonstrate dual-polarization nonlinear frequency division multiplexing using the continuous spectrum in 1680 km of normal dispersion fiber at a burst rate of 128Gbit/s. The DGD penalties are shown to be negligible.

STu4C.4 • 18:00

Polarization Division Multiplexing for Nonlinear Fourier-Based Transmission Schemes, Stella Civelli^{1,2}, Jaroslav E. Prilepsky², Marco Secondini¹, Sergei K. Turitsyn²; ¹Tecip, Scuola Superiore Sant'Anna, Italy; ²Aston Inst. of Photonic Technologies, Aston Univ., UK. A polarization-division multiplexing transmission scheme based on the nonlinear Fourier transform is considered. A new dual-polarization processing technique with reduced complexity, providing 1dB performance improvement, is introduced.

Executive Ballroom
210D

CLEO: Science & Innovations

17:00–19:00

STu4D • Terahertz QCLs

President: Kaushik Sengupta; Princeton Univ., USA

STu4D.1 • 17:00

Octave-spaced on-chip THz frequency combs, Andres Forrer¹, Markus Rösch¹, Mattias Beck¹, Jérôme Faist¹, Giacomo Scalari¹; ¹ETH Zurich, Switzerland. Latest results on frequency combs based on THz quantum cascade lasers will be presented including the monolithic integration of octave-spaced combs at 2.3 THz and 4.6 THz

STu4D.2 • 17:15

Terahertz Dual-Comb Spectroscopy Using Quantum Cascade Laser Frequency Combs, Jonas Westberg¹, Lukasz A. Sterczewski², Yang Yang³, David Burghoff³, Qing Hu³, Gerard Wysocki¹; ¹Dept. of Electrical Engineering, Princeton Univ., USA; ²Faculty of Electronics, Wrocław Univ. of Science and Technology, Poland; ³MIT, USA. We demonstrate THz dual comb spectroscopy of molecular samples using dispersion compensated quantum cascade lasers. The system achieves an optical bandwidth of ~150 GHz at 2.9 THz and is used to measure ammonia in gas phase.

STu4D.3 • 17:30 **Invited**

THz Quantum Cascade Lasers and Combs, Mattias Beck¹, Martin Franckie¹, Lorenzo Bosco¹, Giacomo Scalari¹, Jérôme Faist¹; ¹Inst. for Quantum Electronics, ETH Zurich, Switzerland. Recent developments of THz QCLs based on two-well and four-well active regions will be presented. The two-well structure demonstrated lasing up to 192K. The lasing spectrum of the four-well design spans over a bandwidth of 1.9 THz suitable for comb operation over a spectral bandwidth of 1.1 THz.

STu4D.4 • 18:00

Continuous frequency tuning of Y-branched terahertz quantum cascade lasers with photonic lattice, Iman Kundu¹, Paul Dean¹, Alexander Valavanis¹, Joshua R. Freeman¹, Mark Rosamond¹, Lianhe Li¹, Yingjun Han¹, Edmund H. Linfield¹, Alexander G. Davies¹; ¹Univ. of Leeds, UK. We report electrically-controlled continuous frequency tuning over ~20 GHz by exploiting the additive Vernier tuning effect in a THz QCL based on a longitudinally-coupled Y-branched waveguide.

Executive Ballroom
210E

CLEO: QELS-Fundamental Science

17:00–19:00

FTu4E • Quantum and Non-local Plasmonics

President: Henri Lezec; NIST, USA

FTu4E.1 • 17:00

Engineering Infrared Quantum Fluctuations to Generate Light from UV through Gamma Rays, Nicholas Rivera¹, Liang Jie Wong², John Joannopoulos¹, Marin Soljacic¹, Ido Kaminer³; ¹MIT, USA; ²SimTECH, Singapore; ³Technion Israel Inst. of Technology, Israel. We show that plasmonic vacuum fluctuations can lead to a passive radiation source at UV to gamma ray energies. Its per-electron power is comparable to synchrotrons with a 1 Tesla field and is density-of-states tunable.

FTu4E.2 • 17:15

Nonlinear and Quantum-Light Scattering from Gold Nanorods, Theodore B. Norris¹, Miao-bin Lien¹, Benjamin Girodias¹, Ji-Young Kim¹, Zhen Xu¹, Heather George¹, You-Chia Chang¹, Myung-Geun Han², Yimeizhu², John Schotland¹, Nicolas Kotov¹, Mackillo Kira¹; ¹Univ. of Michigan, USA; ²Brookhaven NL, USA. We study the spectral dependence of the scattered light from Au nanorods illuminated by 50-fs pulses resonant with the longitudinal plasmon, and determine the origin of the scattering in terms of the plasmon modes. We project the expected spectrum under illumination from a squeezed optical pump.

FTu4E.3 • 17:30 **Invited**

Functional Quantum-Plasmonic Metamaterials/ Metasurfaces and Maximizing the Lorentz Nonlinearity, Reuven Gordon¹, Ghazal Hajisalem¹, Dao Xiang¹, Esmail Rahimi¹; ¹Univ. of Victoria, Canada. We present two approaches to achieve massive changes in the optical properties of plasmonic metasurfaces by making use of quantum effects. We also demonstrate ways of maximizing the Lorentz nonlinearity beyond hydrodynamic contributions.

FTu4E.4 • 18:00

Strong Coupling of Excitons, Plasmonic and Photonic Modes in Organic-dye-doped Nanostructures, Ruwen Peng¹, Kun Zhang¹, Mu Wang¹; ¹Nanjing Univ., China. We demonstrate experimentally hybrid strong couplings among molecular excitons, plasmonic and photonic modes in the organic-dye-doped nanostructures. And multiple hybrid polariton bands are observed, which may achieve potential applications on multimode polariton lasers and optical spectroscopy.

Executive Ballroom
210F

CLEO: Science & Innovations

17:00–19:00

STu4F • Nonlinear Optical Phononics & Optomechanics

President: Amol Choudhary; Univ. of Sydney, Australia

STu4F.1 • 17:00 **Tutorial**

Stimulated Brillouin Scattering: Then and Now, Elsa M. Garmire¹; ¹Dartmouth College, USA. Stimulated Brillouin scattering (SBS) is embedded today in a variety of optical systems: advanced lasers, sensors, microwave signal processors, scientific instrumentation and opto-mechanical systems. Optical fibers and micro-resonators generate useful SBS.



Elsa Garmire is retired from Dartmouth College as Professor and Dean of Engineering. Member of National Academy of Engineering, IEEE and OSA Fellow, she studied semiconductor nonlinear optics at USC. As MIT graduate student, she reported the first SBS in liquids; now is writing a book on nonlinear optical technology.

STu4F.2 • 18:00

Brillouin Filtering with Enhanced Noise Performance and Linearity Using Anti-Stokes Interactions, Amol Choudhary¹, Yang Liu¹, David Marpaung¹, Benjamin Eggleton¹; ¹Univ. of Sydney, Australia. The anti-Stokes component of a stimulated Brillouin scattering interaction enabled low-power and high-resolution bandpass filtering, with improvements in linearity and signal-to-noise ratio of upto 3dB and 8dB, respectively when compared to using the Stokes component.

CLEO: QELS-Fundamental Science

CLEO: Applications
& Technology

17:00–19:00

FTu4G • Continuous Variable Quantum Computing

President: Martin Stevens; NIST, USA

FTu4G.1 • 17:00

On-Chip Continuous Variable Squeezing, Jasmin D. Meinecke², Genta Masada^{3,4}, Takahiro Serikawa³, Jeremy L. O'Brien¹, Akira Furusawa³, ¹Centre for Quantum Photonics, Univ. of Bristol, UK; ²Max-Planck-Inst. for Quantum Optics, Germany; ³Dept. Applied Physics, The Univ. of Tokyo, Japan; ⁴Quantum ICT Research Inst., Tamagawa Univ., Japan. We perform a squeezing transformation for continuous variable input states using a measurement-based scheme on chip. Implementing this fundamental transformation is an important building block for fully integrated continuous variable quantum information processing.

FTu4G.2 • 17:15

Multiphoton Hong-Ou-Mandel Interferometry with Entangled Photon-Subtracted States, Omar S. Magana Loaiza¹, Roberto Leon², Armando Perez-Leija³, Alfred U'ren², Kurt Busch³, Adriana E. Lita¹, Sae Woo Nam¹, Richard Mirin¹, Thomas Gerrits¹, ¹NIST, USA; ²Universidad Nacional Autonoma de Mexico, Mexico; ³Max-Born-Institut, Germany. We demonstrate generation of entangled photon-subtracted states and manipulation of their quantum fluctuations. The flexibility of our technique allows us to explore Hong-Ou-Mandel interferometry with mesoscopic states that resemble systems of entangled lasers.

FTu4G.3 • 17:30

Low-Latency Digital Feedforward for Universal Continuous-Variable Quantum Computation in Time Domain, Atsushi Sakaguchi¹, Hisashi Ogawa¹, Masaya Kobayashi¹, Shigenari Suzuki¹, Hidehiro Yonezawa², Elanor Huntington³, Shuntaro Takeda¹, Jun-ichi Yoshikawa¹, Akira Furusawa¹; ¹Dept. of Applied Physics, School of Engineering, Univ. of Tokyo, Japan; ²Centre for Quantum Computation and Communication Technology, School of Engineering and Information Technology, Univ. of New South Wales, Australia; ³College of Engineering and Computer Science, The Australian National Univ., Australia. We demonstrate a programmable optical quantum gate with a 25ns-latency digital feedforward. Such a flexible, stable, and fast feedforward enables large-scale universal continuous-variable quantum computation in time domain.

FTu4G.4 • 17:45

Scalable and Universal Quantum Computing with Continuous-Variable Gate Sequence in a Loop-Based Architecture, Shuntaro Takeda^{1,2}, Akira Furusawa¹; ¹Dept. of Applied Physics, The Univ. of Tokyo, Japan; ²JST, PRESTO, Japan. We propose a scalable scheme for optical quantum computing using continuous-variable quantum gates in a loop-based architecture. This architecture offers a universal gate set for both qubits and continuous variables with almost minimum resources.

FTu4G.5 • 18:00 **Invited**

Continuous-variable Quantum Computing: Scalable Designs and Fault Tolerance, Nicolas Menicucci¹; ¹Physics, RMIT Univ., Australia. Continuous-variable (CV) cluster states are multimode-squeezed states that are resource states for measurement-based quantum computation. I will discuss recent experimental advances in producing large-scale CV cluster states and how to use them for fault-tolerant quantum computation.

17:00–19:00

FTu4H • Novel Solid State Systems for Quantum Optics

President: Marina Radulaski; Stanford Univ., USA

FTu4H.1 • 17:00

Formation of quantum emitter arrays in hexagonal Boron Nitride at room temperature, Nicholas Proscia^{1,2}, Zav Shontan¹, Harishankar Jayakumar¹, Prithvi Reddy³, Michael Dollar¹, Audrius Alkauskas⁴, Marcus Doherty³, Carlos Meriles^{1,2}, Vinod M. Menon^{1,2}; ¹CUNY City College of New York, USA; ²Physics, CUNY Graduate Center, USA; ³Laser Physics Centre, Australian National Univ., Australia; ⁴Center for Physical Science and Technology, Lithuania. Room temperature quantum emitter arrays are created in hexagonal Boron Nitride (hBN) by deterministic activation via strain engineering on a nanopillar substrate. Emitters are localized at pillar edges where the hBN film undergoes maximum strain.

FTu4H.2 • 17:15

Lead-Related Quantum Emitters in Diamond, Matthew Trusheim¹, Noel Wan¹, Girish Malladi², Kevin Chen¹, Benjamin Lienhard¹, Hassaram Bakhrut², Dirk. Englund¹; ¹Electrical Engineering and Computer Science, MIT, USA; ²College of Nanoscale Science and Engineering, Univ. at Albany-State Univ. of New York, USA. We investigate the optical properties of quantum emitters formed in diamond after the implantation of Pb and subsequent high-temperature annealing. We find narrow-band emission in two spectral ranges, indicating multiple classes of Pb-related color centers.

FTu4H.3 • 17:30 **Invited**

A Photonic Link for Donor Spin Qubits in Silicon, Stephanie Simmons¹; ¹Simon Fraser Univ., Canada. This talk presents an approach to scale up donor spin qubits in silicon using the built-in, spin-selective, strong electric dipole (optical) transitions of singly-ionized double donors. This photonic link could enable photonic cavity-QED at 4.2K.

FTu4H.4 • 18:00

Miniaturizing Rare-Earth Ion Microwave to Optical Transducers, John G. Bartholomew¹, Jake Rochman¹, Jonathan Kindem¹, Tian Zhong¹, Ioana Craiciu¹, Andrei Ruskuc¹, Andrei Faraon¹; ¹Caltech, USA. We present the development of an on-chip rare-earth ion architecture that integrates planar microwave elements and photonic structures to realize coherent microwave to optical transduction.

17:00–19:00

ATu4I • Combustion and Hypersonic Flow Diagnostics

President: Brian Simonds; National Inst. of Standards and Tech, USA

ATu4I.1 • 17:00

Spatially-resolved hydrogen atom detection in flames using backward lasing, Maria Ruchkina¹, Pengji Ding¹, Andreas Ehn¹, Marcus L.E. Alden¹, Joakim Boord¹; ¹Lund Univ., Sweden. We report on an experimental demonstration of spatially-resolved detection of atomic hydrogen in flames using a single-ended configuration. The lasing signal in a backward direction is obtained by two-photon pumping with 205-nm femtosecond laser pulses

ATu4I.2 • 17:15 **Invited**

Translating Novel Optical Diagnostics to Air Force-Rellevant Systems, James R. Gord¹; ¹Air Force Research Lab, USA. Measurements with lasers and optics are often ideal for characterizing nonreacting and reacting flows, including those in aero propulsion systems. Approaches based on ultrashort-pulse and burst-mode lasers, especially for multidimensional, high-speed imaging, will be explored.

ATu4I.3 • 17:45

Spatially Resolved Raman Spectra of Diffusion Flame via Compressive Sensing, David J. Starling¹, Joseph Ranalli¹; ¹Univ. College, Penn State Univ., USA. We simulate compressive sensing on spatially resolved Raman scattering measurements of a highly strained diffusion flame. Simulations agree with prior data, enabling the use of lower cost sensors in a simplified form of the experiment.

ATu4I.4 • 18:00

Hypersonic Flow Velocity Measurements Using FLEET, Laura Dogariu^{2,3}, Arthur Dogariu¹, Mike Smith⁴, Eric Marineau⁴, Richard B. Miles^{2,1}; ¹Princeton Univ., USA; ²Plasma TEC, Inc., USA; ³Speckodyne Corp., USA; ⁴AEDC White Oak, USA. We developed and applied a Femtosecond Laser Electronic Excitation Tagging (FLEET) system to nonintrusive flow velocity measurements in a large scale hypersonic wind tunnel. Freestream and boundary layer velocity measurements are compared with model predictions.

Meeting Room
212 A/C

CLEO: Applications
& Technology

17:00–19:00

ATu4J • Medical Devices & Systems

Presider: Ilko Ilev; U.S. Food and Drug Administration, USA

ATu4J.1 • 17:00 **Invited**

Machine Learning and Computation Enabled Microscopy and Sensing for Point-of-Care Medicine and Global Health, Aydogan . Ozcan¹; ¹Univ. of California Los Angeles, USA. We review some of our recent progress on mobile microscopy, sensing and diagnostics technologies that utilize computational photonics and machine learning approaches to address point-of-care medicine and global health related applications.

ATu4J.2 • 17:30 **Invited**

Progress in the Development of All-Solid-State Coherent Sources in the Mid-IR above 5 μm for Surgical Applications, Valentin Petrov¹; ¹Max Born Inst., Germany. I will review the state-of-the-art and the recent progress in all-solid-state parametric frequency down-conversion devices for achieving high pulse energy and average power in the 5 to 8 μm spectral range interesting for medical applications.

ATu4J.3 • 18:00

Microlens-Stabilized Laser Arrays for Short-Pulse, Speckle-Free Imaging, Austin W. Steinforth¹, José A. Rivera¹, J. G. Eden¹; ¹Univ of Illinois at Urbana-Champaign, USA. Microlens-stabilized laser arrays were constructed using solid-state and liquid gain media. Arrays comprised of more than 1,200 beams illuminated motile biological specimens, producing speckle-free video with 15 nanosecond exposure per frame.

Meeting Room
212 B/D

CLEO: Science & Innovations

17:00–19:00

STu4K • Fiber Frequency Combs

Presider: Masaki Tokurakawa; Univ. of Electro-communications, ILS, Japan

STu4K.1 • 17:00

Fast phase locking of a 750-MHz Yb: fiber laser frequency comb using a high-speed piezo-transducer, Yuxuan Ma^{1,2}, Bo Xu^{1,3}, Hiroataka Ishii¹, Fei Meng², Yoshiaki Nakajima^{1,3}, Thomas R. Schibli⁴, Isao Matsushima^{1,3}, Zhigang Zhang², Kaoru Minoshima^{1,3}; ¹Dept. of Engineering Science, Graduate School of Informatics, The Univ. of Electro-Communications, Japan; ²State Key Lab of Advanced Optical Communication System and Networks, School of Electronics Engineering and Computer Science, Peking Univ., China; ³Japan Science and Technology Agency, ERATO Intelligent Optical Synthesizer (IOS) Project, Japan; ⁴Dept. of Physics, Univ. of Colorado at Boulder, USA. We demonstrate a 750-MHz-spaced Yb: fiber frequency comb phase locked to a narrow linewidth CW laser by a single stack PZT actuator. Low phase noise and high stability were achieved by the fast phase locking.

STu4K.2 • 17:15

Generation of 250-MHz electro-optic frequency comb for Doppler-limited spectroscopy, Wang Shuai¹, Xinyu Fan¹, Bingxin Xu¹, Zuyuan He¹; ¹Shanghai Jiao Tong Univ., China. We proposed a cascaded modulation method for electro-optic frequency comb generation. With this method, electro-optic frequency combs with 250-MHz line spacing covering 4,000 teeth were generated, which enable Doppler-limited spectroscopy.

STu4K.3 • 17:30 **Invited**

Precision Measurements with Ultra-Low Noise Frequency Combs, Wolfgang Hänsel¹, Michele Giunta^{1,2}, Katja Beha¹, Matthias Lezius¹, Maurice Lessing¹, Marc Fischer¹, Ronald Holzwarth^{1,2}; ¹Menlo Systems GmbH, Germany; ²Max-Planck Inst. of Quantum Optics, Germany. The advent of long-term stable ultra-low noise (ULN) frequency combs opens new prospects for precision measurements. We characterize the stability of such ULN combs and present dual-comb precision spectroscopy of molecules and cavities.

STu4K.4 • 18:00

All-Polarization-Maintaining Dual-Comb Fiber Laser with Nonlinear Amplifying Loop Mirror, Yoshiaki Nakajima^{1,2}, Yuya Hata¹, Kaoru Minoshima^{1,2}; ¹Univ. of Electro-Communications, Japan; ²IOS Project, Japan. We demonstrate an all-polarization-maintaining dual-comb fiber laser with nonlinear-amplifying-loop-mirror for realizing simple and robust dual-comb spectroscopy using two mutually coherent combs with slightly different repetition rates emitted from the laser cavity without complex servo system.

Marriott
Salon I & II

Joint

17:00–19:00

JTu4L • Symposium on Multimodal and Molecular Contrast Optical Imaging II

Presider: Wolfgang Drexler; Medizinische Universität Wien, Austria

JTu4L.1 • 17:00 **Tutorial**

Bringing Functional High Resolution Diagnostics to the Bedside Using Multimodal, Label-free, Two-photon Imaging, Irene Georgakoudi¹, Dimitra Pouli¹, Zhiyi Liu¹, Mihaela Balu², Bruce Tromberg²; ¹Tufts Univ., USA; ²Univ. of California at Irvine, USA. Changes in optical metabolic signals related to the intensity, lifetime and spatial localization of endogenous fluorescence are associated with alterations in specific biosynthetic and bioenergetic cellular pathways, which can serve as diagnostic and therapeutic targets.



Irene Georgakoudi is a Professor of Biomedical Engineering at Tufts University. Her work focuses on the understanding and exploitation of endogenous fluorescence and scattering signals in two-photon microscopy to extract highly quantitative, functional information regarding cellular metabolism and matrix biomechanics. She is an OSA and AIMBE fellow.

CLEO: Applications
& Technology

17:00–19:00

ATu4M • Thin Film & Metrology for Laser
Processing

Presider: TBD

ATu4M.1 • 17:00 **Invited**

Laser Annealing of Thin Si Films for Displays and Other Applications, James S. Im¹; ¹Columbia Univ., USA. In this talk, we will (1) discuss deciphering the currently utilized excimer-laser annealing (ELA) process, and (2) present a newly developed ultra-high-frequency fiber-laser-based crystallization approach, which is referred to as the spot-beam crystallization (SBC) method.

ATu4M.2 • 17:30

Improved Performance & Thermal Stability in Plasmonic Films with Thinner Adhesion & Capping Layers, William M. Abbott¹, Christopher P. Murray¹, Chuan Zhong¹, Christopher M. Smith¹, David McCloskey¹, John F. Donegan¹; ¹School of Physics, Crann & Amber, Trinity College Dublin, Ireland. Ultrathin (≥ 0.5 nm) adhesion and capping layers were used to inhibit dewetting in 50 nm Au thin films. A 1500x stability enhancement was found over standard 2 nm adhesion Ti layers used in HAMR.

ATu4M.3 • 17:45

Roughness measurements of Al and Cu particles in Laser-Induced forward transferring process, Mohammad Hossein Azhdast¹, Hans Joachim Eichler¹, Klaus-Dieter Lang², Veronika Glaw², Martin Kossatz³; ¹Technical Univ. of Berlin, Germany; ²IZM Fraunhofer, Germany; ³PacTech GMBH, Germany. Cu and Al particles were optimized to create thin films by laser direct transfer on Si-wafer substrate with minimal measured roughness; Cu-LIFT results are especially promising at high repetition rates and minimal pulse energy.

ATu4M.4 • 18:00

Tracking the Morphology Evolution of 3D Selective Laser Melting *in situ* using Inline Coherent Imaging., Tristan G. Fleming¹, Stephen Nestor¹, Mark Boukhaled¹, Troy Allen¹, Nathan Smith¹, James Fraser¹; ¹Queen's Univ., Canada. We demonstrate the utility of inline coherent imaging, an interferometric imaging technique, in monitoring 3D selective laser melting additive manufacturing builds. Interlayer morphology is demonstrated to be a promising candidate for real-time process control.

CLEO: Science & Innovations

17:00–19:00

STu4N • 2D Materials in Photonic Structures

Presider: Luca Sapienza; Univ. of
Southampton, UKSTu4N.1 • 17:00 **Invited**

Nanoscale Optical Field Topology, from Fascination to Application, Laurens K. Kuipers¹; ¹Quantum Nanoscience, Kavli Inst. of Nanoscience Delft, Netherlands. We investigate the distribution of phase singularities and observe their life-long fidelity or promiscuity. We exploit optical spin-momentum locking to create a deterministic interface between valley spin in a 2D material and plasmon propagation direction.

STu4N.2 • 17:30

Monolayer Semiconductor Surface-Emitting Lasers Using 2D Dark Plasmonic Cavities, Chun-Yuan Wang^{2,1}, Jinwei Shi⁴, Soniya S. Raja¹, Chun-An Chen⁶, Xin-Quan Zhang⁶, Chih-Kang Shih², Hyeyoung Ahn⁵, Yi-Hsien Lee⁶, Shangji Gwo^{1,3}; ¹Dept. of Physics, National Tsing-Hua Univ., Taiwan; ²Dept. of Physics, Univ. of Texas at Austin, USA; ³National Synchrotron Radiation Research Center, Taiwan; ⁴Dept. of Physics, Beijing Normal Univ., China; ⁵Dept. of Photonics, National Chiao-Tung Univ., Taiwan; ⁶Dept. of Materials Science and Engineering, National Tsing-Hua Univ., Taiwan. We demonstrated a low-threshold lasing from a monolayer gain medium which is made possible due to 2D feedback mechanism via strong exciton-SPP coupling in both real space and a wide range of momentum space.

STu4N.3 • 17:45

Coupling of Photonic Fano Resonances with MoS₂ Excitons for Enhanced Light Emission and Optical Modulation, Xingwang Zhang¹, Nicolas Biekert¹, Shinhyuk Choi¹, Carl H. Naylor², Chawina De-Eknamkul¹, Wenzhuo Huang¹, Xiaorui Zheng¹, Dake Wang¹, A. T. Charlie Johnson², Ertugrul Cubukcu¹; ¹Univ. of California, San Diego, USA; ²Univ. of Pennsylvania, USA. We demonstrate unidirectional enhanced photoluminescence from a monolayer MoS₂ via Fano resonances in dielectric photonic crystals. The Fano resonances can also be dynamic controlled by optical and electrical tuning of the MoS₂ refractive index.

STu4N.4 • 18:00

Dynamics of Valley-Polarized Exciton-Polaritons in Monolayer MoS₂, Yen-Jung Chen¹, Itamar Balla², Hadalia Bergeron², Lei Liu¹, Mark C. Hersam², Nathaniel P. Stern¹; ¹Physics and Astronomy, Northwestern Univ., USA; ²Materials Science & Engineering, Northwestern Univ., USA. We investigate the dynamics of valley-polarized exciton-polaritons in monolayer MoS₂ embedded in a planar dielectric microcavity. We demonstrate both theoretically and experimentally that valley polarization of exciton-polaritons can be tuned with cavity parameters.

17:00–19:00

STu4O • Laser Facilities

Presider: Thomas Metzger; TRUMPF Scientific
Lasers GmbH + Co. KG, Germany

STu4O.1 • 17:00

Towards Sub-2 cycle, Several-TW, 1kHz OPCPA System Based on Yb:KGW and Nd:YAG Lasers, Tomas Stanislaukas¹, Ignas Balciunas^{1,2}, Rimantas Budriunas^{1,2}, Jonas Adamonis³, Szabolcs Toth⁴, Adam Borzsonyi⁴, Karoly Osvay⁴, Andrejus Michailovas³, Gediminas Veitas¹, Darius Gadonas¹; ¹Light Conversion Ltd., Lithuania; ²Laser Research Center, Vilnius Univ., Lithuania; ³Eksplo Ltd., Lithuania; ⁴ELI-HU Nonprofit Ltd., Hungary. We investigate nonlinear crystal type multiplexing as means of increasing the bandwidth of a parametric amplification system pumped at 532nm. Experimental results and numerical simulations indicate that sub-2 cycle pulse durations and multi-mJ pulse energies will be possible using BBO and LBO.

STu4O.2 • 17:15

Efficient and Wavelength Tunable Extreme-ultraviolet Light Source Used for Tr-ARPES, Zhiqiang Ni¹, Zhonghui Nie¹, Jian Tu¹, Yao Li¹, Xuezhong Ruan¹, Liang He¹, Edmond Turcu¹, Yongbing Xu¹; ¹Nanjing Univ., China. Efficient and wavelength tunable extreme-ultraviolet source is developed through high harmonic generation by a frequency doubled Ti:sapphire and a monochromator with off-plane mount single grating. Photon flux of 1.2×10^{11} photons/s is achieved at 21.7 eV.

STu4O.3 • 17:30 **Invited**

Performance of the 20 fs, 4 PW Ti:Sapphire Laser at CoReLS, Chang Hee Nam^{2,1}; ¹Gwangju Inst of Science & Technology, South Korea; ²Center for Relativistic Laser Science, Inst. for Basic Science, South Korea. One of two petawatt Ti:Sapphire laser beamlines at CoReLS was upgraded to a high-contrast, 4 PW, 20 fs laser with a repetition rate of 0.1 Hz and its performance has been tested for multi-GeV electron acceleration.

STu4O.4 • 18:00

Highly-stable, 1 kHz, 200 mJ, 1.1 ps laser optically synchronized to a photocathode laser for inverse Compton scattering, Kyung-Han Hong^{1,2}, Sandro Klingebiel³, Knut Michel³, Thomas Metzger³, Darius Gadonas⁴, Karolis Neimontas⁴, Vytautas Sinkevicius¹, Lucian Hand⁴, Andrey Senin⁴, Mark R. Holl², William Graves²; ¹RLE, MIT, USA; ²Physics and Bio-design Inst., Arizona State Univ., USA; ³TRUMPF Scientific Lasers GmbH + Co. KG, Germany; ⁴Light Conversion, Lithuania. We demonstrate a highly-stable, 1 kHz, 200 mJ, 1.1 ps, 1030 nm laser with good beam quality as an inverse-Compton-scattering driver, optically synchronized with 33-fs rms jitter to a photocathode laser that triggers electron beams.

CLEO: Science & Innovations

17:00–19:00

STu4P • Advanced Sensing Concepts

President: Adam Fleisher; NIST, USA

STu4P.1 • 17:00

Slow Light Imaging Spectroscopy with a Passive Atomic Filter, Arthur Dogariu¹, Richard B. Miles^{1,2}, ¹Princeton Univ., USA; ²Texas A&M Univ., USA. We demonstrate time delayed imaging with slow light using high positive dispersion of a passive atomic gas. This filter allows for imaging of Raman, Rayleigh, and Thomson scattering without the need of a spectrometer.

STu4P.2 • 17:15

Wide-Range Tunable Refractometer Based on Orbital Angular Momentum of Light, Ahmed Dorrah¹, Michel Zamboni-Rached², Mo Mojahedi¹; ¹Dept. of Electrical and Computer Engineering, Univ. of Toronto, Canada; ²School of Electrical Engineering, Univ. of Campinas, Brazil. We experimentally demonstrate a programmable refractive index sensor utilizing orbital angular momentum of light where the sensitivity, resolution, and dynamic range can be controlled in real-time, thus addressing many challenges in refractometry and remote sensing.

STu4P.3 • 17:30

Coherent Spatiotemporal Phase Control by Combining Optical Frequency Combs and Optical Vortices, Akifumi Asahara^{1,2}, Satoru Shoji^{1,2}, Ken-ichi Kondo^{1,2}, Yue Wang^{1,2}, Kaoru Minoshima^{1,2}; ¹Univ. of Electro-Communications, Japan; ²JST, Intelligent Optical Synthesizer, Japan. "Optical vortex comb" is proposed, that enables coherent spatiotemporal phase control by combining optical frequency combs with optical vortices. The applicability is demonstrated through experiments on optical ring lattice control and optical tweezers.

STu4P.4 • 17:45

Nanoscale isotopic imaging and trace analysis by extreme ultraviolet laser ablation mass spectrometry, Carmen S. Menoni¹, Tyler Green¹, Ilya Kuznetsov¹, Weilun Chao², Jorge Rocca¹, Andrew Duffin³; ¹Colorado State Univ., USA; ²Center for X-Ray Optics, Lawrence Berkeley Lab, USA; ³Pacific Northwest National Lab, USA. Extreme ultraviolet laser ablation mass spectrometry isotopic imaging and analysis with 80 nm spatial resolution are demonstrated.

STu4P.5 • 18:00

Development of a Miniature Laser-induced Fluorescence Sensor Module used for Unmanned Aerial Vehicles, Supriya nagpal¹, Prakash Adhikari¹, William P. Williams³, Gary L. Windham², Gerald A. Matthews², Aionbold O. Gombojav¹; ¹Physics and Astronomy, Mississippi State Univ., USA; ²USDA-ARS, Mississippi state university, USA; ³USDA-ARS, Mississippi State Univ., USA. A versatile sensor module based on laser-induced fluorescence is constructed. The results demonstrate its ability to investigate stress in vegetation. Module is mounted on a quadcopter and flown with pre-planned missions making the task autonomous.

17:00–19:00

STu4Q • UV-visible Semiconductor Lasers

President: Boon Ooi; King Abdullah Univ of Sci & Technology, Saudi Arabia

STu4Q.1 • 17:00 **Tutorial**

III-Nitride Lasers – Challenges and Approaches to Expand the Emission Wavelength into the UV, Thomas Wunderer¹; ¹Palo Alto Research Center, USA. In this tutorial we will review III-Nitride-based laser technology, discuss materials challenges using high band gap semiconductors, and present different approaches and tricks to overcome these barriers (i.e., polarization doping, e-beam excitation and frequency multiplication).



Thomas Wunderer is a Senior Member of Research Staff at the Palo Alto Research Center, CA with a PhD in EE from Ulm University, Germany. Since joining PARC in 2010, he has led various R&D projects developing novel optoelectronic materials, devices and sub-systems (incl. UV lasers for DARPA LUSTER, CMUVT).

STu4Q.2 • 18:00 **Invited**

Recent progress in GaN-based Vertical-Cavity Surface-Emitting Lasers Having Dielectric Distributed Bragg Reflectors, Hiroshi Nakajima¹, Jugo Mitomo¹, Kentaro Fujii¹, Masayuki Tanaka¹, Masamichi Ito¹, Maho Ohara¹, Noriko Kobayashi¹, Hideki Watanabe¹, Tatsushi Hamaguchi¹, Rintaro Koda¹, Hironobu Narui¹; ¹Sony Corporation, Japan. The recent progress in GaN-based vertical-cavity surface-emitting lasers (VCSELs) having dielectric distributed Bragg reflectors, including the device characteristics of GaN-based VCSELs with a newly proposed cavity structure incorporating an atomically smooth curved mirror, is overviewed.

CLEO: QELS-Fundamental
ScienceFTu4A • Quantum Information Processing—
Continued

FTu4A.3 • 18:15

Finding Non-Classical States that do not Generate Entanglement at a Beam Splitter, Aaron Z. Goldberg¹, Daniel James¹; ¹Univ. of Toronto, Canada. A common way to generate modal entanglement uses beam splitters. We find a set of non-classical states that are not entangled by beam splitters. This is crucial for understanding entanglement generation for, e.g., boson sampling.

FTu4A.4 • 18:30

High speed device-independent quantum random number generation without detection loophole, Yang Liu¹, Xiao Yuan^{1,2}, Ming-Han Li¹, Weijun Zhang³, Qi Zhao², Jiaqiang Zhong⁴, Yuan Cao¹, Yu-Huai Li¹, Luo-Kan Chen¹, Tianyi Peng², Yu-Ao Chen¹, Cheng-Zhi Peng¹, Sheng-Cai Shi⁴, Zhen Wang³, Lixing You³, Xiongfang Ma², Jingyun Fan¹, Qiang Zhang¹, Jian-Wei Pan¹; ¹Univ. of Science and Technology of China, China; ²Tsinghua Univ., China; ³Shanghai Inst. of Microsystem and Information Technology, Chinese Academy of Sciences, China; ⁴Purple Mountain Observatory and Key Lab of Radio Astronomy, Chinese Academy of Sciences, China. We report an experimental study of device-independent quantum random number generation based on an detection-loophole free Bell test with entangled photons. After considering fluctuations and applying hashing, we achieve a random bit rate of 114 bits/s, with a failure probability less than 1E-5.

FTu4A.5 • 18:45

Two-Photon N-Party Quantum Secret Sharing, Warren P. Grice¹, Joseph M. Lukens¹, Nicholas A. Peters¹, Brian Williams¹; ¹Oak Ridge National Lab, USA. We describe a multiparty quantum secret sharing protocol utilizing two-photon entangled states in which the source is one of the secret sharing participants. It is experimentally easier to realize than methods using GHZ states.

CLEO: Science & Innovations

STu4B • Wavelength and Phase-sensitive
Integrated Devices—Continued

STu4B.5 • 18:15

Genetically optimized on-chip wideband ultracompact reflectors and Fabry-Pérot cavities, Zejie Yu¹, Haoran Cui¹, Xiankai Sun¹; ¹The Chinese Univ. of Hong Kong, Hong Kong. We propose a new scheme for on-chip reflectors on the prevalent thin-film-on-insulator platform by using genetic algorithm optimization and experimentally demonstrated devices with footprint of 2.16 μ m \times 2.16 μ m and reflectivity >85% in the wavelength range of 1440-1640nm.

STu4B.6 • 18:30

Scalable Optical Phased Array with Sparse 2D Aperture, Reza Fatemi¹, Aroutin Khachaturian¹, Ali Hajimiri¹; ¹California Inst. of Technology, USA. A scalable OPA with sparse 2D aperture is presented, achieving the highest reported grating-lobe-free FOV-to-beamwidth ratio (16°/0.8°). A PWM generator chip is designed to drive compact phase shifters with row-column layout to reduce power consumption.

STu4B.7 • 18:45

Experimental Realization of Floquet Engineered Topological Phase in Periodically-Curved Waveguide Arrays, Chaoshi Zhang¹, Q.Q. Cheng¹, Yiming Pan², Huaiqiang Wang³, Tao Li³, Shining Zhu³; ¹Univ. of Shanghai for Science and Technology, China; ²Tel Aviv Univ., Israel; ³Nanjing Univ., China. A photonic Floquet simulator was designed to investigate the engineered topological phase in a periodically-driven Su-Schrieffer-Heeger model. Experimentally, we firstly observed a new periodically-driven end state (π -mode), which only exists in special Floquet gauges.

STu4C • Nonlinearity Compensation—
Continued

STu4C.5 • 18:15

Experimental Demonstration of Fiber-Nonlinearity Cancellation by Photonic Homodyne Down-Conversion in Conjugated-Paired Radio-on-Fiber System, Takahide Sakamoto¹, Guo-Wei Lu², Naokatsu Yamamoto¹; ¹National Inst of Information & Comm Tech, Japan; ²Tokai Univ., Japan. We experimentally demonstrate fiber nonlinearity cancellation using photonic homodyne down conversion in conjugated-paired radio-on-fiber (C-RoF) system. 20-km SMF transmission of 156-Mb/s BPSK-C-RoF is demonstrated, naturally cancelling nonlinear phase shift without using digital signal processing.

STu4C.6 • 18:30

Signal-to-Idler Conversion Penalty in AlGaAs-on-Insulator Wavelength Converter, Pawel M. Kaminski¹, Francesco Da Ros¹, Edson P. da Silva¹, Minhao Pu¹, Metodij Yankov¹, Elizaveta Semenova¹, Kresten Yvind¹, Leif K. Oxenlowe¹, Søren Forchhammer¹, Michael Galili¹; ¹DTU Fotonik, Denmark. A wavelength converter based on AlGaAsOI waveguide is characterized by varying the input signal quality. Signal-to-idler conversion penalty is measured in terms of effective received SNR, and trade-offs between penalty and converted signal quality are outlined.

CLEO: Science & Innovations

STu4D • Terahertz QCLs—Continued

STu4D.5 • 18:15

Amplitude Stabilization of a Terahertz Quantum Cascade Laser with an External Metamaterial Amplitude Modulator, Binbin Wei¹, Stephen J. Kindness¹, Nikita Almond¹, Robert Wallis¹, Yuqing Wu¹, Yuan Ren², Philipp Braeuninger-Weimer³, Stephan Hofmann³, Harvey Beere¹, David Ritchie¹, Riccardo Degl'Innocenti⁴; ¹*Cavendish Lab, Univ. of Cambridge, UK*; ²*Purple Mountain Observatory, Chinese Academy of Sciences, China*; ³*Dept. of Engineering, Univ. of Cambridge, UK*; ⁴*Dept. of Engineering, Lancaster Univ., UK*. We demonstrate amplitude stabilization of a terahertz quantum cascade laser with a graphene loaded split-ring-resonator array, the transmission of which can be tuned to compensate the laser power fluctuation with a PID loop.

STu4D.6 • 18:30

Graphene Saturable Absorbers at Terahertz Frequency from Liquid Phase Exfoliation of Graphite, Leonardo Viti¹, Veziro Bianchi¹, Tian Carey², Lianhe Li³, Edmund H. Linfield³, Alexander G. Davies³, Alessandro Tredicucci⁵, Duhee Yoon², Panagiotis Karagiannidis², Lucia Lombardi², Flavia Tomarchio², Andrea Carlo Ferrari², Felice Torrisi², Miriam S. Vitiello⁴; ¹*Scuola Normale Superiore, Italy*; ²*Cambridge Graphene Center, Univ. of Cambridge, UK*; ³*School of Electronic and Electrical Engineering, Univ. of Leeds, UK*; ⁴*Nanoscience, CNR, Italy*; ⁵*Fisica, Università di Pisa, Italy*. We report on the development of terahertz (THz) saturable-absorbers exploiting printable graphene inks. The achieved 80% transparency modulation at 3.5 THz makes these devices potential candidates as passive components for THz solid-state lasers.

STu4D.7 • 18:45

Experimental Demonstration of 16dB Isolation at Room Temperature on a Magnetoplasmonic One-Way Mirror Exploiting THz Cyclotron Resonances in Narrow Gap Semiconductors, Oleksandr Stepanenko², Tomáš Horák^{2,1}, Jan Chocholeš^{3,5}, Kamil Postava^{3,4}, Jean-François Lampin², Mathias Vanwolleghem²; ¹*Université de Lille 1, France*; ²*THz Photonics, CNRS IEMN, France*; ³*Nanotechnology Center, Technical Univ. Ostrava, Czechia*; ⁴*IT4Innovations National Supercomputing Center, Czechia*; ⁵*Dept. of Electrical and Computer Engineering, Dalhousie Univ., Canada*. We demonstrate experimentally a nonreciprocal magnetoplasmonic mirror that achieves room temperature isolation with a rejection rate of 16dB by combining the THz plasma frequency of intrinsic small-gap InSb with its strong THz cyclotron effects. At typical THz QCL temperatures this goes up to 25dB.

CLEO: QELS-Fundamental Science

FTu4E • Quantum and Non-local Plasmonics—Continued

FTu4E.5 • 18:15

Cooperative coupling of hot alkali vapors to surface plasmon: Towards room temperature quantum plasmonics with atomic media, Yoel Sebbag¹, Pankaj Arora¹, Yefim Barash¹, Uriel Levy¹; ¹*Applied Physics, The Hebrew Univ. of Jerusalem, Israel, Israel*. We demonstrate cooperative coupling between hot vapors and surface plasmons with three-fold Purcell factor enhancement. Our result can be regarded as a major step in the quest for room temperature quantum plasmonics with atomic media.

FTu4E.6 • 18:30

Ultrabright Room-Temperature Emission from Single Plasmon-Enhanced Nitrogen-Vacancy Centers in Diamond, Simeon Bogdanov¹, Mikhail Y. Shalaginov^{1,2}, Alexei S. Lagutchev¹, Chin-Cheng Chiang¹, Deesha Shah¹, Alexander S. Baburin^{3,4}, Ilya A. Ryzhikov^{3,5}, Ilya A. Rodionov^{3,4}, Alexandra Boltasheva¹, Vladimir M. Shalaev¹; ¹*Purdue Univ., USA*; ²*Maschussets Inst. of Technology, USA*; ³*FMNS REC, Bauman Moscow State Technical Univ., Russia*; ⁴*Dukhov Research Inst. of Automatics, Russia*; ⁵*Inst. for Theoretical and Applied Electromagnetics RAS, Russia*. We report unprecedentedly bright emission from single nitrogen-vacancy centers in nanodiamonds placed in gaps between a metal film and randomly dispersed metal nanoparticles. The detected fluorescence intensity reaches up to 50 million photons per second.

FTu4E.7 • 18:45

Photonic Crystal Slab Nanocavities from Bulk Single-Crystal Diamond, Noel Wan¹, Sara L. Mouradian¹, Dirk Englund¹; ¹*MIT, USA*. We report on the fabrication of high-Q diamond photonic crystal (PC) slab cavities near the optical transition of the NV center. This process, which allows the production of 2D PC slabs directly on bulk diamond, significantly extends the toolbox for controlling light-matter interactions in diamond.

CLEO: Science & Innovations

STu4F • Nonlinear Optical Phononics & Optomechanics—Continued

STu4F.3 • 18:15

Electro-Opto-Mechanical Radio-Frequency Oscillator in a Multi-Core Fiber, Yosef London¹, Hilel Hagai Diamandi¹, Gil Bashan¹, Avi Zadok¹; ¹*Bar-Ilan Univ., Israel*. An electro-opto-mechanical feedback loop is established across two cores of a multi-core fiber. Guided acoustic waves are stimulated into single-mode oscillations at 369 MHz with 400 Hz linewidth. Threshold behavior and spectral narrowing are observed.

STu4F.4 • 18:30

Raman-Dominant Supercontinuum Generation in Nitrogen-Filled Hollow-Core Negative Curvature Fiber Pumped by Picosecond Laser, Yingying Wang¹, Shoufei Gao¹, Pu Wang¹; ¹*Beijing Univ. of Technology, China*. We present a novel scheme of supercontinuum generation in nitrogen-filled hollow-core negative-curvature fiber pumped by a 532 nm picosecond laser. 250 nm to 1200 nm supercontinuum is generated with total energy of tens microjoule.

19:00–20:30 OSA Technical Group Poster Session, Room 230A/B

CLEO: QELS-Fundamental Science

CLEO: Applications
& TechnologyFTu4G • Continuous Variable Quantum
Computing—Continued

FTu4G.6 • 18:30

Invited

Quantum Computing using Squeezed Light, Christian Weedbrook¹; ¹Xanadu, Canada. Integrated photonics based on squeezed light offers a way to build a highly scalable, room temperature and energy efficient quantum computer. We will discuss the advances we are making here at Xanadu based on this exciting architecture.

FTu4H • Novel Solid State Systems for
Quantum Optics—Continued

FTu4H.5 • 18:15

¹⁷¹Yb:YVO for Nanoscale Quantum Interfaces, Jonathan Kindem¹, John G. Bartholomew¹, Jake Rochman¹, Tian Zhong¹, Charles W. Thiel², Philip J. Woodburn², Rufus L. Cone², Andrei Faraon¹; ¹Caltech, USA; ²Physics, Montana State Univ., USA. We report on the optical and spin coherence properties of ¹⁷¹Yb:YVO at cryogenic temperatures. Our results indicate this material is promising for nanoscale quantum memories, microwave-to-optical transduction, and optically addressable single ions.

FTu4H.6 • 18:30

Narrowing of Electromagnetically Induced Transparency in an Inhomogeneously Broadened Solid-State Atomic Ensemble, Haoquan Fan^{1,2}, Elizabeth A. Goldschmidt^{1,2}; ¹USA Army Research Lab, USA; ²Joint Quantum Inst., Univ. of Maryland, USA. We study electromagnetically induced transparency (EIT) in an inhomogeneously broadened solid-state ensemble of europium atoms. We observe agreement with theory including narrowing of the EIT linewidth as a function of the inhomogeneous width.

FTu4H.7 • 18:45

All-Optical Control of Long-lived Spin Coherences in Rare Earth Doped Nanoparticles, Diana Serrano¹, Jenny Karlsson¹, Alexandre Fossati¹, Alban Ferrier¹, Philippe Goldner¹; ¹Institut de Recherche de Chimie Paris, PSL Research Univ., Chimie ParisTech, CNRS, France. We measured nuclear spin coherence lifetimes up to several milliseconds in Eu³⁺ doped Y₂O₃ nanoparticles using all-optical techniques. Combined with narrow optical linewidths, this opens the way to nanoscale light-atom-spin interfaces at the quantum level.

ATu4I • Combustion and Hypersonic Flow
Diagnostics—Continued

ATu4I.5 • 18:15

Intra-pulse Cavity Enhanced Measurements of Carbon Monoxide in a Rapid Compression Machine, Ehsan Nasir¹, Aamir Farooq¹; ¹Clean Combustion Research Center, King Abdullah Univ. of Science and Technology, Saudi Arabia. A laser absorption sensor for CO concentration was developed for a rapid compression machine using a pulsed QCL near 4.89 μm . Cavity enhancement reduced minimum detection limit down to 2.4 ppm. Off-axis alignment and rapid intrapulse down-chirp resulted in effective suppression of cavity noise.

19:00–20:30 OSA Technical Group Poster Session, Room 230A/B

**CLEO: Applications
& Technology**

**ATu4J • Medical Devices & Systems—
Continued**

ATu4J.4 • 18:15

Portable Diagnostic for Malaria Detection in Low-Resource Settings, Samantha McBirney¹, Dongyu Chen¹, Alexis Scholtz², Bernard Chen¹, Andrea M. Armani¹; ¹Univ. of Southern California, USA; ²Johns Hopkins Univ., USA. We have designed a novel device to identify malaria in both symptomatic and asymptomatic populations by detecting the presence of hemozoin. Here, we detect clinically relevant concentrations of β -hematin, a synthetic mimic of hemozoin.

ATu4J.5 • 18:30

Improved Spot Formation through Flexible Multimode Fiber Using a Partial Reflector, Ruo Yu Gu¹, Elaine Chou¹, Cory Rewcastle², Ofer . Levi², Joseph Kahn¹; ¹Stanford Univ., USA; ²Univ. of Toronto, Canada. We describe a method for improving the formation of a spot of light at the distal end of a flexibly perturbed multimode fiber by attaching a structured partial reflector to the distal end.

ATu4J.6 • 18:45

Intracellular Doppler Imaging Clinical Trials in Personalized Cancer Care, David D. Nolte^{1,2}, Zhe Li¹, Honggu Choi¹, Michael Childress¹, Shadia Jalal³, John Turek^{1,2}; ¹Purdue Univ., USA; ²Animated Dynamics Inc., USA; ³Indiana Univ. School of Medicine, USA. Clinical trials of biodynamic digital holography of cancer biopsies identify patients resistant to chemotherapy with 90% accuracy. Translation of this biomedical optical technology to the clinic may transform personalized cancer care.

CLEO: Science & Innovations

**STu4K • Fiber Frequency Combs—
Continued**

STu4K.5 • 18:15

Wavelength Tunable Narrow Linewidth Comb Using Soliton Self-frequency Shift and Spectral Compression Technique, Nozomu Ohta¹, Lei Jin¹, Yoichi Sakakibara², Emiko Omoda², Hiromichi Kataura², Norihiko Nishizawa¹; ¹Nagoya Univ., Japan; ²AIST, Japan. 1.6-1.9 μ m wavelength tunable comb with spectral width of 4 nm was demonstrated using wavelength tunable soliton pulse and comb profile fiber. High SNR of 37 dB was confirmed for generated comb by beat measurement.

STu4K.6 • 18:30

10 W, sub-100 fs Fiber Amplifier Based on a Self-referenced 750-MHz Yb: fiber Laser Frequency Comb, Bo Xu^{1,2}, Yuxuan Ma^{1,3}, Hirotaka Ishii¹, Fei Meng³, Isao Matsushima^{1,2}, Zhigang Zhang³, Kaoru Minoshima^{1,2}; ¹The Univ. of Electro-Communications, Japan; ²ERATO Intelligent Optical Synthesizer (IOS) Project, Japan Science and Technology Agency, Japan; ³State Key Lab of Advanced Optical Communication System and Networks, Peking Univ., China. We developed a polarization maintained Yb: fiber amplifier based on the self-referenced 750-MHz Yb: fiber laser frequency comb. 10 W average power and sub-100 fs pulse were achieved without deteriorating the high coherence of the comb.

Joint

**JTu4L • Symposium on Multimodal and
Molecular Contrast Optical Imaging II—
Continued**

JTu4L.3 • 18:30 **Invited**

On the Road to Optical Biopsy Based on Multimodal Imaging, Thomas Bocklitz¹; ¹IPC, Univ. Jena, Germany. Optical multimodal imaging techniques feature a huge potential as non-invasive optical biopsy and diagnostic tool. These applications require fiber based measurements and image analysis for artefact removal and tissue diagnostics, which are presented herein.

19:00–20:30 OSA Technical Group Poster Session, Room 230A/B

CLEO: Applications
& TechnologyATu4M • Thin Film & Metrology for Laser
Processing—Continued

ATu4M.5 • 18:15

De-Multiplexed Multiwavelength Light Interferometry, Vala Fathipour¹, Zain Zaidi¹, Connie J. Chang-Hasnain¹; ¹EECS, Univ. of California Berkeley, USA. A new ranging technique is proposed using multi-wavelength laser interferometry with wavelength de-multiplexed detectors to alleviate the range-resolution trade-off inherent in many contemporary ranging techniques. We demonstrate 3-mm range and 10-nm resolution with two-wavelengths.

ATu4M.6 • 18:30

Embedding Distributed Temperature and Strain Optical Fiber Sensors in Metal Components Using Additive Manufacturing, Ran Zou¹, Xuan Liang¹, Aidong Yan¹, Mohan Wang¹, Paul Ohodnicki², Albert To¹, Kevin P. Chen¹; ¹Univ. of Pittsburgh, USA; ²National Energy Technology Lab, U.S. Dept. of Energy, USA. A standard telecom-grade single-mode optical fiber was protected and embedded into IN718 components by nickel electroplating to provide distributed real-time temperature and strain sensing in metal additive manufacturing applications with 5 mm spatial resolution.

ATu4M.7 • 18:45

Self-Mixing Vibrometer has picometer sensitivity by exploiting the FM Channel, Silvano Donati¹, Michele Norgia²; ¹Universita degli Studi di Pavia, Italy; ²DEIB, Politecnico di Milano, Italy. By converting the FM modulation of a self-mixing interferometer into an amplitude signal, we demonstrate a noise-equivalent-displacement (NED) of 1.3-pm/√Hz, two orders of magnitude better than AM channel or a normal interferometer.

CLEO: Science & Innovations

STu4N • 2D Materials in Photonic
Structures—Continued

STu4N.5 • 18:15

Circular Polarized Emission of Tungsten Diselenide (WSe₂) Atomic Layers with Plasmonic Metasurface, Hsiang-Ting Lin^{1,2}, Chiao-Yun Chang¹, Pi-Ju Cheng¹, Ming-Yang Li^{1,3}, Chia-Chin Cheng³, Shu-Wei Chang^{1,2}, Lain-Jong Li³, Chih-Wei Chu¹, Min-Hsiung Shih^{1,2}; ¹Research Center for Applied Sciences, Academia Sinica, Taiwan; ²Dept. of Photonics and Inst. of Electro-Optical Engineering, National Chiao Tung Univ., Taiwan; ³Physical Science and Engineering Division, King Abdullah Univ. of Science and Technology, Saudi Arabia. A circularly polarized light emitting device with ultrathin geometry were demonstrated by integrating WSe₂ atomic layers with plasmonic chiral metasurfaces and achieve more than 25% circular dichroism.

STu4N.6 • 18:30

Bright Electroluminescence from Back-Gated WSe₂ P-N Junctions Using Pulsed Injection, Kevin Han¹, Seth Fortuna¹, Matin Amani¹, Sujay Desai¹, Der-Hsien Lien¹, Geun Ho Ahn¹, Eli Yablonovitch¹, Ali Javey¹, Ming C. Wu¹; ¹Univ. of California Berkeley, USA. We demonstrate bright electroluminescence in WSe₂ monolayers using pulsed injection, without the use of split gates, chemical doping, or heterostructures. Electroluminescence quantum efficiency approaches that of photoluminescence, indicating efficient exciton formation with injected carriers.

STu4N.7 • 18:45

Giant Electro-Refractive Modulation of Monolayer WS₂ Embedded in Photonic Structures, Ipshita Datta¹, Sang Hoon Chae¹, Gaurang R. Bhatt¹, James Hone¹, Michal Lipson¹; ¹Columbia Univ., USA. We electrically tune the index of refraction of a monolayer WS₂ index that is integrated on a SiN photonic structure by up to 3%. The loss of WS₂ is electro-statically tuned by less than 0.2 % at 1550 nm.

STu4O • Laser Facilities—Continued

STu4O.5 • 18:15

Compact Photo-Injector and Laser-Heater Drive Laser for the European X-ray Free Electron Laser Facility, Lutz Winkelmann¹, Maik Frede², Christian Mohr¹, Hongwei Chu¹, Chen Li¹, Peng Li^{1,3}, Uwe Grosse-Wortmann¹, Frank Brinker¹, Ingmar Hartl¹, Bastian Schulz²; ¹DESY, Germany; ²neoLASE GmbH, Germany; ³IMRA America, USA. We present a drive laser for the photo-injector of the European XFEL, which delivers up to 25 μJ, ~6 ps, 266 nm pulses at 4.5 MHz repetition frequency in 600 μs long bursts with 0.6 % rms energy instability.

STu4O.6 • 18:30 **Invited**

Status and Development of High Average Power Lasers at HiLASE, Michal Chyla¹, Martin Divoky¹, Martin Smrz¹, Jiri Muzik¹, Amani Reza¹, Pawel Sikocinski¹, Liyuan Chen¹, Patricie Severova¹, Ondrej Novak¹, Hana Turcicova¹, Michal Vyvlecka¹, Lukas Roskot¹, Jaroslav Huynh¹, Siva Nagisetty¹, Jitka Cernohorska¹, Huang Zhou¹, Alina Pranovich¹, Jan Pilar¹, Ondrej Slezak¹, Magdalena Sawicka-Chyla¹, Venkatesan Jambunathan¹, Akira Endo¹, Antonio Lucianetti¹, Danijela Rostohar¹, Paul Mason², Jonathan Phillips², Klaus Ertel², Saumyabrata Banerjee², Jodie Smith², Thomas Butcher², Mariastefania De Vido², Cristina Hernandez-Gomez², Chris Edwards², John Collier², Tomas Mocek¹; ¹HiLASE Centre, Inst. of Physics ASCR v.v.i., Czechia; ²CALTA, Rutherford Appleton Lab, UK. HiLASE facility focuses on development of high average power pulsed lasers with picosecond and nanosecond laser pulses. Current status of 1kW/100J multislabs and 500W/5mJ thin-disk lasers and future plans of the HiLASE facility are presented.

19:00–20:30 OSA Technical Group Poster Session, Room 230A/B

CLEO: Science & Innovations

STu4P • Advanced Sensing Concepts—
Continued

STu4P.6 • 18:15

High-speed Ultra-broadband Fourier-transform CARS Spanning over 3,000 cm^{-1} , Junko Omachi¹, Kazuki Hashimoto^{2,3}, Takuro Ideguchi^{3,4}; ¹*Inst. for Photon Science and Technology, The Univ. of Tokyo, Japan*; ²*Aeronautical Technology Directorate, Japan Aerospace Exploration Agency, Japan*; ³*Dept. of Physics, The Univ. of Tokyo, Japan*; ⁴*PRESTO, Japan Science and Technology Agency, Japan*. We demonstrate ultra-broadband rapid-scan Fourier-transform coherent anti-Stokes Raman scattering spectroscopy spanning over 3,000 cm^{-1} at a scan rate of 24,000 spectra/s with a 6-fs mode-locked laser.

STu4P.7 • 18:30

Real-time Detection of Scaling on Reverse Osmosis Membranes with Raman Spectroscopy, Omkar D. Supekar¹, Joseph J. Brown¹, Alan R. Greenberg¹, Juliet Gopinath^{2,3}, Victor Bright¹; ¹*Dept. of Mechanical Engineering, Univ. of Colorado Boulder, USA*; ²*Dept. of Electrical, Computer, and Energy Engineering, Univ. of Colorado Boulder, USA*; ³*Dept. of Physics, Univ. of Colorado Boulder, USA*. We demonstrate real-time, local detection of the onset of scaling, in addition to chemical quantification, in a reverse osmosis separation system using confocal Raman microscopy. The results show consistent scalant detection.

STu4P.8 • 18:45

Single and double-quantum multidimensional coherent spectroscopy using frequency combs, Bachana Lomsadze¹, Steven T. Cundiff¹; ¹*Univ. of Michigan, USA*. We present a novel experimental approach of multidimensional coherent spectroscopy using frequency combs. We demonstrate its capabilities for probing weak many-body interactions as well as its applications for rapid and high resolution chemical sensing.

STu4Q • UV-visible Semiconductor Lasers—
Continued

STu4Q.3 • 18:30

Direct Pulse Position Modulation of a 410 nm Semipolar GaN Laser Diode for Space Optical Communications, Joseph M. Fridlander¹, Changmin Lee¹, James Speck¹, Steven DenBaars¹, Jonathan Klamkin¹; ¹*UCSB, USA*. A semipolar GaN laser was characterized for space optical communications, achieving a peak power of 160 mW. Periodic and random M-ary pulse position modulation sequences with pulse widths of 5 ns and 10 ns were demonstrated.

STu4Q.4 • 18:45

High Power, High Efficiency Red Laser Diode Structures Grown on GaAs and GaAsP Metamorphic Superlattices, Steven Ruder^{2,1}, Tom Earles^{2,1}, Christian Galstad², Michael Klaus², Don Olson², Luke J. Mawst¹; ¹*Univ. of Wisconsin - Madison, USA*; ²*Compound Photonics, USA*. Red laser diodes were fabricated on GaAs and GaAsP metamorphic-superlattice-substrates. The tensile strained QW on GaAs emitted 45% PCE, 638nm, TM-polarized light at 880mW CW. The compressively strained QW on the metamorphic structure emitted 639nm TE-polarized light with $T_0=90\text{K}$ and $T_1=300\text{K}$.

19:00–20:30 OSA Technical Group Poster Session, Room 230A/B

07:30–18:30 Registration, Concourse Level

08:00–10:00 JW1A • Plenary Session II & International Day of Light, Grand Ballroom

10:00–17:00 Exhibition Open, Exhibit Hall

10:00–11:30 Coffee Break & Exhibit Only Time, Exhibit Hall

Exhibit Hall

11:30–13:00 JW2A • Poster Session II

JW2A.1

Tuning Effective Fiber Radius Variation of SNAP Structures With a Femtosecond Laser, Yu Qi¹, Shen Fangcheng¹, Xu Zuowei¹, Haoran Cao¹, Misha Sumetsky², Shu Xuewen¹; ¹Huazhong Univ. of Science and Technology, China; ²Aston Univ., UK. It is shown that the nanoscale radius variation of the optical fiber can be effectively tuned by introducing variable internal pressure into an optical fiber with a femtosecond laser.

JW2A.2

90 Gb/s PAM4 and OOK Optical Signal Generation by Using the Dual-arm-drive Silicon Mach-Zehnder Modulator, Sizhu Shao^{1,2}, Jianfeng Ding¹, Lingchen Zheng^{1,2}, Lei Zhang¹, Xin Fu¹, Lin Yang^{1,2}; ¹Inst. of Semiconductors, CAS, China; ²Univ. of Chinese Academy of Sciences, China. In this paper, the 90 Gb/s PAM4 and OOK optical signal generation by using a dual-arm-drive silicon Mach-Zehnder modulator is demonstrated. The OOK optical signal generation with speed up to 110 Gb/s is also demonstrated.

JW2A.3

An On-Chip Integrated Dual-Functional Modulator-Detector for Optical Communication, SHUAI SUN¹, Ruoyu Zhang¹, Jiaxin Peng¹, Vikram Narayana¹, Hamed Dalir², Tarek El-Ghazawi¹, Volker J. Sorger¹; ¹George Washington Univ., USA; ²Omega Optics, Inc., USA. We propose a novel integrated broadband hybrid photonic-plasmonic device termed MODetector featuring dual light modulation and detection. With 10 dB extinction ratio and 0.8 dB insertion loss for modulation and 0.7 W/A responsivity for detection.

JW2A.4

Highly-efficient, ultra-broadband and polarization insensitive graphene-silicon based electro-absorption modulator, Yin Xu^{1,2}, Feng Li^{2,3}, Jinhui Yuan^{3,4}, Zhe Kang³, Chao Mei^{3,4}, Xianting Zhang³, P. K. A. Wai³; ¹Dept. of Electrical Engineering, The Hong Kong Polytechnic Univ., China; ²Hong Kong Polytechnic Univ. Shenzhen Research Inst., China; ³Dept. of Electronic and Information Engineering, The Hong Kong Polytechnic Univ., China; ⁴State Key Lab of Information Photonics and Optical Communications, Beijing Univ. of Posts and Telecommunications, China. We propose a highly-efficient, ultra-broadband and polarization-insensitive electro-absorption modulator based on a multilayer graphene-silicon waveguide. A modulation efficiency of ~2.21 dB/μm is obtained for both polarizations within a bandwidth covering from E to U bands.

JW2A.5

Gold based plasmonic stripes co-integrated with low loss Si₃N₄ platform in aqueous environment, Athanasios Manolis^{1,2}, George Dabos^{1,2}, Dimitra Ketzaki^{1,2}, Evangelia Chatzianagnostou^{1,2}, Dimitris Tsiokos^{1,2}, Laurent Markey³, Jean Claude Weeber⁴, Alain Dereux³, Anna-Lena Giesecke⁴, Caroline Porschatis⁴, Bartos Chmielak⁴, Nikos Pleros^{1,2}; ¹Aristotle Univ. of Thessaloniki, Greece; ²Center for Interdisciplinary Research and Innovation, Greece; ³Laboratoire Interdisciplinaire Carnot de Bourgogne, France; ⁴AMO GmbH, Advanced Microelectronic Center Aachen (AMICA), Germany. We demonstrate a butt-coupled interface between LPCVD Si₃N₄ and gold based plasmonic waveguides in aqueous environment, exhibiting 2.3dB coupling loss and 75μm propagation length at 1550nm, towards future employment in biosensing applications.

JW2A.6

Novel Polarization Beam Splitter with High Fabrication Tolerance, Nicolas M. Abadia Calvo^{1,2}, Md Ghulam Saber², Qiaoyin Lu¹, Wei-Hua Guo¹, David V. Plant², John F. Donegan¹; ¹Trinity College Dublin, Canada; ²McGill Univ., Canada. A highly fabrication tolerant polarization beam splitter is presented. The fabrication tolerances are relaxed by adjusting two voltages. Experiments show on-chip losses of 3.5 dB and extinction ratio of 15 dB at C-band.

JW2A.7

Application of High-reflectivity Non-periodic Sub-wavelength Gratings with Small-angle Beam-steering Ability in Fabry-Perot Cavity, Shuai Zhang¹, Xiaofeng Duan¹, Gongqing Li¹, Kai Liu¹, Yongqing Huang¹, Xiaomin Ren¹; ¹Beijing Univ. of Posts and Telecommunications, China. An axisymmetric high-reflectivity non-periodic sub-wavelength gratings (SWG) with small-angle beam-steering ability for reflected light is presented, and it brings a new characteristic of flexibly controlling the width of oscillation optical field for the improved Fabry-Perot (F-P) cavity.

JW2A.8

Ultra-broadband 3dB power splitter based on silicon slot waveguide, Yuguang Zhang^{2,1}; ¹State Key Lab of Optical Communication Technologies and Networks, Wuhan Research Inst. of Posts and Telecommunications, China; ²National Information Optoelectronics Innovation Center, China. We present the design of the ultra-broad bandwidth 3dB splitter based on silicon slot waveguide. The bandwidth of the proposed splitter is simulated as large as 600 nm, with the insertion loss less than 1dB.

JW2A.9

Design of an Ultra-Small Footprint Graphene-based Silicon Photonic Bandgap Modulator, Giannino Dziallas^{2,1}, Lars Zimmermann¹, Klaus Petermann²; ¹IHP GmbH, Germany; ²Inst. of High-Frequency and Semiconductor System Technologies, Technical Univ. of Berlin, Germany. We propose a novel design of an ultra-small footprint silicon photonic. The device length is 6 μm and with 1 V_{pp} the modulator should attain 15 dB extinction due to the photonic bandgap microcavity.

JW2A.10

Ultrafast shifted-core coaxial nano-emitter with tunable Q factor, Xi Li¹, Qing Gu¹; ¹Univ. of Texas at Dallas, USA. We numerically demonstrate a III-V single mode shifted-core coaxial nano-emitter featuring a Purcell factor larger than 600 and tunable Q factor.

JW2A.11

Silicon-Based Nanophotonic Topological Insulators, Kasper E. Lund^{1,2}, Chirag M. Patil¹, Søren Stobbe^{1,2}; ¹The Niels Bohr Inst., Univ. of Copenhagen, Denmark; ²Fotonik, Technical Univ. of Denmark, Denmark. We present the design and fabrication of nanophotonic topological insulators based on photonic crystals. Our work extends recent a proposal silicon photonics in the telecom c-band while taking realistic fabrication parameters into account.

JW2A.12

Demonstration of microring-based WDM-compatible mode-division multiplexing on a silicon chip, Shuang Zheng¹, Xiaoping Cao¹, Jian Wang¹; ¹Wuhan National Lab for Optoelectr, China. Based on silicon chip, we design and fabricate a mode-division (de)multiplexer in conjunction with wavelength-division multiplexing (WDM) by using three single-mode microring resonators. The on-chip device exhibits low mode crosstalk around the wavelength of 1540 nm.

JW2A.13

A 3-Micron-Radius Bend for SOI TE₀/TE₁ Multiplexing, Min Teng¹, Abdullah Al Noman¹, Yun Jo Lee¹, Ziyun Kong¹, Minghao Qi¹; ¹Purdue Univ., USA. We propose a 3-micron-radius, TE₀/TE₁ multiplexed 90-degree bend that numerically exhibits 0.8 dB bending loss and 20 dB crosstalk suppression over 30nm bandwidth on a silicon-on-insulator platform. An S-bend shows >37 dB colorless crosstalk suppression.

JW2A.14

Ultra-compact on-chip mode exchange device using inverse-designed silicon metasurface, Hao Jia^{1,2}, Ting Zhou^{1,2}, Xin Fu^{1,2}, Lin Yang^{1,2}; ¹Inst Semiconductors, CAS, China; ²College of Materials Science and Opto-Electronic Technology, Univ. of Chinese Academy of Sciences, China. We propose and demonstrate an ultra-compact mode exchange device with high efficiency. It is 4×1.6 μm in size and can realize mode exchange between TE₀ and TE₁. Characterization shows its optical bandwidth covers C-band.

JW2A.15

Extending Modulation Bandwidth of SOI Thermo-Optic Phase Shifters Through Digital Pre-Emphasis, Sungwon Chung¹, Hossein Hashemi¹; ¹Univ. of Southern California, USA. We demonstrate a digital pre-emphasis technique for extending the modulation bandwidth of a thermo-optic phase shifter in silicon-on-insulator (SOI) CMOS. The electrical input to the phase shifter is pre-emphasized, increasing 3-dB optical modulation bandwidth 6.3 times from 8.1 kHz to 50.7 kHz.

JW2A.16

Encapsulated Silicon Nitride Nanobeam Cavity for Nanophotonics using Layered Materials, Taylor K. Fryett¹, Yueyang Chen¹, James Whitehead¹, Zane Peycke¹, Xiaodong Xu¹, Arka Majumdar¹; ¹Univ. of Washington, USA. The fragile nature of floating membrane resonators poses a serious problem for constructing a hybrid photonics platform. To overcome this challenge, we design and demonstrate encapsulated silicon nitride nanobeams and demonstrate coupling to layered materials.

JW2A.17

Magnitude and Sign Control of Index-Antiguidded Coupling, Zihe Gao¹, Dominic Siriani², Kent D. Choquette¹; ¹Univ of Illinois at Urbana-Champaign, USA; ²Cisco Systems, USA. We show the first theoretical analysis of the coupling coefficient in passive index-antiguidded coupling. Both magnitude and sign of the coupling coefficient are controlled by the inter-element distance and index, enabling novel photonic applications.

JW2A.18

Design of a Low-threshold Mid-IR Silicon Raman Laser, Behsan Behzadi¹, Ravinder K. Jain¹, Mani Hossein-Zadeh^{1,2}; ¹Center for High Technology Materials, USA; ²ECE, Univ. of New Mexico, USA. We present the design and performance of an integrated all-silicon continuous-wave Mid-IR Raman laser with an estimated threshold power < 100 μ W generating a single line with a linewidth < 10 MHz at 3.278 μ m.

JW2A.19

Chip-Integrated Plasmonic Flat Optics for Mid-infrared Polarization Detection, Jing Bai¹, Chu Wang¹, Xiahui Chen¹, Ali Basiri¹, Chao Wang¹, Yu Yao¹; ¹Arizona State Univ., USA. We present theoretical modeling and experimental demonstration of MIR polarization detection based on monolithically chip-integrated plasmonic metasurfaces. Our technique enables full Stokes Parameters detection for arbitrary polarized states of light in MIR wavelengths.

JW2A.20

Subwavelength grating waveguide based cladding-modulated Bragg reflector in bulk CMOS, Cheng-Tse Tang¹, Tse-Hung Chen¹, Tzu-Hsiang Yen¹, Yung-Jr Hung¹; ¹National Sun Yat-sen Univ., Taiwan. A SWG-based cladding-modulated Bragg reflector implemented in bulk CMOS enables a lower propagation loss (< 30 dB/cm), a higher extinction ratio (24.5 dB) and a less-sensitive temperature coefficient (29.4 $\text{pm}/^\circ\text{C}$) as compared to strip-based counterpart.

JW2A.21

Nanoscale Fingerprinting with Hyperbolic Metamaterials, Zhengyu Huang¹, Evgenii E. Narimanov², Theodore B. Norris¹; ¹Electrical Engineering and Computer Science, Univ. of Michigan, USA; ²Electrical and Computer Engineering, Purdue Univ., USA. We develop a new concept for optical sub-wavelength discrimination of nanostructures positioned on a hyperbolic metamaterial surface using only far-field measurements of the spectral scattered intensity.

JW2A.22

Integrated Optical Power Equalizer Based on a Dual-Polarization Micro-Ring Resonator, Xingyuan Xu¹, Jiayang Wu¹, Thach Nguyen², Sai T. Chu³, Brent Little⁴, Roberto Morandotti⁵, Anan Mitchell², David J. Moss¹; ¹Swinburne Univ. of Technology, Australia; ²RMIT Univ., Australia; ³City Univ. of Hong Kong, Hong Kong; ⁴Chinese Academy of Science, China; ⁵INRS-Énergie, Matériaux et Télécommunications, Canada. We demonstrate an optical power equalizer based on a dual-polarization micro-ring resonator. By controlling the light polarization, a large loss tunable range from -29.3 dB to 30 dB of the equalizer is experimentally achieved.

JW2A.23

A dual-drive DAC-less silicon PAM-4 optical modulator for 100 Gb/s data transmission at C-band, Lingchen Zheng^{1,2}, Jianfeng Ding¹, Sizhu Shao^{1,2}, Lei Zhang¹, Xin Fu¹, Lin Yang^{1,2}; ¹Institute of semiconductor, CAS, China; ²Univ. of Chinese Academy of Sciences, China. A DAC-less silicon PAM-4 optical modulator which is driven by two binary electrical signals is demonstrated. A mathematical analysis for the modulation chirp is established. The device can work at 100 Gb/s.

JW2A.24

High Fidelity MMI Excitation Patterns for Optofluidic Multiplexing, Matthew Stott¹, Vahid Ganjalizadeh², Maclain Olsen¹, Marcos Orfila¹, Johnny McMurray¹, Erik Hamilton¹, Holger Schmidt², Aaron Hawkins¹; ¹Brigham Young Univ., USA; ²Univ. of California, Santa Cruz, USA. High fidelity interference patterns from multimode interference waveguides are needed for multiplexed optofluidic biosensors. Spot pattern fidelity can be optimized by careful design of the single-mode waveguides used to excite the multimode waveguides.

JW2A.25

Experimental Demonstration of Low Temperature Sensitivity SiN Interleaver, Yinglu Zhang¹, Jinsong Xia¹; ¹Wuhan National Lab for Optoelectronics, China. We experimentally demonstrate a low temperature sensitivity SiN interleaver. The FSR is 1.65 nm. The 1-dB bandwidth is 0.62 nm. The crosstalk is less than -15 dB from 1522 nm to 1549 nm. In the temperature from 25°C to 70°C, the temperature sensitivity is within $\pm 7 \text{ pm}/^\circ\text{C}$.

JW2A.26

Apodization techniques for side-lobes suppression in silicon photonics waveguide gratings, Chia-Ju Yu¹, Tzu-Hsiang Yen¹, You-Cheng Lu¹, Bing-Hao Shih¹, Yung-Jr Hung¹; ¹National Sun Yat-sen Univ., Taiwan. We demonstrate c-band and o-band silicon waveguide gratings with a side-lobe suppression ratio of 36.6 and 27.1 dB, respectively, by modulating the corrugation width or grating offset with apodization function while remaining zero-dc effective index change.

JW2A.27

Silicon Nitride Integrated All-optical Switch Assisted by Graphene, Ciyuan Qiu¹, Yuxing Yang¹, Chao Li¹, Yifang Wang¹, Kan Wu², Jianping Chen¹; ¹Shanghai Jiao Tong Univ., China; ²Shanghai Jiao Tong Univ., China. An all-optical switch near 1550nm is realized on a graphene-on-silicon nitride (Si_3N_4) integrated platform with thermo-optic effect. A fast switching time of 253ns is obtained due to the high thermal conductivity of graphene.

JW2A.28

Experimental demonstration of a polarization diversity broadband orbital angular momentum modes emitter, Zhou Nan¹, Shuang Zheng¹, Xiaoping Cao¹, Shengqian Gao², Shimao Li², Mingbo He², Xinlun Cai², Jian Wang¹; ¹Wuhan National Lab for Optoelectronics, China; ²State Key Lab of Optoelectronic Materials and Technologies and School of Physics and Engineering, Sun Yat-sen Univ., China. We simulate, fabricate and demonstrate the silicon-based polarization multiplexing broadband orbital angular momentum (OAM) generator. The generated x-pol OAM_{1,1}, x-pol OAM_{1,2}, y-pol OAM_{1,1}, and y-pol OAM_{1,2} show maximum purity of 0.91, 0.89, 0.92 and 0.92.

JW2A.29

Light Sources for Neuromorphic Computing, Sonia M. Buckley¹, Jeffrey Chiles¹, Adam McCaughan¹, Richard Mirin¹, Sae Woo Nam¹, Jeffrey Shainline¹; ¹NIST, USA. We have demonstrated electrically-injected waveguide-coupled LEDs based on W centers in silicon for neuromorphic computing. We analyze the sources of loss in these LEDs and simulate new designs for scalable, waveguide-coupled devices with several orders of magnitude higher efficiency.

JW2A.30

1550 nm AlGaInAs MQWs 10-channel Laser Array for Optical Interconnects, Mingjin Wang¹, Hailing WANG¹, Ranzhe Meng¹, Aiyi Qi¹, Wan-hua Zheng¹; ¹CAS Inst. of Semiconductors, China. A 10-channel laser array with 3-nm wavelength spacing is presented. The output-power of 20 mW, SMSR of higher than 30 dB, and efficient slope of 0.224 mW/mA for each laser within the array are achieved.

JW2A.31

All-Optical Intensity Modulation in Polymer Waveguides Doped with Si Quantum Dots, Aleksandrs Marinins¹, Aleksjs Udalcovs², Oskars Ozolins², Xiaodan Pang², Jonathan G. Veino³, Gunnar Jacobsen², Ilya Sychugov¹, Jan Linnros¹, Sergei Popov¹; ¹KTH, Sweden; ²RISE Acreo AB, Sweden; ³Univ. of Alberta, Canada. We demonstrate all-optical intensity modulation in integrated PMMA optical waveguides doped with silicon quantum dots. The 1550 nm probe signal is absorbed by free carriers excited in silicon quantum dots with 405 nm pump light.

JW2A.32

Compact Optomechanical Phase Shifter for Visible Light Integrated Photonics, Bruno Figeys¹, Rita Van Hoof¹, Pieter Neutens¹, Bert Du Bois¹, Guilherme Brondani Torri¹, Simone Severi¹, Xavier Rottenberg¹; ¹imec, Belgium. This paper reports on the development of a CMOS compatible capacitively actuated optomechanical phase shifter for visible light, demonstrated on a 200nm PECVD SiN photonic platform. The phase shifting was demonstrated using Mach-Zehnder interferometers.

JW2A.33

Wideband Kerr-comb near visible spectrum in coupling-engineered thin Silicon nitride resonators, Ali Eshaghian Dorche¹, Ali Asghar Eftekhari¹, Ali . Adibi¹; ¹Georgia Inst. of Technology, USA. We present wideband Kerr-comb generation from 650 nm to 1200 nm in a thin silicon-nitride (SiN) platform enabled by enhanced power transfer through the dispersive wave using a dispersion-engineered over-etched SiN waveguide and a coupled-resonator structure.

JW2A.34

On-Chip Adiabatic Couplers for Broadband Quantum-Polarization State Preparation, Yen-Hung Chen¹, Hung-Pin Chung¹, Kuang-Hsu Huang¹, Kai Wang², Sung-Lin Yang¹, Shih-Yuan Yang¹, Chun-I Sung¹, Alexander S. Soltsev^{2,3}, Andrey A. Sukhorukov², Dragomir N. Neshev²; ¹National Central Univ., Taiwan; ²The Australian National Univ., Australia; ³Univ. of Technology Sydney, Australia. We present a unique wavelength-dependent polarization splitter based on asymmetric adiabatic couplers designed for integration with type-II spontaneous parametric-down-conversion sources. The system can be used for preparing different quantum polarization-path states over a broad band.

JW2A.35

Thermal tuning of Brillouin resonance in free standing silicon nanowire, Paul Tiebot^{1,2}, Raphaël Van Laer^{1,3}, Dries Van Thourhout^{1,2}; ¹Photonics Research Group, Ghent Univ.-imec, Belgium; ²Center for Nano and Biophotonics (NB-Photonics), Ghent Univ., Belgium; ³Ginzton Lab, Dept. of Applied Physics, Stanford Univ., USA. We have demonstrate the thermal tuning of the Brillouin resonance in silicon nanowire waveguides using cross phase modulation detection. We also investigate possible use of this effect for locally mapping the width of an extended waveguide.

JW2A.36

Microring Resonator Based Compact On-chip Phase Tuner, Hwaseob Lee¹, Thomas M. Kananen¹, Ranajoy Bose², Raymond Beausoleil², Tingyi Gu¹; ¹Univ. of Delaware, USA; ²Hewlett-Packard Labs, USA. We study the mode-splitting microring resonators for compact and efficient phase tuners. Through optimization of inter-modal and ring-waveguide coupling, 72.535 ps group delay and 1.4208 rad phase shift with 5.83 dB loss are achieved.

JW2A.37

Near-field flat focusing mirrors using a metallic subwavelength grating on top of a plasmonic waveguide, Yu-Chieh Cheng¹, Bo-Zhi Huang¹, Juei-Hung Tsai¹, Yu-Ching Chuang¹; ¹Dept. of Electro-Optical Engineering, National Taipei Univ. of Technology, Taiwan. Flat focusing mirrors without any optical axis have been studied by metallic subwavelength gratings on top of a plasmonic waveguide. The principle is based on an anomalous lateral displacement, leading to a near-field focusing.

JW2A.38

Linewidth-adjustable bandpass filter based on silicon cladding-modulated waveguide moiré Bragg gratings, Tzu-Hsiang Yen¹, Bing-Hao Shih¹, Nai-Wen Cheng¹, Yung-Jr Hung¹; ¹National Sun Yat-sen Univ., Taiwan. We demonstrate linewidth-adjustable (0-1 nm) narrow bandpass filters using silicon cladding-modulated waveguide moiré Bragg gratings. The passband linewidth is controlled by the number of crossovers and the corrugation width of the moiré grating.

JW2A.39

Ge-on-Si wavelength division multiplexing components near 4.7 μm , Aditya Malik¹, Eric J. Stanton¹, Junqian Liu¹, Alexander Spott¹, John E. Bowers¹; ¹*Electrical and Computer Engineering, Univ. of California Santa Barbara, USA.* Wavelength division multiplexing components based on Ge-on-Si waveguides are presented for operation near 4.7 μm wavelength. Transmission characteristics of 1×1 and 2× MZIs (35 dB extinction) and AWGs (25.7 dB cross-talk) are reported.

JW2A.40

Polarization Rotator in Low Index Contrast Substrates for Mid-Infrared Photonic Integration, Swapnajt Chakravarty¹, Jason Midkiff¹, Chi-Jui Chung², Ali Rostamian², Joel Guo², Ray Chen²; ¹*Omega Optics, Inc, USA;* ²*Electrical and Computer Engineering, Univ. of Texas at Austin, USA.* We demonstrate polarization rotators in low index contrast InGaAs-InP material system to enable monolithic integration of quantum cascade lasers and detectors with slotted photonic crystal waveguide gas sensors in the molecular fingerprint region from 1–3–15mm

JW2A.41

Low Loss Etchless Photodefined Polymer Optical Waveguides, Julie I. Frish¹, Kyung-Jo Kim¹, Roland Himmelhuber¹, Sasaan Showghi¹, Robert A. Norwood¹; ¹*Univ. of Arizona, USA.* Etchless photodefined polymer optical waveguides are created through direct-write lithography and commercially available materials. Bypassing wet development provides benefits to optical chip-to-chip devices. At 1550nm telecommunication wavelengths optical propagation loss is less than 1 dB/cm.

JW2A.42

A Dispersion-Compensated Transmitter for All-Pass Radio over Fiber Link with Simultaneous Dispersion Induced Power Fading and Phase Distortion Elimination, Guanyu Han¹, Haojie Wang¹, Shangyuan Li¹, Xiaoxiao Xue¹, Xiaoping Zheng¹, Bingkun Zhou¹; ¹*Tsinghua National Lab for Information Science and Technology, Dept. of Electronic Engineering, Tsinghua Univ., China.* A dispersion-compensated transmitter for the all-pass RoF link is demonstrated. CD-induced power fading and phase distortion are simultaneously eliminated with the bandwidth up to 25-GHz after 40-km SMF transmission. The SFDR is improved by 13.3-dB.

JW2A.43

Generation of Optical Single Sideband OFDM Using a Silicon Microring IQ modulator, Yelong Xu¹, Mingyang Lyu¹, Jiachuan Lin¹, Leslie A. Rusch¹, Wei Shi¹; ¹*Université Laval, Canada.* Optical single-sideband (SSB) OFDM signal is experimentally generated by a silicon microring IQ modulator. 24 Gb/s SSB 8-QAM OFDM is successfully achieved with a BER well below the FEC limit.

JW2A.44

Electro-Optic Aperiodically Poled Lithium Niobate Directional Couplers, Yen-Hung Chen¹, Hung-Pin Chung¹, Shih-Yuan Yang¹, Sung-Lin Yang¹, Tsai-Yi Chien¹, Kuang-Hsu Huang¹; ¹*National Central Univ., Taiwan.* We report the first aperiodically alternating- $\Delta\beta$ directional couplers whose switching behavior can be engineered in great freedom. The fabrication tolerance/working bandwidth of the novel coupler can be increased by 2.7/2.4 times over a conventional coupler.

JW2A.45

Fano Resonance Assisted Tunable Microwave Photonic Phase Shifter in Loaded Ring Resonator, Awanish Pandey¹, Shankar Kumar Selvaraja¹; ¹*Indian Inst. of Science, India.* We demonstrate photonic assisted RF-phase shifter based on an internally loaded ring resonator exhibiting Fano resonance. A phase shift of 0°–172° has been achieved with a power penalty of 0–4.1 dB for 10 GHz (21–31 GHz) of bandwidth.

JW2A.46

Integrated Power Splitters for Mode-Multiplexed Signals, Yuanhang Zhang¹, Mohammed Al-Mumin², Huiyuan Liu¹, Chi Xu¹, Lin Zhang², Patrick L. LiKawWa¹, Guifang Li¹; ¹*Univ. of Central Florida, CREOL, USA;* ²*Tianjin Univ., China;* ³*College of Technological Studies, Kuwait.* An on-chip non-center-feed MMI power splitter for mode-multiplexed signals is proposed and experimentally demonstrated for the first time.

JW2A.47

An Ultra-Compact Colorless Dual-Mode 3 dB Power Splitter Based on Axisymmetrical Subwavelength Structure, Weijie Chang¹, Lulu Lu¹, Deming Liu¹, Minming Zhang¹; ¹*Huazhong Univ. of Science and Tech, China.* A novel ultra-compact colorless dual mode power splitter using inverse design method is proposed and experimentally demonstrated with low crosstalk < 20 dB and a footprint of only 2.88 × 2.88 μm^2 .

JW2A.48

Hybrid Silicon Waveguides for Photonic Quantum Circuits Integrating Quantum State Generation and Manipulation, Lingjie Yu¹, Renduo Qi¹, Wei Zhang¹, Yidong Huang¹; ¹*Tsinghua Univ., China.* We propose a hybrid silicon waveguide structure for photonic quantum circuits, in which biphoton states are generated in the strip waveguide section and manipulated in the shallow-ridge waveguide section.

JW2A.49

Verilog-A Compact Modeling and Simulation of AWGR based All-to-All Optical Interconnects, Kaiqi Zhang¹, Xian Xiao¹, Yu Zhang¹, S. J. Ben Yoo¹; ¹*Univ. of California Davis, USA.* We construct a Verilog-A compact module for all-to-all optically interconnected system. A physics-based model of a cyclic AWGR generate simulation results, which are compared to the measured data of an actual AWGR.

JW2A.50

An Optical Parallel Multiplier Using Nanophotonic Analog Adders and Optoelectronic Analog-to-Digital Converters, Yuuki Imai¹, Tohru Ishihara¹, Hidetoshi Onodera¹, Akihiko Shinya², Shota Kita², Kengo Nozaki², Kenta Takata², Masaya Notomi²; ¹*Kyoto Univ., Japan;* ²*NTT Basic Research Labs, Japan.* We propose an architecture of an optical parallel multiplier based on an optical analog addition. With optoelectronic circuit simulation, we show that the optical multiplier is more than three times faster than the CMOS multiplier.

JW2A.51

Microwave Waveform Generation via Discrete Fourier Transform of Modulated Optical Pulse Train, Qijie Xie¹, Chester Shu¹; ¹*Chinese Univ. of Hong Kong, Hong Kong.* A new scheme of microwave waveform generation is experimentally demonstrated utilizing envelope detection of optical waveform generated from discrete Fourier transform of modulated optical pulse trains. Programmable triangular and rectangular microwave waveforms are synthesized.

JW2A.52

High-Power Integrated Indium Phosphide Transmitter for Free Space Optical Communications, Hongwei Zhao¹, Sergio Pinna¹, Bowen Song¹, Ludovico Megalini¹, Simone Brunelli¹, Larry Coldren¹, Jonathan Klamkin¹; ¹*UC Santa Barbara, USA.* An integrated indium phosphide transmitter is demonstrated for free space optical communications. The transmitter tunes from 1521 nm to 1565 nm, demonstrates performance up to 5 Gbps, and includes an output high-power semiconductor optical amplifier.

JW2A.53

Photonic Microwave Frequency Identification System with a Thermally Tunable Silicon Microring, Xu Wang¹, Feng Zhou¹, Yuhua Yao¹, Xi Xiao², Jianji Dong¹, Xinliang Zhang¹; ¹*Wuhan National Lab for Optoelectronics, China;* ²*Wuhan Research Inst. of Posts & Telecommunications, State Key Lab of Optical Communication Technologies and Networks, China.* A photonic microwave frequency identification system with a thermally tunable silicon microring is proposed and experimentally demonstrated. The system has excellent performance of wide operating bandwidth of 1–30 GHz, high resolution of 375 MHz and multi-frequency measurement capability.

JW2A.54

Machine learning and Silicon Photonic Sensor for Complex Chemical Components Determination, Hui Zhang¹, Muhammad F. Karim¹, Shaonan Zheng^{1,2}, Hong Cai², Yuan Dong Gu², Shoushun Chen¹, Hao Yu³, Ai Qun Liu¹; ¹*School of Electrical and Electronic Engineering, Nanyang Technological Univ., Singapore 639798, Singapore;* ²*Inst. of Microelectronics, A*STAR, Singapore 117685, Singapore;* ³*Dept. of Electrical and Electronic Engineering, Southern Univ. of Science and Technology, China 518055, China.* We propose an integrated microring resonator sensing system based on Backward-Propagation Neural Networks (BPNN)-Adaboost algorithm to predict component fraction in binary liquid mixtures. A minimum absolute error of 0.0023 and mean squared error of 0.000345 is achieved by this training model.

JW2A.55

Integrated Photodiodes for On-chip Semiconductor Optical Amplifier gain measurement, Agnes A. Verdier^{1,2}, Alexandre Garreau¹, Karim Mekhazni¹, Carmen Gomez¹, Hélène Debrégeas¹, Hélène Carrère², Romain Brenot¹; ¹*III-V Lab, Nokia Bell Labs, France;* ²*LPCNO - INSA Toulouse, France.* Two photodiodes are integrated on a semiconductor optical amplifier (SOA) for on-chip measurement of the gain. Coupled waveguides drive fraction of light into photodiodes for gain calculation from photocurrents ratio. The method can easily be implemented in SOA inside photonic integrated circuits.

JW2A.56

Optical frequency comb generation and microwave synthesis with integrated cascaded silicon modulators, Si Qi Liu¹, Kan Wu¹, Linjie Zhou¹, Xu Xiao¹, Yiming Zhong¹, Jianping Chen¹; ¹*Shanghai Jiao Tong Univ., China.* An optical frequency comb with 15 lines, 5 GHz spacing and 6 dB flatness is generated by two cascaded silicon Mach-Zehnder modulator and phase modulator. We also demonstrate microwave synthesis using the generated frequency comb.

JW2A.57

Monolithic 1310nm 1Gb/s Optical Receiver with Schottky Photodiode in 40nm Bulk CMOS, Wouter Diels¹, Michel Steyaert¹, Filip Tavernier¹; ¹*Catholic University Leuven, Belgium.* We present an optical receiver with integrated Schottky photodiode in a standard 40nm bulk CMOS process, suitable for 1310nm communication. The low-noise analog front-end enables receiving 1Gb/s data rates at 3.3dBm sensitivity.

JW2A.58

Side-lobe Level Reduction in Two-dimensional Optical Phased Array Antennas, Julian L. Pitta¹, Ivan A. Aldaya^{2,3}, Octavio Santana², Luis Araujo², Paulo C. Dainese², Lucas Gabrielli¹; ¹*DECOM - FEEC, UNICAMP, Brazil;* ²*DEQ - IFGW, UNICAMP, Brazil;* ³*São João da Boa Vista, UNESP, Brazil.* We experimentally demonstrate that by arranging the array elements according to Fermat's spiral, the side lobe level of an 8-element SOI-array is reduced by 0.9 dB. Additional experiments show a 6.9 dB reduction for 64-elements.

JW2A.59

Broadband efficient coupled-cavity electro-optic modulators based on Q engineering for RF photonics applications, Hayk Gevorgyan¹, Anatol Khilo¹, Milos Popovic¹; ¹*Boston Univ., USA.* We propose a coupled-cavity electro-optic modulator, with tailored supermode Q-factors, for efficient RF-to-optical upconversion of broadband signals. It promises 20–30dB improvement over single-ring modulators and 10–20dB over the state-of-the-art for broadband modulation in high-Q cavities.

JW2A.60

Fully-Automated Grating Coupler Design Through Adjoint Optimization, Logan Su¹, Rahul Trivedi¹, Neil V. Saprà¹, Alexander Y. Piggott¹, Dries Vercrucysse^{1,2}, Jelena Vuckovic¹; ¹*Stanford, USA;* ²*Physics, KU Leuven, Belgium.* By leveraging adjoint optimization, we develop an efficient algorithm for designing 1D grating couplers for different functionalities without any human input and use it to design a fiber-to-chip blazed grating with under 0.18 dB loss.

JW2A.61

Increasing the Sensitivity-Bandwidth Product of Dual Resonant FSR Electro-Optic Modulators Using a Ring Resonator with Waveguide-Coupled Feedback, Yoo Seung Lee¹, Sang-Shin Lee², Chee Wei Wong¹; ¹UCLA, USA; ²Electronic Engineering, Kwangwoon Univ., South Korea. Dual resonant free-spectral-range RF-optic modulators using ring and feedback waveguide have been first proposed and theoretically analyzed to increase the sensitivity–bandwidth product. The sensitivity–bandwidth products are up to 2.5 times larger than conventional ring resonator modulator.

JW2A.62

A monolithic integrated InP few-mode transmitter, Zhao Song Li^{1,2}, Dan Lu¹, Yiming He^{1,2}, Xuliang Zhou¹, Lingjuan Zhao^{1,2}, Jiaoqing Pan^{1,2}; ¹Inst. of Semiconductors, CAS, China; ²College of Materials Science and Opto-Electronic Technology, Univ. of Chinese Academy of Sciences, China. A monolithic integrated InP few-mode transmitter comprising of two directly modulated lasers and a mode converter-multiplexer based on multimode interference coupler was designed and demonstrated. 2×10 Gbps two modes generation and modulation was realized.

JW2A.63

Optimizing Recirculating-Frequency-Shifter performance with Semiconductor Optical Amplifier gain assistance, Xiaoxi Wang¹, Shayan Mookherjee¹; ¹Electrical and Computer Engineering, Univ. of California, San Diego, USA. We show that nonlinear effects—including four wave mixing in chip-based semiconductor optical amplifier gain—impose limits to the wavelength spacing of combs in Recirculating-Frequency-Shifters (RFS), but can be mitigated by operating SOA in deeper saturation.

JW2A.64

Dispersion-engineered high quality lithium niobate microring resonators, Yang He¹, Hanxiao Liang¹, Rui Luo¹, Qiang Lin¹; ¹Univ. of Rochester, USA. We report dispersion-engineered lithium niobate microring resonators with optical Q above one million. In particular, we observed anomalous group-velocity dispersion for all three cavity mode families, with values around -0.5 ps²/m.

JW2A.65

An Efficient Approach to Characterize Low Loss Waveguides Using Bragg Gratings, Yi-Wen Hu¹, Yang Zhang¹, Pradip Gatikine¹, Joss Bland-Hawthorn², Sylvain Veilleux¹, Mario Dagenais¹; ¹Univ. of Maryland, USA; ²Univ. of Sydney, Australia. An efficient approach to measure waveguide loss is developed using record-high Q (>1×10⁶) Bragg grating cavities. Our demo sample's loss is evaluated as 0.24 dB/cm, whereas the measurement limit is estimated as 0.001 dB/cm.

JW2A.66

Low Crosstalk Bent Multimode Waveguide for On-chip Mode-Division Multiplexing Interconnects, Xinru Wu^{1,2}, Wen Zhou¹, Duanni Huang², Zeyu Zhang², Yi Wang¹, John E. Bowers², Hon K. Tsang¹; ¹The Chinese Univ. of Hong Kong, Hong Kong; ²Univ. of California, Santa Barbara, USA. A 90° multimode bent waveguide with a bending radius of 20 μm is proposed and experimentally demonstrated to have -23 dB crosstalk level over 60 nm optical bandwidth for the three supported quasi-TE modes.

JW2A.67

A Sub-Sampling Time-Interleaved Photonic Analog-to-Digital Converter Based on an Optoelectronic Oscillator, Huanfa Peng¹, Rui Guo¹, Huayang Du¹, Yongchi Xu¹, Cheng Zhang¹, Jingbiao Chen¹, Zhangyuan Chen¹; ¹Peking Univ., China. A sub-sampling time-interleaved photonic analog-to-digital converter based on an optoelectronic oscillator is demonstrated. A sampling rate of 20GS/s, analog bandwidth of 8GHz and ENOB of 4.6bits are realized with a test signal of 21.5GHz single-tone.

JW2A.68

Tagging Electronic ICs using Silicon Nitride Photonic Physical Unclonable Functions, Hongcheng Sun¹, Milad Alemohammad¹, Bryan Bosworth¹, A. B. Cooper¹, Mark A. Foster¹, Amy Foster¹; ¹Johns Hopkins Univ., USA. We demonstrate an on-chip photonic physical unclonable function using integrated evanescently coupled multimode spiral waveguides formed in silicon nitride with rich spectral features and validate it for use in an identification tagging application for electronic ICs.

JW2A.69

Pattern enhancement of high speed data modulation through saturating SOA-integrated EAM, Yi-Jen Chiu¹, Rih-Yu Chen¹; ¹National Sun Yat-Sen Univ., Taiwan. An optical modulation scheme by saturating SOA-integrated EAM is used for enhancing high-speed optical waveform. The saturation conditions on devices will have complementary carrier dynamics, thus leading to significant improvement of extinction ratio and also signal-to-noise ratio.

JW2A.70

Geometric Loss Reduction in Tight Bent Waveguides for Silicon Photonics, Makoto Nakai^{2,1}, Tsuyoshi Nomura¹, Sung-Won Chung², Hossein Hashemi²; ¹Toyota Central R&D Labs., INC, Japan; ²Viterbi School of Engineering, Univ. of Southern California, USA. A bent waveguide with a Clothoid shape whose width is adjusted along the curvature is demonstrated. The loss is less than 0.04 dB for a single S-shape bend with a bend radius of 1.6 μm.

JW2A.71

Superchannel Engineering with Microresonator Combs, Óskar B. Helgason¹, Attila Fulop¹, Jochen Schröder¹, Peter A. Andrekson¹, Andrew M. Weiner², Victor Torres-Company¹; ¹Dept. of Microtechnology and Nanoscience, Chalmers Univ. of Technology, Sweden; ²School of Electrical and Computer Engineering, Purdue Univ., USA. We study segmenting the available bandwidth of a WDM system into microcomb-driven superchannels. This solution improves the power per line while using a fraction of the pump power, making it potentially more favorable for integration.

JW2A.72

Fiber to Chip Fusion Splicing for Robust, Low Loss Optical Coupling, Juniyali Nauriyal¹, Jaime Cardenas¹, Meiting Song¹, Raymond Yu¹; ¹Univ. of Rochester, USA. We present a novel method of optical coupling to permanently attach a fiber to a chip using fusion splicing. As proof-of-concept, we achieve 3dB loss per facet between a silicon-nitride chip and a cleaved fiber.

JW2A.73

Photonic Microwave Channelization Based on Frequency Shifted Feedback Laser and Delayed Coherent Detection, Wenhui Hao¹, Yitang Dai¹, Feifei Yin¹, Yue Zhou¹, Jianqiang Li¹, Kun Xu¹; ¹Beijing Univ. of Posts and Telecoms, China. We present a microwave channelizer implemented by frequency shifted feedback laser and I/Q demodulation. The mixing of pulse and its own delay generates a tunable radio frequency local oscillation which can be used for channelization.

JW2A.74

Mode identification for ultra high-Q terahertz whispering-gallery modes, Dominik W. Vogt¹, Rainer Leonhardt¹; ¹Univ. of Auckland, New Zealand. We report on the identification of terahertz whispering-gallery modes using the phase information from coherent continuous-wave spectroscopy. The demonstrated WGM has an ultra high quality factor of 1.5×10⁴ at 0.62THz.

JW2A.75

Graphene Anti-dot Arrays with Self-aligned Gold Disks for Enhanced Excitation of Terahertz Surface Plasmons, Licheng Xiao¹, Xianglong Miao¹, Geng Li¹, Peter Q. Liu¹; ¹Electrical Engineering, Univ. at Buffalo, The State Univ. of New York, USA. A periodic graphene anti-dot array integrated with self-aligned gold disks for enhancing interactions between terahertz graphene surface plasmons and incident light is demonstrated. Experimental results show enhancement of the resonant transmission modulation by ~3 times.

JW2A.76

Efficient Design of Diffractive THz Lenses for Aberration Rectified Focusing via Modified Binary Search Algorithm, Sourangsu Banerji¹, Ashish Chanana¹, Hugo Condori¹, Ajay Nahata¹, Berardi Sensale-Rodriguez¹; ¹Univ. of Utah, USA. We experimentally demonstrate thin, error tolerant, and aberration corrected 3D printed diffractive 1D and 2D THz lenses for focusing THz beams with NA > 0.25 and an average efficiency greater than 75% (for all cases). Our work has relevance to THz lens design, and in general, THz imaging systems.

JW2A.77

Ultrashort Pulsed-Laser Fabrication of Silicon Moth-Eye Structures for Terahertz Anti-Reflection, Haruyuki Sakurai¹, Natsuki Nemoto¹, Kuniaki Konishi¹, Yuki Sakurai¹, Nobu Katayama¹, Tomotake Matsumura¹, Junji Yumoto¹, Makoto Kuwata-Gonokami¹; ¹The Univ. of Tokyo, Japan. We fabricate moth-eye anti-reflection structures for the terahertz region on high-resistivity silicon substrates by ultrashort pulsed-laser ablation. We demonstrate 1.4 times increased THz yield from Mg:LN by using the moth-eye structure as an output coupler.

JW2A.78

Discovery of Phase-matched Stimulated Polariton Scattering near 4 THz in Lithium Niobate, Yen-Chieh Huang¹, Yu Chung Chiu¹, Tsong Dong Wang³, Gang Zhao²; ¹National Tsing Hua Univ., Taiwan; ²Inst. of Heavy Ion Physics, China; ³Chung-Shan Inst. of Science and Technology, Taiwan. We report highly efficient stimulated polariton scattering near 4 THz with a parametric gain overtaking the well-known one near 1.8-THz in lithium niobate by using an off-axis parametric oscillator resonating the THz wave.

JW2A.79

Nano-electrode photomixer free from low-temperature-grown semiconductors for THz detection, Kiwon Moon¹, Il-Min Lee¹, Eui Su Lee¹, Kyung Hyun Park¹; ¹ETRI, South Korea. By manipulating local photocarrier dynamics by means of field enhancement and plasmonic enhanced absorption harnessed by nano-electrode, we demonstrate the photo-conductive detection of continuous-wave THz radiations without using low-temperature-grown optoelectronic materials.

JW2A.80

Generation of Intense Terahertz Pulses with Longitudinal Electric fields, Mizuho Mattoba¹, Natsuki Nemoto¹, Natsuki Kanda^{1,2}, Kuniaki Konishi¹, Junji Yumoto¹, Makoto Kuwata-Gonokami¹; ¹The Univ. of Tokyo, Japan; ²RIKEN Center for Advanced Photonics, Saitama, Japan. We demonstrate a method for converting broadband intense terahertz Gaussian beams into Hermite-Gaussian 01 beams, based on a specially designed prism. The generated longitudinal electric fields by focusing them were observed to be 36 kV/cm.

JW2A.81

High-field Terahertz Pulses Generated in an HMQ-TMS Organic Crystal Pumped by an Amplified Ytterbium Laser, Andrea Rovere¹, Young-Gyun Jeong¹, Riccardo Piccoli¹, Seung-Heon Lee², Seung-Chul Lee², O-Pil Kwon², Mojca Jazbinssek³, Roberto Morandotti^{1,4}, Luca Razzari¹; ¹INRS-Energie Matériaux et Telecom, Canada; ²Ajou Univ., South Korea; ³Zurich Univ. of Applied Science, Switzerland; ⁴National Research Univ. of Information Technologies, Russia. High-peak-electric-field THz pulses (>200 kV/cm) can be efficiently generated in a recently developed organic crystal pumped by a femtosecond ytterbium laser in a collinear configuration.

JW2A.82

Ferroelectric Metasurfaces for THz Wave Manipulation, Jingyul Tian^{1,2}, Fredrik Laurell¹, Valdas Pasiskevicius¹, Min Qiu¹, Hoon Jang¹; ¹Dept. of Applied Physics, Royal Inst. of Technology, KTH, Sweden; ²College of Optical Science and Engineering, Zhejiang Univ., China. We propose ferroelectric metasurfaces based on KTiOPO₄ and demonstrate the fabrication procedures. It will provide a versatile platform for THz wave manipulation and open up new possibilities to monolithically combine it with THz generation.

JW2A.83

Anti-reflection coating design for metallic terahertz metamaterials, Matteo Pancaldi^{2,1}, Ryan Freeman³, Matthias Hudl¹, Matthias C. Hoffmann⁴, Sergei Urazhdin³, Paolo Vavassori², Stefano Bonetti¹; ¹Stockholm Univ., Sweden; ²CIC nanoGUNE, Spain; ³Emory Univ., USA; ⁴SLAC National Accelerator Lab, USA. We demonstrate a silicon-based, single-layer anti-reflection coating that suppresses the reflectivity of metals at near-infrared frequencies, enabling optical probing of nanoscale structures embedded in highly reflective surroundings, paving the way for table-top studies on such systems.

JW2A.84

Terahertz Antireflection Metasurfaces and Application in Narrow Bandpass Filters, Hou-Tong Chen¹, Chun-Chieh Chang¹, Li Huang², John Nogan³; ¹Los Alamos National Lab, USA; ²Harbin Inst. of Technology, China; ³Sandia National Labs, USA. Here we demonstrate bilayer metasurfaces for narrow, dual and broadband terahertz antireflection on a silicon surface. By stacking multiple metasurfaces, we realize narrow bandpass terahertz filters with an extremely clean background.

JW2A.85

Coupled Microring Resonator Lattices as Periodically-Driven Floquet Topological Insulators, Shirin Afzal¹, Vien Van¹; ¹Electrical and Computer Engineering, Univ. of Alberta, Canada. We show that 2D coupled microring lattices represent systems with periodic Hamiltonian and are thus natural structures for realizing photonic Floquet topological insulators. Their topological equivalence to arrays of periodically-coupled waveguides is also established.

JW2A.86

Dispersion engineering with plasmonic nanostructures for enhanced surface plasmon resonance sensing, P. Arora¹, Eliran Talker¹, Noa Mazurski¹, Uriel Levy¹; ¹Dept. of Applied Physics, The Hebrew Univ. of Jerusalem, Israel. We experimentally demonstrate plasmonic resonance narrowing via dispersion engineering using plasmonic nanogratings placed on top of thin metal coated prism. The enhancement in Q factor, combined with strong field localization is attractive for sensing applications.

JW2A.87

Lossless Edge States Protected by PT-Symmetric Phase, Xiang Ni^{1,2}, Daria Smirnova², Alexander N. Poddubny^{3,4}, Daniel Leykam⁵, Yidong Chong⁵, Alexander Khanikaev^{2,1}; ¹Graduate Center of CUNY, USA; ²City College of New York, USA; ³Australian National Univ., Australia; ⁴ITMO Univ., Russia; ⁵Nanyang Technological Univ., Singapore. Parity-time (PT) symmetric interfaces between amplifying and lossy crystals support dissipationless edge states exhibiting gapless spectra in complex band structure if exceptional points (EPs) of edge states exist, which is verified by rigorous full-wave simulations in PT-symmetric photonic graphene

JW2A.88

Billion-times Enhanced 3rd Order Nonlinear Susceptibility Based on Non-resonant Mesoscopic Crystal, Taeyong Chang¹, Jonghwa Shin¹; ¹KAIST, South Korea. We propose a broadband enhancement scheme of optical nonlinearity with mesoscopically structured material. The one billion enhancement is larger than any previous result. The nonlinear susceptibility tensor components can be individually tuned and 18 different crystal classes can be realized.

JW2A.89

Ghost Resonance in Light Scattering, Sanjay Debnath¹, Evgenii E. Narimanov¹; ¹Purdue Univ., USA. We demonstrate the presence of ghost resonance in optical scattering from dielectric systems, and develop the theoretical description of this effect.

JW2A.90

Temporal Metamaterials with Non-Foster Networks, Yasaman Kiasat¹, Victor Pacheo-Pena¹, Brian Edwards¹, Nader Eng-heta¹; ¹Univ. of Pennsylvania, USA. We theoretically explore instantaneous time mirrors (ITM) for real-time amplification of electromagnetic wave using non-Foster networks to engineer the required dispersion. Our analytical and numerical results demonstrate various salient features of this phenomenon.

JW2A.91

Hyperbolic Metamaterials for Quantum Dot Emission Enhancement- Effects of Unit Cell Thickness and Light Outcoupling, Akash Kannegulla¹, Bo Wu¹, Ye Liu¹, Yi-Chieh Wang¹, Li-Jing Cheng¹; ¹Oregon State Univ., USA. We investigated how the unit cell thickness of multilayer hyperbolic metamaterials affects the enhancement of quantum dot emission. A facile outcoupling approach was demonstrated to improve the emission using a large-area nanoparticle-based photonic crystal.

JW2A.92

Slow-light Si-wire Waveguide with Metamaterial, Satoshi Yamasaki¹, Tomohiro Amemiya¹, Zhichen Gu¹, Junichi Suzuki¹, Keisuke Masuda¹, Hibiki Kagami¹, Nobu Nishiyama¹, Shigehisa Arai¹; ¹Tokyo Inst. of Technology, Japan. We propose a novel slow-light Si-wire waveguide using metamaterials, which can be easily integrated with other Si photonics devices, and the group index of more than 40 was obtained in both theoretical and experimental investigations.

JW2A.93

Free-space Optical Mach-Zehnder Modulator based on Two Cascaded Metasurfaces, Nasim Mohammadi Estakhri¹, Nader Eng-heta¹; ¹Univ. of Pennsylvania, USA. An approach to realize Mach-Zehnder type modulators in free-space is presented. Modulation is based on the relative distance between two parallel gradient metasurfaces. We numerically study the device performance and discuss its potential applications.

JW2A.94

Control of Electric and Magnetic Resonances in Nanoparticle Metasurfaces, Viktoriia Babicheva¹, Andrey Evlyukhin^{2,3}; ¹College of Optical Sciences, Univ. of Arizona, USA; ²Laser Zentrum Hannover e.V., Germany; ³ITMO Univ., Russia. We study collective multipole resonances in plasmonic and dielectric nanoparticle arrays. Because of the lattice multipole resonance overlap, the transmission and reflection can be tuned in a given spectral range choosing an appropriate array periodicity.

JW2A.95

Plasmonic Tuning of Effective Phase Transition Temperature and Electrical Conductivity, James Frame¹, Wanaka Kubo^{2,3}, Xu Fang¹; ¹Dept. of Electronics and Computer Science, Univ. of Southampton, UK; ²Dept. of Electrical and Electronic Engineering, Tokyo Univ. of Agriculture and Technology, Japan; ³Metamaterials Lab, RIKEN, Japan. Thermo-plasmonic engineering at the nanoscale can control material properties at the macroscopic scale. We demonstrate utilising plasmonic resonance to tune the effective phase transition temperature and electrical conductivity of vanadium oxide thin films

JW2A.96

Engineering Optical Emission of Sub-diffraction Hyperbolic Metamaterial Resonators, Kaijun Feng¹, Galen Harden¹, Deborah Sivco², Anthony Hoffman¹; ¹Univ. of Notre Dame, USA; ²Princeton Univ., USA. We develop an electrodynamic model for sub-diffraction hyperbolic metamaterial resonators using the modified long wave approximation and verify it via experiment and simulations. We investigate engineering the resonator Q, photon loss and far-field pattern.

JW2A.97

A new method to obtain the phase for designing highly efficient metasurface devices: Local Phase Method, Liyi Hsu¹, Matthieu Dupre¹, Abdoulaye Ndao¹, Boubacar Kante¹; ¹Electrical and Computer Engineering, Univ. of California San Diego, USA. Recently, metasurfaces have attracted significant attention. However, the approach assumes that neighboring elements are identical. We propose a method accounting for near-field coupling with different neighbors. The proposed local phase method paves the way to highly efficient metasurface devices.

JW2A.98

Second Harmonic Generation in Geometric-Phase Resonant Dielectric Metasurfaces, Jonathan Bar-David¹, Uriel Levy¹; ¹Hebrew Univ. of Jerusalem, Israel. We explore the second harmonic generation from resonant dielectric metasurfaces. We experimentally demonstrate that second harmonic radiation intensity and emission patterns can be controlled by metasurface structure and meta-atom symmetries.

JW2A.99

Complex Birefringence with Dielectric Metasurfaces for Non-conventional Polarisation Control, Shaun Lung¹, Kai Wang¹, Andrey A. Sukhorukov¹; ¹Nonlinear Physics Centre, Research School of Physics and Engineering, The Australian National Univ., Australia. We establish that complex birefringence can be efficiently realised with all-dielectric metasurfaces without utilising material losses, enabling new regimes of polarisation control for enhanced measurements and unconventional interference for classical and quantum light.

JW2A.100

Double-Layer USRRs for a Thin Terahertz-Wave Phase Shifter with High Transmission, Zhengli Han¹, Seigo Ohno², Yu Tokizane¹, Kouji Nawata¹, Takashi Notake¹, Yuma Takida¹, Hiroaki Minamide¹; ¹Riken, Japan; ²Tohoku Univ., Japan. Double-layer un-split ring resonators (USRRs) with film metamaterial was developed for a thin THz-wave phase shifter (48µm-thick) with high transmission and polarization independent properties. The film size of 5cm×5cm enables large THz optical components.

JW2A.101

Metasurfaces with wavelength-controlled functions, Zhujun Shi¹, Mohammadreza Khorasaninejad¹, Yao-Wei Huang¹, Charles Roques-Carmes¹, Vyshakh Sanjeev¹, Alexander Zhu¹, Wei-Ting Chen¹, Michele Tamagnone¹, Kundan Chaudhary¹, Cheng-Wei Qiu², Federico Capasso¹; ¹Harvard Univ., USA; ²National Univ. of Singapore, Singapore. We demonstrate single-layer metasurfaces with controllable multi-wavelength functions. A multiwavelength achromatic metalens for red, yellow, green and blue light, and metasurfaces generating focused beams with different orbital angular momentum states are designed and fabricated.

JW2A.102

The Chirality of Exceptional Points – An Experimental Investigation, Samlan C.T.¹, Nirmal K. Viswanathan¹; ¹Univ. of Hyderabad, India. Behavior of exceptional points (EPs) in biaxial crystal is experimentally investigated, as the system is taken from absorption-dominated regime to chirality-dominated, using conoscopic Stokes polarimetry. The resulting chirality-mediated helical trajectory of the EP is reported.

JW2A.103

Position Selective Beam Shaping in Mid-Infrared Regime by All-Dielectric Metasurfaces, Boris Desiatov¹, Marko Loncar¹; ¹Harvard, USA. We demonstrate the design, fabrication and experimental characterization of a dielectric metasurfaces acting as a position selective computer generated hologram operating at mid infrared wavelength of 4.5 micron.

JW2A.104

Difference-Frequency Generation and Frequency Up-Conversion with Polaritonic Nonlinear Metasurfaces, Yingnan Liu¹, Jongwon Lee², Stephen March¹, Nishant Nookala¹, Daniele Palaferri¹, Omri Wolf¹, Igal Brener³, Seth Bank¹, Mikhail A. Belkin¹; ¹The Univ. of Texas at Austin, USA; ²School of Electrical and Computer Engineering, Ulsan National Inst. of Science and Technology, South Korea; ³Sandia National Labs, USA. We report difference-frequency generation in nonlinear metasurfaces based on coupling of electromagnetic nanocavity modes with intersubband nonlinearities in semiconductor heterostructures. Nonlinear susceptibility of $2.7 \times 10^5 \text{ pm/V}$ and the conversion efficiency of 0.13% were measured.

JW2A.105

Influence of geometry on speed of phase-change in GST-based nanorods, Andrea Aboujaoude¹, Joshua Burrow¹, Josh Hendrickson², Imad Agha¹, Andrew Sarangan¹, Joseph W. Haus¹; ¹Univ. of Dayton, USA; ²Air Force Research Lab, USA. We investigate how patterning phase-change materials into nanorods influences the speed of phase-change through a modification of temporal dynamics of heating/cooling. It is shown that a 10-fold improvement over bulk geometry can be achieved.

JW2A.106

Mode hybridization in lattice induced transparency for polarization-insensitive THz metasurfaces, Joshua Burrow¹, Riad Yahiaoui², Andrew Sarangan¹, Jay Mathews¹, Imad Agha¹, Thomas Searles²; ¹Univ. of Dayton, USA; ²Dept. of Physics & Astronomy, Howard Univ., USA. We demonstrate multiple lattice-induced transparencies by decoupling the first-order lattice mode achieving a measured Q factor of 40 and support measurements with numerical calculations revealing bright dipole resonances.

JW2A.107

Revisitation of ZnO random lasers toward optical security, Seung Ho Choi¹, Young Jin Yoo², Jung Woo Leem¹, Jong Heon Lee², Young Min Song², Young L. Kim¹; ¹Purdue Univ., USA; ²GIIST, South Korea. Random lasing with localized modes, governed by the inherent randomness and uncertainty, are genuinely stochastic with high entropy. Such optical chaos generated from ZnO random lasers could be used for healthcare encryption and security applications.

JW2A.108

Pseudocanalization Regime for Surface Waves, Taavi Repän¹, Andrey Novitsky¹, Morten Willatzen¹, Andrei V. Lavrinenko¹; ¹DTU Fotonik, Technical Univ. of Denmark, Denmark. Magnetic properties can be used to reverse phase advancing in the pseudocanalization regime of hyperbolic metamaterials. However, practical implementations of required μ -negative media are challenging. Here we reveal analogous effect for the electromagnetic surface waves in non-magnetic materials.

JW2A.109

Dynamically Tunable, Vanadium Dioxide Huygens Source Metasurfaces, Yaping Ji¹, Adam Ollanik¹, Mason Belue², Matthew D. Escarra¹; ¹Tulane Univ., USA; ²Univ. of Arkansas, USA. An active vanadium dioxide Huygens source metasurface offering >85% near-infrared transmittance modulation over the first 10% of the metal-insulator transition is demonstrated. The fabricated vanadium dioxide Huygens source nanoantennas exhibit experimental results similar to the model.

JW2A.110

Multimodal Parity Conversion in Supersymmetric Optical Potentials for Controlling Random Waves, Sunkyu Yu¹, Xianji Piao¹, Choonlae Cho¹, Namkyoo Park¹; ¹Seoul National Univ., South Korea. Utilizing isospectral and global parity conversion in supersymmetric transformation, we demonstrate multimodal switching with high throughput and isolation. We show that the collective multimode manipulation in supersymmetric harmonic potentials allows random wave switching.

JW2A.111

Metagrating holograms with ultra-wide incident angle tolerances and high diffraction efficiencies, Zi-Lan Deng¹, Junhong Deng², Guo Ping Wang³, Xing Cheng², Guixin Li², Xiangping Li¹; ¹Jinan Univ., China; ²Southern Univ. of Science and Technology, China; ³Shenzhen Univ., China. High-performance meta-holograms are experimentally demonstrated in a near-unity-efficiency metagrating platform without any size or shape variation of the meta-atoms, which is robust against large incident angles, and sustains high diffraction efficiency in a broadband.

JW2A.112

Toroidal Response of Asymmetric Metasurfaces with Multiple High Q-Factor Resonances, Riad Yahiaoui¹, Sirak M. Mekonen¹, Joshua A. Burrow², Pheona Williams¹, Andrew Sarangan², Imad Agha², Jay Mathews², Thomas Searles¹; ¹Howard Univ., USA; ²Univ. of Dayton, USA. We report numerical simulations and experimental investigations of a planar asymmetric terahertz metamaterials exhibiting toroidal response. By inducing symmetry breaking, multiple Fano-like resonances arise in 0.1-2.5 THz frequency range with extremely high Q-factor.

JW2A.113

Manipulation Of The Propagation Of Light In Tunable Nonlinear Bragg Mirrors With Embedded Quantum Wells, Evgeny Sedov^{1,2}, Irina Sedova², Igor Chestnov², Sergey Arakelian², Alexey Kavokin^{1,3}; ¹Univ. of Southampton, UK; ²Vladimir State Univ., Russia; ³St. Petersburg State Univ., Russia. The specially designed nonlinear semiconductor structure with embedded quantum wells possesses a tunable hyperbolic dispersion. We revealed dynamical regimes for localized polariton wave packets resulting from competition of the hyperbolic dispersion and the repulsive nonlinearity

JW2A.114

A Novel Photonic Structure with a Nodal Line of Dirac Cones and a Photonic Topological Insulator that Emerges from it, Ran A. Gladstein Gladstone¹, Gennady Shvets¹; ¹Cornell Univ., USA. We propose a 2D photonic structure with a nodal line of Dirac cones. We then perturb the structure to open a band gap and reveal topologically protected edge states that also support localized slow light.

JW2A.115

X-ray created metamaterials: applications to metal-free structural colors with full chromaticity spectrum and 80 nm spatial resolution., Marcella Bonifazi¹, Valerio Mazzone¹, Andrea Fratolocchi¹; ¹King Abdullah Univ of Sci & Technology, Italy. We created new types of metamaterials by hard X-rays possessing high fluency. We discuss applications in structural colors that show full spectrum of Cyan, Yellow, Magenta, Black (CYMK), realized in transparent dielectrics with 80 nm resolution.

JW2A.116

In-situ Visualization of Multiple Filament Competition Dynamic of Femtosecond Laser, Qi PengFei¹; ¹Nankai Univ., China. The visualization of multiple filamentation competition has been realized performing the three-photon fluorescence. The random changes of multiple filamentation are first observed directly and visually, which can be well explained by a simplified model.

JW2A.117

Laser Absorption and Scaling Behavior in Powder Bed Fusion Additive Manufacturing of Metals, Jianchao Ye¹, Alexander M. Rubenchik¹, Michael F. Crumb¹, Gabe Guss¹, Manyalibo J. Matthews¹; ¹Lawrence Livermore National Lab, USA. The effect of powder bed thickness and laser beam diameter on laser absorptivity is studied using micro-calorimetry. Dimensionless analysis is utilized to consolidate multiple influence factors into a single parameter for comparison between materials and laser parameters.

JW2A.118

Measuring quantum efficiency and background absorption of an Ytterbium-doped ZBLAN fiber, Mostafa Peysokhan¹, Behnam Abaie¹, Esmaeil Mobini¹, Saeid Rostami¹, Arash Mafi¹; ¹Univ. of New Mexico, USA. Laser-induced temperature modulation spectrum (LITMoS) test is performed for an Ytterbium-doped ZBLAN fiber. The quantum efficiency and the background absorption are extracted from the cooling efficiency curve of the LITMoS test.

JW2A.119

Raman Nonlinearity Influence On Temporal Pulse Dynamics And Supercontinuum Generation Under Filamentation In YAG Crystal, Kirill Lvov^{1,2}, Sergey Y. Stremoukhov^{1,2}, Fedor Potemkin¹; ¹M.V. Lomonosov Moscow State Univ., Russia; ²National Research Center "Kurchatov Inst.", Russia. We report an asymmetric Raman-initiated temporal splitting and spectrum transformation of intense 200 fs laser pulses with normal (1.24 μm) and anomalous (1.9 μm) group velocity dispersion in YAG crystal.

JW2A.120

Librations in Water Nanodroplets Confined in DOPC Reverse Micelles, Giulia Folpini¹, Torsten Siebert^{1,4}, Michael Woerner¹, Thomas Elsaesser¹, Stephane Abel², Damien Laage^{3,5}; ¹Max-Born-Institut fuer Nichtlineare Optik und Kurzzeitspektroskopie, Germany; ²ZBC, Universite Paris-Saclay, France; ³Departement de Chemie, Ecole Normale Supérieure, France; ⁴Dept. of Physics, Freie Universität Berlin, Germany; ⁵Sorbonne Université, France. We study the librational absorption spectra of water nanodroplets in reverse micelles by time-domain THz spectroscopy: an additional feature at 830 cm^{-1} is assigned by molecular dynamics simulations to water molecules bonded to phosphate heads.

JW2A.121

Ultrafast pulse generation in the mid-infrared via modulated emissivity, Yuzhe Xiao¹, Nicholas Charipar², Alberto Pique², Mikhail Kats¹; ¹Univ. of Wisconsin-Madison, USA; ²Naval Research Lab, USA. We demonstrate that mid-infrared pulses can be generated by fast emissivity modulation of semiconductors. Ultrafast visible-frequency pulses were used to pump intrinsic unpatterned silicon and gallium arsenide, resulting in nanosecond-scale thermally emitted pulses.

JW2A.122

Calculating Terahertz Near-fields in the Scanning Tunneling Microscope Junction, Peter H. Nguyen¹, Vedran Jelic¹, Graham Hornig¹, Rathje Christopher², Frank A. Hegmann¹; ¹Univ. of Alberta, Canada; ²4th Physical Inst., Univ. of Göttingen, Germany. A finite-element-method model of the terahertz scanning tunneling microscope experiment is built to simulate the propagation and coupling of THz pulses to the STM junction. Simulations are compared with analytical calculations.

JW2A.123

Optical response of crystals with effective models, Rodrigo A. Muniz^{1,2}, Jin-Luo Cheng³, John E. Sipe¹, Mackillo Kira²; ¹Univ. of Toronto, Canada; ²Univ. of Michigan, USA; ³Changchun Inst. of Optics, fine Mechanics and Physics, Chinese Academy of Sciences, China. We present a scheme of using effective models to efficiently compute optical properties of crystals. The dynamics equations depend only on gauge-invariant quantities, and we avoid introducing a position operator.

JW2A.124

Single Exciton Optical Gain in CsPbBr₃ Nanocrystals Uncovered by 2D Electronic Spectroscopy, Wei Zhao¹, Zhengyuan Qin², Chunfeng Zhang², Xingcan Dai¹, Min Xiao^{3,2}; ¹Dept. of Physics, Tsinghua Univ., China; ²National Lab of Solid State Microstructures, School of Physics, and Collaborative Innovation Center of Advanced Microstructures, Nanjing Univ., China; ³Dept. of Physics, Univ. of Arkansas, USA. We study the gain mechanism of CsPbBr₃ colloidal nanocrystals using 2D electronic spectroscopy. Optical gain in single-exciton regime has been observed in fluence-dependent measurements, indicating the promising potential for applying perovskite nanocrystals in laser technology.

JW2A.125

Radiative and Nonradiative Recombination Coefficients of InAs/InAlAs Core-shell Nanowires, Xinxin Li^{1,2}, Kailing Zhang^{1,2}, Fatima Toor^{2,3}, John Prineas^{1,2}, Julian Treu⁴, Lukas Stampfer⁴, Gregor Koblmüller⁴, ¹Physics and Astronomy, Univ. of Iowa, USA; ²Optical Science and Technology Center, Univ. of Iowa, USA; ³Electrical and Computer Engineering, Univ. of Iowa, USA; ⁴Physik Dept., Walter Schottky Institut of Technische Universität München, Germany. Ultrafast and external quantum efficiency measurements were performed on InAs/InAlAs core-shell nanowires. Rates of different recombination mechanisms were determined, and the carrier densities ranges at which each dominates, an important consideration for design of devices

JW2A.126

Plasmon-Induced Hot Electron Transfer in Ag-CsPbBr₃ Hybrid Nanocrystals, Xinyu Huang¹, Hongbo Li², Chunfeng Zhang¹, Zhenda Lu², Min Xiao^{1,3}, ¹National Lab of Solid State Microstructures, School of Physics, and Collaborative Innovation Center of Advanced Microstructures, Nanjing Univ., China; ²National Lab of Solid State Microstructures, College of Engineering and Applied Sciences, Collaborative Innovation Center of Advanced Microstructures and Research Center for Environmental Nanotechnology (ReCENT), Nanjing Univ., China; ³Dept. of Physics, Univ. of Arkansas, USA. We demonstrate plasmon-induced hot-electron transfer in Ag-CsPbBr₃ hybrid nanocrystals. Using transient absorption spectroscopy, we have observed the highly efficient transfer hot electrons from metal Ag to semiconductor CsPbBr₃ in a timescale of sub-100 fs.

JW2A.127

Ultrafast Optical Response Due to Nonlocal Interaction between Light and Excitons in ZnO Thin Films, Masayoshi Ichimiya^{1,3}, Takuya Matsuda², Takashi Kinoshita², Takuya Takahashi¹, Masaaki Nakayama⁴, Hajime Ishihara^{1,2}, Masaaki Ashida¹, ¹Osaka Univ., Japan; ²Osaka Prefecture Univ., Japan; ³The Univ. of Shiga Prefecture, Japan; ⁴Osaka City Univ., Japan. Ultrafast optical response in ZnO thin films has been investigated by the transient grating method. Sub-picosecond radiative recombination caused by radiation-induced interaction between two multipole-type excitons was observed between nano- and micro-scale.

JW2A.128

Transient Electronic Anisotropy in Normal State of Overdoped NaFe_{1-x}Co_xAs Superconductors, Shenghua Liu¹, Chunfeng Zhang¹, Xiaoyong Wang¹, Min Xiao¹, ¹Nanjing Univ., China. We observe anisotropic electronic response in the tetragonal phase of NaFe_{1-x}Co_xAs superconductors by using polarization-dependent pump-probe spectroscopy, which can be scribed as a result of nematic fluctuation driven by an orbital order.

JW2A.129

Carrier Relaxation Dynamics of InGaN/GaN Dot-in-Nanowires, Heather George¹, Yong-Ho Ra², Zetian Mi^{1,2}, Theodore B. Norris¹, ¹EECS, Univ. of Michigan, USA; ²Electrical and Computer Engineering, McGill Univ., Canada. Carrier relaxation was investigated for InGaN/GaN dot-in-nanowires using femtosecond pump-probe in transmission 400nm pump/white light probe. Though bright emitters, the localization of states contributes to relaxation rates which are faster than expected.

JW2A.130

Ultrashort molecular dynamics and flame temperature measurements by hybrid fs/ps CARS spectroscopy, Xia Yuanqin¹, Zhibin Zhang¹, Sheng Zhang¹, Yang Zhao¹, Guozhong Hou¹, ¹Harbin Inst. of Technology, China. We research the molecular dynamics by hybrid femtosecond/picosecond coherent anti-Stokes Raman scattering (fs/ps CARS), and utilize the single-laser-shot CPP (chirped Probe Pulse) fs CARS signals of N₂ to get the temperature information.

JW2A.131

Terahertz Carrier Dynamics in Epitaxial Layered ε-InSe, Wei Lu¹, Zhibin Yang^{2,3}, Jianhuan Hao^{2,3}, Dong Sun^{1,4}, ¹International Center for Quantum Materials, School of Physics, Peking Univ., China; ²Dept. of Applied Physics, The Hong Kong Polytechnic Univ., Hung Hom, China; ³The Hong Kong Polytechnic Univ. Shenzhen Research Inst., China; ⁴Collaborative Innovation Center of Quantum Matter, China. Relaxation of optically excited quasiparticles in ε-InSe is studied by employing ultrafast optical-pump THz-probe spectroscopy. The excited quasiparticles enhance the THz absorption and relax by three processes which occur in few to hundreds of picoseconds.

JW2A.132

Natural Lineshapes by Projecting Multidimensional Spectra, Geoffrey M. Diederich¹, Mark E. Siemens¹, ¹The Univ. of Denver, USA. We take one-dimensional data along arbitrary directions in the t-t plane of a multidimensional coherent spectroscopy experiment to obtain projections in the w₁-w₂ plane, allowing faster data collection and insight into the meaning of lineshapes.

JW2A.133

Dynamic Terahertz Response in the Dirac Semimetal Cd₃As₂ Induced by Ultrafast Optical Excitation, Wei Lu¹, Jiwei Ling², Faxian Xiu², Dong Sun^{1,3}, ¹International Center for Quantum Materials, School of Physics, Peking Univ., China; ²State Key Lab of Surface Physics and Dept. of Physics, Fudan Univ., China; ³Collaborative Innovation Center of Quantum Matter, China. Hot electron relaxation and coupling in Cd₃As₂ is studied by employing ultrafast time-domain THz spectroscopy. The excited carriers enhance the absorption of THz and relax in ps-time scales, the cooling rules consistent with mid-IR spectroscopy.

JW2A.134

Ultrafast Time-Resolved Photocurrent Measurement of Carrier Escape Dynamics in Anisotropic ReS₂, Hyemin Bae¹, Sangwan Sim^{1,2}, Taeyoung Kim¹, Doeon Lee¹, Dong-Hwi Kim^{2,3}, Gwangmook Kim¹, Wooyoung Shim¹, Moon-Ho Jo^{3,2}, Hyunyoung Choi¹, ¹Yonsei Univ., South Korea; ²Inst. for Basic Science, South Korea; ³POSTECH, South Korea. We report the two-pulse time-resolved photocurrent measurements in a group VII ReS₂. The absence of bias dependence on the photocurrent recovery implies that the escape time of photoexcited carrier is much faster than electron-hole recombination.

JW2A.135

The Influence of hBN on the Pump-dependent Time-evolution of Monolayer Photoluminescence in WSe₂, Jan Kuhnert¹, Lorenz M. Schneider¹, Sina Lippert¹, Dylan Renaud¹, Obafunso Ajayi², Young Duck Kim², Wolfram Heimbrot¹, James Hone², Arash Rahimi-Iman¹, ¹Faculty of Physics and Material Science Center, Philipps Universität Marburg, Germany; ²Dept. of Mechanical Engineering, Columbia Univ., USA. We present the influence of hBN buffer layers on the power-dependent time-evolution of the photoluminescence in monolayer WSe₂ on different substrates. An even greater influence is observed when the excitonic Mott transition regime is reached.

JW2A.136

Exciton Dynamics in WSe₂ Monolayers for Different Stacking Schemes Involving h-BN, Lorenz M. Schneider¹, Jan Kuhnert¹, Dylan Renaud¹, Saleh Firoozabadi¹, Obafunso Ajayi², Young Duck Kim², Wolfram Heimbrot¹, James Hone², Arash Rahimi-Iman¹, ¹Philipps-Universität Marburg, Germany; ²Dept. of Mechanical Engineering, Columbia Univ., USA. We present a comparison of tungsten-diselenide monolayers in different stacking configurations with hBN and MoSe₂. A pronounced red-shift is observed when the monolayer is supported or encapsulated by hBN. Furthermore, the excitonic annihilation rate changes.

JW2A.137

The H2020 Project CLONETS: Clock Services over Optical-fibre Networks in Europe, Josef Vojtech¹, Jan Radil¹, Vladimir Smotlacha¹, Radek Velc¹, Przemyslaw Krehlik², Lukasz Sliwczynski², Mauro Campanella³, Davide Calonico⁴, Cecilia Clivati⁴, Filippo Levi⁴, Ondrej Cip⁵, Simon Rerucha⁵, Ronald Holzwarth⁶, Maurice Lessing⁶, Sarah Saint-Jalm⁶, Fabiola Camargo⁷, Bruno Desruelle⁷, Jean Lautier-Gaud⁷, Elizabeth Laier English⁸, Jochen Kronjäger⁸, Peter Whibberley⁸, Eva Bookjans⁹, Paul-Eric Pottie⁹, Philip Tuckey⁹, Tomáš Müller¹⁰, Jiri Stefl¹⁰, Pawel Nogas¹¹, Robert Urbaniak¹¹, Artur Binczewski¹², Wojbor Bogacki¹², Krzysztof Turza¹², ¹CESNET, Czechia; ²AGH Univ. of Science and Technology, Poland; ³Consortium GARR, Italy; ⁴Istituto Nazionale di Ricerca Metrologica, Italy; ⁵Inst. of Scientific Instruments of the ASCR, v.v.i. (IS), Czechia; ⁶Menlo Systems, Germany; ⁷Muquans, France; ⁸National Physical Lab, UK; ⁹LNE-SYRTE, Observatoire de Paris, PSL Research Univ., CNRS, Sorbonne Université, France; ¹⁰OPTOKON, a.s., Czechia; ¹¹Piktime Systems sp. z o.o., Poland; ¹²Poznan Supercomputing and Networking Center, Poland. Time and frequency transfer based on optical fiber links techniques have demonstrated excellent performances. CLONETS is EU project intended to accelerate transfer of related technologies, in order to prepare deployment of technology for sustainable network providing high-performance clock services.

JW2A.138

Commissioning of a Fully-Automated, Pulsed Optical Timing Distribution System at Dalian Coherent Light Source, Haynes P. Cheng¹, Kemal Shafak¹, Anan Dai¹, Johann Derksen¹, Andrej Berlin¹, Erwin Cano¹, Zhichao Chen², Hongli Ding², Dariush Forouher¹, Zhigang He², Xiaoping Liu³, Wahid Nasimzade⁴, Mathias Neuhaus¹, Philipp Schiepel¹, Eduard Seibel¹, Yuhuan Tian², Bo Liu³, Guorong Wu², Franz X. Kaertner^{4,5}, ¹Cycle GmbH, Germany; ²State Key Lab of Molecular Reaction Dynamics, Dalian Inst. of Chemical Physics, China; ³Shanghai Inst. of Applied Physics (SINAP), China; ⁴Deutsches Elektronen Synchrotron (DESY), Germany; ⁵Center for Free Electron Laser Science (CFEL), Germany. We present latest results from the commissioning of China's first multi-link pulse-based optical timing distribution system (TDS). A fully-automated control system, and polarization-maintaining fiber links enable reliable, 24/7 operation of the TDS at user's facility.

JW2A.139

Sub-Shot-Noise Absorption Imaging with a Hybrid Detection Scheme, Javier Sabines-Chesterking¹, Alex McMillan¹, Paul-Antoine Moreau², Sebastian Knauer¹, Eric Johnston¹, Siddarth Joshi^{1,3}, John Rarity¹, Jonathan Matthews¹, ¹Univ. of Bristol, UK; ²Univ. of Glasgow, UK; ³Austrian Academy of Sciences, Austria. We demonstrate a scanning microscopy system for high resolution, sub-shot-noise absorption imaging. A genuine quantum advantage of factor 1.66 in information gained per probe photon, relative to an ideal classical measurement, is demonstrated.

JW2A.140

A Step Forward the Determination of the Anomalous Dispersion on the Er³⁺ in the Tellurite Glass, Luis H. Andrade¹, Ana Paula Langaro¹, Ana Kely Rufino¹, Alex Cesar Pereira Rocha¹, Claudio Y. Morassuti¹, Junior R. Silva¹, Sandro Lima¹, ¹UEMS, Brazil. We report the anomalous dispersion and group refractive index (n_g) of the Er³⁺: tellurite glass measured by Windowed Fourier Transform from interferometric measurements and compared with the dispersion calculated from absorption spectra by known Kramers-Kronig relations.

JW2A.141

Photo-acoustic sensing with fiber-based optical frequency comb cavity, Takeo Minamikawa^{1,2}, Takashi Masuoka^{1,2}, Takashi Ogura¹, Yoshiaki Nakajima^{3,2}, Yoshihisa Yamaoka⁴, Kaoru Minoshima^{3,2}, Takeshi Yasui^{1,2}; ¹Tokushima Univ., Japan; ²JST, ERATO Intelligent Optical Synthesizer Project, Japan; ³Univ. of Electro-Communications, Japan; ⁴Saga Univ., Japan. We proposed a novel photo-acoustic sensing employing an optical-frequency-comb. We utilized an optical-frequency-comb cavity as an acoustic wave sensor, and successfully demonstrated the detection of ultrasound that generated by the laser irradiation on sample.

JW2A.142

A Simplistic Method to Generate Highly Flat Optical Frequency Combs, Thanh Tuan Tran^{2,1}, Minje Song^{3,1}, Minhyup Song¹, Dongsun Seo²; ¹Electronics and Telecommunications Research Inst., South Korea; ²Dept. of Electronics, Myongji Univ., South Korea; ³School of Electronics Engineering, Kyungpook National Univ., South Korea. We demonstrate a simplistic scheme to generate highly flat optical frequency combs. Our results show the spectral flatness within 1 dB for 35 taps and 1.5 dB for 55 taps, where a DP-MZM is combined with 2 and 3 phase modulators, respectively

JW2A.143

Evolution and Performance of High-Speed A-Scan based on Real-Time Optical Spectrum Fourier Transformation, Fabio Falconi², Yongwoo Park³, Jose Azana⁴, Antonella Bogoni¹, Antonio Malacame¹; ¹Scuola Superiore Sant'Anna, Italy; ²CNIT, Italy; ³Automated Precision Inc., USA; ⁴INRS-EMT, Institut National de la Recherche Scientifique, Canada. Advances on a recently proposed approach to obtain reflectivity profiles have been reported. The method has been successfully applied to a 150 μm thick transparent polyvinyl chloride layer. System performance and optimization have been discussed

JW2A.144

Femtosecond Laser-based Atmospheric Frequency Transfer Using Single Electronic Phase Compensator, Dong Hou¹, Danian Zhang¹, Fuyu Sun¹, Jie Tian², Haoyuan Lu³, Jianye Zhao³; ¹Univ. of Elect. Sci. and Tech. of China, China; ²China Academy of Engineering Physics, China; ³Peking Univ., China. We demonstrate a femtosecond laser-based atmospheric radio-frequency transfer with a single electronic phase compensator over 100 m free-space link. The root-mean-square timing fluctuation of transferred microwave signal is about 490 fs within 5000 s.

JW2A.145

Dispersive Tunable Laser Spectroscopy with Ultrahigh Spectral Resolution, Bin Wang¹, Xinyu Fan¹, Wang Shuai¹, Zuyuan He¹; ¹Shanghai Jiao Tong Univ., China. We propose a dispersive spectroscopy with ultrahigh spectral resolution based on an ultra-linearly swept laser. A measurement bandwidth of 98 GHz and a spectral resolution of 11 kHz are achieved without using costly mode-locked laser.

JW2A.146

Refractive-index-sensing RF comb using intra-cavity multi-mode interference fiber sensor, Ryo Oe¹, Kosuke Nagai¹, Takeo Minamikawa¹, Shuji Taue², Hideki Fukano², Yoshiaki Nakajima³, Kaoru Minoshima³, Takeshi Yasui¹; ¹Tokushima Univ., Japan; ²Okayama Univ., Japan; ³The Univ. of Electro-Communications, Japan. We demonstrate refractive index (RI) measurement of liquid sample based on RI/RF conversion in fiber comb cavity including multi-mode interference fiber sensor. RI resolution of 6.6×10^{-6} is achieved at a measurement time of 0.1 s

JW2A.147

Auto-Start Mechanism of a Polarization-Multiplexed Dual-Frequency Femtosecond Fiber Laser, Rongqing Hui¹, Govind Vedala¹; ¹Univ. of Kansas, USA. Mechanism of dual-frequency-combs coexistence in a polarization-multiplexed all-PM femtosecond fiber laser is presented. Balance between mode-locking conditions of the two combs is essential to minimize differential phase change caused by pump power variation.

JW2A.148

Radiation Pressure Assisted Acousto-Optical Transducer, Ke Huang¹, Mani Hossein-Zadeh¹; ¹Univ. of New Mexico, USA. We study the acousto-optical response of the optomechanical resonators in subthreshold regime and demonstrate that the reduced damping due to radiation pressure can be used for high sensitivity detection of acoustic waves.

JW2A.149

Phase Correlation Between Lines of Electro-Optical Frequency Combs, Lars Lundberg¹, Mikael Mazur¹, Attila Fulop¹, Victor Torres-Company¹, Magnus Karlsson¹, Peter A. Andrekson¹; ¹Chalmers Univ. of Technology, Sweden. Simultaneous measurement of the phase noise from 49 electro-optical frequency comb lines show a correlation of over 99.99% between lines. Additionally, the phase noise difference between line pairs is correlated, verifying theoretical predictions.

JW2A.150

Fluorescence Double Resonance Optical pumping spectrum and its application for frequency stabilization in Millimeter scale vapor cell, Eliran Talker¹, Liron Stern¹, Alex Naiman¹, Uriel Levy¹; ¹Hebrew University Of Jerusalem, Israel. We introduce the approach of fluorescence double resonance optical pumping, demonstrate its superior contrast compare with the conventional double resonance optical pumping, and use it for locking at telecom wavelength in mm scale vapor cell.

JW2A.151

Absolute Frequency of Cesium Atom $6S_{1/2}-6D_{3/2}$ Doppler-free Two-photon Transition, Ting-Ju Chen¹, Jeng-En Chen¹, Tze-Wei Liu^{1,2}, Hsin-Hung Yu¹, Ko-Han Chen¹, Ya-Fen Hsiao², Ying-Cheng Chen², Wang-Yao Cheng¹; ¹Physical Dept., National Central Univ., Taiwan; ²Inst. of atomic and molecular science, Academia Sinica, Taiwan. We determined the absolute frequency of ^{133}Cs $6S_{1/2}-6D_{3/2}$ two-photon transition, our novel scheme enabled the resolution to address the nuclear magnetic octupole.

JW2A.152

Frequency dissemination over 1000 km optical fiber with 10^{21} frequency instability, Xing Chen¹, Jianmin Shang², Dongxing Wang², Cheng Ci³, Wanpeng Zhang³, Bo Liu³, Hong Wu³, Song Yu², Zhigang Zhang¹; ¹Peking Univ., China; ²Beijing Univ. of Posts and Telecommunications, China; ³Nankai Univ., China. We demonstrate a frequency transfer scheme for over 1000 km optical fiber link with mode locked pulse train as the frequency carrier. The fractional frequency instability was measured as $2.75 \times 10^{-15}/\text{s}$ and $3.91 \times 10^{-21}/120000$ s.

JW2A.153

Dual-comb spectroscopy of methan based on an Erbium dual-comb fiber laser, Jie Chen¹, Xin Zhao¹, Yuehan Wu¹, Ting Li¹, Ruli Wang¹, Qian Li¹, Siyao Yin¹, Jiansheng Liu¹, Zheng Zheng^{1,2}; ¹School of Electronic and Information Engineering, Beihang Univ., China; ²Collaborative Innovation Center of Geospatial Technology, China. Dual-comb spectroscopy measurement of methan absorption around 1650nm is demonstrated using a dual-wavelength Erbium mode-locked fiber laser, which illustrates the capability of such single-cavity dual-comb sources to cover spectral range well beyond their initial bandwidth.

JW2A.154

Self-controlled Stabilization of a Passively Phase-locked Er:Fiber Frequency Comb, Andreas Liehl¹, David Fehrenbacher¹, Philipp Sulzer¹, Markus Ludwig¹, Felix Ritzkowski¹, Alfred Leitenstorfer¹, Denis Seletskiy^{1,2}; ¹Univ. of Konstanz, Germany; ²École Polytechnique de Montréal, Canada. We demonstrate optical linewidth narrowing and simultaneous repetition rate stabilization of an Er:fiber frequency comb passively phase-locked by ultrabroadband difference frequency mixing. Optical self-control is performed using the original comb from the master oscillator.

JW2A.155

Real-time multi-wavelength digital holography using line-by-line spectral shaping of optical frequency comb, Masatomo Yamagiwa^{1,2}, Takeo Minamikawa^{1,2}, Isao Morohashi³, Norihiko Sekine³, Iwao Hosako³, Hirotsugu Yamamoto^{2,4}, Takeshi Yasui^{1,2}; ¹Tokushima Univ., Japan; ²JST, ERATO MINOSHIMA Intelligent Optical Synthesizer (IOS), Japan; ³National Inst. of Information and Communications Technology, Japan; ⁴Utsunomiya Univ., Japan. Mode-resolved spectrum in optical frequency comb (OFC) is manipulated by a combination of a 2D spectral disperser with a spatial light modulator. The resulting mode-manipulated OFC is effectively applied for real-time multi-wavelength digital holography.

JW2A.156

High-Sensitivity Doppler-Free Optical-Optical Double-Resonance Dual-Comb Spectroscopy, Akiko Nishiyama^{1,2}, Ken'ichi Nakagawa¹, Hiroyuki Sasada^{3,2}, Atsushi Onae^{4,2}, Yoshiaki Nakajima^{1,2}, Kaoru Minoshima^{1,2}; ¹Univ. of Electro-Communications, Japan; ²Japan Science and Technology Agency (JST), Erato Minoshima Intelligent Optical Synthesizer (IOS) Project, Japan; ³Dept. of Physics, Faculty of Science and Technology, Keio Univ., Japan; ⁴National Metrology Inst. of Japan (NMIJ), National Inst. of Advanced Industrial Science and Technology (AIST), Japan. We demonstrate background-free detection schemes in optical-optical double-resonance dual-comb spectroscopy to improve measurement sensitivity. The dual-comb employing modulation spectroscopy and fluorescence detection achieved 4 and 925 times higher SNR than normal dual-comb setup, respectively.

JW2A.157

Free-running, Femtosecond Dual-Comb MIXSEL for Spectroscopy of Acetylene, Jacob Nuernberg¹, Cesare Alfieri¹, Zaijun Chen², Dominik Waldburger¹, Matthias Golling¹, Nathalie Picque², Ursula Keller¹; ¹Inst. of Quantum Electronics, ETH Zurich, Switzerland; ²Max-Planck Inst. of Quantum Optics, Germany. We present dual-comb spectroscopy on acetylene performed with one single free-running modelocked integrated external-cavity surface-emitting laser (MIXSEL). Two intracavity birefringent crystals reduce the difference in repetition rate and solve aliasing issues for broad optical spectra.

JW2A.158

Quantum Interference Control of Injected Photocurrent in an AlGaAs Waveguide, Kai Wang¹, Rodrigo A. Muni², John E. Sipe², Steven T. Cundiff¹; ¹physics, Univ. of Michigan, USA; ²physics, Univ. of Toronto, Canada. We measured the directional photocurrent induced by quantum interference between two- and three-photon absorption in a semiconductor (AlGaAs) waveguide, which allows the design of compact devices for comb offset frequency measurements.

JW2A.159

Determination of the offset frequency of a broadband frequency comb generated in a waveguide-type periodically poled lithium niobate crystal, Kazumichi Yoshii^{1,2}, Junia Nomura^{1,2}, Kaho Taguchi¹, Yusuke Hisai^{1,2}, Feng-Lei Hong^{1,2}; ¹Yokohama National Univ., Japan; ²JST, Erato, Minoshima Intelligent Optical Synthesizer Project, Japan. We generate a broadband frequency comb using a WG-PPLN and measure the offset frequency of the comb by using a frequency-stabilized laser at 532 nm. The visible comb is generated through $\chi^{(2)}$ process.

JW2A.160

A Computational Correction Method for Dual-comb Interferometry, Zebin Zhu¹, Kai Ni², Qian Zhou², Guanhao Wu^{1,2}; ¹Dept. of Precision Instrument, Tsinghua Univ., China; ²Division of Advanced Manufacturing, Graduate School at Shenzhen, Tsinghua Univ., China. We present a post-correction algorithm for dual-comb interferometry that can compensate the carrier phase noise and timing jitter of interferograms. One-hertz linewidth, ~1 ns timing jitter, and 0.4 rad precision of carrier phase are demonstrated.

JW2A.161

Compact GHz Frequency Comb from an Ultrafast Solid-State Laser with Cost-Efficient 3D-Printed Plastic Cavity Base, Sargis Hakobyan¹, Pierre Brochard¹, Valentin J. Wittwer¹, Kutan Gurel¹, Stephane Schilt¹, Thomas Südmeyer¹; ¹Laboratoire Temps-Fréquence, Switzerland. We present a GHz mode-locked laser with a 3D-printed cavity base resulting in substantial noise reduction from the previous use of traditional opto-mechanical mounts. Additionally, the repetition rate is stabilized to a low-noise optically-derived 15-GHz signal.

JW2A.162

Frequency-sweeping interferometry utilizing optical frequency comb and Fourier transform phase retrieving, Weipeng Zhang¹, Haoyun Wei¹, Yan Li¹; ¹Tsinghua Univ., China. A precise 3D surface measurement method for large stepped structures without height ambiguity is proposed based on optical frequency comb referenced frequency-sweeping interferometry and Fourier transformed fractional phase retrieval. Samples of from 1 to 1000 microns were measured.

JW2A.163

A High Performance Clock Laser for Two-Photon Frequency Stabilized Optical Clocks, Matthew S. Bigelow¹, Kyle W. Martin¹, Gretchen Phelps², Nathan D. Lemke²; ¹Applied Technology Associates dba ATA, USA; ²Space Vehicles Directorate, Air Force Research Lab, USA. We describe a simple high-performance all-fiber atomic-line clock laser constructed from commercial off-the-shelf (COTS) components. This laser, based on a frequency-doubled telecom laser, has significantly lower frequency noise compared to direct diode lasers.

JW2A.164

Development and Qualification of UHV-Compatible, Micro-Integrated Optical Setups for Cold Atom Applications, Marc Christ¹, Achim Peters¹, Markus Krutzik¹; ¹Humboldt-Universität zu Berlin, Germany. We present a tool for rapid prototyping and qualification of (electro-) optical components and adhesive integration techniques for micro-integrated assemblies operating in ultra-high vacuum environments.

JW2A.165

Optical Frequency Comb Faraday Rotation Spectroscopy, Alexandra C. Johansson¹, Jonas Westberg², Gerard Wysocki², Aleksandra Foltynowicz¹; ¹Umeå Univ., Sweden; ²Princeton Univ., USA. By combining Faraday rotation spectroscopy with an optical frequency comb Fourier transform spectrometer, we measure background- and calibration-free spectra of the entire Q- and R-branches of the fundamental band of nitric oxide at 1850–1920 cm⁻¹.

JW2A.166

Tunable lower-RIN Brillouin fiber ring laser for BOTDA sensing, Diego Marini¹, Leonardo Rossi^{1,3}, Filippo Bastianini², Gabriele Bolognini¹; ¹CNR, IMM Inst., Bologna, Italy; ²Sestosensor s.r.l., Italy; ³Università degli Studi di Bologna, Italy. In this work we characterize a lower-RIN Brillouin ring-laser technology for Brillouin optical time-domain analysis (BOTDA) sensing. The developed tunable pump-probe light allows for efficient BOTDA over 10 km fiber with 10mε/0.5°C temperature-strain resolutions.

JW2A.167

Multi-point Acoustic Sensing System Using Coherent Phase Detection, Jingyi Wang¹, Fan Ai¹, Yuezheng Sun¹, Hao Li¹, Xiangpeng Xiao¹, Zhijun Yan¹, Deming Liu¹, Qizhen Sun¹; ¹School of Optical and Electronic Information, National Engineering Lab for Next Generation Internet Access System, Huazhong Univ. of Science and Technology, China. A multi-point acoustic sensing system with capacity up to 248 is proposed. The sensitivity of -131.5dB ± 1.5dB re 1rad/μPa in 2.4k–6kHz is achieved in a prototype system with graphene diaphragm based fiber sensors.

JW2A.168

Fiber Optical Sensor for Methane Detection Based on Metal-Organic Framework/Silicone Polymer Coating, Rongtao Cao¹, Hangjun Ding¹, Zhaoqiang Peng¹, Ki-Joong Kim², Paul Ohodnicki², Aidong Yan¹, Kevin P. Chen¹; ¹Univ. of Pittsburgh, USA; ²National Energy Technology Lab, USA. A multimode fiber methane sensor made of polymer/metal-organic framework coated cladding is presented with a low detection limit of 1% (v/v). The detailed sensing mechanism is also analyzed in this paper.

JW2A.169

High-resolution and Large-capacity DBR Fiber Laser Accelerometer Network, Tao Liu¹, Dongdong Lv¹, Yiyang Luo¹, Zhijun Yan¹, Kai Wang², Chengqiang Li², Deming Liu¹, Qizhen Sun¹; ¹Huazhong Univ of Science and Technology, China; ²The 38th Research Inst. of CETC, China. We demonstrate a highly sensitive DBR fiber laser acceleration sensor network with a resolution of 17.86 ng/Hz^{1/2} and accuracy of 10⁻⁶ g. The sensing capacity is increased to 128 by utilizing the hybrid multiplexing technique.

JW2A.170

Ultra-Sensitive Long Period Fiber Gratings Based Sensor for Detection of Adulterator in Ethanol, Krishnendu Dandapat¹, Indrajeet Kumar², Saurabh M. Tripathi^{1,2}; ¹Physics, Indian Inst. of Technology Kanpur, India; ²Centre for Lasers and Photonics, Indian Inst. of Technology Kanpur, India. Using extremely sensitive dual-resonance long-period-fiber-gratings operating close to their turnaround-wavelength, we demonstrate a sensor for accurate and quantitative detection of adulterator in ethanol. Our sensor can detect methanol concentration as small as 0.1% in ethanol.

JW2A.171

Fast Reading of Fiber Bragg Grating Sensors with a Locked Non-Dithered Tunable Laser, Pedro Martín-Mateos¹, Oscar Elias Bonilla-Manrique¹, Pablo Acedo¹, Jose A. Garcia-Souto¹; ¹Universidad Carlos III de Madrid, Spain. We propose a fast reading FBG laser-locked architecture that provides a single output, a wavelength range only limited by the tuning capabilities of the laser and an operation speed only restricted by the servo controller.

JW2A.172

Cost Effective Dual-Polarization Interferometric Fiber Optic Gyroscopes with Ultra-Simple Configuration, Fangyuan Chen¹, Yulin Li¹, Rongya Luo¹, Fang Ben¹, Dong He¹, Chao Peng¹, Zhengbin Li¹; ¹School of Electronics Engineering and Computer Science, Peking Univ., China. A cost effective and ultra-simple dual-polarization interferometric fiber optic gyroscope utilizing single-mode components was proposed and tested, which achieves an overall bias instability below 2 x 10⁻²°/h and a scale factor nonlinearity below 100 ppm.

JW2A.173

Pico-strain Resolution Fiber Grating Sensor with Ultralow Probe Power and Tunable Sensitivity, Shuangxiang Zhao¹, Qingwen Liu¹, Jiageng Chen¹, Zuyuan He¹; ¹State Key Lab of Advanced Optical Communication Systems and Networks, Shanghai Jiao Tong Univ., China. We present here a novel interrogation method for Er³⁺-doped fiber grating sensor with pε resolution, ultralow probe power, large tunable strain sensitivity and capability of multiplexed, static and dynamic sensing.

JW2A.174

Multichannel Fiber Bragg Grating for Temperature Field Monitoring, Wei Zhang¹, Adenowo Gbadebo², Zhikun Xing¹, Desheng Jiang³, Deming Liu¹, Zhijun Yan¹, Qizhen Sun¹; ¹National Engineering Lab for Next Generation Internet Access System, Huazhong Univ. of Science and Technology, China; ²Aston Inst. of Photonic Technologies, Aston Univ., UK; ³National Engineering Lab for Fiber Optic Sensing Technology, Wuhan Univ. of Technology, China. We demonstrated a multichannel FBG based temperature field sensor, in which the grating was designed by pre-compensation layer peeling method. Such system could achieve a real time temperature field monitoring with 3mm high spatial resolution.

JW2A.175

Demonstration of a Plasmomechanical Radiation Detector with Si₃N₄ Waveguide Optical Readout Circuit, Qiancheng Zhao¹, Mohammad W. Khan¹, Parinaz Sadri-Moshkenani¹, Regina Ragan¹, Filippo Capolino¹, Ozdal Boyraz²; ¹Univ. of California, Irvine, USA. A plasmomechanical radiation detector based on suspended nano-antennas with a Si₃N₄ waveguide optical readout circuit has been demonstrated. The responsivity and noise equivalent power of the detector are measured to be 3.954 × 10⁻³ μm²/μW and 3.01 μW/√Hz, respectively.

JW2A.176

Surface Plasmon Resonator Biosensor Spatial Phase Sensitivity Enhancement through Optical Fiber Low Coherence Interferometry, Shih-Hsiang Hsu¹, Hsun-Yuan Hsu¹, Chung-Hsuan Chen¹, Meng-Syuan Jian¹; ¹National Taiwan Univ of Science & Tech, Taiwan. The spatial phase sensitivity on the effective reaction length using optical fiber low coherence interferometry demonstrates 10.4-rad/μM, 34 times more enhancement than the polarized light phase characterization from spectral interferometry based surface plasmon resonance biosensors.

JW2A.177

Ppb-level Detection of Acetylene based on QEPAS Using a Power Amplified Diode Laser, Yufei Ma¹, Yao Tong¹, Ying He¹, Xin Yu¹, Frank Tittel²; ¹Harbin Inst. of Technology, China; ²Rice Univ., USA. An ultra-high sensitive C₂H₂-QEPAS sensor using an EDFA amplified diode laser was demonstrated. The 33.2 ppb detection sensitivity verified that the design of the reported QEPAS method demonstrated significantly enhanced sensor performance.

JW2A.178

Remote, distributed gas sensor based on FEW-QEPAS, Ying He¹, Yufei Ma¹, Yao Tong¹, Xin Yu¹, Frank Tittel²; ¹Harbin Inst. of Technology, China; ²Rice Univ., USA. A remote, distributed gas sensing using fiber evanescent wave quartz-enhanced photoacoustic spectroscopy (FEW-QEPAS) technique was demonstrated. A 3 km single mode fiber with multiple tapers was employed to perform long distance, distributed gas measurements.

JW2A.179

Temperature Sensor Using Fluid-Filled Negative Curvature Fibers, Chengli Wei¹, Joshua Young¹, Curtis R. Menyuk², Jonathan Hu¹; ¹Dept. of Electrical and Computer Engineering, Baylor Univ., USA; ²Dept. of Computer Science and Electrical Engineering, Univ. of Maryland, Baltimore County, USA. We propose a new temperature sensor based on fluid-filled negative curvature fibers. The temperature sensitivity increases from 0.8 nm/°C to 2.5 nm/°C when the refractive index of the fluid increases from 1.30 to 1.42.

11:30–13:00 JW2A • Poster Session II

JW2A.180

Multi-functional cellulose fiber decorated with plasmonic Au nanoparticles for colorimetry and SERS assay, Qian Yu², Xianming Kong², Yibo Ma³, Alan X. Wang¹; ¹Oregon State Univ., USA; ²College of Chemistry, Chemical Engineering and Environment Engineering, Liaoning Shihua Univ., China; ³Aalto Univ., Finland. We fabricated a multi-functional sensor through decorating Au nanoparticles on cellulose fibers. The solid colorimetry and surface-enhanced Raman scattering sensing for water and malachite green were achieved on this device.

JW2A.181

An Optical Microwave Generator based on Stimulated Brillouin Scattering with Fine Tunability, Juanjuan Yan¹, Aihu Liang¹; ¹Beihang Univ., China. In this optical microwave generator, the lower sideband of CS-DSB modulated laser is shifted using SBS in a fiber. Microwaves from 14.67GHz to 30.67GHz are generated by beating the shifted sideband and the upper sideband.

JW2A.182

Strong-field laser initiated H₂ roaming chemistry and the formation of H₃⁺ from organic molecules, Nagitha Ekanayake¹, Muath Nairat¹, Travis Severt², Peyman Feizollah², Bethany Jochim², Balram Kaderiya², Farzaneh Ziaee², Kurtis Borne², Kanaka Raju Pandiri², Kevin Carnes², Daniel Rolles², Artem Rudenko², Itzik Ben-Itzhak², Nicholas Weingartz¹, Benjamin Farris¹, Benjamin Levine¹, James Jackson¹, Marcos Dantus^{1,3}; ¹Dept. of Chemistry, Michigan State Univ., USA; ²J. R. Macdonald Lab, Dept. of Physics, Kansas State Univ., USA; ³Dept. of Physics, Michigan State Univ., USA. H₂ roaming has been recently implicated in H₃⁺ production when certain organic molecules interact with a strong-field laser. Mechanistic details and femtosecond time-resolved dynamics of H₃⁺ formation were obtained on a series of alcohols.

11:30–13:00 Exhibit Hall Free Lunch

12:00–13:00 OSA Photonic Metamaterials Technical Group Tutorial on Metasurface Design and Simulation, Room 230A

CLEO: Science & Innovations

13:00–15:00

SW3A • Microresonator Combs*Presider: Miro Erkintalo; Univ. of Auckland, New Zealand*

SW3A.1 • 13:00

Gallium Phosphide Microresonator Frequency Combs, Dalziel Wilson^{2,1}, Simon Hönl², Katharina Schneider², Paul Seidler², Miles H. Anderson¹, Tobias J. Kippenberg¹; ¹*Inst. of Physics (IPHYs), École Polytechnique Fédérale de Lausanne (EPFL), Switzerland*; ²*Quantum Technologies, IBM Research, Zurich, Switzerland*. We demonstrate the first microresonator frequency combs in GaP, a III-V semiconductor transparent above 549 nm. High Kerr nonlinearity ($>10^{-18}$ m²/W) yields a 10-mW parametric threshold and 100-nm-wide combs with THz spacing, centered at 1550 nm.

SW3A.2 • 13:15

Low Power Generation of Broadband Single Kerr Solitons in Silicon Nitride Resonators, Travis C. Briles¹, Su-Peng Yu¹, Kartik Srinivasan², Scott Diddams¹, Scott Papp¹; ¹*Time and Frequency Division, National Inst. of Standards and Technology, USA*; ²*Center for Nanoscale Science and Technology, National Inst. of Standards and Technology, USA*. We report the generation of broadband, single soliton frequency combs with dual dispersive waves in 1 THz and 333 GHz FSR silicon nitride microresonators using an on-chip pump-power as low as 12 mW.

SW3A.3 • 13:30

Quasi-phase matched multispectral Kerr frequency comb, Shu-Wei Huang¹, Jinghui Yang², Abhinav K. Vinod², Mingbin Yu³, Dim-Lim Kwong³, Chee-Wei Wong²; ¹*Electrical, Computer & Energy Engineering, Univ. of Colorado, Boulder, USA*; ²*Univ. of California, Los Angeles, USA*; ³*Inst. of Microelectronics, Singapore*. We demonstrate a new type of Kerr frequency comb with expanded parametric range, where the momentum conservation is ensured by azimuthal modulation of the cavity dispersion. A coherent multispectral frequency comb covering telecommunication O, C, L, and 2 μ m bands is observed and characterized.

SW3A.4 • 13:45

Synchronization of coupled microresonator frequency combs, Jae K. Jang¹, Alexander Klenner¹, Xingchen Ji^{1,2}, Yoshitomo Okawachi¹, Michal Lipson¹, Alexander L. Gaeta¹; ¹*Columbia Univ., USA*; ²*Cornell Univ., USA*. We experimentally demonstrate passive synchronization of microresonator-based optical frequency combs. By injecting a small fraction of the light from one microresonator to the other, we frequency-lock two combs separated by over 20 m.

13:00–15:00

SW3B • Hybrid Lasers on Silicon*Presider: Tae Joon Seok; Gwangju Inst. of Science and Technol, South Korea*SW3B.1 • 13:00 **Invited**

Quantum Dot Photonic Integrated Circuits on Silicon, John E. Bowers¹, Arthur Gossard¹, Daehwan Jung¹, Justin Norman¹, Yating Wan¹; ¹*Univ. of California Santa Barbara, USA*. Quantum dot lasers, amplifiers, modulators and photodetectors epitaxially grown on Si are promising for photonic integrated circuits on silicon. Laser performance is improving rapidly. This represents a significant stride toward efficient, scalable, and reliable III-V lasers on on-axis Si substrates for photonic integrate circuits that are fully compatible with CMOS foundries.

SW3B.2 • 13:30

Hybrid Integration of Solid-State Quantum Emitters with a Silicon Chip, Jehyung Kim^{1,2}, Shahriar Aghaeimebodi², Christopher Richardson³, Richard Leavitt³, Dirk Englund⁴, Edo Waks²; ¹*UNIST, South Korea*; ²*Univ. of Maryland, USA*; ³*Lab for Physical Sciences, USA*; ⁴*MIT, USA*. Scalable quantum photonic systems require integrated single photon sources with photonic devices. We demonstrate hybrid integration of solid-state quantum dots to a silicon photonic device and perform Hanbury-Brown and Twiss experiments on the silicon chip with integrated quantum emitters.

SW3B.3 • 13:45

Design Principles for Heterogeneously Integrated III-V-on-Silicon Microdisk Unidirectional Singlemode Lasers, Bo Xue Tan¹, Kaiyi WU¹, Yu Zhang², Andrew W. Poon¹; ¹*Hong Kong Univ of Science & Technology, Hong Kong*; ²*Univ. of California, Davis, USA*. We unfold the design principles for heterogeneously integrated III-V-on-silicon microdisk unidirectional singlemode lasers. Our simulations suggest hybrid modes between the vertically coupled III-V and silicon microdisks of different radii. Our experiments reveal unidirectional singlemode lasing.

13:00–15:00

SW3C • High Capacity Transmission*Presider: Yue-Kai Huang; NEC Labs America Inc, USA*

SW3C.1 • 13:00

PM-64QAM Coherent Optical Communications Using a Dark-Pulse Microresonator Frequency Comb, Attila Fulop¹, Mikael Mazur¹, Abel Lorences-Riesgo^{1,2}, Pei-Hsun Wang³, Yi Xuan^{3,4}, Daniel E. Leaird³, Minghao Qi^{3,4}, Peter A. Andrekson¹, Andrew M. Weiner^{3,4}, Victor Torres-Company¹; ¹*Photonics Lab, Chalmers Univ. of Technology, Sweden*; ²*IT-Instituto de Telecomunicações, Portugal*; ³*School of Electrical and Computer Engineering, Purdue Univ., USA*; ⁴*Birk Nanotechnology Center, Purdue Univ., USA*. Dark-pulse microresonator combs exhibit efficient pump-to-comb power conversion. Using on-chip pump powers of 21 dBm, we show 20-channel PM-64QAM-based data transmission. These results represent the highest-order modulation format encoded onto any integrated comb.

SW3C.2 • 13:30

Experimental Investigation of Roll-off Factor and Channel Spacing for >400Gb/s Coherent Optical Systems, Qiang Wang¹, Yang Yue¹, Xuan He¹, Andre Vovan¹, Jon Anderson¹; ¹*Juniper Networks Inc., USA*. Residual skew in coherent transmitter degrades system performance. To increase tolerance to the transmitter skew, roll-off factor of Nyquist pulse shaping, channel spacing are optimized for >400Gb/s coherent optical communications systems

SW3C.3 • 13:45

Mapping options of 4D constant modulus format for multi-subcarrier modulation, Keisuke Kojima¹, Kieran Parsons¹, Toshiaki Koike-Akino¹, David S. Millar¹; ¹*Mitsubishi Electric Research Labs, USA*. We investigate three options of 4D constant modulus modulation format in terms of pairing complementary amplitude signals for multi-subcarrier modulation. Nonlinear transmission simulations indicate these options are almost equally effective, and much better than the conventional modulation format.

CLEO: Science & Innovations

13:00–15:00

SW3D • Terahertz Nano-imaging and Spectroscopy

Presider: Pernille Klarskov Pedersen; Brown Univ., USA

SW3D.1 • 13:00

Terahertz-Pulse-Induced Patterning on the Nanoscale with Terahertz Scanning Tunneling Microscopy, Vedran Jelic¹, Daniel Mildenerberger¹, Peter H. Nguyen¹, Tianwu Wang¹, Frank A. Hegmann¹; ¹Univ. of Alberta, Canada. We demonstrate that ultrafast terahertz pulses focused onto the tip of scanning tunneling microscope (THz-STM) can be used to pattern structures on a silicon surface via field-assisted removal of surface atoms.

SW3D.2 • 13:15

THz Near-Field Nanoscopy at 25 Nanometer Spatial Resolution, Max Eisele¹, Andreas Huber¹, Tobias Gokus¹; ¹neaspec GmbH, Germany. We combine terahertz time-domain spectroscopy with near-field microscopy to achieve extreme sub-wavelength spatial resolution (<25nanometer) in the far-infrared spectral range. We apply our technology to investigate the carrier concentrations in semiconductor devices and single-layer graphene.

SW3D.3 • 13:30

Scattering-type Scanning Near-field Optical Microscope Operating in the Terahertz Regime, Xinzhong Chen¹, Jiawei Zhang¹, Ryan Mescall¹, Mengkun Liu¹; ¹Stony Brook Univ., USA. We demonstrate a home-built terahertz (THz) scattering-type scanning near-field optical microscope (s-SNOM) system and systematically study the THz response of various common lab materials with ~50 nm spatial resolution. The modeling of the THz near-field response will be discussed.

SW3D.4 • 13:45

Reflection type scanning laser terahertz near-field spectroscopy and imaging system for bio-applications, Kosuke Okada¹, Kazunori Serita¹, Iwao Kawayama¹, Hironaru Murakami¹, Masayoshi Tonouchi¹; ¹Osaka Univ., Japan. We developed a reflection type scanning laser THz near-field spectroscopy and imaging system and evaluated its basic performance. We found that this system has huge potential for high-resolution, high-sensitive and high-speed biological measurements.

CLEO: QELS-Fundamental Science

13:00–15:00

FW3E • Frequency Combs & Precision Metrology

Presider: Scott Diddams; NIST, USA

FW3E.1 • 13:00

Octave-spanning dual comb spectroscopy in the molecular fingerprint region, Henry Timmers¹, Abijith Kowligy¹, Alex Lind¹, Flavio Cruz¹, Nima Nader¹, Myles Silfies², Thomas Allison², Gabriel Ycas¹, Peter G. Schunemann³, Scott Papp¹, Scott Diddams¹; ¹NIST, USA; ²Physics Dept., Stony Brook Univ., USA; ³BAE Systems, USA. We present a scheme for generating super-octave, long-wave infrared combs in the molecular fingerprint region using intra-pulse difference frequency generation in an orientation patterned GaP crystal. We demonstrate high resolution dual-comb spectroscopy in methanol vapor.

FW3E.2 • 13:15

Origin of clustered frequency combs in Kerr microresonators, Hoan Pham¹, Noel L. Sayson¹, Karen E. Webb¹, Luke S. Trainor², Harald G. Schwefel², Stephane Coen¹, Miro J. Erkintalo¹, Stuart G. Murdoch¹; ¹Univ. of Auckland, New Zealand; ²Physics, Univ. of Otago, New Zealand. We identify the physical mechanism responsible for the generation of clustered frequency combs in optical microresonators. This theory is validated by experimentally measuring the coherence of such clustered combs in a MgF₂ monolithic microresonator.

FW3E.3 • 13:30

Brillouin Lasers Based on Ultra-low Loss Silicon Nitride Waveguides, Dan J. Blumenthal¹, Sarat Guvandarapu¹, Debapam Bose¹, Grant Huffman¹, Taran Huffman¹, Ryan Buhunin³, Peter T. Rakich²; ¹Univ. of California, Santa Barbara, USA; ²Yale Univ., USA; ³Northern Arizona Univ., USA. We describe a new class of integrated, ultra-low phase noise Brillouin laser. Leveraging new laser dynamics in very-high Q Si₃N₄ waveguide resonators, record low linewidths and noise in cascaded-order operation, with potential operation across the visible to infrared, can be achieved.

13:00–15:00

FW3F • Single-Photon Detectors

Presider: Martin Stevens; NIST, USA

FW3F.1 • 13:00

Fractal superconducting nanowire single-photon detectors with low polarization sensitivity, Chao Gu¹, Xiaoming Chi¹, Yuhao Cheng¹, Julien Zichi², Nan Hu¹, Xiaojian Lan¹, Kai Zou¹, Shufan Chen¹, Zuzeng Lin^{1,2}, Val Zwiller², Xiaolong Hu¹; ¹Tianjin Univ., China; ²Dept. of Applied Physics, Royal Inst. of Technology (KTH), Sweden. We demonstrated a fractal superconducting nanowire single-photon detector and achieved 42% device efficiency and 1.04 polarization sensitivity. The low polarization sensitivity can be maintained for higher-order spatial modes in few-mode optical fibers.

FW3F.2 • 13:15

Photon-Number Resolution in Conventional Superconducting Nanowire Single-photon Detectors: Experimental Demonstration, Clinton T. Cahall¹, Kathryn L. Nicolich², NURUL T. ISLAM¹, Gregory P. Lafyatis¹, Aaron J. Miller³, Daniel J. Gauthier², Jungsang Kim^{1,4}; ¹Duke Univ., USA; ²The Ohio State Univ., USA; ³Quantum Opus, LLC, USA; ⁴IonQ, Inc., USA. We present the first experimental evidence of photon number resolution in a conventional superconducting nanowire single-photon detector. The photon-number-dependent resistance reflected in the rise-time of output pulses is detected using a wideband, low-noise read-out circuit.

FW3F.3 • 13:30

WSi superconducting nanowire single photon detector with a temporal resolution below 5 ps, Boris A. Korzh¹, Qing-Yuan Zhao², Simone Frasca¹, Di Zhu², Edward Ramirez¹, Eric A. Bersin^{1,2}, Marco Colangelo², Andrew Dane², Andrew Beyer¹, Jason Allmaras¹, Emma Wollman¹, Karl K. Berggren², Matthew Shaw¹; ¹Jet Propulsion Lab, USA; ²MIT, USA. Through the use of an impedance matched taper, we demonstrate a reduction of the noise jitter in WSi SNSPDs to a level below the intrinsic effects, resulting in full-width at half-maximum values of 4.8 ps for 532 nm and 10.3 ps for 1550 nm single photons.

FW3F.4 • 13:45

Concept of quantum timing jitter and non-Markovian limits in single photon detection, Li Ping Yang¹, Hong Xing Tang², Jacob Zubin¹; ¹Dept. of Electric and Computer Engineering, Purdue Univ., USA; ²Dept. of Electrical Engineering, Yale Univ., USA. We propose the concept of quantum timing jitter in single-photon detection, based on the observation of a finite rise time in the quantum probabilistic signal transduction (absorption). We also place a fundamental limit on this quantum jitter.

CLEO: QELS-Fundamental Science

CLEO: Science & Innovations

13:00–15:00

FW3G • Nonlinear Nano-optics

President: Bo Zhen; Univ. of Pennsylvania, USA

FW3G.1 • 13:00

Enhanced Second-Harmonic Generation in Broken Symmetry III-V Semiconductor Metasurfaces driven by Fano resonance, Polina Vabishchevich^{1,2}, Sheng Liu^{1,2}, Michael Sinclair¹, Gordon A. Keeler¹, Gregory M. Peake¹, Igal Brener^{1,2}; ¹Sandia National Labs, USA; ²Center for Integrated Nanotechnologies, Sandia National Labs, USA. We use broken symmetry III-V semiconductor Fano metasurfaces to substantially improve the efficiency of second-harmonic generation (SHG) in the near infrared, compared to SHG obtained from metasurfaces created using symmetrical Mie resonators.

FW3G.2 • 13:15

Second-harmonic generations in a plasmonic two-wire transmission-line, Tzu-Yu Chen¹, Julian Obermeier², Fan-Cheng Lin¹, Jer-Shing Huang³, Markus Lippitz², Chen-Bin Huang¹; ¹National Tsing Hua Univ., Taiwan; ²Univ. of Bayreuth, Germany; ³Leibnitz Inst., Germany. A plasmonic two-wire transmission-line is experimentally used for SHG despite of material and geometric symmetries. The resulting SHGs are only coupled into the asymmetric mode. This characteristic is explained through surface nonlinear polarization calculations.

FW3G.3 • 13:30

Collective nonlinear optical effects in plasmonic nanohole ensembles of different rotational symmetries, Godofredo S. Bautista¹, Christoph Dreser^{2,3}, Xiaorun Zang¹, Dieter Kern^{2,3}, Martti Kauranen¹, Monika Fleischer^{2,3}; ¹Lab of Photonics, Tampere Univ. of Technology, Finland; ²Inst. for Applied Physics, Univ. of Tübingen, Germany; ³Center for Light-Matter-Interaction, Sensors and Analytics LISA+, Univ. of Tübingen, Germany. We use cylindrical vector beams to investigate second-harmonic generation from rotationally symmetric arrangements of plasmonic nanoholes. The second-harmonic efficiency is shown to depend strongly on collective interactions between the nanoholes.

FW3G.4 • 13:45 **Invited**

Nonlinear Wave Mixing in Semiconductor Nanoantennas and Metasurfaces, Dragomir N. Neshev¹; ¹Australian National Univ., Australia. We demonstrate how ultra-small dielectric nanoantennas ordered in a metasurface can enable enhanced light-matter interaction for efficient nonlinear wave-mixing and in particular, to enhance the sum-frequency generation and spontaneous parametric down conversion.

13:00–15:00

FW3H • Active and Tunable Metasurfaces

President: Kevin MacDonald; Univ. of Southampton, UK

FW3H.1 • 13:00

Electrical Tuning of Dielectric Metasurfaces at Visible Frequencies Facilitated by Photoalignment of Liquid Crystals, Chengjun Zou¹, Andrei Komar², Stefano Fasold¹, Alexander Muravsky³, Anatoli Murauskii³, Thomas Pertsch¹, Dragomir N. Neshev¹, Isabelle Staude¹; ¹Inst. of Applied Physics, Abbe Center of Photonics, Friedrich Schiller Univ. Jena, Germany; ²Nonlinear Physics Centre, Research School of Physics and Engineering, The Australian National Univ., Australia; ³Inst. of Chemistry of New Materials, National Academy of Sciences of Belarus, Belarus. We experimentally demonstrate the use of photoalignment materials for liquidcrystal based electrical tuning of resonant silicon metasurfaces with a 67% modulation depth at visible frequencies.

FW3H.2 • 13:15

Continuous Angle Beam Steering Using Spatiotemporal Frequency-Comb Control in Dielectric Metasurfaces, Amr Shaltout¹, Konstantinos Lagoudakis¹, Jorik van de Groep¹, Soo Jin Kim¹, Jelena Vuckovic¹, Vladimir M. Shalaev², Mark Brongersma¹; ¹Stanford Univ., USA; ²Purdue Univ., USA. Experimental laser beam steering is demonstrated using light-matter interaction between frequency-comb source and silicon based metasurface. Continuous angular scanning of 25° is successfully achieved over a time interval of 10 ps

FW3H.3 • 13:30

Active Frequency Modulation of Metamaterial/Graphene Optoelectronic Device Using Coupled Resonators, Stephen J. Kindness¹, Nikita Almond¹, Robert Wallis¹, Binbin Wei¹, varun kamboj¹, Philipp Braeuninger-Weimer¹, Stephan Hofmann¹, Harvey Beere¹, David Ritchie¹, Riccardo Degl'Innocenti²; ¹Univ. of Cambridge, UK; ²Lancaster Univ., UK. We present continuous frequency modulation of a metamaterial resonance by selective damping of coupled resonators using electrostatically gated graphene. A frequency tuning range >150 GHz is achieved at 1.5 THz making this device suitable for use as an electrically tunable frequency modulator.

FW3H.4 • 13:45

Dielectric Metasurfaces for Optical Communications and Spatial Division Multiplexing, Sergey S. Kruk¹, Filipe Ferreira², Naoise Mac-Suibhne², Christos Tsekrekos², Ivan Kravchenko³, Andrew Ellis³, Dragomir N. Neshev¹, Sergei K. Turitsyn², Yuri S. Kivshar¹; ¹Australian National Univ., Australia; ²Aston Univ., UK; ³Oak Ridge National Lab, USA. We employ passive dielectric metasurfaces with near-unity transmission to engineer spatial mode profiles for both mode modulation and multiplexing in optical communications. The broadband response of the metasurface covers S, C, and L telecommunication bands.

13:00–15:00

SW3I • Low-dimensional and Phase-change Materials

President: Matthew Escarra; Tulane Univ., USA

SW3I.1 • 13:00 **Tutorial**

Phase Change Photonics for Neuromorphic Computing and Information Displays, Harish Bhaskaran¹; ¹Univ. of Oxford, UK. In this talk, I shall discuss recent developments in phase change photonics, specifically as it relates to on-chip photonics for memory applications as well as applications in emerging areas of computing. I shall talk about how this generic architecture can be applied to a range of functional materials in photonics. The optoelectronic functionality of these devices ("mixed-mode") will also be explored, and specific applications in displays will be briefly introduced.



Harish's research interests are broadly in the area of Nanoscale Engineering, and recently has focused on the use of accumulative materials to create photonic brain-inspired or neuromorphic computing, display applications and ways to manufacture them. He is currently the Professor of Applied Nanomaterials at Oxford, where he holds the EPSRC Fellowship in Manufacturing and leads the £3.1 million Wearable and Flexible Technologies Collaboration (www.waftcollaboration.org), which includes 15 industrial partners. He is the co-founder, and director (currently serving in an Executive capacity as Chief Scientific Officer) of Bodle Technologies Limited, a displays spin-out emerging out of research done in his laboratory at Oxford.

CLEO: Science & Innovations

13:00–15:00

SW3J • Biosensors & Photonic Devices*Presider: Nien-Tsu Huang, National Taiwan Univ., Taiwan*SW3J.1 • 13:00 **Invited**

Point-of-Care Technologies for Infectious Diseases and Nutritional Deficiencies, David Erickson¹; ¹*Cornell Univ., USA*. In this talk I will discuss some of the technologies and approaches to enable point-of-care diagnostics for vitamin and micronutrient deficiencies and infectious disease related cancers like Kaposi's Sarcoma.

SW3J.2 • 13:30

Laser Emission Microscopy: A Novel Tool for High-contrast Cancer Screening with Nuclear Biomarkers, YU-CHENG CHEN¹, Xiaotian Tan¹, Qiusu Chen¹, Xudong Fan¹; ¹*Bio-medical Engineering, Univ. of Michigan, USA*. We developed a scanning laser-emission microscope capable of mapping lasing emission from nuclear biomarkers in both frozen and paraffin-embedded human tissues, which may open a new field in bioimaging with unprecedented contrast for cancer screening, immunodiagnosis, and cell biology.

13:00–15:00

SW3K • Few Mode Fibers and OAM*Presider: Shaif-UI Alam; Univ. of Southampton, UK*

SW3K.1 • 13:00

Robustness of OAM fiber modes to geometric perturbations, Zelin Ma¹, Gautam Prabhakar¹, Patrick Gregg², Sid-dharth Ramachandran¹; ¹*Boston Univ., USA*; ²*Finisar, USA*. We experimentally demonstrate that pure OAM fiber modes are highly robust to out-of-plane bend perturbations in contrast to their vector counterparts (HE/EH) that mix completely, because geometric (Pancharatnam) phase accumulation varies with OAM content.

SW3K.2 • 13:15

Measurement of the Orbital Angular Momentum Spectrum in Twisted Coreless Photonic Crystal Fiber, Paul Roth¹, Gordon K. L. Wong¹, Ramin Beravat¹, Clarissa M. Harvey¹, Michael H. Frosz¹, Rafal Sopalla¹, Philip S. Russell¹; ¹*Max-Planck-Inst Physik des Lichts, Germany*. We present a technique for measuring the phase and amplitude distribution of the light guided in a twisted coreless photonic crystal fiber (or indeed any fiber), enabling full characterization of the orbital angular momentum states.

SW3K.3 • 13:30

All Fiber Orbital Angular Momentum Light Generation and Propagation Using Graded-Index Few Mode Fiber, Jiulin Gan¹, Xiaobo Heng¹, Zhishen Zhang¹, Zhongmin Yang¹; ¹*South China Univ. of Technology, China*. The special designed graded-index few mode fiber can support orbital angular momentum (OAM) light propagation. Stable OAM light generation and propagation using all fiber fused mode selective coupler with 100nm bandwidth has been experimental demonstrated.

SW3K.4 • 13:45

Towards High-Q Microwave Photonic Passband Filters using Few Mode Fibers with Cascaded Long Period Grating Mode Converters, Daniel Nickel¹, Bryan Haas¹; ¹*Naval Research Lab, USA*. We demonstrate single source microwave photonic finite impulse response filters with coherence-free operation and the potential for arbitrarily high numbers of filter taps using few mode fibers with cascaded long period grating mode converters.

13:00–15:00

SW3L • Fiber and Waveguide Sensing*Presider: Todd Stievater; US Naval Research Lab, USA*

SW3L.1 • 13:00

High-resolution, dynamic fiber Bragg grating sensing base on dual-comb spectroscopy with a single fiber laser, Xin Zhao¹, Qian Li¹, Siyao Yin¹, Jie Chen¹, Zheng Zheng^{1,2}; ¹*School of Electronic and Information Engineering, Beihang Univ., China*; ²*Collaborative Innovation Center of Geospatial Technology, China*. Enabled by a dual-comb fiber laser, real-time interrogation of fiber Bragg grating's spectral response is realized using the dual-comb spectroscopy scheme. kHz sampling speed and pm accuracy are simultaneously achieved with a simple fiber-optic setup.

SW3L.2 • 13:15

Ultrahigh-Resolution and High-Dynamic-Range Strain Sensing by Time-of-Flight Detection with Femtosecond-Laser Pulses, Xing Lu², Shuangyou Zhang¹, Dohyeon Kwon¹, Chan-Gi Jeon¹, Bo Liu³, Haifeng Liu³, Jungwon Kim¹, Kebin Shi²; ¹*Korea Advanced Inst of Science & Tech, South Korea*; ²*Peking Univ., China*; ³*Nankai Univ., China*. We demonstrate a new strain sensing method by time-of-flight detection with femtosecond-laser pulses. Strain resolution of 18 pε/Hz^{1/2} at 1-Hz and 1.9 pε/Hz^{1/2} at 3-kHz is demonstrated with large dynamic range of >159 dB at 3-kHz.

SW3L.3 • 13:30

Coherent Brillouin Random Fiber Laser for Application in Phase-sensitive Optical Time Domain Reflectometry, Liang Zhang¹, Yuan Wang^{1,2}, Yanping Xu¹, Song Gao¹, Dapeng Zhou¹, Liang Chen¹, Xiaoyi Bao¹; ¹*Dept. of physics, Univ. of Ottawa, Canada*; ²*Inst. of Optoelectronic Technology, China Jiliang Univ., China*. We report the experimental demonstration of a new fashion of a coherent Brillouin random fiber laser enabled by distributed Rayleigh feedback for distributed acoustic sensor based on phase-sensitive optical time domain reflectometry.

SW3L.4 • 13:45

Porous Silicon Photonics at Unity Confinement Factors for Surface Adlayer Biosensing Applications, Gabriel Allen^{1,2}, William Delaney¹, Judson Ryckman¹; ¹*Clemson Univ., USA*; ²*Western Michigan Univ., USA*. We report a porous silicon photonics platform that addresses the evanescent limitations of guided wave surface adlayer biosensors. Devices are realized through an inverse fabrication process and ultra-high sensitivity to small molecule adlayers is demonstrated.

CLEO: Science & Innovations

CLEO: Applications
& Technology

13:00–15:00

SW3M • Beam Control & Measurement

Presider: Seung-Whan Bahk; Univ. of Rochester, USA

SW3M.1 • 13:00

Elegant Laser Resonator Modes with OAM, Alfonso I. Jaimés-Nájera¹, Sabino Chávez-Cerda¹; ¹INAOE, Mexico. Siegman introduced the elegant beams and proved that they are not eigenmodes of spherical resonators. We demonstrate that by superposing a finite number of elegant Laguerre-Gauss beams we can generate eigenmodes of spherical resonators.

SW3M.2 • 13:15

Novel Method for Generating High Purity Vortex Modes, Robin T. Uren¹, Stephen Beecher¹, Callum Smith¹, William A. Clarkson¹; ¹Univ. of Southampton, UK. A scheme for generating Laguerre-Gaussian vortex modes using a novel astigmatic mode converter based on spherical mirrors is described. A simple method for characterizing mode purity is employed to confirm the benefits of this scheme.

SW3M.3 • 13:30

Optical vortex parametric laser with a versatile orbital angular momentum, Shungo Araki¹, Roukuya Mamuti¹, Kensuke Suzuki¹, Shigeki Nishida¹, Katsuhiko Miyamoto^{1,2}, Takashige Omatsu^{1,2}; ¹Chiba Univ., Japan; ²Molecular chirality research center, Chiba Univ., Japan. We present a tunable optical vortex parametric oscillator with versatile OAM. The OAM mode with a designated topological charge within the range of -1~3 was selectively generated by simply shortening or extending the cavity.

SW3M.4 • 13:45

High-resolution and compact vortex mode sorters based on a spiral transformation, Yuanhui Wen¹, Ioannis Chremmos^{1,2}, Yujie Chen¹, Jiangbo Zhu³, Yanfeng Zhang¹, Siyuan Yu^{1,3}; ¹Sun Yat-sen Univ., China; ²Hellenic Electricity Distribution Network Operator S. A., Greece; ³Univ. of Bristol, UK. We put forward a more generalized spiral transformation for vortex mode sorting with better separation between adjacent modes. We confirm this theoretical prediction with a compact vortex mode sorter fabricated on a thin quartz plate.

13:00–15:00

SW3N • Few-cycle Sources

Presider: Takao Fujii; National Inst.s of Natural Sciences, Japan

SW3N.1 • 13:00

A Robust Two-color-field Driven Hollow-core Fiber Compressor, Yudong Yang^{1,2}, Liwei Song^{1,3}, Fabian Scheiba^{1,2}, Giulio M. Rossi^{1,2}, Roland E. Mainz^{1,4}, Shaobo Fang¹, Oliver Muecke^{1,2}, Franz X. Kaertner^{1,4}; ¹Center for Free-Electron Laser Science CFEL, Deutsches Elektronen-Synchrotron DESY, Germany; ²The Hamburg Centre for Ultrafast Imaging CUI, Univ. of Hamburg, Germany; ³State Key Lab of High Field Laser Physics, Shanghai Inst. of Optics and Fine Mechanics, Chinese Academy of Sciences, China; ⁴Dept. of Physics, Univ. of Hamburg, Germany. We present a robust two-color-field driven hollow-core-fiber compressor. The ~1mJ HCF output covers 300 nm to 950 nm supporting sub-cycle transform-limited pulses with ~2.1fs duration. The spectral phase is characterized with two-dimensional spectral shearing interferometry.

SW3N.2 • 13:15

33-fold pulse compression down to 1.5 cycles in a 6-m-long hollow-core fiber, Young-Gyun Jeong¹, Riccardo Piccoli¹, Denis Ferachou^{1,2}, Vincent Cardin¹, Michael Chini³, Steffen Hädrich⁴, Jens Limpert^{5,6}, Roberto Morandotti^{1,7}, François Légaré¹, Bruno E. Schmidt², Luca Razzari¹; ¹INRS-EMT, Canada; ²few-cycle Inc., Canada; ³Dept. of Physics and CREOL, Univ. of Central Florida, USA; ⁴Active Fiber Systems GmbH, Germany; ⁵Inst. of Applied Physics, Abbe Center of Photonics, Friedrich-Schiller-Universität Jena, Germany; ⁶Fraunhofer Inst. for Applied Optics and Precision Engineering, Germany; ⁷National Research Univ. of Information Technologies, Mechanics and Optics, Russia. We demonstrate 33-fold pulse compression employing a 6-m-long hollow-core fiber and chirped mirrors. 1 mJ, 170 fs pulses at 1030 nm are compressed to 0.65 mJ, 5.1 fs, corresponding to 1.5 optical cycles.

SW3N.3 • 13:30

2.5 Cycle Pulses Obtained With Self Compression At 1.8 μm In Antiresonant Waveguides, Rudrakant Sollaipur¹, Bruno E. Schmidt², Philippe Lassonde³, Shoufei Gao⁴, Yingying Wang⁴, Pu Wang⁴, François Légaré³, Christian Spielmann^{1,5}; ¹Friedrich Schiller Univ. Jena, Germany; ²few-cycle Inc., Canada; ³INRS-EMT, Canada; ⁴Inst. of Laser Engineering, Beijing Univ. of Technology, China; ⁵Helmholtz Inst. Jena, Germany. We report on 2.5 cycle pulse compression from 60 to 15 fs at 1800 nm in the fundamental mode of an Ar-filled low-loss antiresonant hollow-core fiber by pumping close to strand-resonance and zero dispersion wavelength.

SW3N.4 • 13:45

Compression of a Yb:KGW Laser with Multi-Plate and Hollow-Core Fiber Compressors, John E. Beetar¹, Shima Gholam Mirzaeimoghadar¹, Michael Chini^{1,2}; ¹Physics, Univ. of Central Florida, USA; ²CREOL, The College of Optics and Photonics, Univ. of Central Florida, USA. We investigate the potential of multi-plate and hollow-core fiber-based pulse compressors to generate few-cycle pulses from a moderately high energy (400 μJ) and average power (20 W) Yb:KGW laser with 280 fs input duration.

13:00–15:00

AW3O • Optical Enhancement of Photovoltaics

Presider: TBD

AW3O.1 • 13:00

Efficiency Increasing of Single-Junction GaAs Solar Cells Coated with Species of NIR Up-Conversion Phosphors Layer on Front-Side Surface by Spin-On Film Deposition, Jih-Ciang Chen¹, Wen-Jeng Ho¹, Zong-Xian Lin¹, Wen-Bin Bai¹, Guan-Yu Chen¹, Hao-Xiang Zhang¹, Jheng-Jie Liu¹, Hung-Pin Shiao²; ¹National Taipei Univ. of Technology, Taiwan; ²Win Semiconductor Corp., Taoyuan, Taiwan, R.O.C., Taiwan. This study demonstrates high-efficiency (23.72%) single-junction GaAs solar cell coated with species of NIR up-conversion phosphors layer on the front-side surface by spin-on-film deposition, compared to 19.36% efficiency of the reference single-junction GaAs solar cell.

AW3O.2 • 13:15

HIT Solar Cell Performance Enhancement with Luminescent Down Shifting Phenomenon, Albert Lin¹, Chien Y. Huang¹, Parag Parashar¹, Hao-Ming Chou¹, Yi-Shuan Lin¹, Ming-Hsuan Kao², Shih-Wei Chen², Chang-Hong Shen², Jia-Min Shieh², Tzu-Yu Chen¹, Chien-Chung Lin³, Peichen Yu¹, Hao-Chung Kuo¹; ¹National Chiao Tung Univ., Taiwan; ²National Nano Device Labs (NDL), Taiwan; ³Inst. of Photonic System, National Chiao Tung Univ., Taiwan. Luminescent down-shifting (LDS) phenomenon has been employed to enhance the HIT solar cell efficiency. The efficiency and J_{sc} are increased by 2.3% and 11.5% respectively. External quantum efficiency (EQE) data supports our claim.

AW3O.3 • 13:30

Spectrum Splitting Micro-Concentrator Assembly for Laterally-arrayed Multi-Junction Photovoltaic Module, Duanhui Li¹, Rui-Tao Wen², Rushabh Shah¹, Xueying Zhao¹, Haoquan Zhang³, Eugene A. Fitzgerald¹, David J. Perreault², Jurgen Michel¹, Juejun Hu¹, Tian Gu¹; ¹Dept. of Materials Science and Engineering, MIT, USA; ²Materials Research Lab, MIT, USA; ³Dept. of Electrical Engineering and Computer Science, MIT, USA. We demonstrate a novel spectrum-splitting module for integration with laterally-arrayed multi-bandgap micro-scale solar cells. The high-efficiency, low-cost, and low-profile design potentially enables significant improvement on solar module performance and reduction of energy production costs.

AW3O.4 • 13:45

Flexible Integrated Concentrators for Scalable High-Power Generation from Colloidal Quantum Dot Solar Cells, Yida Lin¹, Garrett Ung¹, Botong Qiu¹, Susanna Thon¹; ¹Johns Hopkins Univ., USA. We fabricated economical and scalable compact concentrators using PDMS integrated with QD solar cells. The lenses deliver short circuit currents up to 20 times and powers up to 10 times that of bare solar cells.

Joint

13:00–15:00

JW3P • Symposium on New Advances in Adaptive Optics Retinal Imaging I

President: TBD

JW3P.1 • 13:00 **Invited**

Adaptive Optics Scanning Light Ophthalmoscopy: Beyond Structural Imaging, Alfredo Dubra¹; ¹Stanford Univ., USA. Here we will first review demonstrations of imaging retinal function at the cellular scale using adaptive optics ophthalmoscopy, and then, we will discuss their potential clinical applications.

JW3P.2 • 13:45 **Invited**

Imaging Single Cells in the Living Eye from the Retinal Pigment Epithelium to the Ganglion Cell Layer, Ethan A. Rossi¹; ¹Ophthalmology, Univ. of Pittsburgh, USA. Rapid advances in adaptive optics ophthalmoscopy have allowed additional cell classes to be imaged in the living eye, offering great promise for the study of diseases such as glaucoma and age-related macular degeneration. This presentation will cover some of these and discuss the challenges that remain for widespread clinical deployment.

JW3P.3 • 14:30

CLEO: Science & Innovations

13:00–15:00

SW3Q • Semiconductor Lasers for Integration

President: Kiyoul Yang; Stanford Univ.

SW3Q.1 • 13:00

Room-Temperature Electrically Pumped InP-based Laser Directly Grown on on-axis (001) Silicon, Si Zhu¹, Bei Shi¹, Qiang Li¹, Kei May Lau¹; ¹Hong Kong Univ of Science & Technology, Hong Kong. We report the first InAlGaAs/InP multi-quantum-well lasers grown on (001) silicon by MOCVD. Lasing near 1.5 μm was achieved with a $J_{th} = 3.3 \text{ kA/cm}^2$ and a high T_0 of 133 K.

SW3Q.2 • 13:15

Highly Improved Reliability of Low Threshold 1.3 μm III/V Quantum Dot Laser Epitaxially Grown on On-axis Si, Daehwan Jung¹, Robert Herrick², Justin Norman¹, Catherine Jan², Neil Caranto², Alfredo Torres¹, Yating Wan¹, Arthur Gossard¹, John E. Bowers¹; ¹UCSB, USA; ²Intel Corp., USA. InAs quantum dot Fabry-Perot lasers grown on on-axis (001) Si demonstrate record-low continuous-wave threshold current of 4.8 mA as well as excellent device reliability with extrapolated lifetimes more than ten million hours at 35 °C.

SW3Q.3 • 13:30

Quadruple reduction of threshold current density for micro-ring quantum dot lasers epitaxially grown on (001) Si, Yating Wan¹, Daehwan Jung¹, Justin Norman¹, Kaiyin Feng¹, Aip Dagli¹, Arthur Gossard¹, John E. Bowers¹; ¹UCSB, USA. A quadruple reduction of threshold current density was achieved for electrically pumped quantum-dot micro-rings epitaxially grown on (001) silicon. This was enabled by a low threading dislocation density GaAs buffer layer and a smoothed etching sidewall.

CLEO: Applications & Technology

13:00–15:00

AW3R • A&T Topical Review on Advanced Applications of Laser Radar and Remote Sensing II

President: Fabio Di Teodoro; Raytheon SAS

AW3R.1 • 13:00 **Invited**

LiDAR for Autonomous Vehicles: Challenges and Opportunities for Photonics, Lute Maleki¹; ¹Sensors, GM/Cruise, USA. Autonomous vehicles are arguably the most impactful technology since the advent of the Internet. In this talk challenges and opportunities of LiDAR that pertain to Photonics Technology will be discussed.

AW3R.2 • 13:30

Comparison of cavity enhanced Faraday rotation techniques for oxygen detection, Charles L. Patrick¹, Jonas Westberg¹, Gerard Wysocki¹; ¹Princeton University, USA. Two cavity enhanced Faraday rotation spectroscopic techniques are compared by detection of oxygen around 762 nm. Both techniques demonstrate sensitivities in the 1e-9 rad/ $\sqrt{\text{Hz}}$ range and inherent advantages of the two techniques are discussed.

AW3R.3 • 13:45

Navigation Doppler Lidar for autonomous ground, aerial, and space vehicles, Farzin Amzajerdian¹, Glenn D. Hines¹, Diego F. pierrottet², Bruce W. Barnes¹, Larry B. Petway¹, John M. Carson³; ¹NASA Langley Research Center, USA; ²Coherent Applications, USA; ³NASA Jonsen Space Center, USA. A Doppler lidar instrument has been developed and demonstrated for providing critical vector velocity and altitude/range data for autonomous precision navigation. Utilizing advanced component technologies, this lidar can be adapted to different types of vehicles.

13:00–15:00

AW3S • A&T Topical Review on Advances in Supercontinuum Technologies II: New Application Areas for Supercontinuum Light Sources

President: Adam Devine

AW3S.1 • 13:00 **Invited**

Supercontinuum Applications in High Resolution Non Invasive Optical Imaging, Adrian G. Podoleanu¹, Ole Bang², Peter Moselund³; ¹Univ. of Kent, Canterbury, UK; ²Technical Univ. of Denmark, Denmark; ³NKT Photonics, Denmark. Progress will be presented in adapting supercontinuum sources to optical coherence tomography and photoacoustic applications with emphasis on signal processing procedures customised to alleviate noise and take full advantage of the large bandwidth of the supercontinuum

AW3S.2 • 13:30 **Invited**

Mid-infrared Supercontinuum-based Trace as Sensing, Frans J. M. Harren¹; ¹Radboud Univ., Netherlands. An overview will be given on mid-infrared supercontinuum sources combined with sensitive spectroscopic methods, to trace molecular gases for applications such as food spoilage reduction and high-sensitivity sensing for a safer atmospheric environment.

CLEO: Science & Innovations

SW3A • Microresonator Combs—Continued

SW3A.5 • 14:00

Generation of Multiple Side Lines around Kerr Comb Lines by a Second Pump Coupled into the Soliton Resonance, Peicheng Liao¹, Changjing Bao¹, Kaiheng Zou¹, Arne Kordts², Lin Zhang³, Maxim Karpov², Martin Pfeiffer², Ahmed Almainan¹, Yinwen Cao¹, Fatemeh Alishahi¹, Amirhossein Mohajerin Ariaei¹, Ahmad Fallahpour¹, Moshe Tur⁴, Tobias J. Kippenberg², Alan E. Willner¹, ¹Univ. of Southern California, USA; ²Ecole Polytechnique Federale de Lausanne, Switzerland; ³School of Precision Instrument and Opto-electronics Engineering, China; ⁴Tel Aviv Univ., Israel. We demonstrate the generation of multiple side lines around Kerr comb lines by injecting a second pump into the soliton resonance. The side lines around each comb lines have relatively high power and are stable.

SW3A.6 • 14:15

Direct Generation of Solitons with a Reversed Soliton Step in a Microresonator Pumped by a Phase-Modulated Laser, Daniel C. Cole¹, Jordan Stone¹, Scott Papp¹, ¹NIST Boulder, USA. We demonstrate direct generation of Kerr-microresonator solitons with measured 100 percent success rate using an increasing-frequency scan of a phase-modulated pump laser. A reversed soliton step is observed. The phase modulation controls the solitons' properties.

SW3A.7 • 14:30

Raman comb generation through broadband gain in a silica microresonator, Ryo Suzuki¹, Akihiro Kubota¹, Atsuhiko Hori¹, Shun Fujii¹, Takasumi Tanabe¹, ¹Keio Univ., Japan. We study the dynamics of Raman comb formation in silica rod microresonators. We generated a Raman comb with a smooth spectral envelope and observed the center wavelength transition by controlling the detuning and coupling strength.

SW3A.8 • 14:45

Efficient Mid-Infrared Dispersive Wave Generation in Dispersion-Engineered Si₃N₄ Waveguides Pumped at 2 μm, Eirini Tagkoudi¹, Davide Grassani¹, Hairun Guo², Clemens Herkommer², Tobias J. Kippenberg², Camille-Sophie Bres¹, ¹Ecole Polytechnique Fédérale de Lausanne (EPFL), Photonic Systems Lab (PHOSL), Switzerland; ²Ecole Polytechnique Fédérale de Lausanne (EPFL), Lab for Photonics and Quantum Measurements (LPQM), Switzerland. We demonstrate efficient generation of mid-infrared dispersive wave at 3.5 μm in a Si₃N₄ waveguide pumped by a 2090nm femtosecond mode-locked fiber laser. The 8% maximum efficiency allows for a milliwatt-level average power mid-infrared pulse.

SW3B • Hybrid Lasers on Silicon—Continued

SW3B.4 • 14:00

CMOS-Compatible Tunable Vernier Ring Laser using Erbium Doped Waveguide on a Silicon Photonics Platform, Nanxi Li^{1,2}, Diedrik Vermeulen^{1,3}, Zhan Su^{1,3}, Emir Magden¹, Alfonso Ruocco¹, Neetesh Singh¹, Jelena Notaros¹, Ming Xin¹, Christopher Poulton^{1,3}, Erman Timurdogan^{1,3}, Christopher Baiocco⁴, Michael Watts¹, ¹Research Lab of Electronics, MIT, USA; ²John A. Paulson School of Engineering and Applied Science, Harvard Univ., USA; ³Analog Photonics, USA; ⁴College of Nanoscale Science and Engineering, Univ. at Albany, USA. We demonstrate the first silicon photonic tunable laser with integrated erbium-doped Al₂O₃ waveguides. The laser is designed to have Vernier ring structure for wide tuning operation. It has a 0.23cm² footprint and 1.6mW output power.

SW3B.5 • 14:15

Low Cost 100 Gbps Multicore VCSEL Based Transmitter Module Platform, Teng Li¹, Sander Dorrestein², Wouter Soenen³, Chenhui Li¹, Ripalta Stabile¹, Xin Yin³, Oded Raz¹, ¹Eindhoven Univ. of Technology, Netherlands; ²TE Connectivity, Netherlands; ³Ghent Univ., Belgium. We demonstrate a flexible printed circuit board platform for a 100 Gbps VCSEL based transmitter with direct light launching into a multicore-fiber using a 3D glass interposer as fan-out. Error free operation is demonstrated.

SW3B.6 • 14:30

Silicon Waveguide Coupled III-V Nanowire Lasers with Epitaxial Gain Control, Thomas Stettner^{2,1}, Tobias Kostenbader², Daniel Ruhstorfer^{2,1}, Jochen Bissinger^{2,1}, Andreas Thurn², Hubert Riedl², Michael Kaniber^{2,1}, Gregor Koblmüller^{2,1}, Jonathan J. Finley^{2,1}, ¹Nanosystems Initiative Munich (NIM), Schellingstr. 4, Germany; ²Walter Schottky Institut and Physik Dept., Technische Universität München, Germany. We demonstrate lasing from individual GaAs-based NWs integrated onto Si ridge waveguides. In addition, proof-of-principle coupling emission to the Si WG is shown, with propagation distances of the lasing mode exceeding > 60 μm.

SW3B.7 • 14:45

Microwave Spectral Characteristics of the Three-Section Distributed Feedback Lasers, Chun-Hong Chen¹, Fu-Chun Hsiao², Yao-Zhong Dong³, Yueh-Lin Chan², Yi-Hsun Chen², Yu-Ming Huang², Shun Chieh Hsu², Chung-Ping Huang³, Chien-Chung Lin², ¹College of Photonics, Inst. of Imaging and Biomedical Photonics, National Chiao-Tung Univ., Taiwan; ²College of Photonics, Inst. of Photonic System, National Chiao-Tung Univ., Taiwan; ³College of Photonics, Inst. of Lighting and Energy Photonics, National Chiao-Tung Univ., Taiwan. The three-section DFB lasers are used for RF signal generation. With an extra section, it can tune the RF peak frequency farther than the two-section one, and can also simultaneously generate two single-mode RF signals.

SW3C • High Capacity Transmission—Continued

SW3C.4 • 14:00 Tutorial

Scaling Disparities in Optical Communications – And How to Resolve Them, Peter J. Winzer¹, ¹Nokia Bell Labs, USA. Decades of consistent traffic growth suggest that optical transmission capacities will soon be unable to support demands. New transmission technologies will be needed, based on massive array integration across spatial and wavelength multiplexing dimensions.



Peter Winzer has contributed to many aspects of optical communications and networking, high-speed transmission, and spatial multiplexing to overcome network scalability problems. He has amply published and patented and is actively involved within IEEE and OSA. He is a Highly Cited Researcher, a Fellow of Bell Labs, IEEE, and OSA, and a Member of the NAE.

CLEO: Science & Innovations

SW3D • Terahertz Nano-imaging and Spectroscopy—Continued

SW3D.5 • 14:00 **Invited**

Terahertz Light Fingerprints Biomolecular Dynamics, Yanting Deng¹, Mengyang Xu¹, Katherine Niessen¹, Deepu Koshy George¹, Andrea G. Markelz¹; ¹Physics, Univ. at Buffalo, SUNY, USA. This talk will discuss the limitations of standard THz spectroscopic methods, and how THz polarization techniques can be used to both fingerprint specific biomolecules and reveal their biologically important changes. I will also discuss challenges that must be addressed to fully realize THz light's impact on the biomedical community.

SW3D.6 • 14:30

Control of Spoof Localized Surface Plasmons Using Terahertz Near-field Microscope, Takashi Arikawa¹, Shohei Morimoto¹, Tomoki Hiraoka¹, François Blanchard², Kyosuke Sakai³, Keiji Sasaki³, Koichiro Tanaka⁴; ¹Kyoto Univ., Japan; ²Dept. of Electrical Engineering, École de Technologie Supérieure (ÉTS) Montréal, Canada; ³Research Inst. for Electronic Science, Hokkaido Univ., Japan; ⁴Inst. for Integrated Cell-Material Sciences, Kyoto Univ., Japan. We performed time-resolved terahertz near-field imaging of a gold disk with sub-wavelength periodic grooves and successfully observed spoof localized surface plasmons. A selective excitation method is also demonstrated with orbital angular momentum of light.

SW3D.7 • 14:45

Depth-enhanced terahertz reflection imaging with Bessel beam generated by 3D-printed diffractive element, Liting Niu¹, Qiao Wu¹, Kejia Wang¹, Zhengang Yang¹, Jinsong Liu¹; ¹Huazhong Univ. of Science and Techn., China. We propose a depth-enhanced terahertz reflection imaging system with Bessel beam generated by 3D-printed diffractive element. For testing the imaging quality of this system, a resolution chart is imaged at different transverse planes.

CLEO: QELS-Fundamental Science

FW3E • Frequency Combs & Precision Metrology—Continued

FW3E.4 • 14:00

Electro-optic Frequency Comb Generation in Ultrahigh-Q Integrated Lithium Niobate Micro-resonators, Mian Zhang¹, Cheng Wang¹, Brandon Buscaino², Amirhassan Shams-Ansari^{1,3}, Joseph Kahn², Marko Loncar¹; ¹John A. Paulson School of Applied and Engineering Sciences, Harvard Univ., USA; ²E. L. Ginzton Lab, Dept. of Electrical Engineering, Stanford Univ., USA; ³Dept. of Electrical Engineering and Computer Science, Howard Univ., USA. We generate an electro-optic frequency comb in an integrated lithium niobate ultrahigh-Q microresonator. The comb has more than 250 lines with a line spacing of ~ 25 GHz in the telecom L-band.

FW3E.5 • 14:15

Direct Kerr-frequency-comb atomic stabilization, Liron Stern¹, Jordan Stone¹, Songbai Kang¹, Daniel C. Cole¹, John Kitching¹, Scott A. Diddams¹, Scott Papp¹; ¹Time and Frequency Division, National Inst. for Standards and Technology, USA. We experimentally demonstrate direct Kerr-microresonator frequency-comb atomic spectroscopy, utilizing a cascaded two-photon 1529-nm transition in a rubidium micro-machined vapor cell. The demonstration is a path for compact atomic frequency references and multiphoton-comb-atom interactions.

FW3E.6 • 14:30

Shaping Harmonic Frequency Combs in Quantum Cascade Lasers, Marco Piccardo¹, Paul Chevalier¹, Benedikt Schwarz², Yongrui Wang³, Dmitry Kazakov^{1,4}, Noah A. Rubin¹, Sajant Anand⁵, Enrique A. Mejia⁶, Michele Tamagnone¹, Feng Xie⁷, Kevin Lascola¹, Alexey Belyanin³, Federico Capasso¹; ¹Harvard Univ., USA; ²TU Wien, Austria; ³Texas A&M Univ., USA; ⁴ETH Zurich, Switzerland; ⁵Wake Forest Univ., USA; ⁶Univ. of Texas at Austin, USA; ⁷Thorlabs Quantum Electronics, USA. Controlling the spacing of self-starting harmonic frequency combs in QCLs by design of fundamental laser parameters is arduous. New ways to shape such combs by means of original electrical, optical and radiofrequency techniques are presented.

FW3F • Single-Photon Detectors—Continued

FW3F.5 • 14:00

A Primary Radiation Standard Based on Quantum Nonlinear Optics, Samuel Lemieux¹, Enno Giese¹, Robert Fickler¹, Maria Chekhova², Robert Boyd^{1,3}; ¹Univ. of Ottawa, Canada; ²Max Planck Inst. for the Science of Light, Germany; ³Univ. of Rochester, USA. We introduce spontaneous parametric down-conversion as a light source for intensity calibration of spectrometers solely based on physical principles. The response function of the spectrometer obtained with our technique agrees with the one measured with a NIST-traceable calibration lamp.

FW3F.6 • 14:15

Measuring single photons to bright light with a logarithmic optical detector, Johannes Tiedau¹, Evan Meyer-Scott¹, Thomas Nitsche¹, Sonja Barkhofen¹, Christine Silberhorn¹, Tim J. Bartley¹; ¹Integrated Quantum Optics Group, Applied Physics, Univ. of Paderborn, Germany. We explore the behaviour of a loop detection scheme above the saturation region of single photon detectors. This enables us to measure single photon states and up to 309 nW power with the same device.

FW3F.7 • 14:30

Sub-nanosecond Temporally Resolved Imaging with a Single Pixel Camera, Steven Johnson¹, Matthew Edgar¹, David Phillips², Miles Padgett¹; ¹Univ. of Glasgow, UK; ²Univ. of Exeter, UK. Single pixel cameras with temporal resolution can produce 3D images. We present a single pixel camera that has a temporal resolution of 200 picoseconds, enabling us to resolve the modes from a few-mode optical fibre.

FW3F.8 • 14:45

Harnessing Quantum Wave Nature of Individual Electrons for Single Photon Detection, Yang Zhang¹, Yang Wu², Xiaoxin Wang³, Eric R. Fossum³, Rahul Kumar², Jifeng Liu³, Gregory Salamo², Shui-Qing Yu¹; ¹Dept. of Electrical Engineering, Univ. of Arkansas, USA; ²Dept. of Physics, Univ. of Arkansas, USA; ³Thayer School of Engineering, Dartmouth College, USA. We propose and examine theoretically a new type of photodetector that senses THz single photons by the wavefunction change of a single electron confined in a quantum dot. A possible readout scheme is also presented.

15:00–17:00 Coffee Break & Exhibit Only Time, Exhibit Hall

CLEO: QELS-Fundamental Science

CLEO: Science & Innovations

FW3G • Nonlinear Nano-optics—Continued

FW3G.5 • 14:15

Plasmon Enhanced Third-Harmonic Generation with Graphene Nanoribbons, Irati Alonso Calafell¹, Lee Rozema¹, David Alcaraz², Frank H. Koppens², Philip Walther¹; ¹Univ. of Vienna, Austria; ²ICFO, Spain. Graphene's strong third-order nonlinearity could allow single-photon level interactions. Using third-harmonic generation, we characterize this nonlinearity over a wide wavelength range (1-4 μ m). We study a further plasmon enhancement by resonantly pumping graphene nanoribbons.

FW3G.6 • 14:30

Structured Light for Selective Third-Harmonic Generation in Subwavelength Resonators, Elizaveta V. Melik-Gaykazyan¹, Sergey S. Kruk², Maria del R. Camacho Morales², Lei Xu², Mohsen Rahmani², Khosro Zangeneh Kamali², Aristeidis Lamprianidis², Andrey Miroshnichenko³, Andrey Fedyanin¹, Dragomir N. Neshev², Yuri S. Kivshar²; ¹Faculty of Physics, Lomonosov Moscow State Univ., Russia; ²Nonlinear Physics Centre, Australian National Univ., Australia; ³School of Engineering and Information Technology, Univ. of New South Wales, Australia. We study the third-harmonic generation in subwavelength silicon particles supporting Mie-type optical modes. By tailoring the vectorial structure of the pumping light, we selectively excite electric or magnetic multipoles, also controlling the induced nonlinear response.

FW3H • Active and Tunable Metasurfaces—Continued

FW3H.5 • 14:00 **Invited**

Active and Nonlinear Metasurfaces: From Graphene-Integrated to Photon-Accelerating Semiconductor Nanostructures, Gennady Shvets¹; ¹Cornell Univ., USA. Amplitude and phase shaping of infrared light on a nanosecond scale using graphene-integrated plasmonic metasurfaces will be described. The concept of a Photon-Accelerating Metasurface enabling simultaneously broadband and efficient nonlinear light generation will be introduced

FW3H.6 • 14:30

A Reprogrammable Photonic Meta-platform, Kaichen Dong^{2,1}, Sukjoon Hong^{2,3}, Yang Deng², He Ma¹, Jiachen Li¹, Xi Wang², Junyeob Ye^{2,4}, Letian Wang², Shuai Lou², Kyle Tom^{2,5}, Kai Liu¹, Zheng You¹, Yang Wei¹, Costas P. Grigoropoulos², Jie Yao^{2,5}, Junqiao Wu^{2,5}; ¹Tsinghua Univ., China; ²Univ. of California, Berkeley, USA; ³Hanyang Univ., South Korea; ⁴Kyungpook National Univ., South Korea; ⁵Lawrence Berkeley National Lab, USA. We present an all-solid, reprogrammable meta-platform, which can be rapidly (re)programmed into nearly arbitrary photonic devices by writing/erasing patterns on it. The writing is performed with a low-power laser, and the erasing utilizes global cooling.

FW3H.7 • 14:45

Reflectance Modulation of Metasurface Coupled to Inter-subband Transitions using Voltage Controlled Quantum Tunneling, Raktim Sarma¹, Salvatore Campione¹, Michael Goldflam¹, Loan Te², Mike Lange², Joshua Shank¹, Michael Wanke¹, Jinhyun Noh³, Peide Ye³, Igal Brener¹; ¹Sandia National Labs, USA; ²Northrop Grumman Corporation, USA; ³Purdue Univ., USA. We demonstrate a fundamentally new approach of using voltage controlled quantum tunneling for modulating optical response of a metasurface coupled to intersubband transitions in semiconductor quantum wells.

SW3I • Low-dimensional and Phase-change Materials—Continued

SW3I.2 • 14:00

Adaptive thermal camouflage based on phase-changing material GST, Yurui Qu¹, Qiang Li¹, Lu Cai¹, Meijian Pan¹, Pintu Ghosh¹, Kaikai Du¹, Min Qiu¹; ¹Zhejiang Univ., China. An adaptive thermal camouflage device incorporating phase-changing material Ge₂Sb₂Te₅ (GST) is experimentally demonstrated. Near-perfect thermal camouflage can be achieved continuously for the background temperature ranging from 30 °C to 50 °C.

SW3I.3 • 14:15

Non-Local Detection and Electric Modulation of Valley-Coupled Spin Photocurrents in WSe₂-Bi₂Se₃ Heterostructure Device, Minji Noh¹, Soonyoung Cha¹, Jehyun Kim², Jangyup Son², Hyemin Bae¹, Doeon Lee¹, Hoil Kim³, Jekwan Lee¹, Hoseung Shin¹, Sangwan Sim¹, Seung Hoon Yang⁴, Sooun Lee¹, Gangtae Jin³, Moon-Ho Jo³, Wooyoung Shim¹, Chul-Ho Lee⁴, Junsung Kim³, Dohun Kim², Hyunyoung Choi¹; ¹Yonsei Univ., South Korea; ²Seoul National Univ., South Korea; ³POSTECH, South Korea; ⁴Korea Univ., South Korea. We perform a non-local circular photogalvanic measurement and directly generate the valley-coupled spin currents from WSe₂ to Bi₂Se₃ topological insulators. Our WSe₂-Bi₂Se₃ heterostructure offers a new optoelectronic platform toward the electrically-controllable valley-spin degree of freedom.

SW3I.4 • 14:30

Strain dependent optical helicity in monolayer WSe₂, Jinkang Lim¹, Zhangji Zhao¹, Jin Ho Kang¹, Jiahui Huang¹, Xiangfeng Duan¹, Ali Javey², Chee Wei Wong¹, hyungjin kim²; ¹Univ. of California Los Angeles, USA; ²Electrical Engineering, Univ. of California, Berkeley, USA. We investigate optical helicity of chemical vapor deposition (CVD) grown monolayer WSe₂ samples on fused silica substrates with/without a strain control. 38 (18) % of helicity for the strain controlled (uncontrolled) sample is measured at 77 K.

SW3I.5 • 14:45

Spectroscopic signature of interlayer coupling in Black phosphorus-graphite heterostructure, Zhonghui Nie¹, Hanwen Wang², Weilai Liu², Xiaoping Liu¹, Yongbing Xu¹, Yi Shi¹, Zheng Han², Frank (Fengqiu) Wang¹; ¹Nanjing Univ., China; ²IMR, Chinese Academy of Sciences, China. We reveal a pump-polarization-dependent spectroscopic signature of interlayer coupling in a black phosphorus-graphite heterostructure by probing its ultrafast photo-response. The angle-resolved transients provide new insights into the interfacial carrier dynamics in this emerging hybrid system.

15:00–17:00 Coffee Break & Exhibit Only Time, Exhibit Hall

CLEO: Science & Innovations

SW3J • Biosensors & Photonic Devices—
Continued

SW3J.3 • 14:00

Random Lasing Action in All-Marine Based Materials, Wei-Ju Lin¹, Shih-Yao Lin¹, Cheng Han Chang¹, Yu-Ming Liao¹, Tai-Yuan Lin², Yang-Fang Chen¹; ¹National Taiwan Univ., Taiwan; ²Inst. of Optoelectronic Sciences, National Taiwan Ocean Univ., Taiwan. Towards the sustainable development, optoelectronic devices with biodegradability and biocompatibility have been a desirable but challenging issue for years. In this study, an all-biomaterial random laser device based on all-marine elements has been demonstrated.

SW3J.4 • 14:15

Dense-Wavelength-Division Laser Micro-Particles: Fabrication and Imaging in Tissues, Nicola Martino^{1,2}, Sheldon J. Kwok^{1,3}, Jiamin Wu¹, Andreas C. Liapis^{1,2}, Sun-Joo Jang^{1,2}, Seok-Hyun Yun^{1,2}; ¹Wellman Center for Photomedicine, Massachusetts General Hospital, USA; ²Dept. of Dermatology, Harvard Medical School, USA; ³MIT, USA. Small laser cavities embedded in biological systems are a novel contrast agent for biomedical research. Here we demonstrate the fabrication of highly multiplexed laser particles that can be imaged in tissue.

SW3J.5 • 14:30

Enhanced Fluorescence Spectroscopy and Imaging Immunoassay using Biological Photonic Crystals, Kenny Squire¹, Xianming Kong¹, Paul Leduff¹, Gregory Rorrer¹, Alan X. Wang¹; ¹Oregon State Univ., USA. Utilizing natural photonic crystals, diatoms, we developed immunoassay with efficiently enhanced fluorescence signals. Testing on standard antibody-antigen models achieved unprecedented detection limits of 10^{-16} M and 10^{-14} M using fluorescence spectroscopy and fluorescence imaging respectively.

SW3J.6 • 14:45

Sub-5-nm-nanogap Metasurface for Record-breaking Surface Enhanced Infrared Absorption Spectroscopy, Dengxin Ji¹, Alec R. Cheney¹, Nan Zhang¹, Haomin Song¹, Jun Gao¹, Xie Zeng¹, Haifeng Hu¹, Suhua Jiang¹, Zongfu Yu¹, Qiaoqiang Gan¹; ¹State Univ. of New York at Buffalo, USA. We developed a metamaterial super absorber with sub-5-nanometer gaps and demonstrated its application for record-breaking surface enhanced infrared absorption spectroscopy using its extremely enhanced localized field.

SW3K • Few Mode Fibers and OAM—
ContinuedSW3K.5 • 14:00 **Invited**

Optical fiber designs for MIMO-less SDM, Sophie LaRochelle¹, Alessandro Corsi¹, Reza Mirzaei-Nejad¹, Lixian Wang¹, Xun Guan¹, Jun Ho Chang¹, Jiachuan Lin¹, Leslie Rusch¹; ¹COPL, Université Laval, Canada. We examine polarization maintaining elliptical core fiber designs for space-division-multiplexing (SDM) in short reach links. Linearly polarized vector modes simplify polarization Mux/Demux and MIMO-less transmission is achieved. We discuss scalability of the approach.

SW3K.6 • 14:30

Intermodal Modulation Instability and Four-Wave Mixing in Graded-Index Few-Mode Fibers, Abdelkrim Bendahmane¹, Richard Dupiol^{1,2}, Katarzyna Krupa³, Alessandro Tonello², Julien Fatome¹, Marc Fabert², Bertrand Kibler¹, Thibaut Sylvestre⁴, Alain Barthelemy², Vincent Couderc², Stefan Wabnitz^{1,3}, Guy Millot¹; ¹Laboratoire ICB, UMR CNRS 6303, Université Bourgogne Franche-Comté, France; ²XLIM, UMR CNRS 7252, Université de Limoges, France; ³Università degli Studi di Brescia, Italy; ⁴Institut FEMTO-ST, Université Bourgogne Franche-Comté, France. By controlling pump modes injected in the normal dispersion regime of few-mode graded index optical fiber, we investigated intermodal noise-seeded modulation instability and generation of highly-detuned cascaded intermodal four-wave mixing sidebands.

SW3L • Fiber and Waveguide Sensing—
ContinuedSW3L.5 • 14:00 **Invited**

Thermo-refractive noise at high frequency: Beyond the conventional model, Nicolas Le Thomas¹, Ali Raza¹, Roel Baets¹; ¹Ghent Univ., Belgium. The detection limit of Raman sensors based on waveguides is restricted by a background that exhibits an unconventional exponential decay at high frequency. We discuss a new model that reveals the origin of this background.

SW3L.6 • 14:30

E-beam-lithography free plasmonic slot waveguides for on-chip Raman spectroscopy, Ali Raza¹, Michiel V. Daele¹, Pieter Wuytens¹, Jolien Dendooven¹, Christophe Detavernier¹, Stephane Clemmen¹, Roel Baets¹; ¹Ghent Univ., Belgium. We present nanoplasmonic slot-waveguides interfaced to dielectric photonic waveguides and capable of strongly enhancing Raman scattering. Their e-beam-free fabrication can be scaled to volume manufacturing and makes the plasmonic structure, hence the Raman spectra, reproducible.

SW3L.7 • 14:45

Dynamic Optical Fringe Suppression for Silicon Photonic Sensors, Chu Teng¹, Eric J. Zhang², Chi Xiong², Yifeng Chen¹, Jonas Westberg¹, William Green², Gerard Wysocki¹; ¹Princeton Univ., USA; ²IBM Thomas J. Watson Research Center, USA. We present a new fringe mitigation method based on Fourier decomposition of background optical fringe patterns. Application to a silicon photonic on-chip sensor show order of magnitude improved concentration retrieval stability.

15:00–17:00 Coffee Break & Exhibit Only Time, Exhibit Hall

CLEO: Science & Innovations

CLEO: Applications
& TechnologySW3M • Beam Control & Measurement—
ContinuedSW3M.5 • 14:00 **Invited**

Hartmann Wavefront Sensors for Advanced LIGO, Peter Veitch¹, Aidan Brooks², Won Kim¹, Jesper Munch¹, David Ottaway¹; ¹Univ. of Adelaide, Australia; ²LIGO Lab, USA. The operation and sensitivity of the Advanced LIGO gravitational wave detector are degraded by absorption-induced wavefront distortion. We describe the use of ultra-sensitive Hartmann wavefront sensors to tune detector operation and optimize sensitivity.

SW3M.6 • 14:30

Improved Spatially Dithered Beam Shapers Using Direct Binary Search, Christophe Dorrer¹, Jie Qiao²; ¹Univ. of Rochester, USA; ²Rochester Inst. of Technology, USA. Direct binary search is used to optimize spatially dithered distributions of transparent and opaque pixels for beam shaping, improving the performance of spatial gain precompensation for laser systems, and wavefront metrology by optical differentiation.

SW3M.7 • 14:45

Amplification of Incoherent and Coherently Coupled Higher Order Modes in a Ho:YAG Single Crystal Fiber, Yuan Li¹, Wenzhe Li¹, Keith Miller¹, Eric G. Johnson¹, Subhabrata Bera², Craig Nie², James A. Harrington²; ¹Clemson Univ., USA; ²Rutgers Univ., USA. The simultaneous excitation and amplification of two higher order modes (HOMs) are demonstrated in a Ho:YAG single crystal fiber (SCF) amplifier for both incoherent and coherent mode combing.

SW3N • Few-cycle Sources—Continued

SW3N.5 • 14:00

Greater than 50x solid-state compression of 1030 nm Yb-based laser pulses to single-cycle duration, Chih-Hsuan Lu^{1,2}, Wei-Hsin Wu¹, Shiang-He Kuo¹, Shang-Da Yang¹, Ming-Chang Chen¹, A. H. Kung^{1,2}; ¹National Tsing Hua Univ., Taiwan; ²Inst. of Atomic and Molecular Sciences, Academia Sinica, Taiwan. 170 fs pulses of a 1030 nm Yb-based laser system has been compressed to 3.1 fs at below a single carrier cycle following spectral broadening in a two-stage multiple thin plates arrangement

SW3N.6 • 14:30

Near single-cycle laser pulses at high average power and high repetition rate from an all-solid-state setup, Tobias Witting¹, Chih-Hsuan Lu^{2,3}, Federico J. Furch¹, A. H. Kung^{2,3}, Marc J. Vrakking¹; ¹Max-Born-Inst., Germany; ²Inst. of Photonics Technologies, Taiwan; ³Inst. of Atomic and Molecular Sciences, Taiwan. We demonstrate pulse compression of a high average power 100 kHz NOPCPA laser system with an all solid state setup. Using multiple thin quartz plates we achieve near-single cycle pulses with an average power of over 10 W with excellent long term power and CEP stability.

SW3N.7 • 14:45

Generation of sub-two-cycle, CEP-stable, high-energy, 3.5- μ m pulses by multiple-plate pulse compression, Peiyu Xia¹, Faming Lu¹, Teruto Kanai¹, Nobuhisa Ishii¹, Jiro Itatani¹; ¹Inst. for Solid State Physics, The Univ. of Tokyo, Japan. We demonstrate multiple-plate compression of femtosecond pulses in the mid-infrared region. Using YAG and two Si plates, 1.80-optical-cycle, CEP-stable, intense pulses (21.0 fs, 45 μ J, 3.5 μ m) has been obtained with octave-spanning spectrum.

AW3O • Optical Enhancement of
Photovoltaics—ContinuedAW3O.5 • 14:00 **Invited**

Progress Toward Stationary Concentrator Photovoltaics, Peter Kozodoy¹, John Lloyd¹, Michael Pavilonis¹, Chadwick Casper¹, Kevin Schneider¹, William McMahon², Christopher Gladden¹; ¹Glint Photonics, Inc., USA; ²National Renewable Energy Lab, USA. We present an overview of our research on stationary high-concentration photovoltaic panels with internal micro-tracking. Utilizing multijunction cells, these modules offer the potential for high energy production per unit area at low cost.

AW3O.6 • 14:30

Analysis of an Anti-reflecting Nanowire Transparent Electrode for Solar Cells, Zhixin Zhao¹, Ken X. Wang¹, Shanhui Fan¹; ¹Ginzton Lab, Stanford Univ., USA. We investigate a nanowire transparent electrode that also functions as an anti-reflection coating for solar cells. To provide physical insights into this broadband anti-reflection, we introduce a generalized Fabry-Perot model.

AW3O.7 • 14:45

Experimental Demonstration of 28.2% Thermophotovoltaic Conversion Efficiency, Zunaïd Omair^{1,2}, Gregg Scranton^{1,2}, Luis Pazos-Outon¹, Myles Steiner², Per Peterson⁴, John Holrichter⁵, Eli Yablonovitch^{1,2}; ¹Electrical Engineering and Computer Science, Univ. of California at Berkeley, USA; ²Materials Science Division, Lawrence Berkeley National Lab, USA; ³National Renewable Energy Lab, USA; ⁴Nuclear Engineering, Univ. of California at Berkeley, USA; ⁵Physical Insight Associates, USA. Efficient luminescence extraction enables us to use the photovoltaic band gap as the spectral filter for thermophotovoltaics. Using this concept, we demonstrate a 28.2% conversion efficiency, higher than the previously reported value for the range of the emitter temperature (700C -1250C) used.

15:00–17:00 Coffee Break & Exhibit Only Time, Exhibit Hall

Joint

JW3P • Symposium on New Advances in Adaptive Optics Retinal Imaging I—Continued

Simultaneous Multi-Channel AOSLO Imaging for Visualizing Inner Retina Structures, Mircea Mujat¹, Yang Lu¹, Gopi Maguluri¹, Nicusor Iftimia¹, R. Daniel Ferguson¹; ¹Physical Sciences Inc., USA. A new detection scheme was demonstrated for multiple channels simultaneous imaging that provides isotropic images of inner retina structures free of directionality artifacts. The channels can be combined to reveal additional structural and functional details.

CLEO: Science & Innovations

SW3Q • Semiconductor Lasers for Integration—Continued

SW3Q.4 • 14:00

III-V-on-Silicon Filtered Feedback Discretely Tunable Laser with Nanosecond Switching Times, Sören Dhoore^{1,2}, Abdul Rahim^{1,2}, Gunter Roelkens^{1,2}, Geert Morthier^{1,2}; ¹Photonics Research Group, Belgium; ²Center for Nano- and Biophotonics, Belgium. We demonstrate nanosecond fast wavelength switching with a heterogeneously integrated III-V-on-silicon four-channel filtered feedback tunable laser. High-speed direct modulation at 12.5 Gbit/s of each wavelength channel is achieved.

SW3Q.5 • 14:15

Electrically Pumped Hybrid III-V/Si Photonic Crystal Surface Emitting Lasers with Buried Tunnel-Junction, Shih-Chia Liu¹, Deyin Zhao¹, Carl Reuterskiöld-Hedlund², Mattias Hammar², Weidong Zhou¹; ¹Univ. of Texas at Arlington, USA; ²Dept. of Electronics, KTH-Royal Inst. of Technology, Sweden. We report here an electrically pumped hybrid III-V/Si photonic crystal surface emitting laser (PCSELS) on silicon with a buried tunnel-junction (BTJ). RT CW single mode operation was achieved at 1504 nm for a 80x80 μm^2 laser.

SW3Q.6 • 14:30

An MMI-based Tunable Laser for Integrated Photonic Circuits, Ludovic Caro^{1,2}, Mohamad Dernaika^{1,3}, Frank Peters^{1,2}; ¹Tyndall National Inst., Ireland; ²Physics Dept., Univ. College Cork, Ireland; ³Electrical and Electronic Engineering Dept., Univ. College Cork, Ireland. A single mode, tunable semiconductor laser is presented for the L band. This facetless, regrowth-free laser shows a tuning range extending from 1564nm to 1611nm, with side-mode suppression ratio values over 30dB.

SW3Q.7 • 14:45

Tunable self-injected Fabry-Perot laser diode coupled to an external high-Q Si₃N₄/SiO₂ micro-ring resonator, Yu Li¹, Yuanjue Zhang¹, Minghua Chen¹, Hongwei Chen¹, Sigang Yang¹; ¹Tsinghua Univ., China. We demonstrate a self-injection locking of Fabry-Perot laser diode with narrow linewidth of 8 kHz. The laser has output power of 7 dBm and SMSR of 45 dB with wavelength switchable range of 17 nm.

CLEO: Applications & Technology

AW3R • A&T Topical Review on Advanced Applications of Laser Radar and Remote Sensing II—Continued

AW3R.4 • 14:00 **Invited**

Three-Dimensional Imaging Under Extreme Conditions Using Single-Photon Counting, Gerald S. Buller¹, Abderrahim Halimi¹, Aurora Maccarone¹, Rachael Tobin¹, Peter Connolly¹, Zoe Greener¹, Yoann Altmann¹, Aongus McCarthy¹; ¹Heriot-Watt Univ., UK. Picosecond single-photon timing has been used for depth profiling under extreme environmental conditions. Depth imaging has been examined in a variety of scenarios including multi-kilometer range, in underwater conditions and in the presence of obscurants.

AW3R.5 • 14:30 **Invited**

High Performance Mid-IR Devices and Applications to Gas Sensing, Mariano Troccoli¹, Pietro Patimisco², Angelo Sampaolo², Vincenzo Spagnolo²; ¹Evolution Photonics Inc, USA; ²Dipartimento di Fisica, PolySense Lab - Univ. and Politecnico di Bari, Italy. Manufacturing and deployment of high performance mid-IR devices for demanding sensing applications requires a high degree of control over development and manufacturing of components that can be packaged in a ruggedized, reliable and compact instrument.

AW3S • A&T Topical Review on Advances in Supercontinuum Technologies II: New Application Areas for Supercontinuum Light Sources—Continued

AW3S.3 • 14:00 **Invited**

Biological applications of Supercontinuum lasers in Optical light microscopy, David Castaneda-Castellanos¹; ¹Leica Microsystems, Germany. The integration of a supercontinuum laser in a confocal microscope allows the imaging of biological samples with unprecedented flexibility in confocal and superresolution modes as well as broad applications in precise single molecule lifetime measurements.

AW3S.4 • 14:30 **Invited**

Mid-IR hyperspectral imaging of gases using a supercontinuum source and frequency upconversion, Peter John Rodrigo¹, Peter Tidemand-Lichtenberg¹, Lasse Høgstvedt², Laurent Huot^{1,3}, Christian Pedersen¹; ¹DTU Fotonik, Denmark; ²NLIR, Denmark; ³NKT Photonics, Denmark. We experimentally demonstrate hyperspectral imaging of different gas species by using an all-fiber broadband mid-IR supercontinuum source for illumination and a frequency upconversion based system for detection.

15:00–17:00 **Coffee Break & Exhibit Only Time, Exhibit Hall**

CLEO: Science & Innovations

17:00–19:00

SW4A • High-Q Microcavities*President: Zhihong Huang; Hewlett Packard Labs, USA*

SW4A.1 • 17:00

Achieving Topological Photonics in a Synthetic Space with Dynamically Modulated Ring Resonators, Luqi Yuan¹, Meng Xiao¹, Qian Lin¹, Shanhui Fan¹; ¹Stanford Univ., USA. We implement the two-dimensional Haldane model in the synthetic frequency space in a system composed of several ring resonators undergoing dynamic modulation. It provides a route towards nonreciprocal topological photonics in a miniaturized structure.

SW4A.2 • 17:15

High Q Integrated Photonic Microresonators on 3C SiC-on-Insulator Platform, Tianren Fan¹, Hesam Moradinejad¹, Xi Wu¹, Ali Asghar Eftekhari¹, Ali Adibi¹; ¹Georgia Inst. of Technology, USA. We report for the first time the fabrication of high-Q SiC resonators on a 3C SiC-on-insulator platform (with no undercutting) formed using direct wafer bonding. We demonstrate Q of 42,000 for a 20 μm radius microdonut resonator with a great potential for higher Qs by chemical-mechanical polishing.

SW4A.3 • 17:30 **Invited**

Measurements of Thermodynamical Noise and Drift in Mesoscale Cavities with Quality Factors in Excess of 1 Billion, J. Lim¹, A. A. Savchenkov², W. Liang², W. Wang¹, A. Matsko², L. Maleki², C. W. Wong¹; ¹Mesoscopic Optics and Quantum Electronics Laboratory, University of California, USA; ²OEwaves Inc., USA. We describe the measured noise and drift characteristics of ultrahigh-Q microresonator-stabilized lasers at the thermodynamical limits, achieving a sub-25-Hz linewidth and 32-Hz Allan deviation. Random-walk noise statistics, along with cross-polarization mode temporal correlations, are demonstrated.

17:00–19:00

SW4B • Nitride-based Integrated Photonics*President: Weidong Zhou; Univ. of Texas at Arlington, USA*SW4B.1 • 17:00 **Invited**

III-Nitride Integrated Photonics: Prospects and Challenges, Mohammad Soltani¹; ¹Raytheon BBN Technologies, USA. An integrated photonic platform made of III-Nitrides with their wide bandgap and unique optical/electronic properties enables promising applications over a broad spectral range from ultraviolet to infrared. We review the progress/challenges of developing such platforms.

SW4B.2 • 17:30

Narrow-linewidth, tunable external cavity diode lasers through hybrid integration of quantum-well/quantum-dot SOAs with Si₃N₄ microresonators, Yeyu Zhu¹, Siwei Zeng¹, Xiaolei Zhao¹, Yunsong Zhao¹, Lin Zhu¹; ¹Clemson Univ., USA. We demonstrate hybridly integrated narrow-linewidth, tunable diode lasers via edge coupling. The silicon nitride photonic integrated circuit performs as the tunable external cavity, whereas the gain medium is provided by a quantum-well/quantum-dot semiconductor optical amplifier.

SW4B.3 • 17:45

An unreleased MEMS actuated silicon nitride resonator with bidirectional tuning, Hao Tian¹, Bin Dong¹, Michael Zervas², Tobias J. Kippenberg², Sunil Bhave¹; ¹OxideMEMS Lab, Purdue Univ., USA; ²École Polytechnique Fédérale de Lausanne (EPFL), Switzerland. A silicon nitride photonic resonator is tuned by integrating a piezoelectric MEMS actuator above the resonator. Bidirectional tuning is achieved by controlling voltage polarity and judicious placement of the actuator above the ring.

17:00–19:00

SW4C • Optical Switching*President: David Geisler; Massachusetts Inst of Tech Lincoln Lab, USA*

SW4C.1 • 17:00

Hybrid Flow Switched Network with an Arbitrarily Reconfigurable Optical Switch, Gregory Steinbrecher^{2,1}, Vincent W. Chan¹, Dirk Englund¹, Scott A. Hamilton²; ¹MIT, USA; ²MIT Lincoln Lab, USA. We present a hybrid network based on an integrated photonic switch capable of arbitrary single- and multi-cast transformations. We show bandwidth and latency improvements in a multi-switch network under load from one to several flows.

SW4C.2 • 17:15

On-Chip Switching of Mode- and Polarization-Multiplexed Signals with a 748-Gb/s/λ (8 × 93.5-Gb/s) Capacity, Qingming Zhu¹, Yong Zhang¹, Yu He¹, Shaohua An¹, Ciyuan Qiu¹, Xuhan Guo¹, Yikai Su¹; ¹Shanghai Jiao Tong Univ., China. We experimentally demonstrate an on-chip optical switching scheme for mode- and polarization-multiplexed signals. A quadrupled switching capacity of 748 Gb/s/λ is achieved by routing eight 93.5-Gb/s data channels on two modes and two polarizations.

SW4C.3 • 17:30

Experimental Demonstration of 64-Port Thin-CLOS Architecture for All-to-All Optical Interconnects, Xian Xiao¹, Roberto Proietti¹, Kaiqi Zhang¹, Gengchen Liu¹, Hongbo Lu¹, Jeff Messig², S. J. Ben Yoo¹; ¹Univ. of California, Davis, USA; ²Enablence Technologies, Inc., USA. We designed, assembled, and experimentally demonstrated a 64-port wavelength-routing Thin-CLOS system in a 1U rack using four 32×32 AWGRs. BER measurements show error-free performance under the worst-case intra-band crosstalk scenario.

SW4C.4 • 17:45

OpenFlow-Control of an OAM-Based Two-Layer Switch Supporting 100Gb/s Real Data-Traffic, Mirco Scaffardi¹, Muhammad N. Malik^{1,2}, Francesco Paolucci², Emma Lazzeri², Ning Zhang³, Charalambos Klitis³, Andrea Sgambelluri², Martin Lavery³, Filippo Cugini¹, Marc Sorel³, Antonella Bogoni²; ¹CNIT, Italy; ²Scuola Superiore Sant'Anna, Italy; ³Univ. of Glasgow, UK. A two-layer orbital angular momentum and wavelength based switch is presented and characterized up to 100Gb/s with coherent polarization-multiplexed real data traffic. The switch is successfully reconfigured by applying an OpenFlow based SDN control plane.

CLEO: Science & Innovations

17:00–19:00

SW4D • Novel THz Techniques

President: Ben Ofori-Okai; SLAC National Accelerator Lab, USA

SW4D.1 • 17:00 **Invited**

THz silicon systems on chip: A Moore-Maxwell Approach, Kaushik Sengupta¹; ¹Princeton Univ., USA. In this talk, we will highlight new design methodologies to enable future chip-scale THz architectures in silicon that are multi-functional, programmable and can enable efficient THz technology diversity of applications in sensing, imaging and communication

SW4D.2 • 17:30

Plasmonic Heterodyne Terahertz Spectrometry, Mona Jarrahi¹, Ning Wang¹, Semih Cakmakyapan¹; ¹Univ. of California Los Angeles, USA. We demonstrate a new class of terahertz spectrometers that use plasmonic photomixers as frequency downconverters to offer quantum-level sensitivity at room temperature. We demonstrated double-sideband noise temperatures of 120-270 K over 0.1-2 THz.

SW4D.3 • 17:45

Shaping Terahertz Beams with High-efficiency All-dielectric Metasurfaces, Cheng Zhang¹, Ashish Chanana², Wenqi Zhu¹, Henri Lezec¹, Ajay Nahata², Amit K. Agrawal¹; ¹NIST, USA; ²Univ. of Utah, USA. We demonstrate high-efficiency (>70%) all-dielectric Terahertz metasurfaces operating in the transmission mode. Example devices include high numerical-aperture (NA≈0.9) meta-lenses as well as cylindrical vector beam generator.

CLEO: QELS-Fundamental Science

17:00–19:00

FW4E • Quantum and Nonlinear Phenomena

President: Roberto Morandotti; INRS-Energie Mat & Tele Site Varennes, Canada

FW4E.1 • 17:00

High-efficiency Broadband Single-photon Frequency Upconversion, Huiqin Hu¹, Jianhui Ma¹, Yu Chen¹, Xiuliang Chen¹, Haifeng Pan¹, E Wu¹; ¹East China Normal Univ., China. We demonstrate broad bandwidth single-photon upconversion of femtosecond pulses at telecom wavelength in periodically poled lithium niobate (PPLN) bulk with high conversion efficiency by pumping with a broad bandwidth laser.

FW4E.2 • 17:15

Experimental Demonstration of an Optical-Coherence Converter, Chukwuemeka Okoro¹, Hasan E. Kondacki², Ayman Abouraddy², Kimani C. Toussaint¹; ¹Univ of Illinois at Urbana-Champaign, USA; ²CREOL, The College of Optics & Photonics, USA. By treating coherence as a shareable resource between multiple degrees of freedom (DoFs), we experimentally demonstrate a reversible exchange of coherence between polarization and spatial DoFs using only unitary transformations.

FW4E.3 • 17:30 **Invited**

Single Photon Quantum Frequency Conversion as Tool for Quantum Networks, Christoph Becher¹; ¹Fachbereich Physik, Universität des Saarlandes, Germany. We demonstrate that quantum frequency down-conversion of single photons can be used to interface stationary quantum bits with telecom photons. The preservation of polarization-entanglement and indistinguishability allows for connecting quantum bits across a quantum network.

17:00–19:00

FW4F • Beyond Qubits

President: John Sipe; Univ. of Toronto, Canada

FW4F.1 • 17:00

Temporal-Mode Selective Measurement and Purification of Quantum Light, John M. Donohue¹, Vahid Ansari¹, Markus Allgaier¹, Linda Sansoni¹, Georg Harder¹, Jonathan Roslund², Nicolas Treps², Benjamin Brecht^{3,1}, Christine Silberhorn¹; ¹Integrated Quantum Optics, Paderborn Univ., Germany; ²Laboratoire Kastler Brossel, UPMC, CNRS, ENS-PSL, CC74, France; ³Clarendon Lab, Dept. of Physics, Univ. of Oxford, UK. We employ dispersion-engineered sum-frequency generation to perform temporal-mode selective measurements on quantum light, provably manipulating the structure of multimode downconverted light and demonstrating spectral-phase sensitive seven-dimensional time-frequency quantum state tomography.

FW4F.2 • 17:15

On-chip Entangled D-level Photon States – Scalable Generation and Coherent Processing, Michael Kues¹, Christian Reimer¹, Piotr Roztock¹, Luis Romero Cortés¹, Stefania Sciarra¹, Benjamin Wetzel¹, Young Zhang¹, Alfonso Cino², Sai T. Chu³, Brent E. Little⁴, David J. Moss⁵, Lucia Caspani⁶, Jose. Azana¹, Roberto Morandotti¹; ¹INRS-EMT, Canada; ²Dept. of Energy, Information Engineering and Mathematical Models, Univ. of Palermo, Italy; ³City Univ. of Hong Kong, Dept. of Physics and Material Science, China; ⁴State Key Lab of Transient Optics and Photonics, Xi'an Inst. of Optics and Precision Mechanics, China; ⁵Swinburne Univ. of Technology, Centre for Micro Photonics, Australia; ⁶Inst. of Photonics, Dept. of Physics, Univ. of Strathclyde, UK. Exploiting a micro-cavity-based quantum frequency comb, we demonstrate the on-chip generation of high-dimensional entangled quantum states with a Hilbert-space dimensionality larger than 100, and introduce a coherent control approach relying on standard telecommunications components.

FW4F.3 • 17:30

Stimulated Emission Tomography of Hyperentangled States, Mario A. Ciampini¹, Andrea Gherardi¹, Valeria Cimini¹, John E. Sipe², Chiara Macchiavello³, Marco Liscidini³, Paolo Mataloni¹; ¹Physics, Università Roma La Sapienza, Italy; ²Physics, Univ. of Toronto, Canada; ³Università degli Studi di Pavia, Italy. We demonstrate the generation of states hyperentangled in polarization and path by non-degenerate spontaneous down conversion. We characterize them by quantum state tomography and stimulated emission tomography.

FW4F.4 • 17:45

High-dimensional Entanglement Distribution and Einstein-Podolsky-Rosen Steering Over Deployed Fiber, Catherine Lee^{1,2}, Darius Bunandar², Margaret Pavlovich¹, Matthew E. Grein¹, Ryan Murphy¹, Scott A. Hamilton¹, Dirk J. Englund², P. Ben Dixon¹; ¹Lincoln Lab, USA; ²MIT, USA. We demonstrate the generation of high-dimensional time-frequency entangled photon pair states and the preservation of entanglement after transmission across a 42-km telecom fiber by violating a high-dimensional Einstein-Podolsky-Rosen steering inequality.

CLEO: QELS-Fundamental Science

CLEO: Science & Innovations

17:00–19:00

FW4G • Plasmon-mediated Control of Light Emission

President: TBD

FW4G.1 • 17:00

Self-aligned Fabrication of Microscale Electron Column Array using Plasmonic Enhanced Photoemission, Zhidong Du¹, Ye Wen¹, Liang Pan¹; ¹Purdue Univ., USA. Microcolumns are important for parallel electron-beam lithography because of their compactness. A large array of electrostatic microcolumns is numerically optimized for our recent surface plasmon enhanced photoemission sources and demonstrated using a self-aligned fabrication process.

FW4G.2 • 17:15

Fundamental limits on spontaneous emission and energy loss of free electrons, Yi Yang¹, Aviram Massuda¹, Charles Roques-Carmes¹, Steven E. Kooi¹, Thomas Christensen¹, Steven Johnson¹, John Joannopoulos¹, Owen Miller², Ido Kaminer¹, Marin Soljacic¹; ¹MIT, USA; ²Yale Univ., USA. We derive and experimentally validate limits of electron radiation and energy loss. We show slow electrons generate stronger radiation than relativistic ones at subwavelength separations and bound states in the continuum enable order-of-magnitude radiation enhancement.

FW4G.3 • 17:30

The Role of Surface Roughness in Plasmonically Assisted Internal Photoemission Schottky Photodetectors, Meir Y. Grajower¹, Uriel Levy¹, Jacob Khurgin²; ¹Dept. of Applied Physics, The Benin School of Engineering and Computer Science, The Center for Nanoscience and Nanotechnology, Hebrew Univ. of Jerusalem, Israel; ²Dept. of Electrical and Computer Engineering, Johns Hopkins Univ., USA. We describe the positive roll of roughness in enhancing the efficiency of internal photoemission. We show that roughness provides momentum relaxation enabling the transmission of energetic electrons through the Schottky barrier between metal and silicon.

FW4G.4 • 17:45

Large radiative emission rate of deep ultraviolet emitter with hyperbolic metamaterial structure, Kun-Ching Shen^{1,2}, Chiieh Hsieh¹, Yuh-Jen Cheng¹, Din Ping Tsai^{1,2}; ¹Academia Sinica, Research Center for Applied Sciences, Taiwan; ²National Taiwan Univ., Taiwan. A large radiative emission rate of ultraviolet emitter with hyperbolic metamaterials was demonstrated, where a hybridized plasmon coupling is formed and provides a new path of the photon and thus boosts the radiative rate.

17:00–19:00

FW4H • Shaping Emission Using Metasurfaces

President: Gennady Shvets; Cornell Univ., USA

FW4H.1 • 17:00

Manipulating Smith-Purcell Radiation Polarization with Metasurfaces, Yujia Yang¹, Charles Roques-Carmes¹, Ido Kaminer¹, Aun Zaidi¹, Aviram Massuda¹, Yi Yang¹, Steven E. Kooi¹, Karl K. Berggren¹, Marin Soljacic¹; ¹MIT, USA. Swift electrons moving closely to a periodic structure can generate far-field radiation. The radiated light is usually polarized in the direction of electron propagation. We have demonstrated manipulation of this polarization with properly designed metasurfaces.

FW4H.2 • 17:15

Vortex radiation from a single emitter, Renmin Ma¹; ¹Peking Univ., China. We propose a metamaterial engineered chiral plasmonic nanocavity (CPN) that, for the first time to our knowledge, can twist single emitter radiation to vortex beams with controllable topological charge.

FW4H.3 • 17:30

Spectral and spatial shaping of Smith-Purcell radiation, Roei Remez¹, Niv Shapira¹, Charles Roques-Carmes², Romain Tirole^{2,3}, Yi Yang², Yossi Lereah¹, Marin Soljacic², Ido Kaminer^{2,4}, Ady Arie¹; ¹School of Electrical Engineering, Fleischman Faculty of Engineering, Tel Aviv Univ., Israel; ²Research Lab of Electronics, MIT, USA; ³Dept. of Physics, Faculty of Natural Sciences, Imperial College London, UK; ⁴Dept. of Electrical Engineering, Technion-Israel Inst. of Technology, Israel. The Smith-Purcell effect is observed when an electron beam passes in the vicinity of a periodic structure. We propose a method to shape the spatial and spectral far-field radiation using complex periodic and aperiodic gratings.

FW4H.4 • 17:45

Strong Coupling of Dye Molecules and Cavities: Beyond First Excited State Resonances, Ekemba K. Tanyi¹, Erin Harrison^{2,3}, Cansu On¹, Mikhail A. Noginov¹; ¹Center of Materials Research, Norfolk State Univ., USA; ²Dept. of Psychology and Brain Science, Univ. of Delaware, USA; ³Center of Materials Research, Summer Research Program, Norfolk State Univ., USA. In example of Fabry-Perot cavities filled with dye molecules, we studied a range of strong coupling phenomena in complex systems with multiple exciton and optical resonances, bringing applications of these exciting systems one step closer.

17:00–19:00

SW4I • Silicon Hybrid Integration

President: Shota Kita; Nippon Telegraph & Telephone Corp, Japan

SW4I.1 • 17:00 **Invited**

Monolithic Integration of 1.3 μm III-V Quantum-Dot Lasers on Si for Si Photonics, Huiyun Liu¹; ¹Univ. College London, UK. Quantum-dot (QD) lasers directly grown on Si are the prospective candidate to realize on-chip optical sources for Si photonics. In this paper, the recent progress made in field of Si-based QDs lasers are discussed.

SW4I.2 • 17:30

A Deuterium-Passivated Amorphous Silicon Platform for Stable Integrated Nonlinear Optics, Peter Girouard¹, Lars H. Frandsen¹, Michael Galili¹, Leif K. Oxenlowe¹; ¹DTU Fotonik, Denmark. We report a method to create amorphous silicon waveguides passivated with deuterium and demonstrate stability under moderate continuous-wave power. The waveguides have nonlinear properties comparable to hydrogenated amorphous silicon.

SW4I.3 • 17:45

Gain Characterization and Parameter Extraction of 1.3 μm InAs Quantum Dot Lasers on Silicon, Zeyu Zhang¹, Daehwan Jung¹, Justin Norman¹, Pari Patel¹, Arthur Gossard¹, John E. Bowers¹; ¹UCSB, USA. We report the current and wavelength dependence of gain and transparency current for a variety of quantum dot laser structures. The dependence on number of quantum dot layers and templates for growth are reported.

CLEO: Science & Innovations

17:00–19:00

SW4J • Advanced Microscopy Methods*Presider: Emily Gibson; Univ. of Colorado at Boulder, USA*SW4J.1 • 17:00 **Invited**

Longitudinal Intravital Multi-Photon Imaging of the Femoral Marrow Based on an Implanted GRIN Microendoscope, Raluca Niesner¹; ¹DRFZ, Berlin, Germany. The development of mechano-optical systems which enable highly resolved, dynamic imaging of the bone marrow of long bones is mandatory to understand patho-physiologic phenomena within this important organ. Here we present a longitudinal intravital microendoscopic technology based on GRIN optics to image one and the same region of the mouse femoral bone marrow over up to 158 days.

SW4J.2 • 17:30

Experimental Demonstration of Double Moiré Structured Illumination Microscopy, Doron Shterman¹, Bergin Gjonaj¹, Guy Bartal¹; ¹Electrical Engineering, Technion - Israel Inst. of Technology, Israel. ~ 4 fold resolution enhancement is demonstrated experimentally, with respect to a low NA capabilities, utilizing a novel Double Moiré Structured Illumination Microscopy (DM-SIM) scheme

SW4J.3 • 17:45

Stimulated emission depletion microscopy with polarization-maintaining fiber, Brendan M. Heffernan¹, Stephanie A. Meyer², Diego Restrepo⁵, Mark E. Siemens⁴, Emily A. Gibson², Juliet Gopinath^{3,1}; ¹Univ. of Colorado, Boulder, USA; ²Bioengineering, Univ. of Colorado, Denver, USA; ³Electrical, Computer, and Energy Engineering, Univ. of Colorado, Boulder, USA; ⁴Physics and Astronomy, Denver Univ., USA; ⁵Cell and Developmental Biology, Univ. of Colorado, Denver, USA. Sub-diffraction limited fluorescent images using a fiber-based stimulated emission depletion (STED) microscope are reported. Both excitation and depletion beams are transported through polarization-maintaining fiber and a lateral resolution of 100nm has been achieved.

17:00–19:00

SW4K • Fiber Lasers and Amplifiers*Presider: Gregory Cowle; Lumentum, USA*

SW4K.1 • 17:00

Femtosecond Laser Pulse Generation from Picosecond Laser Source with Self-Similar Amplification, Huanyu Song¹, Wei Chen¹, Youjian Song¹, Minglie Hu¹, Bowen Liu¹; ¹Tianjin Univ., China. We demonstrated femtosecond laser pulse generation from a self-similar amplifier with picosecond laser which delivers ~8-ps pulses with ~0.9-nm bandwidth. The system outputs 87-fs pulses at 30-MHz repetition rate with 4.5-W average power.

SW4K.2 • 17:15

Generation of Wavelength-Tunable Picosecond Pulses with Polarization-Maintaining Yb Figure-Nine Laser for Stimulated Raman Scattering Microscopy, Takuya Asai¹, Hironobu Yoshimi¹, Jingwen Shou¹, Toshiro Fujita¹, Yasuyuki Ozeki¹; ¹The Univ. of Tokyo, Japan. We present an environmentally stable, high-speed wavelength-tunable laser system with a tunability of >280 cm⁻¹. This laser is synchronized to a picosecond Ti:sapphire laser to demonstrate video-rate hyperspectral stimulated Raman imaging of polymer beads.

SW4K.3 • 17:30

Nonlinear Characterization of a Kilowatt-class Amplifier Based on Laser Gain Competition, Brian Anderson¹, Nader A. Naderi¹, Angel Flores¹; ¹AFRL, USA. The scalability of dual wavelength laser gain competition for the design of beam combinable, high power fiber amplifiers is analyzed by characterizing the nonlinear phase accumulated due to self and cross-phase modulation.

SW4K.4 • 17:45

Cladding-Pumped Hybrid Single-and Higher-Order-Mode (HOM) Amplifier, Kazi S. Abedin¹, Raja Ahmad¹, Anthony DeSantolo¹, Jeffrey Nicholson¹, Paul Westbrook¹, Clifford Headley¹, David DiGiovanni¹; ¹OFS Labs, USA. We demonstrate a cladding-pumped hybrid-amplifier for low-power input seed-signals, by concatenating single-mode and HOM Yb-fibers. An 115mW average-power pulsed-source (8ns, 250kHz) was amplified to 52W output, using a 120W, 975nm multimode-pump, yielding 57% slope-efficiency.

17:00–19:15

SW4L • NIR Dual Combs*Presider: Jérôme Genest, Université Laval, Canada*SW4L.1 • 17:00 **Invited**

Length, Time, and Frequency Metrology with Dual Frequency Combs, Katja Beha¹, Wolfgang Hänsel¹, Michele Giunta^{1,2}, Florian Pollinger³, Tobias Meyer³, Ulli Angermüller¹, Matthias Lezius¹, Ronald Holzwarth^{1,2}; ¹Menlo Systems GmbH, Germany; ²Max Planck Inst. of Quantum Optics, Germany; ³Physikalisch-Technische Bundesanstalt, Germany. We present two applications of dual-comb spectroscopy: Real-time precision ranging and high-resolution spectroscopy of acetylene. The measurement system consists of two ultra-low noise optical frequency combs.

SW4L.2 • 17:30

High-speed ultra-broadband dual-comb spectroscopy using electro-optics, David R. Carlson¹, Dan Hickstein¹, Scott Diddams¹, Scott Papp¹; ¹Time & Frequency Division, NIST, USA. Using 10-GHz electro-optic frequency combs and photonic-waveguide supercontinuum, we demonstrate dual-comb spectroscopy across 120 THz of bandwidth in the near infrared with a 32 kHz interferogram refresh rate.

SW4L.3 • 17:45

Hybrid dual comb spectroscopy with largely dissimilar FSR, Hao Liu¹, Shu-Wei Huang^{2,1}, Jinghui Yang¹, Mingbin Yu³, Dim-Lim Kwong³, Chee-Wei Wong¹; ¹UCLA, USA; ²Univ. of Colorado, Boulder, USA; ³The Inst. of Microelectronics, Singapore. We report a novel hybrid dual comb by combining two frequency combs with 19.5GHz and 250MHz repetition rates, respectively, which retains high spectral resolution and large spectral range simultaneously, proved by preliminary characterizations.

CLEO: Science & Innovations

CLEO: Applications
& Technology

17:00–19:00

SW4M • Application of Microresonator Frequency Combs

Presider: Yoshitomo Okawachi; Columbia Univ., USA

SW4M.1 • 17:00

Soliton Microcombs at Gigahertz-Repetition-Rates, Myoung-Gyun Suh¹, Kerry Vahala¹; ¹California Inst. of Technology, USA. Soliton microcombs with repetition rates as low as 1.86 GHz are demonstrated. Low repetition rate frequency combs are important in spectroscopy and relax requirements on comb processing electronics.

SW4M.2 • 17:15

Deterministic single soliton generation via mode-interaction in microresonators, Chengying Bao¹, Yi Xuan¹, Daniel E. Leaird¹, Stefan Wabnitz², Minghao Qi¹, Andrew M. Weiner¹; ¹Purdue Univ., USA; ²Università di Brescia and INO-CNR, Italy. We show that a strong mode-interaction in microcavities can trigger single soliton Kerr combs deterministically. The soliton number tends to be reduced to 1 to decrease the nonlinear loss into mode-interaction induced Cherenkov radiation.

SW4M.3 • 17:30

On-Chip Kerr Frequency Comb Generation in Lithium Niobate Microresonators, Cheng Wang¹, Mian Zhang¹, Rongrong Zhu^{1,2}, Han Hu^{1,2}, Hongsheng Chen², Marko Loncar¹; ¹Harvard Univ., USA; ²Zhejiang Univ., China. We demonstrate Kerr frequency comb generation in high quality factor, dispersion engineered lithium niobate microresonators. The generated combs span over 250 nm in the telecommunication wavelength range.

SW4M.4 • 17:45

Thermally self-stabilized single dissipative Kerr soliton in optical microresonator, Zhe Kang¹, Feng Li¹, Jinhui Yuan¹, Xianting Zhang¹, P. K. A. Wai¹; ¹Hong Kong Polytechnic Univ., Hong Kong. We deterministically excited thermally self-stabilized single dissipative Kerr soliton in a microresonator using an energetic trigger pulse. The soliton automatically balances the thermal perturbation and is stabilized without any active thermal compensation.

17:00–19:00

SW4N • Ultrafast Phenomena

Presider: Lawrence Shah; Luminar Technologies, Inc., USA

SW4N.1 • 17:00

Electric-field induced second-harmonic generation of femtosecond laser pulses in atmospheric air, Gunter Steinmeyer^{1,2}; ¹Max Born Inst., Germany; ²Inst. of Physics, Humboldt-Universität, Germany. We demonstrate frequency-doubling of an amplified femtosecond laser with electric-field induced second-harmonic generation in air. The method promises application with unattenuated terawatt lasers and offers wavelength conversion beyond the ultraviolet limit of nonlinear crystals.

SW4N.2 • 17:30

Phase Lock in Four-Wave Raman Mixing in the Ultraviolet Region, Yoshifumi Mori¹, Totaro Imasaka¹; ¹Kyushu Univ., Japan. Raman emissions generated by four-wave mixing in hydrogen were coherently phased against the probe beam emitting at 267 nm by molecular phase modulation induced by a two-color pump beam emitting at 800/1200 nm.

SW4N.3 • 17:45

Demonstration of Subluminal and Superluminal Group Velocities of Diffraction-Free Space-Time Light Sheets in Free Space, Hasan E. Kondakci¹, Ayman Abouraddy¹; ¹CREOL, Univ. of Central Florida, USA. We report on an experimental study to control the group velocity of diffraction-free space-time light sheets propagating in free space. We demonstrate pulsed light sheets with speeds exceeding 30c and going below 0.5c. We also show space-time light sheets with negative group velocity.

17:00–19:00

AW4O • Novel Laser Characterization

Presider: Paul Williams; NIST, USA

AW4O.1 • 17:00

Process-oriented adaptive optics control method in the multi-pass amplifiers, Qiao Xue¹; ¹Research Center of Laser Fusion, China. We propose and demonstrate the process-oriented adaptive optics wavefront control method. The experiments validate that the novel approach can effectively prevent the beam quality from worsening and ensure the successful reality of multi-pass amplification.

AW4O.2 • 17:15

Multiplexed Two-color Phase-and-amplitude Characterization of Harmonic Up-conversion in OAM Beams using Ptychography, Yuka Esashi¹, Bin Wang¹, Nathan Brooks¹, Kevin Dorney¹, Chen-Ting Liao¹, Carlos Hernandez-Garcia², Henry Kapteyn¹, Daniel Adams¹, Margaret Murnane¹; ¹Univ. of Colorado at Boulder, USA; ²Universidad de Salamanca, Spain. We present high-resolution, simultaneous two-color phase-and-amplitude characterization of 2nd harmonic up-conversion in OAM beams by ptychography. We measure topological charge conservation during 2nd harmonic generation process, which can be extended to high-order harmonic upconversion.

AW4O.3 • 17:30

Beam Quality Factor Analysis of On-Wafer Vertical Cavity Surface Emitting Lasers, Kirk A. Ingold¹, Joshua Tate¹, Joshua B. Groen¹, Brian Souhan¹, James Raftery¹; ¹Photonics Research Center, USA Military Academy, USA. We report on a method for analyzing the beam quality factor of on-wafer vertical cavity surface emitting lasers (VCSEL) leading to an M² min-max for each measured device due to asymmetry in the beam profile.

AW4O.4 • 17:45

Polarimetry Using Graphene-Integrated Anisotropic Metasurface, Minwoo Jung¹, Shourya Dutta-Gupta², Gennady Shvets³; ¹Dept. of Physics, Cornell Univ., USA; ²Materials Science and Metallurgical Engineering, Indian Institute of Technology Hyderabad, India; ³School of Applied and Engineering Physics, Cornell Univ., USA. We have demonstrated polarimetry using an anisotropic metasurface on gate-tunable monolayer graphene as an electro-optic modulator. Operating by electric gate-tuning, our device measures polarization ellipse of mid-infrared light and successfully distinguishes two circular polarization states.

Joint

CLEO: Science & Innovations

17:00–19:00
JW4P • Symposium on New Advances in Adaptive Optics Retinal Imaging II
Presider: TBD

17:00–19:00
SW4Q • Novel Semiconductor Emitters
Presider: Qing Gu; The Univ. of Texas at Dallas, USA

JW4P.1 • 17:00 **Invited**
Adaptive Optics Scanning Laser Ophthalmoscopy in Retinal Degenerations: New Insights in Structure and Function, Jacque Duncan¹; ¹*Ophthalmology, Univ. of California San Francisco, USA*. Retinal degenerations cause progressive death of photoreceptors. Imaging photoreceptors in eyes with retinal degeneration yields insights into how genetic mutations affect photoreceptor structure and function. High-resolution images can provide sensitive measures of photoreceptor survival.

SW4Q.1 • 17:00
Demonstration of Electrically Injected Parity-Time-Symmetric Microring Lasers, William Hayenga¹, Enrique Sanchez Cristobal¹, Hipolito Garcia-Gracia¹, Midya Parto¹, Hossein Hodaie¹, Jinhan Ren¹, Patrick LiKamWa¹, Demetrios N. Christodoulides¹, Mercedeh Khajavikhan¹; ¹*Univ. of Central Florida, CREOL, USA*. Single-mode lasing is demonstrated in an electrically injected coupled microring arrangement at telecommunication wavelengths by exploiting the unique physics associated with parity-time-symmetry.

SW4Q.2 • 17:15
Electro-Optical Bistability in Semiconductor Laser, Curtis Wang¹, Milton Feng¹, Nick Holonyak, Jr.¹; ¹*Electrical Engineering, Univ. of Illinois at Urbana-Champaign, USA*. Optical bistability in a single semiconductor transistor laser are realized and demonstrated based on the modulation of cavity photon density via the base quantum-wells for photon-generation and collector intra-cavity photon assisted tunneling for photon-absorption.

SW4Q.3 • 17:30 **Invited**
Optimized photonics: from on-chip nonclassical light sources to circuits, Jelena Vuckovic¹; ¹*Stanford Univ., USA*. Quantum emitters in semiconductors, such as quantum dots and color centers, have been used to demonstrate nonclassical light sources with high purity, indistinguishability, and efficiency. Further improvements can be achieved by employing photonics optimization techniques.

JW4P.2 • 17:45 **Invited**
Progress on functional retinal imaging with OCT: recent advancements in measurements and modeling of photoreceptor optophysiology, Robert J. Zawadzki^{1,2}; ¹*Ophthalmology & Vision Science, Univ. of California Davis, USA*; ²*Cell Biology and Human Anatomy, Univ. of California Davis, USA*. I will review recent advances in the development of Optical Coherence Tomography based retinal imaging systems in the context of its applications to study light-induced functional responses of the retina.

CLEO: Science & Innovations

SW4A • High-Q Microcavities—Continued

SW4A.4 • 18:00

High Q AlGaAs-On-Sapphire Microresonators, Yi Zheng¹, Minhao Pu¹, Hitesh K. Sahoo¹, Elizaveta Semenova¹, Kresten Yvind¹; ¹Technical Univ. of Denmark, Denmark. We demonstrate an AlGaAs-on-sapphire (AlGaAsOS) microresonator with intrinsic quality factor(Q) as high as 460,000 and investigate the thermal property of this platform. The realization of the AlGaAsOS platform opens new prospects for AlGaAs devices applications in the mid-infrared wavelength range.

SW4A.5 • 18:15

Droplet-Induced Optical Resonator in a Silica Microcapillary, Tabassom Hamidfar^{2,1}, Kirill Tokmakov², Brian Mangan³, Robert Windeler³, Artemiy Dmitriev^{4,2}, Dashiell Vitullo², Pablo Bianucci¹, Misha . Sumetsky²; ¹Concordia Univ., Canada; ²Aston Univ., UK; ³OFS Labs, USA; ⁴Univ. of Birmingham, UK. We show that light circulating in a silica microcapillary can be fully localized by evanescent coupling to a water droplet forming a high Q-factor microresonator. The discovered phenomenon suggests an advanced method for microfluidics sensing.

SW4A.6 • 18:30

Differential Tuning of Coupled SNAP Microresonators on a Capillary Surface, Dashiell L. Vitullo¹, Sajid Zaki¹, Gabriella Gardosi¹, Brian Mangan², Robert Windeler², Michael Brodsky³, Misha . Sumetsky¹; ¹Aston Univ., UK; ²OFS Labs, USA; ³U. S. Army Research Lab, USA. We fabricate two coupled SNAP microresonators on the surface of a capillary fiber and demonstrate fine differential tuning near the resonance anticrossing point by heating with a nonuniformly-etched metal wire positioned inside the capillary.

SW4A.7 • 18:45

Phase-locked Two-Color Soliton Microcombs, Gregory Moille^{1,2}, Qing Li^{1,2}, Sangsik Kim³, Kartik Srinivasan¹; ¹CNST, National Inst. of Standards and Technology, USA; ²Maryland NanoCenter, Univ. of Maryland, USA; ³Dept. of Electrical and Computer Engineering, Texas Tech Univ., USA. We design a dispersion-engineered Si₃N₄ microresonator to support two-color soliton states. The directly-pumped 1550 nm soliton is phase-locked to a second color whose center wavelength can be tailored between 750 nm to 3000 nm.

SW4B • Nitride-based Integrated Photonics—Continued

SW4B.4 • 18:00

Dispersion Engineering of High-Q Si₃N₄ Microdisk Resonators, Kaiyi Wu¹, Andrew W. Poon¹; ¹HKUST, Hong Kong. We demonstrate Si₃N₄ waveguide-coupled microdisk resonators with a loaded Q-factor of 2.4×10^6 at 1550 nm. We tailor the cavity dispersion by increasing the Si₃N₄ microdisk thickness and using a thin oxide cladding.

SW4B.5 • 18:15

Long-Range Static and Dynamic Thermal Crosstalk in Silicon-Nitride (SiNx) Photonic Integrated Circuits, Siva Yegnanarayanan¹, Ryan Maxson¹, Cheryl Sorace-Agaskar¹, Dave Kharas¹, Paul W. Juodawlkis¹; ¹Massachusetts Inst of Tech Lincoln Lab, USA. We experimentally investigate long-range (> 1-mm) static and dynamic thermal crosstalk in a silicon-nitride photonic integrated circuit (PIC) platform and identify a thermal crosstalk floor that depends strongly on modulation frequency and buried oxide thickness.

SW4B.6 • 18:30

High-Quality Hybrid Double-layer-Silicon on Silicon Nitride Platform for Integrated Photonic Applications, Tianren Fan¹, Hesam Moradinejad¹, Amir H. Hosseinnia¹, Xi Wu¹, Ali Asghar Eftekhari¹, Ali . Adibi¹; ¹Georgia Inst. of Technology, USA. We demonstrate a hybrid double-layer-crystalline-silicon on silicon nitride platform formed by a two-step of bonding process. We report high Q of 400,000 for a 40 μm radius microresonator in the platform using evanescent coupling between different layers.

SW4B.7 • 18:45

Polarization-Independent Silicon Nitride 3-dB Coupler for Potential Matrix Switches Application, Jijun Feng¹, Xiaoyu Sun¹, Ryoichi Akimoto², Heping Zeng³; ¹Univ. of Shanghai for Sci.&Technol., China; ²National Inst. of Advanced Industrial Science and Technology, Japan; ³East China Normal Univ., China. A polarization-independent 3-dB coupler was experimentally demonstrated with a 580-nm-thick, 700-nm-wide Si₃N₄ waveguide. By consisting a MZI structure, both TE and TM light can output from the cross port, confirming the polarization-independent performance of the device.

SW4C • Optical Switching—Continued

SW4C.5 • 18:00

Optically switched 56 Gb/s PAM-4 using a hybrid InP-TriPLEX integrated tunable laser based on silicon nitride micro-ring resonators, Colm Browning¹, Marco Ruffini², Yi Lin¹, Roelof Timens³, Douwe Geuzebroek³, Chris Roeloffzen³, Dimitri Geskus³, Ruud Oldenbeuving³, Rene Heideman³, Youwen Fan⁴, Klaus Boller³, Liam Barry¹; ¹Dublin City Univ., Ireland; ²Trinity College Dublin, Ireland; ³LioniX International, Netherlands; ⁴Univ. of Twente, Netherlands. Tunable lasers are key elements for switching fabrics in future datacenter networks. Experimental results show transmission of 56 Gb/s PAM-4 data in a switching environment using an integrated silicon nitride micro-ring resonator based tunable laser.

SW4C.6 • 18:15

On-chip 2x2 four-mode global optical mode switch, Ting Zhou^{1,2}, Lin Yang^{1,2}, Hao Jia^{1,2}, Shanglin Yang^{1,2}, Jianfeng Ding¹, Xin Fu^{1,2}, Lei Zhang^{1,2}; ¹Institute of semiconductor, CAS, China; ²College of Materials Science and Opto-Electronic Technology, Univ. of Chinese Academy of Sciences, China. We proposed a general architecture for on-chip global optical mode switching. A silicon thermo-optic 2x2 four-mode optical switch capable of performing the global optical mode switch functionality is experimentally demonstrated.

CLEO: Science & Innovations

SW4D • Novel THz Techniques—Continued

SW4D.4 • 18:00

Terahertz Light Amplification by Current-Driven Plasmon Instabilities in Graphene, Stephane Boubanga-Tombet¹, Deepika Yadav¹, Wojciech Knap², Vyacheslav Popov³, Taiichi Otsuji¹, ¹RIEC, Tohoku Univ., Japan; ²Lab Charles Coulomb, Univ. of Montpellier and CNRS, France; ³Kotelnikov Inst. of Radio Engineering and Electronics (Saratov Branch), Russian Academy of Sciences, Russia. This paper reports on room-temperature frequency tunable terahertz light amplification by current-driven plasmon instabilities produced in a graphene metasurface implemented in an asymmetric dual-grating-gate graphene field effect transistor.

SW4D.5 • 18:15

Fast Differential Absorption Measurement with Self-Frequency-Switched Double Terahertz-Wave Pulse, Yuma Takida¹, Toshiyuki Ikeo², Kouji Nawata¹, Yasuhiro Higashi², Hiroaki Minamide¹, ¹RIKEN, Japan; ²RIKOH COMPANY, LTD, Japan. We demonstrate fast differential absorption measurement by using self-frequency-switched double terahertz (THz)-wave pulse with 11-GHz center frequency difference and 200- μ s time interval. Our system is capable of detecting the THz-wave differential absorption signal every 20 milliseconds.

SW4D.6 • 18:30

Active high-Q dielectric terahertz supercavities, Hansong Han^{1,2}, Longqing Cong^{1,2}, Yogesh Srivastava^{1,2}, Bo Qiang^{3,2}, Mikhail Rybin^{5,4}, Wenxiang Lim^{1,2}, Qijie Wang³, Yuri S. Kivshar^{6,5}, Ranjan Singh^{1,2}, ¹School of Physical and Mathematical Science, Nanyang Technological Univ., Singapore; ²Centre for Disruptive Photonic Technologies, The Photonics Inst., Nanyang Technological Univ., Singapore; ³Nanyang Technological Univ., School of Electrical and Electronic Engineering & The Photonics Inst., Singapore; ⁴Ioffe Inst., Russia; ⁵Dept. of Nanophotonics and Metamaterials, ITMO Univ., Russia; ⁶Nonlinear Physics Center, Australian National Univ., Australia. We report the observation of extremely high-quality factors in all-dielectric subwavelength terahertz metasurfaces. We further demonstrate an active ultrafast switching of the high-Q resonances via direct optical excitation of the supercavities.

SW4D.7 • 18:45

Extraordinary Optical Reflection and Giant Goos-Hänchen Effect from a Periodic Array of Thin Metal Plates, Wei Zhang¹, Rajind Mendis¹, Aaron Charous¹, Masaya Nagai², Daniel M. Mittleman¹, ¹School of Engineering, Brown Univ., USA; ²Graduate School of Engineering Science, Osaka Univ., Japan. We theoretically and experimentally study the optical properties of a periodic array of thin metal plates at THz frequencies. Narrow extraordinary optical reflection resonances and a giant Goos-Hänchen effect are observed in the structure.

CLEO: QELS-Fundamental Science

FW4E • Quantum and Nonlinear Phenomena—Continued

FW4E.4 • 18:00

Wavefront Analysis of White-light Supercontinuum, Emma Kueny^{1,2}, Anne-Laure Calendron^{1,3}, Xavier Levecq⁴, Nadezda Varkentina⁴, Joachim Meier^{1,2}, Franz X. Kaertner^{1,2}, ¹Deutsches Elektronen Synchrotron (DESY), Germany; ²Dept. of Physics, Universität Hamburg, Germany; ³The Hamburg Centre for Ultrafast Imaging, Universität Hamburg, Germany; ⁴Imagine Optic, France. The characterization of the wavefront of a white-light supercontinuum generated by sub-picosecond pulses in YAG at 1030 nm shows a good quality and little dependence on the wavelength.

FW4E.5 • 18:15

Noise-seeded Backward Stimulated Raman Scattering in Gas-filled Hollow-Core Fibers, Manoj K. Mridha¹, David Novoa¹, Philip S. Russell¹, ¹Russell Division, Max Planck Inst. for the Science of Light, Germany. We study, experimentally and theoretically, noise-seeded backward SRS in gas-filled hollow-core fibers. The spatio-temporal dynamics of the Raman coherence makes the backward Stokes signal stronger than the forward, despite a low backward/forward gain ratio.

FW4E.6 • 18:30

Tailor-made Raman-resonant four-wave-mixing processes and their applications to optical devices, Masayuki Katsuragawa^{1,2}, Chiaki Ohae^{1,2}, Jian Zheng¹, Masaru Suzuki¹, Kaoru Minoshima^{1,2}, ¹Univ. of Electro-Communications, Japan; ²ERATO, MINOSHIMA Intelligent Optical Synthesizer Project, JST, Japan. We theoretically and experimentally show the tailor-made Raman-resonant four-wave-mixing process. We also demonstrate an attractive application of this tailored nonlinear frequency mixing as an optical device, namely, nonlinear Mach-Zehnder interferometer in the frequency domain.

FW4E.7 • 18:45

Pressure-Tunable Third Harmonic Generation in Tapered Solid-Core Fiber, Jonas Hammer^{1,2}, Riccardo Pennetta¹, Philip S. Russell^{1,2}, Nicolas Y. Joly^{1,2}, ¹Max-Planck Inst., Germany; ²Univ. of Erlangen-Nuremberg, Germany. Third-harmonic phase-matching in tapered silica fiber is tuned by introducing a high pressure gas around the taper waist. This offers a new means of achieving precise control over the dispersion in tapered fibers.

FW4F • Beyond Qubits—Continued

FW4F.5 • 18:00

Demonstration of Adaptive Optics Compensation for Emulated Atmospheric Turbulence in a Two-Orbital-Angular-Momentum Encoded Free-Space Quantum Link at 10 Mbits/s, Cong Liu¹, Kai Pang¹, Yongxiong Ren¹, Jia-peng Zhao², Guodong Xie¹, Yinwen Cao¹, Hao Song¹, Zhe Zhao¹, Haoqian Song¹, Long Li¹, Runzhou Zhang¹, Jing Du¹, Seyed M. Rafsanjani², Guillaume Labroille³, Pu Jian³, Dmitry Starodubov¹, Robert Boyd², Moshe Tur⁴, Alan E. Willner¹, ¹Univ. of Southern California, USA; ²The Inst. of Optics, Univ. of Rochester, USA; ³CALabs, France; ⁴School of Electrical Engineering, Tel Aviv Univ., Israel. We experimentally demonstrate adaptive-optics compensation of emulated atmospheric turbulence for an OAM-based quantum communication link with a classical Gaussian beam used as probe. The turbulence-induced quantum-symbol-error-rate is reduced by $\approx 76\%$ with the compensation.

FW4F.6 • 18:15

Detection of Orbital Angular Momentum of Light Using Cavity Optomechanics, Hamidreza Kaviani^{1,2}, Marcellu Wu^{1,2}, Aaron Hryciw^{2,3}, Roohollah Ghobadi¹, Sonny Vo⁴, David Fattal⁴, Paul E. Barclay^{1,2}, ¹Inst. for Quantum Science and Technology, Univ. of Calgary, Canada; ²NRC-National Inst. for Nanotechnology, Canada; ³nanoFAB, Univ. of Alberta, Canada; ⁴Leia Inc., USA. We introduce a nanoscale cavity-optomechanical device for non-destructively measuring the orbital angular momentum of light (OAM) by detecting torque on a subwavelength grating. The device can measure the torque produced by a change $\Delta l = 1$ in OAM from a beam with power $P_{\min} \sim 2$ mW at $T=4$ k.

FW4F.7 • 18:30

Single-shot measurement of the orbital-angular-momentum spectrum of light, Girish Kulkarni¹, Rishabh Sahu¹, Omar Magana-Loaiza², Robert Boyd², Anand Jha¹, ¹Indian Inst. of Technology, Kanpur, India; ²Univ. of Rochester, USA. We propose a single-shot scheme to measure the orbital-angular-momentum (OAM) spectrum of a partially coherent field. We first test the scheme for a known field, and then use it to measure the OAM spectrum of the signal-idler field from parametric down-conversion with Schmidt number $K=82.1$.

FW4F.8 • 18:45

Generation and Detection of 256 Photonic Quantum States Using Deformable-Mirror-Based Adaptive Optics and Its Application to Quantum Secure Authentication, Naoto Namekata¹, Masahito Ohya¹, Jun Nishikawa², Shuichiro Inoue¹, ¹Nihon Univ., Japan; ²National Astronomical Observatory of Japan, Japan. 90-dimensional and spatially phase-modulated quantum states were generated and detected using deformable-mirror-based adaptive optics. The number of controllable states was increased up to 256, which enabled us to demonstrate a quantum secure authentication.

19:30–20:30 Conference Reception, Grand Ballroom

CLEO: QELS-Fundamental Science

CLEO: Science & Innovations

FW4G • Plasmon-mediated Control of Light Emission—Continued

FW4G.5 • 18:00

Plasmon Enhanced Upconversion in Water-Dispersible Metal-Insulator-Metal Nanostructures, Ananda Das¹, Chenchen Mao¹, Suehyun Cho¹, Wounjhang Park¹; ¹CU Boulder, USA. We present results on enhanced upconversion of NaYF₄:Er³⁺, Yb³⁺ nanoparticles using a metal-insulator-metal structure that can eventually be dispersed in solution. Enhancement of 1200x in photoluminescence and 3.8x in energy transfer rate is observed.

FW4G.6 • 18:15

Inhibition of the Concentration Quenching of HITC Dye in Nonlocal Plasmonic Environments, Srujana Prayakarao¹, Samantha R. Koutsares¹, Carl E. Bonner¹, Mikhail A. Noginov¹; ¹Norfolk State Univ., USA. The long-range inhibition of the luminescence concentration quenching in heavily doped HITC:PMMA polymeric films in the vicinity of lamellar hyperbolic metamaterials and metallic surfaces is tentatively explained in terms of the strong exciton-plasmon coupling.

FW4G.7 • 18:30

Manipulation of Quenching and Strong Coupling via Detuned Nanoantenna-Microresonator Hybrid Systems, Burak Gurlek^{1,2}, Vahid Sandoghdar^{1,2}, Diego Martin-Cano¹; ¹Max Planck Inst. for the Science of Light, Germany; ²Friedrich Alexander Univ. Erlangen—Nuremberg, Germany. We show that a broadband Fabry-Perot cavity can control the radiative and nonradiative channels of an emitter next to a nanoantenna and assist the emitter to enter into strong coupling regime.

FW4G.8 • 18:45

Modification of Photoluminescence via Strong Coupling of Vibronic Transitions in Organic Molecules to Surface Plasmons, Rahul Deshmukh^{1,2}, Paulo Marques¹, Anurag Panda³, Stephen R. Forrest³, Vinod M. Menon^{1,2}; ¹City College of New York, USA; ²Physics, The Graduate Center of the City Univ. of New York, USA; ³Univ. of Michigan, USA. We demonstrate redistribution of the spectral intensities of the luminescence associated with different vibronic transitions in organic molecule, Diindenoperylene through strong coupling of excitons to surface plasmons.

FW4H • Shaping Emission Using Metasurfaces—Continued

FW4H.5 • 18:00

Optical Power Limiting from Plasmonic Metasurfaces Coupled to Intersubband Transitions, Nishant Nookala¹, Peter Chang¹, Dimitrios Sounas¹, Omri Wolf¹, Stephen March¹, Seth Bank¹, Igal Brener², Andrea Alù¹, Mikhail A. Belkin¹; ¹Univ. of Texas at Austin, USA; ²Sandia National Labs, USA. We report power limiting metasurfaces based on saturable absorption of the intersubband transition in n-doped multi-quantum wells. Experimentally, we note a 20% decrease in reflectivity with an increase of the pump intensity.

FW4H.6 • 18:15

Directional Spontaneous Emission of Dye on Top of Silver Grating Metasurface, Ekembu K. Tanyi¹, Soheila Mashhad¹, Sahana Bhattacharyya², Tal Galfsky², Vinod M. Menon², Evan Simmons³, Viktor A. Podolskiy³, Natalia Noginova¹, Mikhail A. Noginov¹; ¹Center for Materials Research, NSU, USA; ²City College of New York, USA; ³Univ. of Massachusetts, USA. We have observed double crescent patterns in the TE polarized spontaneous emission of rhodamine 6G dye deposited onto silver grating metasurface. It originates from the surface wave characterized by the effective index of refraction $n=1.03$.

FW4H.7 • 18:30

Graphene Metamaterials for Intense, Tunable and Compact EUV and X-Sources, Andrea Pizzi¹, Gilles D. Rosolen², Liang Jie Wong³, Rasmus Ischebeck⁴, Marin Soljagic⁵, Thomas Feuerer⁶, Ido Kaminer^{7,8}; ¹Dept. of Applied Science and Technology, Politecnico di Torino, Italy; ²Micro and Nanophotonic Materials Group, Univ. of Mons, Belgium; ³Singapore Inst. of Manufacturing Technology, Singapore; ⁴Paul Scherrer Inst. (PSI), Switzerland; ⁵Dept. of Physics, MIT, USA; ⁶Inst. of Applied Physics, Univ. of Bern, Switzerland; ⁷Dept. of Electrical Engineering, Technion – Israel Inst. of Technology, Israel. We present a bright X-ray source based on free electron-plasmon interactions inside graphene metamaterials, showing with *ab initio* simulations how the structure scales up the intensity and the tunability of the source.

FW4H.8 • 18:45

Shaping InAs quantum dot photoluminescence using GaAs nanoresonator arrays, Aleksandr Vaskin¹, Sheng Liu², Matthias Zilk¹, Benjamin Leung², Miao-Chan Tsai², Yuanmu Yang², Polina Vabishchevich², Xiaowei He³, Younghee Kim³, Nicolai F. Hartmann³, Sadvikas Addamane⁴, Gordon A. Keeler², George Wang², Han Htoon³, Stephen Doorn³, Ganesh Balakrishnan⁴, Thomas Pertsch¹, Michael Sinclair², Igal Brener^{2,5}, Isabelle Staude¹, Stefano Fasold¹; ¹Inst. of Applied Physics, Friedrich Schiller Univ., Germany; ²Sandia National Labs, USA; ³Center for Integrated Nanotechnologies, Los Alamos National Lab, USA; ⁴Center for High Technology Materials, Univ. of New Mexico, USA; ⁵Center for Integrated Nanotechnologies, Sandia National Labs, USA. We study photoluminescence from arrays of GaAs nanoresonators incorporating self-assembled InAs quantum dots. We experimentally observe spectral and spatial reshaping of the quantum dot photoluminescence by the resonant nanostructure.

SW4I • Silicon Hybrid Integration—Continued

SW4I.4 • 18:00 **Invited**

A Hybrid SiN-QDOT Platform for Visible Photonics, Dries VanThourhout¹, Lukas Elsinger¹, Yunpeng Zhu¹, Weiqiang Xie¹, Ivo Tanghe¹, Suzanne Bisschop², Vignesh Chandrasekaran², Pieter Geiregat², Edouard Brainin², Zeger Hens²; ¹Photonics Research Group, Ghent Univ. / IMEC, Belgium; ²Physics and Chemistry of Nanostructures, Ghent Univ., Belgium. We developed a hybrid SiN-QDOT platform by embedding quantum dots in a SiN waveguide. Low loss waveguiding, high modal gain and lasing from mikrodisk and DFB-type devices was demonstrated.

SW4I.5 • 18:30

Seed-Layer Free Cerium-Doped Terbium Iron Garnet on Non-Garnet Substrates for Photonic Isolators, Karthik Srinivasan¹, Thomas E. Gage², Bethanie J. Stadler^{1,2}; ¹Electrical and Computer Engineering, Univ. of Minnesota, USA; ²Chemical Engineering and Materials Science, Univ. of Minnesota, USA. Novel seed-layer free cerium-doped terbium iron garnet with high gyrotropy is grown on non-garnet substrates for integration with photonics integrated circuits, whose performance can be tuned by varying the dopant concentration and annealing parameters.

SW4I.6 • 18:45

O-band and C/L-band emission of InAs QDs monolithically grown on Ge and U-shape Si (001) platform, Ting Wang¹; ¹Inst. of Physics, CAS, China. Here, the C/L-band light emission (1.53 μm -1.63 μm) of InAs/In_{0.25}Ga_{0.75}As quantum dots (QDs) epitaxially grown on both Ge (001) and on-axis U-shape Si (001) substrates by molecular beam epitaxy are reported.

19:30–20:30 Conference Reception, Grand Ballroom

CLEO: Science & Innovations

SW4J • Advanced Microscopy Methods—
Continued

SW4J.4 • 18:00

Localized Plasmonic Structured Illumination Microscopy, Anna Bezryadina¹, Junxiang Zhao¹, Zhaowei Liu¹; ¹Electrical and Computer Engineering, Univ. of California San Diego, USA. Localized plasmonic structured illumination microscopy (LPSIM) has tremendous ability to improve resolution of fluorescent microscopy. We analyzed and tested new approach to push resolution limit significantly below 50nm for wide-field of view high-speed biological imaging.

SW4J.5 • 18:15

Three-photon fluorescence microscopic imaging by a compact Er-doped fiber laser at 1.6 μm , Jiqiang Kang¹, Cihang Kong¹, Pingping Feng¹, Can Li¹, Zhichao Luo^{1,2}, Edmund Y. Lam¹, Kevin K. Tsia¹, Kenneth Kin-Yip Wong¹; ¹Univ. of Hong Kong, Hong Kong; ²South China Normal Univ., China. We report a high energy pulse generation scheme for three-photon fluorescence microscopy (3PM) by leveraging an L-band Er-doped fiber laser and chirped pulse amplifier. 3PM imaging is demonstrated on a mouse kidney slice.

SW4J.6 • 18:30

Adaptively Scanned Compressive Multiphoton Microscopy, Milad Alemohammad¹, Jaewook Shin¹, Mark A. Foster¹; ¹Johns Hopkins Univ., USA. A depth sectioning, compressive multiphoton microscope based on spatio-temporal focusing of patterned fs-laser pulses has been demonstrated. Adaptive fluorescence sampling is used to achieve random access imaging across a wide field of view.

SW4J.7 • 18:45

Electrowetting Prism for Scanning in Two-photon Microscopy, Omkar D. Supekar², Baris N. Ozbay¹, Mo Zohrabi³, Philip D. Nystrom², Gregory L. Futia¹, Diego Restrepo⁴, Emily A. Gibson¹, Juliet Gopinath^{3,5}, Victor Bright²; ¹Dept. of Bioengineering, Univ. of Colorado Anschutz Medical Campus, USA; ²Dept. of Mechanical Engineering, Univ. of Colorado Boulder, USA; ³Dept. of Electrical, Computer, and Energy Engineering, Univ. of Colorado Boulder, USA; ⁴Dept. of Cell and Developmental Biology, Univ. of Colorado Anschutz Medical Campus, USA; ⁵Dept. of Physics, Univ. of Colorado Boulder, USA. We have demonstrated an electrowetting prism as a lateral scanning element for a 2-photon excitation microscope. We show imaging of mouse hippocampal neurons, with a field of view of 130 \times 130 μm^2 .

SW4K • Fiber Lasers and Amplifiers—
Continued

SW4K.5 • 18:00

110 W High-Efficiency Er-Nanoparticle-Doped Fiber Laser, Huaqin Lin¹, Colin Baker², Zhimeng Huang¹, Shankar Pidishety¹, Yutong Feng¹, E. Joseph Friebele³, Ashley Burdett⁴, Dan Rhonehouse², Brandon Shaw², Jas Sanghera², Johan Nilsson¹; ¹Optoelectronics Research Centre, Univ. of Southampton, UK; ²Naval Research Lab, USA; ³KeyW Corp, USA; ⁴Univ. Research Foundation, USA. An Er-nanoparticle-doped fiber laser cladding-pumped at 975 nm generates 110 W at 1605 nm with 40.6% slope efficiency and $M^2 \sim 7$. High Er-concentration (4×10^{25} ions/m³) and pump brightness allows for adequate pump absorption even without Yb-codoping.

SW4K.6 • 18:15

1.3kW Single-mode All-fiber MOPA Based on Low-NA Trench-assisted Ytterbium-doped Fiber, Fangfang Zhang¹, Yehui Liu¹, Lei Liao¹, Yingbin Xing¹, Jinyan Li^{1,2}; ¹Wuhan National Lab for Optoelectronics (WNLO), Huazhong Univ. of Science and Technology, China; ²School of Optical and Optoelectronic Information, Huazhong Univ. of Science and Technology, China. A newly designed and fabricated trench-assisted low-NA (~ 0.04) fiber was reported. An output power up to 1.3kW with $M^2 < 1.1$ was achieved in an all-fiber MOPA based on the fabricated low-NA fiber.

SW4L • NIR Dual Combs—Continued

SW4L.4 • 18:00

Free-running, All-fiber Dual Electro-optic Frequency Comb System for the Precision Spectroscopy and Sensing of H¹³CN, Philippe Guay^{1,2}, Jérôme Genest¹, Adam J. Fleisher²; ¹Université Laval, Canada; ²National Inst. for Standards and Technology, USA. We demonstrate precision spectroscopy of H¹³CN where successive interferograms were phase-corrected in post-processing, averaged, and normalized to yield the complex transmission spectrum of several transitions within the 2_{v3} band centered near $\lambda = 1545$ nm.

SW4L.5 • 18:15

Low-Noise Dual-Comb Platform Based on Mode-Locked Lasers in a Multi-Waveguide Chip, Nicolas Bourbeau Hebert¹, David Lancaster², George Chen², Jérôme Genest¹; ¹Université Laval, Canada; ²Univ. of South Australia, Australia. We analyze the frequency noise of a free-running dual-comb source based on two adjacent waveguide lasers in the same glass chip. We demonstrate high rejection of environmental noise and an exceptionally low frequency noise floor.

SW4L.6 • 18:30

Dual Comb Spectroscopy with Free-Running Bidirectional Mode-Locked Laser at 1.9 μm , Md Imrul Kayes¹, Nurmemet Abdikerim¹, Alexandre Rekiik¹, Martin Rochette¹; ¹McGill Univ., Canada. We demonstrate a dual-comb spectrometer based on a free-running mode-locked laser that operates bidirectionally at 1.9 μm . Since both signals are emitted from a common cavity, the mutual coherence requirement for dual-comb spectroscopy is satisfied.

SW4L.7 • 18:45

Broadband Cavity-Enhanced Dual-Comb Spectroscopy of Multiple Trace Gas Species, Nazanin Hoghooghi¹, Robert Wright¹, William C. Swann², Ian R. Coddington², Nathan R. Newbury², Gregory B. Rieker¹; ¹Univ. of Colorado Boulder, USA; ²National Inst. of Standard and Technology, USA. We report compact and broadband near infrared cavity-enhanced dual-comb spectroscopy (CE-DCS) with 60 nm transmitted bandwidth and pathlength enhancement factor of 11,000 for CE-DCS. Simultaneous trace detection of four gas species is demonstrated.

19:30–20:30 Conference Reception, Grand Ballroom

CLEO: Science & Innovations

CLEO: Applications
& TechnologySW4M • Application of Microresonator
Frequency Combs—Continued

SW4M.5 • 18:00

Dual-cavity scanning comb spectroscopy, Mengjie Yu^{1,2}, Yoshitomo Okawachi¹, Chaitanya Joshi¹, Xingchen Ji^{2,3}, Michal Lipson³, Alexander L. Gaeta¹; ¹*Applied Physics and Mathematics, Columbia Univ., USA*; ²*Electrical Engineering, Cornell Univ., USA*; ³*Electrical Engineering, Columbia Univ., USA*. We present a novel approach for microresonator-based gas-phase spectroscopy without use of an external laser source. The absorption spectrum of acetylene is measured with high spectral resolution using an integrated heater in a fiber-microresonator dual-cavity scheme.

SW4M.6 • 18:15

Counter-propagating soliton frequency microcombs, Qifan Yang¹, Xu Yi¹, Ki Youl Yang¹, Kerry Vahala¹; ¹*California Inst. of Technology, USA*. Counter-propagating dissipative Kerr solitons are generated in a single silica microresonator. A relative soliton rate-locking phenomenon is observed and it provides dual-comb pulse streams with different repetition rates and a high-level of mutual coherence.

SW4M.7 • 18:30

Spatially-Multiplexed Solitons in Optical Microresonators, Erwan Lucas¹, Grigory Lihachev^{2,3}, Michael Gorodetsky^{2,3}, Tobias J. Kippenberg¹; ¹*Ecole Polytechnique Fédérale de Lausanne, Switzerland*; ²*Physics, Moscow State Univ., Russia*; ³*Russian Quantum Center, Russia*. We simultaneously create stable solitons in up to three distinct mode families of a single crystalline MgF₂ microresonator. The resulting Kerr combs are mutually coherent and have distinct repetition rates and are thus well suited for dual-comb applications.

SW4N • Ultrafast Phenomena—Continued

SW4N.4 • 18:00

Self-Healing Property of Space-Time Light Sheets, Hasan E. Kondakci¹, Ayman Abouraddy¹; ¹*CREOL, Univ. of Central Florida, USA*. We experimentally demonstrate self-healing of diffraction-free space-time light sheets propagating through one-dimensional beam blocks. Diffraction-free space-time beams are produced by introducing hyperbolic correlations in their spatio-temporal spectra.

SW4N.5 • 18:15

Mid-IR Ultrafast Carrier Dynamics in Black Phosphorus Observed Above and Below the Bandgap, Yigit Aytac¹, Martin Mittendorff¹, Thomas E. Murphy¹; ¹*Univ. of Maryland, USA*. We employ pump-probe measurements to study the carrier dynamics in layers of black phosphorus. By tuning the probe wavelength above and below the bandgap we unambiguously quantify the interband and intraband transitions and relaxation rates.

SW4N.6 • 18:30

The Picoseconds Structure of Ultrafast Rogue Waves, Moti Fridman¹; ¹*Bar Ilan Univ., Israel*. We suggest a new mechanism for ultrafast rogue waves in fiber lasers. We claim that ultrafast patterns arise from the non-instantaneous relaxation of the saturable absorber together with the polarization mode dispersion of the cavity.

SW4N.7 • 18:45

Single Shot Magnetization Reversal of Micron Size Magnetic Domains in a Pt/Co/Pt Ferromagnetic Stack, Mircea Vomir¹, Michèle Albrecht¹, Gilles Versini¹, Jean-Yves Bigot¹; ¹*Université de Strasbourg and CNRS, France*. We show that the magnetization reversal of a Pt/Co/Pt ferromagnetic stack can be triggered by a single femtosecond laser pulse if the switched spot is comparable to the size of the intrinsic magnetic domains.

AW4O • Novel Laser Characterization—Continued

AW4O.5 • 18:00

Metasurface-integrated Fully CMOS-compatible Phase Gradient Photodetector, Evgeniy Panchenko¹, Lukas Wesemann¹, Timothy Davis¹, Daniel Gomez², Ann Roberts¹; ¹*The Univ. of Melbourne, Australia*; ²*RMIT Univ., Australia*. Here we present a fully CMOS compatible photodetector with embedded plasmonic metasurfaces capable of detecting a local phase gradient. This device could form the basis of novel wavefront sensing systems for imaging, communications and astronomy.

AW4O.6 • 18:15

Impacting Factors in Linewidth Measurement of Single-Frequency Lasers, Songsong Sun¹, Yong Wang¹, Wei Yan¹; ¹*Laser Research Inst., Qilu Univ of Technology(Shandong Academy of Sciences), China*. Linewidth measurement of single-frequency laser using self-heterodyne method is studied. 1/f noise and the noise caused by double Rayleigh scattering in delayed fiber can affect the shape of linewidth, which introduces inaccuracy in linewidth measurement.

AW4O.7 • 18:30

Experimental Access to the Instantaneous Spectrum of MEMS-Based Swept Source, John O. Gerguis², Yasser Sabry^{1,3}, Diaa Khalil^{1,3}; ¹*Faculty of Engineering, Egypt*; ²*Faculty of Engineering, Egypt*; ³*Si-Ware Systems, Egypt*. This work presents a novel technique for measuring the spectral response of high-speed swept laser using the convolution between this spectrum and a reference filter. The method is successfully used to characterize MEMS-based swept source

19:30–20:30 Conference Reception, Grand Ballroom

Joint

CLEO: Science & Innovations

JW4P • Symposium on New Advances in Adaptive Optics Retinal Imaging II—Continued

SW4Q • Novel Semiconductor Emitters—Continued

JW4P.3 • 18:30

Multimodality Imaging Guided Retichoroidal Neovascularization in a Rabbit Model, Phuc Nguyen^{2,1}, Yannis M. Paulus^{2,1}, Xueding Wang^{1,3}, Yanxiu Li^{2,1}, Wei Zhang^{1,4}; ¹Univ. of Michigan, USA; ²Dept. of Ophthalmology and Visual Sciences, Kellogg Eye Center, USA; ³Dept. of Biomedical Engineering, USA; ⁴Dept. of Radiology, University of Michigan, USA. The current study presents a novel multimodal photoacoustic microscopy (PAM), optical coherence tomography (OCT), and fluorescein angiography (FA) molecular imaging system to diagnose wet aged related macular degeneration (AMD) at an earlier stage.

SW4Q.4 • 18:00

Development of Efficient Electrically Pumped Nanolasers based on InAlGaAs Tunnel Junction, Cheng-Yi Fang¹, Felipe Vallini³, Abdelkrim El Amili³, Antti Tukiainen², Jari Lyytikäinen², Mircea D. Guina², Yeshaiahu Fainman³; ¹Materials Science and Engineering Program, UC San Diego, USA; ²Optoelectronic Research Centre, Tampere Univ. of Technology, Finland; ³Dept. of Electrical & Computer Engineering, U C San Diego, USA. We propose and experimentally demonstrate a metallo-dielectric nanolasers utilizing an InAlGaAs tunnel junction for efficient carrier injection, which reduce the complexity when optimizing the metal contact, and reduces the device resistance.

SW4Q.5 • 18:15

Electrically Pumped Metallic Coaxial Nanolasers, Enrique Sanchez Cristobal¹, William Hayenga¹, Hipolito Garcia-Gracia¹, Mohammad Parvinnezhad Hokmabadi¹, Patrick LiKamWa¹, Mercedeh Khajavikhan¹; ¹CREOL, USA. We present our progress towards the realization of room temperature current-injected coaxial nanolasers. Laser action is demonstrated in a subwavelength coaxial resonator up to a temperature of 140 K.

SW4Q.6 • 18:30

Synchronized Narrow Linewidth Laser and High Quality Microwave Signal Generation using Optically Mutual-Injection-Locked DFB Lasers with Optoelectronic Feedback, Guangcan Chen^{1,2}, Dan Lu^{1,2}, Song Liang^{1,2}, Lu Guo^{1,2}, Wu Zhao^{1,2}, Lingjuan Zhao^{1,2}; ¹CAS Inst. of Semiconductors, China; ²College of Materials Science and Opto-Electronic Technology, Univ. of Chinese Academy of Sciences, China. Synchronized dual-wavelength narrow-linewidth laser and high-quality microwave signal generation is demonstrated using mutual-injection-locked DFB lasers with optoelectronic feedback. Two synchronized lasers with linewidth down to kHz and beating frequency of 23.3 GHz is realized.

SW4Q.7 • 18:45

Mode Locking at THz Repetition Frequencies using Lasers with Phase Shifted Sampled Gratings, Lianping Hou¹, Song Tang¹, Bin Hou¹, John Marsh¹; ¹Univ. of Glasgow, UK. Mode-locking at repetition frequencies of 800 GHz and 1 THz is reported in pi-phase-shifted sampled grating distributed-Bragg-reflector (DBR) lasers. The effective coupling coefficient of the phase-shifted gratings is twice that of conventional sampled grating DBRs.

19:30–20:30 Conference Reception, Grand Ballroom

Executive Ballroom
210AExecutive Ballroom
210BExecutive Ballroom
210C

CLEO: Science & Innovations

08:00–10:00

STh1A • Novel Structures and Devices*Presider: Takasumi Tanabe; Keio Univ., Japan***STh1A.1 • 08:00**

3D-Printed Ultra-Broadband Highly Efficient Out-of-Plane Coupler for Photonic Integrated Circuits, Matthias Blaicher¹, Muhammad R. Billah¹, Tobias Hoose¹, Philipp-Immanuel Dietrich¹, Andreas Hofmann¹, Sebastian Randel¹, Wolfgang Freude¹, Christian Koos¹; ¹*Karlsruhe Inst. of Technology, Germany*. We demonstrate a 3D printed ultra-broadband and highly efficient out-of-plane coupler for photonic integrated circuits. The coupling efficiency at 1550 nm is -0.8 dB with a 1 dB bandwidth exceeding 100 nm.

STh1A.2 • 08:15

Broadband Mode Router Based on Three-Dimensional Mach-Zehnder Interferometer and Waveguide Branches, Quandong Huang¹, Yunfei Wu¹, Wei Jin¹, Kin S. Chiang¹; ¹*City Univ. of Hong Kong, Hong Kong*. We demonstrate a broadband mode router based on integrating a 3D thermo-optic Mach-Zehnder interferometer and a 3D mode demultiplexer. The device can dynamically route four spatial modes of a few-mode waveguide into four single-mode waveguides.

STh1A.3 • 08:30

Multiresonant Optical Response in Quasi-3D Multilayer Metal-Insulator-Metal Nanoplasmonic Crystals, Junyeob Song¹, Wonil Nam¹, Wei Zhou¹; ¹*Virginia Tech, USA*. Quasi-3D multilayer Metal-Insulator-Metal (MIM) nanoplasmonic crystals sitting on dielectric nanopillar arrays show unique multiresonant optical response from localized and delocalized surface plasmon modes both in far-field and near-field.

STh1A.4 • 08:45

Compact Narrow-Linewidth Integrated Laser Based on Low-Loss Silicon Nitride Ring Resonator, Brian Stern^{1,2}, Xingchen Ji^{1,2}, Avik Dutt^{1,2}, Michal Lipson²; ¹*Cornell Univ., USA*; ²*Columbia Univ., USA*. We demonstrate an integrated silicon nitride/III-V laser leveraging the narrowband backreflection of a high-Q microring resonator for output coupling and feedback. We measure a 13 kHz linewidth with 1.7 mW output power around 1550 nm.

08:00–10:00

STh1B • Integrated Photonic Sensors*Presider: Qiaoqiang Gan; State Univ. of New York at Buffalo, USA***STh1B.1 • 08:00**

Mid-infrared (MIR) Mach-Zehnder Silicon Modulator at 2 μ m Wavelength based on Interleaved PN Junction, Wanjun Wang¹, Zecen Zhang¹, Xin Guo¹, Jin Zhou¹, Sia Jia B. Xu¹, Mohamed S. Rouifed¹, Chongyang Liu¹, Callum Littlejohns^{1,2}, Graham T. Reed², Hong Wang¹; ¹*Nanyang Technological Univ., Singapore*; ²*Optoelectronics Research Centre, Univ. of Southampton, UK*. In this paper, a MIR silicon modulator operating at 2 μ m wavelength is experimentally demonstrated. The modulator shows 9.7 GHz 3-dB electro-optic bandwidth at $V_{\text{bias}} = -3$ V. We also present optical modulation at 12.5 Gb/s.

STh1B.2 • 08:15

Methane Absorption Spectroscopy with a Hybrid III-V Silicon External Cavity Laser, Eric J. Zhang¹, Laurent Schares¹, Jason S. Orcutt¹, Yves Martin¹, Chi Xiong¹, Marwan Khater¹, Tymon Barwicz¹, William Green¹; ¹*IBM T. J. Watson Research Center, USA*. We present line-scanned methane absorption spectroscopy at 1656.5 nm using a multi-section hybrid III-V silicon external-cavity laser. The laser demonstrates > 2 nm tunability and single-mode operation with SMSR > 50 dB for high-resolution spectroscopy.

STh1B.3 • 08:30

Widely Tunable III-V-on-silicon Vernier Lasers Operating in the 2.3 μ m Wavelength Range, Ruijun Wang¹, Stephan Sprengel², Gerhard Boehm², Roel Baets¹, Markus Amann², Gunther Roelkens¹; ¹*Photonics Research Group, Ghent Univ.-imec, Belgium*; ²*Walter Schottky Institut, Technische Universität München, Germany*. We report widely tunable III-V-on-silicon lasers with more than 40 nm tuning range near 2.35 μ m wavelength. By combining two lasers with different distributed Bragg reflectors, a tuning range of more than 70 nm is achieved.

08:00–10:00

STh1C • Machine Learning for Communication*Presider: Francesco Da Ros; DTU Fotonik, Denmark***STh1C.1 • 08:00** **Invited**

Learning of Laser Dynamics using Bayesian Inference, Darko Zibar¹, Christian Schaeffer², Jesper Mork¹; ¹*Danmarks Tekniske Universitet, Denmark*; ²*Helmut-Schmidt-Universität, Germany*. Techniques from Bayesian machine learning and digital coherent detection are applied to perform frequency noise characterization. Significant advantage of the presented techniques are high-sensitivity and direct access to the uncertainty of the frequency noise measurement.

STh1C.2 • 08:30

Complex Neural Network Equalization of Optical SSB PAM-4 Signal in Direct-Detection Kramers-Kronig Receiver, hao ying¹, Mingyue Zhu¹, Stylianos Sygletos², Xingwen Yi^{1,3}, Jing Zhang¹, Xiatao Huang¹; ¹*Univ. of Electronics Science & Tech, China*; ²*Aston Inst. of Photonic Technologies,, Aston Univ., UK*; ³*School of Electronics and Information Technology, Sun Yat-Sen Univ., China*. We propose a complex neural network equalizer in a Kramers-Kronig receiver to process the complex signals. Improved performance is demonstrated in a transmission of 56-Gb/s optical SSB PAM-4 signal over 800-km SSMF.

STh1C.3 • 08:45

Joint Estimation of IQ Phase and Gain Imbalances Using Convolutional Neural Networks on Eye Diagrams, Stefano Savian^{1,2}, Júlio Diniz¹, Alan Pak Tao Lau³, Faisal Nadeem Khan³, Simone Gaiarin¹, Rasmus Thomas Jones¹, Darko Zibar¹; ¹*Fotonik, DTU, Denmark*; ²*Computer Science, The Free Univ. of Bozen-Bolzano, Italy*; ³*Electrical Engineering, The Hong Kong Polytechnic Univ., Hong Kong*. A machine learning-based low-cost monitoring technique for transmitter IQ phase and gain imbalances is proposed. Simulations with formats up to NRZ-64QAM (28 Gb/s) show 95%-confidence estimation within 1.5° for phase and 0.06 for gain imbalances.

Executive Ballroom
210DExecutive Ballroom
210EExecutive Ballroom
210F

CLEO: QELS-Fundamental Science

08:00–10:00

FTh1D • Nonlinear Metamaterials and Metasurfaces*Presider: Rafael Piestun; Univ. of Colorado at Boulder, USA***FTh1D.1 • 08:00****Nonlinear Tunability and Mechanical Actuation in Photonically Doped ENZ Metasurfaces**, Ehsan Nahvi¹, Inigo Liberal^{1,2}, Nader Engheta¹; ¹Univ. of Pennsylvania, USA; ²Public Univ. of Navarra, Spain. Built upon the photonic doping concept we introduced recently [Science 355, 1058 (2017)], we numerically demonstrate how nonlinearity of the single dielectric rod and its mechanical actuation enable tunability of transmission through Epsilon-Near-Zero (ENZ) metasurfaces**FTh1D.2 • 08:15****Nonlinear Manifestations of Photon Acceleration in Rapidly Evolving Semiconductor Metasurfaces**, Maxim R. Shcherbakov¹, Kevin Werner², Zhiyuan Fan¹, Noah Talisa², Enam Chowdhury², Gennady Shvets¹; ¹Cornell Univ., USA; ²The Ohio State University, USA. We report an experimental observation of photon acceleration in mid-infrared semiconductor metasurfaces manifested as blue-shifted third harmonic generation at carrier frequencies of up to 3.1 ω .**FTh1D.3 • 08:30** **Invited****Nonlinear Optics on Demand**, Haim Suchowski¹; ¹Tel Aviv Univ., Israel. Nonlinear metasurfaces expand the possibilities of optical response resulting in intriguing and rich optical phenomena. Recent advances in controlling the generation and understanding of optical nonlinearities via single and collective metasurfaces designs will be presented.

08:00–10:00

FTh1E • Nonlinear Optics in Microresonator Systems*Presider: Scott Diddams; NIST, USA***FTh1E.1 • 08:00** **Invited****Nonlinear and Quantum Optics within Whispering Gallery Mode Resonators**, Harald G. Schwefel^{1,2}, Luke S. Trainor^{1,2}, Alfredo Rueda³, Florian Sedlmeir³; ¹Univ. of Otago, New Zealand; ²Dodd-Walls Centre for Photonics and Quantum Technology, New Zealand; ³Max Planck Inst. for the Science of Light, Germany. I present the current state of nonlinear and quantum optics within WGM resonators with particular emphasis on frequency conversion. This includes electro-optic microwave to optics transduction as well as parametric photon triplet generation.**FTh1E.2 • 08:30****Polarization Effects and Nonlinear Mode Coupling in Kerr Microresonators**, Tobias Hansson¹, Martino Bernard¹, Stefan Wabnitz^{1,2}; ¹Dipartimento di Ingegneria dell'Informazione, Università degli Studi di Brescia, Italy; ²CNR-INO, Italy. We model optical frequency comb generation in the presence of nonlinear polarization effects. We make an in-depth study of the modulational instability and demonstrate the appearance of novel types of instabilities and frequency comb states.**FTh1E.3 • 08:45****Type-1 and type-2 satellites in Kerr frequency combs**, Jinghui Yang¹, Shu-Wei Huang², Zhenda Xie³, Mingbin Yu⁴, Dim-Lim Kwong⁴, Chee-Wei Wong¹; ¹Electrical Engineering, Univ. of California, Los Angeles, USA; ²Electrical, Computer & Energy Engineering, Univ. of Colorado, Boulder, USA; ³Nanjing Univ., China; ⁴Inst. of Microelectronics, Singapore. We report Kerr frequency combs with two types of satellites, enabled by multiple phase matching in microcavities. Satellite comb clusters at ≈ 1.3 mm and 2.0 mm regimes are simultaneously generated with the central comb, with a demonstrated high external conversion efficiency reaching up to 30dB.

08:00–10:00

FTh1F • Novel Phenomena in van der Waals Heterostructure*Presider: Steven Cundiff; Univ. of Michigan, USA***FTh1F.1 • 08:00****Room-temperature optoelectronic detection of valley-locked spin photocurrent in WSe₂-graphene-Bi₂Se₃ heterostructures**, Soonyoung Cha¹, Minji Noh¹, Je-hyun Kim², Jangyup Son^{2,3}, Hyemin Bae¹, Doeon Lee¹, Hoil Kim⁴, Jekwan Lee¹, Hoseung Shin¹, Sangwan Sim¹, Seunghoon Yang⁵, Chul-Ho Lee⁵, Moon-Ho Jo^{6,7}, Junsung Kim⁴, Dohun Kim², Hyunyong Choi¹; ¹Yonsei Univ., South Korea; ²Seoul National Univ., South Korea; ³Univ. of Illinois at Urbana-Champaign, USA; ⁴Postech, South Korea; ⁵Korea Univ., South Korea; ⁶Center for artificial low dimensional electronics systems, Inst. for Basic Science, South Korea; ⁷Division of Advanced Materials Science, POSTECH, South Korea. Using a lateral WSe₂-graphene-Bi₂Se₃ heterostructure, we generate the valley-locked spin photocurrent in ion-liquid gated WSe₂ transistor by the circular photogalvanic effect and extract the spin-polarized current in the Bi₂Se₃ topological insulator using the spin-momentum locking.**FTh1F.2 • 08:15****Probing Charge Transfer States in Polymer:Fullerene – MoS₂ van der Waals Heterostructures**, Christopher Petouk-hoff¹, Damien Voiry², Ibrahim Bozkurt², Manish Chowhalla², Keshav M. Dani¹; ¹Femtosecond Spectroscopy Unit, Okinawa Inst. of Science and Technology, Japan; ²Materials Science and Engineering, Rutgers Univ., USA. Using transient absorption spectroscopy, we observe the formation of long-lived charge transfer states in polymer:fullerene – MoS₂ van der Waals heterostructures at sub-picosecond timescales.**FTh1F.3 • 08:30** **Invited****2D Magnets and Heterostructures**, Xiadong Xu¹; ¹Univ. of Washington, USA. Since the discovery of graphene, the family of two-dimensional (2D) materials has grown to encompass a broad range of electronic properties. However, until recently 2D crystals with intrinsic magnetism were still lacking. In this talk, I will describe our recent magneto-optical spectroscopy experiments on van der Waals magnets, chromium(III) iodide CrI₃, and their heterostructures with other non-magnetic 2D materials.

Executive Ballroom
210G

Executive Ballroom
210H

Meeting Room
211 B/D

CLEO: QELS-Fundamental Science

CLEO: Science & Innovations

08:00–10:00

FTh1G • Integrated Quantum Sources

Presider: John Sipe; Univ. of Toronto, Canada

FTh1G.1 • 08:00

Spectrally Unentangled Photon Pairs from Microring Resonators using Pump-pulse Tailoring, Jesper B. Christensen¹, Jacob G. Koefoed¹, Colin McKinstrie¹, Karsten Rottwitt¹; ¹Technical Univ. of Denmark, Denmark. We show that a tailored pump-pulse spectrum can be used to completely eliminate spectral correlation in photon pairs generated from spontaneous four-wave mixing in nonlinear microring resonators.

FTh1G.2 • 08:15

Photonic Crystal Waveguides As Integrated Sources of Counterpropagating Factorizable Photon Pairs, Sina Saravi¹, Thomas Pertsch¹, Frank Setzpfandt¹; ¹Abbe Center of Photonics, Friedrich Schiller Univ. Jena, Germany. We show that counterpropagating phase-matching reached in photonic crystal waveguides, without periodic poling, can be used in spontaneous parametric down-conversion to engineer the generation of photon pairs factorizable in the spectral degree of freedom.

FTh1G.3 • 08:30

Visible-Telecom Photon Pair Generation with Silicon Nitride Nanophotonics, Xiyuan Lu¹, Qing Li¹, Gregory Moille¹, Anshuman Singh¹, Daron Westly¹, Kartik Srinivasan¹; ¹NIST, USA. We demonstrate a silicon nanophotonic chip that generates high-quality, narrowlinewidth photon pairs that link the visible and telecommunications bands. This device has potential for use in communication and entanglement of remote quantum systems

FTh1G.4 • 08:45

High CAR and low $g^{(2)}(0)$ of 1.55 μm entangled photon-pairs generated by a silicon microring resonator, Chaoxuan Ma¹, Malhar Jere¹, Xiaoxi Wang¹, Shayan Mookherjee¹; ¹Univ. of California, San Diego, USA. Silicon microring photon-pair and heralded single-photon generation is reported with a spectral brightness of 1.6×10^8 pairs/s/GHz/mW², achieving record CAR > 12,000 and heralded second-order self-correlation $g^{(2)}(0) < 0.006$. Franson interferometry was used to verify time-energy entanglement.

08:00–10:00

FTh1H • Quantum Interference, Imaging and Spectroscopy

Presider: Sergey Polyakov; NIST, USA

FTh1H.1 • 08:00

Sub-cycle Control of Optical Response by Using a Terahertz Excitonic Dressed State, Hideki Hirori¹, Kento Uchida¹, Tomohito Otake², Toshimitsu Mochizuki³, Changsu Kim⁴, Masahiro Yoshita⁴, Koichiro Tanaka¹, Akifumi Akiyama⁴, L. N. Pfeiffer⁵, K. W. West⁵; ¹Kyoto Univ., Japan; ²Kansai Photon Science Inst., Japan; ³National Inst. of Advanced Industrial Science and Technology, Japan; ⁴Univ. of Tokyo, Japan; ⁵Princeton Univ., USA. We observed optical absorption strengths modulated on a sub-cycle timescale in a GaAs quantum well in the presence of a multi-cycle terahertz driving pulse using a near-infrared probe pulse.

FTh1H.2 • 08:15

Stern-Gerlach Effect for Photons, Aviv Karnieli¹, Ady Arie²; ¹Raymond and Beverly Sackler School of Physics and Astronomy, Tel Aviv Univ., Israel; ²School of Electrical Engineering, Iby and Aladar Fleischman Faculty of Engineering, Tel Aviv Univ., Israel. We demonstrate theoretically the existence of a Stern-Gerlach effect for single photons in a quadratic nonlinear medium. The new effect enables the spatial separation of orthogonal frequency superposition states and might open new possibilities for the manipulation of bichromatic qubits.

FTh1H.3 • 08:30

Few Photons Correlation Measurement of a Thermally Populated Cavity, Francesca F. Settembrini¹, Ileana-Cristina Benea-Chelmus¹, Jérôme Faist¹; ¹ETH Zürich, Switzerland. In the THz range, correlation measurements have been implemented exploiting electrooptic sampling and femtosecond pulses. We present the field correlation measurement of few photons populating the modes of a cavity (nonlinear crystal) at room temperature.

FTh1H.4 • 08:45

Interfering Photons in Orthogonal States, Alexander Jones^{2,1}, Adrian Menssen¹, Helen Chrzanowski¹, Valery Shchesnovich³, Ian Walmsley¹; ¹Univ. of Oxford, UK; ²Imperial College London, UK; ³Federal Univ. of ABC, Brazil. Here we show that multi-particle quantum interference still occurs even when some of the particles involved are in orthogonal states. We experimentally demonstrate this with four photons.

08:00–10:00

STh11 • Novel Fabrication Methods

Presider: Roberto Paiella; Boston Univ., USA

STh11.1 • 08:00

Photonic Damascene process with reflow step for ultra-smooth Si₃N₄ waveguides, Martin Pfeiffer¹, Junqiu Liu¹, Tiago Morais¹, Bahareh Ghadiani¹, Tobias J. Kippenberg¹; ¹Ecole Polytechnique Federale de Lausanne, Switzerland. We present ultra-smooth silicon nitride waveguides fabricated by the photonic Damascene process extended with a novel reflow step. This leads to record Q-factors for tightly confining waveguides with anomalous dispersion.

STh11.2 • 08:15

Single-Step Fabrication of Multispectral Filter Arrays Using Grayscale Lithography and Metal-Insulator-Metal Geometry, Calum Williams¹, George S. Gordon¹, Timothy D. Wilkinson¹, Sarah E. Bohndiek²; ¹Dept. of Engineering, Univ. of Cambridge, UK; ²Dept. of Physics, Univ. of Cambridge, UK. Metal-insulator-metal geometries can provide optical transmission filtering, with peak wavelength dependent on insulator thickness. Using grayscale electron beam lithography to control insulator thickness, we fabricate multispectral filter arrays, whereby dose determines wavelength

STh11.3 • 08:30 **Invited**

Silicon and Germanium based Waveguide Platforms for the Long Wave Infrared, Milos Nedeljkovic¹, Jordi Soler Penades¹, Alejandro Sánchez-Postigo², J. Gonzalo Wangüemert Pérez², Alejandro Ortega-Moñux², Robert Halir², Pavel Cheben³, Iñigo Molina-Fernández², Vinita Mittal¹, Ganapathy S. Murugan¹, Ali Z. Khokhar¹, Callum Littlejohns¹, Yolanda Xu¹, Zhibo Qu¹, Ahmed Osman¹, Wei Cao¹, Lewis G. Carpenter¹, Corin Gawith¹, James S. Wilkinson¹, Goran Mashanovich¹; ¹Univ. of Southampton, UK; ²Universidad de Malaga, Spain; ³National Research Council of Canada, Canada. We report on low-loss light propagation at mid-infrared wavelengths above 7 μm in a) suspended silicon waveguides with metamaterial claddings, and b) germanium-on-silicon waveguides. These waveguides enable new sensing circuits for this wavelength range.

Meeting Room
212 A/C

CLEO: Science & Innovations

08:00–10:00

STh1J • OCT & Biomedical Imaging

Presider: Raluca Niesner; Charité-Univ. Medicine Berlin, USA

STh1J.1 • 08:00 **Tutorial**

Case Studies in Bringing Biophotonics Devices from Concept to Medical Product, Dennis L. Matthews¹; ¹Univ. of California Davis, USA. In this presentation, I will review the history of development for a couple of technologies that we have brought from the idea stage to a successful commercial product (superresolution Structured Illumination Microscope) or about to be a product (Personal Blood Count Monitor). I will also describe a couple of other projects which haven't yet reached a product status or that failed to reach such a status. My lecture is meant to provide examples of successful and not-so-successful strategies and some lessons learned. Biophotonics is a relatively mature field of research with lots of successful technology development, but the translation to the marketplace, especially in clinical medicine, has been limited. I will provide some insight into this situation along with some predictions of a bright future for the adoption of biophotonics technologies into various market sectors including medicine.



Dennis Matthews, Ph.D., is the Emeritus Director of the NSF Center for Biophotonics Science and Technology, and the previous Associate Director for Biomedical Technology for the Integrated Cancer Center at the University of California at Davis. He is an emeritus professor in the UC Davis Department of Neurological Surgery and a member of the Biomedical Engineering, Applied Sciences and Clinical Sciences Graduate Groups. He is also a previous Program Leader and Division Leader at Lawrence Livermore National Laboratory. He is the co-founder and Chief Scientist of the Tahoe institute for Rural Healthcare Research, the Univ of CA Biophotonics Alliance and the Biophotonics4Life Worldwide Consortium. He is also the sole proprietor of LifeLight Resources LLC, a biophotonics-based consulting company. He has also recently become the Chief Science and Operations Officer in a radar-based heart monitoring startup company called Cardiac Motion LLC. While he is credited for inventing and developing x-ray wavelength lasers at Lawrence Livermore National Laboratory, Dr. Matthews' continuing interest is in the translation and commercialization of new physical science and engineering technologies for grand challenges in medicine and the life sciences. His current interests are in developing optical, RF and x-ray technologies for disease diagnosis and treatment. He is a Fellow of the American Physical Society, the Society of Photo and Industrial Engineers and the Optical Society. He has more than 295 publications and >30 patents and is the co-editor of the Journal of Biophotonics. Dr. Matthews is credited for raising more than \$225M in grant and investor funds in his career, helping create 14 startup companies.

Meeting Room
212 B/DCLEO: QELS-Fundamental
Science

08:00–10:00

FTh1K • Optical Near-field and Thermal Imaging

Presider: Chengjun Zou; Friedrich Schiller Univ. Jena, Germany

FTh1K.1 • 08:00

Nanoscale Field Mapping of Interfering Beams from Nomarski Prism Using Photo-Induced Force Microscopy, Mohsen Rajaei¹, Mohammad Kamandi¹, Mohammad Al-booyeh¹, Mina Hanifeh¹, Filippo Capolino¹, Hemantha K. Wickramasinghe¹; ¹Univ. of California, Irvine, USA. We map the near-field distribution of a linearly-polarized light transmitting through a Nomarski prism. We show how translating the prism changes the near-field profile. This setup has potential applications in phase detection of molecular responses.

FTh1K.2 • 08:15

Enantio-specific Detection of Chirality at Nanoscale Using Photo-induced Force, Mohammad Kamandi¹, Mohammad Albooyeh¹, Mohsen Rajaei¹, Jinwei Zeng¹, Caner Guclu¹, Mehdi Veysi¹, Hemantha K. Wickramasinghe¹, Filippo Capolino¹; ¹Univ. of California, Irvine, USA. We propose a high-resolution scanning-tip microscopy technique for enantio-specific detection of nanoscale samples (down to sub-100-nm size) by measuring the photo-induced force exerted on an achiral probe in the vicinity of a chiral sample, under circularly polarized excitation beams.

FTh1K.3 • 08:30

High Coupling Efficiency Adiabatic Near-field Transducer for HAMR, Chuan Zhong¹, Patrick Flanigan¹, Nicolás Abadía¹, Brian D. Jennings¹, Frank Bello¹, Gwenael Atcheson¹, Jing Li¹, Jian-Yao Zheng¹, Richard Hobbs¹, David McCloskey¹, John F. Donegan¹; ¹Trinity College Dublin, Ireland. The literature reports NFT with size below 1 micron are found to be thermo-mechanically unstable and low coupling efficiency. We demonstrate a 6 μm long adiabatic taper. A maximum coupling efficiency of 90.8% is achieved.

FTh1K.4 • 08:45

Cryogenic Near-Field Imaging and Spectroscopy at the 10-Nanometer-Scale, Max Eisele¹, Andreas Huber¹, Tobias Gokus¹; ¹neaspec GmbH, Germany. We extend conventional near-field microscopy at ambient conditions to the cryogenic temperature range (<10-300K). We will present first nano-optical measurements on semiconductor samples and single-layer materials highlighting the novel insights attainable by our cryo-neasSNOM.

Marriott
Salon I & II

CLEO: Science & Innovations

08:00–10:00

STh1L • MIR to the THz Dual Combs

Presider: Ian Coddington; NIST, USA

STh1L.1 • 08:00

Mid-Infrared Frequency Comb Generation with In-Line Frequency Stabilization, Alexander Lind^{1,2}, Abijith Kowligy¹, Henry Timmers¹, Nima Nader³, Flavio Cruz¹, Gabriel Ycas³, Scott Papp¹, Scott Diddams^{1,2}; ¹Time and Frequency, NIST, USA; ²Physics, Univ. of Colorado, Boulder, USA; ³Applied Physics, NIST, USA. We demonstrate a simple mid-infrared comb source via intra-pulse difference frequency generation in periodically poled lithium niobate crystals. This technique generates an offset frequency beat in the mid-infrared, which we use for comb stabilization.

STh1L.2 • 08:15

Mid-Infrared Dual-Comb Spectroscopy of Liquid-Phase Samples using Attenuated Total Reflectance, Daniel I. Herman^{1,2}, Gabriel Ycas¹, Fabrizio Giorgetta¹, Eleanor Waxman¹, Esther Baumann¹, Ian R. Coddington¹, Nathan R. Newbury¹; ¹NIST, USA; ²Physics, Univ. of Colorado at Boulder, USA. Mid-infrared dual-comb spectroscopy (DCS) is performed on liquid isopropanol from 3.0-3.75 μm with a 1.5-second acquisition time. This experiment is a first step towards viewing liquid-phase reactions in real time using DCS.

STh1L.3 • 08:30 **Invited**

Dual THz Comb Spectroscopy, Takeshi Yasui^{1,2}; ¹Tokushima Univ., Japan; ²JST, ERATO MINOSHIMA Intelligent Optical Synthesizer, Japan. We combine dual-comb spectroscopy with spectrally interleaving in terahertz (THz) region, enabling us to achieve the spectral sampling interval equal to linewidth of the comb tooth in the low-pressure gas spectroscopy in THz region.

**Marriott
Salon III**

**CLEO: QELS-Fundamental
Science**

08:00–10:00

FTh1M • Nonlinear Dynamics in Resonators and Fibers

Presider: Arash Mafi; Univ. of New Mexico, USA

FTh1M.1 • 08:00

10-GHz Femtosecond Degenerate Optical Parametric Oscillator, Richard A. McCracken¹, Yuk Shan Cheng¹, Derryck T. Reid¹; ¹Heriot-Watt Univ., UK. We report a synchronously pumped degenerate optical parametric oscillator (DRO) with a 90-nm bandwidth at 1.634 μm , producing 400-mW average power femtosecond pulses at 10 GHz, the highest repetition frequency femtosecond DRO demonstrated to date.

FTh1M.2 • 08:15

Exotic Nonlinear Effects by Inserting a Low Finesse Resonator in a Mode-Locked Laser Cavity, James Hendrie¹, Ning Hsu¹, Jean-Claude M. Diels¹, Matthias Lenzner², Ladan Arisshian¹; ¹Univ. of New Mexico, USA; ²Lenzner Research LLC, USA. Intracavity comb multiplication is demonstrated by inserting a low finesse resonator in a mode-locked laser. Control of the comb in frequency and repetition rate is demonstrated.

FTh1M.3 • 08:30

Accelerating nonlinear interactions in tapered multimode fibers, Mohammad Amin Eftekhari¹, Zeinab Sanjabi Eznaveh¹, Jose Enrique Antonio-Lopez¹, Helena E. Lopez Aviles¹, Sepehr Benis¹, Miroslav Kolesik², A. Schülzgen¹, Frank W. Wise³, Rodrigo Amezcua Correa¹, Demetrios N. Christodoulides¹; ¹CREOL, Univ. of Central Florida, USA; ²College of Optical Sciences, The Univ. of Arizona, USA; ³School of Applied and Engineering Physics, Cornell Univ., USA. We theoretically and experimentally demonstrate that the processes of multimode soliton fission and dispersive wave generation in parabolic-index multimode fibers are substantially altered when the rate of intermodal nonlinear interactions is progressively increased during propagation.

FTh1M.4 • 08:45

Phase Conjugation in OAM fiber modes via Stimulated Brillouin Scattering, Gautam Prabhakar¹, Xiao Liu¹, Jeffrey Demas¹, Patrick Gregg¹, Siddharth Ramachandran¹; ¹Boston Univ., USA. We report the first demonstration of phase conjugation in OAM fiber modes via SBS. Acoustic and optical angular-momentum selection rules facilitate this even for monomode launch, in contrast to the traditional need for multimode inputs.

**Marriott
Salon IV**

CLEO: Science & Innovations

08:00–10:00

STh1N • Ultrafast Applications

Presider: Christophe Dorrer; Univ. of Rochester, USA

STh1N.1 • 08:00 Tutorial

THz Driven Accelerators and X-ray Sources, Franz X. Kaertner^{1,2}; ¹Center for Free-Electron Laser Science, Deutsches Elektronen Synchrotron, Germany; ²Physics Dept., Universität Hamburg, Germany. Approaches towards a linear THz accelerator technology are discussed. Theoretical and first experimental results on laser based high energy THz generation, guns, accelerators as well as compact X-ray sources based on these devices are presented.



Franz Kärtner heads the Ultrafast Optics and X-rays Group at the Center for Free-Electron Laser Science at DESY and is Professor of Physics at University of Hamburg. Within an ERC Synergy Grant, he and colleagues pursue Terahertz acceleration and coherent X-ray sources. He is a fellow of OSA and IEEE.

**Marriott
Salon V**

**CLEO: Applications
& Technology**

08:00–10:00

ATH1O • Trace Gas Detection

Presider: Paul Williams; NIST, USA

ATH1O.1 • 08:00

Optical re-injection in Off-Axis Integrated Cavity Output Spectroscopy, modelling and experiments, Faisal Nadeem¹, Julien Mandon¹, Simona M. Cristescu¹, Frans J. M. Harren¹; ¹Radboud Univ., Netherlands. A 3-D ray-tracing model is developed, to model reinjection in Off-Axis Cavity Enhanced Spectroscopy. Modelling and experiments demonstrate, at near-IR laser wavelengths, a 38-times enhancement, corresponding to a NEAS of $1.1 \times 10^{-9} \text{ cm}^{-1} \text{ Hz}^{-1/2}$

ATH1O.2 • 08:15

Detection of Trace Amounts of Volatile Organic Compounds via Laser-Induced Condensation, Valentina Shumakova¹, Mary Matthews², Tadas Balciunas², Skirmantas Ališauskas¹, Elise Schubert², Audrius Pugzlys^{1,3}, Andrius Baltuska¹, Jerome Kasparian², Jean-Pierre Wolf²; ¹Vienna Univ. of Technology, Austria; ²Université de Genève, Switzerland; ³Center for Physical Sciences & Technology, Lithuania. Laser-induced condensation allows to detect volatile organic compounds with concentrations below 1 ppb. Lab experiments and comparison with quantitative photo-ionization detection measurements were performed. The method is sensitive to excitation wavelength in 1.6-2.0 μm range.

ATH1O.3 • 08:30

Mid-Infrared Photothermal Interferometric Gas Sensing in Hollow-Core Optical Fibers, Chenyu Yao¹, Zhili Li², Fan Yang³, Wei Jin³, Wei Ren¹; ¹The Chinese Univ. of Hong Kong, Hong Kong; ²Univ. of Electronic Science and Technology-Zhongshan Inst., China; ³The Hong Kong Polytechnic Univ., Hong Kong. We developed a photothermal interferometry-based trace gas sensor by coupling a mid-infrared pump laser and a near-infrared probe laser into a hollow-core optical fiber.

ATH1O.4 • 08:45

Parts-Per-Billion Carbon Monoxide Sensing in Silicon-on-Sapphire Mid-Infrared Photonic Crystal Waveguides, Ali Rostamian², Joel Guo², Swapnajit Chakravarty¹, Chi-Jui Chung², Duy Nguyen¹, Ray Chen^{2,1}; ¹Omega Optics, Inc, USA; ²Electrical and Computer Engineering, Univ. of Texas at Austin, USA. We experimentally detect 3 ppm carbon monoxide via optical absorbance in a 1mm long slotted photonic crystal waveguide in silicon-on-sapphire at wavelength $\lambda = 4.55\text{mm}$. Feasibility of low ppb sensing will be shown by design modifications.

Marriott
Salon VI

Marriott
Willow Glen

**CLEO: QELS-Fundamental
Science**

**CLEO: Applications
& Technology**

08:00–10:00
**FTh1P • Engineering and Metrology of
Thermal Radiation**
Presider: Gururaj Naik; Rice Univ., USA

08:00–10:00
**ATh1Q • A&T Topical Review on
Neurophotonics I**
Presider: Chris Xu; Cornell Univ., USA

FTh1P.1 • 08:00 Tutorial
**Nanophotonic Control of Thermal Radiation for Energy
Applications**, Shanhui Fan¹; ¹*Stanford Univ., USA*. The ability
to control thermal radiation plays a fundamentally important
role in a wide range of energy technology. Nanophotonic
structures provide enhanced capabilities for controlling thermal
radiation, which is leading to new energy applications.

ATh1Q.1 • 08:00 Tutorial
The Challenge of Large-scale Neuronal Imaging, Jerome
C. Mertz¹; ¹*Boston Univ., USA*. Fast, large-scale, volumetric,
in-vivo neuronal imaging has long been a challenge for
microscopists. I will discuss some of the issues involved and
review various strategies to address this challenge.



Shanhui Fan is a Professor of Electrical Engineering and the Director of the Ginzton Laboratory, at Stanford University. He received his Ph. D in 1997 from Massachusetts Institute of Technology (MIT). His research interests are in fundamental physics of nanophotonic structures, and their applications in energy and information technology.



Jerome Mertz is currently a professor of Biomedical Engineering at Boston University. His interests are in the development and applications of novel optical microscopy techniques for biological imaging. He is also author of a textbook entitled Introduction to Optical Microscopy.

CLEO: Science & Innovations

STh1A • Novel Structures and Devices—Continued

STh1A.5 • 09:00

Spectral Engineering Based on Mode Splitting in Integrated Cascaded Sagnac Loop Reflectors, Jiayang Wu¹, Tania Moein¹, Xingyuan Xu¹, David J. Moss¹; ¹*Swinburne Univ. of Technology, Australia*. We propose and experimentally demonstrate mode splitting in integrated cascaded Sagnac loop reflectors (SLRs). By changing the number and reflectivity of the SLRs, rich filtering characteristics for spectral engineering are experimentally achieved and show good agreement with theory.

STh1A.6 • 09:15

Integrated Amorphous Silicon-Aluminum Long-Range Surface Plasmon Polaritons (LR-SPP) Waveguides, Boaz Sturlesi¹, Meir Grajower¹, Noa Mazurski¹, Uriel Levy¹; ¹*the Hebrew Univ. of Jerusalem, Israel*. We demonstrate Long Range Surface Plasmon Polaritons waveguide with aluminum embedded in amorphous silicon. It operates in the telecom band and is compatible with backend CMOS process. Transmission and near field measurement results are reported.

STh1A.7 • 09:30

Radiation-Free, Sub-Wavelength Optical Resonator based on All-Evanescent Confinement in a High-Index Core Material, Imbert Wang¹, Milos Popovic¹; ¹*Electrical Engineering, Boston Univ., USA*. We propose a radiation-free dielectric nanocavity with all-evanescent confinement, based on perfect mode-matching and minimal use of negative permittivity. A record-low mode volume within high-index core material, supporting high-Q(Q/V), may enable efficient active nanophotonic components.

STh1A.8 • 09:45

Interface Passivation for Realizing High Efficiency Direct Band Gap Emission from Ge MOS Tunneling Diode, Min Xie¹, Yi Zhao¹; ¹*Zhejiang Univ., China*. We demonstrated room temperature Ge surface-emitting diode with 1.5-1.6 μm strong infrared emission using a metal/graphene/high-k/interface layer (IL)/n-Ge MOS tunneling structure, without introducing strain or extra-doping.

STh1B • Integrated Photonic Sensors—Continued

STh1B.4 • 09:00

Monolithic Integration of Quantum Cascade Laser, Quantum Cascade Detector and Slotted Photonic Crystal Waveguide for Absorbance Sensing from l=3-15mm, Swapnajt Chakravarty¹, Jason Mickiff¹, Ali Rostamian², Joel Guo², Ray Chen^{2,1}; ¹*Omega Optics, Inc, USA*; ²*Electrical and Computer Engineering, Univ. of Texas at Austin, USA*. We demonstrate monolithic integration of quantum cascade laser and detector and slotted photonic crystal waveguide on a single epitaxial heterostructure for on-chip slow light enhanced absorption sensing. Designs can cover l=3-15mm wavelengths without wafer bonding.

STh1B.5 • 09:15

Demonstration of 2-μm on-chip two-mode division multiplexing using tapered directional coupler-based mode (de) multiplexer, Shuang Zheng¹, Meng Huang¹, Xiaoping Cao¹, Lulu Wang¹, Zhengsen Ruan¹, Li Shen¹, Jian Wang¹; ¹*Wuhan National Lab for Optoelectr, China*. We design and fabricate a four-mode division (de)multiplexer for chip-scale optical data transmission in 2 μm waveband for the first time. The on-chip device exhibits low mode crosstalk and wide bandwidth over the wave band.

STh1B.6 • 09:30

Coupled Resonator Optical Waveguide Filter Based on Sagnac Loop Mirrors, Renyou Ge¹, Xinlun Cai¹; ¹*Sun Yat-Sen Univ., China*. We designed and fabricated a novel coupled resonator optical waveguide filter based on Sagnac loop mirrors on silicon-on-insulator platform. We can achieve extinction ratio of >50 dB by tuning reflections of the Sagnac loop mirrors.

STh1B.7 • 09:45

Quantum cascade multi-spectral laser with integrated beam combiner on silicon, Eric J. Stanton¹, Alexander Spott¹, Jon Peters¹, Michael Davenport¹, Nicolas Volet¹, Aditya Malik¹, Junqian Liu¹, Charles D. Merritt², William W. Bewley², Igor Vurgaftman², Chul Soo Kim², Jerry R. Meyer², John E. Bowers¹; ¹*Univ. of California Santa Barbara, USA*; ²*Code 5613, Naval Research Lab, USA*. A multi-spectral quantum cascade laser is demonstrated on SOI, emitting at 4.6–4.7 μm with an integrated multiplexer. Low-loss spectral beam combining to a single-mode waveguide efficiently scales the output power.

STh1C • Machine Learning for Communication—Continued

STh1C.4 • 09:00

Performance Improvement of Nyquist DP-16QAM Over 600km System Using ANN-enhanced Post-equalization, C.P. Tsekrekos¹, Christian Sánchez Costa¹, Mohammad A. Al-Khateeb¹, Feng Wen¹, Oleg Sidelnikov², Stylianos Sygletos¹; ¹*Inst. of Photonic Technologies, Aston Univ., UK*; ²*Inst. of Computational Technologies, Russia*. Performance improvement of up to 1.2 dB in Q²-factor is experimentally demonstrated in single-carrier dual-polarization 2x28-Gbaud 16QAM 6x100 km EDFA-amplified transmission with digital post-equalization enhanced with an artificial neural network.

STh1C.5 • 09:15

Affinity propagation clustering for blind nonlinearity compensation in coherent optical OFDM, Elias Giacomidis¹, Ivan A. Aldaya², Jinlong Wei³, Christian Sánchez Costa⁴, Hichem Mrabet⁵, Liam Barry¹; ¹*Dublin City Univ., Ireland*; ²*Univ. of Campinas, Brazil*; ³*Huawei Technologies Düsseldorf GmbH, Germany*; ⁴*Aston Univ., UK*; ⁵*Saudi Electronic Univ., Saudi Arabia*. The first blind nonlinear equalizer using affinity propagation (AP) clustering is experimentally demonstrated for single-channel and WDM CO-OFDM. AP outperforms fuzzy-logic c-means clustering and digital-back propagation for both QPSK and 16-QAM formats.

10:00–15:00 Exhibition Open, Exhibit Hall

10:15–13:00 Technology Transfer Program, Exhibit Hall Theater

10:00–11:30 Coffee Break & Exhibit Only Time, Exhibit Hall

CLEO: QELS-Fundamental Science

FTh1D • Nonlinear Metamaterials and Metasurfaces—Continued

FTh1D.4 • 09:00

Field- and Carrier-Induced Nonlinear Metamaterials, Mohammad Taghinejad¹, Wenshan Cai¹; ¹Georgia Inst. of Technology, USA. We explore active and nonlinear plasmonic metamaterials by leveraging the field-induced disruption of the inversion symmetry for second-order optical processes, and exploiting the hot-carrier-induced perturbation of the dielectric permittivity for ultrafast all-optical modulation.

FTh1D.5 • 09:15

Asymmetric Light Transport at Nonlinear Metasurfaces, Nir Shitrit¹, Jeongmin Kim¹, David Barth¹, Hamidreza Ramezani¹, Yuan Wang¹, Xiang Zhang^{1,2}; ¹Univ. of California at Berkeley, USA; ²Materials Sciences Division, Lawrence Berkeley National Lab, USA. We report asymmetric transport of free-space light at nonlinear metasurfaces and the derivation of the nonlinear generalized Snell's laws. Asymmetric transport at metasurfaces opens a new paradigm for ultrathin lightweight optical devices with one-way operation.

FTh1D.6 • 09:30

Homogenization and Nonlinearity Enhancement of 2D Graphene-Based Metasurfaces, Jian Wei You¹, Nicolae C. Panoiu¹; ¹EEE, Univ. College London, UK. A general homogenization technique is developed to study the optical properties of 2D graphene-based metasurfaces. The results show the effective nonlinear susceptibilities of graphene metasurfaces can be enhanced by more than two orders of magnitude.

FTh1D.7 • 09:45

Structural Second Order Nonlinearity in Metamaterials, Brian Wells^{2,1}, Anton Y. Bykov³, Giuseppe Marino³, Mazhar Nasir³, Anatoly Zayats³, Viktor A. Podolskiy¹; ¹Univ. of Massachusetts Lowell, USA; ²Dept. of Physics, Univ. of Hartford, USA; ³Dept. of Physics, Kings College London, UK. We demonstrate that second harmonic generation in plasmonic nanowire composites can be described by an effective bulk χ^2 susceptibility which depends on the geometry of the composite, and present an analytical description of this phenomenon

FTh1E • Nonlinear Optics in Microresonator Systems—Continued

FTh1E.4 • 09:00

Dynamics of Coupled Microresonator-Based Degenerate Optical Parametric Oscillators, Jae K. Jang¹, Yoshitomo Okawachi¹, Alexander L. Gaeta¹; ¹Columbia Univ., USA. We theoretically study a network of microresonator-based $\chi^{(3)}$ degenerate optical parametric oscillators (DOPOs). We investigate the influence of coupling on the global oscillation condition and show that the system can emulate the Ising model.

FTh1E.5 • 09:15

Mid-wavelength Infrared Supercontinuum Generation Spanning 1.4 Octaves in a Silicon-Germanium Waveguide, Milan Sinobad^{2,1}, Christelle Monat¹, Barry Luther-Davies³, Pan Ma³, Stephen Madden³, David J. Moss⁴, Aman Mitchell², Regis Orobtschouk¹, Salim Boutami⁵, Jean-Michel Hartmann⁵, Jean-Marc Fedeli⁵, Christian Grillet¹; ¹Lyon Inst. of Nanotechnology, France; ²School of Engineering, RMIT Univ., Australia; ³Laser Physics Centre, Australian National Univ., Australia; ⁴Centre for Microphotonics, Swinburne Univ. of Technology, Australia; ⁵CEA-Leti, France. We report mid-wavelength infrared supercontinuum generation, from 2.6 to 7.3 μm , in a CMOS compatible low loss silicon-germanium waveguide pumped using a tunable OPA laser delivering ~ 200 fs pulses at 4.15 μm .

FTh1E.6 • 09:30

Dissipative Kerr Soliton States in Hybridized Microresonator Modes, Maxim Karpov¹, Martin Pfeiffer¹, Junqiu Liu¹, Anton Lukashchuk¹, Tobias J. Kippenberg¹; ¹Lab. of Photonics and Quantum Measurement, Switzerland. We experimentally demonstrate that the formation of dissipative Kerr soliton states can be achieved in hybridized microresonator modes by exploring their strong local anomalous group velocity dispersion, enabling arbitrary center wavelength operation.

FTh1E.7 • 09:45

Dynamics of laser with an integrated nonlinear waveguide, A. Aadhi¹, Michael Kues^{2,3}, Anton V. Kovalev², Piotr Roztock¹, Christian Reimer¹, Young Zhang¹, Toa Wang¹, Sai T. Chu⁵, David J. Moss⁴, Zhiming Wang¹, Evgeny A. Viktorov², Roberto Morandotti^{1,2}; ¹INRS EMT, Canada; ²ITMO Univ., Russia; ³Univ. of Glasgow, UK; ⁴Inst. of Fundamental and Frontier Sciences, Univ. of Electronic Science and Technology of China, China; ⁵City Univ. of Hong Kong, Hong Kong; ⁶Swinburne Univ. of Technology, Australia. Exploiting a single figure-eight laser configuration that uses a highly nonlinear on-chip spiral waveguide, we experimentally demonstrate several mode-locking dynamics. We adjust the mode-locking pulse profiles in a controlled manner by varying the polarization.

FTh1F • Novel Phenomena in van der Waals Heterostructure—Continued

FTh1F.4 • 09:00

Designer Photocurrents, Perry T. Mahon², Rodrigo A. Muniz^{3,1}, John E. Sipe²; ¹Univ. of Toronto, Canada; ²Dept. of Physics, Univ. of Toronto, Canada; ³Univ. of Michigan, USA. Using transition metal dichalcogenides as an example, we show that the coherent control of injected carriers via 2- and 3-photon absorption processes leads to controllable, highly localized carrier distributions in the Brillouin zone.

FTh1F.5 • 09:15

Enhanced Luminescence of MoS₂, WS₂ and WSe₂, Direct Band Gap Semiconductor Heterostructures, Jin-Kyu So¹, Shoujun Zheng¹, Fucai Liu², Zheng Liu², Nikolay I. Zheludev^{1,3}, Hong Jin Fan^{1,4}; ¹Centre for Disruptive Photonic Technologies, TPI, SPMS, Nanyang Technological Univ., Singapore; ²School of Materials Science and Engineering, Nanyang Technological Univ., Singapore; ³Optoelectronics Research Centre & Centre for Photonic Metamaterials, Univ. of Southampton, UK; ⁴Division of Physics and Applied Physics, School of Physical and Mathematical Sciences, Nanyang Technological Univ., Singapore. We introduce van der Waals heterostructures to amplify the otherwise negligible cathodoluminescence from monolayer transition metal dichalcogenides, which allowed to visualize the nanoscale variation of strain and photonic modes in the monolayer on engineered surfaces.

FTh1F.6 • 09:30

Suppression of Excitonic Absorption by Thickness Variation in Few-layer GaSe, Arne Budweg¹, Dinesh Yadav^{1,2}, Alexander Grupp¹, Alfred Leitenstorfer¹, Maxim Trushin^{1,3}, Fabian Pauly^{1,2}, Daniele Brida¹; ¹Dept. of Physics and Center for Applied Photonics, Univ. of Konstanz, Germany; ²Okinawa Inst. of Science and Technology Graduate Univ., Japan; ³Centre for Advanced 2D Materials, National Univ. of Singapore, Singapore. We study the optical absorption of GaSe via sensitive differential transmission measurements while controlling the sample thickness with individual layer precision. Below a critical value of eight layers, suppression of the excitonic transitions is observed.

FTh1F.7 • 09:45

Photon Correlation of Photoluminescence Emission of a Monolayer WS₂, Jiahui Huang¹, Ibrahim Sarpkaya², Jinkang Lim¹, Sung-Joon Lee¹, Xiangfeng Duan¹, Chee Wei Wong¹, Han Htoon²; ¹Univ. of California, Los Angeles, USA; ²Los Alamos National Lab, USA. We observed the photon bunching of photoluminescence emission from a Tungsten disulfide monolayer by photon correlation measurements. The mixture of spectral diffusion and thermal light emission is considered to explain the bunching signature.

10:00–15:00 Exhibition Open, Exhibit Hall

10:15–13:00 Technology Transfer Program, Exhibit Hall Theater

10:00–11:30 Coffee Break & Exhibit Only Time, Exhibit Hall

Executive Ballroom
210GExecutive Ballroom
210HMeeting Room
211 B/D

CLEO: QELS-Fundamental Science

CLEO: Science & Innovations

FTh1G • Integrated Quantum Sources—
Continued

FTh1G.5 • 09:00

Indistinguishable Photon-Pairs from Pure and Bright Silicon Micro-ring Resonator Sources, Imad Faruque¹, Daniel M. Llewellyn¹, Yunhong Ding^{2,3}, Stefano Paesani¹, Raffaele Santagati¹, Damien Bonneau¹, Gary Sinclair¹, Davide Bacco^{2,3}, Karsten Rottwitt^{2,3}, Leif K. Oxenlowe^{2,3}, Jeremy O'Brien¹, Jianwei Wang¹, John Rarity¹, Mark G. Thompson¹; ¹Univ. of Bristol, UK; ²Dept. of Photonics Engineering, Technical Univ. of Denmark, Denmark; ³Center for Silicon Photonics for Optical Communication (SPOC), Technical Univ. of Denmark, Denmark. We report on-chip interference fringes of very high visibility 89% from heralded single photons from separate ultra-bright silicon micro-ring resonator sources as 4-fold coincidences. The reconfigurable chip is also used to measure multipair fringes and conditional $g^{(2)}(0)$ of single photons.

FTh1G.6 • 09:15

Percolation Based Cluster State Generation by Photon-Mediated Entanglement, Mihir Pant¹, Hyeonrak Choi¹, Saikat Guha², Dirk Englund¹; ¹MIT, USA; ²Optical Sciences, Univ. of Arizona, USA. We present an architecture for creating large entangled cluster states for quantum computing and simulation with nitrogen vacancy centers in diamond within the experimentally demonstrated coherence time using percolation theory.

FTh1G.7 • 09:30

Generation and Manipulation of Multi-Photon Entangled States on a Silicon Photonic Device, Daniel M. Llewellyn¹, Yunhong Ding^{2,3}, Imad Faruque¹, Stefano Paesani¹, Raffaele Santagati¹, Jake Kennard¹, Davide Bacco^{2,3}, Karsten Rottwitt^{2,3}, Leif K. Oxenlowe^{2,3}, Jeremy L. O'Brien¹, Jianwei Wang¹, Mark G. Thompson¹; ¹Univ. of Bristol, UK; ²Dept. of Photonics Engineering, Technical Univ. of Denmark, Denmark; ³Center for Silicon Photonics for Optical Communication, Technical Univ. of Denmark, Denmark. We experimentally demonstrate the generation and manipulation of entangled photons-pairs from an array of bright and pure photon micro-ring sources, and realise the teleportation of unknown quantum states on a reconfigurable silicon photonic quantum device.

FTh1G.8 • 09:45

Integrated silicon nitride time-bin entanglement circuits, Xiang Zhang¹, Bryn A. Bell¹, Andri Mahendra¹, Chunle Xiong¹, Philip Leong¹, Benjamin J. Eggleton¹; ¹Univ. of Sydney, Australia. Time-bin entangled states are generated and analyzed in an integrated silicon nitride chip. Quantum state tomography indicates 91% fidelity to the ideal state, demonstrating its potential for applications in quantum communication networks.

FTh1H • Quantum Interference, Imaging
and Spectroscopy—Continued

FTh1H.5 • 09:00

Randomness Extraction From Chsh Violation Without Fair Sampling Assumptions With A Continuous Wave Source, Alessandro Cerè¹, Lijiong Shen^{1,2}, Jianwei Lee¹, Le Phuc Thinh¹, Jean-Daniel Bancal³, Valerio Scarani¹, Christian Kurtsiefer^{1,2}; ¹Centre for Quantum Technologies, NUS, Singapore; ²Dept. of Physics, National Univ. of Singapore, Singapore; ³Dept. of Physics, Univ. of Basel, Switzerland. We demonstrate a detection loophole-free Bell violation using a photonic system based on a continuous wave source, and show that it allows to increase the randomness generation rate compared to pulsed systems.

FTh1H.6 • 09:15

Quantum Interference in a Room Temperature InAs/InP Quantum Dot Semiconductor Optical Amplifier, Igor Khanonkin¹, Akhilesh K. Mishra¹, Ouri Karni², Johann P. Reithmaier³, Gadi Eisentein¹; ¹Technion-Israel Inst. of Technology, Israel; ²Stanford Univ., USA; ³Univ. of Kassel, Germany. Ramsey interference were observed in an inhomogeneously broadened InAs/InP quantum dot semiconductor optical amplifier operating at room temperature. The imprint of the Ramsey fringes on pulse intensity, phase and temporal position were demonstrated.

FTh1H.7 • 09:30

Quasimomentum Distribution and Free Expansion of an Anyonic Gas, Tena Dubček¹, Bruno Klajn¹, Robert Pezer², Hrvoje Buljan¹, Dario Jukić³; ¹Dept. of Physics, Faculty of Science, Univ. of Zagreb, Croatia; ²Faculty of Metallurgy, Univ. of Zagreb, Croatia; ³Faculty of Civil Engineering, Univ. of Zagreb, Croatia. We point out that the momentum distribution is not a proper observable for anyons in two dimensions. We define the quasimomentum distribution as the asymptotic single-particle density after free expansion (time-of-flight measurements), as a means to measure the anyonic statistics.

STh11 • Novel Fabrication Methods—
Continued

STh11.4 • 09:00

In-situ "Point-and-Shoot" Fabrication of Metallic Rings for Mid-IR/Visible Sensing, Bharath Bangalore Rajeeva¹, Zilong Wu¹, Andrew F. Briggs¹, Palash V. Acharya¹, Vaibhav Bahadur¹, Seth Bank¹, Yuebing Zheng¹; ¹The Univ. of Texas at Austin, USA. We utilize "point-and-shoot" strategy to achieve single-step fabrication of silver ring arrays from its precursor ink within spatially-constrained environments. We further utilize the substrates to demonstrate dual-mode sensing in mid-IR and visible regimes.

STh11.5 • 09:15

Template assisted dewetting of optical glasses for large area, flexible and stretchable all dielectric metasurfaces, Tapajyoti Das Gupta¹, Louis Martin-Monier¹, Arthur Lebris¹, Wei Yan¹, Tung Nguyen¹, Alexis Page¹, Yunpeng Qu¹, Fabien Sorin¹; ¹Ecole Polytechnique Federale de Lausanne, Switzerland. We propose for the first time template-assisted dewetting of high-index chalcogenide glasses for low-cost manufacturing of all-dielectric metasurfaces on large-area flexible and stretchable substrates.

STh11.6 • 09:30

Centimeter-scale Superfine 3D Printing, Wei Chu¹, Yuanxin Tan¹, Jintian Lin¹, Jinping Yao¹, Ya Cheng^{1,2}; ¹Shanghai Inst of Optics & Fine Mechanics, China; ²School of Physics and Materials Science, East China Normal Univ., China. We present a method based on simultaneous spatiotemporal focusing (SSTF) of the femtosecond laser pulses that enables to fabricate 3D structures on the centimeter scale with TPP. Several Centimeter-scale structures were fabricated using this method.

STh11.7 • 09:45

On-demand lens fabrication by liquid phase molding with gallium and Polydimethylsiloxane, Keisuke Nakakubo¹, Hiroaki Nomada¹, Hiroaki Yoshioka¹, Kinichi Morita², Yuji Oki¹; ¹Kyushu Univ., Japan; ²Ushio, Inc., Japan. A new on-demand lens fabrication with gallium molding was proposed and demonstrated. A convex and concave surface of liquid gallium is transferred to Polydimethylsiloxane. The curvature can be controlled between $\pm 0.37 \text{ mm}^{-1}$

10:00–15:00 Exhibition Open, Exhibit Hall

10:15–13:00 Technology Transfer Program, Exhibit Hall Theater

10:00–11:30 Coffee Break & Exhibit Only Time, Exhibit Hall

CLEO: Science & Innovations

STh1J • OCT & Biomedical Imaging—
Continued

STh1J.2 • 09:00

Multimodal deep tissue imaging using Wavelength Modulated Spatially Offset Raman Spectroscopy and Optical Coherence Tomography, Mingzhou Chen¹, Josep Mas¹, Lindsey H. Forbes², Melissa Andrews³, Kishan Dholakia¹; ¹School of Physics and Astronomy, Univ. of St Andrews, UK; ²Scho, Univ. of St Andrews, UK; ³Biological Sciences, Univ. of Southampton, UK. We demonstrate a multimodal system integrating optical coherence tomography (OCT) with wavelength modulated spatially offset Raman spectroscopy. This has the capability to detect co-registered Raman and OCT signals from targets deeply embedded in tissue.

STh1J.3 • 09:15

Non-Iterative Holographic Image Reconstruction and Phase Retrieval Using a Deep Convolutional Neural Network, Yair Rivenson¹, Yibo Zhang¹, Harun Günaydin¹, Da Teng¹, Aydogan Ozcan¹; ¹Univ. of California Los Angeles, USA. We demonstrate a non-iterative holographic image reconstruction and phase retrieval framework based on deep learning. After its training, a deep convolutional neural network rapidly recovers phase and amplitude images of specimen from a single hologram.

STh1J.4 • 09:30

Chip-Based Frequency Combs for High-Resolution Optical Coherence Tomography, Xingchen Ji^{1,2}, Alexander Klenner¹, Xinwen Yao¹, Yu Gan¹, Alexander L. Gaeta¹, Christine Hendon¹, Michal Lipson¹; ¹Columbia Univ., USA; ²Cornell Univ., USA. We present a source for OCT based on chip-scale microresonators for sub-micrometer axial resolution and deep tissue penetration. Using the microresonators, we acquire OCT images of human tissue and show compatibility with standard OCT systems.

STh1J.5 • 09:45

High-throughput 3D Tracking of Sperm Locomotion Reveals Head Spin and Flagellar Beating Patterns, Mustafa Daloglu¹, Wei Luo¹, Faizan Shabbir¹, Francis Lin¹, Kevin Kim¹, Inje Lee¹, Jiaqi Jiang¹, Wenjun Cai¹, Vishwajith Ramesh¹, Mengyuan Yu¹, Aydogan Ozcan¹; ¹Univ. of California, Los Angeles, USA. Dual-view on-chip holographic imaging enabled high-throughput tracking of the complete 3D locomotion of bovine sperms, including the translational and rotational (i.e., spin) motion of the sperm head and the 3D beating of the flagellum.

CLEO: QELS-Fundamental
ScienceFTh1K • Optical Near-field and Thermal
Imaging—Continued

FTh1K.5 • 09:00

Sum rules & power-bandwidth limits to near-field optical response, Hyungki Shim^{1,2}, Lingling Fan^{1,3}, Steven Johnson⁴, Owen Miller¹; ¹Dept. of Applied Physics and Energy Sciences Inst., Yale Univ., USA; ²Dept. of Physics, Yale Univ., USA; ³School of Physics and National Lab of Solid State Microstructures, Nanjing Univ., China; ⁴Dept. of Mathematics, MIT, USA. We not only derive a sum rule for near-field optical response integrated over all frequencies, but also establish a general framework yielding a geometry-independent limit on bandwidth-averaged response, which we call the power-bandwidth limit.

FTh1K.6 • 09:15

Imaging of Ultra-Confined Phonon Polaritons in Hexagonal Boron Nitride on Gold, Antonio Ambrosio^{2,3}, Michele Tamagnone¹, Kundan Chaudhary¹, Luis Jauregui³, Philip Kim³, William L. Wilson², Federico Capasso¹; ¹School of Engineering and Applied Sciences, Harvard Univ., USA; ²Center for Nanoscale Physics, Harvard Univ., USA; ³Dept. of Physics, Harvard Univ., USA. We investigated infrared phonon polariton on thin hexagonal boron nitride flakes on gold. We successfully imaged ultraslow guided modes in both retransmission bands, using photo-induced force microscopy and scattering type near field scanning optical microscopy

FTh1K.7 • 09:30

Ultrasensitive localization of plasmonic nanoparticles by dual optical lock-in interferometric imaging and photothermal excitation, Seweryn Morawiec¹, Patrycja Stremplewski^{2,1}, Maciej Wojtkowski^{2,1}, Ireneusz Grulkowski¹; ¹Inst. of Physics, Nicolaus Copernicus Univ., Poland; ²Inst. of Physical Chemistry, Polish Academy of Sciences, Poland. Dual optical lock-in (DOLI) interferometric imaging method allowing for simultaneous detection of scattering and absorption depth profiles is proposed and used for highly sensitive localization of gold nanorods in colloidal solution via photothermal excitation.

FTh1K.8 • 09:45

Thermoreflectance Imaging of Optically Pumped Gap Plasmon Structures, Di Wang^{1,2}, Kerry Maize^{1,2}, Maowen Song^{2,3}, Alexandra Boltasseva^{1,2}, Vladimir M. Shalaev^{1,2}, Ali Shakouri^{1,2}, Alexander Kildishev^{1,2}; ¹Electrical and Computer Engineering, Purdue Univ., USA; ²Birck Nanotechnology Center, Purdue Univ., USA; ³Key Lab of Optoelectronic Technology and Systems of Education Ministry of China, Chongqing Univ., China. We developed a fast, high-resolution thermoreflectance imaging-based technique to map the temperature distribution of gap plasmon structures subject to laser irradiation, and observed 120 K temperature rise with 3 mW/μm² irradiance.

CLEO: Science & Innovations

STh1L • MIR to the THz Dual Combs—
Continued

STh1L.4 • 09:00

Dual-comb spectroscopy in the spectral fingerprint region using OPGaP optical parametric oscillators, Oguzhan Kara¹, Luke Maidment¹, Tom Gardiner², Peter G. Schunemann³, Deryck T. Reid¹; ¹Heriot-Watt Univ., UK; ²National Physical Lab (NPL), UK; ³BAE Systems, Inc., USA. Dual-comb spectroscopy using OPGaP optical parametric oscillators is demonstrated with cross-correlation-based spectral averaging to obtain high-fidelity spectra of H₂O and CH₄ at approximately 0.3 cm⁻¹ resolutions from 1285–1370 cm⁻¹ and 1500–1585 cm⁻¹.

STh1L.5 • 09:15

Quantum Cascade Laser-based Dual-Comb Spectroscopy in the Mid-Infrared, Jonas Westberg¹, Lukasz A. Sterczewski^{1,2}, Filippos Kapsalidis³, Yves Bidaux³, Johanna Wolf³, Mattias Beck³, Jérôme Faist³, Gerard Wysocki¹; ¹Dept. of Electrical Engineering, Princeton Univ., USA; ²Faculty of Electronics, Wrocław Univ. of Science and Technology, Poland; ³Institut für Quantenelektronik, ETH Zürich, Switzerland. We demonstrate sub-millisecond response time dual-comb spectroscopy using quantum cascade lasers by measurements of Bromomethane and Freon 134a around 7.7 μm. The system achieves a noise-equivalent absorption of 1×10^{-3} Hz^{-1/2} and an optical bandwidth of ~25 cm⁻¹.

STh1L.6 • 09:30

Massively Parallel Detection of Trace Molecules in a Mixture With An Ultra-Broadband Mid-IR Subharmonic Dual Comb, Andrey Muraviev¹, Viktor O. Smolski², Zachary E. Loparo¹, Konstantin L. Vodopyanov¹; ¹Univ. of Central Florida, CREOL, USA; ²Mid-Infrared Lasers, IPG Photonics, USA. We use a pair of highly-coherent GaAs subharmonic OPOs with instantaneous span 3.1–5.5 μm to demonstrate fast acquisition of 350,000 mode-resolved spectral data points and perform parallel detection in a mixture of 22 molecular species

10:00–15:00 Exhibition Open, Exhibit Hall

10:15–13:00 Technology Transfer Program, Exhibit Hall Theater

10:00–11:30 Coffee Break & Exhibit Only Time, Exhibit Hall

**Marriott
Salon III**

**CLEO: QELS-Fundamental
Science**

**FTh1M • Nonlinear Dynamics in Resonators
and Fibers—Continued**

FTh1M.5 • 09:00

Harmonic dissipative soliton resonance passively mode-locked fiber laser, Georges Semaan¹, Alioune Niang¹, Mohamed Salhi¹, François Sanchez¹; ¹Laboratoire de Photonique d'Angers, France. We experimentally demonstrate for the first time a harmonic mode-locked dissipative soliton resonance square pulses fiber oscillator. High energy stable pulses up to the 13th order of harmonic have been obtained without wave-breaking.

FTh1M.6 • 09:15

Diverse Solitons Interactions in the Formation of Dissipative Optical Soliton Molecules, Junsong Peng¹, Heping Zeng¹; ¹East China Normal Univ., China. Using real-time measurement techniques, we firstly unveil four nonlinear stages in the build-up of soliton molecules in an ultrafast fiber laser, which are modulation instability, mode locking, soliton fission and diverse solitons interactions.

FTh1M.7 • 09:30

Demonstration of Spatial Riemann Waves and Inviscid Burgers' Equation Dynamics in Nonlinear Optics, Domenico Bongiovanni¹, Benjamin Wetzel², Yi Hu³, Pengzhen Yang³, Yujie Qiu³, Jingjun Xu³, Stefan Wabnitz⁵, Zhigang Chen^{4,3}, Roberto Morandotti¹; ¹INRS, Canada; ²School of Mathematical and Physical Sciences, Univ. of Sussex, UK; ³TEDA Applied Physics Inst. and School of Physics, Nankai Univ., China; ⁴Dept. of Physics & Astronomy, San Francisco State Univ., USA; ⁵Dipartimento di Ingegneria dell'Informazione, Università degli Studi di Brescia, Italy. We report on observation of spatial Riemann wave dynamics in a nonlinear m-resol/nylon thermal solution, obtained by properly tailoring the initial optical beam. Experimental results show controllable steepening and shock formation, in good agreement with theory.

FTh1M.8 • 09:45

Observation of a Period-doubling Dynamics of the Modulation Instability Induced Temporal Pattern in a Dispersion Oscillating Fiber-ring Cavity, Francois Copie¹, Matteo Conforti², Alexandre Kudlinski¹, Stefano Trillo³, Arnaud Musot¹; ¹PhLAM, France; ²CNRS, France; ³Dept. of Engineering, Univ. of Ferrara, Italy. We provide a clear demonstration of a period-doubling phenomenon associated to the modulation instability in dispersion oscillating fiber cavities. This has been done by performing roundtrip-to-roundtrip measurements of the temporal pattern generated through the instability.

**Marriott
Salon IV**

CLEO: Science & Innovations

STh1N • Ultrafast Applications—Continued

STh1N.2 • 09:00

1 MHz Ultrafast Cascaded VUV Generation in Negative Curvature Hollow Fibers, Sterling J. Backus¹; ¹KMLabs, USA. We demonstrate 3 tier cascaded harmonic generation to 9th harmonic (115nm) of 1040nm in a negative curvature hollow fiber filled with Xenon gas at a 1MHz repetition rate.

STh1N.3 • 09:15

High Photon Flux XUV Source Driven by Few Cycle Pulses from a Bandwidth-Optimized High Energy Yb-Doped Fiber Amplifier at 1.03 μm , Aura I. Gonzalez^{2,1}, Loïc Lavenu^{2,3}, Florent Guichard³, Yoann Zaouter³, Patrick Georges², Marc Hanna², Thierry Ruchon¹; ¹Amplitude Technologies, France; ²Laboratoire Charles Fabry, Institut d'Optique Graduate School, France; ³Amplitude Systemes, France; ⁴LIDYL, CEA, CNRS, Université Paris-Saclay, France. We report on the advantage of high harmonic generation XUV source driven by a high repetition rate few-cycle ytterbium-doped fiber-laser. We achieve a photon energy cutoff of 140 eV with photon flux of 10¹² photons/s/eV.

STh1N.4 • 09:30

Photon-Induced Near-Field and Far-Field Electron Microscopy, Kangpeng Wang¹, Giovanni M. Vanacore², Enrico Pomarico², Ivan Madan², Gabriele Berruto², Francisco Javier García de Abajo^{3,4}, Ido Kaminer¹, Fabrizio Carbone²; ¹Faculty of Electrical Engineering, Technion - Israel Inst. of Technology, Israel; ²École Polytechnique Fédérale de Lausanne (EPFL), Switzerland; ³The Barcelona Inst. of Science and Technology, Spain; ⁴ICREA - Institució Catalana de Recerca i Estudis Avançats, Spain. We present developments in the technique of photo-induced near-field electron microscopy (PINEM). We image the electron interaction with a far-field plane wave reflected from a mirror, and with the near-field resonance of a plasmonic nanowire.

STh1N.5 • 09:45

Ultrafast spectro-temporal analyzer for the multi-scale laser dynamics studies, Ying Yu¹, Bowen Li¹, Xiaoming Wei², Chi Zhang³, Kevin K. Tsia¹, Kenneth Kin-Yip Wong¹; ¹Univ. of Hong Kong, Hong Kong; ²California Inst. of Technology, USA; ³Huazhong Univ. of Science and Technology, China. We propose a real-time optical spectro-temporal analyzer (ROSTA), which simultaneously provides single-shot temporal and spectral information for multiple time-scale radiance. By using ROSTA, new complex dynamic phenomena during the birth of passive mode-locking is observed.

**Marriott
Salon V**

**CLEO: Applications
& Technology**

ATh1O • Trace Gas Detection—Continued

ATh1O.5 • 09:00

A new Method to Determine the Resonance Frequency in QEPAS, Philipp Breitegger¹, Benjamin Lang¹, Alexander Bergmann¹; ¹TU Graz, Austria. We present a novel method to determine the resonance frequency and Q factor of a quartz tuning fork (QTF) in quartz-enhanced photoacoustic spectroscopy (QEPAS) in a few seconds. A CHIRP modulates a laser diode.

ATh1O.6 • 09:15

GaSb Diode Lasers for QEPAS Sensor Applications, Tobias Milde¹, Morten Hoppe^{1,2}, Herve Tatenguem Fankem¹, Wolfgang Schade³, Joachim Sacher¹; ¹Sacher Lasertechnik GmbH, Germany; ²Technische Hochschule Mittelhessen, Germany; ³Technische Universität Clausthal, Germany. Newly developed tunable single mode laser diodes based on GaSb material system in the wavelength range 1.6 $\mu\text{m} \leq \lambda \leq 4 \mu\text{m}$ are combined with the QEPAS technique for trace gas detection.

ATh1O.7 • 09:30

Fiber Laser Intracavity Quartz-Enhanced Photoacoustic Gas Sensor, Qiang Wang¹, Zhen Wang¹, Pietro Patimisco², Angelo Sampaolo², Vincenzo Spagnolo², Wei Ren¹; ¹The Chinese Univ. of Hong Kong, Hong Kong; ²Politecnico di Bari, Italy. We report a novel photoacoustic trace gas sensor by using a custom-designed quartz tuning fork inside a fiber ring laser cavity for sensitive gas detection with a large dynamic range.

ATh1O.8 • 09:45

Sub-Parts-Per-Trillion Sensitivity in Trace Gas Detection by Cantilever-Enhanced Photo-Acoustic Spectroscopy, Teemu Tomberg¹, Markku M. Vainio^{1,2}, Tuomas Hieta³, Lauri Halonen¹; ¹Dept. of Chemistry, Univ. of Helsinki, Finland; ²Lab of Photonics, Tampere Univ. of Technology, Finland; ³Gasera Ltd., Finland. We report a simple cantilever-enhanced photoacoustic detector, which reaches exceptionally good sensitivity in trace gas detection of hydrogen fluoride by using a highly stable narrow-linewidth optical parametric oscillator at 2.476 μm .

10:00–15:00 Exhibition Open, Exhibit Hall

10:15–13:00 Technology Transfer Program, Exhibit Hall Theater

10:00–11:30 Coffee Break & Exhibit Only Time, Exhibit Hall

**CLEO: QELS-Fundamental
Science**

**FTh1P • Engineering and Metrology of
Thermal Radiation—Continued**

FTh1P.2 • 09:00

Demonstration of On-Chip Thermocouple Photodetector in Infrared Regime through Field Enhancement by Plasmonic Nano Focusing, Orián Keneth¹, P. Arora¹, Noa Mazurski¹, Uriel Levy¹; ¹*Applied Physics, Hebrew Univ. of Jerusalem, Israel.* <div style="direction: ltr;">On-chip thermocouple photodetector is realized for near infrared regime. Conversion of electromagnetic field to heat was performed through plasmonic mode which leads to joule heating at the metal. The responsivity of the device is $32 \pm 1 \text{ mV/W}$.</div>

FTh1P.3 • 09:15 **Invited**

Thermal Homeostasis and Hybrid Optothermal Logic, Michelle L. Povinelli¹, Ahmed Morsy¹, Shao-Hua Wu¹, Mingkun Chen¹, Michael Barako², Vladan Jankovic², Philip W. Hon², Luke Sweatlock²; ¹*Univ. of Southern California, USA*; ²*NG Next, Northrop Grumman Corporation, USA*. We exploit the co-design of optical and thermal properties for microphotonic applications. We design a material that passively regulates its temperature by switching on/off its thermal emission. We experimentally demonstrate a hybrid optothermal logic device.

FTh1P.4 • 09:45

Single-molecule Thermometry by Carbon Nanotube Excitons Coupled to Plasmonic Nanocavities, Yue Luo^{1,4}, Ehsaneh D. Ahmadi¹, Kamran Shayan^{1,4}, Yichen Ma^{1,4}, Kevin S. Mistry², Changjian Zhang³, James Hone³, Jeffrey L. Blackburn², Stefan Strauf^{1,4}; ¹*Dept. of Physics, Stevens Inst. of Technology, USA*; ²*National Renewable Energy Lab, USA*; ³*Dept. of Mechanical Engineering, Columbia Univ., USA*; ⁴*Center for Quantum Science and Engineering, USA*. In a unique interplay of excitons, phonons, and plasmons, we demonstrate plasmonic thermometry at the single-molecule level by detecting the plasmonically induced heat from SWCNT excitons coupled to plasmonic nanocavity arrays.

**CLEO: Applications
& Technology**

**ATh1Q • A&T Topical Review on
Neurophotonics I—Continued**

ATh1Q.2 • 09:00

Ultrasonic Guiding and Steering of Light in Scattering Tissue, Matteo Giuseppe Scopelliti¹, Maysam Chamanzar¹; ¹*Carnegie Mellon Univ., USA*. We present a novel technique for guiding and steering photons in multiply scattering brain tissue by using ultrasound waves to sculpt refractive index contrast profiles that define and control the trajectory of light within tissue.

ATh1Q.3 • 09:30

Spectral Multiplexing of Optogenetic Switch by Stimulated Emission Depletion Quenching, Alexei Goun¹; ¹*Princeton Univ., USA*. We demonstrate that stimulated emission depletion quenching allows for higher fidelity control of optogenetic switching

ATh1Q.4 • 09:45

Attojoule Modulators for Photonic Neuromorphic Computing, Rubab Amin¹, Jonathan George¹, Jacob Khurgin², Tarek El-Ghazawi¹, Paul R. Prucnal³, Volker J. Sorger¹; ¹*George Washington Univ., USA*; ²*Johns Hopkins Univ., USA*; ³*Princeton Univ., USA*. We show how the nonlinear transfer function of electrooptic modulators enables vector matrix multiplications of photonic neural networks. Here the modulators energy-per-bit function and signal-to-noise ratio are critical factors impacting system performance.

10:00–15:00 **Exhibition Open**, *Exhibit Hall*

10:15–13:00 **Technology Transfer Program**, *Exhibit Hall Theater*

10:00–11:30 **Coffee Break & Exhibit Only Time**, *Exhibit Hall*

JTh2A.1

Limits on manipulating conditional photon statistics of lasers via interference and post-selections, Kang-Hee Hong¹, Jisung Jung², Young-Wook Cho², Sang-Wook Han², Sung Moon², Kyunghwan Oh³, Yong-Su Kim², Yoon-Ho Kim¹; ¹Pohang Univ. of Sci & Tech (POSTECH), South Korea; ²Korea Inst. of Science and Technology (KIST), South Korea; ³Yonsei Univ., South Korea. Recently it has been reported that photon anti-bunching can be obtained via interference of lasers. We provide counter-evidence by theoretical analysis on the limits of manipulating conditional photon statistics of lasers via interference and post-selections.

JTh2A.2

Photon-Pair State Engineering in Raman-Mediated Four-Wave Mixing, Kai B. Shinbrough¹, Bin Fang¹, Yanting Teng¹, Yujie Zhang¹, Offir Cohen¹, Virginia O. Lorenz¹; ¹Univ. of Illinois Urbana-Champaign, USA. Towards delayed-choice generation of single photons in pure quantum states, we measure and model the purity of Stokes photons scattered from sapphire, measuring a maximum purity of 0.99±0.03 and high quantum correlation with anti-Stokes photons.

JTh2A.3

Mechanically Tunable Photonic Crystal Cavity with High Quality Factor and Small Mode Volume, Xiruo Yan^{1,2}, Jingda Wu^{1,2}, Ryan Watt¹, Megan Nantel¹, Lukas Chrostowski^{2,3}, Jeff Young^{1,2}; ¹Physics and Astronomy, Univ. of British Columbia, Canada; ²Stewart Blusson Quantum Matter Inst., Canada; ³Electrical and Computer Engineering, Univ. of British Columbia, Canada. A fractured planar photonic crystal microcavity is designed to be mechanically tunable while maintaining a quality factor of >1×10⁵, and a mode volume ~0.3 (λn)³. Its optomechanical coefficient is ~15GHz/nm, at mid-IR wavelengths.

JTh2A.4

Sorting Laguerre-Gaussian modes by radial quantum number, Yiyu Zhou¹, Mohammad Mirhosseini¹, Dongzhi Fu^{1,2}, Jiapeng Zhao¹, Seyed Mohammad Hashemi Rafsanjani¹, Alan E. Willner³, Robert Boyd^{1,4}; ¹The Inst. of Optics, Univ. of Rochester, USA; ²Key Lab for Quantum Information and Quantum Optoelectronic Devices, Dept. of Applied Physics, Xi'an Jiaotong Univ., China; ³Dept. of Electrical Engineering, Univ. of Southern California, USA; ⁴Dept. of Physics, Univ. of Ottawa, Canada. An efficient sorter based on the fractional Fourier transform is realized to detect the radial quantum number of the Laguerre-Gaussian modes. The reported scheme can, in principle, have unit efficiency and no cross-talk.

JTh2A.5

Sub-Poissonian Twin-Beam Correlations at Blue and Red Wavelengths from Four-Wave Mixing, Jason D. Mueller^{1,1}, Alex McMillan¹, Paul-Antoine Moreau³, Javier Sabines-Chesterking¹, John Rarity¹, Peter J. Mosley², Jonathan Matthews¹; ¹Quantum Engineering Technology Labs, Univ. of Bristol, UK; ²Centre for Photonics and Photonic Materials, Univ. of Bath, UK; ³School of Physics and Astronomy, Univ. of Glasgow, UK; ⁴Quantum Engineering Centre for Doctoral Training, Univ. of Bristol, UK. We demonstrate sub-Poissonian intensity correlations of twin beams at short wavelengths: 442nm and 665nm. The beams are generated via four-wave mixing in photonic crystal fiber, measured with a CCD camera.

JTh2A.6

Towards a Waveguide-based Single Photon Detector for Integrated Quantum Photonics Platforms, Salih Yanikgonul^{1,2}, Jun Rong Ong³, Victor Leong¹, Leonid Krivitskiy¹; ¹Advanced Concepts and Nanotechnology, Data Storage Inst. (DSI) of A*STAR, Singapore; ²Centre for Disruptive Photonic Technologies, Nanyang Technological Univ., Singapore; ³Electronics and Photonics, Inst. of High Performance Computing, Singapore. We design a waveguide-based Geiger-mode silicon single-photon avalanche diode (SPAD), optimized for visible wavelengths. We simulate photon detection efficiency and timing jitter with 2D Monte Carlo simulator for SPADs with different widths and bias voltages.

JTh2A.7

Ghost Imaging with Paired X-ray Photons, Aviad Schori^{1,2}, Denis Borodin^{1,2}, Kenji Tamasaku², Sharon Shwartz^{1,2}; ¹Bar-Ilan Univ., Israel; ²RIKEN SPring-8 Center, Japan. We observed of ghost imaging with parametrically down-converted x-ray photons pairs. We reconstructed the image of slits with nominally zero background levels. Our procedure can lead to the observation of quantum phenomena at x-ray wavelengths.

JTh2A.8

Photon-Number Resolution in Conventional Superconducting Nanowire Single-Photon Detectors: Theoretical Predictions, Kathryn Nicolich¹, Clinton T. Cahall², Nurul T. Islam³, Gregory P. Lafyatis¹, Jungsang Kim^{2,4}, Daniel J. Gauthier¹; ¹Dept. of Physics, Ohio State Univ., USA; ²Dept. of Electrical and Computer Engineering, Duke Univ., USA; ³Dept. of Physics, Duke Univ., USA; ⁴IonQ Inc., USA. We demonstrate theoretically that a conventional single-pixel superconducting nanowire single-photon detector can resolve photon number by sensing changes in the rising edge of the electrical readout pulse

JTh2A.9

Passive State Preparation in Continuous Variable Quantum Key Distribution, Bing Qi¹, Phil Evans¹, Warren Grice¹; ¹Oak Ridge National Lab, USA. We propose a passive continuous-variable quantum key distribution scheme, where Alice splits the output of a thermal source into two spatial modes, measures one locally and transmits the other mode to Bob after applying attenuation.

JTh2A.10

Security verification for vacuum fluctuation based quantum random number generator, Arne Kordts¹, Cosmo Lupo², Dino Solar¹, Tobias Gehring¹, Ulrik L. Andersen¹; ¹Danmarks Tekniske Universitet, Denmark; ²Univ. of York, UK. We demonstrate a gigahertz source of verifiable quantum random numbers based on homodyne detection of the vacuum state. Using a whitening filter, we generate iid samples with a potential randomness rate of 20Gbit/s.

JTh2A.11

Multipartite Quantum Entanglement and Quantum Correlation from cascaded Four-wave Mixing Processes with spatial multiplexing, Jietai Jing¹, Shuchao Lv¹, Kai Zhang¹, Wei Wang¹, Hailong Wang¹, Jun Xin¹, Leiming Cao¹, Sijin Li¹, Li Wang¹, Jinjian Du¹; ¹East China Normal Univ., China. Four-wave mixing (FWM) process with spatial multiplexing is a promising candidate for building quantum network. We experimentally investigate multipartite quantum correlation and theoretically study multipartite quantum entanglement from cascaded FWM processes.

JTh2A.12

1.064-μm-band Up-conversion Single-photon Detector, Fei Ma¹, Ming-Yang Zheng², Quan Yao³, Xiu-Ping Xie², Qiang Zhang^{1,3}, Jian-Wei Pan¹; ¹Hefei National Lab for Physical Sciences at Microscale and Dept. of Modern Physics, Univ. of Science and Technology of China, China; ²Shandong Inst. of Quantum Science and Technology Co., Ltd., China; ³Jinan Inst. of Quantum Technology, China. We demonstrate an up-conversion single-photon detection at 1.064-μm band using a PPLN waveguide. By employing two kinds of filtering schemes, we achieve the detection efficiency of 32.5% and 38% with noise count rate of 45 cps and 700 cps respectively.

JTh2A.13

Performance Improvement of Discrete-Modulation Continuous-Variable Quantum Key Distribution by Using the Machine-Learning-Based Detector, Jiawei Li¹, Duan Huang¹, Cailiang Xie¹, Ling Zhang¹, Ying Guo¹; ¹School of Information Science and Engineering, Central South Univ., China. The discrete-modulation continuous-variable quantum key distribution is proposed using the machine-learning-based detector to preprocess the signal before the reconciliation, which would mitigate the burden of error correction reconciliation and further improve the system performance.

JTh2A.14

Generation of Multi-mode NOON States with Arbitrary N, Lu Zhang¹, Kam Wai C. Chan¹; ¹Univ. of Oklahoma, USA. We present three methods of generating multi-mode NOON states with arbitrary photon number using either coherent states or Fock states along with single photons. Generation probabilities are calculated to show their efficiencies.

JTh2A.15

Experimental Demonstration of a 20-Mbit/s per Channel Free-Space Bi-directional Quantum Communication Link Using Orbital-Angular-Momentum Encoding and Multi-Port Mode Converters, Cong Liu¹, Kai Pang¹, Hao Song¹, Guodong Xie¹, Jiapeng Zhao², Yongxiong Ren¹, Haoqian Song¹, Zhe Zhao¹, Runzhou Zhang¹, Long Li¹, Jing Du¹, Seyed Rafsanjani², Guillaume Labroille³, Pu Jian³, Robert Boyd², Moshe Tur¹, Alan E. Willner¹; ¹Univ. of Southern California, USA; ²The Inst. of Optics, Univ. of Rochester, USA; ³CALabs, France; ⁴School of Electrical Engineering, Tel Aviv Univ., Israel. We experimentally demonstrate a free-space, bi-directional quantum communication link encoded by two OAM states using multi-port mode converters. We achieve a quantum-symbol-error-rate of ≈ 0.058 for each channel at 20 Mbit/s/channel when OAM mode-spacing is 4.

JTh2A.16

Spectral Resolution of Second-Order Coherence of Broad-band Biphotons, Ashutosh Rao¹, Nima Nader², Thomas Gerits², Martin J. Stevens², Omar S. Magana Loaiza², Guillermo Camacho-Gonzalez¹, Jeffrey Chiles², Amirmahdi Honardoost¹, Marcin Malinowski¹, Richard Mirin², Sasan Fathpour¹; ¹CREOL, Univ. Central Florida, USA; ²NIST, USA. We spectrally resolve the second-order coherence of biphoton pairs using a time-of-flight fiber spectrometer. Spectrally resolved coincidence-to-accidental ratios of over 300 are measured using a thin-film lithium niobate waveguide source on a silicon chip.

JTh2A.17

One-Way Noise Measurement of Deployed Optical Fiber for Quantum Networks Using Mode-Locked Lasers, Helena Zhang^{1,2}, Matthew E. Grein³, Scott A. Hamilton³, Issac Chuang^{2,1}; ¹Research Lab of Electronics, MIT, USA; ²Dept. of Physics, MIT, USA; ³Lincoln Lab, MIT, USA. One-way noise across a 42-km deployed optical fiber link is measured using two different techniques employing referenced mode-locked lasers. We compare the two techniques and assess their suitability for stabilizing the fiber for quantum networks.

JTh2A.18

Determining Full Parameters of U-Matrix for Reconfigurable Boson Sampling Circuits using Machine Learning, Lingxiao Wan¹, Hui Zhang¹, Jianguo Huang¹, Gong Zhang¹, Leong Chuan Kwek², Joseph F. Fitzsimons³, Yidong Chong¹, Jiangbin Gong², Alexander Szameit⁴, Xiaoqi Zhou⁵, Man-Hong Yung⁶, Xianmin Jin⁷, Xiaolong Su⁸, Wee Ser¹, WeiBo Gao¹, Aiqun Liu¹; ¹Nanyang Technological Univ., Singapore; ²National Univ. of Singapore, Singapore; ³Singapore Univ. of Technology and Design, Singapore; ⁴Univ. of Rostock, Germany; ⁵Sun Yat-sen Univ., China; ⁶Southern Univ. of Science and Technology, China; ⁷Shanghai Jiaotong Univ., China; ⁸Shanxi Univ., China. A method of tuning a reconfigurable silicon photonic circuit into an arbitrary unitary operator with machine learning was proposed to bypass the traditional phase-voltage calibration process and make the prediction of applied heating voltage directly.

JTh2A.19

Performance analysis of d-dimensional quantum cryptography with mode-dependent diffraction, Jiapeng Zhao², Mohammad Mirhosseini¹, Yiyu Zhou², Seyed Mohammad Hashemi Rafsanjani², Yongxiong Ren³, Nicholas Steinhoff⁴, Glenn Tyler⁴, Robert Boyd²; ¹California Inst. of Technology, USA; ²Univ. of Rochester, USA; ³Univ. of Southern California, USA; ⁴The Optical Science Company, USA. We analyze the degraded performance of QKD that results from mode-dependent diffraction in spatial-mode-encoded QKD systems. A pre-compensation method is proposed to solve this problem without sacrificing the security.

JTh2A.20

Quantum temporal imaging and gravitational wave detection, Dmitri Horoshko^{2,1}, Giuseppe Patera², Mikhail I. Kolobov², B. I. Stepanov *Inst. of Physics, NASB, Belarus*; ²CNRS, UMR 8523 - PhLAM, Univ. of Lille, France. We study the quantum field evolution in a temporal imaging system, including the vacuum noise due to finite time aperture. We show how the gravitational wave detector signal can be transmitted to a higher frequency.

JTh2A.21

Purification of Photon Subtraction from Continuous Squeezed Light by Filtering, Jun-ichi Yoshikawa¹, Warit Asavanant¹, Akira Furusawa¹; ¹Univ. of Tokyo, Japan. We show that Schrödinger cat states, generated by photon subtraction from squeezed states with conventional continuous-wave methods, have an inherent impurity. Furthermore, we show that the impurity is arbitrarily suppressed by optical filtering.

JTh2A.22

Quantum-Classical Transmission on Single Wavelength, Rupesh Kumar¹, Adrian Wonfor², Richard V. Pentyl², Ian White²; ¹Quantum Communication Hub, UK; ²Univ. of Cambridge, UK. We demonstrate, for the first time, simultaneous generation, transmission and reception of quantum signals and classical signals on a single wavelength. 61.6kbps Quantum key and 590kbps classical data rates are estimated.

JTh2A.23

Quantum monitored long-distance secure optical network, Yupeng Gong¹, Rupesh Kumar², Adrian Wonfor¹, Richard V. Pentyl¹, Ian White¹; ¹Univ. of Cambridge, UK; ²Univ. of York, UK. We report a method for monitoring physical layer attacks in optical fiber communication using a modulated quantum signal. This system utilizes the quantum noise of the quadrature components of coherent states to monitor fiber links with quantum sensitivity.

JTh2A.24

High-Speed Quantum Key Distribution with Wavelength-Division Multiplexing on Integrated Photonic Devices, Alasdair Price^{1,2}, Philip Sibson¹, Chris Erven¹, John Rarity¹, Mark G. Thompson¹; ¹Centre for Quantum Photonics, Univ. of Bristol, UK; ²Quantum Engineering Centre for Doctoral Training, Univ. of Bristol, UK. We experimentally implement a compact and practical solution for wavelength-division multiplexed quantum key distribution using integrated photonics. This increases secret key rates and allows for greater operational flexibility to meet network user requirements.

JTh2A.25

Quantum-Enhanced Optomechanical Magnetometry, Jan Bilek¹, BeiBei Li², Ulrich B. Hoff¹, Lars Madsen², Stefan Forstner², Varun Prakash², Clemens Schäfermeier¹, Tobias Gehring¹, Warwick Bowen², Ulrik L. Andersen¹; ¹Technical Univ. of Denmark, Denmark; ²The Univ. of Queensland, Australia. Quantum-enhanced measurements of magnetic fields are experimentally demonstrated using a microcavity optomechanical magnetometer and squeezed states of light. We attain an improvement of the magnetic field sensitivity of 20% using 2.2dB phase-squeezed states.

JTh2A.26

Breaking up the Anapole: or How to Separate Toroidal and Electric Dipole Excitations in Matter, Vassili Savinov¹, Wei-Yi Tsai^{1,2}, Din Ping Tsai^{3,2}, Nikolay I. Zheludev^{1,4}; ¹Univ. of Southampton, UK; ²Dept. of Physics, National Taiwan Univ., Taiwan; ³Research Center for Applied Sciences, Academia Sinica, Taiwan; ⁴Centre for Disruptive Photonic Technologies, Nanyang Technological Univ., Singapore. Increasing interest in electrodynamics and spectroscopy of toroidal excitations in matter has initiated a discussion on independent physical significance of toroidal and electric dipole excitations. Here we introduce three Gedanken-Experiments that reveal their fundamental differences.

JTh2A.27

On-Chip Electro-Mechanical Routing of Single Photons from an Embedded Quantum Emitter, Zofia K. Bishop¹, Andrew P. Foster¹, Benjamin Royall¹, Christopher Bentham¹, Ed Clarke², Maurice S. Skolnick¹, Luke R. Wilson¹; ¹Physics and Astronomy, The Univ. of Sheffield, UK; ²Electronic and Electrical Engineering, The Univ. of Sheffield, UK. We demonstrate on-chip routing of single photons using a III-V semiconductor-based electro-mechanical system with embedded quantum dots. Switching is achieved by electro-mechanical actuation of an integrated directional coupler.

JTh2A.28

Certification of high-dimensional entanglement and Einstein-Podolsky-Rosen steering with quantum memory, Mateusz Mazelanik¹, Michal Dabrowski¹, Michal Parniak¹, Adam Leszczynski¹, Michal Lipka¹, Wojciech Wasilewski¹; ¹Univ. of Warsaw, Poland. We experimentally generate a spatially-entangled state using a Raman multimode quantum memory setup and characterize it with the entropic EPR-steering inequality. We obtain genuine violation of 1.06 ± 0.05 bits and certify entanglement of formation of at least 0.70 ± 0.04 ebits.

JTh2A.29

Ultrafast leakage suppression in weakly nonlinear atomic qubits, Hanlae Jo¹, Yunheung Song¹, Jaewook Ahn¹; ¹Korean Adv Inst of Science and Tech, South Korea. We propose and experimentally demonstrate ultrafast coherent control scheme for leakage transition suppression through inducing destructive interference of constituent two-photon pathways in a three-level system of atomic rubidium, without disturbing resonant two-level qubit subspace operations.

JTh2A.30

Fiber-Integrated Single Photon Devices with High Efficiency and Directional Emission, Changmin Lee¹, Mustafa A. Buyukkaya¹, Edo Waks^{1,2}; ¹Univ. of Maryland, USA; ²Joint Quantum Inst., Univ. of Maryland and National Inst. of Standard and Technology, USA. Fiber-integrated single photon device based on quantum dot nanobeam and fiber taper is proposed and calculated. Total collection efficiency of 88% is achieved into one arm of fiber taper. Broadband and robust operation of the system is also confirmed.

JTh2A.31

Improving Squeezed Vacuum Generation via Spatial Mode Shaping in Hot Rb Vapor, Irina Novikova¹, Mi Zhang¹, Melissa A. Guidry¹, Eugeniy Mikhailov¹, R N. Lanning², Zhihao Xiao², Jonathan P. Dowling²; ¹College of William & Mary, USA; ²Physics, Louisiana State Univ., USA. Achievable squeezed vacuum may be limited by contamination of the output fields with higher-order spatial modes. Squeezing can be improved by multipass interactions with a less optically-dense medium or by spatial tailoring of the input.

JTh2A.32

An 8-branch optical frequency comb for laser frequency stabilization and measurement in optical lattice clocks, Yusuke Hisai^{1,2}, Daisuke Akamatsu², Takumi Kobayashi², Sho Okubo², Hajime Inaba², Kazumoto Hosaka², Feng-Lei Hong¹, Masami Yasuda²; ¹Yokohama National Univ., Japan; ²National Metrology Inst. of Japan, National Inst. of Advanced Industrial Science and Technology, Japan. We have developed an 8-branch fiber comb for frequency stabilization and measurement of multiple lasers. Seven lasers used in the Sr and Yb optical lattice clocks are frequency stabilized or measured using the developed comb.

JTh2A.33

Spatially-resolved spin manipulation using ac-Stark effect, Adam Leszczynski¹, Mateusz Mazelanik¹, Michal Parniak¹, Michal Dabrowski¹, Michal Lipka¹, Wojciech Wasilewski¹; ¹Inst. of Experimental Physics, Facul, Poland. We used a Zeeman-like ac-Stark shift to perform spatially-resolved rotations of spins in cold rubidium. Using SLM we extended coherent spins oscillations time and imprinted comb-like patterns on the atomic ensemble.

JTh2A.34

Charging Dynamics of Single InGaAs Quantum Dots under Resonant Excitation, Gary R. Lander¹, Samantha D. Isaac¹, Disheng Chen¹, Glenn S. Solomon², Edward Flagg¹; ¹West Virginia Univ., USA; ²Joint Quantum Inst., National Inst. of Standards and Technology, USA. We investigate the rates of charge fluctuation in single quantum dots under resonant excitation, with additional modulated low-power above-band excitation. Time-resolved fluorescence is fit using stretched/compressed exponentials, indicating a continuum of relaxation and charging rates.

JTh2A.35

Integrated Photonic Platform for Scalable Ion-Qubits towards Quantum Information Networking, Youngmin M. Kim¹, Shahriar Aghaieimobodi¹, Edo Waks¹; ¹Univ. of Maryland, USA. We propose a SiN photonic platform where ion-qubits can be effectively coupled to polarization insensitive photonic circuits. Our approach aims to improve scalability of ion-qubit system via integration with photonic devices which could form a base architecture for realizing a quantum network.

JTh2A.36

Dissipation-enhanced optomechanically induced transparency, Yong-Chun Liu¹, Cuicui Lu¹, Li You¹; ¹Tsinghua Univ., China; ²Qian Xuesen Lab of Space Technology, China. We find that dissipation can be utilized as a resource to enhance optomechanically induced transparency in the unresolved sideband regime. This positive effect of dissipation holds potential for applications including high-precision measurements and slow light.

JTh2A.37

Highly Directional Single Photon Source Based on Nitrogen Vacancy Centers, Niko Nikolay¹, Boaz Lubotzky², Alexander Dohms¹, Hamza Abudayyeh², Nikola Sadzak¹, Florian M. Böhm¹, Bernd Sontheimer¹, Ronen Rapaport², Oliver Benson¹; ¹Humboldt-Universität zu Berlin, Germany; ²Hebrew Univ. of Jerusalem, Israel. A stable single photon device consisting of a nitrogen vacancy center coupled to a bulls-eye grating will be presented. Beside the highly directional emission pattern, we will report on the functionalization technique using electrostatic forces.

JTh2A.38

Nitrogen-Vacancy Based Spectroscopy and Control of the Local Paramagnetic Spin Bath in Nitrogen-15 Delta-Doped Diamond, Florian M. Böhm¹, Nikola Sadzak¹, Claudia Widmann², Christoph Nebel², Oliver Benson¹; ¹Humboldt-Universität zu Berlin, Germany; ²Fraunhofer-Institut für Angewandte Festkörperphysik, Germany. We present the spectroscopy of the local paramagnetic spin bath in nitrogen-15 delta-doped (111) diamond using single shallow nitrogen-vacancy centers as sensors and probe the spin bath dynamics with double spin resonance schemes.

JTh2A.39

Towards Light Storage and Retrieval from a Solid-State Atomic Ensemble at the Single-Photon Level, Kumel Kagalwala¹, Elizabeth A. Goldschmidt², Sergey Polyakov^{3,1}, Alan Migdal^{3,1}; ¹Joint Quantum Inst., UMCP, USA; ²US Army Research Labs, USA; ³National Inst. of Standards and Technology, USA. We report progress towards the implementation of a quantum memory in a rare-earth ion-doped crystal. Toward that goal, we demonstrate a narrowband spectral filter for our memory, and measure the optical correlations.

JTh2A.40

Observation of plasmonic enhanced EIT and velocity selective optical pumping measurements with atomic vapor, Eliran Talker¹, P. Arora¹, Yefim Barash¹, Liron Stern¹, Uriel Levy¹; ¹Dept. of Applied Physics, 91904, Israel, The Benin School of Engineering and Computer Science, The Center for Nanoscience and Nanotechnology, The Hebrew Univ. of Jerusalem, Israel. We demonstrate theoretically and experimentally for the first time nanoscale plasmonic enhanced electromagnetically induced transparency and velocity selective optical pumping effects in miniaturized integrated quantum plasmonic device for D₂ transitions in rubidium with V-type system

JTh2A.41

Probing dipole-dipole interaction at cold-atom density range using optical two-dimensional coherent spectroscopy, Shaogang Yu^{1,2}, Michael Titzel¹, XiaoJun Liu², Hebin Li¹; ¹Dept. of physics, Florida International Univ., USA; ²Wuhan Inst. of Physics and Mathematics, Chinese Academy of Sciences, China. We experimentally demonstrate that the dipole-dipole interaction in a potassium vapor at cold atom density can be observed using optical 2D coherent spectroscopy. This paves the way to implement 2D spectroscopy in cold atoms.

JTh2A.42

Coherent Population Trapping in Cs-filled Kagome Hollow Core Fibers, Marcelo A. Gouveia^{1,2}, Thomas Bradley¹, Mohsin Hajji², Natalie Wheeler¹, Yong Chen¹, Seyed Sandoghchi¹, David Richardson¹, Patrick Gill², Marco Petrovich¹; ¹Optoelectronics Research Centre, UK; ²Quantum Metrology Inst., National Physical Lab, UK. We report for the first time Coherent Population Trapping (CPT) in Cs-filled Kagome Hollow Core Fibers. Dark resonance contrasts of up to 9 % and linewidths as narrow as 1.8 MHz were observed.

JTh2A.43

Novel nonlinear collective effects in hybrid quantum systems: relaxation to negative temperatures, William Munro^{1,2}, Yusuke Hama², Kae Nemoto²; ¹NTT Basic Research Labs, Japan; ²National Inst. of Informatics, Japan. Nonlinear systems are known to exhibit interesting and important phenomena that have profoundly changed our technological landscape. They can now be explored in quantum hybrid systems and here we discuss novel effects such as superradiance induced negative temperature relaxation in such systems.

JTh2A.44

Spontaneous and Stimulated Emission from Quantum Optical Systems, Rahul Trivedi^{2,1}, Kevin Fischer², Shanshan Xu³, Shanhui Fan², Jelena Vuckovic²; ¹Stanford Univ., USA; ²Electrical Engineering, Stanford, USA; ³Physics, Stanford, USA. We develop a method based on the input-output formalism to analyze stimulated emission of photons by a low-dimensional quantum optical system into 1D loss channels (e.g. waveguides) or a spatial continuum (e.g. free space, photonic crystals).

JTh2A.45

Channeling of Spontaneous Emission from an Atom into the Fundamental and Higher-Order Modes of a Vacuum-Clad Ultrathin Optical Fiber, Fam Le Kien¹, Sahar Hejazi¹, Thomas Busch¹, Viet Giang Truong¹, Sile Nic Chormaic¹; ¹Okina Inst of Sci and Tech Grad Univ, Japan. We study spontaneous emission from a multilevel atom into the fundamental and higher-order modes of a vacuum-clad ultrathin optical fiber. We examine the dependencies of the rate on the type of modes, the position of the atom, and the fiber radius.

JTh2A.46

Photostable Single-Photon Emission from Organic Nanocrystals, Sofia Pazzagli^{1,2}, Pietro Lombardi^{2,3}, Daniele Martella³, Maja Colautti³, Bruno Tiribilli⁴, Francesco Cataliotti^{1,2}, Costanza Toninelli^{2,3}; ¹Dept. of Physics and Astrophysics, Univ. of Florence, Italy; ²National Inst. of Optics, INO-CNR, Italy; ³European Lab for Nonlinear Spectroscopy (LENS), Italy; ⁴Inst. of Complex Systems, ISC-CNR, Italy. We report on organic nanocrystals doped with tunable concentration of fluorescent molecules, grown with an easy and inexpensive method and performing as bright and photostable single-photon sources at both room and cryogenic temperatures.

JTh2A.47

Exceptional Points in Passive Plasmonic Nanostructure for Sensing, Jun-Hee Park¹, Ashok Kodigala¹, Abdoulaye Ndao¹, Boubacar Kante¹; ¹Univ. of California San Diego, USA. We propose a passive plasmonic nanostructures sensor operated at an exceptional point (EP), that fundamentally shift more than conventional resonances and will pave the way to highly sensitive plasmonic devices.

JTh2A.48

Spin Hall Effect from Achiral Nanohole Arrays, Chao Liu¹, Xiaoyu Guo¹, H. C. Ong¹; ¹Chinese Univ. of Hong Kong, Hong Kong. We continuously steer the propagation direction of the degenerate (-1, ±1) surface plasmon on circular nanohole arrays under an elliptical polarization. The directionality has been attributed to the coherent control of the dark and bright modes.

JTh2A.49

Angular sensitivity of PT-symmetric optical lattices, Konstantinos Makris¹, Stylianos Miliotis², Ioannis Komis¹; ¹Univ. of Crete, Greece; ²Inst. for Theoretical Physics, Vienna Univ. of Technology, Austria. We investigate the sensitivity of the diffraction pattern in PT optical lattices near exceptional points. We examine the range of excitation angles, in one and two-dimensional lattices, that leads to the maximum sensitivity.

JTh2A.50

Surface Emitting Plasmonic Laser with Distributed Feedback, Ekemba K. Tanyi³, Soheila Mashhadi³, Cansu On^{3,2}, Md Omar Faruq³, Erin Harrison^{1,2}, Mikhail A. Noginov^{3,2}; ¹Univ. of Delaware, USA; ²Summer Research Program, Center for Materials Research, NSU, USA; ³Center for Materials Research, NSU, USA. We have demonstrated the novel low-threshold surface-emitting plasmonic laser and explained its performance in terms of the distributed feedback mechanism, providing a new degree of freedom to the laser design.

JTh2A.51

Hybrid-plasmonic gold coated GaAs nanowire lasers, Fatemesadat Mohammadi¹, Mykhaylo Lysevych², Hoe Tan², Chennupati Jagadish², Martin Fraenzl³, Hans Peter Wagner¹; ¹Dept. of Physics, Univ. of Cincinnati, USA; ²Dept. of Electronic Materials Engineering, The Australian National Univ., Australia; ³Dept. of Physics, Univ. of Leipzig, Germany. Hybrid plasmonic lasing from zinc doped GaAs nanowires which were coated with a 10 nm thick granular gold layer was observed. The result suggests that hybrid-plasmonic lasing is achievable despite of a non-continuous metal surface.

JTh2A.52

Tunable Random Lasing Emissions by Manipulating Plasmonic Coupling Strengths on Flexible Substrates, TingWei Yeh¹, ChunYang Chou¹, ZuPo Yang², Nguyen Thi Bich Hanh¹, YungChi Yao¹, Meng-Tsan Tsai^{3,4}, Hao-Chung Kuo⁵, Ya-Ju Lee¹; ¹National Taiwan Normal Univ., Taiwan; ²National Chiao-Tung Univ., Taiwan; ³Chang Gung Univ., Taiwan; ⁴Chang Gung Memorial Hospital, Taiwan; ⁵National Chiao Tung Univ., Taiwan. We experimentally demonstrated flexible random lasers fabricated on the PET substrate with tunable emissions. Lasing wavelength is blue-shifted with the bending strains exerted on the PET, and the maximum shift of ~15 nm was achieved.

JTh2A.53

Optical properties of graphene flakes and organic molecules, Rodrigo A. Muniz¹, Zahene S. Sadeq¹, John E. Sipe¹; ¹Univ. of Toronto, Canada. We compute the electronic states of graphene flakes and organic molecules including electron correlations beyond the mean field level. We analyze the linear and nonlinear optical properties of these systems and discuss their implications.

JTh2A.54

Highly Sensitive Refractive Index Sensing with Silicon-Based Dielectric Metasurfaces, Adam Ollanik¹, Matthew D. Escarra¹; ¹Tulane Univ., USA. We design and simulate microfluidic refractive index sensors based on optical dielectric metasurfaces comprised of resonant silicon nanoantennas. Sensitivity as high as 10^7 RIU is modeled; experimental realization is in progress with biomarker of interest.

JTh2A.55

Highly Compact Structure for Near-total Absorption in a Graphene Monolayer in the Visible, Amirreza Mahigiri¹, Georgios Veronis¹; ¹Louisiana State Univ., USA. We propose a highly compact structure consisting of a subwavelength grating covered with a graphene monolayer to achieve near-total absorption in the graphene monolayer in the visible without the need for thick multilayer dielectric mirrors.

JTh2A.56

Tunable plasmonic subwavelength grating using electrically controlled conductive oxide, Erwen Li¹, Qian Gao¹, Alan X. Wang¹; ¹Oregon State Univ., USA. We design and experimentally demonstrate an electrically tunable plasmonic subwavelength grating at telecommunication wavelength based on a metallic subwavelength slit array coupled with a Si/SiO₂/ITO semiconductor-oxide-metal (MOS) capacitor, achieving 32%-56% transmission-reflection modulation.

JTh2A.57

Generation of Surface Plasmon Polaritons in Graphene-Semiconductor Structure with Distributed Feedback, Igor O. Zolotovskii¹, Yuliya S. Dadoenkova¹, Aleksei S. Kadochkin¹, Sergey G. Moiseev¹; ¹Ulyanovsk State Univ, Russia. We have shown the possibility of surface plasmon polaritons generation in a waveguiding system containing semiconductor film and graphene single-layer.

JTh2A.58

Scanning Light-Diffracted Microscopy, Hira Farooq¹, Sueli Skinner-Ramos¹, Luis Grave de Peralta¹; ¹Physics and Astronomy, Texas Tech Univ., USA. We simulated and experimentally demonstrated a novel subwavelength resolution microscopy technique by illuminating the sample with the hollow-cone of light produced by a ring-shaped condenser and scanning the diffracted light using a slit.

JTh2A.59

Generation of Prescribed Optical Orbital Angular Momentum Spectrum with Spiral Polarization Modulation, Chenhao Wan¹, Xiahui Tang¹, Yingxiong Qin¹, Yu Xiao¹, Qiwen Zhan²; ¹Huazhong Univ. of Science & Technology, China; ²Dept. of Electro-Optics and Photonics, Univ. of Dayton, USA. We report a method to generate prescribed optical orbital angular momentum (OAM) spectrum with spiral polarization modulation. The generated OAM spectrum contains 11 OAM states of equal intensity and various linear polarization angles.

JTh2A.60

High Q Si Slot Waveguide Ring Resonators for Gas Sensing Application, Yuki Tomono¹, Hiromasa Shimizu¹; ¹Tokyo Univ. of Agri. and Tech., Japan. We fabricated Si slot waveguide ring resonators having Q factor of 2.5x10⁴. Based on the resonance characteristics, refractive index sensitivity Dn of 1x10⁻⁵ was theoretically estimated by the difference of transmitted optical intensity at the resonance wavelength.

JTh2A.61

Determination of Complex Hermitian and Anti-Hermitian Interaction Constants from a Coupled System via Coherent Control, Xiaoyu Guo¹, Zhaolong Cao¹, H. C. Ong¹; ¹The Chinese Univ. of Hong Kong, Hong Kong. We devise a new method to determine the complex Hermitian and anti-Hermitian coupling constants from a coupled system via coherent control. The method is verified numerically and experimentally on various photonic and electronic systems.

JTh2A.62

Integrated Plasmonic Waveguide at the Mid-Infrared, Bingqing Zhu¹, Wen Zhou¹, Hon Ki Tsang¹; ¹Chinese Univ. of Hong Kong, Hong Kong. We demonstrate an integrated plasmonic waveguide fabricated on the silicon-on-insulator platform at the mid-infrared range. Experimentally, the metal-insulator-metal mode propagation loss is 1.16 dB/μm, and the Si-to-SPP mode converter loss is 4.1 dB/interface.

JTh2A.63

Excitation Light-Induced Anisotropies in LSP-Enhanced SHG from Au Nanoprisms, Atsushi Sugita¹, Hirofumi Yogo¹, Shohei Hamada¹, Atsushi Ono¹, Yoshimasa Kawata¹; ¹Shizuoka Univ., Japan. We report excitation light-induced anisotropies in polarized SHG for Au nanoprisms at LSP resonances. The anisotropies were pronounced more in higher excitation powers. The phenomena were explained by taking account of 2nd and 4th-order nonlinearities.

JTh2A.64

Graphene Plasmonic in-Plane Cherenkov Radiation, Jin Tao¹, Lin Wu¹, ZiChen Liu¹, Quan You¹, Qi Yang¹, Guoxing Zheng², ¹State Key Lab of Optical Communication Technologies and Networks, Wuhan Research Inst. of Posts & Telecommunications, China; ²Wuhan Univ., China. We theoretically study the Cherenkov plasmonic radiation in/parallel graphene plane by a moving electron, which provides a versatile, tunable mechanism for plasmonic cherenkov effect in active integrated photonic applications.

JTh2A.65

Graded-Index Plasmonic Nanoparticles: Light Scattering Characteristics and Peculiarities, Dimitrios Tzarouchis¹, Ari Sihvola¹, ¹Aalto Univ., Finland. Light scattering by sub-wavelength spheres exhibiting a radially inhomogeneous permittivity are presented. The theoretical model for power-law, exponential, and Drude-like inhomogeneous profiles are discussed, generalizing the concept of polarizability for graded-index nanoparticles.

JTh2A.66

Multifrequency Near Field Scanning Optical Microscopy (MF-SNOM), Hadar Greener¹, Michael Mrejen¹, Uri Arieli¹, Haim Suchowski¹, ¹Tel Aviv Univ., Israel. We introduce a novel excitation and detection scheme in near-field optical microscopy based on a multifrequency method. Using this method, we experimentally demonstrate enhanced sensitivity, implying improved spatial resolution in optical measurements.

JTh2A.67

Thermal Scan of Metal Based Metasurface and Evidence of Circular Dichroism and Optothermal Anisotropy, Grigore Leahu¹, Alessandro Belardini¹, Emilija Petronijevic¹, Roberto Li Voti¹, Concita Sibilia¹, Tiziana Cesca², Giovanni Mattei², ¹Univ degli Studi di Roma La Sapienza, Italy; ²Università di Padova, Italy. Photothermal and photoacoustic techniques are utilized to explore the thermal properties of metal based metasurfaces. We experimentally evidence the role of the symmetry in the heat transport and its relation with the optical circular dichroism.

JTh2A.68

Electric Field Enhancement by Two-scale Structure, Mahsa Darvishzadeh Varcheie¹, William John Thrift¹, Mohammad Kamandi¹, Regina Ragan¹, Filippo Capolino¹, ¹Univ. of California Irvine, USA. We propose a novel multi-length-scale architecture for giant electric field enhancement. We investigate the capability of our structure to boost the electric field analytically and using full-wave simulations and verify our results with surface-enhanced Raman spectroscopy experiment.

JTh2A.69

Plasmonic enhancement and control of optical nonlinearity in monolayer WS₂, Wei-Yun Liang¹, Hyeyoung Ahn¹, Yungang Sang², Yanrong Wang², Jinwei Shi², Soniya S. Raja³, Yi-Hsien Lee⁴, Shangji Gwo⁵, ¹National Chiao Tung Univ., Taiwan; ²Dept. of Physics and Applied Optics, Beijing Normal Univ., China; ³Inst. of NanoEngineering and MicroSystems, National Tsing Hua Univ., Taiwan; ⁴Dept. of Materials Science and Engineering, National Tsing Hua Univ., Taiwan; ⁵Dept. of Physics, National Tsing Hua Univ., Taiwan. A giant SHG enhancement is achieved from monolayer-WS₂ incorporated onto 2D plasmonic metasurfaces (Ag-nanogroove-grating) in resonance with the excitonic resonance of monolayer-WS₂. An optical encoding technique is demonstrated based on plasmonic manipulation of SHG polarization.

JTh2A.70

Integrated resonant units of metasurface for broadband efficiency and phase modulation, Ren Jie Lin¹, Hui-Hsin Hsiao², Yu Han Chen¹, Bo Han Chen¹, Pin Chieh Wu³, Yi-Chieh Lai¹, Shuming Wang⁴, Din Ping Tsai^{1,3}, ¹Dept. of Physics, National Taiwan Univ., Taiwan; ²Graduate Inst. of Biomedical Optomechatronics, Taipei Medical Univ., Taiwan; ³Research Center for Applied Sciences, Academia Sinica, Taiwan; ⁴School of Physics, Nanjing Univ., China. Integrated-resonant units (IRUs) provide additional degree of freedom to control the phase compensation and enhance the conversion efficiency over a broad bandwidth of light. In this work, we demonstrated achromatic metalens in visible range and broadband versatile polarization generator.

JTh2A.71

Enhanced Harmonic Generation in Metal-Insulator-Metal Nanostructures, Mallik Mohd Raihan Hussain¹, Zhengning Gao², Domenico de Ceglia³, Maria A. Vincenti⁴, Andrew Sarangan¹, Imad Agha¹, Michael Scalora⁵, Parag Banerjee^{2,6}, Joseph Haus⁵, ¹Dept. of Electro-Optics and Photonics, Univ. of Dayton, USA; ²Inst. of Materials Science and Engineering, Washington Univ., USA; ³Dept. of Information Engineering, Univ. of Padova, Italy; ⁴Dept. of Information Engineering, Univ. of Brescia, Italy; ⁵Charles M. Bowden Research Lab, US Army AMRDEC, USA; ⁶Dept. of Mechanical Engineering & Materials Science, Washington Univ., USA. We experimentally observed no change in second-harmonic signal and an enhancement of the third-harmonic signal from metal-insulator-metal nanostructures, which are consistent with the nonlinear photon-assisted electron tunneling current flowing through them.

JTh2A.72

Scattering near-field mid-infrared microscopy using self-mixing in quantum cascade lasers, Mingzhou Jin¹, Mikhail A. Belkin¹, ¹Univ. of Texas at Austin, USA. We demonstrated scattering near-field mid-infrared imaging via the self-mixing in a quantum cascade laser used as both a light source and a detector. The experimental setup and preliminary results on gold/sapphire samples are presented.

JTh2A.73

Strong Mode Coupling and High-Q Supercavity Modes in Subwavelength Dielectric Resonators, Kirill Koshelev^{1,3}, Andrey Bogdanov^{1,2}, Sergey Gladyshev¹, Zarina Sadrieva¹, Mikhail Rybin^{1,2}, Kirill Samusev^{1,2}, Mikhail Limonov^{1,2}, Yuri S. Kivshar^{1,3}, ¹Dept. of Nanophotonics and Metamaterials, ITMO Univ., Russia; ²Ioffe Inst., Russia; ³Nonlinear Physics Centre, Australian National Univ., Australia. We reveal that isolated subwavelength dielectric resonators support states with giant Q-factors similar to bound states in the continuum formed via destructive interference between strongly coupled eigenmodes and characterized by singularities of the Fano parameters

JTh2A.74

Hybrid Metal-Dielectric Metasurfaces For Refractive Index Sensing, Debdatta Ray¹, TV Raziman¹, Christian Santschi¹, Andreas Tittl¹, Dordaneh Etezadi¹, Hatice Altug¹, Olivier Martin¹, ¹EPFL, Switzerland, Switzerland. The utilization of a hybrid metal-dielectric metasurface for sensing is demonstrated experimentally. We show how the hybridization between the different modes supported by the structure determines the overall sensitivity of the system.

JTh2A.75

Optimization of Titanium Nitride Films using Plasma Enhanced Atomic Layer Deposition, Ray R. Secondo¹, Vitaliy Avrutin¹, Umit Ozgur¹, Nathaniel Kinsey¹, ¹Virginia Commonwealth Univ., USA. We investigate the quality of atomic layer deposited Titanium nitride thin films and find metallicity close to high quality sputtered films on both sapphire and silicon for a deposition temperature of 375°C.

JTh2A.76

InGaAs/InP Multi-quantum-well Nanowires Directly Grown on SOI Substrates and Optical Property Characterizations, Mengqi Wang^{1,2}, Zhibo Li^{1,2}, Xuliang Zhou^{1,2}, Yajie Li^{1,2}, Pengfei Wang^{1,2}, Hongyan Yu^{1,2}, Wei Wang^{1,2}, Jiaqing Pan^{1,2}, ¹Inst. of Semiconductors, Chinese Academy of Sciences, China; ²College of Materials Science and Opto-Electronic Technology, Univ. of Chinese Academy of Sciences, China. InGaAs/InP MQW nanowires were directly grown on SOI substrates by ART technique. Multiple characterizations which applied to reveal the material quality and optical properties, had proved that such MQW nanowire was capable of an active waveguide cavity for potential photonic applications.

JTh2A.77

Yb-doped Large-Mode-Area Al-P-Silicate Laser Fiber fabricated by MCV, Arindam Halder¹, Lin Di¹, Andrey A. Umnikov¹, N. J. Ramirez-Martinez², Martin M. Núñez-Velázquez¹, Pranabesh Barua¹, Shaif-Ul Alam¹, Jayanta K. Sahu¹, ¹Univ. of Southampton, UK. We demonstrate an efficient ytterbium-doped aluminophospho-silicate low-NA fiber fabricated by modified solution-doping process that shows continuous-wave laser efficiency of 81%. In ps-MOPA, the fiber provides 35kW peak power with repetition-rate 1.46MHz, and average power 9.1W.

JTh2A.78

Hybrid h-BN/Graphene/h-BN Silicon Device for Electro-optic Modulation, Tianren Fan¹, Amir H. Hosseini¹, Hesam Moradinejad¹, Ali Asghar Eftekhari¹, Ali A. Adibi¹, ¹Georgia Inst. of Technology, USA. We integrate hexagonal boron nitride (h-BN)-encapsulated graphene on top of a compact silicon microdisk resonator for modulation applications. We demonstrate reduced graphene resistance through h-BN encapsulation and showed active tuning of the optical mode through voltage-gated graphene.

JTh2A.79

Investigation of High Temperature Photoluminescence Efficiency from InGaN/GaN MQWs, Abbas F. Sabbar¹, Syam Madhusoodhanan¹, Sattar Al-Kabi¹, Binzhong Dong², Jiangbo Wang³, Shui-Qing Yu¹, Zhong Chen¹, ¹Dept. of Electrical Engineering, Univ. of Arkansas, Fayetteville, USA; ²HC SemiTek, China; ³HC SemiTek, China. Temperature and power dependent photoluminescence (PL) measurements from InGaN/GaN MQWs, which was grown on a sapphire substrate were performed to extract the PL efficiency.

JTh2A.80

Numerical Characterization of Monolayer Ink-Jet Printed Polystyrene Lattice, Ray R. Secondo¹, Karam Nashwan Al-Milaji¹, Tse Nga Ng², Hong Zhao¹, Nathaniel Kinsey¹, ¹Virginia Commonwealth Univ., USA; ²Univ. of California San Diego, USA. We investigate the color of polystyrene metasurfaces printed via a novel dual-droplet ink-jet technique resulting in a closely-packed hexagonal formation through self-assembly. Simulations, Mie Theory, and Bragg Diffraction calculations are utilized for spectra validation.

JTh2A.81

Highly Transparent Organic Microdisk Cavity in Visible Range by the Ink-jet Printing Method, Taku Takagishi¹, Hiroaki Yoshioka¹, Shintaro Mitsui¹, Yuya Mikami¹, Naoya Nishimura², Yuji Oki¹, ¹Kyushu Univ., Japan; ²Nissan chemical industries, Ltd, Japan. We experimentally demonstrated the fabrication and the fundamental lasing evaluation of a printed microdisk cavity by focusing on a fluorinated spherical polymer FZ-001 to achieve a microdisk with small absorption loss in the visible range.

JTh2A.82

Stable, inkjet printed temperature- and humidity-resistant black phosphorus for ultrafast lasers, Xinxin Jin¹, Guohua Hu², Meng Zhang¹, Yuwei Hu¹, Qing Wu¹, T. Albrow-Owen², R Howe², T Wu², Zheng Zheng¹, Tawfique Hasan²; ¹Beihang Univ., China; ²Cambridge Graphene Centre, UK. We demonstrate an inkjet-printed temperature- and humidity-resistant black phosphorus saturable absorber, enabling stable continuous mode-locking over 210 hours. Our work highlights the potential of BP-based devices for photonic applications operating under challenging environmental conditions.

JTh2A.83

Inkjet-printed optically uniform transition metal dichalcogenide saturable absorbers, Qing Wu¹, Guohua Hu², Meng Zhang¹, Xinxin Jin¹, Yuwei Hu¹, Ting Li¹, T. Albrow-Owen², R Howe², T Wu², Zheng Zheng¹, Tawfique Hasan²; ¹Beihang Univ., China; ²Cambridge Graphene Centre, UK. We report self-starting mode-locking in all-fiber erbium-doped lasers utilizing inkjet-printed transition metal dichalcogenide saturable absorbers, exhibiting highly optical uniformity, with <5% standard deviations.

JTh2A.84

Single Crystal Growth of BaGa₂S₃ and BaGa₂Se₃ by the Horizontal Gradient Freeze Technique, Peter G. Schunemann¹, Kevin Zawilski¹; ¹BAE Systems Inc, USA. Horizontal gradient freeze growth in transparent furnaces yields extremely favorable crystallization of high-optical quality barium thiogallate and selenogallate: two new nonlinear optical crystals with wide band gaps, deep infrared transparency, and moderately high nonlinear coefficients.

JTh2A.85

Auger Recombination in Mid-Infrared Active Regions, Kenneth J. Underwood¹, Andrew F. Briggs², Scott D. Sifferman², Seth Bank², Juliet Gopinath¹; ¹Univ. of Colorado at Boulder, USA; ²Dept. of Electrical and Computer Engineering, Univ. of Texas at Austin, USA. We study strain effects on Auger recombination in GaInAsSb/GaSb multiple quantum well structures emitting ~3 μm, using differential reflection pump-probe and photoluminescence spectroscopy; results suggest increasing strain decreases Auger and increases radiative recombination strength.

JTh2A.86

Novel spectroscopic transparent/scattering material for 260/280nm ultraviolet optical detection, Keisuke Nakakubo¹, Junfeng Zhu¹, Yuya Mikami¹, Kinichi Morita^{2,1}, Hiroaki Yoshioka¹, Yuji Oki¹; ¹Kyushu Univ., Japan; ²Ushio, Inc, Japan. Novel type of wavelength filter was proposed and demonstrated. Polydimethylsiloxane was mixed with CaF₂ particles. This scattering material of 30wt% provided transparency at specified wavelength of 259 nm and 278nm.

JTh2A.87

Enhanced Spontaneous Emission of Quantum Emitters in the Vicinity of TiN Thin Films, Shaimaa I. Azzam¹, Motoharu Saito², Shunsuke Murai², Satoshi Ishii³, Katsuhisa Tanaka², Alexander Kildishev¹; ¹Purdue Univ., USA; ²Kyoto Univ., Japan; ³National Inst. for Materials Science, Japan. We report on the enhancement of spontaneous emission from organic dyes on top of TiN films. Up to 200-fold Purcell enhancement is achieved. The proposed structures are modeled in the time domain and validated experimentally.

JTh2A.88

Dissolvable and Recyclable Random Lasers, Shih-Yao Lin¹, Yu-Ming Liao¹, Hung-I Lin¹, Wei-Ju Lin¹, Yang-Fang Chen¹, Tai-Yuan Lin², Wei-Cheng Liao¹, Yuan-Fu Huang¹, Ying-Chih Lai³, Zhaona Wang⁴, Xiaoyu Shi⁴, Cheng-Han Chang¹; ¹National Taiwan Univ., Taiwan; ²National Taiwan Ocean Univ., Taiwan; ³National Chung Hsing Univ., Taiwan; ⁴Beijing Normal Univ., China. The dissolvable and recyclable random laser can be dissolved in water, accompanying the decay of emission intensity and the increment in lasing threshold. It can be reused after deionized treatment, exhibiting reproducibility with recycling processes.

JTh2A.89

All Inorganic Perovskite Quantum Dots Hybrid Green Light-Emitting Diode with Stable Performance, Chung-Ping Yu³, Meng-Ting Chung¹, Tzu-Yu Chen², Yu-Ming Huang³, Chung-Ping Huang⁵, Shu-Hsiu Chang⁴, Shun Chieh Hsu³, Teng-Ming Chen¹, Hao-Chung Kuo², Chien-Chung Lin³; ¹Dept. of Applied Chemistry, National Chiao-Tung Univ., Taiwan; ²Inst. of Electro-Optical Engineering, National Chiao-Tung Univ., Taiwan; ³Inst. of Photonic System, National Chiao-Tung Univ., Taiwan; ⁴Inst. of Imaging and Biomedical Photonics, National Chiao-Tung Univ., Taiwan; ⁵Inst. of Lighting and Energy Photonics, National Chiao-Tung Univ., Taiwan. A silica-coated inorganic perovskite quantum dot hybrid light-emitting diodes is aged continuously in high and low light intensity conditions. Both blue and ultra-violet-pumped samples showed stable performances up to 104 hours.

JTh2A.90

Planar Focusing Element Based on Scattering Structures in a Dielectric Waveguide, Brian D. Jennings¹, David McCloskey¹, Alexander Krichchevsky², Christopher Wolf², Frank Bello¹, Ertugrul Karademir¹, John F. Donegan¹; ¹Univ. of Dublin Trinity College, Ireland; ²Western Digital Corporation, USA. Focusing elements in integrated optics are required for localised high intensities and coupling between certain components. Here, a focusing element is designed using analytical approximations, simulated using FDTD and characterised using far-field optical imaging. Focusing below λ/2 is predicted.

JTh2A.91

KW-level Yb/Ce-codoped Aluminosilicate Fiber Fabricated by Chelate Precursor Doping Technique, Yuwei Li¹, Huan Zhan¹, Kun Peng¹, Shuang Liu¹, Xiaolong Wang¹, Li Ni¹, Shihao Sun¹, Jiali Jiang¹, Lei Jiang¹, Juan Yu¹, Jianjun Wang¹, Feng Jing¹, Aoxiang Lin¹; ¹China Academy of Engineering Physics, China. By chelate precursor doping technique, an Yb/Ce-codoped aluminosilicate fiber was fabricated and reported. The fiber showed excellent laser stability at 1850W for over 500 minutes with small power degradation of <1.04%.

JTh2A.92

Linear and Nonlinear Optical Response of Monolayer Two-dimensional Transition Metal Dichalcogenide MoSe₂ and WSe₂, Yanxiao Sun¹, Boyang Zhao², Jintao Bai¹, Yang Bai¹, Jiming Zheng¹; ¹Northwest Univ., China; ²Xi'an Jiaotong Univ., China. Linear and nonlinear optical properties of CVD-fabricated monolayer MoSe₂ and WSe₂ are studied, which showed nonlinear saturable absorption, reverse saturable absorption and two photon absorption. Band structure of the materials are investigated by simulation and experiments.

JTh2A.93

Fiber fuse in GeAsSe photonic crystal fiber and its impact on undamaged segment, Sida Xing¹, Svyatoslav Kharitonov¹, Jianqi Hu¹, Camille-Sophie Bres¹; ¹École polytechnique fédérale de Lausanne, Switzerland. We observe, for the first-time, fiber fuse in non-silica fiber. Images of the photonic crystal fiber show smooth discrete voids in the solid core region. Significant dispersion modifications of the undamaged fiber section are measured.

JTh2A.94

Electric Field Control of the Ferro-paraelectric Phase Transition in Cu:KTN Crystals, Xin Zhang^{1,2}, Hongliang Liu^{1,2}, Zhuan Zhao^{1,2}, Xuping Wang³, Pengfei Wu^{1,2}; ¹Key Lab of Optical Information Science and Technology, Ministry of Education, Inst. of Modern Optics, Nankai Univ., China; ²Tianjin Key Lab of Optoelectronic Sensor and Sensing Network Technology, China; ³Advanced Materials Inst., Shandong Academy of Sciences, China. We demonstrate an efficient ferro-paraelectric phase transition in Cu-doped KTa_{1-x}Nb_xO₃ crystals using AC electric fields. The dynamic process is probed by a laser beam and characterized by a microscope and an X-ray diffractometer.

JTh2A.95

Raman determination of the rate of α-chymotrypsin-catalyzed reaction, Irina Shpachenko¹, Nikolay Brandt¹, Andrey Chikishev²; ¹Lomonosov Moscow State Univ., Russia; ²International Laser Center of Moscow State Univ., Russia. We apply the method of Raman spectroscopy to the study of enzyme kinetics. It is shown that Raman spectroscopy data can be used for calculation of chemical reaction rates and catalytic activity of α-chymotrypsin.

JTh2A.96

Characterization of the Photonic Response in Nitzschia Filiformis Phytoplankton, Yannick D'Mello¹, Dan Pretescu¹, James Skorica¹, Melissa Campbell¹, Mark Andrews¹, David V. Plant¹; ¹McGill Univ., Canada. The optical response of the phytoplankton species *Nitzschia filiformis*, specifically its silica shell, is investigated by correlating SEM, AFM, SNOM, and HSI microscopy techniques. Our results demonstrate its behavior as a passive optical device.

JTh2A.97

Double-clad hypocycloid core-contour Kagome hollow-core photonic crystal fiber, Frédéric Delahaye¹, Martin Maurer^{1,2}, Matthieu Chafer^{1,2}, Foued Amrani¹, Benoit Debord^{1,2}, Frédéric Gérôme^{1,2}, Fetha Benabid^{1,2}; ¹GPPMM, XLIM, UMR 7252 Univ. de Limoges, France; ²GloPhotonics, France. We report on the design and fabrication of the first double-clad hypocycloid core-contour Kagome fiber optimized for guidance in air-core at 1 μm via Inhibited-Coupling and in a cladding silica ring via total-internal-reflection.

JTh2A.98

Ultrasound Sensing with a Photonic Crystal Slab, Eric Y. Zhu¹, Cory Rewcastle¹, Raanan Gad¹, Li Qian¹, Ofer Levi¹; ¹Univ. of Toronto, Canada. We experimentally demonstrate a compact architecture for ultrasound sensing based upon a photonic crystal slab (PCS) fabricated on top of a thin mechanically pliable silicon membrane. A noise-equivalent pressure of 2.0 kPa (0.072 kPa/rt Hz) at 5 MHz is observed.

JTh2A.99

Optical Trapping of Living Bacteria in 2D Hollow Photonic Crystal Cavities, Rita Therisod¹, Manon Tardif^{2,3}, Pierre Marcoux⁴, Emmanuel Picard³, Emmanuel Hadji³, David Peyrade², Romuald Houdré¹; ¹Institut de Physique, Ecole Polytechnique Fédérale de Lausanne (EPFL), Switzerland; ²CNRS-LTM - Micro and Nanotechnologies for Health, Univ. Grenoble Alpes, France; ³CEA-INAC-PHELIQS-SINAPS, Univ. Grenoble Alpes, France; ⁴CEA-LETI-DTBS-SBSC-LCMI/LBAM, Univ. Grenoble Alpes, France. We report on the optical trapping of seven types of living bacteria in 2D hollow photonic crystal cavities. The possibility of distinction of bacteria via the interaction effects with the trapping field will be discussed.

JTh2A.100

Optofluidic SERS in a Microcapillary Coated with a Graphene Oxide/Gold Nanorod Nanocomposite, Pilar Gregory Vianna¹, Daniel Grasseschi¹, Sergio Domingues¹, Cristiano de Matos¹; ¹MackGrappe - Graphene and Nanomaterials Research Center, Mackenzie Univ., Brazil. We demonstrate a re-usable microcapillary fiber with a graphene oxide/gold nanorod nanocomposite inner coating for optofluidic SERS. Rhodamine detection is performed with <1sec integration times down to 10⁻⁹M in samples of few hundreds of nanoliters.

JTh2A.101

3D Hydrodynamic Focusing for Optofluidics Using a Stacked Channel Design, Erik Hamilton¹, Joel G. Wright¹, Matthew Stott¹, Jennifer A. Black², Holger Schmidt², Aaron Hawkins¹; ¹Brigham Young Univ., USA; ²Univ. of California, Santa Cruz, USA. We present a 3D hydrodynamic focusing design suitable for optofluidic devices allowing planar fabrication and velocity independent particle focusing. Simulations are presented and fabrication outlined with evidence that stacked SU8 layers are suitable building blocks.

JTh2A.102

Triple Fluorescence SPIM Using a Single Camera Detection, Israel Rocha¹, Jacob Licea-Rodriguez¹, Alfredo Figueroa¹, Meritxell Riquelme¹; ¹CICESE Ensenada, Mexico. Three color SPIM is performed using three sequential cw-lasers pulsed trains in the excitation synchronized with the acquisition frame rate of a single camera. Multicolor images of living hyphae of *Neurospora crassa* are acquired.

JTh2A.103

Effect of Viscosity on Fluorescence Lifetime Measured Using Flow Cytometry, Faisal H. Alturkistany¹, Kapil Nichani¹, Wenyang Li¹, Jessica P. Houston¹; ¹New Mexico State Univ., USA. The effect of viscosity on Dronpa-3 fluorescence protein kinetics is studied using time resolved flow cytometry (TRFC). Phasor analysis and Förster Hoffman relation analysis provide the basis of studying intracellular viscosity in high throughput manner.

JTh2A.104

Mode and sensing properties of the deformed microdroplet, Meng Zhang¹, Jiansheng Liu¹, Weifeng Cheng², Jiangtao Cheng², Hongwen Zhou¹, Haitao Liu¹, Jie Chen¹, Qing Wu¹, Yuhang Wan¹, Zheng Zheng¹; ¹Beihang Univ., China; ²Virginia Tech, USA. The resonant mode along meridian of a deformed droplet on a hydrophilic substrate with different contact angle CA is investigated. A relatively large Q ~ 2000 and a sensitivity S ~ 550 nm/RIU can still be achieved even with CA down to 1500.

JTh2A.105

Hyperspectral and multimodal CARS microscopy of structured endogenous biomolecules in *Euglena gracilis*, Joel T. Tabaranga¹, Jeremy G. Porquez¹, Aaron D. Slepko¹; ¹Trent Univ., Canada. Using hyperspectral CARS and SHG microscopies we image and fingerprint an intriguing biomolecule in phototrophic *Euglena gracilis*. The large CARS signal strength of this endogenous biomolecule opens new opportunities in label-free, live biological imaging.

JTh2A.106

Imaging of 3D Molecular Orientations by Polarization-Controlled Coherent Raman Microscopy, Young J. Lee¹; ¹NIST, USA. A new optical imaging method determines the 3D angles of molecular orientation by concurrent polarization analysis of multiple Raman modes. Theoretical description and data analysis results of a high-density polyethylene film will be presented.

JTh2A.107

Flexible Mid-infrared Photonic Chips for Real-time and Label-Free Biochemical Detection, Pao T. Lin¹; ¹Texas A&M Univ., USA. Chip-scale biomedical chemical sensors were demonstrated using mid-infrared flexible aluminum nitride waveguides. Ethanol and water real-time detection was conducted by measuring waveguide light at $\lambda=2.7 \mu\text{m}$ corresponding to the characteristic -OH absorption.

JTh2A.108

All-optical wavelength-tunable narrow-linewidth fiber laser, Yujia Li¹, Tao Zhu¹, Shihong Huang¹, Lei Gao¹, Tianyi Lan¹, Yulong Cao¹; ¹Chongqing Univ., China. We propose an optical-controlled wavelength-tunable narrow-linewidth fiber laser based on graphene's optical-thermal effect, which has the properties of wavelength fast-scanning, low to ~750 Hz linewidth, wavelength stability of 0.4 pm and so on.

JTh2A.109

Spatially Gain-Tailored Fiber Raman Laser Cladding-Pumped by Multimode Disk Laser at 1030 nm, Yutong Feng¹, Sheng Zhu¹, Soonki Hong¹, Huaqin Lin¹, Pranabesh Barua¹, Jayanta K. Sahu¹, Johan Nilsson¹; ¹Univ. of Southampton, UK. A spatially gain-tailored fiber Raman laser with Ge-doped core and P-doped inner cladding generates 46 W of instantaneous power at 1084 nm with 64% slope efficiency when cladding-pumped by a 1030-nm quasi-cw multimode disk laser.

JTh2A.110

Numerical Analysis on the Influence of Photo Darkening Heating Induced Phase Distortion on Fiber Coherent Combining CPA Scheme, Yujun Feng¹, Betty M. Zhang¹, Johan Nilsson¹; ¹Univ. of Southampton, UK. We use numerical simulations to investigate the effects of photodarkening (PD) on single-channel and coherently combined Yb-doped Fiber CPA Systems. The system design optimizing for the lossy fiber caused by PD at ending of life shows improvements on both pulse compression and combining efficiency.

JTh2A.111

Generation of Octave Spanning Spectra Directly from a Fiber Oscillator with Self-Similar Pulse Evolution, Ankita N. Khanolkar¹, Chunyang Ma², Andy Chong^{1,2}; ¹Electro Optics and Photonics, Univ. of Dayton, USA; ²Dept. of Physics, Univ. of Dayton, USA; ³Electronic Science and Engineering, Jilin Univ., China. A mode-locked fiber laser with a strong self-similar evolution in a gain segment and spectral broadening in a photonic crystal fiber was simulated to generate nearly octave spanning spectra.

JTh2A.112

Stable microwave signal generation from PM dual-wavelength single-frequency Er-doped DBR fiber laser utilizing superimposed FBGs, Yubin Hou¹, Qian Zhang¹, Shuxian Qi¹, Xian Feng¹, Pu Wang¹; ¹Beijing Univ. of Technology, China. We demonstrate a PM dual-wavelength single-frequency Er-doped DBR fiber laser as a stable microwave generation source. The beat frequency of the dual-wavelength is 28.4474 GHz with the linewidth less than 0.3 kHz.

JTh2A.113

Spatial-Mode Switchable Ring Fiber Laser Based on Low Crosstalk Few-mode Fiber and Mode MUX/DEMUX, Yu Yang¹, Juhao Li¹, Fang Ren², Jinglong Zhu¹, Yongqi He¹, Zhanguan Chen¹, Zhengbin Li¹; ¹Peking Univ., China; ²Univ. of Science and Technology Beijing, China. A spatial-mode switchable ring fiber laser based on low mode-crosstalk few-mode fiber and mode multiplexer/demultiplexer (MUX/DEMUX) is proposed. We experimentally demonstrate that output lasing mode can be switched among the three lowest-order LP modes.

JTh2A.114

Efficient Frequency Doubling of an Ytterbium-Doped Fiber Ring Laser Using an Internal Enhancement Cavity, Stanislav K. Vassilev¹, William A. Clarkson¹; ¹Optoelectronics Research Centre, UK. A novel fiber laser geometry incorporating an internal resonant enhancement cavity to generate visible output via second harmonic generation is presented. Preliminary experiments using an Yb-fiber gain medium yielded 17W of single-mode output at 540nm.

JTh2A.115

Generation and Amplification of First Order OAM with Fused Taper Coupler, Jianxiang Wen¹; ¹Shanghai Univ., China. We demonstrated a vortex beams coupler which can generate at range of 1480–1640 nm and built up an all-fiber vortex amplification system, which is of the higher gain and better flatness of OAM.

JTh2A.116

All-fiber Laser Source at 1.7 μm for Photoacoustic Microscopy in Lipid Detection, Nan Chen¹, Can Li¹, Bowen Li¹, Kenneth Kin-Yip Wong¹; ¹The Univ. of Hong Kong, China. Multi-wavelength all-fiber laser source in 1.7- μm regime combining parametric oscillation and thulium-doped fiber amplification is reported. Its high flexibility facilitates itself of high performance in high-speed OR-PAM for lipid detection in the first overtone wavelength.

JTh2A.117

Distributed Measurement of Bending-Induced Birefringence in Single-Mode Fibers with PA-OFDR, Yanling Shang¹, Ting Feng¹, Xichen Wang¹, Anton Khomenko², James Chen², Xiaotian S. Yao^{1,2}; ¹Hebei Univ., China; ²General Photonics Corporation, USA. We demonstrate the distributed bending-induced birefringence measurement in single-mode fibers with high spatial resolution using a polarization-analyzing optical frequency domain reflectometry. The bending-induced birefringence coefficient of $5.499 \times 10^{-10} \text{ m}^2$ is accurately obtained.

JTh2A.118

Implementation of linearly-polarized LP₀₁ modes to any azimuthally-orientated LP₁₁ modes conversion, lipeng feng¹, Yan Li¹, Sihan Wu¹, Xinglin Zeng¹, Wei Li¹, Rongsheng Chen², Jifang Qiu¹, Xiaobin Hong¹, Ian P. Giles², Jian Wu¹; ¹Beijing Univ. of Posts and telecom, China; ²Phoenix Photonics, UK. We propose a scheme that converts fundamental modes of different polarization to asymmetrical spatial modes of different orientation, of utility in exchange data between preceding PDM and rising MDM optical networks.

JTh2A.119

Multiplexed mode-locked fiber laser emitting dissipative and conventional solitons, Bowen liu¹, Yiyang Luo¹, Yang Xiang¹, Zhijun Yan¹, Yingxiong Qin¹, Qizhen Sun¹, Xiahui Tang¹; ¹Huazhong Univ. of Science and Technology, China. We report a bidirectional passively mode-locked fiber laser supporting both dissipative and conventional soliton emission in different propagating directions. Moreover, broadband wavelength-tunable solitons, dual-wavelength solitons and wavelength-tunable noise-like pulses are respectively obtained.

JTh2A.120

High Peak Power Single-Frequency Amplifier Based on a Er-Yb Doped Polarization Maintaining LMA Fiber, Anne Durécu¹, Pierre Bourdon¹, François Gustave¹, Hermance Jacquemin¹, Julien Le Gouët¹, Laurent Lombard¹; ¹ONERA, France. We report on single-frequency fiber amplifiers based on PM Er-Yb doped P₂O₅-Al₂O₃-SiO₂ fibers. Peak power up to 700W at 1545nm for 730ns pulse duration was obtained with a good beam quality and a 17dB PER.

JTh2A.121

Bidirectional, Er-doped, Dual-comb Fiber Laser with Carbon Nanotube Polyimide Film, Shuto Saito¹, Lei Jin¹, Yoichi Sakakibara², Emiko Omoda², Hiromichi Kataura², Norihiko Nishizawa¹; ¹Nagoya Univ., Japan; ²AIST, Japan. Bi-directional, Er-doped dual comb fiber laser was demonstrated using polyimide film dispersed with single wall carbon nanotube. Difference of repetition frequency was temporally stable and it could be tuned continuously by pump power control.

JTh2A.122

Directly modified single mode fiber as an intermodal interferometer based on single femtosecond-laser induced line, Pengcheng Chen¹, Shu Xuwen¹; ¹Huazhong Univ. of Sci. & Tech., China. We demonstrate a novel Mach-Zehnder interferometer based on a single femtosecond-laser induced positive refractive index-modified line created in the core of a single-mode fiber. The device is extremely simple in structure and very efficient in manufacturing.

JTh2A.123

Dispersion Engineering Analysis of Er-Fiber Based Comb Amplification in All-Fiber Configuration, Ken Kashiwagi^{1,2}, Hajime Inaba^{1,2}; ¹National Inst. of Advanced Industrial Science and Technology, Japan; ²JST, ERATO, MINOSHIMA Intelligent Optical Synthesizer (IOS), Japan. We experimentally and numerically investigated dispersion engineering of amplification of erbium-fiber based comb. Spectral narrowing in a fiber amplifier increased the effective gain and enhanced the peak power at fiber-based dispersion compensator output.

JTh2A.124

Super-resolution electro-optic dual-comb spectroscopy, Wang Shuai¹, Xinyu Fan¹, Bingxin Xu¹, Zuyuan He¹; ¹Shanghai Jiao Tong Univ., China. We demonstrate an electro-optic dual-comb spectroscopy with 1-MHz spectral resolution. By using quasi-integer-ratio multiheterodyne approach, 36000 electro-optic comb lines were well resolved with an increased measurement speed of 3000.

JTh2A.125

Design of a Dual-Channel Modelocked Fiber Laser that Avoids Multi-Pulsing, Xianting Zhang¹, Shaokang Wang², Feng Li², Curtis R. Menyuk², P. K. A. Wai¹; ¹Dept. of Electronic and Information Engineering, The Hong Kong Polytechnic Univ., Hong Kong; ²Dept. of Computer Science and Electrical Engineering, Univ. of Maryland Baltimore County, USA. Multi-pulsing competes with multi-channel modelocking in fiber lasers and can suppress it. We study the conditions to achieve stable dual-channel modelocking, and we propose a design that avoids multi-pulsing.

JTh2A.126

Rogue waves in an ultrafast fiber laser under chaotic dissipative soliton buildup regime, Zhichao Luo^{1,2}, Jiqiang Kang¹, Meng Liu², Can Li¹, Cihang Kong¹, Kenneth Kin-Yip Wong¹; ¹Univ. of Hong Kong, Hong Kong; ²South China Normal Univ., China. We report on the observation of optical rogue waves (RWs) in a net-normal dispersion fiber laser during the chaotic dissipative soliton buildup process. These findings indicate a promising approach for optical RW generation.

JTh2A.127

Optical Computing Based on Recirculating Frequency Shifter, Zhiqiang Qin¹, Qizhuang Cen¹, Yitang Dai¹, Feifei Yin¹, Kun Xu¹; ¹Beijing Univ. of Posts and Telecommunications, China. Optical computing is an effective technique to accelerate the computing process. Here, an optical computing scheme based on recirculating frequency shifter is proposed and experimentally demonstrated. Matrix multiplication can be realized based on our scheme.

JTh2A.128

High Damage Threshold Semiconductor Saturable Absorber Mirror for Fiber Lasers, Yan Wang¹, Nan Lin², Wanli Gao¹, Huanyu Song³, Minglie Hu³, Haiming Li⁴, Wenxia Bao⁵, Xiaoyu Ma², Zhigang Zhang¹; ¹Peking Univ., China; ²Inst. of Semiconductors, Chinese Academy of Sciences, China; ³Tianjin Univ., China; ⁴LZ Lasers, China. We demonstrate a high damage threshold semiconductor saturable absorber mirror for mode-locked fiber lasers, with a damage threshold of 9.5 mJ/cm², a modulation depth of 11.5%, a saturation fluence of 39.3 mJ/cm², an ISA coefficient of 6.3×10² mJ/cm².

JTh2A.129

Fabrication of Low Loss Low-NA Highly Yb-doped Alumino-phosphosilicate Fiber for High Power Fiber Lasers, Raghuraman Sidharthan¹, Serene Huiting Lim², Kang Jie Lim², Daryl Ho¹, Chun Ho Tse¹, Junhua Ji¹, Huizi Li¹, Yue Men Seng¹, Song Liang Chua², Seongwoo Yoo¹; ¹Nanyang Technological Univ., Singapore; ²DSO National Labs, Singapore. We report fabrication and characterization of photodarkening-suppressed highly Yb-doped step-index fibers. The fiber contains 2.9wt% of Yb and has background loss of ~10dB/km. The fiber generates >100 W laser output power with 75% slope efficiency.

JTh2A.130

An Er Fiber Laser Generating Multi-Milliwatt Picosecond Pulses with Nearly Shot-Noise-Limited Intensity Noise, Hironobu Yoshimi¹, Kazuhiko Sumimura², Yasuyuki Ozeki¹; ¹The Univ. of Tokyo, Japan; ²Kokyo Inc., Japan. We demonstrate a polarization-maintaining fiber laser generating 8.4-ps pulses at 40 MHz with an average power of ~5 mW. Its intensity noise is measured to be only 2.4-dB higher than the shot noise limit.

JTh2A.131

Localization of light and transport of infrared optical image in a tellurite optical fiber with transversely-disordered refractive index profile, Hoang Tuan Tong¹, Shunei Kuroyanagi¹, Kenshiro Nagasaka¹, Takenobu Suzuki¹, Yasutake Ohishi¹; ¹Toyota Technological Inst., Japan. By numerical calculations and experiments, we demonstrate that tellurite optical fibers with transverse-disordered refractive index profile can be used to obtain the localization of light and to transport infrared optical images at 1.55 μm.

JTh2A.132

All-Polarization-Maintaining One- and Two-Stage Holmium-doped Fiber Amplifiers at 2051 nm, Robert E. Tench¹, Clement Romano^{1,2}, Jean-Marc Delavaux¹, Benoit Cadier², Thierry Robin², Arnaud Laurent²; ¹Cybel, LLC, USA; ²Institut Telecom/Paris Telecom Tech, France; ³IXBlue Photonics, France. We report the performance of one- and two-stage single clad polarization-maintaining (PM) Ho-doped fiber amplifiers (HDFAs) at λ_s = 2051 nm, pumped at λ_p = 1950 nm. We show that the Ho-doped fiber has a slope efficiency η = 70 %, and demonstrate an output power P_{out} of 3.5 W and a gain G = 43 dB.

JTh2A.133

Cladding Pumped EDFAs with Annular Erbium Doping, Charles Matte-Breton¹, Haoshuo Chen², Nicolas K. Fontaine², Roland Ryf², René-Jean Essiambre², Younés Messaddeq¹, Sophie LaRochelle¹; ¹Université Laval, Canada; ²Nokia Bell Labs, USA. We present simulation, fiber design and experimental characterization of a cladding pumped EDFA with erbium doping in the cladding. The approach is of interest for future development of multi-core EDFAs with increased saturation output power.

JTh2A.134

Gain-Switched Thulium-Doped Fiber Laser with Electrically Tuning at 1690-1765 nm, Can Li¹, Nan Chen¹, Zhichao Luo^{1,2}, Kenneth Kin-Yip Wong¹; ¹Univ. of Hong Kong, Hong Kong; ²Guangzhou Key Lab for Special Fiber Photonic Devices and Applications, South China Normal Univ., China. We demonstrate a gain-switched thulium-doped fiber laser with electrically tuning at 1690-1765 nm. Stable laser pulse with duration of 190 ns, average power of 654 mW, and pulse energy of 2.2 μJ is achieved.

JTh2A.135

Dual Pumping Scheme for Efficient 4 μm Operation of a Ho:InF₃ Glass Fiber Laser, Richard S. Quimby¹; ¹Worcester Polytechnic Inst., USA. Numerical modeling shows that pumping a Ho-doped fluorindate fiber laser at both 910 and 2100 nm will give a cw output at 4100 nm with a slope efficiency of ~17%.

JTh2A.136

Fiber-based Picosecond Source with Variable Transform Limited Linewidth and Flexible Repetition Rate, Daniel Kiefer¹, Thomas Walther¹; ¹TU Darmstadt, Laser and Quantum Optics, Germany. We present a 1028-nm master oscillator power amplifier system generating transform limited pulses with adjustable duration (250 and 735 ps) and repetition rate (1 and 10 MHz).

JTh2A.137

Off-resonance long-period fiber gratings and spin-optics response, Moti Fridman¹; ¹Bar Ilan Univ., Israel. We investigated the spectral response of strong long-period fiber gratings (LPFGs) and found an off-resonance spectral response including a spin-optics coupling between polarization and modes for asymmetric LPFGs.

JTh2A.138

Probabilistic Phase Control for Coherent Beam Combining, Henrik Tuennermann¹, Akira Shirakawa¹; ¹Univ. of Electro-Communications, Japan. Using probabilistic phase control, we realize coherent beam combining without using explicit modulation or polarization for error signal generation. Furthermore, the technique allows fusing multiple types of sensor data.

JTh2A.139

Polarization-maintaining, dual-wavelength, dual-comb mode-locked fiber laser, Ruli Wang¹, Xin Zhao¹, Weinan Bai¹, Jie Chen¹, Zheng Zheng^{1,2}; ¹School of Electronic and Information Engineering, Beihang Univ., China; ²Collaborative Innovation Center of Geospatial Technology, China. A self-starting, dual-wavelength, dual-comb mode-locked fiber laser based on all polarization-maintaining parts and a carbon nanotube modelocker is demonstrated, and dual-wavelength operation is realized through spatial filtering facilitated by waveplates in the cavity.

JTh2A.140

Timing Stabilization of Solid-State Yb-Based Laser System, Stefano Valente^{1,2}, Anne-Laure Calendron^{1,3}, Joachim Meier¹, Emma Kueny^{1,2}, Huseyin Cankaya^{1,2}, Nicholas H. Matlis¹, Giovanni Cirri^{1,3}, Franz X. Kaertner^{1,2}; ¹Center for Free Electron Laser Science, Deutsches Elektronen Synchrotron (DESY), Germany; ²Dept. of Physics, Univ. of Hamburg, Germany; ³The Hamburg Centre for Ultrafast Imaging, Univ. of Hamburg, Germany. We present a tight optical timing stabilization to 10 fs RMS jitter between two compressed branches of a sub-picosecond Yb based laser system operating at 1 kHz

JTh2A.141

Extension of the Stable Operation of an all Polarization Maintaining Mode-Locked Fiber Laser, Hanieh Afkhamiardakani¹, Mehran Tehrani¹, Jean-Claude M. Diels¹; ¹Univ. of New Mexico, USA. We present an all-polarization maintaining mode-locked fiber laser at 1532 nm with enhanced stability by cooling of the carbon nanotube saturable absorber. The laser output power ranges from 50uW to 200uW depending on the cooling.

JTh2A.142

Pulse-Chirp Instability and Issues for Its Measurement, Rana Jafari¹, Rick Trebino¹; ¹Georgia Inst. of Technology, USA. Pulses often possess random amounts of linear chirp. We find that SPIDER cannot detect this variation, yielding instead a shorter, flat-phase, coherent artifact. SHG FROG can and provides a better estimate of the average pulse.

JTh2A.143

Ultrafast Broadband Photodetectors Based on Three-Dimensional Dirac Semimetal Cd₃As₂, Jiawei Lai¹, Qingsheng Wang¹, Cai-Zhen Li², Shaofeng Ge¹, Jin-Guang Li², Wei Lu¹, Xuefeng Liu¹, Junchao Ma¹, Da-Peng Yu^{2,3}, Zhi-Min Liao^{2,3}, Dong Sun^{1,3}; ¹International Center for Quantum Materials, School of Physics, Peking Univ., China; ²State Key Lab for Mesoscopic Physics, School of Physics, Peking Univ., China; ³Collaborative Innovation Center of Quantum Matter, China. In this work, we report the realization of an ultrafast broadband photodetector based on Cd₃As₂ with a high sensitivity, high responsivity and high speed (~145 GHz) over a broad wavelength range.

JTh2A.144

Ultralow-Noise and Agile Microwave Synthesizer Based on a Femtosecond Mode-Locked Fiber Laser, Juan Wei^{1,2}, Dohyeon Kwon¹, Shilong Pan², Jungwon Kim¹; ¹Korea Advanced Inst of Science & Tech, South Korea; ²Nanjing Univ. of Aeronautics and Astronautics, China. We demonstrate a microwave synthesizer based on a mode-locked fiber laser and all-fiber photonics, which outputs 9-11 GHz signals with integrated timing jitter of 7.6-fs to 9.1-fs [integration bandwidth: 10 Hz-10 MHz] and frequency switching time of 135-ns.

JTh2A.145

Simplified Pre-Characterization of Chirped Pulses in Single-shot Supercontinuum Spectral Interferometry, Dinhduy Vu¹, Dogeun Jang¹, Ki-Yong Kim¹; ¹Univ. of Maryland at College Park, USA. We develop a method to pre-characterize a chirped pulse in single-shot supercontinuum spectral interferometry (SSSI). In this method, the spectral phase of both modulated (probe) and unmodulated (reference) pulses can be determined simultaneously.

JTh2A.146

Optical Repetition Rate Locking of Ultrafast SESAM-Based Yb-Doped All-Fiber Oscillator for High Intensity OPCPA Systems, Karolis Madeikis^{1,2}, Karolis Viskontas¹, Rokas Danilevicius^{1,2}, Tadas Bartulevicius^{1,2}, Laurynas Veselis^{1,2}, Andrejus Michailovas^{1,2}, Nerijus Rusteika^{1,2}, ¹Ekspla Ltd., Lithuania; ²Dept. of Laser Technology, State research Inst. Center for Physical Sciences and Technology, Lithuania. We demonstrate all-fiber ultrafast SESAM-based optically repetition rate locked oscillator concept designed for high intensity OPCPA systems. Pump induced refractive index change in the active erbium fiber for precise delay line was tested.

JTh2A.147

Femtosecond laser delivery and coupling via dual hollow-core anti-resonant fiber, Xiaosheng Huang¹, Seongwoo Yoo¹, Dingyuan Tang¹, Jie Ma¹; ¹Nanyang Technological Univ., Singapore. We design, fabricate and characterize dual hollow-core anti-resonant fibers (DHAFs) that function as air core fiber couplers. The applications of DHAFs in fiber laser and ultrafast pulse delivery and power coupling are demonstrated.

JTh2A.148

Dual-comb spectrally encoded confocal microscopy, Pingping Feng¹, Jiqiang Kang¹, Sisi Tan¹, Xi Zhou², Chi Zhang², Kenneth Kin-Yip Wong¹; ¹The Univ. of Hong Kong, Hong Kong; ²Huazhong Univ. of Science and Technology, China. We report a dual-comb spectrally encoded confocal microscopy (DC-SECM) at 3-MHz frame rate and 8.8- μ m resolution. Comparing with mode-locked laser based SECM, DC-SECM features with lower detection bandwidth and higher power efficiency.

JTh2A.149

An aberration-free ultrafast optical oscilloscope with large temporal window, Liao Chen¹, Yuhua Duan¹, Xi Zhou¹, Chi Zhang¹, Xinliang Zhang¹; ¹Huazhong Univ. of Science and Technology, Wuhan National Lab for Optoelectronics & School of Optical and Electronic Information, China. We report an aberration-free ultrafast optical oscilloscope based on the time-to-frequency conversion. It achieves 430-fs temporal resolution over 14-ns temporal window, which represents the largest record-length-to-resolution ratio (3.2×10^9) of any single-shot-capable ultrafast oscilloscope.

JTh2A.150

High-Speed "Multi-Grid" Pulse-Retrieval Algorithm for Frequency-Resolved Optical Gating, Rana Jafari¹, Rick Trebino¹; ¹Georgia Inst. of Technology, USA. We improved the FROG-algorithm convergence speed for complex pulses using a "multi-grid" technique. We achieved a factor of ~7 improvement for cross-correlation FROG for pulses with time-bandwidth products from 40 to 90.

JTh2A.151

Ultrafast Coherent Hole Transfer in Non-Fullerene OPV Blends, Rui Wang¹, Chunfeng Zhang¹, Zhiguo Zhang², Yongfang Li², Xiaoyong Wang¹, Min Xiao^{1,3}; ¹National Lab of Solid State Microstructures, School of Physics, and Collaborative Innovation Center of Advanced Microstructures, Nanjing Univ., China; ²Beijing National Lab for Molecular Science, CAS Key Lab of Organic Solids, Inst. of Chemistry, Chinese Academy of Science, China; ³Dept. of Physics, Univ. of Arkansas, USA. We study the ultrafast hole transfer process in the OPV blends of J71/ITIC utilizing two-dimensional electronic spectroscopy. The results show coherent vibronic coupling plays a critical role in ultrafast hole transfer process.

JTh2A.152

Mode-Locked all-fiber laser using Two-Dimensional Perovskite in C and L band, Seongjin Hong¹, Ferdinand Iedee², Jaedock Park³, Sanggwon Song¹, Dong-il Yeom³, Emmanuelle Deleporte², Kyunghwan Oh¹; ¹Yonsei Univ., South Korea; ²Université Paris-Sud, France; ³Ajou Univ., South Korea. Using two-dimensional (2D) hybrid organic-inorganic (C₆H₅C₂H₄NH₃)₂PbI₄ perovskite thin film as an in-line saturable absorber, we experimentally demonstrate an all-fiber mode-locked laser with 381 fs in both C and L band.

JTh2A.153

Scaling of High Repetition Rate Mode-Locked Tm-doped Fiber Lasers, Junjie Zeng¹, Ahmet E. Akosman¹, Michelle Y. Sander^{1,2}; ¹Electrical and Computer Engineering, Boston Univ., USA; ²Materials Science and Engineering, Boston Univ., USA. Scaling of a compact linear soliton mode-locked Tm-doped fiber lasers with repetition rates of 531.9 MHz, 704.3 MHz, and 969.0 MHz with transform limited pulse durations down to 358 fs is demonstrated.

JTh2A.154

Compact High Average Power High Energy CPA Laser System Based on Yb Fiber Seeder and Yb:YAG Amplifier, Laurynas Veselis^{1,2}, Tadas Bartulevicius^{1,2}, Karolis Madeikis^{1,2}, Rokas Danilevicius^{1,2}, Andrejus Michailovas^{1,2}, Nerijus Rusteika^{1,2}; ¹R&D, Ekspla Ltd, Lithuania; ²Dept. of Laser Technology, Center for Physical Sciences and Technology, Lithuania. We presented a compact sub-ps high average power (20 W) and energy (100 μ J) laser based on the matched pair of chirped fiber Bragg grating and chirped volume Bragg grating for pulse stretching and compression.

JTh2A.155

Soliton molecule vibration in mode-locked fiber lasers, Yiyang Luo¹, Yang Xiang¹, Tao Liu¹, Bowen Liu¹, Zhijun Yan¹, Yingxiang Qin¹, Qizhen Sun¹, Xiahui Tang¹; ¹Huazhong Univ of Science and Technology, China. Atom-like behaviors make the bound solitons akin to molecules. Here, we report on the experimental observation of soliton molecule vibration in mode-locked fiber lasers with time-stretch technique to deepen our understanding of soliton complexes.

JTh2A.156

Four-Prism-Pumped All-Gold-Mirror Femtosecond Optical Parametric Oscillator Based on an Yb-doped Fiber Laser, Jun Zhao¹, Jintao Fan¹, Chenglin Gu¹, Wu Liu¹, Chingyue Wang¹, Ming-lie Hu¹; ¹Tianjin Univ., China. We report a four-prism-pumped all-gold-mirror idler resonant optical parametric oscillator (OPO) driven by an Yb-fiber femtosecond laser. The idler is tuned from 2560-4180 nm, with the corresponding signal covering 1380-1825 nm.

JTh2A.157

Generation of a CEO-stabilized optical frequency comb with programmable sub-MHz FSR using spectral self-imaging, Mohamed Seghilani¹, Xiao-Zhou Li¹, Reza M. Qartavol¹, Luis Romero Cortés¹, Jose A. Azana¹; ¹INRS-EMT, Canada. We demonstrate a low noise, CEO-stabilized optical frequency comb (OFC) with a programmable sub-MHz FSR through suitable temporal phase modulation of a 250-MHz OFC. The method preserves the energy and the full bandwidth of the input OFC.

JTh2A.158

21-fs Kerr-lens Mode-locked Yb:CaYAlO₄ Laser, Jie Ma^{2,1}, Xiaodong Xu², Deyuan Shen², Dingyuan Tang¹; ¹Nanyang Technological Univ., Singapore; ²Jiangsu Normal Univ., China. We experimentally demonstrated the generation of 5.87-optical-cycle pulses from a Kerr-lens mode-locked Yb:CaYAlO₄ (Yb:CYA) laser. Pumped by a 976 nm fiber laser, stable ultrashort pulses with a repetition rate of ~114 MHz were obtained around 1077 nm.

JTh2A.159

Continuous Generation of Ultrafast Arbitrary Optical Waveform with a Repetition Rate Exceeding 100 THz, Chiaki Ohae^{1,2}, Trivikramarao Gavara¹, Kaoru Minoshima^{1,2}, Masayuki Katsuragawa^{1,2}; ¹Univ. of Electro-Communications, Japan; ²JST, ERATO, MINOSHIMA Intelligent Optical Synthesizer, Japan. We generate the five phase-locked harmonics having an exact integer frequency ratio 1 ω , 2 ω , 3 ω , ... with a controlled carrier-envelope-phase. We also demonstrate the continuous generation of ultrafast optical amplitude waveforms with a repetition rate exceeding 100 THz.

JTh2A.160

Dissipative Kerr Soliton mode-locking and breather states in 19 GHz Si₃N₄ microresonator, Wenting Wang¹, Abhinav K. Vinod¹, Jinghui Yang¹, Mingbin Yu², Dim-Lim Kwong², Chee-Wei Wong¹; ¹Mesoscopic Optics and Quantum Electronics Lab, Univ. of California, Los Angeles, USA; ²Technology and Research (A*STAR), Inst. of Microelectronics, Singapore. We observed chaotic state, breather comb, and dissipative Kerr soliton (DKS) with repetition rate of 19 GHz in dispersion-managed Si₃N₄ microresonator. The DKS pulse train is characterized by SHG noncollinear autocorrelator and frequency-resolved optical gating.

JTh2A.161

Multiplexed Signal Recovery for Ultrafast Waveform Measurement, Daniel J. Kane¹; ¹Mesa Photonics, LLC, USA. We demonstrate a combined optical and electronic system for measuring optical waveforms at bandwidths up to 2 THz. The technique uses sonogram decomposition of the waveform to reduce the optical bandwidth to levels measurable with current electronics.

JTh2A.162

Tightly Synchronized Two-color Femtosecond Source Based on Low-noise SPM-enabled Spectral Selection, Yi Hua¹, Gengji Zhou¹, Wei Liu¹, Franz X. Kaertner¹, Guoqing Chang¹; ¹Center for Free-Electron Laser Science, DESY, Germany. We demonstrate that SPM-enabled spectral selection generates low noise high-energy wavelength tunable femtosecond pulses that exhibit sub-fs relative timing jitter and therefore are tightly synchronized to the source laser pulse.

JTh2A.163

Temporal Super-Resolution, Moti Fridman¹; ¹Bar Ilan Univ., Israel. We investigated the resolution limits of time-lenses and developed a super-resolution technique in the time domain based on localization microscopy algorithm, demonstrating an improved resolution by a factor of two.

JTh2A.164

Phase Lock in Four-Wave Raman Mixing in the Near-Infrared Region, Yuta Nakano¹, Totaro Imasaka²; ¹Dept. of Applied Chemistry, Graduate School of Engineering, Kyushu Univ., Japan; ²Division of International Strategy, Center of Future Chemistry, Kyushu Univ., Japan. The Raman emission generated by four-wave mixing was verified to be coherently phased against the pump beams, suggesting the generation of an ultrashort optical pulse train by superimposing the Raman emission and the pump beams.

JTh2A.165

Ultralarge Dispersion of Microwave Signals, Jilong Li¹, Yan Zheng¹, Yitang Dai¹, Feifei Yin¹, Kun Xu¹; ¹Beijing Univ of Posts & Telecom, China. We propose and demonstrate a novel microwave signal processing scheme to achieve ultralarge dispersion amounts approaching 10 ns/GHz. We achieve this by magnifying limited optical dispersion amounts (around 32.3 ps/nm) 390,000 times

JTh2A.166

Progress Towards Full Stabilization of an Injection Locked 10GHz Chip-Scale Mode-Locked Laser on InP, Michael E. Plascak², Ricardo Bustos Ramirez², Marcin Malinowski², Jean-Etienne Tremblay¹, Ashish Bhardwaj³, Gloria Hoefler³, Sasan Fathpour², Ming C. Wu¹, Peter Delfyett²; ¹Dept. of Electrical Engineering and Computer Science, Univ. of California at Berkeley, USA; ²CREOL, The College of Optics & Photonics, Univ. of Central Florida, USA; ³Infinera Corporation, USA. Repetition rate stabilization of an injection locked chip-scale mode-locked laser and progress towards carrier envelope offset frequency stabilization using chalcogenide waveguides for supercontinuum generation and a bulk PPLN for second harmonic generation are presented.

JTh2A.167

Harmonic Injection Locking for a Direct Optical to RF Link, Ricardo Bustos Ramirez², Michael E. Plascak², Ashish Bhardwaj¹, Gloria Hoefler¹, Fred Kish¹, Peter Delfyett²; ¹Infinera Corporation, USA; ²CREOL, The College of Optics and Photonics, USA. We demonstrate a chip-scale direct optical to RF link, that down-converts 60GHz optical frequency combs to 10GHz, using harmonic multi-tone injection locking. A minimum injection power of 10μW and locking bandwidth of 4.3MHz is observed.

JTh2A.168

Photonic Measurement of Broadband Microwave Bursts, Yihan Li¹, Naoya Kuse¹, Martin E. Ferrmann²; ¹IMRA America, Inc., BRL, USA; ²IMRA America, Inc., USA. We report a photonic-assisted system for broadband microwave burst measurements. By deploying a dual coherent electro-optical comb and optical storage, wavelength and time-division multiplexings are enabled simultaneously to offer broad bandwidth and fast acquisition speed.

JTh2A.169

4D Pulse Shaping of Discretized Beam Arrays, Wei Liu¹, Joseph Robinson¹, Alan Fry¹, Sergio Carabajo¹; ¹Stanford Univ. SLAC National Accelerator, USA. We report on a novel ultrafast laser architecture capable of generating 4D arbitrarily distributed beams based on an array of coherently combined fibers, each containing femtosecond pulses with controlled intensity, wavefront, and polarization vector distribution.

JTh2A.170

Spectrally sampled second-harmonic interferometric autocorrelation for 3.5 fs pulse measurement, Heng-Jia Liu¹, An-Chia Hsu¹, Chung-Lo Chen¹, Shang-Da Yang¹; ¹National Tsing Hua Univ., Taiwan. We demonstrate that two interferometric autocorrelation traces obtained by sampling two second-harmonic tones around the carrier would be sufficient to algebraically retrieve the spectral phase of a 3.5 fs pulse.

JTh2A.171

Directly Determining the Coefficient of Thermal Expansion of High-power Light-emitting Diodes by Optical Coherence Tomography, TingWei Yeh¹, Chun-Yang Chou¹, Chun-Ying Huang^{2,3}, YungChi Yao¹, YiKai Haung¹, Meng-Tsan Tsai^{4,5}, Ya-Ju Lee¹; ¹National Taiwan Normal Univ., Taiwan; ²Univ. of Washington, USA; ³National Chi Nan Univ., Taiwan; ⁴Chang Gung Univ., Taiwan; ⁵Chang Gung Memorial Hospital, Taiwan. We used optical coherence tomography to measure CTE of high-power LEDs encapsulated in polystyrene resin. This work validates OCT can provide an alternative way to directly and nondestructively determine spatially resolved CTE of packaged LEDs.

JTh2A.172

A Fast, Accurate and Widely Applicable Computer Algorithm for Estimating Layer Number of Two-Dimensional Materials, Seungwan Cho¹, Jekwan Lee¹, Soohyun Park¹, Hyemin Bae¹, Minji Noh¹, Beom Kim¹, Chihun In¹, Seung Hoon Yang², Sooun Lee³, Seung Young Seo⁴, Jehyun Kim⁵, Chul-Ho Lee², Wooyoung Shim³, Moon-Ho Jo^{4,6}, Dohun Kim⁵, Hyunyoung Choi¹; ¹Electrical and Electronic Engineering, Yonsei Univ., South Korea; ²KU-KIST Graduate School of Converging Science and Technology, Korea Univ., South Korea; ³Dept. of Materials Science and Engineering, Yonsei Univ., South Korea; ⁴Dept. of Materials Science and Engineering, Pohang Univ. of Science and Technology, South Korea; ⁵Dept. of Physics and Astronomy, Seoul National Univ., South Korea; ⁶Center for Artificial Low Dimensional Electronic Systems, Inst. for Basic Science, South Korea. We present a computer algorithm for layer number estimation of few-layered two-dimensional materials. Based on the optical contrast method, this algorithm analyzes an optical microscope image in a few seconds with high accuracy over 90%.

JTh2A.173

Characterizing Chromatic Dispersion of Multiple Few-Mode Fibers Using Bidirectional OTDR Technique, Huiyuan Liu^{2,1}, Haoshuo Chen², Jiaxiong Li², Nicolas K. Fontaine², Roland Ryf², Guifang Li¹; ¹Univ. of Central Florida, USA; ²Nokia Bell Labs, USA. We use bidirectional OTDR technique to measure effective areas of two LP modes at four discrete wavelengths in cascaded few-mode fibers, with the help of mode-selective photonic lanterns, and calculate the chromatic dispersion.

JTh2A.174

The Reliability Assessment of Interferometric Fiber Optical Gyroscopes Based on Bayesian Estimation, Kun Ma¹, Jing Jin¹, Jing Ma¹, Ningfang Song¹; ¹Beihang Univ., China. With the combination of priori distribution and likelihood function, the joint posterior distribution of interferometric fiber optical gyroscopes (IFOGs) is obtained based on Bayesian estimation and the reliability of IFOGs is assessed.

JTh2A.175

Using Two-Photon Absorption Pulsed-Laser Excitation to Simulate Radiation Effects in Microelectronics, Joel M. Hales^{1,2}, Ani Khachatryan^{1,2}, Stephen Buchner¹, Nicolas J. Roche¹, Jeffrey Warner¹, Veronique Ferlet-Cavrois³, Dale McMorro¹; ¹Naval Research Lab, USA; ²Sotera Defense Solutions, USA; ³European Space Agency, Netherlands. By accurately characterizing and simulating the charge deposited in a device using two-photon absorption, this laser-based approach is used for quantitatively predicting radiation effects induced by heavy-ion excitation.

JTh2A.176

Study on Improved Object Identification by Using a Fused Image from Hyper-Spectral IR Images, Do-Hwi Kim¹, Changwon Kim¹, Kuk-Il Han¹, Jun-Hyuk Choi¹, Tae-Kuk Kim¹; ¹Chung Ang Univ., South Korea. We developed a method for fusion of hyper-spectral IR images by emphasizing the feature points determined from the gray scale analysis. The proposed image fusion method resulted in an increased contrast up to 46% as compared to the previous methods.

JTh2A.177

Simultaneous Identification of Size and Complex Refractive Index of a Single Microbead via Mie Scattering, Benjamin Mills¹, James Grant-Jacob¹, Bharat Pant¹, Daniel Heath¹, Peter Horak¹, Matthew Loxham¹, Robert Eason¹; ¹Univ. of Southampton, UK. The comparison of a single experimental diffraction pattern with simulations produced using Mie theory enables the precise and simultaneous determination of size and complex refractive index of a polystyrene microbead. Results agree with tabulated values.

JTh2A.178

An broadband terahertz metamaterial filter based on multiplexed metallic bar resonators, Zi jie Dai¹, Jing Yang², Qiang Su¹, Pengfei Qi¹, Dan Lu¹, Cheng Gong¹, Lu Sun¹, Weiwei Liu¹; ¹Nankai Univ., China; ²Shanghai Inst. of Applied Physics, China. An ultrabroad terahertz metamaterial filter based on multiplexed metallic bar resonators is designed and fabricated. The bandwidth of terahertz filter can be significantly broadened by the multiplexed configurations.

JTh2A.179

Broadband Wavelength Tunable Mode-Locked Tm-Doped Fiber Laser Based on Carbon Nanotubes, Bo Fu¹, Syed Hussain¹, Giancarlo Soavi¹, Baicheng Yao¹, Daniel Popa¹, Andrea Ferrari¹; ¹Cambridge Graphene Centre, UK. We report a broadband tunable Tm-doped fiber laser mode-locked by carbon nanotubes. The wavelength tunability is achieved by introducing a polarization-maintaining isolator and two polarization controllers and the tunable range is up to 60 nm.

JTh2A.180

A Raman Spectroscopy and Optical Microscopy System for Studies at Low Temperatures and High Magnetic Fields, Todd Sayles¹; ¹Quantum Design, USA. We present an optical probe for the PPMS for temperatures from 1.8 to 350 K and magnetic fields up to 16 T with XYZ motion control and integrated camera for fluorescence, Raman spectroscopy, and microscopy

JTh2A.181

Generation of wavelength- and orbital-angular-momentum-tunable vortex beam in Yb:CALGO laser, Yijie Shen¹, Mali Gong¹; ¹Tsinghua Univ., China. A dual-off-axis pumping scheme is presented to generate orbital-angular-momentum (OAM) beam in Yb:CALGO laser. The wavelength-tunable width about 10 nm and the OAM-tunable range from ±1h to ±15h, controlled by the off-axis-displacements and pump power.

JTh2A.182

Ultra-Thin Films with Eu³⁺ Ions for Probing Effects of Local Environment, Alexis D. Bullock^{1,2}, Marvin c. Clemmons^{1,2}, Mohammad Shahabuddin^{1,2}, Soheila Mashhadi¹, Chi Yang^{1,2}, Carl E. Bonner^{1,2}, Natalia Noginova^{1,2}; ¹Center of Materials Research, USA; ²Material Science and Engineering, Norfolk State Univ., USA. Ultra-thin films of Eu(TTA)₃(L1a) have been fabricated by Langmuir-Blodgett technique on plasmonic and dielectric substrates and used to probe the effect of local environment on magnetic dipole emission and charge transfer processes.

JTh2A.183

A Novel Scheme Based on Composite Frame and Correlation for OTN Fiber Link In-Service Monitoring, Jinhao Du¹, Yan Zhang¹, Zhiliang Ren², Xue Chen¹; ¹Beijing Univ. of Posts and Telecommunications, China; ²ZTE Corporation, China. Using correlation technique and composite frame formed by OTN OSC channel and M sequence, we demonstrate an in-service monitoring scheme for OTN fiber link, which has the benefit of large dynamic range and without waveform distortion in service signal.

JTh2A.184

Real-time loop gain and bandwidth measurement of phase-locked loop for mode-locked laser in full frequency range, Dong Hou¹, Jie Tian², Fuyu Sun¹, Qingsong Bai¹, Haoyuan Lu², Jianye Zhao³; ¹Univ. of Elect. Sci. and Tech. of China, China; ²Inst. of Electronic Engineering-CAEP, China; ³Peking Univ., China. We demonstrate a technique for directly and real-time measuring the loop gain and bandwidth of a phase-locking loop for mode-locked laser in full frequency range. The agreement of measurement and theoretical calculation proves the validity.

JTh2A.185

Precision visible comb from an Er fiber laser, Antoine Rolland¹, Peng Li¹, Marco Cassinero¹, Jie Jiang¹, Martin E. Ferrmann¹; ¹IMRA, USA. We report a highly coherent octave spanning visible optical frequency comb from a doubled Er fiber laser. The fractional residual instability is lower than 6x10⁻¹⁸ at 1s and reaches 3x10⁻¹⁸ after 1000 s of averaging time.

JTh2A.186

High-performance and cost-effective C-OTDR employing polarization independent coherent detection, Yan Zhao¹, Yang Tao¹, Ke Yan¹, Zhiliang Ren², Xue Chen¹; ¹State Key Lab of Information Photonics and Optical Communications, Beijing Univ. of Posts and Telecommunications, China; ²ZTE corporation, China. We propose a novel C-OTDR scheme which not only achieves large dynamic range but also solves the problem of polarization dependence. Simulation and experimental results demonstrate its feasibility and potentiality in ultra-long fiber link monitoring.

JTh2A.187

Non-mechanical Beam-steer Lidar System Based on Swept-laser Source, Yuyao N. Zhai¹, qingwen liu¹, Zuyuan He¹, He Li¹, Dian Chen¹; ¹Shanghai Jiao Tong Univ., China. We have proposed a non-mechanical beam-steer lidar system, in which laser sweeps to realize 1-D beam steering and ranging simultaneously. Steering resolution of 0.19° over 3.3° and distance resolution of 1.8mm over 1m is achieved.

JTh2A.188

Computation of Refractive Index and Optical Parameters for Stretched Polymer Films, KEUMCHEOL KWAK¹, Jung-Gu Lim^{1,2}, Jang-Kun Song¹; ¹Sungkyunkwan Univ., South Korea; ²Advanced Materials R&D Center, Dongwoo Fine Chem. Co., Ltd., South Korea. We report a theoretical calculation process without empirical databases to predict the refractive index, including wavelength dispersions and optical retardation of stretched polymer films using polarizability tensor, molecular volume for periodic units of polymers.

JTh2A.189

Dual-chirped OPA based pumping source for generation multicycle tunable terahertz pulses, Gyorgy Toth², József A. Fülöp¹, Máté Baditz², János Hebling²; ¹MTA-PTE High-Field THz Research Group, Hungary; ²Inst. of Physics, Univ. of Pécs, Hungary. The superposition of signal and idler in dual-chirped OPA is proposed to produce intensity-modulated pulses with constant period. The modulation period can be tuned by changing the chirp and/or the delay between pump and signal.

JTh2A.190

Single-cycle attosecond pulse generation by Thomson scattering of terahertz pulses, Gyorgy Toth², Zoltan Tibai², Ashutosh Sharma³, József A. Fülöp^{1,3}, János Hebling²; ¹MTA-PTE High-Field THz Research Group, Hungary; ²Inst. of Physics, Univ. of Pécs, Hungary; ³ELI-ALPS, ELI-Hu Nkft., Hungary. Single-cycle attosecond pulses can be generate by Thomson scattering of terahertz pulses on ultrathin electron layers, produced by a laser-plasma wakefield accelerator. According to our calculations, the energy can achieve more than 1 nJ.

JTh2A.191

Efficient semiconductor source of multicycle terahertz pulses using intensity-modulated pump, Gyorgy Toth², Pryo S. Nugraha², Mátyás I. Mechler², Gergo Krizsán², Gyula Polónyi², János Hebling², József A. Fülöp¹; ¹MTA-PTE High-Field THz Research Group, Hungary; ²Inst. of Physics, Univ. of Pécs, Hungary. Up to 5% conversion efficiency is predicted by numerical simulations for optimized GaP contact-grating THz sources based on optical rectification. Easy control of multicycle THz waveforms is enabled by a flexible dual-chirped OPA pump source.

JTh2A.192

A Continuously Tunable Optical Filter System in Broad Spectral Range, Mi-Yun Jeong¹; ¹Gyeongsang National Univ., South Korea. Optical notch and band pass filter systems with continuous fine tuning resolution in broad spectral range are realized by combining left- and right-handed cholesteric liquid crystal wedge cells.

JTh2A.193

Nano-membrane based Plasmonic Devices for Surface-Enhanced Infrared Absorption Gas Sensing, Xinyuan Chong¹, Yujing Zhang¹, Ki-joong Kim², Erwen Li¹, Paul Ohodnicki², Chih-hung Chang¹, Alan X. Wang¹; ¹Oregon State Univ., USA; ²National Energy Technology Lab, USA. Surface-enhanced infrared absorption for gas sensing is still not successful due to the intrinsically weak light-matter interaction. Herein, we demonstrate a plasmonic device integrated with metal-organic framework on Si₃N₄ membrane substrate for CO₂ sensing.

JTh2A.194

Detection of O18 and D Isotopes in Water Vapor using a Fiber-Coupled Tunable Diode Laser Absorption Spectroscopy Multi-Pass Cell, Allan S. Chang¹, Ate Visser¹, Erik Oerter¹, Tiziana Bondi¹; ¹Lawrence Livermore National Lab, USA. We have demonstrated detection of water isotopologues (H16OH, H18OH and HDO) by a compact fiber-coupled tunable diode laser absorption spectroscopy setup. The measured results agree well with HITRAN simulation.

JTh2A.195

28Gbps PAM4 60GHz Radio over Fiber System by Injection Locking Two-Tone Light to Directly-Modulated Laser, Guo-Wei Lu^{1,2}, Ruben S. Luis², Hiroyuki Toda³, Jiabin Cui⁴, Takahide Sakamoto², Hongxiang Wang⁴, Yuefeng Ji⁴, Naokatsu Yamamoto²; ¹Tokai Univ., Japan; ²National Inst. of Information and Communication Technology, Japan; ³Doshisha Univ., Japan; ⁴Beijing Univ. of Posts and Telecommunications, China. A 28Gbps PAM4 60GHz radio-over-fiber system is proposed and experimentally demonstrated by injection locking a two-tone light to a directly-modulated laser. Experimental results show negligible power penalty for the obtained PAM4 after the injection locking.

JTh2A.196

Visible to Mid-infrared Supercontinuum Generation Using a Gas-filled Hollow-core Fiber, MD Selim Habib¹, Christos Markos², A. Isa Adamu², Jose Enrique Antonio-Lopez¹, Rodrigo Amezcua Correa¹; ¹CREOL, Univ. of Central Florida, USA; ²Dept. of Photonics Engineering, Technical Univ. of Denmark, Denmark. Broadband supercontinuum generation spanning 0.58-5.0 μm is numerically presented using a Xe-filled nested hollow-core anti-resonant fiber under 7 bar pressure, pumped at 3 μm with 100 fs pulses and 15 μJ pulse energy.

CLEO: Science & Innovations

Joint

14:00–16:00

STh3A • Photonic Crystals

President: Kengo Nozaki; NTT Basic Research Labs, Japan

STh3A.1 • 14:00

CMOS-Compatible High-Q Photonic Crystal Cavities, Delphin Dodane¹, Jérôme Bourderionnet¹, Sylvain Combré¹, Alfredo De Rossi¹; ¹Thales Research & Technology, France. All-Solid Cladding Photonic Crystal Cavities have been fabricated in CMOS foundry. A recent design concept resulted into a measured Q-factor of 0.6 million (4.1x10⁵ in average). Statistical analysis leads to an estimate of the fabrication disorder of 1.2 nm.

STh3A.2 • 14:15

High-Contrast Resonance Excitation in Photonic Crystal Nanobeams via Side-Coupling and Wave-Vector Matching, Francis Afzal¹, Sami Halimi¹, Sharon M. Weiss¹; ¹Vanderbilt Univ., USA. Photonic crystal nanobeams engender exceptional high Q/V devices but suffer broadband signal loss off-resonance and low on-resonance transmission. We demonstrate drastically improved transmission metrics without compromising Q-factor using side-coupled excitation with optical momentum matching.

STh3A.3 • 14:30 **Invited**

InP Membrane Photonic Crystal Fano Devices, Kresten Yvind¹, Yi Yu¹, Dagmawi Bekele¹, Thorsten S. Rasmussen¹, Aurimas Sakanas¹, Andrey Marchevsky¹, Kristoffer S. Mathiesen¹, Hitesh K. Sahoo¹, Luisa Ottaviano¹, Elizaveta Semenova¹, Jesper Mork¹; ¹DTU Fotonik, Technical Univ. of Denmark, Denmark. Membrane photonic crystals offer many possibilities for designing small energy efficient devices like switches and lasers. We will present theoretical and experimental results on devices based on Fano resonances in photonic crystals.

STh3A.4 • 15:00

Lasing in a topological photonic crystal nanocavity, Yasutomo Ota¹, Ryota Katsumi¹, Katsuyuki Watanabe¹, Satoshi Iwamoto¹, Yasuhiko Arakawa¹; ¹Univ. of Tokyo, Japan. We report lasing oscillation in a zero-dimensional edge state formed at the boundary of two photonic crystal nanobeams with distinct band topologies. The topological origin of the nanocavity mode ensures a single mode operation.

14:00–16:00

STh3B • Networks on a Chip

President: Ruijun Wang; Ghent Univ.-imec, Belgium

STh3B.1 • 14:00 **Invited**

Microring Weight Banks for Neuromorphic Silicon Photonics, Alexander Tait¹, Thomas Ferreira de Lima¹, Mitchell Nahmias¹, Bhavin Shastri¹, Paul R. Prucnal¹; ¹Princeton Univ., USA. Research in photonic information processing has experienced a recent resurgence. Microring weight banks enable reconfigurable neural network approaches on silicon photonics. We discuss the latest results in neuromorphic silicon photonic networks and microring weight banks.

STh3B.2 • 14:30

Thermally Tunable III-V Photonics Architecture for Coherent Nonlinear Optical Circuits, Marina Radulaski^{1,2}, Ranojoy Bose², Tho Tran², Thomas Van Vaerenbergh², David Kielpin-ski², Raymond Beausoleil²; ¹Stanford Univ., USA; ²Hewlett Packard Enterprise, USA. We develop a thermally tunable hybrid photonics architecture integrating GaAs photonic crystal cavities, SiN_x grating couplers and waveguides, and chromium microheaters. We demonstrate external signal coupling to frequency-synchronized microcavities connected by a bus waveguide.

STh3B.3 • 14:45

Design, Fabrication and Demonstration of a Chip-Scale Reconfigurable Photonic Signal Processor, Xiaoping Cao¹, Shuang Zheng¹, Yun Long¹, Yan Luo¹, Li Shen¹, Jian Wang¹; ¹WNLO, China. Inspired by electronic Field Programmable Gate Arrays, we experimentally demonstrate a reconfigurable hexagonal mesh processor based on silicon platform. Assisted by tunable Mach-Zehnder couplers, numerous topologies and functions can be implemented with favorable performances.

STh3B.4 • 15:00

Reconfigurable Silicon Photonic Signal Processor Based on the SCOW Resonant Structure, Liangjun Lu¹, Lin Shen¹, linjie zhou¹, Jianping Chen¹; ¹Shanghai Jiao Tong Univ., China. We propose a reconfigurable silicon photonic signal processor composed of three stages of self-coupled optical waveguide (SCOW) resonators. The processor can be configured to ring resonator and MZI-based optical filters.

14:00–16:00

JTh3C • Symposium on Integrated Sources of Non-Classical Light: Perspectives and Challenges I

President: Marco Liscidini; Università degli Studi di Pavia, Italy

JTh3C.1 • 14:00 **Invited**

Photon-pair Generation and Quantum-classical Correspondence in Nonlinear Nanostructures, Andrey A. Sukhorukov¹; ¹Nonlinear Physics Centre, RSPE, The Australian National Univ., Australia. We present theoretical and experimental advances towards efficient photon-pair generation through spontaneous parametric down-conversion in nonlinear nanostructures and metasurfaces, enabling quantum entanglement engineering at sub-wavelength scale for photon generation with tailored polarization and spatial correlations.

JTh3C.2 • 14:30

Photon Pair Generation on a Silicon Chip Using Nanophotonic Periodically-Poled Lithium Niobate Waveguides, Ashutosh Rao¹, Nima Nader², Martin J. Stevens², Thomas Gerrits², Omar S. Magana Loaiza², Guillermo Camacho-Gonzalez¹, Jeffrey Chiles², Amirmahdi Honardoost¹, Marcin Malinowski¹, Richard Mirin², Sasan Fathpour¹; ¹CREOL, Univ. Central Florida, USA; ²NIST, USA. We present a new class of photon pair sources on a silicon chip. The source is based on nanophotonic periodically poled lithium niobate waveguides and presents MHz rate pair generation.

JTh3C.3 • 14:45

A Nanophotonic Platform Integrating Quantum Memories and Single Rare-earth Ions, Tian Zhong^{1,2}, Jonathan Kindem¹, Jake Rochman¹, John G. Bartholomew¹, Andrei Faraon¹; ¹California Inst. of Technology, USA; ²Univ. of Chicago, USA. We demonstrate a quantum nanophotonic platform integrating on-chip quantum memories and optically addressable single rare-earth ions. We show near-transform-limited, high-purity single photon emissions from individual rare-earth ions.

JTh3C.4 • 15:00 **Invited**

Tailoring radiative emission in integrated quantum light sources, Andrea Fiore¹, Daniele Pellegrino¹, Michele Cotrufo¹, Ewold Verhagen^{1,2}, Robert Johne³, Maurangelo Petruzzella¹, Francesco Pagliano¹, Frank van Otten¹; ¹Dep. Applied Physics, Eindhoven Univ. of Technology, Netherlands; ²AMOLF, Netherlands; ³Max Planck Inst. for the Physics of Complex Systems, Germany. An approach to the real-time control of the exciton-photon interaction rate in solid-state systems will be discussed. It enables the temporal shaping of single photons and the coherent coupling of excitons and phonons.

Joint

14:00–16:00

JTh3D • Symposium on Advances in Integrated Microwave Photonics I

Presider: José Capmany; *Universidad Politecnica de Valencia, Spain* and David Marpaung; *University of Twente, Netherlands*

JTh3D.1 • 14:00 **Invited**

Advanced Microwave Photonics Applications and Routes to Hybrid Integration, Richard DeSalvo¹, Anthony Klee¹, Charles Middleton¹, Kristina Bagnell¹, Elliott Grafer¹, Alex Cramer¹; ¹Harris Corporation, USA. We review recent advances in microwave photonic systems for wideband spectral awareness and down-conversion. Progress is shown toward hybrid integration of these systems with the latest chip-scale technologies to reduce SWaP and improve performance.

JTh3D.2 • 14:30 **Invited**

Integrated Microwave Photonics for 5G, Chris Roeloffzen¹, Ilka Visscher¹, Caterina Taddei¹, Dimitri Gekus¹, Ruud Oldenbeuving¹, Jörn Epping¹, Roelof Timens¹, Paul van Dijk¹, René Heideman¹, Marcel Hoekman¹, Robert Grootjans¹, Laurens Bliet², Sander Wahls², Michel Verhaegen²; ¹LioniX International, Netherlands; ²Delft Center for Systems and Control, Delft Univ. of Technology, Netherlands. This paper describes the design, fabrication, packaging, testing and automated tuning of an integrated 1x4 optical beamforming network. It consists of hybridly integrated InP and TriPleX chips, where end-facet coupling is used for optical interfacing.

JTh3D.3 • 15:00

Fast and Broadband SOI Photonic Integrated Microwave Phase Shifter, Giovanni Serafino¹, Claudio Porzi¹, Marc Sans², Fabio Falconi³, Sergio Pinna¹, Vito Sorianello³, John Mitchell², Marco Romagnoli³, Antonella Bogoni^{1,3}, Paolo Ghelfi²; ¹TeCIP, Scuola Superiore Sant'Anna, Italy; ²Dept. of Electronic and Electrical Engineering, Univ. College London, UK; ³National Photonics Labs, CNIT, Italy. An integrated silicon-on-insulator microwave photonic phase shifter based on an optical deinterleaver and a reverse-biased pn-junction waveguide providing broadband phase shift up to more than 400° with fast reconfiguration time of 1 ns is demonstrated.

CLEO: QELS-Fundamental
Science

14:00–16:00

FTh3E • Non-diffracting and Vortex Beams

Presider: Zhigang Chen; *San Francisco State Univ., USA*

FTh3E.1 • 14:00

Spatiotemporal diffraction-free pulsed beams in free-space of the Airy and Bessel type, Nikolaos K. Efremidis^{1,2}; ¹Univ. of Crete, Greece; ²Inst. of Applied and Computational Mathematics, Foundation for Research and Technology - Hellas (FORTH), Greece. We find new classes of optical spatiotemporal waves with one transverse direction that propagate in space-time in a diffraction-free fashion. These waves take the form of Airy, Bessel, and modified Bessel functions.

FTh3E.2 • 14:15

Observation of a Bessel beam soliton, Mariano Flammini¹, Giuseppe Di Domenico^{1,2}, Davide Pierangeli^{1,3}, Fabrizio Di Mei¹, Aharon Agranat¹, Eugenio DelRe^{1,5}; ¹Dept. of Physics, Univ. of Rome "La Sapienza", Italy; ²Center for Life Nano Science@Sapienza, Istituto Italiano di Tecnologia, Italy; ³Collaborative Innovation Center for Optoelectronic Science & Technology, College of Optoelectronic Engineering-Shenzhen Univ., China; ⁴Dept. of Applied Physics, Hebrew Univ. of Jerusalem, Israel; ⁵ISC-CNR, Università di Roma "La Sapienza", Italy. We have demonstrated experimentally and numerically that a Bessel-Beam propagating in a strongly self-focusing medium undergoes relevant dynamics along the propagation axis that ultimately cause it to self-trap into a periodic breather.

FTh3E.3 • 14:30

Nonlinear Optical Conversion of Photon Spin to Orbital Angular Momentum, Alex M. Wilhelm¹, David Schmidt¹, Charles Durfee¹; ¹Colorado School of Mines, USA. We demonstrate, to our knowledge, the first optical spin-to-orbital angular momentum conversion using second harmonic generation in underdense plasmas, enabling the generation of arbitrary orbital angular momentum beams using a single focusing optic.

FTh3E.4 • 14:45

Demonstration of pseudospin-to-orbital angular momentum conversion in photonic graphene, Xiuying Liu¹, Dao-Hong Song^{1,2}, Shiqi Xia¹, Zhixuan Dai¹, Liqin Tang¹, Jingjun Xu¹, Zhigang Chen^{1,3}; ¹The MOE Key Lab of Weak-Light Nonlinear Photonics, TEDA Applied Physics Inst. and School of Physics, Nankai Univ., China; ²Collaborative Innovation Center of Extreme Optics, Shanxi Univ., China; ³Dept. of Physics and Astronomy, San Francisco State Univ., USA. Momentum-matched selective excitation of two sublattices with vortex beams leads to direct observation of pseudospin-dependent conical diffraction and topological charge transformation, including spin-orbital angular momentum conversion arising from inherent degree-of-freedom in photonic graphene.

FTh3E.5 • 15:00

Tunable Vortex Beam, Singly-Resonant Ultrafast Optical Parametric Oscillator, Varun Sharma¹, S. C. Kumar², G. K. Samanta¹, M. Ebrahim-Zadeh^{2,3}; ¹Photonics Sciences Lab., Physical Research Lab, India; ²CFO-Institut de Ciències Fotoniques, Spain; ³Instituto Catalana de Recerca i Estudis Avançats (ICREA), Spain. We demonstrate the direct transfer of pump vortex mode to the idler beam in a singly-resonant optical parametric oscillator, generating ultrafast vortex beam of order as high as l=3, tunable across 1109-1209 nm.

CLEO: Science & Innovations

14:00–16:00

STh3F • Mid-IR Nonlinear Devices

Presider: Shu-Wei Huang; *Univ. of Colorado at Boulder, USA*

STh3F.1 • 14:00

Suspended-Si waveguides for spectral engineering of mid-IR frequency combs, Nima Nader¹, Jeff Chiles¹, Abijith Kowligy², Henry Timmers², Sae Woo Nam¹, Scott Diddams², Richard Mirin¹; ¹Applied Physics Division, NIST, USA; ²Time and Frequency Measurements Division, NIST, USA. Suspended-silicon waveguides are used for broadband mid-IR supercontinuum with low input power. Pumped with 100 fs, 3 μm pulses, these devices extend the mid-IR comb coverage across 126 THz from 1.74 μm to 6 μm.

STh3F.2 • 14:15

Picosecond fiber-laser-pumped widely tunable, narrow-linewidth, high-peak-power, mid-infrared OP-GaAs OPA, Qiang Fu¹, Lin Xu¹, Sijing Liang¹, David Shepherd¹, David Richardson¹, Shaif-Ul Alam¹; ¹Optoelectronics Research Centre, UK. We demonstrate a narrow-linewidth, mid-infrared OP-GaAs cascaded OPG-OPA with a widely tunable output of 2552-2960 nm (signal) and 5733-8305 nm (idler), and with a maximum peak power of 11.1 kW (signal) and 4.5 kW (idler).

STh3F.3 • 14:30 **Invited**

Chalcogenide-based devices for mid-infrared waveguide photonics, Martin Rochette¹; ¹McGill Univ., Canada. This talk will feature recent achievements of the Nonlinear Photonics Group at McGill Univ. towards the fabrication of chalcogenide-based mid-infrared optical fiber components such as nonlinear gain media, optical fiber couplers and optical filters.

STh3F.4 • 15:00

Octave-Spanning Mid-Infrared Supercontinuum Generation and Self-Compression in $\chi^{(2)}$ -Structured Rb-Doped KTP, Anne-Lise Viotti¹, Robert Lindberg¹, Andrius Zukauskas¹, Rimantas Budriunas^{3,2}, Dainius Kucinskas^{3,2}, Tomas Stanislaukas², Carlota Canalias¹, Fredrik Laurell¹, Valdas Pasiskevicius¹; ¹Royal Inst. of Technology, Sweden; ²Light Conversion, Lithuania; ³Vilnius Univ. Laser Research Center, Lithuania. We experimentally demonstrate octave-spanning supercontinuum generation and nonlinear pulse compression, down to sub-20-fs, in periodically poled Rb-doped KTP. The results of a detailed numerical study provide excellent agreement with the experiments.

CLEO: Science & Innovations

14:00–16:00

STh3G • Quantum Information Processing on Photonic Nanostructures

Presider: Mark Thompson; University of Bristol, UK

STh3G.1 • 14:00 **Tutorial**

Recent Advances in Quantum Information Science Using Quantum Optical Systems, Mikhail Lukin¹; ¹Harvard Univ., USA. We will discuss a new scientific interface between quantum optics, many-body physics, nanophotonics and quantum information science. Examples include manipulating arrays of individually trapped cold neutral atoms and atom-like emitters in diamond.



Mikhail Lukin received the Ph.D. degree from Texas A&M University in 1998. He has been a Professor of Physics at Harvard since 2004, where he is currently a co-Director of Harvard-MIT Center for Ultracold Atoms. His research interests include quantum optics, quantum metrology, nanophotonics, and quantum information science.

STh3G.2 • 15:00

Silicon on Silicon Carbide Ring Resonators for Coupling to Color Centers, Chuting Wang¹, Evan Miyazono¹, Ioana Craciun¹, Jake Rochman¹, Jonathan Kindem¹, Tian Zhong¹, John G. Bartholomew¹, Andrei Faraon¹; ¹California Inst. of Technology, USA. We present hybrid crystalline-silicon (c-Si) ring resonators on top of 4H silicon carbide with measured quality factor ~9600 for coupling to spin qubits like divacancies and Cr ions for future applications in quantum information networks.

CLEO: Applications & Technology

14:00–16:00

ATH3H • Control of Quantum Optical and Opto-mechanical Systems

Presider: Thomas Purdy; NIST, USA

ATH3H.1 • 14:00

Spin-Photon Interface Controlled Optical Switching in a Nanobeam Waveguide, Tim Schröder¹, Alisa Javadi¹, Dapeng Ding¹, Martin Hayhurst Appel¹, Sahand Mahmoodian¹, Matthias Löbl², Immo Söllner², Rüdiger Schott², Camille Papon¹, Tommaso Pregnolato¹, Søren Stobbe¹, Leonardo Midolo¹, Andreas Wieck³, Arne Ludwig³, Richard Warburton², Peter Lodahl¹; ¹Niels Bohr Inst., Denmark; ²Dept. of Physics, Univ. of Basel, Switzerland; ³Ruhr Universität Bochum, Germany. We demonstrate a single InGaAs quantum dot electron spin controlled photon switch in a nanobeam waveguide with 4-fold switching ratio, a spin-state preparation fidelity of 96%, and a lifetime T_1 approaching 5 μ s.

ATH3H.2 • 14:15

Electromechanically Tunable Diamond Color Centers Coupled to Nanophotonic Waveguides, Bartholomeus J. Machielse¹, Michael J. Burek², Srujan Meesala², Cleaven Chia², Young-Ik Sohn², Haig Atikian², Linbo Shao², Smarak Maity², Mikhail Lukin¹, Marko Loncar²; ¹Dept. of Physics, Harvard Univ., USA; ²John A Paulson School of Engineering and Applied Sciences, Harvard Univ., USA. We present a platform for the generation and high-efficiency collection of indistinguishable photons from spatially separated silicon-vacancy (SiV) color centers by use of waveguide-coupled nanoelectromechanical systems (NEMS).

ATH3H.3 • 14:30

Spectral Tuning of Multiple Germanium Vacancy Centers in Diamond with Mechanical Strain, Smarak Maity¹, Linbo Shao¹, Young-Ik Sohn¹, Srujan Meesala¹, Bartholomeus J. Machielse¹, Edward Bielejec², Marko Loncar¹; ¹Harvard Univ., USA; ²Sandia National Labs, USA. We experimentally demonstrate spectral tuning of the optical transitions of the germanium vacancy (GeV) center using strain in a diamond microcantilever. The GeV shows a large strain susceptibility on the order of PHz/strain. Spectral alignment of two initially spectrally separated GeVs is achieved.

ATH3H.4 • 14:45

Quantum Measurement of Membrane's Vibration, Jiteng Sheng¹, Xinrui Wei¹, Shuhui Wu¹, Haibin Wu¹; ¹East China Normal Univ., China. We demonstrate that the sub-shot-noise measurement of membrane's displacement can be realized with the cooperation of membrane-based interferometer and quantum correlated light. This provides a new strategy to study cavity optomechanics with squeezed light.

ATH3H.5 • 15:00

Quantum Optomechanics with Ultracoherent Soft-Clamped Resonators, Junxin Chen¹, Massimiliano Rossi¹, David Mason¹, Yeghishe Tsaturyan¹, Yannick Seis¹, Albert Schliesser¹; ¹Niels Bohr Inst., Denmark. Soft-clamped mechanical resonators realise quality factors $Q \sim 10^8$ and quantum cooperativities $C_c \sim 60$ already in a moderate cryogenic environment (e.g. a 4.2 K flow cryostat). This enables both sideband and feedback cooling to the mechanical quantum ground state.

CLEO: Science & Innovations

14:00–16:00

STh3I • Integrated Photonic Platforms

Presider: Tian Gu; MIT, USA

STh3I.1 • 14:00

Highly Nonlinear Gallium Nitride Waveguides, Erik Stassen¹, Minhao Pu¹, Elizaveta Semenova¹, Evgeniy Zavarin², Wsevolod Lundin², Kresten Yvind¹; ¹Technical Univ. of Denmark, Denmark; ²Ioffe Inst., Russia. We demonstrate a high effective nonlinearity in high refractive-index-contrast gallium nitride waveguides by performing four-wave mixing characterization. The intrinsic material nonlinearity (n_2) of gallium nitride is extracted at telecom wavelengths.

STh3I.2 • 14:15

InGaN-ZnSnN₂ Quantum Wells for High Efficiency Light Emitters Beyond Green, Md Rezaul Karim¹, Hongping Zhao^{1,2}; ¹Dept. of Electrical and Computer Engineering, The Ohio State Univ., USA; ²Dept. of Materials Science and Engineering, The Ohio State Univ., USA. A novel quantum well design based on InGaN-ZnSnN₂ structures is promising to address the existing challenge to realize high performance InGaN based visible light emitters emitting beyond green spectral regime (3-order enhancement in spontaneous emission).

STh3I.3 • 14:30

Four-Wave Mixing in a High-Q Aluminum Oxide Microcavity on Silicon, Henry C. Frankis¹, Zhan Su^{2,3}, Nanxi Li^{2,5}, Emir Magden^{2,4}, Mengyuan Ye¹, Michael Watts^{2,3}, Jonathan Bradley^{1,2}; ¹McMaster Univ., Canada; ²MIT, USA; ³Analog Photonics, USA; ⁴Koç Univ., Turkey; ⁵Harvard Univ., USA. We demonstrate Q factors of $> 10^8$ and parametric frequency conversion in Al₂O₃ micro-trench resonators co-integrated with Si₃N₄ waveguides on silicon. Under 1550-nm pumping we show oscillation at wavelengths ranging from 1135 to 2445 nm

STh3I.4 • 14:45

Arbitrary Vertical Low-Loss Waveguides in Deposited Oxide of Optical Interposers for Low-Loss 3D Photonic Packaging, Yi-Chun Ling¹, Yu Zhang¹, S. J. Ben Yoo¹; ¹Univ. of California, Davis, USA. We first demonstrate a low-loss flexible 3D waveguide on deposited oxide cladding for 3D photonic packaging using ultrafast laser inscription. Waveguide propagation loss, excess bending loss and coupling loss to SiN waveguide were characterized.

STh3I.5 • 15:00

Four-Wave Mixing in a Multi-Layer SiN_x/a-Si:H Photonic Chip, Michael Kossey¹, Kangmei Li¹, Hongcheng Sun¹, Amy Foster¹; ¹Johns Hopkins Univ., USA. We demonstrate four-wave mixing (FWM) in a-Si:H waveguides in a multi-layer integrated photonic chip. The a-Si:H waveguides are accessed through interlayer couplers from waveguides composed of SiN_x and exhibit 0.45±0.05 dB loss per transition.

CLEO: Science & Innovations

14:00–16:00

STh3J • Optofluidics & High Throughput Fluorescence

President: Andreu Llobera; Carl Zeiss Vision GmbH, Germany

STh3J.1 • 14:00 **Invited**

Light Controlled Cellular Surgery and Intracellular Delivery, Pei-Yu Chiou¹; ¹Univ. of California Los Angeles, USA. Delivery of large-sized extracellular cargo into live cells has been a major technical barrier. Here, we present an optofluidics platform for high efficiency delivery of cargo of size up to micrometers into mammalian cells.

STh3J.2 • 14:30 **Invited**

Optofluidic Platforms for Applications in Cancer Research, Alexandre Brolo¹, America Palacios¹, Karolina Papera Valente¹; ¹Univ. of Victoria, Canada. We will describe a microfluidic chip designed to study the diffusion of nanoparticles in cancer tissues. We will also demonstrate an optical trap to study the effect of radiation on cancer cells by Raman scattering.

STh3J.3 • 15:00

Frequency Doubled High Speed Fluorescence Lifetime Imaging, Sebastian Karpf¹, Bahram Jalali¹; ¹Univ. of California, Los Angeles, USA. We present high speed fluorescence lifetime imaging in the visible enabled by broadband frequency-doubling of the SLIDE technique (1P-SLIDE). Fluorescence Lifetime imaging at 88 million pixels per second is demonstrated.

14:00–16:00

STh3K • Multimode Fiber Optics

President: Sophie LaRoche; Université Laval, Canada

STh3K.1 • 14:00 **Tutorial**

Multimode Nonlinear Fiber Optics: New perspectives, opportunities & challenges, Siddharth Ramachandran¹; ¹Boston Univ., USA. Multimode fibers experience intra- and inter-modal nonlinear interactions, facilitating new degrees of design freedom as well as nonlinear effects not seen in single mode systems. We review the physics and applications of this emerging platform.



Dr. Siddharth Ramachandran started his scientific career as a Member of Technical Staff at Bell Laboratories in 1998, followed by continuing, in 2002, with its fiber-optics-related spin-off, OFS Laboratories. In 2010, he moved back to academics and is now a Professor in the Department of Electrical Engineering at Boston University.

STh3K.2 • 15:00

Multimode random fiber laser for speckle free imaging, Rui Ma¹, Yun Jiang Rao¹, Wei Li Zhang¹, Bo Hu¹; ¹Univ of Electronic Science & Tech China, China. It is the first time that a multi transverse mode random fiber laser with high radiance and low coherence is used for speckle-free imaging, which is ideal for wide field or high-speed imaging applications.

14:00–16:00

STh3L • Imaging and Ranging

President: Waruna Kulatilaka; Texas A&M Univ., USA

STh3L.1 • 14:00 **Invited**

Deep Learning Smart Microscope, Bahram Jalali¹, Ata Mahjoubfar¹, Claire L. Chen¹; ¹Univ. of California Los Angeles, USA. We describe a microscope featuring artificial intelligence (AI), time stretch, quantitative phase imaging and optofluidics. Capturing images at 50 GigaPixels per seconds, the system has shown record performance in classification of cancer in blood.

STh3L.2 • 14:30

Speckle-based wavelength measurement at femtometer resolution using a multimode fibre, Mingzhou Chen¹, Graham D. Bruce¹, Kishan Dholakia¹; ¹School of Physics and Astronomy, Univ. of St Andrews, UK. We demonstrate an approach to accurately measure the wavelength of light at femtometer resolution using the speckle output from a multimode fibre. Our approach can be used to measure a single wavelength, or distinguish between two wavelengths co-propagating through the fibre.

STh3L.3 • 14:45

Dual-Comb Microscopy for Scanless Confocal Phase Imaging, Eiji Hase^{1,2}, Shuji Miyamoto^{1,2}, Takahiko Mizuno^{1,2}, Takeo Minamikawa^{1,2}, Hirotsugu Yamamoto^{3,2}, Takeshi Yasui^{1,2}; ¹Tokushima Univ., Japan; ²JST, ERATO MINOSHIMA Intelligent Optical Synthesizer, Japan; ³Utsunomiya Univ., Japan. Two-dimensional image pixels of a sample are encoded onto optical frequency comb modes via spectral encoding, and the resulting mode-resolved amplitude and phase spectra are used to decode full-field confocal and phase images without scanning.

STh3L.4 • 15:00

Subwavelength Optical Focusing in Scattering Media with Optically Detectable Magnetic Resonance, Donggyu Kim^{1,2}, Dirk Englund^{3,2}; ¹Dept. of Mechanical Engineering, MIT, USA; ²Research Lab of Electronics (RLE), MIT, USA; ³Dept. of Electrical Engineering and Computer Science, MIT, USA. We introduce a new wavefront shaping technique guided by optically detectable magnetic resonance (ODMR). We present subwavelength light focusing in scattering media with our ODMR-guided wavefront shaping, which paves the way for subwavelength quantum sensing in deep-tissue.

CLEO: QELS-Fundamental
Science

14:00–16:00

FTh3M • Chirality Vortices and Topological
Effects

Presider: Amr Shaltout; Purdue Univ., USA

FTh3M.1 • 14:00

Disorder Topological Defects Induce Photonic Phase Transition, Bo Wang¹, Elhanan Maguid¹, Michael Yannai¹, Arkady Faerman¹, Vladimir Kleiner¹, Erez Hasman¹; ¹*Technion-Israel Inst. of Technology, Israel*. We report on the observation of photonic phase transition emerging from disorder topological defects in geometric phase metasurfaces. Low defect concentration induces isolated vortices, whereas high disorder leads to a random vortex interaction.

FTh3M.2 • 14:15

Topological photonic crystals in the visible: design and angle-resolved characterization of the bulk and edge states, Siying Peng¹, Nick Schilder², Xiang Ni³, Sophie Meuret², Hugo Doleman², Toon Coenen^{2,4}, Femius Koenderink², Alexander Khanikaev³, Andrea Alù⁵, Harry Atwater¹, Albert Polman²; ¹*Applied physics, California Inst. of Technology, USA*; ²*Center for Nanophotonics, AMOLF, Netherlands*; ³*Dept. of Electrical Engineering, City Univ. of New York, USA*; ⁴*Delmic B.V., Netherlands*; ⁵*Dept. of Electrical and Computer Engineering, Univ. of Texas at Austin, USA*. We fabricated and characterized photonic crystals with topological bulk states and pseudo-time-reversal-symmetry protected helical edge states in the visible regime. With a 30kV electron beam, we excite cathodoluminescence in the nanostructured material and derive photonic band structures.

FTh3M.3 • 14:30

Metasurfaces and Ultrafast Dynamics for High Angular Momentum Compound Optical Fileds, Grisha Spektor¹, Deirdre Kilbane², Anna-Katharina Mahro³, Michael Hartelt³, Eva Prinz³, Martin Aeschlimann³, Meir Orenstein¹; ¹*Technion Israel Inst. of Technology, Israel*; ²*School of Physics, Univ. College Dublin, Ireland*; ³*Dept. of Physics, Univ. of Kaiserslautern, Germany*. Employing unique metasurface-based plasmonic generators and an ultrafast probing technique, we experimentally demonstrate plasmonic vortex compounds carrying arbitrary orbital angular momentum. These can be used for functional near-field shaping and sculpting of optical potentials.

FTh3M.4 • 15:00

Controlling the topology of plasmonic vortex lattices, Shai Tseses¹, Kobi Cohen¹, Evgeny Ostrovsky¹, Bergin Gjonaj^{1,2}, Guy Bartal¹; ¹*Technion-Israeli Inst. of technology, Israel*; ²*Medical Sciences, Albanian Univ., Albania*. We experimentally demonstrate creation of two-dimensional plasmonic vortex lattices, while controlling the lattice topology. These lattices could drive many nanophotonic applications and bear an uncanny similarity to recently observed magnetic skyrmion lattices.

CLEO: Science & Innovations

14:00–16:00

STh3N • Ultrafast Metrology I

Presider: Gunter Steinmeyer; Max Born Inst., Germany

STh3N.1 • 14:00

Spatio-temporal characterization of few-cycle laser pulses by SEA-F-SPIDER and time-domain ptychography, Tobias Witting¹, Federico J. Furch¹, Marc J. Vrakking¹; ¹*Max-Born-Inst., Germany*. We review the self-referenced spatio-temporal characterization of few-cycle laser pulses. In particular we show results obtained from high average power NOPA based laser systems using the single-shot SEA-F-SPIDER technique and spatially multiplexed time-domain ptychography.

STh3N.2 • 14:15

Spatio-temporal Characterization and Optimization of a 200-kHz OPCPA Laser System, Sara Mikaelsson¹, Miguel Miranda¹, Anne Harth^{1,2}, Chen Guo¹, Thomas Binhammer³, Yu-Chen Cheng¹, Arthur Losquin¹, Christoph Heyl^{1,4}, Alexander Pape³, Jan Ahrens³, Oliver Prochnow³, Uwe Morgner³, Anne L'Huillier¹, Cord Arnold¹; ¹*Dept. of Physics, Lund Univ., Sweden*; ²*Max-Planck-Institut für Kernphysik, Germany*; ³*Laser Quantum, Germany*; ⁴*JILA, USA*; ⁵*Institut of Quantum Optics, Germany*. We present measurements on a few cycle OPCPA laser chain where due to careful characterization and compensation of the spectral phase and spatio-temporal couplings, we are able achieve efficient HHG with very low pulse energy.

STh3N.3 • 14:30

Characterization of Spatiotemporal Coupling with a Hyper-spectral Hartmann Wavefront Sensor, Christophe Dorrier¹, Seung-Whan Bahk¹; ¹*Univ. of Rochester, USA*. A broadband optical source is directly characterized using a Hartmann wavefront sensor implemented with a custom hyperspectral camera, yielding the accurate experimental characterization of radial group delay and pulse-front tilt.

STh3N.4 • 14:45

Spectrally-Resolved, Single-Shot Wavefront Sensing of Broadband High-Harmonic Sources, Matthijs Jansen^{2,1}, Lars Freisem^{2,1}, Denis Rudolf^{2,1}, Kjeld S. Eikema^{1,2}, Stefan Witte^{2,1}; ¹*Physics and Astronomy, Vrije Universiteit Amsterdam, Netherlands*; ²*Advanced Research Center for Nanolithography, Netherlands*. A novel grating-based Hartmann-type wavefront sensor is developed and used to measure wavefronts of nine high-harmonics at 25–49 nm wavelength simultaneously. Pulse front tilts of the high-harmonic beam are measured in a single exposure.

STh3N.5 • 15:00 **Invited**

Temporal Imaging in Three Dimensions, Moti Fridman¹; ¹*Bar-Ilan Univ., Israel*. We adopted the concept of three-dimensional (3D) imaging into the time domain, providing a new dimension in temporal optics. We demonstrated depth imaging in time and developed the concept of non-flat signals.

CLEO: Applications
& Technology

14:00–16:00

ATH3O • Novel Spectroscopic Approaches I

Presider: Brian Simonds; NIST, USA

ATH3O.1 • 14:00

Longwave Infrared Lidar Based on Parametric Sources for Standoff Detection of Gaseous Chemicals, Julie Ar-mougom¹, Jean-Michel Melkonian¹, Myriam Raybaut¹, Jean-Baptiste Dherbecourt¹, Guillaume Gorju¹, Antoine Godard¹, Riaan Stuart Coetzee², Valdas Pasiskevicius², Jiri Kadlčák³; ¹*ONERA - The French Aerospace Lab, France*; ²*Dept. of Applied Physics, Royal Inst. of Technology, Sweden*; ³*CBRN Protection Division, Military Research Inst., Czechia*. We report on a longwave infrared lidar, tailored for detection of chemical warfare agents in the gaseous phase. The emitter is based on single-frequency 2 μm parametric oscillator/amplifier systems followed by a ZnGeP2 downconversion stage.

ATH3O.2 • 14:15

Towards Broadband Multi-species Trace Gas Detection Using a Mid-infrared Supercontinuum Source, Qing Pan¹, Khalil E. Jahromi¹, Ali Abbas¹, Amir Khodabakhsh¹, Simona M. Cristescu¹, Frans J. M. Harren¹; ¹*Radboud Univ., Netherlands*. We present mid-infrared trace gas sensing based on a supercontinuum source combined with direct absorption spectroscopy and sum-frequency upconversion, showing broadband detection with a 10⁴ Hz^{-1/2} noise equivalent absorbance sensitivity.

ATH3O.3 • 14:30

Infrared metrology using visible photons, Anna Paterova^{1,2}, Hongzhi Yang¹, Chengwu An¹, Dmitry Kalashnikov¹, Leonid Krivitskiy¹; ¹*Data Storage Inst., Singapore*; ²*School of EEE, Nanyang Technological Univ., Singapore*. We exploit the nonlinear interference of correlated photons to demonstrate a new infrared metrology technique using detection of visible photons. The technique applies to infrared spectroscopy, optical coherence tomography, and imaging.

ATH3O.4 • 14:45

Self-heterodyne and dual-comb spectroscopy using acousto-optic frequency combs, Vicente Duran¹, Leo Djevarhidjian¹, Come Schnebelin¹, Kanagaraj Nithyanandan¹, Samir Kassi¹, Guillaume Mejean¹, Daniele Romanini¹, Hugues Guillet de Chatellus¹; ¹*LIPhy, France*. We demonstrate that repetitive frequency shifts of a CW laser in an acousto-optic modulator generate frequency combs with > 1000 mutually coherent lines. We report self-heterodyne interferometry with 500-kHz resolution, and precise dual-comb molecular spectroscopy.

ATH3O.5 • 15:00

An FPGA Based Algorithm to Study and Characterize Gas Mixtures: CH₄/CO₂ Case Study, Fatemeh Yazdandoust¹, Herve Tatenguem Fankem¹, Tobias Milde¹, Alvaro Jimenez¹, Joachim Sacher¹; ¹*Sacher Lasertechnik GmbH, Germany*. This study reports on the development and validation of a real-time algorithm, for measuring the peak area of molecular transitions. The proposed algorithm is then successfully used to characterize a gas mixture of CH₄/CO₂ in different proportions.

CLEO: Applications
& Technology

14:00–16:00

**ATH3P • Sensing in Extreme Environments
& Organic Optical Materials***Presider: David Bomse; Mesa Photonics, LLC, USA*

ATH3P.1 • 14:00

HO₂ Detection in a Photolysis Reactor Using Faraday Rotation Spectroscopy, Chu Teng¹, Chao Yan¹, Aric Rousso¹, Timothy Chen¹, Yiguang Ju¹, Gerard Wysocki¹; ¹Princeton Univ., USA. We perform Faraday rotation spectroscopy at 7.2 μm to quantify HO₂ formation from the reaction between excited singlet O(¹D) atoms and C₂H₂. A digitally balanced detection scheme is employed to suppress spectral interferences from diamagnetic C₂H₂.

ATH3P.2 • 14:15

Criegee Intermediates Dynamic Analysis based on Dual Optical Frequency Combs Spectrometer, Haoyuan Lu¹, Dawei Li², Jy Zhao¹, Peng Zuo³; ¹School of Electronics Engineering and Computer Science, Peking Univ., China; ²Biomedical engineering Dept., Johns Hopkins Univ., USA; ³College of environment sciences and engineering, Peking Univ., China. We propose a Fourier transform spectrometer based on dual optical frequency comb structure. The spectrum resolution can reach 0.001 nm with 71.5 microseconds time resolution. It can be used for precisely analyzing the spectrum dynamic process of Criegee intermediates.

ATH3P.3 • 14:30 **Invited**

Single-particle fluorescence detection of biological particles in the atmosphere, Anne Perring^{1,2}; ¹Chemical Sciences Division, NOAA Earth System Research Lab, USA; ²Cooperative Inst. for Research in Environmental Sciences, Univ. of Colorado, Boulder, USA. Single-particle fluorescence sensors, such as the Wide-Band Integrated Bioaerosol Sensor (WIBS), allow real-time detection of atmospheric primary biological particles. In this talk I discuss instrumental and methodological developments and present key findings from ambient studies.

ATH3P.4 • 15:00

Ultrafast Laser Enhanced Rayleigh Backscattering on Silica Fiber for Distributed Sensing under Harsh Environment, Mohan Wang¹, Mohamed Zaghoul¹, Sheng Huang¹, Aidong Yan¹, Shuo Li¹, Ran Zou¹, Paul Ohodnicki², Michael Buric², Ming-Jun Li³, David Carpenter⁴, Joshua Daw⁵, Kevin P. Chen¹; ¹Univ. of Pittsburgh, USA; ²National Energy Technology Lab, USA; ³Corning Research and Development Corporation, USA; ⁴MIT Nuclear Reactor Lab, USA; ⁵Idaho National Lab, USA. This paper reports an ultrafast laser processing method to improve the high temperature stability, radiation resilience, and measurement sensitivity in silica optical fiber distributed temperature sensing with optical frequency domain reflectometry (OFDR).

14:00–16:00

**ATH3Q • A&T Topical Review on
Neurophotonics II***Presider: TBD*

ATH3Q.1 • 14:00

An Active Visible Nanophotonics Platform for Sub-Millisecond Deep Brain Neural Stimulation, Aseema Mohanty^{1,2}, Qian Li³, Mohammad Amin Tadayon¹, Gaurang R. Bhatt¹, Euijae Shim¹, Xingchen Ji^{1,2}, Jaime Cardenas^{4,1}, Steven A. Miller¹, Adam Kepecs³, Michal Lipson¹; ¹Columbia Univ., USA; ²Cornell Univ., USA; ³Cold Spring Harbor Lab, USA; ⁴Univ. of Rochester, USA. We demonstrate the first visible-range nanophotonic switch network and create an implantable probe for in-vivo deep-brain stimulation. The probe enables stimulation patterns of single neurons with the timing and spatial precision to decode animal behavior.

ATH3Q.2 • 14:30

Energy-Efficient and High-Throughput Nanophotonic Neuromorphic Computing, Mohammadamin Nazirzadeh¹, Mohammadsadegh Shamsabardeh¹, S. J. Ben . Yoo¹; ¹Univ. of California Davis, USA. High-efficient bio-inspired nanophotonic neuromorphic computing is discussed. Using reconfigurable photonic interconnects combined by optical 2D and 3D integrated circuits, more than 500× improvement in energy consumption is predicted compared to the state-of-the-art implementations of SNNs.

ATH3Q.3 • 14:45

Liquid-level Sensor Using Optical Microfiber Probe, Junjie Wang¹, Yanpeng Li¹, Lingduo Li¹, Wei Zhang¹, Zhijun Yan¹, Qizhen Sun¹, Deming Liu¹; ¹School of Optical and Electronic Information, National Engineering Lab for Next Generation Internet Access System, Huazhong Univ. of Science and Technology, China. A liquid-level sensor using reflective optical microfiber probe as the sensing element is proposed and experimentally demonstrated. By monitoring the reflection wavelength shift, an ultra-high liquid-level sensitivity of ~153.5 nm/mm is achieved.

ATH3Q.4 • 15:00

Third Harmonic Generation Microscopy for Label-free Human Brain Imaging, Sandeep Chakraborty¹, Hao-Cheng Gao¹, Chen-Tung Yen¹, Hsin-Yi Huang², Chi-Kuang Sun¹; ¹National Taiwan Univ., Taiwan; ²Pathology, National Taiwan Univ. Hospital, Taiwan. Third harmonic generation microscopy (THG) was used for high-resolution label-free human brain imaging. The THG images of human brain tissues show neuronal soma, dendrites, and lipofuscin in gray matter while myelinated axons in white matter.

CLEO: Science & Innovations

Joint

STh3A • Photonic Crystals—Continued

STh3A.5 • 15:15

Slow Light Dispersion Engineering of Active Photonic Crystal Cavities for Compact and Integrated Mode-Locked Lasers, Malik Kemiche¹, Jérémy Lhuillier¹, Thomas Wood¹, Aziz Benamrouche¹, Philippe Regreny¹, Radoslaw Mazurczyk¹, Pedro Rojo-Romeo¹, Xavier Letartre¹, Ségolène Callard¹, Christelle Monat¹; ¹INL - CNRS UMR5270 - Ecole Centrale de Lyon, France. We realize compact active photonic crystal cavities for miniaturized chip-based pulsed lasers. We experimentally validate our approach relying on slow-light dispersion engineering for sustaining the intended regular comb of modes from a 30 μ m long cavity.

STh3A.6 • 15:30

Transmission Experiments on Photonic-Crystal Waveguides With a Symmetry-Protected Dirac Point, Chirag M. Patil¹, Xiaoyan Zhou¹, Morten Herskind¹, Kasper E. Lund^{1,2}, Søren Stobbe^{1,2}; ¹Niels Bohr Inst., Denmark; ²DTU Fotonik, Denmark. Slow-light photonic-crystal waveguides suffer from Anderson localization and propagation losses due to fabrication imperfections. Here we investigate a novel photonic system exhibiting a symmetry-protected two-dimensional Dirac-point feature and observe a >50-fold group-velocity slowdown.

STh3A.7 • 15:45

Complete photonic bandgaps in supercell photonic crystals, Alexander Cerjan¹, Shanhui Fan¹; ¹Stanford Univ., USA. We develop a class of supercell photonic crystals supporting complete photonic bandgaps based on breaking spatial symmetries. One member of this class supports a complete bandgap for $n_{\text{high}}/n_{\text{low}}=2.1$ the lowest known index-contrast ratio in 2D.

STh3B • Networks on a Chip—Continued

STh3B.5 • 15:15

Inter Symbol Interference Correction Based on Zero-forcing Equalization for Time Interleaved Photonic Analog to Digital Converter, Zhengtao Jin¹, Guiling Wu¹, Cheng Wang¹, Jianping Chen¹; ¹Shanghai Jiao Tong Univ., China. A zero-forcing equalization based inter symbol interference correction method is proposed to overcome the limitation to single-channel sampling rate for the finite backend electric bandwidth in TIPADCs. The correction method is verified experimentally.

STh3B.6 • 15:30

Crosstalk-aware Calibration for Fast and Automated Functionalization of Photonic Integrated Switch Fabrics, Yishen Huang¹, Qixiang Cheng¹, Keren Bergman¹; ¹Columbia Univ., USA. Intelligent calibration technique coordinating thermo- and electro-optic phase shifters for simultaneous phase-error and power-imbalance corrections is first introduced, capable of determining driving conditions for optimized crosstalk across entire photonic switch without built-in power monitors.

STh3B.7 • 15:45

All-optical Ternary Content Addressable Memory (T-CAM) Cell for ultra-fast Address Look-ups in Router Applications, George Mourgiyas-Alexandris¹, Christos Vagionas¹, Apostolos Tsakyridis¹, Pavlos Maniotis¹, Nikos Pleros¹; ¹Dep. of Informatics, Aristotle Univ. of Thessaloniki, Greece. We experimentally demonstrate the first all-optical Ternary Content Addressable Memory (T-CAM) cell based on two monolithic integrated InP Flip-Flops and a SOA-MZI XOR-gate, achieving 10Gb/s error-free operation during Content-Addressing and Write functionalities.

JTh3C • Symposium on Integrated Sources of Non-Classical Light: Perspectives and Challenges I—Continued

JTh3C.5 • 15:30

Diamond Color Center Integration with a Silicon Carbide Photonics Platform, Marina Radulaski¹, Yan-Kai Tzeng¹, Jingyuan Linda Zhang¹, Hitoshi Ishiwata¹, Konstantinos Lagoudakis¹, Constantin Dory¹, Kevin Fischer¹, Yousif Kelaita¹, Shuo Sun¹, Peter Maurer¹, Kassem Alasaad², Gabriel Ferro², Zhu-Xun Shen¹, Nicholas Melosh¹, Steven Chu¹, Jelena Vuckovic¹; ¹Stanford Univ., USA; ²Univ. of Lyon, France. We develop hybrid microresonators composed of the color center-rich nanodiamonds and silicon carbide microdisks fabricated on a silicon wafer. We demonstrate up to five-fold resonant enhancement of diamond silicon-vacancy and chromium-related color center emission.

JTh3C.6 • 15:45

Covalent Defects of Carbon Nanotubes: Room Temperature, 1.5 μ m Single Photon Emitters for Integrated Photonics, Han Htoon¹; ¹Center for Integrated Nanotechnologies, Los Alamos National Lab, USA. We demonstrate room-T single photon emission at 1.55 μ m telecommunication wavelength with 99% single-photon purity and the shot-noise limited emission stability from covalently-introduced aryl sp³ defect sites of single-wall carbon nanotubes.

16:00–16:30 Coffee Break, Concourse Lobby

Executive Ballroom
210D

Joint

JTh3D • Symposium on Advances in
Integrated Microwave Photonics I—
Continued

JTh3D.4 • 15:15

Automated Initialization of Reconfigurable Silicon-Nitride (SiN) Filters, Siva Yegnanarayanan¹, Ryan Maxson¹, Cheryl Sorace-Agaskar¹, Dave Kharas¹, Gregory Steinbrecher¹, Paul W. Juodawlkis¹; ¹Massachusetts Inst of Tech Lincoln Lab, USA. We demonstrate automated initialization of tunable optical filters consisting of an initial feed-forward step followed by iterative feedback. Rapid convergence is demonstrated on high-order all-pass-filter (APF) structures in a silicon-nitride photonic integrated circuit (PIC).

JTh3D.5 • 15:30 **Invited**

Integrated Microwave Photonic Component Technologies, Jonathan Klamkin¹, Yuan Liu¹, Bowen Song¹, Fengqiao Sang¹, Brandon Isaac¹; ¹Univ. of California Santa Barbara, USA. Key integrated microwave photonic component technologies are presented including low-loss waveguide true time delays for optical signal processing functions and high-performance hybrid integrated active devices.

Executive Ballroom
210E

CLEO: QELS-Fundamental
Science

FTh3E • Non-diffracting and Vortex
Beams—Continued

FTh3E.6 • 15:15

Landau-Zener-Bloch oscillations and valley-dependent vortex generation in photonic graphene, Yong Sun^{1,2}, Daniel Leykam^{3,4}, Stephen Nenni¹, Daohong Song⁵, Hong Chen², Y. D. Chong^{4,6}, Zhigang Chen^{1,5}; ¹Dept. of Physics and Astronomy, San Francisco State Univ., USA; ²MOE Key Lab of Advanced Micro-Structured Materials, School of Physics Science and Engineering, Tongji Univ., China; ³Center for Theoretical Physics of Complex Systems, Inst. for Basic Science, South Korea; ⁴Division of Physics and Applied Physics, School of Physical and Mathematical Sciences, Nanyang Technological Univ., Singapore; ⁵MOE Key Lab of Weak-Light Nonlinear Photonics, TEDA Applied Physics Inst. and School of Physics, Nankai Univ., China; ⁶Centre for Disruptive Photonic Technologies, Nanyang Technological Univ., Singapore. We observe Bloch oscillations and Landau-Zener-tunneling at Dirac points in photonic graphene. The non-adiabatic wave dynamics depend anisotropically on the direction of an applied index gradient, resulting in imperfect Landau-Zener-tunneling and valley-dependent vortex generation.

FTh3E.7 • 15:30

Launching Electromagnetic Donuts: Non-transverse electromagnetic pulses, Apostolos Zdagkas¹, Parik Moitra¹, Oleksander Buchnev¹, Nikitas Papasimakis¹, Nikolai I. Zheludev^{1,2}; ¹Univ. of Southampton, UK; ²Nanyang Technological Univ., Singapore. We demonstrate experimentally for the first time the generation of electromagnetic “Flying Donuts”, few-cycle pulses of toroidal topology with non-separable spatial and temporal structure, and discuss applications in the study of anapole excitations in matter.

FTh3E.8 • 15:45

Generation of Vector Vortex Beam From Doubly-Resonant Nanosecond Optical Parametric Oscillator., Varun Sharma³, S. C. Kumar¹, A Aadhi³, H. Ye¹, G. K. Samanta³, M. Ebrahim-Zadeh^{1,2}; ¹ICFO-Institut de Ciències Fotoniques, Spain; ²Institucio Catalana de Recerca i Estudis Avancats (ICREA), Spain; ³Photonic Sciences Lab, Physical Research Lab, India. We demonstrate a novel experimental scheme to generate tunable vector vortex beam directly from an optical parametric oscillator (OPO). Using a nanosecond doubly-resonant OPO, we produce vector vortex beam tunable across 964-990 nm.

Executive Ballroom
210F

CLEO: Science & Innovations

STh3F • Mid-IR Nonlinear Devices—
Continued

STh3F.5 • 15:15

Generation of coherent mid-IR light by parametric four-wave mixing in alkali vapor, Yoel Sebbag¹, Yefim Barash¹, Uriel Levy¹; ¹Applied Physics, The Hebrew Univ. of Jerusalem, Israel, Israel. We demonstrate the generation of coherent mid-infrared light at 5.23 μm in hot rubidium vapor by parametric four wave mixing. Different regimes of competition between amplified spontaneous emission and four wave mixing are observed.

STh3F.6 • 15:30

Generation of high power, higher order, continuous-wave optical vortices tunable in the mid-IR wavelength ranges, A. Aadhi¹, Varun Sharma¹, G. K. Samanta¹; ¹Physical Research Lab, India. We report on direct transfer of vortices at near-IR to the mid-IR wavelengths using a dual-crystal singly-resonant optical parametric oscillator producing vortices of order up to $l=6$ and power of 6 W across 2270-3560 nm.

16:00–16:30 Coffee Break, Concourse Lobby

CLEO: Science & Innovations

Sth3G • Quantum Information Processing
on Photonic Nanostructures—Continued

Sth3G.3 • 15:15

Single-Photon Detection by Cavity-Assisted All-Optical Gain, Christopher L. Panuski¹, Mihir Pant¹, Mikkel Heuck², Dirk . Englund¹; ¹Dept. of Electrical Engineering and Computer Science, MIT, USA; ²Dept. of Photonics Engineering, Technical Univ. of Denmark, Denmark. Considering the free-carrier dispersion effect at the limit of a single photoexcited charge carrier pair suggests the possibility of realizing single-photon detection through a high-Q/V semiconductor cavity.

Sth3G.4 • 15:30

Switching radiative processes via mode field modulation, Daniele Pellegrino¹, Francesco Pagliano^{1,2}, Armando Genco¹, Maurangelo Petruzzella^{1,2}, Frank van Otten¹, Andrea Fiore¹; ¹Eindhoven Univ. of Technology, Netherlands; ²nanoPHAB, Netherlands. We experimentally demonstrate the control over the emission of quantum dots embedded in photonic molecules via mode field modulation. By locally changing the cavity frequencies we control, and even suppress, spontaneous emission.

Sth3G.5 • 15:45

Chiral quantum optics in hot vapor cladded waveguide, Roy T. Zekter¹, Eliran Talker¹, Yefim Barash¹, Noa Mazurski¹, Uriel Levy¹; ¹The Hebrew Univ. of Jerusalem, Israel. We demonstrate a strong magneto optic effect in chip scale integrated atomic cladded waveguides. Chiral effects and non-reciprocity of the integrated waveguide-atomic vapor system is observed. Possible applications such as isolators are discussed

CLEO: Applications
& TechnologyAth3H • Control of Quantum Optical and
Opto-mechanical Systems—Continued

Ath3H.6 • 15:15

Elastic Strain Engineering for Exceptional Mechanical Coherence, Nils Johan Engelsen¹, Amir Ghadimi¹, Sergey A. Fedorov¹, Mohammad J. Beryhi¹, Ryan Schilling¹, Dalziel Wilson^{2,1}, Tobias J. Kippenberg¹; ¹Physics, École polytechnique fédérale de Lausanne, Switzerland; ²IBM Research, Switzerland. We utilized strain engineering combined with soft-clamping to realize exceptionally high Q Si₃N₄ nanomechanical oscillators. The quality factors (>400 million) and Qxf products (approaching 10¹⁵ Hz) are both unprecedented for any room temperature mechanical oscillator.

Ath3H.7 • 15:30

Frequency Conversion of a Quantum Dot Single-Photon Source on a Nanophotonic Chip, Anshuman Singh^{1,2}, Qing Li^{1,2}, Jin Liu³, Xiyuan Lu^{1,2}, Christian Schneider⁴, Sven Höfling⁴, Kartik Srinivasan¹; ¹NIST-CNST, USA; ²Maryland NanoCenter, Univ. of Maryland College Park, USA; ³School of Physics, Sun-Yat Sen Univ., China; ⁴Technische Physik, Universität Würzburg, Germany. We report frequency conversion of single photons from a quantum dot using four-wave-mixing Bragg scattering in a Si₃N₄ microring. We measure an on-chip conversion efficiency >10%, and frequency-converted light that is antibunched with g⁽²⁾(0) <0.5.

Ath3H.8 • 15:45

Single-Photon-Level Interface for Linking Sr⁺ Transition at 422nm with The Telecommunications C-band, Thomas A. Wright¹, Robert J. Francis-Jones¹, Corin Gawith³, Jonas N. Becker², Patrick Ledingham², Ian Walmsley², Benjamin Brecht², Joshua Nunn¹, Peter J. Mosley¹; ¹Univ. of Bath, UK; ²Univ. of Oxford, UK; ³Univ. of Southampton, UK. We present a single-stage bi-directional interface capable of linking Sr⁺ trapped ion qubits emitting single photons at 422 nm with the telecoms C-band. We achieve external up(down) conversion efficiencies of 9.4%(1.1%).

CLEO: Science & Innovations

Sth3I • Integrated Photonic Platforms—
Continued

Sth3I.6 • 15:15

GaP-On-Insulator as a Platform for Integrated Photonics, Simon Hönl¹, Katharina Schneider¹, Pol Welter¹, Yannick Baumgartner¹, Herwig Hahn¹, Lukas Czornomaz¹, Dalziel Wilson¹, Paul Seidler¹; ¹IBM Research -- Zurich, Switzerland. We present a complete process flow for fabrication of integrated GaP-on-insulator photonic devices via direct wafer bonding of epitaxial films. High-fidelity patterning enables a range of applications, such as waveguide resonators and photonic crystal cavities.

Sth3I.7 • 15:30

A Widely Tunable Vernier Filter on a Ge-on-SOI Platform for Sensing Applications, Sanja Radosavljevic¹, Nuria Teiggell Beneitez¹, Andrew Katumba¹, Muhammad Muneeb¹, Michael Vanslebrouck¹, Bart Kuyken¹, Gunther Roelkens¹; ¹Universiteit Gent, Belgium. We present a Vernier tunable racetrack resonator filter on Ge-on-SOI, with 110nm FSR at 5µm. The racetrack has a Q-factor of 20000 and side-peak suppression >20dB, sufficient for wavelength selection in an external cavity laser.

Sth3I.8 • 15:45

Silicon nitride metalenses for unpolarized high-NA visible imaging, Zhi-Bin Fan¹, Zeng-Kai Shao¹, Ming-Yuan Xie¹, Xiao-Ning Pang¹, Wen-Sheng Ruan¹, Fu-Li Zhao¹, Yu-Jie Chen¹, Si-Yuan Yu¹, Jianwen Dong¹; ¹Sun Yat-Sen Univ., China. We experimentally demonstrate the high-NA silicon nitride metalenses with centimeter aperture and micro size in visible region, fabricated by 695-nm-thick hexagonal silicon nitride arrays. The potential application of wide viewing-angle functionality has also been shown.

16:00–16:30 Coffee Break, Concourse Lobby

CLEO: Science & Innovations

STh3J • Optofluidics & High Throughput
Fluorescence—Continued

STh3J.4 • 15:15

A Novel Cell and Particle Sorting Approach Based on Fluorescence Dynamics, Jianzhi Li¹, Jessica P. Houston¹; ¹New Mexico State Univ., USA. Fluorescence activated cell sorting (FACS) is an approach that is based solely on detection of the amount of fluorescence emitted. We advance FACS with a unique phase mixing approach to enable separation based on fluorescence dynamics.

STh3J.5 • 15:30

Microfluidic Diatomite Analytical Devices for Ultra-Sensitive Detection of Hazardous Chemicals, Xianming Kong¹, Kenny Squire¹, Alan X. Wang¹; ¹Oregon State Univ., USA. We report microfluidic diatomite analytical devices (μ DADs), which consist of highly porous photonic crystal biosilica microchannels, as an innovative lab-on-a-chip platform to detect hazardous chemicals with the sensitivity down to ppb level.

STh3J.6 • 15:45

Optical Lattice-Based Cell Guiding and Stretching Using Integrated Vertical Multimode-Interference Waveguides, Zhanshi Yao¹, Andrew W. Poon¹; ¹Hong Kong Univ. of Sci. and Tech., Hong Kong. We report our recent progress in optical lattice-based cell guiding and stretching using integrated SU8-filled vertically embedded multimode-interference waveguides. We obtain a throughput of ~ 6 cells/s for the deformability characterization of rabbit red blood cells.

STh3K • Multimode Fiber Optics—
Continued

STh3K.3 • 15:15

Imaging Beyond a Multimode Fibre with Time of Flight Depth Information, Daan Stellinga¹, David Phillips², Matthew Edgar¹, Sergey Turtaev^{3,4}, Tomáš Čizmár^{3,4}, Miles Padgett¹; ¹Univ. of Glasgow, UK; ²Univ. of Exeter, UK; ³Univ. of Dundee, UK; ⁴Leibniz Inst. of Photonic Technology, Germany. Imaging through a multimode fibre can be achieved using a DMD. Using a Q-switched laser we extend this to include the time of flight as a first step towards 3D imaging through a fibre.

STh3K.4 • 15:30

Time-Domain Interference of Nonlinearly Interacting Spatial Modes in a Multimode Fiber, Sai Kanth Dacha¹, Thomas E. Murphy¹; ¹Univ. of Maryland at College Park, USA. The study of nonlinear optics in multimode fibers has gathered considerable interest recently. We report experimental observation of time-domain interference between nonlinearly interacting co-polarized spatial modes of a graded-index multimode fiber at 1550nm.

STh3K.5 • 15:45

Mode Scrambler Using CO₂-laser Inscribed Long-period Gratings, Yunhe Zhao¹, Haoshuo Chen², Nicolas K. Fontaine², Jiaxiong Li², Roland Ryf², Yunqi . Liu¹; ¹Shanghai Univ., China; ²Bell labs, Nokia, USA. We demonstrate a mode scrambler using CO₂-laser inscribed long-period gratings for mixing 3 spatial modes. The mode-dependent loss and modal transfer matrices versus wavelength are characterized using a swept-wavelength interferometer.

STh3L • Imaging and Ranging—Continued

STh3L.5 • 15:15

Controlled Transmission Through Highly Scattering Media Using Semi-Definite Programming as a Phase Retrieval Computation Method, Moussa N'Gom¹; ¹Univ. of Michigan, USA. An SLM in a simple optical setup is used to generate a random wavefronts. The transmitted speckle patterns are acquired on a camera. The semi-definite algorithm allows computation of the complex transmission matrix of the system. Arbitrary intensity profiles can then be generated.

STh3L.6 • 15:30

One-shot three-dimensional imaging with a paired filter and chirped-frequency combs, Takashi Kato^{1,2}, Megumi Uchida^{1,2}, Yurina Tanaka^{1,2}, Kaoru Minoshima^{1,2}; ¹The Univ. of Electro-Communications, Japan; ²JST, ERATO MINOSHIMA Intelligent Optical Synthesizer (IOS), Japan. One-shot three-dimensional imaging with chirped-frequency comb interferometry was demonstrated using 2D spectral imaging technique with a paired spectral filter. Non-scanning image measurement of a target 3D surface profile with 120-pixels square area was demonstrated.

STh3L.7 • 15:45

Overcoming the Coherence Distance Barrier in Long-Range FMCW LIDAR, Taehwan Kim¹, Pavan Bhargava¹, Vladimir Stojanovic¹; ¹UC Berkeley, USA. Coherence distance has been considered as a hard limit for FMCW LIDAR range. We show laser characterization and a detection algorithm tailored to laser properties can significantly improve the accuracy, extending the range beyond coherence distance.

16:00–16:30 Coffee Break, Concourse Lobby

CLEO: QELS-Fundamental
ScienceFTh3M • Chirality Vortices and Topological
Effects—Continued

FTh3M.5 • 15:15

Giant intrinsic chiro-optical activity in planar nanostructures, Alexander Y. Zhu¹, Wei-Ting Chen¹, Aun Zaidi¹, Yao-Wei Huang¹, Mohammadreza Khorasaninejad¹, Vyshakh Sanjeev², Cheng-Wei Qiu², Federico Capasso¹; ¹Harvard Univ., USA; ²National Univ. of Singapore, Singapore; ³Univ. of Waterloo, Singapore. We demonstrate near-unity circular dichroism in planar dielectric nanostructures, with approximately 90% of the incident light of the chosen helicity being transmitted at normal incidence at 540nm. Such strong intrinsic chiral behavior exists due to the excitation of giant higher-order multipoles.

FTh3M.6 • 15:30

Microscopic Origin of the Chiroptical Response of Plasmonic Media, Matthew Davis^{1,2}, Jay Lee¹, Henri Lezec², Amit K. Agrawal^{2,3}; ¹Syracuse Univ., USA; ²Center for Nanoscale Science and Technology, USA; ³Maryland Nanocenter, USA. Plasmonic systems hold potential for amplifying chiroptical signals of molecular systems, however a comprehensive understanding of this effect does not exist. We discuss the common origin of chiroptical response in two-dimensional and three-dimensional plasmonic systems.

FTh3M.7 • 15:45

A chiral waveguide directional coupler using transition metal dichalcogenide monolayers, Zhili Yang¹, Edo Waks¹; ¹Univ. of Maryland, College Park, USA. We demonstrated an on-chip broadband input-polarization-dependent directional coupler with a directionality of 0.3 based on coupling between a glide-plane photonic crystal waveguide and WSe₂ monolayers.

CLEO: Science & Innovations

STh3N • Ultrafast Metrology I—Continued

STh3N.6 • 15:30

Spatio-temporally wideband ultrafast imaging, Cihang Kong¹, Xiaoming Wei^{1,2}, Kevin K. Tsia¹, Kenneth Kin-Yip Wong¹; ¹Univ. of Hong Kong, Hong Kong; ²Dept. of Medical Engineering, California Inst. of Technology, USA. We present a 10's-MHz imaging system through a simple spatio-temporally sweeping unit which is constructed with incremental optical fibers. It is demonstrated that this imaging modality can be performed over an ultrawide wavelength range, i.e., 500-2000 nm.

STh3N.7 • 15:45

Cascading Nonlinearity Inside a Spectrometer (CaNIS) for Ultrashort Pulse Diagnostics, Ning Hsu¹, Luke Horstman¹, Jean-Claude M. Diels¹; ¹Univ. of New Mexico, USA. An ultrashort pulse is characterized by using spectra only. Second harmonic and cascading spectra are manipulated with a grating spectrometers to determine the original pulse's spectral phase, and hence achieve complete field reconstruction.

CLEO: Applications
& TechnologyATh3O • Novel Spectroscopic Approaches
I—Continued

ATh3O.6 • 15:15

Wavelength calibration of high-performance spectrometers with a stabilized optical comb from an ultrafast semiconductor disk laser, Antoine Jallageas¹, Jacob Nuernberg², Cesare Alfieri², Dominik Waldburger², Sandro M. Link², Florian Emaury², Jacques Morel¹, Ursula Keller²; ¹Federal Institut of Metrology METAS, Switzerland; ²Inst. of Quantum Electronics, ETH Zurich, Switzerland. We demonstrate for the first time that a fully stabilized ultrafast semiconductor disk laser is a suitable tool to perform wavelength calibration of high-performance spectrometers, opening new possibilities for wider and more accurate instruments calibrations.

ATh3O.7 • 15:30

Noise Correlation Spectroscopy for spectroscopic measurements of low energy modes, Giorgia Sparapassi¹, Jonathan O. Tollerud¹, Filippo Glerean¹, Daniele Fausti^{1,2}; ¹Università degli Studi di Trieste, Italy; ²Elettra Sincrotrone Trieste S.C.p.A., Italy. Noise Correlation Spectroscopy (NCS) is a technique exploiting statistical correlations imprinted onto spectral components of shaped ultrashort light pulses by a light-matter inelastic scattering process, in order to measure low energy eigenmodes of a material.

CLEO: Applications
& TechnologyATH3P • Sensing in Extreme Environments
& Organic Optical Materials—Continued

ATH3P.5 • 15:15

Passive radiative cooling structure with vivid colors, Gil Ju Lee¹, Hyun Myung Kim¹, Yeong Jae Kim¹, Young Min Song¹; ¹GIST, South Korea. A colored passive radiative cooler can widen the applicability of passive cooling strategy. This photonic structure is based on 1D structure/thermal emitter polymer and can be easily fabricated by metal/dielectric deposition and polymer coating.

ATH3P.6 • 15:30

Observation of Coherent Perfect Absorption in Resonant Organic Materials, Ali Kazemi Jahromi¹, Lorelle N. Pye¹, Soroush Shabahang¹, Massimo Villinger¹, Joshua Perlstein¹, Ayman Abouraddy¹; ¹Univ. of Central Florida, CREOL, USA. By judiciously devising mirror reflectivities of a cavity containing an absorber, we experimentally demonstrate coherent perfect absorption in a resonant organic dye, even though the material's intrinsic absorption significantly varies across the dye absorption bandwidth.

ATH3P.7 • 15:45

Silk is a natural metamaterial for self-cooling: An oxymoron?, Seung Ho Choi¹, Zahyun Ku², Seong-Ryul Kim³, Kwang-Ho Choi³, Augustine Urbas², Young L. Kim¹; ¹Purdue Univ., USA; ²Air Force Research Lab, USA; ³National Inst. of Agricultural Sciences, South Korea. As light transmittance in silk is suppressed by Anderson localization, its reflectance is drastically enhanced. A further combination with the high emissivity from the biomolecules of silk in infrared radiation results in passive radiative cooling.

ATH3Q • A&T Topical Review on
Neurophotonics II—Continued

ATH3Q.5 • 15:30

Identification of Biomarker (L-2HG) in Real Human Brain Glioma by Terahertz Spectroscopy, Yan Peng¹, Wanqing Chen¹, Yiming Zhu¹; ¹Univ of Shanghai for Science & Tech, China. L-2-Hydroxyglutaric acid disodium salt (L-2HG), a unique biomarker in glioma, has been detected effectively in real human brain glioma by THz time-domain spectroscopy (THz-TDS), which is especially meaningful for the diagnose and treatments of glioma.

ATH3Q.6 • 15:45

Neurite Outgrowth and Retraction Caused by Combined Optical and Chemical Stimulations, Yu-Chiu Kao¹, Yu-Cing Liao^{1,2}, Chau-Hwang Lee^{1,2}; ¹Research Center for Applied Sciences, Academia Sinica, Taiwan; ²Inst. of Biophotonics, National Yang-Ming Univ., Taiwan. We demonstrated that a 473 nm light spot caused neurite retraction of a neuroblastoma cell; while a 650 nm light spot on soma plus a myosin II inhibitor stimulated the neurite re-growth effectively.

16:00–16:30 Coffee Break, Concourse Lobby

CLEO: Science & Innovations

Joint

16:30–18:30

STh4A • Waveguide Structures

President: Ali Adibi; Georgia Inst. of Technology, USA

STh4A.1 • 16:30

High-Density Photonic Chip with All-Dielectric Metamaterials, Sangsik Kim^{1,2}, Saman Jahani^{2,3}, Jonathan Atkinson³, Justin Wirth², Farid Kalhor^{2,3}, Abdullah Al Noman², Ward Newman^{2,3}, Prashant Shekhar³, Kyunghun Han², Vien Van³, Raymond G. Decorbey³, Lukas Chrostowski⁴, Minghao Qi², Zubin Jacob^{2,3}; ¹Electrical and Computer Engineering, Texas Tech Univ., USA; ²Electrical and Computer Engineering, Purdue Univ., USA; ³Electrical and Computer Engineering, Univ. of Alberta, Canada; ⁴Electrical and Computer Engineering, Univ. of British Columbia, Canada. We present an extreme skin-depth (e-skin) waveguide scheme, whose evanescent field is suppressed significantly. We demonstrate it on a monolithic silicon chip, reducing the waveguide crosstalk and bending loss for a high-density photonic chip integration.

STh4A.2 • 16:45

Fast adiabatic mode evolution based on geometry-induced suppression of nearest-mode crosstalk, Josep Fargas Cabanillas¹, Milos Popovic¹; ¹Dept. of Electrical and Computer Engineering, Boston Univ., USA. A new degree of freedom in the design of adiabatic mode-evolution structures allows dramatic length reduction while maintaining the characteristic large bandwidth and insensitivity, leading to a 10x shorter ultrabroadband, low-loss 2x2 3dB coupler design

STh4A.3 • 17:00

Curvature Control in a Segmented Beam Expander - Emergence of a Semi-lens, Siamak Abbaslou¹, Robert Gatdula¹, Ming Lu², Aaron Stein², Wei Jiang¹; ¹Rutgers Univ., USA; ²Brookhaven National Lab, USA. We introduce direct curvature control in optimizing a segmented beam expander that maintains width continuity. Unexpectedly, the optimization algorithm yields a structure with abrupt width discontinuity. Spatial phase analysis reveals the emergence of a semi-lens.

STh4A.4 • 17:15

Double-Inverse Tapers for Efficient Light Coupling with Arbitrary Polarization, Junqiu Liu¹, Arslan Raja¹, Martin Pfeiffer¹, Clemens Herkommer¹, Hairun Guo¹, Michael Zervas^{1,2}, Michael Geiselmann^{1,2}, Tobias J. Kippenberg¹; ¹EPFL, Switzerland; ²LIGENEC SA, Switzerland. Efficient light coupling to integrated photonic devices is vital. We present novel, double-inverse tapers, which can achieve optimum coupling with arbitrary polarization. Reduced lithography requirement makes the double-inverse tapers promising for operation at near-IR and visible wavelengths.

STh4A.5 • 17:30

On-Chip Polarization Control Using Augmented Low Index Guiding Platform, Xiao Sun¹, J. Stewart Aitchison¹, Mo Mojahedi¹; ¹Univ. of Toronto, Canada. The Augmented Low-index Guiding Waveguide can confine the two orthogonal polarization modes in different layers. We present our recent theoretical and experimental results on several polarization manipulation devices enabled by such a platform.

16:30–18:30

STh4B • On-chip and Offchip Coupling Schemes

President: Qiaoqiang Gan; State Univ. of New York at Buffalo, USA

STh4B.1 • 16:30

On-chip optical interconnect on silicon by transfer printing, Lei Liu¹, Ruggero Loi¹, Brendan Roycroft¹, James O'Callaghan¹, John Justice¹, Antonio Jose Trindade², Stephen Kelleher², Agnieszka Gocalinska¹, Kevin Thomas¹, Emanuele Pelucchi¹, Christopher A. Bower², Brian Corbett¹; ¹Tyndall National Inst., Ireland; ²X-Celeprint Limited, Ireland. On-chip optical interconnects consisting of transfer-printed micro-LEDs and photodiodes are presented. Static and dynamic data transmission and bi-directional interconnect are demonstrated. The results show the potential for cost-effective and small form-factor on-chip opto-isolators.

STh4B.2 • 16:45

Optical Equalization Using Spatial Phase Manipulation for VCSEL-MMF Based Links, Chenyu Liang¹, Wenjia Zhang¹, Shun Yao^{2,3}, Qing Wang^{2,3}, Zuyuan He¹; ¹Shanghai Jiaotong Univ., China; ²Inst. of Laser Engineering, Beijing Univ. of Technology, China; ³Sino-semiconductor Photonics Integrated Circuit Co., Ltd., China. We propose an optical equalization scheme for VCSEL and MMF based link by using spatial phase manipulation. Over 2-dB power penalty improvement is achieved by experiment for 25-Gb/s 300m transmission.

STh4B.3 • 17:00

Fabrication Constrained Inverse Design of a 3-channel Wavelength Demultiplexer, Alexander Y. Piggott¹, Logan Su¹, Neil V. Saprà¹, Jan Petykiewicz¹, Jelena Vuckovic¹; ¹Stanford Univ., USA. We have implemented an automated nanophotonic design algorithm with fabrication constraints. This was used to demonstrate a compact 3-channel wavelength demultiplexer with a channel spacing of 40nm, insertion loss <2.29dB, and under 10.7dB crosstalk.

STh4B.4 • 17:15

Ultra-broadband Compact Adiabatic Coupler in Silicon-on-Insulator for Joint Operation in the C- and O-Bands, Heba Tamazin¹, Eslam Elfiky¹, Yun Wang¹, Yannick D'Mello¹, David Patel¹, Amar Kumar¹, David V. Plant¹; ¹McGill Univ., Canada. An ultra-broadband, compact adiabatic coupler in silicon-on-insulator platform is presented. It has 70 μm coupling length and a splitting ratio of 3±0.8 dB over bandwidth > 160 nm measured jointly in the C- and O-bands.

STh4B.5 • 17:30

Direct coupling between 2D-PDA and triangular/square shape aligned MCF for universal SDM photoreceiver, Toshimasa Umezawa¹, Takahide Sakamoto¹, Atsushi Kanno¹, Naokatsu Yamamoto¹, Tetsuya Kawanishi^{1,2}; ¹National Inst of Information & Comm Tech, Japan; ²Waseda Univ., Japan. We successfully achieved the high coupling efficiencies and alignment tolerances between a newly developed 10-GHz 32-pixel two dimensional photodetector array (2D-PDA) and triangular- and square-shape-aligned multi-core fiber (MCF) for universal SDM photoreceivers.

16:30–18:30

JTh4C • Symposium on Integrated Sources of Non-Classical Light: Perspectives and Challenges II

President: Alireza Marandi, USA

JTh4C.1 • 16:30 **Invited**

Nonclassical Light Sources for Silicon Photonics, Matteo Galli¹; ¹Universita degli Studi di Pavia, Italy. Silicon photonics has rapidly become the platform of choice for on-chip integration of high performing photonic devices, now extending their functionalities to quantum-based applications. We review recent progress in this growing field and highlight the challenges that need to be overcome to make quantum photonics a reliable and widespread technology.

JTh4C.2 • 17:00 **Invited**

Scalable On-chip Generation and Coherent Control of Complex Optical Quantum States, Piotr Roztockii¹, Michael Kues^{1,3}, Christian Reimer¹, Luis Romero Cortés¹, Stefania Sciarra^{1,4}, Benjamin Wetzels^{1,5}, Young Zhang¹, Alfonso Cino⁴, Sai T. Chu⁶, Brent E. Little⁷, David J. Moss⁸, Lucia Caspani⁹, Jose . Azana¹, Roberto Morandotti^{1,2}; ¹INRS-Energie Mat & Tele Site Varennes, Canada; ²National Research Univ. of Information Technologies, Mechanics and Optics, Russia; ³Univ. of Glasgow, UK; ⁴Univ. of Palermo, Italy; ⁵Univ. of Sussex, UK; ⁶City Univ. of Hong Kong, China; ⁷Xi'an Inst. of Optics and Precision Mechanics, Chinese Academy of Science, China; ⁸Swinburne Univ. of Technology, Australia; ⁹Univ. of Strathclyde, UK. Integrated quantum frequency combs provide access to multi-photon and high-dimensional entangled states, and their control via standard telecommunications components, and can thus open paths for reaching the state complexities required for meaningful quantum information science.

JTh4C.3 • 17:30

Monolithic Source of Entangled Photons with Integrated Pump Rejection, Cale M. Gentry¹, Omar S. Magana Loaiza², Mark T. Wade¹, Fabio Pavanello¹, Thomas Gerrits², Sen Lin³, Jeffrey Shainline², Shellee Dyer², Sae Woo Nam², Richard Mirin², Milos Popovic^{4,1}; ¹Univ. of Colorado Boulder, USA; ²National Inst. of Standards and Technology, USA; ³Univ. of California Berkeley, USA; ⁴Boston Univ., USA. We demonstrate a photon pair source with pump rejection filter on a single CMOS chip. Cascaded microring-based filters exhibit >95 dB pump extinction, providing a raw visibility in time-energy entanglement of 81.4% ± 2.3%.

Executive Ballroom
210D

Joint

16:30–18:30

JTh4D • Symposium on Advances in Integrated Microwave Photonics II

President: Maurizio Burla; ETH Zurich, Switzerland and David Marpaung; University of Twente, Netherlands

JTh4D .1 • 16:30 **Invited**

Photonic Integrated Circuits for Microwave Signal Generation and Processing, Jianping Yao¹; ¹Univ. of Ottawa, Canada. Silicon photonic integrated circuits (PICs) for the implementation of microwave photonic systems to perform functions including microwave signal processing based on a reconfigurable grating, and microwave signal generation based on an optoelectronic oscillator are discussed.

JTh4D .2 • 17:00 **Invited**

Microcomb Engine for Microwave Photonics, Xiaoxiao Xue¹, Xiaoping Zheng¹, Andrew M. Weiner²; ¹Tsinghua Univ., China; ²Purdue Univ., USA. We review recent advances in microcomb generation for microwave photonic applications including microwave generation, programmable signal processing, and true-time-delay beamforming. The key challenges and future research opportunities are also discussed.

JTh4D .3 • 17:30

Injection Locking of Dissipative Kerr Solitons, Wenle Weng¹, Erwan Lucas¹, Hairun Guo¹, Grigory Lihachev^{2,3}, Valery Lobanov², Michael Gorodetsky^{2,3}, Tobias J. Kippenberg¹; ¹EPFL, Switzerland; ²Russian Quantum Center, Russia; ³Faculty of Physics, M.V. Lomonosov Moscow State Univ., Russia. We report a radio frequency injection locking technique with amplitude modulation of pump laser for suppressing fluctuations of the repetition rate of a microresonator-based dissipative Kerr soliton frequency comb.

Executive Ballroom
210E

CLEO: QELS-Fundamental
Science

16:30–18:30

FTh4E • Multimode Nonlinear Fiber Optics

President: Arash Mafi; Univ. of New Mexico, USA

FTh4E.1 • 16:30 **Invited**

Spatiotemporal Phenomena in Multimode Fibers, Frank W. Wise¹; ¹Cornell Univ., USA. New phenomena observed recently in multimode optical fibers will be reviewed, and their relevance to applications will be discussed.

FTh4E.2 • 17:00

Universal Entropic Response of Nonlinear Multimode Optical Systems, Fan Wu¹, Absar U. Hassan¹, Mohammad Amin Eftekhari¹, Demetrios N. Christodoulides¹; ¹Univ. of Central Florida, USA. We show that the mode occupancies in nonlinear multimode optical systems follow a universal behavior that tends to maximize the system's entropy at steady-state. This thermodynamic response occurs irrespective of the type of nonlinearities involved.

FTh4E.3 • 17:15

Intermodal Raman Scattering of Ultrashort Pulses in Multimode Fibers, Aku J. Antikainen¹, Boyin Tai², Lars Rishøj², Siddharth Ramachandran², Govind P. Agrawal^{1,2}; ¹Univ. of Rochester, USA; ²Boston Univ., USA. We study numerically the competition between intramodal and intermodal Raman scattering of ultrashort pulses in a multimode fiber. Considerable pulse energy can be transferred between different modes depending on the extent of group velocity matching.

FTh4E.4 • 17:30

Nonlinear Wave Collapse in Coupled Fiber Systems, Andre Luiz M. Muniz¹, Martin Wimmer¹, Arstan Bisianov¹, Demetrios N. Christodoulides², Roberto Morandotti³, Ulf Peschel¹; ¹Friedrich-Schiller-Universität Jena, Germany; ²Univ. of Central Florida, College of Optics and Photonics, USA; ³Energie, Matériaux et Télécommunications, Institut national de la recherche scientifique, Canada. We experimentally demonstrate nonlinear wave collapse at mW-power levels in a genuine 1D system formed by coupled optical fibers. Based on time-multiplexing we realize an effective two-dimensional lattice and observe strong nonlinearly driven field compression.

Executive Ballroom
210F

CLEO: Science & Innovations

16:30–18:30

STh4F • Optical Parametric Oscillators

President: Markku Vainio; Univ. of Helsinki, Finland

STh4F.1 • 16:30

HVPE of Orientation-Patterned Gallium Phosphide (OP-GaP) with Novel Quasi-Phase-matched Device Structures, Peter G. Schunemann¹, Daniel J. Magarrell¹, Leonard A. Pomeranz²; ¹BAE Systems Inc, USA. We report the successful growth and fabrication of engineered quasi-phase-matched grating structures - parallel gratings, tandem gratings, linear and curved fan gratings, and chirped gratings - in the new nonlinear optical semiconductor OP-GaP.

STh4F.2 • 16:45

Efficient Backward-Wave Optical Parametric Oscillator with 500 nm-periodicity PPRKTP, Riaan Stuart Coetzee¹, Andrius Zukauskas¹, Carlota Canalias¹, Valdas Pasiskevicius¹; ¹Royal Inst. of Technology (KTH), Sweden. Backward-wave OPO with forward mid-infrared idler and backward signal generation is demonstrated in 500- μ m-periodicity PPRKTP. The output energy of 2.39mJ and efficiency of 46.4% is obtained. This design has potential for broad tunability in mid-infrared.

STh4F.3 • 17:00 **Invited**

Optical Parametric Oscillation in Random Polycrystalline $\chi^{(2)}$ Medium, Konstantin L. Vodopyanov¹, Qitian Ru¹, Nathaniel Lee¹, Xuan Chen¹, Kai Zhong², Sergey Vasilyev³, Mike Mirov³, Sergey Mirov^{3,4}; ¹Univ. of Central Florida, CREOL, USA; ²College of Precision Instrum. and Optoe. Eng., Tianjin Univ., China; ³Mid-Infrared Lasers, IPG Photonics, USA; ⁴Dept. of Physics, Univ. of Alabama at Birmingham, USA. We demonstrate the first OPO based on random phase matching. The OPO was based on ZnSe ceramic pumped by 62-fs, $\lambda=2.35\text{-}\mu\text{m}$ Cr:ZnS laser pulses, had 90-mW pump threshold and produced an ultra-broad spectrum spanning 3-7.5 μm .

STh4F.4 • 17:30

Half-watt average power compact femtosecond source with a bandwidth of 3–8 μm based on subharmonic GaAs OPO, Viktor O. Smolski¹, Sergey Vasilyev¹, Igor Moskalev¹, Mike Mirov¹, Qitian Ru², Andrey Muraviev², Peter G. Schunemann³, Sergey Mirov^{3,4}, Valentin Gapontsev⁵, Konstantin L. Vodopyanov²; ¹IPG Photonics, USA; ²Univ. of Central Florida, CREOL, USA; ³BAE Systems, USA; ⁴Univ. of Alabama at Birmingham, USA; ⁵IPG Photonics, USA. High-power (0.5 W) mid-IR output suitable for ultra-broadband frequency comb generation was produced in a subharmonic GaAs optical parametric oscillator that was synchronously pumped by a compact 0.9 GHz, 6 W femtosecond Cr:ZnS (2.35 μm) MOPA.

CLEO: QELS-Fundamental Science

CLEO: Science & Innovations

16:30–18:30

FTh4G • Cats and Kets

President: Martin Stevens; NIST, USA

FTh4G.1 • 16:30

Experimental Test of Bell's Inequality for Temporal Orders, Giulia Rubino¹, Lee Rozema¹, Francesco Massa¹, Mateus Araujo¹, Magdalena Zych², Caslav Brukner¹, Philip Walther¹; ¹Univ. of Vienna, Austria; ²Univ. of Queensland, Australia. Bell's inequality has been violated using different physical systems, but never for the temporal order between events. Here we present such a Bell inequality and experimentally violate it by entangling the temporal order between events.

FTh4G.2 • 16:45

A Four-Photon Graph State Generator in Silicon, Jeremy C. Adcock¹, Caterina Vigliar¹, Raffaele Santagati¹, Joshua W. Silverstone¹, Mark G. Thompson¹; ¹Univ. of Bristol, UK. We present a four-photon, four-qubit graph state generator in Silicon quantum photonics, achieving, for the two and four qubit cases respectively, fidelities of 0.931 ± 0.004 and 0.62 ± 0.04 , and a visibility of 0.85 ± 0.03 .

FTh4G.3 • 17:00

A Broadband All-Fiber SU(1,1) Interferometer, Joseph M. Lukens¹, Raphael C. Pooser^{1,2}, Nicholas A. Peters^{1,3}; ¹Oak Ridge National Lab, USA; ²Dept. of Physics, Univ. of Tennessee, USA; ³Bredesen Center, Univ. of Tennessee, USA. We describe an SU(1,1) interferometer based on highly nonlinear optical fiber, attaining >97% peak interference visibility and >90% visibility over a 554 GHz optical band.

FTh4G.4 • 17:15

Rabi-like Oscillations in Photon Pair Correlations, Steven Rogers¹, Austin Graf¹, Usman Javid¹, Qiang Lin¹; ¹Univ. of Rochester, USA. We have produced a new quantum coherence phenomenon via photon generation within ultra-high-Q silicon microdisks. The Rayleigh-scattering-induced strong coupling of counterpropagating modes leads to Rabi-like oscillations in the biphoton second-order coherence.

FTh4G.5 • 17:30 **Invited**

Schrödinger Cats for Quantum Internet, Alexander I. Lvovsky^{2,1}, Alexander Ulanov², Demid Sychev², Anastasia A. Pushkina^{2,1}, Egor Tiunov², Valery Novikov²; ¹Univ. of Calgary, Canada; ²Russian Quantum Center, Russia. We generate and characterize an entangled state between qubits encoded in single-photon polarizations and superpositions of opposite-amplitude coherent states. We demonstrate its application for exchanging quantum information between discrete- and continuous-variable encodings of quantum information.

16:30–18:30

FTh4H • Nanophotonic Emitters, Detectors and Modulators

President: Cheng Zhang; NIST, USA

FTh4H.1 • 16:30

Bypassing Loss in Plasmonic Modulators, Christian Haffner¹, Daniel Chelladurai¹, Yuriy Fedoryshyn¹, Arne Josten¹, Benedikt Baeuerle¹, Wolfgang Heni¹, Tatsuhiro Watanabe¹, Tong Cui¹, Bojun Cheng¹, Soham Saha², Delwin Elder³, Larry R. Dalton³, Alexandra Boltasseva², Vladimir M. Shalaev², Nathaniel Kinsey⁴, Juerg Leuthold¹; ¹ETH Zurich, Switzerland; ²School of Electrical & Computer Engineering and Brick Nanotechnology Center, Purdue Univ., USA; ³Dept. of Chemistry, Univ. of Washington, USA; ⁴Electrical and Computer Engineering, Virginia Commonwealth Univ., USA. We show that Ohmic losses in plasmonic modulators can be bypassed by using a resonant scheme. This enables the first modulator that unites low-loss, high-speed, compact footprint and low-electrical energy consumption.

FTh4H.2 • 17:00

Electro-Absorption Waveguide Modulator Performance, Rubab Amin¹, Jacob Khurgin², Volker J. Sorger¹; ¹The George Washington Univ., USA; ²Johns Hopkins Univ., USA. A holistic analysis for waveguide-based electro-absorption modulators demonstrates that all materials with direct interband absorption show comparable performance from the fundamental point of view. Only reducing the effective waveguide area can lead to reduced switching energy and wide bandwidth.

FTh4H.3 • 17:15

High responsivity and bias-free graphene photodetector with nano-grating contact electrodes, Mona Jarrahi¹, Semih Cakmakyan¹; ¹Univ. of California Los Angeles, USA. We present a high responsivity and bias-free graphene photodetector with responsivity levels as high as 225 mA/W at 800 nm wavelength, which uses nano-grating contact electrodes to enhance optical absorption and photocarrier extraction.

FTh4H.4 • 17:30 **Invited**

Integrated Quantum Optics: From Emitters to Detectors, Val Zwiller¹; ¹Technische Universiteit Delft, Netherlands. We develop quantum devices to generate quantum states of light with semiconductor quantum dots, superconducting single photon detectors and on-chip circuits to filter and route light.

16:30–18:30

STh4I • Mid-IR Optoelectronics

President: Frank (Fengqiu) Wang; Nanjing Univ., China

STh4I.1 • 16:30 **Invited**

Epitaxy-free Direct Bandgap GeSn Materials and Devices for Facile 3D Photonic Integration, Jifeng Liu¹, Xiaoxin Wang¹; ¹Dartmouth College, USA. We present direct bandgap GeSn crystallized on dielectric layers at <450 °C with room-temperature photoluminescence, ~0.1 ns transient optical gain >4000/cm at $\lambda=2100\text{--}2350$ nm, and a photoconductive responsivity of ~10 mA/W @1V at $\lambda=2180$ nm.

STh4I.2 • 17:00

Systematic Study of Ge_{0.89}Sn_{0.11} Photodiodes for Low-Cost Shortwave Infrared Imaging, Huong Tran¹, Thach Pham¹, Wei Du², Yang Zhang¹, Seyed Ghetmiri³, Perry Grant^{1,4}, Joshua Grant¹, Greg Sun⁴, Richard Soref⁴, Joe Margetis⁵, John Tolle⁵, Baohua Li⁶, Mansour Mortazavi³, Shui-Qing Yu¹; ¹Univ. of Arkansas, USA; ²Wilkes Univ., USA; ³Univ. of Arkansas Pine Bluff, USA; ⁴Univ. of Massachusetts Boston, USA; ⁵ASM, USA; ⁶Arkonics, USA. The characteristics Ge_{0.89}Sn_{0.11} photodiodes were systematically investigated. A cutoff wavelength of 2.65 μm at 300 K and the peak detectivity of 4.3×10^9 Jones at 77 K were achieved. An infrared imaging of an object was demonstrated using the single Ge_{0.89}Sn_{0.11} photodiode.

STh4I.3 • 17:15

Dilute-Bismide Alloys for GaSb-based Mid-Infrared Semiconductor Lasers, Scott D. Sifferman¹, Marcin Motyka², Andrew F. Briggs¹, Kenneth J. Underwood³, Kyle M. Mc-Nicholas¹, Robert Kudrawiec², Juliet Gopinath^{3,4}, Seth Bank¹; ¹Microelectronics Research Center, Univ. of Texas at Austin, USA; ²Wroclaw Univ. of Technology, Poland; ³Dept. of Physics, Univ. of Colorado Boulder, USA; ⁴Dept. of Electrical, Computer and Energy Engineering, Univ. of Colorado Boulder, USA. Incorporation of bismuth into III-V emitters typically results in dramatically reduced luminescence efficiency. We present type-I dilute-bismide III-V quantum wells exhibiting enhanced photoluminescence near 4 μm , suggesting a viable route to extend diode laser emission.

STh4I.4 • 17:30

Direct Bandgap Type-I GeSn Quantum Well toward Si-based Optoelectronics, Perry C. Grant^{2,1}, Joe Margetis⁵, Yiyin Zhou^{2,1}, Wei Dou¹, Grey Abernathy¹, Andrian Kuchuk¹, Wei Du⁴, Seyed Ghetmiri², Baohua Li², John Tolle³, Jifeng Liu⁶, Greg Sun⁷, Richard Soref⁷, Mansour Mortazavi⁵, Shui-Qing Yu¹; ¹Univ. of Arkansas, USA; ²Arkonics LLC., USA; ³ASM, USA; ⁴Wilkes Univ., USA; ⁵Univ. of Arkansas-Pine Bluff, USA; ⁶Dartmouth College, USA; ⁷Univ. of Massachusetts-Boston, USA. GeSn single quantum well on relaxed GeSn and Ge buffered Si substrate was investigated. The direct bandgap well and type-I band alignment were achieved, which were confirmed by calculation and photoluminescence studies.

CLEO: QELS-Fundamental
Science

16:30–18:30

FTh4J • Random and Alternative Materials
Metasurfaces

Presider: Otto Muskens; Univ. of Southampton, UK

FTh4J.1 • 16:30

Tunable topology of photonic systems based on transparent conducting oxides, Zhaxylyk A. Kudyshev¹, Alexander Kildishev¹, Alexandra Boltasseva¹, Vladimir M. Shalaev¹; ¹Purdue, USA. Here we show that by integrating transparent conducting oxides with a photonic waveguide array it is possible to realize ultrafast control over topology of photonic system. This precise control is highly important for topologically protected memory devices and quantum communication applications.

FTh4J.2 • 16:45

Chip-scale atomic diffractive optical elements, Liron Stern¹, Douglas Bopp¹, Vincent N. Maurice¹, John Kitching¹; ¹Time & Frequency Division, National Inst. of Standards and Technology (NIST), USA. We experimentally explore the spatial and spectral response of a chip-scale hybrid atomic-dielectric grating. Spectral control of the diffracting orders mediated by the atomic vapor paves the path to a variety of novel atomic-controlled diffractive-optical-elements.

FTh4J.3 • 17:00

Gain tunable all-dielectric metasurfaces incorporating III-V semiconductors, Hang Li¹, Ruizhe Yao¹, Jun Ding², Wei Guo¹, Hualiang Zhang¹; ¹Univ. of Massachusetts Lowell, USA; ²School of Information and Science Technology, East China Normal Univ., China. In this work, we present a tunable all-dielectric metasurface based on III-V semiconductors (InGaAs/GaAs). Active amplitude tuning of reflected optical wave using the proposed metasurface has been demonstrated through both numerical simulation and experiment.

FTh4J.4 • 17:15

III-V semiconductor metasurface as the optical metamixer, Polina Vabishchevich¹, Sheng Liu¹, Aleksandr Vaskin², John Reno^{1,3}, Gordon A. Keeler¹, Michael Sinclair¹, Isabelle Staudé², Igal Brener^{1,3}; ¹Sandia National Labs, USA; ²Inst. of Applied Physics, Abbe Center of Photonics, Friedrich-Schiller-Universität Jena, Germany; ³Center for Integrated Nanotechnologies, Sandia National Labs., USA. In this work, we experimentally demonstrate simultaneous occurrence of second-, third-, fourth-harmonic generation, sum-frequency generation, four-wave mixing and six-wave mixing processes in III-V semiconductor metasurfaces with spectra spanning from the UV to the near-IR.

FTh4J.5 • 17:30

High-efficiency and low-loss dielectric metasurfaces on a gallium nitride platform, Naresh K. Emani¹, Egor Khaidarov^{1,2}, Ramon Paniagua-Dominguez¹, Yuan Hsing Fu¹, Vytautas Valuckas¹, Shunpeng Lu², Xueliang Zhang², Swee Tiam Tan², Hilmi Volkan Demir^{2,3}, Arseniy Kuznetsov¹; ¹Data Storage Inst., Singapore; ²Nanyang Technological Univ., Singapore; ³Bilkent Univ., Turkey. Epitaxial GaN on sapphire is a promising material platform for low-loss, nonlinear and active metasurfaces at visible wavelengths. We experimentally demonstrate high efficiency dielectric metasurfaces with beam bending and polarization splitting functionalities on this platform.

CLEO: Science & Innovations

16:30–18:30

STh4K • Long Wavelength Fiber Sources

Presider: Camille-Sophie Bres; Ecole Polytechnique Federale de Lausanne, Switzerland

STh4K.1 • 16:30

Few-Cycle Pulse Generation from a 3 μm Fiber Laser, Robert I. Woodward¹, Darren Hudson¹, Alex Fuerbach¹, Stuart D. Jackson¹; ¹Macquarie Univ., Australia. We demonstrate the generation of 70-fs pulses (~7 optical-cycles) from a mid-infrared mode-locked Ho:ZBLAN fiber laser using nonlinear compression with step-index chalcogenide fiber. Experiments are supported by numerical modelling, confirming the scalability of this approach.

STh4K.2 • 17:00

High Power Splice-less Fiber Laser at 2825 nm, Yigit O. Aydin¹, Vincent Fortin¹, Réal Vallée¹, Martin Bernier¹; ¹Centre d'Optique, Photonique et Laser (COPL), Université Laval, Canada. A passively cooled 2825 nm splice-less erbium-doped fluoride fiber laser delivering 20 W output power in continuous wave operation was reported. This result represents the highest mid-IR output power obtained from a splice-less laser cavity.

STh4K.3 • 17:15

Emission Beyond 4 μm and Mid-infrared Lasing from a Dy³⁺:InF₃ Fiber, Matthew Majewski¹, Robert I. Woodward¹, Jean-Yves Carree², Marcel Poulain², Samuel Poulain², Stuart D. Jackson¹; ¹Macquarie Univ., Australia; ²Le Verre Fluore, France. We present a dysprosium-doped InF₃ fiber exhibiting emission beyond 4 microns; the longest wavelength to date from a fluoride-based fiber. Laser emission around 3 μm is also demonstrated.

STh4K.4 • 17:30

Yb-doped Fiber Laser Based Coherent Mid-Infrared Frequency Comb at λ = 4.5 μm for CRDS application, Lei Jin¹, Volker Sonnenschein¹, Ryohei Terabayashi¹, Noriyoshi Hayashi¹, Shusuke Kato¹, Masahito Yamanaka¹, Hideki Tomita¹, Tetsuo Iguchi¹, Atsushi Sato², Kohei Nozawa², Kenji Yoshida², Norihiko Nishizawa¹; ¹Nagoya Univ., Japan; ²Sekisui Medical Co. Ltd., Japan. An offset free mid-infrared optical frequency comb was generated based on an Yb-doped fiber laser system with tunability of 3.9-4.7 μm. Cavity ring down spectroscopy measurement was demonstrated with QCL and MIR comb reference.

16:30–18:30

STh4L • Optical Sensing in Combustion

Presider: Brian Brumfield; Pacific Northwest National Lab, USA

STh4L.1 • 16:30 **Invited**

Probing Soot Formation and Chemical Evolution During Combustion, Hope A. Michelsen¹; ¹Sandia National Labs, USA. There are gaps in the understanding of soot formation during combustion, which are largely attributable to a limited ability to probe relevant particle parameters during formation. This talk will describe approaches to developing appropriate diagnostics.

STh4L.2 • 17:00

Investigation of Multi-Photon Excitation Schemes for Detecting Atomic Hydrogen in Flames, Ayush Jain¹, Waruna Kulatilaka¹; ¹Texas A&M Univ., USA. **Abstract:** We investigate two-photon and three-photon excitation schemes for ultra-short pulse LIF detection of atomic hydrogen in flames. Three-photon (λ=307.7nm) scheme was demonstrated successfully for the first time and various interferences effects are studied.

STh4L.3 • 17:15

CO₂ Measurement in Laminar Premixed Flames Using Heterodyne Phase-Sensitive Dispersion Spectroscopy, Zhen Wang¹, Liuha Ma¹, Kin-Pang Cheong¹, Wei Ren¹; ¹The Chinese Univ. of Hong Kong, Hong Kong. We measured CO₂ concentrations in laminar premixed flames using heterodyne phase sensitive dispersion spectroscopy by directly modulating the injection current of an interband cascade laser.

STh4L.4 • 17:30 **Tutorial**

Development and Application of Laser Diagnostic Techniques for Combustion Studies, Marcus L.E. Alden¹; ¹Dept of Physics, Lund Univ., Sweden. The present talk will present some advancement in laser diagnostics in combustion environments. Several techniques will be described and the talk will also include new developments addressing some of the challenges in the field

continued on page 211

CLEO: QELS-Fundamental
Science

16:30–18:30

FTh4M • Functional Nanophotonics Using
Metasurfaces

Presider: Godofredo Bautista; Tampere Univ.
of Technology, Finland

FTh4M.1 • 16:30

Active Tuning of Reflectance at Long Infrared Wavelengths using Strongly Coupled Metasurface-Semiconductor Hybrid Structures, Raktim Sarma¹, Salvatore Campione¹, michael goldflam¹, Joshua Shank¹, Sean Smith¹, Jinhyun Noh², Peide Ye², Michael Sinclair¹, Igal Brener¹; ¹Sandia National Labs, USA; ²Purdue Univ., USA. We experimentally demonstrate spectral tuning and amplitude modulation of reflectance at long infrared wavelengths using a complementary metasurface strongly coupled to an epsilon-near-zero (ENZ) mode in an ultrathin InGaAs layer with a reflecting backplane.

FTh4M.2 • 16:45

Wavelength-dependent Optical-rotation Manipulation for Active Color Display and Highly Secure Encryption, Maowen Song^{1,2}, Alexander Kildishev^{1,3}, Di Wang^{1,3}, Zhuoxian Wang^{1,3}, Yi Xuan¹, Alexandra Boltasseva^{1,3}, Honglin Yu², Vladimir M. Shalaev^{1,3}; ¹Birck Nanotechnology Center, Purdue Univ., USA; ²Key Lab of Optoelectronic Technology and Systems of Education Ministry of China, Chongqing Univ., China; ³School of Electrical and Computer Engineering, Purdue Univ., USA. We present a silica coated aluminum metamirror with wavelength-dependent optical rotation effect. Excitation of localized surface plasmons maps discrete polarizations into diverse colors, broadly increasing the encoded information space.

FTh4M.3 • 17:00 **Invited**

Broadband Hot Electron Creation in Nanoscale Gap Plasmon Metasurfaces, Gary Wiederrecht¹; ¹Argonne National Lab, USA. We report experimental and theoretical results on the use of broadband plasmonic nanopatch metasurfaces to produce large concentrations of hot electrons. Transient absorption spectroscopy enables the detection of hot electron populations and their decay pathways.

FTh4M.4 • 17:30

Ultrafast Tunable Metasurface with Transparent Conducting Oxide Antenna Array, Soham Saha^{1,2}, Aveek Dutta^{1,2}, Clayton DeVault^{1,2}, Vladimir M. Shalaev^{1,2}, Alexandra Boltasseva^{1,2}; ¹Birck Nanotechnology Center, USA; ²Purdue Univ., USA. We demonstrate large reflection and transmission modulation and femtosecond relaxation times in undoped zinc oxide films. Using these experimental results, we designed an optically tunable, terahertz-speed metasurface with a 17.4dB extinction ratio at 1.30 μm .

CLEO: Science & Innovations

16:30–18:30

STh4N • Ultrafast Metrology II

Presider: Jose Azana; INRS-Energie Materiaux
et Telecom, Canada

STh4N.1 • 16:30

Deep Learning Reconstruction of Ultrashort Pulses, Tom Zahavy¹, Alex Dikopoltsev¹, Oren Cohen¹, Shie Mannor¹, Mordechai Segev¹; ¹Technion, Israel. We propose and demonstrate, numerically and experimentally, the first deep neural network technique to reconstruct the amplitude and phase of ultrashort optical pulses. We anticipate that this approach will enable diagnostics of very weak pulses.

STh4N.2 • 16:45

Differential Evolution for Robust Phase Retrieval in Ultrafast Pulse Characterization, Gunter Steinmeyer¹; ¹Max Born Inst., Germany. We demonstrate pulse retrieval from dispersion-scan and FROG traces using a genetic algorithm. The algorithm is extremely robust even for complex pulse shapes, resilient to noise, and can reliably compensate for spectral efficiency variations.

STh4N.3 • 17:00 **Invited**

Ultra-short Optical Pulses for Coherent Ultra-wide Band RF Signal Sampling, Daniel Onori¹, Filippo Scotti¹, Giovanni Serafino², Paolo Ghelfi¹, Antonella Bogoni^{1,2}; ¹CNIT, Italy; ²Sant'Anna School of Advanced Studies, Italy. The importance of ultra-short and stable optical pulses for ultra-wide band RF signal sampling is demonstrated through the implementation and comparison of different solutions of RF scanning receiver based on photonics.

STh4N.4 • 17:30

All-linear Phase Retrieval of a Single-soliton Kerr Comb, Ziyun Kong¹, Chengying Bao¹, Oscar Sandoval¹, Bohao Liu¹, Minghao Qi¹, Andrew M. Weiner¹; ¹Purdue Univ., USA. We demonstrate all-linear phase retrieval of a single-soliton Kerr comb via dual-comb electric field cross-correlation (EFXC). This approach greatly lowers the power needed for ultrafast waveform reconstruction of optical frequency combs.

CLEO: Applications
& Technology

16:30–18:30

Ath4O • Novel Spectroscopic Approaches II

Presider: Paul Williams; NIST, USA

Ath4O.1 • 16:30

High-resolution and Large Tunable Range Nanophotonic Spectrometer Using a Microring Resonator, Shaonan Zheng^{1,2}, Yangyang Chen³, Hong Cai², Yuandong Gu², Zhenchun Yang³, Y. L. Hao³, D.L. Kwong², Aiqun Liu¹; ¹Nanyang Technological Univ., Singapore; ²Inst. of Microelectronics, Singapore; ³Peking Univ., China. An integrated high-resolution on-chip spectrometer with Ge-on-Si photodetector is demonstrated. The robust spectrometer has high resolution, high compactness, low cost and CMOS-compatibility. It has high potential to be used in integrated sensing and spectroscopy systems.

Ath4O.2 • 16:45

High-resolution and Large-bandwidth On-chip Microring Resonator Cavity-enhanced Fourier-transform Spectrometer, Shaonan Zheng^{1,2}, Yangyang Chen³, Hong Cai², Yuandong Gu², Aiqun Liu¹; ¹Nanyang Technological Univ., Singapore; ²Agency for Science, Technology and Research (A*STAR), Singapore; ³Peking Univ., China. A high-resolution (0.47 nm) and large-bandwidth (150 nm) on-chip Fourier-transform spectrometer (FTS) enhanced with a microring resonator (MRR) cavity is demonstrated. It is promising to be applied in applications such as on-chip chemical and biological sensing systems.

Ath4O.3 • 17:00

Self-expanding fabricated bubble resonators used as whispering gallery modes sensors, Hongwen Zhou¹, Jiansheng Liu¹, Meng Zhang¹, Jie Chen¹, Xiaosheng Liu¹, Qing Wu¹, Zheng Zheng¹; ¹Beihang Univ., China. Employing low-cost high borosilicate glass capillaries, self-expanding bubble resonator fabrication method based on air thermal expansion is demonstrated. Detected quality factor Q is as high as 10⁵. 54 pm light perturbation mode shift was sensed.

Ath4O.4 • 17:15

A High-resolution Dual-microring-based Silicon Photonic Sensor using Electronic Integrated Circuit, Hui Zhang¹, Muhammad F. Karim¹, Shaonan Zheng^{1,2}, Hong Cai², Yuan Dong Gu², Shoushun Chen¹, Hao Yu³, Aiqun Liu¹; ¹School of Electrical and Electronic Engineering, Nanyang Technological Univ., Singapore 639798, Singapore; ²Inst. of Microelectronics, A*STAR, Singapore 117685, Singapore; ³Dept. of Electrical and Electronic Engineering, Southern Univ. of Science and Technology, China 518055, China. A high-resolution dual-microring based silicon photonic sensor is demonstrated with an electronic integrated circuit. For refractive index sensing in sodium chloride solution, a high sensitivity of 0.153 RIU/W and a detection limit of 0.34 μRIU are achieved.

Ath4O.5 • 17:30

Combined Laser-Induced Breakdown Spectroscopy and MIR Quantum Cascade Laser Reflectance Spectroscopy for Elemental and Molecular Characterization, Francis Vanier¹, Christian Padioulet¹, Mohamad Sabsabi¹, Alain Blouin¹; ¹National Research Council Canada, Canada. We combine laser-based mid-infrared reflectance measurements using tunable quantum cascade lasers and laser-induced breakdown spectroscopy to get both the elemental and molecular compositions of a sample. Results for mineral ore characterization are shown.

CLEO: Applications
& Technology

16:30–18:30

ATH4P • Environmental Greenhouse Gas Sensing*Presider: Mark Zondlo; Princeton Univ., USA*ATH4P.1 • 16:30 **Invited**

Bringing Laser Spectroscopy to the Deep Sea, Anna P. Michel¹; ¹WHOI, USA. By coupling laser-based techniques to gas extraction techniques, gases critical for understanding ocean processes such as methane and carbon dioxide can be measured. Recent advances in oceanographic chemical sensing using laser-based techniques will be presented.

ATH4P.2 • 17:00

Compact Amplitude-Modulated, Phase-Analyzed Spectroscopy (CAMPAS) for Gas Analysis, David Bomse¹; ¹Mesa Photonics, LLC, USA. Optical absorption in gases within an integrating sphere is determined by phase shifts of amplitude modulated laser light. This technique could achieve performance advantages similar to those of FM radio over AM radio.

ATH4P.3 • 17:15

Quantifying methane emissions among simulated gas wells with a dual-frequency comb spectrometer, Sean C. Coburn¹, Caroline Alden^{1,2}, Robert Wright¹, Esther Baumann³, Kevin Cossel³, Nathan R. Newbury³, Kuldeep Prasad⁴, Ian R. Codrington³, Gregory B. Rieker¹; ¹Univ. of Colorado at Boulder, USA; ²CIRES, USA; ³NIST, USA; ⁴NIST, USA. We present the results of a single-blind field test assessing the capability of a dual-frequency comb spectrometer coupled with atmospheric inversion methods for detecting and quantifying methane emissions from natural gas production infrastructure.

ATH4P.4 • 17:30 **Invited**

Recent Advancement in Cavity Ringdown Spectroscopy in Measuring Effects of Natural Gas Industry, Tracy Tsai¹; ¹Picarro, USA. Natural gas is a growing energy source, but to minimize environmental impact and safety risks, the natural gas infrastructure must be monitored for methane emissions. I will present field results collected with a cavity ring-down based spectrometer.

16:30–18:30

ATH4Q • A&T Topical Review on Scientific and Commercial Progress in Semiconductor Laser Technology I*Presider: Bojan Resan; Univ. of Applied Sciences FHNW, Switzerland*ATH4Q.1 • 16:30 **Invited**

Progress in VECSELS: from Gain Mirror Technology to New Applications, Mircea D. Guina^{1,2}; ¹Tampere Univ. of Technology, Finland; ²VEXLUM Ltd, Finland. We review recent progress in VECSEL technology in connection to new milestones that continue to pave the way for practical use in emerging applications. We focus on wavelength extension and applications in quantum technology, dermatology, or spectroscopy.

ATH4Q.2 • 17:00 **Invited**

Commercial Semiconductor Disk Lasers, Nils Hempler¹, David Paboeuf¹, Tiago Ortega¹, Robin Head¹, Walter Lubeigt¹, Gareth Maker¹, Graeme Malcolm¹; ¹M Squared Lasers, UK. This paper will present the development of commercial semiconductor disk lasers undertaken at M Squared Lasers mainly for microscopy and quantum applications.

ATH4Q.3 • 17:30

First demonstration of O-band grating-assisted microcylinder surface-emitting laser, Xiang Ma¹, Quanan Chen¹, Wei Sun¹, Ye Liu¹, Gongyuan Zhao¹, Gonghai Liu¹, Qiaoyin Lu¹, Weihua Guo¹; ¹Wuhan National Lab for Optoelectronics, Huazhong Univ. of S & T, China. Grating-assisted microcylinder surface-emitting laser (GAMSEL) in the O-band was demonstrated. Continuous-wave working with side-mode suppression-ratio >40dB has been realized and the output beam is radially polarized.

CLEO: Science & Innovations

Joint

STh4A • Waveguide Structures—Continued

STh4A.6 • 17:45

Large Bandwidth Waveguide Spectral Splitters Using Higher-Order Mode Evolution, Jean-Etienne Tremblay¹, Marcin Malinowski², Guillermo Camacho-Gonzalez², Sasan Fathpour², Ming C. Wu¹; ¹Univ. of California, Berkeley, USA; ²CREOL, Univ. of Central Florida, USA. Broadband spectral filters separating 1 μ m/2 μ m wavelengths of octave-spanning frequency combs have been realized using mode evolution to high-order modes. The splitters are fabricated in chalcogenide glass (Ge₂₃Sb₇S₇₀) and can be readily integrated with supercontinuum sources.

STh4A.7 • 18:00

Ultra-Broadband and Compact Asymmetrical Beam Splitter Enabled by Angled Sub-Wavelength Grating MMI, Eslam Elfiky¹, Yannick D'Mello¹, Yun Wang¹, Md Ghulam Saber¹, Amar Kumar¹, James Skoric¹, Alireza Samani¹, Luhua Xu¹, Rui Li¹, David Patel¹, David V. Plant¹; ¹McGill Univ., Canada. We present an ultra-broadband and compact asymmetrical beam splitter using subwavelength grating based multi-mode interference coupler. We experimentally demonstrate splitting ratios from 50:50 to 90:10 over 100 nm bandwidth using a 24 μ m x 3 μ m design.

STh4A.8 • 18:15

Arbitrary Ratio, Wavelength-insensitive 2x2 MMI Coupler in SOI with Enhanced Fabrication Tolerance, Jin Zhang¹, Liangshun Han¹, Bill P. Kuo¹, Stojan Radic¹; ¹Univ. of California, San Diego, USA. We present a new arbitrary-ratio 2x2 MMI coupler design. The design demonstrated 2.6 times lower coupling ratio variation across extended C-band, and 2.2 times ratio error reduction when subjected to ± 10 nm thickness and width deviations.

STh4B • On-chip and Offchip Coupling Schemes—Continued

STh4B.6 • 17:45

Efficient coupling of ultra-high Q crystalline microresonators to integrated photonic waveguides, Miles H. Anderson¹, Nikolay Pavlov^{2,5}, John Jost¹, Grigory Lihachev^{3,5}, Junqiu Liu¹, Tiago Morais¹, Michael Zervas¹, Michael Gorodetsky^{3,5}, Tobias J. Kippenberg¹; ¹Inst. of Physics, Ecole Polytechnique Federale de Lausanne, Switzerland; ²Moscow Inst. of Physics and Technology, Russia; ³Faculty of Physics, M. V. Lomonosov Moscow State Univ., Russia; ⁴LiGenTec, SA, Switzerland; ⁵Russian Quantum Center, Russia. We present a new integrated photonic chip solution for coupling light to ultra-high quality factor (Q) crystalline microresonators, which is in the form of an index-matching suspended silica beam-waveguide. The scheme enables coupled Q-factors exceeding 100 million near critical coupling.

STh4B.7 • 18:00

3D Photonic Structure for Plug-and-Play Fiber to Waveguide Coupling, Oscar Jimenez¹, Mohammad Amin Tadayon¹, You-Chia Chang¹, Michal Lipson¹; ¹Columbia Univ., USA. We show a 3D photonic structure for passive high alignment tolerance fiber to waveguide coupling. We measured a coupling efficiency of 2.5dB \pm 0.4dB from fiber to a polymeric waveguide for fiber misalignments within a 17 μ m diameter.

STh4B.8 • 18:15

Automated Assembly of Duplex Fiber Connectors to Photonic Chips in Standard Microelectronic Tools, Ted Lichoulas¹, Eddie Kimbrell¹, Alexander Janta-Polczynski², Elaine Cyr², Paul Fortier², Nicolas Boyer², Tymon Barwicz³; ¹AFL Telecommunications, USA; ²IBM, Canada; ³IBM, USA. We demonstrate self-aligned assembly of LC-terminated fibers to chips in a manner compatible with standard microelectronics assembly lines. We show -1.5dB peak transmission to chip with 0.9dB penalty over a 100nm bandwidth and all polarization.

JTh4C • Symposium on Integrated Sources of Non-Classical Light: Perspectives and Challenges II—Continued

JTh4C.4 • 17:45

Unidirectional Frequency Conversion in Silicon-based Double-Ring Microresonator, Mikkel Heuck¹, Yunhong Ding¹, Lars H. Frandsen¹, Jacob G. Koefoed¹, Jesper B. Christensen¹, Karsten Rottwitz¹; ¹Dept. of Photonics Engineering, Technical Univ. of Denmark, Denmark. We experimentally study four-wave-mixing frequency conversion in two coupled silicon ring-resonators. The asymmetric super-mode structure causes highly directional conversion and enables near-unity efficiency which is important for photonic quantum information technology.

JTh4C.5 • 18:00 **Invited**

Nonlinear Quantum Optics in Si₃N₄ micro-ring resonators, Sven Ramelow¹; ¹Humboldt Universität zu Berlin, Germany. Si₃N₄ is a promising platform for nonlinear quantum optics. Here, I will summarize experimental results and future perspectives on implementing bright and narrowband entangled photon sources in different wavelengths regimes and realizing strong nonlinear coupling due to induced photon interaction.

18:30–20:00 **Emerging Trends in Nonlinear Optics – A Review of CLEO: 2018**, Room 230A

18:30–20:00 **Dinner Break** (on your own)

20:00–22:00 **Postdeadline Paper Sessions**, Location TBD

Executive Ballroom
210D

Joint

JTh4D • Symposium on Advances in
Integrated Microwave Photonics II—
Continued

JTh4D.4 • 17:45

Ultra-Compact Optical True Time Delay Lines Featuring Fishbone-Like One-Dimensional Photonic Crystal Waveguide, Chi-Jui Chung¹, Xiaochuan Xu², Gencheng Wang³, Zeyu Pan¹, Ray Chen^{1,2}, ¹Dept. of Electrical and Computer Engineering, Univ. of Texas at Austin, USA; ²Omega Optics, Inc, USA; ³College of Information Science and Electronic Engineering and the Cyrus Tang Center for Sensor Materials and Applications, Zhejiang Univ., China. An ultra-compact on-chip optical true-time-delay line features the slow light enhanced fishbone-like one-dimensional photonic crystal waveguide is proposed. A delay time of 65 ps/mm which corresponds to group index of 19.47 is observed experimentally.

JTh4D.5 • 18:00 **Invited**

Plasmonics for RF Photonics, Juerg Leuthold¹, Yannick Saramin¹, Romain Bonjour¹, Arne Josten¹, Benedikt Baeuerle¹, Alexander Dorodny¹, Yuriy Fedoryshyn¹, Ping Ma¹, Delwin Elder², Larry R. Dalton², ¹ETH Zurich, Switzerland; ²Univ. of Washington, USA. Plasmonics is a solution to replace active photonics. If properly designed, plasmonic devices offer highly integrated circuits on a micrometer footprint with THz frequency responses. In this talk we will review opportunities for RF plasmonics

Executive Ballroom
210E

CLEO: QELS-Fundamental
Science

FTh4E • Multimode Nonlinear Fiber
Optics—Continued

FTh4E.5 • 17:45

Optical Trapping and Manipulation of Multiple Microparticles Using SDM Fibers, Joel A. Hernández-García¹, Amado M. Velazquez-Benitez¹, Yanin Guerra-Santillán², Raúl Caudillo-Viurquez², Jose Enrique Antonio-Lopez², Rodrigo Amezcua Correa³, Juan Hernandez-Cordero⁴, ¹CCADET-UNAM, Mexico; ²Facultad de Ciencias, UNAM, Mexico; ³CREOL, UCF, USA; ⁴IIM, UNAM, Mexico. We demonstrate optical trapping and dynamic manipulation of microparticles using multicore and few-mode fibers. Tuning of the input state of polarization of the trapping beam allows for particle rotation and adjustable trapping distances.

FTh4E.6 • 18:00

Analysis of Parametric Instabilities in Parabolic Multimode Fibers under High Intensity Conditions, Helena E. Lopez Aviles¹, Fan Wu¹, Zeinab Sanjabi Eznaveh¹, Mohammad Amin Eftekhar¹, Frank W. Wise², Rodrigo Amezcua Correa¹, Demetrios N. Christodoulides¹, ¹Univ. of Central Florida, USA; ²School of Applied and Engineering Physics, Cornell Univ., USA. We systematically study geometric parametric instabilities in parabolic multimode fibers. We show, both analytically and experimentally, that global dispersion processes and self-focusing effects can substantially affect the spectral positions and widths of the generated sidebands.

FTh4E.7 • 18:15

Mode-Resolved Control and Measurement of Nonlinear Pulse Propagation in Multimode Fibers, Zimu Zhu¹, Logan Wright¹, Joel Carpenter², Dan Nolan³, Ming-Jun Li³, Demetrios N. Christodoulides⁴, Frank W. Wise¹, ¹Cornell Univ., USA; ²The Univ. of Queensland, Australia; ³Corning Incorporated, USA; ⁴Univ. of Central Florida, USA. We demonstrate use of spatial light modulators to control modal excitation and make mode-resolved measurements of nonlinear pulse propagation in multimode fiber, and present a representative experiment wherein we observe discrete Raman beam clean-up.

Executive Ballroom
210F

CLEO: Science & Innovations

STh4F • Optical Parametric Oscillators—
Continued

STh4F.5 • 17:45

Femtosecond mid-IR difference-frequency generation in BaGa₂GeSe₆ from a 40 MHz optical parametric oscillator pumped at 1035 nm, Gero Stibenz², Marcus Beutler², Ingo Rimke², Valeriy Badikov³, Dmitrii Badikov³, Valentin Petrov¹; ¹Max Born Inst., Germany; ²APE, Germany; ³Kuban State Univ., Russia. Mixing the signal and idler pulses near 2 μm from a femtosecond synchronously-pumped optical parametric oscillator in a BaGa₂GeSe₆ crystal we generate mid-IR pulses tunable up to 10 μm with 45% maximum internal quantum efficiency.

STh4F.6 • 18:00

Pulsed Optical Parametric Generation and Oscillation in Orientation-Patterned Gallium Phosphide, Hanyu Ye¹, Chaitanya Kumar Suddapalli², Junxiong Wei¹, Peter G. Schunemann³, Majid Ebrahim-Zadeh^{1,4}, ¹ICFO-Institut de Ciències Fotòniques, Spain; ²Radiantis, Spain; ³BAE Systems, Incorporated, USA; ⁴Instituto Catalana de Recerca i Estudis Avancats (ICREA), Spain. We report a Nd:YAG-laser-pumped pulsed OPG/OPO based on OP-GaP. The OPG and singly-resonant OPO spanning 2.8 μm-3.1 μm provide up to ~2 mW and ~20 mW idler power, respectively. Crystal thermal effects are also investigated.

STh4F.7 • 18:15

Critically Phase-Matched Deep-Infrared Femtosecond Optical Parametric Oscillator Based on CdSiP₂, Callum F. O'Donnell^{1,2}, Chaitanya Kumar Suddapalli¹, Kevin Zawilski³, Peter G. Schunemann³, M. Ebrahim-Zadeh², ¹Radiantis, Spain; ²ICFO - Institut de Ciències Fotòniques, Spain; ³BAE Systems, USA. We report a femtosecond optical parametric oscillator across 6654–8329 nm based on critically phase-matched CdSiP₂. Directly pumping with a Ti:sapphire laser, we generate 19 mW of average power in ~300-fs pulses at 80.5 MHz.

18:30–20:00 Emerging Trends in Nonlinear Optics – A Review of CLEO: 2018, Room 230A

18:30–20:00 Dinner Break (on your own)

20:00–22:00 Postdeadline Paper Sessions, Location TBD

CLEO: QELS-Fundamental Science

CLEO: Science & Innovations

FTh4G • Cats and Kets—Continued

FTh4G.6 • 18:00

Generation of Schrodinger's cat state in an optical double sideband mode, Takahiro Serikawa¹, Jun-ichi Yoshikawa¹, Hidehiro Yonezawa², Timothy Ralph³, Eleanor Huntington⁴; ¹Univ. of Tokyo, Japan; ²The Univ. of New South Wales, Australia; ³Univ. of Queensland, Australia; ⁴Australian National Univ., Australia. An optical Schrodinger's cat state is generated in 500.6MHz double sideband mode of continuous wave light. We used phase modulation to selectively subtract a photon from sideband. The reconstructed Wigner function exhibits a significant negativity of -0.088 without any correction.

FTh4G.7 • 18:15

Amplifying Schrödinger cat state with an optical parametric amplifier, Meihong Wang¹, Zhongzhong Qin¹, Miao Zhang¹, Li Zeng¹, Xiaolong Su¹, Changde Xie¹, Kunchi Peng¹; ¹Shanxi Univ., China. We experimentally demonstrate the deterministic amplification of an optical Schrödinger cat state by an optical parametric amplifier. The results provide an efficient way to amplify the amplitude of an optical cat state.

FTh4H • Nanophotonic Emitters, Detectors and Modulators—Continued

FTh4H.5 • 18:00

Circularly Polarized Light Detection Based on Efficient Chip-Integrated Metasurface, Ali Basiri^{1,2}, Xiahui Chen^{1,2}, Pouya Amrollahi³, Jing Bai^{1,2}, Chao Wang^{1,4}, Yu Yao^{1,2}; ¹School of Electrical, Computer and Energy Engineering, Arizona State Univ., USA; ²The Center for Photonics Innovation, Arizona State Univ., USA; ³School for Engineering of Matter, Transport & Energy, Arizona State Univ., USA; ⁴Biodesign Center for Molecular Design & Biomimetics, Arizona State Univ., USA. We report a hybrid metal-dielectric metasurface to realize on-chip detection of circularly polarized light at telecommunication wavelengths. Preliminary experimental results show extinction ratios close to 10 dB and efficiencies up to 90% at designed wavelengths.

FTh4H.6 • 18:15

Extraordinary Properties of Epsilon-Near-Zero and Low-Index Chalcogenide Metamaterials, Davide Piccinotti¹, Behrad Gholipour¹, Jin Yao¹, Kevin F. MacDonald¹, Brian E. Hayden¹, Nikolay I. Zheludev^{1,2}; ¹Univ. of Southampton, UK; ²Nanyang Technological Univ., Singapore. 'Laminar flow' transmission, suppression of plasmonic powerflow vortices, and absorption decreasing with increasing Joule losses can be observed in metamaterials combining plasmonic nanostructures with chalcogenide inclusions exhibiting epsilon-near-zero and sub-unitary refractive index behaviors.

STh4I • Mid-IR Optoelectronics—Continued

STh4I.5 • 17:45

Quantum Dot Quantum Cascade Detector on Si Substrate, Jian Huang¹, Daqian Guo², Deng Zhuo¹, Wei Chen¹, Tinghui Wu¹, Yaojiang Chen¹, Huiyun Liu², Jiang Wu², Baile Chen¹; ¹SIST, ShanghaiTech Univ., China; ²Dept. of Electronic and Electrical Engineering, Univ. College London, UK. We demonstrate a quantum cascade detector monolithic grown on Si substrate for mid infrared application. Sub-monolayer dots were used as absorption region for normal incidence light detection around 6 μ m.

STh4I.6 • 18:00

Low-Threshold Lasing in Strained Germanium under Optical Pumping, Donguk Nam^{1,4}, Shuyu Bao¹, Daeik Kim⁴, Chibuzo Onwukaeme⁴, Shashank Gupta², Krishna Saraswat², Kwang Hong Lee³, Yeji Kim⁴, Dabin Min⁴, Yongduck Jung⁴, Haodong Qiu¹, Hong Wang¹, Eugene Fitzgerald³, Chuan Seng Tan¹; ¹Nanyang Technological Univ., Singapore; ²Stanford Univ., USA; ³Singapore-MIT Alliance for Research and Technology (SMART), Singapore; ⁴Inha Univ., South Korea. We report the first experimental observation of low-threshold lasing in strained germanium nanowires. The lasing threshold is ~3.0 kW cm⁻² which is more than one order of magnitude lower than the state-of-the-art germanium-tin Fabry-Perot laser.

18:30–20:00 Emerging Trends in Nonlinear Optics – A Review of CLEO: 2018, Room 230A

18:30–20:00 Dinner Break (on your own)

20:00–22:00 Postdeadline Paper Sessions, Location TBD

**CLEO: QELS-Fundamental
Science**

CLEO: Science & Innovations

**FTh4J • Random and Alternative Materials
Metasurfaces—Continued**

FTh4J.6 • 17:45

Mid-infrared Magnetic Mirror Based on a Hybrid Metal/Dielectric Metasurface, Ming Ye¹, Shiqiang Li¹, Yang Gao¹, Vivek R. Shrestha¹, Kenneth B. Crozier¹; ¹*The Univ. of Melbourne, Australia*. We propose a hybrid metal/dielectric metasurface that functions as a mid-infrared magnetic mirror. It consists of amorphous silicon cuboids on gold. The physical mechanism is explained by image theory. Measured reflection spectra agree with simulations.

FTh4J.7 • 18:00

Towards Random Metasurface based Devices, Matthieu Dupre¹, Junhee Park¹, Liji Hsu¹, Abdoulaye Ndao¹, Boubacar Kante¹; ¹*UCSD, USA*. Using full wave simulations and a transmission matrix approach, we design and then realize random metasurface lenses with anisotropic nanorods, and show that we can obtain a diffraction limited focal spot for all polarizations.

FTh4J.8 • 18:15

Disordered Geometric Phase: Photonic Transition from Spin Hall to Random Rashba Effect, Elhanan Maguid¹, Michael Yannai¹, Arkady Faerman¹, Igor Yulevich¹, Vladimir Kleiner¹, Erez. Hasman¹; ¹*Technion-Israel Inst. of Technology, Israel*. We report on photonic spin-symmetry breaking and unexpected optical transport phenomena arising from disordered geometric phase structures. Weak disorder induces a photonic spin Hall effect, whereas strong disorder leads to a random Rashba effect.

**STh4K • Long Wavelength Fiber Sources—
Continued**

STh4K.5 • 17:45

Generation of sub-100 fs pulses tunable from 1.8 to 2.0 μm from an All-fiber, All-PM Source Pumped at 1560 nm, Grzegorz J. Sobon¹, Tadeusz Martynkien³, Karol Tarnowski³, Pawel Mergo², Jaroslaw Sotor¹; ¹*Faculty of Electronics, Wrocław Univ. of Science and Technology, Poland*; ²*Maria Curie-Skłodowska Univ., Poland*; ³*Faculty of Fundamental Problems of Technology, Wrocław Univ. of Science and Technology, Poland*. An all-fiber, all-PM source of widely tunable (1800 – 2000 nm) ultrashort pulses seeded by an Er-doped fiber laser is presented. The system delivers sub-100 fs pulses with 400 mW average power and >8 nJ energy.

STh4K.6 • 18:00

Dual Comb Spectroscopy with a Free-Running Bi-Directional Mode-Locked Thulium Fiber Laser, Joshua Olson¹, Yi-Hsin Ou¹, Ali Azarm¹, Khanh Q. Kieu¹; ¹*Univ. of Arizona, USA*. We present a Thulium fiber laser mode-locked bi-directionally with a carbon nanotube saturable absorber and demonstrate single-shot dual-comb spectroscopy of H₂O in the short-wave infrared (SWIR) with the laser.

STh4K.7 • 18:15

15 GHz actively mode-locked fiber laser at 2 micron, Jiarong Qin¹, Ruihong Dai¹, Yafei Meng¹, Wenbin Gao¹, Yongbing Xu¹, Yao Li¹, Shining Zhu¹, Frank (Fengqiu) Wang¹; ¹*Nanjing Univ., China*. We demonstrate a 15-GHz actively-mode-locked thulium fiber laser. The repetition-rate is improved by one order of magnitude compared with existing results and such a source can be used for 2 μm optical data-communication and processing.

**STh4L • Optical Sensing in Combustion—
Continued**



Marcus Aldén is professor/Head of the Division of Combustion Physics at Lund University and Program director of the Swedish Centre in Combustion Science and Technology. Prof. Aldén has co-authored 395 papers and is a member of the Royal Swedish Academy of Engineering Sciences and the Royal Swedish Academy of Sciences.

18:30–20:00 **Emerging Trends in Nonlinear Optics – A Review of CLEO: 2018**, Room 230A

18:30–20:00 **Dinner Break** (on your own)

20:00–22:00 **Postdeadline Paper Sessions**, Location TBD

CLEO: QELS-Fundamental
ScienceFTh4M • Functional Nanophotonics Using
Metasurfaces—Continued

FTh4M.5 • 17:45

Magnetic Plasmon Hybridization in Vertically Stacked Double-gap Nanocavities, Seied Ali Safiabadi Tali¹, Wei Zhou¹; ¹Virginia Tech, USA. In vertically stacked double-gap nanocavities, the strong magnetic-optical interaction between magnetic plasmon modes in individual gap nanocavities can lead to new hybridized bonding and antibonding modes with a tunable splitting energy.

FTh4M.6 • 18:00

Perovskite Nanostructures and Metasurfaces Enhanced by Mie Resonances, Sergey Makarov¹, Ekaterina Tigunseva¹, Anvar Zakhidov^{3,1}, Yuri S. Kivshar^{2,1}; ¹ITMO Univ., Russia; ²Australian National Univ., Australia; ³Univ. of Texas at Dallas, USA. We study resonant properties of nanoantennas and nanostructured metasurfaces made of halide perovskites and demonstrate experimentally the photoluminescence enhancement near the dipolar and multipolar Mie resonances for both visible and near-infrared frequency ranges.

FTh4M.7 • 18:15

Bifunctional Gap-Plasmon Metasurfaces for Visible Light, Fei Ding¹, Rucha Deshpande¹, Sergey I. Bozhevolnyi¹; ¹Univ. of Southern Denmark, Denmark. We design, fabricate and experimentally demonstrate bifunctional gap-plasmon metasurfaces for visible light, allowing simultaneous polarization-controlled unidirectional surface plasmon polariton (SPP) excitation and beam steering at normal incidence.

CLEO: Science & Innovations

STh4N • Ultrafast Metrology II—Continued

STh4N.5 • 17:45

Cross-spectrum approach for absolute timing jitter measurement of mode-locked lasers, Alexis Casanova^{1,2}, Benoit Trophez¹, Antoine Courjaud¹, Giorgio Santarelli²; ¹Ampitude Systemes, France; ²Université de Bordeaux, France. A combination of cross-spectral analysis and balanced optical cross-correlation techniques is proposed to access the absolute timing jitter of one laser mode-locked solid-state laser. This method gives a record jitter detection floor.

STh4N.6 • 18:00

Waveform characterization of optical pulses by plasma luminescence of gas, Nariyuki Saito¹, Nobuhisa Ishii¹, Teruto Kanaï¹, Jiro Itatani¹; ¹Univ. of Tokyo, Japan. We propose and demonstrate a new all-optical method to characterize an optical waveform using plasma luminescence of gas. Our technique is based on simple physics, and applicable to compact pulse diagnostics and petahertz time-domain spectroscopy.

STh4N.7 • 18:15

Intrapulse Coherence for Gauging the Quality of Passive Carrier-Envelope Phase Stabilization, Gunter Steinmeyer¹; ¹Max Born Inst., Germany. The intrapulse coherence is introduced as a measure for judging a fixed phase relation between different spectral components within a laser pulse. This new criterion plays an important role for passive CEP stabilization of OPA systems.

CLEO: Applications
& TechnologyAth4O • Novel Spectroscopic Approaches
II—Continued

Ath4O.6 • 17:45

Identification of white powder samples using broadband coherent light in the molecular fingerprint region, Luke Maidment¹, Richard A. McCracken¹, Oguzhan Kara¹, Peter G. Schunemann², Derryck T. Reid¹; ¹Heriot-Watt Univ., UK; ²BAE Systems, USA. Stand-off Fourier-transform spectroscopy of eleven white powder samples illuminated by a broadband femtosecond source was used to construct a library of spectra, which are demonstrated to enable automated chemical detection using a simple correlation algorithm.

Ath4O.7 • 18:00

Edible Oils Sensing Setup Based on a Core-Offset Mach-Zehnder Interferometer With Single Mode Fiber, Leidy J. Cuchimaque Lugo¹, Rafael Castro-López², Maria E. Sosa Morales², Juan M. Sierra Hernandez¹, Julian M. Estudillo Ayala¹, Daniel Jauregui¹, Juan Hernandez Garcia¹, Roberto Rojas Laguna¹; ¹Departamento de Ingeniería Electrónica, División de Ingenierías, Campus Irapuato-Salamanca, Universidad de Guanajuato, Comunidad de Palo Blanco, Salamanca, Gto., C.P. 36885, México., Mexico; ²Departamento de Alimentos, División de Ciencias de la Vida, Campus Irapuato-Salamanca, Universidad de Guanajuato, Carretera Irapuato-Silao km 9, Irapuato, Gto. 36500 México., Mexico. Peroxides are compounds related to rancidity in oils. A peroxides index sensing setup based on a Mach-Zehnder interferometer is presented. The output power spectrum shift occurs from 1490 to 1580 [nm] with sensitivity of 0.88 [nm/meq/kg].

Ath4O.8 • 18:15

Alpha Radiation Induced Luminescence in Solar Blind Spectral Region, Thomas H. Kerst^{1,2}, Juha Toivonen¹; ¹Tampere Univ. of Technology, Finland; ²Helsinki Inst. of Physics, Finland. Intense luminescence in the solar blind spectral region is produced by modifying the gas atmosphere around an alpha emitter. This enables standoff detection of alpha radiation under daylight conditions.

18:30–20:00 Emerging Trends in Nonlinear Optics – A Review of CLEO: 2018, Room 230A

18:30–20:00 Dinner Break (on your own)

20:00–22:00 Postdeadline Paper Sessions, Location TBD

CLEO: Applications & Technology

ATH4P • Environmental Greenhouse Gas Sensing—Continued

ATH4P.5 • 18:00

Effect of tuning characteristics of continuous wave quantum cascade laser on detection of CH₄ and N₂O in mid-IR region, May Hlaing^{1,2}, Mohammad A. Khan¹; ¹Delaware State Univ., USA; ²Optical Science Center for Applied Research, USA. We report studies of tuning characteristics and modulation properties of a distributed feedback continuous wave quantum cascade laser centered at 7.83 μm in detection of mid-IR line transitions of methane, nitrous-oxide and water-vapor.

ATH4P.6 • 18:15

Mid-infrared Photonic Chips for Real-time Gas Mixture Analysis, Pao T. Lin¹; ¹Texas A&M Univ., USA. Real-time gas analysis on-a-chip was demonstrated using a mid-infrared microcavity. Optical apertures were made of ultrathin membranes using the CMOS process. CH₄, CO₂, and N₂O were selected as analytes due to their strong absorption bands at λ = 3.25 - 3.50 μm, 4.20 - 4.35 μm.

ATH4Q • A&T Topical Review on Scientific and Commercial Progress in Semiconductor Laser Technology I—Continued

ATH4Q.4 • 17:45

Far field control of large-area surface-emitting photonic crystal quantum cascade laser, Yong Liang¹, Zhixin Wang¹, Johanna Wolf¹, Emilio Gini¹, Mattias Beck¹, Jérôme Faist¹; ¹ETH Zurich, Switzerland. Large-area single-mode lasing is demonstrated within surface-emitting photonic-crystal quantum cascade lasers, at room temperature, with narrow divergence (<1°) and 175 mW peak power. Single-lobed far-field is realized by optimizing the pillar shape.

ATH4Q.5 • 18:00

Frequency Comb Formation Over the Entire Lasing Range of Quantum Cascade Lasers, Yang Yang¹, David Burghoff¹, John Reno², Qing Hu¹; ¹MIT, USA; ²Sandia National Labs, USA. By incorporating a two-section geometry featuring an electrically tunable dispersion compensator, we demonstrate terahertz quantum cascade lasers exhibiting comb operation from I_{th} to I_{max}, covering the entire bias range of lasing.

ATH4Q.6 • 18:15

Direct Measurement of the Phase Coherence of Quantum Cascade Comb Sources, Saverio Bartalini^{1,2}, Luigi Consolino¹, Francesco Cappelli¹, Giulio Campo¹, Iacopo Galli^{1,2}, Davide Mazzotti^{1,2}, Pablo Cancio^{1,2}, Giacomo Scalari³, Jérôme Faist³, Paolo De Natale^{1,2}; ¹CNR-INO, Italy; ²ppqSense Srl, Italy; ³Inst. for Quantum Electronics, ETH Zürich, Switzerland. Thanks to a novel method for directly and simultaneously measuring the instantaneous phases of the modes of mid-infrared and THz quantum cascade lasers combs, the phase coherence of these sources is presented and discussed.

18:30–20:00 Emerging Trends in Nonlinear Optics – A Review of CLEO: 2018, Room 230A

18:30–20:00 Dinner Break (on your own)

20:00–22:00 Postdeadline Paper Sessions, Location TBD

Executive Ballroom
210ACLEO: Science &
Innovations

08:00–10:00

SF1A • Si Photonics

Presider: Qiang Lin; Univ. of Rochester, USA

SF1A.1 • 08:00

High-resolution on-chip digital Fourier transform spectroscopy, Derek Kita¹, Brando Miranda¹, David Favela¹, David Bono¹, Jérôme Michon¹, Hongtao Lin¹, Tian Gu¹, Juejun Hu¹; ¹MIT, USA. We experimentally demonstrate a high-resolution, on-chip digital Fourier transform (dFT) spectrometer using a reconfigurable Mach-Zehnder interferometer. The dFT architecture claims the multiplex advantage for signal enhancement, with a resolution that scales exponentially with device footprint.

SF1A.2 • 08:15

Silicon Linear Optical Logic Gates for Low-Latency Computing, Shota Kita^{1,2}, Kengo Nozaki^{1,2}, Kenta Takata^{1,2}, Akihiko Shinya^{1,2}, Masaya Notomi¹; ¹NTT Nanophotonics Center, Nippon Telegraph & Telephone Corp, Japan; ²NTT Basic Research Labs., Nippon Telegraph and Telephone corp., Japan. We demonstrate 3 μm -long linear optical logic gates with a bias input. The binary contrasts of AND/NOR operations can be 9.5 dB without signal attenuation. This may open up a new boundary for ultralow-latency computing.

SF1A.3 • 08:30

Microdisk-Based Full Adders for Optical Computing in Silicon Photonics, Zhoufeng Ying¹, Zheng Wang¹, Zheng Zhao¹, Shoung Dhar¹, David Pan¹, Richard Soref², Ray Chen¹; ¹The Univ. of Texas at Austin, USA; ²Univ. of Massachusetts Boston, USA. We experimentally demonstrate a two-bit thermal-optic ripple-carry full adder based on microdisk resonators in silicon photonics with the advantages of large bandwidth, low power consumption, and high scalability, paving the way to future optical computing.

Executive Ballroom
210BCLEO: QELS-
Fundamental Science

08:00–10:00

FF1B • Quantum Enhanced
Measurements

Presider: Raphael Pooser; Oak Ridge National Lab, USA

FF1B.1 • 08:00

Resolution-enhanced imaging with quantum correlations, Ermes Toninelli¹, Paul-Antoine Moreau¹, Adam Mihalyi¹, Thomas Gregory¹, Matthew Edgar¹, Miles Padgett¹; ¹The Univ. of Glasgow, UK. The resolution of optical systems is limited by diffraction. We exploit the spatial properties of correlated photon-pairs to reconstruct a super-resolved image made of bisectant pixel-coordinates, achieving 40% of the theoretical $\sqrt{2}$ optical resolution enhancement.

FF1B.2 • 08:15

Imaging incoherent point sources with quantum-inspired measurements, Kent Fisher¹, Hugo Ferretti¹, Edwin (Weng-Kian) Tham¹, Aephraim M. Steinberg^{1,2}; ¹Physics, Univ. of Toronto, Canada; ²Canadian Inst. for Advanced Research, Canada. We present straightforward measurements, involving only π -phase shifts and single-mode fiber coupling, to estimate the separation and relative intensities of two incoherent point sources. We show Monte Carlo results demonstrating an advantage over direct imaging.

FF1B.3 • 08:30

Super-Resolution Localization and Readout of Individual Solid State Qubits, Eric A. Bersin¹, Michael Walsh¹, Sara L. Mouradian¹, Matthew Trusheim¹, Tim Schröder², Dirk Englund¹; ¹MIT, USA; ²Niels Bohr Inst., Denmark. We demonstrate super-resolution imaging and readout of solid state defect centers. Multiple nitrogen vacancy centers within 130 nm are resolved. Simultaneous control sequences are performed to demonstrate protection of nearby NV states during readout.

Executive Ballroom
210C

Joint

08:00–10:00

JF1C • Symposium on Lasers
in Accelerator Science and
Technology I

Presider: Sergio Carbajo; Stanford University and SLAC National Accelerator Laboratory, US

JF1C.1 • 08:00 **Invited**

Photonics-based Laser-driven Particle Acceleration: from proof-of-concept structures to the accelerator on a chip, Peter Hommelhoff¹; ¹Physics Dept., Friedrich Alexander Univ. Erlangen-Nurnberg, Germany. Demonstrating a photonics-based particle accelerator is the goal of the "Accelerator on a Chip International Collaboration" (ACHIP). Half way into the program, the current status is discussed.

JF1C.2 • 08:30 **Invited**

X-ray laser based on Inverse Compton Scattering, William Graves¹; ¹Arizona State Univ., USA. A compact XFEL based on inverse Compton scattering is described. A novel method allows coherent control of the phase, bandwidth, and pulse length of the x-ray pulses, and enables multi-color experiments with precisely tunable femtosecond delays.

Executive Ballroom
210DCLEO: QELS-
Fundamental Science

08:00–10:00

FF1D • Ultrafast Spectroscopy
of 2D Materials

Presider: Jigang Wang; Iowa State Univ., USA

FF1D.1 • 08:00

Spectroscopic signature of chiral phonons in 2D materials, Hanyu Zhu¹, Jun Yi¹, Ming-Yang Li², Jun Xiao¹, Lifa Zhang³, Chih-Wen Yang², Yuan Wang^{1,4}, Robert Kaindl⁴, Lain-Jong Li², Xiang Zhang^{1,4}; ¹Univ. of California Berkeley, USA; ²King Abdullah Univ. of Science and Technology, Saudi Arabia; ³Nanjing Normal Univ., China; ⁴Lawrence Berkeley National Lab, USA. The chiral phonons at the corners of the Brillouin zone in inversion asymmetric 2D atomic lattices were revealed by the circular-polarization selection rules and the spectrum of the indirect intervalence band transition.

FF1D.2 • 08:15

Homogeneous Linewidth of Encapsulated MoSe₂ Monolayer Revealed using Multi-dimensional Coherent Spectroscopy, Eric Martin¹, Jason Horng¹, Hanna G. Ruth¹, Eunice Paik¹, Michael-Henr Wentzel¹, Hui Deng¹, Steven T. Cundiff¹; ¹Dept. of Physics, Univ. of Michigan, USA. We use a collinear multidimensional coherent spectroscopic technique to measure van der Waals structures with a nearly diffraction-limited spot size. Encapsulation by boron nitride narrows both the homogeneous and inhomogeneous linewidths of MoSe₂.

FF1D.3 • 08:30

Intrinsic Homogeneous Linewidth of Trions in Monolayer MoSe₂, Michael Titze¹, Bo Li², Pulickel Ajayan^{2,3}, Hebin Li¹; ¹Florida International Univ., USA; ²Dept. of Materials Science and NanoEngineering, Rice Univ., USA; ³Dept. of Chemistry, Rice Univ., USA. We have measured the intrinsic homogeneous linewidth of trions in monolayer MoSe₂ using two-dimensional spectroscopy. The linewidth is 3.60 meV, corresponding to a decoherence time of 182 fs.

Executive Ballroom
210E

CLEO: QELS-Fundamental Science

08:00–10:00

FF1E • THz Generation and Novel Phenomena

Presider: Mona Jarrahi; Univ. of California Los Angeles, USA

FF1E.1 • 08:00

Silicon nitride-based deep sub- λ slit for ultra-broadband THz coherent detection, Alessandro Tomasino^{1,2}, Riccardo Piccoli¹, Yoann Jestin¹, Alessandro Busacca², Sebastien Delprat¹, Mohamed Chaker¹, Marco Pecciant³, Matteo Clerici⁴, Luca Razzari¹, Roberto Morandotti^{1,5}; ¹INRS-EMT, Canada; ²DEIM, Univ. of Palermo, Italy; ³Dept. of Physics and Astronomy, Univ. of Sussex, UK; ⁴School of Engineering, Univ. of Glasgow, UK; ⁵National Research Univ. of Information Technologies, Russia. We report on the characterization of a new type of CMOS-compatible device for terahertz solid-state biased coherent detection, which relies on a 1- μ m-wide metallic slit embedded in a thin film of PECVD-grown silicon nitride.

FF1E.2 • 08:15

Observation of Strong THz Fields from Mid-Infrared Two-Color Laser Filaments, Anastasios D. Koulouklidis^{1,2}, Claudia Gollner³, Valentina Shumakova³, Vladimir Fedorov^{2,4}, Audrius Pugzlys^{3,5}, Andrius Baltuska^{3,5}, Stylianos Tzortzakidis^{1,2}; ¹Inst. of Electronic Structure and Laser (IESL), Foundation for Research and Technology/Hellas (FORTH), Greece; ²Science Program, Texas A&M Univ. at Qatar, Qatar; ³Photonics Inst., TU Wien, Austria; ⁴P. N. Lebedev Physical Inst. of the Russian Academy of Sciences, Russia; ⁵Center for Physical Sciences & Technology, Lithuania. We demonstrate, strong THz emission from two-color mid-infrared (3.9 μ m) femtosecond laser filaments. The conversion efficiency approaches the percent level, at least one order of magnitude higher than the previously reported for plasma-based THz sources.

FF1E.3 • 08:30

Towards Millijoule Narrowband Terahertz Pulses Using the Chirp-and-Delay Technique, Spencer W. Jolly^{1,2}, Frederike Ahr^{3,4}, Nicholas H. Matlis⁵, Vincent Leroux^{1,2}, Timo Eichner¹, Koustuban Ravi⁵, Hideki Ishizuki⁶, Takunori Taira⁶, Franz X. Kaertner^{3,4}, Andreas R. Maier¹; ¹CFEL and Univ. of Hamburg, Germany; ²ELI - Beamlines, Czechia; ³DESY and CFEL, Germany; ⁴Dept. of Physics, Univ. of Hamburg, Germany; ⁵RLE, MIT, USA; ⁶Laser Research Center, Inst. for Molecular Sciences, Japan. We show generation of THz pulses of combined energy above 0.5 mJ at 0.361 THz using the chirp-and-delay technique.

Executive Ballroom
210F

08:00–10:00

FF1F • Spatial and Temporal Control of Light Using Metasurfaces

Presider: Martti Kauranen; Tampere University of Technology, Finland

FF1F.1 • 08:00

Femtosecond Pulse Shaping by Metasurfaces, Shawn Divitt^{1,2}, Wenqi Zhu^{1,2}, Cheng Zhang^{1,2}, Henri Lezec², Amit K. Agrawal^{1,2}; ¹Univ. of Maryland College Park, USA; ²National Inst. of Standards and Technology, USA. Metasurfaces provide extremely fine spatial control over the amplitude and phase of incident light. Here, we demonstrate shaping of <15 femtosecond ultrafast laser pulses using a metasurface as a spectral phase mask.

FF1F.2 • 08:30

A Photonic Crystal Slab Laplace Differentiator, Cheng Guo¹, Meng Xiao¹, Momchil Minkov¹, Yu Shi¹, Shanhui Fan¹; ¹Stanford Univ., USA. We propose an implementation of a Laplace differentiator based on a photonic crystal slab that operates at transmission mode. Such a device may facilitate nanophotonics-based optical analog computing for image processing.

Executive Ballroom
210G

CLEO: Science & Innovations

08:00–10:00

SF1G • Surface Emitting Lasers

Presider: Eric Tournie; Univ. of Montpellier, France

SF1G.1 • 08:00

Photonic crystal diode laser arrays integrated with a phase shifter designed for narrow far-field angle, Xuyan Zhou¹, Xiaolong Ma¹, Shaoyu Zhao¹, Hongwei Qu¹, Aiyi Qi¹, Wanhua Zheng¹; ¹Inst. of Semiconductors, CAS, China. Edge-emitting photonic crystal laser arrays integrated with a phase-shifter are investigated to obtain narrow far field in lateral and vertical directions. More than 500 mW/facet continuous-wave power, FWHM of $1.5^\circ \times 12^\circ$, and single-lobe pattern are achieved.

SF1G.2 • 08:15

Ultrafast Quantum Dot VECSELs: Record Performance Depending on Growth Techniques, Cesare Alfieri¹, Dominik Waldburger¹, Jacob Nürnberg¹, Matthias Golling¹, Ursula Keller¹; ¹ETH, Switzerland. We present the extended potentialities of quantum dots (QDs) as active media for semiconductor disk lasers. Self-assembled QDs efficiently reach the shortest sub-200-fs pulses, while submonolayer QDs deliver record output powers in continuous wave operation.

SF1G.3 • 08:30

10 W High-Power and High-Beam-Quality Pulsed Operation of Double-Hole Photonic-Crystal Surface-Emitting Lasers, Masahiro Yoshida¹, Menaka D. Zoysa¹, Kenji ishizaki¹, Yoshinori Tanaka¹, Ranko Hatsuda¹, Masato Kawasaki^{1,3}, Bong-Shik Song^{1,2}, Susumu Noda¹; ¹Kyoto Univ., Japan; ²Sungkyunkwan Univ., South Korea; ³Mitsubishi Electric Corporation, Japan. We develop high-power, high-beam-quality photonic-crystal lasers with double-hole structures. We demonstrate broad-area coherent lasing in a circular region with a 500 μ m diameter, and 10 W peak powers with very narrow far-field angles (< 0.3°).

Executive Ballroom
210H

CLEO: QELS-Fundamental Science

08:00–10:00

FF1H • Nanophotonic Strategies for Controlling Light-Matter Interaction

Presider: Haim Suchowski; Tel Aviv Univ., Israel

FF1H.1 • 08:00 **Invited**

New All-optical and Plasmonic Strategies for Controlling Light on a Silicon Chip, Otto L. Muskens¹, Bigeng Chen¹, Nicholas Dinsdale¹, Roman Bruck¹, David J. Thomson¹, Goran Mashanovich¹, Graham T. Reed¹, Kevin Vynck², Philippe Lalanne²; ¹Univ. of Southampton, UK; ²LP2N, Institut Optique d'Aquitaine, France. We explore the integration of nanophotonic and plasmonic concepts with the silicon photonics platform. I will present hybrid plasmonic antennas on a silicon ring resonator and all-optical wave-front shaping in a multimode device.

Meeting Room
211 B/DMeeting Room
212 A/CMeeting Room
212 B/DMarriott
Salon III

CLEO: Science & Innovations

CLEO: Applications
& Technology

08:00–10:00

SF11 • Perovskites and Organics

Presider: Thomas Murphy; Univ. of Maryland at College Park, USA

08:00–10:00

SF1J • Metasurfaces

Presider: Takasumi Tanabe; Keio Univ., Japan

08:00–10:00

SF1K • Hollow Core Fibers

Presider: Sze Set; Univ. of Tokyo, Japan

08:00–10:00

AF1M • Fiber-Optic Based Sensing

Presider: Gregory Rieker; Univ. of Colorado at Boulder, USA

SF11.1 • 08:00

Invited

Toward Hybrid Organic-Inorganic Perovskite Diode Lasers, Noel C. Giebink¹; ¹Pennsylvania State Univ., USA. Hybrid organic-inorganic perovskites represent a promising, wavelength-tunable materials platform for a future diode laser. This talk will present progress toward this goal, including continuous-wave lasing and high-brightness perovskite light emitting diodes.

SF1J.1 • 08:00

Dynamic Dielectric Metasurfaces Incorporating Phase-Change Material, Sajjad AbdollahRamezani¹, Hossein Taghinejad¹, Yashar Kiarashi Nejad¹, Ali Asghar Eftekhari¹, Ali . Adibi¹; ¹Georgia Inst. of Technology, USA. We present a highly-reconfigurable metasurface with unprecedented efficiency for spatial and spectral manipulation of optical wavefronts, leveraging control over the overlapped Mie-dipolar-modes of dielectric nanorings and large refractive index tunability granted by GeSbTe phase-change material.

SF1K.1 • 08:00

45W 2 μ m Nanosecond Pulse Delivery Using Antiresonant Hollow-core Fiber, Elizabeth M. Lee^{2,1}, Jiaqi Luo^{2,1}, Biao Sun², Vincent Larry Ramalingam^{2,1}, Xia Yu², Qijie Wang¹, Fei Yu³, Jonathan C. Knight²; ¹School of Electrical & Electronic Engineering, Nanyang Technological Univ., Singapore; ²Precision Measurements Group, Singapore Inst. of Manufacturing Technology, Singapore; ³Centre for Photonics and Photonic Materials, Dept. of Physics, Univ. of Bath, UK. We demonstrated the highest reported transmission of 44.9W average power from a 1980nm 1.2ns source using an antiresonant hollow-core delivery fiber with good output beam quality.

AF1M.1 • 08:00

Invited

Optical Sensing Systems for Industrial and Medical Process Monitoring, Guido Perrone¹; ¹Politecnico di Torino, Italy. The paper reviews how photonic sensors, and those based on fiber optics in particular, can enable new applications in the framework of the so-called "industry 4.0" and in the biomedical field.

SF1J.2 • 08:15

MEMS-tunable dielectric metasurface lens, Ehsan Arbabi¹, Amir Arbabi², Seyedeh Mahsa Kamali¹, Yu Horie¹, MohammadSadeq Faraji-Dana¹, Andrei Faraon¹; ¹California Inst. of Technology, USA; ²Electrical Engineering, Univ. of Massachusetts Amherst, USA. We report a micro-electromechanically tunable metasurface doublet composed of a moving metasurface on a membrane and a stationary one. The doublet provides more than 180 diopters change in the optical power.

SF1K.2 • 08:15

2-3 μ m wavelength-range low-loss inhibited-coupling hollow-core fiber, Martin Maurel^{1,2}, Frédéric Delahaye¹, Foued Amrani¹, Benoit Debord^{1,2}, Frédéric Gérôme^{1,2}, Fetah Benabid^{1,2}; ¹GPPMM, Xlim, CNRS UMR 7252, Limoges Univ, France; ²GLPhotonics SAS, France. We report on ultra-broad transmission guiding large-mode area inhibited-coupling HC-PCFs. The fibers guidance spans from 500 nm to 3300 nm and exhibits losses in the range of 25-50 dB/km in the 2-3 μ m wavelength range.

SF11.2 • 08:30

Lasing from high-quality lead halide perovskite single crystal microparticles, Sangyeon Cho^{2,1}, Seok-Hyun Yun^{2,1}; ¹Harvard-MIT Health Sciences and Technology, MIT, USA; ²Wellman Center for Photomedicine, Massachusetts General Hospital and Harvard Medical School, USA. We have synthesized CsPbBr₃ and CH₃NH₃PbBr₃ single-crystal microplates with improved surface quality and obtained whispering-gallery mode lasing from a size of 2 μ m. The method can produce high-quality perovskite microlasers in large quantity within minutes.

SF1J.3 • 08:30

Continuous Gradient Dielectric Metasurfaces for Non-discrete Spatial Light Manipulation, Masashi Miyata¹, Mitsumasa Nakajima¹, Toshikazu Hashimoto¹; ¹NTT Device Technology Labs., Japan. We demonstrate continuous gradient metasurfaces that can form a non-discrete one-dimensional phase pattern on a surface. The capability of our approach for wavefront shaping is demonstrated in efficient and versatile optical multi-beam splitters.

SF1K.3 • 08:30

1 km fiber with losses at the fundamental Rayleigh scattering limit in the green wavelength range, Matthieu Chafer^{1,2}, Frédéric Delahaye¹, Foued Amrani¹, Benoit Debord^{1,2}, Frédéric Gérôme^{1,2}, Fetah Benabid^{1,2}; ¹GPPMM, Xlim, CNRS UMR 7252, Limoges Univ, France; ²GLPhotonics, France. We report losses at the Rayleigh scattering limit of silica at 539 nm in a tubular HC-PCF with value of 13.8 dB/km. The fiber was drawn over 1 km with \pm 0.6% fluctuation.

AF1M.2 • 08:30

A Family of Interferometric Fiber Optic Gyroscopes for Miniaturized Satellites, Jing Jin¹, Kun Ma¹, Cai Wei¹, Linghai Kong¹; ¹Beihang Univ., China. The compact interferometric fiber optical gyroscope configurations and components, efficient and reliable parameters monitoring and fault diagnosis, performances and in-orbit tests of miniaturized products for space use are presented in this paper.

Marriott Salon IV	Marriott Salon VI	Marriott Willow Glen
CLEO: Science & Innovations	CLEO: QELS-Fundamental Science	CLEO: Applications & Technology
<p>08:00–10:00 SF1N • Ultrafast Mid-IR Sources <i>Presider: Igor Jovanovic; Univ. of Michigan, USA</i></p> <p>SF1N.1 • 08:00 Generation of 1 mJ, 85 fs, 2.5 μm Pulses from a $\text{Cr}^{2+}:\text{ZnSe}$ Chirped Pulse Amplifier, Lam H. Mach¹, Xiaoming Ren¹, Yanchun Yin¹, Yang Wang¹, Zenghuo Chang¹; ¹CREOL and Dept. of Physics, Univ. of Central Florida, USA. We demonstrate the generation of 1 mJ, 85 fs, 2.5 μm pulses with 300 nm of available bandwidth at 1 kHz of repetition rate from a Chirped Pulse Amplifier based on the $\text{Cr}^{2+}:\text{ZnSe}$ gain medium.</p> <p>SF1N.2 • 08:15 8.6 MHz Extended Cavity Cr:ZnS Chirped-pulse Oscillator, Nikolai Tolstik^{1,2}, Cherrie S. Lee¹, Evgeni Sorokin³, Irina Sorokina^{1,2}; ¹Norges Teknisk Naturvitenskapelige Univ, Norway; ²Atla Lasers AS, Norway; ³Vienna Univ. of Technology, Austria. We report the first extended cavity Cr:ZnS chirped-pulse oscillator mode-locked by graphene. We demonstrate 415 mW average power at 8.6 MHz repetition rate which results in 48 nJ pulse energy.</p> <p>SF1N.3 • 08:30 High Energy, Few-Cycle Parametric Source Tunable in the 5–11 μm Window, Driven by an Yb Bulk CPA System, Giedre M. Archipovaite¹, Guangyu Fan², Pavel Malevich², Tan Lihao³, Stéphane Petit¹, Jean-Christophe Delagnes¹, Eric Cormier¹, Giedrius Andriukaitis², Edgar Kaksis², Andrius Baltuska², Tadas Balciunas²; ¹CELIA, France; ²Vienna Univ. of Technology, Austria; ³DSO National Labs, Singapore. We demonstrate an efficient difference frequency generation in the 5–11 μm spectral range. A KTA-AGS based parametric source is driven by 14 mJ Yb:CPA and provides 150 μJ pulses with up to 3 μm bandwidth.</p>	<p>08:00–10:00 FF1P • Attosecond and X-Ray Spectroscopy <i>Presider: Ming-Chang Chen; National Tsing Hua University, Taiwan</i></p> <p>FF1P.1 • 08:00 Invited Femtosecond Response of Atoms and Molecules to Ultra-Intense X-rays, Rebecca Boll¹; ¹European XFEL, Germany. The interaction of heavy atoms and small molecules with very intense soft and hard X-ray FEL pulses is discussed, and comprehensive results from several recent experiments at the LCLS are presented.</p> <p>FF1P.2 • 08:30 Attosecond Transient Absorption and Four-Wave Mixing with Tunable IR Pulses, Nathan Harkema¹, Jens E. Bækhoj², Kenneth J. Schafer², Mette B. Gaarde², Arvinder S. Sandhu¹; ¹Univ. of Arizona, USA; ²Louisiana State Univ., USA. We extend the technique of attosecond transient absorption spectroscopy by incorporating tunable IR pulses from an OPA. This technique is used to control Autler-Townes splitting and drive XUV four-wave mixing processes in Helium.</p>	<p>08:00–10:00 AF1Q • A&T Topical Review on Scientific and Commercial Progress in Semiconductor Laser Technology II <i>Presider: Bojan Resan; Univ. of Applied Sciences FHNW, Switzerland</i></p> <p>AF1Q.1 • 08:00 Invited New Platform for High Power IR and Visible Diode Laser Modules: Towards Yellow Wavelengths., Peter Skovgaard¹, Danny Noordegraaf¹, Mathias Christensen^{1,2}, Mariafernanda Vilera Suarez¹, Thomas Buss¹, Peter E. Andersen², Ole B. Jensen²; ¹Norlase ApS, Denmark; ²Fotonik, DTU, Denmark. A new platform of Watt-class, visible lasers is presented. Enabled by tapered diodes and highly efficient frequency conversion, visible laser modules are realized. Such lasers are inherently robust and can be made in unusual wavelengths, such as 577 nm.</p> <p>AF1Q.2 • 08:30 A Widely-Tunable High-SMSR Narrow-Line-width Laser Heterogeneously Integrated on Silicon, Minh Tran¹, Tin Komljenovic¹, Duanni Huang¹, Linjun Liang¹, MJ Kennedy¹, John E. Bowers¹; ¹Univ. of California Santa Barbara, USA. A heterogeneously-integrated widely-tunable semiconductor laser utilizing unbalanced MZI filter assisted Vernier ring resonators is demonstrated. A wavelength tuning range of 55 nm, SMSR greater than 50 dB and spectral linewidth of 50–85 kHz over this range was achieved.</p>

Executive Ballroom
210ACLEO: Science &
Innovations

SF1A • Si Photonics—Continued

SF1A.4 • 08:45

128x128 Silicon Photonic MEMS Switch with Scalable Row/Column Addressing, Kyungmok Kwon¹, Tae Joon Seok², Johannes Henriksson¹, Jianheng Luo¹, Lane Ochikubo³, John Jacobs³, Richard Muller¹, Ming C. Wu¹; ¹UC Berkeley, USA; ²Gwangju Inst. of Science and Technology, South Korea; ³TSI Semiconductors, USA. 128x128 silicon photonic switch with 16,384 MEMS-actuated switching elements and row/column addressing scheme have been successfully integrated on a 16x17mm² chip. The maximum (minimum) on-chip loss is 22.7 dB (4.8 dB).

SF1A.5 • 09:00 **Invited**

Monolithically Integrated Photonics with Silicon Nanoelectronics in Advanced Bulk CMOS Process Nodes for Next-Generation Systems-on-Chip, Milos Popovic¹, Fabio Pavanello⁴, Amir H. Atabaki², Sajjad Moazeni³, Hayk Gevorgyan¹, Jelena Notaras^{4,2}, Luca Alloatti², Mark T. Wade⁴, Chen Sun³, Seth Kruger⁵, Kenaish Al Qubaisi¹, Imbert Wang¹, Bohan Zhang¹, Anatol Khilo¹, Christopher Baiocco⁵, Vladimir Stojanovic³, Rajeev Jagga Ram²; ¹Boston Univ., USA; ²MIT, USA; ³Univ. of California Berkeley, USA; ⁴Univ. of Colorado Boulder, USA; ⁵SUNY Polytechnic Inst., USA. We demonstrate microring-based, 10Gbps single-chip electronic-photonic transceivers for dense WDM links that are monolithically integrated in a new 65nm bulk-CMOS microelectronics-derivative process on 300mm wafers. The polysilicon platform includes waveguides/resonators, modulators, and sensitive avalanche photodetectors.

Executive Ballroom
210BCLEO: QELS-
Fundamental ScienceFF1B • Quantum Enhanced
Measurements—Continued

FF1B.4 • 08:45

Super-Resolution Quantum Imaging at the Heisenberg Limit, Manuel Unternährer¹, Bänz Bessire¹, Leonardo Gasparini², Matteo Perenzoni², André Stefanov¹; ¹IAP, Univ. of Bern, Switzerland; ²Fondazione Bruno Kessler FBK, Italy. The theory of optical centroid measurement, having shown N -fold spatial resolution using entangled N -photon states, is formulated in the framework of an imaging formalism. An exemplary experiment using photon pairs demonstrates double resolution and uses a newly developed integrated detector array.

FF1B.5 • 09:00

Direct quantum process tomography via measuring sequential weak values, Yosep Kim¹, Yong-Su Kim², Sang-Yun Lee², Sang-Wook Han², Sung Moon², Yoon-Ho Kim¹, Young-Wook Cho²; ¹POSTECH, South Korea; ²Korea Inst. of Science and Technology (KIST), South Korea. We demonstrate measurement of the sequential weak value of two incompatible observables by making use of two-photon quantum interference. We also demonstrate direct quantum process tomography of a qubit channel using the sequential weak value.

FF1B.6 • 09:15

Quantum Measurements in weak coupling regime: from Sequential weak values to Protective measurements, Marco Genovese¹, Fabrizio Piacentini¹, Alessio Avella¹, Enrico Rebuffello¹, Salvatore Virzi¹, Ivo Degiovanni¹, Marco Gramengna¹, Giorgio Brida¹; ¹INRIM, Italy. Quantum measurements in weak coupling regime represent a new interesting paradigm with significant applications both conceptual and practical. Here we present several experimental achievements exploiting weak values, and the first realization of protective measurements.

Executive Ballroom
210C

Joint

JF1C • Symposium on Lasers
in Accelerator Science and
Technology I—Continued

JF1C.3 • 09:00

Characterizing isolated attosecond pulses with angular streaking, Siqi Li^{2,1}, Zhaoheng Guo³, R. Coffee^{4,5}, Kareem Hegazy^{1,4}, Zhirong Huang², Adi Natan⁴, Timur Osipov⁵, Dipanwita Ray⁵, Agostino Marinelli², James Cryan⁴; ¹Physics, Stanford Univ., USA; ²SLAC National Accelerator Lab, USA; ³Applied Physics, Stanford Univ., USA; ⁴Stanford Pulse Inst., USA; ⁵LCLS, SLAC National Accelerator Lab, USA. We present a robust reconstruction algorithm for isolated attosecond pulses, which exploits the phase-dependent energy modulation of a photoelectron ionized in the presence of a circularly polarized laser field.

JF1C.4 • 09:15

High-repetition rate, TW-class, picosecond CO₂ laser for a variable species ion source, Jeremy Pigeon¹, Sergei Tochitsky¹, Eric Welch¹, Chan Joshi¹; ¹UCLA, USA. A CO₂ laser driven, high-brightness, H, He, C, Ne ion source from a gas jet plasma is being developed. The high-repetition rate, 0.5 TW, picosecond, CO₂ laser driver is described.

Executive Ballroom
210DCLEO: QELS-
Fundamental ScienceFF1D • Ultrafast Spectroscopy
of 2D Materials—Continued

FF1D.4 • 08:45

Ultrafast Linewidth and Resonant Energy Dynamics of Anisotropic Excitons in Atomically Thin ReS₂, Ho-Seung Shin¹, Sangwan Sim^{1,2}, Doeun Lee¹, Seungwan Cho¹, Sooun Lee³, Seung Hoon Yang³, Wooyoung Shim³, Chul-Ho Lee³, Hyunyoung Choi¹; ¹School of Electrical and Electronic Engineering, Yonsei Univ., South Korea; ²Center for Artificial Low Dimensional Electrical Systems, Institution for Basic Science (IBS), Pohang Univ. of Science and Technology, South Korea; ³Dept. of Materials Science and Engineering, Yonsei Univ., South Korea; ⁴KU-KIST Graduate School of Converging Science and Technology, Korea Univ., South Korea. We investigate the anisotropic exciton dynamics of bilayer ReS₂ using time-resolved pump-probe spectroscopy. In contrast to conventional 2D materials, we identify that the exciton resonance broadening strongly depends on the exciton-longitudinal optical (LO) phonon coupling.

FF1D.5 • 09:00

Direct time-domain observation of ultrafast exciton formation in monolayer MoS₂, Chiara Trovatiello¹, Stefano Dal Conte¹, Giulio Cerullo^{1,4}, Kaiyuan Yao^{2,3}, Nick Borys², Francesco Scotognella^{1,2}, Ilka Kriegel², P. James Schuck^{2,3}; ¹Dipartimento di Fisica, Politecnico di Milano, Italy; ²Molecular Foundry Division, Lawrence Berkeley National Lab, USA; ³Dept. of Mechanical Engineering, Columbia Univ., USA; ⁴IFN-CNR, Italy. We study the transient optical response of monolayer MoS₂ with an unprecedented temporal resolution. From the build-up dynamics of the transient signal around A/B excitonic peaks we directly extract the characteristic time-scale for exciton formation process, which ranges between 15 and 35 fs.

FF1D.6 • 09:15

Tuning Exciton-polaritons in Monolayer WS₂ Using Electrical Field Gating, Biswanath Chakraborty¹, Jie Gu¹, Mandeep Khantoria¹, Zheng Sun², Vinod M. Menon¹; ¹The City College of New York, USA; ²Dept. of Physics and Astronomy, Univ. of Pittsburgh, USA. We demonstrate the tuning of the exciton-polaritons in monolayer WS₂ embedded in a microcavity via electrostatic gating at room temperature. Under high electron doping the formation of polaritons with the charged excitons is observed.

CLEO: QELS-Fundamental Science

FF1E • THz Generation and Novel Phenomena—Continued

FF1E.4 • 08:45

Excitation Wavelength Dependence of a High-Q Nanocavity-based Raman Silicon Laser, Daiki Yamashita¹, Takashi Asano², Susumu Noda², Yasushi Takahashi¹; ¹Osaka Prefecture Univ., Japan; ²Kyoto Univ., Japan. We investigate the excitation wavelength dependence of the laser emission from a nanocavity-based Raman silicon laser with a technique called Raman-scattering-luminescence excitation. This technique provides an overview of the Raman gain including nonlinear optical losses.

FF1E.5 • 09:00

Bloch oscillations of a free electron in a strong field, Adi Pick^{1,2}, Ori Reinhardt¹, Liang Jie Wong³, Yonatan Plotnik⁴, Ido Kaminer^{1,4}; ¹Electrical Engineering, Technion-Israel Inst. of Technology, Israel; ²Chemistry, Technion-Israel Inst. of Technology, Israel; ³Singapore Inst. of Manufacturing Technology, Singapore; ⁴Physics, Technion-Israel Inst. of Technology, Israel. We find that electrons in strong electromagnetic fields exhibit Bloch oscillations, in analogy to light propagation in index-gradient waveguide arrays. Our relativistic non-perturbative approach generalizes to multifrequency fields, producing rich variety of oscillations.

FF1E.6 • 09:15

Resonant harmonic generation in AlGaAs nanoantennas using cylindrical vector beams, Maria del R. Camacho Morales¹, Godofredo S. Bautista², Xiaorun Zang², Lei Xu¹, Léo Turquet², Andrey Miroshnichenko¹, Aristeidis Lamprianidis¹, Mohsen Rahmani¹, Dragomir N. Neshev¹, Martti Kauranen²; ¹Nonlinear Physics Centre, Research School of Physics and Engineering, The Australian National Univ., Australia; ²Lab of Photonics, Tampere Univ. of Technology, Finland. We use second- and third-harmonic generation with cylindrical vector beams to investigate AlGaAs nanodisks. The nonlinear emission is found to depend strongly on the interplay between tensorial nonlinearities, focal-field symmetries and resonant multipolar excitations.

CLEO: Science & Innovations

FF1F • Spatial and Temporal Control of Light Using Metasurfaces—Continued

FF1F.3 • 08:45

Broadband Achromatic Metalenses, Yu Han Chen¹, Pin Chieh Wu^{2,1}, Shuming Wang³, Ren Jie Lin¹, Jia Wern Chen¹, Yi-Chieh Lai¹, Cheng Hung Chu², Bo Han Chen¹, Shining Zhu³, Tao Li³, Zhenlin Wang³, Din Ping Tsai^{1,2}; ¹National Taiwan Univ., Taiwan; ²Research Center for Applied Sciences, Academia Sinica, Taiwan; ³College of Engineering and Applied Sciences, School of Physics, Nanjing Univ., China. We propose a design principle to realize achromatic metasurface devices which successfully eliminate the chromatic aberration over a continuous wavelength regions from 400 to 660 nm and 1200 to 1680 nm in a transmission and reflection scheme, respectively.

FF1F.4 • 09:00

Aberration Corrected Metalenses for Imaging, Sajan Shrestha¹, Adam Overvig¹, Nanfang Yu¹; ¹Columbia Univ., USA. We experimentally demonstrated chromatic aberration correction in converging and diverging metalenses up to wavelength range of ~450 nm in the near-infrared by utilizing dispersion engineering of meta-units.

FF1F.5 • 09:15

Angle-multiplexed metasurfaces, Seyedeh Mahsa Kamali¹, Ehsan Arbabi¹, Amir Arbabi², Yu Horie¹, MohammadSadegh Faraji-Dana¹, Andrei Faraon¹; ¹California Inst. of Technology, USA; ²UMass Amherst, USA. We introduce angle-multiplexed metasurfaces for encoding independent wavefronts in a single metasurface under different illumination angles. As proof of concept, we demonstrate an angle-multiplexed hologram, which projects different images under normal and oblique illumination angles.

CLEO: QELS-Fundamental Science

SF1G • Surface Emitting Lasers—Continued

SF1G.4 • 09:00

Asymmetric beam generation in an on-chip 2D-pattern-projecting lasers, Kazuyoshi Hirose¹, Yoshitaka Kurosaka¹, Yu Takiguchi¹, Takahiro Sugiyama¹, Yoshiro Nomoto¹, So Uenoyama¹; ¹Hamamatsu Photonics K.K., Japan. We successfully generate an asymmetric beam pattern in integrable phase-modulating surface-emitting lasers, which showed static, arbitrary, two-dimensional beam pattern from on-chip size, while symmetric beam patterns are obtained in the conventional device.

SF1G.5 • 09:15

Direct generation of Laguerre-Gaussian beam with holographical phase-modulated surface-emitting lasers, Yu Takiguchi¹, Kazuyoshi Hirose¹, Takahiro Sugiyama¹, So Uenoyama¹, Yoshiro Nomoto¹, Yoshitaka Kurosaka¹; ¹Hamamatsu Photonics K.K., Japan. Holographically-designed Laguerre-Gaussian beam generation with surface emitting semiconductor lasers are demonstrated. Holographic information was inserted as resonator between the cladding layers. The Laguerre-Gaussian holograms was calculated in the form of complex-amplitude phase hologram.

CLEO: QELS-Fundamental Science

FF1H • Nanophotonic Strategies for Controlling Light-Matter Interaction—Continued

FF1H.3 • 08:45

In situ Real-Time Beam Monitoring with Dielectric Meta-Holograms, Yoav Blau¹, Michal Eitan¹, Victor Egorov¹, Amir Boag¹, Yael Hanein¹, Jacob Scheuer¹; ¹Tel-Aviv Univ., Israel. We propose and demonstrate novel meta-holograms for laser beam monitoring. These devices project a portion of the beam power to a screen, allowing for real-time monitoring of laser beam properties - position, astigmatism, and spot-size.

FF1H.4 • 09:00 **Invited**

Coherent Control of Light-matter Interactions in Standing Waves, Kevin F. MacDonald¹, Eric Plum¹, Daniele Faccio², Nikolay I. Zheludev^{1,3}; ¹Univ. of Southampton, UK; ²Univ. of Glasgow, UK; ³Nanyang Technological Univ., Singapore. In standing wave light fields, 'coherent control' of energy exchange, in ultrathin films and metasurfaces, between incident and scattered waves leads to new technological opportunities relevant to optical data processing, spectroscopy, and nonlinear/quantum optics applications.

Meeting Room
211 B/DMeeting Room
212 A/CMeeting Room
212 B/DMarriott
Salon III

CLEO: Science & Innovations

CLEO: Applications
& TechnologySF11 • Perovskites and
Organics—Continued

SF11.3 • 08:45

Highly Sensitive UV-Vis-NIR Inorganic Perovskite Quantum Dot Phototransistors Based on Layered Heterojunctions, Chen Zou¹, Yuyin Xi², Lilo D. Pozzo², Lih Y. Lin¹; ¹Electrical Engineering, Univ. of Washington, USA; ²Chemical Engineering, Univ. of Washington, USA. We report a high-performance phototransistor based on a layered heterojunction composed of all-inorganic perovskite quantum dots (IPQDs) and a narrow-bandgap conjugated polymer DPP-DTT. The device exhibits stable and excellent optoelectronic properties with broadband photodetection range.

SF11.4 • 09:00

Low Coherence Illumination of Flexible Perovskite Random Lasers, Yu-Chi Wang¹, Yu-Heng Hong¹, Kuo-Bin Hong¹, Tsung-Sheng Kao¹, Tien-Chang Lu¹; ¹National Chiao Tung Univ., Taiwan. We demonstrated that the methylammonium metal-halide perovskites can be exploited as a random laser source for the advanced speckle-free imaging. Furthermore, the lasing performance can be actively controlled via the mechanical modulation of supporting substrates.

SF11.5 • 09:15

Highly Efficient Energy Transfer Between TMDCs and Organic Materials, Chehsuan Cheng¹, Zidong Li¹, Parag Deotare¹; ¹Univ. of Michigan, USA. We demonstrate MoS₂ photodetectors sensitized with highly absorbing organic π -aggregate thin films. Förster resonance energy transfer (FRET) radius of 1.649 nm was estimated across the hybrid organic-inorganic interface.

SF11J • Metasurfaces—
Continued

SF11J.4 • 08:45

Large Area Tunable Alvarez Metalens via Stepper Photolithography, Shane A. Colburn¹, Alan Zhan¹, Arka Majumdar¹; ¹Univ. of Washington, USA. Using inexpensive and high-throughput stepper lithography, we design and fabricate 1 cm wide tunable metalenses which exhibit a focal length change of 162%, more than 6 cm, with only 2.4 mm lateral actuation.

SF11J.5 • 09:00

Directional Plasmonic Image Sensors for Lens-Free Compound-Eye Vision, Leonard Kogos¹, Lei Tian¹, Roberto Paiella¹; ¹Boston Univ., USA. We describe a novel lens-free camera technology inspired by the compound-eye vision modality that combines ultrathin plasmonic metasurfaces to enable angle-resolved photodetection with computational imaging for wide field-of-view image reconstruction.

SF11J.6 • 09:15

Intra-cavity metasurfaces for topologically spin-controlled laser modes, Elhanan Maguid¹, Ronen Chriki², Michael Yannai¹, Chene Tradonsky², Vladimir Kleiner¹, Erez Hasman¹, Asher Friesem², Nir Davidson²; ¹Technion-Israel Inst. of Technology, Israel; ²Dept. of Physics of Complex Systems, Weizmann Inst. of Science, Israel. We present the incorporation of a metasurface involving spin-orbit interaction phenomenon into a laser cavity paving the way for the generation of spin-controlled intra-cavity modes with different topologies.

SF11K • Hollow Core Fibers—
Continued

SF11K.4 • 09:00

Hollow-Core Negative-Curvature Fiber for High Energy Pulse Delivery at UV Wavelength, Shoufei Gao¹, Yingying Wang¹, Pu Wang¹, Wei Ding²; ¹Beijing Univ. of Technology, China; ²Lab of Optical Physics, Inst. of Physics, Chinese Academy of Sciences, China. We report a UV guiding hollow-core negative-curvature fiber with loss of 0.2 dB/m at 355 nm. This fiber enables, for the first time, picosecond pulse delivery up to 160 μ J at 355 nm with no damage observed.

SF11K.5 • 09:15

Polarization Evolution in Antiresonant Hollow Core Fibers, Nikhil Jayakumar¹, Rudrakant Sollapur¹, Andreas Hoffmann¹, Teodora Grigorova¹, Alexander Hartung², Anka Schwuchow², Joerg Bierlich², Jens Kobelke², Markus Schmidt^{2,3}, Christian Spielmann^{1,4}; ¹Friedrich Schiller Univ. Jena, Germany; ²Leibniz Inst. of Photonic Technology, Germany; ³Otto Schott Inst. of Material Research, Germany; ⁴Helmholtz Inst. Jena, Germany. We experimentally demonstrate that the ellipticity of light exiting antiresonant hollow core fibers is a function of the input polarization which manifests as ellipticity varying with the azimuthal periodicity of the cornered core.

AF11M • Fiber-Optic Based
Sensing—Continued

AF11M.3 • 08:45

Sensing applications of double hollow-core anti-resonant fiber based modal interferometer, Xiaosheng Huang¹, Seongwoo Yoo¹, Jichao Zang¹; ¹Nanyang Technological Univ., Singapore. In this work, sensing application of dual hollow-core anti-resonant fibers (DHAFs) is studied. DHAF based gas pressure sensor with 40 nm/MPa ultrahigh sensitivity is demonstrated.

AF11M.4 • 09:00

Angular Dependence in Coupling Lamb Waves to Optical Fiber Guided Modes, Junghyun Wee¹, Drew Hackney¹, Kara Peters¹; ¹North Carolina State Univ., USA. We investigate directional differences when coupling Lamb waves in a structure to guided modes in an optical fiber sensor for detection of the ultrasonic wave propagation through the structure.

AF11M.5 • 09:15

Multimode Interference Dynamic Light Scattering, Jose Guzman-Sepulveda¹, Aristide Dogariu¹; ¹CREOL, The College of Optics and Photonics, Univ. of Central Florida, USA. We present a robust implementation of a fiber-based, single-mode, common-path interferometer assisted by multimode interference effects in which light is efficiently collected from larger coherent regions while keeping a high signal-to-noise ratio.

CLEO: Science &
InnovationsSF1N • Ultrafast Mid-IR
Sources—Continued

SF1N.4 • 09:00

An all-fiber mid-infrared (6 – 9 μm) source based on difference frequency generation in OP-GaP crystal, Jaroslaw Z. Sotor¹, Tadeusz Martynkien¹, Peter G. Schunemann², Pawel Mergo³, Grzegorz J. Sobon¹; ¹Politechnika Wroclawska, Poland; ²BAE Systems, Inc, USA; ³Lab of Optical Fiber Technology, Maria Curie-Sklodowska Univ., Poland. We present an all-fiber source generating laser pulses in the 6 – 9 μm spectral range. The developed setup is based on difference frequency generation in the OP-GaP crystal and delivers 7.4 mW at 7600 nm.

SF1N.5 • 09:15

Generation of high-energy mid-infrared pulses at 3.3 μm by dual-chirped optical parametric amplification, Yuxi Fu¹, Kataro Nishimura¹, Bing Xue¹, Akira Suda², Katsumi Midorikawa¹, Eiji J. Takahashi¹; ¹RIKEN, Japan; ²Tokyo Univ. of Science, Japan. We generated 31 mJ mid-infrared pulses near 3.3 μm using a dual-chirped optical parametric amplification scheme. The pulse was compressed to 70 fs. We will further increase the energy to obtain multi-TW, few-cycle mid-infrared pulses.

CLEO: QELS-
Fundamental ScienceFF1P • Attosecond and X-Ray
Spectroscopy—Continued

FF1P.3 • 08:45

Attosecond Transient Absorption Spectroscopy near the $L_{2,3}$ -edge of Argon, Andrew Chew², Nicolas Douguet², Coleman Cariker², Jie Li², Xiaoming Ren², yanchun yin², Luca Argenti², Zenghu Chang², Wendell Hill¹; ¹Physics, Univ. of Maryland, College Park, USA; ²CREOL and Physics, Univ. of Central Florida, USA. We present an experimental investigation of attosecond transient absorption spectroscopy near the $L_{2,3}$ -edge of argon gas by using an attosecond pulse in the 240-250 eV range.

FF1P.4 • 09:00

Electron dynamics in transition metal dichalcogenides utilizing attosecond transient absorption spectroscopy, Alexander Guggenmos¹, Hung-Tzu Chang¹, Michael Zürich¹, Diana Y. Qiu^{2,3}, Romain Geneaux¹, Yen-Chang Chen^{4,5}, Xuan Wei⁵, Chang-Ming Jiang^{6,7}, Yufeng Liang⁴, Felipe H. da Jornada^{2,3}, Adam Schwartzberg⁴, David Prendergast⁴, Vincent C. Tung⁵, Steven G. Louie^{2,3}, Daniel M. Neumark^{1,6}, Stephen R. Leone^{1,2}; ¹Dept. of Chemistry, Univ. of California, Berkeley, USA; ²Dept. of Physics, Univ. of California, Berkeley, USA; ³Materials Sciences Division, Lawrence Berkeley National Lab, USA; ⁴Molecular Foundry, Lawrence Berkeley National Lab, USA; ⁵School of Engineering, Univ. of California, Merced, USA; ⁶Chemical Sciences Division, Lawrence Berkeley National Lab, USA; ⁷Joint Center of Artificial Photosynthesis, Lawrence Berkeley National Lab, USA. Strong enhancement of exciton binding has been observed in valence-excitons in the optical regime of 2D materials. We report direct observation of long-lived core-exciton states in transition metal dichalcogenides by attosecond transient absorption spectroscopy in the XUV.

FF1P.5 • 09:15

Optical Chirality for High Harmonic Generation, Ofer Neufeld^{1,2}, Oren Cohen^{1,2}; ¹Physics, Technion, Israel; ²Solid State Inst., Technion, Israel. We link the chirality of attosecond pulses with the chirality of the pump that drives them by extending the theory of optical chirality. We propose a chiral tri-circular pump that generates tunable highly helical attopulses.

CLEO: Applications
& TechnologyAF1Q • A&T Topical Review
on Scientific and Commercial
Progress in Semiconductor
Laser Technology II—Continued

AF1Q.3 • 08:45

Increase in Output Power of 8 μm Quantum Cascade Spiral Cavity Superluminescent Devices by Active Region Doping, Yezhezi M. Zhang¹, Mei C. Zheng¹, Abigail R. Pitarresi^{1,2}, Sara Kacmoli¹, Abanti Basak^{1,3}, Deborah Sivco^{1,4}, Claire F. Gmachl¹; ¹Princeton Univ., USA; ²Lafayette College, USA; ³Univ. of California, Santa Barbara, USA; ⁴Trumpf Photonics, Inc., USA. We report on 8 μm quantum cascade superluminescent emitters. Doping in the active region contributed to higher SL power of 7.5 mW; we obtained a coherence length of ~346 μm at maximum SL power.

AF1Q.4 • 09:00

Mid-infrared saturable absorber mirror (MIR-SAM) based on Dirac semimetal thin films, Lei Huang¹, Jiarong Qin¹, Yafei Meng¹, Chunhui Zhu¹, Yao Li¹, Yongbing Xu¹, Yi Shi¹, Frank (Fengqiu) Wang¹; ¹Nanjing Univ., China. We have for the first time fabricated a Dirac semimetal saturable absorber with a mirror structure. The centimeter-scale, SESAM-like device can operate across 3-5 μm , and mid-infrared pump-probe spectroscopy is used to study the nonlinear absorption characteristics.

AF1Q.5 • 09:15

Optically Pumped GeSn-edge-emitting Laser with Emission at 3 μm for Si Photonics, Wei Dou¹, Yiyin Zhou^{1,7}, Joe Margetis², Seyed Ghetmiri³, Wei Du⁴, Jifeng Liu⁵, Greg Sun⁶, Richard Soref⁶, John Tolle², Baohua Li⁷, Mansour Mortazavi³, Shui-Qing Yu¹; ¹Univ. of Arkansas, USA; ²ASM, LLC, USA; ³Dept. of Chemistry and Physics, Univ. of Arkansas at Pine Bluff, USA; ⁴Dept. of Electrical Engineering, Wilkes Univ., USA; ⁵Thayer School of Engineering, Dartmouth College, USA; ⁶Dept. of Engineering, Univ. of Massachusetts Boston, USA; ⁷Arktonics, LLC, USA. We presented optically pumped edge-emitting GeSn laser with 22.3% world-record maximum Sn content and 3 μm emission wavelength. Lasing threshold of 139 kW/cm² at 77 K and maximum operating temperature of 150 K were achieved.

Executive Ballroom
210ACLEO: Science &
Innovations

SF1A • Si Photonics—Continued

SF1A.6 • 09:30

Monolithically Integrated Holmium Lasers on Silicon Chips, Nanxi Li^{1,2}, Emir Magden¹, Zhan Su^{1,3}, Neetesh Singh¹, Alfonso Ruocco¹, Ming Xin¹, Matthew Byrd^{1,3}, Patrick Callahan¹, Jonathan Bradley^{1,4}, Diedrik Vermeulen^{1,3}, Michael Watts¹; ¹Research Lab of Electronics, MIT, USA; ²John A. Paulson School of Engineering and Applied Science, Harvard Univ., USA; ³Analog Photonics, USA; ⁴Dept. of Engineering Physics, McMaster Univ., Canada. We demonstrate holmium-doped DFB lasers monolithically integrated on silicon. Single mode lasing at wavelength from 2.02 to 2.10 μm with 15 mW maximum output power are reported. This work extends silicon-photonic microsystems beyond 2 μm .

SF1A.7 • 09:45

Quantum-dot nanolasers on Si photonic circuits, Alto Osada¹, Yasutomo Ota¹, Ryota Katsumi², Katsuyuki Watanabe¹, Satoshi Iwamoto^{1,2}, Yasuhiko Arakawa^{1,2}; ¹Inst. for Nano Quantum Information Electronics, The Univ. of Tokyo, Japan; ²Inst. of Industrial Science, The Univ. of Tokyo, Japan. We report the hybrid integration of quantum dot nanolasers on silicon photonic circuits using transfer printing. The pick-and-place assembly method facilitates the integration of two nanolasers on a single CMOS-processed waveguide that supports two-wavelength output.

Executive Ballroom
210BCLEO: QELS-
Fundamental ScienceFF1B • Quantum Enhanced
Measurements—Continued

FF1B.7 • 09:30

Distributed Quantum Sensing Using Continuous-Variable Multipartite Entanglement, Quntao Zhuang¹, Zhesen Zhang^{1,2}, Jeffrey H. Shapiro¹; ¹MIT, USA; ²Dept. of Materials Science and Engineering, Univ. of Arizona, USA. Continuous-variable multipartite entanglement, obtained from dividing a squeezed state between multiple nodes, is shown to enhance distributed field-quadrature displacement sensing. In the lossless case, its performance has Heisenberg scaling in the number of nodes.

FF1B.8 • 09:45

Manipulation of Two-Photon Interference by Entanglement, Polina Sharapova¹, Kai Hong Luo¹, Harald Herrmann¹, Matthias Reichelt¹, Torsten Meier¹, Christine Silberhorn¹; ¹Univ. of Paderborn, Germany. We demonstrate that entangled states are able to significantly extend the functionality of integrated Hong-Ou-Mandel interferometers and give rise an antibunching peak and rapid oscillation fringes with twice the optical frequency in the coincidence probability.

Executive Ballroom
210C

Joint

JF1C • Symposium on Lasers
in Accelerator Science and
Technology I—ContinuedJF1C.5 • 09:30 **Invited**

Linear-Field Particle Acceleration in Free Space by Spatiotemporally Structured Laser Pulses, Liang Jie Wong¹, Kyung-Han Hong², Sergio Carbajo³, Arya Fallahi⁴, Philippe Piot⁵, Marin Soljagic², John Joannopoulos³, Franz X. Kaertner⁴, Ido Kaminer⁶; ¹SIMTech, Singapore; ²MIT, USA; ³Stanford SLAC, USA; ⁴CFEL, Germany; ⁵Northern Illinois Univ., USA; ⁶Technion, Israel. We show that net energy transfer via linear-field forces, between a laser pulse and a bunch of multiple interacting electrons, can be realized in unbounded free space by engineering the spatiotemporal structure of light.

Executive Ballroom
210DCLEO: QELS-
Fundamental ScienceFF1D • Ultrafast Spectroscopy
of 2D Materials—Continued

FF1D.7 • 09:30

Ultrafast Dynamical Evolution of Anisotropic Response of Black Phosphorus under Magnetic Field, Wei Lu^{1,2}, Xuefeng Liu^{1,2}, Xiaoying Zhou^{3,4}, Yang Zhou³, Chenglong Zhang^{1,2}, Jiawei Lai^{1,2}, Shaofeng Ge^{1,2}, M. Chandra Sekhar^{1,2}, Shuang Jia^{1,2}, Kai Chang³, Dong Sun^{1,2}; ¹International Center for Quantum Materials, School of Physics, Peking Univ., China; ²Collaborative Innovation Center of Quantum Matter, China; ³SKLSM, Inst. of Semiconductors, Chinese Academy of Sciences, China; ⁴Dept. of Physics, Hunan Normal Univ., China. The dynamical evolution of anisotropy properties of black phosphorus (BP) under magnetic field is studied by polarization resolved mid-IR ultrafast transient reflection spectroscopy. We found magnetic field can efficiently adjust the anisotropy response of BP.

FF1D.8 • 09:45

Ultrafast quantum beats of linearly polarized excitons in two-dimensional ReS₂, Sangwan Sim^{1,3}, Doeon Lee¹, Artur Trifonov², Taeyoung Kim¹, Soonyoung Cha¹, Ji Ho Sung³, Sungjun Cho¹, Wooyoung Shim¹, Moon-Ho Jo³, Hyunyoung Choi¹; ¹Yonsei Univ., South Korea; ²Spin Optics Lab, Russia; ³Center for Artificial Low Dimensional Electronics Systems, IBS, South Korea. We observe quantum beats of excitons in atomically thin ReS₂. Our observation directly confirms the quantum coherence between anisotropic excitons which are linearly polarized with different orientations.

10:00–10:30 Coffee Break, Concourse Level

Executive Ballroom
210E

CLEO: QELS-Fundamental Science

FF1E • THz Generation and Novel Phenomena—Continued

FF1E.7 • 09:30

Optimizing the Nonlinear Optical Response of Plasmonic Metasurfaces, Yael Blechman¹, Euclides C. Almeida¹, Basudeb Sain¹, Yehiam Prior¹; ¹Weizmann Inst. of Science, Israel. We demonstrate that the enhancement of nonlinear optical processes in plasmonic nanomaterials cannot be fully predicted by their linear properties.

FF1E.8 • 09:45

Probing free-carrier recombination in silicon strip nano-waveguides, Ivan A. Aldaya^{1,2}, Andres Gil-Molina^{1,3}, Julian Pita³, Lucas Gabrielli³, Hugo Fragnito^{1,4}, Paulo C. Dainese¹; ¹Inst. of Physics, Univ. of Campinas, Brazil; ²State Univ. of Sao Paulo, Brazil; ³School of Electrical Engineering, Univ. of Campinas, Brazil; ⁴Mackgraphe, Mackenzie Presbyterian Univ., Brazil. We analyze recombination dynamics of photo-generated free-carriers in strip silicon nanowaveguides, revealing a highly nonlinear decay dynamics with a time-dependent lifetime ranging from 800ps at the beginning to 300ns at the end of the decay.

Executive Ballroom
210F

CLEO: QELS-Fundamental Science

FF1F • Spatial and Temporal Control of Light Using Metasurfaces—Continued

FF1F.6 • 09:30

Two-Color and 3D Phase-Amplitude Modulation Holograms, Adam C. Overvig¹, Sajjan Shrestha¹, Chang Xiao¹, Changxi Zheng¹, Nanfang Yu¹; ¹Columbia Univ., USA. We report a high-efficiency dielectric metasurface with continuous and arbitrary control of both amplitude and phase of one or two colors simultaneously. We numerically and experimentally demonstrate 2D and 3D holograms using such metasurfaces.

FF1F.7 • 09:45

Large-scale Metasurface Design using the Adjoint Sensitivity Technique, Mahdad Mansouree¹, Amir Arbabi¹; ¹Univ. of Massachusetts at Amherst, USA. We introduce a general technique for the design of metasurfaces composed of a large number of meta-atoms that enables efficient multifunctional metasurfaces. As a proof-of-concept, we demonstrate a metalens with 0.78NA and 74% focusing efficiency.

Executive Ballroom
210G

CLEO: Science & Innovations

SF1G • Surface Emitting Lasers—Continued

SF1G.6 • 09:30

Mixed-Cation Organic-Inorganic Halide Perovskite Thin Film Surface-Emitting Laser Enabled by Excitonic Gain, Songtao Chen¹, Arto Nurmikko¹; ¹Engineering, Brown Univ., USA. Cesium incorporated mixed-cation perovskite thin films are demonstrated as source of excitonic optical gain media, embedded within monolithic vertical cavity exploiting sputtered dielectric HfO₂/SiO₂ DBRs, realizing robust low threshold green lasing under optical pumping.

SF1G.7 • 09:45

A violet III-nitride vertical-cavity surface-emitting laser with a MOCVD-grown tunnel junction contact, Seunggeun Lee¹, Charles Forman², Changmin Lee², Jared Kearns², John T. Leonard², Daniel Cohen², James Speck², Shuji Nakamura^{1,2}, Steven DenBaars^{1,2}; ¹Dept. of Electrical and Computer Engineering, Univ. of California, Santa Barbara, USA; ²Materials Dept., Univ. of California, Santa Barbara, USA. We demonstrated a violet III-nitride vertical-cavity surface-emitting laser (VCSEL) with a GaN tunnel junction (TJ) contact grown by a metal-organic chemical vapor deposition (MOCVD) technique. A peak output power of 319 uW was achieved.

Executive Ballroom
210H

CLEO: QELS-Fundamental Science

FF1H • Nanophotonic Strategies for Controlling Light-Matter Interaction—Continued

FF1H.5 • 09:30

Physical random bit generation using mesoscopic chaos in silicon optomechanical oscillators, Ciwei Luo¹, Jia-Gui Wu^{1,2}, Shaojie Wang¹, Yongjiao Niu¹, Jaime G. Flor Flores², Mingbin Yu³, Guoqiang Lo³, Dim-Lim Kwong³, Shukai Duan¹, Chee-Wei Wong²; ¹Southwest Univ., College of Electronic and Information Engineering, China; ²Univ. of California, Los Angeles, Fang Lu Mesoscopic Optics and Quantum Electronics Lab, USA; ³Inst. of Microelectronics, Singapore. We propose a new physical random bit (PRB) generator using silicon micro-oscillator, which is configured with photonic-crystal optomechanical microcavity and fabricated with CMOS process. 200Mbit/s PRB was obtained and passed tests of NIST-SP800-22

FF1H.6 • 09:45

Nanophotonic light sails for relativistic spaceflight by high-power laser beams, Ognjen Ilic¹, Cora Went¹, Harry Atwater¹; ¹California Inst. of Technology, USA. We show that designed nanophotonic structures could become multiband building-block elements of a relativistic light sail, due to their ability to achieve substantial reflectivity and low absorption in the near-IR, significant emissivity in the mid-IR, and a very low mass.

10:00–10:30 Coffee Break, Concourse Level

Meeting Room
211 B/DMeeting Room
212 A/CMeeting Room
212 B/DMarriott
Salon III

CLEO: Science & Innovations

CLEO: Applications
& TechnologySF11 • Perovskites and
Organics—Continued

SF11.6 • 09:30 **Invited**
Patterning of Organic Micro/Nano-crystals for High-Performance Optoelectronic Devices, Jiansheng Jie¹; ¹*Inst. of Functional Nano and Soft Materials Lab (FUNSOM), Soochow Univ., China*. Organic micro/nanocrystals (OMNCs) are promising system to construct new-generation optoelectronic devices. However, the scale-up of OMNCs for technological applications is difficult. We developed a series of simple methods to produce patterned OMNCs for device applications.

SF1J • Metasurfaces—
Continued

SF1J.7 • 09:30
Bianisotropic All-dielectric Metasurfaces for Efficient Diffraction of Mid-infrared Electromagnetic Waves, Zhiyuan Fan¹, Maxim R. Shcherbakov¹, Gennady Shvets¹; ¹*Cornell Univ., USA*. We design and experimentally demonstrate a bianisotropic all-silicon metasurface with a near unity diffraction by implementing a 4-mode interference in the far field. Resonant and non-resonant properties of the modes and interactions can be mediated by sculpting meta-atoms of the metasurface.

SF1J.8 • 09:45
Self-Aligned Nano-Transfer of Metasurface Polarimeter to an Optical Fiber Tip using UV-Curable Hybrid Polymer, Michael Juhl^{1,2}, Carlos Mendoza¹, J. P. Balthasar Mueller³, Federico Capasso³, Kristjan Leosson^{1,2}; ¹*Innovation Center Iceland, Iceland*; ²*Univ. of Iceland, Iceland*; ³*Harvard John A. Paulson School of Engineering and Applied Sciences, USA*. We present a novel method of patterning an optical fiber facet using self-aligned nano-transfer of a gold pattern to a UV-curable hybrid polymer. We experimentally demonstrate a metasurface polarimeter on a 1550 nm single-mode fiber.

SF1K • Hollow Core Fibers—
Continued

SF1K.6 • 09:30
Mode transformation in an inhibited-coupling guiding asymmetric tubular hollow fiber, Jonas H. Osório¹, Matthieu Chafer^{1,2}, Benoît Debord^{1,2}, Fabio Giovanardi³, Martin Cordier⁴, Frédéric Delahaye¹, Luca Vincetti³, Frédéric Gérôme^{1,2}, Fetah Benabid^{1,2}; ¹*GPPMM Group, XLIM Research Inst., Univ. of Limoges, France*; ²*GLO Photonics, France*; ³*Univ. of Modena and Reggio Emilia, Italy*; ⁴*Télécom ParisTech, Université Paris-Saclay, France*. We report on mode transformation in an asymmetric tubular hollow fiber. We theoretically and experimentally show that LP₀₁ and LP₁₁ modes superposition entails an output profile with unusual spatially-separated orthogonal polarization sites.

SF1K.7 • 09:45
Low-Frequency Suppression of Classical Laser Fluctuations Using Hollow-Core Fibre, Euan Allen¹, Giacomo Ferranti¹, Dylan H. Mahler¹, Kristina Rusimova², Peter J. Mosley², Jonathan Matthews¹; ¹*Univ. of Bristol, UK*; ²*Univ. of Bath, UK*. We demonstrate classical laser amplitude noise suppression at 4.5 MHz using hollow-core free-boundary fibre. We attain suppression of 2.0 dB and get to within 0.2 dB of the shot-noise limit.

AF1M • Fiber-Optic Based
Sensing—Continued

AF1M.6 • 09:30
Inherent Signal Distortion in Dynamic Fiber-optic Interrogators Employing Frequency Scanning, Hari D. Bhatta¹, Roy Davidi¹, Moshe Tur¹; ¹*Tel Aviv Univ., Israel, Israel*. It is shown, theoretically and experimentally, that signal distortion is inherently present in dynamic fiber-optic strain sensing techniques, which use frequency scanning to determine the value of the measurand. The resulting harmonic distortion and ways to reduce it are described.

AF1M.7 • 09:45
Temperature-sensitivity enhancement in a tapered dual-core As₂Se₃-PMMA fiber with an antisymmetric long-period grating, Song Gao¹, Chams Baker¹, Liang Chen¹, Xiaoyi Bao¹; ¹*Univ. of Ottawa, Canada*. We report sensitivity enhancement of temperature measurement by a factor of 4.0 based on effective group-velocity matching between the even and odd modes of a dual-core chalcogenide-PMMA taper that is inscribed with an antisymmetric long-period grating.

10:00–10:30 Coffee Break, Concourse Level

Marriott
Salon IVCLEO: Science &
InnovationsSF1N • Ultrafast Mid-IR
Sources—Continued

SF1N.6 • 09:30

High Power Offset-free Ultrafast Mid-IR Source Harnessing SPM-enabled Spectral Selection, Gengji Zhou^{1,2}, Franz X. Kaertner^{1,2}, Guoqing Chang^{1,2}; ¹CFEL/DESY, Germany; ²Physics Dept., Universität Hamburg, Germany. We demonstrate a novel fiber approach for power scaling difference-frequency-generation based ultrafast mid-IR laser sources that are tunable from 7.4 μm to 16.8 μm with up to 5.3-mW average power at 9.3 μm .

SF1N.7 • 09:45

High-Power Harmonic Frequency Comb Covering the Mid-Infrared Molecular Fingerprint Region, Christian Gaida¹, Tobias Heuermann^{1,2}, Martin Gebhardt^{1,2}, Thomas Butler³, Daniel Gerz⁴, Lenard Vamos⁴, Ferenc Krausz^{3,4}, Jens Limpert^{1,5}, Joachim Pupeza³; ¹Inst. of Applied Physics, Germany; ²Helmoltz-Inst. Jena, Germany; ³Max Planck Inst. of Quantum Optics, Germany; ⁴Ludwig Maximilians Univ. Munich, Germany; ⁵Fraunhofer Inst. for Applied Optics and Precision Engineering, Germany. We present a multi-channel, 0.1 mW/THz-level, 50 MHz-repetition-rate harmonic frequency comb covering the spectral range 18.5 – 85 THz (or 3.5 – 16 μm , or 625 – 2860 cm^{-1}), based on intrapulse difference-frequency mixing within few-cycle, high-power 1.96 μm pulses.

Marriott
Salon VICLEO: QELS-
Fundamental ScienceFF1P • Attosecond and X-Ray
Spectroscopy—Continued

FF1P.6 • 09:30

Ultrafast Photo-Isomerization Dynamics Probed via Time-Resolved High-Harmonic Spectroscopy, Keisuke Kaneshima¹, Yuki Ninota¹, Taro Sekikawa¹; ¹Division of Applied Physics, Hokkaido Univ., Japan. Time-resolved high-harmonic spectroscopy (TR-HHS) of the photo-isomerization dynamics of 1,3-cyclohexadiene is demonstrated. The present results show that TR-HHS can track both the electronic and the nuclear dynamics, and is useful for unveiling ultrafast photochemical reactions.

Marriott
Willow GlenCLEO: Applications
& TechnologyAF1Q • A&T Topical Review
on Scientific and Commercial
Progress in Semiconductor
Laser Technology II—Continued

AF1Q.6 • 09:30

Room Temperature Operation of Directly Patterned Perovskite Distributed Feedback Light Source under Continuous-Wave Optical Pumping, Abouzar Gharajeh¹, Ross Haroldson¹, Zhitong Li¹, Jiyoung Moon¹, Balasubramaniam Balachandran¹, Walter Hu^{1,2}, Anvar Zakhidov^{1,3}, Qing Gu¹; ¹The Univ. of Texas at Dallas, USA; ²Microelectronics Dept., Fudan Univ., China; ³ITMO Univ., Russia. We report the first directly patterned perovskite distributed feedback (DFB) resonator with a narrow amplified spontaneous emission (ASE) at pump powers as low as 0.1W/cm², under continuous-wave (CW) optical pumping condition at room temperature.

AF1Q.7 • 09:45

Unusual Scaling Laws for Plasmonic Nanolasers, Suo Wang¹, Xing-Yuan Wang¹, Hua-Zhou Chen¹, Yi-Lun Wang¹, Lun Dai¹, Rupert Oulton², Renmin Ma¹; ¹Peking Univ., China; ²Imperial College London, UK. We report unusual scaling laws allowing plasmonic lasers with superior performances over photonic lasers at the nanoscale, which clarifies the long-standing debate over the viability of metal confinement and feedback strategies in laser technology.

10:00–10:30 Coffee Break, Concourse Level

Executive Ballroom
210ACLEO: Science &
Innovations

10:30–12:30

SF2A • Nonlinear Photonics in
Integrated Structures

Presider: Gregory Moille; NIST/
UMD, USA

SF2A.1 • 10:30

Quantum frequency conversion using nano-photonics, Qing Li^{1,2}, Anshuman Singh^{1,2}, Xiyuan Lu^{1,2}, Varun Verma³, Richard Mirin³, Sae Woo Nam³, Kartik Srinivasan¹; ¹CNST, NIST, USA; ²Univ. of Maryland, USA; ³PML, NIST, USA. We demonstrate quantum frequency conversion of photon pairs, with both pair generation and frequency conversion implemented in Si₃N₄ microrings. Quantum correlations between the signal and idler are preserved, with an on-chip conversion efficiency around 25%.

SF2A.2 • 11:00

Observation of Second Harmonic and Sum Frequency in an Optically Poled Si₃N₄ Waveguide, Davide Grassani¹, Adrien Bilal¹, Martin Pfeiffer², Tobias J. Kippenberg², Camille-Sophie Bres³; ¹Photonic System Lab (PHOSL), Ecole Polytechnique Federale de Lausanne, Switzerland; ²Lab for Photonics and Quantum Measurements (LPQM), Ecole Polytechnique Federale de Lausanne, Switzerland. Enhanced second order nonlinear processes in a Si₃N₄ waveguide following optically induced $\chi^{(2)}$ is demonstrated, enabling the detection of a frequency doubled pulsed train and SFG with >-37 dB conversion efficiency for 18 W pump peak power.

Executive Ballroom
210B

Joint

10:30–12:30

JF2B • Symposium on Emerging
Quantum Sensing Techniques
and Applications I

Presider: TBD

JF2B.1 • 10:30 **Invited**

Quantum Sensing and Imaging with Diamond Spins, Ania Bleszynski Jayich¹, Alec Jenkins¹, Susanne Baumann¹, Dolev Bluvstein¹, Simon Meynell¹, Amila Ariyaratne¹; ¹Univ. of California Santa Barbara, USA. The diamond nitrogen-vacancy (NV) center quantum sensor features excellent spatial resolution, sensitivity, and versatility. I discuss recent developments in NV-based imaging of condensed matter systems and ongoing developments in improving the NV center's functionality.

JF2B.2 • 11:00 **Invited**

Quantum Metrology with Rydberg Atoms, Sebastien Gleyzes¹, Eva-Katharina Dietsche¹, Arthur Larrouy¹, Serge Haroche¹, Jean-Michel Raimond¹, Michel Brune¹; ¹Laboratoire Kastler Brossel, Collège de France, CNRS, ENS-PSL Univ., Sorbonne Université, France. I will present how we can use non-classical states of Rydberg atom to measure fast variations of the electric or magnetic field with a precision close to the Heisenberg limit.

Executive Ballroom
210C

10:30–12:30

JF2C • Symposium on Lasers
in Accelerator Science and
Technology II

Presider: Peter Hommelhoff,
Friedrich-Alexander-Universität
Erlangen, Germany

JF2C.1 • 10:30 **Invited**

Laser-shaping of Electron Beams for X-ray Free-electron Laser Applications, Agostino Marinelli¹; ¹SLAC National Accelerator Lab, USA. From seeding to laser-based electron bunch compression, to the generation of attosecond X-ray pulses, conventional lasers are ubiquitous in X-ray free-electron laser facilities. In my talk I will give an overview of advanced XFELs schemes involving the use of high-power lasers.

JF2C.2 • 11:00

Multi-kW Average Power Thin Disk -Slab Ti:Sa Amplifiers, Vladimir V. Chvykov¹, Roland Nagymihály¹, Huabao Cao¹; ¹ELI-HU Non-Profit Ltd., Hungary. Ti:Sapphire thin disc is suitable for ultrafast lasers of kW average power, Js pulse energy. Simulations show the changing geometry of direct CW diodes pumped amplifiers from TD to slab can improve efficiency and heating extraction.

Executive Ballroom
210DCLEO: QELS-
Fundamental Science

10:30–12:30

FF2D • THz Electrodynamics
and control of Electronic
Degrees of Freedom

Presider: Bachana Lomsadze;
Univ. of Michigan, USA

FF2D.1 • 10:30

Coherent Terahertz Excitation of Magnons to 30 T, Gary T. Noe¹, Xinwei Li¹, Jeffrey Horowitz¹, Katsumasa Yoshioka², Ning Yuan³, Maolin Xiang³, Kai Xu³, Zuanming Jin³, Shixun Cao³, Hiroyuki Nojiri⁴, Ikufumi Katayama², Jun Takeda², Dmitry Turchinovich^{5,6}, Junichiro Kono¹; ¹Rice Univ., USA; ²Yokohama National Univ., Japan; ³Shanghai Univ., China; ⁴Tohoku Univ., Japan; ⁵Univ. Duisburg-Essen, Germany; ⁶Max Planck Inst. for Polymer Research, Germany. We have performed terahertz time-domain magneto-spectroscopy measurements on canted antiferromagnet YFeO₃ in pulsed high magnetic fields up to 30 T, observing coherent magnon oscillations and frequency splitting.

FF2D.2 • 10:45

Magneto -THz spectroscopy in spinel superconductors LiTi₂O₄ thin films, Yue Huang¹, Jie Yuan², Kui Jin², Wei Zhang¹, Kimberly Reichel¹, Daniel M. Mittleman¹; ¹Brown Univ., USA; ²Inst. of Physics, Chinese Academy of Sciences, China. We observed a clear superconducting gap at 2.0meV and a coherent peak in the strong spin fluctuation compounds LiTi₂O₄ using continuous wave (CW) terahertz spectroscopy. The superconducting state was strongly suppressed by magnetic fields.

FF2D.3 • 11:00 **Invited**

Quantum Manipulation of Competing Phases by Terahertz Pulses, Jigang Wang¹; ¹Iowa State Univ., USA. We reveal a hidden quantum phase of prethermalized, gapless electron fluid, which evolves following single-cycle, resonant terahertz quench of the SC gap above a critical fluence and implies novel organization principles beneath superconductivity.

CLEO: QELS-Fundamental Science

CLEO: Science & Innovations

CLEO: QELS-Fundamental Science

10:30–12:30

FF2E • Novel Nonlinear Optical Materials

Presider: David Hagan; CREOL, Univ. of Central Florida, USA

FF2E.1 • 10:30

Enhancement Mechanism of Nonlinear Optical Response of Transparent Conductive Oxides at Epsilon-Near-Zero, Sepehr Benis¹, David J. Hagan¹, Eric W. Van Stryland¹; ¹Univ. of Central Florida, CREOL, USA. Transient nondegenerate nonlinear refraction of Indium Tin Oxide has been characterized in the near-infrared using femtosecond Beam-Deflection with independently tuned excitation and probe. ENZ enhancement depends more strongly on the probe wavelength than the excitation.

FF2E.2 • 10:45

Graphene Electrically Tuneable Third Harmonic Generation, Giancarlo Soavi¹, Gang Wang¹, Habib Rostami², David Purdie³, Domenico De Fazio¹, Teng Ma¹, Birong Luo¹, Junjia Wang¹, Anna K. Ott¹, Duhee Yoon¹, Sean Bourelle¹, Jakob E. Muench¹, Ilya Goykhman³, Stefano Dal Conte⁴, Michele Celebrano⁴, Andrea Tomadin⁵, Marco Polini⁵, Giulio Cerullo⁴, Andrea Ferrari¹; ¹Cambridge Graphene Centre, Univ. of Cambridge, UK; ²Nordic Inst. for Theoretical Physic, Sweden; ³Electrical Engineering, Israel Inst. of Technology, Israel; ⁴Dipartimento di Fisica, Politecnico di Milano, Italy; ⁵Istituto Italiano di Tecnologia, Graphene Labs, Italy. Graphene displays electrically and broadband tunable third order nonlinear susceptibility. Third harmonic generation efficiency in graphene can be tuned by two orders of magnitude by controlling the Fermi energy and the incident photon energy.

FF2E.3 • 11:00

Electrically Tunable Nonlinear Refraction and Absorption in Graphene-covered SiN Waveguides, Koen Alexander^{1,2}, Bart Kuyken^{1,2}, Dries VanThourhout^{1,2}; ¹Photonics Research Group, INTEC, Ghent Univ.-imec, Belgium; ²Center for Nano- and Biophotonics (NB-Photonics), Ghent Univ., Belgium. The real and imaginary part of the third-order nonlinearity of a gate-tunable graphene-covered SiN waveguide are measured through cross-phase and cross-amplitude modulation. A strong dependence on pump-probe detuning and Fermi energy is demonstrated.

10:30–12:30

FF2F • Fundamental Nanophotonics: Sensing and Infrared Applications

Presider: Ognjen Ilic; California Inst. of Technology, USA

FF2F.1 • 10:30

Revisiting the Photon-Drag Effect in Thin Metal Films, Jared Strait¹, Glenn Holland¹, B. Robert Ilic¹, Amit K. Agrawal^{1,2}, Domenico Pacifici^{1,3}, Henri Lezec¹; ¹Center for Nanoscale Science and Technology, National Inst. of Standards and Technology, USA; ²Maryland NanoCenter, Univ. of Maryland, USA; ³School of Engineering and Dept. of Physics, Brown Univ., USA. We demonstrate that the sign of the photon-drag effect in smooth gold films is crucially dependent on the surface environment and contrary to the prevailing intuitive model of direct momentum transfer to free electrons.

FF2F.2 • 10:45

Plasmon Drag Effect and Opportunities for Sensing Applications, Natalia Noginova¹, Tejaswini Ronurpraful¹, Nelly Jerop¹, David Keene¹, Maxim Durach²; ¹Norfolk State Univ., USA; ²Georgia Southern Univ., USA. Photoinduced voltages in profile-modulated plasmonic surfaces demonstrate sharp dependence on the incidence angle and are very sensitive to dielectric environment, which provides opportunities for applications in compact plasmonic sensors with electrical detection.

FF2F.3 • 11:00

Optical Sensing with Anderson-Localized Light, Oliver J. Trojak¹, Tom Crane¹, Luca Sapienza¹; ¹Dept. of Physics and Astronomy, Univ. of Southampton, UK. We demonstrate optical sensing with Anderson-localized visible light on scalable silicon nitride photonic crystal waveguides. For a refractive index change of ≈ 0.38 , we measure 15.2 nm wavelength shifts of an optical resonance 0.15 nm broad.

10:30–12:30

SF2G • Mid-infrared Semiconductor Lasers

Presider: Dan Botez; Univ. of Wisconsin-Madison, USA

SF2G.1 • 10:30

Dual-comb spectroscopy with passively mode-locked interband cascade laser frequency combs, Lukasz A. Sterczewski^{1,2}, Jonas Westberg¹, Mahmood Bagheri², Clifford Frez², Igor Vurgafman³, Chadwick Canedy³, William W. Bewley³, Charles D. Merritt³, Chul Soo Kim³, Mijin Kim⁴, Jerry R. Meyer³, Gerard Wysocki⁵; ¹Princeton Univ., USA; ²Jet Propulsion Lab, California Inst. of Technology, USA; ³Naval Research Lab, USA; ⁴Sotera Defense Solutions, USA. We demonstrate dual comb spectroscopy using free running passively mode-locked interband cascade laser frequency combs by measuring methane around 3.6 μm with 100 μs acquisition time and an instantaneous optical bandwidth of 570 GHz.

SF2G.2 • 10:45

Ring Interband Cascade Lasers, Martin Holzbauer¹, Borislav Hinkov¹, Rolf Szedlak¹, Hermann Detz², Robert Weih³, Sven Höfling^{4,5}, Werner Schrenk¹, Erich Gornik¹, Johannes Koeth³, Gottfried Strasser¹; ¹TU Wien, Austria; ²Austrian Academy of Sciences, Austria; ³nanoplus Nanosystems and Technologies GmbH, Germany; ⁴Univ. of Würzburg, Germany; ⁵Univ. of St Andrews, UK. We present ring-shaped interband cascade lasers with light emission through the GaSb substrate. Measurements of the projected nearfields revealed a radial polarization, owing to the nature of the optical interband transitions.

SF2G.3 • 11:00 **Invited**

Mid-IR Optoelectronic Devices Epitaxially Grown on Silicon, Eric Tournie¹; ¹Univ. of Montpellier, France. Integrated optoelectronic devices are key technologies for Si photonics. I will review recent results in show that GaSb-based mid-IR devices epitaxially grown on Si substrates which exhibit high performances and are promising candidates for future on-chip sensing solutions.

10:30–12:30

FF2H • Interference and Localization Phenomena in Complex Media

Presider: Alexey Yamilov; Missouri Univ. of Science & Technology, USA

FF2H.1 • 10:30

Wide spectral tuning range in an Anderson localizing fiber laser, Behnam Abaie¹, Thomas Hawkins^{1,2}, John Ballato², Arash Mafi¹; ¹Univ. of New Mexico, USA; ²Clemson Univ., USA. Wavelength sensitivity of Anderson localized modes in a disordered optical fiber is exploited to obtain a tunable fiber laser. The lasing wavelength varies upon excitation of various localized modes across the fiber.

FF2H.2 • 10:45

Eradicated Coherent Backscattering of Anderson Localized Modes, Alex Dikopoltsev¹, Hanan Herzig Sheinfux^{2,1}, Mordechai Segev¹; ¹Technion, Israel; ²ICFO, Spain. Coherent backscattering is a recognized precursor of Anderson localization. But, we show that waves in certain types of disordered potentials can undergo Anderson localization, without exhibiting any coherent backscattering at all

FF2H.3 • 11:00 **Tutorial**

Wave Engineering in Complex Media, Stefan Rotter¹; ¹Technische Universität Wien, Austria. I will give an overview of new concepts for engineering light waves in complex media based on shaping either their external wave-front or the spatial structure of gain and loss components inside these media.



Stefan Rotter is professor for Theoretical Physics at Vienna University of Technology (TU Wien) in Austria. After studies in Vienna and Lausanne, he worked as a postdoc at Yale. Since 2011 he runs his own group focused on waves in disordered media, non-Hermitian physics, and quantum optics.

Friday, 10:30–12:30

CLEO: Science & Innovations

CLEO: QELS-
Fundamental Science

10:30–12:30
SF21 • **Electrooptic and Nanophotonic Materials**
President: Tian Gu; MIT, USA

SF21.1 • 10:30
A Breakthrough leading to a New Type of E-O Materials Electro-Elasto-Optical Properties of EEO Crystals (PMN-PT Based Relax Ferroelectric Crystals) by Special Modifications, Pengdi Han¹; ¹EEOptics Corp., USA. Important findings from a systematic investigation on Electro-Elasto-Optical characterization for PMN-PT based ferroelectric crystals. The new E-O material is biaxial EEO crystal with $N_o=2.564$, $N_m=2.558$, $N_p=2.545$, $2V=109^\circ$ and effective EO-coefficient g_c over 300~600pm/V and V_p less than 100V.

SF21.2 • 10:45
Periodic Poling of Ion-Sliced X-Cut Magnesium Oxide Doped Lithium Niobate Thin Films, Jonathan T. Nagy¹, Ronald M. Reano¹; ¹The Ohio State Univ., USA. We fabricate and periodically pole 700 nm thick ion-sliced x-cut magnesium oxide doped lithium niobate thin films. Uniform domains with 50% duty cycle are imaged by piezo-response force microscopy.

SF21.3 • 11:00
Ultrahigh-Q Lithium Niobate Microring Resonator, Mian Zhang¹, Cheng Wang¹, Rebecca Cheng^{1,2}, Amirhassan Shams-Ansari^{1,3}, Marko Loncar¹; ¹John A. Paulson School of Applied and Engineering Sciences, Harvard Univ., USA; ²Dept. of Physics, Brown Univ., USA; ³Dept. of Electrical Engineering and Computer Science, Howard Univ., USA. We demonstrate ultralow loss monolithic integrated lithium niobate photonic platform consisting of dry-etched subwavelength waveguides. We show microring resonators with a quality factor of 10^7 and waveguides with propagation loss as low as 2.7 dB/m.

10:30–12:30
SF2J • **Cavity Optomechanics**
President: Karen Grutter; Univ. of Maryland at College Park, USA

SF2J.1 • 10:30
Optomechanically Mediated Wavelength Conversion in Diamond Microdisks, Matthew Mitchell^{1,2}, David P. Lake^{1,2}, Paul E. Barclay^{1,2}; ¹Inst. for Quantum Science & Tech., Canada; ²NRC - National Inst. for Nanotechnology, Canada. Optomechanically mediated wavelength conversion in a single-crystal diamond microdisk operating in the resolved sideband regime is demonstrated. Frequency down-conversion is demonstrated with an expected internal conversion efficiency of ~ 45%.

SF2J.2 • 11:00
Diamond Optomechanical Crystals at Cryogenic Temperatures, Cleaven Chia¹, Srujan Meesala¹, Nayera El-Sawah^{1,2}, Bartholomeus J. Machielse³, Michael J. Burek¹, Marko Loncar¹; ¹John A. Paulson School of Engineering and Applied Sciences, Harvard Univ., USA; ²Univ. of Waterloo, Canada; ³Dept. of Physics, Harvard Univ., USA. We investigate the properties of optomechanical crystals (OMCs) fabricated in single-crystal diamond in a cryogenic environment (T ~ 5K). We demonstrate high mechanical Q-factors (> 100,000) from localized OMC mechanical modes at 5 & 8 GHz, a 30x improvement from room temperature.

10:30–12:30
SF2K • **Novel Fiber Technology**
President: Sze Set; Univ. of Tokyo, Japan

SF2K.1 • 10:30 **Invited**
SNAP: Subangstrom Precise and Ultralow Loss Nanophotonic Platform, Misha Sumetsky¹; ¹Aston Univ., UK. The review of fundamentals, recent results, and prospects of Surface Nanoscale Axial Photonics (SNAP), which includes ultralow-loss slow light delay lines and buffers, tunable, optomechanical and optofluidic microresonators, microlasers, and frequency comb generators, is presented.

SF2K.2 • 11:00
Harmonic SNAP Bottle Microresonators Produced via Tapering of Optical Fibers, Dashiell L. Vitullo¹, Gabriella Gardosi¹, Sajid Zaki¹, Kirill Tokmakov¹, Michael Brodsky², Misha Sumetsky¹; ¹Aston Univ., UK; ²U.S. Army Research Lab, USA. We demonstrate fabrication of SNAP microresonators with parabolic profiles via fiber tapering with a laser-heated microfurnace. The developed method enables simple and convenient fabrication of prospective frequency comb generators and miniature dispersionless SNAP delay lines.

10:30–12:30
FF2L • **Polaritons in 2D Materials**
President: Peter Liu; Sandia National Labs Albuquerque, USA

FF2L.1 • 10:30
Valley-controlled directional coupling to plasmonic nanowire modes, Su-Hyun Gong^{1,2}, Filippo Alpeggiani^{1,2}, Beniamino Sciacca², Erik C. Garnett², Laurens K. Kuipers^{1,2}; ¹Delft Univ. of Technology, Netherlands; ²AMOLF, Netherlands. We demonstrate the valley/spin-dependent directional emission of transition metal chalcogenides (TMDs) into plasmonic eigenstates of a silver nanowire through spin-orbit coupling of light.

FF2L.2 • 10:45
Topological Valley Transport of Infrared Plasmons on a Nanoscale in Metagated Graphene, Minwoo Jung², Zhiyuan Fan¹, Gennady Shvets¹; ¹School of Applied and Engineering Physics, Cornell Univ., USA; ²Dept. of Physics, Cornell Univ., USA. We propose an electrically tunable plasmonic platform for valleytronics---a monolayer graphene with its chemical potential controlled by a periodically structured metagate. Topologically protected edge states show reflection-free propagation around sharp corners.

FF2L.3 • 11:00
Inducing Indirect Optical Transitions Using Graphene Plasmons, Yaniv Kurman¹, Nicholas Rivera², Thomas Christensen², Shai Tseses¹, Meir Orenstein¹, Marin Soljacic², John Joannopoulos², Ido Kaminer^{1,2}; ¹Electrical Engineering, Israel Inst. of Technology, Israel; ²Physics, MIT, USA. We show that graphene placed near a quantum-well induces a pronounced shift in the emission/absorption frequency. The high momenta of graphene plasmons reaches the electron's momenta, enabling indirect optical transitions and inducing structural nonlocal properties.

Marriott
Salon III

CLEO: Applications
& Technology

10:30–12:30

AF2M • Imaging & Microscopy

President: Kara Peters; North
Carolina State Univ., USA

AF2M.1 • 10:30

Broadband spectral-focusing CARS of pharmaceutical drugs, Jeremy G. Porquez¹, Aaron D. Slepko¹, ¹Trent Univ., Canada. We apply supercontinuum-Stokes-based spectral-focusing CARS hypermicroscopy for chemical identification and 3D imaging of pharmaceutical powder samples. A wide spectral scan range, combined with facile epi-detection, allows for strong progress toward quantitative drug assaying with CARS.

AF2M.2 • 10:45

Distributed Pulsation Waveform Inspection to Radial Artery with Shadow Moiré fringe, Chun-Hsiung Wang¹, Yu-Hsiang Hsu¹, Shu-Sheng Lee², Wen-Jung Wu¹, Chih-Kung Lee¹; ¹National Taiwan Univ., Taiwan; ²National Taiwan Ocean Univ., Taiwan. A non-invasive full-field arterial-induced skin vibration inspection system is developed based on Shadow Moiré, 2D Continuous Wavelet Transform and Region of Interest techniques. Pulsation profiles obtained can be used for potential diagnostic use.

AF2M.3 • 11:00

Deep tissue, wide-field multiphoton imaging using TEMPIX, Adria Escobet-Montalban¹, Roman Spesyvtsev¹, Mingzhou Chen¹, Wardiya Afshar², Melissa Andrews³, Simon Herrington⁴, Michael Mazilu¹, Kishan Dholakia¹; ¹School of Physics and astronomy, Univ. of St Andrews, Univ. of St Andrews, UK; ²School of Medicine, Univ. of St Andrews, UK; ³Biological Sciences, Univ. of Southampton, UK; ⁴Inst. of Genetics and Molecular Medicine, Univ. of Edinburgh, UK. We demonstrate a new approach, temporal focusing microscopy with single-pixel detection (TEMPPIX), for wide-field multiphoton imaging through scattering media without any *a priori* knowledge or requirement to determine the properties of the media.

Marriott
Salon IV

CLEO: Science & Innovations

10:30–12:30

SF2N • Ultrafast Oscillators

President: Bojan Resan; Univ.
of Applied Sciences FHNW,
Switzerland

SF2N.1 • 10:30

Sub-100 fs pulse generation from a Tm,Ho:CALYO laser mode-locked by a GaSb-based SESAM at ~2043 nm, Yongguang Zhao^{2,1}, Yicheng Wang², Xuzhao Zhang³, Xavier Mateos³, Zhongben Pan^{1,2}, Pavel Loiko⁵, Wei Zhou¹, Xiaodong Xu¹, Xu Jun⁶, Deyuan Shen¹, Soile Suomalainen⁷, Antti Härkönen⁷, Mircea D. Guina⁷, Uwe Griebner², Valentin Petrov²; ¹Jiangsu Normal Univ., Germany; ²Max-Born-Inst. for Non-linear Optics and Ultrafast Spectroscopy, Germany; ³Universitat Rovira i Virgili (URV), Spain; ⁴China Academy of Engineering Physics, China; ⁵ITMO Univ., Russia; ⁶Tongji Univ., China; ⁷Tampere Univ. of Technology, Finland. We report on the first sub-100-fs mode-locked Ho³⁺-laser in the 2- μ m spectral range. The disordered co-doped Tm,Ho:CaYAlO₄ (Tm,Ho:CALYO) crystal produced pulses as short as 87 fs with 27-mW average output power at 80.45-MHz repetition rate.

SF2N.2 • 10:45

Sub-120 fs Kerr-lens Mode-locked Tm:Sc₂O₃ Laser In-band pumped by an Er:Yb fiber MOPA, Masaki Tokurakawa¹, Eisuke Fujita¹, Christian Kraenkel^{2,3}; ¹Univ. of Electro-communications, ILS, Japan; ²Zentrum für Lasermaterialien, Leibniz-Institut für Kristallzüchtung, Germany; ³Institut für Laser-Physik, Universität Hamburg, Germany. We demonstrate a Kerr-lens mode-locked Tm:Sc₂O₃ laser in-band pumped by a 1611 nm Er-fiber laser. 115 fs pulses with 42.6 nm spectral bandwidth are obtained. The output power and repetition rate are 420 mW and 95 MHz, respectively.

SF2N.3 • 11:00 **Invited**

Frontiers in Ultrafast Thin-Disk Laser Oscillators, Clément Paradis¹, Norbert Modsching¹, Maxim Gaponenko¹, François Labaye¹, Valentin J. Wittwer¹, Thomas Südmeyer¹; ¹Laboratoire Temps-Fréquence, Université de Neuchâtel, Switzerland. Ultrafast thin-disk lasers continue achieving higher average powers and pulse energies than other oscillator technologies. We discuss performance scaling and the ongoing race towards shorter durations, which recently resulted in 30-fs from Yb-based thin-disk lasers.

Marriott
Salon VI

CLEO: QELS-
Fundamental Science

10:30–12:30

FF2P • High-order Harmonic
Generation in Solids

President: Alexis Chacon; Los
Alamos National Lab , USA

FF2P.1 • 10:30 **Tutorial**

High Harmonics from Solids and Gases., Paul B. Corkum^{1,2}; ¹Univ. of Ottawa, Canada; ²National Research Council of Canada, Canada. Experiments and models show that intense light irradiating transparent solids or gases creates a sequence of harmonics extending to photon energies >1 keV in gases and >H₂₉ in solids. The same process creates attosecond pulses.



Corkum holds a Canada Research Chair at the University of Ottawa and directs the Joint NRC/University of Ottawa Attosecond Science Laboratory. He is a member of the Royal Societies of London and of Canada, also a foreign member of the US National Academy of Science and of the Austrian Academy of Science.

Marriott
Willow Glen

CLEO: Applications
& Technology

10:30–12:30

AF2Q • A&T Topical Review
on Time-Stretch Technology:
Principles and Applications I

President: Hongwei Chen;
Tsinghua University, China

AF2Q.1 • 10:30 **Invited**

Real-time Measurements of Nonlinear Instabilities in Optical Fibers, Piotr Ryzkowski¹, Mikko Närhi¹, Cyril Bilet², Jean-Marc Merolla², John M. Dudley², Goëry Genty¹; ¹Tampereen Teknillinen Yliopisto, Finland; ²Institut FEMTO ST, France. We review recent advances in the real-time characterization of instabilities in nonlinear fiber optics systems. In particular, we show how these techniques can provide novel insight into the dynamics of ultrafast complex optical systems.

AF2Q.2 • 11:00 **Invited**

Demonstration of GHz-band RF receiver and spectrometer using random speckle patterns, Adam Scofield¹; ¹The Aerospace Corporation, USA. We report experimental demonstrations of compressive sensing with photonic systems in which the measurement matrices are implemented using speckle in multimode waveguides. We calibrate by measuring a dictionary of single frequency RF sinusoids.

Friday, 10:30–12:30

Executive Ballroom
210A

CLEO: Science &
Innovations

SF2A • Nonlinear Photonics
in Integrated Structures—
Continued

SF2A.3 • 11:15

Broadband parametric down-conversion in an X-cut lithium niobate microresonator, Rui Luo¹, Haowei Jiang^{1,2}, Steven Rogers¹, Hanxiao Liang¹, Yang He¹, Qiang Lin¹; ¹Univ. of Rochester, USA; ²Shanghai Jiao Tong Univ., China. We report spontaneous parametric down-conversion with a bandwidth of about 400 nm in a high-Q lithium niobate microdisk resonator. The broadband feature is enabled by cyclic phase matching in an X-cut microresonator.

SF2A.4 • 11:30

Four-Wave Mixing in GaN Waveguides, Dvir Munk¹, Moshe Katzman¹, Ohad Westreich^{3,2}, Moran Bin Nun², Yedidya Lior², Noam Sicon³, Yossi Paltiel², Avi Zadok¹; ¹Bar-Ilan Univ., Israel; ²Hebrew Univ., Israel; ³Soreq NRC, Israel. Four-wave mixing at 1550 nm wavelength is demonstrated in a GaN ridge waveguide for the first time. A nonlinear coefficient of 1.6 ± 0.45 [W²m]⁻¹ is measured. The nonlinear parameter of GaN is estimated as $3.4 \pm 1e-18$ [m²/W].

SF2A.5 • 11:45

CMOS-compatible, low-loss deuterated silicon nitride photonic devices for optical frequency combs, Jeff Chiles¹, Nima Nader¹, Daniel Hickstein¹, Su Peng Yu¹, Travis C. Briles¹, David R. Carlson¹, Hojoong Jung¹, Jeffrey Shainline¹, Scott A. Diddams¹, Scott Papp¹, Sae Woo Nam¹, Richard Mirin¹; ¹NIST, USA. We demonstrate plasma-deposited (temperature < 300°C), deuterated silicon nitride waveguides with 0.22 dB/cm propagation loss at $\lambda = 1552$ nm. Pumping at $\lambda = 1560$ nm, we obtain a 550 nm-bandwidth Kerr-microcomb and octave-spanning supercontinuum.

Executive Ballroom
210B

Joint

JF2B • Symposium on Emerging
Quantum Sensing Techniques
and Applications I—Continued

JF2B.3 • 11:30

Atomic Force Microscopy Beyond the Standard Quantum Limit, Benjamin Lawrie¹, Raphael C. Pooser¹; ¹Quantum Information Science Group, Oak Ridge National Lab, USA. We explore the impact of quantum noise reduction on force microscopy for broadband off-resonant materials characterization by integrating a multi-spatial-mode squeezed state as the readout field in a commercially available microscope.

JF2B.4 • 11:45

Quantum Enhanced Joint Multi-Parameter Measurement, Jiamin Li¹, Yuhong Liu¹, Liang Cui¹, Nan Huo¹, Xiaoying Li¹, Z.Y. Ou^{2,1}; ¹Tianjin Univ., China; ²Indiana Univ.-Purdue Univ. Indianapolis, USA. We study simultaneously measure the multiple non-commuting observables by using the SU(1,1) nonlinear interferometer, and show that joint measurement of each non-commuting observables can achieve a sensitivity beating the standard quantum limit.

Executive Ballroom
210C

JF2C • Symposium on Lasers
in Accelerator Science and
Technology II—Continued

JF2C.3 • 11:15

Laser Heater Shaping for Microbunching Instability Suppression in Free Electron Lasers, Nikolas Liebster^{1,2}, Jingyi Tang^{1,2}, Zhirong Huang^{1,2}, Daniel Ratner^{1,2}, Wei Liu^{1,2}, Sharon Vetter^{1,2}, Sergio Carbajo^{1,2}; ¹SLAC National Accelerator Lab, USA; ²Stanford Univ., USA. We present two laser heater shaping solutions based on Laguerre-Gaussian and discrete beamlet array distributions that significantly outperform current microbunching instability suppression approaches in free-electron lasers

JF2C.4 • 11:30

Invited
Light Sources from Laser Wakefield Acceleration: Development and Applications, F elicie Albert¹; ¹Lawrence Livermore National Lab, USA. This talk reviews x-ray and gamma-ray sources driven by laser wakefield acceleration. They provide broadband radiation from keV to MeV energies, and can be used for applications in high energy density science.

Executive Ballroom
210D

CLEO: QELS-
Fundamental Science

FF2D • THz Electrodynamics
and control of Electronic
Degrees of Freedom—
Continued

FF2D.4 • 11:30

Ultrafast Semiconducting to Metallic Terahertz Responses in the Topological Insulator Bi₂Se₃, Seungmin Lee¹, Sangwan Sim¹, Jisoo Moon², Soonyoung Cha¹, Ho-seung Shin¹, Soohyun Park¹, Woosun Jang³, Myungwoo Son⁴, Hyunseung Jung⁵, Seung Young Seo⁶, Aloysius Soon³, Moon-Ho Ham⁴, Hojin Lee⁵, Moon-Ho Jo^{6,7}, Seongsik Oh², Hyunyoung Choi¹; ¹School of Electrical and Electronic Engineering, Yonsei Univ., South Korea; ²Dept. of Physics and Astronomy, Rutgers, The State Univ. of New Jersey, USA; ³Dept. of Materials Science and Engineering, Yonsei Univ., South Korea; ⁴School of Materials Science and Engineering, Gwangju Inst. of Science & Technology (GIST), South Korea; ⁵School of Electronic Engineering, Soongsil Univ., South Korea; ⁶Dept. of Materials Science and Engineering, Pohang Univ. of Science and Technology (POSTECH), South Korea; ⁷Division of Advanced Materials Science, Pohang Univ. of Science and Technology (POSTECH), South Korea. We present the photoinduced terahertz responses of topological insulators Bi₂Se₃. The photoconductance sign is determined by the competition between the topological surface state and the bulk response in *n*-type, *p*-type and bulk-insulating Bi₂Se₃.

FF2D.5 • 11:45

Formation Dynamics of Indirect Excitons and Electron Hole Droplets in InSb, Xu Yang^{1,2}, Chirag Vaswani^{1,2}, Xin Zhao^{1,2}, Yongxin Yao^{1,2}, Cai-Zhuang Wang^{1,2}, Kai-Ming Ho^{1,2}, Jigang Wang^{1,2}; ¹Iowa State Univ., USA; ²Ames Lab, USA. Direct band-gap semiconductor InSb is studied under intense electric fields leading to impact ionization followed by intervalley scattering. Further, fast formation of indirect excitons and Electron Hole Droplets(EHDs) is shown by time-resolved conductivity measurements.

CLEO: QELS-Fundamental Science

FF2E • Novel Nonlinear Optical Materials—Continued

FF2E.4 • 11:15

Nanophotonic Waveguides for Extreme Nonlinear Optics, Dan Hickstein¹, David R. Carlson¹, Abijith Kowligy¹, Scott Domingue², Matt Kirchner², Henry Timmers¹, Nima Nader¹, Alex Lind¹, Hairun Guo³, Clemens Herkommer³, Tobias J. Kippenberg³, Margaret Murnane^{4,2}, Henry Kapteyn^{4,2}, Scott Papp^{1,5}, Scott A. Diddams^{1,5}, ¹NIST, USA; ²KM-Labs, USA; ³Ecole Polytechnique Federale de Lausanne, Switzerland; ⁴JILA - Univ. of Colorado and NIST, USA; ⁵Physics, Univ. of Colorado, USA. We demonstrate nanophotonic waveguides for mid-infrared supercontinuum generation and high-harmonic generation. The waveguide geometry enables phase-matching of harmonic generation to higher-order modes. Simulations reveal how periodic poling enables harmonic generation through a cascaded mechanism.

FF2E.5 • 11:30

Photorefractive quenching in high quality LiNbO₃ photonic crystal nanocavities, Hanxiao Liang¹, Rui Luo¹, Mingxiao Li¹, Yang He¹, Haowei Jiang¹, ¹Univ. of Rochester, USA. We report extremely strong cavity tuning by photorefractive in LiNbO₃ photonic crystal nanocavities, with a tuning rate up to ~84 MHz/photon. In particular, we report for the first time intriguing quenching of photorefractive in these devices.

FF2E.6 • 11:45

Broadband mid-infrared frequency combs in quasi-phase-matched lithium niobate waveguides, Abijith Kowligy¹, Alex Lind^{1,2}, Henry Timmers¹, Dan Hickstein¹, David R. Carlson¹, Nima Nader³, Flavio Cruz¹, Gabriel Ycas³, Scott Papp¹, Scott Diddams¹; ¹Time and Frequency Division, NIST, USA; ²Dept. of Physics, Univ. of Colorado, USA; ³Applied Physics Division, NIST, USA. We experimentally demonstrate broadband mid-infrared (3–5 mm) frequency combs in quasi-phase-matched lithium niobate waveguides leveraging cascaded-c⁽²⁾ supercontinuum generation and difference-frequency generation pumped by an Er:fiber laser.

FF2F • Fundamental Nanophotonics: Sensing and Infrared Applications—Continued

FF2F.4 • 11:15

Narrowband Plasmonic Metamaterial Absorber Integrated Pyroelectric Detectors Towards Infrared Gas Sensing, Xiaohao Tan¹, Junyu Li¹, Ao Yang¹, Huan Liu¹, Fei Yi^{1,2}; ¹School of Optical and Electronic Information, Huazhong Univ. of Science and Technology, China; ²Shenzhen R & D Center of Huazhong Univ. of Science and Technology, China. We proposed using narrowband absorption filter integrated lithium tantalate (LT) based pyroelectric detector array as spectroscopic sensor for NDIR gas sensing. Measured absorption spectra of the narrowband absorber and calculated thermal responses are provided.

FF2F.5 • 11:30

Sub-wavelength field enhancement in mid-IR: Phononics vs Plasmonics vs Phononics, Tengfei Li¹, Vivek Nagal², David Gracias², Jacob Khurgin¹; ¹Electrical and Computer Engineering, Johns Hopkins Univ., USA; ²Chemical and Biomolecular Engineering, Johns Hopkins Univ., USA. We compare different means for the mid-infrared light enhancement on sub-wavelength scale. Depending on whether the magnitude of the bandwidth of enhancement is important, metallic or phononic structures are preferable.

FF2F.6 • 11:45

Metal-insulator-metal Metamaterial Absorbers with Optical Absorption Tailored by Embedded Phonons, Junyu Li¹, Rulai Gan¹, Huan Liu¹, Fei Yi^{1,2}; ¹School of Optical and Electronic Information, Huazhong Univ. of Science and Technology, China; ²Shenzhen R & D Center of Huazhong Univ. of Science and Technology, China. We demonstrated that the coupling of the plasmonic resonances of gold nanodisk antennae and naonrod antennae with the optical phonons in the dielectric spacer such as SiO₂, Si₃N₄ and PDMS can broaden the absorption band.

CLEO: Science & Innovations

SF2G • Mid-infrared Semiconductor Lasers—Continued

SF2G.4 • 11:30

InP-based Quantum Cascade Lasers Monolithically Integrated onto Si and GaAs Substrates, Rowel Go¹, H. Krysiak², M. Fetters², Pedro Figueiredo¹, Matthew Suttinger¹, Jason Leshin¹, X. M. Fang², Joel Fastenau², D. Lubyshchev², Amy Liu², A. Eisenbach², M. Furlong², Arkadiy Lyakh¹; ¹Univ. of Central Florida, USA; ²IQE, USA. Operation of InP-based quantum cascade lasers (QCL) processed from structures grown on 6-inch Si and GaAs substrates with metamorphic buffers are reported. Results pave the way for the development of ultra-compact Si-based platforms comprising QCLs.

SF2G.5 • 11:45

Monolithic integration of mid-infrared quantum cascade lasers coupled with passive InGaAs waveguides, Seungyong Jung^{2,1}, Daniele Palaferri¹, Jiaming Xu¹, Feng Xie³, Yae Okuno³, Christopher Pinzone³, Kevin Lascola³, Mikhail A. Belkin¹; ¹Univ. of Texas at Austin, USA; ²TransWave Photonics, LLC, USA; ³Thorlabs Quantum Electronics, USA. We experimentally demonstrate lasing and mode coupling of mid-infrared quantum cascade lasers monolithically integrated with passive InGaAs waveguides for integrated-photonics applications. A waveguide-coupled device produced 30 mW peak power with J_{th}=3.5 kA/cm² at room-temperature.

CLEO: QELS-Fundamental Science

FF2H • Interference and Localization Phenomena in Complex Media—Continued

CLEO: Science & Innovations

CLEO: QELS-
Fundamental ScienceSF21 • Electrooptic and
Nanophotonic Materials—
Continued

SF21.4 • 11:15

Foundry-compatible Hybrid Silicon / Lithium Niobate Electro-Optic Modulator, Peter Weigel¹, Jie Zhao¹, Douglas Trotter², Dana Hood², John Mudrick², Christina Dallo², Andrew Pomerene², Andrew Starbuck², Christopher DeRose², Anthony Lentine², Shayan Mookherjee¹; ¹Univ. of California San Diego, USA; ²Applied Microphotonics Systems, Sandia National Labs, USA. A foundry-compatible hybrid silicon-lithium niobate electro-optic modulator with an optical bandwidth greater than 6 GHz is presented. Wafer-scale photolithography processing is used to fabricate silicon features before bonding to a 600 nm lithium niobate film.

SF21.5 • 11:30

Measurement of Nonlinear Refractive Index of Solids in the Mid-Infrared, Gauri Patwardhan^{1,2}, Jared Ginsberg², M. Mehdi Jadidi², Xiaohui Gao², Alexander L. Gaeta²; ¹Applied and Engineering Physics, Cornell Univ., USA; ²Applied Physics and Applied Mathematics, Columbia Univ., USA. We report experimental measurements of nonlinear refractive index of solids in the mid-infrared. Here we present our results for fused silica at wavelength of 2.3 and 3.5 μm , and for silicon at 2.3 μm .

SF21.6 • 11:45

Super Absorbing Nano-gap Metasurface With Sub-5-nm Gaps for Extreme Light Confinement, Dengxin Ji¹, Alec R. Cheney¹, Nan Zhang¹, Haomin Song¹, Jun Gao², Xie Zeng¹, Haifeng Hu³, Suhua Jiang², Zongfu Yu⁴, Qiaoqiang Gan¹; ¹Univ. at Buffalo, USA; ²Fudan Univ., China; ³Northeastern Univ., China; ⁴Univ. of Wisconsin-Madison, USA. We report a metamaterial super absorber structure with sub-5-nm gaps fabricated using atomic layer deposition processes for extreme light confinement. Light trapping efficiency of 81% is experimentally demonstrated at mid-infrared wavelengths.

SF2J • Cavity Optomechanics—
Continued

SF2J.3 • 11:15

High Harmonic Generation Via an Electro-Optomechanical Oscillator, Turker Beyazoglu¹, Clark T. Nguyen¹; ¹UC Berkeley, USA. We present an Electro-Opto-Mechanical Oscillator achieving 270 harmonics from a 37-MHz mechanical oscillation, more than 2x larger in harmonic number and 1000x higher in frequency compared to the previous mark. This is achieved by producing large oscillation amplitude with a unique device design

SF2J.4 • 11:30

NEMS with Co-Localized Optical and Electric Forces, Marcel W. Pruessner¹, Doewon Park¹, Dmitry Kozak¹, Todd Stievater¹, William Rabinovich¹; ¹US Naval Research Lab, USA. Recently, there has been significant interest in nano-electro-mechanics (NEMS). By co-localizing optical and electric actuation, enhanced functionality can be achieved. We demonstrate NEMS-cavity tuning using electric forces and NEMS-resonance excitation using optical forces.

SF2J.5 • 11:45

Reconfigurable Optical Circulator In An Optomechanical Microresonator, Zhen Shen¹, Yan-Lei Zhang¹, Yuan Chen¹, Fang-Wen Sun¹, Xu-Bo Zou¹, Guang-Can Guo¹, Chang-Ling Zou¹, Chun-Hua Dong¹; ¹Univ. of Science and Technology of China, China. We experimentally demonstrate a reconfigurable non-reciprocal device with alternative functions as either a circulator or a directional amplifier via optomechanically induced coherent photon-phonon conversion or gain.

SF2K • Novel Fiber
Technology—ContinuedSF2K.3 • 11:15 **Invited**

Ultra-low Loss Silica Core Fiber for Long Haul Transmission, Yoshiaki Tamura¹, Hiro-taka Sakuma¹, Yoshinori Yamamoto¹, Takemi Hasegawa¹; ¹Sumitomo Electric Industry, Japan. We review recent advances in optical fiber technologies that realize ultra-low losses as low as 0.142 dB/km including pure-silica core and reduction of microscopic density fluctuation.

SF2K.4 • 11:30

Integration of High-performance Optoelectronic Nanowire-based Devices at Optical Fiber Tips, Wei Yan¹, Tapajyoti Das Gupta¹, Inès Richard¹, Fabien Sorin¹; ¹Ecole Polytechnique Federale de Lausanne, Switzerland. We establish a facile and robust approach to integrate high-performance semiconducting nanowire-based optoelectronic devices at optical fiber tips. The multi-functional fibers exhibit excellent optical and optoelectronic properties, leading to unique applications in fluorescence imaging.

FF2L • Polaritons in 2D
Materials—Continued

FF2L.4 • 11:15

Ultrafast and energy-efficient all-optical modulator based on deep-subwavelength graphene-loaded plasmonic waveguides, Masaaki Ono^{1,2}, Masanori Hata^{2,3}, Masato Tsunekawa^{2,3}, Kengo Nozaki^{1,2}, Hisashi Sumikura^{1,2}, Masaya Notomi^{1,2}; ¹Nanophotonics Center, NTT Corporation, Japan; ²NTT Basic Research Labs, NTT Corporation, Japan; ³Dept. of Physics, Tokyo Inst. of Technology, Japan. We have demonstrated ultracompact all-optical modulators by deep-subwavelength graphene-loaded plasmonic waveguides (60 x 40 nm²), and achieved an ultrafast response time (2.2 ps) with a substantially small consumption energy (155 fJ) for the first time.

FF2L.5 • 11:30

Graphene-induced tunable Lamb shifts beyond atomic fine structure, Cyuan-Han Chang¹, Nicholas Rivera¹, John Joannopoulos¹, Marin Soljagic¹, Ido Kaminer^{1,2}; ¹Dept. of Physics, MIT, USA; ²Dept. of Electrical Engineering, Israel Inst. of Technology, Israel. We show that highly tunable atomic energy levels can be achieved by exploiting plasmonic Lamb shifts. The shifts can be larger than fine-structure shifts and potentially larger than the Coulomb interactions at certain Fermi energies.

FF2L.6 • 11:45

Broadband Negative Refraction of Hyperbolic Highly Squeezed Graphene Plasmons, Jing Jiang¹, Xiao Lin¹, Yi Yang², Ido Kaminer³, Marin Soljagic³, Baile Zhang¹; ¹Nanyang Technological Univ., Singapore; ²Electrical Engineering and Computer Science, MIT, USA; ³Physics, MIT, USA. The array of graphene nanoribbons provides a versatile platform to enable all-angle negative refraction of hyperbolic highly squeezed graphene plasmons in a broad bandwidth.

Marriott
Salon III

CLEO: Applications
& Technology

AF2M • Imaging &
Microscopy—Continued

AF2M.4 • 11:15

FPGA-based high-speed real-time line-scan imager via Fourier spectrum acquisition, Tianhua Fang¹, Jiajie Teng¹, Hongwei Chen¹, Qiang Guo¹, Minghua Chen¹, Sigang Yang¹, Shizhong Xie¹; ¹*Tsinghua Univ., China*. A FPGA-based high-speed real-time line-scan imager with Fourier spectrum acquisition is demonstrated, which allows image acquisition at a frame rate of 400 kHz in real-time and the imaging data processing with only microseconds delay.

AF2M.5 • 11:30

Wide-Field Surface-Enhanced Raman Scattering from Ferroelectrically Defined Au Nanoparticle Microarrays for Optical Sensing, Nebras Alattar^{2,3}, Rusul M. Al-Shammari¹, Michele Manzo⁴, Katia Gallo⁴, Brian Rodriguez¹, James Rice¹; ¹*School of Physics, Univ. College Dublin, Ireland*; ²*School of biosystems & food engineering, Univ. College Dublin, Ireland*; ³*Laser and Optoelectronics Engineering Dept., Univ. of Technology, Iraq*; ⁴*Royal Inst. of Technology, Sweden*. The acquisition-time in optical sensors using SERS is vital value. Wide-field SERS is used to perform high-density of hot-spots of GNPs photodeposition on a periodically-proton-exchanged-LiNbO₃ which, leads to increase the sensitivity at ultralow probe concentrations <10⁻⁹–10⁻¹³M

AF2M.6 • 11:45

A hyperspectral camera based on ghost imaging via sparsity constraints with a flat-field grating, Liu S. Ying^{1,2}; ¹*Shanghai Inst of Optics and Fine Mech, China*; ²*Univ. of Chinese Academy of Sciences, China*. We propose a hyperspectral camera based on ghost imaging via sparsity constraints with a flat-field grating, which can greatly improve spectral resolution and optimize the measurement matrix according to optical fields with different wavelengths.

Marriott
Salon IV

CLEO: Science &
Innovations

SF2N • Ultrafast Oscillators—
Continued

SF2N.4 • 11:30

Discrete similariton regime for energy scaling of modelocked thin-disk lasers, F. Ömer Ilday², Martin Hoffmann¹, Clara J. Saraceno¹; ¹*Ruhr Universität Bochum, Germany*; ²*Bilkent Univ., Turkey*. We investigate energy scaling of modelocked thin-disk lasers via modelocking regimes which are more tolerant in terms of maximum nonlinearity than soliton modelocking. Our numerical results show promise for mJ-level pulse energies without requiring vacuum.

SF2N.5 • 11:45

Kerr-Lens Mode-Locked Yb:Lu₂O₃ Ceramic Thin-Disk Laser, Shotaro Kitajima¹, Akira Shirakawa¹, Hideki Yagi², Takagimi Yanagitani²; ¹*Univ. of Electro-communications, Japan*; ²*Konoshima Chemical Co., Ltd., Japan*. The first Kerr-lens mode-locked Yb:Lu₂O₃ ceramic thin-disk laser was demonstrated. The shortest pulse duration was 177 fs with 3.2 W output power. The output power of 17 W with 588 fs pulses was also demonstrated.

Marriott
Salon VI

CLEO: QELS-
Fundamental Science

FF2P • High-order Harmonic
Generation in Solids—
Continued

FF2P.2 • 11:30

High-harmonic generation from crystalline silicon driven by sub-cycle mid-infrared pulses, Hideto Shirai¹, Fumitoshi Kumaki^{1,2}, Yutaka Nomura^{1,2}, Takao Fujii^{1,2}; ¹*Inst. for Molecular Science, Japan*; ²*The Graduate Univ. for Advanced Studies (SOKENDAI), Japan*. Carrier-envelope phase controlled sub-cycle mid-infrared pulses generated through two-color filamentation have been applied for high harmonic generation from crystalline silicon membrane. The high harmonic spectrum reaches the ultraviolet region.

FF2P.3 • 11:45

Polarimetry of High Harmonics in Bulk Crystals, Yongsing You¹, Eric Cunningham¹, Christian Rödel¹, David Reis¹, Shambhu Ghimire¹; ¹*SLAC National Lab, USA*. We measure the polarization of extreme ultraviolet high-harmonics from a MgO crystal pumped by strong infrared laser pulses. We find that the polarization depends strongly on crystal orientation and harmonic order.

Marriott
Willow Glen

CLEO: Applications
& Technology

AF2Q • A&T Topical Review
on Time-Stretch Technology:
Principles and Applications I—
Continued

AF2Q.3 • 11:30 **Invited**

Studying Nonlinear Pulse Interactions using Time Stretch, Ray Man¹, Mary Fung¹, Kevin Lui¹, K.S. Tsang¹; ¹*Amonics Ltd, Hong Kong*. Single shot measurements unveil valuable information about laser performance. We report characterization of ultrafast optical system using the first commercial time stretch instrument.

Executive Ballroom
210A

CLEO: Science &
Innovations

SF2A • Nonlinear Photonics
in Integrated Structures—
Continued

SF2A.6 • 12:00

Stability of cnoidal wave frequency combs in microresonators, Zhen Qi¹, Shaokang Wang¹, José Jaramillo-Villegas², Minghao Qi², Andrew M. Weiner², Giuseppe D'Aguanno³, Curtis R. Menyuk¹; ¹Univ. of Maryland Baltimore County, USA; ²Purdue Univ., USA; ³Univ. of Texas at Austin, USA. We determine the regions in the parameter space of microresonators where cnoidal waves (Turing rolls) are stable; solitons are included as a special limit. Conditions to obtain broadband frequency combs are identified.

SF2A.7 • 12:15

Non-Hermiticity in Weakly Coupled Semiconductor Laser Arrays, Zihao Gao¹, Matthew T. Johnson², Harshil Dave¹, Bradley J. Thompson¹, Kent D. Choquette¹; ¹Univ of Illinois at Urbana-Champaign, USA; ²USA Air Force Academy, USA. Coupled semiconductor laser arrays are naturally non-Hermitian optical systems. We show that in a weakly coupled semiconductor laser array, the control for gain/loss is dominated by the nonlinearities, rather than simply following the pump profile.

Executive Ballroom
210B

Joint

JF2B • Symposium on Emerging
Quantum Sensing Techniques
and Applications I—Continued

JF2B.5 • 12:00

Optomechanical Quantum Thermometry, Thomas Purdy¹, Robinjeet Singh^{1,2}, Nikolai Klimov^{1,2}, Zeeshan Ahmed¹, Karen Grutter^{1,4}, Kartik Srinivasan¹, Jacob Taylor^{1,3}; ¹NIST, USA; ²Joint Quantum Inst., USA; ³JQI and QULCS, USA; ⁴Lab for Physical Sciences, USA. We demonstrate quantum-backaction-noise-calibrated Brownian motion thermometry as a metrological application of quantum optomechanics. We present recent work as well as on-going efforts to enhance the bandwidth, sensitivity, and range of these devices.

JF2B.6 • 12:15

Quantum-Enhanced Ultrasound Detection with Plasmonic Sensors, Ashok Kumar¹, Mohammadjavad Dowran¹, Benjamin Lawrie², Raphael C. Pooser², Alberto M. Marino¹; ¹Univ. of Oklahoma, USA; ²Oak Ridge National Lab, USA. We implement a quantum-enhanced plasmonic sensor with a 56% sensitivity enhancement with respect to the shot-noise limit when used to detect ultrasound waves. The sensor is probed with twin beams with 9dB of intensity-difference squeezing.

Executive Ballroom
210C

JF2C • Symposium on Lasers
in Accelerator Science and
Technology II—Continued

JF2C.5 • 12:00 **Invited**

Recent Progress on High-Repetition Rate Laser-Plasma Acceleration, Jerome Faure^{1,2}; ¹Laboratoire d'Optique Appliquée, France; ²Ecole Polytechnique, France. We have used kHz single cycle laser pulses in order to resonantly drive a plasma wakefield, resulting in the acceleration of relativistic electron beams with 5 MeV energies and >20 pC/shot charges. Simulations indicate that the electron bunch duration can be as short as 1 femtosecond, making this source unique for probing structural dynamics on ultrafast time scales.

Executive Ballroom
210D

CLEO: QELS-
Fundamental Science

FF2D • THz Electrodynamics
and control of Electronic
Degrees of Freedom—
Continued

FF2D.6 • 12:00

Vacuum Bloch-Siegert Shift in Landau Polaritons with Ultrahigh Cooperativity, Xinwei Li¹, Motoaki Bamba², Qi Zhang³, Saeed Fallahi⁴, Geoff Gardner⁴, Weilu Gao¹, Minhan Lou¹, Katsumasa Yoshioka⁵, Michael J. Manfra⁴, Junichiro Kono^{1,6}; ¹Dept. of Electrical and Computer Engineering, Rice Univ., USA; ²Dept. of Material Engineering Science, Osaka Univ., Japan; ³Argonne National Labs, USA; ⁴Dept. of Physics and Astronomy, Purdue Univ., USA; ⁵Dept. of Physics, Yokohama National Univ., Japan; ⁶Dept. of Physics and Astronomy, Rice Univ., USA. Terahertz spectroscopy of Landau polaritons reveals a shift induced by the ultrastrong coupling of cyclotron-orbiting electrons with the counter-rotating component of the vacuum fluctuation field, evidencing the nonvacuum of the rotating wave approximation.

FF2D.7 • 12:15

Ultrafast THz Fingerprints of Large Polaron Formation in Lead-Halide Perovskites, Eugenio L. Cinquanta^{1,2}, Daniele Meggiolaro^{3,4}, Marina Gandini⁵, Edoardo Mosconi^{2,4}, Silvia Motti⁵, Marcello Alcocer¹, Cristian Manzoni², Caterina Vozzi², Annamaria Petrozza⁵, Filippo De Angelis^{3,4}, Salvatore Stagira¹; ¹Politecnico di Milano, Italy; ²CNR-IFN, Italy; ³CNR-ISM, Italy; ⁴IIT, Italy; ⁵IIT, Italy. Ultrafast THz spectroscopy combined with DFT calculations demonstrates the formation of large polaron in CsPbPr₃ nanocrystals. Our results explain their fascinating dielectric properties that makes hybrid perovskites a promising platform for next-generation high-performances optoelectronics devices.

12:30–14:00 Lunch Break (on your own)

CLEO: QELS-Fundamental Science

CLEO: Science & Innovations

CLEO: QELS-Fundamental Science

FF2E • Novel Nonlinear Optical Materials—Continued

FF2F • Fundamental Nanophotonics: Sensing and Infrared Applications—Continued

SF2G • Mid-infrared Semiconductor Lasers—Continued

FF2H • Interference and Localization Phenomena in Complex Media—Continued

FF2E.7 • 12:00

Optical Magnetic Force Induces Molecular Rotations, Tuan M. Trinh¹, Krishnandu Makhal¹, Elizabeth Dreyer¹, Stephen Rand¹; ¹Univ. of Michigan, USA. Optical interactions involving both electric and magnetic fields in two-photon scattering can stimulate molecular librations/rotations, via torque-enhanced magnetic transitions. Here we report ultrafast observations of magneto-electrically-induced vibrations and rotations

FF2F.7 • 12:00

Surface-Enhanced Infrared Absorption Spectroscopy via Coaxial Zero-Mode Resonators with Sub-10-nm Gaps, Daehan Yoo¹, Daniel A. Mohr¹, Ferran Vidal-Codina², Aurelian John-Herpin³, Minsik Jo^{4,5}, Sung-hwan Kim^{4,5}, Joseph Matson⁶, Joshua D. Caldwell⁶, Ngoc-Cuong Nguyen², Luis Martin-Moreno^{7,8}, Jaime Peraire², Hatice Altug³, Sang-Hyun Oh¹; ¹Dept. of Electrical and Computer Engineering, Univ. of Minnesota, USA; ²Dept. of Aeronautics and Astronautics, MIT, USA; ³Inst. of BioEngineering, École Polytechnique Fédérale de Lausanne, Switzerland; ⁴Dept. of Physics, Ajou Univ., South Korea; ⁵Dept. of Energy Systems Research, Ajou Univ., South Korea; ⁶Dept. of Mechanical Engineering, Vanderbilt Univ., USA; ⁷Instituto de Ciencia de Materiales de Aragón, Spain; ⁸Departamento de Física de la Materia Condensada, CSIC-Universidad de Zaragoza, Spain. We demonstrate high-contrast infrared absorption spectroscopy on ultrathin protein films enabled by coaxial nanogap resonators, where light can be efficiently coupled with vibrational modes of proteins at the zeroth-order Fabry-Perot resonance condition.

FF2F.8 • 12:15

Generating Spin Current from Mid Infrared Plasmonic Metamaterial Absorbers, Satoshi Ishii¹, Ken-ichi Uchida¹, Thang Dao¹, Yoshiki Wada¹, Eiji Saitoh², Tadaaki Nagao¹; ¹National Inst. for Materials Science, Japan; ²Tohoku Univ., Japan. Wavelength selective spin current is generated in the mid infrared range by combining plasmonic metamaterial absorbers with platinum/yttrium-iron-garnet spintronic devices. The wavelength selectivity is attributed to the plasmonic resonance of the metamaterial absorber.

SF2G.6 • 12:00

External cavity GaSb-based cascade diode lasers with tuning range of 280 nm centered near 3.13 μm ., Meng Wang¹, Tao Feng¹, Takashi Hosoda¹, Gela Kipshidze¹, Jiang Jiang¹, Leon Shterengas¹, Gregory Belenky¹; ¹Stony Brook Univ., USA. Cascade type-I quantum well GaSb-based laser heterostructures with broad optical gain demonstrated tuning from 2.99 to 3.27 μm (above 35 meV) in Littrow external cavity configuration. The devices generated up to 5 mW of the narrow spectrum output power in continuous wave regime at room temperature

SF2G.7 • 12:15

Pure Amplitude or Frequency Modulation of a Quantum Cascade Laser by Use of an Integrated Heater, Atif Shehzad¹, Pierre Brochard¹, Renaud Matthey¹, Alfredo Bismutto², Stephane Blaser², Tobias Gresch², Richard Maulini², Antoine Muller², Thomas Südmeyer¹, Stephane Schilt¹; ¹Univ. of Neuchâtel, Switzerland; ²Alpes Lasers, Switzerland. We present pure amplitude and frequency modulation realized electrically in a quantum cascade laser (QCL) equipped with an integrated heater (IH), achieved by simultaneously modulating the QCL and IH currents with proper amplitudes and phases.

FF2H.4 • 12:00

Diffusion in Translucent Media, Azriel Z. Genack^{1,2}, Zhou Shi^{1,3}; ¹Queens College of the City Univ. of New York, USA; ²Physics, The Graduate Center of the City Univ. of New York, USA; ³Chiral Photonics, USA. We show in optical measurements and simulations that the scaling of transmission, intensity profiles of transmission eigenchannels, and the statistics of transmission eigenvalues are the same in translucent and opaque media.

FF2H.5 • 12:15

High-Quality Confinement of Visible Light in Disordered Photonic Crystal Waveguides in the Anderson-Localized Regime, Oliver J. Trojak¹, Tom Crane¹, Luca Sapienza¹; ¹Dept. of Physics and Astronomy, Univ. of Southampton, UK. We demonstrate Anderson localization of visible light in silicon nitride photonic crystal waveguides. We measure photoluminescence resonances due to disorder-induced light localization showing quality factors of $\sim 10^4$ that exceed engineered 2D photonic crystal cavities.

12:30–14:00 Lunch Break (on your own)

Meeting Room
211 B/D

Meeting Room
212 A/C

Meeting Room
212 B/D

Marriott
Salon I & II

CLEO: Science & Innovations

CLEO: QELS-
Fundamental Science

SF21 • Electrooptic and
Nanophotonic Materials—
Continued

SF21.7 • 12:00

Engineering the Coupling Between the Berreman Mode and Nanobar Antennas in Epsilon-near-zero Materials, Owen Dominguez², Leland J. Nordin¹, Daniel Wasserman¹, Anthony Hoffman²; ¹Electrical and Computer Engineering, Univ. of Texas at Austin, USA; ²Electrical Engineering, Univ. of Notre Dame, USA. We design, fabricate and characterize the coupling between nanobar antennas and optical modes on epsilon-near-zero thin AlN films. Reflection measurements and simulations indicate that the interaction can be controlled via incident angle and antenna length.

SF21.8 • 12:15

Memetic Algorithm Optimization of Thin-film Photonic Structures for Thermal and Energy Applications, Yu Shi¹, Wei Li¹, Aaswath Raman¹, Shanhui Fan¹; ¹Electrical Engineering, Stanford Univ., USA. We present an effective thin-film optimization method using the memetic algorithm for thermal and energy applications. This method rigorously treats broadband material dispersion and produces structures with superior performances than their counterparts in the literature.

SF2J • Cavity Optomechanics—
Continued

SF2J.6 • 12:00

Integrated Brillouin microcavity laser with sub-milliwatt threshold, Ki Y. Yang¹, Boqiang Shen¹, Heming Wang¹, Qifan Yang¹, Xu Yi¹, Seung Hoon Lee¹, Dong Yoon Oh¹, Kerry Vahala¹; ¹California Inst. of Technology, USA. A Brillouin laser featuring an ultra-high-Q silica cavity monolithically integrated with a silicon-nitride waveguide is demonstrated. The device features a sub-milliwatt threshold pump power and provides high-coherence output for on-chip sources, gyroscopes, and microwave generation

SF2J.7 • 12:15

Electromechanically Induced Brillouin Scattering in AlN Optomechanical Waveguides, Qiyu Liu¹, Huan Li¹, Mo Li¹; ¹Univ. of Minnesota, USA. We experimentally demonstrate electromechanically induced Brillouin scattering in a photonic waveguide fabricated on aluminum nitride thin film, and show single sideband modulation due to the non-reciprocal acousto-optic phase matching conditions.

SF2K • Novel Fiber
Technology—Continued

FF2L • Polaritons in 2D
Materials—Continued

FF2L.7 • 12:00

Indirect excitons in van der Waals heterostructures at room temperature, Erica V. Calman¹, Michael Fogler¹, Leonid Butov¹, Sheng Hu², Artem Mishchenko², Andre Geim²; ¹UC San Diego, USA; ²Univ. of Manchester, UK. Indirect excitons (IXs) are observed at room temperature in a van der Waals MoS₂/hBN heterostructure. IX lifetimes are orders of magnitude longer than direct exciton lifetimes and IX energy is controllable by voltage.

FF2L.8 • 12:15

Coupling Single Defect Emissions From 2-Dimensional Semiconductors into Long-Range Propagating Gap Plasmons in Metal-Insulator-Metal Waveguides, Subhojit Dutta¹, Tao Cai¹, Edo Waks¹; ¹Inst. for Research in Electronics and Applied Physics, Univ. of Maryland, College Park, USA. We demonstrate coupling of single defect emissions from the 2-D transition metal dichalcogenide (TMDC), Tungsten diselenide (WSe₂) into propagating surface plasmon modes in lithographically fabricated silver-air-silver, metal-insulator-metal (MIM) waveguides.

Friday, 10:30–12:30

12:30–14:00 Lunch Break (on your own)

Marriott
Salon III

CLEO: Applications
& Technology

AF2M • Imaging &
Microscopy—Continued

AF2M.7 • 12:00

Increasing the Speed of CCD-based Thermoreflectance Imaging: An Experimental and Theoretical Demonstration, Mark Hallman¹, Kyle Allison¹, Johanna Hardin², Ami Radunskaya², Janice A. Hudgings¹; ¹Physics and Astronomy Dept., Pomona College, USA; ²Mathematics Dept., Pomona College, USA. To increase the speed of thermoreflectance imaging, we derive detailed statistical models of both the conventional imaging algorithm and our proposed higher speed technique, and we experimentally confirm both the models and resulting speed enhancement.

AF2M.8 • 12:15

High-Resolution and Real-Time W-Band Imaging Radar Based on Photonics for Security Check, Shaowen Peng¹, Shangyuan Li¹, Xuedi Xiao¹, Dexin Wu¹, Xiaoxiao Xue¹, Xiaoping Zheng¹; ¹Tsinghua National Lab for Information Science and Technology, Dept. of Electronic Engineering, Tsinghua Univ., China. We present a photonics-based W-band imaging radar for non-cooperative and non-contact security check with a two-dimension imaging resolution of $\sim 1.9\text{cm} \times \sim 1.6\text{cm}$ and an image frame rate of 200 fps.

Marriott
Salon IV

CLEO: Science &
Innovations

SF2N • Ultrafast Oscillators—
Continued

SF2N.6 • 12:00

Nonlinear-Mirror Modelocked 323-fs Thin-Disk Oscillator, Francesco Saltarelli¹, Andreas Diebold¹, Ivan J. Graumann¹, Christopher R. Phillips¹, Ursula Keller¹; ¹ETH Zurich, Switzerland. We present the first nonlinear-mirror modelocked thin-disk laser, delivering 21 W at 323 fs pulse duration. This opens a new chapter for the nonlinear-mirror technique which, until now, only modelocked few-ps bulk oscillators.

SF2N.7 • 12:15

Repetition-Rate Stabilized 10-GHz Straight-Cavity SESAM-Modelocked Yb:CALGO Laser, Léonard M. Krüger¹, Aline S. Mayer¹, Christopher R. Phillips¹, Valentin J. Wittwer², Olga Razkazovskaya², Thomas Südmeyer², Ursula Keller¹; ¹ETH Zurich, Switzerland; ²Univ. of Neuchâtel, Switzerland. We present a repetition-rate stabilized SESAM-modelocked 10-GHz Yb:CALGO laser using a self-defocussing straight-cavity that suppresses Q-switching and delivered 171 fs pulses at 1.44 W, and even 104 fs at 0.81 W with a dispersion-compensating output coupler.

Marriott
Salon VI

CLEO: QELS-
Fundamental Science

FF2P • High-order Harmonic
Generation in Solids—
Continued

FF2P.4 • 12:00

Observation of selection rules for circularly polarized high harmonics from a solid, Nariyuki Saito¹, Peiyu Xia¹, Faming Lu¹, Nobuhisa Ishii¹, Teruto Kanai¹, Jiro Itatani¹; ¹Univ. of Tokyo, Japan. We report on the observation of selection rules for circularly polarized high harmonics from solids driven by single-color circularly polarized mid-infrared pulses. Our result offers a novel way to produce circularly polarized short wavelength light.

FF2P.5 • 12:15

A real space perspective of high harmonic generation in crystalline solids, Harshit Lakhota¹, Minjie Zhan¹, Hee-Yong Kim¹, Eleftherios Goulielmakis¹; ¹Max Planck Inst. of Quantum Optics, Hans-Kopfermann-Str. 1 D-85748, Garching, Germany. We present a real space picture for high harmonic generation in solids. We studied the crystal orientation dependence of extreme ultraviolet high harmonics in MgF₂.

Marriott
Willow Glen

CLEO: Applications
& Technology

AF2Q • A&T Topical Review
on Time-Stretch Technology:
Principles and Applications I—
Continued

AF2Q.4 • 12:00

Ultrafast Optical Sampling Spectroscopy Based on Dispersive Fourier Transformation, Srikanth Soundararajan¹, Lin Yang¹, Lingze Duan¹; ¹Univ. of Alabama in Huntsville, USA. Time-wavelength optical sampling combines ultrafast optical sampling and dispersive Fourier transform and has been demonstrated for real-time absorption spectroscopy with a low-pressure C₂H₂ sample.

AF2Q.5 • 12:15

Dynamic Dispersion via Acousto-Optic Angular Excitation of Multimode Waveguides, Jacky Chan¹, Sebastian Karpf¹, Bahram Jalali¹; ¹Univ. of California, Los Angeles, USA. To enable tunable temporal engineering in optical communications and processing systems, we integrate RF and wavelength control of mode excitation angle in a multimode waveguide. Dynamic tunability of dispersion is demonstrated over 1.27 ns and 40 nm of optical bandwidth.

12:30–14:00 Lunch Break (on your own)

Friday, 10:30–12:30

Executive Ballroom
210A

CLEO: Science & Innovations

14:00–16:00

SF3A • Integrated Photonics (III-V Heterogeneous)

Presider: Ali Adibi; Georgia Inst. of Technology, USA

SF3A.1 • 14:00

Room temperature lasing from InP/InGaAs nano-ridges at telecom-bands, Yu Han¹, Chao Ma², Wai Kit Ng², Qiang Li¹, Kam Sing Wong², Kei May Lau¹; ¹Dept. of Electronic and Computer Engineering, Hong Kong Univ. of Science and Technology, Hong Kong; ²Dept. of Physics, Hong Kong Univ. of Science and Technology, Hong Kong. Densely packed InP/InGaAs nano-ridges are selectively grown on patterned (001) Si substrates. We demonstrate room temperature lasing at telecom-wavelengths under optical pumping from InGaAs QW nano-ridges transferred onto SiO₂/Si substrates.

SF3A.2 • 14:15

Graphene nano-optomechanical resonators on an integrated photonic platform, Xiang Xi¹, Zefeng Chen¹, Jingwen Ma¹, Jian-Bin Xu¹, Xiankai Sun¹; ¹The Chinese Univ. of Hong Kong, Hong Kong. Graphene nano-optomechanical resonators are demonstrated for the first time on an integrated photonic platform. A flexural mode with effective mass 4.5 fg and frequency 8.1 MHz was measured in air with mechanical Q of ~28.

SF3A.3 • 14:30

Ultra-compact O-E-O converter based on fF-capacitance nanophotonic integration, Kengo Nozaki¹, Shinji Matsuo¹, Takuro Fujii¹, Koji Takeda¹, Eiichi Kuramochi¹, Akihiko Shinya¹, Masaya Notomi¹; ¹NTT Nanophotonics Center, Japan. A nanocavity-based modulator is closely integrated with a nano-photodetector to form an ultra-compact O-E-O converter. The femto-joule energy operation proves the opto-electronic integrability with a femto-farad capacitance, for the first time.

Friday, 14:00–16:00

Executive Ballroom
210B

Joint

14:00–16:00

JF3B • Symposium on Emerging Quantum Sensing Techniques and Applications II

Presider: TBD

JF3B.1 • 14:00 **Invited**

The LIGO Squeezed Light Upgrade, Lee McCuller¹; ¹MIT Kavli Inst. for Astrophysics and Space Research, USA. Squeezed light sources are being commissioned for operation during the third observing run of advanced LIGO. I overview the implementation and optomechanical tradeoffs of continuous squeezed states for interferometers as gravitational wave observatories.

JF3B.2 • 14:30

Cavity-Enhanced Nitrogen-Vacancy Ensemble Magnetometry, Sepehr Ahmadi¹, Haitham A. R. El-Ella¹, Adam M. Wojciechowski¹, Tobias Gehring¹, Jörn O. Hansen¹, Alexander Huck¹, Ulrik L. Andersen¹; ¹Danmarks Tekniske Universitet, Denmark. We demonstrate magnetic-field sensing using the intrinsic nitrogen-vacancy concentration of a single-crystal diamond placed in an optical cavity resonant with the pump field. We investigate two approaches based on fluorescence detection and pump absorption, respectively.

JF3B.3 • 14:45

Optically Levitated Torque Sensor and Ultrafast Nanomechanical Rotor, Tongcang Li¹, Jonghoon Ahn¹, Zhuojing Xu¹, Jaehoon Bang¹; ¹Purdue Univ., USA. We propose to optically levitate a nonspherical nanoparticle in vacuum to detect the quantum vacuum torque (Casimir torque). We have levitated nonspherical nanoparticles in vacuum and driven them to mechanically rotate at several hundred MHz.

Executive Ballroom
210C

CLEO: QELS-Fundamental Science

14:00–16:00

FF3C • Optimization and Design of Metasurfaces

Presider: Viktor Podolskiy; Univ. of Massachusetts Lowell, USA

FF3C.1 • 14:00

High Efficiency Aperiodic Metasurfaces Based on Variable Phase Shifting Element Spacing, Jiaqi Jiang¹, Thaibao Phan¹, Jonathan Fan¹; ¹Electrical Engineering, Stanford Univ., USA. We report new method for designing high efficiency aperiodic metasurfaces by approximating the desired phase profile with linear sections and optimizing the spacing between subwavelength-scale phase shifter elements within each section.

FF3C.2 • 14:15

Multifunctional Silicon Metagratings, David Sell¹, Jianji Yang¹, Sage Doshay¹, Evan W. Wang¹, Thaibao Phan¹, Jonathan Fan¹; ¹Stanford Univ., USA. We design highly efficient multi-functional silicon metagratings based on adjoint-based optimization and experimentally demonstrate devices exhibiting negative refraction and wavelength sorting capabilities.

FF3C.3 • 14:30

Solving Equations with Waves in Collections of Mach-Zehnder Interferometers, Mario Junior Mencagli¹, Nasim Mohammadi Estakhri¹, Brian Edwards¹, Nader Engheta¹; ¹Univ. of Pennsylvania, USA. We present how waves in ensembles of Mach-Zehnder interferometers (MZIs) can be utilized to perform mathematical operations and solve integral equations with kernels that can be re-configured by adjusting phases in such MZIs.

FF3C.4 • 14:45

Non-local computing metasurfaces performing mathematical operations, Concetto Eugenio Andrea Cordaro^{1,2}, Hoyeong Kwon³, Dimitrios Sounas³, Albert Polman¹, Andrea Alù³; ¹AMOLF, Netherlands; ²Universiteit van Amsterdam, Netherlands; ³The Univ. of Texas at Austin, USA. We present Si-based metasurfaces with suitably engineered spatial dispersion and non-locality that can perform even and odd mathematical operations on an input image, enabling all-analog signal processing and on-the-fly edge detection.

Executive Ballroom
210D

14:00–16:00

FF3D • Spectroscopy of Low Dimensional Systems

Presider: Rohit Prasankumar; Los Alamos National Lab, USA

FF3D.1 • 14:00

Selective Observation of Nonradiative Electronic States in Silicon-Vacancy Centers in Diamond, Christopher L. Smallwood¹, Matthew W. Day¹, Travis Autry^{2,3}, Geoffrey M. Diederich⁴, Ronald Ulbricht^{2,3}, Tim Schröder⁵, Edward Bielejec⁶, Mark E. Siemens⁴, Steven T. Cundiff²; ¹Physics, Univ. of Michigan, USA; ²JILA, Univ. of Colorado / NIST, USA; ³Physics, Univ. of Colorado, USA; ⁴Physics and Astronomy, Univ. of Denver, USA; ⁵Electrical Engineering and Computer Science, MIT, USA; ⁶Sandia National Labs, USA. Multidimensional coherent spectroscopy measurements of SiV⁻ centers in diamond reveal a previously unexamined population of silicon-based defect states, which are not detected in photoluminescence and which exhibit a substantial degree of inhomogeneous broadening.

FF3D.2 • 14:15

Exploring the State Structure of Quantum Dot/Quantum Well Systems by Two-Dimensional Coherent Spectroscopy with White Pulses, Mirco Kolarczik¹, Sophia Helmrich¹, Kevin Thomas¹, Bastian Herzog¹, Nina Owschmikow¹, Ulrike K. Woggon¹; ¹IOAP, Technical Univ. Berlin, Germany. Coulomb-bound states of mixed dimensionality (Crossed Excitons) are directly observed in In(Ga)As quantum dot/quantum well systems by coherent two-dimensional spectroscopy. The setup incorporates collinear geometry, inversion control by electrical carrier injection, and white supercontinuum pulses.

FF3D.3 • 14:30

Vibrational Interferometry Enables Single-Scan Acquisition of all x⁽³⁾ Multi-Dimensional Coherent Spectral Maps, Travis Autry¹, Galan Moody¹, Corey McDonald^{1,3}, James M. Fraser^{1,2}, Richard Mirin¹, Kevin L. Silverman¹; ¹NIST, USA; ²Queen's Univ., Canada; ³Physics, Univ. of Colorado, USA. We demonstrate a new method for multidimensional coherent spectroscopy of nanostructures. We use a heterodyne technique implemented with a confocal microscope to record the amplitude and phase of all degenerate third-order wave-mixing processes.

FF3D.4 • 14:45

Sub-Cycle Effects in Carrier-Envelope-Phase-Sensitive Photoemission from Plasmonic Nanoparticles, William Putnam^{1,2}, Phillip D. Keathley¹, Richard Hobbs^{1,3}, Praful Vasireddy¹, Karl K. Berggren¹, Franz X. Kaertner^{1,4}; ¹Massachusetts Inst. of Technology, USA; ²NG Next, Northrop Grumman Corp., USA; ³Chemistry, Trinity College Dublin, Ireland; ⁴Physics, Univ. Of Hamburg, Germany. We study carrier-envelope-phase-sensitive (CEP-sensitive) photoemission from plasmonic nanoparticles illuminated with few-cycle laser pulses of varying intensity. The CEP-sensitive photocurrent exhibits antiresonant-like behavior due to competing emission from different optical half-cycles.

CLEO: QELS-Fundamental Science

14:00–16:00

FF3E • Photon-Phonon Interactions and Cooling

Presider: Peter Rakich; Yale Univ., USA

FF3E.1 • 14:00 **Invited**

Optical Refrigeration Advances: Solid-State Cryocoolers and Athermal Disk Laser, Mansoor . Sheik-Bahae¹, Junwei Meng¹, Zhou Yang¹, Alexander Albrecht¹, Eric Lee¹, Richard Epstein¹, Markus Hehnen^{1,2}; ¹Univ. of New Mexico, USA; ²Los Alamos National Lab, USA. Having reached record temperatures <90K in Yb:YLF, cryogenic optical refrigeration of an arbitrary load has been demonstrated for the first time. In parallel, research on radiation-balanced-lasers has led to demonstration of athermal rare-earth-doped thin-disk lasers.

14:00–16:00

FF3F • Optomechanical Interactions and Single Particle Tracking

Presider: Luca Sapienza; Univ. of Southampton, UK

FF3F.1 • 14:00

Experimental realization of Feynman's ratchet with an optically trapped microsphere, Jaehoon Bang¹, Rui Pan², Thai M. Hoang¹, Jonghoon Ahn¹, Christopher Jarzynski³, Hai Tao Quan², Tongcang Li¹; ¹Purdue Univ., USA; ²Peking Univ., China; ³Univ. of Maryland, USA. Feynman's ratchet is a microscopic heat engine that was proposed by Richard Feynman. Here we experimentally realize Feynman's ratchet for the first time with a colloidal particle in a feedback controlled one dimensional optical trap.

FF3F.2 • 14:15

Opto-Thermophoretic Trapping in Simple Polar Liquids, Xiaolei Peng¹, Linhan Lin^{1,2}, Yuebing Zheng^{1,2}; ¹Materials Science & Engineering Program and Texas Materials Inst., The Univ. of Texas at Austin, USA; ²Dept. of Mechanical Engineering, The Univ. of Texas at Austin, USA. We experimentally demonstrate opto-thermophoretic trapping of particles in several simple polar liquids with a dominant interfacial-entropy-driven force, which is determined by the surface chemistry of the particles and physical properties of the solvents

FF3E.2 • 14:30

Interaction of light with thin liquid membranes, Anatoly Patsyk¹, Miguel Bandres¹, Mordechai Segev¹; ¹Technion-Israel Inst. of Technology, Israel. We study the interaction of light with liquid thin soap membranes experimentally. We observe optical beams form liquid waveguides, bulges, and trigger nucleation of crystals in the membrane due to absorption and surface tension effects.

FF3E.3 • 14:45

Brillouin cooling in a linear waveguide through dispersive symmetry breaking, Nils T. Otterstrom¹, Eric Kittlaus¹, Ryan O. Behunin², Peter T. Rakich¹; ¹Applied Physics, Yale Univ., USA; ²Dept. of Physics and Astronomy, Northern Arizona Univ., USA. Here, we experimentally demonstrate Brillouin cooling in a linear waveguide for the first time. Leveraging the dispersive symmetry breaking of inter-modal Brillouin scattering, we achieve Brillouin cooling without an optical cavity or discrete acoustic modes.

CLEO: Science & Innovations

14:00–16:00

SF3G • Quantum Cascade Lasers

Presider: Seungyong Jung; Univ. of Texas at Austin, USA

SF3G.1 • 14:00 **Invited**

High-Power, High-Efficiency Mid-Infrared Quantum Cascade Lasers, Dan Botez¹, Jeremy D. Kirch¹, Colin Boyle¹, Kevin M. Oresick¹, Chris Sigler¹, Don F. Lindberg III², Thomas L. Earles², Luke J. Mawst¹; ¹Univ. of Wisconsin-Madison, USA; ²Intraband, LLC, USA. Carrier-leakage suppression and fast carrier extraction allow quantum cascade lasers to reach internal efficiencies close to fundamental limits (~ 90 %). Then, CW wallplug efficiencies ≥ 40 % and powers ≥ 10 W become possible.

SF3G.2 • 14:30

Phase Measurement of a QCL Comb in the Mid-IR, Matthew Singleton¹, Pierre Jouy¹, Mattias Beck¹, Jérôme Faist¹; ¹ETH Zurich, Switzerland. QCL combs arise through cascaded four-wave mixing, with simulations suggesting a strongly frequency modulated field. Experimentally, we show that QCL combs can possess a linear chirp, and demonstrate that the comb states are reproducible.

SF3G.3 • 14:45

Tuning the multimode dynamics of Fabry-Perot quantum cascade laser devices with optical injection, Paul Chevalier¹, Marco Piccardo¹, Sajant Anand^{1,2}, Enrique A. Mejia^{1,3}, Yongrui Wang¹, Tobias S. Mansuripur⁴, Feng Xie⁵, Kevin Lascola⁵, Alexey Belyanin⁶, Federico Capasso¹; ¹Harvard Univ., USA; ²Dept. of Physics, Wake Forest Univ., USA; ³Univ. of Texas at Austin, USA; ⁴Dept. of Physics and Astronomy, Texas A&M Univ., USA; ⁵Thorlabs Quantum Electronics (TQE), USA; ⁶Pendar Technologies, USA. With the external injection of an optical seed, we demonstrate how to control the spectrum of multimode Fabry-Perot quantum cascade lasers by reaching a watt-level single-mode emission and tunable harmonic comb regime.

CLEO: QELS-Fundamental Science

14:00–16:00

FF3H • Wavefront Shaping in Complex Media

Presider: Viktoriia Babicheva; Georgia State University, USA

FF3H.1 • 14:00

Wavefront Shaping with the Generalized Wigner-Smith Operator, Philipp Ambichl¹, Andre Brandstötter¹, Matthias Kühmayer¹, Michael Horodyski¹, Julian Böhm², Ulrich Kuhl², Stefan Rotter¹; ¹Technische Universität Wien, Austria; ²Université Côte d'Azur, France. We introduce a wave front shaping protocol based on a generalization of the Wigner-Smith time-delay operator. This tool is used to create light fields with desired properties at a predetermined target embedded inside a medium.

FF3H.2 • 14:15

Temporal Focusing of Total Transmission through Multimode Fibers with Random Mode Mixing, Wen Xiong¹, Chia Wei Hsu¹, Hui Cao¹; ¹Yale Univ., USA. We demonstrate the temporal focusing of optical pulses through multimode fibers with strong mode mixing. The focusing efficiency varies strongly with the focus time, which can be explained by the time-dependent correlations between output channels.

FF3H.3 • 14:30

Constant Pressure Sound Waves in Non-Hermitian Disordered Media, Etienne Rivet², Andre Brandstötter¹, Konstantinos Makris³, Herve Lissek², Stefan Rotter¹, Romain Fleury²; ¹Technische Universität Wien, Austria; ²EPFL, Switzerland; ³Univ. of Crete, Greece. Theory shows that waves with constant intensity can perfectly transmit through a disordered medium with a tailored distribution of gain and loss. We present the first experimental realization of this concept using an acoustic waveguide.

FF3H.4 • 14:45

Tailoring Spatial Intensity-Correlations of Speckle Patterns, Nicholas Bender¹, Hasan Yilmaz¹, Yaron Bromberg², Hui Cao¹; ¹Yale Univ., USA; ²Racah Inst. of Physics, The Hebrew Univ. of Jerusalem, Israel. We present a general framework for customizing the spatial intensity-correlations of speckle patterns without altering the spatial field-correlations. We experimentally generate speckles possessing long-range intensity-correlations by synthesizing non-Gaussian random phase patterns on a SLM.

CLEO: Science & Innovations

CLEO: Applications
& Technology

14:00–16:00

SF31 • Materials for Fiber and Solid State Lasers

Presider: TBD

SF31.1 • 14:00

5 kW 30/600Yb-doped Aluminophosphosilicate Laser Fiber, Cong Gao¹, Chengyu Li¹, Yuying Wang¹, Huan Zhan¹, Kun Peng¹, Lihua Zhang¹, Li Ni¹, Xiaolong Wang¹, Lei Jiang¹, Yuwei Li¹, Shuang Liu¹, Jianjun Wang¹, Feng Jing¹, Aoxiang Lin¹; ¹Laser Fusion Research Center, China Academy of Engineering Physics, China. A 30/600 Yb-doped aluminophosphosilicate fiber was fabricated and presented 5.17 kW laser output at 1064 nm with slope efficiency of 85.69%. Stable operation at 5 kW was demonstrated for 10 hours.

SF31.2 • 14:15

Novel Fabrication Technique for Highly Efficient Tm-doped Fibers, Norberto J. Ramirez-Martinez¹, Martín M. Núñez-Velázquez¹, Andrey A. Umnikov¹, Jayanta K. Sahu¹; ¹Optoelectronics Research Centre, Univ. of Southampton, UK. Thulium-doped aluminosilicate fiber fabricated by MCVF process combining both solution doping and gas phase. Laser characterization report a slope efficiency of ~72% with respect to launched pump power at 2069nm emission wavelength.

SF31.3 • 14:30

Cladded Single Crystal Fibers for All-Crystalline Fiber Lasers, Brandon Shaw¹, Shyam Bayya¹, Woohong Kim¹, Jason Myers¹, Dan Rhonehouse¹, Noor Qadri¹, Charles Askins², John Peele², Rajesh Thapa², Dan Gibson¹, Rafael Gattass¹, Joseph Kolis³, Brad Stadleman³, Jas Sanghera¹; ¹US Naval Research Lab, USA; ²Sotera Defense Solutions, USA; ³Clemson Univ., USA. We report on fabrication of crystalline cladded single crystal Yb:YAG fiber. Net gain has been demonstrated in hydrothermal grown cladded Yb:YAG fiber structures

SF31.4 • 14:45

Hybrid mode-locked erbium-doped fiber laser with black phosphorus saturable absorber, Yuwei Hu¹, Xinxin Jin¹, Guohua Hu², Meng Zhang¹, Qing Wu¹, Zheng Zheng¹, Tawfique Hasan²; ¹Beihang Univ., China; ²Cambridge Graphene Centre, UK. We demonstrate a self-starting erbium-doped fiber laser mode-locked by the hybrid mode-locking mechanism consisting of a nonlinear amplifying loop mirror and a black phosphorus saturable absorber, producing 100 fs pulses at 45.9 MHz repetition rate.

14:00–16:00

SF3J • Mid IR Sensing and Optical Forces

Presider: Kenneth Crozier, Australia

SF3J.1 • 14:00

Optomechanically coupled glass nanopike array on the endface of a multicore fiber, Zheqi Wang¹, Shangran Xie¹, Xin Jiang¹, Riccardo Pennetta¹, Johannes R. Koehler¹, Philip S. Russell¹; ¹Max Planck Inst. for the Science of Light, Germany. We report the fabrication and characterization of an optomechanically coupled array of glass nanopikes on the endface of a germanate multicore fiber. Strong optical gradient forces drive the mechanical motion of the free-standing nanopikes.

SF3J.2 • 14:15

Soft Optical Contact Sensing based on On-Demand Drawn, High Aspect-Ratio Elastomeric Micropillars, Qiang Li¹, Jaeyoun Kim¹; ¹Iowa State Univ., USA. We demonstrate on-demand fabrication of high aspect-ratio, microsphere-tipped elastomeric micropillars on various structures with uncommon geometries. A fiber optic contact sensor is realized by integrating a micropillar onto the end facet of an optical fiber.

SF3J.3 • 14:30

Controlled optical trapping and transport of a single 100 nm particle across an array of silicon nanoantennas, Zhe Xu¹, Kenneth B. Crozier^{1,2}; ¹School of Physics, Univ. of Melbourne, Australia; ²Dept. of Electrical and Electronic Engineering, Univ. of Melbourne, Australia. We experimentally demonstrate the optical trapping and transport of a single 100 nm polystyrene nanosphere across an array of silicon nanoantennas. Our device is all silicon and produces negligible local heating.

SF3J.4 • 14:45

Waveguide Polarimetry using Belinfante Forces, Vincent Giniis^{1,2}, Lulu Liu^{1,3}, Alan She¹, Federico Capasso¹; ¹Harvard SEAS, USA; ²Applied Physics, Vrije Universiteit Brussel, Belgium; ³MIT Lincoln Lab, USA. We reveal the surprising polarization dependence of lateral forces acting on resonant Mie particles in evanescent fields. This effect can be utilized to retrieve the polarization state of light inside birefringent waveguides.

14:00–16:00

SF3K • Mode-Locked Fiber Lasers

Presider: Kazi Abedin; OFS Labs, USA

SF3K.1 • 14:00

Spectral dynamics of dual-color-soliton intracavity collision, Yuan Wei¹, Bowen Li¹, Xiaoming Wei^{1,2}, Ying Yu¹, Kenneth Kin-Yip Wong¹; ¹Univ. of Hong Kong, Hong Kong; ²California Inst. of Technology, USA. By using the dispersive Fourier transform (DFT), we unveil the collision-induced soliton spectral dynamics, which features evolving spectral fringes over the soliton main lobe, and the rebuilding of Kelly sidebands with wavelength drifting.

SF3K.2 • 14:15

Ultrafast dispersion-managed fiber laser mode-locked by black phosphorus saturable absorber, Xinxin Jin¹, Guohua Hu², Meng Zhang¹, Yuwei Hu¹, Qing Wu¹, T Albrow-Owen², R Howe², T Wu², Zheng Zheng¹, Tawfique Hasan²; ¹Beihang Univ., China; ²Cambridge Graphene Centre, UK. We demonstrate an all-fiber erbium-doped laser mode-locked by an inkjet-printed black phosphorus saturable absorber, delivering 102 fs pulses with 40 nm spectral width. Our work highlights the potential of BP-based devices for future photonic technologies.

SF3K.3 • 14:30

Spatiotemporal Mode-Locking, Logan Wright¹, Demetrios N. Christodoulides², Frank W. Wise¹; ¹Cornell Univ., USA; ²College of Optics and Photonics, CREOL, Univ. of Central Florida, USA. We describe, through multiple theoretical and experimental realizations, spatiotemporal mode-locking (STML), the most general form of self-organization in optical oscillators. We discuss qualitatively new kinds of mode-locking, and routes to ultrahigh power, compact lasers.

14:00–16:00

AF3M • Instruments and Components for Spectroscopy

Presider: Kara Peters; North Carolina State Univ., USA

AF3M.1 • 14:00

Experimental Demonstration of Mid-Infrared Computational Spectroscopy with a Plasmonic Filter Array, Benjamin J. Craig¹, Vivek R. Shrestha¹, Jiajun Meng¹, Kenneth B. Crozier¹; ¹Univ. of Melbourne, Australia. We demonstrate mid-infrared plasmonic filters. We experimentally determine the spectrum of a mid-infrared light source using an algorithm whose inputs are the total power transmitted by each filter and the transmission spectrum of each filter.

AF3M.2 • 14:15

Phase-type zigzag grating for suppression high order diffraction, Ziwei Liu^{1,2}, Tanchao Pu^{1,2}, Lina Shi¹, Changqing Xie¹; ¹Inst. of Microelectronics of CAS, China; ²Univ. of Chinese Academy of Sciences, China. We present a novel design of phase-type diffraction grating for spectrum measurement from soft x-ray to far infrared. The 0, 2n, 3n order diffractions can be suppressed and the absolute diffraction efficiency is 27.72%.

AF3M.3 • 14:30

Folded planar metasurface spectrometer, MohammadSadegh Faraji-Dana¹, Ehsan Arbabi¹, Amir Arbabi², Seyedeh Mahsa Kamali¹, Hyounghan Kwon¹, Andrei Faraon¹; ¹T. J. Watson Lab of Applied Physics, California Inst. of Technology, USA; ²Electrical and Computer Engineering, Univ. of Massachusetts Amherst, USA. We present a folded planar spectrometer based on dielectric metasurfaces operating in the near-IR range (760nm-860nm) and achieving ~1.22nm spectral resolution. The planar and compact shape makes the demonstrated spectrometer well-suited for applications requiring integrated and portable spectrometers

Marriott
Salon IV

CLEO: Science &
Innovations

14:00–16:00

SF3N • Ultrafast Pulse
Manipulation

Presider: Alan Fry; SLAC National
Accelerator Lab, USA

SF3N.1 • 14:00

6 GHz Repetition Rate Photocathode Laser for Multi-Bunch Operation of a Relativistic Electron Gun, Chen Li¹, Lutz Winkelmann¹, Ingmar Hartl¹; ¹Deutsches Elektronen-Synchrotron, Germany. We report a new photocathode laser with 6 GHz repetition rate, generated by an electro-optic modulator comb. The laser is amplified by an Yb: fiber amplifier to 10 W and will be converted to UV for photoelectron generation.

SF3N.2 • 14:15

Space-Time Control of Broadband Light in a Multimode Fiber, Bohao Liu¹, Andrew M. Weiner¹; ¹Purdue Univ., USA. Strong modal dispersion of a highly multimode fiber causes a space-time scrambled output field. Using pulse shaping, impulse responses at specific output spots can be characterized and spatial-temporal focusing can be achieved.

SF3N.3 • 14:30

Generation of 1.4-fs Ultrafast Single-Cycle Pulses with a Repetition Rate Exceeding 100 THz by Arbitrarily Manipulating Amplitude and Phase, Chuan Zhang¹, Kazumichi Yoshii^{1,2}, Dmitry Tregubov¹, Chiaki Ohae^{1,2}, Masaru Suzuki¹, Kaoru Minoshima^{1,2}, Masayuki Katsuragawa^{1,2}; ¹The Univ. of Electro-Communications, Japan; ²JST, ERATO MINOSHIMA Intelligent Optical Synthesizer Project (IOS), Japan. We report a new optical technology which enables arbitrarily manipulating amplitudes and phases of a highly-discrete optical spectrum and its application to generating a train of 1.4-fs ultrafast pulses with a repetition-rate exceeding 100 THz.

SF3N.4 • 14:45

Carrier-Envelope Phase Control and Single-Cycle Autocorrelation in Attosecond Coherent Nanotransport, Markus Ludwig¹, Tobias Rybka¹, Felix Ritzkowski¹, Alfred Leitenstorfer¹, Daniele Brida¹; ¹Univ. of Konstanz, Germany. We employ a pair of single-cycle near-infrared pulses to control coherent transfer of single electrons between the contacts of a plasmonic nanocircuit. As a result, attosecond highly nonlinear phenomena manifest themselves at pJ pulse energies.

Marriott
Salon VI

CLEO: QELS-
Fundamental Science

14:00–16:00

FF3P • Strong-field Physics in
Solids

Presider: Shambhu Ghimire; SLAC
National Accelerator Lab, USA

FF3P.1 • 14:00 **Invited**

HHG in Solids: Influence of Band Structure on Harmonic Spectral and Temporal Properties, Mette B. Gaarde¹; ¹Louisiana State Univ., USA. I will discuss how the spectral and temporal properties of harmonic radiation from solids are closely connected to their band structure. I will compare predictions for yields, cutoff energies and orientation-dependence to recent experimental results.

FF3P.2 • 14:30

Disentangling surface and bulk contributions to high-harmonic generation from solids, Giulio Vampa¹, Hanzhe Liu¹, Tony F. Heinz¹, David Reis^{1,2}; ¹Stanford PULSE Inst., USA; ²Dept. of Applied Physics and Photon Science, Stanford Univ., USA. We demonstrate that surface space-charges alter the large amplitude oscillations of electron-hole pairs during high-harmonic generation from silicon, resulting in the emission of weak even-order harmonics. Our results extend surface nonlinear optics to the non-perturbative regime.

FF3P.3 • 14:45

Enhanced Solid-State High-Harmonic Generation from a Silicon Metasurface, Hanzhe Liu^{1,2}, Cheng Guo^{3,4}, Giulio Vampa¹, Jingyuan Linda Zhang^{3,4}, Tomas Sarmiento^{4,5}, Meng Xiao⁴, Philip Bucksbaum^{1,2}, Jelena Vuckovic^{3,4}, Shanhui Fan^{3,4}, David Reis^{1,3}; ¹Stanford Pulse Inst., USA; ²Physics, Stanford Univ., USA; ³Applied Physics, Stanford Univ., USA; ⁴E. L. Ginzton Lab, USA; ⁵Electrical Engineering, Stanford Univ., USA. We report resonantly enhanced non-perturbative high-harmonic emission by more than two orders of magnitude from a Si metasurface that possesses a Fano-like resonance resulting from a classical analog of electromagnetically induced transparency.

Marriott
Willow Glen

CLEO: Applications
& Technology

14:00–16:00

AF3Q • A&T Topical Review
on Time-Stretch Technology:

Principles and Applications II

Presider: Cheng Lei; University of
Tokyo, Japan

AF3Q.1 • 14:00 **Invited**

Coherent RogueScope, Dale Capewell¹, Bahram Jalali², Mohamad Asghari³; ¹RogueScope, USA; ²UCLA, USA; ³Loyola Marymount Univ., USA. Photonic time stretch has enabled new scientific discoveries, and new industrial and biomedical applications. RogueScope is its first commercial product. It measures full-field optical spectra in real-time at MHz refresh rates and millions of frames record length.

AF3Q.2 • 14:30 **Invited**

Large-scale, Deep Single-cell Analysis by All-optical Laser-scanning Imaging Cytometry, Kevin K. Tsia¹; ¹The Univ. of Hong Kong, Hong Kong. Two techniques enabling ultralarge-scale multi-scale single-cell analysis (through biophysical and biochemical phenotyping) with the unprecedented combination of imaging resolution, contrast, and speed are introduced: interferometry-free quantitative phase time-stretch imaging and free-space angular-chirp-enhanced delay (FACED) imaging.

Executive Ballroom
210A

CLEO: Science &
Innovations

SF3A • Integrated Photonics
(III-V Heterogeneous)—
Continued

SF3A.4 • 15:00

An Aluminum Nitride Integrated Photonics Platform for the Ultraviolet to Visible Spectrum, Tsung-Ju Lu¹, Michael Fanto^{2,3}, Hyeonrak Choi¹, Paul Thomas², Jeffrey Steidle², Sara L. Mouradian¹, Wei Kong¹, Di Zhu¹, Hyowon Moon¹, Karl K. Berggren¹, Jeehwan Kim¹, Mohammad Soltani⁴, Stefan Preble², Dirk Englund¹; ¹Research Lab of Electronics, MIT, USA; ²Microsystems Engineering, Rochester Inst. of Technology, USA; ³Air Force Research Lab, USA; ⁴Raytheon BBN Technologies, USA. We demonstrate a wide-bandgap semiconductor photonics platform based on aluminum nitride on sapphire. We measure ring resonators with quality factor >140,000 at 638 nm and >20,000 down to 369 nm, which shows a promising path for low-loss integrated photonics in the ultraviolet and visible spectrum.

SF3A.5 • 15:15

III-V Photonic Circuits with Waveguide-Integrated LED Source and WSi Nanowire Detectors, Corey McDonald^{2,1}, Sonia Buckley¹, Sae Woo Nam¹, Richard Mirin¹, Galan Moody¹, Jeffrey Shainline¹, Kevin L. Silverman¹; ¹NIST, USA; ²Physics, Univ. of Colorado Boulder, USA. We describe the fabrication and testing of photonic circuits using a III-V LED light source coupled to waveguide-integrated WSi single photon detectors for use in advanced computing and on-chip quantum optics experiments.

SF3A.6 • 15:30

Non-volatile All-Optical Quasi-Continuous Switching in GST-on-Silicon Microring Resonators, Jiajiu Zheng¹, Amey Khanolkar¹, Peipeng Xu^{2,1}, Shane A. Colburn¹, Sanchit Deshmukh³, Jason Myers⁴, Jesse Frantz⁴, Eric Pop³, Nicholas Boechler¹, Arka Majumdar¹; ¹Univ. of Washington, Seattle, USA; ²Ningbo Univ., China; ³Stanford Univ., USA; ⁴US Naval Research Lab, USA. Based on GST-on-silicon hybrid nanophotonic integrated circuits, we demonstrate a non-volatile reprogrammable platform, where we achieve all-optical quasi-continuous tuning of microring resonators with switching extinction ratio up to 33dB by controlling a pulsed laser.

Executive Ballroom
210B

Joint

JF3B • Symposium on Emerging
Quantum Sensing Techniques
and Applications II—Continued

JF3B.4 • 15:00 **Invited**

Optimal and Secure Measurement Protocols for Quantum Sensor Networks, Alexey Gorshkov¹; ¹Joint Quantum Inst., USA. We find the optimal entanglement-enhanced protocol for measuring linear combinations of the values of a field (e.g. magnetic or electric) at different spatial points. This has potential applications in chemistry, biology, medicine, geodesy, and geophysics.

JF3B.5 • 15:30 **Invited**

Quantum Sensing with Extreme-coherence Spin Ensembles, Morgan Mitchell¹, Silvana Palacios¹, Simon Coop¹, Pau Gomez², Thomas Vanderbruggen², Natali M. de Escobar³, Martijn Jasperse⁴; ¹ICFO -The Inst. of Photonic Sciences, Spain; ²Koheron, Centre scientifique d'Orsay, France; ³Lone Star College, Univ. Park, USA; ⁴The Univ. of Melbourne, Australia. We demonstrate an ultra-cold magnetic spin ensemble with seemingly-unlimited coherence time. We discuss its use as an extreme magnetic sensor.

Executive Ballroom
210C

CLEO: QELS-Fundamental Science

FF3C • Optimization and Design
of Metasurfaces—Continued

FF3C.5 • 15:00

Robust Design for Topology Optimized Metasurfaces, Evan W. Wang¹, David Sell², Jianji Yang¹, Jonathan Fan¹; ¹Dept. of Electrical Engineering, Stanford Univ., USA; ²Dept. of Applied Physics, Stanford Univ., USA. We implement robustness control in topology-optimized metasurfaces and show that robust metasurfaces are relatively insensitive to geometric erosion and dilation. We also explore the physical mechanisms enabling robustness through a coupled mode analysis.

FF3C.6 • 15:15

Metasurface Lenses Based on Topology-Optimized Wavelength-Scale Building Blocks, Thaibao Phan¹, David Sell¹, Jianji Yang¹, Sage Doshay¹, Jonathan Fan¹; ¹Stanford Univ., USA. We develop a new technique for improving the performance of planar, high numerical aperture metamaterial lenses by combining wavelength-scale diffractive elements designed using topology optimization.

FF3C.7 • 15:30

Scaling Laws for Inverse-Designed Metadevices, Philip Camayd-Muñoz¹, Andrei Faraon¹; ¹California Institute of Technology, USA. Metasurface designs are typically limited to single functions. We use an inverse design method to optimize device performance across multiple tasks, and investigate limits on performance based on effective degrees of freedom in the system.

Executive Ballroom
210D

FF3D • Spectroscopy of
Low Dimensional Systems—
Continued

FF3D.5 • 15:00

All-Optical Determination of 3-Dimensional Alignment of Crystal Axis of Single Colloidal Quantum Dots for Control of Ultrafast Spin Dynamics, Pascal Gumbscheimer¹, Christopher Hinz¹, Yannic Behovits¹, Florian Werschler¹, Christian Traum¹, Denis Seletskiy^{2,1}, Alfred Leitenstorfer¹; ¹Universität Konstanz, Germany; ²École Polytechnique de Montréal, Canada. The spatial alignment of the crystallographic axes of single colloidal quantum dots is determined by purely optical means. This capability allows maximizing the Zeeman interaction in a magnetic field which is vital e.g. for efficient and ultrafast single-photon amplification.

FF3D.6 • 15:15

Probing the Influence of Shell Configurations on the Exciton Dephasing of CdSe Colloidal Quantum Dots Using Multidimensional Coherent Spectroscopy, Diogo Almeida¹, Albert Liu¹, Wan Ki Bae³, Lazaro Padilha², Steven T. Cundiff¹; ¹Univ. of Michigan, USA; ²Universidade Estadual de Campinas, Brazil; ³Korea Inst. of Science and Technology, South Korea. Using multidimensional coherent spectroscopy, measurements of exciton dephasing, acoustic phonon confinement and fine structure splitting were obtained for CdSe colloidal quantum dots with different shell configurations, enabling identification of the shell's influence over these properties.

FF3D.7 • 15:30

Evidence of Non-Markovian Dynamics in CdSe/CdZnS Colloidal Quantum Dots Revealed by 2D Coherent Spectroscopy, Albert Liu¹, Diogo Almeida¹, Wan Ki Bae², Lazaro Padilha³, Steven T. Cundiff¹; ¹The Univ. of Michigan, USA; ²Korea Inst. of Science and Technology, South Korea; ³Universidade Estadual de Campinas, Brazil. We present evidence of non-Markovian dynamics of interband coherences in CdSe/CdZnS colloidal quantum dots by using the 0-quantum 2D coherent spectroscopy technique at cryogenic temperatures.

CLEO: QELS-Fundamental Science

FF3E • Photon-Phonon Interactions and Cooling—Continued

FF3E.4 • 15:00

Investigation of solid state laser cooling in Ytterbium-doped silica fibers, Esmail Mobini¹, Mostafa Peysokhan¹, Behnam Abaie¹, Arash Mafi¹; ¹Univ. of New Mexico, USA. The possibility of solid-state laser cooling (SSLC) in a single mode Yb-doped silica fiber is investigated. The results show that the material is a viable candidate for SSLC and radiation-balanced lasers.

FF3E.5 • 15:15

Effect of Thermal Nonlinearities on Sideband Asymmetry Measurements in Quantum Optomechanics, Itay Shomroni¹, Liu Qiu¹, Marie Ioannou¹, Daniel Malz², Andreas Nunnenkamp², Tobias J. Kippenberg¹; ¹EPFL, Switzerland; ²Cavendish Lab, Univ. of Cambridge, UK. Probing an optomechanical crystal cavity with two optical tones leads to generation of multiple asymmetric mechanical sidebands. This occurs due to nonlinear thermal effects in the cavity, that interfere with the optomechanical scattering.

FF3E.6 • 15:30

Measuring the spin-dependent lateral force in evanescent fields, Lulu Liu¹, Andrea Di Donato¹, Vincent Ginis^{1,2}, Simon Kheifets¹, Arman Amirzhan¹, Federico Capasso¹; ¹Harvard SEAS, USA; ²Applied Physics, Vrije Universiteit Brussel, Belgium. We report the quantitative measurement of the out-of-plane spin-dependent optical force acting on a microsphere in evanescent fields. The measurement was made via a thermally-limited floating-probe detection scheme with extreme sensitivity and high dynamic range.

CLEO: Science & Innovations

FF3F • Optomechanical Interactions and Single Particle Tracking—Continued

FF3F.4 • 15:00

Synthetic Optical Anisotropy via Plasmonic Resonant Tuning of Nanorod Orientation, Huizhong Xu¹, Trevor S. Kelly¹, Pepito J. Alvaro¹, Yu-Xuan Ren¹, Chensong Zhang¹, Yinxiao Xiang¹, Zhigang Chen^{1,2}; ¹Dept. of Physics & Astronomy, San Francisco State Univ., USA; ²TEDA Applied Physics Inst. and School of Physics, Nankai Univ., China. We demonstrate tunable orientation of gold nanorods in colloidal suspensions via plasmonic resonant solitons. Wavelength-dependent polarizability and optical torque lead to synthetic anisotropic optical properties (birefringence and dichroism) of the nanorods along the soliton channel.

FF3F.5 • 15:15

Programmable Transport of Nanoparticles Based on a Plasmonic Metasurface, Min Jiang¹, Guanghui Wang¹, Wenhao Xu¹, Xuping Zhang¹; ¹Nanjing Univ., China. Plasmonic nano-ellipses metasurface are designed for the realization of programmable two-dimensional transport of nanoparticles through rotating the polarization of an excitation beam, which can be used in lab-on-a-chip applications.

FF3F.6 • 15:30

Long-range Laser-induced Self-assembly via Plasmon Radiative Interactions and the Lorentz Force, Haojie Ji¹, Jacob Trevino^{2,3}, Raymond Tu^{4,3}, Ellen Knapp⁴, Farzad Mashayek⁵, Vitaliy Yurkiv⁵, Luat Vuong^{1,6}; ¹Queens College of CUNY, USA; ²Chemistry, The Graduate Center of the City Univ. of New York, USA; ³Advanced Science Research Center of the Graduate Center at the City Univ. of New York, USA; ⁴Chemical Engineering, City College of New York, USA; ⁵Mechanical and Industrial Engineering, Univ. of Illinois at Chicago, USA; ⁶Physics, The Graduate Center of the City Univ. of New York, USA. We report on the light-induced formation of gold-nanoparticle chains as long as 200 μ m, aligned perpendicular to the illuminating linear polarization. The long-range self-assembly is shown to arise from plasmon radiation and the Lorentz force.

CLEO: QELS-Fundamental Science

SF3G • Quantum Cascade Lasers—Continued

SF3G.4 • 15:00

The Role of Spatial and Spectral Hole Burning in QCL Frequency Comb Formation, Nathan C. Henry¹, Jacob Khurgin¹; ¹Johns Hopkins Univ., USA. We investigate theoretically formation of frequency comb in Quantum Cascade Lasers operating in mid-IR and THz regions and show that spectral and spatial hole burning mitigation favors pseudo-random frequency modulation format.

SF3G.5 • 15:15

Raman Emission From An Electrically Pumped Phonon Polariton Laser, Keita Ohtani¹, Lorenzo Bosco¹, Mattias Beck¹, Martin Franckie¹, Camille Ndebeka-Bandou¹, Jérôme Faist¹; ¹ETH Zurich, Switzerland. We demonstrate an electrically pumped laser that generates phonon polaritons. The emission also appears directly on a Raman spectrum measurement exhibiting a Stokes and anti-Stokes component with the expected shift of 48meV.

SF3G.6 • 15:30

Surface-Emitting Terahertz Quantum-Cascade Laser with 170 mW Output Power in a Single Lobed Beam, Yuan Jin¹, Liang Gao¹, Ji Chen¹, Chongzhao Wu¹, John Reno², Sushil Kumar¹; ¹Lehigh Univ., USA; ²Sandia National Labs, USA. A fourth-order Bragg grating scheme is developed to achieve single-lobed emission and increased radiative efficiencies from surface-emitting semiconductor lasers. Record-high peak output power of 170mW is demonstrated for a single-mode 3.4THz quantum-cascade laser at 62K.

CLEO: QELS-Fundamental Science

FF3H • Wavefront Shaping in Complex Media—Continued

FF3H.5 • 15:00 **Invited**

Adaptive Wave-front shaping in Linear and Nonlinear Complex Media, Omer Tzang¹, Antonio Caravaca-Aguirre¹, Kelvin Wagner¹, Rafael . Piestun¹; ¹Univ. of Colorado Boulder, USA. We present wave-front-shaping (WFS) methodologies for controlling light propagation in complex nonlinear media. We demonstrate linear and nonlinear photoacoustic feedback for focusing through scattering media and control nonlinear interactions along multimode fibers.

FF3H.6 • 15:30

Coherent Injection of Light into Lossy Micro-Porous Scattering Medium, Alexey G. Yamilov¹, Raktim Sarma², Vladislav Yakovlev³, Hui Cao²; ¹Missouri Univ of Science & Technology, USA; ²Yale Univ., USA; ³Texas A&M Univ., USA. We demonstrate a possibility of efficient injection of light into scattering lossy medium by coupling to eigenchannels confined to a micro-pore. Evidence of enhanced injection past absorption length is obtained in wave-front shaping experiments.

CLEO: Science & Innovations

CLEO: Applications
& TechnologySF31 • Materials for Fiber and
Solid State Lasers—Continued

SF31.5 • 15:00

Crystal growth, spectroscopy and femto-second laser performance of Tm,Na:CNGG disordered garnet crystal, Zhongben Pan^{1,2}, Yicheng Wang¹, Yongguang Zhao^{1,3}, Hualei Yuan², Xiaojun Dai², Huaqiang Cai², Ji Eun Bae⁴, Sun Young Choi⁴, Fabian Rotermund⁴, Xavier Mateos⁵, Josep Maria Serres⁵, Pavel Loiko⁶, Uwe Griebner¹, Valentin Petrov¹; ¹Max-Born-Inst. for Nonlinear Optics and Short Pulse Spectroscopy, Germany; ²Inst. of Chemical Materials, China Academy of Engineering Physics, China; ³Jiangsu Key Lab of Advanced Laser Materials and Devices, Jiangsu Normal Univ., China; ⁴Dept. of Physics, Korea Advanced Inst. of Science and Technology (KAIST), South Korea; ⁵Física i Cristallografia de Materials i Nanomaterials (FICMA-FICNA)-EMaS, Dept. Química Física i Inorgànica, Universitat Rovira i Virgili (URV), Campus Sescelades, Spain; ⁶ITMO Univ., Russia. We report on the crystal growth, spectral properties, and mode-locked laser operation of Tm,Na:CNGG, generating pulses as short as 84 fs at ~2018 nm using single-walled carbon nanotubes as a saturable absorber.

SF31.6 • 15:15

Reduced loss in SiGe-core optical fibers, Trygve Sörgård¹, Korbinian Mühlberger², Wu Wei¹, Xiong Yang², Thomas Hawkins³, John Ballato³, Fredrik Laurell², Michael Fokine², Ursula J. Gibson^{1,2}; ¹Norges Teknisk Naturvitenskapelige Univ, Norway; ²Applied Physics, KTH, Sweden; ³Clemson Univ., USA. We investigate CO₂ laser processing of SiGe-core glass fibers, and show that homogeneous, low optical loss cores can be made. Coaxial Ge-rich centers within the semiconductor cores can also be fabricated.

SF31.7 • 15:30

Efficient High Power Yellow Tb³⁺:LiLuF₄ Laser, Elena Castellano-Hernández¹, Maksim Dzemesh⁴, Hiroki Tanaka², Christian Kränkel^{1,3}; ¹Leibniz Inst. for Crystal Growth, Germany; ²Dept. of Electronics and Electrical Engineering, Keio Univ., Japan; ³Inst. of Laser Physics, Univ. of Hamburg, Germany; ⁴Center for Optical Materials and Technologies, Belarusian National Technical Univ., Belarus. We report on yellow Tb³⁺:LiLuF₄ solid-state lasers. Under 2.1 W of 2ω-OPSL-pumping at 486.2 nm the laser delivers 0.45 W of cw output at a wavelength of 587.5 nm and a slope efficiency of 23%

SF3J • Mid IR Sensing and
Optical Forces—Continued

SF3J.5 • 15:00

Thin-Film Magnetless Faraday Rotators for Heterogeneously Integrated On-Chip Optical Isolators, Miguel Levy¹, Dolendra Karki¹, Vincent Stenger², Andrea Pollock²; ¹Michigan Technological Univ., USA; ²Srco, Inc, USA. This article describes the processing, characterization, and transfer of 26 μm-thick by 480 μm-long iron-garnet Faraday rotator films onto semiconductor substrates. Insertion losses below 0.1 dB and extinction ratios of -30 dB are achieved. No magnets are needed.

SF3J.6 • 15:15

Mid-Infrared Silicon-on-Sapphire Polarization Rotator, Joel Guo², Ali Rostamian², Swapnajat Chakravarty¹, Hai Yan², Chi-Jui Chung², Elham Heidari², Ray Chen^{2,1}; ¹Omega Optics, Inc, USA; ²Electrical and Computer Engineering, Univ. of Texas at Austin, USA. We experimentally demonstrate mid-infrared polarization rotators in silicon-on-sapphire at wavelength λ = 4.55mm to enable integration of quantum cascade lasers and detectors with slotted photonic crystal waveguide gas sensors. Polarization selective grating couplers are also demonstrated.

SF3J.7 • 15:30

Mid-infrared integrated photonic elements and efficient couplers on fusion-bonded, suspended silicon membranes, Jeff Chiles¹, Nima Nader¹, Scott A. Diddams¹, Sae Woo Nam¹, Richard Mirin¹; ¹NIST, USA. Using all-silicon fusion-bonded membrane waveguides, we demonstrate efficient input/output couplers with 1.8 dB loss at λ = 3.06 μm, 1×2 power splitters (Y- and MML-type), 25 μm bends, and 0.35 dB transitions to fusion-sealed micro-channels.

SF3K • Mode-Locked Fiber
Lasers—Continued

SF3K.4 • 15:00

Figure-9 Fiber Laser with Phase Bias by Frequency Shifter, Yuki Shirakura¹, Koji Takiguchi¹, Shinji Yamashita¹, Sze Y. Set¹; ¹The Univ. of Tokyo, Japan. We propose a novel figure-9 fiber laser using a frequency shifter to produce phase bias. Mode-locking operation is successfully achieved, and arbitrary phase bias can be produced by changing the frequency shift.

SF3K.5 • 15:15

Reduction of Intensity Noise in Mode-Locked Er-Fiber Oscillators and Amplifiers by Optical Bandpass Filtering, Dohyun Kim¹, Shuangyou Zhang¹, Jungwon Kim¹; ¹Korea Advanced Inst of Science & Tech, South Korea. Relative-intensity-noise (RIN) of <140 dB/Hz over broad offset frequency (20 Hz – 1 MHz) of mode-locked Er-fiber oscillator output is demonstrated by optical bandpass filtering. Optical filtering also reduces the Er-doped fiber amplifier output RIN by ~10-dB.

SF3K.6 • 15:30

Gate controllable and stabilized ultrafast fiber lasers based on graphene, Baicheng Yao¹, Giancarlo Soavi¹, Teng Ma¹, Xiao Zhang¹, Bo Fu¹, Duhee Yoon¹, Syed Hussain¹, Antonio Lombardo¹, Daniel Popa¹, Andrea Ferrari¹; ¹Cambridge graphene center, Univ. of Cambridge, UK. We report an all-fiber graphene-based gate tunable saturable absorber, dispersion controller and electrical feedback acceptor, for mode-locked lasers, enabling tunable repetition rate up to 348 GHz, with minimized supermode noise <-50 dB and timing jitter <6.62×10⁻¹⁷ s.

AF3M • Instruments and
Components for Spectroscopy—
Continued

AF3M.4 • 15:00

Impact of Tapered Nano-Slits Grating on The Optical Enhancement of Photo-Sensing Devices, Ahmad A. Darweesh¹, Stephen Bauman¹, Joseph Herzog¹; ¹Univ. of Arkansas, USA. A nano-grating structure with a 5nm slit and 15 nm thickness was simulated. Optical enhancement, which can be harnessed to improve photo-sensing devices such as photodetectors and biosensors, was calculated for various tapered nanoslits.

AF3M.5 • 15:15

Wavefront Aberration Compensation Method to Fabricate Large Gratings with Low Spacing Error Using Broad-beam Scanning Exposure, Yuxuan Zhao¹, Lijiang Zeng¹; ¹Tsinghua Univ., China. A wavefront aberration compensation method is proposed to reduce the spacing error accumulation in broad-beam scanning exposure. A 200 mm × 100 mm grating with a spacing error of 0.07 λ was fabricated.

AF3M.6 • 15:30

Goddard Laser for Absolute Measurement of Radiance for Instrument Calibration in the Ultraviolet to Short Wave Infrared, Brendan McAndrew¹, Joel McCorkel¹, Timothy Shuman², Barbara Zukowski³, Aboubakar Traore⁴, Michael Rodriguez⁵, Steven Brown⁶, John Woodward⁶; ¹NASA Goddard Space Flight Center, USA; ²Fibertek, USA; ³Ball Aerospace, USA; ⁴NASA Langley Research Center, USA; ⁵Sigma Space Corporation, USA; ⁶NIST, USA. A description of the Goddard Laser for Absolute Calibration of Radiance, a tunable, narrow linewidth spectroradiometric calibration tool, and results from calibration of an earth science satellite instrument from ultraviolet to short wave infrared wavelengths.

**CLEO: Science &
Innovations**

**SF3N • Ultrafast Pulse
Manipulation—Continued**

SF3N.5 • 15:00

Three-octave-wide Phase-stable Seeding Scheme for Parallel Parametric Waveform Synthesizers, Roland E. Mainz^{1,2}, Giulio M. Rossi^{1,2}, Yudong Yang^{1,2}, Oliver Muecke^{1,2}, Giovanni Cirmi^{1,2}, Franz X. Kaertner^{1,2}; ¹Center for Free-Electron Laser Science, Deutsches Elektronen-Synchrotron DESY, Germany; ²Univ. of Hamburg, Physics Dept. and The Hamburg Centre for Ultrafast Imaging, Germany. We present a three-octave-wide phase-stable seeding scheme using separate supercontinua in bulk driven by a CEP-stable laser and its second harmonic to provide optimized seeds for each spectral channel of a parallel parametric waveform synthesizer.

SF3N.6 • 15:15

Flexible Width Nyquist Pulse Based on a Single Mach-Zehnder Modulator, Jianqi Hu¹, Simon J. Fabbri¹, Camille-Sophie Bres¹; ¹EPFL, Switzerland. We present a Nyquist pulse generation technique based on a single Mach-Zehnder modulator driven by a multi-harmonic electrical signal. The direct control of the RF components yields a range of 10 GHz sinc-shaped pulse train.

SF3N.7 • 15:30

On-the-fly Recovery of Arbitrary Waveforms from In-band Noise by Linear Coherent Spectral Energy Re-distribution, Benjamin G. Crockett¹, Luis Romero Cortés¹, Jose . Azana¹; ¹INRS, Canada. We introduce a novel concept for in-band noise mitigation applicable to non-repetitive events, through linear spectral and temporal phase control. We demonstrate recovery of broadband optical waveforms, with unknown characteristics, buried under noise.

**CLEO: QELS-
Fundamental Science**

**FF3P • Strong-field Physics in
Solids—Continued**

FF3P.4 • 15:00

Controlling High Harmonic Generation in Tailored Semiconductors, Marco Taucer^{1,3}, Murat Sivas^{2,3}, Giulio Vampa^{1,3}, Kyle Johnston^{1,3}, André Staudte^{1,3}, Andrei Naumov^{1,3}, David Villeneuve^{1,3}, Claus Ropers², Paul B. Corkum^{1,3}; ¹Univ. of Ottawa, Canada; ²Georg-August Univ., Germany; ³National Research Council of Canada, Canada. Here, we use nanofabrication tools to demonstrate the potential to tailor semiconductor targets for high harmonic generation. Morphology and local composition can localize light fields and enhance emission, which can be used to realize new high harmonic devices.

FF3P.5 • 15:15

Strong-Field Polarization-State Control of Higher Harmonics Generated in Crystalline Solids, Nicolai Klemke^{1,2}, Nicolas Tancogne-Dejean^{3,4}, Giulio M. Rossi^{1,2}, Yudong Yang^{1,2}, Roland E. Mainz^{1,2}, Giuseppe Di Sciacca¹, Eliza Casandru¹, Angel Rubio^{3,4}, Franz X. Kaertner^{1,2}, Oliver Muecke^{1,5}; ¹Center for Free-Electron Laser Science CFEL, Deutsches Elektronen Synchrotron DESY, Germany; ²Physics Dept., Univ. of Hamburg, Germany; ³Max Planck Inst. for the Structure and Dynamics of Matter, Germany; ⁴European Theoretical Spectroscopy Facility (ETSF), Germany; ⁵The Hamburg Centre for Ultrafast Imaging, Germany. We demonstrate that the polarization states of higher harmonics emitted from crystalline solids (here silicon, quartz) are determined by both crystal symmetry and nonperturbative dynamics, opening the door to strong-field control of the harmonics' polarization states.

FF3P.6 • 15:30

Anisotropic Polarization Dependent High Harmonic Generation in the Ferroelectric Crystal BaTiO₃, Shima Gholam Mirzaeimoghaddar¹, Erin Crites¹, John E. Beetar¹, Aiping Chen³, Michael Chini^{1,2}; ¹Physics, Univ. of Central Florida, USA; ²CREOL, the College of Optics and Photonics, Univ. of Central Florida, USA; ³Center for Integrated Nanotechnologies, Los Alamos National Lab, USA. We generate high-order harmonics from femtosecond mid-IR pulses in ferroelectric BaTiO₃ crystals. We find that odd and even harmonics' intensity and polarization behave differently when rotating the input polarization with respect to the crystal axes.

**CLEO: Applications
& Technology**

**AF3Q • A&T Topical Review
on Time-Stretch Technology:
Principles and Applications II—
Continued**

AF3Q.3 • 15:00 **Invited**

Optofluidic Time-stretch Microscopy for Precision Medicine, Cheng Lei¹, Yasuyuki Ozeki², Keisuke Goda¹; ¹Dept. of Chemistry, The Univ. of Tokyo, Japan; ²Dept. of Electrical Engineering and Information Systems, The Univ. of Tokyo, Japan. We present the principle of optofluidic time-stretch microscopy and its application to precision medicine. Its ability to perform multiparametric image-based profiling of numerous single cells enables biomedical data mining with the help of machine learning.

AF3Q.4 • 15:30

Introduction to Time-folded Optics; Spatial Compression of Paraxial Optics Using Time, Barmak Heshmat¹, Matthew Tancik¹, Guy Satat¹, Ramesh Raskar¹; ¹MIT, USA. We exploit the high time resolution of ultrafast imaging sensors to fold and modify the imaging optics of the camera. We demonstrate an order of magnitude compression in lens-sensor distance using a time-folded design.

Executive Ballroom
210A

CLEO: Science &
Innovations

SF3A • Integrated Photonics
(III-V Heterogeneous)—
Continued

SF3A.7 • 15:45

A multifunctional micro-electro-opto-mechanical (MEOM) platform based on phase-transition materials, Xi Wang¹, Kaichen Dong^{1,2}, Hwan Sung Choe^{1,2}, HuiLi Liu^{1,2}, Shuai Lou¹, Kyle Tom^{1,2}, Hans Bechtel⁴, Zheng You³, Junqiao Wu^{1,2}, Jie Yao^{1,2}; ¹Univ. of California, Berkeley, USA; ²Materials Sciences Division, Lawrence Berkeley National Lab, USA; ³Dept. of Precision Instrument, Tsinghua Univ., China; ⁴Advanced Light Source Division, Lawrence Berkeley National Lab, USA. We demonstrate a new MEOM multifunctional platform activated by the structural phase transition of an embedded vanadium dioxide layer. Its diverse stimuli and > 50% optical modulation depth over a broad wavelength range promise versatile applications.

Executive Ballroom
210B

Joint

JF3B • Symposium on Emerging
Quantum Sensing Techniques
and Applications II—Continued

Executive Ballroom
210C

CLEO: QELS-Fundamental Science

FF3C • Optimization and Design
of Metasurfaces—Continued

Executive Ballroom
210D

FF3D • Spectroscopy of
Low Dimensional Systems—
Continued

FF3D.8 • 15:45

A Near Deterministic Plasmonic Quantum Zeno Gate using Graphene Nanoribbons, Irati Alonso Calafell¹, Joel Cox², Milan Radonjic¹, José Ramón Martínez Saavedra², Javier García de Abajo³, Lee Rozema¹, Philip Walther¹; ¹Univ. of Vienna, Austria; ²ICFO, Spain. The scalability of photonic quantum-computation is limited by the low success probability of two-qubit logic gates. We propose a root-SWAP gate based on graphene nanoribbons, where the strong two-plasmon absorption boosts its success above 90%.

Executive Ballroom
210E

CLEO: QELS-Fundamental Science

FF3E • Photon-Phonon Interactions and Cooling—Continued

FF3E.7 • 15:45

Observation of stimulated Brillouin scattering and Brillouin frequency comb generation in diamond, Zhenxu Bai^{1,2}, Robert J. Williams¹, Ondrej Kitzler¹, Soumya Sarang¹, Richard P. Mildren¹; ¹Macquarie Univ., Australia; ²Harbin Inst. of Technology, China. We report evidence for stimulated Brillouin scattering in diamond using an intense Raman-generated intracavity pump. Configurations are described for producing a single Stokes line and a Brillouin frequency comb containing up to the 22 orders spaced over 1.55 THz.

Executive Ballroom
210F

FF3F • Optomechanical Interactions and Single Particle Tracking—Continued

FF3F.7 • 15:45

All-optical Light Control in Dielectric Bilayer Optical Surfaces via Optomechanical Interaction, Carol Bibiana Rojas Hurtado¹, Johannes Dickmann¹, Walter Dickmann², Thomas Siefke³, Stefanie Kroker^{1,2}; ¹Physikalisch-Technische Bundesanstalt, Germany; ²Technische Universität Braunschweig, Germany; ³Friedrich-Schiller-Universität Jena, Germany. We propose a bilayer Gamma-shape grating structure as a novel nano-optomechanical system promising for all-optical modulation in a frequency range of a few MHz up to a few 100 MHz.

Executive Ballroom
210G

CLEO: Science & Innovations

SF3G • Quantum Cascade Lasers—Continued

SF3G.7 • 15:45

Difference-Frequency Generation Terahertz Quantum Cascade Lasers with Surface Grating Outcouplers, Jae Hyun Kim¹, Seungyong Jung¹, Yifan Jiang¹, Kazuo Fujita², Masahiro Hitaka², Akio Ito², Tadataka Edamura², Mikhail A. Belkin¹; ¹Univ. of Texas at Austin, USA; ²Hamamatsu Photonics K.K., Japan. We report terahertz quantum cascade laser sources based on intra-cavity difference-frequency generation processed into double-metal waveguides with surface-grating outcouplers. Over 112 μ W of peak power output is produced at room temperature at 1.9 THz.

Executive Ballroom
210H

CLEO: QELS-Fundamental Science

FF3H • Wavefront Shaping in Complex Media—Continued

FF3H.7 • 15:45

Broadband perfect transmission through non-Hermitian disordered media, Konstantinos Makris¹, Andre Brandstotter², Stefan Rotter²; ¹Univ. of Crete, Greece; ²Inst. for Theoretical Physics, Vienna Univ. of Technology, Austria. We examine the resonance properties of a novel type of waves, the constant-intensity (CI) waves in one-dimensional non-Hermitian disordered media. Such CI waves propagate perfectly through a scattering landscape without any reflection.

Friday, 14:00–16:00

Meeting Room
211 B/D

Meeting Room
212 A/C

Meeting Room
212 B/D

Marriott
Salon III

CLEO: Science & Innovations

CLEO: Applications
& Technology

SF3I • Materials for Fiber and
Solid State Lasers—Continued

SF3J • Mid IR Sensing and
Optical Forces—Continued

SF3K • Mode-Locked Fiber
Lasers—Continued

AF3M • Instruments and
Components for Spectroscopy—
Continued

SF3I.8 • 15:45

Direct generation of a 'bottle beam' from an end-pumped Nd:YVO₄ laser with second-harmonic generation, Jung-Chen Tung¹, Yuan-Yuan Ma¹, Yung-Fu Chen², Kai-Feng Huang², Takashige Omatsu¹; ¹Chiba Univ., Taiwan; ²National Chiao Tung Univ., Taiwan. We have demonstrated, for the first time, the generation of an optical 'bottle beam' with a 'zero-intensity' region surrounded by three-dimensional bright regions from an intra-cavity frequency-doubled Nd:YVO₄ laser with a nearly hemispherical cavity configuration.

SF3J.8 • 15:45

Long-Wave Infrared Germanium-on-Silicon Waveguides Beyond 10 μm, Dmitry Kozak¹, Todd H. Stievater¹, Rita Mahon¹, Marcel W. Pruessner¹, William S. Rabinovich¹; ¹US Naval Research Lab, USA. We show low-loss propagation in germanium-on-silicon (GOS) waveguides from 6.85 μm to 11.25 μm. The loss is as low as a few dB/cm at a wavelength of 10 μm for both the quasi-TE₀₀ and quasi-TM₀₀ modes.

AF3M.7 • 15:45

Peculiarities of near-room-temperature thermal-emission measurements using FTIR spectroscopy, Yuzhe Xiao¹, Alireza Shahsafi¹, Patrick Roney¹, Chenghao Wan¹, Graham Joe¹, Zhaoning Yu¹, Jad Salman¹, Mikhail Kats¹; ¹Univ. of Wisconsin-Madison, USA. We investigated the impact of multi-source background emission on thermal-emission measurements using FTIR spectroscopy. We found that a backward-emitting background in the interferometer can lead to partial or total cancellation of the measured thermal emission.

Friday, 14:00–16:00

Marriott
Salon IV

**CLEO: Science &
Innovations**

SF3N • Ultrafast Pulse
Manipulation—Continued

Marriott
Salon VI

**CLEO: QELS-
Fundamental Science**

FF3P • Strong-field Physics in
Solids—Continued

FF3P.7 • 15:45

Wannier-Stark Localization in Bulk Gallium Arsenide Induced by Extreme Mid-Infrared Fields, Johannes Bühler¹, Christian Schmidt¹, Alexander-Cornelius Heinrich¹, Jonas Allerbeck¹, Reinold Podzinski², Daniel Berghoff², Torsten Meier², Wolf G. Schmidt², Christian Reichl³, Werner Wegscheider³, Daniele Brida¹, Alfred Leitenstorfer¹; ¹Dept. of Physics and Center for Applied Photonics, Univ. of Konstanz, Germany; ²Dept. of Physics and Center for Optoelectronics and Photonics Paderborn, Univ. of Paderborn, Germany; ³Solid State Physics Lab, ETH Zurich, Switzerland. Sub-cycle transmission measurements of bulk gallium arsenide biased by intense mid-infrared transients reveal a strong blue-shift of the optical absorption when the peak electric field reaches 10 MV/cm, indicating 2D-localization of electronic wave functions.

Marriott
Willow Glen

**CLEO: Applications
& Technology**

AF3Q • A&T Topical Review
on Time-Stretch Technology:
Principles and Applications II—
Continued

AF3Q.5 • 15:45

High-resolution time-stretch microscopy based on asynchronous optical sampling, Xi Zhou¹, Xin Dong¹, Jiqiang Kang², Liao Chen¹, Chi Zhang¹, Kenneth Kin-Yip Wong², Xinliang Zhang¹; ¹Wuhan National Lab for Optoelectronics, China; ²Dept. of Electrical and Electronic Engineering, The Univ. of Hong Kong, Hong Kong. We propose and demonstrate an ultrafast time-stretch microscopy based on asynchronous optical sampling (ASOPS) with 92-MHz sampling rate and 10-kHz frame rate, and this microscopy achieves 2.3- μ m lateral resolution leveraging 1.9-MHz acquisition bandwidth.

Friday, 14:00–16:00

Key to Authors and Presiders

A

A. Burrow, Joshua - JW2A.112
A. R. El-Ella, Haitham - JF3B.2
A. Viktorov, Evgeny - FTh1E.7
Aadhi, A. - FTh1E.7, FTh3E.8, STh3F.6
Aasmul, Soren - ATu3L.5
Abadia Calvo, Nicolas M. - JW2A.6
Abadia, Nicolás M. - FTh1K.3
Abaie, Behnam - FF2H.1, FF3E.4, JW2A.118, STu3K.2
Abbas, Ali - Ath3O.2
Abbaslou, Siamak - STh4A.3
Abbott, William M. - ATu4M.2
Abdelaziz, Abdallah M. - JTu2A.46
Abdi-Jalebi, Mojtaba - FM4F.2
AbdollahRamezani, Sajjad - SF1J.1
Abdou Ahmed, Marwan - SM1N.4
Abdulkarim, Nurmemet - SW4L.6
Abe, Hiroshi - SM2B.5
Abedin, Kazi S. - SF3K, SM3K.6, SW4K.4
Abel, Stephane - JW2A.120
Abernathy, Grey - STh4I.4
Aboujaoude, Andrea - JTu2A.6, JW2A.105
Abouraddy, Ayman - Ath3P.6, FM4E.4, FW4E.2, SW4N.3, SW4N.4
Abraham, Eitan - JTu2A.115
Abrams, Nathan - JTu2A.45
Abudayyeh, Hamza - JTh2A.37
Abuduweili, Abulikemu - SM1L.2
Acedo, Pablo - JW2A.171, STu3N.6
Acharya, Palash V. - STh1I.4
Acuna, Guillermo - AM1J.4
Adamonis, Jonas - STu4O.1
Adams, Daniel - AW4O.2
Adams, David - AM1J.6
Adamu, A. Isa - JTh2A.196
Adcock, Jeremy C. - FTh4G.2
Addamane, Sadhvikas - FW4H.8
Adel, Peter - STu3P.2
Adelung, Johanna - STu3P.2
Adhikari, Prakash - STu4P.5
Adibi, Ali - JTh2A.78, JTu2A.85, JW2A.33, SF1J.1, SF3A, SM1I.1, STh4A, SW4A.2, SW4B.6
Aeschlimann, Martin - FTh3M.3
Afkhamiardakani, Hanieh - JTh2A.141
Aflatouni, Firooz - SM3L.2
Afshar, Wardiya - AF2M.3
Afzal, Francis - STh3A.2
Afzal, Shirin - JW2A.85
Aggarwal, Ishwar D. - SM1N.1
Agha, Imad - JTh2A.71, JTu2A.6, JW2A.105, JW2A.106, JW2A.112
Aghaeimeibodi, Shahriar - JTh2A.35, SW3B.2
Agranat, Aharon - FM3E.2, FTh3E.2
Agranat, Aharon J. - SM4N.4
Agrawal, Amit K. - FF1F.1, FF2F.1, FTh3M.6, SW4D.3
Agrawal, Govind P. - FTh4E.3, SM3D.7
Agrell, Erik - SM4C.3
Aguiló, Magdalena - SM2N.6
Aharonovich, Igor - SM1O.5
Ahasan, Sohail - JTu2A.81, SM3I.2
Ahmad, Raja - SM3K.6, SW4K.4
Ahmadi, Ehsaneh D. - FTh1P.4
Ahmadi, Sepehr - JF3B.2
Ahmed, Zeeshan - JF2B.5
Ahn, Geun Ho - STu4N.6
Ahn, Hyeyoung - JTh2A.69, STu4N.2
Ahn, Jaewook - FM2H.7, JTh2A.29
Ahn, Jonghoon - FF3F.1, JF3B.3
Aho, Antti - JTu2A.28
Ahr, Frederike - FF1E.3
Ahrens, Jan - STh3N.2
Ai, Fan - JW2A.167
Aikawa, Kazuhiko - JTu2A.52
Aikawa, Masaki - JTu2A.12

Aitchison, J. Stewart - STh4A.5
Ajayan, Pulickel - FF1D.3
Ajayi, Obafunso - JW2A.135, JW2A.136
Akahane, Kouichi - JTu2A.15
Akamatsu, Daisuke - JTh2A.32
Akabba, Enis - SM2C.4
Akel, Hatem - SM2C.4
Akimoto, Ryoichi - SW4B.7
Akiyama, Akifumi - FTh1H.1
Akiyama, Jun - SM4N.6
Akopian, Nika - FM4J.1
Akosman, Ahmet E. - JTh2A.153
Aktas, Ozan - SM3D.5
Aktürk, Selçuk - SM3O.3
Akulov, Katherine - FM2F.2
Al Alshaykh, Mohammed S. - FM4G.2, JTu2A.112
Al Noman, Abdullah - JW2A.13, SM1B.1, STh4A.1
Al Qubaisi, Kenaish - SF1A.5
Alam, Shaif-UI - ATu3S.3, JTh2A.77, SM4K.2, SM4K.5, STh3F.2, SW3K
Alassaad, Kassem - JTh3C.5
Alattar, Nebras - AF2M.5
Albert, Félicie - JF2C.4
Albooyeh, Mohammad - FTh1K.1, FTh1K.2
Albrecht, Alexander - FF3E.1, JTu2A.14, SM4N.5
Albrecht, Daniel - AM1M.4
Albrecht, Manfred - FM4F.3
Albrecht, Michèle - SW4N.7
Albrow-Owen, T. - JTh2A.82, JTh2A.83, SF3K.2
Alcaraz, David - FW3G.5
Alcocer, Marcelo - FF2D.7
Aldaya, Ivan A. - FF1E.8, JTu2A.71, JW2A.58, STh1C.5
Alden, Caroline - Ath4P.3
Aldén, Marcus - FM1Q.5
Alden, Marcus L.E. - ATu4I.1, STh4L.4
Alegre, Thiago P. - JTu2A.111
Aleksandrov, Veselin - JTu2A.69
Alemohammad, Milad - JW2A.68, SW4J.6
Alexaline, Olivier - JTu2A.88
Alexander, Koen - FF2E.3
Alfano, Robert - JTu2A.97
Alfieri, Cesare - Ath3O.6, JW2A.157, SF1G.2, SM4L.7
Alfredsson, Arni - SM4C.3
Alghoniemy, Masoud - JTu2A.46
Alhabebe, Mohamed - FM2G.7
Alic, Nikola - STu4B.3
Ališauskas, Skirmantas - Ath1O.2, FM1Q.1
Alishahi, Fatemeh - JTu2A.49, JTu2A.53, SM1D.2, SW3A.5
Al-Kabi, Sattar - JTh2A.79
Alkauskas, Audrius - FTu4H.1
Al-Khateeb, Mohammad A. - SM2C.6, STh1C.4
Alkhazraji, Emad - JTu2A.34
Allegro, Isabel - SM4I.6
Allen, Euan - SF1K.7
Allen, Gabriel - SW3L.4
Allen, Jeffery W. - JTu2A.77
Allen, Monica S. - JTu2A.77
Allen, Taylor - JTu2A.59
Allen, Troy - ATu4M.4
Allison, Thomas - FW3E.1
Allmaras, Jason - FW3F.3
Alloatti, Luca - SF1A.5
Almairan, Ahmed - JTu2A.49, JTu2A.53, SM1D.2, SW3A.5
Almási, Gábor - SM3A.2
Almeida, Diogo - FF3D.6, FF3D.7
Almeida, Euclides C. - FF1E.7

Almeida, Gustavo - JTu2A.1
Almeida, Juliana - JTu2A.1
Almond, Nikita - FW3H.3, STu4D.5
Al-Mumin, Mohammed - JW2A.46
Alonso Calafell, Irati - FF3D.8, FW3G.5
Alpeggiani, Filippo - FF2L.1, FM2G.1, FW4G
Alperin, Samuel N. - FTu3E.6
Al-Qadi, Mustafa A. - JTu2A.35
Al-Shammari, Rusul M. - AF2M.5
Alshebeili, Saleh - JTu2A.34
Alt, Wolfgang - FM2H.3
Altmann, Yoann - AW3R.4
Altug, Hatic - FF2F.7, JTh2A.74
Alturkistany, Faisal H. - JTh2A.103
Alù, Andrea - FF3C.4, FM3Q.6, FTh3M.2, FW4H.5
Alvarado Zacarias, Juan Carlos - FM1E.2, SM3C.1
Alvaro, Pepito J. - FF3F.4
Alves, Luis Lemos - SM2N.2
Amani, Matin - STu4N.6
Amann, Markus - STh1B.3
Ambichl, Philipp - FF3H.1
Ambrosio, Antonio - FTh1K.6
Amemiya, Tomo - FM3J.7
Amemiya, Tomohiro - JW2A.92
Amezua Correa, Rodrigo - FM1E.2, FTh1M.3, FTh4E.5, FTh4E.6, JTh2A.196, SM2K.6, SM3C.1, STu3K.2, STu3K.3
Ami, Udi Ben - STu3K.5
Amin, Rubab - Ath1Q.4, FTh4H.2, SM1I.5
Amirzhan, Arman - FF3E.6
Amo, Alberto - FM3Q.4
Amrani, Foued - JTh2A.97, SF1K.2, SF1K.3, SM2N.2
Amrollahi, Pouya - FTh4H.5
Amzajerdian, Farzin - AW3R.3
An, Chengwu - Ath3O.3
An, Kyungwon - FM2H.5
An, Shaohua - SW4C.2
An, Xin - JTu2A.99
Anagnosti, Maria - SM1B.1
Anand, Sajant - FW3E.6, SF3G.3
Andaji-Garmaroudi, Zahra - FM4F.2
Andersen, David - AM2P.3
Andersen, Peter E. - AF1Q.1
Andersen, Ulrik L. - JF3B.2, JTh2A.10, JTh2A.25
Anderson, Brian - SW4K.3
Anderson, Jon - JTu2A.43, SW3C.2
Anderson, Miles H. - SM4K.7, STh4B.6, SW3A.1
Andrade, Luis H. - JW2A.140
Andrade, Nicolas M. - SM4I.3, SM4I.5
Andre, Paulo S. - JTu2A.50
Andrekson, Peter A. - JW2A.71, JW2A.149, STu3F.1, SW3C.1
Andrews, Mark - JTh2A.96
Andrews, Melissa - AF2M.3, STh1J.2
Andriukaitis, Giedrius - FM3M.2, SF1N.3, SM4M.1
Angermüller, Ulli - SW4L.1
Anjum, Dalaver - JTu2A.91
Anopchenko, Aleksei - FM4J.2
Ansari, Wahid - FW4F.1
Anstie, James - STu3P.3
Antier, Marie - SM2N.8
Antikainen, Aku J. - FTh4E.3, SM3D.7
Antipenkov, Roman - STu3M.2
Anton, Carlos - FTu3H.6, FTu3H.7
Antonelli, Cristian - STu3C.3
Antonio-Lopez, Jose - STu3K.2
Antonio-Lopez, Jose Enrique - FM1E.2, FTh1M.3, FTh4E.5, JTh2A.196, SM2K.6, SM3C.1, STu3K.3
Antony, Cleitus - SM2C.2

Aparanji, Santosh - JTu2A.70, SM1K.4
Appel, Stefan - FM1H.4
Arai, Shigehisa - FM3J.7, JW2A.92
Arakawa, Yasuhiko - FM1H.5, SF1A.7, STh3A.4
Arakelian, Sergey - JW2A.113
Araki, Shungo - SW3M.3
Arashida, Yusuke - JM2A.1
Araujo, Luis - JW2A.58
Araujo, Mateus - FTh4G.1
Arbabi, Amir - AF3M.3, FF1F.5, FF1F.7, SF1J.2
Arbabi, Ehsan - AF3M.3, FF1F.5, SF1J.2
Archipovaite, Giedre M. - SF1N.3
Arenskötter, Jan - FM2H.6
Argenti, Luca - FF1P.3
Arie, Ady - FTh1H.2, FW4H.3
Arieli, Uri - JTh2A.66
Arikawa, Takashi - SW3D.6
Arissian, Ladan - FTh1M.2, SM1O.7
Ariyaratne, Amila - JF2B.1
Arkinstall, Jake - FM3Q.2
Armani, Andrea M. - ATu3J, ATu4J.4
Armougom, Julie - Ath3O.1
Arndt, Catherine - FM4J.2
Arnold, Cord - STh3N.2
Arora, P. - FTh1P.2, JTh2A.40, JW2A.86
Arora, Pankaj - FTu4E.5
Arrizabalaga, O. - SM2K.6
Arrospide, E. - SM2K.6
Arteaga-Sierra, Francisco R. - SM3D.7
Arun, S. - JTu2A.70, SM1K.4
Asahara, Akifumi - STu4P.3
Asai, Takuya - SW4K.2
Asano, Takashi - FF1E.4
Asavanant, Warit - JTh2A.21
Asghar, Haroon - JTu2A.31
Asghari, Mohamad - AF3Q.1
Ashida, Masaaki - JW2A.127
Askins, Charles - SF3I.3
Aßmann, Christian - JTu2A.162
Astrauskas, Ignas - SM4M.1
Atabaki, Amir H. - STu4P.3
Atakhodjaev, Iskandar - FM1G.4
Atature, Mete - FM1H.1
Atcheson, Gwenael - FTh1K.3
Atikian, Haig - Ath3H.2, STu3F.6
Atkin, Joanna M. - JM1A.2
Atkinson, Jonathan - STh4A.1
Atwater, Harry - FF1H.6, FM3J.5, FTh3M.2
Auffeves, Alexia - FTu3H.6, FTu3H.7
Autry, Travis - FF3D.1, FF3D.3
Avella, Alessio - FF1B.6
Avrutin, Vitaliy - JTh2A.75
Awaji, Yoshinari - JTu2A.52, SM4C.1
Axner, Ove - STu3P.4
Aydin, Yigit O. - STh4K.2
Aytaç, Yigit - SW4N.5
Azana, Jose - FW4F.2, JTh2A.157, JTh4C.2, JTu2A.51, JW2A.143, SF3N.7, STh4N
Azarm, Ali - STh4K.6
Azhadast, MOHAMMAD HOSSEIN - ATu4M.3
Azzam, Shaimaa I. - FM2G.7, JTh2A.87

B

Baba, Toshihiko - SM2B.5
Babicheva, Viktoriia - JW2A.94
Baburin, Alexander S. - FTu4E.6
Bacco, Davide - FTh1G.5, FTh1G.7
Bacher, Andreas - STu3D.4
Bachmann, Dominic - SM3L.6
Backus, Sterling J. - STh1N.2
Badikov, Dmitrii - STh4F.5
Badikov, Valeriy - STh4F.5
Baditz, Máté - JTh2A.189
Bae, Hyemin - FM1F.1, FTh1F.1, JTh2A.172, JW2A.134, SW3I.3

- Bae, Ji Eun - SF3I.5
 Bae, Sanghoon - JTu2A.7
 Bae, Wan Ki - FF3D.6, FF3D.7
 Baek, Jieun - JTu2A.96
 Bækhoj, Jens E. - FF1P.2
 Baets, Roel - ATu3I.5, SM1B.3, STh1B.3, SW3L.5, SW3L.6
 Baeuerle, Benedikt - FTh4H.1, JTh4D.5, SM1I.4, SM4B.1
 Bagheri, Mahmood - SF2G.1
 Bagnell, Kristina - JTh3D.1
 Bahadur, Vaibhav - STh1I.4
 Bahari, Babak - FM4Q.8
 Bahk, Seung-Whan - STh3N.3, STu3M.6, SW3M
 Bahl, Gaurav - FM3E.1
 Bai, Jing - FTh4H.5, JW2A.19
 bai, jintao - JTh2A.92, JTu2A.95
 Bai, Lin - JTu2A.36
 Bai, Qingsong - JTh2A.184
 Bai, Weinan - JTh2A.139
 Bai, Wen-Bin - AW3O.1
 Bai, Xiaolei - SM2N.7
 Bai, Yang - JTh2A.92
 Bai, Zhenxu - FF3E.7
 Baiocco, Christopher - SF1A.5, SM3L.1, SW3B.4
 Bajoni, Daniele - JTu2A.128, STu3F.2
 Baker, Chams - AF1M.7
 Baker, Christopher A. - AM3P.2
 Baker, Colin - SW4K.5
 Baker, Robert D. - SM2K.1
 Bakhru, Hassaram - FTu4H.2
 Balachandran, Balasubramaniam - AF1Q.6
 Balaghi, Leila - JM2A.3
 Balakrishnan, Ganesh - FW4H.8
 Balaswamy, V - JTu2A.70, SM1K.4, SM1K.5
 Balch, Halleh B. - AM4P.2
 Balciunas, Ignas - STu4O.1
 Balciunas, Tadas - Ath1O.2, FM3M.2, SF1N.3, SM4M.1, SM4M.3
 Balembois, François - SM4M.4
 Balla, Itamar - STu4N.4
 Ballato, John - FF2H.1, SF3I.6, SM3D.5, STu3K.6
 Baltuska, Andrius - Ath1O.2, FF1E.2, FM1Q.1, FM1Q.2, FM3M.2, SF1N.3, SM4M.1, SM4M.3
 Balu, Mihaela - JTu4L.1
 Bamba, Motoaki - FF2D.6, FM2F.3
 Bancal, Jean-Daniel - FTh1H.5
 Bandres, Miguel A. - FF3E.2, FM1E.8, FM2E.3, FM2E.5
 Banerjee, Parag - JTh2A.71
 Banerjee, Saumyabrata - STu4O.6
 Banerji, Sourangsu - JW2A.76
 Bang, Jaehoon - FF3F.1, JF3B.3
 Bang, Ole - AW3S.1, JTu2A.109, SM3D.2, SM4K.1
 Bangalore Rajeeva, Bharath - STh1I.4
 Bank, Seth - FW4H.5, JTh2A.85, JW2A.104, STh1I.4, STh4I.3
 Banzer, Peter - FM2G.4
 Bao, Changjing - JTu2A.49, JTu2A.53, SW3A.5
 Bao, Chengying - STh4N.4, SW4M.2
 Bao, Shuyu - STh4I.6
 Bao, Wei - FM2F.4, SM4I.1
 Bao, Wenxia - JTh2A.128
 bao, xiaoyi - AF1M.7, SW3L.3
 Bapty, Rupert - SM4O.3
 Barako, Michael - FTh1P.3
 Barash, Yefim - FTu4E.5, JTh2A.40, SM3L.5, STh3F.5, STh3G.5
 Barclay, Paul E. - FW4F.6, SF2J.1
 Bar-David, Jonathan - JW2A.98
 Barh, Ajanta - SM4D.4
 Barkhofen, Sonja - FW3F.6
 Barner-Kowollik, Christopher - SM4O.5
 Barnes, Bruce W. - AW3R.3
 Barry, Liam - STh1C.5, SW4C.5
 Bartal, Guy - FM2Q.5, FTh3M.4, SW4J.2
 Bartalini, Saverio - Ath4Q.6
 Bartels, Randy A. - ATu3J.3
 Barth, David - FTh1D.5
 Barthelemy, Alain - SM3D.3, SW3K.6
 Bartholomew, John G. - FTu4H.4, FTu4H.5, JTh3C.3, STh3G.2
 Bartley, Tim J. - FW3F.6
 Bartolucci, Stephen - JTu3O.7
 Barton, Jennifer - SM1K.2
 Bartulevicius, Tadas - JTh2A.146, JTh2A.154
 Barua, Pranabesh - JTh2A.109, JTh2A.77
 Barwicz, Tymon - STh1B.2, STh4B.8
 Baryshnikova, Marina - JTu2A.21
 Basak, Abanti - AF1Q.3
 Bashan, Gil - JTu2A.80, SM3K.1, SM3K.7, STu4F.3
 Bashkansky, Mark - FM2H.4
 Basiri, Ali - FTh4H.5, JW2A.19
 Basov, Dimitri - JM1A.5
 Bastianini, Filippo - JW2A.166
 Bastos, Ana R. - JTu2A.50
 Bate, Timothy - JTu2A.19, JTu2A.27
 Batjargal, Orkhongua - SM1K.2
 Batysta, Frantisek - STu3M.2
 Bäuerle, Benedikt - SM2I.3
 Bauman, Stephen - AF3M.4
 Baumann, Esther - Ath4P.3, SM4L.1, STh1L.2
 Baumann, Susanne - JF2B.1
 Baumgarten, Cory - SM1N.5
 Baumgartner, Yannick - STh3I.6
 Bautista, Godofredo S. - FF1E.6, FTh4M, FW3G.3
 Bauwelinck, Johan - SM4C.4
 Bayya, Shyam - SF3I.3
 Beausoleil, Raymond - JW2A.36, STh3B.2
 Becher, Christoph - FW4E.3
 Bechtel, Hans - SF3A.7
 Beck, Mattias - Ath4Q.4, SF3G.2, SF3G.5, STh1L.5, STu4D.1, STu4D.3
 Becker, Jonas N. - Ath3H.8
 Becker, Simon F. - JTu2A.136
 Beckerwerth, Tobias - STu3B.4
 Bedrosian, P. S. - STu3C.7
 Beecher, Stephen - SW3M.2
 Beere, Harvey - FW3H.3, STu4D.5
 Beetar, John E. - FF3P.6, SW3N.4
 Begishev, Ildar - SM1N.7
 Beha, Katja - STu4K.3, SW4L.1
 Behovits, Yannic - FF3D.5
 Behunin, Ryan O. - FF3E.3, SM3K.5
 Behzadi, Behsan - JW2A.18
 Bekele, Dagmawi - STh3A.3
 Belardini, Alessandro - JTh2A.67
 belenky, gregory - SF2G.6
 Beling, Andreas - SM2I.1, SM2L.2, STu3B.5
 Belkin, Mikhail A. - FW4H.5, JTh2A.72, JW2A.104, SF2G.5, SF3G.7
 Bell, Bryn - FM4E.6
 Bell, Bryn A. - FTh1G.8
 Bell, Teboho - JTu2A.177
 Bellanger, Séverine - SM2N.8
 Belli, Federico - ATu3S.2, SM4M.2
 Bello, Frank - FTh1K.3, JTh2A.90
 Bello, Leon - FM1G.7
 Belov, Pavel - FM3Q.6
 Belue, Mason - JW2A.109
 Belyanin, Alexey - FW3E.6, SF3G.3
 Ben, Fang - JW2A.172
 Benabid, Fetah - FM4G.4, JTh2A.97, SF1K.2, SF1K.3, SF1K.6, SM2N.2, SM3L.3, SM3L.4
 Benalcazar, Wladimir A. - FM2Q.2
 Benamrouche, Aziz - STh3A.5
 Bencheikh, Kamel - SM4I.7
 Bendahmane, Abdelkrim - SW3K.6
 Bender, Nicholas - FF3H.4
 Benea-Chelms, Ileana-Cristina - FTh1H.3
 Ben-Hamida, Naim - SM3B.7
 Benis, Sepehr - FF2E.1, FTh1M.3, JTu2A.59
 Ben-Itzhak, Itzik - JW2A.182
 Benney, Lucas - SM3I.7
 Benson, Oliver - JTh2A.37, JTh2A.38
 Bentham, Christopher - JTh2A.27
 Benudiz, Yehuda - STu3K.5
 Bera, Subhabrata - SW3M.7
 Beravatt, Ramin - SW3K.2
 Bereyhi, Mohammad J. - Ath3H.6
 Bergé, Luc - JTu2A.121, JTu2A.160
 Bergeron, Hadallia - STu4N.4
 Bergeron, Hugo - SM1L.3
 Berggren, Karl K. - FF3D.4, FW3F.3, FW4H.1, SF3A.4, SM4I.2
 Berghoff, Daniel - FF3P.7
 Bergman, Arik - JTu2A.63
 Bergman, Keren - JTu2A.45, STh3B.6
 Bergmann, Alexander - Ath1O.5
 Berlin, Andrej - JW2A.138
 Bernard, Martino - FTh1E.2
 Bernhard, Christian - FM1F.5
 Bernier, Martin - STh4K.2
 Berrou, Antoine - SM3N.1
 Berruto, Gabriele - STh1N.4
 Bersin, Eric A. - FF1B.3, FM1H.3, FW3F.3
 Bertram, Rainer - SM4N.2
 Bertrand, Maxime - SM3B.4
 Bessire, Bänz - FF1B.4
 Beutler, Marcus - STh4F.5
 Bewley, William W. - SF2G.1, STh1B.7, STu3N.1
 Beyazoglu, Turker - SF2J.3
 Beyer, Andrew - FW3F.3
 Beyer, Sabrina - SM3N.4
 Bezryadina, Anna - SW4J.4
 Bhardwaj, Ashish - JTh2A.166, JTh2A.167
 Bhargava, Pavan - STh3L.7
 Bhaskaran, Harish - SW3I.1
 Bhatt, Gaurang R. - Ath3Q.1, FTu3E.2, STu4N.7
 Bhatta, Hari D. - AF1M.6
 Bhattacharyya, Sahana - FW4H.6
 Bhawe, Sunil - SW4B.3
 Bhokari, Hussai - SM2O.7
 Biancalana, Fabio - JTu2A.115
 Bianchi, Vezio - STu4D.6
 Bianucci, Pablo - SW4A.5
 Bidaux, Yves - STh1L.5
 Biekert, Nicolas - STu4N.3
 Bielejec, Edward - Ath3H.3, FF3D.1
 Bienfang, Joshua - FM1G, FM3G, FM4G
 Bierlich, Joerg - SF1K.5
 Bigelow, Matthew S. - JW2A.163
 Bigot, Jean-Yves - SW4N.7
 Bilek, Jan - JTh2A.25
 Billah, Muhammad R. - STh1A.1
 Billat, Adrien - SF2A.2
 Billet, Cyril - AF2Q.1
 Bin Nun, Moran - SF2A.4
 Binczeski, Artur - JW2A.137
 Binhammer, Thomas - STh3N.2
 Birks, Tim - SM3D.4
 Bishop, Zofia K. - JTh2A.27
 Bisianov, Arstan - FM1E.1, FTh4E.4
 Bismutto, Alfredo - SF2G.7
 Bissinger, Jochen - AM2M.6
 Bisschop, Suzanne - SW4I.4
 Blau, Federico - ATu3S.2, SM4M.2
 Bittner, Stefan - FM3E.6
 Black, Adam T. - FM2H.4
 Black, Adam T. - FM4H
 Black, Charles T. - FM3J.6
 Black, Dylan S. - FM3M.7
 Black, Jennifer A. - JTh2A.101
 Blackburn, Jeffrey L. - FTh1P.4
 Blaicher, Matthias - SM4I.6, STh1A.1
 Blanchard, François - SW3D.6
 Bland-Hawthorn, Joss - JW2A.65
 Blasco, Eva - SM4O.5
 Blaser, Stephane - SF2G.7
 Blau, Werner - AM2M.6
 Blau, Yoav - FF1H.3
 Blechman, Yael - FF1E.7
 Bleszynski Jayich, Ania - JF2B.1
 Bliker, Laurens - JTh3D.2
 Bloch, Immanuel - FTu4A.1
 Bloch, Jacqueline - FM3Q.4
 Blouin, Alain - Ath4O.5
 Blumenstein, Andreas - SM1N.8
 Blumenthal, Dan J. - FW3E.3
 Bluvstein, Dolev - JF2B.1
 Bo, Fang - JTu2A.139
 Boag, Amir - FF1H.3
 Bocklitz, Thomas - JTu4L.3
 Boechler, Nicholas - SF3A.6
 Boehm, Gerhard - STh1B.3
 Boehmke, Alexandra - FM2F.6
 Boes, Andreas - STu3F.5
 Bogacki, Wojbor - JW2A.137
 Bogdanov, Andrey - JTh2A.73
 Bogdanov, Simeon - FTu4E.6
 Bogoni, Antonella - JTh3D.3, JW2A.143, STh4N.3, SW4C.4
 Böhm, Florian M. - JTh2A.37, JTh2A.38
 Böhm, Julian - FF3H.1
 Bohndiek, Sarah E. - STh1I.2
 Boll, Rebecca - FF1P.1
 Boller, Klaus - SW4C.5
 Bolognini, Gabriele - JW2A.166
 Boltasseva, Alexandra - FM2G.7, FM3E.5, FM3J, FTh1K.8, FTh4H.1, FTh4J.1, FTh4M.2, FTh4M.4, FTu4E.6, SM4D.7
 Bömer, Christina - FM1Q.7
 Bomsse, David - Ath3P, Ath4P.2
 Bonamis, Guillaume - AM2M.4
 Bonato, Luiz G. - JTu2A.114
 Bono, Tiziana - JTh2A.194
 Bondu, Magalie - ATu3S.4
 Bonetti, Stefano - JW2A.83
 bongiovanni, domenico - FTh1M.7
 Bonifazi, Marcella - JW2A.115
 Bonilla-Manrique, Oscar Elias - JW2A.171
 Bonjour, Romain - JTh4D.5
 Bonn, D. - FM1F.7
 Bonneau, Damien - FTh1G.5
 Bonner, Carl E. - FW4G.6, JTh2A.182
 Bono, David - SF1A.1
 Bonsma-Fisher, Kent - FF1B.2
 Bony, Pierre-Yves - SM2C.3
 Bood, Joakim - ATu4I.1, FM1Q.5
 Booker, Henry T. - SM3D.2
 Bookjans, Eva - JW2A.137
 Boppe, Douglas - FTh4J.2
 borge, Ted - STu3M.2
 Borne, Kurtis - JW2A.182
 Borodin, Denis - FM1Q.7, JTh2A.7
 Borsch, Markus - FM2F.8
 Bortolozzo, Umberto - STu3M.4
 Borys, Nick - FF1D.5
 Borzsonyi, Adam - SM4N.7, STu3M.3, STu4O.1
 Boschini, F. - FM1F.7
 Bosco, Lorenzo - SF3G.5, STu4D.3
 Bose, Debapam - FW3E.3
 Bose, Ranjoy - JW2A.36, STh3B.2
 Bosworth, Bryan - FM1G.4, JW2A.68
 Botez, Dan - SF2G, SF3G.1
 Boubanga-Tombet, Stephane - SW4D.4
 Bouchard, Romain - SM2L.5
 Bougeard, Michel - JTu2A.150
 Boukhalel, Mark - ATu4M.4
 Bountis, Tassos - JTu2A.123, JTu2A.124
 Bourbeau Hebert, Nicolas - SW4L.5
 Bourderionnet, Jérôme - SM2N.8, STh3A.1
 Bourdon, Pierre - JTh2A.120
 Bourelle, Sean - FF2E.2
 Bouscher, Shlomi - FM2F.1
 Boutami, Salim - FTh1E.5
 Bowden, Audrey - JTu3L.3
 Bowen, Patrick - ATu3S.4
 Bowen, Warwick - JTh2A.25
 Bower, Christopher A. - STh4B.1
 Bowers, John E. - AF1Q.2, JW2A.39, JW2A.66, SM2I.6, STh1B.7, STu3F.5, STu3N.1, SW3B.1, SW3Q.2, SW3Q.3, SW4I.3
 Boyd, Robert - FTu3G.4, FW3F.5, FW4F.5, FW4F.7, JTh2A.15, JTh2A.19, JTh2A.4
 Boyer, Nicolas - STh4B.8
 Boyle, Alexis - JTu2A.170
 Boyle, Colin - SF3G.1

- Boyras, Ozdal - JW2A.175
 Bozhvelnyh, Sergey I. - FTh4M.7
 Bozkurt, Ibrahim - FTh1F.2
 Bradley, Jonathan - SF1A.6, STh3I.3
 Bradley, Thomas - JTh2A.42
 Braeuninger-Weimer, Philipp - FW3H.3, STu4D.5
 Brainis, Edouard - SW4I.4
 Brandstötter, Andre - FF3H.1, FF3H.3, FF3H.7
 Brandt, Nikolay - JTh2A.95
 Brauner, Sebastian - FM1G.3
 Brecht, Benjamin - Ath3H.8, FW4F.1
 Breitegger, Philipp - Ath1O.5
 Brener, Igal - FTh4J.4, FTh4M.1, FW3G.1, FW3H.7, FW4H.5, FW4H.8, JW2A.104
 Brenot, Romain - JW2A.55
 Bres, Camille-Sophie - JTh2A.93, SF2A.2, SF3N.6, SM1C.1, STh4K, SW3A.8
 Breuer, Steffen - STu3D.5
 Brewer, Nicholas - FM4H.2, SM2D.4
 Brida, Daniele - FF3P.7, FTh1F.6, SF3N.4
 Brida, Giorgio - FF1B.6
 Bridges, Denzel - FTu3H.4
 Briggs, Andrew F. - JTh2A.85, STh11.4, STh4I.3
 Bright, Victor - STu4P.7, SW4J.7
 Brignon, Arnaud - SM2N.8
 Briles, Travis C. - SF2A.5, SW3A.2
 Brilland, Laurent - SM4K.1
 Brinker, Frank - STu4O.5
 Brisset, Jean-Gabriel - JTu2A.168, JTu2A.88
 Brochard, Pierre - JW2A.161, SF2G.7, SM4L.6
 Brodbeck, Sebastian - FM2F.1
 Brodsky, Michael - FTu3G, FTu3G.7, FTu4A, SF2K.2, SW4A.6
 Brolo, Alexandre - STh3J.2
 Bromage, Jake - SM1N.7, SM3N, STu3M.5, STu3M.6
 Bromberg, Yaron - FF3H.4
 Brondani Torri, Guilherme - JW2A.32
 Brongersma, Mark - FW3H.2
 Brooks, Aidan - SW3M.5
 Brooks, Nathan - AW4O.2
 Brown, Joseph J. - STu4P.7
 Brown, Richard - SM1N.2
 Brown, Steven - AF3M.6
 Browning, Colm - SW4C.5
 Bruce, Graham D. - STh3L.2
 Bruck, Roman - FF1H.1
 Brukner, Caslav - FTh4G.1
 Brumfield, Brian - STh4L, STu3N.4
 Brune, Michel - JF2B.2
 Brunelli, Simone - JW2A.52
 Bruno, Vincenzo - FM3E.5, SM4D.7
 Buchler, Ben C. - FM1G.5
 Buchner, Stephen - JTh2A.175
 Buchnev, Oleksander - FTh3E.7
 Bucht, Sara - STu3M.5
 Buchvarov, Ivan C. - JTu2A.69
 Buckley, Sonia M. - JW2A.29, SF3A.5
 Bucksbaum, Phillip - FM4F.5, FF3P.3
 Budko, Serguei - FM1F.6
 Budriunas, Rimantas - STh3F.4, STu4O.1
 Budweg, Arne - FTh1F.6
 Bühler, Johannes - FF3P.7
 Buhunin, Ryan - FW3E.3
 Bulgakova, Nadezhda M. - SM3O.3
 Buljan, Hrvoje - FTh1H.7
 Buller, Gerald S. - AW3R.4
 Bullock, Alexis D. - JTh2A.182
 Bunandar, Darius - FW4F.4
 Burdett, Ashley - SW4K.5
 Burek, Michael J. - Ath3H.2, FTu3H.5, SF2J.2
 Burenkov, Ivan A. - FM2H.2
 Burger, Milos - FM1Q.4, SM3O.6
 Burghoff, David - Ath4Q.5, STu4D.2
 Buric, Michael - Ath3P.4
 Burke, John H. - AM2P.1
 Burla, Maurizio - JTh4D, JTh4D.5
 Burrow, Joshua - JTu2A.6, JW2A.105, JW2A.106
 Burton, Clement - STu3C.7
 Busacca, Alessandro - FF1E.1
 Buscaino, Brandon - FW3E.4
 Busch, Kurt - FTu4G.2
 Busch, Thomas - JTh2A.45
 Buss, Thomas - AF1Q.1
 Busse, Lynda E. - SM1N.1
 Bustos Ramirez, Ricardo - JTh2A.166, JTh2A.167, STu3F.4
 Butcher, Thomas - STu4O.6
 Butler, Thomas - SF1N.7
 Butov, Leonid - FF2L.7, FM3H.3
 Buyukkaya, Mustafa A. - JTh2A.30
 Byer, Robert L. - FM3M.7
 Byers, James - SM3B.5
 Bykov, Alexander - JTu2A.102
 Bykov, Anton Y. - FTh1D.7
 Byrd, Matthew - ATu3R.2, SF1A.6, SM3I.5, STu4B.2
- C**
- C.T., Samlan - JW2A.102
 Cabello, Neil - STu3Q.6
 Cadier, Benoit - JTh2A.132
 Cadusch, Jasper - SM2I.4
 Cahall, Clinton T. - FTu3G.3, FW3F.2, JTh2A.8
 Cai, Hao - AM4P.7
 Cai, Hong - Ath4O.1, Ath4O.2, Ath4O.4, JW2A.54
 Cai, Huaqiang - SF3I.5
 Cai, Lu - SW3I.2
 Cai, MengQiang - JTu2A.141
 Cai, Shanyong - JTu2A.37
 Cai, Tao - FF2L.8
 Cai, Wenjun - STh1J.5
 Cai, Wenshan - FTh1D.4
 Cai, Xinlun - JW2A.28, STh1B.6, STu3B.2
 Cakmakcapan, Semih - FTh4H.3, SW4D.2
 Caldwell, Joshua D. - FF2F.7
 Calegari, Francesca - JTu2A.158
 Calendron, Anne-Laure - FW4E.4, JTh2A.140, SM4A.4
 Califa, Ran - JTu2A.101
 Callahan, Patrick - SF1A.6, SM3L.1
 Callard, Ségolène - STh3A.5
 Calman, Erica V. - FF2L.7
 Calonico, Davide - JW2A.137
 Calvi, Chase - STu3M.1
 Calzada, Jesus A. - JM2A.2
 Camacho Morales, Maria del R. - FF1E.6, FW3G.6
 Camacho-Gonzalez, Guillermo - JTh2A.16, JTh3C.2, SM1B.2, STh4A.6, STu3F.4
 Camargo, Fabiola - JW2A.137
 Camayd-Muñoz, Philip - FF3C.7
 Campanella, Mauro - JW2A.137
 Campbell, Joe C. - SM2L.2, SM2L.3, STu3B.5
 Campbell, Melissa - JTh2A.96
 Campione, Salvatore - FTh4M.1, FW3H.7
 Campling, Joseph - SM3D.5
 Campman, Kenneth - FM3H.3
 Campo, Giulio - Ath4Q.6
 Canalias, Carlota - STh3F.4, STh4F.2
 Cancio, Pablo - Ath4Q.6
 Canedy, Chadwick - SF2G.1
 Canfield, Paul - FM1F.6
 Cankaya, Huseyin - JTh2A.140, JTu2A.116, SM4A.4
 Cano, Erwin - JW2A.138
 Cao, Bin - FM3H.2
 Cao, Haoran - JW2A.1
 Cao, Huabao - JF2C.2, SM4N.7
 Cao, Hui - FF3H.2, FF3H.4, FF3H.6, FM3E.4, FM3E.6
 Cao, Leiming - JTh2A.11
 Cao, Lin - FTu3G.2
 Cao, Qian - AM1J.2, SM4K.4
 Cao, Rongtao - JW2A.168
 Cao, Shixun - FF2D.1
 Cao, Wei - STh1I.3
 Cao, Xiaoping - JW2A.12, JW2A.28, STh1B.5, STh3B.3
 Cao, Yinwen - FTu3G.4, FW4F.5, JTu2A.49, JTu2A.53, SM1D.2, SW3A.5
 Cao, Yuan - FTu4A.4
 Cao, Yulong - JTh2A.108
 Cao, Zhaolong - JTh2A.61
 Capasso, Federico - AM1J.6, FF3E.6, FM3J.1, FTh1K.6, FTh3M.5, FW3E.6, JW2A.101, SF1J.8, SF3G.3, SF3J.4
 Capewell, Dale - AF3Q.1
 Caplan, David O. - STu3C.7
 Capmany, José - JTh3D
 Capmany, Juan - SM4D.3
 Capolino, Filippo - FM3Q.5, FTh1K.1, FTh1K.2, JTh2A.68, JW2A.175
 Cappelli, Francesco - Ath4Q.6
 Caranto, Neil - SW3Q.2
 Caravaca-Aguirre, Antonio - FF3H.5
 Carbajo, Sergio - JF1C, JF1C.5, JF2C.3, JTh2A.169
 Carbone, Fabrizio - STh1N.4
 Cardenas, Jaime - Ath3Q.1, JW2A.72, SM3D.1
 Cardin, Vincent - FM3M.2, SM4M.3, SW3N.2
 Carey, Tian - STu4D.6
 Careker, Coleman - FF1P.3
 Carletti, Luca - FM2E.2
 Carlos, Luis D. - JTu2A.50
 Carlson, David R. - FF2E.4, FF2E.6, SF2A.5, SM4L.1, SW4L.2
 Carmody, Neil - SM4N.3
 Carnemolla, Enrico Giuseppe - SM4D.7
 Carson, Kevin - JW2A.182
 caro, Ludovic - SW3Q.6
 Carpenter, David - Ath3P.4
 Carpenter, Joel - FTh4E.7
 Carpenter, Lewis G. - STh1I.3
 Carpintero del Barrio, Guillermo - JTu2A.162
 Carras, Mathieu - JTu2A.24
 Carree, Jean-Yves - STh4K.3
 Carrère, Hélène - JW2A.55
 carson, John M. - AW3R.3
 Carter, Richard - AM1M.1, AM1M.5
 Casale, Marco - JTu2A.120
 Casandruc, Eliza - FF3P.5
 Casanova, Alexis - STh4N.5
 Caspani, Lucia - FW4F.2, JTh4C.2, SM4D.7
 Casper, Chadwick - AW3O.5
 Cassano, Paolo - AM3P.1
 Cassinerio, Marco - JTh2A.185
 Castaneda, Mario A. - FM3G.3
 Castaneda-Castellanos, David - AW3S.3
 Castellano-Hernández, Elena - SF3I.7, SM1N.6
 Castro-López, Rafael - Ath4O.7
 Castrovilli, Mattea C. - JTu2A.158
 Cataliotti, Francesco - JTh2A.46
 Catrysse, Peter B. - FTu3E.7
 Cătuneanu, Mircea - SM3B.6
 Caudillo- Viurquez, Raúl - FTh4E.5
 Cavalcante, Fabio - JTu2A.151
 Cavaliere, Fabio - STu3C.1
 Cavillon, Maxime - STu3K.6
 Ceballos, Andrew - FM3M.7
 Cebrano, Michele - FF2E.2
 Cen, Qizhuang - JTh2A.127
 Cepe, Jean-Baptiste - SM4I.7
 Cerè, Alessandro - FTh1H.5
 Cerjan, Alexander - FM2Q.4, FM3Q.2, STh3A.7
 Cermak, Michael - SM1L.3
 Cernohorska, Jitka - STu4O.6
 Cerullo, Giulio - FF1D.5, FF2E.2
 Cesca, Tiziana - JTh2A.67
 Cha, Soonyoung - FF1D.8, FF2D.4, FTh1F.1, SW3I.3
 Chacon, Alexis A. - FF2P, FM3F.2
 Chae, Jongjae - AM1J.4
 Chae, Sang Hoon - STu4N.7
 Chafer, Matthieu - FM4G.4, JTh2A.97, SF1K.3, SF1K.6
 Chaker, Mohamed - FF1E.1
 CHAKRABORTY, BISWANATH - FF1D.6
 Chakraborty, Sandeep - Ath3Q.4
 Chakravarthi, Srivatsa - FM1H.2
 Chakravarty, Swapnajit - Ath1O.4, JW2A.40, SF3J.6, STh1B.4
 Chamanzar, Maysam - Ath1Q.2
 Chan, Chun-Kit - JTu2A.41, SM4B.4
 Chan, Jacky - AF2Q.5
 Chan, Kam Wai C. - JTh2A.14
 Chan, Ming-Che - JTu2A.93
 Chan, Vincent W. - SW4C.1
 Chan, Yueh-Lin - SW3B.7
 Chanana, Ashish - JW2A.76, SW4D.3
 Chandrasekaran, Vignesh - SW4I.4
 Chandrasekhar, Sethumadhavan - SM3B.4
 Chang, Allan S. - JTh2A.194
 Chang, Cheng Han - AM4P.4, SW3J.3
 Chang, Cheng-Han - JTh2A.88
 Chang, Chia-Kai - JTu2A.100
 Chang, Chiao-Yun - SM2O.4, STu4N.5
 Chang, Chih-hung - JTh2A.193
 Chang, Chun-Chieh - JW2A.84
 Chang, Cyuhan-Han - FF2L.5
 Chang, Guoqing - AM1J.2, JTh2A.162, SF1N.6, SM4K.4
 Chang, Hung-Tzu - FF1P.4
 Chang, Jun Ho - SW3K.5
 Chang, Kai - FF1D.7
 Chang, Lin - STu3F.5
 Chang, Peter - FW4H.5
 Chang, Shu-Hsiu - JTh2A.89
 Chang, Shu-Wei - STu4N.5
 Chang, Taeyong - JW2A.88
 Chang, Tsu-Chi - JTu2A.9
 Chang, Weijie - JW2A.47
 Chang, Wei-Zung - SM3D.4
 Chang, Wen-Hao - JTu2A.4
 Chang, You-Chia - FTu4E.2, STh4B.7
 Chang, Zenghu - FF1P.3, FM3M.1, SF1N.1
 Chang-Hasnain, Connie J. - ATu4M.5, STu3Q, STu3Q.3, STu3Q.5, STu3Q.6
 Chanteloup, Jean-Christophe - SM2N.8
 Chao, Weulun - STu4P.4
 Charalambidis, Dimitris - STu3M.3
 Charczun, Dominik - STu3N.8, STu3P.5
 Charipar, Nicholas - JW2A.121, SM2O.1
 Charous, Aaron - SW4D.7
 Chatzianagnostou, Evangelia - JW2A.5
 Chaudhary, Kostas - FTh1K.6, JW2A.101
 Chaudhuri, Krishnakali - FM2G.7
 Chávez-Cerda, Sabino - SW3M.1
 Chavez-Pirson, arturo - SM2N.4
 Cheben, Pavel - SM2B.1, STh1I.3
 Chekhova, Maria - FW3F.5
 Chelladurai, Daniel - FTh4H.1
 Chemla, Yoav - JTu2A.107
 Chen, Aiping - FF3P.6
 Chen, Baile - STh4I.5
 Chen, Bernard - ATu4J.4
 Chen, Bigeng - FF1H.1
 Chen, Bo Han - FF1F.3, JTh2A.70
 Chen, Chang J. - FM4G.7, FM4G.8
 Chen, Changchen - FM3G.4, FTu3G.5
 Chen, Che - SM2B.3
 Chen, Chun-An - STu4N.2
 Chen, Chung-Hsuan - JW2A.176
 Chen, Chung-Lo - JTh2A.170
 Chen, Chun-Hong - SW3B.7
 Chen, Claire L. - STh3L.1
 Chen, Deying - JTu2A.175
 Chen, Dian - JTh2A.187
 Chen, Disheng - JTh2A.34
 Chen, Dongyu - ATu4J.4
 Chen, Fangyuan - JW2A.172
 Chen, Feng - SM3O.1, SM3O.2
 Chen, Genfu - FM1F.4
 Chen, George - SW4L.5
 Chen, Guangcan - SW4Q.6
 Chen, Guan-Yu - AW3O.1
 Chen, Hao W. - JTu2A.95

- Chen, Haoshuo - JTh2A.133, JTh2A.173, SM3C.1, SM4C.2, STh3K.5
 Chen, Hong - FM4Q.1, FTh3E.6
 Chen, Hongsheng - FM3Q.8, FM4J.6, SW4M.3
 Chen, Hongwei - AF2M.4, AF2Q, SM1D.3, SW3Q.7
 Chen, Hou-Tong - JW2A.84
 Chen, Huan - JTu2A.42
 Chen, Hua-Zhou - AF1Q.7
 Chen, James - JTh2A.117
 Chen, Jeng-En - JW2A.151
 Chen, Jihh-Ciang - AW3O.1
 Chen, Ji - SF3G.6
 Chen, Jia Wern - FF1F.3
 Chen, Jiageng - JW2A.173
 Chen, Jiajia - SM4C.4, SM4C.5
 Chen, Jian - SM4C.2
 Chen, Jianping - JW2A.27, JW2A.56, STh3B.4, STh3B.5
 Chen, Jie - ATH4O.3, JTh2A.104, JTh2A.139, JW2A.153, SW3L.1
 Chen, Jingbiao - JW2A.67
 Chen, Jiming - JTu2A.149
 Chen, Junxin - ATH3H.5
 Chen, Jyehong - JTu2A.39, JTu2A.58
 Chen, Kaixin - STu4B.4
 Chen, Ke - SM1I.2
 Chen, Kevin - FTu4H.2
 Chen, Kevin P. - Ath3P4, ATu4M.6, FM3Q.2, JW2A.168
 Chen, Ko-Han - JW2A.151
 Chen, Lei - JTu2A.98
 chen, Liang - AF1M.7, SW3L.3
 Chen, Lian-Kuan - JTu2A.41
 Chen, Liao - AF3Q.5, JTh2A.149
 Chen, Liyuan - STu4O.6
 Chen, Luo-Kan - FTu4A.4
 Chen, Ming-Chang - FF1P, SW3N.5
 Chen, Minghua - AF2M.4, SM1D.3, SW3Q.7
 Chen, Mingkun - FTh1P.3
 Chen, Mingzhou - AF2M.3, ATu3I.3, STh1J.2, STh3L.2
 Chen, Nan - JTh2A.116, JTh2A.134
 Chen, Pengcheng - JTh2A.122
 Chen, Qiushu - SW3J.2
 Chen, Qunan - Ath4Q.3, SM4B.7
 Chen, Ray - Ath1O.4, JTh4D.4, JW2A.40, SF1A.3, SF3J.6, SM1I.2, SM1I.3, SM1I.6, STh1B.4
 Chen, Rih-You - JW2A.69
 Chen, Rongsheng - JTh2A.118
 Chen, Shih-Wei - AW3O.2
 Chen, Shoushun - Ath4O.4, JW2A.54
 Chen, Shufan - FW3F.1
 Chen, Songtao - SF1G.6
 Chen, Teng-Ming - JTh2A.89
 Chen, Timothy - Ath3P.1
 Chen, Ting-Ju - JW2A.151
 Chen, Tse-Hung - JW2A.20
 Chen, Tzu-Yu - AW3O.2, FW3G.2, JTh2A.89
 Chen, Wanqing - Ath3Q.5
 Chen, Wei - JTu2A.137, STh4I.5, SW4K.1
 Chen, Wei Li - AM2J.4
 Chen, Weidong - SM2N.6
 Chen, Wei-Ting - FM3J.1, FTh3M.5, JW2A.101
 Chen, Wenjuan - STu3B.3
 Chen, Xi - SM2C, SM3B.4
 Chen, Xiahui - FTh4H.5, JW2A.19
 Chen, Xianfeng - STu3F.3
 Chen, Xing - JW2A.152, SM1L.2
 Chen, Xinzhong - SW3D.3
 Chen, Xiuliang - FW4E.1
 Chen, Xuan - STh4F.3
 Chen, Xue - JTh2A.183, JTh2A.186, JTu2A.37, JTu2A.42
 Chen, Yang-Fang - AM4P.4, JTh2A.88, SW3J.3
 Chen, Yangyang - Ath4O.1, Ath4O.2
 Chen, Yanyu - AM4P.5
 Chen, Yaojiang - STh4I.5
 Chen, Yen-Chang - FF1P.4
 Chen, Yen-Chun - JTu2A.4
 Chen, Yen-Hung - JW2A.34, JW2A.44
 Chen, Yen-Jung - STu4N.4
 Chen, Yifeng - SW3L.7
 Chen, Yi-Hsun - SW3B.7
 Chen, Ying-Cheng - JW2A.151
 Chen, Yong - JTh2A.42
 Chen, Yu - FW4E.1
 Chen, Yu Han - FF1F.3, JTh2A.70
 Chen, Yu Tung - AM2J.4
 Chen, Yuan - SF2J.5
 Chen, Yu-Ao - FTu4A.4
 Chen, Yu-Chen - AM2M.3, JTu2A.25
 CHEN, YU-CHENG - SW3I.2
 Chen, Yueyang - JW2A.16
 Chen, Yuhao - AM2M.2
 Chen, Yujie - SW3M.4
 Chen, Yu-Jie - STh3I.8
 Chen, Yu-Ling - JTu2A.4
 Chen, Yung-Fu - SF3I.8
 Chen, Yung-Tsan - JTu2A.40
 Chen, Yunxiang - JTu2A.73
 Chen, Yuping - STu3F.3
 Chen, Zaijun - JW2A.157
 Chen, Zefeng - SF3A.2
 Chen, Zhangyuan - JTh2A.113, JW2A.67
 Chen, Zhaowei - FM2Q.6
 Chen, Zhichao - JW2A.138
 Chen, Zhigang - FF3F.4, FM1E.7, FM4Q.1, FTh1M.7, FTh3E, FTh3E.4, FTh3E.6, JTu2A.139
 Chen, Zhijiang - SM4A.5
 Chen, Zhong - JTh2A.79
 Chen, Zhongping - JTu3L.4
 Cheney, Alec R. - SF2I.6, SW3J.6
 Cheng, Bojun - FTh4H.1, SM2I.3
 CHENG, CHE-HSUAN - SF1I.5
 Cheng, Chen - SM3O.2
 Cheng, Chia-Chin - STu4N.5
 Cheng, Haynes P. - JW2A.138
 cheng, jiangtao - JTh2A.104
 Cheng, Jin-Luo - JW2A.123
 Cheng, Ji-Xin - AM3P.4
 Cheng, Li-Jing - ATu3J.2, JW2A.91
 Cheng, Mengfan - SM1C.5
 Cheng, Nai-Wen - JW2A.38
 Cheng, Pi-Ju - STu4N.5
 Cheng, Q.Q. - STu4B.7
 Cheng, Qixiang - STh3B.6
 Cheng, Rebecca - SF2I.3
 Cheng, Tonglei - JTu2A.117
 Cheng, Wang-Yao - JW2A.151
 Cheng, Weifeng - JTh2A.104
 Cheng, Xiaojun - FM4Q.2
 Cheng, Xing - JW2A.111
 Cheng, Xue M. - JTu2A.95
 Cheng, Ya - JTu2A.149, STh1I.6
 Cheng, Yi-Shing L. - JTu3L.2
 Cheng, Yu-Chen - STh3N.2
 Cheng, Yu-Chieh - JW2A.37
 Cheng, Yuhao - FW3F.1
 Cheng, Yuh-Jen - FW4G.4
 Cheng, Yu-Hsiang - FM2H.2
 Cheng, Yuk Shan - FTh1M.1
 Cheng, Zhi - FM3M.3
 Cheong, Kin-Pang - STh4L.3
 Cheriaux, Gilles - STu3M.2
 Chervinskii, Semyon - JTu2A.134
 Chestnov, Igor - JW2A.113
 Chevalier, Paul - FW3E.6, SF3G.3
 Chew, Andrew - FF1P.3
 Chhowalla, Manish - FTh1F.2
 Chi, Han - SM1N.5
 Chi, San-Hui - JTu2A.59
 Chi, Xiaoming - FW3F.1, JTu2A.138
 Chia, Cleaven - Ath3H.2, SF2J.2
 Chiang, An-Chung - JTu2A.83
 Chiang, Chin-Cheng - FTu4E.6
 Chiang, Kin S. - JTu2A.147, STh1A.2, STu4B.4
 Chien, Tsai-Yi - JW2A.44
 Chikishev, Andrey - JTh2A.95
 Childress, Michael - ATu4J.6
 Chiles, Jeff - SF2A.5, SF3J.7, SM4L.1, STh3F.1, STu3F.5
 Chiles, Jeffrey - JTh2A.16, JTh3C.2, JW2A.29
 Chini, Michael - FF3P.6, SW3N.2, SW3N.4
 Chiou, Pei-Yu - STh3J.1
 Chisholm, Matthew - FM1G.6, FTu3H.4
 Chiu, Yi-jeu - JW2A.69
 Chiu, Yu Chung - JW2A.78
 Chmielak, Bartos - JW2A.5
 Cho, Choonlae - JW2A.110
 Cho, Sangyeon - FM2G.6, SF1I.2
 Cho, Seungwan - FF1D.4, FM1F.2, JTh2A.172
 Cho, Shigeki - JTu2A.126
 Cho, Suehyun - FW4G.5
 Cho, Sungjun - FF1D.8
 Cho, Young-Wook - FF1B.5, JTh2A.1
 Chochol, Jan - STu4D.7
 Choe, Hwan Sung - SF3A.7
 Choi, Honggu - ATu4J.6
 Choi, Hyeonrak - FM1H.6, FTh1G.6, SF3A.4
 Choi, Hyunyoung - FF1D.4, FF1D.8, FF2D.4, FM1F.1, FM1F.2, FTh1F.1, JTh2A.172, JW2A.134, SW3I.3
 Choi, Il Woo - JTu2A.140
 Choi, Junho - SM2B.2
 Choi, Jun-Hyuk - JTh2A.176
 Choi, Kwang-Ho - Ath3P.7
 Choi, Seung Ho - Ath3P.7, JW2A.107
 Choi, Shinhyuk - STu4N.3
 CHoi, Sun Young - SF3I.5
 Choi, Sunjak - JTu2A.96
 Choi, Youngwoon - JTu2A.105, JTu2A.94
 Chong, Andy - JTh2A.111
 Chong, Xinyuan - JTh2A.193
 Chong, Y. D. - FTh3E.6
 Chong, Yidong - FM1G.2, FM3Q.2, FTu3G.2, JTh2A.18, JW2A.87
 Choquette, Kent D. - JW2A.17, SF2A.7, STu3Q.4, STu3Q.7
 Chou, ChunYang - JTh2A.52
 Chou, Chun-Yang - JTh2A.171
 Chou, Elaine - ATu4J.5
 Chou, Han-Yi - AM4P.4
 Chou, Hao-Ming - AW3O.2
 Chou, Ming-Hsien - AM2M.3
 Choudhary, Amol - SM2D, STu4F, STu4F.2
 Choudhury, Vishal - SM1K.5
 Chow, Chi-Wai - JTu2A.39, JTu2A.58
 Chow, Philippe - JTu3O.6, JTu3O.7
 Chow, Weng - FM4E.5
 Chowdhury, Enam - FTh1D.2, JTu2A.125, SM3O.7
 Chremmos, Ioannis - SW3M.4
 Chriki, Ronen - SF1J.6
 Christ, Marc - JW2A.164
 Christen, Ian - FM1H.2
 Christensen, Erik N. - FM3G.3
 Christensen, Jesper B. - FM3G.3, FTh1G.1, JTh4C.4
 Christensen, Mathias - AF1Q.1
 Christensen, Thomas - FF2L.3, FW4G.2
 Christodoulides, Demetrios N. - FM1E.2, FM2E.3, FM2E.5, FM2G.5, FM4E.1, FM4E.3, FM4E.5, FM4E.7, FTh1M.3, FTh4E.2, FTh4E.4, FTh4E.6, FTh4E.7, SF3K.3, SW4Q.1
 Christopher, Rathje - JW2A.122
 Chrostowski, Lukas - JTh2A.3, STh4A.1
 Chrzanoski, Helen - FTh1H.4
 Chu, Cheng Hung - FF1F.3
 Chu, Chih-Wei - STu4N.5
 Chu, Hongwei - STu4O.5
 Chu, Hsu-Hsin - FM3M.3
 Chu, Qian - AM4P.7
 Chu, Sai T. - FTh1E.7, FW4F.2, JTh4C.2, JW2A.22, SM1B.4, SM1B.5, STu3F.7
 Chu, Steven - AM2J.3, FTu3H.5, JTh3C.5
 Chu, Wei - JTu2A.149, STh1I.6
 Chu, Yiwen - SM1O.2
 Chua, Song Liang - JTh2A.129
 Chuang, Chun-Yen - JTu2A.39, JTu2A.58
 Chuang, Issac - JTh2A.17
 CHUANG, YU-CHING - JW2A.37
 Chung, Chi-Jui - Ath1O.4, JTh4D.4, JW2A.40, SF3J.6, SM1I.2
 CHUNG, HSIANG-YU - AM1J.2, SM4K.4
 Chung, Hung-Pin - JW2A.34, JW2A.44
 Chung, Meng-Ting - JTh2A.89
 Chung, SungWon - JW2A.15, JW2A.70
 Chvykov, Vladimir V. - JF2C.2, SM4N.7
 Chyla, Michal - STu4O.6
 Ci, Cheng - JW2A.152, SM1L.2
 Ciampini, Mario A. - FW4F.3
 Cimini, Valeria - FW4F.3
 Cino, Alfonso - FW4F.2, JTh4C.2
 Cinquanta, Eugenio L. - FF2D.7
 Čip, Ondrej - JW2A.137
 Ciriolo, Anna Gabriella - JTu2A.156
 Cirmi, Giovanni - JTh2A.140, SF3N.5
 Civelli, Stella - STu4C.4
 Čizmár, Tomáš - STh3K.3
 Clarke, Ed - JTh2A.27
 Clarke, Robert - JTu2A.170
 Clarkson, William A. - JTh2A.114, SW3M.2
 Clementi, Marco - STu3F.2
 Clemmen, Stephane - FM3G.2, SM1B.3, SW3L.6
 Clemmons, Marvin C. - JTh2A.182
 Clerici, Matteo - FF1E.1, FM3E.5, SM4D.7
 Clivati, Cecilia - JW2A.137
 Coburn, Sean C. - Ath4P.3
 Cocker, Tyler - FM3F.1, JM1A, JM2A.4, STu3D
 Coddington, Ian R. - Ath4P.3, SM4L.1, STh1L, STh1L.2, SW4L.7
 Coen, Stephane - FW3E.2, JTu2A.119, JTu2A.137, SM2D.2, SM4K.7
 Coenen, Toon - FTh3M.2
 Coetzee, Riaan Stuart - Ath3O.1, STh4F.2
 Coffee, R. - FM1F.7, JF1C.3
 Cohen, Daniel - SF1G.7
 Cohen, Kobi - FTh3M.4
 Cohen, Nadav - JTu2A.49
 Cohen, Offir - JTh2A.2
 Cohen, Oren - FF1P.5, STh4N.1
 Colangelo, Marco - FW3F.3
 Colautti, Maja - JTh2A.46
 Colburn, Shane A. - SF1J.4, SF3A.6
 Coldren, Larry - JW2A.52, STu3Q.5
 Coldren, Larry A. - ATu3R.3
 Cole, Daniel C. - FW3E.5, SM1D.1, SW3A.6
 Cole, Garrett - JTu2A.14, SM3L.6
 Collett, Oliver J. - SM3N.1
 Collier, John - JTu2A.170, STu4O.6
 Collins, Steve - FM1Q.7
 Collinson, Robert - SM2O.7
 Colvin, Vicki - JM1A.1
 Combrí, Sylvain - STh3A.1
 Comby, Antoine - JTu2A.150
 Condori, Hugo - JW2A.76
 Cone, Rufus L. - FTu4H.5
 Conforti, Matteo - FTh1M.8
 Cong, Kankan - FM2F.7
 Cong, Longqing - SW4D.6
 Connolly, Peter - AW3R.4
 Consentino, Albert - SM1N.7
 Consolino, Luigi - Ath4Q.6
 Conti, Claudio - FM3E.2
 Cook, Gary - SM3O.5
 Cook, Kevin T. - STu3Q.6
 Cook, Kevin T. - STu3Q.3, STu3Q.5
 Coop, Simon - JF3B.5
 Cooper, A. B. - FM1G.4, JW2A.68
 Copie, Francois - FTh1M.8
 Coppola, Guillaume - FTu3H.6, FTu3H.7
 Corato-Zanarella, Mateus - JTu2A.110
 Corbett, Brian - STh4B.1
 Corcoran, Bill - SM1C.2
 Cordaro, Concetto Eugenio Andrea - FF3C.4
 Cordier, Martin - FM4G.4, SF1K.6

- Corkum, Paul B. - FF2P.1, FF3P.2
 Cormann, Mirko - SM1O.1
 Cormier, Eric - SF1N.3, STu3M.3
 Corsi, Alessandro - SW3K.5
 Coslovich, G. - FM1F.7
 Cossel, Kevin - Ath4P.3
 Cotrufo, Michele - JTh3C.4
 Couderc, Vincent - SM3D.3, SM3D.6, SW3K.6
 Courjaud, Antoine - JTu2A.168, JTu2A.88, STh4N.5
 Cowle, Gregory - SW4K
 Cox, Joel - FF3D.8
 Craiciu, Ioana - FTu4H.4, STh3G.2
 Craig, Benjamin J. - AF3M.1
 Cramer, Alex - JTh3D.1
 Crane, Tom - FF2F.3, FF2H.5
 Crippa, Gabriele - JTu2A.156
 Cristescu, Simona M. - Ath1O.1, Ath3O.2
 Cristofori, Valentina - SM2C.5, STu4C.1
 Crites, Erin - FF3P.6
 Crockett, Benjamin G. - SF3N.7
 Crozier, Kenneth B. - AF3M.1, FTh4J.6, SF3J, SF3J.3, SM2L.4
 Crumb, Michael F. - JW2A.117
 Cruz, Carlos Henrique B. - JTu2A.114
 Cruz, Flavio - FF2E.6, FW3E.1, STh1L.1
 Cryan, James - FM4F.5, JF1C.3
 Cubukcu, Ertugrul - STu4N.3
 Cuchimaque Lugo, Leidy J. - Ath4O.7
 Cuenca, Rodrigo - JTu3L.2
 Cuffney, Robert - SM1N.7
 Cugini, Filippo - SW4C.4
 Cui, Bianxiao - AM4P.2
 Cui, Haoran - STu4B.5
 Cui, Jiabin - JTh2A.195, JTu2A.36
 Cui, Kaiyu - JTu2A.138
 Cui, Liang - JF2B.4
 Cui, Nan - JTu2A.47
 Cui, Tong - FTh4H.1
 Cui, Wenwen - JTu2A.148, JTu2A.56
 Cundiff, Steven T. - FF1D.2, FF3D.1, FF3D.6, FF3D.7, FM2F.8, FM4F.7, FTh1F, JW2A.158, STu4P.8
 Cunningham, Eric - FF2P.3
 Curic, Tatjana - AM1P.1
 Curtis, Alden - STu3M.1
 Cygan, Agata - STu3N.8
 Cyr, Elaine - STh4B.8
 Czornomaz, Lukas - STh3L.6
- D**
 da Jornada, Felipe H. - FF1P.4
 Da Ros, Francesco - SM2C.3, SM2C.5, STh1C, STu3D.1, STu4C.1, STu4C.2, STu4C.6
 da Silva Neto, E.H. - FM1F.7
 da Silva, Edson P. - STu4C.1, STu4C.2, STu4C.6
 Dabos, George - JW2A.5
 Dabrowski, Michal - FM4H.6, JTh2A.28, JTh2A.33
 Dacha, Sai Kanth - STh3K.4
 Dadoenkova, Yuliya S. - JTh2A.57
 Daele, Michiel V. - SW3L.6
 Dagenais, Mario - JW2A.65
 Dagli, Aip - SW3Q.3
 D'Aguzzo, Giuseppe - SF2A.6
 Dai, Anan - JW2A.138
 Dai, Jianming - SM4A.1
 Dai, Liang Yuan - JTu2A.45
 Dai, Lun - AF1Q.7
 Dai, Nengli - STu3K.4
 Dai, Ruihong - STh4K.7
 Dai, Xiaojun - SF3L.5
 Dai, Xingcan - JW2A.124
 Dai, Yaomin - FM1F.4
 Dai, Ye - JTu3O.2
 Dai, Yitang - JTh2A.127, JTh2A.165, JW2A.73
 Dai, Zhixuan - FTh3E.4
 Dai, Zi jie - JTh2A.178
- Dainese, Paulo C. - FF1E.8, JTu2A.71, JW2A.58
 Dakovski, G.L. - FM1F.7
 Dal Conte, Stefano - FF1D.5, FF2E.2
 Dalacu, Dan - FTu3H.2
 Dalir, Hamed - JW2A.3, SM11.2, SM11.5, SM11.6
 Dallo, Christina - SF2L.4
 Daloglu, Mustafa - STh1J.5
 Dalton, Larry R. - FTh4H.1, JTh4D.5, SM11.4, SM4B.1
 Damascelli, A. - FM1F.7
 Damiano, Eugenio - SM4N.2
 Dandapat, Krishnendu - JW2A.170
 Dane, Andrew - FW3F.3
 Dangovski, Rumen R. - FM1Q.3
 Dani, Keshav M. - FM4F.2, FM4F.6, FTh1F.2
 Danialut, Louis - SM2N.8
 Danilevicius, Rokas - JTh2A.146, JTh2A.154
 Dannenberg, Paul - JTu2A.23
 Dantus, Marcos - JW2A.182
 Danylo, Rostyslav - FM1Q.8
 Dao, Thang - FF2F.8, SM3A.5
 Darvishzadeh Varcheie, Mahsa - JTh2A.68
 Darweesh, Ahmad A. - AF3M.4
 Das Gupta, Tapajyoti - SF2K.4, STh1L.5
 Das, Ananda - FW4G.5
 Das, Subrata - JTu2A.77
 Dasa, Manoj Kumar - JTu2A.109
 Datta, Ipshita - STu4N.7
 Datta, Shubhashish - SM2L.5
 Dave, Harshil - SF2A.7, STu3Q.4, STu3Q.7
 Davenport, Michael - STh1B.7
 Davidi, Roy - AF1M.6
 Davidson, Nir - SF1J.6
 Davidson, Roderick - FTu3H.4
 Davies, Alexander G. - STu4D.4, STu4D.6
 Davila-Rodriguez, Josue - SM1L.4, SM2L.3
 Davis, Alex O. - FM4G.1
 Davis, Matthew - FTh3M.6
 Davis, Timothy - AW4O.5
 Davoine, Xavier - JTu2A.160
 Daw, Joshua - Ath3P.4
 Dawson, Jay - SM4M.6
 Day, Matthew W. - FF3D.1
 De Angelis, Costantino - FM2E.2
 De Angelis, Filippo - FF2D.7
 de Boer, Johannes - JTu4L.2
 de Ceglia, Domenico - JTh2A.71
 de Escobar, Natali M. - JF3B.5
 De Fazio, Domenico - FF2E.2
 de la Zerda, Adam - AM2J.3, JTu3L.1
 De Leon, Israel - FM2G.4
 de Matos, Cristiano - JTh2A.100
 de Melis, Mirko - ATu3L.5
 De Natale, Paolo - Ath4Q.6
 De Rossi, Alfredo - STh3A.1
 De Santis, Lorenzo - FTu3H.6, FTu3H.7
 De Vido, Mariastefania - STu4O.6
 Dean, Paul - STu4D.4
 Debayle, Arnaud - JTu2A.160
 Debnath, Kapil - SM3B.5, STu3F.2
 Debnath, Sanjay - JW2A.89
 Debord, Benoit - FM4G.4, JTh2A.97, SF1K.2, SF1K.3, SF1K.6, SM2N.2, SM3L.3, SM3L.4
 Debrégeas, Hélène - JW2A.55
 Deby, Stanislas - AM2J.5
 Dechard, Jeremy - JTu2A.160
 Deckoff-Jones, Skylar - SM2L.8
 Decorby, Raymond G. - STh4A.1
 Deeb, Claire - FM2G.3
 De-Eknankul, Chawina - STu4N.3
 Degiovanni, Ivo - FF1B.6
 Degli'Innocenti, Riccardo - FW3H.3, STu4D.5
 Degnan, John - ATu3R.4
 Dehak, Najim - FM1G.4
 Dehghanasiri, Razi - SM11.1
 Dehne, Kristian - SM1N.5
 Deka, Suruj - JTu2A.30
 Del Bino, Leonardo - FM3E.3, SM1D.4
 Delagnes, Jean-Christophe - SF1N.3
- Delahaye, Frédéric - JTh2A.97, SF1K.2, SF1K.3, SF1K.6, SM2N.2
 Delaney, William - SW3L.4
 Delavaux, Jean-Marc - JTh2A.132
 Delaye, Philippe - FM4G.4
 Delen, Xavier - SM4M.4
 Deleporte, Emmanuelle - JTh2A.152
 Delfyett, Peter - JTh2A.166, JTh2A.167, STu3F.4
 Delgado, Manuel C. - AM2J.6
 Delgrange, Maxime - SM3L.3, SM3L.4
 Del'Haye, Pascal - FM3E.3, SM1D.4
 Delprat, Sebastien - FF1E.1
 DelRe, Eugenio - FM3E.2, FTh3E.2
 Delva, Justin - SM3L.7
 Demas, Jeffrey - FTu1M.4
 Demetriou, Giorgos - JTu2A.115
 Demir, Hilmi Volkan - FTh4J.5
 Demko, Andrew - STu3N.3
 Dempsey, Dennis - JTu2A.3
 Demur, Romain - SM4D.2
 DenBaars, Steven - SF1G.7, STu4Q.3
 Dendooven, Jolien - SW3L.6
 Deng, Hui - FF1D.2
 Deng, Huiyang - FM3M.7
 Deng, Junhong - JW2A.111
 Deng, Lei - SM1C.5
 Deng, Lu - ATu3J.7
 Deng, Wentao - SM4B.5
 Deng, Yang - FW3H.6
 Deng, Yanting - SW3D.5
 Deng, Zi-Lan - JW2A.111
 Dennis, Allison - FF1H.2
 Deotare, Parag - SF1I.5
 Dereux, Alain - JW2A.5
 Derksen, Roderick - JW2A.138
 Dernaika, Mohamad - SW3Q.6
 DeRose, Christopher - SF2L.4
 Desai, Sujay - STu4N.6
 DeSalvo, Richard - JTh3D.1
 DeSantolo, Anthony - SM1K.3, SW4K.4
 Deschènes, Jean-Daniel - SM1L.3
 Deshmukh, Rahul - FW4G.8
 Deshmukh, Sanchit - SF3A.6
 Deshpande, Rucha - FTh4M.7
 Desiatov, Boris - JW2A.103
 Desruelle, Bruno - AM1P.2, JW2A.137
 Detavernier, Christophe - SW3L.6
 Detlefs, Blanka - FM1Q.7
 Detz, Hermann - SF2G.2
 Deutsch, Christoph - SM3L.6
 DeVault, Clayton - FM3E.5, FTh4M.4, SM4D.7
 Devetta, Michele - JTu2A.156
 Devi, Kavita - JTu2A.67
 Devine, Adam - ATu3S, ATu3S.4, AW3S
 Dhar, Shounak - SF1A.3
 Dherbecourt, Jean-Baptiste - Ath3O.1, STu3N.7
 Dholakia, Kishan - AF2M.3, ATu3L.3, STh1J.2, STh3L.2
 Dhoore, Sören - SW3Q.4
 Di Domenico, Giuseppe - FTh3E.2
 Di Donato, Andrea - FF3E.6
 Di Mei, Fabrizio - FM3E.2, FTh3E.2
 Di Sciacca, Giuseppe - FF3P.5
 Di Teodoro, Fabio - AW3R
 Di, Li - SM1C.5
 Di, Lin - JTh2A.77
 Diamandi, Hilel Hagai - JTu2A.80, SM3K.1, SM3K.7, STu4F.3
 Diamanti, Eleni - FM4G.4
 Diaz Tormo, Alejandro - AM1J.3
 Diaz, Francisc - SM2N.6
 Dickmann, Johannes - FF3F.7
 Dickmann, Walter - FF3F.7
 Diddams, Scott A. - FF2E.4, FF2E.6, FTh1E, FW3E, FW3E.1, FW3E.5, SF2A.5, SF3J.7, SM1L.4, SM2L.3, SM4L.1, STh1L.1, STh3F.1, STu3F.5, SW3A.2, SW4L.2
 Didierjean, Julien - SM4M.4
 Diebold, Andreas - SF2N.6, SM3N.5
- Diederich, Geoffrey M. - FF3D.1, JW2A.132
 Diels, Jean-Claude M. - FTh1M.2, JTh2A.141, JTu2A.161, SM1O.7, STh3N.7
 Diels, Wouter - JW2A.57
 Dietrich, Philipp-Immanuel - STh1A.1
 Dietrich, Tom - SM1N.4
 Dietsche, Eva-Katharina - JF2B.2
 DiGiovanni, David - SM3K.6, SW4K.4
 Dikopoltsev, Alex - FF2H.2, STh4N.1
 Dimakis, Emmanouil - JM2A.3
 Ding, Dapeng - Ath3H.1
 Ding, Fei - FTh4M.7
 Ding, Hangjun - JW2A.168
 Ding, Hongli - JW2A.138
 Ding, Jianfeng - JW2A.2, JW2A.23, SW4C.6
 ding, jun - FM4Q.5, FTh4J.3
 Ding, Pengji - ATu4L.1, FM1Q.5
 Ding, Wei - SF1K.4
 Ding, Xiaoyue - SM3D.4
 Ding, Xun - STu3A.3
 Ding, Yihang - JTu2A.89
 Ding, Yunhong - FTh1G.5, FTh1G.7, JTh4C.4
 Diniz, Júlio - STh1C.3
 Dinsdale, Nicholas - FF1H.1
 Disque, Spencer - ATu3R.4
 Dissanayake, Senali - JTu3O.6
 Ditmire, Todd - STu3M.2
 Divitt, Shawn - FF1F.1
 Divoky, Martin - STu4O.6
 Dixon, P. Ben - FW4F.4
 Djevarhijian, Leo - Ath3O.4
 Djupsjöbacka, Anders - SM4C.5
 D'Mello, Yannick - JTh2A.96, STh4A.7, STh4B.4
 Dmitriev, Artemiy - SW4A.5
 Dodane, Delphin - STh3A.1
 Doeleman, Hugo - FTh3M.2
 Dogariu, Aristide - AF1M.5
 Dogariu, Arthur - ATu4L.4, STu4P.1
 Dogariu, Laura - ATu4L.4
 Doherty, Marcus - FTu4H.1
 Dohms, Alexander - JTh2A.37
 Doiron, Chloe - FTu3E.3
 Dollar, Michael - FTu4H.1
 Domingue, Scott - FF2E.4
 Domingues, Sergio - JTh2A.100
 Dominguez Bucio, Thalia - STu3F.2
 Dominguez, Owen - SF2L.7
 Donath, Sascha - STu3P.2
 Donati, Silvano - ATu4M.7
 Donegan, John F. - ATu4M.2, FTh1K.3, JTh2A.90, JTu2A.26, JW2A.6
 Dong, Bin - SW4B.3
 Dong, Binzhong - JTh2A.79
 Dong, Chun-Hua - SF2J.5
 Dong, Jianji - JW2A.53
 Dong, Jianwen - STh3I.8
 Dong, Kaichen - FW3H.6, SF3A.7
 Dong, Po - SM2B.4, SM4B.3
 Dong, Xin - AF3Q.5
 Dong, Yao-Zhong - SW3B.7
 Donohue, John M. - FW4F.1
 Donvalkar, Prathamesh - FM3G.5
 Doolittle, Lawrence - SM4M.6
 Doorn, Stephen - FW4H.8
 Dorney, Kevin - AW4O.2
 Dorodny, Alexander - JTh4D.5
 Dorrah, Ahmed - JTu2A.110, STu4P.2
 Dorrer, Christophe - SM1N.2, SM1N.7, STh1N, STh3N.3, STu3M.5, SW3M.6
 Dorrestein, Sander - SW3B.5
 Dory, Constantin - FTu3H.1, FTu3H.5, JTh3C.5
 Doshay, Sage - FF3C.2, FF3C.6
 Dou, Wei - AF1Q.5, STh4I.4
 Douquet, Nicolas - FF1P.3
 Douplik, Alexandre - JTu2A.107
 Dowling, Jonathan P. - JTh2A.31
 Dowran, Mohammadjavad - JF2B.6
 Drag, Cyril - STu3N.7

- Dragic, Peter - STu3K.6
 Dreser, Christoph - FW3G.3
 Drexler, Wolfgang - JTu3L, JTu4L
 Dreyer, Elizabeth - FF2E.7
 Druon, Frédéric - SM4M.4
 Du Bois, Bert - JW2A.32
 Du, Huayang - JW2A.67
 Du, Jing - FW4F.5, JTh2A.15, SM3C.4
 Du, Jinhao - JTh2A.183
 Du, Jinjian - JTh2A.11
 Du, Kaikai - SW3I.2
 Du, Qiang - SM4M.5, SM4M.6
 Du, Wei - AF1Q.5, STh4I.2, STh4I.4
 Du, Zhidong - FW4G.1
 Duan, Lingze - AF2Q.4
 Duan, Shukai - FF1H.5, SM1B.6
 Duan, Xiangfeng - FTh1F.7, SW3I.4
 Duan, Xiaofeng - JW2A.7
 Duan, Yuhua - JTh2A.149
 Dubček, Tena - FTh1H.7
 Dubietis, Audrius - FM3E.5
 Dubra, Alfredo - JW3P.1
 Dudley, John M. - AF2Q.1
 Duffin, Andrew - STu4P.4
 Dumeige, Yannick - SM4I.7
 Dumitrescu, Eduard - JTu3O.6
 Dumitrescu, Eugene - FM1G.6, FTu3H.4
 Duncan, Jacque - JW4P.1
 Duperron, Matthieu - ATu3I.5
 Dupiol, Richard - SM3D.6, SW3K.6
 Dupre, Matthieu - FTh4J.7, JW2A.97
 Durach, Maxim - FF2F.2
 Duran, Vicente - ATH3O.4
 Durand, Eric - SM2N.8
 Durand, Magali - JTu2A.168, JTu2A.88
 Durécu, Anne - JTh2A.120
 Durfee, Charles - FTh3E.3
 Dutt, Avik - STh1A.4
 Dutta, Aavek - FTh4M.4
 Dutta, Rebecca - AM2J.3
 Dutta, Subhojit - FF2L.8
 Dutta-Gupta, Shourya - AW4O.4
 Dyer, Shellie - JTh4C.3
 Dynes, James F. - FTu3G.6
 Dzemes, Maksim - SF3I.7
 Dziallas, Giannino - JW2A.9
- E**
 E, Yiwen - SM4A.1
 Earles, Thomas L. - SF3G.1
 Earles, Tom - STu4Q.4
 Easo, Sajjan - FM4J.6
 Eason, Robert - JTh2A.177, SM1O.4, SM4O.3
 Ebrahim-Zadeh, M. - FTh3E.5, FTh3E.8, JTu2A.61, JTu2A.67, STh4F.7
 Ebrahim-Zadeh, Majid - JTu2A.60, STh4F.6
 Edamura, Tadataka - SF3G.7
 Eden, J. G. - ATu4J.3
 Edgar, Matthew - FF1B.1, FW3F.7, STh3K.3
 Edstrom, Steve - SM3A.1
 Edwards, Brian - FF3C.3, JW2A.90
 Edwards, Chris - STu4O.6
 Edwards, Matthew - JTu2A.159
 Efremidis, Nikolaos K. - FTh3E.1
 Eftekhar, Ali Asghar - JTh2A.78, JTu2A.85, JW2A.33, SF1J.1, SM1I.1, SW4A.2, SW4B.6
 Eftekhar, Mohammad Amin - FTh1M.3, FTh4E.2, FTh4E.6
 Eggleton, Benjamin J. - FM4E.6, FTh1G.8, STu4F.2
 Egorov, Victor - FF1H.3
 Ehn, Andreas - ATu4I.1, FM1Q.5
 Eich, Pascal - FM2H.6
 Eichler, Hans Joachim - ATu4M.3
 Eichner, Timo - FF1E.3, JTu2A.171
 Eigner, Christof - FM1G.3
 Ekema, Kjeld S. - STh3N.4
 Eisele, Max - FTh1K.4, SW3D.2
 Eisenbach, A. - SF2G.4
 Eisentent, Gadi - FTh1H.6
 Eitan, Michal - FF1H.3
- Ekanayake, Nagitha - JW2A.182
 El Amili, Abdelkrim - FM4Q.8, JTu2A.30, SW4Q.4
 El Dirani, Houssein - JTu2A.120
 Elafandy, Rami - JTu2A.91
 Elder, Delwin - FTh4H.1, JTh4D.5, SM1I.4, SM4B.1
 Elder, Ian - AM1M.1
 Eleuch, Hichem - FM4H.4
 Elfiky, Eslam - STh4A.7, STh4B.4
 El-Ganainy, Rami - FM3Q.1, FM4E.2, FM4E.7, FM4Q.6
 El-Ghazawi, Tarek - ATH1Q.4, JW2A.3
 Ellis, Andrew - FW3H.4, SM2C.6
 Elsaesser, Thomas - FM4F.4, JW2A.120
 El-Sawah, Nayera - SF2J.2
 El-Shimy, Mohamed - JTu2A.46
 Elsing, Lukas - SW4I.4
 Emani, Naresh K. - FTh4J.5
 Emaury, Florian - Ath3O.6
 Emboras, Alexandros - SM2I.3
 Emmons, Erik - STu3N
 Enderlein, Martin - SM1K.3
 Endo, Akira - STu4O.6
 Endo, Mamoru - SM2L.4
 Eng, Lukas - JM2A.3
 Engelsen, Nils Johan - Ath3H.6
 Enghtae, Nader - FF3C.3, FM4Q.7, FTh1D.1, JW2A.90, JW2A.93
 England, Duncan - FM4G.6
 Englund, Dirk - FF1B.3, FM1H.3, FM1H.6, FTh1G.6, FTu4E.7, FTu4H.2, FW4F.4, SF3A.4, STh3G.3, STh3L.4, SW3B.2, SW4C.1
 Epping, Jörn - JTh3D.2
 Epstein, Richard - FF3E.1
 Erdogan, Sedef - JTu2A.105
 Erickson, David - SW3J.1
 Erkintalo, Miro J. - FW3E.2, JTu2A.119, JTu2A.137, SM1D.5, SM2D.2, SM4K.7, SW3A
 Erskine, Jennifer - FM4G.6
 Ertel, Klaus - STu4O.6
 Erven, Chris - JTh2A.24
 Esashi, Yuka - AW4O.2
 Escarrat, Matthew D. - JTh2A.54, JW2A.109, SW3I
 Eschner, Jürgen - FM2H.6
 Escobet-Montalban, Adria - AF2M.3
 Eshaghian Dorche, Ali - JTu2A.85, JW2A.33
 Esmail, Maged - JTu2A.34
 Esser, M J Daniel - AM1M.1, SM3N.1
 Essiambre, René-Jean - JTh2A.133, SM3C.2
 Estudillo Ayala, Julian M. - Ath4O.7
 Etcheverry, Sebastian - AM4P.6
 Etezadi, Dordaneh - JTh2A.74
 Eto, Motohiko - STu4B.3
 Evans, Christopher C. - STu3N.1
 Evans, Dean - JTu3O.3
 Evans, Phil - FM1G.6, FTu3H.4, JTh2A.9
 Evlyukhin, Andrey - JW2A.94
- F**
 Fabbri, Simon J. - SF3N.6, SM1C.1
 Fabert, Marc - SM3D.6, SW3K.6
 Fabre, Claude - SM4D.2
 Facciola, Davide - JTu2A.156
 Faccio, Daniele - FF1H.4, FM3E.5, SM4D.7
 Faerman, Arkady - FTh3M.1, FTh4J.8, FTu3E.5
 Fainman, Yeshaiahu - FM4Q.8, JTu2A.30, SW4Q.4
 Faist, Jérôme - Ath4Q.4, Ath4Q.6, FTh1H.3, SF3G.2, SF3G.5, STh1L.5, STu4D.1, STu4D.3
 Fakhari, Moien - SM4A.4
 Falconi, Fabio - JTh3D.3, JW2A.143
 Fallahi, Arya - JF1C.5, SM4A.4
 Fallahi, Saeed - FF2D.6
 Fallahpour, Ahmad - JTu2A.49, JTu2A.53, SM1D.2, SW3A.5
 Fan, Guangyu - FM3M.2, SF1N.3, SM4M.3
- Fan, Haoquan - FTu4H.6
 Fan, Hong Jin - FTh1F.5
 Fan, Jingyun - FTu4A.4
 Fan, Jintao - JTh2A.156
 Fan, Jonathan - FF3C.1, FF3C.2, FF3C.5, FF3C.6
 Fan, Lingling - FTh1K.5
 Fan, Shanhui - AW3O.6, FF1F.2, FF3P.3, FM1E.4, FM2Q.4, FM3Q.7, FTh1P.1, FTu3E.2, FTu3E.7, JTh2A.44, JTu2A.13, SF2I.8, STh3A.7, SW4A.1
 Fan, Tianren - JTh2A.78, SM1I.1, SW4A.2, SW4B.6
 Fan, Wei - JTu2A.163
 Fan, Wentao - FM4J.5
 Fan, Xinyu - JTh2A.124, JW2A.145, SM3K.4, STu4K.2
 Fan, Xudong - SW3J.2
 fan, Yingwei - JTu2A.99
 Fan, Youwen - SW4C.5
 Fan, Zhengquan - FM1Q.8
 Fan, Zhi-Bin - STh3I.8
 Fan, Zhiyuan - FF2L.2, FTh1D.2, SF1J.7
 Fancher, Charles T. - FM2H.4
 Fang, Bin - FM3G.7, JTh2A.2
 Fang, Cheng-Yi - SW4Q.4
 Fang, Shaobo - SW3N.1
 Fang, Tianhua - AF2M.4
 Fang, X. M. - SF2G.4
 Fang, Xu - JW2A.95
 Fangcheng, Shen - JW2A.1
 Fanto, Michael - SF3A.4
 Faraji-Dana, MohammadSadeq - AF3M.3, FF1F.5, SF1J.2
 Faraon, Andrei - AF3M.3, FF1F.5, FF3C.7, FTu4H.4, FTu4H.5, JTh3C.3, SF1J.2, STh3G.2
 Fargas Cabanillas, Josep - STh4A.2
 Farooq, Aamir - ATu4I.5
 Farooq, Hira - JTh2A.58
 Farris, Benjamin - JW2A.182
 Farsi, Alessandro - FM3G.2
 Faruk, Md Omar - JTh2A.50
 Faruque, Imad - FTh1G.5, FTh1G.7
 Faryadras, Sanaz - FM4E.7
 Fasold, Stefano - FW3J.1, FW4H.8
 Fastenau, Joel - SF2G.4
 Fatemi, Fredrik K. - FM2H.4
 Fatemi, Reza - SM3B.6, STu4B.6
 Fathallah, Habib - JTu2A.34
 Fathipour, Vala - ATu4M.5
 Fathpour, Sasan - JTh2A.16, JTh2A.166, JTh3C.2, SM1B.2, STh4A.6, STu3F.4
 Fatome, Julien - JTu2A.119, SW3K.6
 Fattal, David - FW4F.6
 Faure, Jerome - JF2C.5
 Fausti, Daniele - Ath3O.7
 Favela, David - SF1A.1
 Fedeli, Jean-Marc - FTh1E.5
 Feder, Kenneth - SM3K.6
 Fedorov, Sergei V. - FM1E.5
 Fedorov, Sergey A. - Ath3H.6
 Fedorov, Vladimir - FF1E.2, FM1Q.1, FM1Q.2, JTu2A.113
 Fedoryshyn, Yuriy - FTh4H.1, JTh4D.5, SM1I.4, SM2I.3, SM4B.1
 Fedyanin, Andrey - FW3G.6
 Fehrenbacher, David - JW2A.154
 Fei, Yueyang - STu3A.3
 Feist, Armin - FM4F.1
 Feizollah, Peyman - JW2A.182
 Fejer, M. M. - FTu4A.2, SM2D.5
 Feldman, Matthew A. - FM1G.6, FTu3H.4
 Fendel, Peter - ATu3I
 Feng, Chengyong - JTu2A.161
 Feng, Jijun - SW4B.7
 Feng, Jing - STu4B.4
 Feng, Kaijun - JW2A.96
 Feng, Kaiyin - SW3Q.3
 Feng, Liang - FM2Q.6, FM3Q, FM3Q.1, FM4Q.6
 Feng, Lipeng - JTh2A.118
 Feng, Milton - SW4Q.2
- Feng, Pingping - JTh2A.148, SW4J.5
 Feng, Tao - SF2G.6
 Feng, Ting - JTh2A.117, JTu2A.98
 Feng, Xian - JTh2A.112
 Feng, Xianglian - JTu2A.54
 Feng, Yujun - JTh2A.110, SM2K.7
 Feng, Yutong - JTh2A.109, SM1K.6, SW4K.5
 Ferachou, Denis - SM4M.3, SW3N.2
 Ferdinandus, Manuel R. - JTu2A.130
 Ferguson, R. Daniel - JW3P.3
 Ferlet-Cavrois, Veronique - JTh2A.175
 Fermann, Martin E. - JTh2A.168, JTh2A.185
 Fernandez, Hervé - AM2J.5
 Féron, Patrice - SM4I.7
 Ferranti, Giacomo - SF1K.7
 Ferrara, Marcello - FM3E.5, SM4D.7
 Ferrari, Andrea - FF2E.2, JTh2A.179, SF3K.6
 Ferrari, Andrea Carlo - STu4D.6
 Ferreira de Lima, Thomas - STh3B.1
 Ferreira, Filipe - FW3H.4
 Ferreira, Maria R. - JTu2A.50
 Ferretti, Hugo - FF1B.2
 Ferrier, Alban - FTu4H.7
 Ferro, Gabriel - JTh3C.5
 Fettes, M. - SF2G.4
 Feurer, Thomas - FW4H.7
 Fickler, Robert - FW3F.5
 Field, Jeff - ATu3J.3
 Figeys, Bruno - JW2A.32
 Figueiredo, Pedro - SF2G.4
 Figueiroa, Alfredo - JTh2A.102
 Filipsson, Anna - STu3P.4, STu3P.6
 Finley, Jonathan - FM1H.4, FTu3H.1, JTu2A.8
 Finley, Jonathan J. - SW3B.6
 Fiore, Andrea - JTh3C.4, STh3G.4
 Firoozabadi, Saleh - JW2A.136
 Fischer, Kevin - FM1H.4, FM3H.4, FTu3H.1, FTu3H.5, JTh2A.44, JTh3C.5
 Fischer, Marc - SM1L.5, SM2L.5, STu4K.3
 Fitzgerald, Eugene A. - AW3O.3
 Fitzgerald, Eugene A. - STh4I.6
 Fitzsimons, Joseph F. - FM1G.2, FTu3G.2, JTh2A.18
 Flach, Sergej - FM1E.7
 Flagg, Edward - JTh2A.34
 Flammini, Mariano - FM3E.2, FTh3E.2
 Flanigan, Patrick - FTh1K.3
 Fleischer, Monika - FW3G.3
 Fleisher, Adam J. - STu3N.5, STu4P, SW4L.4
 Fleming, Tristan G. - ATu4M.4
 Fleury, Romain - FF3H.3
 Flom, Steven R. - SM1N.1
 Flores, Angel - SW4K.3
 Flores, Jaime G. Flor - FF1H.5, SM1B.6
 Flores-Bravo, J. A. - SM2K.6
 Flöry, Tobias - SM4M.1
 Foerster, Daniel J. - AM1M.3
 Fogler, Michael - FF2L.7, FM3H.3
 Fokine, Michael - SF3I.6
 Follman, David - JTu2A.14, SM3L.6
 Folpini, Giulia - JW2A.120
 Foltynowicz, Aleksandra - JW2A.165, STu3P.4, STu3P.6
 Fontaine, Nicolas K. - JTh2A.133, JTh2A.173, SM3C.1, SM4C.2, STh3K.5
 Fontana, Jacob - SM2O.1
 Forbes, Lindsey H. - STh1J.2
 Forchhammer, Søren - STu4C.6
 Forestieri, Enrico - STu3C.1
 Forget, Nicolas - STu3M.4
 Forman, Charles - SF1G.7
 Forouher, Dariush - JW2A.138
 Forrer, Andres - STu4D.1
 Forrest, Stephen R. - FW4G.8
 Forstner, Stefan - JTh2A.25
 Fortier, Paul - STh4B.8
 Fortier, Tara M. - SM1L.4, SM2L, SM2L.3
 Fortin, Vincent - STh4K.2
 Fortuna, Seth - SM4I.3, SM4I.5, STu4N.6
 Forward, Sarah - ATu3J.6

- Fossati, Alexandre - FTu4H.7
 Fossum, Eric R. - FW3F.8
 Foster, Amy - FM1G.4, JW2A.68, SM1D.7, STh3I.5
 Foster, Andrew P. - JTh2A.27
 Foster, Mark A. - FM1G.4, JW2A.68, SW4J.6
 Fraenzl, Martin - JTh2A.51
 Fragnito, Hugo - FF1E.8, JTu2A.71
 Frame, James - JW2A.95
 Francis-Jones, Robert J. - Ath3H.8
 Frankie, Martin - SF3G.5, STu4D.3
 Frandsen, Lars H. - JTh4C.4, SW4I.2
 Frankis, Henry C. - STh3I.3
 Frantz, Jesse - SF3A.6, SM1N.1
 Frasca, Simone - FW3F.3
 Fraser, James M. - ATu3I.1, ATu4M.4, FF3D.3
 Frassetto, Fabio - JTu2A.158
 Fratolocchi, Andrea - JW2A.115
 Frede, Maik - STu4O.5
 Freeman, Joshua R. - STu4D.4
 Freeman, Ryan - JW2A.83
 Freisem, Lars - STh3N.4
 Freiwang, Peter - FTu3G.1
 Fresi, Francesco - STu3C.1
 Freude, Wolfgang - SM3B.1, SM3B.3, SM4I.6, STh1A.1, STu3D.4
 Frez, Clifford - SF2G.1
 Fridlander, Joseph M. - STu4Q.3
 Fridman, Moti - JTh2A.137, JTh2A.163, STh3N.5, SW4N.6
 Friebele, E. Joseph - SW4K.5
 Friedman, Gavin - STu3M.2
 Friesem, Asher - SF1J.6
 Friis, Søren M. - FM3G.3
 Frish, Julie I. - JW2A.41
 Frish, Michael B. - STu3N.1
 Fröch, Johannes E. - SM1O.5
 Fröhlich, Bernd - FTu3G.6
 Frosz, Michael H. - SM2K.5, SW3K.2
 Fry, Alan - JTh2A.169, SF3N
 Fryett, Taylor K. - JW2A.16
 Frysliet, Stewart - STu3Q.4, STu3Q.7
 Fsaifes, Hsan - SM2N.8
 Fu, Bo - JTh2A.179, SF3K.6
 Fu, Dong - JTu2A.32
 Fu, Dongzhi - JTh2A.4
 Fu, Kai-Mei - FM1H.2
 Fu, Liang - FM2Q.3
 Fu, Qiang - ATu3S.3, SM4K.2, SM4K.5, STh3F.2
 Fu, Shijie - SM2N.7
 Fu, Songnian - SM1C.5, SM4C.4, SM4C.5, STu3C.6
 Fu, Walter P. - SM2N.1, SM4K.3
 Fu, Xin - JW2A.14, JW2A.2, JW2A.23, SW4C.6
 Fu, Xuelei - JTu2A.66
 Fu, Yuan Hsing - FTh4J.5
 Fu, Yuxi - JTu2A.155, SF1N.5
 Fuerbach, Alex - STh4K.1
 Fuji, Takao - FF2P.2, SW3N
 Fujii dos Santos, Lais - JTu2A.111
 Fujii, Kentaro - STu4Q.2
 Fujii, Shun - SW3A.7
 Fujii, Takuro - SF3A.3
 Fujita, Eisuke - SF2N.2
 Fujita, Kazuue - SF3G.7
 Fujita, Toshiro - SW4K.2
 Fukano, Hideki - JW2A.146
 Fukuda, Hiroshi - SM2I.5
 Fulop, Attila - JW2A.149, JW2A.71, STu3F.1, SW3C.1
 Fülöp, József A. - JTh2A.189, JTh2A.190, JTh2A.191, SM3A.2
 Fulop, Lajos - STu3M.3
 Fung, Mary - AF2Q.3
 Furch, Federico J. - JTu2A.151, STh3N.1, SW3N.6
 Furlong, M. - SF2G.4
 Furukawa, Hideaki - JTu2A.52
 Furusawa, Akira - FTu4G.1, FTu4G.3, FTu4G.4, JTh2A.21
 Futami, Fumio - JTu2A.57
 Futia, Gregory L. - SW4J.7
- G**
- Gaarde, Mette B. - FF1P.2, FF3P.1
 Gabriel, Tobias - AM1M.7
 Gabrielli, Lucas - FF1E.8, JTu2A.71, JW2A.58
 Gad, Raanan - JTh2A.98
 Gadonas, Darius - STu4O.1, STu4O.4
 Gaeta, Alexander L. - FM3G.2, FM3G.5, FTh1E.4, JTu2A.72, SF2I.5, SM1D.6, SM3D.1, SM4L.7, STh1J.4, STu3F.6, SW3A.4, SW4M.5
 Gaeta, Alexander L. - FM1Q
 Gage, Thomas E. - SW4I.5
 Gaierin, Simone - STh1C.3
 Gaida, Christian - SF1N.7
 Gajda, Andrzej - STu4C.1
 Galfsky, Tal - FW4H.6
 Galili, Michael - JTu2A.68, SM2C.3, STu3D.1, STu4C.1, STu4C.2, STu4C.6, SW4I.2
 Galimberti, Marco - JTu2A.170
 Gallego, Jose - FM2H.3
 Galli, Iacopo - Ath4Q.6
 Galli, Mara - JTu2A.158
 Galli, Matteo - JTh4C.1, JTu2A.128, STu3F.2
 Gallo, Katia - AF2M.5
 Galstad, Christian - STu4Q.4
 Galvanauskas, Almantas - SM4M.6
 Gan, Jiulin - SW3K.3
 Gan, Lin - SM4C.4, SM4C.5
 Gan, Qiaoqiang - SF2I.6, STh1B, STh4B, SW3J.6
 Gan, Rulei - FF2F.6
 Gan, Yu - STh1J.4
 Gandini, Marina - FF2D.7
 Ganija, Miftar - SM4N.3
 Ganjalizadeh, Vahid - JW2A.24
 Gao, Cong - SF3I.1
 Gao, Fan - STu3C.6
 Gao, Fei - FM4J.8, FM4Q.4
 Gao, Hao-Cheng - Ath3Q.4
 Gao, Jun - SF2I.6, SW3J.6
 Gao, Lei - JTh2A.108
 Gao, Liang - SF3G.6
 Gao, Qian - JTh2A.56, SM1I.3, SM4B.2
 Gao, Shengqian - JW2A.28, STu3B.2
 Gao, Shiming - JTu2A.54
 Gao, Shoufei - SF1K.4, STu4F.4, SW3N.3
 Gao, Shuang - JTu2A.41
 Gao, Song - AF1M.7, SW3L.3
 Gao, Wanli - JTh2A.128
 Gao, Weibo - FM1G.2, FTu3G.2, JTh2A.18
 Gao, Weilu - FF2D.6, FM2F.3, FTu3E.3
 Gao, Wenbin - STh4K.7
 Gao, Xiaohui - SF2I.5
 Gao, Yang - FTh4J.6
 Gao, Yun - SM2I.7
 Gao, Zhengning - JTh2A.71
 Gao, Zhihe - JW2A.17, SF2A.7, STu3Q.4, STu3Q.7
 Gaoneng, Dong - SM4B.5
 Gaponenko, Maxim - SF2N.3
 Gapontsev, Valentin - STh4F.4
 Garbin, Bruno - JTu2A.119
 García de Abajo, Francisco Javier - STh1N.4
 García de Abajo, Javier - FF3D.8
 Garcia-Gracia, Hipolito - SW4Q.1, SW4Q.5
 Garcia-Souto, Jose A. - JW2A.171
 Gardes, Frederic - SM3B.5, STu3F.2
 Gardiner, Tom - STh1L.4
 Gardner, Geoff - FF2D.6
 Gardosi, Gabriella - SF2K.2, SW4A.6
 Garlapati, Suresh Kumar - STu3D.4
 Garmire, Elsa M. - STu4F.1
 Garnett, Erik C. - FF2L.1
 Garreau, Alexandre - JW2A.55
 Gasparini, Leonardo - FF1B.4
 Gasser, Christoph - AM2M.7
 Gatdula, Robert - STh4A.3
 Gatkine, Pradip - JW2A.65
 Gattass, Rafael - SF3I.3
 Gaul, Erhard W. - SM1N, STu3M.2
 Gauthier, Daniel J. - FTu3G.3, FW3F.2, JTh2A.8
 Gavara, Trivikramarao - JTh2A.159
 Gawith, Corin - Ath3H.8, STh1I.3
 Gazzano, Olivier - FM3H.2, SM1O.6
 Gbadebo, Adenowo - JW2A.174
 Ge, Renyou - STh1B.6
 Ge, Shaofeng - FF1D.7, JTh2A.143
 Ge, Xiaochen - JTu2A.13
 Gebhardt, Martin - SF1N.7
 Gehring, Tobias - JF3B.2, JTh2A.10, JTh2A.25
 Geim, Andre - FF2L.7
 Geiregat, Pieter - SW4I.4
 Geiselmann, Michael - STh4A.4
 Geisler, David - STu3C, SW4C
 Gemechu, Wasyhun A. - STu4C.3
 Genack, Azriel Z. - FF2H.4, FM4Q.2
 Genco, Armando - STh3G.4
 Gene, Jinhwa - SM2N.5
 Geneaux, Romain - FF1P.4
 Genest, Jérôme - SW4L, SW4L.4, SW4L.5
 Genestie, Catherine - AM2J.5
 Geng, Yong - JTu2A.148, JTu2A.56, SM4K.6, STu3C.4
 Geng, Zihan - SM1C.2
 Gengler, Jamie - JTu2A.130
 Genner, Andreas - AM2M.7
 Genovese, Marco - FF1B.6
 Gentry, Cale M. - JTh4C.3
 Genty, Goëry - AF2Q.1
 Georgakoudi, Irene - AM2J, JTu4L.1
 George, Deepu Koshy - SW3D.5
 George, Heather - FTu4E.2, JW2A.129
 George, Jonathan - Ath1Q.4
 Georges, Patrick - JTu2A.150, SM4M.4, STh1N.3
 Georgiev, Kaloyan - JTu2A.69
 Gerald, Andrea - FW4F.3
 Gerguis, John O. - AW4O.7
 Gérôme, Frédéric - FM4G.4, JTh2A.97, SF1K.2, SF1K.3, SF1K.6, SM2N.2, SM3L.3, SM3L.4
 Gerrits, Thomas - FTu4G.2, JTh2A.16, JTh3C.2, JTh4C.3
 Gershoni, David - FTu3H.3
 Gertler, Shai - SM1I.8
 Gerz, Daniel - SF1N.7
 Geskus, Dimitri - JTh3D.2, SW4C.5
 Geuzebroek, Douwe - SW4C.5
 Gevorgyan, Hayk - JW2A.59, SF1A.5
 Ghadiani, Bahareh - STh1I.1
 Ghadimi, Amir - Ath3H.6
 Gharajeh, Abouzar - AF1Q.6
 Ghelfi, Paolo - JTh3D.3, STh4N.3
 Ghetmiri, Seyed - AF1Q.5, STh4I.2, STh4I.4
 Ghimire, Shambhu - FF2P.3, FF3P, FM3F.5
 Ghobadi, Roohollah - FW4F.6
 Gholam Mirzaeimoghadar, Shima - FF3P.6, SW3N.4
 Gholipour, Behrad - FTh4H.6, SM4O.3
 Ghosh, Anirban - JTu2A.142
 Ghosh, Pintu - SW3I.2
 Ghosh, Samir - SM4B.6
 Giacomuidis, Elias - STh1C.5
 Gianardi, Don - JTu2A.19
 Giannetti, C. - FM1F.7
 Gibson, Dan - SF3I.3
 Gibson, Emily A. - SW4J, SW4J.3, SW4J.7
 Gibson, Ursula J. - SF3I.6, SM3D.5
 Giebink, Noel C. - SF1I.1
 Giese, Enno - FW3F.5
 Giesecke, Anna-Lena - JW2A.5
 Giesz, Valerian - FTu3H.6
 Giles, Ian P. - JTh2A.118
 Gill, Patrick - JTh2A.42
 Gil-Molina, Andres - FF1E.8, JTu2A.71
 Gini, Emilio - Ath4Q.4
 Ginis, Vincent - FF3E.6, SF3J.4
 Ginsberg, Jared - SF2I.5
 Giorgetta, Fabrizio - STh1L.2
 Giovanardi, Fabio - SF1K.6
 Girodias, Benjamin J. - FTu4E.2, JTu2A.146
 Girouard, Peter - SW4I.2
 Giunta, Michele - SM1L.5, SM2L.5, STu4K.3, SW4L.1
 Gjonaj, Bergin - FTh3M.4, SW4J.2
 Gladden, Christopher - AW3O.5
 Gladstein Gladstone, Ran A. - JW2A.114
 Gladyshev, Alexey - FM4G.7, FM4G.8
 Gladyshev, Sergey - JTh2A.73
 Glaw, Uwe - AM1M.7
 Glaw, Veronika - ATu4M.3
 Glenzer, Siegfried - SM3A.1, SM4A.5
 Glerean, Filippo - Ath3O.7
 Gleyzes, Sebastien - JF2B.2
 Globisch, Bjoern - STu3D.5
 Glowina, James - FM4F.5
 Gluckman, Joshua - ATu3R.4
 Gmachl, Claire F. - AF1Q.3, FM4J.5
 Gnilitzkiy, Iaroslav - AM1M.6, JTu3O.1
 Go, Rowel - SF2G.4
 Gocalinska, Agnieszka - STh4B.1
 Goda, Keisuke - AF3Q.3
 Godard, Antoine - Ath3O.1, STu3N.7
 Gogotsi, Yury - FM2G.7
 Goh, Takashi - SM1C.4
 Gokus, Tobias - FTh1K.4, SW3D.2
 Golberg, Mark - JTu2A.101
 Goldberg, Aaron Z. - FTu4A.3
 Goldflam, Michael - FTh4M.1, FW3H.7
 Goldner, Philippe - FTu4H.5
 Goldschmidt, Elizabeth A. - FM1H, FTu4H.6, JTh2A.39
 Goldstein, Jonathan - SM3O.5
 Golling, Matthias - JW2A.157, SF1G.2
 Gollner, Claudia - FF1E.2, FM1Q.2
 Golombek, Adina - FM2F.2
 Gombojav, Aiunbold O. - STu4P.5
 Gomes, Jean-Thomas - SM4M.4
 Gomez, Carmen - JW2A.55
 Gomez, Daniel - AW4O.5
 Gomez, Pau - JF3B.5
 Gong, Cheng - JTh2A.178
 Gong, Jiangbin - FM1G.2, FTu3G.2, JTh2A.18
 Gong, Mali - AM2M.5, JTh2A.181
 Gong, Qihuang - FM1Q.8
 Gong, Su-Hyun - FF2L.1
 Gong, Yupeng - JTh2A.23
 González de Alaiza Martínez, Pedro - JTu2A.121
 Gonzalez, Aura I. - JTu2A.150, STh1N.3
 Gonzalo, Ivan Bravo - JTu2A.109
 Gossens, Jan-Willem - STu4C.3
 Gopinath, Juliet - JTh2A.85, STh4I.3, STu4P.7, SW4J.3, SW4J.7
 Gord, James R. - ATu4I.2
 Gordon, George S. - STh1I.2
 Gordon, Reuven - FTu4E.3
 Gorju, Guillaume - Ath3O.1
 Gornik, Erich - SF2G.2
 Göröcs, Zoltán - AM1J.5
 Gorodetsky, Michael - JTh4D .3, STh4B.6, SW4M.7
 Gorse, Alexandre - FM4G.4
 Gorshkov, Alexey - JF3B.4
 Gorywoda, Marek - AM1M.7
 Gossard, Arthur - FM3F.4, FM3H.3, SM2I.6, SW3B.1, SW3Q.2, SW3Q.3, SW4I.3
 Gotoh, Hideki - JTu2A.153, SM4L.5
 Gould, Michael - FM1H.2
 Goulielmakis, Eleftherios - FF2P.5
 Goun, Alexei - Ath1Q.3
 Gouveia, Marcelo A. - JTh2A.42
 Goykhan, Ilya - FF2E.2
 Gracias, David - FF2F.5
 Graf, Austin - FTh4G.4
 Graf, Thomas - SM1N.4
 Grafer, Elliott - JTh3D.1
 Grajower, Meir Y. - FW4G.3, STh1A.6
 GRAMEGNA, MARCO - FF1B.6

- Grange, Thomas - FTu3H.6
 Grant, Joshua - STh4I.2
 Grant, Perry C. - STh4I.4
 Grant, Perry C. - STh4I.2
 Grant-Jacob, James - JTh2A.177, SM10.4, SM40.3
 Grass, Tobias - FM3H.2
 Grassani, Davide - SF2A.2, SW3A.8
 Grasseschi, Daniel - JTh2A.100
 Graumann, Ivan J. - SF2N.6, SM3N.5
 Grave de Peraltá, Luis - JTh2A.58
 Graves, William - JF1C.2, STu4O.4
 Gray, Stephen K. - SM2O.3
 Grebing, Christian - SM3N.4
 Green, Tyler - STu4P.4
 Green, William - STh1B.2, SW3L.7
 Greenberg, Alan R. - STu4P.7
 Greene, Jonathan T. - STu3M.2
 Greener, Hadar - JTh2A.66
 Greener, Zoe - AW3R.4
 Gregg, Patrick - FTh1M.4, SW3K.1
 Gregory Vianna, Pilar - JTh2A.100
 Gregory, Thomas - FF1B.1
 Grein, Matthew E. - FW4F.4, JTh2A.17
 Greinert, Rüdiger - AM1J.2
 Gremillet, Laurent - JTu2A.160
 Gresch, Tobias - SF2G.7
 Grewal, Raghvinder S. - JTu2A.142
 Grice, Warren P. - FTu4A.5
 Grice, Warren P. - JTh2A.9
 Griebner, Uwe - SF2N.1, SF3I.5, SM2N.6
 Grigoropoulos, Costas P. - FW3H.6
 Grigoroza, Teodora - ATu3S.2, SF1K.5, SM4M.2
 Grigoryan, Vladimir - STu4C
 Grillet, Christian - FTh1E.5
 Grillot, Frédéric - JTu2A.24
 Grisard, Arnaud - SM4D.2
 Groen, Joshua B. - AW4O.3
 Grootjans, Robert - JTh3D.2
 Grosse-Wortmann, Uwe - STu4O.5
 Grotti, Jacopo - SM1L.6
 Grubel, Brian - FM1G.4
 Gulkowski, Ireneusz - FTh1K.7
 Grupp, Alexander - FTh1F.6
 Grutter, Karen - JF2B.5, SF2J
 Gruzdev, Vitaly - AM1M.6, AM3P.5, SM3O.4
 Grynko, Rostislav - JTu2A.132, JTu2A.3
 Gu, Chao - FW3F.1
 Gu, Chenglin - JTh2A.156
 Gu, Jie - FF1D.6, FM2F.6
 Gu, Qing - AF1Q.6, JTu2A.30, JW2A.10, SW4Q
 Gu, Ruo Yu - ATu4J.5
 Gu, Tian - AW3O.3, SF1A.1, SF2I, STh3I
 Gu, Tingyi - JW2A.36, SM2B.4
 Gu, Xiaodong - JTu2A.11, SM3I.4
 Gu, Yuan Dong - Ath4O.4, JW2A.54
 Gu, Yuandong - Ath4O.1, Ath4O.2
 Gu, Zhichen - FM3J.7, JW2A.92
 Guan, Pengyu - SM2C.3, STu3D.1
 Guan, Xianchao - JTu2A.164
 Guan, Xun - SW3K.5
 Guardalben, Mark J. - STu3M.5
 Guay, Philippe - SW4L.4
 Guazzotti, Stefano - FM3E.6
 Guclu, Caner - FTh1K.2
 Guddala, Sriram - SM2O.7
 Guerra-Santillán, Yanin - FTh4E.5
 Guggenmos, Alexander - FF1P.4
 Guha, Saikat - FTh1G.6
 Gui, Tao - SM3K.3, STu4C.3
 Guichard, Florent - STh1N.3
 Guidry, Melissa A. - JTh2A.31
 Guilhabert, Benoît - SM2B.6
 Guillet de Chatellus, Hugues - Ath3O.4, SM1B.7
 Guina, Mircea D. - Ath4Q.1, JTu2A.10, JTu2A.17, JTu2A.28, SF2N.1, SW4Q.4
 Gumbsheimer, Pascal - FF3D.5
 Günaydin, Harun - AM1J.5, STh1J.3
 Guo, Chen - STh3N.2
 Guo, Cheng - FF1F.2, FF3P.3
 Guo, Daqian - STh4I.5
 Guo, Guang-Can - SF2J.5
 Guo, Hairun - FF2E.4, JTh4D.3, STh4A.4, SW3A.8
 Guo, Hsuan-Tse - AM2M.3
 Guo, Huiyong - SM2K.3
 Guo, Jingjing - JTu2A.89
 Guo, Joel - Ath1O.4, JW2A.40, SF3J.6, STh1B.4
 Guo, Lu - SW4Q.6
 Guo, Nan - SM3K.3
 Guo, Qiang - AF2M.4
 Guo, Rui - JW2A.67
 guo, wei - FM4Q.5, FTh4J.3, JTu2A.7
 Guo, Weihua - Ath4Q.3, JTu2A.22, SM4B.7
 Guo, Wei-Hua - JTu2A.26, JW2A.6
 Guo, Xiaowen - STu3F.5
 Guo, Xiaoyu - JTh2A.48, JTh2A.61
 Guo, Xin - STh1B.1
 Guo, Xuhan - SW4C.2
 Guo, Yajing - JTu2A.178
 Guo, Ying - JTh2A.13
 Guo, Zhaocheng - JF1C.3
 Gupta, Shashank - STh4I.6
 Gurel, Kutan - JW2A.161, SM4L.2, SM4L.6
 Gurlek, Burak - FW4G.7
 Gurung, Sudip - FM4J.2
 Guss, Gabe - JW2A.117
 Gustave, François - JTh2A.120
 Guvandarapu, Sarat - FW3E.3
 Guzman-Sepulveda, Jose - AF1M.5
 Gwo, Shangjr - JTh2A.69, SM2B.2, STu4N.2
- H**
- Haas, Bryan - SW3K.4
 HABIB, MD SELIM - JTh2A.196
 Hachisu, Hidekazu - SM1L.1
 Hachtel, Jordan - FM1G.6, FTu3H.4
 Hackney, Drew - AF1M.4
 Hadji, Emmanuel - JTh2A.99
 Hädrich, Steffen - SM4M.3, SW3N.2
 Hafermann, Hartmut - STu4C.3
 Hafezi, Mohammad - FM3H.2
 Haffner, Christian - FTh4H.1, SM1I.4, SM4B.1
 Häfner, Sebastian - SM1L.6
 Hagan, David J. - FF2E, FF2E.1, JTu2A.59
 Hage, Arvid - SM3N.2
 Hagley, Edward W. - ATu3J.7
 Haglund, Richard - FM1G.6, FTu3H.4
 Hahn, Herwig - STh3I.6
 Hahn, Lothar - SM4I.6, STu3D.4
 Haie-Meder, Christine - AM2J.5
 Haji, Mohsin - JTh2A.42
 Hajimiri, Ali - SM3B.6, STu4B.6
 Hajisalem, Ghazal - FTu4E.3
 Hakobyan, Sargis - JW2A.161
 Halas, Naomi - JTu2A.82
 Halder, Arindam - JTh2A.77
 Halder, Matthäus - STu3P.2
 Hales, Joel M. - JTh2A.175, JTu2A.59
 Halimi, Abderrahim - AW3R.4
 Halimi, Sami - STh3A.2
 Halir, Robert - STh1I.3
 Hallman, Mark - AF2M.7
 Halonen, Lauri - Ath1O.8
 Ham, Moon-Ho - FF2D.4, FM1F.1
 Hama, Yusuke - JTh2A.43
 Hamada, Shohei - JTh2A.63
 Hamaguchi, Tatsushi - STu4Q.2
 Hamerly, Ryan - FTu4A.2
 Hamidfar, Tabassom - SW4A.5
 Hamilton, Erik - JTh2A.101, JW2A.24
 Hamilton, Scott A. - FW4F.4, JTh2A.17, STu3C.7, SW4C.1
 Hammack, Aaron - FM3H.3
 Hammar, Mattias - SW3Q.5
 Hammer, Jonas - FW4E.7
 Hammer, Larissa - SM4O.5
 Han, Guanyu - JW2A.42
 Han, Kevin - SM4I.3, SM4I.5, STu4N.6
 Han, Kuk-Il - JTh2A.176
 Han, Kyunghun - SM1B.1, STh4A.1
 Han, Liangshun - STh4A.8, STu4B.3
 Han, Myung-Geun - FTu4E.2
 Han, Pengdi - SF2I.1
 Han, Sang-Wook - FF1B.5, JTh2A.1
 Han, Song - SW4D.6
 Han, Xu - JTu2A.12
 Han, Yingjun - STu4D.4
 Han, Yu - SF3A.1
 Han, Yuchen - FM4Q.4
 Han, Zheng - SW3I.5
 Han, Zhengli - JW2A.100
 Hanado, Yuko - SM1L.1
 Hanawa, Masanori - JTu2A.38
 Hand, Duncan P. - AM1M.1, AM1M.5
 Hand, Lucian - STu4O.4
 Hanein, Yael - FF1H.3
 Hanh, Nguyen Thi Bich - JTh2A.52
 Hanifteh, Mina - FTh1K.1
 Hanna, Marc - JTu2A.150, STh1N.3
 Hanschke, Lukas - FM1H.4, FTu3H.1
 Hänsel, Wolfgang - SM1L.5, SM2L.5, STu4K.3, SW4L.1
 Hansen, Jörn O. - JF3B.2
 Hansson, Tobias - FTh1E.2
 Hao, Jianhuan - JW2A.131
 Hao, Wenhui - JW2A.73
 Hao, Y. L. - Ath4O.1
 Hao, Zhenzhong - JTu2A.139
 Hara, Kazutaka - SM4L.5
 Harada, Yoichi - JTu2A.152
 Haraguchi, Eisuke - JTu2A.152
 Harari, Gal - FM2E.3, FM2E.5, FM4E.5
 Harden, Galen - JW2A.96
 Harder, Georg - FW4F.1
 Hardin, Johanna - AF2M.7
 Hardy, W. - FM1F.7
 Hare, Alva - SM3I.7
 Hariki, Takuya - SM4L.3
 Harilal, Sivanandan S. - STu3N.4
 Hariri, Lida - AM1J.6
 Harkema, Nathan - FF1P.2
 Härkönen, Antti - SF2N.1
 Haroche, Serge - JF2B.2
 Haroldson, Ross - AF1Q.6
 Harren, Frans J. M. - Ath1O.1, Ath3O.2, AW3S.2
 Harrington, James A. - SW3M.7
 Harrington, Kerianne - SM3D.4
 Harris, Gary - STu3F.6
 Harris, James S. - FM3M.7, STu3A.3
 Harrison, Erin - FW4H.4, JTh2A.50
 Hartelt, Michael - FTh3M.3
 Harter, Tobias - STu3D.4
 Harth, Anne - STh3N.2
 Hartin, Anthony - JTu2A.116
 Hartl, Ingmar - SF3N.1, STu3P.5, STu4O.5
 Hartmann, Jean-Michel - FTh1E.5, FTu3E.2
 Hartmann, Nicolai F. - FW4H.8
 Hartung, Alexander - SF1K.5
 Harvey, Clarissa M. - SW3K.2
 Hasan, Tawfique - JTh2A.82, JTh2A.83, SF3I.4, SF3K.2
 Hase, Eiji - STh3L.3
 Hasegawa, Takemi - SF2K.3
 Hashemi Rafsanjani, Seyed Mohammad - JTh2A.19, JTh2A.4
 Hashemi, Hossein - JW2A.15, JW2A.70
 Hashimoto, Kazuki - STu4P.6
 Hashimoto, Toshikazu - SF1J.3, SM1C.4
 Hasman, Erez - FTh3M.1, FTh4J.8, FTu3E.5, SF1J.6
 Hassan, Absar U. - FM4E.5, FTh4E.2
 Hata, Masanori - FF2L.4
 Hata, Yuya - STu4K.4
 Hatami, Fariba - FM1H.2
 Hatsuda, Ranko - SF1G.3
 Haub, John - SM4N.3
 Hauf, Christoph - FM4F.4
 Haung, YiKai - JTh2A.171
 Haus, Joseph W. - JTh2A.71, JW2A.105
 Hausmaninger, Thomas - STu3P.4
 Havelund, Jesper F. - AM3P.5
 Haw, Jing Yan - FTu3G.2
 Hawkins, Aaron - JTh2A.101, JW2A.24
 Hawkins, Peter G. - FM3F.1
 Hawkins, Thomas - FF2H.1, SF3I.6, SM3D.5, STu3K.6
 Hawthorn, D.G. - FM1F.7
 Hayasaka, Natsuki - JTu2A.12
 Hayashi, Kesuke - JTu2A.92
 Hayashi, Neisei - SM3K.2
 Hayashi, Noriyoshi - STh4K.4
 Hayat, Alex - FM2F.1
 Hayden, Brian E. - FTh4H.6
 Hayden, Jakob - STu3N.2, STu3N.6
 Hayenga, William - FM2G.5, SW4Q.1, SW4Q.5
 Hayhurst Appel, Martin - Ath3H.1
 He, Bo - JTu2A.95
 He, Dong - JW2A.172
 He, Hongwei - JTu2A.54
 He, Liang - STu4O.2
 He, Mingbo - JW2A.28, STu3B.2
 He, Susu - JTu2A.62
 He, Xiaowei - FW4H.8
 He, Xuan - JTu2A.43, SW3C.2
 He, Yang - FF2E.5, JTu2A.79, JW2A.64, SF2A.3
 He, Yiming - JW2A.62
 He, Ying - JW2A.177, JW2A.178
 He, Yongqi - JTh2A.113
 He, Yu - SW4C.2
 He, Yunxiao - FM3M.3
 He, Zhigang - JW2A.138
 He, Zuyuan - JTh2A.124, JTh2A.187, JW2A.145, JW2A.173, SM3K.4, STh4B.2, STu4K.2
 Head, Robin - Ath4Q.2
 Headley, Clifford - SW4K.4
 Heath, Daniel - JTh2A.177, SM1O.4, SM4O.3
 Hebling, János - JTh2A.189, JTh2A.190, JTh2A.191, SM3A.2
 Heffernan, Brendan M. - SW4J.3
 Hegazy, Kareem - JF1C.3
 Hegmann, Frank A. - JM2A.2, JM2A.5, JW2A.122, SM3A.6, SW3D.1
 Hehlen, Markus - FF3E.1
 Heidari, Elham - SF3J.6
 Heideman, Rene - SW4C.5
 Heideman, René - JTh3D.2
 Heigl, Michael - FM4F.3
 Heilmann, Anke - SM2N.8
 Heimbrod, Wolfram - JW2A.135, JW2A.136
 Heinrich, Alexander-Cornelius - FF3P.7
 Heinz, Tony F. - FF3P.2
 Hejazi, Sahar - JTh2A.45
 Helgason, Óskar B. - JW2A.71, STu3F.1
 Helm, Manfred - JM2A.3
 Helmrich, Sophia - FF3D.2
 Hemmer, Michael - SM4A.4
 Hemming, Alexander - SM4N.3
 Hempler, Nils - Ath4Q.2
 Hen, Mirit - JTu2A.63
 Hendon, Christine - STh1J.4
 Hendrickson, Josh - JTu2A.6, JW2A.105
 Hendrie, James - FTh1M.2
 Hendry, Ian - JTu2A.137
 Heng, Xiaobo - SW3K.3
 Hengster, Julia - JTu2A.157
 Heni, Wolfgang - FTh4H.1, SM1I.4, SM2I.3, SM4B.1
 Henrad, Luc - SM1O.1
 Henriksson, Johannes - SF1A.4, STu4B.1
 Henry, Didier - STu3N.7
 Henry, Nathan C. - SF3G.4
 Hens, Zeger - SW4I.4
 Hensley, Joel M. - STu3N.1
 Her, Tsing-Hua - JTu2A.4, SM4O
 Herbers, Sofia - SM1L.6
 Herd, Jeffrey - SM3I.1
 Herdzik, Krzysztof P. - ATu3S.3
 Herkommer, Clemens - FF2E.4, STh4A.4, SW3A.8

- Herman, Daniel I. - STh1L.2
 Hernandez Garcia, Juan - Ath4O.7
 Hernandez Salvador, Antonio-Andres - FM4F.4
 Hernandez-Cordero, Juan - FTh4E.5
 Hernandez-Garcia, Carlos - AW4O.2
 Hernández-García, Joel A. - FTh4E.5
 Hernandez-Gomez, Cristina - JTu2A.170, STu4O.6
 Herrick, Robert - SW3Q.2
 Herrington, Simon - AF2M.3
 Herrmann, Harald - FF1B.8, FM1G.3
 Hersam, Mark C. - STu4N.4
 Herskind, Morten - STh3A.6
 Herzog Sheinfux, Hanan - FF2H.2, FM2Q.5
 Herzog, Bastian - FF3D.2
 Herzog, Joseph - AF3M.4
 Heshmat, Barmak - AF3Q.4
 Hess, Ortwin - FM3E.6
 Hestroffer, Karine - FM1H.2
 Hettel, W. - FM1F.7
 Heu, Paula - JTu2A.14, SM3L.6
 Heuck, Mikkel - JTh4C.4, STh3G.3
 Heuermann, Tobias - SF1N.7
 Heyes, Jane E. - FTu3G.5
 Heyl, Christoph - STh3N.2
 Hibino, Hiroki - JTu2A.153
 Hickstein, Dan - FF2E.4, FF2E.6, SW4L.2
 Hickstein, Daniel - SF2A.5, SM4L.1, STu3F.5
 Hieta, Tuomas - Ath1O.8
 Higashi, Yasuhiro - JTu2A.165, SW4D.5
 High, Alexander - FM3H.3
 Hill, Elizabeth - SM1N.7
 Hill, Wendell - FF1P.3
 Hillerkuss, David - SM11.4
 Himmelhuber, Roland - JW2A.41
 Hines, Glenn D. - AW3R.3
 Hinkov, Borislav - SF2G.2
 Hinsdale, Taylor - JTu3L.2
 Hinz, Christopher - FF3D.5
 Hiraoka, Tomoki - SW3D.6
 Hirori, Hideki - FTh1H.1
 Hirose, Kazuyoshi - SF1G.4, SF1G.5
 Hisai, Yusuke - JTh2A.32, JW2A.159
 Hitachi, Kenichi - SM4L.5
 Hitaka, Masahiro - SF3G.7
 Hlaing, May - Ath4P.5
 Ho, Daryl - AM2M.2, JTh2A.129, STu3K.5
 Ho, Kai-Ming - FF2D.5, FM1F.6
 Ho, Wen-Jeng - AW3O.1
 Ho, Zeuku - SM31.4
 Hoa, Nguyen Phuoc Trung - JTu2A.126, JTu2A.143
 Hoang, Thai M. - FF3F.1
 Hobbs, Richard - FF3D.4, FTh1K.3
 Hodaiei, Hossein - FM2E.5, SW4Q.1
 Hoefler, Gloria - JTh2A.166, JTh2A.167, SM1B.1
 Hoekman, Marcel - JTh3D.2
 Hoenninger, Clemens - AM2M.4
 Hoff, Dominik - JTu2A.151
 Hoff, Ulrich B. - JTh2A.25
 Hoffman, Anthony - JW2A.96, SF21.7
 Hoffmann, Andreas - SF1K.5
 Hoffmann, Martin - SF2N.4
 Hoffmann, Matthias C. - JW2A.83, SM3A.1, SM4A.3, SM4A.5, SM4A.6
 Höfling, Sven - Ath3H.7, FM2F.1, SF2G.2
 Hofmann, Andreas - STh1A.1
 Hofmann, Stephan - FW3H.3, STu4D.5
 Hoghooghi, Nazanin - SW4L.7
 Høgstædt, Lasse - AW3S.4, SM4D.4
 Hohage, Thorsten - FM4F.1
 Holl, Mark R. - STu4Q.4
 Holland, Glenn - FF2F.1
 Hollinge, Reed - STu3M.1
 Holonyak, Jr., Nick - SW4Q.2
 Holtz, Marcel - FM4F.4
 Holzbauer, Martin - SF2G.2
 Holzrichter, John - AW3O.7
 Holzwarth, Ronald - JW2A.137, SM1L.5, SM2L.5, STu3P.2, STu4K.3, SW4L.1
 Hommelhoff, Peter - JF1C.1, JF2C.1
 Hon, Philip W. - FTh1P.3
 Honardoost, Amirmahdi - JTh2A.16, JTh3C.2, SM1B.2
 Hone, James - FTh1P.4, JW2A.135, JW2A.136, STu4N.7
 Hong, Feng-Lei - JTh2A.32, JW2A.159, STu3P.1
 Hong, Kang-Hee - JTh2A.1
 Hong, Kuo-Bin - JTu2A.9, SF11.4
 Hong, Kyung-Han - FM3M, JF1C.5, STu4O.4
 Hong, Minghui - SM3O.1
 Hong, Seongjin - JTh2A.152
 Hong, Soonki - JTh2A.109, SM1K.6
 Hong, Sukjoon - FW3H.6
 Hong, Xiaobin - JTh2A.118
 Hong, Yang - JTu2A.41
 Hong, Yu-Heng - SF11.4
 Honjo, Toshimori - JTu2A.87
 Hönl, Simon - STh31.6, SW3A.1
 Hood, Dana - SF21.4
 Hoogland, Heinar - STu3P.2
 Hooper, Lucy - ATu3S.4
 Hoose, Tobias - STh1A.1
 Hooten, Sean M. - SM41.3, SM41.5
 Hoppe, Morten - Ath1O.6
 Horak, Peter - JTh2A.177, SM3D.5
 Horák, Tomáš - STu4D.7
 Hori, Atsuhiko - SW3A.7
 Horie, Yu - FF1F.5, SF1J.2
 Horng, Jason - AM4P.2, FF1D.2
 Hornig, Graham - JW2A.122
 Horodyski, Michael - FF3H.1
 Horoshko, Dmitri - JTh2A.20
 Horowitz, Jeffrey - FF2D.1
 Horstman, Luke - STh3N.7
 Horvath, Andrew - STu3C.7
 Hosaka, Kazumoto - JTh2A.32
 Hosako, Iwao - JW2A.155
 Hosoda, Takashi - SF2G.6
 Hosseini, Ehsan - ATu3R.2, SM31.7
 Hosseini, Seyedreza - SM3B.6
 Hosseinnia, Amir H. - JTh2A.78, SM11.1, SW4B.6
 Hossein-Zadeh, Mani - JW2A.148, JW2A.18
 Hou, Bin - SW4Q.7
 Hou, Dong - JTh2A.184, JW2A.144
 Hou, Guozhong - JW2A.130
 Hou, Lianping - SW4Q.7
 Hou, Yubin - JTh2A.112
 Houard, Aurélien - FM1Q.8
 Houdré, Romuald - JTh2A.99
 Houston, Jessica P. - JTh2A.103, STh3J.4
 Howe, R. - JTh2A.82, JTh2A.83, SF3K.2
 Hryciw, Aaron - FW4F.6
 Hsiao, Fu-Chun - SW3B.7
 Hsiao, Hui-Hsin - JTh2A.70
 Hsiao, Ya-Fen - JW2A.151
 Hsieh, Chieh - FW4G.4
 Hsu, An-Chia - JTh2A.170
 Hsu, Cheng-Wei - AM2M.3, JTu2A.131
 Hsu, Chia Wei - FF3H.2, FM2Q.3
 Hsu, Hsun-Yuan - JW2A.176
 Hsu, Liyi - FTh4J.7, JW2A.97
 Hsu, Ming-Yang - JTu2A.25
 Hsu, Ning - FTh1M.2, STh3N.7
 Hsu, Shih-Hsiang - JW2A.176
 Hsu, Shun Chieh - JTh2A.89, SW3B.7
 Hsu, Ting Way - AM2J.4
 Hsu, Ting-Wei - AM2J.6
 Hsu, Yu-Hsiang - AF2M.2
 Hsu, Yung - JTu2A.39, JTu2A.58
 Htoon, Han - FTh1F.7, FW4H.8, JTh3C.6
 Hu, Anming - FTu3H.4
 Hu, Bo - STh3K.2
 Hu, Guohua - JTh2A.82, JTh2A.83, SF31.4, SF3K.2
 Hu, Haifeng - SF21.6, SW3J.6
 Hu, Han - SW4M.3
 Hu, Hao - STu3D.1
 Hu, Huiqin - FW4E.1
 Hu, Jianqi - JTh2A.93, SF3N.6, SM1C.1
 Hu, Jie - SM2C.1
 Hu, Jiuning - FM3H.2
 Hu, Jonathan - JW2A.179
 Hu, Juejun - AW3O.3, SF1A.1, SM21.8
 Hu, Minglie - JTh2A.128, SW4K.1
 Hu, Ming-lie - JTh2A.156
 Hu, Nan - FW3F.1
 Hu, Qing - Ath4Q.5, STu4D.2
 Hu, Sheng - FF2L.7
 Hu, Walter - AF1Q.6
 Hu, Xiaolong - FW3F.1, JTu2A.138
 Hu, Xiaonan - FM3E.6
 Hu, Yaowen - SM11.7
 Hu, Yi - FTh1M.7, JTu2A.139
 Hu, Yi-Wen - JW2A.65
 Hu, Yuwei - JTh2A.82, JTh2A.83, SF31.4, SF3K.2
 Hu, Zhouyi - JTu2A.41, SM4B.4
 Hua, Jianfei - FM3M.3
 Hua, Yi - JTh2A.162, SM4A.4
 Huang, Bo-Zhi - JW2A.37
 Huang, Chen-Bin - FW3G.2
 Huang, Cheng-Yi - JTu2A.40
 Huang, Chia-Yen - JTu2A.9
 Huang, Chien Y. - AW3O.2
 Huang, Chung-Ping - JTh2A.89, SW3B.7
 Huang, Chun-Ying - JTh2A.171
 Huang, Dajie - JTu2A.163
 Huang, Duan - JTh2A.13
 Huang, Duanni - AF1Q.2, JW2A.66
 Huang, Gang - SM4M.6
 Huang, Hao - SM2C.4
 Huang, Haoyu - FM3F.3
 Huang, Hsin-Yi - Ath3Q.4
 Huang, Jer-Shing - FW3G.2
 Huang, Jiahui - FTh1F.7, SW31.4
 Huang, Jian - STh41.5
 Huang, Jianguo - AM4P.5, FM1G.2, JTh2A.18
 Huang, Jian-Jang - JTu2A.40
 Huang, Kai-Feng - SF31.8
 Huang, Ke - JW2A.148
 Huang, Kuang-Hsu - JW2A.34, JW2A.44
 Huang, Lei - AF1Q.4
 Huang, Li - JW2A.84
 Huang, Meng - STh1B.5
 Huang, Nien-Tsu - ATu3J.4, SW3J
 Huang, Qingqing - SM4C.2
 Huang, Quandong - STh1A.2
 Huang, Sheng - Ath3P.4, FM3Q.2
 Huang, Sheng Lung - AM2J.4, AM2J.6, JTu2A.100
 Huang, Shihong - JTh2A.108
 Huang, Shu-Wei - FTh1E.3, JTu2A.56, STh3F, SW3A.3, SW4L.3
 Huang, Tingrui - JTu2A.163
 Huang, Wenfa - JTu2A.163
 Huang, Wenzhuo - STu4N.3
 Huang, Xiaosheng - AF1M.3, JTh2A.147, STu3K.5
 Huang, Xiatao - JTu2A.56, STh1C.2
 Huang, Xinyu - JW2A.126
 Huang, Xuettian - JTu2A.44
 Huang, Yao-Wei - AM1J.6, FTh3M.5, JW2A.101
 Huang, Yen-Chieh - JW2A.78
 Huang, Yidong - JW2A.48, SM41.4
 Huang, Yiping - JTu2A.173
 Huang, Yishen - STh3B.6
 Huang, Yongqing - JW2A.7
 Huang, Yuan-Fu - JTh2A.88
 HUANG, YUE - FF2D.2
 Huang, Yue-Kai - SW3C
 Huang, Yu-Ming - JTh2A.89, SW3B.7
 Huang, Yusheng - AM2M.5
 Huang, Zhengyu - JW2A.21
 Huang, Zhihong - SM21, SW4A
 Huang, Zhilei - STu4B.1
 Huang, Zhimeng - SW4K.5
 Huang, Zhirong - JF1C.3, JF2C.3
 Huang, Zongyuan - SM2C.1
 Huber, Andreas - FTh1K.4, SW3D.2
 Huber, Rupert - FM3F.1, FM4F, JM2A.4
 Huber, Tobias - FM3H.2, FTu3H.2, SM1O.6
 Hübner, René - JM2A.3
 Huck, Alexander - JF3B.2
 Hudgings, Janice A. - AF2M.7
 Hudl, Matthias - JW2A.83
 Hudson, Darren - STh4K.1
 Hudspeth, Quentin - JTu3O.6, JTu3O.7
 Huet, Vincent - SM41.7
 Huffman, Grant - FW3E.3
 Huffman, Taran - FW3E.3
 Hughes, Taylor L. - FM2Q.2
 Hui, Rongqing - JTu2A.35, JW2A.147
 Hummon, Matthew - SM3L.5
 Hung, Yung-Jr - JW2A.20, JW2A.26, JW2A.38
 Huntington, Elanor - FTh4G.6, FTu4G.3
 Huo, Li - JTu2A.103, JTu2A.99
 Huo, Nan - JF2B.4
 Huo, Yijie - STu3A.3
 Huo, Yuandong - SM1D.3
 Huot, Laurent - AW3S.4
 Husain, Muhammad K. - SM3B.5
 Hussain, Mallik Mohd Raihan - JTh2A.71
 Hussain, Syed - JTh2A.179, SF3K.6
 Hutchins, Romanus - AM3P.3
 Huttner, Ulrich - FM3F.1
 Huyen, Jaroslav - JTu4O.6
 Hyeon, Min Gyu - JTu2A.94
- I
- Iakovlev, Vladimir - JTu2A.10
 Ichijo, Mitsuki - SM4O.4
 Ichimiya, Masayoshi - JW2A.127
 Ideguchi, Takuro - STu4P.6
 Idjadi, Mohamad Hossein - SM3L.2
 Ido, Tetsuya - SM1L.1
 Iftimia, Nicusor - JW3P.3
 Iguchi, Tetsuo - STh4K.4
 Ihn, Yong Sup - FM4G.5
 Ikeda, Kazuhiro - STu3Q.2
 Ikeo, Toshiyuki - JTu2A.165, SW4D.5
 Ikuta, Takuya - JTu2A.87
 Ilday, F. Ömer - SF2N.4
 Ilev, Ilko - AM1J, AM4P, ATu4J
 Ilic, B. Robert - FF2F.1
 Ilic, Ognjen - FF1H.6, FF2F
 Ili, James S. - ATu4M.1
 Imai, Yuuki - JW2A.50
 Imany, Poolad - FM4G.2, FM4G.3
 Imasaka, Tataro - JTh2A.164, SW4N.2
 In, Chihun - FM1F.1, JTh2A.172
 Inaba, Hajime - JTh2A.123, JTh2A.32, STu3P.1
 Inaba, Kensuke - JTu2A.87
 Inagaki, Takahiro - FTu4A.2, JTu2A.87
 Inga, Marvyn - JTu2A.111
 Ingold, Kirk A. - AW4O.3
 Inoue, Daisuke - FM3J.7
 Inoue, Shuichiro - FW4F.8
 Inubushi, Masanobu - SM1C.4
 Ioannou, Marie - FF3E.5
 Ippen, Erich - SM3L.1
 Isaac, Brandon - JTh3D.5
 Isaac, Samantha D. - JTh2A.34
 Ischebeck, Rasmus - FW4H.7
 Ishaaya, Amiel - STu3K.5
 Ishihara, Hajime - JW2A.127
 Ishihara, Tohru - JW2A.50
 Ishii, Hirotaka - STu4K.1, STu4K.6
 Ishii, Nobuhisa - FF2P.4, FM3M.6, JTu2A.154, STh4N.6, SW3N.7
 Ishii, Satoshi - FF2F.8, JTh2A.87
 Ishikawa, Atsushi - FM3J.7
 Ishikawa, Jun - STu3P.1
 Ishikawa, Yuya - JTu2A.104
 Ishiwata, Hitoshi - JTh3C.5
 Ishizaki, Kenji - SF1G.3
 Ishizawa, Atsushi - SM4L.5
 Ishizuki, Hideki - FF1E.3
 ISLAM, NURUL T. - FTu3G.3, FW3F.2, JTh2A.8
 Itatani, Jiro - FF2P.4, FM3M.6, JTu2A.154, STh4N.6, SW3N.7
 Ito, Akio - SF3G.7

- Ito, Hiroyuki - SM2B.5
Ito, Masamichi - STu4Q.2
Iwamoto, Satoshi - FM1H.5, SF1A.7, STh3A.4
Izumura, Hideyuki - STu3P.1
- J
- Jackson, James - JW2A.182
Jackson, Stuart D. - STh4K.1, STh4K.3
Jackson, Stuart D. - SM2K
Jacob, Zubin - FTu3E, FTu3E.4, STh4A.1
Jacobs, John - SF1A.4, STu4B.1
Jacobsen, Gunnar - JW2A.31, SM2C.5, SM4C.4, SM4C.5, STu3D.1
Jacqmin, Hermance - JTh2A.120
Jadidi, M. Mehdi - SF2I.5
Jaeggi, Beat - AM1M.3
Jafari, Rana - JTh2A.142, JTh2A.150
Jagdish, Chennupati - JTh2A.51
Jahanbakhsh, Amir - AM1M.5
Jahani, Saman - STh4A.1
Jahromi, Khalil E. - Ath3O.2
Jaimes-Nájera, Alfonso I. - SW3M.1
Jain, Ayush - STh4L.2
Jain, Deepak - JTu2A.109
Jain, Gaurav - JTu2A.26
Jain, Ravinder K. - JW2A.18
Jalal, Shadia - ATu4J.6
Jalali, Bahram - AF2Q.5, AF3Q.1, SM4D.5, STh3J.3, STh3L.1
Jalas, Sören - JTu2A.171
Jallageas, Antoine - Ath3O.6
Jambunathan, Venkatesan - STu4O.6
James, Daniel - FTu4A.3
jamshidi, kambiz - SM3B.6
Jan, Catherine - SW3Q.2
Jang, Dogeun - JTh2A.145
Jang, Dong-Hoon - JTu2A.23
Jang, Hoon - JW2A.82
Jang, Jae K. - FTh1E.4, SW3A.4
Jang, Sun-Joo - SW3J.4
Jang, Woosun - FF2D.4, FM1F.1
Janjua, Bilal - JTu2A.91
Jankovic, Vladan - FTh1P.3
Jansen, Matthijs - STh3N.4
Janta-Polczynski, Alexander - STh4B.8
Jaouen, Yves - STu4C.3
Jaramillo-Villegas, José - SF2A.6
Jargot, Gaëtan - JTu2A.150
Jarrahi, Mona - FF1E, FTh4H.3, SM2K.1, SW4D.2
Jarzynski, Christopher - FF3F.1
Jaspere, Martijn - JF3B.5
Jauregui, Daniel - Ath4O.7
Jauregui, Luis - FTh1K.6
Javadi, Alisa - Ath3H.1, FM1H.7
Javaloyes, Julien - JTu2A.137
Javey, Ali - STu4N.6, SW3I.4
Javid, Usman - FTh4G.4
Jayakumar, Harishankar - FTu4H.1
Jayakumar, Nikhil - SF1K.5
Jazbinsek, Mojca - JW2A.81
Jelic, Vedran - JM2A.2, JW2A.122, SW3D.1
Jen, Alex K. - JTu2A.147
Jenkins, Alec - JF2B.1
Jennings, Brian D. - FTh1K.3, JTh2A.90
Jensen, Ole B. - AF1Q.1
Jeon, Chan-Gi - SM4L.4, SW3L.2
Jeon, Cheonha - JTu2A.140
Jeon, Jinwoo - JTu2A.51
Jeong, Mi-Yun - JTh2A.192
Jeong, Young-Gyun - JW2A.81, SM4M.3, SW3N.2
Jere, Malhar - FTh1G.4
Jerop, Nelly - FF2F.2
Jestin, Yoann - FF1E.1
Jha, Anand - FW4F.7
Ji, Dengxin - SF2I.6, SW3J.6
Ji, Haojie - FF3F.6
Ji, Junhua - JTh2A.129, STu3K.5
Ji, Wei - JTu2A.115
- Ji, Xingchen - Ath3Q.1, JTu2A.72, SM1D.6, SM3D.1, SM4L.7, STh1A.4, STh1J.4, SW3A.4, SW4M.5
Ji, Yaping - JW2A.109
Ji, Yuefeng - JTh2A.195, JTu2A.36
Jia, Baohua - SM1I.2, STu3F.7
Jia, Hao - JW2A.14, SW4C.6
Jia, Shi - STu3D.1
Jia, Shuang - FF1D.7
Jia, Xiaojun - FM4H.7, FTu3G.2
Jian, Meng-Syuan - JW2A.176
Jian, Pu - FW4F.5, JTh2A.15
Jiang, Chang-Ming - FF1P.4
Jiang, Chen - SM2K.2
Jiang, Desheng - JW2A.174
Jiang, Haitao - FM4Q.1
Jiang, Haowei - FF2E.5, SF2A.3, STu3F.3
Jiang, Hexin - JTu2A.54
Jiang, Hongbing - FM1Q.8
Jiang, Jiali - JTh2A.91
jiang, jiang - SF2G.6
Jiang, Jiaqi - FF3C.1, STh1J.5
Jiang, Jie - JTh2A.185
Jiang, Jing - FF2L.6
Jiang, Lei - JTh2A.91, SF3I.1
Jiang, Lin - JTu2A.48
Jiang, min - FF3F.5
Jiang, Qing - JTu2A.178
Jiang, Suhua - SF2I.6, SW3J.6
Jiang, Wei - SM3I, STh4A.3
Jiang, Xiao - STu3A.3
Jiang, Xin - SF3J.1
Jiang, Yifan - SF3G.7
Jiang, Yunshan - SM4D.5
Jie, Jiansheng - SF1I.6
Jimenez Galindo, Alvaro - JTu2A.162
Jimenez, Alvaro - Ath3O.5
Jimenez, Oscar - STh4B.7
Jin, Chao - SM3K.3
Jin, Gangtae - SW3I.3
Jin, Jing - AF1M.2, JTh2A.174
Jin, Kui - FF2D.2
Jin, Lei - JTh2A.121, STh4K.4, STu4K.5
Jin, Mingzhou - JTh2A.72
Jin, Qi - SM4A.1
Jin, Wei - Ath1O.3, STh1A.2
Jin, Xianmin - FM1G.2, JTh2A.18
Jin, Xinxin - JTh2A.82, JTh2A.83, SF3I.4, SF3K.2
Jin, Yuan - SF3G.6
Jin, Zhengtao - STh3B.5
Jin, Zhiqiang - AM4P.7
Jin, Zuanming - FF2D.1
Jing, Feng - JTh2A.91, SF3I.1
Jing, Jietai - JTh2A.11
Jo, Hanlae - FM2H.7, JTh2A.29
Jo, Javier A. - JTu3L.2
Jo, Minsik - FF2F.7
Jo, Moon-Ho - FF1D.8, FF2D.4, FM1F.1, FTh1F.1, JTh2A.172, JW2A.134, SW3I.3
Joannopoulos, John - FF2L.3, FF2L.5, FM2Q.3, FM3H.5, FM4J.6, FM4J.8, FTu4E.1, FW4G.2, JF1C.5, SM2O.6
Jobe, R. Keith - SM3A.1
Jochim, Bethany - JW2A.182
Jochmann, Axel - STu3M.2
Joe, Graham - AF3M.7
Johansson, Alexandra C. - JW2A.165, STu3P.4, STu3P.6
John, Robert - JTh3C.4
John-Herpin, Aurelian - FF2F.7
Johns, Paul - SM2O.1
Johnson, A. T. Charlie - STu4N.3
Johnson, Adrea R. - SM4L.7
Johnson, Eric G. - SW3M.7
Johnson, Matthew T. - SF2A.7
Johnson, Steven - FTh1K.5, FW3F.7, FW4G.2
Johnston, Eric - JW2A.139
Johnston, Peter - FF3P.4
Jojart, Kyle - SM4N.7
Jolly, Spencer W. - FF1E.3, JTu2A.171
- Joly, Nicolas Y. - FW4E.7
Jones, Alexander - FTh1H.4
Jones, Daniel E. - FTu3G.7
Jones, Rasmus Thomas - STh1C.3
Jornod, Nayara - SM4L.6
Joseph, Hodges - STu3N.5
Joshi, Abhai - SM2L.5
Joshi, Chaitali - FM3G.2, FM3G.5
Joshi, Chaitanya - SW4M.5
Joshi, Chan - FM3M.3, FM3M.4, JF1C.4
Joshi, Siddarth - JW2A.139
Jost, John - STh4B.6
Josten, Arne - FTh4H.1, JTh4D.5, SM1I.4, SM2I.3, SM4B.1
Jouini, Jenny - SM3L.3, SM3L.4
Jouy, Pierre - SF3G.2
Jovanovic, Igor - FM1Q.4, SF1N, SM3O.6
Ju, Yiguang - Ath3P.1
Juhl, Michael - SF1J.8
Jukić, Dario - FTh1H.7
Jullien, Aurelie - STu3M.4
Jun, xu - SF2N.1
Jung, Daehwan - SM2I.6, SW3B.1, SW3Q.2, SW3Q.3, SW4I.3
Jung, Hojoong - SF2A.5
Jung, Hyunseung - FF2D.4, FM1F.1, FM3J.8
Jung, Jisung - JTh2A.1
Jung, Minhyoung - JTu2A.96
Jung, Minwoo - AW4O.4, FF2L.2
Jung, Sangyoon - JTu2A.96
Jung, Seungyong - SF2G.5, SF3G, SF3G.7
Jung, Yongduck - STh4I.6
Jung, Yongmin - ATu3S.3
Juodawlkis, Paul W. - JTh3D.4, SM3I.1, SW4B.5
Justice, John - STh4B.1
- K
- Kacmoli, Sara - AF1Q.3
Kaderiya, Balram - JW2A.182
Kadláček, Jiri - Ath3O.1
Kadochkin, Aleksei S. - JTh2A.57
Kadoya, Hiroki - JTu2A.92
Kaenders, Wilhelm - AM1P, AM2P
Kaertner, Franz X. - AM1J.2, FF1E.3, FF3D.4, FF3P.5, FM3F.3, FW4E.4, JF1C.5, JTh2A.140, JTh2A.162, JTu2A.116, JTu2A.157, JW2A.138, SF1N.6, SF3N.5, SM3L.1, SM4A.2, SM4A.4, SM4K.4, STh1N.1, SW3N.1
Kagalwala, Kumel - JTh2A.39
Kagami, Hibiki - JW2A.92
Kaganovskii, Yuri - JTu2A.63
Kahn, Joseph - ATu4J.5, FW3E.4
Kaindl, Robert - FF1D.1, FM1F, FM1F.7
Kaksis, Edgar - FM3M.2, SF1N.3, SM4M.1
Kakuda, Masahiro - FM1H.5
Kalashnikov, Dmitry - Ath3O.3
Kalashnikov, Mikhail - SM1N.8, SM4N.7, STu3M.3
Kalchenko, Vyacheslav - JTu2A.102
Kalhor, Farid - STh4A.1
Kamada, Naoki - JTu2A.12
Kamali, Seyedeh Mahsa - AF3M.3, FF1F.5, SF1J.2
Kamandi, Mohammad - FTh1K.1, FTh1K.2, JTh2A.68
Kambe, Eiji - STu3P.1
Kamboj, Varun - FW3H.3
Kamel, Ayman N. - JTu2A.120
Kaminer, Ido - FF1E.5, FF2L.3, FF2L.5, FF2L.6, FM1Q.3, FM1Q.6, FM2G.2, FM3H.5, FM4J.6, FM4J.8, FTu4E.1, FW4G.2, FW4H.1, FW4H.3, FW4H.7, JF1C.5, SM2O.6, SM4I.2, STh1N.4
Kamins, Theodore I. - STu3A.3
Kaminski, Pawel M. - STu4C.1, STu4C.6
Kamperidis, Christos - STu3M.3
Kanai, Teruto - FF2P.4, FM3M.6, JTu2A.154, STh4N.6, SW3N.7
Kananen, Thomas M. - JW2A.36, SM2B.4
Kanzawa, Toru - FM3J.7
- Kanda, Natsuki - JW2A.80
Kane, Daniel J. - JTh2A.161
Kaneshima, Keisuke - FF1P.6, FM3M.6, JTu2A.152
Kanetake, Tomoki - JTu2A.92
Kang, Donghyun - JTu2A.96
Kang, Jin ho - SW3I.4
Kang, Jin U. - JTu2A.106
Kang, Jiqiang - AF3Q.5, JTh2A.126, JTh2A.148, SW4J.5
Kang, Moon Sung - FM3J.8
Kang, Songbai - FW3E.5
Kang, Yuhao - FM4Q.2
Kang, Zhe - JW2A.4, SW4M.4
Kaniber, Michael - JTu2A.8, SW3B.6
Kannari, Fumihiko - SM1N.6
Kannegulla, Akash - ATu3J.2, JW2A.91
Kanno, Atsushi - STh4B.5
Kante, Bouacar - FM4Q.8, FTh4J.7, JTh2A.47, JW2A.97
Kantola, Emmi L. - JTu2A.10, JTu2A.17
Kao, Hsuan-Yun - JTu2A.40
Kao, Ming-Hsuan - AW3O.2
Kao, Tsung-Sheng - SF1I.4
Kao, Yu-Chiu - Ath3Q.6
Kapraun, Jonas - STu3Q.3, STu3Q.5
Kapsalidis, Filippos - STh1L.5
Kapteyn, Henry - AW4O.2, FF2E.4
Kar, Ajoy K. - JTu2A.115, SM3D.2
KARA, OGUZHAN - Ath4O.6, STh1L.4
Karademir, Ertugrul - JTh2A.90
Karagiannidis, Panagiotis - STu4D.6
Karim, Faisal - STu3P.3
Karim, Md Rezaul - STh3I.2
Karim, Muhammad F. - Ath4O.4, JW2A.54
Karki, Dolendra - SF3J.3
Karlsson, Jenny - FTu4H.7
Karlsson, Magnus - JW2A.149, SM4C.3
Karni, Ouri - FTh1H.6
Karnieli, Aviv - FTh1H.2
Karpf, Sebastian - AF2Q.5, STh3J.3
Karpov, Maxim - FTh1E.6, SM1D.2, SW3A.5
Kartashov, Danil - FM1Q.2
Kase, Kiwamu - ATu3I.6
Kashiwagi, Ken - JTh2A.123, STu3P.1
Kasparian, Jerome - Ath1O.2
Kaspi, Ron - JTu2A.19, JTu2A.27
Kassi, Samir - Ath3O.4
Kataoka, Shunji - JTu2A.92
Kataura, Hiromichi - FM2F.7, JTh2A.121, STu4K.5
Katayama, Ikufumi - FF2D.1, JM2A.1, SM3A.5
Katayama, Nobu - JW2A.77
Kato, Keiko - JTu2A.153
Kato, Shusuke - STh4K.4
Kato, Takashi - STh3L.6
Kats, Mikhail - AF3M.7, JW2A.121
Katsumi, Ryota - FM1H.5, SF1A.7, STh3A.4
Katsuragawa, Masayuki - FW4E.6, JTh2A.159, SF3N.3
Katumba, Andrew - STh3I.7
Katzman, Moshe - JTu2A.63, SF2A.4
Kauffmann, Paul - JTu2A.72
Kauranen, Martti - FF1E.6, FF1F, FW3G.3, JTu2A.134
Kaviani, Hamidreza - FW4F.6
Kavokin, Alexey - JW2A.113
Kawanishi, Tetsuya - STh4B.5
Kawasaki, Masato - SF1G.3
Kawata, Yoshimasa - JTh2A.63
Kawato, Sakae - JTu2A.92
Kawayama, Iwao - SW3D.4
Kayes, Md Imrul - SW4L.6
Kazakov, Dmitry - FW3E.6
Kazansky, Peter - FM4G.7, FM4G.8
Kazemi Jahromi, Ali - Ath3P.6, FM4E.4
Kazi, Mohiyuddin - SM4B.6
Keams, Jared - SF1G.7
Keathley, Phillip D. - FF3D.4
Keeler, Gordon A. - FTh4J.4, FW3G.1, FW4H.8
Keene, David - FF2F.2

- Kehr, Susanne - JM2A.3
 Keilmann, Fritz - JM1A.4
 Kelaita, Youisif - FTu3H.5, JTh3C.5
 Kelleher, Stephen - STh4B.1
 Keller, Ursula - Ath3O.6, JW2A.157, SF1G.2, SF2N.6, SF2N.7, SM3N.5, SM4L.7
 Kelly, Trevor S. - FF3F.4
 Kelsey, Adam - SM3I.7
 Kemal, Juned N. - SM3B.1, SM3B.3, STu3D.4
 Kemiche, Malik - STh3A.5
 Keneth, Orian - FTh1P.2
 Kennard, Jake - FTh1G.7
 Kennedy, MJ - AF1Q.2, SM2I.6, STu3F.5
 Kentaro, Nakamura - SM3K.2
 Kepecs, Adam - Ath3Q.1
 Kerdiles, Sébastien - JTu2A.120
 Kern, Dieter - FW3G.3
 Kerst, Thomas H. - Ath4O.8
 Ketzaki, Dimitra - JW2A.5
 Keyvaninia, Shahram - STu3B.4
 Kfir, Ofer - FM4F.3
 Khachatrian, Ani - JTh2A.175
 Khachaturian, Aroutin - SM3B.6, STu4B.6
 Khader, Isaac - SM1L.3
 Khaidarov, Egor - FTh4J.5
 Khajavikhan, Mercedeh - FM1E.2, FM2E.3, FM2E.5, FM2G.5, FM4E.3, FM4E.5, FM4E.7, JTu2A.86, SW4Q.1, SW4Q.5
 Khalkenkov, Dmitry - AM1J.3
 Khalil, Diaa - AW4O.7
 Khalil, Mostafa - JTu2A.46
 Khan, Faisal Nadeem - STh1C.3
 Khan, Mohammad A. - Ath4P.5
 Khan, Mohammad W. - JW2A.175
 Khan, Mohammed - JTu2A.29
 Khan, Mohammed Zahed - JTu2A.34
 Khan, Muhammed Talal - JTu2A.34
 Khan, Saeed - STu3F.4
 Khan, Sikandar - SM1I.5
 Khanal, Sudeep - JTu2A.24
 Khanikaev, Alexander B. - FM3Q.6, FM4Q.2, FTh3M.2, JW2A.87
 Khanolkar, Arney - SF3A.6
 Khanolkar, Ankita N. - JTh2A.111
 Khanonkin, Igor - FTh1H.6
 Kharas, Dave - JTh3D.4, SM3I.1, SW4B.5
 Kharel, Prashanta - SM1I.8, SM1O.2
 Kharitonov, Svyatoslav - JTh2A.93
 Khatana, Sunil - SM2C.4
 Khater, Marwan - STh1B.2
 KHATONIAN, MANDEEP - FF1D.6, SM2O.7
 Kheifets, Simon - FF3E.6
 Khilo, Anatol - JW2A.59, SF1A.5
 Khmaladze, Jarji - FM1F.5
 Khodabakhsh, Amir - Ath3O.2
 Khodakovskiy, Nikita - SM1N.8
 Khokhar, Ali Z. - SM3B.5, STh1I.3
 Khomenko, Anton - JTh2A.117
 Khorasaninejad, Mohammadreza - AM1J.6, FTh3M.5, JW2A.101
 Khoshnagar, Milad - FTu3H.2
 Khurgin, Jacob - Ath1Q.4, FF2F.5, FTh4H.2, FW4G.3, SF3G.4
 Kiarashi Nejad, Yashar - SF1J.1
 Kiasat, Yasaman - JW2A.90
 Kibler, Bertrand - SW3K.6
 Kiefer, Daniel - JTh2A.136
 Kielpinski, David - STh3B.2
 Kieninger, Clemens - SM3B.1, SM3B.3
 Kieu, Khanh Q. - SM1K.2, SM2K.1, STh4K.6
 Kifle, Esrom - SM2N.6
 Kilbane, Deirdre - FTh3M.3
 Kildishev, Alexander - FM2G.7, FM4J.7, FTh1K.8, FTh4J.1, FTh4M.2, JTh2A.87
 Kim, Beom - FM1F.1, JTh2A.172
 Kim, Beop-Min - JTu2A.105, JTu2A.94
 Kim, Bok Young - FM3G.5
 Kim, Changsu - FTh1H.1
 Kim, Chang-won - JTh2A.176
 Kim, Chul Soo - SF2G.1, STh1B.7, STu3N.1
 Kim, Daeh - STh4I.6
 Kim, Dohun - FM1F.1, FM1F.2, FTh1F.1, JTh2A.172, SW3I.3
 Kim, Do-Hwi - JTh2A.176
 Kim, Dohyun - SF3K.5
 Kim, Donggyu - STh3L.4
 Kim, Dong-Hwi - JW2A.134
 Kim, Gwangmook - JW2A.134
 Kim, Hee-Yong - FF2P.5
 Kim, Hoil - FM1F.2, FTh1F.1, SW3I.3
 Kim, Hyewon - JM1A.1
 Kim, Hyun Myung - Ath3P.5
 Kim, Hyungjin - SW3I.4
 Kim, Hyung-Jin - JTu2A.94
 Kim, Jae Hyun - SF3G.7
 Kim, Jaeyoung - SF3J.2
 Kim, Jaehwan - JTu2A.7, SF3A.4
 Kim, Jehyun - FM1F.2, JTh2A.172, SW3I.3
 Kim, Je-hyun - FTh1F.1
 Kim, Jeyung - SW3B.2
 Kim, Jeongmin - FTh1D.5, SM4I.1
 Kim, Ji In - JTu2A.166
 Kim, Jin-Hun - FM4G.5
 Kim, Ji-Young - FTu4Q.2
 Kim, Jongbum - SM4D.7
 Kim, Jungsang - FTu3G.3, FW3F.2, JTh2A.8
 Kim, Jungwon - JTh2A.144, SF3K.5, SM3L.7, SM4L, SM4L.4, SW3L.2
 Kim, Junki - FM2H.5
 Kim, Junsung - FM1F.2, FTh1F.1, SW3I.3
 Kim, Kevin - STh1J.5
 Kim, Ki-joong - JTh2A.193, JW2A.168
 Kim, Ki-Yong - JTh2A.145, SM4A.7
 Kim, Kwangwoong - SM4B.3
 Kim, Kyungduk - FM3E.6
 Kim, Kyung-Jo - JW2A.41
 Kim, Mijin - SF2G.1
 Kim, Minji - JTu2A.94
 Kim, Philip - FTh1K.6
 Kim, Richard H. - FM1F.6
 Kim, Sangheon - JTu2A.96
 Kim, Sangsik - STh4A.1, SW4A.7
 Kim, Sejeong - SM1O.5
 Kim, Seong-Ryul - Ath3P.7
 Kim, Seung Kwan - SM2N.5
 Kim, Seungkyeum - AM1J.4
 Kim, Soo Jin - FW3H.2
 Kim, sunghwan - FF2F.7
 Kim, Taehwan - STh3L.7
 Kim, Tae-Kuk - JTh2A.176
 Kim, Taeyoung - FF1D.8, JW2A.134
 Kim, Won - SW3M.5
 Kim, Woohong - SF3I.3
 Kim, Yeji - STh4I.6
 Kim, Yeong Gyu - JTu2A.166
 Kim, Yeong Jae - Ath3P.5
 Kim, Yong-Su - FF1B.5, JTh2A.1
 Kim, Yoon-Ho - FF1B.5, FM4G.5, JTh2A.1
 Kim, Yosep - FF1B.5
 Kim, Young Duck - JW2A.135, JW2A.136
 Kim, Young L. - Ath3P.7, FM2G.7, JW2A.107
 Kim, Younghee - FW4H.8
 Kim, Young-Kyu - JTu2A.105
 Kim, Youngmin M. - JTh2A.35
 Kim, Yunjo - JTu2A.7
 Kimbrell, Eddie - STh4B.8
 Kindem, Jonathan - FTu4H.4, FTu4H.5, JTh3C.3, STh3G.2
 Kindness, Stephen J. - FW3H.3, STu4D.5
 Kinezuka, Yoshinori - SM4O.4
 Kinoshita, Takashi - JW2A.127
 Kinsey, Nathaniel - FTh4H.1, JTh2A.75, JTh2A.80, JTu2A.130
 Kippenberg, Tobias J. - Ath3H.6, FF2E.4, FF3E.5, FTh1E.6, JTh4D.3, SF2A.2, SM1D.2, STh1I.1, STh4A.4, STh4B.6, SW3A.1, SW3A.5, SW3A.8, SW4B.3, SW4M.7
 Kipshidze, Gela - SF2G.6
 Kira, Mackillo - FM2F.8, FM3F.1, FM4F.7, FTu4E.2, JTu2A.146, JW2A.123
 Kirby, Brian T. - FTu3G.7
 Kirby, Jeremy D. - SF3G.1
 Kirchen, Manuel - JTu2A.171
 Kirchner, Matt - FF2E.4
 Kirsanské, Gabija - FM1H.7
 Kish, Fred - JTh2A.167, SM1B.1
 Kiss, Balint - STu3M.3
 Kita, Derek - SF1A.1, SM2I.8
 Kita, Shota - JW2A.50, SF1A.2, SW4I
 Kita, Tomohiro - JTu2A.15
 Kitada, Takahiro - JTu2A.20
 Kitajima, Masahiro - SM3A.5
 Kitajima, Shotaro - SF2N.5
 Kitching, John - FTh4J.2, FW3E.5, SM3L.5
 Kittlaus, Eric - FF3E.3, SM1I.8, SM3K.5
 Kitzler, Ondrej - FF3E.7
 Kivshar, Yuri S. - FM2E.2, FM2E.4, FM3Q.6, FTh4M.6, FW3G.6, FW3H.4, JTh2A.73, SM4D.6, SW4D.6
 Klajn, Bruno - FTh1H.7
 Klamkin, Jonathan - ATu3R.3, JTh3D.5, JW2A.52, STu4Q.3
 Klarskov Pedersen, Pernille - JM1A.1, JM1A.3, SW3D
 Klaus, Michael - STu4Q.4
 Klee, Anthony - JTh3D.1
 Klein, Julian - JTu2A.8
 Kleiner, Vladimir - FTh3M.1, FTh4J.8, FTu3E.5, SF1J.6
 Klejs, Frederik - JTu2A.68
 Klemke, Nicolai - FF3P.5, FM3F.3
 Klenner, Alexander - SM4L.7, STh1J.4, SW3A.4
 Klimm, Detlef - SM4N.2
 Klimov, Nikolai - JF2B.5
 Kling, Laurent - FM1G.1
 Klingebiel, Sandro - STu4O.4
 Klittis, Charalambos - SM2B.6, SW4C.4
 Klötzer, Robert - STu3B.4
 Knap, Wojciech - SW4D.4
 Knapp, Ellen - FF3F.6
 Knauer, Sebastian - JW2A.139
 Knight, Jonathan C. - SF1K.1
 Kobayashi, Masaya - FTu4G.3
 Kobayashi, Noriko - STu4Q.2
 Kobayashi, Ryo - JTu2A.92
 Kobayashi, Takayoshi - JTu2A.104
 Kobayashi, Takumi - JTh2A.32
 Kobelke, Jens - SF1K.5
 Koblmüller, Gregor - JW2A.125, SW3B.6
 Koch, Jürgen - AM1M.4
 Koch, Philip - SM3L.6
 Koch, Stephan W. - FM3F.1
 Koda, Rintaro - STu4Q.2
 Kodama, Takahiro - JTu2A.38
 Kodanev, Anna - FM2Q.5
 Kodigala, Ashok - JTh2A.47
 Koefoed, Jacob G. - FM3G.3, FTh1G.1, JTh4C.4
 Koehler, Johannes R. - SF3J.1
 Koenderink, Femius - FM3J.5, FTh3M.2
 Koeth, Johannes - SF2G.2
 Kogos, Leonard - FF1H.2, SF1J.5
 Kogure, Shigeru - ATu3I.6
 Kohler, Daria - SM4I.6
 Kohlhaas, Robert - STu3D.5
 Köhnlé, Kira - STu3D.4
 Koike-Akino, Toshiaki - SW3C.3
 Koivusalo, Eero - JTu2A.28
 Kojima, Keisuke - SW3C.3
 Kolarczik, Mirco - FF3D.2
 Kolesik, Miroslav - FTh1M.3
 Kolev, Emil - STu3Q.3, STu3Q.5
 Kolis, Joseph - SF3I.3
 Kolkowski, Radoslaw - FM2Q.5
 Koller, Silvio - SM1L.6
 Kolobov, Mikhail I. - JTh2A.20
 Komachi, Yuichi - ATu3I.6
 Komar, Andrei - FW3H.1
 Kominis, Yannis - JTu2A.123, JTu2A.124
 Komis, Ioannis - JTh2A.49
 Komljenovic, Tin - AF1Q.2
 Kondakci, Hasan E. - FW4E.2, SW4N.3, SW4N.4
 Kondo, Keisuke - SM3I.4
 Kondo, Ken-ichi - STu4P.3
 Kong, Cihang - JTh2A.126, STh3N.6, SW4J.5
 Kong, Deming - SM1C.2
 Kong, Linghai - AF1M.2
 Kong, Lingjie - JTu2A.89
 Kong, Wei - SF3A.4
 Kong, Xianming - JW2A.180, STh3J.5, SW3J.5
 Kong, Ziyun - JW2A.13, STh4N.4
 Konishi, Kuniaki - JW2A.77, JW2A.80
 Kono, Junichiro - FF2D.1, FF2D.6, FM2F.3, FM2F.7, FTu3E.3, SM3A.3
 Koo, Jaemok - FM3J.8
 Kooi, Steven E. - FW4G.2, FW4H.1, SM4I.2
 Koos, Christian - SM3B.1, SM3B.3, SM4I.6, STh1A.1, STu3D.4
 Koots, Rian - FM2F.6
 Koppens, Frank H. - FW3G.5
 Koralek, J.D. - FM1F.7
 Kordts, Arne - JTh2A.10, SM1D.2, SW3A.5
 Korkin, Dmitry - AM3P.5
 Korn, Georg - SM3N.4
 Korzh, Boris A. - FW3F.3
 Koshelev, Kirill - FM2E.2, JTh2A.73, SM4D.6
 Koskinen, Kalle O. - JTu2A.134
 Kossatz, Martin - ATu4M.3
 Kossey, Michael - FM1G.4, SM1D.7, STh3I.5
 Kostenbader, Tobias - SW3B.6
 Kotov, Nicolas - FTu4E.2
 Koulouklidis, Anastasios D. - FF1E.2
 Koushyari, Farzard - SM1I.6
 Koutsares, Samantha R. - FW4G.6
 Kovanis, Vassilios I. - JTu2A.123, JTu2A.124
 Kowalski, Ben - JTu3O.3
 Kowligy, Abijith - FF2E.4, FF2E.6, FW3E.1, STh1L.1, STh3F.1, STu3F.5
 Kowzan, Grzegorz A. - STu3N.8, STu3P.5
 Koyama, Fumio - JTu2A.11, SM3I.4
 Kozak, Dmitry - FM2H.4, SF2J.4, SF3J.8
 Kozawa, Yuichi - JTu2A.16, SM4O.2
 Kozina, Michael - SM4A.6
 Kozodoy, Peter - AW3O.5
 KP, Nagarjun - SM2D.1
 Kraenkel, Christian - SF2N.2, SM4N.1
 Kramer, Daniel - STu3M.2
 Kränkel, Christian - SF3I.7, SM1N.6, SM4L.6
 Krasnok, Alexandr - SM2B.2
 Krausz, Ferenc - SF1N.7
 Kravchenko, Ivan - FM2E.4, FW3H.4, SM4D.6
 Krehlik, Przemyslaw - JW2A.137
 Krein, Douglas - SM3O.5
 Kresch, Matthias - FM2H.6
 Kremer, Mark - FM1E.1
 Krenser, Malte - JTu2A.8
 Krich, Jacob - JTu3O.6
 Krichevsky, Alexander - JTh2A.90
 Kriegel, Ilka - FF1D.5
 Krieger, Axel - JTu2A.106
 Krishnaswamy, Harish - JTu2A.81, SM3I.2
 Krivitskiy, Leonid - Ath3O.3, JTh2A.6
 Krizsán, Gergo - JTh2A.191
 Kroker, Stefanie - FF3F.7
 Kronjäger, Jochen - JW2A.137
 Krüger, Léonard M. - SF2N.7
 Kruger, Seth - SF1A.5
 Kruk, Sergey S. - FM2E.4, FW3G.6, FW3H.4, SM4D.6
 Krupa, Katarzyna - SM3D.3, SM3D.6, SW3K.6
 Kruschwitz, Brian - STu3M.6
 Krutzik, Markus - JW2A.164
 Krysiak, H. - SF2G.4
 Ku, Zahun - Ath3P.7
 Kubo, Wanaka - JW2A.95
 Kubota, Akihiro - SW3A.7
 Kucera, Courtney - STu3K.6
 Kucera, Stephan - FM2H.6
 Kuchuk, Andrian - STh4I.4
 Kucinskas, Dainius - STh3F.4

- Kudlinski, Alexandre - FTh1M.8
 Kudrawiec, Robert - STh4I.3
 Kudyshvay, Zhaxylyk A. - FM4J.7, FTh4J.1
 Kueny, Emma - FW4E.4, JTh2A.140
 Kues, Michael - FTh1E.7, FW4F.2, JTh4C.2
 Kuhl, Ulrich - FF3H.1
 Kühmayer, Matthias - FF3H.1
 Kuhnert, Jan - JW2A.135, JW2A.136
 Kuipers, Laurens K. - FF2L.1, FM2G.1, STu4N.1
 Kulatilaka, Waruna - STh3L, STh4L.2, STu3N.3
 Kulkarni, Girish - FW4F.7
 Kum, Hyun - JTu2A.7
 Kumagai, Naoto - JTu2A.20
 Kumaki, Fumitoshi - FF2P.2
 Kumar, Amar - STh4A.7, STh4B.4
 Kumar, Ashok - JF2B.6
 Kumar, Indrajeet - JW2A.170
 Kumar, Prem - FM4H.8
 Kumar, Rahul - FW3F.8
 Kumar, Rupesh - JTh2A.22, JTh2A.23
 Kumar, S. C. - FTh3E.5, FTh3E.8
 Kumar, Sushil - SF3G.6
 Kundu, Iman - STu4D.4
 Kunert, Bernardette - JTu2A.21
 Kung, A. H. - JTu2A.151, SW3N.5, SW3N.6
 Kuo, Bill P. - STh4A.8, STu4B.3
 Kuo, Hao-Chung - AW3O.2, JTh2A.52, JTh2A.89, JTu2A.9, SM2O.4
 Kuo, Paulina S. - SM2D.5
 Kuo, Shiang-He - SW3N.5
 Kupchak, Connor - FM4G.6
 Kuramochi, Eiichi - SF3A.3
 Kurman, Yaniv - FF2L.3
 Kurosaka, Yoshitaka - SF1G.4, SF1G.5
 Kuroyanagi, Shunei - JTh2A.131
 Kurtsiefer, Christian - FTh1H.5
 Kuse, Naoya - JTh2A.168
 Kutuvantavida, Yasar - SM3B.1, SM3B.3, STu3D.4
 Kuwata-Gonokami, Makoto - JW2A.77, JW2A.80
 Kuyken, Bart - FF2E.3, STh3I.7
 Kuznetsov, Arseniy - FTh4J.5
 Kuznetsov, Ilya - STu4P.4
 KWAK, KEUMCHEOL - JTh2A.188
 Kwapisz, Jaroslaw - SM3C.3
 Kwek, Leong Chuan - FM1G.2, FTu3G.2, JTh2A.18
 Kwok, Sheldon J. - ATu3J.6, JTu2A.23, SW3J.4
 Kwon, Dohyeon - JTh2A.144, SM3L.7, SW3L.2
 Kwon, Hoyeong - FF3C.4
 Kwon, Younghang - AF3M.3
 Kwon, Kyungmok - SF1A.4, STu4B.1
 Kwon, O-Pil - JW2A.81
 Kwong, D.L. - Ath4O.0
 Kwong, Dim-Lim - FF1H.5, FTh1E.3, JTh2A.160, JTu2A.76, SM1B.6, SW3A.3, SW4L.3
- L**
 Laage, Damien - JW2A.120
 Labaye, François - SF2N.3
 Labroille, Guillaume - FW4F.5, JTh2A.15
 Lacava, Cosimo - JTu2A.64
 Lafyatis, Gregory P. - FW3F.2, JTh2A.8
 Lagoudakis, Konstantinos - FTu3H.5, FW3H.2, JTh3C.5
 Lagutchev, Alexei S. - FTu4E.6
 Lai, Jiawei - FF1D.7, JTh2A.143
 Lai, Jui-Yu - AM2M.3, JTu2A.131
 Lai, Kueifu - FM4Q.4
 Lai, Yi-Chieh - FF1F.3, JTh2A.70
 Lai, Ying-Chih - JTh2A.88
 Laier English, Elizabeth - JW2A.137
 Laine, J P. - SM3I.7
 Lake, David P. - SF2J.1
 Lakhotia, Harshit - FF2P.5
 Lakomy, Katherine - STu3Q.7
 Lal, Vikrant - SM1B.1
 Lalanne, Philippe - FF1H.1
 Lallier, Eric - SM2N.8, SM4D.2
 Lam, Edmund Y. - SW4J.5
 Lam, Ping Koy - FTu3G.2
 Lamb, Robert - AM1M.1
 Lambin, Philippe - SM1O.1
 Lambropoulos, John - AM1M.2
 Lampin, Jean-François - STu4D.7
 Lamprianidis, Aristeidis - FF1E.6, FW3G.6
 Lan, Tianyi - JTh2A.108
 Lan, Xiaojian - FW3F.1
 Lancaster, David - SW4L.5
 Lanco, Loic - FTu3H.7
 Landau, Nadav - FM2F.1
 Lander, Gary R. - JTh2A.34
 Landes, Christie - FF3F.3
 Lane, Benjamin F. - SM3I.7
 Lang, Benjamin - Ath1O.5
 Lang, Denny - JM2A.3
 Lang, Klaus-Dieter - ATu4M.3
 Langaro, Ana Paula - JW2A.140
 Lange, Christoph - FM3F.1
 Lange, Mike - FW3H.7
 Langer, Fabian - FM3F.1
 Langrock, Carsten - SM2D.5
 Lanning, R N. - JTh2A.31
 Lanzara, Alessandra - FM1F.3
 Lapointe, Jean - FTu3H.2
 Larat, Christian - SM2N.8
 LaRochelle, Sophie - JTh2A.133, STh3K, SW3K.5
 Larrouy, Arthur - JF2B.2
 Lascola, Kevin - FW3E.6, SF2G.5, SF3G.3
 Lassonde, Philippe - SW3N.3
 Latawiec, Pawel - STu3F.6
 Lau, Kei may - SF3A.1, SW3Q.1
 Laueremann, Matthias - SM3B.1
 Laurell, Fredrik - AM4P.6, JW2A.82, SF3I.6, STh3F.4
 Laurent, Arnaud - JTh2A.132
 Lautier-Gaud, Jean - JW2A.137
 Lavenu, Loïc - STh1N.3
 Lavery, Martin - SW4C.4
 Lavrinenko, Andrei V. - FM4J.1, JW2A.108
 Lawrie, Benjamin - FM1G.6, FTu3H.4, JF2B.3, JF2B.6
 Lazzeri, Emma - SW4C.4
 Le Coq, Yann - SM2L.5
 Le Dortz, Jérémy - SM2N.8
 Le Gouët, Julien - JTh2A.120
 Le Gratiot, Luc - FM3Q.4
 Le Jeannic, Hanna - FM1H.7
 Le Kien, Fam - JTh2A.45
 Le Thomas, Nicolas - AM1J.3, SW3L.5
 Le, Hanh N. - JTu2A.106
 Leahu, Grigore - JTh2A.67
 Leaird, Daniel E. - FM4G.2, FM4G.3, JTu2A.112, SM1B.1, SW3C.1, SW4M.2
 Leavitt, Richard - SW3B.2
 Lebris, Arthur - STh1I.5
 Ledee, Ferdinand - JTh2A.152
 Ledingham, Patrick - Ath3H.8
 Leduff, Paul - SW3J.5
 Lee, Byounggwak - SM3A.4, SM3A.7
 Lee, Catherine - FW4F.4
 Lee, Changmin - JTh2A.30, SF1G.7, STu4Q.3
 Lee, Chau-Hwang - Ath3Q.6
 Lee, Cheol J. - SM1I.5
 Lee, Cherrie S. - SF1N.2
 Lee, Chih-Kung - AF2M.2
 Lee, Chi-sen - FM4Q.5
 Lee, Chul-Ho - FF1D.4, FTh1F.1, JTh2A.172, SW3I.3
 Lee, Doeon - FF1D.4, FF1D.8, FTh1F.1, JW2A.134, SW3I.3
 Lee, Elizabeth M. - SF1K.1
 Lee, Eric - FF3E.1, FM3J.1
 Lee, Eui Su - JW2A.79
 Lee, Gil Ju - Ath3P.5
 Lee, Han-gyeol - FM2H.7
 Lee, Ho Wai H. - FM4J.2
 Lee, Hojin - FF2D.4, FM1F.1, FM3J.8
 Lee, Huai-chuan - JTu2A.169
 Lee, Hwang Woon - JTu2A.140, JTu2A.166
 Lee, Hwaseob - JW2A.36
 Lee, Il-Min - JW2A.79
 Lee, Inje - STh1J.5
 Lee, Jay - FTh3M.6
 Lee, Jekwan - FM1F.2, FTh1F.1, JTh2A.172, SW3I.3
 Lee, Jianwei - FTh1H.5
 Lee, Jong Heon - JW2A.107
 Lee, Jongwon - JW2A.104
 Lee, Junho - JTu2A.96
 Lee, Kim F. - FM4H.8
 Lee, Kwang Hong - STh4I.6
 Lee, Kyungmin - JTu3O.3
 Lee, Nathaniel - STh4F.3
 Lee, Sang-Shin - JW2A.61
 Lee, Sang-Yun - FF1B.5
 Lee, Seong Geun - JTu2A.140
 Lee, Seong Ku - JTu2A.140, JTu2A.166
 Lee, Seung Hoon - SF2J.6
 Lee, Seung-Chul - JW2A.81
 lee, seunggeun - SF1G.7
 Lee, Seung-Heon - JW2A.81
 Lee, Seungmin - FF2D.4
 Lee, Shu-Sheng - AF2M.2
 Lee, Sooun - FF1D.4, FM1F.2, JTh2A.172, SW3I.3
 Lee, Sung-Joon - FTh1F.7
 Lee, Wonwoo - FM3J.8
 Lee, Ya-Ju - JTh2A.171, JTh2A.52
 Lee, Yeji - JTu2A.96
 Lee, Yi-Hsien - JTh2A.69, STu4N.2
 Lee, Yong-Hee - JTu2A.23
 Lee, Yoo Seung - JTu2A.62, JW2A.61
 Lee, Young J. - JTh2A.106
 Lee, Yun Jo - JW2A.13
 Lee, Yun-Shik - SM3A.4, SM3A.7
 Leedle, Kenneth - FM3M.7
 Leem, Jung Woo - JW2A.107
 Leemans, Wim - SM4M.5, SM4M.6
 Légaré, François - FM3M.2, JTu2A.158, SM3N.2, SM4M.3, SW3N.2, SW3N.3
 Légaré, Katherine - FM3M.2
 Lei, Cheng - AF3Q, AF3Q.3
 Lei, Mingwei - FM1Q.8
 Leinonen, Tomi - JTu2A.10, JTu2A.17
 Leitenstorfer, Alfred - FF3D.5, FF3P.7, FTh1F.6, JW2A.154, SF3N.4
 Lemaitre, Aristide - FM3Q.4, FTu3H.6, FTu3H.7
 Lemieux, Samuel - FW3F.5
 Lemke, Nathan D. - JW2A.163
 Lendl, Bernhard - AM2M.7, STu3N.2, STu3N.6
 Leng, Yuxin - SM4D.1
 Lentine, Anthony - SF2I.4
 Lenzer, Matthias - FTh1M.2, SM1O.7
 Léo, François - JTu2A.119
 Leon, Roberto - FTu4G.2
 Leonard, Jason R. - FM3H.3
 Leonard, John T. - SF1G.7
 Leonard, Simon - JTu2A.106
 Leone, Stephen R. - FF1P.4
 Leong, Philip - FTh1G.8
 Leong, Victor - JTh2A.6
 Leonhardt, Rainer - JW2A.74
 Leopardi, Holly F. - SM1L.4, SM2L.3
 Leosson, Kristjan - SF1J.8
 Lereah, Yossi - FW4H.3
 Leroux, Vincent - FF1E.3, JTu2A.171
 Leshin, Jason - SF2G.4
 Lesparre, Fabien - SM4M.4
 Lessard, Stéphane - STu3C.1
 Lessing, Maurice - JW2A.137, SM2L.5, STu4K.3
 Leszczynski, Adam - FM4H.6, JTh2A.28, JTh2A.33
 Letartre, Xavier - STh3A.5
 Lett, Paul D. - FM4H.2, SM2D.4
 Leung, Benjamin - FW4H.8
 Leuthold, Juerg - FTh4H.1, JTh4D.5, SM1I.4, SM2I.3, SM4B.1
 Levanon, Assaf - FM2F.5
 Levecq, Xavier - FW4E.4
 Levenson, Ariel - SM4I.7
 Leventhal, Ed - ATu3R.4
 Levi, Filippo - JW2A.137
 Levi, Ofer - AM4P.1, ATu4J.5, JTh2A.98
 Leviandier, Luc - SM4D.2
 Levine, Benjamin - JW2A.182
 Levy, Miguel - SF3J.5
 Levy, Uriel - FTh1P.2, FTu4E.5, FW4G.3, JTh2A.40, JW2A.150, JW2A.86, JW2A.98, SM3L.5, STh1A.6, STh3F.5, STh3G.5
 Lew, Matthew D. - AM2J.3
 Leykam, Daniel - FTh3E.6, JW2A.87
 Lezec, Henri - FF1F.1, FF2F.1, FTh3M.6, FTu4E, SW4D.3
 Lezius, Matthias - SM1L.5, SM2L.5, STu4K.3, SW4L.1
 L'Huillier, Anne - STh3N.2
 Lhuillier, Jérémy - STh3A.5
 Li Voti, Roberto - JTh2A.67
 Li, Baohua - AF1Q.5, STh4I.2, STh4I.4
 Li, BeiBei - JTh2A.25
 Li, Bo - FF1D.3
 Li, Bowen - JTh2A.116, SF3K.1, SM1K.7, STh1N.5
 Li, Cai-Zhen - JTh2A.143
 Li, Can - JTh2A.116, JTh2A.126, JTh2A.134, SW4J.5
 Li, Chao - JW2A.27
 Li, Chen - SF3N.1, STu4O.5
 Li, Chengqiang - JW2A.169
 Li, Chengyu - SF3I.1
 Li, Chenhui - SW3B.5
 Li, Da - JTu2A.169
 Li, Dan - AM2M.5
 Li, Dawei - Ath3P.2
 Li, Denghui - FM1E.7
 Li, Duanhui - AW3O.3, SM2I.8
 Li, Erwen - JTh2A.193, JTh2A.56, SM1I.3, SM4B.2
 Li, Fei - FM3M.3
 Li, Feng - JTh2A.125, JW2A.4, SW4M.4
 Li, Geng - JW2A.75
 Li, Gongqing - JW2A.7
 Li, Guifang - JTh2A.173, JW2A.46
 Li, Guixin - JW2A.111
 Li, Haoming - JTh2A.128
 Li, Haiqing - STu3K.4
 Li, Hang - FM4Q.5, FTh4J.3
 Li, Hao - JW2A.167
 Li, He - JTh2A.187
 Li, Hebin - FF1D.3, JTh2A.41
 Li, Hongbo - JW2A.126
 Li, Huan - SF2J.7
 Li, Huizi - JTh2A.129, JTu2A.174
 Li, Jiachen - FW3H.6, SM1D.3
 Li, Jiamin - JF2B.4
 Li, Jianqiang - JW2A.73, STu3C.6
 Li, Jianzhi - STh3J.4
 Li, Jiawei - JTh2A.13
 Li, Jiaxiong - JTh2A.173, STh3K.5
 Li, Jie - FF1P.3
 Li, Jilong - JTh2A.165
 Li, Jing - FTh1K.3
 Li, Jingang - JTu2A.2
 Li, Jin-Guang - JTh2A.143
 Li, Jinyan - STu3K.4, SW4K.6
 Li, Juhao - JTh2A.113
 Li, Juntao - FM3J.3
 li, Junyu - FF2F.4, FF2F.6
 Li, Kangmei - SM1D.7, STh3I.5
 Li, Kejia - SM2C.4
 Li, Lain-Jong - FF1D.1, STu4N.5
 Li, Lianhe - STu4D.4, STu4D.6
 Li, Lingduo - Ath3Q.3
 Li, Long - FTu3G.4, FW4F.5, JTh2A.15, SM3C.4
 Li, Ming-Han - FTu4A.4
 Li, Ming-Jun - Ath3P.4, FTh4E.7
 Li, Mingxiao - FF2E.5, JTu2A.79
 Li, Ming-Yang - FF1D.1, STu4N.5

- Li, Mo - SF2J.7, SM2B.3
 Li, Nanxi - SF1A.6, SM3L.1, STh3I.3, STu4B.2, SW3B.4
 Li, Peng - JTh2A.185, JTu2A.99, STu4O.5
 Li, PingPing - JTu2A.141
 Li, Qian - Ath3Q.1, JW2A.153, SW3L.1
 Li, Qiang - SF3A.1, SF3J.2, SW3I.2, SW3Q.1
 Li, Qin - JTu3O.2
 Li, Qing - Ath3H.7, FTh1G.3, SF2A.1, SW4A.7
 Li, Qinglong - SM2I.1
 Li, Quanwei - FM2F.4
 Li, Renkai - SM3A.1
 Li, Rui - STh4A.7
 Li, Shangyuan - AF2M.8, JW2A.42
 Li, Shimao - JW2A.28, STu3B.2
 Li, ShiQiang - FTh4J.6
 Li, ShuHui - SM2C.1
 Li, Shujing - FM4H.5
 Li, Shuo - Ath3P.4
 Li, Shuoran - ATu3J.5
 Li, Sijin - JTh2A.11
 Li, Siqi - JF1C.3
 Li, Tao - FF1F.3, STu4B.7
 Li, TENG - SW3B.5
 Li, TENGFEI - FF2F.5
 Li, Ting - JTh2A.83, JW2A.153
 Li, Tongcang - FF3F.1, JF3B.3
 Li, Wei - JTh2A.118, SF2I.8
 Li, Wenkai - SM4D.1
 Li, Wenping - JTu2A.98
 Li, Wenyang - JTh2A.103
 Li, Wenzhe - SW3M.7
 Li, Xi - JW2A.10
 Li, Xiang - STu3C.6
 Li, Xiangping - JW2A.111
 Li, Xiaoqing - SM2B.2
 Li, Xiaoying - JF2B.4
 Li, Xiao-Zhou - JTh2A.157
 Li, Xinbai - JTu2A.74
 Li, Xinwei - FF2D.1, FF2D.6, FM2F.3, FTu3E.3
 Li, Xinxin - JW2A.125
 Li, Xiuling - JTu2A.13
 Li, XuDong - JTu2A.175
 Li, Xuechun - JTu2A.163
 Li, Yajie - JTh2A.76
 Li, Yan - JTh2A.118, JW2A.162
 Li, Yanlu - ATu3I.5
 Li, Yanpeng - Ath3Q.3
 Li, Yanxiu - JW4P.3
 Li, Yanyan - SM4D.1
 Li, Yao - AF1Q.4, STh4K.7, STu4O.2
 Li, Yihan - JTh2A.168
 Li, Yongfang - JTh2A.151
 Li, YongNan - JTu2A.141
 Li, Yu - SM1D.3, SW3Q.7
 Li, Yuan - FM4Q.1, SW3M.7
 Li, Yu-Huai - FTu4A.4
 Li, Yujia - JTh2A.108
 Li, Yulin - JW2A.172
 Li, Yunhui - FM4Q.1
 Li, Yuwei - JTh2A.91, SF3I.1
 Li, Yvonne Y. - ATu3J.7
 Li, Zhaohui - STu3B.2
 Li, Zhaosong - JW2A.62
 Li, Zhe - ATu4J.6
 Li, Zhengbin - JTh2A.113, JW2A.172
 Li, ZHENYU - AM4P.5
 Li, Zhibo - JTh2A.76
 Li, Zhili - Ath1O.3
 Li, Zhitong - AF1Q.6
 Li, Zidong - SF1I.5
 Li, Ziqi - SM3O.2
 Liang, Aihu - JW2A.181
 Liang, Chenyu - STh4B.2
 Liang, Di - SM2I.6
 Liang, Hanxiao - FF2E.5, JTu2A.79, JW2A.64, SF2A.3, STu3F.3
 Liang, Haowen - FM3J.3
 Liang, Houkun - JTu2A.65
 Liang, Linjun - AF1Q.2
 Liang, Qingqing - FM1Q.8
 Liang, R. - FM1F.7
 Liang, Sijing - ATu3S.3, SM4K.2, SM4K.5, STh3F.2
 Liang, Song - SW4Q.6
 Liang, Wei-Yun - JTh2A.69
 Liang, Xuan - ATu4M.6
 Liang, Yize - SM2C.1
 Liang, Yong - Ath4Q.4
 Liang, Yufeng - FF1P.4
 Liao, Chen-Ting - AW4O.2
 Liao, Hongen - JTu2A.99
 Liao, Lei - SW4K.6
 Liao, Peicheng - JTu2A.49, JTu2A.53, SM1D.2, STu3Q.4, SW3A.5
 Liao, Wei-Cheng - JTh2A.88
 Liao, Yu-Cing - Ath3Q.6
 Liao, Yu-Ming - AM4P.4, JTh2A.88, SW3J.3
 Liao, Zhi-Min - JTh2A.143
 Liapis, Andreas C. - ATu3J.6, FM2G.6, FM3J.6, JTu2A.23, SW3J.4
 Liba, Orly - AM2J.3
 Liberal, Inigo - FTh1D.1
 Licea-Rodriguez, Jacob - JTh2A.102
 Lichoulas, Ted - STh4B.8
 Liebermeister, Lars - STu3D.5
 Liebig, Carl M. - SM3O, SM3O.5
 Liebster, Nikolas - JF2C.3
 Liehl, Andreas - JW2A.154
 Lien, Der-Hsien - STu4N.6
 Lien, Miao-bin - FTu4E.2
 Lienau, Christoph - JTu2A.136
 Lienhard, Benjamin - FTu4H.2
 Liewald, Clemens - JM1A.4
 Light, Philip - STu3P.3
 Lihachev, Grigory - JTh4D.3, STh4B.6, SW4M.7
 Lihao, Tan - SF1N.3
 LiKamWa, Patrick - JTu2A.86, SW4Q.1, SW4Q.5
 LiKawWa, Patrick L. - JW2A.46
 Lillieholm, Mads - JTu2A.68, SM2C.3
 Lim, Charles - FTu3G.3
 Lim, Jinkang - FTh1F.7, SW3I.4
 Lim, Jung-Gu - JTh2A.188
 Lim, Kang Jie - JTh2A.129
 Lim, Serene Huiting - JTh2A.129
 Lim, Shao Qi - JTu3O.6
 Lim, Sun Do - SM2N.5
 Lim, Wenxiang - SW4D.6
 Lima, Mário - JTu2A.50
 Lima, Sandro - JW2A.140
 Limonov, Mikhail - JTh2A.73
 Limpert, Jens - SF1N.7, SM4M.3, SW3N.2
 Lin, Albert - AW3O.2
 Lin, Aoxiang - JTh2A.91, SF3I.1
 Lin, Bo - AM4P.7
 Lin, Chen-An - SM2O.4
 Lin, Chi-Chen - ATu3J.4
 Lin, Chien-Chung - AW3O.2, JTh2A.89, SW3B.7
 Lin, Chih-Hsuan - SM1O.3
 Lin, Fan-Cheng - FW3G.2
 Lin, Francis - STh1J.5
 Lin, Gray - JTu2A.25
 Lin, Haifeng - SM2N.6
 Lin, Hongtao - SF1A.1, SM2I.8
 Lin, Hsiang-Ting - SM2O.4, STu4N.5
 Lin, Huaqin - JTh2A.109, SM2K.7, SW4K.5
 Lin, Hung-I - JTh2A.88
 Lin, Jiachuan - JTu2A.55, JW2A.43, SW3K.5
 Lin, Jing-Jie - JTu2A.9
 Lin, Jintian - STh1I.6
 Lin, Lih Y. - SF1I.3
 Lin, Linhan - FF3F.2, JTu2A.2, SM2O.5
 Lin, M.-F. - FM1F.7
 Lin, Nan - JTh2A.128
 Lin, Pao T. - Ath4P.6, JTh2A.107
 Lin, Qian - SW4A.1
 Lin, Qiang - FTh4G.4, JTu2A.79, JW2A.64, SF1A, SF2A.3, STu3F.3
 Lin, Qiaoling - FM3J.3
 Lin, Ren Jie - FF1F.3, JTh2A.70
 Lin, Rui - SM4C.4, SM4C.5
 Lin, Sen - JTh4C.3
 Lin, Shih-Yao - JTh2A.88, SW3J.3
 Lin, Tai-Yuan - JTh2A.88, SW3J.3
 Lin, Tong - FTu3E.2
 Lin, Tung-Ching - JTu2A.40
 Lin, Wei-Ju - AM4P.4, JTh2A.88, SW3J.3
 Lin, Xiao - FF2L.6, FM4J.6, FM4J.8
 Lin, Yen-Yin - JTu2A.83
 Lin, Yi - SW4C.5
 Lin, Yida - AW3O.4
 Lin, Yi-Shiuan - AW3O.2
 Lin, YuanYao - JTu2A.172
 Lin, Yu-Chieh - JTu2A.83
 Lin, Yu-Hong - JTu2A.40
 Lin, Zhoubin - SM2N.6
 Lin, Zong-Xian - AW3O.1
 Lin, Zuzeng - FW3F.1
 Lind, Alex - FF2E.4, FF2E.6, FW3E.1
 Lind, Alexander - STh1L.1
 Lindberg III, Don F. - SF3G.1
 Lindenberg, Aaron - SM3A.1
 Lindt, Daniel - SM3B.1
 Linfield, Edmund H. - STu4D.4, STu4D.6
 Ling, Jiwei - JW2A.133
 Ling, Yi-Chun - SM3I.6, STh3I.4
 Ling, Yun - JTu2A.148, JTu2A.56
 Link, Sandro M. - Ath3O.6
 Linnros, Jan - JW2A.31
 Lior, Yedidya - SF2A.4
 Lipka, Michal - FM4H.6, JTh2A.28, JTh2A.33
 Lipovskii, Andrey - JTu2A.134
 Lippert, Sina - JW2A.135
 Lippitz, Markus - FW3G.2
 Lipson, Michal - Ath3Q.1, ATu3S.1, FTu3E.2, JTu2A.72, JTu2A.81, SM1D.6, SM3D.1, SM3I.2, SM4L.7, STh1A.4, STh1J.4, STh4B.7, STu4N.7, SW3A.4, SW4M.5
 Lisak, Daniel - STu3N.8
 Liscidini, Marco - FM3G.7, FW4F.3, JTh3C, STu3F.2
 Lisdat, Christian - SM1L.6
 Lison, Frank - SM1K.3
 Lissek, Herve - FF3H.3
 Lita, Adriana E. - FTu4G.2
 Litchiniser, Natalia - FM3J.4, FM4Q.3
 Little, Brent - JW2A.22, SM1B.4, SM1B.5, STu3F.7
 Little, Brent E. - FW4F.2, JTh4C.2
 Littlejohns, Callum - SM3B.5, STh1B.1, STh1I.3
 Liu, Ai qun - Ath4O.4, JW2A.54
 Liu, Aiqun - AM4P.5, Ath4O.1, Ath4O.2, FM1G.2, JTh2A.18
 Liu, Ai-Qun - FTu3G.2
 Liu, Albert - FF3D.6, FF3D.7
 Liu, Amy - SF2G.4
 Liu, Bo - JW2A.138, JW2A.152, SM1L.2, SW3L.2
 Liu, Bohao - SF3N.2, STh4N.4
 Liu, Bowen - JTh2A.119, JTh2A.155, SW4K.1
 Liu, Boyuan - FM3Q.8
 Liu, Chao - JTh2A.48
 Liu, Cheng - JTu2A.65
 Liu, Che-Yu - JTu2A.9
 Liu, Chongyang - STh1B.1
 Liu, Cong - FTu3G.4, FW4F.5, JTh2A.15, SM3C.4
 Liu, Deming - Ath3Q.3, JTu2A.122, JW2A.167, JW2A.169, JW2A.174, JW2A.47, SM1C.5, SM4C.4, SM4C.5
 Liu, Fang - SM4I.4
 Liu, Fucai - FTh1F.5
 Liu, Gengchen - SW4C.3
 Liu, Gonghai - Ath4Q.3, JTu2A.22, SM4B.7
 Liu, GuiGeng - JTu2A.141
 Liu, Haifeng - SW3L.2
 Liu, Haitao - JTh2A.104
 Liu, Hanzhe - FF3P.2, FF3P.3
 Liu, Hao - JTu2A.103, JTu2A.62, JTu2A.99, SW4L.3
 Liu, Heng-Jia - JTh2A.170
 Liu, Hongliang - JTh2A.94, SM3O.1
 Liu, Huan - FF2F.4, FF2F.6
 Liu, Huaping - FM2F.7
 Liu, Huili - SF3A.7
 Liu, Huiyuan - JTh2A.173, JW2A.46
 Liu, Huiyun - STh4I.5, SW4I.1
 Liu, Jheng-Jie - AW3O.1
 Liu, Jiansheng - Ath4O.3, JTh2A.104, JW2A.153
 Liu, Jie - JTu2A.66, SM4B.4, STu3B.2
 Liu, Jifeng - AF1Q.5, FW3F.8, STh4I.1, STh4I.4
 Liu, Jin - Ath3H.7
 Liu, Jinsong - SW3D.7
 Liu, Junqian - JW2A.39, STh1B.7
 Liu, Junqiu - FTh1E.6, STh1I.1, STh4A.4, STh4B.6
 Liu, Kai - FW3H.6, JW2A.7
 Liu, Kun - JTu2A.65
 Liu, Lei - STh4B.1, STu4N.4
 Liu, Liu - STu3B.2
 Liu, Lulu - FF3E.6, SF3J.4
 Liu, Meng - JTh2A.126
 Liu, Mengkun - SW3D.3
 Liu, Min - JTu2A.44
 Liu, Minwen - SM4C.2
 Liu, Peter - FF2L
 Liu, Peter Q. - JW2A.75
 Liu, Qingwen - JTh2A.187, JW2A.173
 Liu, Qiyu - SF2J.7
 Liu, Ren-Bao - FM3F.4
 Liu, Rongjuan - FM3Q.8
 Liu, Sheng - FTh4J.4, FW3G.1, FW4H.8
 Liu, Shenghua - JW2A.128
 Liu, Shengying - AF2M.6
 Liu, Shih-Chia - SW3Q.5
 Liu, Shuang - FM3M.3, JTh2A.91, SF3I.1
 Liu, Si qi - JW2A.56
 Liu, Suling - JTu2A.98
 Liu, Tao - JTh2A.155, JW2A.169
 Liu, Tze-Wei - JW2A.151
 Liu, Wei - AM1J.2, JF2C.3, JTh2A.162, JTh2A.169, SM4K.4
 Liu, Weilai - SW3I.5
 Liu, Weiwei - JTh2A.178
 Liu, Wu - JTh2A.156
 Liu, Xiao - FTh1M.4
 Liu, Xiaojun - JTh2A.41
 Liu, Xiaoping - SW3I.5
 Liu, Xiaoqing - JW2A.138
 Liu, Xiaosheng - Ath4O.3
 Liu, Xiaoze - FM2F.4, SM4I.1
 Liu, Xiuying - FM1E.7, FTh3E.4
 Liu, Xu - JTu2A.139
 Liu, Xuan - JTu2A.108
 Liu, Xuefeng - FF1D.7, JTh2A.143
 Liu, Yang - FTu4A.4, STu4F.2
 Liu, Ye - Ath4Q.3, ATu3J.2, JW2A.91, SM4B.7
 Liu, Yehui - SW4K.6
 Liu, Yi - FM1Q.5, FM1Q.8, SM2K.3
 Liu, Yingnan - JW2A.104
 Liu, Yong-Chun - JTh2A.36
 Liu, Yuan - JTh3D.5
 Liu, Yuhong - JF2B.4
 Liu, Yun - SM1N.3
 Liu, Yunqi - SM2K.2, STh3K.5
 Liu, Zhaowei - SW4J.4
 Liu, Zhaoxiang - JTu2A.149
 Liu, Zheng - FTh1F.5
 Liu, Zhiyi - JTu4L.1
 Liu, Zichen - JTh2A.64
 Liu, Zimei - AF3M.2
 Llewellyn, Daniel M. - FTh1G.5, FTh1G.7
 Llobera, Andreu - STh3J
 Lloyd, John - AW3O.5
 Lo, Guoqiang - FF1H.5, SM1B.6
 Lobanov, Valery - JTh4D.3
 Lobet, Michaël - SM1O.1
 Löbl, Matthias - Ath3H.1, FM1H.7

- Lodahl, Peter - ATH3H.1, FM1H.7, FM3H.1, FTu3H
- Loh, William - SM2L.1
- Loi, Ruggero - STh4B.1
- Loiko, Pavel - SF2N.1, SF3I.5, SM2N.6
- Loke, Thomas - FM1G.1
- Lombard, Laurent - JTh2A.120
- Lombardi, Lucia - STu4D.6
- Lombardi, Pietro - JTh2A.46
- Lombardo, Antonio - SF3K.6
- Lomsadze, Bachana - FF2D, STu4P.8
- Loncar, Marko - ATH3H.2, ATH3H.3, FTu3H.5, FW3E.4, JW2A.103, SF2I.3, SF2J.2, SM1I.7, SM3B.4, STu3F.6, SW4M.3
- London, Yosef - JTu2A.80, SM3K.1, SM3K.7, STu4F.3
- Long, Yun - STh3B.3
- Loparo, Zachary E. - STh1L.6
- Lopatin, Sergei - JTu2A.91
- Lopez Aviles, Helena E. - FTh1M.3, FTh4E.6
- Lopez, Helena - FM1E.2
- Lopez, Josue - SM3I.1
- Lopez-Martens, Rodrigo - SM1N.8, STu3M.3
- Lorences-Riesgo, Abel - SW3C.1
- Lorenz, Virginia O. - FM2H, FM3G.7, JTh2A.2
- Losquin, Arthur - STh3N.2
- Lou, Minhan - FF2D.6
- Lou, Shuai - FW3H.6, SF3A.7
- Louie, Steven G. - FF1P.4
- Lounis, Ibrahim - FTu3H.2
- Lowery, Arthur - SM1C.2
- Loxham, Matthew - JTh2A.177
- Lozano, Magali - SM1N.8
- LU, Chao - SM3K.3
- Lu, Chaoyang - STu3A.2
- Lu, Chih-Hsuan - JTu2A.151, SW3N.5, SW3N.6
- Lu, Ching-Ying - STu3A.3
- Lu, Chunte - JTu2A.19, JTu2A.27
- Lu, Cuicui - JTh2A.36
- Lu, Dan - JTh2A.178, JW2A.62, SW4Q.6
- Lu, Faming - FF2P.4, JTu2A.154, SW3N.7
- Lu, Guo-Wei - JTh2A.195, JTu2A.36, SM3B.2, STu4C.5
- Lu, Haoyuan - ATH3P.2, JTh2A.184, JW2A.144
- Lu, Hongbo - SW4C.3
- Lu, Hsuan-Hao - FM4G.2
- Lu, Jiafeng - JTu3O.2
- Lu, Jian - FM3F.5
- Lu, Liangjun - STh3B.4
- Lu, Ling - FM3Q.8
- Lu, Luluzi - JW2A.47
- Lu, Ming - STh4A.3
- Lu, Qiaoyin - Ath4Q.3, JTu2A.22, JTu2A.26, JW2A.6, SM4B.7
- Lu, Shunpeng - FTh4J.5
- Lu, Tien-Chang - JTu2A.9, SF1I.4
- Lu, Tsung-Ju - SF3A.4
- Lu, Wei - FF1D.7, FM3M.3, JTh2A.143, JW2A.131, JW2A.133
- Lu, Xiangmeng - JTu2A.20
- Lu, Xing - SW3L.2
- Lu, Xinghua - JTu2A.163
- Lu, Xiyuan - Ath3H.7, FTh1G.3, SF2A.1
- Lu, Yang - JW3P.3
- Lu, You-Cheng - JW2A.26
- Lu, Zhenda - JW2A.126
- Lubeigt, Walter - Ath4Q.2
- Lubotzky, Boaz - JTh2A.37
- Lubyshev, D. - SF2G.4
- Lucamarini, Marco - FTu3G.6
- Lucas, Erwan - JTh4D.3, SW4M.7
- Lucianetti, Antonio - STu4O.6
- Lück, Harald - SM3L.6
- Ludwig, Arne - Ath3H.1, FM1H.7
- Ludwig, Markus - JW2A.154, SF3N.4
- Luhn, Jannik - FTu3G.1
- Lui, Kevin - AF2Q.3
- Luis, Ruben S. - JTh2A.195, JTu2A.52, SM4C.1, SM4C.3
- Luiten, Andre N. - STu3P.3
- Lukashchuk, Anton - FTh1E.6
- Luke, Kevin - JTu2A.72
- Lukens, Joseph M. - FTh4G.3, FTu4A.5
- Lukin, Daniil - FM1H.4
- Lukin, Mikhail - Ath3H.2, STh3G.1
- Lumer, Yaakov - FM4Q.7
- Lund, Kasper E. - JW2A.11, STh3A.6
- Lundberg, Lars - JW2A.149
- Lundin, Wsevolod - STh3I.1
- Lung, Shaun - JW2A.99
- Luning, Jan - FM3M.2
- Luo, Bin - JTu2A.48
- Luo, Birong - FF2E.2
- Luo, Chih Wei - JTu2A.4, JTu2A.5, SM1O
- Luo, Ciwei - FF1H.5
- Luo, Jian-Fu - ATu3J.4
- Luo, Jianheng - SF1A.4, STu4B.1
- Luo, Jiaqi - SF1K.1
- Luo, Jingdong - JTu2A.147
- Luo, Kai Hong - FF1B.8
- Luo, Kai-Hong - FM1G.3
- Luo, Ming - STu3C.6
- Luo, Rongya - JW2A.172
- Luo, Rui - FF2E.5, JTu2A.79, JW2A.64, SF2A.3, STu3F.3
- Luo, Site - JTu2A.103, JTu2A.99
- Luo, Wei - AM1J.4, STh1J.5
- Luo, Xing - JTu2A.143
- Luo, Yan - SM2C.1, STh3B.3
- Luo, Yang - JM2A.2
- Luo, Yiyang - JTh2A.119, JTh2A.155, JW2A.169
- Luo, Yue - FTh1P.4
- Luo, Zhichao - JTh2A.126, JTh2A.134, SW4J.5
- Luong, Sanh - JTu2A.19, JTu2A.27
- Lupo, Cosmo - JTh2A.10
- Lustig, Eran - FM1E.6, FM1E.8, FM3Q.3
- Luther, Bradley - STu3M.1
- Luther-Davies, Barry - FTh1E.5, SM4D.6
- Lv, Dongdong - JW2A.169
- Lv, Shuchao - JTh2A.11
- Lvov, Kirill - JW2A.119
- Lvovsky, Alexander I. - FTh4G.5
- Lyakh, Arkadiy - SF2G.4
- Lysevych, Mykhaylo - JTh2A.51
- Lyu, Jiaqi - JTu2A.141
- Lyu, Mingyang - JW2A.43
- Lyytikäinen, Jari - SW4Q.4
- M**
- M. Mekonen, Sirak - JW2A.112
- M. Wojciechowski, Adam - JF3B.2
- Ma, Chao - SF3A.1
- Ma, Chaouxuan - FTh1G.4
- Ma, Chunyang - JTh2A.111
- Ma, Fei - JTh2A.12
- Ma, He - FW3H.6
- Ma, Jianhui - FW4E.1
- Ma, Jianjun - STu3D.2
- Ma, Jie - JTh2A.147, JTh2A.158, JTu2A.174
- Ma, Jing - JTh2A.174
- Ma, Jingwen - SF3A.2
- Ma, Junchao - JTh2A.143
- Ma, Kun - AF1M.2, JTh2A.174
- Ma, Lihao - STh4L.3
- Ma, Pan - FTh1E.5
- Ma, Ping - JTh4D.5, SM2I.3
- Ma, Renmin - AF1Q.7, FW4H.2
- Ma, Rui - STh3K.2
- Ma, Teng - FF2E.2, SF3K.6
- Ma, Xiang - Ath4Q.3, SM4B.7
- Ma, Xiaolong - SF1G.1
- Ma, Xiaoyu - JTh2A.128
- Ma, Xiongfeng - FTu4A.4
- Ma, Yibo - JW2A.180
- Ma, Yichen - FTh1P.4
- Ma, Yuan-Yuan - SF3I.8
- Ma, Yue - FM3M.3
- Ma, Yufei - JW2A.177, JW2A.178
- Ma, Yuxuan - STu4K.1, STu4K.6
- Ma, Zelin - SW3K.1
- Mabuchi, Hideo - FM3G.6
- Maccaroni, Aurora - AW3R.4
- Macchiavello, Chiara - FW4F.3
- MacDonald, Kevin F. - FF1H.4, FTh4H.6, FW3H
- Mach, Lam H. - SF1N.1
- Macha, Tobias - FM2H.3
- Machielse, Bartholomeus J. - Ath3H.2, Ath3H.3, SF2J.2
- Mack, Shawn - FM3F.4
- Mackenzie, Mark - SM3D.2
- Mac-Suibhne, Naoise - FW3H.4
- Madan, Ivan - STh1N.4
- Madden, Stephen - FTh1E.5
- Madeikis, Karolis - JTh2A.146, JTh2A.154
- Madeo, Julien - FM4F.2, FM4F.6
- Madhusoodhanan, Syam - JTh2A.79
- Madsen, Lars - JTh2A.25
- Maes, Bjorn - FM1Q.6
- Maestre, Haroldo - SM4D.3
- Mafi, Arash - FF2H.1, FF3E.4, FTh1M, FTh4E, JW2A.118, STu3K.2
- Magana Loaiza, Omar S. - FTu4G.2, JTh2A.16, JTh3C.2, JTh4C.3
- Magana-Loaiza, Omar - FW4F.7
- Magarrell, Daniel J. - STh4F.1
- Magden, Emir - SF1A.6, SM3L.1, STh3I.3, STu4B.2, SW3B.4
- Maguid, Elhanan - FTh3M.1, FTh4J.8, FTu3E.5, SF1J.6
- Maguluri, Gopi - JW3P.3
- Mahajan, sumeet - ATu3S.3
- Mahendra, Andri - FTh1G.8
- Mahigir, Amirreza - JTh2A.55
- Mahjoubfar, Ata - STh3L.1
- Mahler, Dylan H. - SF1K.7
- Mahmoodian, Sahand - Ath3H.1
- Mahon, Perry T. - FTh1F.4
- Mahon, Rita - FM2H.4, SF3J.8
- Mahro, Anna-Katharina - FTh3M.3
- Mai, Andreas - STu4C.1
- Maidment, Luke - Ath4O.6, STh1L.4
- Maier, Andreas R. - FF1E.3, JTu2A.171
- Maier, Robert R. - AM1M.5
- Mainz, Roland E. - FF3P.5, JTu2A.157, SF3N.5, SW3N.1
- Maitland, Kristen C. - JTu3L.2
- Maity, Smarak - Ath3H.2, Ath3H.3
- Maize, Kerry - FTh1K.8
- Majedi, Hamed - FTu3H.2
- Majérus, Bruno - SM1O.1
- Majewski, Matthew - STh4K.3
- Majumdar, Arka - JW2A.16, SF1J.4, SF3A.6
- Makarov, Sergey - FTh4M.6
- Maker, Gareth - Ath4Q.2
- Makhal, Krishnandu - FF2E.7
- Makris, Konstantinos - FF3H.3, FF3H.7, FM3E, FM4E.2, JTh2A.49
- Malacarne, Antonio - JW2A.143
- Malcolm, Graeme - Ath4Q.2
- Maleki, Lute - AW3R.1
- Malevich, Pavel - SF1N.3, SM4M.1
- Malik, Aditya - JW2A.39, STh1B.7
- Malik, Bilal H. - JTu3L.2
- Malik, Muhammad N. - SW4C.4
- Malinowski, Marcin - JTh2A.16, JTh2A.166, JTh3C.2, SM1B.2, STh4A.6, STu3F.4
- Malladi, Girish - FTu4H.2
- Mallett, Benjamin - FM1F.5
- Malz, Daniel - FF3E.5
- Malzard, Simon - FM4Q.6
- Mamuti, Roukuya - SW3M.3
- Man, Michael - FM4F.2, FM4F.6
- Man, Ray - AF2Q.3
- Mandel, Olaf - STu3P.2
- Mandel, Yossi - JTu2A.107
- Mandon, Julien - Ath1O.1
- Manek-Hoenninger, Inka - AM2M.4
- Manfra, Michael J. - FF2D.6
- Mangan, Brian - SW4A.5, SW4A.6
- Maniotis, Pavlos - STh3B.7
- Mannenbach, Ehren - SM3A.1
- Mannor, Shie - STh4N.1
- Manolis, Athanasios - JW2A.5
- Mans, Torsten - SM3N.2
- Mansoureh, Mahdad - FF1F.7
- Månsson, Erik - JTu2A.158
- Mansuripur, Tobias S. - SF3G.3
- Manurkar, Paritosh - SM4L.1
- Manzo, Michele - AF2M.5
- Manzoni, Cristian - FF2D.7
- Mao, Chenchen - FW4G.5
- Mao, Dun - SM2B.4
- Marandi, Alireza - FTu4A.2, JTh4C
- Marangoni, Marco - STu3P
- March, Stephen - FW4H.5, JW2A.104
- Marchevsky, Andrey - STh3A.3
- Marcoux, Pierre - JTh2A.99
- Margetis, Joe - AF1Q.5, STh4I.2, STh4I.4
- Margulis, Walter - AM4P.6
- Maria, Michael - JTu2A.109
- Marineau, Eric - ATu4I.4
- Marinelli, Agostino - JF1C.3, JF2C.1
- Marini, Diego - JW2A.166
- Marinins, Aleksandrs - JW2A.31
- Marino, Alberto M. - JF2B.6
- Marino, Giuseppe - FTh1D.7
- Markelz, Andrea G. - SW3D.5
- Markelz, Andrea G. - SM3A
- Markey, Laurent - JW2A.5
- Markos, Christos - JTh2A.196, JTu2A.109
- Maroto-Valer, Mercedes - AM1M.5
- Marpaung, David - JTh3D, JTh4D, STu4F.2
- Marquardt, Christoph - SM2D.3
- Marques, Paulo - FW4G.8
- Marsh, John - SW4Q.7
- Marshall, Graham - FM1G.1
- Marsik, Premysl - FM1F.5
- Martella, Daniele - JTh2A.46
- Mårtensson, Jonas - SM4C.5
- Martial, Igor - SM4M.4
- Martin, Eric - FF1D.2, FM2F.8
- Martin, Kyle W. - JW2A.163
- Martin, Olivier - JTh2A.74
- Martin, Yves - STh1B.2
- Martín-Cano, Diego - FW4G.7
- Martínez Saavedra, José Ramón - FF3D.8
- Martinez Vazquez, Rebecca - JTu2A.156
- Martinez, Amos - FTu3G.6
- Martinez-Dorantes, Miguel - FM2H.3
- Martin-Mateos, Pedro - JW2A.171, STu3N.6
- Martin-Monier, Louis - STh1I.5
- Martin-Moreno, Luis - FF2F.7
- Martino, Nicola - ATu3J.6, JTu2A.23, SW3J.4
- Martins, Renato - JTu2A.1
- Martynkien, Tadeusz - SF1N.4, STh4K.5
- Maryuwa, Ryo - JTu2A.52
- Mas, Josep - ATu3I.3, STh1J.2
- Masada, Genta - FTu4G.1
- Mashanovich, Goran - FF1H.1, STh1I.3
- Mashayek, Farzad - FF3F.6
- Mashhadi, Soheila - FW4H.6, JTh2A.182, JTh2A.50
- Mashiko, Hiroki - JTu2A.153
- Maslowski, Piotr - STu3N.8, STu3P.5, STu3P.6
- Mason, David - Ath3H.5
- Mason, Paul - STu4O.6
- Massa, Francesco - FTh4G.1
- Masselink, W. T. - JTu2A.18
- Massler, Hermann - FTu3D.4
- Massuda, Aviram - FW4G.2, FW4H.1, SM4I.2
- Mastronardi, Lorenzo - SM3B.5
- MASUDA, KEIGO - SM4O.4
- Masuda, Keisuke - JW2A.92
- Masuda, Shin-ichi - FM3M.5
- Masuoka, Takashi - JW2A.141
- Mataloni, Paolo - FW4F.3
- Mateos, Xavier - SF2N.1, SF3I.5, SM2N.6
- Mathews, Jay - JW2A.106, JW2A.112

- Mathiesen, Kristoffer S.- STh3A.3
 Mathine, David - SM1B.1
 Matlis, Nicholas H.- FF1E.3, JTh2A.140, JTu2A.116, SM4A.4
 Matoba, Mizuho - JW2A.80
 Mátrón, Zsuzsanna - SM3A.2
 Matson, Joseph - FF2F.7
 Matsuda, Takuya - JW2A.127
 Matsumoto, Atsushi - JTu2A.15
 Matsumoto, Masayuki - SM1C, STu3C.5
 Matsumoto, Morio - JTu2A.126
 Matsumura, Tomotake - JW2A.77
 Matsuo, Shinji - SF3A.3, SM2I.5
 MATSUOKA, Yohei - JTu2A.18
 Matsusaka, Shugo - SM4O.2
 Matsushima, Isao - STu4K.1, STu4K.6
 Matsutani, Akihiro - SM3I.4
 Matsuura, Motoharu - SM1C.3
 Matte-Breton, Charles - JTh2A.133
 Mattei, Giovanni - JTh2A.67
 Matthews, Dennis L.- STh1J.1
 Matthews, Gerald A.- STu4P.5
 Matthews, Jonathan - FM1G.1, JTh2A.5, JW2A.139, SF1K.7, STu3A
 Matthews, Manyalibo J.- JW2A.117
 Matthews, Mary - Ath1O.2
 Matthey, Renaud - SF2G.7
 Maulini, Richard - SF2G.7
 Maurel, Martin - JTh2A.97, SF1K.2
 Maurer, Joshua - JTu3O.7
 Maurer, Peter - JTh3C.5
 Maurice, Vincent N.- FTh4J.2
 Mawst, Luke J.- SF3G.1, STu4Q.4
 Maxson, Ryan - JTh3D.4, SW4B.5
 May, Eric - STu3P.3
 May, Stuart - JTu2A.64, SM2B.6
 Mayer, Aline S.- SF2N.7, SM4L.7
 Mazelanik, Mateusz - FM4H.6, JTh2A.28, JTh2A.33
 Mazilu, Michael - AF2M.3
 Mazur, Mikael - JW2A.149, SW3C.1
 Mazurczyk, Radoslaw - STh3A.5
 Mazurski, Noa - FTh1P.2, JW2A.86, SM3L.5, STh1A.6, STh3G.5
 Mazzone, Valerio - JW2A.115
 Mazzotti, Davide - Ath4Q.6
 McAndrew, Brendan - AF3M.6
 McBirney, Samantha - ATu4J.4
 McCCarthy, Aongus - AW3R.4
 McCaughan, Adam - JW2A.29
 McCloskey, David - ATu4M.2, FTh1K.3, JTh2A.90
 McCorkel, Joel - AF3M.6
 McCracken, Richard A.- Ath4O.6, FTh1M.1
 McCuller, Lee - JF3B.1
 McDanniel, Sean - SM3O.5
 McDonald, Corey - FF3D.3, SF3A.5
 McGuire, Allister - AM4P.2
 McInerney, John - JTu2A.31
 McKinstrie, Colin - FTh1G.1
 McKinzie, Keith A.- SM1B.1
 McMahan, Peter L.- FTu4A.2
 McMahan, William - AW3O.5
 McMillan, Alex - JTh2A.5, JW2A.139
 McMorrow, Dale - JTh2A.175, JTu2A.59
 McMurray, Johnny - JW2A.24
 McNicholas, Kyle M.- STh4I.3
 McPhillim, John - SM2B.6
 McQuade, James - JTu2A.145
 Mechler, Máttyás I.- JTh2A.191
 Meccozzi, Antonio - STu3C.3
 Mecseki, Katalin - SM4A.3
 Meesala, Srujan - Ath3H.2, Ath3H.3, SF2J.2
 Megalini, Ludovico - JW2A.52
 Meggiolaro, Daniele - FF2D.7
 Meglinski, Igor - JTu2A.102
 Mei, Chao - JW2A.4
 Meier, Joachim - FW4E.4, JTh2A.140
 Meier, Torsten - FF1B.8, FF3P.7, FM1G.3
 Meier, William R.- FM1F.6
 Meinecke, Jasmin D.- FTu4G.1
 Meissner, Helmut E.- JTu2A.169
 Meissner, Stephanie K.- JTu2A.169
 Mejean, Guillaume - Ath3O.4
 Mejia, Enrique A.- FW3E.6, SF3G.3
 Mekhazni, Karim - JW2A.55
 Melen, Gwenaelle - FTu3G.1
 Melik-Gaykazyan, Elizaveta V.- FW3G.6
 Melikyan, Argishti - SM4B.3
 Melkonian, Jean-Michel - Ath3O.1, STu3N.7
 Melosh, Nicholas - FTu3H.5, JTh3C.5
 Mencagli, Mario Junior - FF3C.3
 Mendis, Rajind - SW4D.7
 Mendonca, Cleber R.- JTu2A.1
 Mendoza, Carlos - SF1J.8
 Meng, Fei - STu4K.1, STu4K.6
 Meng, Jiajun - AF3M.1, SM2I.4
 Meng, Junwei - FF3E.1, SM4N.5
 Meng, Ran zhe - JW2A.30
 Meng, Xiangeng - FM2G.7
 Meng, Yafei - AF1Q.4, STh4K.7
 Menicucci, Nicolas - FTu4G.5
 Menon, Vinod M.- FF1D.6, FM2F, FM2F.6, FTu4H.1, FW4G.8, FW4H.6, SM2O.7
 Menoni, Carmen S.- JTu2A.151, STu3M.1, STu4P.4
 Menotti, Matteo - FM3G.7
 Menssen, Adrian - FTh1H.4
 Menyuk, Curtis R.- JTh2A.125, JW2A.179, SF2A.6
 Mercier, Brigitte - SM1N.8
 Mergo, Pawel - SF1N.4, STh4K.5
 Meriles, Carlos - FTu4H.1
 Merkouche, Sofiane - FM4G.1
 Merolla, Jean-Marc - AF2Q.1
 Merritt, Charles D.- SF2G.1, STh1B.7, STu3N.1
 Mertz, Jerome C.- Ath1Q.1
 Mescall, Ryan - SW3D.3
 Meschede, Dieter - FM2H.3
 Messaddeq, Younès - JTh2A.133
 Messig, Jeff - SW4C.3
 Messner, Philipp - JTu2A.171
 Metzger, Thomas - SM3N.4, STu4O, STu4Q.4
 Meuret, Sophie - FM3J.5, FTh3M.2
 Meyer, Jerry R.- SF2G.1, STh1B.7, STu3N.1
 Meyer, Ralf - STu3Q.1
 Meyer, Stephanie A.- SW4J.3
 Meyer, Tobias - SW4L.1
 Meyer-Scott, Evan - FW3F.6
 Meynell, Simon - JF2B.1
 Mi, Zetian - JW2A.129
 Miao, Pei - FM3Q.1, FM4Q.6
 Miao, Xianglong - JW2A.75
 Miao, Yu - FM3M.7
 Michael, Yoand H.- FM4H.3
 Michailovas, Andrejus - JTh2A.146, JTh2A.154, STu4O.1
 Michel, Anna P.- Ath4P.1
 Michel, Jurgen - AW3O.3
 Michel, Knut - SM3N.4, STu4O.4
 Michelsen, Hope A.- STh4L.1
 Michikawa, Takashi - ATu3I.6
 Michon, Jérôme - SF1A.1
 Middleton, Charles - JTh3D.1
 Midkiff, Jason - JW2A.40, STh1B.4
 Midolo, Leonardo - Ath3H.1, FM1H.7
 Midorikawa, Katsumi - ATu3I.6, JTu2A.155, SF1N.5
 Migdall, Alan - JTh2A.39
 Mihalji, Adam - FF1B.1
 Mikaelsson, Sara - STh3N.2
 Mikami, Yuya - JTh2A.81, JTh2A.86
 Mikhailov, Eugeniy - JTh2A.31
 Mikhailova, Julia - JTu2A.159
 Milde, Tobias - Ath1O.6, Ath3O.5, JTu2A.162
 Mildenerberger, Daniel - JM2A.2, SW3D.1
 Mildren, Richard P.- FF3E.7
 Miles, Richard B.- ATu4I.4, STu4P.1
 Milicevic, Marijana - FM3Q.4
 Miliotis, Stylianos - JTh2A.49
 Millar, David S.- SW3C.3
 Miller, Aaron J.- FW3F.2
 Miller, Keith - SW3M.7
 Miller, Owen - FTh1K.5, FW4G.2
 Miller, Steven A.- Ath3Q.1
 Millot, Guy - SM3D.3, SM3D.6, SW3K.6
 Mills, Benjamin - JTh2A.177, SM1O.4, SM4O.3
 Mills, Matthew S.- JTu3O.3
 Min, Dabin - STh4I.6
 Minami, Yasuo - JTu2A.20, SM3A.5
 Minamide, Hiroaki - JTu2A.118, JTu2A.165, JW2A.100, SW4D.5
 Minamikawa, Takeo - JW2A.141, JW2A.146, JW2A.155, STh3L.3
 Minitti, M.P. - FM1F.7
 Minkov, Momchil - FF1F.2, FM1E.4, JTu2A.13
 Minola, Matteo - FM1F.5
 Minoshima, Kaoru - FW4E.6, JTh2A.159, JW2A.141, JW2A.146, JW2A.156, SF3N.3, SM4L.3, STh3L.6, STu3P.1, STu3P.5, STu4K.1, STu4K.4, STu4K.6, STu4P.3
 Miranda, Brando - SF1A.1
 Miranda, Miguel - STh3N.2
 Mircovich, Matthew - JTu2A.6
 Mirhosseini, Mohammad - JTh2A.19, JTh2A.4
 Mirin, Richard - FF3D.3, FTu4G.2, JTh2A.16, JTh3C.2, JTh4C.3, JW2A.29, SF2A.1, SF2A.5, SF3A.5, SF3J.7, STh3F.1
 Miroshnichenko, Andrey - FF1E.6, FW3G.6
 Mirov, Mike - STh4F.3, STh4F.4
 Mirov, Sergey - STh4F.3, STh4F.4
 Mirzaei-Nejad, Reza - SW3K.5
 Mishchenko, Artem - FF2L.7
 Mishchik, Konstantin - AM2M.4
 Mishra, Akhilesh K.- FTh1H.6
 Mistry, Kevin S.- FTh1P.4
 Mitchell, Arnan - FTh1E.5, JW2A.22, SM1B.4, SM1B.5
 Mitchell, John - JTh3D.3
 Mitchell, Matthew - SF2J.1
 Mitchell, Morgan - JF3B.5
 Mitomo, Jugo - STu4Q.2
 Mitrofanov, Alexander - FM1Q.2
 Mitsui, Shintaro - JTh2A.81
 Mittal, Vinita - STh1I.3
 Mittendorff, Martin - SW4N.5
 Mittleman, Daniel M.- FF2D.2, JM1A.1, JM1A.3, JM2A, STu3D.2, SW4D.7
 Miura, Eisuke - FM3M.5
 Miura, Hiroki - SM3B.2, SM3B.3
 Miyamoto, Katsuhiko - SM4O.4, SW3M.3
 Miyamoto, Shuji - STh3L.3
 Miyata, Masashi - SF1J.3
 MIYAZAKI, JUN - JTu2A.104
 Miyazono, Evan - STh3G.2
 Mizuno, Takahiko - STh3L.3
 Mizuno, Tomoya - FM3M.6
 Mizuno, Yosuke - SM3K.2
 Mlynarczyk, Jacqueline - SM3I.7
 Moazeni, Sajjad - SF1A.5
 Mobini, Esmaeil - FF3E.4, JW2A.118
 Mocek, Tomas - STu4O.6
 Mochizuki, Toshimitsu - FTh1H.1
 Modotto, Daniele - SM3D.3, SM3D.6
 Modsching, Norbert - SF2N.3, SM4L.6
 Moein, Tania - STh1A.5
 Moeller, Lothar - STu3D.2
 Moeller, S.P. - FM1F.7
 Mohajerin Ariaei, Amirhossein - JTu2A.49, JTu2A.53, SM1D.2, SW3A.5
 Mohammadi Estakhri, Nasim - FF3C.3, JW2A.93
 Mohammadi, Fatemesadat - JTh2A.51
 Mohanty, Aseema - Ath3Q.1, FTu3E.2
 Mohr, Christian - STu4O.6
 Mohr, Daniel A.- FF2F.7
 Moille, Gregory - FTh1G.3, SF2A, SW4A.7
 Moiseev, Sergey G.- JTh2A.57
 Moitra, Parik - FTh3E.7
 Mojahedi, Mo - FM2G, JTu2A.110, STh4A.5, STu4P.2
 Molina-Fernández, Inigo - STh1I.3
 Molisch, Andreas F.- SM3C.4
 Mollaei, Masoud - SM2N.4
 Möller, Ian M.- AM3P.5
 Molodij, Guillaume - JTu2A.102
 Moloney, Jerome - FM3M.4
 Monat, Christelle - FTh1E.5, STh3A.5
 Monreal, Javier G.- JTu2A.101
 Montambaux, Gilles - FM3Q.4
 Moody, Galan - FF3D.3, SF3A.5
 Mookherjee, Shayan - FTh1G.4, JW2A.63, SF2I.4
 Moon, Geol - FM2H.7
 Moon, Hyowon - SF3A.4
 Moon, Jisoo - FF2D.4, FM1F.1
 Moon, Jiyoung - AF1Q.6
 Moon, Kiwon - JW2A.79
 Moon, Sung - FF1B.5, JTh2A.1
 Mooney, Brian P.- AM3P.5
 Mootz, Martin - FM1F.6
 Moradinejad, Hesam - JTh2A.78, SM1I.1, SW4A.2, SW4B.6
 Morais, Tiago - STh1I.1, STh4B.6
 Morandotti, Roberto - FF1E.1, FTh1E.7, FTh1M.7, FTh4E.4, FW4E, FW4F.2, JTh4C.2, JW2A.22, JW2A.81, SM1B.4, SM1B.5, SM4M.3, STu3F.7, SW3N.2
 Morassutti, Claudio Y.- JW2A.140
 Morawiec, Seweryn - FTh1K.7
 Morea, Matthew - STu3A.3
 Moreau, François - AM2J.5
 Moreau, Paul-Antoine - FF1B.1, JTh2A.5, JW2A.139
 Morel, Jacques - Ath3O.6
 Moretti Sala, Marco - FM1Q.7
 Morgan, Jesse S.- STu3B.5
 Morgner, Uwe - STh3N.2
 Mori, Warren B.- FM3M.3
 Mori, Yoshifumi - SW4N.2
 Morimoto, Shohei - SW3D.6
 Morinaga, Mizuki - JTu2A.11
 Morioka, Motoki - JTu2A.92
 Morioka, Toshio - SM2C.3, STu3D.1
 Morita, Ken - JTu2A.20
 Morita, Kinichi - JTh2A.86, STh1I.7
 Mork, Jesper - STh1C.1, STh3A.3
 Morohashi, Isao - JW2A.155
 Morris, Daniel - SM3N.1
 Morris, James - SM3D.2
 Morsy, Ahmed - FTh1P.3
 Morsy-Osman, Mohamed - STu3C.1
 Mortazavi, Mansour - AF1Q.5, STh4I.2, STh4I.4
 Morthier, Geert - SW3Q.4
 Mortier, Michel - SM4I.7
 Morvan, Loic - SM4D.2
 Mosconi, Edoardo - FF2D.7
 Moselund, Peter - ATu3S.4, AW3S.1, JTu2A.109, SM4K.1
 Moser, Harald - AM2M.7
 Moses, Jeffrey - SM3D.4
 Moshfeghi, Darius - AM2J.3
 Moskalev, Igor - STh4F.4
 Mosley, Peter J.- Ath3H.8, JTh2A.5, SF1K.7
 Moss, Benjamin - ATu3R.2
 Moss, David J.- FTh1E.5, FTh1E.7, FW4F.2, JTh4C.2, JW2A.22, SM1B.4, SM1B.5, STh1A.5, STu3F.7
 Mottay, Eric - AM2M.4
 Motti, Silvia - FF2D.7
 Motyka, Marcin - STh4I.3
 Mou, Chengbo - SM2K.2
 Moulton, Peter F.- SM3N.3
 Mouradian, Sara L.- FF1B.3, FM1H.3, FTu4E.7, SF3A.4
 Mourgias-Alexandris, George - STh3B.7
 Mousavi, Hossein - FM3Q.6
 Mousavian, Ali - SM3A.4, SM3A.7
 Mrabet, Hichem - STh1C.5
 Mrejan, Michael - FM2F.5, JTh2A.66
 Mridha, Manoj K.- FW4E.5

- Mudrick, John - SF2I.4
Muecke, Oliver - FF3P.5, FM3F.3, JTu2A.157, SF3N.5, SW3N.1
Muehlbrandt, Sascha - STu3D.4
Mueller, J. P. Balthasar - SF1J.8
Mueller, Jason D. - JTh2A.5
Mueller, Patrick - SM4O.5
Mueller, Rouven - SM4O.5
Muench, Jakob E. - FF2E.2
Mühlberger, Korbinian - SF3I.6
Mujat, Mircea - JW3P.3
Muller, Antoine - SF2G.7
Müller, Kai - FM1H.4, FTu3H.1, JTu2A.8
Müller, Philipp - FM2H.6
Muller, Richard - SF1A.4, STu4B.1
Müller, Tomáš - JW2A.137
Munch, Jesper - SM4N.3, SW3M.5
Muneeb, Muhammad - STh3I.7
Munekata, Hiro - JTu2A.129
Munera, Natalia - JTu2A.59
Muniz, Andre Luiz M. - FTh4E.4
Muniz, Rodrigo A. - FM4F.7, FTh1F.4, JTh2A.53, JW2A.123, JW2A.158
Munk, Dvir - JTu2A.63, SF2A.4
Munro, William - JTh2A.43
Murai, Shunsuke - JTh2A.87
Murakami, Hironaru - SW3D.4
Murakami, Takeharu - ATu3I.6
Murauski, Anatoli - FW3H.1
Muraviev, Andrey - STh1L.6, STh4F.4
Muravsky, Alexander - FW3H.1
Murdoch, Stuart G. - FW3E.2, JTu2A.119, JTu2A.137, SM2D.2, SM4K.7
Murmane, Margaret - AW4O.2, FF2E.4
Murphy, Ryan - FW4F.4
Murphy, Thomas E. - STh3K.4, SW4N.5
Murphy, Thomas E. - SF1I
Murray, Christopher P. - ATu4M.2
Murugan, Ganapathy S. - STh1I.3
Musgrave, Ian O. - JTu2A.170
Muskens, Otto L. - FF1H.1, FTh4J
Mussot, Arnaud - FTh1M.8
Mutschall, Sven - STu3B.4
Muzik, Jiri - STu4O.6
Myers, Jason - FM4J.2, SF3A.6, SF3I.3
Myszyrowicz, André - FM1Q.8
- N**
- Naciri, Jawad - SM2O.1
Nada, Mohamed Y. - FM3Q.5
Nadeem, Faisal - Ath1O.1
Nader, Nima - FF2E.4, FF2E.6, FW3E.1, JTh2A.16, JTh3C.2, SF2A.5, SF3J.7, STh1L.1, STh3F.1, STu3F.5
Naderi, Nader A. - SW4K.3
Nadri, Souheil - SM2I.1
Nagai, Kosuke - JW2A.146
Nagai, Masaya - SW4D.7
Nagai, Vivek - FF2F.5
Nagamine, Gabriel - JTu2A.114
Nagao, Tadaaki - FF2F.8, SM3A.5
Nagar, Garima C. - JTu2A.132, JTu2A.3
Nagasaka, Kenjiro - JTh2A.131, JTu2A.126, JTu2A.127, JTu2A.143
Nagisetty, Siva - STu4O.6
Naggal, Supriya - STu4P.5
Nagy, Jonathan T. - SF2I.2
Nagy, Tamas - SM1N.8
Nagyimihály, Roland - JF2C.2, SM4N.7
Nahata, Ajay - JW2A.76, SW4D.3
Nahear, Rotem - SM4N.4
Nahmias, Mitchell - STh3B.1
Nahvi, Ehsan - FTh1D.1
Naik, Gururaj - FTh1P, FTu3E.3
Naiman, Alex - JW2A.150
Nairat, Muath - JW2A.182
Nakagawa, Fumimaru - SM1L.1
Nakagawa, Ken'ichi - JW2A.156
Nakahama, Masanori - JTu2A.11
Nakai, Makoto - JW2A.70
Nakajima, Hiroshi - STu4Q.2
Nakajima, Mitsumasa - SF1J.3, SM1C.4
Nakajima, Naoya - JTu2A.92
Nakajima, Yoshiaki - JW2A.141, JW2A.146, JW2A.156, SM4L.3, STu4K.1, STu4K.4
Nakakubo, Keisuke - JTh2A.86, STh1I.7
Nakamura, Keisuke - STu3P.1
Nakamura, Shuji - SF1G.7
Nakano, Shogo - SM4O.4
Nakano, Yoshiaki - SM4B.6
Nakano, Yuta - JTh2A.164
Nakayama, Masaaki - JW2A.127
Nam, Chang Hee - JTu2A.140, JTu2A.166, STu4O.3
Nam, Donguk - STh4I.6
Nam, Sae Woo - FTu4G.2, JTh4C.3, JW2A.29, SF2A.1, SF2A.5, SF3A.5, SF3J.7, STh3F.1
Nam, Wonil - STh1A.3
Namekata, Naoto - FW4F.8
Nan, Fan - SM2O.2
Nan, Zhou - JW2A.28
Nandy, Biplob K. - JTu2A.60
Nantel, Megan - JTh2A.3
Nara, Yuki - JTu2A.16
Narayana, Vikram - JW2A.3
Närhi, Mikko - AF2Q.1
Narimanov, Evgenii E. - FM4J.3, JTu2A.144, JW2A.21, JW2A.89
Narui, Hironobu - STu4Q.2
Nash, Kelly L. - AM3P.2
Nashwan Al-Milaji, Karam - JTh2A.80
Nasimzada, Wahid - JW2A.138
Nasir, Ehsan - ATu4I.5
Nasir, Mazhar - FTh1D.7
Natan, Adi - FM4F.5, JF1C.3
Naumov, Andrei - FF3P.4
Nauriyal, Juniyali - JW2A.72
Nawata, Kouji - JTu2A.118, JTu2A.165, JW2A.100, SW4D.5
Naylor, Carl H. - STu4N.3
Nazac, André - AM2J.5
Nazirzadeh, Mohammadamin - Ath3Q.2
Ndao, Abdoulaye - FM4Q.8, FTh4J.7, JTh2A.47, JW2A.97
Ndebeka-Bandou, Camille - SF3G.5
Nebel, Christoph - JTh2A.38
Nedeljkovic, Milos - STh1I.3
Nees, John - SM3O.6
Negro, Matteo - JTu2A.156
Neimontas, Karolis - STu4O.4
Nellen, Simon - STu3D.5
Nellikka, Apurv Chaitanya - FM2G.4
Nelson, Karl D. - AM2P.4
Nelson, Keith - FM2Q.3, SM4A.5
Nemirovski, Yonatan - FM1E.3
Nemoto, Kae - JTh2A.43
Nemoto, Masaya - SM2K.4
Nemoto, Natsuki - JW2A.77, JW2A.80
Nenni, Stephen - FTh3E.6
Neshev, Dragomir N. - FF1E.6, FM4E.6, FW3G.4, FW3G.6, FW3H.1, FW3H.4, JW2A.34
Nestor, Stephen - ATu4M.4
Neuenschwander, Beat - AM1M.3
Neufeld, Ofer - FF1P.5
Neuhaus, Mathias - JW2A.138
Neumann, Tanja - JTu2A.157
Neumark, Daniel M. - FF1P.4
Neutens, Pieter - JW2A.32
Newbury, Nathan R. - Ath4P.3, SM1L.3, SM4L.1, STh1L.2, SW4L.7
Newell, Dave - FM3H.2
Newell, Timothy C. - JTu2A.19, JTu2A.27
Newman, Ward - STh4A.1
Ng, Edwin - FM3G.6, FTu4A.2
Ng, Mili - FM4G.8
Ng, Tien Khee - JTu2A.29, JTu2A.91
Ng, Wai Kit - SF3A.1
Nga Ng, Tse - JTh2A.80
N'Gom, Moussa - STh3L.5
Nguyen, Alisee - JTu2A.121
Nguyen, Clark T. - SF2J.3
Nguyen, Duy - Ath1O.4
Nguyen, Hoa P. - JTu2A.127
Nguyen, Minh - SM1O.5
Nguyen, Ngoc-Cuong - FF2F.7
Nguyen, Peter H. - JM2A.2, JW2A.122, SW3D.1
Nguyen, Phuc - JW4P.3
Nguyen, Thach - JW2A.22, SM1B.4, SM1B.5
Nguyen, Tung - STh1I.5
Ni, Kai - ATu3I.4, JW2A.160
Ni, Li - JTh2A.91, SF3I.1
Ni, Ni - FM1F.4
Ni, Xiang - FM3Q.6, FM4Q.2, FTh3M.2, JW2A.87
Ni, Zhiqiang - STu4O.2
Niang, Alioune - FTh1M.5
Nic Chormaic, Sile - JTh2A.45
Nichani, Kapil - JTh2A.103
Nicholson, Jeffrey - SM1K.3, SW4K.4
Nickel, Daniel - SW3K.4
Nicolich, Kathryn L. - FW3F.2, JTh2A.8
Nicolodi, Daniele - SM2L.5
Nie, Craig - SW3M.7
Nie, Zan - FM3M.3
Nie, Zhonghui - STu4O.2, SW3I.5
Nielsen, Henri T. - FM1H.7
Niemi, Nicholas - STu3N.3
Niesner, Raluca - STh1J, SW4J.1
Niessen, Katherine - SW3D.5
Nikolay, Niko - JTh2A.37
Nilsson, Johan - JTh2A.109, JTh2A.110, SM1K.6, SM2K.7, SW4K.5
Ning, Xiaonan - FM3M.3
Ninota, Yuki - FF1P.6
Nisaka, Kunpei - STu3Q.2
Nishi, Hidetaka - SM2I.5
Nishida, Shigeki - SW3M.3
Nishikawa, Jun - FW4F.8
Nishikawa, Tadashi - SM4L.5
Nishimura, Kataro - JTu2A.155, SF1N.5
Nishimura, Naoya - JTh2A.81
Nishiyama, Akiko - JW2A.156, SM4L.3, STu3P.5
Nishiyama, Nobu - FM3J.7, JW2A.92
Nishizawa, Norihiko - JTh2A.121, STh4K.4, STu4K.5
Nishizawa, Nozomi - JTu2A.129
Nisoli, Mauro - JTu2A.158
Nithyanandan, Kanagaraj - Ath3O.4
Nitsche, Thomas - FW3F.6
Niu, Liting - SW3D.7
Niu, Yongjiao - FF1H.5
Noach, Salman - SM4N.4
Noda, Susumu - FF1E.4, SF1G.3
Noe II, G. Timothy - FM2F.7
Noe, Gary T. - FF2D.1
Nogan, John - JW2A.84
Nogas, Pawel - JW2A.137
Noginov, Mikhail A. - FM4J, FW4G.6, FW4H.4, FW4H.6, JTh2A.50
Noginova, Natalia - FF2F.2, FW4H.6, JTh2A.182
Nogueira, Ana Flávia - JTu2A.114
Noh, Jiho - FM2Q.2
Noh, Jinyun - FTh4M.1, FW3H.7
Noh, Minji - FTh1F.1, JTh2A.172, SW3I.3
Nojiri, Hiroyuki - FF2D.1
Nolan, Dan - FTh4E.7
Nolte, David D. - ATu4J.6
Nomada, Hiroaki - STh1I.7
Nomoto, Yoshiro - SF1G.4, SF1G.5
Nomura, Junia - JW2A.159
Nomura, Tsuyoshi - JW2A.70
Nomura, Yutaka - FF2P.2
Nong, Zhichao - STu3B.2
Nookala, Nishant - FW4H.5, JW2A.104
Noordegraaf, Danny - AF1Q.1
Nordin, Leland J. - SF2I.7
Norgia, Michele - ATu4M.7
Norman, Justin - SM2I.6, SW3B.1, SW3Q.2, SW3Q.3, SW4I.3
Norris, Theodore B. - FTu4E.2, JW2A.129, JW2A.21
Northup, Tracy - FM3H
Norwood, Robert A. - JW2A.41
Notake, Takashi - JW2A.100
Notaras, Jelena - SF1A.5, SM3I.5, STu4B.2, SW3B.4
Notcutt, Mark - SM1L
Notomi, Masaya - FF2L.4, FM2Q.7, JW2A.50, SF1A.2, SF3A.3, SM2I.5
Novak, Ondrej - STu4O.6
Novikov, Valery - FTh4G.5
Novikova, Irina - JTh2A.31
Novitsky, Andrey - JW2A.108
Novoa, David - FW4E.5
Nozaki, Kengo - FF2L.4, JW2A.50, SF1A.2, SF3A.3, STh3A
Nozawa, Kohei - STh4K.4
Nuernberg, Jacob - Ath3O.6, JW2A.157
Nugraha, Pryo S. - JTh2A.191
Núñez-Velázquez, Martín M. - JTh2A.77, SF3I.2
Nunn, Joshua - Ath3H.8
Nunnenkamp, Andreas - FF3E.5
Nurmikko, Arto - SF1G.6
Nürnberg, Jacob - SF1G.2, SM4L.7
Nystrom, Philip D. - SW4J.7
- O**
- O'Brien, Peter - ATu3I.5
Obermeier, Julian - FW3G.2
O'Brien, Jeremy L. - FM1G.1, FTh1G.5, FTh1G.7, FTu4G.1
O'Callaghan, James - STh4B.1
Ochikubo, Lane - SF1A.4, STu4B.1
Odele, Ogaga D. - FM4G.2, FM4G.3
O'Donnell, Callum F. - JTu2A.61, STh4F.7
Oe, Ryo - JW2A.146
Oerter, Erik - JTh2A.194
Ofori-Okai, Ben - SM3A.1, SM4A.5, SW4D
O'Gara, Sean - FM1G.1
Ogawa, Hisashi - FTu4G.3
Ogura, Takashi - JW2A.141
Oguri, Katsuya - JTu2A.153
Oh, Dong Yoon - SF2J.6
Oh, Kyungwhan - JTh2A.1, JTh2A.152
Oh, Sang Soon - FM3E.6
Oh, Sang-Hyun - FF2F.7
Oh, Seongshik - FM1F.1
Oh, Seongsik - FF2D.4
Oh, Seunghoon - FM2H.5
Ohae, Chiaki - FW4E.6, JTh2A.159, SF3N.3
Ohara, Maho - STu4Q.3
Ohishi, Yasutake - JTh2A.131, JTu2A.117, JTu2A.126, JTu2A.127, JTu2A.143
Ohno, Seigo - JW2A.100
Ohodnicki, Paul - Ath3P.4, ATu4M.6, JTh2A.193, JW2A.168
Ohta, Nozomu - STu4K.5
Ohtani, Keita - SF3G.5
Ohya, Masahito - FW4F.8
Oikonomov, Michail - JTu2A.45
Okada, Kosuke - SW3D.4
Okawachi, Yoshitomo - FTh1E.4, SM1D, SM1D.6, SM3D.1, SM4L.7, STu3F.6, SW3A.4, SW4M, SW4M.5
Oki, Yuji - JTh2A.81, JTh2A.86, STh1I.7
Okoro, Chukwuemeka - FW4E.2
Oksman, Mark - JTu2A.63
Okubo, Sho - JTh2A.32, STu3P.1
Okuno, Yae - SF2G.5
Oldenbeuving, Ruud - JTh3D.2, SW4C.5
Oliveira, Vinicius S. - STu3P.5
Oliver, Jim - STu3M.6
Oliviera, Pedro - JTu2A.170
Ollanik, Adam - JTh2A.54, JW2A.109
Olsen, Maclain - JW2A.24
Olson, Don - STu4Q.4
Olson, Joshua - STh4K.6
Omachi, Junko - STu4P.6
Omar, Zunaid - AW3O.7
Omatsu, Takashige - SF3I.8, SM4O.1, SM4O.4, SW3M.3
Omoda, Emiko - JTh2A.121, STu4K.5
On, Cansu - FW4H.4, JTh2A.50
Onae, Atsushi - JW2A.156
O'Neil, Morgan - STu3N.3

- Ong, H C.- JTh2A.48, JTh2A.61
 Ong, Jun Rong - JTh2A.6
 Ono, Atsushi - JTh2A.63
 Ono, Masaaki - FF2L.4, SM2I.5
 Onodera, Hidetoshi - JW2A.50
 Onodera, Tatsuhiro - FM3G.6, FTu4A.2
 Onori, Daniel - STh4N.3
 Onuki, Yuya - JTu2A.12
 Onwukaeme, Chibuzo - STh4I.6
 Ooi, Boon S.- JTu2A.29, JTu2A.91, STu4O
 Opfermann, Justin - JTu2A.106
 Oppo, Gian-Luca - JTu2A.119, JTu2A.137
 Orazi, Leonardo - AM1M.6
 Orcutt, Jason S.- STh1B.2
 Oreffo, Richard - SM1O.4
 Oren, Dikla - FTu3E.5
 Orenstein, Meir - FF2L.3, FM2Q.5, FTh3M.3
 Oresick, Kevin M.- SF3G.1
 Orfila, Marcos - JW2A.24
 Orioux, Adeline - FM4G.4
 Origlia, Stefano - SM1L.6
 Orobtkhouk, Regis - FTh1E.5
 Ortega, Tiago - ATH4Q.2
 Ortega-Moñux, Alejandro - STh1I.3
 Osada, Alto - SF1A.7
 Osellame, Roberto - JTu2A.156
 Osipov, Timur - JF1C.3
 Osman, Ahmed - STh1I.3
 Osório, Jonas H.- SF1K.6
 Ostrovsky, Evgeny - FTh3M.4
 Osvay, Karoly - SM4N.7, STu3M.3, STu4O.1
 Ota, Yasutomo - FM1H.5, SF1A.7, SM4I, STh3A.4
 Othman, Mohamed A.- FM3Q.5
 Otohe, Tomohito - FTh1H.1
 Otsuji, Taiichi - SW4D.4
 Ott, Annika K.- FF2E.2
 Ottaviano, Luisa - STh3A.3
 Ottaway, David - SW3M.5
 Otterstrom, Nils T.- FF3E.3, SM1I.8, SM3K.5
 Ou, Jun-Yu - FM4J.4
 Ou, Yi-Hsin - STh4K.6
 Ou, Yiwen - SM2K.3
 Ou, Z.Y. - JF2B.4
 Oubei, Hassan - JTu2A.29
 Oulton, Rupert - AF1Q.7
 Ouyang, Xing - SM2C.2
 Overmeyer, Ludger - AM1M.4
 Overvig, Adam C.- FF1F.4, FF1F.6
 Oxenhimikow, Nina - FF3D.2
 Oxenlowe, Leif K.- FTh1G.5, FTh1G.7, JTu2A.120, JTu2A.68, SM2C.3, SM2C.5, STu3D.1, STu4C.1, STu4C.2, STu4C.6, SW4I.2
 Ozana, Nisan - AM4P.3
 Ozawa, Tomoki - FM3Q.4
 Ozbay, Baris N.- SW4J.7
 Ozcan, Aydogan - AM1J.4, AM1J.5, AM1J.7, ATu3J.5, ATu4J.1, STh1J.3, STh1J.5
 Ozeki, Yasuyuki - AF3Q.3, JTh2A.130, SW4K.2
 Ozigur, Umit - JTh2A.75
 Ozolins, Oskars - JW2A.31, SM2C.5, SM4C.4, SM4C.5, STu3D.1
- P**
 P, Semstiv, Mykhaylo - JTu2A.18
 Paboouf, David - Ath4Q.2
 Pacheco-Pena, Victor - JW2A.90
 Pacifici, Domenico - FF2F.1
 Padgett, Miles - FF1B.1, FW3F.7, STh3K.3
 Padihye, Anuja - JTu2A.67
 Padilha, Lazaro - FF3D.6, FF3D.7, JTu2A.114
 Padioleau, Christian - Ath4O.5
 Paesani, Stefano - FTh1G.5, FTh1G.7
 Page, Alexis - STh1I.5
 Pagliano, Francesco - JTh3C.4, STh3G.4
 Pahlevaninezhad, Hamid - AM1J.6
 Pai, Chih-Hao - FM3M.3
 Paiella, Roberto - FF1H.2, SF1J.5, STh1I
 Paik, Eunice - FF1D.2
 Paik, Seung-ho - JTu2A.105
 Paillet, Matthieu - SM1O.1
 Pajković, Rastko - SM3B.1
 Palacios, America - STh3J.2
 Palacios, Silvana - JF3B.5
 Palaferri, Daniele - JW2A.104, SF2G.5
 Pálfalvi, László - SM3A.2
 Palomino, Robert - JTu2A.27
 Paltiel, Yossi - SF2A.4
 Pan, Chien-Hung - JTu2A.25
 Pan, Ci-Ling - SM1O.3
 Pan, David - SF1A.3
 Pan, Haifeng - FW4E.1
 Pan, Jian-Wei - FTu4A.4, JTh2A.12, STu3A.3
 Pan, Jiaoqing - JTh2A.76, JW2A.62
 Pan, Liang - FW4G.1
 Pan, Meiyang - SW3I.2
 Pan, Mingsen - FM3Q.1
 Pan, Qing - Ath3O.2
 Pan, Rui - FF3F.1
 Pan, Shilong - JTh2A.144, STu3B.3
 Pan, Si Hui - JTu2A.30
 Pan, Wei - JTu2A.48
 Pan, Yan - JTu2A.48
 Pan, Yiming - STu4B.7
 Pan, Yue - JTu2A.141
 Pan, Zeyu - JTh4D.4, SM1I.2, SM1I.6
 Pan, Zhongben - SF2N.1, SF3I.5
 Panagiotopoulos, Paris - FM3M.4
 Pancaldi, Matteo - JW2A.83
 Panchenko, Evgeniy - AW4O.5
 Panda, Anurag - FW4G.8
 Pandey, Awanish - JW2A.45
 PANDEY, DEEPAK - FM2H.3
 Pandiri, Kanaka Raju - JW2A.182
 Pandya, Aditya - JTu2A.107
 Pang, Fufei - JTu2A.173, JTu3O.2
 Pang, Kai - FTu3G.4, FW4F.5, JTh2A.15, SM3C.4
 Pang, Shuo - STu3K.3
 Pang, Xiaodan - JW2A.31, SM2C.5, SM4C.4, SM4C.5, STu3D.1
 Pang, Xiao-Ning - STh3I.8
 Paniagua-Dominguez, Ramon - FTh4J.5
 Panna, Dimitry - FM2F.1
 Panoiu, Nicolae C.- FTh1D.6
 Pant, Bharat - JTh2A.177
 Pant, Mihir - FTh1G.6, STh3G.3
 Pantouvaki, Marianna - JTu2A.21
 Panuski, Christopher L.- STh3G.3
 Paoletta, Therese - JTu2A.61
 Paolucci, Francesco - SW4C.4
 Papasimakis, Nikitas - FTh3E.7
 Papazoglou, Dimitris - FM1Q.1
 Pape, Alexander - STh3N.2
 Papon, Camille - Ath3H.1
 Papp, Scott - FF2E.4, FF2E.6, FW3E.1, FW3E.5, SF2A.5, SM1D.1, SM4L.1, STh1L.1, STu3F.5, SW3A.2, SW3A.6, SW4L.2
 Paradis, Clément - SF2N.3, SM4L.6
 Parapurath, Nikhil - FM2G.1
 Parashar, Parag - AW3O.2
 Pareek, Vivek - FM4F.2, FM4F.6
 Park, Doewon - FM2H.4, SF2J.4
 Park, Jaedoek - JTh2A.152
 Park, Junhee - FTh4J.7
 Park, Jun-Hee - JTh2A.47
 Park, Kyung Hyun - JW2A.79
 Park, Namkyoo - JTu2A.136, JW2A.110
 Park, Soohyun - FF2D.4, FM1F.2, JTh2A.172
 Park, Su Ji - SM3A.1
 Park, Sunghee - JTu2A.105
 Park, Sungjun - FM1F.2
 Park, Wounghang - FW4G.5
 Park, Yongwoo - JW2A.143
 Parniak, Michal - FM4H.6, JTh2A.28, JTh2A.33
 Parsons, Kieran - SW3C.3
 Parto, Midya - FM1E.2, FM2E.3, FM2E.5, FM2G.5, FM4E.3, SW4Q.1
 Parvinnezhad Hokmabadi, Mohammad - FM4E.3, FM4E.5, FM4E.7, SW4Q.5
 Parvizi, Mahdi - SM3B.7
 Pascal, Remy - STu3M.4
 Pashkin, Oleksiy - JM2A.3
 Pasiskevicius, Valdas - Ath3O.1, JW2A.82, STh3F.4, STh4F.2
 Passian, Ali - FM1G.6
 Patel, David - SM3B.7, STh4A.7, STh4B.4
 Patel, Pari - SW4I.3
 Patera, Giuseppe - JTh2A.20
 Paterova, Anna - Ath3O.3
 Patil, Chirag M.- JW2A.11, STh3A.6
 Patimisco, Pietro - Ath1O.7, AW3R.5
 Patrick, Charles L.- AW3R.2, STu3N.2
 Patsyk, Anatoly - FF3E.2
 Patwardhan, Gauri - SF2I.5
 Paul, McManamon - ATu3R.1
 Paulus, Gerhard G.- JTu2A.151
 Paulus, Yannis M.- JW4P.3
 Pauly, Fabian - FTh1F.6
 Pavanello, Fabio - JTh4C.3, SF1A.5
 Pavilonis, Michael - AW3O.5
 Pavlov, Nikolay - STh4B.6
 Pavlovich, Margaret - FW4F.4
 Pazos-Outon, Luis - AW3O.7
 Pazzagli, Sofia - JTh2A.46
 Peacock, Anna C.- SM3D.5, SM4K, STu3K.1
 Peake, Gregory M.- FW3G.1
 Peccianti, Marco - FF1E.1
 Peczek, Anna - STu4C.1
 Pedersen, Christian - AW3S.4, SM4D.4
 Peele, John - SF3I.3
 Pe'er, Avi - FM1G.7, FM4H.3
 Pejkić, Ana - STu4B.3
 Pelc, Jason - SM2D.5
 Pellegrino, Daniele - JTh3C.4, STh3G.4
 Peller, Dominik - FM3F.1, JM2A.4
 Pelucchi, Emanuele - STh4B.1
 Peng, Chao - FM2Q.3, JW2A.172
 Peng, Cheng-Zhi - FTu4A.4
 Peng, Huanfa - JW2A.67
 Peng, Jiaxin - JW2A.3
 Peng, Junsong - FTh1M.6
 Peng, Kun - JTh2A.91, SF3I.1
 Peng, Kunchi - FTh4G.7
 Peng, Ruoming - SM2B.3
 Peng, Ruwen - FTu4E.4
 Peng, Shaowen - AF2M.8
 Peng, Siying - FM3J.5, FTh3M.2
 Peng, Tao - FM4H.4
 Peng, Tianyi - FTu4A.4
 Peng, Xiaolei - FF3F.2, JTu2A.2, SM2O.5
 Peng, Yan - Ath3Q.5
 Peng, Yujie - SM4D.1
 Peng, Zhaoqiang - JW2A.168
 PengFei, Qi - JW2A.116
 Pennetta, Riccardo - FW4E.7, SF3J.1
 Penttinen, Jussi-Pekka - JTu2A.17
 Penty, Richard V.- JTh2A.22, JTh2A.23, SM1B, STu3B
 Peraire, Jaime - FF2F.7
 Perakis, Ilias E.- FM1F.6
 Pereira Lopes, Diogo - JTu2A.156
 Perenzoni, Matteo - FF1B.4
 Perez, Edgar - SM4L.1
 Perez, Max - AM1P.3
 Perez-Leija, Armando - FTu4G.2
 Periyanyagam, Gandhi Kallarasan - JTu2A.12
 Perlstein, Joshua - Ath3P.6
 Perreault, David J.- AW3O.3
 Perrella, Chris - STu3P.3
 Perring, Anne - Ath3P.3
 Perrone, Guido - AF1M.1
 Perry, Joseph W.- JTu2A.59
 Pertsch, Thomas - FM2H.1, FTh1G.2, FW3H.1, FW4H.8
 Peschel, Ulf - FM1E.1, FTh4E.4
 Petermann, Klaus - JW2A.9, STu4C.1
 Peters, Achim - JW2A.164
 Peters, Frank - SW3Q.6
 Peters, Jon - STh1B.7
 Peters, Kara - AF1M.4, AF2M, AF3M
 Peters, Nicholas A.- FTh4G.3, FTu4A.5
 Peters, Sven - JTu2A.118
 Petersen, Christian R.- JTu2A.109, SM3D.2, SM4K.1
 Petersen, Eric - STu3N.3
 Peterson, Kristen - SM1O.7
 Peterson, Per - AW3O.7
 Petit, Stéphane - SF1N.3
 Petoukhoff, Christopher - FM4F.2, FTh1F.2
 Petrescu, Dan - JTh2A.96
 Petronijević, Emilija - JTh2A.67
 Petropoulos, Periklis - JTu2A.64
 Petrov, Valentin - ATu4J.2, SF2N.1, SF3I.5, SM2N.6, STh4F.5
 Petrovich, Marco - JTh2A.42
 Petrozza, Annamaria - FF2D.7
 Petruzzella, Maurangelo - JTh3C.4, STh3G.4
 Petway, Larry B.- AW3R.3
 Petykiewicz, Jan - STh4B.3
 Peucheret, Christophe - SM2C.5
 Peycke, Zane - JW2A.16
 Peyghambarian, Nasser - SM2N.4
 Peyrade, David - JTh2A.99
 Peysokhan, Mostafa - FF3E.4, JW2A.118, STu3K.2
 Pezer, Robert - FTh1H.7
 Pfeiffer, L. N. - FTh1H.1
 Pfeiffer, Martin - FTh1E.6, SF2A.2, SM1D.2, STh1I.1, STh4A.4, SW3A.5
 Pham, Hoan - FW3E.2, SM2D.2
 Pham, Thach - STh4I.2
 Phan, Thibao - FF3C.1, FF3C.2, FF3C.6
 Phare, Christopher T.- JTu2A.81, SM3I.2
 Phelps, Gretchen - JW2A.163
 Phillips, Christopher R.- SF2N.6, SF2N.7, SM3N.5
 Phillips, David - FW3F.7, STh3K.3
 Phillips, Ian - SM2C.6
 Phillips, Jonathan - STu4O.6
 Phillips, Mark - STu3N.4
 Phillips, Zeph - JTu2A.105
 PIACENTINI, FABRIZIO - FF1B.6
 Piao, Xianji - JW2A.110
 Picard, Emmanuel - JTh2A.99
 Piccardo, Marco - FW3E.6, SF3G.3
 Piccinotti, Davide - FTh4H.6
 Piccoli, Riccardo - FF1E.1, JW2A.81, SM4M.3, SW3N.2
 Pick, Adi - FF1E.5
 Picque, Nathalie - JW2A.157, STu3F.6
 Pidshety, Shankar - SW4K.5
 Pihler, Stefan - SM1N.4
 Pierangeli, Davide - FM3E.2, FTh3E.2
 Pierangelo, Angelo - AM2J.5
 Pierrrottet, Diego F.- AW3R.3
 Piestun, Rafael - FF3H.5, FTh1D
 Pigeon, Jeremy - JF1C.4
 Piggott, Alexander Y.- JTu2A.84, JW2A.60, STh4B.3
 Pilar, Jan - STu4O.6
 Pinhas, Hadar - JTu2A.107
 Pinna, Sergio - ATu3R.3, JTh3D.3, JW2A.52
 Pinzone, Christopher - SF2G.5
 Piot, Philippe - JF1C.5
 Pique, Alberto - JW2A.121
 Pita, Julian L.- FF1E.8, JTu2A.71, JW2A.58
 Pitarresi, Abigail R.- AF1Q.3
 Pizzi, Andrea - FW4H.7
 Pizzuto, Angela C.- JM1A.1, JM1A.3
 PLant, David V.- JTh2A.96, JW2A.6, SM3B.7, STh4A.7, STh4B.4, STu3C.1
 Plascak, Michael E.- JTh2A.166, JTh2A.167, STu3F.4
 Pleros, Nikos - JW2A.5, STh3B.7
 Plews, Alan - FTu3G.6
 Plotnik, Yonatan - FF1E.5, FM1E.3, FM1E.8
 Plum, Eric - FF1H.4
 Poddubny, Alexander N.- FM2E.4, FM2H.1, JW2A.87

- Podoleanu, Adrian G.- AW3S.1
 Podolskiy, Viktor A.- FF3C, FTh1D.7, FW4H.6
 Podzimski, Reinold - FF3P.7
 Pogorelsky, Igor - FM3M.4
 Polani, Sagi - JTu2A.101
 Poletto, Luca - JTu2A.158
 Polini, Marco - FF2E.2
 Pollick, Andrea - SF3J.5
 Pollinger, Florian - SW4L.1
 Polman, Albert - FF3C.4, FM3J.5, FTh3M.2
 Polónyi, Gyula - JTh2A.191
 Polster, Robert - JTu2A.45
 Polyakov, Sergey - FM2H.2, FTh1H, JTh2A.39
 Polyanskiy, Misha - FM3M.4
 Polzin, Wayne - SM3A.1
 Pomarico, Enrico - STh1N.4
 Pomerantz, Michael - AM1M.2
 Pomeranz, Leonard A.- STh4F.1
 Pomerene, Andrew - SF2L.4
 Poole, Philip - FTu3H.2
 Poon, Andrew W.- STh3J.6, SW3B.3, SW4B.4
 Pooser, Raphael C.- FF1B, FTh4G.3, FTu3H.4, JF2B.3, JF2B.6
 Pop, Eric - SF3A.6
 Popa, Daniel - JTh2A.179, SF3K.6
 Popov, Alexey - JTu2A.102
 Popov, Sergei - JW2A.31, SM2C.5, SM4C.4, SM4C.5, STu3D.1
 Popov, Vyacheslav - SW4D.4
 Popovic, Milos - JTh4C.3, JW2A.59, SF1A.5, STh1A.7, STh4A.2
 Porquez, Jeremy G.- AF2M.1, JTh2A.105
 Porsandeh Khial, Parham - SM3B.6
 Porschatis, Caroline - JW2A.5
 Porzi, Claudio - JTh3D.3
 Postava, Kamil - JTu2A.47
 Potemkin, Fedor - JW2A.119
 Poti, Luca - STu3C.1
 Pottie, Paul-Eric - JW2A.137
 Poulain, Marcel - STh4K.3
 Poulain, Samuel - STh4K.3
 Pouli, Dimitra - JTu4L.1
 Poulin, Michel - SM3B.7
 Poulton, Christopher V.- ATu3R.2, SM3I.5, SM3I.7, STu4B.2, SW3B.4
 Povinelli, Michelle L.- FTh1P.3
 Power, Michael - SM1O.2
 Pozzo, Lilo D.- SF1I.3
 Prabaswara, Aditya - JTu2A.91
 Prabhakar, Gautam - FTh1M.4, SW3K.1
 Prakash, Roopa - SM2D.1
 Prakash, Varun - JTh2A.25
 Pramod, Mysore - SM1L.6
 Pranovich, Alina - STu4O.6
 Prasad, Kuldeep - Ath4P.3
 Prasankumar, Rohit P.- FF3D, FM1F.4
 Prayakara, Srujana - FW4G.6
 Preble, Stefan - SF3A.4
 Predojević, Ana - FTu3H.2
 Pregnolato, Tommaso - Ath3H.1, FM1H.7
 Prendergast, David - FF1P.4
 Preter, Eyal - SM3K.7
 Previde Massara, Micol - JTu2A.128
 Priante, Davide - JTu2A.91
 Price, Alasdair - JTh2A.24
 Price, Jonathan H.- ATu3S.3
 Priebe, Katharina E.- FM4F.1
 Prilepsky, Jaroslav E.- STu4C.4
 Prilmüller, Maximilian - FTu3H.2
 Primov-Fever, Adi - AM4P.3
 Prineas, John - JW2A.125
 Prinz, Eva - FTh3M.3
 Prior, Yehiam - FF1E.7
 Probst, Rafael - STu3P.2
 Prochnow, Oliver - STh3N.2
 Proietti, Roberto - SW4C.3
 Prokopeva, Ludmila J.- FM4J.7
 Proscia, Nicholas - FTu4H.1
 Prucnal, Paul R.- Ath1Q.4, STh3B.1
- Pruessner, Marcel W.- FM2H.4, SF2J.4, SF3J.8
 Pryor, Brian - AM3P
 Pu, Minhao - JTu2A.120, SM2C.3, STh3I.1, STu4C.6, SW4A.4
 Pu, Tanchao - AF3M.2
 Pugzlys, Audrius - Ath1O.2, FF1E.2, FM1Q.1, FM1Q.2, SM4M.1
 Pupeza, Ioachim - SF1N.7
 Purdie, David - FF2E.2
 Purdy, Thomas - Ath3H, JF2B.5
 Purschke, David - SM3A.6
 Pusala, Aditya - JTu2A.156
 Pushkina, Anastasia A.- FTh4G.5
 Putnam, William - FF3D.4
 Puttnam, Benjamin - JTu2A.52, SM4C.1, SM4C.3
 Pye, Lorelle N.- Ath3P.6
- Q**
- Qadri, Noor - SF3I.3
 Qartavol, Reza M.- JTh2A.157, JTu2A.51
 Qi, Aiyi - JW2A.30, SF1G.1
 Qi, Bing - FTu3G.3, JTh2A.9
 Qi, Jipeng - STu3Q.3, STu3Q.6
 Qi, Minghao - JW2A.13, SF2A.6, SM1B.1, STh4A.1, STh4N.4, SW3C.1, SW4M.2
 Qi, Pengfei - JTh2A.178
 Qi, Renduo - JW2A.48
 Qi, Shuxian - JTh2A.112
 Qi, Yu - JW2A.1
 Qi, Zhen - SF2A.6
 Qian, Li - FM4G.7, FM4G.8, JTh2A.98, SM2K.3
 Qiang, Bo - SW4D.6
 Qiang, Xiaogang - FM1G.1
 Qiao, Jie - AM1M.2, SW3M.6
 Qiao, Wenchao - JTu2A.116
 Qin, Huaqiang - JTu2A.167
 Qin, Jiarong - AF1Q.4, STh4K.7
 Qin, Yandong - AM2J.6
 Qin, Yingxiong - JTh2A.119, JTh2A.155, JTh2A.59
 Qin, Zhengyuan - JW2A.124
 Qin, Zhiqiang - JTh2A.127
 Qin, Zhongzhong - FTh4G.7
 Qiu, Botong - AW3O.4
 Qiu, Cheng-Wei - AM1J.6, FTh3M.5, JW2A.101
 Qiu, Ciyuan - JW2A.27, SW4C.2
 Qiu, Diana Y.- FF1P.4
 Qiu, Feng - SM3B.2
 Qiu, Haodong - STh4I.6
 Qiu, Jifang - JTh2A.118
 Qiu, Kun - JTu2A.148, JTu2A.32, JTu2A.56, SM4K.6
 Qiu, Liu - FF3E.5
 Qiu, Min - JW2A.82, SW3I.2
 Qiu, Xianggang - FM1F.4
 Qiu, Yujie - FTh1M.7
 Qu, Hongwei - SF1G.1
 Qu, Shizhen - JTu2A.65
 Qu, Yunpeng - STh1I.5
 Qu, Yurui - SW3I.2
 Qu, Zhibo - STh1I.3
 Quan, Hai Tao - FF3F.1
 Quimby, Richard S.- JTh2A.135
 Quinlan, Franklyn - SM1L.4, SM2L.3
- R**
- Ra, Yong-Ho - JW2A.129
 Rabe, Martina - SM4N.2
 Rabinovich, William S.- SF2J.4, SF3J.8
 Rademacher, Georg - JTu2A.52, SM4C.3
 Rademacher, Georg F.- SM3C.2, SM4C.1
 Radic, Stojan - STh4A.8, STu4B.3
 Radil, Jan - JW2A.137
 Radonjic, Milan - FF3D.8
 Radosavljevic, Sanja - STh3I.7
 Radulaski, Marina - FTu3H.5, FTu4H, JTh3C.5, STh3B.2
 Radunskaya, Ami - AF2M.7
 Rafsanjani, Seyed M.- FW4F.5, JTh2A.15
- Raftery, James - AW4O.3
 Ragan, Regina - JTh2A.68, JW2A.175
 Ragheb, Amr - JTu2A.34
 Rahim, Abdul - SW3Q.4
 Rahimi, Esmail - FTu4E.3
 Rahimi-Iman, Arash - JW2A.135, JW2A.136
 Rahmani, Mohsen - FF1E.6, FW3G.6
 Rai, Ashish - SM3L.6
 Raimond, Jean-Michel - JF2B.2
 Raja, Arslan - STh4A.4
 Raja, Soniya S.- JTh2A.69, STu4N.2
 Rajaei, Mohsen - FTh1K.1, FTh1K.2
 Rakhman, Abdurrahim - SM1N.3
 Rakich, Peter T.- FF3E, FF3E.3, FW3E.3, SM1I.8, SM1O.2, SM3K.5
 Ralph, Timothy - FTh4G.6
 Ram, Rajeev Jagga - SF1A.5, STu3A.5
 Ramachandran, Ajith - FM1E.7
 Ramachandran, Siddharth - FTh1M.4, FTh4E.3, SM1K.1, SM1K.4, SM3K, STh3K.1, SW3K.1
 Ramalingam, Vincent Larry - SF1K.1
 Raman, Aaswath - SF2I.8
 Ramasesh, Vinay - FM3H.4
 Ramelow, Sven - FM3G.2, JTh4C.5, JTu2A.72
 Ramesh, Vishwajith - STh1J.5
 Ramezani, Hamidreza - FM2Q.1, FTh1D.5
 Ramirez, Edward - FW3F.3
 Ramírez-Martínez, N. J. - JTh2A.77
 Ramirez-Martinez, Norberto J.- SF3I.2
 Rana, Taimoor - SM4O.3
 Ranalli, Joseph - ATu4I.3
 Rand, Stephen - FF2E.7
 Randel, Sebastian - SM3B.1, SM3B.3, STh1A.1, STu3D.4
 Ranta, Sanna - JTu2A.17
 Rantamäki, Antti - JTu2A.10
 Rao, Ashutosh - JTh2A.16, JTh3C.2, SM1B.2, STu3F.4
 Rao, Yun Jiang - STh3K.2
 Rapaport, Ronen - JTh2A.37
 Rarity, John - FTh1G.5, JTh2A.24, JTh2A.5, JW2A.139
 Raskar, Ramesh - AF3Q.4
 Rasmussen, Thorsten S.- STh3A.3
 Rastegari, Ali - JTu2A.161, SM1O.7
 Rathje, Christopher - FM4F.1
 Ratner, Daniel - JF2C.3
 Rau, Markus - FTu3G.1
 Raval, Manan - SM3I.5
 Ravi, Koustuban - FF1E.3, SM4A.2
 Ray, Aniruddha - ATu3J.5
 Ray, Debdatta - JTh2A.74
 Ray, Dipanwita - JF1C.3
 Raybaut, Myriam - Ath3O.1, STu3N.7
 Raz, Oded - SW3B.5
 Raz, Ali - SM1B.3, SW3L.5, SW3L.6
 Raza, Daniel - AM2J.1
 Raziman, T.V - JTh2A.74
 Razkazovskaya, Olga - SF2N.7
 Razzari, Luca - FF1E.1, JW2A.81, SM4M.3, SW3N.2
 Reagan, Brendan - SM1N.5
 Reano, Ronald M.- SF2I.2
 REBUFELLO, ENRICO - FF1B.6
 Rechtsman, Mikael C.- FM1E, FM2E.5, FM2Q.2
 Rechtsman, Mikael C.- FM2E, FM3Q.2
 Reckinger, Nicolas - SM1O.1
 Reddy, Jay W.- AM3P.6
 Reddy, Prithvi - FTu4H.1
 Reed, Graham T.- FF1H.1, JTu2A.64, SM3B.5, STh1B.1
 Regreny, Philippe - STh3A.5
 Rehbinder, Jean - AM2J.5
 Reichel, Kimberly - FF2D.2
 Reichelt, Matthias - FF1B.8
 Reichl, Christian - FF3P.7
 Reid, Alexander H.- SM3A.1
 Reid, Derryck T.- Ath4O.6, FTh1M.1, STh1L.4
- Reimer, Christian - FTh1E.7, FW4F.2, JTh4C.2
 Reinhardt, Ori - FF1E.5
 Reis, David - FF2P.3, FF3P.2, FF3P.3, FM3F.5
 Reithmaier, Johann P.- FTh1H.6
 Rekić, Alexandre - SW4L.6
 Remez, Roei - FW4H.3
 Ren, Fang - JTh2A.113
 Ren, haonan - SM3D.5
 Ren, Jinhua - FM2E.3, FM2E.5, FM4E.3, FM4E.5, SW4Q.1
 Ren, Wei - Ath1O.3, Ath1O.7, STh4L.3
 Ren, Xiaomin - JW2A.7
 Ren, Xiaoming - FF1P.3, SF1N.1
 Ren, Yongxiong - FTu3G.4, FW4F.5, JTh2A.15, JTh2A.19
 Ren, Yuan - STu4D.5
 Ren, Yu-Xuan - FF3F.4
 Ren, Zhaoyu - JTu2A.95
 Ren, Zhiliang - JTh2A.183, JTh2A.186
 Renaud, Dylan - JW2A.135, JW2A.136
 Reno, John - Ath4Q.5, FTh4J.4, SF3G.6
 Repán, Taavi - JW2A.108
 Repp, Jascha - FM3F.1, JM2A.4
 Rerucha, Simon - JW2A.137
 Resan, Bojan - AF1Q, Ath4Q, SF2N
 Residori, Stefania - STu3M.4
 Restouin, Christine - SM3L.4
 Restrepo, Diego - SW4J.3, SW4J.7
 Reuterskiöld-Hedlund, Carl - SW3Q.5
 Rewcastle, Cory - ATu4J.5, JTh2A.98
 Reza, Amani - STu4O.6
 Reznichenkov, Bogdan - FTu3H.7
 Rhonehouse, Dan - SF3I.3, SW4K.5
 Riazi, Arash - FM4G.7, FM4G.8
 Ribeill, Guilhem - SM1I.7
 Rice, James - AF2M.5
 Richard, Inès - SF2K.4
 Richardson, Christopher - SW3B.2
 Richardson, David - ATu3S.3, JTh2A.42, JTu2A.64, SM4K.2, SM4K.5, STh3F.2
 Richardson, Kathleen - STu3F.4
 Ricken, Raimund - FM1G.3
 Rico, Maria Luisa - SM4D.3
 Riedl, Hubert - SW3B.6
 Rieffel, Eleanor - FTu4A.2
 Rieker, Gregory B.- AF1M, Ath4P.3, SW4L.7
 Rigatti, Amy - STu3M.6
 Rigaud, Philippe - JTu2A.150
 Rimke, Ingo - STh4F.5
 Riquelme, Meritxell - JTh2A.102
 Rishøj, Lars - FTh4E.3, SM1K.1
 Ritchie, David - FW3H.3, STu4D.5
 Rittershofer, Jonas - SM3B.1
 Rittmann, Thomas - FM4F.1
 Ritzkowski, Felix - JW2A.154, SF3N.4
 Rivensown, Yair - AM1J.5, STh1J.3
 Rivera, José A.- ATu4J.3
 Rivera, Nicholas - FF2L.3, FF2L.5, FM1Q.3, FM1Q.6, FM2G.2, FM3H.5, FTu4E.1, SM2O.6
 Rivet, Etienne - FF3H.3
 Roberts, Ann - AW4O.5
 Roberts, Samantha - FTu3E.2
 Robin, Thierry - JTh2A.132
 Robinson, Joseph - JTh2A.169
 Rocca, Jorge - SM1N.5, STu3M.1, STu4P.4
 Rocha, Alex Cesar Pereira - JW2A.140
 Rocha, Israel - JTh2A.102
 Rocha, Jaqueline O.- JTu2A.114
 Rochard, Philippe - SM4I.7
 Roche, Nicolas J.- JTh2A.175
 Rochette, Martin - STh3F.3, SW4L.6
 Rochman, Jake - FTu4H.4, FTu4H.5, JTh3C.3, STh3G.2
 Röcker, Christoph - SM1N.4
 Rockwood, Alex - STu3M.1
 Rödel, Christian - FF2P.3
 Ródenas, Airán - SM2N.6
 Rodionov, Ilya A.- FTu4E.6
 Rodrigo, Peter John - AW3S.4

- Rodrigues Jr., Jose J.- JTu2A.1
 Rodriguez, Brian - AF2M.5
 Rodriguez, Michael - AF3M.6
 Roelkens, Gunther - STh1B.3, STh3I.7, SW3Q.4
 Roeloffzen, Chris - JTh3D.2, SW4C.5
 Roger, Thomas - FM3E.5, SM4D.7
 Rogers, Edward T.- FM3J.2
 Rogers, John - AM3P.3
 Rogers, Katrina S.- FM3J.2
 Rogers, Steven - FTh4G.4, SF2A.3
 Rojas Hurtado, Carol Bibiana - FF3F.7
 Rojas Laguna, Roberto - Ath4O.7
 Rojo-Romeo, Pedro - STh3A.5
 Rolland, Antoine - JTh2A.185
 Rolland, Claude - SM3B.7
 Rolles, Daniel - JW2A.182
 Romagnoli, Marco - JTh3D.3
 Romanini, Daniele - Ath3Q.4
 Romano, Clement - JTh2A.132
 Romero Cortés, Luis - FW4F.2, JTh2A.157, JTh4C.2, SF3N.7
 Romero, Carolina - SM3O.2
 Romkey, Barry R.- STu3C.7
 Roney, Patrick - AF3M.7
 Rong, Yanhong - JTu2A.44
 Ronurpraful, Tejaswini - FF2F.2
 Ropers, Claus - FF3P.4, FM4F.1, FM4F.3
 Ropers, Greta - STu3B.4
 Ropp, Chad - FM2F.4
 Roques-Carmes, Charles - FM3H.5, FW4G.2, FW4H.1, FW4H.3, JW2A.101, SM4I.2
 Rorrer, Gregory - SW3J.5
 Rosamond, Mark - STu4D.4
 Rosanov, Nikolay N.- FM1E.5
 Rösch, Markus - STu4D.1
 Rosenbluh, Michael - FM4H.3, JTu2A.63
 Rosenfeld, Wenjamin - FTu3G.1
 Roskot, Lukas - STu4O.6
 Roslund, Jonathan - FW4F.1
 Rosolen, Gilles D.- FM1Q.6, FW4H.7
 Rossi, Ethan A.- JW3P.2
 Rossi, Giulio M.- FF3P.5, SF3N.5, SW3N.1
 Rossi, Leonardo - JW2A.166
 Rossi, Massimiliano - Ath3H.5
 Rostami, Habib - FF2E.2
 Rostami, Saied - JW2A.118
 Rostamian, Ali - Ath1O.4, JW2A.40, SF3J.6, STh1B.4
 Rostohar, Danijela - STu4O.6
 Rotenberg, Nir - FM1H.7
 Rotermund, Fabian - SF3I.5
 Roth, Paul - SW3K.2
 Rottenberg, Xavier - JW2A.32
 Rotter, Stefan - FF2H.3, FF3H.1, FF3H.3, FF3H.7, FM4E
 Rottwitt, Karsten - FM3G.3, FTh1G.1, FTh1G.5, FTh1G.7, JTh4C.4
 Roudas, Ioannis G.- SM3C.3
 Rouified, Mohamed S.- STh1B.1
 Roussel, Stéphane - AM2J.5
 Rousso, Aric - Ath3P.1
 Rovere, Andrea - JW2A.81
 Royall, Benjamin - JTh2A.27
 Roycroft, Brendan - STh4B.1
 Rozema, Lee - FF3D.8, FTh4G.1, FW3G.5
 Rozenman, Georgi - FM2F.2
 Roztocky, Piotr - FTh1E.7, FW4F.2, JTh4C.2
 Ru, Qitian - STh4F.3, STh4F.4
 Ruan, Wen-Sheng - STh3I.8
 Ruan, Xuezhong - STu4O.2
 Ruan, Zhngsen - STh1B.5
 Rubenchik, Alexander M.- JW2A.117
 Rubin, Noah A.- FW3E.6
 Rubino, Giulia - FTh4G.1
 Rubio, Angel - FF3P.5, FM3F.3
 Ruchkina, Maria - ATu4I.1, FM1Q.5
 Ruchon, Thierry - JTu2A.150, STh1N.3
 Rudenko, Artem - JW2A.182
 Ruder, Steven - STu4Q.4
 Rudolf, Denis - STh3N.4
 Rueda, Alfredo - FTh1E.1
 Ruehl, Axel - STu3P.5
 Ruffini, Marco - SW4C.5
 Rufino, Ana Kely - JW2A.140
 Ruhstorfer, Daniel - SW3B.6
 Rumpel, Martin - SM1N.4
 Runge, Antoine - SM3D.5
 Runge, Patrick - STu3B.4
 Ruocco, Alfonso - SF1A.6, SM3L.1, SW3B.4
 Rus, Bedrich - STu3M.2
 Rusch, Leslie A.- JTu2A.55, JW2A.43, SW3K.5
 Rusimova, Kristina - SF1K.7
 Ruskuc, Andrei - FTu4H.4
 Russell, Brandon - SM4A.5
 Russell, Philip S.- FW4E.5, FW4E.7, SF3J.1, SM2K.5, SW3K.2
 Russo, Peter - ATu3R.2
 Rusteika, Nerijus - JTh2A.146, JTh2A.154
 Ruth, Hanna G.- FF1D.2
 Rutkowski, Lucile - STu3P.4, STu3P.6
 Rybak, Leonid - FM2F.1
 Rybin, Mikhail - JTh2A.73, SW4D.6
 Rybka, Tobias - SF3N.4
 Ryckman, Judson - SM1I, SW3L.4
 Ryzckowski, Piotr - AF2Q.1
 Ryf, Roland - JTh2A.133, JTh2A.173, SM3C.1, SM3C.2, SM4C.2, STh3K.5
 Ryzhikov, Ilya A.- FTu4E.6
- S**
- S, Arun - SM1K.5
 Sabattoli, Federico - JTu2A.128
 Sabbar, Abbas F.- JTh2A.79
 Saber, Md Ghulam - JW2A.6, STh4A.7
 Sabines-Chesterking, Javier - JTh2A.5, JW2A.139
 Sabry, Yasser - AW4O.7
 Sabsabi, Mohamad - Ath4O.5
 Sacher, Joachim - Ath1O.6, Ath3O.5, JTu2A.162
 Sadeq, Zaheen S.- JTh2A.53
 Sadravia, Zarina - JTh2A.73
 Sadrri-Moshkenani, Parinaz - JW2A.175
 Sadzak, Nikola - JTh2A.37, JTh2A.38
 Safiabadali Tali, Seied Ali - FTh4M.5
 Sagnes, Isabelle - FM3Q.4
 Saha, Soham - FTh4H.1, FTh4M.4
 Sahoo, Hitesh K.- STh3A.3, SW4A.4
 Sahu, Jayanta K.- JTh2A.109, JTh2A.77, SF3I.2
 Sahu, Rishabh - FW4F.7
 Sain, Basudeb - FF1E.7
 Saini, Than Singh - JTu2A.143
 Saint-Jalm, Sarah - JW2A.137
 Saito, Lúcia - SM2N.3
 Saito, Motoharu - JTh2A.87
 Saito, Nariyuki - FF2P.4, STh4N.6
 Saito, Norihito - ATu3I.6, JTu2A.176
 Saito, Shinichi - SM3B.5
 Saito, Shuto - JTh2A.121
 Saitoh, Eiji - FF2F.8
 Sakaguchi, Atsushi - FTu4G.3
 Sakai, Kyosuke - SW3D.6
 Sakakibara, Yoichi - JTh2A.121, STu4K.5
 Sakamoto, Takahide - JTh2A.195, STh4B.5, STu4C.5
 Sakanas, Aurimas - STh3A.3
 Sakashita, Michio - ATu3I.6
 Sakuma, Hirota - SF2K.3
 Sakurai, Haruyuki - JW2A.77
 Sakurai, Yuki - JW2A.77
 Salamin, Yannick - JTh4D.5, SM2I.3
 Salamo, Gregory - FW3F.8
 Salehi, Maryam - FM1F.1
 Salhi, Mohamed - FTh1M.5
 Salman, Jad - AF3M.7
 Saltarelli, Francesco - SF2N.6, SM3N.5
 Samani, Alireza - STh4A.7
 Samanta, G. K. - FTh3E.5, FTh3E.8, STh3F.6
 Samanta, Goutam K.- JTu2A.142
 Sampaolo, Angelo - Ath1O.7, AW3R.5
 Samusev, Kirill - JTh2A.73
 Sánchez Costa, Christian - SM2C.6, STh1C.4, STh1C.5
 Sanchez Cristobal, Enrique - FM2G.5, SW4Q.1, SW4Q.5
 Sanchez, François - FTh1M.5
 Sánchez-Postigo, Alejandro - STh1I.3
 Sander, Michelle Y.- JTh2A.153, SM3D, SM4D
 Sandhu, Arvinder S.- FF1P.2
 Sandoghchi, Seyed - JTh2A.42
 Sandoghdar, Vahid - FM3G.1, FW4G.7
 Sandoval, Oscar - STh4N.4
 Sang, Fengqiao - JTh3D.5
 Sang, Yungang - JTh2A.69
 Sanghera, Jas - SF3I.3, SM1N.1, SW4K.5
 Sangla, Damien - JTu2A.88
 Sanjabi Eznaveh, Zeinab - FTh1M.3, FTh4E.6, SM3C.1
 Sanjeev, Vyshakh - FM3J.1, FTh3M.5, JW2A.101
 Sano, Tyler - SM4M.5
 Sans, Marc - JTh3D.3
 Sansone, Giuseppe - STu3M.3
 Sansoni, Linda - FW4F.1
 Santagati, Raffaele - FM1G.1, FTh1G.5, FTh1G.7, FTh4G.2
 Santana, Octavio - JW2A.58
 Santarelli, Giorgio - SM2L.5, STh4N.5
 Santschi, Christian - JTh2A.74
 Sapienza, Luca - FF2F.3, FF2H.5, FF3F, STu3A.4, STu4N
 Sapra, Neil V.- JTu2A.84, JW2A.60, STh4B.3
 Saraceno, Clara J.- SF2N.4, SM3N.5
 Saraceno, Clara J. - SM4N
 Sarang, Soumya - FF3E.7
 Sarangan, Andrew - JTh2A.71, JTu2A.6, JW2A.105, JW2A.106, JW2A.112
 Saraswat, Krishna - STh4I.6
 Saravi, Sina - FM2H.1, FTh1G.2
 Sarma, Raktim - FF3H.6, FTh4M.1, FW3H.7
 Sarmiento, Tomas - FF3P.3
 Sarpkaya, Ibrahim - FTh1F.7
 Sasada, Hiroyuki - JW2A.156
 Sasaki, Keiji - SW3D.6
 Satat, Guy - AF3Q.4
 Sato, Atsushi - STh4K.4
 Sato, Shunichi - JTu2A.16, SM4O.2
 Sato, Toru - JTu2A.92
 Sato, Yoichi - SM4N.6
 Savian, Stefano - STh1C.3
 Savinov, Vassili - FM4J.4, JTh2A.26
 Sawicka-Chyla, Magdalena - STu4O.6
 Sayles, Todd - JTh2A.180
 Sayson, Noel L.- FW3E.2
 Sayson, Noel Lito B.- SM2D.2
 Scaffardi, Mirco - SW4C.4
 Scalari, Giacomo - Ath4Q.6, STu4D.1, STu4D.3
 Scalora, Michael - JTh2A.71
 Scarani, Valerio - FTh1H.5
 Scarcelli, Giuliano - AM1J.1
 Schade, Wolfgang - Ath1O.6
 Schaefer, Jochen - STu3D.4
 Schaeffer, Christian - STh1C.1
 Schaffer, Kenneth J.- FF1P.2
 Schäfer, Sascha - FM4F.1
 Schäfermeier, Clemens - JTh2A.25
 Schares, Laurent - STh1B.2
 Schatz, Richard - SM2C.5, SM4C.4, SM4C.5
 Scheiba, Fabian - SW3N.1
 Schelkanova, Irina - JTu2A.107
 Schell, Felix - JTu2A.151
 Schepler, Kenneth - SM1B.2
 Scherbak, Sergey - JTu2A.134
 Scherm, Florian - AM1M.7
 Scheuer, Jacob - FF1H.3
 Schibli, Thomas R.- SM2L.4, STu4K.1
 Schiepel, Philipp - JW2A.138
 Schilder, Nick - FM3J.5, FTh3M.2
 Schiller, Stephan - SM1L.6
 Schilling, Ryan - Ath3H.6
 Schilt, Stephane - JW2A.161, SF2G.7, SM4L.2, SM4L.6
 Schlauderer, Stefan - FM3F.1
 Schlessler, Albert - Ath3H.5
 Schmid, Christoph P.- FM3F.1
 Schmidgall, Emma - FM1H.2
 Schmidt, Bruno E.- FM3M.2, SM3N.2, SM4M.3, SW3N.2, SW3N.3
 Schmidt, Christian - FF3P.7
 Schmidt, David - FTh3E.3
 Schmidt, Holger - JTh2A.101, JW2A.24
 Schmidt, Markus - SF1K.5
 Schmidt, Wolf G.- FTu3P.7
 Schmidtman, Sebastian - JTu2A.162
 Schmittberger, Bonnie L.- FM4H.2, SM2D.4
 Schnebelin, Come - Ath3O.4, SM1B.7
 Schneider, Christian - Ath3H.7, FM2F.1
 Schneider, Harald - JM2A.3
 Schneider, Katharina - STh3I.6, SW3A.1
 Schneider, Kevin - AW3O.5
 Schneider, Lorenz M.- JW2A.135, JW2A.136
 Schneider, Tobias - AM1M.4
 Schnepf, Matthias - JTu2A.171
 Schoelkopf, Robert J.- SM1O.2
 Scholten, Sarah - FTu3P.7
 Scholtz, Alexis - ATu4J.4
 Schomerus, Henning - FM3Q.1, FM4Q.6
 Schori, Aviad - FM1Q.7, JTh2A.7
 Schotland, John - FTu4E.2
 Schott, Rüdiger - Ath3H.1, FM1H.7
 Schramm, Malte - STu3P.1
 Schrenk, Werner - SF2G.2
 Schröder, Jochen - JW2A.71
 Schröder, Sven - SM3L.6
 Schröder, Tim - Ath3H.1, FF1B.3, FF3D.1, FM1H.3
 Schubert, Elise - Ath1O.2
 Schuck, P. James - FF1D.5
 Schüler, Ralf - ATu3I.5
 Schultze, Marcel - SM3N.4
 Schulz, Bastian - STu4O.5
 Schulz, Claus P.- JTu2A.151
 Schülzgen, A. - FTh1M.3, SM2K.6, STu3K.2, STu3K.3
 Schunemann, Peter G.- Ath4O.6, FW3E.1, JTh2A.84, JTu2A.116, JTu2A.67, SF1N.4, STh1L.4, STh4F.1, STh4F.4, STh4F.6, STh4F.7
 Schwartz, Tal - FM2F.2
 Schwartzberg, Adam - FF1P.4
 Schwarz, Benedikt - FW3E.6
 Schwefel, Harald G.- FTh1E.1, FW3E.2, SM2D.2
 Schweinsberg, Aaron - JTu2A.125
 Scully, Marlan - FM4H.4
 Sciacca, Beniamino - FF2L.1
 SCIANCALEPPORE, Corrado - JTu2A.120
 Sciarra, Stefania - FW4F.2, JTh4C.2
 Scofield, Adam - AF2Q.2
 Scopelliti, Matteo Giuseppe - Ath1Q.2
 Scotognella, Francesco - FF1D.5
 Scott, Ryan - SM4C
 Scotti, Filippo - STh4N.3
 Scranton, Gregg - AW3O.7
 Scully, Marlan - FM4H.4
 Sdobnov, Anton U.- JTu2A.102
 Seaberg, M.H. - FM1F.7
 Searles, Thomas - JW2A.106, JW2A.112
 Sebbag, Yoel - FTu4E.5, STh3F.5
 Secondini, Marco - STu3C.1, STu4C.4
 Secondo, Ray R.- JTh2A.75, JTh2A.80
 Sedlmeir, Florian - FTh1E.1
 Sedov, Evgeny - JW2A.113
 Sedova, Irina - JW2A.113
 Seeger, Angela - STu3B.4
 Segev, Mordechai - FF2H.2, FF3E.2, FM1E.3, FM1E.6, FM1E.8, FM2E.1, FM2E.3, FM2E.5, FM2Q.5, FM3Q.3, FTu3E.5, STh4N.1
 Seghilani, Mohamed - JTh2A.157
 Segura, Tatiana - ATu3J.5
 Seibel, Eduard - JW2A.138

- Seidler, Paul - STh3I.6, SW3A.1
 Seis, Yannick - Ath3H.5
 Sekhar, M. Chandra - FF1D.7
 Sekikawa, Taro - FF1P.6, JTu2A.152
 Sekine, Norihiko - JW2A.155
 Sekine, Yoshiaki - JTu2A.153
 Seletskiy, Denis - FF3D.5, JW2A.154
 Sell, David - FF3C.2, FF3C.5, FF3C.6
 Selvaraja, Shankar Kumar - JW2A.45, SM2D.1
 Semaan, Georges - FTh1M.5
 Semenova, Elizaveta - SM2C.3, STh3A.3, STh3I.1, STu4C.6, SW4A.4
 Sen, Debasish - AM2J.3
 Senellart, Pascale - FTu3H.6, FTu3H.7
 Seng, Yue Men - JTh2A.129
 Sengupta, Kaushik - STu4D, SW4D.1
 Senin, Andrey - STu4O.4
 Sensale-Rodriguez, Berardi - JW2A.76
 Seo, Dongsun - JW2A.142
 Seo, Seung Young - FF2D.4, FM1F.1, JTh2A.172
 Seok, Tae Joon - SF1A.4, STu4B.1, SW3B
 Sepherian, Hassan - JTu2A.55
 Ser, Wee - FM1G.2, FTu3G.2, JTh2A.18
 Serafino, Giovanni - JTh3D.3, STh4N.3
 Sergaeva, Olga - SM3O.4
 Serikawa, Takahiro - FTh4G.6, FTu4G.1
 Serita, Kazunori - SW3D.4
 Serrano, Diana - FTu4H.7
 Serres, Josep Maria - SF3I.5
 Set, Sze Y. - SF1K, SF2K, SF3K.4, SM3K.2
 Settembrini, Francesca F. - FTh1H.3
 Setzpfandt, Frank - FM2H.1, FTh1G.2
 Severi, Simone - JW2A.32
 Severova, Patricie - STu4O.6
 Severt, Travis - JW2A.182
 Sevillano, Pierre - JTu2A.168, JTu2A.88
 Sevison, Gary A. - JTu2A.6
 Sgambelluri, Andrea - SW4C.4
 Shabahang, Soroush - Ath3P.6
 Shabbir, Faizan - STh1J.5
 Shafak, Kemal - JW2A.138
 Shah, Deesha - FTu4E.6
 Shah, Lawrence - SW4N
 Shah, Rushabh - AW3O.3
 Shahabuddin, Mohammad - JTh2A.182
 Shahpari, Ali - JTu2A.50
 Shahsafi, Alireza - AF3M.7
 Shaikh, Waseem - JTu2A.170
 Shainline, Jeffrey - JTh4C.3, JW2A.29, SF2A.5, SF3A.5
 Shaked, Yaakov - FM1G.7
 Shakouri, Ali - FTh1K.8
 Shalaby, Hossam M. - JTu2A.46
 Shalae, Mikhail I. - FM4Q.3
 Shalae, Vladimir M. - FM2G.7, FM3E.5, FTh1K.8, FTh4H.1, FTh4J.1, FTh4M.2, FTh4M.4, FTu4E.6, FTh3H.2, SM4D.7
 Shalaginov, Mikhail Y. - FTu4E.6
 Shaltout, Amr - FTh3M, FW3H.2, SM4D.7
 Shamim, Md. Hosne Mobarok - JTu2A.29
 Shamoan, Asaf - JTu2A.107
 Shamsabardeh, Mohammadsadegh - Ath3Q.2
 Shams-Ansari, Amirhassan - FW3E.4, SF2I.3, SM1I.7, SM3B.4, STu3F.6
 Shang, Chen - SM2I.6
 Shang, Jianmin - JW2A.152, SM1L.2
 Shang, Kuanping - SM3I.6
 Shang, Qisong - JTu2A.47
 Shang, Yanling - JTh2A.117
 Shank, Joshua - FTh4M.1, FW3H.7
 Shao, Linbo - Ath3H.2, Ath3H.3
 Shao, Sizhu - JW2A.2, JW2A.23
 Shao, Zeng-Kai - STh3I.8
 Shapira, Niv - FW4H.3
 Shapiro, Jeffrey H. - FF1B.7, FM3G.4, FTu3G.5
 Sharabi, Yonatan - FM1E.3, FM3Q.3
 Sharapova, Polina - FF1B.8, FM1G.3
 Sharma, Ashutosh - JTh2A.190
 Sharma, Jahnavi - JTu2A.81, SM3I.2
 Sharma, Varun - FTh3E.5, FTh3E.8, STh3F.6
 Sharpe, Andrew W. - FTu3G.6
 Shastri, Bhavin - STh3B.1
 Shaw, Brandon - SF3I.3, SM1N.1, SW4K.5
 Shaw, Matthew - FW3F.3
 Shayan, Kamran - FTh1P.4
 Shchelokova, Alena - FM3Q.6
 Shcherbakov, Maxim R. - FTh1D.2, SF1J.7
 Shchesnovich, Valery - FTh1H.4
 She, Alan - SF3J.4
 Shehzad, Atif - SF2G.7
 Sheik-Bahae, Mansoor - FF3E.1, JTu2A.14, SM4N.5
 Shekhar, Prashant - STh4A.1
 Shemis, Mohamed - JTu2A.29, JTu2A.34
 Shen, Bing - FM1F.4
 Shen, Boqiang - JTu2A.74, SF2J.6
 Shen, Chang-Hong - AW3O.2
 Shen, Chao - JTu2A.29
 Shen, Deyuan - JTh2A.158, SF2N.1
 Shen, Huitao - FM2Q.3
 Shen, kun-ching - FW4G.4
 Shen, Li - SM3D.5, STh1B.5, STh3B.3
 Shen, Lijiong - FTh1H.5
 Shen, Lin - STh3B.4
 Shen, Xiaozhe - SM3A.1
 Shen, Yichen - FM4J.6
 Shen, Yijie - JTh2A.181
 Shen, Zhen - SF2J.5
 Shen, Zhu-Xun - FTu3H.5, JTh3C.5
 Sheng, Jiteng - Ath3H.4
 Sheng, Quan - SM2N.7
 Shepherd, David - ATu3S.3, SM4K.2, SM4K.5, STh3F.2
 Sher, Renee - JTu3O
 Sher, Renee - JTu3O.6
 Sherman, Jeff - SM1L.4
 Sherwin, Mark S. - FM3F, FM3F.4
 Shi, Bei - SW3Q.1
 Shi, Chen - JTu2A.42
 Shi, Fan - JTu2A.173
 Shi, Jinwei - JTh2A.69, SM2B.2, STu4N.2
 Shi, Kebin - SW3L.2
 Shi, Lina - AF3M.2
 Shi, Lingyan - JTu2A.97
 Shi, Sheng-Cai - FTu4A.4
 Shi, Siyuan - FM4H.8
 Shi, Wei - JTu2A.55, JW2A.43
 Shi, Xiaoyu - JTh2A.88
 Shi, Xihang - FM4J.8
 Shi, Yi - AF1Q.4, SW3I.5
 Shi, Yu - FF1F.2, SF2I.8
 Shi, Yuting - JTu2A.21
 Shi, Zhou - FF2H.4
 Shi, Zhujun - AM1J.6, JW2A.101
 Shiao, Hung-Pin - AW3O.1
 Shieh, Jia-Min - AW3O.2
 Shields, Andrew - FTu3G.6
 Shih, Bing-Hao - JW2A.26, JW2A.38
 Shih, Chih-Kang - SM2B.2, STu4N.2
 Shih, Min-Hsiung - SM2O.4, STu4N.5
 Shim, Bonggu - JTu2A.132, JTu2A.3
 Shim, Euijae - Ath3Q.1
 Shim, Hyungki - FTh1K.5
 Shim, Wooyoung - FF1D.4, FF1D.8, FM1F.2, JTh2A.172, JW2A.134, SW3I.3
 Shimizu, Hiromasa - JTh2A.60
 Shimomura, Kazuhiko - JTu2A.12
 Shimura, Keisuke - JTu2A.11
 Shin, Heedeuk - FM4G.5
 Shin, Hoseung - FTh1F.1, SW3I.3
 Shin, Ho-seung - FF1D.4, FF2D.4
 Shin, Jaewook - SW4J.6
 Shin, Jonghwa - JW2A.88
 Shin, Min Chul - SM3I.2
 Shimbrough, Kai B. - JTh2A.2
 Shinozaki, Ryo - SM4O.4
 Shinya, Akihiko - JW2A.50, SF1A.2, SF3A.3
 Shir, Daniel - AM1J.4
 Shirahata, Takuma - ATu3I.2
 Shirai, Hideto - FF2P.2
 Shirakawa, Akira - JTh2A.138, SF2N.5
 Shirakura, Yuki - SF3K.4
 Shitrit, Nir - FTh1D.5
 Shoji, Satoru - STu4P.3
 Shoji, Tyko D. - SM2L.4
 Shomroni, Itay - FF3E.5
 Shorokhov, Alexander - FM2E.4
 Shotan, Zav - FTu4H.1
 Shou, Jingwen - SW4K.2
 Showghi, Sasaan - JW2A.41
 Shpachenko, Valery - JTh2A.95
 Shrestha, Rabi - STu3D.2
 Shrestha, Sajjan - FF1F.4, FF1F.6
 Shrestha, Vivek R. - AF3M.1, FTh4J.6
 Shtauf, Mark - STu3C.3
 Shterengas, Leon - SF2G.6
 Shterman, Doron - SW4J.2
 Shtyrkova, Katia - SM3L.1
 Shu, Chester - JTu2A.66, JW2A.51, SM2I.7, SM4B.4, STu3C.2
 Shuai, Wang - JTh2A.124, JW2A.145, STu4K.2
 Shuai, Yichen - SM1O.6
 Shugaev, Maxim - JTu3O.1
 Shumakov, Valentina - Ath1O.2, FF1E.2, FM1Q.1, FM1Q.2
 Shuman, Timothy - AF3M.6
 Shutov, Anton - JTu2A.75
 Shutova, Mariia - JTu2A.135, JTu2A.75
 Shvets, Gennady - AW4O.4, FF2L.2, FM4Q.4, FTh1D.2, FW3H.5, FW4H, JW2A.114, SF1J.7
 Shwartz, Sharon - FM1Q.7, JTh2A.7
 Sibilia, Concita - JTh2A.67
 Sibson, Philip - JTh2A.24
 Sicron, Noam - SF2A.4
 Siddiqi, Irfan - FM3H.4
 Sidelnikov, Oleg - STh1C.4
 Siders, Craig W. - AM2M.1
 Sidharthan, Raghuraman - AM2M.2, JTh2A.129, STu3K.5
 Sidorenko, Pavel - SM2N.1
 Siebert, Torsten - JW2A.120
 Siefke, Thomas - FF3F.7
 Siemens, Mark E. - FF3D.1, FTu3E.6, JW2A.132, SW4J.3
 Sierra Hernandez, Juan M. - Ath4O.7
 Sifferman, Scott D. - JTh2A.85, STh4I.3
 Sigger, Florian - JTu2A.8
 Sigler, Chris - SF3G.1
 Sihvola, Ari - JTh2A.65
 Sikocinski, Pawel - STu4O.6
 Silberhorn, Christine - FF1B.8, FM1G.3, FW3F.6, FW4F.1
 Silfies, Myles - FW3E.1
 Silies, Martin - JTu2A.136
 Silva, Junior R. - JW2A.140
 Silver, Jonathan M. - FM3E.3, SM1D.4
 Silverman, Kevin L. - FF3D.3, SF3A.5
 Silverstone, Joshua W. - FTh4G.2
 Sim, Hyeonuk - JTu2A.96
 Sim, Sangwan - FF1D.4, FF1D.8, FF2D.4, FM1F.1, FM1F.2, FTh1F.1, JW2A.134, SW3I.3
 Simakov, Nikita - SM4N.3
 Simmet, Tobias - FTu3H.1
 Simmons, Evan - FW4H.6
 Simmons, Stephanie - FTu4H.3
 Simon, Peter - SM1N.8
 Simon-Boisson, Christophe - SM2N.8
 Simonds, Brian - Ath3O, ATu4I
 Simpson, M. C. - FM1F.5
 Sinclair, Gary - FTh1G.5
 Sinclair, Laura C. - SM1L.3, SM3L
 Sinclair, Michael - FTh4J.4, FTh4M.1, FW3G.1, FW4H.8
 Singh, Anshuman - Ath3H.7, FTh1G.3, SF2A.1
 Singh, Neetesh - SF1A.6, SM3L.1, SW3B.4
 Singh, Ranjan - SW4D.6
 Singh, Robinjeet - JF2B.5
 Singleton, Matthew - SF3G.2
 Sinkevicius, Vytautas - STu4O.4
 Sinobad, Milan - FTh1E.5
 Sipe, John E. - FM3G.7, FM4F.7, FM4G.7, FTh1F.4, FTh1G, FW4F, FW4F.3, JTh2A.53, JW2A.123, JW2A.158
 Siqueira, Jonathas - JTu2A.1
 Sirbu, Alexei - JTu2A.10
 Siriani, Dominic - JW2A.17
 Sirica, Nicholas - FM1F.4
 Sirota, Jacobo Marcos - ATu3R.4
 Sisler, Jared - FM3J.1
 Sivco, Deborah - AF1Q.3, FM4J.5, JW2A.96
 Sivas, Murat - FF3P.4, FM4F.3
 Sjaardema, Tracy - SM1B.2
 Skinner-Ramos, Sueli - JTh2A.58
 Skirlo, Scott - SM3I.1
 Skirtach, Andre G. - AM1J.3
 Skolnick, Maurice S. - JTh2A.27
 Skoric, James - JTh2A.96, STh4A.7
 Skovgaard, Peter - AF1Q.1
 Skrodzki, Patrick J. - FM1Q.4, SM3O.6
 Skupin, Stefan - JTu2A.121
 Slepuk, Aaron D. - AF2M.1, JTh2A.105
 Slezak, Ondrej - STu4O.6
 Sliwczynski, Lukasz - JW2A.137
 Sloan, Jamison M. - SM2O.6, SM3I.1
 Slobozhanyuk, Alexey - FM2E.4, FM3Q.6
 Smallwood, Christopher L. - FF3D.1
 Smirnova, Daria - FM2E.4, FM3Q.6, JW2A.87
 Smith, Brian J. - FM4G.1
 Smith, Christopher M. - ATu4M.2
 Smith, Jodie - STu4O.6
 Smith, Mike - ATu4I.4
 Smith, Nathan - ATu4M.4
 Smith, Sean - FTh4M.1
 Smith, Thomas - AM1M.2
 Smith, Callum - SW3M.2
 Smolski, Viktor O. - STh1L.6, STh4F.4
 Smotlacha, Vladimir - JW2A.137
 Smrz, Martin - STu4O.6
 So, Jin-Kyu - FTh1F.5
 Soares, Jorge H. - JTu2A.111
 Soavi, Giancarlo - FF2E.2, JTh2A.179, SF3K.6
 Sobon, Grzegorz J. - SF1N.4, STh4K.5
 Socquet-Clerc, Carole - JTu2A.120
 Soenen, Wouter - SW3B.5
 Sogawa, Tetsuomi - SM4L.5
 Sohn, Young-ik - Ath3H.2, Ath3H.3
 Sokolov, Alexei V. - JTu2A.135, JTu2A.75
 Solar, Dino - JTh2A.10
 Soler Penades, Jordi - STh1I.3
 Solgaard, Olav - FM3M.7
 Soljagic, Marin - FF2L.3, FF2L.5, FF2L.6, FM1Q.3, FM1Q.6, FM2G.2, FM2Q.3, FM3H.5, FM4J.6, FM4J.8, FTu4E.1, FW4G.2, FW4H.1, FW4H.3, FW4H.7, JF1C.5, SM2O.6, SM3I.1, SM4I.2
 Sollarup, Rudrakant - SF1K.5, SW3N.3
 Söllner, Immo - Ath3H.1, FM1H.7
 Solntsev, Alexander S. - FM4E.6, JW2A.34
 Solomon, Glenn S. - FM3H.2, JTh2A.34, SM1O.6
 Soltani, Mohammad - FM4E.5, SF3A.4, SM1I.7, SW4B.1
 Somaschi, Niccolo - FTu3H.6, FTu3H.7
 Son, Jangyup - FTh1F.1, SW3I.3
 Son, Myungwoo - FF2D.4, FM1F.1
 Song, Alex Y. - FM4J.5, FTu3E.7
 Song, Bong-Shik - SF1G.3
 Song, Bowen - ATu3R.3, JTh3D.5, JW2A.52
 Song, Chuang - JTu2A.44
 Song, Daohong - FM1E.7, FTh3E.4, FTh3E.6
 Song, Hao - FTu3G.4, FW4F.5, JTh2A.15, SM3C.4
 Song, Haomin - SF2I.6, SW3J.6
 Song, Haoqian - FTu3G.4, FW4F.5, JTh2A.15, SM3C.4
 Song, Hongshen - SM3O.2
 Song, Huan-yu - JTh2A.128, SW4K.1
 Song, Jang-Kun - JTh2A.188
 Song, Jin Dong - STu3A.4

- Song, Junyeob - STh1A.3
 Song, Kang-Il - JTu2A.105
 Song, Liwei - FM3F.3, SM4K.4, SW3N.1
 Song, Maowen - FTh1K.8, FTh4M.2
 Song, Meiting - JW2A.72
 Song, Mengdi - STu4C.3
 Song, Minhyup - JW2A.142
 Song, Minje - JW2A.142
 Song, Ningfang - JTh2A.174
 Song, Sanggwon - JTh2A.152
 Song, Youjian - SW4K.1
 Song, Young Min - Ath3P.5, JW2A.107
 Song, Yufeng - JTu2A.73
 Song, Yunheung - FM2H.7, JTh2A.29
 Sonnenschein, Volker - STh4K.4
 Sonthemer, Bernd - JTh2A.37
 Soon, Aloysius - FF2D.4, FM1F.1
 Sooudi, Ehsan - JTu2A.31
 Sopalla, Rafal - SW3K.2
 Sorace-Agaskar, Cheryl - JTh3D.4, SM3I.1, SW4B.5
 Sordillo, Laura - JTu2A.97
 Sordillo, Peter - JTu2A.97
 Soreff, Richard - AF1Q.5, SF1A.3, STh4I.2, STh4I.4
 Sorel, Marc - JTu2A.64, SM2B.6, SW4C.4
 SoRelle, Elliott - AM2J.3
 Sørsgård, Trygve - SF3I.6
 Sorger, Volker J. - Ath1Q.4, FTh4H.2, JW2A.3, SM1I.5, SM1I.6
 Sorianoello, Vito - JTh3D.3
 Sorin, Fabien - SF2K.4, STh1I.5
 Sorokin, Evgeni - SF1N.2
 Sorokina, Irina - SF1N.2
 Sorokina, Mariia - SM4K.6
 Sosa Morales, Maria E. - Ath4O.7
 Sotor, Jaroslaw - STh4K.5
 Sotor, Jaroslaw Z. - SF1N.4
 Sottile, Alberto - SM4N.2
 Sotto, Moise - STu3F.2
 Soufan, Ranya - AM2J.5
 Souhan, Brian - AW4O.3
 Sounas, Dimitrios - FF3C.4, FW4H.5
 Soundararajan, Rajendran - AM2J.6
 Soundararajan, Srikanal - AF2Q.4
 Spagnolo, Vincenzo - Ath1O.7, AW3R.5
 Sparapassi, Giorgia - Ath3O.7
 Späth, Luisa - SM2K.5
 Speck, James - SF1G.7, STu4Q.3
 Spector, Steven - SM3I.7
 Spektor, Grisha - FTh3M.3
 Spencer, Daryl - STu3F.5
 Spesyvsev, Roman - AF2M.3
 Spielmann, Christian - SF1K.5, SW3N.3
 Spinka, Thomas - SM2N, STu3M
 Spitz, Olivier - JTu2A.24
 Spott, Alexander - JW2A.39, STh1B.7, STu3N.1
 Sprengel, Stephan - STh1B.3
 Spring, Andrew - SM3B.2
 Squier, Jeff - ATu3J.3
 Squire, Kenny - STh3J.5, SW3J.5
 Srinivasan, Karthik - SW4I.5
 Srinivasan, Kartik - Ath3H.7, FTh1G.3, JF2B.5, SF2A.1, SM4L.1, STu3F, SW3A.2, SW4A.7
 Sriramoju, Vidyasagar - JTu2A.97
 Srinavastava, Abneesh - STu3N.5
 Srinavastava, Yogesh - SW4D.6
 Stabile, Ripalta - SW3B.5
 Stace, Tom - STu3P.3
 Stadleman, Brad - SF3I.3
 Stadler, Bethanie J. - SW4I.5
 Stagira, Salvatore - FF2D.7, JTu2A.156
 Stampfer, Lukas - JW2A.125
 Stanislauskas, Tomas - STh3F.4, STu4O.1
 Stankevicius, Evaldas - JTu3O.4
 Stanton, Eric J. - JW2A.39, STh1B.7
 Starbuck, Andrew - SF2I.4
 Starling, David J. - ATu4I.3
 Starodubov, Dmitry - FW4F.5, JTu2A.49
 Stassen, Erik - STh3I.1
 Staude, Isabelle - FTh4J.4, FW3H.1, FW4H.8
 Staudte, André - FF3P.4
 Stav, Tomer - FTu3E.5
 Steele, Aubrey - JTu3O.3
 Stefanov, André - FF1B.4
 Steffl, Jiri - JW2A.137
 Steidle, Jeffrey - SF3A.4
 Stein, Aaron - STh4A.3
 Steinberg, Aephrim M. - FF1B.2
 Steinberg, David - SM2N.3
 Steinbrecher, Gregory - JTh3D.4, SW4C.1
 Steiner, Johannes T. - FM3F.1
 Steiner, Myles - AW3O.7
 Steinforth, Austin W. - ATu4J.3
 Steinhoff, Nicholas - JTh2A.19
 Steinmetz, Tilo - STu3P.2
 Steinhilber, Gunter - STh3N, STh4N.2, STh4N.7, SW4N.1
 Stellinga, Daan - STh3K.3
 Stenger, Vincent - SF3J.5
 Stepanenko, Oleksandr - STu4D.7
 Sterczewski, Lukasz A. - SF2G.1, STh1L.5, STu4D.2
 Stern, Brian - SM1D.6, STh1A.4
 Stern, Liron - FTh4J.2, FW3E.5, JTh2A.40, JW2A.150, SM3L.5
 Stern, Nathaniel P. - STu4N.4
 Sterr, Uwe - SM1L.6
 Stettner, Thomas - SW3B.6
 Stevens, Mark L. - STu3C.7
 Stevens, Martin J. - FTh4G, FTu4G, FW3F, JTh2A.16, JTh3C.2
 Steyaert, Michiel - JW2A.57
 St-Gelais, Raphael - FTu3E.2
 Stibenz, Gero - STh4F.5
 Stickel, Andrew D. - SM3A.4, SM3A.7
 Stievater, Todd H. - FM2H.4, SF2J.4, SF3J.8, SW3L
 Stobbe, Søren - Ath3H.1, JW2A.11, STh3A.6
 Stockton, Patrick - ATu3J.3
 Stojanovic, Vladimir - SF1A.5, STh3L.7
 Stone, Jordan - FW3E.5, SM1D.1, SW3A.6
 Stott, Matthew - JTh2A.101, JW2A.24
 Stoyanov, Velizar - JTu2A.69
 Strain, Michael J. - SM2B.6
 Strait, Jared - FF2F.1
 Stranks, Samuel D. - FM4F.2
 Strasser, Gottfried - SF2G.2
 Straubinger, Christian - JTu2A.8
 Strauf, Stefan - FTh1P.4
 Stremoukhov, Sergey Y. - JW2A.119
 Stremplewski, Patrycjusz - FTh1K.7
 Sturlesi, Boaz - STh1A.6
 Su, Hongpeng - SM4D.1
 Su, Logan - JTu2A.84, JW2A.60, STh4B.3
 Su, Qiang - JTh2A.178
 Su, Qianqian - FM3M.3
 Su, Xiaolong - FM1G.2, FTh4G.7, FTu3G.2, JTh2A.18
 Su, XINzhou - SM2C.1
 Su, Ya - JTu2A.98
 Su, Yikai - SM3C, SW4C.2
 Su, Zhan - ATu3R.2, SF1A.6, STh3I.3, STu4B.2, SW3B.4
 Subedi, Ram Chandra - JTu2A.91
 Sublemontier, Olivier - JTu2A.150
 Suchkov, Sergey V. - FM4E.1
 Suchowski, Haim - FF1H, FM2F.5, FTh1D.3, JTh2A.66, SM3D.4
 Suda, Akira - JTu2A.153, JTu2A.155, SF1N.5
 Suddapalli, Chaitanya Kumar - JTu2A.60, JTu2A.61, STh4F.6, STh4F.7
 Südmeyer, Thomas - JW2A.161, SF2G.7, SF2N.3, SF2N.7, SM4L.2, SM4L.6
 Suess, Ryan J. - SM2O.1
 Sugiki, Fumihiko - JTu2A.92
 Sugita, Aitsushi - JTh2A.63
 Sugiyama, Hirokazu - JTu2A.12
 Sugiyama, Masakazu - SM4B.6
 Sugiyama, Takahiro - SF1G.4, SF1G.5
 Suh, Myoung-Gyun - SW4M.1
 Sukhorukov, Andrey A. - FM2H.1, FM4E.1, FM4E.6, JTh3C.1, JW2A.34, JW2A.99
 Sulzer, Philipp - JW2A.154
 Sumetsky, Misha - JW2A.1, SF2K.1, SF2K.2, STu3K, SW4A.5, SW4A.6
 Sumikura, Hisashi - FF2L.4
 Sumimura, Kazuhiko - JTh2A.130
 Sun, Biao - SF1K.1
 Sun, Chen - SF1A.5
 Sun, Chi-Kuang - Ath3Q.4
 Sun, Dong - FF1D.7, JTh2A.143, JW2A.131, JW2A.133
 Sun, Fang-Wen - SF2J.5
 Sun, Fuyu - JTh2A.184, JW2A.144
 Sun, Greg - AF1Q.5, STh4I.2, STh4I.4
 Sun, Hongcheng - JW2A.68, STh3I.5
 Sun, Jingbo - FM3J.4
 Sun, Keye - SM2L.1, SM2L.2, STu3B.5
 Sun, Liuyang - SM2B.2
 Sun, Lu - JTh2A.178
 Sun, Qian - FM3J.3
 Sun, Qizhen - Ath3Q.3, JTh2A.119, JTh2A.155, JW2A.167, JW2A.169, JW2A.174
 Sun, Shihao - JTh2A.91
 SUN, SHUAI - JW2A.3, SM1I.6
 Sun, Shuo - FTu3H.5, JTh3C.5
 Sun, Songsong - AW4O.6
 Sun, Wei - Ath4Q.3, SM4B.7
 Sun, Xiankai - SF3A.2, STu4B.5
 Sun, Xiao - STh4A.5
 Sun, Xiaoyu - SW4B.7
 Sun, Yangyang - STu3K.3
 Sun, Yanxiao - JTh2A.92
 Sun, Yong - FM4Q.1, FTh3E.6
 Sun, Yuezhen - JW2A.167
 SUN, ZHENG - FF1D.6
 Sung, Chun-I - JW2A.34
 Sung, Jae Hee - JTu2A.140, JTu2A.166
 Sung, Ji Ho - FF1D.8
 Suomalainen, Soile - JTu2A.28, SF2N.1
 Supekar, Omkar D. - STu4P.7, SW4J.7
 Supradeepa, V R - JTu2A.70, SM1K.4, SM1K.5, SM2D.1
 Šušnjić, Peter - JTu2A.151
 Sussman, Ben - FM4G.6
 Suter, Melissa - AM1J.6
 Sutherland, James - JTu2A.3
 Suttinger, Matthew - SF2G.4
 Suttman, Oliver - AM1M.4
 Suzuki, Junichi - JW2A.92
 Suzuki, Kensuke - SW3M.3
 Suzuki, Masaru - FW4E.6, SF3N.3
 Suzuki, Ryo - SW3A.7
 Suzuki, Shigenari - FTu4G.3
 Suzuki, Takenobu - JTh2A.131, JTu2A.117, JTu2A.126, JTu2A.127, JTu2A.143
 Svidzinsky, Anatoly A. - FM4H.4
 Swann, William C. - SM1L.3, SW4L.7
 Sweatlock, Luke - FTh1P.3
 Sychev, Demid - FTh4G.5
 Sychugov, Ilya - JW2A.31
 Sygletos, Stylianos - SM4K.6, STh1C.2, STh1C.4
 Sylvestre, Thibaut - SW3K.6
 Szameit, Alexander - FM1E.1, FM1E.8, FM1G.2, FM4E.1, FTu3G.2, JTh2A.18
 Szedlak, Rolf - SF2G.2
 Tait, Alexander - STh3B.1
 Takagishi, Taku - JTh2A.81
 Takahashi, Eiji J. - FM3M.5, JTu2A.155, SF1N.5
 Takahashi, Takuya - JW2A.127
 Takahashi, Yasushi - FF1E.4
 Takata, Kenta - FM2Q.7, JW2A.50, SF1A.2
 Takeda, Jun - FF2D.1, JM2A.1, SM3A.5
 Takeda, Koji - SF3A.3
 Takeda, Shuntaro - FTu4G.3, FTu4G.4
 Takesue, Hiroki - FTu4A.2, JTu2A.87
 Takeuchi, Kengo - FM3M.6
 Takida, Yuma - JTu2A.118, JTu2A.165, JW2A.100, SW4D.5
 Takiguchi, Koichi - STu3D.3
 Takiguchi, Koji - SF3K.4
 Takiguchi, Yu - SF1G.4, SF1G.5
 Talisa, Noah - FTh1D.2, JTu2A.125, SM3O.7
 Talker, Eliran - JTh2A.40, JW2A.150, JW2A.86, STh3G.5
 Talli, Giuseppe - SM2C.2
 Talmon, Ronen - FM1E.6
 TAM, Hwa-Yaw - SM3K.3
 Tam, Winnie - FTu3G.6
 Tamagnone, Michele - FTh1K.6, FW3E.6, JW2A.101
 Tamamitsu, Miu - AM1J.7
 Tamarat, Philippe - FTu3H.2
 Tamasaku, Kenji - JTh2A.7
 Tamazin, Heba - STh4B.4
 Tamura, Yoshiaki - SF2K.3
 Tan, Bo Xue - SW3B.3
 Tan, Chuan Seng - STh4I.6
 Tan, Hoe - JTh2A.51
 Tan, Jie - AM4P.7
 Tan, Sisi - JTh2A.148
 Tan, Swee Tiam - FTh4J.5
 Tan, Xiaohao - FF2F.4
 Tan, Xiaotian - SW3J.2
 Tan, Yuanxin - STh1I.6
 Tanabe, Takasumi - SF1J, STh1A, SW3A.7
 Tanaka, Hiroki - SF3I.7, SM1N.6
 Tanaka, Katsuhisa - JTh2A.87
 Tanaka, Koichiro - FTh1H.1, SW3D.6
 Tanaka, Masayuki - STu4Q.2
 Tanaka, Shunta - JTu2A.117
 Tanaka, Takuo - FM3J.7
 Tanaka, Yoshinori - SF1G.3
 Tanaka, Yosuke - SM2K.4
 Tanaka, Yurina - STh3L.6
 Tancik, Matthew - AF3Q.4
 Tancogne-Dejean, Nicolas - FF3P.5, FM3F.3
 Tanemura, Takuo - SM4B.6
 Tang, Cheng-Tse - JW2A.20
 Tang, Dingyuan - AM2M.2, JTh2A.147, JTh2A.158, JTu2A.174
 Tang, Hong Xing - FW3F.4
 Tang, Jingyi - JF2C.3
 Tang, Liqin - FM1E.7, FTh3E.4
 Tang, Ming - SM1C.5, SM4C.4, SM4C.5
 Tang, Shunxing - JTu2A.178
 Tang, Song - SW4Q.7
 Tang, Xiahui - JTh2A.119, JTh2A.155, JTh2A.59
 Tang, Xianfeng - JTu2A.47
 Tanghe, Ivo - SW4I.4
 Tanizawa, Ken - JTu2A.57
 Tanyi, Ekembu K. - FW4H.4, FW4H.6, JTh2A.50
 Tanzid, Mehbuba - JTu2A.82
 Tao Lau, Alan Pak - STh1C.3, STu4C.3
 Tao, Jin - JTh2A.64
 Tao, Long - FM4J.2
 Tao, Yang - JTh2A.186, JTu2A.42
 Tardif, Manon - JTh2A.99
 Tarnowski, Karol - STh4K.5
 Tate, Joshua - AW4O.3
 Tatebe, Tomoki - SM2B.5
 Tatenguem Fankem, Herve - Ath1O.6, Ath3O.5, JTu2A.162
 Taucer, Marco - FF3P.4
 Taue, Shuji - JW2A.146

- Tavani, Andrea - FM3E.2
 Tavella, Franz - SM4A.3
 Tavernier, Filip - JW2A.57
 Taylor, Jacob - JF2B.5
 Taylor, Lauren L. - AM1M.2
 Taylor, Toni - FM1F.4
 Te, Loan - FW3H.7
 Tehrani, Mehran - JTh2A.141
 Teigell Beneitez, Nuria - STh3I.7
 Teimourpour, Mohammad H. - FM3Q.1, FM4Q.6
 Teitelbaum, Samuel - SM4A.5
 Tek, Sumeyra - AM3P.2
 Tench, Robert E. - JTh2A.132
 Teng, Chu - Ath3P.1, SW3L.7
 Teng, Da - STh1J.3
 Teng, Jiajie - AF2M.4
 TENG, Min - JW2A.13
 Teng, Yanting - JTh2A.2
 Teo, Stephanie - SM4A.5
 Terabayashi, Ryohei - STh4K.4
 Tessmann, Axel - STu3D.4
 Tham, Edwin (Weng-Kian) - FF1B.2
 Thapa, Rajesh - SF3I.3
 Thelen, Jay J. - AM3P.5
 Therisod, Rita - JTh2A.99
 Thiel, Charles W. - FTu4H.5
 Thiel, Valerian - FM4G.1
 Thiele, Illia - JTu2A.121
 Thinh, Le Phuc - FTh1H.5
 Thomas, Kevin - STh4B.1
 Thomas, Paul - SF3A.4
 Thomas, Philippe - SM3L.3, SM3L.4
 Thommes, Kevin - FF3D.2
 Thompson, Bradley J. - SF2A.7, STu3Q.4, STu3Q.7
 Thompson, Jonathan - JTu2A.75
 Thompson, Mark G. - FM1G.1, FTh1G.5, FTh1G.7, FTh4G.2, JTh2A.24, STh3G, STu3A.1
 Thomson, David J. - FF1H.1, SM3B.5
 Thomson, Robert R. - AM1M.1
 Thon, Susanna - AW3O.4
 Thoroh de Souza, Eunézio - SM2N.3
 Thrift, William John - JTh2A.68
 Thurn, Andreas - SW3B.6
 Tian, Hao - SW4B.3
 Tian, Jiading - AM2M.5
 Tian, Jie - JTh2A.184, JW2A.144
 Tian, Jingyi - JW2A.82
 Tian, Lei - SF1J.5
 Tian, Long - FM4H.5
 Tian, Yuhuan - JW2A.138
 Tibai, Zoltan - JTh2A.190
 Tidemand-Lichtenberg, Peter - AW3S.4, SM4D.4
 Tiebot, Paul - JW2A.35
 Tiedau, Johannes - FW3F.6
 Tigtunseva, Ekaterina - FTh4M.6
 Tikhonchuk, Vladimir - FM1Q.8
 Timens, Roelof - JTh3D.2, SW4C.5
 Timmers, Henry - FF2E.4, FF2E.6, FW3E.1, STh1L.1, STh3F.1
 Timurdogan, Erman - ATu3R.2, SW3B.4
 Tingzon, Philippe - STu3Q.5
 Tinnefeld, Philip - AM1J.4
 Tiribilli, Bruno - JTh2A.46
 Tirole, Romain - FW4H.3
 Titchener, James - FM4E.1, FM4E.6
 Tittel, Frank - JW2A.177, JW2A.178
 Tittl, Andreas - JTh2A.74
 Titze, Michael - FF1D.3, JTh2A.41
 Tiunov, Egor - FTh4G.5
 To, Albert - ATu4M.6
 Tobin, Rachael - AW3R.4
 Tochitsky, Sergei - FM3M.4, JF1C.4
 Toda, Hiroyuki - JTh2A.195
 Toivonen, Juha - Ath4O.8
 Tokizane, Yu - JTu2A.118, JW2A.100
 Tokmakov, Kirill - SF2K.2, SW4A.5
 Tokodi, Levente - SM3A.2
 Toktamis, Melek Merve - SM1N.8
 Tokurakawa, Masaki - SF2N.2, STu4K
- Tolle, John - AF1Q.5, STh4I.2, STh4I.4
 Tollerud, Jonathan O. - Ath3O.7
 Tolstik, Nikolai - SF1N.2
 Tom, Kyle - FW3H.6, SF3A.7
 Tomadin, Andrea - FF2E.2
 Tomarchio, Flavia - STu4D.6
 Tomasino, Alessandro - FF1E.1
 Tomberg, Teemu - Ath1O.8
 Tomita, Hideki - STh4K.4
 Tomono, Yuki - JTh2A.60
 Tondiglia, Vincent - JTu3O.3
 Tonelli, Mauro - SM4N.2
 Tonello, Alessandro - SM3D.3, SM3D.6, SW3K.6
 Tong, Hoang Tuan - JTh2A.131, JTu2A.127
 Tong, Weijun - SM4C.4, SM4C.5
 Tong, Yao - JW2A.177, JW2A.178
 Tong, Yeyu - SM4B.4
 Toninelli, Costanza - JTh2A.46
 Toninelli, Ermes - FF1B.1
 Tonouchi, Masayoshi - SM4A, SW3D.4
 Toor, Fatima - JW2A.125
 Torfs, Guy - SM4C.4
 Torregrosa, Adrian J. - SM4D.3
 Torres, Alfredo - SW3Q.2
 Torres-Company, Victor - JW2A.149, JW2A.71, STu3F.1, SW3C.1
 Torrisi, Felice - STu4D.6
 Tossoun, Bassem - STu3B.5
 Tóth, György - JTh2A.189, JTh2A.190, JTh2A.191, SM3A.2,
 Toth, Milos - SM1O.5
 Toth, Szabolcs - STu4O.1
 Toufanian, Reyhaneh - FF1H.2
 Toume, Kento - JTu2A.153
 Tournie, Eric - SF1G, SF2G.3
 Toussaint, Kimani C. - FW4E.2
 Townsend, Paul - SM2C.2
 Trabold, Barbara M. - SM2K.5
 Tradonsky, Chene - SF1J.6
 Trainor, Luke S. - FTh1E.1, FW3E.2, SM2D.2
 Tran, Huong - STh4I.2
 Tran, Minh - AF1Q.2
 Tran, Thanh Tuan - JW2A.142
 Tran, Tho - STh3B.2
 Traore, Aboubakar - AF3M.6
 Traum, Christian - FF3D.5
 Travers, John C. - ATu3S.2, SM4M.2
 Trawinski, Ryszard S. - STu3N.8, STu3P.5
 Trebino, Rick - JTh2A.142, JTh2A.150
 Tredicucci, Alessandro - STu4D.6
 Tregubov, Dmitry - SF3N.3
 Tremblay, Jean-Etienne - JTh2A.166, STh4A.6, STu3F.4
 Tremblin, Pierre-Alaine - SM2L.5
 Treps, Nicolas - FW4F.1, SM4D.2
 Treu, Julian - JW2A.125
 Trevino, Jacob - FF3F.6, SM2O.7
 Trifonov, Anton - JTu2A.60
 Trifonov, Artur - FF1D.8
 Trillo, Stefano - FTh1M.8
 Trindade, Antonio Jose - STh4B.1
 Trinh, Tuan M. - FF2E.7
 Tripathi, Saurabh M. - JW2A.170
 Trivedi, Rahul - FM3H.4, JTh2A.44, JTu2A.84, JW2A.60
 Troccoli, Mariano - AW3R.5
 Trojak, Oliver J. - FF2F.3, FF2H.5, STu3A.4
 Trojek, Pavel - STu3M.2
 Tromberg, Bruce - JTu4L.1
 Tropheme, Benoit - JTu2A.168, STh4N.5
 Trotter, Douglas - SF2I.4
 Troughton, Michael - AM1M.1
 Trovatiello, Chiara - FF1D.5
 Trugman, Stuart - FM1F.4
 Truong, Gar-Wing - STu3P.3
 Truong, Viet Giang - JTh2A.45
 Trusheim, Matthew - FF1B.3, FM1H.3, FTu4H.2
 Trushin, Maxim - FTh1F.6
 Tsai, Din Ping - FF1F.3, FM4J.4, FW4G.4, JTh2A.26, JTh2A.70
 Tsai, Juei-Hung - JW2A.37
- Tsai, Meng-Tsan - JTh2A.171, JTh2A.52
 Tsai, Miao-Chan - FW4H.8
 Tsai, Tracy - Ath4P.4
 Tsai, Wei-Yi - FM4J.4, JTh2A.26
 Tsakiridis, Apostolos - STh3B.7
 Tsang, Hon K. - JW2A.66
 Tsang, Hon Ki - JTh2A.62, JTu2A.39, JTu2A.58, SM2I.7, SM4B.4
 Tsang, K.S. - AF2Q.3
 Tsauryan, Yeghishe - Ath3H.5
 Tse, Chun Ho - JTh2A.129
 Tsegaye, Tedros - SM2C.4
 Tsekrekos, C P. - STh1C.4
 Tsekrekos, Christos - FW3H.4
 Tsekrekos, Christos P. - SM4K.6
 Tseng, Derek - AM1J.4
 Tseng, Ya-Hsin - JTu2A.4, JTu2A.5
 Tsesse, Shai - FF2L.3, FM2F.1, FM2Q.5, FTh3M.4
 Tsia, Kevin K. - AF3Q.2, STh1N.5, STh3N.6, SW4J.5
 Tsiokos, Dimitris - JW2A.5
 Tsuchizawa, Tai - SM2I.5
 Tsunekawa, Masato - FF2L.4
 Tsutsui, Hironori - STu3P.1
 Tu, ChengHou - JTu2A.141
 Tu, Jian - STu4O.2
 Tu, Raymond - FF3F.6
 Tuan, Tong Hoang - JTu2A.126, JTu2A.143
 Tuckey, Philip - JW2A.137
 Tuennermann, Henrik - JTh2A.138
 Tukiainen, Antti - SW4Q.4
 Tung, Jung-Chen - SF3I.8
 Tung, Vincent C. - FF1P.4
 Tur, Moshe - AF1M.6, FTu3G.4, FW4F.5, JTh2A.15, JTu2A.49, SM3C.4, SW3A.5
 Turchinovich, Dmitry - FF2D.1
 Turcicova, Hana - STu4O.6
 Turcu, Edmond - STu4O.2
 Turek, John - ATu4J.6
 Turitsyn, Sergei K. - FW3H.4, SM4K.6, STu4C.4
 Turner, J.J. - FM1F.7
 Turquet, Léo - FF1E.6
 Turtaev, Sergey - STh3K.3
 Turza, Krzysztof - JW2A.137
 Tyler, Glenn - JTh2A.19
 Tyumenev, Rinat - SM2K.5
 Tzang, Omer - FF3H.5
 Tzarouchis, Dimitrios - JTh2A.65
 Tzeng, Yan-Kai - FTu3H.5, JTh3C.5
 Tzortzakakis, Stylianos - FF1E.2, FM1Q.1, FM1Q.2, JTu2A.113
- U**
- Uchida, Kazuki - JTu2A.12
 Uchida, Ken-ichi - FF2F.8
 Uchida, Kento - FTh1H.1
 Uchida, Megumi - STu3L.6
 Udalcovs, Aleksejs - JW2A.31, SM2C.5, SM4C.4, SM4C.5
 Uenoyama, So - SF1G.4, SF1G.5
 Ulanov, Alexander - FTh4G.5
 Ulbricht, Ronald - FF3D.1
 Umezawa, Toshimasa - JTu2A.15, STh4B.5
 Ummethala, Sandeep - STu3D.4
 Umnikov, Andrey A. - JTh2A.77, SF3I.2
 Underwood, Kenneth J. - JTh2A.85, STh4I.3
 Ung, Garrett - AW3O.4
 Unger, Claudia - AM1M.4
 Ünlü, M. Selim - ATu3J.1
 Unternährer, Manuel - FF1B.4
 Uphues, Thorsten - JTu2A.157
 Urakami, Tatsuhiro - FM3J.7
 Urashdin, Sergei - JW2A.83
 Urbanek, Karel - FM3M.7
 Urbaniak, Robert - JW2A.137
 Urbas, Augustine - Ath3P.7, JTu2A.130
 U'ren, Alfred - FTu4G.2
 Uren, Robin T. - SW3M.2
 Urick, Vincent J. - SM1C.6
 Utsunomiya, Shoko - FTu4A.2
- V**
- V. Kovalev, Anton - FTh1E.7
 Vabishechich, Polina - FTh4J.4, FW3G.1, FW4H.8
 Vagionas, Christos - STh3B.7
 Vahala, Kerry - JTu2A.74, SF2J.6, SW4M.1, SW4M.6
 Vainio, Markku M. - Ath1O.8, STh4F
 Valavanis, Alexander - STu4D.4
 Valente, Karolina Papera - STh3J.2
 Valente, Stefano - JTh2A.140
 Valenzuela, Anthony - JTu2A.125
 Vallée, Réal - STh4K.2
 Vallini, Felipe - FM4Q.8, SW4Q.4
 Valovcin, Darren C. - FM3F.4
 Valuckas, Vytautas - FTh4J.5
 Vamos, Lenard - SF1N.7
 Vampa, Giulio - FF3P.2, FF3P.3, FF3P.4
 Van Campenhout, Joris - JTu2A.21
 van de Groep, Jorik - FW3H.2
 van Dijk, Paul - JTh3D.2
 van Gorsel, Rik - AM1P.4
 Van Hoof, Rita - JW2A.32
 van Howe, James - JTu2A.51
 Van Kerrebrouck, Joris - SM4C.4
 Van Laer, Raphaël - JW2A.35
 Van Mechelen, Todd F. - FTu3E.4
 van Otten, Frank - JTh3C.4, STh3G.4
 Van Stryland, Eric W. - FF2E.1, JTu2A.59
 Van Vaerenbergh, Thomas - STh3B.2
 Van, Vien - JW2A.85, STh4A.1
 Vanacore, Giovanni M. - STh1N.4
 Vanderbruggen, Thomas - JF3B.5
 Vanderhoef, Laura - JTu2A.125
 Vanier, Francis - Ath4O.5
 Vanslebrouck, Michael - STh3I.7
 VanThourhout, Dries - FF2E.3, JTu2A.21, JW2A.35, SW4I.4
 Vanwolleghem, Mathias - STu4D.7
 Varallyay, Zoltan - STu3M.3
 Varju, Katalin - STu3M.3
 Varkentina, Nadezda - FW4E.4
 Vasilyev, Michael - JTu2A.77
 Vasilyev, Sergey - STh4F.3, STh4F.4
 Vasireddy, Praful - FF3D.4
 Vaskin, Aleksandr - FTh4J.4, FW4H.8
 Vasquez, Heriberto - JTu2A.145
 Vassilev, Stanislav K. - JTh2A.114
 Vaswani, Chirag - FF2D.5, FM1F.6
 Vavassori, Paolo - JW2A.83
 Vázquez de Aldana, Javier - SM2N.6, SM3O.2
 Vedala, Govind - JTu2A.35, JW2A.147
 Veerarahgavan, Ashok - JTu2A.82
 Veilleux, Sylvain - JW2A.65
 Veinot, Jonathan G. - JW2A.31
 Veitas, Gediminas - STu4O.1
 Veitch, Peter - SM4N.3, SW3M.5
 Velazquez-Benitez, Amado M. - FTh4E.5
 Velc, Radek - JW2A.137
 Venkataraman, Vivek - STu3F.6
 Venturelli, Davide - FTu4A.2
 Vercruyse, Dries - JTu2A.84, JW2A.60
 Verdier, Agnes A. - JW2A.55
 Veretenov, Nikolay A. - FM1E.5
 Verhaegen, Michel - JTh3D.2
 Verhagen, Ewold - FM2G.1, JTh3C.4
 Verma, Varun - SF2A.1
 Vermeulen, Diederik - ATu3R.2, SF1A.6, SM3L.1, SW3B.4
 Veronis, Georgios - JTh2A.55
 Versini, Gilles - SW4N.7
 Vertchenko, Larissa - FM4J.1
 Veselis, Laurynas - JTh2A.146, JTh2A.154
 Vetter, Sharon - JF2C.3
 Veyssi, Mehdi - FTh1K.2
 Vezzoli, Stefano - FM3E.5, SM4D.7
 Vidal, Yehuda - SM4N.4
 Vidal-Codina, Ferran - FF2F.7
 Vietz, Carolin - AM1J.4
 Vigilante, Gregory - JTu2A.90
 Vigiari, Caterina - FTh4G.2
 Viheriälä, Jukka - JTu2A.28

- Vikram, B S - SM2D.1
 Vilera Suarez, Mariafernanda - AF1Q.1
 Villalba, Jesus - FM1G.4
 Villatoro, Joel - SM2K.6
 Villeneuve, David - FF3P.4
 Villiger, Martin - AM2J.2
 Villinger, Massimo - ATH3P.6
 Vincent, Brandy A. - AM3P.2
 Vincenti, Maria A. - JTh2A.71
 Vincetti, Luca - SF1K.6
 Vinod, Abhinav K. - JTh2A.160, JTu2A.76, SW3A.3
 Viotti, Anne-Lise - STh3F.4
 VIRZI', SALVATORE - FF1B.6
 Viskontas, Karolis - JTh2A.146
 Visscher, Ilka - JTh3D.2
 Visser, Ate - JTh2A.194
 Viswanathan, Nirmal K. - JW2A.102
 Viti, Leonardo - STu4D.6
 Vitiello, Miriam S. - STu4D.6
 Vitullo, Dashiell L. - SF2K.2, SW4A.5, SW4A.6
 Vizet, Jérémy - AM2J.5
 Vo, Sonny - FW4F.6
 Vodopyanov, Konstantin L. - STh1L.6, STh4F.3, STh4F.4
 Vogl, Tobias - FTu3G.1
 Vogt, Dominik W. - JW2A.74
 Vogt, Stefan - SM1L.6
 Voiry, Damien - FTh1F.2
 Voitech, Josef - JW2A.137
 Volet, Nicolas - STh1B.7, STu3F.5
 Vomir, Mircea - SW4N.7
 von Finck, Alexander - SM3L.6
 Voronin, Alexander - FM1Q.2
 Vovan, Andre - JTu2A.43, SW3C.2
 Vozzi, Caterina - FF2D.7, JTu2A.156
 Vrakking, Marc J. - JTu2A.151, STh3N.1, SW3N.6
 Vu, Dinhduy - JTh2A.145
 Vuckovic, Jelena - FF3P.3, FM1H.4, FM3H.4, FTu3H.1, FTu3H.5, FW3H.2, JTh2A.44, JTh3C.5, JTu2A.84, JW2A.60, STh4B.3, SW4Q.3
 Vuong, Luat - FF3F.6, JTu2A.145
 Vurgafman, Igor - SF2G.1, STh1B.7, STu3N.1
 Vyhlidka, Stepan - STu3M.2
 Vynck, Kevin - FF1H.1
 Vyylecka, Michal - STu4O.6
- W**
- Wabnitz, Stefan - FTh1E.2, FTh1M.7, SM3D.3, SM3D.6, STu4C.3, SW3K.6, SW4M.2
 Wacławek, Johannes P. - AM2M.7
 Wada, Naoya - JTu2A.52, SM4C.1
 Wada, Satoshi - ATu3I.6, JTu2A.176
 Wada, Yoshiki - FF2F.8
 Wade, Mark T. - JTh4C.3, SF1A.5
 Wagner, Hans Peter - JTh2A.51
 Wagner, Kelvin - FF3H.5
 Wagner, Omer - JTu2A.107
 Wahls, Sander - JTh3D.2
 Wai, P. K. A. - JTh2A.125, JW2A.4, SW4M.4
 Waks, Edo - FF2L.8, FTh3M.7, JTh2A.30, JTh2A.35, SW3B.2
 Walasik, Wiktor - FM4Q.3
 Waldburger, Dominik - Ath3O.6, JW2A.157, SF1G.2, SM4L.7
 Wallace, Michael J. - JTu2A.26
 Wallis, Robert - FW3H.3, STu4D.5
 Walmsley, Ian - Ath3H.8, FTh1H.4
 Walsh, Michael - FF1B.3, FM1H.3
 Walter, Guillaume - STu3N.7
 Walther, Martin - STu3D.4
 Walther, Philip - FF3D.8, FTh4G.1, FW3G.5
 Walther, Thomas - JTh2A.136
 Wan, Chenghao - AF3M.7
 Wan, Chenhao - JTh2A.59
 Wan, Lingxiao - FM1G.2, JTh2A.18
 Wan, Noel - FM1H.3, FTu4E.7, FTu4H.2
 Wan, Yang - FM3M.3
 Wan, Yating - SM2I.6, SW3B.1, SW3Q.2, SW3Q.3
 Wan, Yuhang - JTh2A.104
 Wandel, Scott - FM1F.7
 Wang, Alan X. - JTh2A.193, JTh2A.56, JW2A.180, SM1I.3, SM4B.2, STh3J.5, SW3J.5
 Wang, Bin - AW4O.2, JW2A.145, SM3K.4
 Wang, Bo - FTh3M.1
 Wang, Cai-Zhuang - FF2D.5, FM1F.6
 Wang, Chao - FTh4H.5, JW2A.19
 Wang, Cheng - FW3E.4, SF2I.3, SM1I.7, SM3B.4, STh3B.5, SW4M.3
 Wang, Chingyue - JTh2A.156
 Wang, Chu - JW2A.19
 Wang, Chun-Hsiung - AF2M.2
 Wang, Chunhua - JTu3O.2
 Wang, Chun-Yuan - SM2B.2, STu4N.2
 Wang, Chuting - STh3G.2
 Wang, Cong - SM1B.1
 Wang, Curtis - SW4Q.2
 Wang, Dake - STu4N.3
 Wang, Dan - JTu2A.141
 Wang, Danshi - JTu2A.44
 Wang, Di - FTh1K.8, FTh4M.2
 Wang, Donglin - JTu2A.103
 Wang, Dongxing - JW2A.152
 Wang, Evan W. - FF3C.2, FF3C.5
 Wang, Fang - SM4C.2
 Wang, Feng - AM4P.2
 Wang, Frank (Fengqiu) - AF1Q.4, STh4I, STh4K.7, SW3I.5
 Wang, Gang - FF2E.2
 Wang, Gaozhong - AM2M.6
 Wang, Gencheng - JTh4D.4
 Wang, George - FW4H.8
 Wang, Guanghui - AM4P.7, FF3F.5
 Wang, Guo Ping - JW2A.111
 Wang, Hai - FM4H.5
 WANG, Hailing - JW2A.30
 Wang, Hailong - JTh2A.11
 Wang, Hanchen - SM1N.5
 Wang, Hanwen - SW3I.5
 Wang, Haojie - JW2A.42
 Wang, Heming - JTu2A.74, SF2J.6
 Wang, Hong - STh1B.1, STh4I.6
 Wang, Hongda - AM1J.5, AM1J.7
 Wang, Hongjie - JTu2A.98
 Wang, Hongxiang - JTh2A.195, JTu2A.36
 Wang, Huaiqiang - STu4B.7
 Wang, HuiTian - JTu2A.141
 Wang, Imbert - SF1A.5, STh1A.7
 Wang, Jade P. - STu3C.7
 Wang, Jian - JW2A.12, JW2A.28, SM2C.1, SM3B, SM4B, STh1B.5, STh3B.3
 Wang, Jiangbo - JTh2A.79
 Wang, Jiangfeng - JTu2A.163
 Wang, Jianjun - JTh2A.91, SF3I.1
 Wang, Jianwei - FM1G.1, FTh1G.5, FTh1G.7
 Wang, Jiaying - STu3Q.3, STu3Q.5, STu3Q.6
 Wang, Jigang - FF1D, FF2D.3, FF2D.5, FM1F.6
 Wang, Jingbo - FM1G.1
 Wang, Jingyi - JW2A.167
 Wang, Jun - JTu2A.174
 Wang, Junjia - FF2E.2
 Wang, Junjie - Ath3Q.3
 Wang, Jyhpyng - FM3M.3
 Wang, Kai - FM4E.1, FM4E.6, FM4F.7, JW2A.158, JW2A.169, JW2A.34, JW2A.99
 Wang, Kangpeng - AM2M.6, STh1N.4
 Wang, Kejia - SW3D.7
 Wang, Ken X. - AW3O.6
 Wang, Lei - SM4D.6
 Wang, Letian - FW3H.6
 Wang, Li - JTh2A.11
 WANG, Liang - SM3K.3
 Wang, Liqian - JTu2A.42
 Wang, Lixian - SW3K.5
 Wang, Lon A. - ATu3J.4
 Wang, Lulu - STh1B.5
 Wang, Meihong - FTh4G.7
 Wang, Meng - SF2G.6
 Wang, Mengqi - JTh2A.76
 Wang, Mengxuan - SM4I.4
 WANG, Mingjin - JW2A.30
 Wang, Mohan - Ath3P.4, ATu4M.6
 Wang, Mu - FTu4E.4
 Wang, Ning - SW4D.2
 Wang, Pan - JTu2A.167
 Wang, Pei-Hsun - SW3C.1
 Wang, Pengfei - JTh2A.76, SM4D.1
 Wang, Pu - JTh2A.112, SF1K.4, STu4F.4, SW3N.3
 Wang, Qiang - Ath1O.7, JTu2A.43, SW3C.2
 Wang, Qijie - FM3E.6, JTu2A.65, SF1K.1, SW4D.6
 Wang, Qing - STh4B.2
 Wang, Qinsheng - JTh2A.143
 Wang, Rui - JTh2A.151, SM1I.6
 Wang, Ruijun - STh1B.3, STh3B
 Wang, Ruli - JTh2A.139, JW2A.153
 Wang, Shaojie - FF1H.5
 Wang, Shaokang - JTh2A.125, SF2A.6
 Wang, Sheng - SM1K.7
 Wang, Shoujun - STu3M.1
 Wang, Shuming - FF1F.3, JTh2A.70
 Wang, Suo - AF1Q.7
 Wang, Teng - JTu2A.173
 Wang, Tianshu - JTu2A.54
 Wang, Tianwu - JM2A.2, SW3D.1
 Wang, Ting - SW4I.6
 Wang, Tingyun - JTu2A.173, JTu3O.2, SM2K.2
 Wang, Toa - FTh1E.7
 Wang, Tsong Dong - JW2A.78
 Wang, Wanjun - STh1B.1
 Wang, Wei - JTh2A.11, JTh2A.76
 Wang, Wen - JTu2A.147
 Wang, Wenting - JTh2A.160, JTu2A.76
 Wang, Xi - FW3H.6, SF3A.7
 Wang, Xiaolong - JTh2A.91, SF3I.1
 Wang, Xiaowei - FF1H.2
 Wang, Xiaoxi - FTh1G.4, JW2A.63
 Wang, Xiaoxin - FW3F.8, STh4I.1
 Wang, Xiaoyong - JTh2A.151, JW2A.128
 Wang, Xichen - JTh2A.117
 Wang, Xijie - SM3A.1
 Wang, Xing-Yuan - AF1Q.7
 Wang, Xu - JW2A.53
 Wang, Xueding - JW4P.3
 Wang, Xuejiao - AM2M.5
 Wang, Xuping - JTh2A.94
 Wang, Yadong - JTu2A.119, JTu2A.137, SM4K.7
 Wang, Yaguo - SM1I.2
 Wang, Yahui - JTu2A.108
 Wang, Yan - JTh2A.128
 Wang, Yang - SF1N.1
 Wang, Yanrong - JTh2A.69
 Wang, Ye - SM2I.1
 Wang, Yi - JW2A.66
 Wang, Yicheng - SF2N.1, SF3I.5
 Wang, Yi-Chieh - JW2A.91
 Wang, Yifang - JW2A.27
 Wang, Yi-Lun - AF1Q.7
 Wang, Yin - FM3J.3
 Wang, Yingying - SF1K.4, STu4F.4, SW3N.3
 Wang, Yong - AW4O.6, STu3M.1
 Wang, Yongrui - FW3E.6, SF3G.3
 Wang, Youmin - SM3I.3
 Wang, Yu - JTu2A.115
 Wang, Yuan - FF1D.1, FM2F.4, FM2Q, FTh1D.5, SM4I.1, SW3L.3
 Wang, Yu-Chi - SF1I.4
 Wang, Yue - STu4P.3
 Wang, Yun - STh4A.7, STh4B.4
 Wang, Yuying - SF3I.1
 Wang, Zehui - AM2M.5
 Wang, Zhaona - JTh2A.88
 Wang, Zhen - Ath1O.7, FTu4A.4, STh4L.3
 Wang, Zheng - SF1A.3, SM3K.5
 Wang, Zhenlin - FF1F.3
 Wang, Zheqi - SF3J.1
 Wang, Zhiqun - FM4H.4
 Wang, Zhiming - FTh1E.7
 Wang, Zhixin - Ath4Q.4
 Wang, Zhong - FM3Q.8
 Wang, Zhuoxian - FM2G.7, FTh4M.2
 Wangüemert Pérez, J. Gonzalo - STh1I.3
 Wanie, Vincent - JTu2A.158
 Wanke, Michael - FW3H.7
 Warburton, Richard - Ath3H.1, FM1H.7
 Ware, Matthew - FM4F.5
 Warner, Jeffrey - JTh2A.175
 Warrender, Jeffrey - JTu2A.90, JTu3O.5, JTu3O.6, JTu3O.7
 Wasilewski, Wojciech - FM4H.6, JTh2A.28, JTh2A.33
 Wasserman, Daniel - SF2I.7
 Watanabe, Hideki - STu4Q.2
 Watanabe, Katsuyuki - SF1A.7, STh3A.4
 Watanabe, Tatsuhiko - FTh4H.1, SM1I.4, SM4B.1
 Watt, Ryan - JTh2A.3
 Watts, Michael - ATu3R.2, SF1A.6, SM3I.5, SM3I.7, SM3L.1, STh3I.3, STu4B.2, SW3B.4
 Waxman, Eleanor - STh1L.2
 Weathersby, Stephen - SM3A.1
 Webb, Benjamin - STu3M.5
 Webb, Karen E. - FW3E.2, SM2D.2
 Wee, Jungyun - AF1M.4
 Weeber, Jean Claude - JW2A.5
 Weedbrook, Christian - FTu4G.6
 Wegener, Martin - SM4O.5
 Wegscheider, Werner - FF3P.7
 Wei, Binbin - FW3H.3, STu4D.5
 Wei, Cai - AF1M.2
 Wei, Chengli - JW2A.179
 Wei, Dong - STu3P.3
 Wei, Haoyun - JW2A.162
 Wei, Jinlong - STh1C.5
 Wei, Juan - JTh2A.144
 Wei, Junxiang - STh4F.6
 Wei, Liang-Yu - JTu2A.39
 Wei, Qingshan - AM1J.4
 Wei, Shi - SM2N.7
 Wei, Shuwen - JTu2A.106
 Wei, Wu - SF3I.6
 Wei, Xiaoming - SF3K.1, STh1N.5, STh3N.6
 Wei, Xinrui - Ath3H.4
 Wei, Xuan - FF1P.4
 Wei, Yang - FW3H.6
 Wei, Yuan - SF3K.1
 Weigel, Peter - SF2I.4
 Weih, Robert - SF2G.2
 Weiks, Gregor - FTu3H.2
 Weikle, Robert M. - SM2I.1
 Weimann, Steffen - FM1E.8, FM4E.1
 Weiner, Andrew M. - FM4G.2, FM4G.3, JTh4D.2, JTu2A.112, JW2A.71, SF2A.6, SF3N.2, SM1B.1, STh4N.4, SW3C.1, SW4M.2
 Weinfurter, Harald - FTu3G.1
 Weingartz, Nicholas - JW2A.182
 Weiss, Sharon M. - STh3A.2
 Welch, Eric - FM3M.4, JF1C.4
 Welch, G. - FM1F.7
 Wells, Brian - FTh1D.7
 Welter, Pol - STh3I.6
 Wen, Feng - SM4K.6, STh1C.4
 Wen, Jianxiang - JTh2A.115
 Wen, Rui-Tao - AW3O.3
 Wen, Ye - FW4G.1
 Wen, Yuanhui - SW3M.4
 Weng, Wenle - JTh4D.3
 Wenner, Brett R. - JTu2A.77
 Went, Cora - FF1H.6
 Wentzel, Michael-Henr - FF1D.2
 Werle, Christian - JTu2A.171
 Werley, Christopher - SM4A.5
 Werner, Kevin - FTh1D.2, JTu2A.125, SM3O.7
 Wernsing, Keith - ATu3J.3

- Werschler, Florian - FF3D.5
 Wesemann, Lukas - AW4O.5
 West, K. W. - FTh1H.1
 Westberg, Jonas - AW3R.2, JW2A.165, SF2G.1, STh1L.5, STu3N.2, STu4D.2, SW3L.7
 Westbrook, Paul - SW4K.4
 Westergren, Urban - SM4C.4
 Westly, Daron - FTh1G.3, SM4L.1
 Westreich, Ohad - SF2A.4
 Wetzel, Benjamin - FTh1M.7, FW4F.2, JTh4C.2
 Wheeler, Natalie - JTh2A.42
 Whibberley, Peter - JW2A.137
 white, Andrew - FTu3H.7
 White, Ian - JTh2A.22, JTh2A.23
 White, Timothy - JTu3O.3
 White, Tommi - AM1M.6, JTu3O.1
 Whitehead, James - JW2A.16
 Whitson, Michael - ATu3R.2
 Wickramasinghe, Hemantha K. - FTh1K.1, FTh1K.2
 Widmann, Claudia - JTh2A.38
 Wieck, Andreas - Ath3H.1, FM1H.7
 Wiederhecker, Gustavo S. - JTu2A.111
 Wiederrecht, Gary - FTh4M.3
 Wiersma, kort - SM2N.4
 Wierzbowski, Jakob - FTu3H.1, JTu2A.8
 Wilcox, Russell - SM4M.5, SM4M.6
 Wilhelm, Alex M. - FTh3E.3
 Wilkes, Callum - FM1G.1
 Wilkins, Matthew - JTu3O.6
 Wilkinson, James S. - STh1L.3
 Wilkinson, Timothy D. - STh1L.2
 Willatzen, Morten - JW2A.108
 Williams, Benjamin - JTu2A.24
 Williams, Brian - FTu4A.5
 Williams, Calum - STh1L.2
 Williams, Jim - JTu3O.6
 Williams, Jonathan - AM3P.3
 Williams, Kaia - SM4A.1
 Williams, Paul - Ath1O, Ath4O, AW4O
 Williams, Pheona - JW2A.112
 Williams, Robert J. - FF3E.7
 Williams, William P. - STu4P.5
 Willner, Alan E. - FTu3G.4, FW4F.5, JTh2A.15, JTh2A.4, JTu2A.49, JTu2A.53, SM1D.2, SM3C.4, STu3B.1, STu3Q.4, SW3A.5
 Wilmer, Brian - JTu2A.125
 Wilson, Christopher - SM1N.1
 Wilson, Dalziel - Ath3H.6, STh3L.6, SW3A.1
 Wilson, Luke R. - JTh2A.27
 Wilson, William L. - FTh1K.6
 Wimmer, Martin - FTh4E.4
 Winchester, Andrew - FM4F.2, FM4F.6
 Windeler, Matthew - SM4A.3
 Windeler, Robert - SW4A.5, SW4A.6
 Windham, Gary L. - STu4P.5
 Winkelmann, Lutz - SF3N.1, STu4O.5
 Winkler, Paul - JTu2A.171
 Winnerl, Stephan - JM2A.3
 Winzer, Peter J. - SM3B.4, SW3C.4
 Wirth, Justin - STh4A.1
 Wise, Frank W. - FTh1M.3, FTh4E.1, FTh4E.6, FTh4E.7, SF3K.3, SM2N.1, SM3D.4, SM4K.3
 Wisk, Patrick - SM1K.3
 Witte, Stefan - STh3N.4
 Wittek, Steffen - FM2E.3, FM2E.5, FM4E.3
 Witting, Tobias - JTu2A.151, SM4M, STh3N.1, SW3N.6
 Wittwer, Valentin J. - JW2A.161, SF2N.3, SF2N.7, SM4L.6
 Wlodarczyk, Krystian L. - AM1M.5
 Woerner, Michael - FM4F.4, JW2A.120
 Woggon, Ulrike K. - FF3D.2
 Wojtkowski, Maciej - FTh1K.7
 Wolf, Christopher - JTh2A.90
 Wolf, Jean-Pierre - Ath1O.2, FM3M.2
 Wolf, Johanna - Ath4Q.4, STh1L.5
 Wolf, Michael - AM4P.3
 Wolf, Omri - FW4H.5, JW2A.104
 Wolfe, Christopher - JTu2A.125
 Wollman, Emma - FW3F.3
 Wondimu, Sentayehu Fetene - SM4I.6
 Wonfor, Adrian - JTh2A.22, JTh2A.23
 Wong, Chee Wei - FTh1F.7, JTu2A.24, JTu2A.56, JTu2A.62, JTu2A.76, JW2A.61, SW3L.4, SW4A.3
 Wong, Chee-Wei - FF1H.5, FTh1E.3, JTh2A.160, JTu2A.148, SM1B.6, SW3A.3, SW4L.3
 Wong, E Laine - FM4F.2, FM4F.6
 Wong, Franco N. - FM3G.4, FTu3G.5
 Wong, Gordon K. L. - SW3K.2
 Wong, Jinghao - JTu2A.122
 Wong, Kam Sing - JTu2A.133, SF3A.1
 Wong, Kenneth Kin-Yip - AF3Q.5, JTh2A.116, JTh2A.126, JTh2A.134, JTh2A.148, SF3K.1, SM1K, SM1K.7, STh1N.5, STh3N.6, SW4J.5
 Wong, Liang Jie - FF1E.5, FM1Q.6, FM2G.2, FTu4E.1, FW4H.7, JF1C.5
 Wood, Thomas - STh3A.5
 Woodburn, Philip J. - FTu4H.5
 Woodhead, Christopher - STu3A.4
 Woodley, Michael T. - FM3E.3, SM1D.4
 Woodward, John - AF3M.6
 Woodward, Robert I. - STh4K.1, STh4K.3
 Wörner, Hans Jakob - SM3N.2, SM4M.3
 Wozniak, Pawel - FM2G.4
 Wright, Joel G. - JTh2A.101
 Wright, John - JTu3L.2
 Wright, Logan - FTh4E.7, SF3K.3, SM2N.1, SM3D.4
 Wright, Robert - Ath4P.3, SW4L.7
 Wright, Thomas A. - Ath3H.8
 Wu, Baojian - JTu2A.148, JTu2A.32, JTu2A.56, SM4K.6
 Wu, Bo - ATu3J.2, JTu2A.147, JW2A.91
 Wu, Chengyin - FM1Q.8
 Wu, Chongzhao - SF3G.6
 Wu, Dexin - AF2M.8
 Wu, Dong-Yi - AM2M.3
 Wu, E - FW4E.1
 Wu, Fan - FTh4E.2, FTh4E.6
 Wu, Guan hao - ATu3I.4, JW2A.160
 Wu, Guiling - STh3B.5
 Wu, Guorong - JW2A.138
 Wu, Haibin - Ath3H.4
 Wu, Hong - JW2A.152
 Wu, Jiagui - JTu2A.24
 Wu, Jia-Gui - FF1H.5, SM1B.6
 Wu, Jiamin - SW3J.4
 Wu, Jian - JTh2A.118
 Wu, Jiang - STh4I.5
 Wu, Jiayang - JW2A.22, SM1B.4, SM1B.5, STh1A.5, STu3F.7
 Wu, JieYun - JTu2A.147
 Wu, Jingda - JTh2A.3
 Wu, Junqiao - FW3H.6, SF3A.7
 Wu, Kaiyi - SW3B.3, SW4B.4
 Wu, kan - JW2A.27, JW2A.56
 Wu, Lin - JTh2A.64
 Wu, Marcelu - FW4F.6
 Wu, Meng-Chang - FM4H.2, SM2D.4
 Wu, Ming C. - JTh2A.166, SF1A.4, SM3I.3, SM4I.3, SM4I.5, STh4A.6, STu3F.4, STu4B.1, STu4N.6
 Wu, Pengfei - JTh2A.94, SM3O.1
 Wu, Pin Chieh - FF1F.3, JTh2A.70
 Wu, Qiao - SW3D.7
 Wu, Qile - FM3F.4
 Wu, Qing - Ath4O.3, JTh2A.104, JTh2A.82, JTh2A.83, SF3I.4, SF3K.2
 Wu, Sarah - ATu3J.6
 Wu, Shao-Hua - FTh1P.3
 Wu, Shuhui - Ath3H.4
 Wu, Sihan - JTh2A.118
 Wu, T - JTh2A.82, JTh2A.83, SF3K.2
 Wu, Tinghui - STh4I.5
 Wu, Wei-Hsin - SW3N.5
 Wu, Wen-Jung - AF2M.2
 Wu, Wentao - JTu2A.175
 Wu, Xi - SW4A.2, SW4B.6
 Wu, Xiaohua - FTu3H.2
 Wu, Xiaojun - SM4A.4
 Wu, Xinru - JTu2A.39, JTu2A.58, JW2A.66, SM4B.4
 Wu, Xiong - STu3B.2
 Wu, Yang - FW3F.8
 Wu, Yichen - AM1J.7
 Wu, Yipeng - FM3M.3
 Wu, Yuanjie - STu3P.2
 Wu, Yuehan - JW2A.153
 Wu, Yunfei - STh1A.2
 Wu, Yuqing - STu4D.5
 Wu, Zhihang - JTu2A.54
 Wu, Zilong - STh1I.4
 Wunderer, Thomas - STu4Q.1
 Wünsch, Sebastian - STu3B.4
 Wuytens, Pieter - SW3L.6
 Wyatt, Adam - JTu2A.170
 Wysocki, Gerard - Ath3P.1, AW3R.2, JW2A.165, SF2G.1, STh1L.5, STu3N.2, STu4D.2, SW3L.7
 X
 Xi, Lixia - JTu2A.47
 Xi, Xiang - SF3A.2
 Xi, Yuyin - SF1I.3
 Xia, Jinsong - JW2A.25
 Xia, Peiyu - FF2P.4, JTu2A.154, SW3N.7
 Xia, Shiqi - FM1E.7, FTh3E.4
 Xia, Shiqiang - FM1E.7
 Xiang, Dao - FTu4E.3
 Xiang, Maolin - FF2D.1
 Xiang, Yang - JTh2A.119, JTh2A.155
 Xiang, Yinxiao - FF3F.4
 Xiao, Chang - FF1F.6
 XIAO, JUN - FF1D.1
 Xiao, Licheng - JW2A.75
 Xiao, Meng - FF1F.2, FF3P.3, FM2Q.4, FM3Q.7, SW4A.1
 Xiao, Min - JTh2A.151, JW2A.124, JW2A.126, JW2A.128
 Xiao, Qirong - AM2M.5
 Xiao, Xi - JW2A.53
 Xiao, Xian - JW2A.49, SW4C.3
 Xiao, Xiangpeng - JW2A.167
 Xiao, Xiaosheng - JTu2A.167, JTu2A.89
 Xiao, Xu - JW2A.56
 Xiao, Xuedi - AF2M.8
 Xiao, Yu - JTh2A.59
 Xiao, Yuzhe - AF3M.7, JW2A.121
 Xiao, Zhihao - JTh2A.31
 Xie, Caifang - JTh2A.13
 Xie, Changde - FTh4G.7
 Xie, Changqing - AF3M.2
 Xie, Feng - FW3E.6, SF2G.5, SF3G.3
 Xie, Guodong - FTu3G.4, FW4F.5, JTh2A.15, SM3C.4
 Xie, Huikai - JTu2A.103, JTu2A.99
 Xie, Linli - SM2I.1
 Xie, Min - STh1A.8
 Xie, Ming-Yuan - STh3I.8
 Xie, Qijie - JW2A.51
 Xie, Shangran - SF3J.1
 Xie, Shizhong - AF2M.4
 Xie, Weiqiang - SW4I.4
 Xie, Xiaojun - SM2L.2, SM2L.3
 Xie, Xiaopeng - SM2L.5
 Xie, Xiaoya - JTu2A.138
 Xie, Xiu-Ping - JTh2A.12
 Xie, Zhaoxin - SM2N.7
 Xie, Zhenda - FTh1E.3
 Xin, Jun - JTh2A.11
 Xin, Ming - SF1A.6, SM3L.1, SW3B.4
 Xing, Chenyang - JTu2A.73
 Xing, Sida - JTh2A.93
 Xing, Yingbin - SW4K.6
 Xing, Zhikun - JW2A.174
 Xiong, Chi - STh1B.2, SW3L.7
 Xiong, Chunle - FTh1G.8
 Xiong, Qihua - AM4P.5
 Xiong, Wen - FF3H.2
 Xiong, Zeng - SM2K.3
 Xiu, Faxian - JW2A.133
 Xu, Bing - FM1F.4
 Xu, Bingxin - JTh2A.124, STu4K.2
 Xu, Bo - JTu2A.149, JTu2A.32, STu4K.1, STu4K.6
 Xu, Chi - JTu2A.86, JW2A.46
 Xu, Chris - Ath1Q
 Xu, Hengying - JTu2A.47
 Xu, Huizhong - FF3F.4
 Xu, Jiaming - SF2G.5
 Xu, Jian-Bin - SF3A.2
 Xu, Jing - AM1M.2
 Xu, Jingjun - FTh1M.7, FTh3E.4, JTu2A.139
 Xu, Kai - FF2D.1
 Xu, Kun - JTh2A.127, JTh2A.165, JW2A.73
 Xu, Lei - FF1E.6, FW3G.6
 Xu, Lin - ATu3S.3, SM4K.2, SM4K.5, STh3F.2
 Xu, Luhua - STh4A.7
 Xu, Mengyang - SW3D.5
 Xu, Mingyu - FM1F.6
 Xu, Peipeng - SF3A.6
 Xu, Shanhui - JTu2A.164
 Xu, Shanshan - JTh2A.44
 Xu, Sia Jia B. - STh1B.1
 Xu, Wenhao - FF3F.5
 Xu, Xiaodong - FTh1F.3
 Xu, Xiaochuan - JTh4D.4, SM1I.2, SM1I.6
 Xu, Xiaodong - JTh2A.158, JW2A.16, SF2N.1
 Xu, Xingyuan - JW2A.22, SM1B.4, SM1B.5, STh1A.5, STu3F.7
 Xu, Yanping - SW3L.3
 Xu, Yelong - JTu2A.55, JW2A.43
 Xu, Yin - JW2A.4
 Xu, Yolanda - STh1I.3
 Xu, Yongbing - AF1Q.4, STh4K.7, STu4O.2, SW3I.5
 Xu, Yongchi - JW2A.67
 Xu, Zhe - SF3J.3
 Xu, Zhen - FTu4E.2
 Xu, Zhongxiao - FM4H.5
 Xu, Zhuojing - JF3B.3
 Xuan, Yi - FTh4M.2, SW3C.1, SW4M.2
 Xue, Bing - SF1N.5
 Xue, Muyu - STu3A.3
 Xue, Qiao - AW4O.1
 Xue, Xiaoxiao - AF2M.8, JTh4D.2, JW2A.42
 Xuwen, Shu - JTh2A.122, JW2A.1
 Y
 Yablonovitch, Eli - AW3O.7, SM4I.3, SM4I.5, STu4N.6
 Yacomotti, Alejandro - SM4I.7
 Yadav, Deepika - SW4D.4
 Yadav, Dinesh - FTh1F.6
 Yadgarov, Lena - FM2F.5
 Yagi, Hideki - SF2N.5
 Yahiaoui, Riad - JW2A.106, JW2A.112
 Yair, Or - FM1E.6
 Yakovlev, Vladislav - FF3H.6
 Yalunin, Sergey V. - JTu2A.15
 Yamada, Hirohito - JTu2A.15
 Yamagiwa, Masatomo - JW2A.155
 Yamamoto, Hiroki - STu3P.1
 Yamamoto, Hirotsugu - JW2A.155, STh3L.3
 Yamamoto, Naokatsu - JTh2A.195, JTu2A.15, STh4B.5, STu4C.5
 Yamamoto, Yoshihisa - FTu4A.2
 Yamamoto, Yoshinori - SF2K.3
 Yamanaka, Masahito - STh4K.4
 Yamaoka, Yoshihisa - JW2A.141
 Yamasaki, Satoshi - FM3J.7, JW2A.92
 Yamashita, Daiki - FF1E.4
 Yamashita, Shinji - ATu3I.2, SF3K.4, SM3K.2
 Yamilov, Alexey G. - FF2H, FF3H.6
 Yan, Aidong - Ath3P.4, ATu4M.6, JW2A.168
 Yan, Chao - Ath3P.1
 Yan, Hai - SF3J.6, SM1I.2
 Yan, Juanjuan - JW2A.181
 Yan, Ke - JTh2A.186
 Yan, Lianshan - JTu2A.48
 Yan, Libin - FM1G.2

- Yan, Man - SM1K.3
 Yan, Ping - AM2M.5
 Yan, Qinghui - FM3Q.8
 Yan, Renpeng - JTu2A.175
 Yan, Wei - AW4O.6, SF2K.4, STh11.5
 Yan, Xiruo - JTh2A.3
 Yan, Zhijun - Ath3Q.3, JTh2A.119, JTh2A.155, JW2A.167, JW2A.169, JW2A.174
 Yan, Zhongbo - FM3Q.8
 Yan, Zijie - SM2O, SM2O.2
 Yanagimoto, Ryotatsu - FM3G.6
 Yanagitani, Takagimi - SF2N.5
 Yang, Ao - FF2F.4
 Yang, Changsheng - JTu2A.164
 Yang, Changxi - JTu2A.89
 Yang, Chan-Shan - SM1O.3
 Yang, Chi - JTh2A.182, JTu2A.19, JTu2A.27
 Yang, Chih-Wen - FF1D.1
 Yang, Daeho - FM2H.5
 Yang, Fan - Ath1O.3
 Yang, Guoqing - JTu2A.98
 Yang, Hongzhi - Ath3O.3
 Yang, Hung - JTu2A.5
 Yang, Jianji - FF3C.2, FF3C.5, FF3C.6
 Yang, Jie - SM3A.1
 Yang, Jing - JTh2A.178
 Yang, Jinghui - FTh1E.3, JTh2A.160, JTu2A.62, JTu2A.76, SW3A.3, SW4L.3
 Yang, Kiyoul - JTu2A.74, SF2J.6, SW3Q, SW4M.6
 Yang, Li Ping - FW3F.4
 Yang, Lin - AF2Q.4, JTu2A.178, JW2A.14, JW2A.2, JW2A.23, SW4C.6
 Yang, Lingxiao - SM1K.7
 Yang, Luyun - STu3K.4
 Yang, Pengzhen - FTh1M.7
 Yang, Qi - JTh2A.64
 Yang, Qifan - JTu2A.74, SF2J.6, SW4M.6
 Yang, Run - FM1F.4
 Yang, Seung Hoon - FF1D.4, JTh2A.172, SW3I.3
 Yang, Seunghoon - FTh1F.1
 Yang, Shang-Da - AM2M.3, JTh2A.170, JTu2A.131, SW3N.5
 Yang, Shanglin - SW4C.6
 Yang, Shih-Yuan - JW2A.34, JW2A.44
 Yang, Sigang - AF2M.4, SM1D.3, SW3Q.7
 Yang, Sui - SM4I.1
 Yang, Sung-Lin - JW2A.34, JW2A.44
 Yang, Wenjie - JTu3O.6
 Yang, Xiong - SF3I.6
 Yang, Xu - FF2D.5, FM1F.6
 Yang, Yang - Ath4Q.5, STu4D.2
 Yang, Yawei - SM4M.6
 Yang, Yi - FF2L.6, FW4G.2, FW4H.1, FW4H.3, SM4I.2
 Yang, Yu - JTh2A.113
 Yang, Yuanmu - FW4H.8
 Yang, Yudong - FF3P.5, JTu2A.157, SF3N.5, SW3N.1
 Yang, Yujia - FW4H.1, SM4I.2
 Yang, Yunyi - STu3F.7
 Yang, Yuxing - JW2A.27
 Yang, Zhaoju - FM4J.8
 Yang, Zhenchun - Ath4O.1
 Yang, Zhengang - SW3D.7
 Yang, Zhibin - JW2A.131
 Yang, Zhili - FTh3M.7
 Yang, Zhongmin - JTu2A.164, SW3K.3
 Yang, Zhou - FF3E.1, JTu2A.14, SM4N.5
 Yang, ZuPo - JTh2A.52, JTu2A.93
 Yanikgonul, Salih - JTh2A.6
 Yankov, Metodi - STu4C.2, STu4C.6
 Yannai, Michael - FTh3M.1, FTh4J.8, SF1J.6
 Yao, Baicheng - JTh2A.179, SF3K.6
 Yao, Chenyu - Ath1O.3
 Yao, Jianping - JTh4D.1
 Yao, Jianquan - SM2N.7
 Yao, Jie - FW3H.6, SF3A.7
 Yao, Jin - FTh4H.6
 Yao, Jinping - JTu2A.149, STh11.6
 Yao, Kaiyuan - FF1D.5
 Yao, Quan - JTh2A.12
 Yao, Ruizhe - FM4Q.5, FTh4J.3, JTu2A.7
 Yao, Shun - STh4B.2
 Yao, Xiaotian S. - JTh2A.117, JTu2A.98
 Yao, Xinwen - STh1J.4
 Yao, Yongxin - FF2D.5, FM1F.6
 Yao, Yu - FTh4H.5, JW2A.19
 Yao, Yuhan - JW2A.53
 Yao, YungChi - JTh2A.171, JTh2A.52
 Yao, Zhanshi - STh3J.6
 Yardimci, Nezh T. - SM2K.1
 Yarotski, Dmitry - FM1F.4
 Yasaka, Hiroshi - STu3Q.2
 Yasuda, Masami - JTh2A.32
 Yasui, Takeshi - JW2A.141, JW2A.146, JW2A.155, STh1L.3, STh3L.3
 Yazdandoust, Fatemeh - Ath3O.5
 Ycas, Gabriel - FF2E.6, FW3E.1, STh1L.1, STh1L.2
 Ye, H. - FTh3E.8
 Ye, Hanyu - JTu2A.60, STh4F.6
 Ye, Jianchao - JW2A.117
 Ye, Mengyuan - STh3I.3
 Ye, Ming - FTh4J.6
 Ye, Peide - FTh4M.1, FW3H.7
 Ye, Yu - SM4I.4
 Ye, Zhichao - STu3F.1
 Yegnanarayanan, Siva - JTh3D.4, SW4B.5
 Yeh, Chien-Hung - JTu2A.39, JTu2A.58
 Yeh, TingWei - JTh2A.171, JTh2A.52
 YeHui, Liu - STu3K.4
 Yen, Chen-Tung - Ath3Q.4
 Yen, Tzu-Hsiang - JW2A.20, JW2A.26, JW2A.38
 Yeo, Junyeob - FW3H.6
 Yeom, Dong-il - JTh2A.152, SM2N.5
 Yi, Anlin - JTu2A.48
 Yi, Fei - FF2F.4, FF2F.6
 Yi, Hongming - STu3N.5
 Yi, Jipeng - STu3Q.5
 Yi, Jun - FF1D.1
 Yi, Xingwen - JTu2A.56, STh1C.2, STu3C.4
 Yi, Xu - JTu2A.74, SF2J.6, SW4M.6
 Yi, Zhenhuan - FM4H.4
 Yibo, Wang - STu3K.4
 Yilmaz, Hasan - FF3H.4, FM3E.6
 Yin, Feifei - JTh2A.127, JTh2A.165, JW2A.73
 Yin, Liang - SM1N.5
 Yin, Siyao - JW2A.153, SW3L.1
 Yin, Xiaobo - FM4Q, FTu3E.1
 Yin, Xin - SM4C.4, SW3B.5
 yin, yanchun - FF1P.3, SF1N.1
 Yin, Yu-Feng - JTu2A.40
 Ying, Hao - STh1C.2
 Ying, Zhoufeng - SF1A.3
 Yogo, Hirofumi - JTh2A.63
 Yokota, Nobuhide - STu3Q.2
 Yokoyama, Shiyoshi - SM3B.2, SM3B.3
 Yonezawa, Hidehiro - FTh4G.6, FTu4G.3
 Yoo, Daehan - FF2F.7
 Yoo, Je Yoon - JTu2A.166
 Yoo, Kyungwan - JTu2A.136
 Yoo, S. J. Ben - Ath3Q.2, JW2A.49, SM3I.6, STh3I.4, SW4C.3
 Yoo, Seongwoo - AF1M.3, AM2M.2, JTh2A.129, JTh2A.147, JTu2A.174, STu3K.5
 Yoo, Young Jin - JW2A.107
 Yoo, Yung Jun - SM4A.7
 Yoon, Duhee - FF2E.2, SF3K.6, STu4D.6
 Yoon, Jin Woo - JTu2A.166
 Yoon, Yoseob - FM2Q.3
 Yoshida, Kenji - STh4K.4
 Yoshida, Masahiro - SF1G.3
 Yoshii, Kazumichi - JW2A.159, SF3N.3
 Yoshikawa, Jun-ichi - FTh4G.6, FTu4G.3, JTh2A.21
 Yoshimi, Hironobu - JTh2A.130, SW4K.2
 Yoshioka, Hiroaki - JTh2A.81, JTh2A.86, STh1I.7
 Yoshioka, Katsumasa - FF2D.1, FF2D.6, JM2A.1
 Yoshita, Masahiro - FTh1H.1
 You, Jian Wei - FTh1D.6
 You, Li - JTh2A.36
 You, Lixing - FTu4A.4
 You, Qun - JTh2A.64
 You, Yongsang - FF2P.3, FM3F.5
 You, Zheng - FW3H.6, SF3A.7
 You, Zi-Xuan - JTu2A.40
 Youn, Inchan - JTu2A.105
 Young, Brenton C. - AM2P.2
 Young, Jeff - JTh2A.3
 Young, Joshua - JW2A.179
 Young, Robert - STu3A.4
 Yousefi, Mansoor I. - STu4C.3
 Yu, Cheng-Li - SM2O.4
 Yu, Chia-Ju - JW2A.26
 Yu, Chung-Ping - JTh2A.89
 Yu, Da-Peng - JTh2A.143
 Yu, Fei - SF1K.1
 Yu, Hao - Ath4O.4, JW2A.54
 Yu, honglin - FTh4M.2
 Yu, Hongyan - JTh2A.76
 Yu, Hsin-Hung - JW2A.151
 Yu, Juan - JTh2A.91
 Yu, Kyoungsik - SM3I.3
 Yu, Lingjie - JW2A.48
 Yu, Mengjie - SM3D.1, STu3F.6, SW4M.5
 Yu, Mengyuan - STh1J.5
 Yu, Mingbin - FF1H.5, FTh1E.3, JTh2A.160, JTu2A.76, SM1B.6, SW3A.3, SW4L.3
 Yu, Nanfang - FF1F.4, FF1F.6
 Yu, Nanjie - STu3K.6
 Yu, Peichen - AW3O.2
 Yu, Ping - AM3P.3, JM2A.4
 Yu, Qian - JW2A.180
 Yu, Qianhuan - SM2I.1, SM2L.2
 Yu, Raymond - JW2A.72
 Yu, Shaogang - JTh2A.41
 Yu, Shui-Qing - AF1Q.5, FW3F.8, JTh2A.79, STh4I.2, STh4I.4
 Yu, Siyuan - SW3M.4
 Yu, Si-Yuan - STh3I.8, STu3B.2
 Yu, Song - JW2A.152, SM1L.2
 Yu, Su Peng - SF2A.5
 Yu, Sunkyu - JTu2A.136, JW2A.110
 Yu, Su-Peng - SW3A.2
 Yu, Wen - STu3B.2
 Yu, Xia - SF1K.1
 Yu, Xianbin - STu3D.1
 Yu, Xin - JW2A.177, JW2A.178
 Yu, Yang - FM4Q.4
 Yu, Yi - STh3A.3
 Yu, Ying - SF3K.1, STh1N.5
 Yu, Yu - SM2L.2
 Yu, Zejie - STu4B.5
 Yu, Zhaoning - AF3M.7
 Yu, Zongfu - SF2I.6, SW3J.6
 Yuan, Guanghui - FM3J.2
 Yuan, Hualei - SF3I.5
 Yuan, Jie - FF2D.2
 Yuan, Jinhui - JW2A.4, SW4M.4
 Yuan, Luqi - FM2Q.4, SW4A.1
 Yuan, Ning - FF2D.1
 Yuan, Xiao - FTu4A.4
 Yuan, Zhiliang - FTu3G.6
 Yuanqin, Xia - JW2A.130
 Yudovich, Shimon - FM1Q.7
 Yue, Yang - JTu2A.43, SW3C.2
 Yulevich, Igor - FTh4J.8
 Yumoto, Junji - JW2A.77, JW2A.80
 Yumoto, Masaki - JTu2A.176
 Yun, Seok-Hyun - ATu3J.6, FM2G.6, FM3J.6, JTu2A.23, SF1I.2, SW3J.4
 Yung, Man-Hong - FM1G.2, JTh2A.18
 Yurkiv, Vitaliy - FF3F.6
 Yvind, Kresten - JTu2A.120, SM2C.3, STh3A.3, STh3I.1, STu4C.6, SW4A.4
- Z**
- Zach, Armin - SM1K.3
 Zach, Shlomo - JTu2A.49
 Zadok, Avi - JTu2A.63, JTu2A.80, SF2A.4, SM3K.1, SM3K.7, STu4F.3
 Zaghloul, Mohamed - Ath3P.4
 Zahavy, Tom - STh4N.1
 Zaidi, Aun - FTh3M.5, FW4H.1, SM4I.2
 Zaidi, Zain - ATu4M.5
 Zakhidov, Anvar - AF1Q.6, FTh4M.6
 Zaki, Sajid - SF2K.2, SW4A.6
 Zalevsky, Zeev - AM4P.3, JTu2A.101, JTu2A.107
 Zamboni-Rached, Michel - JTu2A.110, STu4P.2
 Zang, Jichao - AF1M.3, STu3K.5
 Zang, Jizhao - SM2I.1, SM2L.2, STu3B.5
 Zang, Kai - STu3A.3
 Zang, Xiaorun - FF1E.6, FW3G.3
 Zangeneh Kamali, Khosro - FW3G.6
 Zaouter, Yoann - STh1N.3
 Zapata, Juan - SM2N.3
 Zapata, Luis - SM4A.4
 Zaquine, Isabelle - FM4G.4
 Zarubin, Vera - JTu2A.145
 Zavarin, Evgeniy - STh3I.1
 Zawadzki, Robert J. - JW4P.2
 Zawilski, Kevin - JTh2A.84, JTu2A.116, STh4F.7
 Zayats, Anatoly - FTh1D.7
 Zayko, Sergey - FM4F.3
 Zaytsev, Alexey - SM1O.3
 Zdagkas, Apostolos - FTh3E.7
 Zederbauer, Tobias - SM3L.6
 Zektzer, Roy T. - SM3L.5, STh3G.5
 Zeng, Heping - FTh1M.6, SW4B.7
 Zeng, Jinwei - FTh1K.2
 Zeng, Junjie - JTh2A.153
 Zeng, Li - FTh4G.7
 Zeng, Lijiang - AF3M.5
 Zeng, Siwei - SW4B.2
 Zeng, Xianglong - JTu2A.173, JTu3O.2
 Zeng, Xie - SF2I.6, SW3I.6
 Zeng, Xinglin - JTh2A.118
 Zeng, Yongquan - FM3E.6
 Zepeda, Andre' - SM2B.2
 Zervas, Michael - STh4A.4, STh4B.6, SW4B.3
 Zhai, Liang - FM1H.7
 Zhai, Yuyao N. - JTh2A.187
 Zhan, Alan - SF1J.4
 Zhan, Huan - JTh2A.91, SF3I.1
 Zhan, Minjie - FF2P.5
 Zhan, Qiwen - JTh2A.59
 Zhan, Yueying - JTu2A.44
 Zhang, An - FM1Q.8
 Zhang, Baile - FF2L.6, FM4J.6, FM4J.8, FM4Q.4
 Zhang, Betty M. - JTh2A.110
 Zhang, Bohan - SF1A.5
 Zhang, Changjian - FTh1P.4
 Zhang, Chaojie - FM3M.3
 Zhang, Chaoshi - STu4B.7
 Zhang, Cheng - FF1F.1, FTh4H, JW2A.67, SW4D.3
 Zhang, Chenglong - FF1D.7
 Zhang, Chensong - FF3F.4
 Zhang, Chi - AF3Q.5, JTh2A.148, JTh2A.149, SM1K.7, STh1N.5
 Zhang, Chong - SM2I.6
 ZHANG, CHUAN - SF3N.3
 Zhang, Chunfeng - JTh2A.151, JW2A.124, JW2A.126, JW2A.128
 Zhang, Danian - JW2A.144
 Zhang, Dongfang - SM4A.4
 Zhang, Eric J. - STh1B.2, SW3L.7
 Zhang, Fangfang - STu3K.4, SW4K.6
 Zhang, Ge - SM2N.6
 Zhang, Gong - AM4P.5, FM1G.2, FTu3G.2, JTh2A.18
 Zhang, Han - JTu2A.73
 Zhang, Haoquan - AW3O.3
 Zhang, Hao-Xiang - AW3O.1
 Zhang, Helena - JTh2A.17
 Zhang, Hualiang - FM4Q.5, FTh4J.3, JTu2A.7
 Zhang, Hui - Ath4O.4, JTh2A.18, JW2A.54
 Zhang, Jiawei - SW3D.3

- Zhang, Jie - FM3M.3
 Zhang, Jin - STh4A.8, STu4B.3
 Zhang, Jing - FM4H.1, STh1C.2, STu3C.4
 Zhang, Jingyuan Linda - FF3P.3, FTu3H.5, JTh3C.5
 Zhang, Kai - JTh2A.11
 Zhang, Kailing - JW2A.125
 Zhang, Kaiqi - JW2A.49, SW4C.3
 Zhang, Kun - FTu4E.4
 Zhang, Lei - JW2A.2, JW2A.23, SW4C.6
 Zhang, Liang - SM2K.2, SW3L.3
 Zhang, Lifa - FF1D.1
 Zhang, Lifu - FM3E.2
 Zhang, Lihua - SF3I.1
 Zhang, Lin - JTu2A.97, JW2A.46, SW3A.5
 Zhang, Ling - JTh2A.13
 Zhang, Lizhen - SM2N.6
 Zhang, Lu - JTh2A.14, SM4C.4
 Zhang, Meng - Ath4O.3, JTh2A.104, JTh2A.82, JTh2A.83, SF3I.4, SF3K.2
 Zhang, Mengying - JTu2A.174
 Zhang, Mi - JTh2A.31
 Zhang, Mian - FW3E.4, SF2I.3, SM1I.7, SM3B.4, SW4M.3
 Zhang, Miao - FTh4G.7
 Zhang, Min - JTu2A.32, JTu2A.44
 Zhang, Minming - JTu2A.122, JW2A.47
 Zhang, Nan - SF2I.6, SW3J.6
 Zhang, Nannan - JTu2A.47
 Zhang, Ning - JTu2A.66, SM2B.6, SW4C.4
 Zhang, Qi - FF2D.6
 Zhang, Qian - JTh2A.112, JTu2A.95
 Zhang, Qiang - FTu4A.4, JTh2A.12, STu3A.3
 Zhang, Qianwu - SM4C.2
 Zhang, Qiulin - STu3C.2
 Zhang, Runzhou - FTu3G.4, FW4F.5, JTh2A.15, SM3C.4
 Zhang, Ruoyu - JW2A.3
 Zhang, Sheng - JW2A.130
 Zhang, Shuai - JW2A.7
 Zhang, Shuangyou - FM3E.3, SF3K.5, SM1D.4, SW3L.2
 Zhang, Tingting - SM2C.6
 Zhang, Wanpeng - JW2A.152, SM1L.2
 Zhang, Wei - Ath3Q.3, FF2D.2, JW2A.174, JW2A.48, JW4P.3, SM2I.8, SW4D.7
 Zhang, Wei Li - STh3K.2
 Zhang, Weijun - FTu4A.4
 Zhang, Weipeng - JW2A.162
 Zhang, Weiwei - SM3B.5
 Zhang, Wenbo - JTu2A.47
 Zhang, Wenjia - STh4B.2
 Zhang, Xiang - FF1D.1, FM1Q.8, FM2F.4, FTh1D.5, FTh1G.8, SM4I.1
 Zhang, Xianting - JTh2A.125, JW2A.4, SW4M.4
 Zhang, Xiao - SF3K.6
 Zhang, Xiaoguang - JTu2A.47
 Zhang, Xiaosheng - SM3I.3
 Zhang, Xicheng - SM4A.1
 Zhang, Xin - JTh2A.94
 Zhang, Xingwang - STu4N.3
 Zhang, Xinliang - AF3Q.5, JTh2A.149, JW2A.53, SM2I.2, SM4B.5
 Zhang, Xin-Quan - STu4N.2
 Zhang, Xueliang - FTh4J.5
 Zhang, Xuping - AM4P.7, FF3F.5
 Zhang, Xuzhao - SF2N.1
 Zhang, Yali - JTu3O.2
 Zhang, Yan - JTh2A.183
 Zhang, Yanfeng - SW3M.4
 Zhang, Yang - FW3F.8, JW2A.65, STh4I.2
 Zhang, Yan-Lei - SF2J.5
 Zhang, Yezhezi M. - AF1Q.3, FM4J.5
 Zhang, Yibo - AM1J.5, AM1J.7, STh1J.3
 Zhang, Ying - JTu2A.65, JTu2A.95
 Zhang, Yinglu - JW2A.25
 Zhang, Yong - SW4C.2
 Zhang, Young - FTh1E.7, FW4F.2, JTh4C.2
 Zhang, Yu - JW2A.49, SM3I.6, STh3I.4, SW3B.3
 Zhang, Yuanhang - JW2A.46
 Zhang, Yuanjue - SW3Q.7
 Zhang, Yuguang - JW2A.8
 Zhang, Yujie - JTh2A.2
 Zhang, Yujing - JTh2A.193
 Zhang, Zecen - STh1B.1
 Zhang, Zeyu - JW2A.66, SW4I.3
 Zhang, Zheshen - FF1B.7, FTu3G.5
 Zhang, Zhibin - JW2A.130
 Zhang, Zhifeng - FM3Q.1
 Zhang, Zhigang - JTh2A.128, JW2A.152, SM1L.2, STu4K.1, STu4K.6
 Zhang, Zhiguo - JTh2A.151, JTu2A.37
 Zhang, Zhishen - SW3K.3
 Zhao, Bo - FTu3E.2
 Zhao, Boyang - JTh2A.92
 Zhao, Chao - JTu2A.91
 Zhao, Deyin - SW3Q.5
 Zhao, Fu-Li - STh3I.8
 Zhao, Gang - JW2A.78, STu3P.4
 Zhao, Gongyuan - Ath4Q.3, JTu2A.22, SM4B.7
 Zhao, Haitao - AM4P.5
 Zhao, Han - FM2Q.6, FM4Q.6
 Zhao, Haolan - SM1B.3
 Zhao, Hong - JTh2A.80
 Zhao, Hongping - STh3I.2
 Zhao, Hongwei - JW2A.52
 Zhao, Hui - JTu2A.103
 Zhao, Jian - JTu2A.41, SM2C.2, STu3K.2, STu3K.3
 Zhao, Jianye - JTh2A.184, JW2A.144
 Zhao, Jiapeng - FTu3G.4, FW4F.5, JTh2A.15, JTh2A.19, JTh2A.4
 Zhao, Jie - SF2I.4
 Zhao, Jun - JTh2A.156
 Zhao, Junxiang - SW4J.4
 Zhao, Jy - Ath3P.2
 Zhao, Lingjuan - JW2A.62, SW4Q.6
 Zhao, Lingxiao - FM1F.4
 Zhao, Nan - STu3K.4
 Zhao, Qi - FTu4A.4
 Zhao, Qiancheng - JW2A.175
 Zhao, Qing-Yuan - FW3F.3
 Zhao, Rongkuo - SM4I.1
 Zhao, Ruogang - FM2Q.6
 Zhao, Shaoyu - SF1G.1
 Zhao, Shuangxiang - JW2A.173
 Zhao, Wei - JW2A.124
 Zhao, Wei ke - STu4B.4
 Zhao, Wu - SW4Q.6
 Zhao, Xiaolei - SW4B.2
 Zhao, Xin - FF2D.5, FM1F.6, JTh2A.139, JW2A.153, SW3L.1
 Zhao, Xingchen - FM4H.4
 Zhao, Xueying - AW3O.3
 Zhao, Yan - JTh2A.186
 Zhao, Yang - JW2A.130
 Zhao, Yi - STh1A.8
 Zhao, Yifan - SM2C.1
 Zhao, Yingxin - SM1L.2
 Zhao, Yongguang - SF2N.1, SF3I.5
 Zhao, Yun - FM3G.5
 Zhao, Yunhe - SM2K.2, STh3K.5
 Zhao, Yunsong - SW4B.2
 Zhao, Yuxuan - AF3M.5
 Zhao, Zhangji - SW3I.4
 Zhao, Zhe - FTu3G.4, FW4F.5, JTh2A.15, SM3C.4
 Zhao, Zheng - SF1A.3
 Zhao, Zhixin - AW3O.6
 Zhao, Zhuan - JTh2A.94
 Zhdanova, Alexandra A. - JTu2A.135, JTu2A.75
 Zheltikov, Aleksei - FM1Q.2
 Zheludev, Nikolai I. - FTh3E.7
 Zheludev, Nikolay I. - FF1H.4, FM3J.2, FM4J.4, FTh1F.5, FTh4H.6, JTh2A.26
 Zhen, Bo - FM2Q.3, FW3G
 Zheng, Bowen - JTu2A.7
 Zheng, Changxi - FF1F.6
 Zheng, Donghui - STu3K.3
 Zheng, Guoxing - JTh2A.64
 Zheng, Hanyu - SM2I.8
 Zheng, Jiajiu - SF3A.6
 Zheng, Jian - FW4E.6
 Zheng, Jian-Yao - FTh1K.3
 Zheng, Jiming - JTh2A.92
 Zheng, Lingchen - JW2A.2, JW2A.23
 Zheng, Mei C. - AF1Q.3
 Zheng, Ming-Yang - JTh2A.12
 Zheng, Shaonan - Ath4O.1, Ath4O.2, Ath4O.4, JW2A.54
 Zheng, Shoujun - FTh1F.5
 Zheng, Shuang - JW2A.12, JW2A.28, STh1B.5, STh3B.3
 Zheng, Tianzhe - STu3A.3
 Zheng, Wanhua - SF1G.1
 Zheng, Wan-hua - JW2A.30
 Zheng, Xiaoping - AF2M.8, JTh4D.2, JW2A.42
 Zheng, Xiaorui - STu4N.3
 Zheng, Ximeng - SM3L.3, SM3L.4
 Zheng, Yan - JTh2A.165
 Zheng, Yi - SM2C.3, SW4A.4
 Zheng, Yuebing - FF3F.2, JTu2A.2, SM2O.5, STh1I.4
 Zheng, Zheng - Ath4O.3, JTh2A.104, JTh2A.139, JTh2A.82, JTh2A.83, JW2A.153, SF3I.4, SF3K.2, SW3L.1
 Zheng, Zhou - SM2K.3
 Zheng, Zibo - JTu2A.47
 Zhigilei, Leonid - JTu3O.1
 Zhong, Chuan - ATu4M.2, FTh1K.3
 Zhong, Jiaqiang - FTu4A.4
 Zhong, Kai - STh4F.3
 ZHONG, QI - FM4E.2
 Zhong, Tian - FTu4H.4, FTu4H.5, JTh3C.3, STh3G.2
 Zhong, Yiming - JW2A.56
 Zhong, Zheqiang - SM4A.7
 Zhou, Bingkun - JW2A.42
 Zhou, Ciming - SM2K.3
 Zhou, Dapeng - SW3L.3
 Zhou, De - SM2I.2
 Zhou, Feng - ATu3J.7, JW2A.53
 Zhou, Gan - STu3B.4
 Zhou, Gengji - JTh2A.162, SF1N.6
 Zhou, Guangya - SM3I.3
 Zhou, Heng - JTu2A.148, JTu2A.56, STu3C.4
 Zhou, Hengyun - FM2Q.3
 Zhou, Hongwen - Ath4O.3, JTh2A.104
 Zhou, Huang - STu4O.6
 Zhou, Jin - STh1B.1
 Zhou, Linjie - JW2A.56, STh3B.4
 Zhou, Qian - ATu3I.4, JW2A.160
 Zhou, Ting - JW2A.14, SW4C.6
 Zhou, Tong - SM4M.5, SM4M.6
 Zhou, Wei - FTh4M.5, SF2N.1, SM2C.1, STh1A.3
 Zhou, Weidong - JTu2A.13, SM2B, SW3Q.5, SW4B
 Zhou, Wen - JTh2A.62, JW2A.66
 Zhou, Xi - AF3Q.5, JTh2A.148, JTh2A.149
 Zhou, Xiaoci - FM1G.1, FM1G.2, FTu3G.2, JTh2A.18
 Zhou, Xiaoyan - STh3A.6
 Zhou, Xiaoying - FF1D.7
 Zhou, Xingyu - SM4K.6
 Zhou, Xuliang - JTh2A.76, JW2A.62
 Zhou, Xuyan - SF1G.1
 Zhou, Yang - FF1D.7
 Zhou, Yiyin - AF1Q.5, STh4I.4
 Zhou, Yiyu - JTh2A.19, JTh2A.4
 Zhou, Yue - JW2A.73
 Zhou, Zhiping - JTu2A.74
 Zhu, Alexander - AM1J.6, FM3J.1, JW2A.101
 Zhu, Alexander Y. - FTh3M.5
 Zhu, Baoqiang - JTu2A.178
 Zhu, Binghui - JTh2A.62
 Zhu, Chunhui - AF1Q.4
 Zhu, Dan - STu3B.3
 Zhu, Di - FM1H.6, FW3F.3, SF3A.4
 Zhu, Eric Y. - ATu3J.7, FM4G.7, FM4G.8, JTh2A.98
 Zhu, Hanyu - FF1D.1
 Zhu, Jiangbo - SW3M.4
 Zhu, Jianxiu - FM1F.4
 Zhu, Jinghao - ATu3I.5
 Zhu, Jinglong - JTh2A.113
 Zhu, Junfeng - JTh2A.86
 Zhu, Lin - SW4B.2
 Zhu, Mingyue - STh1C.2, STu3C.4
 Zhu, Qingming - SW4C.2
 Zhu, Rongrong - SW4M.3
 Zhu, Sheng - JTh2A.109
 Zhu, Shining - FF1F.3, STh4K.7, STu4B.7
 Zhu, Si - SW3Q.1
 Zhu, Tao - JTh2A.108
 Zhu, Wenqi - FF1F.1, SW4D.3
 Zhu, Xiushan - SM2N.4
 Zhu, Yeyu - SW4B.2
 Zhu, Yimei - FTu4E.2
 Zhu, Yiming - Ath3Q.5
 Zhu, Yunpeng - SW4I.4
 Zhu, Yuntao - STu3B.2
 Zhu, Zebin - ATu3I.4, JW2A.160
 Zhu, Zheyuan - STu3K.3
 Zhu, Zimu - FTh4E.7
 Zhuang, Quntao - FF1B.7, FTu3G.5
 Zhukov, Vladimir P. - SM3O.3
 Zhuo, Deng - STh4I.5
 Zhuo, Guan-Yu - JTu2A.93
 Zia, Nouman - JTh2A.28
 Ziaee, Farzaneh - JW2A.182
 Zibar, Darko - STh1C.1, STh1C.3, STu3D.1
 Zich, Julien - FW3F.1
 Zilk, Matthias - FW4H.8
 Zimmermann, Lars - JW2A.9, STu4C.1
 Zohrabi, Mo - SW4J.7
 Zolotovskii, Igor O. - JTh2A.57
 Zondlo, Mark - Ath4P
 Zong, Jie - SM2N.4
 Zou, Chang-Ling - SF2J.5
 Zou, Chen - SF1I.3
 Zou, Chengjun - FTh1K, FW3H.1
 Zou, Kai - FW3F.1
 Zou, Kaiheng - JTu2A.49, JTu2A.53, SW3A.5
 Zou, Ran - Ath3P.4, ATu4M.6
 Zou, Xiao - JTu2A.65
 Zou, Xu-Bo - SF2J.5
 Zoysa, Menaka D. - SF1G.3
 Zuba, Viktor - SM4N.7
 Zubia, J. - SM2K.6
 Zubin, Jacob - FW3F.4
 Zukauskas, Andrius - STh3F.4, STh4F.2
 Zukowski, Barbara - AF3M.6
 Zuo, Peng - Ath3P.2
 Zuo, Yan - SM2I.2
 Zuowei, Xu - JW2A.1
 Zürich, Michael - FF1P.4
 Zwick, Thomas - STu3D.4
 Zwickel, Heiner - SM3B.1, SM3B.3, STu4B
 Zwiller, Val - FTh4H.4, FW3F.1
 Zych, Magdalena - FTh4G.1

